



**BRITISH  
COLUMBIA**

**Ministry of Employment and Investment  
Energy and Minerals Division  
Geological Survey Branch**

# **GEOLOGICAL FIELDWORK 1997**

**A Summary of Field Activities  
and Current Research**

**PAPER 1998-1**



**BRITISH  
COLUMBIA**

**Ministry of Employment and Investment  
Energy and Minerals Division  
Geological Survey Branch**

# **GEOLOGICAL FIELDWORK 1997**

**A Summary of Field Activities  
and Current Research**

**PAPER 1998-1**

# Energy and Minerals Division

## Geological Survey Branch

Parts of this publication may be quoted or reproduced if credit is given. The following is the recommended format for referencing individual works contained in this publication:

MacIntyre, D.G. and Struik, L.C. (1998): Nechako NATMAP Project, 1997 Overview, in Geological Fieldwork 1997, *British Columbia Ministry of Employment and Investment*, Paper 1998-1, pages 1-1 to 1-8.

### British Columbia Cataloguing in Publication Data

Main entry under title:

Geological fieldwork: - 1974 -

Annual.

Issuing body varies

Vols. For 1978-1996 issued in series: Paper / British Columbia. Ministry of Energy, Mines and Petroleum Resources; vols for 1997- , Paper / British Columbia. Ministry of Employment and Investment.

Includes Bibliographical references.

ISSN 0381-243X = Geological fieldwork

1. Geology - British Columbia - Periodicals. 2. Mines and mineral resources - British Columbia - Periodicals. 3. Geology, Economic - British Columbia - Periodicals. 4. British Columbia. Geological Survey Branch - Periodicals. I. British Columbia. Geological Division. II. British Columbia. Geological Branch. III. British Columbia. Geological Survey Branch. IV. British Columbia. Department of Mines and Petroleum Resources. V. British Columbia. Ministry of Energy, Mines and Petroleum Resources. VI. British Columbia. Ministry of Employment and Investment. VII. Series: Paper (British Columbia. Ministry of Energy, Mines and Petroleum Resources). VIII. Series: Paper (British Columbia. Ministry of Employment and Investment).

QE187.G46

553'.09711

C76-083084-3 (Rev.)



VICTORIA  
BRITISH COLUMBIA  
CANADA

JANUARY 1998

## FOREWORD

---

Geological Fieldwork: A Summary of Fieldwork and Current Research, 1997 is the twenty-third edition of this annual publication. It contains reports of Geological Survey Branch activities and projects during 1997. The base budget of the Branch for the 1997-98 fiscal year was \$4.6 million, down from \$6.6 million the previous year. The Branch also received \$135 000 from the Corporate Resource Inventory Initiative to maintain the Mineral Potential database of the province and for mineral potential studies of the Cassiar-Iskut-Stikine planning area. In addition, a new Geoscience Partnership Program with external clients was initiated in 1997. Results of the Moyie Partnership are reported on in this volume.

The contents of this year's volume reflect the emphasis of Branch programs. Highlights were:

- Continuation of the Nechako Plateau NATMAP project, which is a collaborative effort with the Geological Survey of Canada and various universities. The focus of GSB work is the Babine porphyry belt with its important mineral potential;
- Regional geochemical sampling of the Mesilinka River Map Sheet (94C) in east central British Columbia;
- Year 2 of the multidisciplinary Eagle Bay Project which is utilizing surficial geology and geochemistry to look for clues for buried mineral deposits in the Adams Plateau area;
- The Moyie industrial partnership project which will result in new 1:50 000 scale compilation maps for areas underlain by the Aldridge Formation;
- The Devonian-Mississippian VMS project which continued to test potential extensions of strata that host the Kudze Kayah and Wolverine deposits in northern British Columbia; and
- The McConnell Range regional mapping project which extended existing coverage of the Toadoggonne volcanic belt southward from the area of the Kemess deposit.

A variety of mineral deposits and deposit types are profiled in this year's volume, including a stratabound zinc deposit in the Caribou terrane, an epithermal gold deposit in northern-most British Columbia, nickel mineralization in the Turnagain Alaskan ultramafic complex, sediment-hosted gold mineralization near Watson Bar and mineral occurrences near Bella Coola. There is also a report on Tertiary mineralization in the Queen Charlotte Islands and results of a study of the Slocan camp, as well as three reports on mineral deposit studies and age dating from MDRU at the University of British Columbia.

The Mineral Potential project completed coverage of the Queen Charlotte Islands, hence the province is now completely covered at 1:250 000 scale. Much information from the project is posted on the Ministry Internet site (address: <http://ei.gov.bc.ca/geology>). The intent is to have geology, mineral potential estimates, MINFILE, mineral titles information and other data available on the Internet. Through the Map Guide viewer (downloadable at the site) data posted may be viewed and manipulated. The geology and some associated datasets may also be downloaded in Arc Export (EOO) format from the site.

The Branch is now employing print-on-demand technology for its geoscience publications. Material will also be posted on the Ministry Internet site for viewing or downloading. Production of Geological Fieldwork to the camera-ready stage has been done in Microsoft WORD by the authors using a template prepared by Brian Grant and updated by Dave Lefebure and Bill McMillan. Thanks are due to Dave Lefebure and Bill McMillan for editing and guiding the process, and Dorthe Jakobsen for administrative backup to ensure completion of this report on schedule.

*W.R. Smyth*  
*Chief Geologist*  
*Geological Survey Branch*



# TABLE OF CONTENTS

|                                                                                                                                                                                                                               | Page |                                                                                                                                                                                                                                  | Page |
|-------------------------------------------------------------------------------------------------------------------------------------------------------------------------------------------------------------------------------|------|----------------------------------------------------------------------------------------------------------------------------------------------------------------------------------------------------------------------------------|------|
| <b>FOREWORD</b> .....                                                                                                                                                                                                         | i    |                                                                                                                                                                                                                                  |      |
| <b>REGIONAL MAPPING</b>                                                                                                                                                                                                       |      |                                                                                                                                                                                                                                  |      |
| <b>D.G. MacIntyre and L.C. Struik:</b> Nechako NATMAP<br>Project, 1997 Overview .....                                                                                                                                         | 1-1  | <b>M. Smith and D.A. Brown:</b> Preliminary Report on a<br>Proterozoic (?) Stock in the Purcell Supergroup<br>and Comparison to the Cretaceous White Creek<br>Batholith, Southeastern British Columbia<br>(82F/16, 82K/01) ..... | 11-1 |
| <b>D.G. MacIntyre:</b> Babine Porphyry Belt: Bedrock<br>Geology of the Nakinilerak Lake Map Sheet<br>(93M/8), British Columbia .....                                                                                          | 2-1  | <b>R. Woodfill:</b> Purcell Gravity Anomaly - Implications<br>for Mineral Exploration .....                                                                                                                                      | 12-1 |
| <b>D.G. MacIntyre, P. Schiarizza and L.C. Struik:</b><br>Preliminary Bedrock Geology of the<br>Tochcha Lake Map Area (93K/13),<br>British Columbia .....                                                                      | 3-1  | <b>ECONOMIC GEOLOGY</b>                                                                                                                                                                                                          |      |
| <b>P. Schiarizza, N. Massey and D. MacIntyre:</b> Geology of<br>the Sitlika Assemblage in the Takla Lake Area<br>(93N/3, 4, 5, 6, 12) .....                                                                                   | 4-1  | <b>T. Höy and F. Ferri:</b> Stratabound Base Metal Deposits<br>of the Barkerville Subterrane, Central British<br>Columbia (093A/NW) .....                                                                                        | 13-1 |
| <b>V.M. Levson, A.J. Stumpf and A.J. Stuart:</b> Quaternary<br>Geology and Ice-Flow Studies in the Smithers and<br>Hazelton Map Areas (93 L and M): Implications for<br>Exploration .....                                     | 5-1  | <b>T. Höy and F. Ferri:</b> Zn-Pb Deposits in the Cariboo<br>Subterrane, Central British Columbia<br>(93A/NW) .....                                                                                                              | 14-1 |
| <b>M.G. Mihalynuk, J. Nelson and R.M. Friedman:</b><br>Regional Geology and Mineralization of the Big<br>Salmon Complex (104N NE and 1040 NW) .....                                                                           | 6-1  | <b>R.E. Lett, P. Bobrowsky, M. Cathro and A. Yeow:</b><br>Geochemical Pathfinders For Massive Sulphide<br>Deposits in the Southern Kootenay Terrane .....                                                                        | 15-1 |
| <b>J. Nelson, T. Harms and J. Mortensen:</b> Extensions<br>and Affiliates of the Yukon-Tanana Terrane in<br>Northern British Columbia .....                                                                                   | 7-1  | <b>R.C. Paulen, P.T. Bobrowsky, E.C. Little,<br/>A.C. Prebble and A. Ledwon:</b> Surficial Deposits<br>in the Louis Creek and Chu Chua Creek Area .....                                                                          | 16-1 |
| <b>L.J. Diakow and C. Rogers:</b> Toodoggone - McConnell<br>Project: Geology of the McConnell Range -<br>Serrated Peak to Jensen Creek, Parts of<br>NTS 94E/2 and 94D/15 .....                                                | 8a-1 | <b>H. Plint, W.J. McMillan, J. Nelson and A. Panteleyev:</b><br>The Nizi Property: A Classic (Eocene?)<br>Epithermal Gold System in Far Northern<br>British Columbia .....                                                       | 17-1 |
| <b>A.S. Legun:</b> Toodoggone - McConnell Project: Geology<br>of the McConnell Range - Jensen Creek to Johanson<br>Creek, Parts of the NTS 94D/9, 10, 15, 16 .....                                                            | 8b-1 | <b>G.T. Nixon:</b> Ni-Cu Sulfide Mineralization in the<br>Turnagain Alaskan-Type Complex: A Unique<br>Magmatic Environment .....                                                                                                 | 18-1 |
| <b>D.A. Brown and R.D. Woodfill:</b> The Moyie Industrial<br>Partnership Project: Geology and Mineralization of<br>the Yahk-Moyie Lake Area, Southeastern British<br>Columbia (82F/01E, 82G/04W, 82F/08E, 82G/05W) .....      | 9-1  | <b>D.V. Lefebure:</b> Epithermal Gold Deposits of the<br>Queen Charlotte Islands .....                                                                                                                                           | 19-1 |
| <b>D.A. Brown and T. Termuende:</b> The Findlay Industrial<br>Partnership Project: Geology and Mineral<br>Occurrences of the Findlay - Doctor Creek Areas,<br>Southeastern British Columbia (parts of 82F/16,<br>82K/1) ..... | 10-1 | <b>G.E. Ray, J.A. Brown and R.M. Friedman:</b><br>Geology of the Nifty Zn-Ba-Ag Prospect Bella<br>Coola District, British Columbia .....                                                                                         | 20-1 |
|                                                                                                                                                                                                                               |      | <b>M.S. Cathro, R.M. Dürfeld and G.E. Ray:</b> Epithermal<br>Mineralization on the Watson Bar Property<br>(92/01E), Clinton Mining Division, Southern B.C. ....                                                                  | 21-1 |
|                                                                                                                                                                                                                               |      | <b>B.N. Church:</b> Metallogeny of the Slocan City Mining<br>Camp (82F11/14) .....                                                                                                                                               | 22-1 |

**B.N. Church and G.H. Klein:** The Allin Property and Equity-type Mineralization, Central British Columbia.....23-1

**SELECTED MINERAL DEPOSIT PROFILES**

**D. Lefebure:** British Columbia Mineral Deposit Profiles..... 24  
**E.A.G. Trueman:** Carbonate Hosted Cu+Pb+Zn ..... 24 a  
**Z.D. Hora:** Bentonite.....24 b  
**Z.D. Hora:** Sedimentary Kaolin ..... 24 c  
**G.J. Simandl and K. Hancock:** Sparry Magnesite.....24 d  
**S. Paradis, G.J. Simandl, D. MacIntyre and G.J. Orris:** Sedimentary-Hosted, Stratiform Barite ..... 24 e  
**R.H. McMillan:** Unconformity-Associated U.....24 f  
**G.E. Ray:** Au Skarns ..... 24 g  
**G.E. Ray:** Garnet Skarns ..... 24 h  
**G.A. Gross, C.F. Gower and D.V. Lefebure:** Magmatic Ti-Fe+V Oxide Deposits .....24 i  
**Z.D. Hora:** Ultramafic-Hosted Chrysotile Asbestos.....24 j  
**J. Pell:** Kimberlite-Hosted Diamonds ..... 24 k  
**J. Pell:** Lamproite-Hosted Diamonds.....24 l  
**Z.D. Hora:** Andalusite Hornfels ..... 24m  
**G.J. Simandl and W.M. Kenan:** Microcrystalline Graphite.....24 n  
**G.J. Simandl and W.M. Kenan:** Crystalline Flake Graphite..... 24 o  
**G.J. Simandl and W.M. Kenan:** Vein Graphite in Metamorphic Terrains ..... 24 p

**INDUSTRIAL MINERALS**

**G.J. Simandl, G. Payie and B. Wilson:** Blue Beryl/ Aquamarine Occurrences in the Horseranch Range, North Central British Columbia .....25-1  
**G.J. Simandl, P. Jones, J.W. Osborne, G. Payie, and J. McLeod:** Use of Heavy Minerals in Exploration for Sapphires, Empress Cu-Au-Mo Deposit, British Columbia.....26-1

**B. Ryan, J. Gransden and J. Price:** Fluidity of Western Canadian Coals and its Relationship to Other Coal and Coke Properties ..... 27-1

**B. Ryan and M. Khan:** Maceral Affinity of Phosphorus in Coals From the Elk Valley Coalfield, British Columbia ..... 28-1

**B. Ryan and A. Ledda:** A Review of Sulphur in Coal: With Specific Reference to the Telkwa Deposit, North-Western British Columbia..... 29-1

**A. Matheson, R. Paulen, P.T. Bobrowsky and N. Massey:** Okanagan Aggregate Potential Project ..... 29a-1

**REGIONAL GEOCHEMISTRY PROGRAM**

**W. Jackaman, S. Cook and R.E. Lett:** Regional Geochemical Survey Program: Review of 1997 Activities..... 30-1

**MINERAL DEPOSIT RESEARCH UNIT  
THE UNIVERSITY OF BRITISH COLUMBIA**

**C.L. Deyell, J.F.H. Thompson, L.A. Groat, J.K. Mortensen, R.M. Friedman and W.D. Tompson:** The Style and Origin of Alternation on the Limonite Creek Property, Central British Columbia (93L/12) ..... 31-1

**M.E. Lepitre, J.K. Mortensen and R.M. Friedman:** Geology and U-Pb Geochronology of Intrusive Rocks Associated with Mineralization in the Northern Tahtsa Lake District, West-Central British Columbia..... 32-1

**R.J. Whiteaker, J.K. Mortensen and R.M. Friedman:** U-Pb Geochronology, Pb Isotopic Signatures and Geochemistry of an Early Jurassic Alkalic Porphyry System Near Lac La Hache, B.C..... 33-1



## Regional Mapping

# NECHAKO NATMAP PROJECT - 1997 OVERVIEW

By D.G. MacIntyre and L.C. Struik (GSC, Vancouver)

*A Contribution to the Nechako NATMAP Project*

**KEYWORDS:** Nechako plateau, Eocene, extension, Natmap, Babine porphyry belt, Sitlika Assemblage, Nechako map, Fort Fraser map, Endako, plutonism, multidisciplinary, bedrock mapping, surficial mapping, biogeochemistry, till geochemistry, geochronology, conodonts, radiolarian, geophysics.

## INTRODUCTION

The Nechako NATMAP project is a joint mapping venture between the GSC, BCGSB, universities and industry (McMillan and Struik; 1996, Struik and McMillan, 1996; Struik and MacIntyre, 1997; MacIntyre and Struik, 1997; Struik and MacIntyre, 1998). The project encompasses over 30,000 square kilometres in central British Columbia (Figures 1-1, 1-2). Its main focus is to improve the quality and detail of bedrock and surficial maps to help resolve several geological problems. In particular it addresses the following questions: 1) the extent and nature of Tertiary crustal extension, 2) Mesozoic compression and the manner of accretion of exotic terranes, 3) the geological and geophysical definition of the terranes, 4) the sequence of changing Pleistocene glacial ice flow directions, and 5) the character and dispersion of glacial deposits.

In this third field season of the Nechako NATMAP project, bedrock mapping was done in eleven NTS map areas and surficial mapping was done in five (Figure 1-2). The scale of mapping varied from 1:20 000 to regional 1:100 000 scales. In addition, detailed sampling, and stratigraphic studies were undertaken in these map areas. Samples were collected for till, silt, lake, biological and lithological chemistry, paleomagnetic studies and paleontological and radioisotopic geochronology. Stratigraphic studies concentrated on sections within the Cache Creek Group near Fort St. James and mainly volcanic sequences of the Ootsa Lake and Endako groups. Digital GIS projects included compilation of mapping data from Placer Dome Incorporated, construction and addition to the digital field mapping databases, cartography of geological maps, and the initiation of the internet GIS data sharing (Figure 1-3).

This paper outlines research that in many cases is preliminary. References are given to more in depth summaries in this volume and Current Research of the Geological Survey of Canada. The continuing research will lead to more comprehensive government and journal reports and maps. No analytical data is reported in this paper.

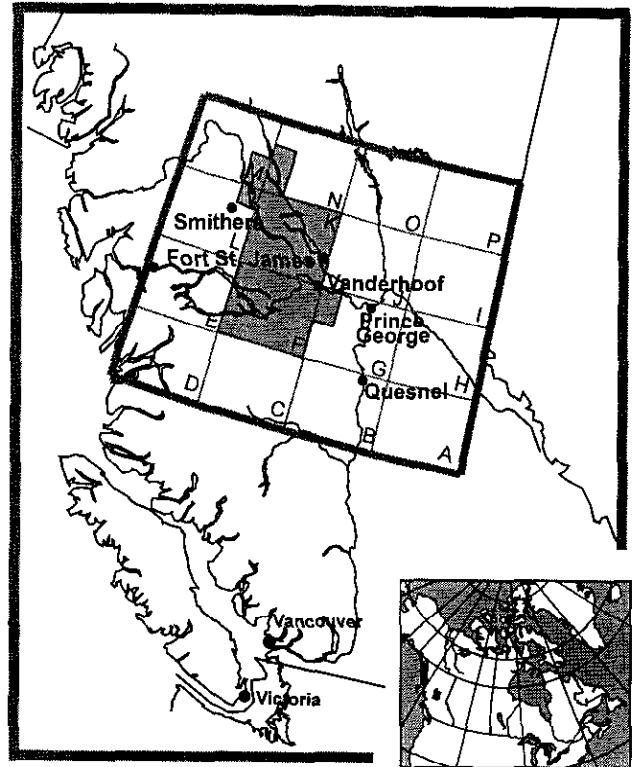


Figure 1-1. Location of the Nechako Natmap project.

## BEDROCK MAPPING

### Babine Porphyry Belt and Sitlika Studies

Bedrock mapping in the Babine-Takla lakes area built on previous mapping by Don MacIntyre and crew in the 93L/16 and 93M/1 map sheets of the Babine Porphyry belt (MacIntyre *et al.*, 1996; MacIntyre *et al.*, 1997) and Paul Schiarizza and crew in the 93N/12 and 93N/13 maps sheets of the Sitlika belt east of Takla Lake (Schiarizza and Payie, 1997). Don MacIntyre, Paul Schiarizza, and Nick Massey of the BCGSB were the project leaders in 1997. Excellent geological field assistance was provided by summer students Michele Lepitre (UBC), Ryanne Metcalf (UBC), Sheldon Modeland (UVIC), Stephen Munzar (UBC) and Deanne Tackaberry (UVIC). From late June until the end of

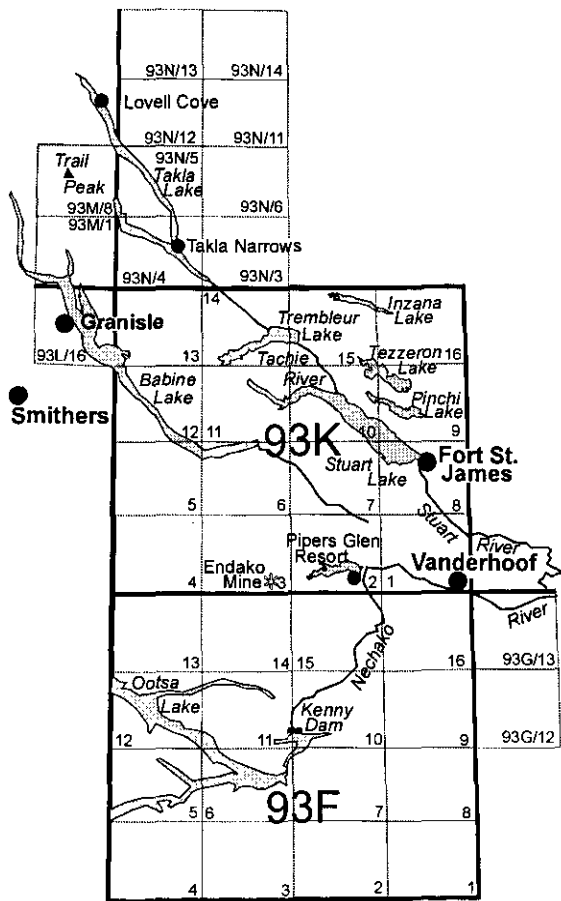


Figure 1-2. Geographic localities referred to in text

August this crew completed bedrock mapping of NTS map sheets 93M/8, 93N/5 and 93K/13 plus most of 93N/4 and parts of 93M/7, 93N/6, 93N/12 and 93N/3 (Figures 1-2,1-3).

Helicopter service was provided by Pacific Western Helicopters from their base at Lovell Cove. Daily set-outs and pickups were used to cover less accessible areas. Other areas were mapped using logging road access. A 17 foot zodiac was used to map extensive rock exposures along the shores of Takla Lake and the B.C. Rail line, which is located along the east shore of Takla Lake. Base camp for the project was at the Takla Rainbow lodge situated at Takla Narrows.

Bedrock mapping in the project area was done at 1:50 000 scale in 93M/8 and 93N/5, and at a more regional 1:100,000 scale in 93N/4 and 93K/13 (MacIntyre, 1998; MacIntyre *et al.*, 1998; Schiarizza *et al.*, 1998). Samples were collected throughout the map area for micro and macro paleontology, isotopic age dating, paleomagnetic determinations, whole rock and trace element geochemistry. All mineralized outcrops were sampled to determine base and precious metal content.

The following are the main highlights of the Babine and Sitlika mapping of 1997:

1. the Trail Peak and Nak porphyry copper deposits, are associated with northwest trending biotite-feldspar porphyry dikes that are part of the Eocene Babine Intrusions. The dikes cut

both an earlier granodiorite to quartz diorite phase and hornfelsed Hazelton Group volcanics and sediments. High angle normal faults, which are Eocene or younger, offset the intrusions and surrounding rocks (MacIntyre, 1998).

2. the belt of Lower to Middle Jurassic bimodal volcanics, first recognized in the area west of Granisle in 1995, was traced into the 93M/8 map sheet. However the unit appears to be thinning and contains less felsic volcanics going northward toward the Bowser Basin. This coincides with a general change in the nature of Lower to Middle Jurassic sediments from shallow to deep water facies.
3. an area of hornblende-biotite-feldspar porphyry flows was mapped northwest of Trail Peak. These rocks are tentatively correlated with the Late Cretaceous Kasalka Group. Previous mapping suggested these flows were part of the Tertiary Babine Intrusive suite.
4. a large stock of porphyritic quartz monzonite with a border phase of hornblende diorite was mapped east of Tochcha Lake in the 93K/13 map area. This stock, which does not appear on previous maps, is considered part of the Topley suite; it intrudes volcanics of the Takla Group. Other large plutons north and south of the northwest arm of Takla lake in the 93N/4 map sheet also intrude Takla rocks and have similar lithologies to the Topley suite with which they are tentatively correlated (MacIntyre *et al.*, 1998).
5. the three lithologic divisions of the Sitlika assemblage were traced southward from 93N/12, through 93N/5 and into the northern part of 93N/4 (MacIntyre *et al.*, 1998). The western clastic unit traces into rocks previously included in the Upper Triassic Takla Group. Because lithologically similar sedimentary rocks are intercalated with typical Takla Group volcanics, it is suspected that the western clastic unit is not Sitlika but might be a fault-bounded sliver of Takla rocks. The Sitlika volcanic unit and overlying eastern clastic unit were traced southwards into volcanic and sedimentary rocks that had previously been mapped as Cache Creek Group.
6. the ultramafic unit that marks the boundary between the Sitlika assemblage and Cache Creek Group in 93N/12 and 13 continues southward through 93N/5 and into 93N/4. This unit is a serpentinite melange in the north, but to the south includes relatively coherent intervals of tectonized harzburgite and dunite, confirming an ophiolitic origin for the ultramafic belt.
7. the contact between the Cache Creek Group and Sitlika assemblage was observed east of Tsayta Lake (93N/5) where it is a low-angle fault that places the Cache Creek ultramafic unit above Sitlika eastern clastic unit. This fault

contact is truncated by monzogranite of the Mitchell pluton (Schiarizza *et al.*, 1998).

8. Sitlika assemblage in 93N/4 and 5 is separated from the Upper Triassic Takla Group of Stikine Terrane by a system of north to northwest-striking faults of uncertain sense of displacement. This fault system is truncated by the north-striking Takla Fault, which marks the western boundary of the Sitlika assemblage in 93N/12 and 13.

## Cache Creek Group Tectono-Stratigraphic Studies in Northeastern Fort Fraser Map Area

Studies in the Cache Creek Group of eastern Fort Fraser map area consisted of bedrock mapping, biostratigraphy, lithochemistry, and geochronological sampling. This work was conducted by Bert Struik (GSC), Hiroyoshi Sano (Kyushu University, Japan), Mike Orchard (GSC), Fabrice Cordey (Universite Claude Bernard a Lyon, France), Wayne Bamber (GSC), Henriette LaPierre (Universite Claude Bernard a Lyon, France) and Marc Tardy (Universite de Savoie, France). Excellent geological mapping assistance was provided by students Mike Hrudehy (Univ. of Alberta), Crystal Huscroft (UBC), Andrew Blair (Okanogan College), Angelique Justafsen (Camosun College), and Samara Lewis (UBC). Primary access was by forest service roads branching from Fort St. James, and the extensive lake system.

Bedrock mapping of sheets 93K/9, 10, and 15 was completed at 1:100 000 scale (Figure 1-3). That mapping built on recent mapping by Ash *et al.* (1993) in 93K/9, 10 and Nelson *et al.* (1993) in 93K/16. Hiroyoshi Sano spent 3.5 weeks doing detailed biostratigraphic mapping of the Cache Creek Group's Mount Pope formation near Fort St. James. Mike Orchard, Fabrice Cordey and Wayne Bamber joined Hiroyoshi Sano to map and sample Cache Creek Group limestones and cherts for conodont, radiolarian and coral assemblages in the context of the sedimentological environments interpreted from depositional textures (Orchard *et al.*, 1998; Sano, 1998). Lithochemical sampling of basalts of the Cache Creek and Takla Group was done by Henriette LaPierre and Marc Tardy to constrain the basalt petrogenesis.

The following are the main highlights of the Cache Creek studies of 1997:

1. Upper Triassic and possibly Lower Jurassic basalt tuff, greywacke, siltstone, conglomerate and minor limestone straddle the Pinchi Fault zone along Pinchi and Tezzeron lakes. These rocks formerly mapped as Takla Group are tentatively differentiated as the Tezzeron assemblage. They are interpreted to have been an overlap assemblage onto oceanic assemblages of the Cache Creek Group.
2. the Pinchi Fault probably cuts the former suture between the oceanic Cache Creek Group and the island arc Takla Group. The suture itself is

exposed along Pinchi Lake as the blueschist terrane documented by Patterson (1973). Cache Creek Group ultramafic rocks overthrust Tezzeron assemblage tuff and greywacke on either side of the Pinchi Fault.

3. all of the contacts of the Mount Pope formation, which consists of limestone, chert and minor basalt, are probably thrust faults. Where the Mount Pope limestone and underlying units have been dated, the underlying rocks are younger.
4. the limestone of the Cache Creek Group has been constrained to three time intervals: earliest Upper Carboniferous to Early Permian, Late Permian and Early Triassic.
5. Upper Carboniferous to Early Permian Cache Creek Group limestone is generally clastic, formed in shallow to moderately shallow water and thought to have developed on basaltic ocean islands.
6. diorite, and quartz diorite plutons intrude a large area of the Cache Creek Group near Tachie River north of Stuart Lake. These plutons called the McElvey and Tachie plutons are generally unfoliated and cross-cut all structures in the Cache Creek Group including metasediments of the Middle and Upper Triassic Sowchea assemblage (Hrudehy and Struik, 1998).
7. new lithochemistry of Cache Creek Group basalts indicate they are mainly ocean island type.

## Endako Plutonism and Tectonics

Detailed bedrock mapping of the Endako map area (93K/3) was conducted at 1:50 000 scale using previous Endako Mines mapping (Kimura *et al.* 1980; G. Johnson, personal communication, 1997) as a guide and template. Joe Whalen (GSC) and Bert Struik (GSC) ably assisted by Nancy Grainger (Univ. of Alberta) and the student assistants of the Cache Creek Group-east study. They concentrated on the intrusive and genetic relationships of the Jura-Cretaceous plutonic suites and tectono-stratigraphy of the Tertiary volcanic rocks. Randy Enkin and Judith Baker (GSC) continued Tertiary paleomagnetic tilt studies in the Endako area (Lowe *et al.*, 1998). Carmel Lowe (GSC) interpreted the magnetic signature of the Endako molybdenum camp (Lowe *et al.*, 1998). The area was accessed through forest roads and highways.

Sufficient geological data was gathered to complete a detailed bedrock map of the Endako map area (93K/3) (Whalen *et al.*, 1998). Stratigraphic sequences in the Ootsa Lake and Endako groups were constrained within the limits of the poor exposure. Nancy Grainger and Mike Villeneuve (GSC) sampled igneous suites for U-Pb and Ar-Ar isotopic dating throughout the area concentrating on the Tertiary volcanic units to constrain their stratigraphy and the tectonic events that generated them. Representative samples of each of the Tertiary

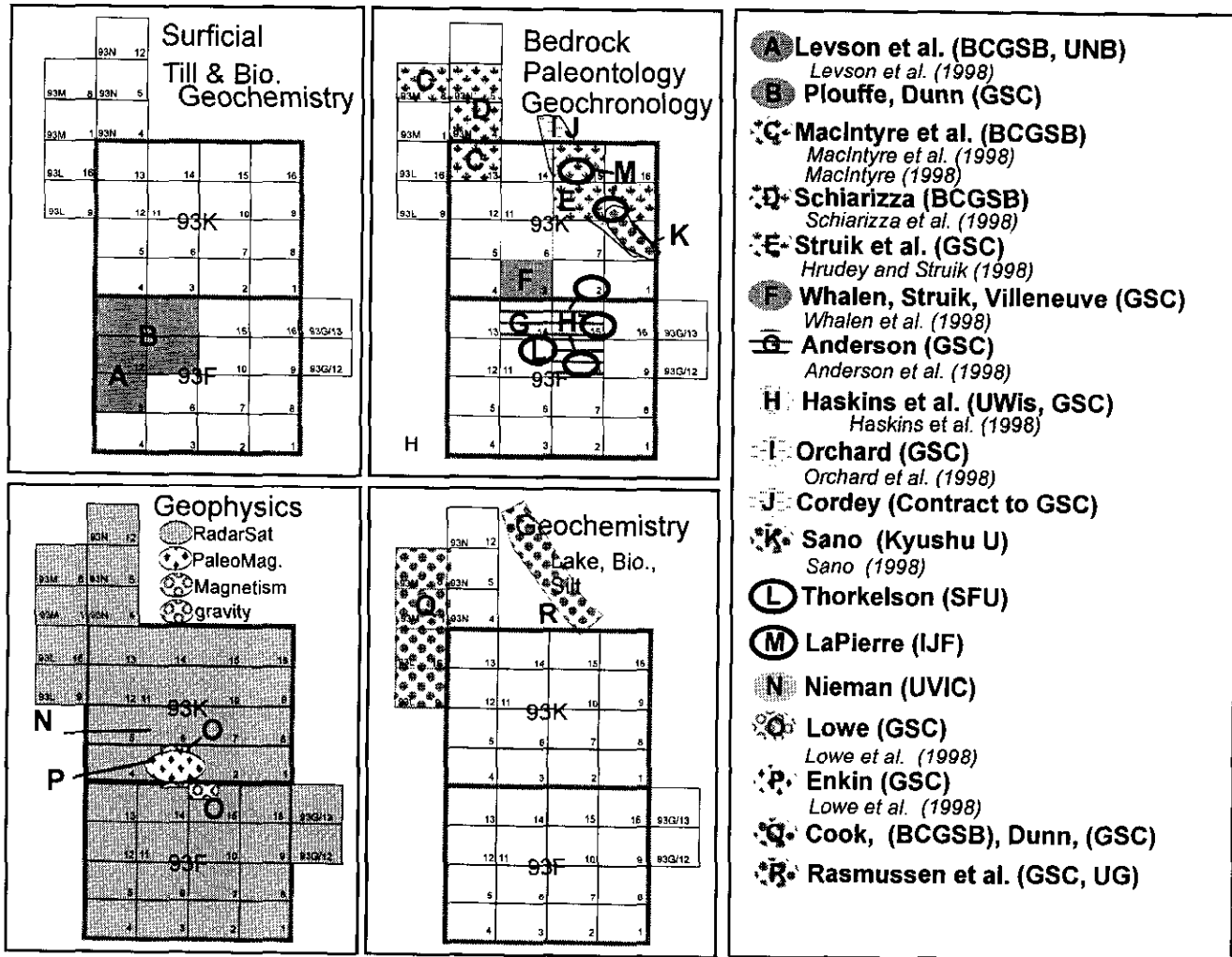


Figure 1-3. Projects active in the Nechako Natmap area in 1997. See text for details.

volcanic units and the Jura-Cretaceous plutonic phases were taken for detailed litho-geochemistry to constrain interpretations of the genetic history of those rocks. Samples were taken by backpack diamond drilling from within the Endako Mine and from Tertiary dikes and flows of the surrounding area for paleomagnetic measurements to quantitatively constrain Tertiary block rotations about horizontal and vertical axes.

The following are the main highlights of the Endako study of 1997:

1. Endako Group basalt occurs in small areas mainly in the southern and central Endako map area. In the central part of the sheet, the basalt forms a thick hyaloclastite breccia overlying andesite and biotite-hornblende-plagioclase

dacite of the Ootsa Lake Group (Whalen *et al.*, 1998).

2. The Eocene age Ootsa Lake Group in the Endako area contains transitions from andesite through rhyolite to dacite crystal tuffs, conglomerates and basalts. Contacts between mafic to intermediate ash flow and lahar, and rhyodacitic crystal tuffs were observed, and these units were in turn intruded by Eocene quartz-feldspar rhyolite dikes. A chert, andesite, dacite clast conglomerate to sandstone unit was found interlayered with Eocene rhyolite and rhyodacite in the eastern part of the map area.
3. Regional tilting of the Endako and Ootsa Lake Groups as determined from bedding attitudes

has been confirmed by paleomagnetic measurements of Eocene dikes within the Endako Mine. The tilting is controlled by closely spaced extensional faults across which block rotations vary from 10 to 40 degrees (Enkin *et al.*, 1997; Lowe *et al.*, 1998).

4. the Francois Lake and Endako phases of the Late Jurassic Francois Lake plutonic suite appear to be the same age and may be regionally indistinguishable from one another (Whalen *et al.*, 1998). The Endako phase is the host rock for the molybdenum of the Endako Mine.
5. The Francois Lake and Glenannon granodiorite phases each appear to have finely crystalline subphases (Whalen *et al.* 1998). Mirolitic subvolcanic granodiorite east of Endako Mine may be the carapace to the Francois Lake phase.

### Nechako River Map Area

Bedrock mapping in the Nechako River (NTS 93F) map area was done by Bob Anderson (GSC) and crew. The crew was comprised of senior mapper Lori Snyder (Univ. of Wisconsin), and junior mappers Jonah Resnick (UBC) and Shireen Wearmouth (Upper Caledonia College, Kamloops) and was reinforced by volunteers Elspeth Barnes (exchange student from University of Glasgow), Michelle Haskin (Univ. of Wisconsin), and Samara Lewis and Shin Yi Siew (exchange students from University of Melbourne). They concentrated on the Hallett Lake (NTS 93F/15), Big Bend (NTS 93F/10) and Knapp Lake (93F/14) map areas (Anderson and Snyder, 1998; Anderson *et al.*, 1998a; Anderson *et al.* 1998b). This work linked with previous mapping in the south (93F/07) by Diakow (1997), to the east (93F/09 and 16) by Wetherup (1997), and to the north in 93K/2 by Struik *et al.* (1997) and in 93K/3 by Whalen *et al.* (1998).

Stratigraphic sections of the Endako Group basalts were measured in detail at Mount Greer (93F/15), Nautley (93K/2), and Kenney Dam (93F/10)(Haskin *et al.*, 1998). These units were also extensively sampled for litho-geochemistry and Ar-Ar age dating. In addition a concerted effort was made to visit all outcrops located by the surficial mapping crew.

Nancy Grainger, Mike Villeneuve and Bob Anderson re-examined some of these contacts as well as the nature and relationships between Ootsa Lake Group and Eocene(?) Copley Lake pluton as part of Nancy Graingers reconnaissance for her 1998 Masters thesis research. Derek Thorkelson (Simon Fraser Univ.) completed a 2 week reconnaissance of Tertiary volcanic rocks in the Cheslatta Lake (93F/10) map area which will be one focus of mapping in 1998.

The following are the main highlights of the Nechako River mapping of 1997:

1. Moderately- to steeply-dipping and deformed volcanic and sedimentary rocks of the undivided Hazelton Group, Naglico Formation, and Bowser

Lake Group were extended north from NTS 93F/07 (Diakow *et al.*, 1995a,b, 1997) in the Big Bend Creek map area (Anderson *et al.*, 1998a). A system of Tertiary block faults deform Mesozoic and Tertiary basement rocks as a north-trending graben developed synchronously with eruption of the Endako Group.

2. In Hallett Lake area (Anderson and Snyder, 1998), Tertiary faults have protracted down-to-the-southeast motion predating and synchronous with Ootsa Lake and Endako Group volcanism. These faults apparently localized the distribution of the Tertiary volcanic units and may be an upper plate manifestation of northwesterly-directed ductile extension recorded in the western part of the structurally lower, Eocene Vanderhoof Metamorphic Complex as described by Wetherup (1997).
3. Preliminary mapping in the Knapp Lake area (Anderson *et al.*, 1998b) revealed significant variations in Ootsa Lake Group stratigraphy noted in the Endako map area (93K/03) to the north. The group rests unconformably on Lower and Middle Hazelton Group rocks. Chilcotin Group olivine-phyric and nodule-bearing glassy basalt is widespread in the southern part of Knapp Lake map area and is mineralogically distinct from Eocene Endako Group clinopyroxene-plagioclase-phyric basalt.
4. Detailed studies of Eocene Endako Group basalts in the Nechako River and southern Fort Fraser areas (Haskin *et al.*, 1998) established the rocks as aphyric to plagioclase-, pyroxene-, and rarely olivine-phyric and commonly amygdaloidal. The Kenney Dam (NTS 93F/10) locality provides the thickest section of Endako Group basalt.

## SURFICIAL MAPPING

### Nechako River Map Area

Surficial mapping concentrated on the northwest quadrant of Nechako River map area and the north half of 93F/05 and provided ground verification of aerial photograph interpretations. That work was done by Alain Plouffe (GSC) and student assistant Jean Bjornson (UO) and in the southwest by Andrew Stumpf (UNB) and Vic Levson (BCGSB) (Levson *et al.*, 1998).

During the 1997 field season, Alain Plouffe and Jean Bjornson (Univ. of Ottawa) completed the surficial geology mapping of the northwestern sector of Nechako River map sheet (93F/11, F/13, and F/14). More than 180 till samples were collected and the extent of glacial lake sediments was mapped in the lowest valleys of this region including the Francois Lake valley. This summer's findings corroborate the observations by Plouffe (1997) that the maximum elevation of continuous glacial lake sediment cover decreases to the west. Sites interpreted to be susceptible to instability

when disturbed were investigated in conjunction with the British Columbia Ministry of Forests.

Abundant striated outcrops in this region reveal a general ice movement to the east and northeast with minor local fluctuations. Very little Quaternary stratigraphy is exposed and no pre-Fraser sediments (pre-late-Wisconsinan) were found.

## **GEOCHEMICAL STUDIES**

Steve Cook (BCGSB) conducted various geochemical studies as followups to previous surveys done in the Nechako NATMAP project area.

### **RGS Interpretation Studies**

As an assessment of the usefulness of element sum ranking in the search for volcanogenic massive sulphide (VMS) deposits in Carboniferous-Jurassic Cache Creek Group and Upper Triassic Kutcho Formation rocks, two Takla Lake area watersheds identified as being in the top five percentiles of the combined Cu-Zn-Pb-Ag data ranking for the western half of the Manson River (NTS 93N) map area were investigated and resampled.

### **Till Dispersal Studies**

Till dispersal studies in cooperation with Vic Levson were carried out in the vicinity of Babine Porphyry Belt copper prospects. The study, initiated in 1996, continued in 1997 near the Dorothy and Hearne Hill prospects. Till and profile sampling was conducted at these sites to document glacial dispersal, and copper concentrations in various soil horizons. Previous work in the Babine Porphyry Belt was conducted near the Nak, Trail Peak and Lennac prospects.

### **Lake Sediment Orientation Studies:**

#### **Hill-Tout Lake**

Lake sediment orientation studies conducted in 1992 at Hill-Tout Lake, near the Dual porphyry copper prospect, identified wide variations in sediment metal concentrations between the three distinct sub-basins of the lake. An Open File documenting these variations, and their implications for regional geochemical exploration, is currently being prepared. Original water samples collected at the lake were analyzed by ICP-ES methods. Fieldwork this season obtained additional surface and bottom-water samples to be analyzed by ICP-MS methods, which yield superior data for trace elements such as copper.

### **Biogeochemical Surveys**

Colin Dunn (GSC) and Rob Scagel (Pacific Phytometric Consultants, Surrey, BC) conducted a reconnaissance level, lodgepole pine sampling program (late July). The sampling extends 1996 northeastern

coverage throughout the northwest quadrant of Nechako River. Samples were the outer bark of lodgepole pine. Samples were collected from 282 sites; 265 at 2 km intervals along all driveable roads and trails, and 17 from sites remote from trails (by Alain Plouffe).

Biogeochemical work with Bob Anderson is testing the possibility of 'fingerprinting' pluton compositions. Vegetation was collected from sites on plutons where samples for lithogeochemical analysis were previously obtained. In particular we will look at rare earth elements (REE) and high field strength elements (HFSE) to determine their patterns. If this technique works, it will provide a quick and economical means to help differentiate underlying rock types (where overburden is thin).

Follow-up sampling was done of last year's reconnaissance biogeochemical survey along the Kluskus forest service road in northeast Nechako River map area (NTS 93F/9, 16). This was to establish the source of Co and Cr enrichment in samples from this area. Enquiries at local forestry offices found that prior to about 1990 parts of the Kluskus road were paved with oxidized volcanic rocks (basaltic) from borrow pits at km 35 and km 36. Samples of the oxidized material and road dust were collected to test for enrichment in Co and Cr. Vegetation was sampled at several sites eastward from the road for a distance of 1 km to ascertain the potential maximum extent of contamination by road dust.

### **Metals in the Environment (MITE)**

As part of the GSC Metals in the Environment (MITE) Initiative, reconnaissance field work was conducted in August 1997 by Colin Dunn, Pat Rasmussen (GSC), and Alain Plouffe in the area of the old Takla Bralorne mercury mine, located approximately 4 km northwest of the confluence of Silver and Kwanika creeks, on the 93N/11 NTS map sheet.

The main purpose of the work undertaken by A. Plouffe was to (1) determine if there is any anthropogenic mercury in the humus horizon; (2) identify the different phases of mercury in soil profiles developed on till and glaciofluvial sediments; (3) establish the mobility of these phases; (4) develop criteria to distinguish between natural and anthropogenic mercury; and (5) provide a framework to measurement of mercury flux to the atmosphere (by Pat Rasmussen). This summer, humus, B-horizon, and, till and/or glaciofluvial sediments were sampled at a total of 13 sites in the Silver Creek and Kwanika Creek valleys, and detailed sampling of soil profiles was done at two sites.

Pat Rasmussen, Colin Dunn and Grant Edwards (Univ. of Guelph, School of Engineering) collected biogeochemical samples at the same sites as Alain Plouffe and at additional sites along the Pinchi fault zone as part of a nation-wide survey of natural mercury emissions to the atmosphere. Results will be used to evaluate the Takla Bralorne site and other areas as potential mercury flux monitoring sites.

## INDUSTRIAL MINERALS INVESTIGATIONS

Dani Hora and George Simandl (BCGSB) continued followup on both previously known and newly located industrial mineral and precious stone sites in the Nechako project area. Dimension stone, decomposed lapilli tuffs (for clays), ornamental and landscaping rock (basalts mainly), perlite, vermiculite, opal, and agate were investigated.

## GEOGRAPHIC INFORMATION SYSTEMS

Stephen Williams (GSC) and Nicki Hastings (GSC) continued to develop the Nechako Project digital point, line and areal database and query system. Work focussed on digital integration of the bedrock mapping data donated by Placer Dome Ltd, the digitization and cartography of geological maps, and the initiation of an internet GIS data sharing system.

Some of the accomplishments to date include;

1. Creation of a GIS data base of the Placer Dome bedrock geology maps for the Endako Mine and surrounding region has been completed. This database includes half of the field notes gathered during that project. All of this information will be combined with Nechako Project mapping.
2. Several new geological maps are in the process of production as coloured 1:100 000 and 1:50 000 scale bedrock maps.
3. This summer the Nechako Project supported and initiated the acquisition and installation of MapGuide and its appropriate server hardware and software at the Vancouver Office. MapGuide is a collection of software packages (Server, Author and Reader) that provides real-time WEB browser access to maps and their associated databases. MapGuide has been used extensively by the BCGSB to make the Mineral Potential of British Columbia project-data accessible over the World Wide Web. We hope to use MapGuide first to distribute the digital data for the Nechako Project to its participants to facilitate research. Later we hope to be able to use it for broader distribution of the data.

For monthly updates in Nechako NATMAP Project developments, see the Nechako Newsletters posted on the Nechako Project website ([ei.gov.bc.ca/natmap.html](http://ei.gov.bc.ca/natmap.html)) during the life of the project.

## ACKNOWLEDGMENTS

We would like to thank all those people who worked hard to make this project a reality and for the support of the GSC, BCGSB and geoscience community. We make a special note of thanks to Glen Johnston of Endako Mines for his hospitality and

generosity with his ideas, and Ed Kimura and Sharon Gardner of Placer Dome Inc. for their contribution to Canadian geoscience community through the donation of their geological maps of the Fort Fraser and Nechako River map areas. In addition we thank the many companies working in the Babine Porphyry Belt for their cooperation and generosity in permitting access to their properties and sharing their geological ideas for the area. Lori and Ken Lindenberger of Pipers Glen RV park provided generous support to the GSC crew throughout June to August.

## REFERENCES

- Anderson, R.G. and Snyder, L.D. (1998): Jurassic to Tertiary volcanic, sedimentary and intrusive rocks in the Hallett Lake area, central British Columbia; *in* Current Research 1998-A; *Geological Survey of Canada*.
- Anderson, R.G., Snyder, L.D., Resnick, J., and Barnes, E. (1998a): Geology of the Big Bend Creek map area, central British Columbia; *in* Current Research 1998-A; *Geological Survey of Canada*.
- Anderson, R.G., Snyder, L.D., Resnick, J., and Barnes, E. (1998b): Geology of the Knapp Lake map area, central British Columbia; *in* Current Research 1998-E; *Geological Survey of Canada*.
- Ash, C.H., MacDonald, R.W.J., and Paterson, I.A. (1993): Geology of the Stuart - Pinchi Lakes area, central British Columbia; *British Columbia Ministry of Energy, Mines and Petroleum Resources*, Open File 1993-9.
- Diakow, L.J., Webster, I.C.L., Richards, T.A., and Tipper, H.W. (1997): Geology of the Fawnie and Nechako Ranges, southern Nechako Plateau, central British Columbia (93F/2,3,6,7); *in* Interior Plateau Geoscience Project: Summary of Geological, Geochemical and Geophysical Studies, L.J. Diakow and J.M. Newell (ed.); *British Columbia Geological Survey Branch Open File 1996-2 and Geological Survey of Canada*, Open File 3448, p. 7-30.
- Diakow, L.J., Webster, I.C.L., Whittles, J.A., and Richards, T.A. (1995a): Stratigraphic highlights of bedrock mapping in the Southern Nechako Plateau, Northern Interior Plateau Region; *in* Geological Fieldwork 1994, B. Grant and J.M. Newell (ed.); *British Columbia Ministry of Energy, Mines and Petroleum Resources*, Paper 1995-1, p. 171-176.
- Diakow, L.J., Webster, I.C.L., Whittles, J.A., Richards, T.A., Giles, T.R., Levson, V.M., and Weary, G.F. (1995b): Bedrock and surficial geology of the Chedakuz Creek map area (NTS 93F/7); *British Columbia Ministry of Energy, Mines and Petroleum Resources*, Open File 1995-17.
- Enkin, R.J., Baker, J., Struik, L.C., Wetherup, S., and Selby, D. (1997): Paleomagnetic determination of post-Eocene tilts in the Nechako Region; *in* Abstracts Volume, *Geological Association of*

- Canada and Mineralogical Association of Canada*, Annual Meeting, May 19-21, 1997, p. A46.
- Haskin, M.L., Snyder, L.D., and Anderson, R.G. (1998): Tertiary Endako Group volcanic and sedimentary rocks at four sites in the Nechako River and Fort Fraser map areas, central British Columbia; in Current Research 1998-A; *Geological Survey of Canada*.
- Hrudey, M.G. and Struik, L.C. (1998): Field observations of the Tachie Pluton near Fort St. James, central British Columbia; in Current Research 1998-A; *Geological Survey of Canada*.
- Kimura, E.T., Bysouth, G.D., Cyr, J., Buckley, P., Peters, J., Boyce, R., and Nilsson, J. (1980): Geology of parts of southeast Fort Fraser and northern Nechako River map areas, central British Columbia; *Placer Dome Incorporated*, Internal Report and Maps, Vancouver, British Columbia.
- Levson, V., Stumpf, A., and Stuart, A. (1998): Quaternary geology studies in the Smithers and Hazelton map areas (93L and M): Implications for exploration; in Geological Fieldwork 1997; *British Columbia Ministry of Employment and Investment*, Paper 1998-1.
- Lowe, C., Enkin, R.J., and Dubois, J. (1998): Magnetic and paleomagnetic constraints on Tertiary deformation in the Endako region, central British Columbia; in Current Research 1998-A; *Geological Survey of Canada*.
- MacIntyre, D.G. (1998): Babine Porphyry Belt Project: Bedrock geology of the Nakinilerak Lake map sheet (93M/8), British Columbia; in Geological Fieldwork 1997; *British Columbia Ministry of Employment and Investment*, Paper 1998-1.
- MacIntyre, D.G. and Struik, L.C. (1998): Nechako Natmap Project: 1997 Overview; in Geological Fieldwork 1997; *British Columbia Ministry of Employment and Investment*, Paper 1998-1.
- MacIntyre, D.G., Schiarizza, P. and Struik L.C. (1998): Preliminary bedrock geology of the Tochcha Lake map sheet (93K/13), British Columbia; in Geological Fieldwork 1997; *British Columbia Ministry of Employment and Investment*, Paper 1998-1.
- McMillan, W.M. and Struik, L.C. (1996): NATMAP: Nechako Project, central British Columbia; in Geological Fieldwork 1995, B. Grant and J.M. Newell (ed.); *British Columbia Ministry of Energy, Mines and Petroleum Resources*, Paper 1996-1, p. 3-9.
- Nelson, J.L., Bellefontaine, K.A., Green, K.C., and Maclean, M.E. (1991): Geology and mineral potential of Wittsichica Creek and Tezzeron Creek map areas; *British Columbia Ministry of Energy, Mines and Petroleum Resources*, Open File 1991-3.
- Orchard, M.J., Struik, L.C., and Taylor, H. (1998): New conodont data from the Cache Creek Group, central British Columbia; in Current Research 1998-A; *Geological Survey of Canada*.
- Paterson, I.A. (1973): The geology of the Pinchi Lake area, central British Columbia; Ph.D. thesis, *University of British Columbia*, Vancouver, British Columbia, 263 p.
- Plouffe, A. (1997): Ice flow and late glacial lakes of the Fraser Glaciation, central British Columbia; in Current Research 1997-A; *Geological Survey of Canada*, p. 133-144.
- Sano, H. (1998): Preliminary report on resedimented carbonates associated with basaltic rocks of Cache Creek Group near Spad Lake, east of Fort St. James, central British Columbia; in Current Research 1998-A; *Geological Survey of Canada*.
- Schiarizza, P., Massey, N.W.D., and MacIntyre, D.G. (1998): Geology of the Sitlika assemblage in the Takla Lake area (93N/3,4,5,6,12); in Geological Fieldwork 1997; *British Columbia Ministry of Employment and Investment*, Paper 1998-1.
- Struik, L.C. and McMillan, W.J. (1996): Nechako Project Overview, central British Columbia; in Current Research 1996-A; *Geological Survey of Canada*, p. 57-62.
- Struik, L.C. and MacIntyre, D.G. (1997): Nechako Plateau NATMAP Project Overview, central British Columbia, year two; in Current Research 1997-A; *Geological Survey of Canada*, p. 57-64.
- Struik, L.C., Whalen, J.B., Letwin, J.M., and L'Heureux, R. (1997): General geology of southeast Fort Fraser map area, central British Columbia; in Current Research 1997-A, *Geological Survey of Canada*, p. 65-75.
- Wetherup, S. (1997): Geology of the Nulki Hills and surrounding area (NTS 93F/9 and F/16), central British Columbia; in Current Research 1997-A; *Geological Survey of Canada*, p. 125-132.
- Whalen, J.B., Struik, L.C., and Hrudey, M.G. (1998): Bedrock geology of the Endako map area, central British Columbia; in Current Research 1998-A; *Geological Survey of Canada*.
- Whalen, J.B. and Struik, L.C. (1998): ?? in Current Research 1998-A; *Geological Survey of Canada*.



**BABINE PORPHYRY BELT PROJECT: BEDROCK GEOLOGY OF THE  
NAKINILERAK LAKE MAP SHEET (93M/8), BRITISH COLUMBIA**

By Don MacIntyre

*(British Columbia Geological Survey Branch contribution to the Nechako NATMAP Project)*

**KEYWORDS:** bedrock mapping, Nechako NATMAP, Nakinilerak Lake, Babine Porphyry Belt, Eocene extension, Babine Igneous Suite, Babine Intrusions, Ootsa Lake group, porphyry copper deposits, Nak, Trail Peak.

**INTRODUCTION**

The Nechako National Mapping Program (NATMAP) project, which began in 1995, is a joint mapping and geoscientific research project between the British Columbia Geological Survey Branch (BCGSB) and the Geological Survey of Canada (GSC) that also includes participation by universities and industry (McMillan and Struik, 1996; MacIntyre and Struik, 1997, MacIntyre and Struik (this volume). The co-coordinators of this project are Don MacIntyre (BCGSB) and Bert Struik (GSC). Work done by BCGSB field crews is funded wholly by the Energy and Minerals Division of the Ministry of Employment and Investment; GSC funding is from the Cordilleran division in Vancouver supplemented with additional funding from the National Mapping Program (NATMAP).

The Babine porphyry belt project, which is a multidisciplinary project with separate components for bedrock and surficial geology, till and silt geochemistry is part of the Nechako NATMAP project (Figure 2-1). The primary objectives of this project are to improve the geological database in the Babine Porphyry belt, to define new areas with potential for additional deposits and to attract new exploration expenditures in the district. To meet these objectives we will produce 1:50 000-scale bedrock and surficial geology maps of the Fulton Lake (93L/16), Old Fort Mountain (93M/1) and Nakinilerak Lake (93M/8) map sheets (Figure 2-1) and define areas of possible buried metallic mineral deposits using till, lake and silt geochemistry. This report summarizes the results of bedrock mapping completed in 1997 and builds on previous reports that describe the results of mapping done in the Fulton Lake (MacIntyre *et al.*, 1996) and Old Fort Mountain (MacIntyre *et al.*, 1997) map sheets.

**PROJECT DESCRIPTION**

The Babine porphyry belt is located in west-central British Columbia and is centered on the northern third of Babine Lake (Figure 2-1). The belt is approximately 80

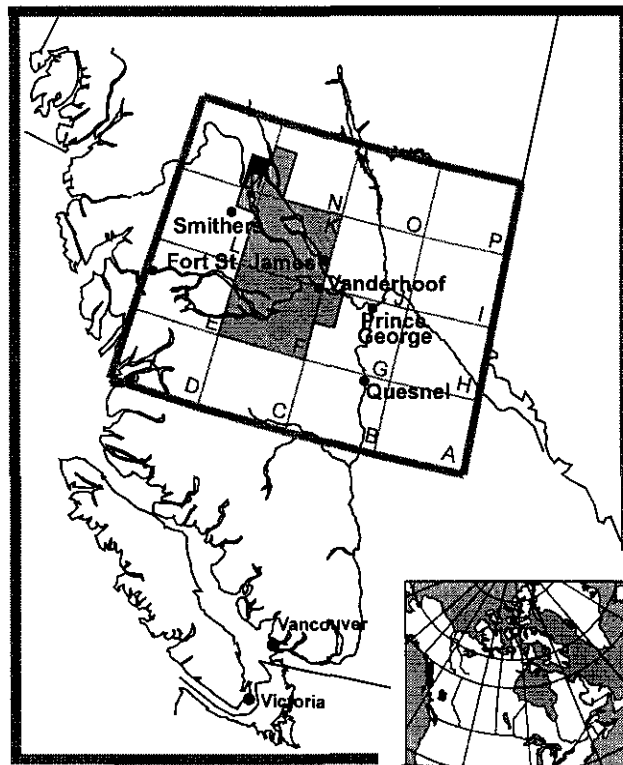


Figure 2-1. Location of the Nechako Natmap project, central British Columbia. Dark grey area was mapped in 1997 and is the subject of this report.

kilometres long and includes twelve significant porphyry copper deposits and prospects including the Bell and Granisle past producers. Previous work and access routes into the Babine Porphyry belt have been described in detail in previous reports (MacIntyre *et al.*, 1995, 1996).

One of the objectives of the current project is to stimulate additional exploration in the belt by providing an integrated package of geoscientific maps. Bedrock and surficial mapping in the belt is now complete. In addition there are completed lake geochemical and till geochemical surveys that cover the entire belt. Most of this data has now been released or is in preparation for release. The Quaternary geology and till and lake geochemical sampling completed in 1995, 1996 and 1997 are discussed in separate reports (Huntley *et al.*, 1996, Stumpf *et al.*, 1996, Levson *et al.*, 1997, Levson *et al.* (this volume) and Cook *et al.*, 1997, Jackaman *et al.* (this volume).

The 1997 bedrock mapping crew consisted of Don MacIntyre and student field assistants RYANNE METCALF,

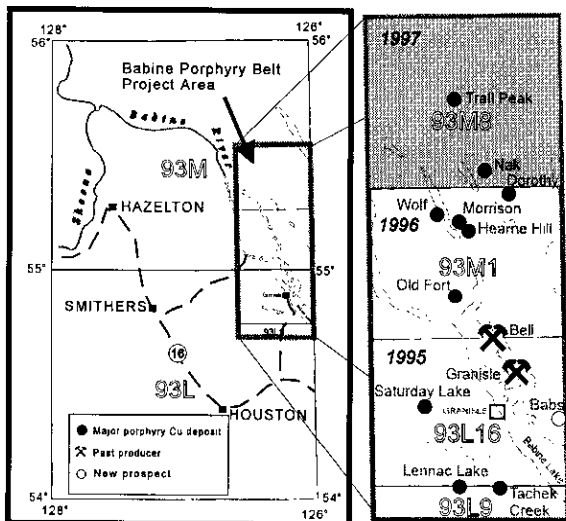


Figure 2-2. Location of the Babine Porphyry Belt project area and major porphyry copper deposits in the district. Shaded area is the Nakinilerak Lake map sheet (93M/8) which was mapped in 1997.

Stephan Munzar and Deanne Tackaberry. This crew spent approximately 4 weeks working in the Babine Porphyry Belt. Logging roads provided access to the east side of the Netalzul Mountain (93M/7) and southeast and southwest corners of the Nakinilerak Lake (93M/8) map sheets. The remaining part of the area was mapped using daily helicopter set-outs and pickups from a base camp located at Takla Narrows on Takla Lake. In addition, Mike Villeneuve and Nancy Grainger of the Geological Survey of Canada helped field crews collected samples for Ar-Ar and U-Pb radiometric dating. Randy Enkin and Judith Baker also visited the project area and did sampling for paleomagnetic studies.

## ACCOMPLISHMENTS

Major geological accomplishments made during the 1997 field season are summarized below.

- revised the geology, stratigraphy and structure of the east side of the Netalzul Mountain (93M/7) and all of the Nakinilerak Lake (93M/8) map sheets.
- the Trail Peak and Nak porphyry copper deposits, which are the most important mineral properties in the 93M/8 map area, were examined and mapped.
- the belt of Lower to Middle Jurassic bimodal volcanic rocks first recognized in the area west of Granisle in 1995 was extended into the 93M/8 map sheet. However the unit appears to be thinning and contains less felsic volcanic rocks going northward. This coincides with a general change in the nature of Lower to Middle Jurassic sedimentary rocks from shallow to deep water facies.
- an area of rhyolitic ash flows and vesicular basalt belonging to the Eocene Ootsa Lake and Endako groups respectively was mapped in the low lying

region west of Takla Lake in the 93M/8 map area and along the southern edge of the 93K/13 map sheet. These areas represent zones of Tertiary extension and volcanism and may have some epithermal potential. Two Ar-Ar isotopic age date samples were collected from the ash flow members of the Ootsa Lake group.

- Randy Enkin and Judith Baker collected core samples from three sites in the Upper Cretaceous sedimentary rocks of the Sustut Group for paleomagnetic studies. These samples may shed light on Tertiary displacements and rotations in the area near the Takla fault.

## FUTURE PLANS

Bedrock mapping in the Babine Porphyry Belt has now been completed. Any additional work in 1998 will focus on mineral deposits in the belt and on areas where more fill-in mapping or sampling is needed.

## REGIONAL GEOLOGIC SETTING

The Babine Porphyry Belt is entirely within Stikinia, the largest terrane of the Intermontane tectonic belt. This terrane includes Early Devonian to Middle Jurassic volcanic and sedimentary strata of the Asitka, Stuhini, Takla, Lewes River and Hazelton assemblages and related comagmatic plutonic rocks. East and in fault contact with Stikina are Paleozoic and Mesozoic oceanic rocks of the Cache Creek terrane; to the west are the Mesozoic and Cenozoic plutonic and metamorphic rocks of the Coast Belt.

## LITHOLOGIC UNITS

The geology of the study area, based on mapping completed in 1997 and the earlier mapping of Carter (1973), Tipper and Richards (1976) and Richards (1980; 1990), is shown in Figure 2-3. Figure 2-4 illustrates our current understanding of the stratigraphic relationships between the different map units.

The physiography of the Babine Lake area reflects the effects of Tertiary extension. A northwest trending range in the center of the Nakinilerak Lake map sheet is an uplifted, tilted and folded block of Jurassic volcanic and sedimentary rocks. The uplift forms a broad, fault bounded syncline with an axial fault that cuts Middle Jurassic sedimentary rocks of the Nilkitkwa and Ashman formations in its core. These rocks overlie Lower Jurassic volcanic rocks of the Telkwa Formation which are exposed on the east and west limbs of the syncline. To the west and east of this uplift are low lying, downdropped areas that are underlain by Cretaceous and Tertiary sedimentary and volcanic rocks of the Skeena, Sustut, Ootsa Lake and Endako groups and their comagmatic intrusive equivalents. These grabens, are

truncated and offset by northeast and northwest-trending high angle faults of Eocene or younger age.

## **Lower to Middle Jurassic Hazelton Group**

The oldest rocks in the Nakinilerak Lake map area are part of the Hazelton Group. The Hazelton Group (Leach, 1910) is a calcalkaline island-arc assemblage that evolved in Early to Middle Jurassic time. In the Babine Lake area, and McConnell Creek map area to the north (94D), it sits unconformably to disconformably on volcanic and sedimentary strata of the Upper Triassic Takla Group (MacIntyre *et al.*, 1996).

Tipper and Richards (1976) divided the Hazelton Group into the Telkwa, Nilkitkwa and Smithers Formations based on lithology, fossil assemblages and stratigraphic position. The Lower Jurassic Telkwa Formation is comprised of subaerial to submarine, predominantly calcalkaline volcanic rocks, the Lower Jurassic Nilkitkwa Formation is mainly marine sedimentary and volcanic rocks and the Middle Jurassic Smithers Formation is mainly shallow water, marine sedimentary rocks. In the Babine lake area there is also a Lower to Middle Jurassic, marine to subaerial volcanic succession which Richards called the Saddle Hill volcanics. In the Nakinilerak Lake area the lower part of the Hazelton succession is not well-exposed and the predominant formations are the Saddle Hill volcanics and the Smithers Formation (Figure 2-4).

### ***Lower Jurassic Telkwa Formation***

The best exposures of the Telkwa Formation crop out along the crest and east facing slopes of a north trending ridge that extends from Sinta Creek to Frypan Peak (Figure 2-2) The predominant lithology, which is typical of the upper part of the Telkwa Formation, is amygdaloidal basalt with areas of strong flow top brecciation. Interbedded with the flows are maroon lapilli and crystal tuffs, volcanic wacke and volcanic conglomerate. The volcanic members are overlain, apparently conformably, by well-bedded siltstones, wackes and pebble conglomerates of the Nilkitkwa Formation. To the east, the Telkwa volcanic rocks are in fault contact with a downdropped area of Tertiary volcanic rocks.

The best exposure of Telkwa Formation volcanic rocks is in the vicinity of Frypan Peak. Here, a moderately west dipping section of basaltic flows and lapilli tuffs is overlain by well-bedded siltstones and mudstones of the Nilkitkwa Formation. The contact runs across the top of Frypan Peak. Correlation of the volcanic strata with the Telkwa Formation is based on a fossil locality east of Frypan Peak (GSC locality C-90981) which is reported to be Late Sinemurian in age.

### ***Lower Jurassic Nilkitkwa Formation***

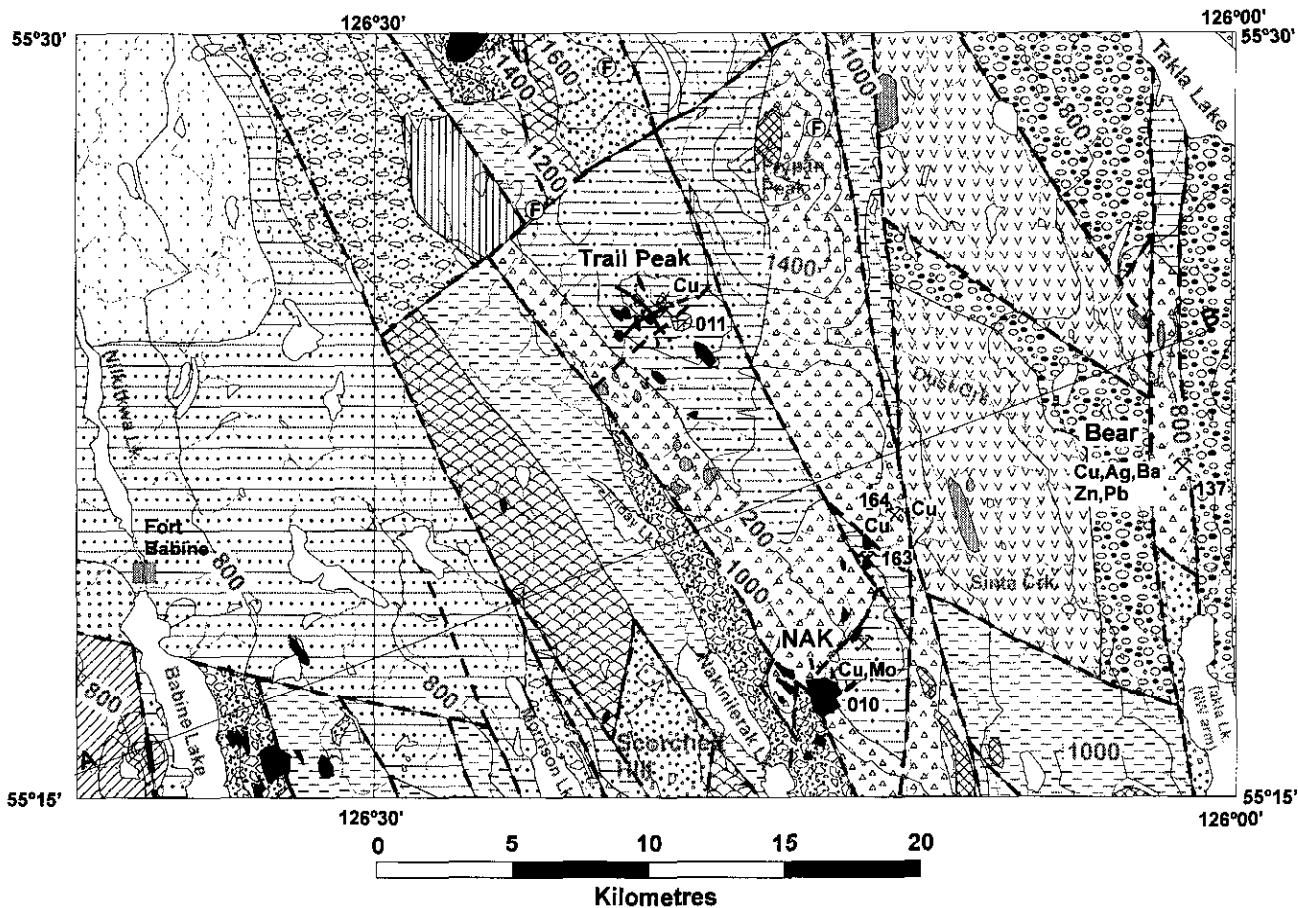
Tipper and Richards (1976) assigned thick sections of Pliensbachian to Toarcian shale, greywacke, red tuff, breccia and minor limestone to the Nilkitkwa Formation. This succession is well exposed in the Nilkitkwa and Bait ranges, the type area, which is just north of the map area. Here, the formation is as much as 1000 metres thick. Limestone and chert beds in the lower part of the section help distinguish Nilkitkwa rocks from younger, lithologically similar formations. Shallow-water, fossiliferous limestone, with interbedded pebble conglomerate and feldspathic sandstone, is a particularly common sequence where Nilkitkwa sedimentary rocks onlap Telkwa volcanic rocks.

The best exposure of the Nilkitkwa Formation in the current study area occurs on the west side of Frypan Peak. Here, moderately west dipping, well bedded, siltstone, mudstone, cherty argillite, and calcarenite with minor volcanic pebble conglomerate and occasional tuff beds conformably overlie Telkwa volcanic rocks. Both the volcanic and sedimentary rocks are intruded by a number of fine-grained, greenish grey diorite sills. Further south, similar, well-bedded sedimentary rocks are exposed in near continuous outcrop (1500 metres) in Sinta Creek. Unlike exposures of Nilkitkwa sedimentary rocks in the Old Fort Mountain map sheet (93M/1) to the south, which are typically shallow water, fossiliferous beds, those in the Nakinilerak Lake map area are fossil poor and appear to represent a deeper, water, finer-grained marine facies. The only known fossil localities in the Nilkitkwa Formation in the current study area are on a ridge 3 kilometres northwest of Frypan Peak where dark grey siltstones interbedded with amygdaloidal, chloritized submarine basaltic flows are reported to contain Middle Toarcian macrofossils (GSC fossil localities C90984, C90949). These volcanic rocks, which are characterized by the presence of submarine basaltic flows and flow top breccias, were mapped previously as the Ankwel Member of the Nilkitkwa Formation (Richards, 1990).

### ***Lower to Middle Jurassic Saddle Hill volcanics***

The Saddle Hill volcanics, as defined by Richards (1990), consist of Early to Middle Jurassic, interbedded, reddish, subaerial tuffaceous mudstone, basalt to rhyolitic flows, ash-flows, ash and lapilli tuff, breccia, lahar and minor volcanoclastic sedimentary rocks. In the type area, at Saddle Hill, which is located in the Old Fort Mountain map sheet south of the current study area (MacIntyre *et al.*, 1996), the volcanic rocks overlie Nilkitkwa Formation and are overlain by Aalenian to Bajocian sedimentary rocks of the Smithers Formation. Zircons extracted from rhyolitic ash flows interbedded with basalts west of the town of Granisle gave a 184.5 Ma U-Pb isotopic age. The Saddle Hill volcanics are therefore Toarcian in age based on stratigraphic position and limited age dating.

## Nakinilerak Lake 93M/8



### Cross Section A-B



Figure 2-3. Generalized geology of the Nakinilerak Lake map area (93M/8)

In the current study area, rocks lithologically similar to the Saddle Hill volcanics are well-exposed near the southern end of the Bait Range. Here, massive flows of chloritized basalt and basalt breccia with calcareous siltstone interbeds form the core of an anticline. The anticline is asymmetrical with a moderately east dipping eastern limb and a nearly vertical to slightly overturned western limb. On the east side of the ridge well-bedded siltstones, mudstones and shales conformably overlie the volcanic rocks. Numerous feldspar porphyry dikes and sills cut the sedimentary section. According to GSC

records, Early Bajocian fossils occur at GSC locality C-91067 which is up section and to the east of the volcanic-sedimentary contact. Therefore, based on the occurrence of these fossils, the sedimentary rocks are mapped as Smithers Formation. Richards (1990) previously mapped the volcanic rocks as the Ankwil member of the Nilkitwa Formation which is predominantly subaqueous basalt of Middle Toarcian age. Based on apparent age, stratigraphic position and lithology we correlate these volcanic rocks with the Saddle Hill volcanics. Overall, there appears to be a

## LEGEND FOR FIGURE 2-3

### EOCENE

#### *Ootsa Lake Group*

-  rhyodacite, andesite and basalt flows, tuffs &, volcanics
-  vesicular basalt, bladed porphyry, breccia, volcanics
-  bt-hb phyric rhyodacite domes

#### *Babine Igneous Suite*

-  Newman volcanics: porphyritic andesite, breccia
-  Babine Intrusions: bt±hb-fd porphyry, qz-fd porphyry, bt-hb qz. diorite

### PALEOCENE-EOCENE

-  siltstone, shale, mudstone, conglomerate

### UPPER CRETACEOUS

#### *Kasalka Group*

-  porphyritic andesite

#### *Sustut Group*

-  Tango Crk. Fm.: chert pebble conglomerate, sandstone

#### *Skeena Group*

-  Red Rose Fm.: sandstone, siltstone, conglomerate
-  Hanawald conglomerate: chert pebble conglomerate, sandstone
-  Rocky Ridge volcanics: alkaline basalt, tuff, rhyolite
-  Kitsuns Creek Fm.: siltstone, mudstone, conglomerate, coal

### MIDDLE CRETACEOUS

-  biotite hornblende granodiorite, hornblende diorite

### MIDDLE to UPPER JURASSIC

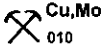
#### *Bowser Lake Group*

-  Trout Creek Fm.: heterolithic conglomerate, sandstone
-  Ashman Fm: siltstone, argillite, shale (Callovian-Oxfordian)

### LOWER to MIDDLE JURASSIC

#### *Hazelton Group*

-  Smithers Fm: feldspathic sandstone, siltstone (Aalenian-Bajocian)
-  Saddle Hill volcanics: basalt, breccia, limy siltstone (Toarcian)
-  Nilkitkwa Fm: wacke, siltstone, argillite, basalt (Pliensbachian)
-  Telkwa Fm: basalt, andesite, maroon tuff, volcanics (Sinemurian)

-  Fossil locality
-  Fault trace
-  Minfile showing

trend from a thick bimodal, partly subaerial section near the type area in the 93M/1 map sheet, to a thinner, predominantly submarine basalt section in the Bait Range to the north.

### ***Smithers Formation***

The Lower to Middle Jurassic Saddle Hill volcanics are conformably overlain by green to dark grey, marine sedimentary rocks of the Smithers Formation. In the 93M/1 map sheet, the Smithers Formation is very fossiliferous and contains abundant bivalves, ammonites and belemnites that indicate an Early Bajocian age. In the current study area, the best exposures of this formation occur on Scorched Hill, west of Nakinilerak lake and at the south end of the Bait Range (Figure 2-3). Bajocian age fossils have been collected from both areas. In general, the Smithers Formation appears to become finer-grained and more deep water going northward towards the Bowser Basin. Fine-grained, well-bedded siltstones and shales at the south end of the Bait Range were mapped by Tipper and Richards (1976) as the Bait member to distinguish them from more shallow water, fossiliferous, coarser-grained and poorly bedded members of the Smithers Formation.

### **Upper Jurassic to Lower Cretaceous Bowser Lake Group**

The Bowser Lake Group, as defined by Tipper and Richards (1976), includes marine sedimentary rocks and minor volcanic rocks ranging in age from Late Bajocian to Kimmeridgian. The group is thickest and most continuous in the Bowser basin located northwest of the current study area. Within the Bowser Basin fine-grained clastic rocks of Late Bajocian to Early Oxfordian age are mapped as Ashman Formation (Tipper and Richards, 1976). Along the southern margin of the basin Late Oxfordian conglomerates overlie Ashman Formation and are mapped as the Trout Creek Formation.

### ***Ashman Formation***

The Ashman Formation is the basal member of the Bowser Lake group and was deposited during an extensive mid to late Jurassic marine transgression that ultimately covered all of west central British Columbia including the Skeena Arch. The formation, which ranges in age from Late Bajocian to Early Oxfordian, consists predominantly of fine-grained dark grey to black shale, with lesser feldspathic to quartzose siltstone and greywacke. On Ashman Ridge, the type area for the Ashman Formation, it sits conformably on the Smithers Formation. South of Ashman Ridge and along the southern margin of the Skeena Arch the Ashman Formation is as old as Late Bajocian and is a more fossiliferous, coarser clastic shallow water facies. The Ashman formation is overlain by Late Jurassic to Early Cretaceous, westward prograding, non-marine clastic sedimentary rocks that were derived from rising

landmasses north, east and southeast of the Bowser Basin.

In the current study area, the Ashman Formation, which is predominantly dark grey, fine-grained siltstone, is sporadically exposed in the core of a northwest trending, uplifted syncline that extends from the Bait Range to the southern limit of the Nakinilerak lake map sheet. Early Callovian to Early Oxfordian fossils have been collected at three localities, two east of Scorched Hill (C-89593, C89648) and the other just north of Trail Peak (C90816). These ages are similar to those obtained in the 93M/1 map sheet. Like the Smithers and Nilkitkwa formations, the Ashman Formation appears to become finer-grained and more deep water moving northward toward the Bowser Basin.

### ***Trout Creek Formation***

The Trout Creek Formation includes coarse sandstone and conglomerate beds containing mid to late Oxfordian bivalves that overlie fine-grained clastics of the Ashman Formation (Tipper and Richards, 1976). These rocks represent a period of marine regression in mid Oxfordian time and a coincident shedding of coarse volcanic detritus northward into the Bowser Basin. Lithologies include marine and non-marine thick-bedded conglomerate, sandstone, siltstone, shale and coal. The conglomerates contain predominantly volcanic clasts mixed with chert but locally contain granitic clasts as well. Cross-bedding and channel cut and fill structures are common and characterize deltaic sequences. The Trout Creek rocks are overlain and in part interbedded with Upper Jurassic basalt and andesite of the subaerial Netalzul volcanics.

In the current study area, good exposures of conglomerates that occur on a ridge immediately east of Friday Lake were previously mapped by Richards (1990) as Trout Creek Formation. Here, thick beds of heterolithic conglomerate containing feldspar phyric volcanic and chert clasts up to 20 centimetres in diameter are exposed at the top of the ridge. The conglomerate beds, which are locally cross-bedded and fill channels in finer-grained beds, dip around 60 degrees to the northeast. The stratigraphic position of these beds is uncertain due to lack of outcrop away from the ridge. Presumably they are underlain by Ashman Formation to the west and are in fault contact with older Telkwa Formation volcanic rocks to the east. Alternatively, they may be younger and correlative with Lower Cretaceous Skeena Group conglomerates.

### **Lower Cretaceous Skeena Group**

The Skeena Group (Leach, 1910) is characterized by well-bedded, quartz, feldspar and muscovite-bearing, marine sedimentary rocks that overlap Jurassic and older rocks along the southern margin of the Bowser Basin. The main Skeena lithologies are dark grey shaly siltstone, greywacke, carbonaceous mudstone and chert-pebble conglomerate. These sedimentary rocks were deposited in a fluviodeltaic, near-shore to shallow

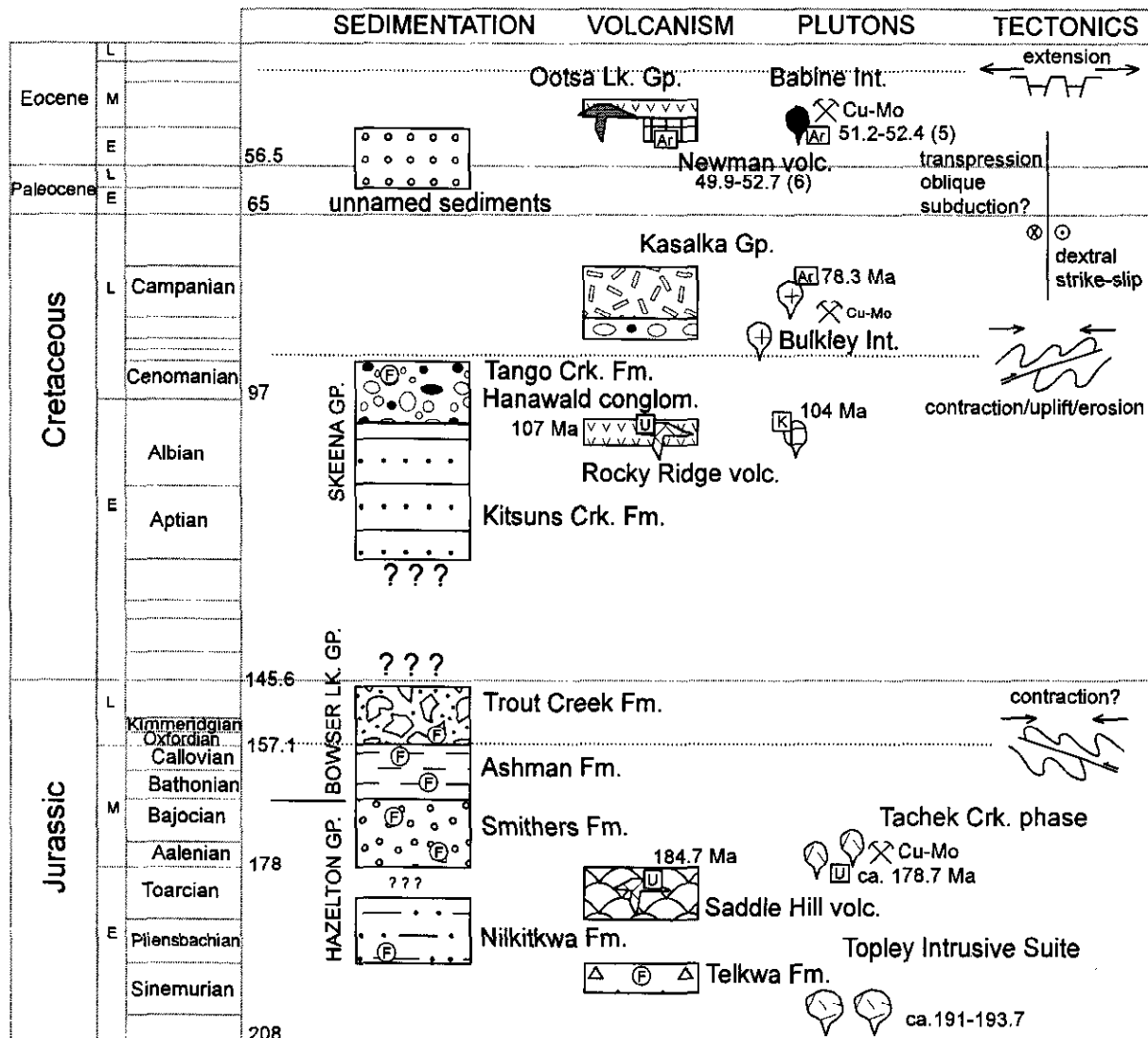


Figure 2-4. Generalized stratigraphy for the Nakinilerak Lake map area, 93M/8. See Figure 2-3 for legend.

marine environment (Basset, 1991). Although fossils are rare, the Skeena Group appears to range from Hauterivian to late Albian or early Cenomanian in age. Paleocurrent measurements indicate south, east and northeast sediment transport with the source area located in the Omineca belt. Bassett and Kleinspehn (1996) suggest that this belt was the main axis of a mid-Cretaceous continental arc and that the Skeena Group is a forearc succession. The Skeena rocks were folded, uplifted and eroded during a mid to late Cretaceous

contractional event related to evolution of the Skeena Fold Belt.

Richards (1990) subdivides Skeena Group rocks in the Hazelton map area (93M) into six formations or mappable units. These are from oldest to youngest the Kitsuns Creek Formation, the Kitsumkalum shale, the Hanawald conglomerate, an unnamed unit of subaqueous volcanic and volcanoclastic rocks, the Rocky Ridge Formation and the Red Rose Formation. In a recent paper Bassett and Kleinspehn (1996) propose a

new stratigraphic nomenclature based on lithofacies. These are the fluvial to deltaic Rocher Deboule Formation which would include both the Red Rose Formation and Hanawald conglomerate, the volcanic arc Rocky Ridge Formation, the deltaic Bulkley Canyon Formation which includes the fluvial Kitsuns Creek Member and the subtidal, turbiditic Couture Formation. Table 2-1 attempts to rationalize this new stratigraphic nomenclature with that of Richards (1990).

**Table 2-1. Skeena Group facies and comparison of stratigraphic divisions used by Richards (1990) and Bassett & Kleinspehn (1996). Age ranges and facies from Bassett & Kleinspehn (1996).**

| Richards (1990)       | Bassett & Kleinspehn (1996) | Facies               | Age Range          |
|-----------------------|-----------------------------|----------------------|--------------------|
| Red Rose Fm.          | Rocher Deboule Fm.          | fluvial, deltaic     | Albian-Cenomanian  |
| Hanawald conglomerate |                             |                      |                    |
| Rocky Ridge volcanics | Rocky Ridge Fm.             | volcanic arc         |                    |
| Kitsuns Creek Fm      | Bulkley Canyon Fm.          | deltaic              | Hauterivian-Albian |
|                       | Kitsuns Creek Mbr.          | fluvial, estuary     |                    |
| Kitsumkalum shale     | Couture Fm.                 | subtidal, turbiditic | Hauterivian-Albian |

Skeena Group sedimentary rocks in the Nakimilerak Lake map sheet have previously been correlated with the Kitsuns Creek Formation, the Hanawald conglomerate and the Red Rose Formation or mapped as undivided Skeena Group. A small area of alkaline basalt and rhyolite in the southwest and southeast corners of the map area, have been mapped as Rocky Ridge Formation.

In the current study area, Skeena Group sedimentary rocks are generally poorly exposed because they are only preserved in down-dropped fault blocks or grabens which tend to be low-lying areas with extensive cover. Although exposure is limited the broad valley extending from the end of the northwest arm of Babine Lake northward along the Babine River appears to be filled with Skeena Group sedimentary rocks. The Skeena rocks are folded and have a moderate to steep dip.

### ***Kitsuns Creek Formation***

The Kitsuns Creek Formation, which includes feldspathic and volcanic sandstone, siltstone, shale and polymictic, volcanic clast conglomerate underlies a large, relatively flat area extending from Fort Babine to the northern limit of mapping. Although these rocks are poorly exposed, good outcrops do occur along the Morrison Main and Nilkitwa haulage roads and near the height of land just east of the Fort Babine village. These feldspathic sedimentary rocks are apparently

overlain by the Hanawald conglomerate; the Rocky Ridge Formation and Kitsumkalum shale members appear to be missing.

### ***Rocky Ridge Formation***

The Rocky Ridge Formation includes Early Albian to Early Cenomanian submarine alkali basalt flows, breccias and lapilli tuffs that were erupted along the southern margin of the Bowser Basin (Bassett and Kleinspehn, 1996). In the Old Fort Mountain map sheet (93M/1), a chain of rhyolite domes that intrude marine sedimentary rocks of the Skeena Group have U-Pb isotopic ages around 107 Ma (mid Albian) suggesting they are also correlative with the Rocky Ridge Formation. These rhyolite domes will be the subject of a B.Sc. thesis by Deanne Tackaberry at the University of Victoria. Rhyolite domes in the southwest corner of the study area are also mapped as part of the Rocky Ridge Formation.

### ***Hanawald Conglomerate***

In the Hazelton map area fluvial-deltaic chert pebble conglomerate beds of the Hanawald Conglomerate member are interbedded with, and overlie, feldspathic clastic sedimentary rocks of the Kitsuns Creek formation (Richards, 1990) and, where present, the Rocky Ridge Formation. The conglomerates are thick-bedded and are more resistant than finer-grained beds of the Kitsuns Creek Formation. The interval of conglomerate beds is probably not more than 200 metres thick at its maximum. The age of the conglomerates, based on stratigraphic position, is late Albian to early Cenomanian. They are, in part, interpreted to be correlative with Sustut Group chert-pebble conglomerates (Tango Creek Formation) which are found on the east side of the map area.

In the current study area, the Hanawald conglomerate member is exposed in road cuts along the Morrison main haulage road near the western edge of the 93M/8 map sheet, as a series of northwest trending hogback ridges located east of the northern end of Morrison Lake and in Tahlo Creek. Unlike Trout Creek conglomerates which have a high proportion of volcanic clasts relative to chert, the Hanawald conglomerate is composed mainly of well-rounded clasts of dark and light grey chert and white quartz. Locally there are also clasts of soft, altered felsic volcanic or intrusive rocks, chloritized granite and feldspar porphyry. Carbonaceous wood fragments are also common. The conglomerate can be either clast or matrix supported and is poorly sorted with clast sizes ranging from 1 to 6 centimetres in diameter. The matrix is predominantly greenish-grey sand and is less resistant to weathering than the clasts. The conglomerates are interbedded with brown weathering greenish grey wackes and granule conglomerates of a similar composition.

The Hanawald conglomerate was probably deposited in a near shore, deltaic to fluvial environment along the northwestern edge of a landmass. Facies

changes to the northwest suggest deeper water, marine conditions in that direction (Bassett and Kleinspehn, 1996). The composition of the Hanawald conglomerate suggests a source area with abundant chert and quartz, possibly the Cache Creek terrane to the southeast.

### **Red Rose Formation**

The Red Rose Formation sits stratigraphically above the Rocky Ridge Formation and includes well-bedded, quartzo-feldspathic and muscovite bearing sandstone, siltstone, argillite, chert-pebble conglomerate, reddish sandstone and gritty mudstone (Richards, 1990). It is mainly fluvial and is in part correlative with the Tango Creek Formation of the Sustut Group. The formation is found mainly west of the map area and is probably the distal, finer-grained equivalent of the Hanawald conglomerate. The only strata mapped as Red Rose formation in the current study area are located in the northeast corner of the 93M/7 map sheet. Bassett and Kleinspehn (1996) have redefined the Red Rose Formation and Hanawald conglomerate as the Rocher Deboule Formation.

### **Mid Cretaceous Intrusions**

Other than the rhyolite domes mentioned earlier under Rocky Ridge Formation, intrusions of Mid Cretaceous age are rare in west central British Columbia. However, in the current study area, Carter (1976) reported a K-Ar isotopic age of  $105 \pm 4$  Ma (revised decay constants) for an equigranular biotite granodiorite stock exposed at Trail Peak. The stock is cut by a mineralized, biotite-feldspar porphyry dike that gave a  $49.8 \pm 4$  Ma K-Ar isotopic age (Carter, 1976). The older age is very similar to the age determined for feldspar porphyry flows at the former Bell mine and rhyolite domes elsewhere in the Old Fort Mountain map sheet (MacIntyre *et al.*, 1997) and is coeval with Rocky Ridge volcanism in west central British Columbia. The close spatial association of intrusions with such disparate ages suggests reactivation of magmatic centers after a lull of some 50 million years.

### **Lower to Upper Cretaceous Sustut Group**

The Sustut Group includes Cretaceous and Tertiary non-marine clastic rocks that overlap rocks of the Stikine Terrane and the Bowser Lake Group. The areal distribution of these rocks defines the northwest trending Sustut Basin which extends from the Stikine River in the northwest to Takla Lake in the southeast. The type area is along the Sustut River in the McConnell Creek map area (Lord, 1948). The Sustut Group is divisible into the Tango Creek and Brothers Peak formations (Eisbacher, 1974). Only the Tango Creek Formation is present in the Nakinilerak Lake map area.

### **Tango Creek Formation**

The Tango Creek Formation includes poorly sorted non marine conglomerates, sandstones and mudstones that sit unconformably on Bowser Lake Group and older rocks. Spores and pollen collected from the formation indicate an age range from mid-Albian to Campanian (late Early to middle Late Cretaceous). Paleocurrent directions indicate an eastern to northeastern source area as does the presence of metamorphic chert clasts which are probably derived from the Cache Creek terrane. The formation thickens westward to a maximum of 1500 metres as a prograding deltaic sequence.

Chert pebble conglomerates of the Tango Creek Formation underlie the northeast corner of the current map area. The best exposures are on the shores of Takla Lake and in the area along the eastern edge of the Nakinilerak Lake map sheet. Here, the conglomerates dip moderately to the northeast and form a series of sparsely timbered hogback ridges between the two arms of Takla Lake, a distance of 15 kilometres. This 4 kilometre wide, north trending panel is bounded to the east by the Takla fault and to the west by an unnamed fault. Both of these faults have strong topographic linears and are presumably high angle. The Takla Fault juxtaposes Tango Creek conglomerates against an uplift of Late Triassic Takla volcanic rocks; the western fault separates the conglomerates from a narrow, fault bounded uplifted slice of Lower Jurassic volcanic and sedimentary rocks. This uplift or horst, is bounded on both sides by Tango Creek chert pebble conglomerates and can be traced northward across Takla Lake, and into the Lovell Cove area where Middle Jurassic Smithers Formation sedimentary rocks are exposed in the uplift. On the east shore of Takla Lake, the fault bounded panel is exposed at Red Bluff where it contains a highly fractured, sheared and brecciated, pink weathering monzonite intrusion that is probably Jurassic in age and related to the Topley intrusions. Along the shore, north of White Bluff, white weathering chert pebble conglomerates are overturned and dip steeply to the east. Distinctive beds of red weathering siltstone or tuff occur in the conglomerate section and were sampled for paleomagnetic studies by Randy Enkin of the Geological Survey of Canada. The steep dipping, overturned orientation of these conglomerate beds may be due to drag on a nearby high angle normal or reverse fault that bounds the north trending uplift.

Northeast-dipping beds of chert pebble conglomerate are also exposed in several other localities in the northeast corner of the study area where they are partly overlain by relatively flat-lying Tertiary volcanic rocks.

Assuming no structural repeats, the Tango Creek conglomerate section exposed along the eastern edge of the map area could be up to 5 kilometres thick. This sedimentary succession becomes finer-grained up section and consists predominantly of mudstone and siltstone where it is exposed on the shores of Takla Lake. Well-preserved plant fossils have been collected from these rocks and have previously been identified as

Cenomanian in age (Armstrong, 1949) suggesting the underlying chert pebble conglomerates are Cenomanian or older.

In the current study area, the Tango Creek Formation is predominantly poorly to moderately sorted, moderate to thick bedded, brown to grey weathering conglomerates that were probably deposited in a fluvial environment. The conglomerates contain well-rounded pebble to cobble sized clasts of chert and quartz of a probable metamorphic provenance with lesser mafic and felsic volcanic and granitic clasts in a gritty, sandstone matrix of similar composition. Conglomerate beds are often cross-bedded especially where they fill channels in underlying strata and typically fine upward into intervals of granule conglomerate and quartz sandstone. Thin beds of red weathering siltstone or tuff are locally present and were the target of paleomagnetic sampling by Randy Enkin of the Geological Survey of Canada.

### Upper Cretaceous Kasalka Group

The Kasalka Group, as defined by MacIntyre (1985), is comprised of calc-alkaline continental volcanic rocks that sit with angular discordance on Skeena Group and older strata. The type area for the Kasalka Group is at Tahtsa Lake where a volcanic section up to 1500 metres thick overlies a basal conglomerate member. These volcanic rocks are part of a north-trending continental volcanic arc that transected west-central British Columbia in Late Cretaceous time. The predominant rock types are hornblende-feldspar-phryic latite-andesite and andesite, volcanic breccia, lapilli tuff and lahar. Sutherland Brown (1960) mapped similar rocks as the Brian Boru Formation in the Rocher Déboulé Range north of Smithers, and MacIntyre and Desjardins (1988) documented Kasalka Group rocks in the Babine Range west of the study area.

In the northwest corner of the Nakinilerak Lake map sheet, coarse porphyritic andesite flows are exposed along a northwest-trending fault scarp and in clear-cuts east of the scarp. These rocks, which apparently unconformably overlie Lower Cretaceous chert pebble conglomerates, are lithologically identical to flows near the Lennac Lake porphyry prospect described in a previous report (MacIntyre *et al.*, 1996). The flows, which display sheeted jointing and are generally unaltered and unmineralized, contain 25 to 30 percent hornblende laths, biotite "books" and equant plagioclase in a finer-grained, greenish grey groundmass. Although previously mapped as a Babine intrusion, the coarse porphyritic texture and presence of books of biotite are features atypical of the Eocene Babine intrusions. Rather, these features are more characteristic of Kasalka Group volcanic rocks and related Bulkley Intrusions. A 2 to 3 metre wide, northeast-trending dike of similar composition to the flows was observed cutting the underlying chert pebble conglomerates and may have been a feeder to the flows.

### Late Cretaceous Bulkley Intrusions

The term Bulkley Intrusions was first used by Kindle (1954) for granitic rocks in the Hazelton area. This suite of intrusions is Late Cretaceous in age and includes large porphyritic and equigranular stocks of quartz monzonite, granodiorite and quartz diorite and smaller plutons and dikes of feldspar porphyry, hornblende-biotite-quartz-feldspar porphyry and quartz porphyry. Potassium argon isotopic ages range from 70 to 84 Ma (Carter, 1976). The plutons define a north-trending belt that extends from north of the Babine River southward to the Eutsuk Lake area. They are believed to be the exhumed roots of an Andean type magmatic arc that formed during a period of oblique plate subduction in Late Cretaceous time. Volcanic centers were probably localized in areas of crustal extension along dextral strike slip faults.

The only intrusions in the Babine Lake area that are known to be part of this suite are exposed at the Lennac Lake porphyry copper prospect (MacIntyre *et al.*, 1996). One of these intrusions was dated using the laser Ar-Ar technique at  $78.3 \pm 0.8$  Ma (MacIntyre *et al.*, 1996), identical to a previous  $78.3 \pm 2.5$  Ma K-Ar age determined by Carter (1973). There are no known occurrences of Bulkley Intrusions in the Nakinilerak Lake map area.

### Cretaceous to Tertiary Intrusions

Several small stocks, sills and dikes of medium to coarse-grained greenish grey diorite and gabbro crop out in the map area. Best exposures are on Frypan peak and in the southern Bait Range where diorite sills up to 10 metres thick intrude Lower and Middle Jurassic sedimentary rocks and volcanic rocks. For the most part the intrusions have been emplaced passively with little disruption of regional bedding attitudes. Zones of biotite hornfels are locally present, especially around larger bodies. In places the diorite contains 1 to 2 millimetre phenocrysts of feldspar and less commonly pyroxene and hornblende. Generally the diorite is weakly to moderately chloritized and in places has poorly developed mineral lineation. Compositionally these intrusions range from gabbro to granodiorite, but most are apparently true diorites or quartz diorites.

The age of diorite intrusions in the map area is uncertain. They are found cutting rocks ranging from Early Jurassic through to Early Cretaceous in age. Therefore, assuming there is only one episode of dioritic magmatism, these intrusions must be Early Cretaceous or younger. It is possible, however, that some of the diorite intrusions are Eocene, and represent the earliest, least differentiated phases of the Babine Intrusions.

### Eocene Babine Igneous Suite

The Babine Igneous Suite is divisible into two main units - the Babine Intrusions and the Newman volcanics (Carter, 1976; 1981; Ogryzlo, 1994). Both are early Eocene in age as indicated by isotopic age dating

(Villeneuve and MacIntyre, 1997). New isotopic dating as part of the Nechako Natmap project suggests the Babine Igneous Suite is slightly older (2-3 million years?) than the Ootsa Lake Group volcanic rocks (Mike Villeneuve, personal communication).

### ***Babine Intrusions***

The Babine Intrusions include small plugs and dikes of crowded biotite±hornblende feldspar porphyry, quartz±biotite feldspar porphyry and equigranular hornblende-biotite granodiorite to quartz diorite that occur as multi-phase intrusive centres in a north-trending belt that extends from Fulton Lake to Trail Peak (Figure 2-1). Potassium-argon isotopic ages biotite and hornblende phyrical phases range from 50.2 to 55.8 indicating the intrusions are early Eocene in age (Villeneuve and MacIntyre, 1997). The intrusions, which are believed to be the subvolcanic roots of a calcalkaline magmatic arc, cut volcanic and sedimentary strata ranging in age from Triassic to Early Cretaceous. The Newman volcanics are the extrusive equivalents of the intrusions and these rocks are preserved close to intrusive centres on the Newman Peninsula and at Saturday Lake. The fact that the volcanic edifices have not been completely removed by erosion is further evidence that the Babine intrusions and associated porphyry copper deposits such as Bell and Granisle are exposed at a subvolcanic level.

Compositionally, the Babine intrusions and Newman volcanics are very similar to the older Bulkley intrusions and Kasalka volcanic rocks found further to the west. This suggests similar, transtensional, volcanic environments prevailed during the Late Cretaceous and, into the early Eocene, and that locus of volcanism moved progressively eastward with time.

### ***Biotite-hornblende quartz diorite to granodiorite***

Stocks of medium-grained, equigranular to subporphyritic biotite-hornblende quartz diorite to granodiorite are exposed at the Nak and Trail Peak properties and in the southeast corner of the 93M/7 map sheet (Figure 2-2). Zones of biotite hornfels and disseminated and fracture controlled pyrite, up to several hundred metres in width enclose the equigranular stocks. Although the equigranular phase of the Babine intrusions can host low-grade copper mineralization, better grades are typically associated with younger porphyritic phases.

### ***Biotite-feldspar porphyry***

The most characteristic rock type of the Babine intrusive suite is a crowded, dark grey biotite-feldspar porphyry which typically occurs as small plugs and dikes. This rock type contains 40 to 60 percent of 2 to 3-millimetre phenocrysts of biotite, plagioclase and rarely hornblende and quartz, in a groundmass of plagioclase, quartz, biotite and minor potassium feldspar. The porphyries are quartz diorite to granodiorite in

composition and are typical of plutonic rocks found in a continental calcalkaline magmatic arc environment.

Northeast to north trending dikes of biotite-feldspar porphyry cut earlier equigranular granodiorite and quartz diorite stocks and surrounding wall rocks at the Nak and Trail Peak porphyry copper prospects. These dikes have associated copper mineralization and are locally strongly altered.

### ***Quartz-biotite-feldspar porphyry and quartz feldspar porphyry***

Quartz-phyric intrusions, with or without biotite, post-date the main phase of stockwork mineralization at the Bell mine and apparently cut the earlier biotite-feldspar porphyry phase (Dirom *et al.*, 1995). The quartz-phyric rocks, which contain partially resorbed quartz phenocrysts, are weakly mineralized relative to the biotite-feldspar porphyry phase. This intrusive phase is most common around the Bell pit but also occurs as small stocks and dikes in the Old Fort Mountain map sheet (Figure 2-2). No quartz phyrical Babine intrusions were mapped in the Nakinilerak Lake map sheet.

### ***Newman Volcanics***

In the Babine Lake area, calc-alkaline, hornblende-biotite-feldspar porphyry flows, breccias and lahars sit with angular discordance on folded Triassic, Jurassic and Lower Cretaceous volcanic and sedimentary rocks. These volcanic rocks were given the name Newman volcanics by Tipper and Richards (1976) because they are well-exposed on both sides of the Newman Peninsula in the Fulton Lake map sheet (93L/16). The Newman volcanics are Early Eocene, with Ar-Ar isotopic ages ranging from 49.9±0.6 to 52.7±0.6 Ma. (Villeneuve and MacIntyre, 1997). These ages overlap those determined for lithologically identical porphyries of the Babine Intrusions and the volcanic rocks are, therefore, considered to be the extrusive equivalent of these rocks (Villeneuve and MacIntyre, 1997). Typical hornblende-biotite-feldspar phyrical andesites of the Newman Volcanics crop out sporadically along the western shore of Babine Lake and on Bear Island in the 93L/16 and 93M/1 map sheets. The only known occurrence of Newman volcanics in the Nakinilerak Lake map sheet is at Trail Peak where hornblende-biotite-feldspar porphyry flows cap the ridge southeast of the main showings.

### ***Eocene Ootsa Lake Group***

The Ootsa Lake Group, as defined by Duffell (1959), is a succession of continental calcalkaline volcanic rocks with minor nonmarine sedimentary interbeds. In the type area around Ootsa Lake, the volcanic members are basalts, andesites, dacites and rhyolites. The dacites and rhyolites occur both as flows and flow-breccia dome complexes of limited areal extent; the andesites and tuffs are more extensively distributed. Several dates determined in the Whitesail

Lake area indicate that the Ootsa Lake volcanic rocks erupted 50 million years ago for a period as short as 1 million years (Diakow and Mihalyuk, 1987).

In the relatively flat, northeast corner of the current study area, brown, maroon and red weathering aphanitic to feldspar phyric vesicular and amygdaloidal basalt flows, flow top breccias, maroon lapilli tuffs and volcanic conglomerates are exposed in road cuts and along the north banks of Sinta Creek. Although exposures are poor, these mafic volcanics appear to be relatively flat lying and sit unconformably on chert pebble conglomerates of the Upper Cretaceous Tango Creek Formation and fossiliferous siltstones of the Middle to Upper Jurassic Smithers and Ashman formations (Figure 2-3). The basaltic flows have a strong aeromagnetic response relative to underlying sedimentary rocks and this has been used to define their areal extent in areas lacking outcrop. A distinctive lithology within this succession is a basalt flow with 5 to 10 millimetre, aligned plagioclase laths. The flows are very vesicular in places and locally have calcite and chlorite filled amygdules that are flattened and elongated parallel to flow directions. These basaltic rocks are tentatively correlated with the Ootsa Lake Group based on stratigraphic position and lithology.

Rhyolite to rhyodacite flows, breccias and intrusive domes occur sporadically in the northeast corner of the Nakinilerak Lake map sheet and in an area north of Friday Lake. These rocks are also tentatively correlated with the Ootsa Lake Group. The rhyolites are cream to white weathering, flow banded and have 10 to 15 percent of 2 to 3 millimetre phenocrysts of biotite, hornblende and plagioclase in a pink to grey, siliceous aphanitic groundmass. The rhyolitic rocks occur both as flows interbedded with vesicular basalt and as subcircular, columnar-jointed domes that form isolated topographic highs.

In the northeast corner of the map area, near Takla Lake, a biotite-hornblende-feldspar phyric rhyodacitic ash flow is well exposed on a northwest trending scarp and appears to be in fault contact with chert pebble conglomerates of the Tango Creek Formation. A sample was collected from the ash flow for Ar-Ar isotopic age dating.

## STRUCTURE

The structure of the Babine Lake area reflects the effects of at least four major tectonic events. The oldest took place in mid to late Jurassic time when rocks of the Hazelton and Takla Groups were folded and uplifted in response to the collision of Stikinia with the Cache Creek Terrane. This was followed in mid Cretaceous time by a contractional event that produced northwest-trending folds and northeast directed thrust faults. In the Bowser Basin and in the current study area, rocks as young as Cenomanian were involved in this folding event. In the southern part of the Bowser Basin, just north of the study area, folds are cut by plutons as old as 82 Ma thus constraining deformation to the early part of

the Late Cretaceous. This is consistent with observations in the Tahtsa Lake area, where relatively flat-lying Late Cretaceous volcanic rocks of the Kasalka Group sit with angular discordance on Albian Skeena Group rocks (MacIntyre, 1985). The unconformity is marked by an erosional conglomerate. Crustal extension and development of north trending grabens and horsts took place in Late Cretaceous to Eocene time during a period of oblique subduction and transpression along the Skeena Arch. The latest episodes of block faulting are Eocene or younger because Late Cretaceous and Eocene plutons and their extrusive equivalents, the Kasalka and Newman volcanics, have been truncated and displaced by high angle faults that bound the grabens. Within the grabens, the younger rocks can have moderate tilts and form broad open folds. This contrasts with Cenomanian and older rocks which are more tightly folded, and in part, imbricated by thrust faults. The latest event, which may be as young as Miocene, involved northwest-southeast crustal extension and tilting of fault blocks between north to northwest trending strike slip faults. In general, because of the Eocene and younger subsidence of fault blocks, younger rocks typically occur at lower elevations within north trending valleys while older rocks compose the ridges that bound the valleys.

## MINERAL OCCURRENCES

The most important mineral occurrences in the Babine Lake area are porphyry copper deposits associated with the Eocene Babine intrusions and Late Cretaceous Bulkley intrusions (Carter, 1981; Carter *et al.*, 1995). The Nak and Trail Peak properties are the main porphyry copper occurrences in the 1997 study area (Table 2-2). In addition, the Bear Hill epithermal prospect occurs near the eastern boundary of the map area.

### Nak (Minfile 93M 010)

The Nak porphyry copper prospect is located approximately 3 kilometres east of Nakinilerak lake (Figure 2-2) and is accessible by helicopter or via an overgrown foot trail connecting to the end of the Nak haulage road. Noranda exploration first explored the property between 1960 and 1970, during the main phase of porphyry exploration in the district. Over this time period they did geochemical, geophysical and geological surveys and drilled 28 holes totaling 1837 metres. Tri Alpha Investments acquired the property and cut a new grid in 1992 and 1993, but subsequently cancelled their program. Hera Resources Inc. subsequently restaked the ground and completed induced polarization and magnetic surveys in late 1994 and early 1995. Their work defined a large, chargeability low rimmed by an area of higher chargeability that coincided with the known distribution of disseminated pyrite. Hera then drilled 43 BQ size holes totaling 8007 metres in 1995 and an additional 28 holes totaling 5304 metres in 1996. The property was not active in 1997.

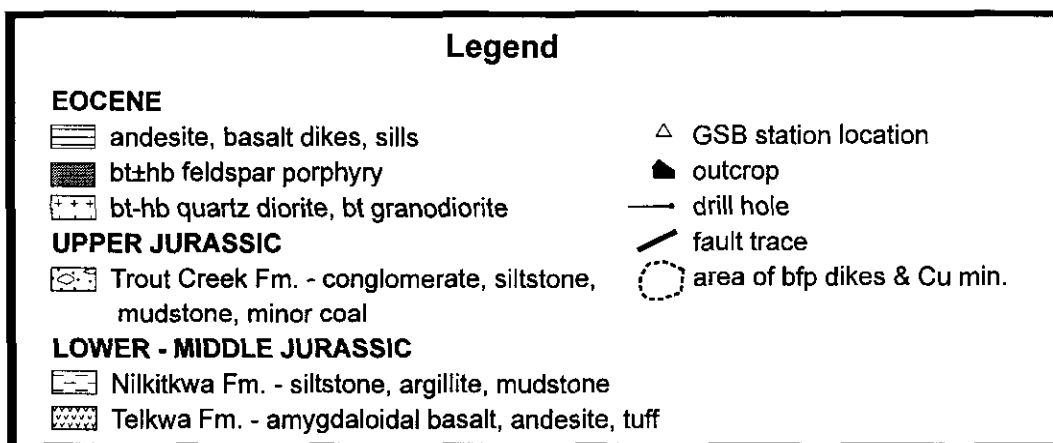
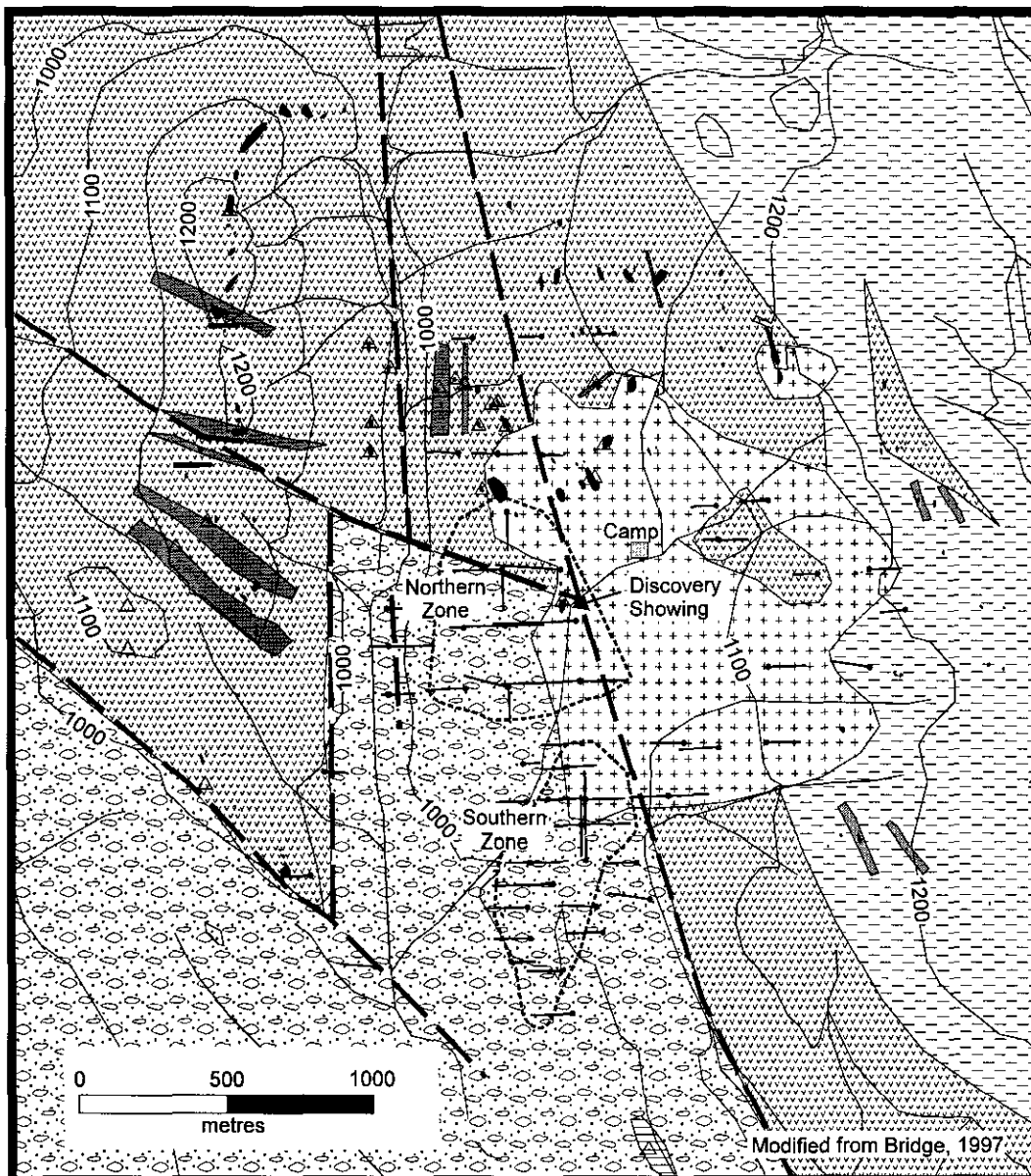


Figure 2-5. Generalized geology of the Nak property. See Figure 2-3 for property location.

Volcanic rocks also crop out sporadically in the area north and northeast of the stock. The volcanic rocks at Nak are tentatively correlated with the Lower Jurassic Telkwa Formation based on lithologic similarity. This correlation implies a high angle fault contact with younger Upper Jurassic Trout Creek sedimentary rocks that were intersected in drilling between the two ridges and also crop out to the west along the shores of Nakinilerak Lake. Both the volcanic rocks and sedimentary rocks are cut and have been hornfelsed by several northwest trending, moderately northeast dipping dikes or sills of biotite-feldspar porphyry that are typical of the Eocene Babine Intrusions.

The geology of the Nak property, based on company reports (Bridge, 1997) and mapping done in 1995 and 1997, is shown in Figure 2-5. The property covers the area between two north trending ridges that are located east of Nakinilerak Lake. Here, porphyry copper mineralization is associated with north to northwest trending biotite-feldspar porphyry dikes and a subcircular stock of biotite quartz diorite to granodiorite that intrude volcanic and sedimentary rocks of the Lower Jurassic Telkwa and Nilkitkwa formations and sedimentary rocks of the Upper Jurassic Trout Creek Formation. The volcanic rocks crop out on the western ridge, which is an uplifted block bounded by north-trending high angle faults and in the area north of the quartz diorite stock. Good exposures of amygdaloidal, feldspar phyric andesite or basalt, with varying amounts of chlorite and epidote alteration and disseminated pyrite occur along the crest of the ridge. The south end of the ridge is truncated by a regional, northwest trending fault that is the contact between volcanic rocks exposed on the ridge and conglomerates and sandstones that crop out down slope towards Nakinilerak Lake. The sedimentary rocks are tentatively mapped as Late Jurassic Trout Creek Formation. Drill hole (N96-61), which was collared in volcanic rocks on the southeast nose of the ridge and drilled to the west at a -56 degree inclination, intersected the sedimentary rocks at depth suggesting the fault contact dips moderately to the north and places older rocks over younger.

The eastern ridge has less outcrop but appears to be a northeast dipping section of hornfelsed fragmental volcanic rocks that, near the crest of the ridge, are overlain by mudstone, siliceous shale, and siltstone of the Nilkitkwa or Ashman Formation. These rocks have up to 5 percent disseminated pyrite and chlorite-epidote veinlets.

The main area of copper mineralization is located in the drainage basin between the two north trending ridges. Sporadic outcrop and drill intersections indicate that a semi-circular, hornblende quartz diorite stock, 1.0 kilometres in diameter, intrudes and has hornfelsed volcanic rocks and sedimentary rocks of probable Late Jurassic age. The contact of the quartz diorite stock apparently dips steeply outward as indicated by drilling (Bridge, 1997). A small stock of hornblende diorite crops out in the northeast corner of the property and may be an early phase of the Babine Intrusions or an older Cretaceous intrusion.

The western side of the quartz diorite stock is cut by a north trending, high angle fault that is coincident with a prominent topographic lineament. Drill holes intersected this fault, and other parallel faults in the ravine along the western side of the deposit (Bridge, 1997). These faults are mineralized indicating they predate or are the same age as the main period of sulphide mineralization. Retrograde, late stage clay alteration, observed in drill core, may be associated with circulation of low temperature fluids along these fault conduits as the porphyry system cooled.

Drill holes located southwest of the quartz diorite stock intersected mainly siltstones, sandstones and mudstones that are interbedded with heterolithic pebble to cobble conglomerate. These rocks have pervasive argillic and phyllic alteration, and are cut by north trending faults and dikes of biotite feldspar porphyry. These sedimentary rocks, which are in a fault bounded graben, are mapped as Trout Creek Formation because of the presence of poorly sorted, clast to matrix supported heterolithic conglomerate beds and the absence of marine fossils.

The discovery outcrop on the Nak property is located just north of a small creek that drains the mineralized area. This outcrop is a biotite feldspar porphyritic quartz diorite or granodiorite with moderate to strong clay alteration and pyrite, chalcopyrite and minor bornite disseminations, fracture coatings and quartz veinlets.

Drilling has defined two main zones of copper mineralization - the Northern and Southern zones, both of which are situated west of the quartz diorite stock (Figure 2-5). The southern zone is at the southwest corner of the quartz diorite stock and is defined by the presence of potassic alteration superimposed on hornfelsed sedimentary rocks with disseminations and veinlets of chalcopyrite, bornite, molybdenite and magnetite. Mineralization is spatially associated with a swarm of biotite-feldspar porphyry dikes of uncertain orientation. A resource estimate for this zone is 54 million tonnes grading 0.17 percent Cu and 0.254 grams per tonne Au (Bridge, 1997). The northern zone is immediately west of the quartz diorite stock and is defined by disseminated, fracture and vein controlled chalcopyrite, bornite and molybdenite in zones of potassic, phyllic and argillic alteration. Mineralization and alteration are spatially associated with biotite-feldspar porphyry dikes that cut volcanic and sedimentary rocks and the quartz diorite stock. Like the southern zone, a late, fault-controlled argillic alteration has been superimposed on the earlier alteration and mineralization. A resource estimate for the northern zone, which is gold poor relative to the southern zone, is 217 million tonnes grading 0.187 percent Cu and 0.0398 grams per tonne Au (Bridge, 1997).

A north trending vein or tabular zone of high grade copper was intersected southwest of the quartz diorite stock. The discovery hole (N96-58) intersected the vein obliquely and returned 2.614 percent Cu and 0.143 grams per tonne Au over a 12.5 metre intersection. A second hole (N96-65) collared 200 metres further north

**Table 2-2. MINFILE Mineral Occurrences**

| NO. | PROPERTY NAME | STATUS  | METALS              | TYPE       |
|-----|---------------|---------|---------------------|------------|
| 010 | NAK           | Showing | Cu,Mo,Au<br>Zn,Pb   | Porphyry   |
| 011 | Trail Peak    | Showing | Ag,Zn,Cu,<br>Pb     | Porphyry   |
| 137 | Bear Hill     | Showing | Cu,Ag,Ba,<br>Zn, Pb | Shear vein |
| 163 | Friday Green  | Showing | Cu                  | ?          |
| 164 | Friday Red    | Showing | Cu                  | ?          |

and drilled in the opposite direction intersected a conglomerate partially replaced with tourmaline and chalcopryrite that graded 1.318 percent Cu over 18.28 metres (Bridge, 1997). This intersection is on strike with the vein intersected in hole N96-58. Other than these high grade intersections, the best and longest intersection obtained in 1996 was drill hole N96-55 which is located southwest of the quartz diorite stock. This hole had a 24.69 metre intersection grading 0.439 percent Cu and 0.704 grams per tonne gold.

Alteration at Nak is comprised of an early prograde potassic alteration overprinted by a late stage, retrograde phyllic to argillic alteration. The potassic alteration is characterized by the presence of veinlets of biotite and K-feldspar, accompanied by magnetite, quartz, chalcopryrite, pyrite, bornite and rare molybdenite in hornfelsed sedimentary rocks along the southern contact of the quartz diorite stock.

Advanced argillic alteration is peripheral to and superimposed on the potassic zone. It extends north and south of the zone along northerly trending faults. This alteration assemblage includes pervasive, feldspar destructive clay-quartz-tourmaline alteration and veinlets of quartz and tourmaline with or without chalcopryrite, pyrite, magnetite and sericite. Argillic alteration is also common in the fault zone and consists of clay-carbonate alteration with rare arsenopyrite-pyrite-calcite with or without quartz veins. Trace amounts of dumortierite are reported to occur in sedimentary rocks west of the quartz diorite stock (Bridge, 1997).

Phyllic alteration is also common and is characterized by light grey zones of sericite and quartz associated with carbonate-pyrite-chalcopryrite-bornite veins that cut dark grey, biotite hornfelsed volcanic and sedimentary rocks.

Propylitic alteration, which is comprised of chlorite, epidote, calcite and pyrite veinlets and disseminations, occurs mainly in volcanic rocks on the west, north and east sides of the property.

### **Trail Peak (Minfile 93M 011)**

The Trail Peak porphyry copper prospect (CAVZ), which is located approximately 13 kilometres north of Nakinilerak Lake, is an isolated, conical, topographic high on a broad northwest trending uplift. Texas Gulf

Sulphur Company conducted geological mapping, geophysical and soil surveys, bulldozer trenching and 1080 metres of diamond drilling in 12 holes between 1968 and 1975.

Most of the Trail Peak property is at or above tree line. Good exposures of bedrock occur on Trail Peak and on a lower, parallel ridge to the east. Gossanous outcrops on Trail Peak are hornfelsed siliceous siltstones with disseminated pyrite. Crystal lithic tuffs are interbedded with the siltstones west of Trail Peak. The sedimentary rocks are mapped as part of the Middle to Late Jurassic Ashman Formation (Richards, 1990). Siltstone and mudstones that crop out in the southeast corner of the property and these may be an inlier of Skeena Group rocks (Carter, 1990).

A small stock of biotite granodiorite crops out on the south end of Trail Peak and is exposed in a series of east west trending trenches downslope to the south. Both the hornfelsed sedimentary rocks and granodiorite stock are cut by north to northwest trending, altered biotite-feldspar porphyry dikes. Carter (1976) reports a 105±4 Ma K-Ar isotopic age for the granodiorite stock and a 49.8±4 Ma K-Ar isotopic age for one of the biotite-feldspar porphyry dikes.

Hornblende-feldspar phyrlic andesite, with crude columnar jointing caps the ridge southeast of Trail Peak. These rocks may be the extrusive equivalent of the porphyry intrusions and therefore, correlative with the Newman volcanics. If this correlation is correct, it implies that the northeast trending faults that cut the property bound successively downdropped fault blocks going to the southeast.

Although disseminated pyrite is widespread in hornfelsed sedimentary rocks at Trail Peak, chalcopryrite and minor bornite are only found as fracture controlled disseminations and in quartz-tourmaline veinlets near and within biotite-feldspar porphyry dikes and along northeast trending fault zones (Carter, 1990). Potassic alteration is coincident with copper mineralization and is comprised of secondary biotite, some K-feldspar and sericite. Pervasive retrograde clay alteration, similar to that observed at Nak, appears to be spatially associated with late, northeast-trending faults.

### **Bear Hill (Minfile 93M 137)**

The Bear Hill property is located in the northeast corner of the map area, approximately 5 kilometres north of the end of Takla Lake (Northwest Arm). The main area of interest is around Bear Hill, a small, northerly elongate knoll of Lower Jurassic Telkwa Formation volcanic rocks protruding from a broad, flat, north trending valley (Findlay and Hoffman, 1981). Bear Hill is one of a chain of knolls that occur along a long, narrow, north-trending, uplifted fault block of Jurassic and older volcanic and sedimentary rocks. This fault block, which at its maximum is 4 kilometres wide, can be traced from the end of the Northwest Arm of Takla Lake to around Lovell Cove, a distance of 30 kilometres. It is bounded to the east and west by downdropped blocks of Late Cretaceous Sustut chert pebble

conglomerate and Eocene Ootsa Lake Group and Endako Group volcanic rocks (Figure 2-2).

The Bear Hill property was first staked by BP Minerals Limited in late 1980 after they located malachite and pyrolusite staining in fractured andesitic volcanic rocks on Bear Hill. They subsequently did geological mapping and sampling in 1981. Placer Development Limited optioned the property in late 1981 and in 1982 did an induced polarization survey and additional geochemical sampling in the vicinity of Bear Hill. Placer then drilled two west dipping holes approximately 100 metres apart near the base of Bear Hill on its eastern side. This drilling intersected a steep, east dipping zone of barite and quartz veining with minor chalcopyrite, galena, sphalerite and rare bornite, tetrahedrite and cuprite. The mineralization occurs as tiny grains, blebs and stringers in intensely fractured and locally silicified andesitic to dacitic flows and volcanoclastic rocks (Gareau and Kimura, 1982). One of the higher grade chip samples from the property assayed 0.73 percent Cu, 117 grams per tonne Ag, and 5.4 percent Ba across 5 metres (Kimura *et al.*, 1982). The main commodity of interest on the property is silver.

The mineralogy and style of alteration and veining at Bear Hill suggests the mineralization is epithermal. Hydrothermal activity was apparently localized along, steep, north trending fault zones that bound a long, narrow, uplifted block of Jurassic volcanic and sedimentary rocks. These faults, which are Eocene or younger in age, might be favourable targets for additional epithermal mineralization elsewhere in the area.

### Friday Green (Minfile 93M 163)

The Friday Green occurrence is approximately 5 kilometres northeast of the Nak porphyry copper occurrence. The property is underlain by gently dipping mudstones and siltstones of the Early Jurassic Nilkitkwa Formation that are intruded by small dikes of biotite-feldspar porphyry presumably related to the Eocene Babine Intrusions. The porphyry, which contains minor disseminated chalcopyrite, has locally hornfelsed the sedimentary rocks. Pyrite occurs on fractures in the hornfels.

### Friday Red (Minfile 93M 164)

The Friday Red occurrence is located approximately 7 kilometres northeast of the Nak porphyry copper occurrence. The property is underlain by green volcanic flows, tuffs, tuff-breccia and minor intercalated mudstones of the Lower Jurassic Telkwa Formation. These rocks are intruded by a strongly magnetic feldspar porphyry dike that has been mapped as an Eocene Babine Intrusion. Trace amounts of disseminated chalcopyrite are reported to occur in the amygdaloidal flows.

## ACKNOWLEDGMENTS

The author acknowledges the excellent assistance provided this summer by youth employment students Ryanne Metcalf, Stephen Munzar and Deanne Tackaberry. Their enthusiasm and positive attitude under less than ideal working conditions were exceptional. In addition, the author acknowledges the excellent service provided by Pacific Western Helicopters, in particular pilot Bob Wellington from their base at Lovell Cove.

## REFERENCES

- Bassett, K.N. (1991): Preliminary Results of the Sedimentology of the Skeena Group in West-central British Columbia; in *Current Research, Part A, Geological Survey of Canada, Paper 91-1A*, pages 131-141.
- Bassett, K.N. and Kleinspehn, K.L. (1996): Mid-Cretaceous transtension in the Canadian Cordillera: Evidence from the Rocky Ridge volcanics of the Skeena Group; *Tectonics*, Volume 15, No. 4, pages 727-746
- Bridge, D. (1997): Geological and drilling report on the NAK 95-1, 95-3, NAK 4-11, SNAK and SNAK 1 mineral claims, Omineca Mining division, North-central British Columbia, NTS 93M/1 and 8; *B.C. Ministry of Employment and Investment, Assessment Report 24928*
- Carter, N.C. (1973): Geology of the Northern Babine Lake Area; *B.C. Ministry of Energy, Mines and Petroleum Resources, Preliminary Map 12 (93L)*.
- Carter, N.C. (1976): Regional Setting of Porphyry Deposits in West-central British Columbia; in *Porphyry Deposits of the Canadian Cordillera*, Sutherland Brown, A., Editor, *Canadian Institute of Mining and Metallurgy, Special Volume 15*, pages 245-263.
- Carter, N.C. (1981): Porphyry Copper and Molybdenum Deposits West Central British Columbia; *B.C. Ministry of Energy, Mines and Petroleum Resources, Bulletin 64*.
- Carter, N.C. (1990): Trail Peak Property; *B.C. Ministry of Employment and Investment, Assessment Report 19557*.
- Carter, N.C., Dirom, G.E., and Ogryzlo, P.L. (1995): Porphyry Copper-gold Deposits, Babine Lake Area, West-central British Columbia; in *Porphyry Deposits of the Northwestern Cordillera of North America*, Schroeter, T.G., Editor, *Canadian Institute of Mining, Metallurgy and Petroleum, Special Volume 46*.
- Cook, S., Jackaman, W., Sibbick, S. and Lett, R. (1997): Regional Geochemical Survey Program - Review of 1996 Activities; in *Geological Fieldwork 1996, B.C. Ministry of Employment and Investment, Paper 1997-1*.
- Diakow, L. and Mihalynuk, M. (1987): Geology of Whitesail Reach and Troitsa Lake Map Areas; in *Geological Fieldwork 1986, B.C. Ministry of*

- Energy, Mines and Petroleum Resources*, Paper 1987-1, pages 171-180.
- Dirom, G.E., Dittrick, M.P., McArthur, D.R., Ogryzlo, P.L., Pardoe, A.J. and Stothart, P.G. (1995): Bell and Granisle Porphyry Copper-Gold Mines, Babine Region, West-central British Columbia; in *Porphyry Deposits of the Northwestern Cordillera of North America*, Schroeter, T.G., Editor, *Canadian Institute of Mining, Metallurgy and Petroleum*, Special Volume 46.
- Duffell, S. (1959): Whitesail Lake Map-area, British Columbia; *Geological Survey of Canada*, Memoir 299.
- Eisbacher, G.H. (1974): Sedimentary and tectonic evolution of the Sustut and Sifton Basins, north-central British Columbia; *Geological Survey of Canada*, Paper 72-31.
- Evenchick, C. A. (1990): Structural relationships of the Skeena Fold Belt west of the Bowser Basin, northwest British Columbia; *Canadian Journal of Earth Sciences*, Volume 28, pages 973-983.
- Findlay, A.R. and Hoffman, S.J. (1981): Geological and geochemical Report on the Takla Lake property; *B.C. Ministry of Employment and Investment*, Assessment Report 9892
- Gabrielse, H. (1991): Structural Styles, Chapter 17; in *Geology of the Cordilleran Orogen in Canada*, Gabrielse, H. and Yorath, C.J., Editors, *Geological Survey of Canada*, Geology of Canada, Number 4, pages 571-675.
- Gareau, M.B. and Kimura, E.T. (1982): Diamond drilling report on the Bear Hill Property; *B.C. Ministry of Employment and Investment*, Assessment Report 10790
- Huntley, D.H., Stumpf, A., Levson, V.M. and Broster, B.E. (1996): Babine Porphyry Belt Project: Quaternary Geology and Regional Till Geochemistry Sampling in the Old Fort Mountain (93M/1) and Fulton Lake (93L/16) Map Areas, British Columbia; in *Geological Fieldwork 1995*, Grant, B. and Newell, J.M., Editors, *B.C. Ministry of Energy, Mines and Petroleum Resources*, Paper 1996-1, pages 45-53.
- Jackaman, W., Cook, S. And Lett, R. (1998): Regional Geochemical Survey program: Review of 1997 activities; in *Geological Fieldwork 1997*, *B.C. Ministry of Employment and Investment*, Paper 1998-1 (this volume).
- Kimura, E.T., Cannon, R.W. and Gareau, M.B. (1982): Geochemical and geophysical reports on Bear Hill property; *B.C. Ministry of Employment and Investment*, Assessment Report 10791.
- Kindle, E.D. (1954): Mineral Resources, Hazelton and Smithers Areas, Cassiar and Coast Districts, British Columbia; *Geological Survey of Canada*, Memoir 223.
- Leach, W.W. (1910): The Skeena River District; *Geological Survey of Canada*, Summary Report 1909.
- Levson, V.M., Meldrum, D.G., Cook, S.J., Stumpf, A., O'Brien E.K., Churchill, C., Coneys, A.M. and Broster, B.E. (1997): Quaternary Geology and Till Geochemical Studies, Babine Copper Porphyry Belt, British Columbia (NTS 93L/16, M/1, M/8); in *Geological Fieldwork 1996*, *B.C. Ministry of Employment and Investment*, Paper 1997-1, pages 427-438.
- Levson, V., Stumpf, A. and Stuart, A. (1998): Quaternary Geology Studies in the Smithers and Hazelton Map Areas (93 L and M): Implications for Exploration; in *Geological Fieldwork 1997*, *B.C. Ministry of Employment and Investment*, Paper 1998-1 (this volume).
- MacIntyre, D.G. (1985): Geology and Mineral Deposits of the Tahtsa Lake District, West Central British Columbia; *B.C. Ministry of Energy, Mines and Petroleum Resources*, Bulletin 75.
- MacIntyre, D.G. and Desjardins, P. (1988): Geology of the Silver King - Mount Cronin Area; *B.C. Ministry of Energy, Mines and Petroleum Resources*, Open File 1988-20.
- MacIntyre, D.G., Webster, I.C.L., and Bellefontaine, K. (1996): Geology of the Fulton Lake Map Sheet (93L/16); *B.C. Ministry of Energy, Mines and Petroleum Resources*, Open File map, 1996-29, pages 11-36.
- MacIntyre, D.G., Webster, I.C.L. and Villeneuve, M. (1997): Babine Porphyry Belt Project: Bedrock Geology of the Old Fort Mountain Area (93M/1), British Columbia; in *Geological Fieldwork 1996*; *B.C. Ministry of Employment and Investment*, Paper 1997-1, pages 47-68.
- MacIntyre, D.G. and Struik, L.C., (1997): Nechako NATMAP Project - 1996 Overview; in *Geological Fieldwork 1996*, Grant, B. and Newell, J.M., Editors, *B.C. Ministry of Employment and Investment*, Paper 1997-1, pages 39-46.
- MacIntyre, D.G. and Struik, L.C. (1998): Nechako Natmap Project: 1997 Overview; in *Geological Fieldwork 1997*, *B.C. Ministry of Employment and Investment*, Paper 1998-1 (this volume).
- McMillan, W.J. and Struik, L.C., (1996): NATMAP: Nechako Project, Central British Columbia; in *Geological Fieldwork 1995*, Grant, B. and Newell, J.M., Editors, *B.C. Ministry of Energy, Mines and Petroleum Resources*, Paper 1996-1, pages 3-10.
- Ogryzlo, P.L. (1994): Hearne Hill, British Columbia, Canada: Collapse Brecciation in a Continental volcano-Plutonic Arc; unpublished M.Sc. thesis, *University of Regina*, 221 pages.
- Richards, T.A. (1980): Geology of the Hazelton Map Area (93M); *Geological Survey of Canada*, Open File 720.
- Richards, T.A. (1990): Geology of the Hazelton Map Area (93M); *Geological Survey of Canada*, Open File 2322.
- Stumpf, A.J., Huntley, D.H., Broster, B.E. and Levson, V.M. (1996): Babine Porphyry Belt Project: Detailed Drift Exploration Studies in the Fulton Lake (93L/16) and Old Fort Mountain (93M/01) Map Areas; in *Geological Fieldwork 1995*, Grant, B. and Newell, J.M., Editors, *B.C. Ministry of*

- Energy, Mines and Petroleum Resources*, Paper 1996-1, pages 37-44.
- Sutherland Brown, A. (1960): Geology of the Rocher Déboulé Range; *B.C. Ministry of Energy, Mines and Petroleum Resources*, Bulletin 43.
- Tipper, H.W. and Richards, T.A. (1976): Jurassic Stratigraphy and History of North-Central British Columbia; *Geological Survey of Canada*, Bulletin 270, 73 pages.
- Villeneuve, M.E. and MacIntyre, D.G., 1997: Laser  $^{40}\text{Ar}/^{39}\text{Ar}$  Ages of the Babine Porphyries and Newman Volcanics, Fulton Lake map area (93L/16), west central British Columbia; in Radiogenic Age and Isotopic Studies: Report 10, *Geological Survey of Canada*, Current Research 1996-F.



# PRELIMINARY BEDROCK GEOLOGY OF THE TOCHCHA LAKE MAP AREA (93K/13), BRITISH COLUMBIA

By D.G. MacIntyre, P. Schiarizza and L.C. Struik (GSC)

(British Columbia Geological Survey Branch contribution to the Nechako NATMAP Project)

**KEYWORDS:** bedrock mapping, Nechako NATMAP, Tochcha Lake, Tertiary volcanic rocks, Takla Group, Topley Intrusions, Cache Creek Group, Sitlika assemblage, Ootsa Lake Group, Endako Group, Mac porphyry molybdenum deposit.

## INTRODUCTION

The Tochcha Lake map area (93K/13), which is located east of the Babine porphyry belt project (MacIntyre, 1998, this volume) and south of the Sitlika project area (Schiarizza *et al.*, 1998, this volume), was mapped at 1:100,000 scale during the 1997 field season as part of the Nechako Natmap project (MacIntyre and Struik, 1998, this volume). Prior to the current mapping, the only published geologic maps for this area were by Armstrong, (1949) as part of his Fort St. James compilation. Don MacIntyre, Ryanne Metcalf, Stephan Munzar, and Deanne Tackaberry spent approximately 3 weeks mapping the Tochcha Lake maps area. They were assisted by Paul Schiarizza and Michele Lepitre of the B.C. Geological Survey Branch and Bert Struik of the GSC and his mapping crew for 5 days in late August. This report describes the results of this mapping. The information contained in this report is preliminary; samples submitted for radiometric dating and microfossil extraction have not yet been processed. This new information may significantly change the conclusions put forth in this paper.

## PROJECT LOCATION

The Tochcha Lake map area (93K/13) is located in central British Columbia (Figure 3-1) between Babine and Takla Lakes. The closest towns are Burns Lake and Granisle. Tochcha Lake is located in the northwest corner of the map sheet in an area of rolling hills. This area has been extensively logged and is accessible via a network of private logging roads that connect to the barge crossing at Nose Bay on Babine Lake. The highest ground in this area is Deescius Mountain which is located east of the lake. The southeast, central and southwest parts of the map area are accessible by private logging roads which connect to Burns Lake via the southern barge crossing on Babine Lake. A northwest trending range, which includes Tsitsutl Mountain, crosses the northeast quadrant of the map area. This area was mapped by helicopter from a base camp located at Takla Narrows on Takla Lake.

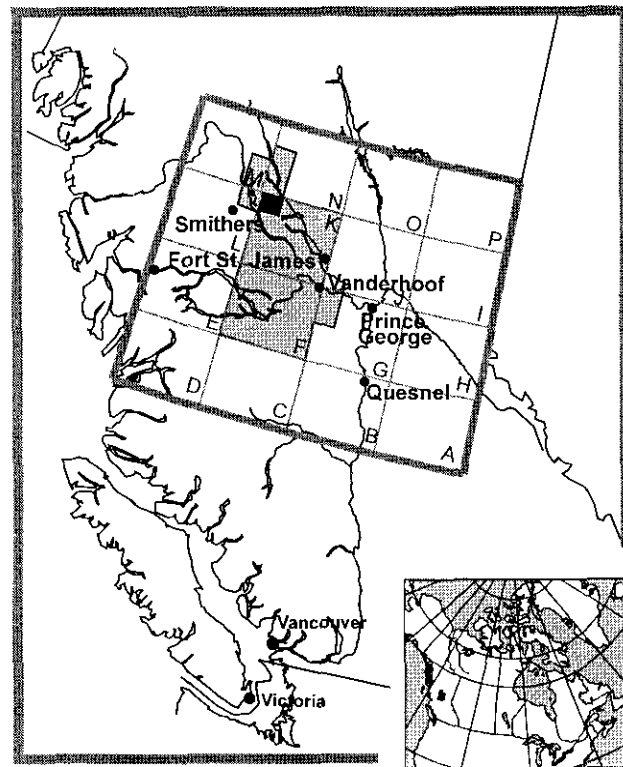


Figure 3-1. Location of the Nechako Natmap Project area (light grey shading), central British Columbia. Dark grey square is the Tochcha Lake map sheet (93K/13) which was mapped in 1997 and is the subject of this report.

## ACCOMPLISHMENTS

Major geological accomplishments made during the 1997 field season in the Tochcha Lake area are as follows:

- completed bedrock mapping of the Tochcha Lake map sheet at 1:100,000 scale.
- mapped several new intrusions of monzonite to quartz monzonite with hornblende diorite border phases between Tochcha Lake and Deescius Mountain. These intrusions, which do not appear on previous maps, cut Takla volcanic rocks and are correlative with the Topley intrusions mapped in the 93L/16 map sheet. They were sampled for Ar-Ar isotopic dating.
- mapped a belt of Takla volcanic rocks in the western half of the map area. Several limestone beds were located and sampled for conodonts. Coarse augite

phyric flows were also sampled for Ar-Ar isotopic dating.

- mapped a belt of Cache Creek rocks underlying the eastern half of the map sheet. Several limestone beds were located and sampled for conodonts. Large plutons cutting the Cache Creek section were sampled for Ar-Ar dating.
- mapped a narrow belt of clastic rocks correlative with the Sitlika assemblage between the Cache Creek and Takla Groups. This indicates that Sitlika rocks extend further south than was originally thought. A limestone member was sampled for conodonts.
- mapped Tertiary volcanic rocks correlative with the Ootsa Lake and Endako Groups in the southwest corner and along the southern boundary of the map area. These rocks unconformably overlie Topley and Takla Group rocks

## FUTURE PLANS

We plan to extend regional bedrock mapping eastward and southward into the 93K/14, 93K/12 and 93K/11 map sheets in 1998. The objective of this work will be to complete mapping of the northwest quadrant of the Fort Fraser map sheet (93K) to evaluate its mineral potential and to tie in with ongoing mapping by the GSC as part of the Nechako Natmap project.

## REGIONAL GEOLOGIC SETTING

The northwest-trending boundary between the Stikine and Cache Creek terrane cuts diagonally across the map area. Rocks west of the boundary include basaltic volcanic rocks and interbedded sedimentary rocks of the Upper Triassic Takla Group. These rocks are cut by monzonite, quartz monzonite and hornblende diorite of the Late Triassic to Middle Jurassic Topley intrusions. Cache Creek rocks include metavolcanic, metasedimentary and ultramafic rocks that are cut by post deformation plutons of Jurassic or younger age. Separating the strongly deformed Cache Creek rocks and Takla Group volcanic rocks of Stikinia is a belt of metasedimentary rocks correlated with part of the Permian and younger Sitlika assemblage. Both Stikine and Cache Creek Terrane rocks are overlapped by relatively flat-lying Tertiary volcanic rocks of the Ootsa Lake and Endako Groups to the south. The Cache Creek rocks have a strong northwest trending, steeply dipping, bedding parallel foliation. These rocks are strongly deformed, often to the point that their protolith is unrecognizable. This deformation may be related to southwest directed structural transport. Rocks of the Stikine Terrane are folded and cut by high angle faults but otherwise are not penetratively deformed.

The current physiography of the study area is due to Tertiary block faulting. Strong northeast trending linears truncate the north to northwest trending ranges and appear to offset geologic units as well. Along the southern border of the map area, a high angle normal fault marks the boundary between uplifted Takla and Topley intrusive

rocks, and low lying regions covered by Tertiary volcanic rocks of probable Eocene age. A downward vertical displacement of Eocene rocks is indicated south of the fault suggesting it is Eocene or younger.

## LITHOLOGIC UNITS

The geology of the study area, based on mapping completed in 1997 is shown in Figure 3-2. Figure 3-3 illustrates our current understanding of the stratigraphic relationships between the different map units.

### Stikine Terrane

Rocks exposed in the western part of the Tochcha Lake map sheet are part of the Stikine Terrane, the largest terrane of the Intermontane Belt. This terrane includes Lower Devonian to Middle Jurassic volcanic and sedimentary strata of the Asitka, Stuhini, Takla, Lewes River and Hazelton assemblages along with comagmatic plutonic rocks. Along the eastern margin of the Stikine Terrane the oldest rocks exposed are late Paleozoic carbonates and island-arc volcanic and volcanoclastic rocks of the Asitka Group. Overlying the Asitka Group are basaltic calc-alkaline to alkaline island arc volcanic and sedimentary rocks of the Late Triassic Takla Group and mafic to intermediate calc-alkaline volcanic and sedimentary rocks of the Lower to Middle Jurassic Hazelton Group. Overlap assemblages include Middle Jurassic to Early Cretaceous sedimentary rocks of the Bowser Lake and Skeena Groups and Late Cretaceous and Eocene volcanic rocks of the Kasalka, Ootsa Lake and Endako Groups.

### Late Paleozoic Asitka Group

Although Upper Pennsylvanian to Lower Permian limestones are exposed in a small uplifted thrust plate in the Fulton Lake map sheet (MacIntyre *et al.*, 1996) which lies immediately west of the study area, no correlative rocks were observed in the Tochcha Lake map area.

### Upper Triassic Takla Group

The Takla Group was first defined by Armstrong (1946, 1949) in the Fort St. James map-area. The type area is located west of Takla Lake in the 93N/4 and 93N/5 map sheets (Armstrong, 1949). As originally defined, the Takla Group included upper and lower divisions of arc related volcanic and sedimentary rocks ranging in age from late Triassic to late Jurassic, a subdivision also used by Lord (1948) in the McConnell Creek map area. Monger (1976) and Monger and Church (1977) redefined the Takla Group to include only sedimentary and basaltic volcanic rocks of Late Triassic age; the Jurassic part of the Takla Group was assigned to the Hazelton Group. Monger and Church further subdivided the Takla Group into the Dewar, Savage Mountain and Moosevale Formations. The Dewar Formation, which occurs at the base, is the most widespread, and includes thin to medium-bedded dark grey or greenish grey, brown weathering volcanic sandstone or

bedded tuff, siltstone and interbedded argillite. It is a marine turbiditic succession up to 300 metres thick, and, near its base, consists mainly of graphitic and pyritic argillite with silty and sandy laminae and interbeds of argillaceous limestone and cherty argillite. Fossils collected from the Dewar Formation are upper Carnian in age (Monger and Church, 1977).

The Dewar Formation is overlain by and in part interbedded with the Savage Mountain Formation. This succession is up to 3000 metres thick and includes massive submarine volcanic breccias, aphanitic and augite-feldspar phyric pillowed and massive basalt flows and minor interbedded volcanoclastic sedimentary rocks and tuffs. The volcanic rocks are characterized by the presence of augite phenocrysts, which occasionally reach 1 centimetre in diameter. Coarse, bladed feldspar phyric basalt flows, with feldspar phenocrysts up to 3 centimetres, are also locally present.

The Savage Mountain Formation, which in places becomes subaerial near its upper contact, is overlain by the Moosevale Formation. The contact varies from gradational to sharp. Fossils from the Moosevale Formation, which is up to 1800 metres thick, are Late Triassic (Norian). Overall, the formation is more intermediate in composition than the underlying Savage Mountain Formation, and includes varying amounts of massive, red, green and maroon volcanic breccia, graded red and grey sandstone, argillite, fossiliferous mudstone, red volcanic conglomerate and lahar. Clasts in the fragmental volcanic rocks and conglomerates are typical of the underlying Savage Mountain Formation. The Moosevale Formation is mainly marine near its base, becoming non-marine up section.

Augite phyric dark green to grey basaltic flows, volcanic breccias, tuffs and minor interbedded volcanoclastic sedimentary rocks crop out along the western half of the Tochcha Lake map sheet and are correlated with the Savage Mountain Formation of the Takla Group. These rocks are at the southern end of a 65 kilometre long belt that can be traced northward into the 93N/4 and 93N/5 map sheets, terminating at Takla Landing on Takla Lake. East of Tochcha lake the basaltic flows are cut by hornblende diorite and pink weathering monzonite to quartz monzonite. Although there are not yet any isotopic dates available for these intrusions, similar intrusions to the west, which are part of the Topley Intrusions, give Late Triassic and Early Jurassic ages and are clearly intrusive into volcanic rocks that have a 208 Ma Ar-Ar isotopic age (MacIntyre *et al.*, 1996). Similar cross-cutting relationships are implied for the Tochcha Lake area.

The best exposures of Takla Group rocks in the Tochcha Lake area are on the west slope of Deescius Mountain where several hundred metres of massive flows are exposed. Thin sedimentary interbeds between flows indicate the succession dips moderately to the northeast. The volcanic rocks apparently overlie a lower sedimentary succession which is exposed along logging roads at the south end of Deescius Mountain. These sedimentary rocks may correlate with the Dewar Formation of the Takla Group. Near the western base of Deescius Mountain, at the

top of a large clearcut, a thin foliated conglomerate that contains flattened clasts of limestone and chert is interbedded with massive augite phyric flows and volcanic breccias. The limestone and chert clasts may be derived from the Late Paleozoic Asitka Group. A sample of limestone clasts extracted from the conglomerate will be processed for conodonts.

### *Late Triassic to Middle Jurassic Topley Intrusive Suite*

The Topley intrusions, as defined by Carter (1981), include quartz diorite to quartz monzonite of Late Triassic to Early Jurassic age. Earlier studies (Carr, 1965; Kimura *et al.*, 1976) used the term Topley intrusions for granite, quartz monzonite, granodiorite, quartz diorite, diorite and gabbro intrusions of probable Jurassic age that intrude Triassic volcanic rocks from Babine Lake to Quesnel. Included in this Topley suite were high-potassium intrusions associated with the Endako porphyry molybdenum deposit. However, subsequent K-Ar isotopic dating showed most of these high-K intrusions were Late Jurassic to Early Cretaceous in age. Consequently, the intrusions around Endako were renamed the Francois Lake intrusions to distinguish them from the older Topley suite.

Potassium-argon isotopic dates for the Topley intrusions, as defined by Carter (1981), would include ages as young as 178 Ma, but most are between 199 and 210 Ma using the old decay constants (MacIntyre *et al.*, 1996). Most of these dates are from large plutons in the Topley area and southwest of Babine Lake. In the current study, we consider the Topley intrusions to be an intrusive suite that is characterized by typically pink, potassium feldspar rich granite, quartz monzonite and monzonite of apparent Late Triassic to Middle Jurassic age. We consider the type area to be the southeast corner of the Fulton Lake map sheet where a large, composite intrusive body, the Tachek stock, is well exposed in clear-cuts and along the shores of Babine Lake. The high-potassium composition of these rocks distinguishes them from younger plutonic suites in Babine Lake area, that are mainly granodiorite to quartz diorite. Isotopic dating as part of the Babine project indicates that there is a significantly younger suite of intrusions with isotopic ages ranging from 179-169 Ma. (MacIntyre *et al.*, 1996) These intrusions are spatially associated with, and are lithologically similar to older phases of the Topley intrusive suite but are at least 20 million years younger. They are discussed below as the Tachek Creek phase.

Previous (Wanless, 1974; Carter, 1974) and current isotopic dating (MacIntyre *et al.*, 1996) suggest that the Topley suite is divisible into 4 main phases. These are;

- an early hornblende diorite phase that occurs as a border phase of large, composite stocks in the Tochcha Lake (93K/13) and Takla Lake areas (93N/4, 5). May also occur as smaller, isolated intrusions. Limited isotopic dating indicates a Late Triassic age (ca 219 Ma?).
- megacrystic granite as an early to intermediate phase of the Tachek stock (ca 215 Ma?)

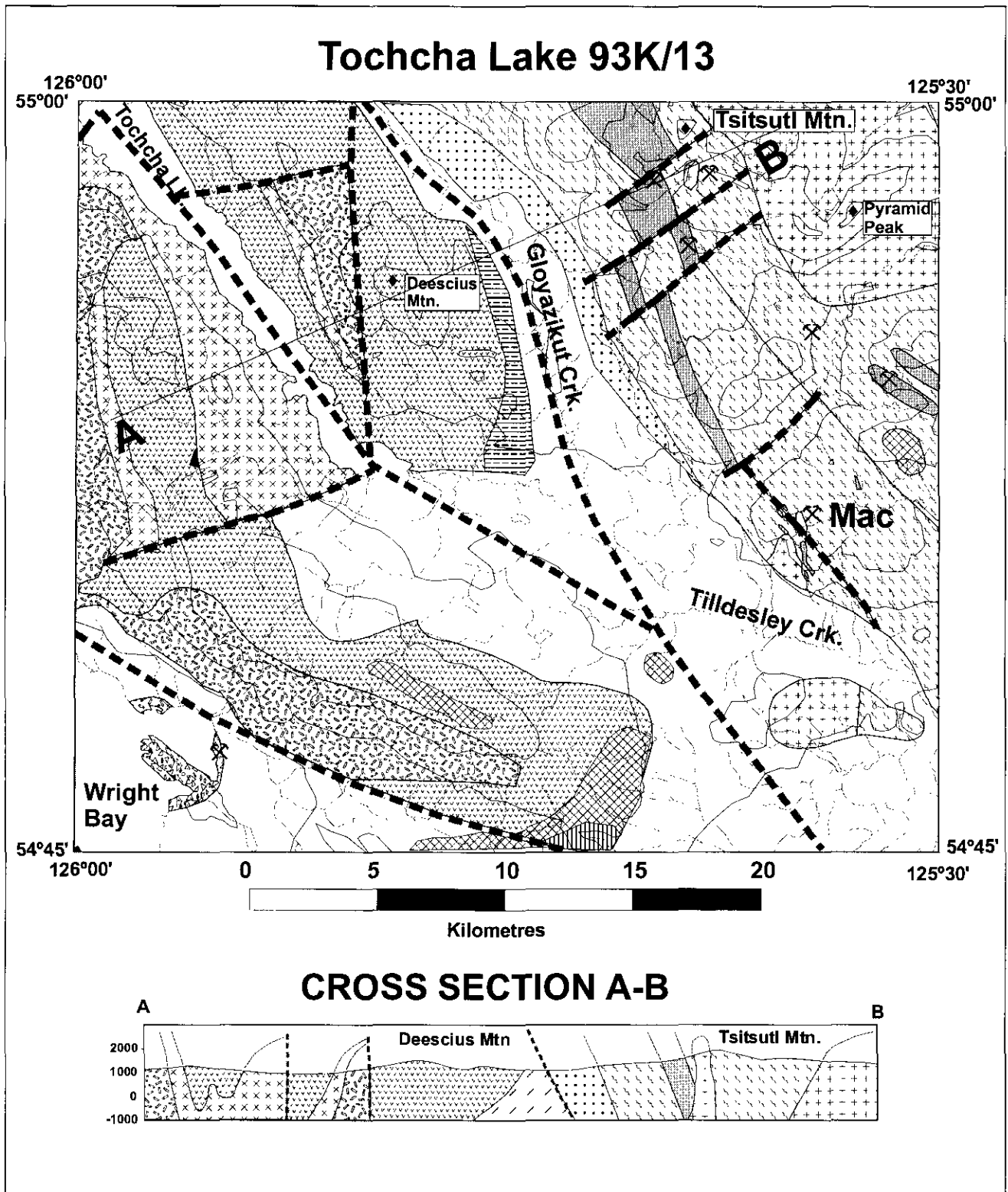


Figure 3-2. Generalized geology of the Tochcha Lake map area (93K/13).

## Legend for Figure 3-2

### TERTIARY

-  Endako Group: basalt, andesite
-  Ootsa Lake Group: rhyodacite, andesite
-  Wright Bay volcanics: lapilli tuff, breccia, basalt

### JURASSIC-CRETACEOUS

-  granodiorite, porphyritic quartz monzonite

### LATE TRIASSIC-MIDDLE JURASSIC

#### Topley Intrusive Suite

-  porphyritic quartz monzonite (Middle Jurassic)
-  granite, monzonite, quartz monzonite, aplite
-  hornblende diorite

### LATE TRIASSIC

#### Takla Group

-  augite basalt, breccia, tuff
-  siltstone, argillite, limestone, conglomerate

### PENNSYLVANIAN-JURASSIC

#### Sitlika Assemblage

-  sandstone, siltstone, slate, limestone

#### Cache Creek Group

-  metavolcanics, metasediments
-  ultramafic rocks

 mineral occurrence

- porphyritic monzonite to quartz monzonite, as a late phase in large stocks and as isolated dikes cutting Takla Group rocks. These intrusions give isotopic ages between 194-191 Ma.
- pink aplitic to rhyolitic dikes and small porphyritic quartz monzonite to granite stocks cutting the Tachek stock and Takla Group volcanic rocks. These intrusions, named here the Tachek Creek phase, are the youngest intrusions of the Topley suite and have isotopic ages ranging from 179-169 (Middle Jurassic). Porphyry copper mineralization is associated with dikes of this age at Tachek Creek (Carter, 1981; MacIntyre *et al.*, 1995)

Locally the Topley Intrusive suite contains numerous xenoliths. The xenoliths vary from a few centimetres to several metres in diameter and are composed either of mafic volcanic rocks of probable Triassic age or an earlier hornblende diorite phase. In one locality, a xenolith of dark grey mafic volcanic flow, with 1 to 2-millimetre feldspar laths, grades into a fine-grained flow-top breccia with recessive calcite-filled cavities. Such lithologies are typical of the Upper Triassic Takla Group.

Most of the Topley intrusive rocks have some degree of alteration, the most common being chlorite after biotite and hornblende. This has made it difficult to find material suitable for Ar-Ar isotopic dating. In addition, fractures

sometimes have potassium feldspar alteration envelopes around them, typically a few millimetres wide. This alteration is probably related to discharge of volatile-rich fluids during the final stages of crystallization. Epidote veins and clots are locally observed and generally have no consistent orientation. Rarely a criss-crossing network of chloritic veinlets penetrates the rock.

The high potassium content of the Topley intrusions is reflected in the presence of potassium feldspar either as 2 to 3-centimetre equant megacrysts or as a major component of the groundmass. Previous workers (Carter, 1981) felt these intrusions were comagmatic with the Lower Jurassic Telkwa Formation but isotopic dating indicates that the Topley suite, for the most part, is older and is probably coeval if not comagmatic with the Takla Group. Younger phases of the Topley suite may be comagmatic with the Telkwa Formation and Saddle Hill volcanics of the Hazelton Group but this seems unlikely since both of these volcanic successions are predominantly low-K basalt and andesite. However, since the Topley intrusive suite is only found intruding Takla volcanic rocks and direct links with younger strata which may, at one time, have overlain the Takla rocks, are no longer observable, the nature of extrusive equivalents to the Topley intrusive suite is unknown.

#### Hornblende Diorite Phase

Hornblende diorite, locally with a weak mineral lineation, is well exposed in clearcuts east and west of Tochcha Lake. The diorite occurs both as isolated intrusions and as a relatively narrow border phase to large monzonite to quartz monzonite stocks. The contact between the two phases is a zone of intense diking with fingers of pink monzonite to quartz monzonite injected into the diorite. There is some evidence of cooling and thermal metamorphism associated with the dikes, indicating the diorite was largely crystallized and cooled prior to intrusion of the monzonite phase. The diorite has intruded and thermally metamorphosed Takla Group volcanic and sedimentary rocks. Similar intrusive relationships were observed further to the north in the area between the two arms of Takla Lake (Scharizza *et al.*, 1997, this volume).

Medium-grained equigranular, hornblende-biotite diorite underlies the hills along the west side of Tochcha lake. Here, the diorite has a pronounced mineral lineation that is defined by the alignment of hornblende and biotite. Xenoliths of biotite microdiorite, up to 10 centimetres in diameter, have indistinct (resorbed?) margins and are abundant in the intrusive. Fine-grained, pink aplitic dikes cut the diorite. An Ar-Ar isotopic age of  $219 \pm 2$  Ma was determined on hornblende collected from this locality in 1995 (MacIntyre *et al.*, 1996). If this age is representative of the hornblende diorite found elsewhere in the Tochcha Lake area it indicates that the diorite is approximately the same age as the Takla volcanic rocks that it intrudes and may be comagmatic with the volcanic rocks. Additional dating is required to verify this correlation. The 219 Ma Ar-Ar isotopic age is similar to dates determined for

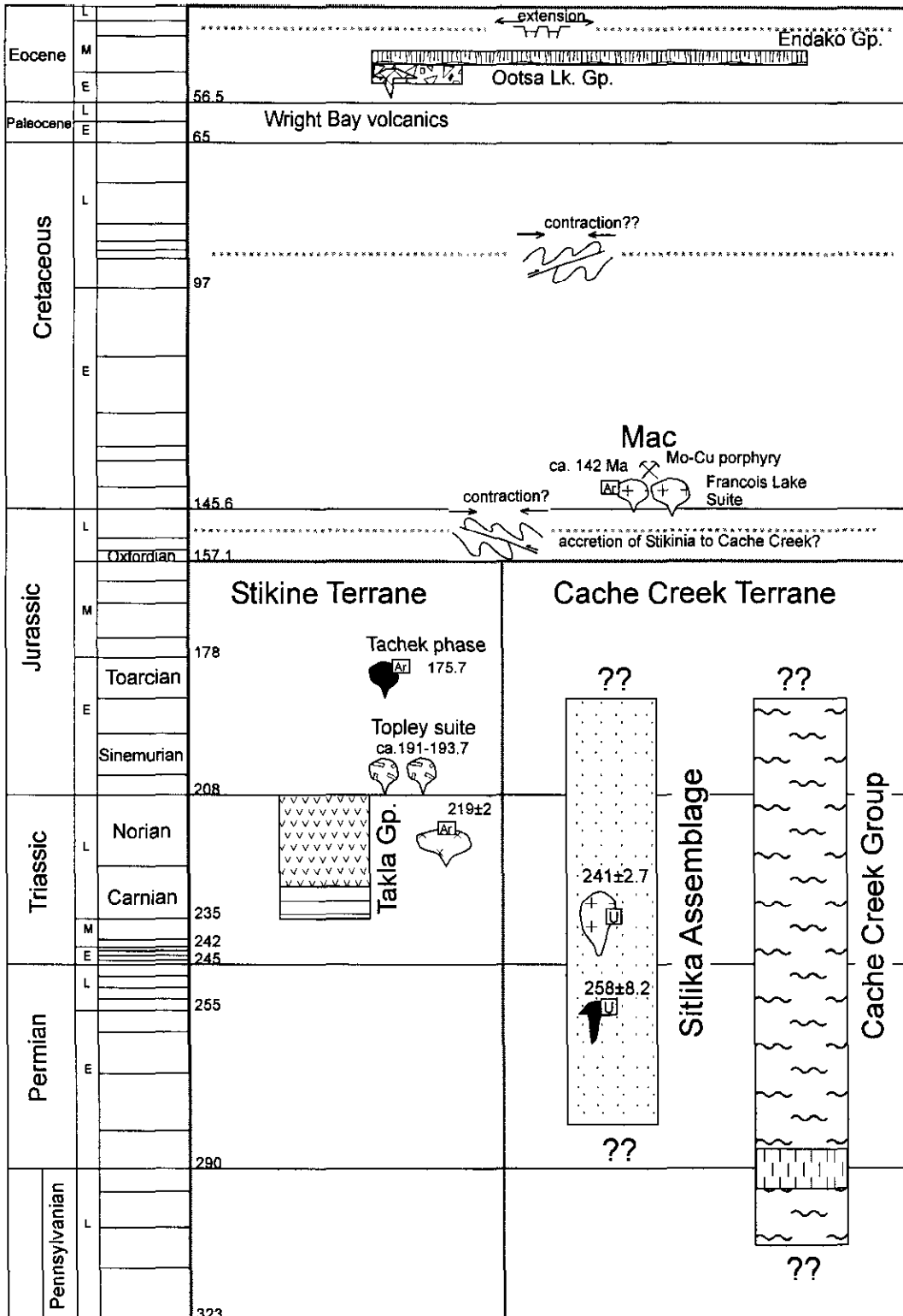


Figure 3-3. Generalized stratigraphy for the Tocha Lake Map area (93K/13)

diorites of the Boer Lake intrusive suite in the Endako area (Mike Villeneuve, personal communication, 1997).

**Granite Phase**

The granite phase comprises the largest proportion of the Tacheke stock and is well exposed east and west of

Babine Lake (MacIntyre *et al.*, 1996). The granite is more monotonous in composition and visual appearance than the quartz monzonite phase. It typically has a medium to coarse-grained equigranular texture and weathers pale pink. Locally the granite is sparsely porphyritic with scattered orthoclase megacrysts up to 2 centimetres long. Quartz phenocrysts up to 1 centimetre long occur as

irregular, elongate crystals that are intergrown with a groundmass of orthoclase, plagioclase and lesser quartz. This phase also carries up to 2 percent biotite and/or hornblende phenocrysts. A very weak foliation, defined by the alignment of quartz and mafic minerals, locally occurs in the granite. The granite phase is not well represented in the Tochcha Lake area and only crops out sporadically in the southwest corner of the map sheet.

The granite phase of the Tachek stock is not well dated. In 1995, a sample for U-Pb isotopic dating was collected from an excellent exposure in a quarry near the Port Arthur landing on the west shore of Babine Lake, south of Topley Landing. This sample gave a poorly defined Late Triassic U-Pb isotopic age of 215 to 230 Ma (MacIntyre *et al.*, 1996). The Tachek stock intrudes Takla Group volcanic rocks, which are presumed to have a similar Late Triassic age.

### ***Monzonite to Quartz Monzonite Phase***

The early granite and hornblende diorite phases of the Topley suite are intruded by a younger, leucocratic, medium to coarse-grained, equigranular to plagioclase-phyric phase that is monzonite to quartz monzonite in composition. This phase is locally porphyritic and contains 10 to 15 percent, 2 to 8 millimetre plagioclase phenocrysts, and up to 3 percent biotite and rare hornblende in a groundmass of intergrown potassium feldspar and quartz. Mirolitic cavities, which range from several millimetres to 2 centimetres in diameter, are also common. The cavities are typically filled with terminated quartz crystals which may have a black coating, and less frequently with epidote crystals.

The monzonite to quartz monzonite phase occupies the eastern part of the Tachek stock on the Fulton Lake map sheet (93L/16). It typically weathers orange and forms some of the conspicuous, large orange outcrops seen in clear-cuts on the east side of Babine Lake. The Tachek stock extends eastward into the Tochcha Lake area. This phase is also exposed in clearcuts east of Tochcha Lake where it intrudes an earlier hornblende diorite border phase. This composite intrusion was not shown on previous geologic maps of the area.

Currently there are only two isotopic age dates for this phase of the Topley intrusions. An Ar-Ar age of  $191.1 \pm 1.9$  Ma was determined on biotite from the quartz monzonite phase of the Tachek stock, east of Babine Lake (MacIntyre *et al.*, 1997). This age is close to another Ar-Ar age of  $193 \pm 1.9$  Ma determined on hornblende from a biotite-hornblende porphyritic monzonite dike that intrudes Takla volcanic rocks north of Granisle. In the current study area, an Ar-Ar sample was collected from the quartz monzonite stock east of Tochcha Lake but results are not yet available.

### ***Pink Aplite to Rhyolite Phase***

There are several later dike phases that intrude both the quartz monzonite and granite phases of the Tachek stock and surrounding rocks. The dikes appear to have a potassium-rich composition like the main granitoid phases

and are therefore included as part of the intrusive suite. They typically have vertical contacts and predominantly northeast and northwest trends. All of the dikes have an aphanitic to sugary-textured groundmass that can be pink, orange, orange-brown, orange-tan or light grey in colour. The dikes are locally sparsely porphyritic with two distinct phenocryst assemblages. One has orthoclase phenocrysts up to 4 millimetres long, the other has both orthoclase and glassy quartz eyes up to 3 millimetres. The latter may be part of the younger Tachek Creek phase.

The composition of these fine-grained, dense rocks is difficult to determine. Rock names such as aplite, rhyolite, syenite and monzonite all seem appropriate, depending on the colour of the rock, its mineralogy and grain size. This apparent variation in dike chemistry may mimic the range of compositions in the main phases of the Topley suite. In several localities, the borders of dikes are flow banded and/or spherulitic, suggesting these are high-level, volatile-rich intrusions.

### ***Tachek Creek Phase***

The Tachek Creek phase, as defined here, includes rocks that are lithologically similar to older phases of the Topley suite but are Middle Jurassic in age and therefore some 20 million years younger. This phase, like older phases, is only observed cutting Takla Group volcanic rocks even though it is young enough to cut Hazelton Group strata as well. It also has the same areal extent as older phases, extending from Topley Landing on Babine Lake to north of Takla Landing in the Takla Lake area.

Carter (1981) first recognized intrusions of Middle Jurassic age at the Tachek Creek porphyry copper prospect where biotite from a biotite-quartz-feldspar porphyry dike gave a  $176 \pm 7$  Ma (178 Ma revised) K-Ar isotopic age. This age is similar to two other isotopic dates determined as part of the Babine project. Hornblende from a small hornblende feldspar porphyritic monzonite stock exposed in a clearcut west of Tochcha Lake gave an Ar-Ar isotopic age of  $175.7 \pm 1.7$  Ma. (MacIntyre *et al.*, 1996) Zircon extracted from a biotite granite phase within the Tachek stock east of Babine Lake gave a U-Pb isotopic age of  $178.7 \pm 0.5$  Ma. Further north, in the Takla Lake area, Schiarizza and Payie (1997) describe a red to pink-weathering granite cut by feldspar porphyry dikes just east of the Takla Fault. Zircons extracted from this intrusion gave a U-Pb isotopic age of  $169.1 \pm 1.0 / -4.8$  Ma (Schiarizza *et al.*, 1998, this volume), slightly younger than ages determined for similar intrusions in the Babine and Tochcha lake areas. This age is also similar to the Stag Lake-Twenty-six Mile Lake plutonic suite in the Hallet Lake area (Anderson *et al.*, 1997) although this suite is predominantly hornblende diorite and therefore, lithologically different from the Tachek Creek phase of the Topley Intrusive suite.

The Topley Intrusive suite is part of a long lived, magmatic arc that was active periodically over a time span of up to 60 million years. Its close spatial association with Takla and possibly Hazelton Group volcanic rocks suggests it is genetically associated with formation of these volcanic terranes. Although orientation of subduction

zones is difficult to establish because of post Jurassic strike slip fault displacements, it is permissible that the Topley Intrusive suite is part of a Late Triassic to earliest Cretaceous magmatic arc that formed above an east dipping subduction zone. In terms of age, composition and geologic setting the Topley Intrusive suite is similar to composite stocks of the Hogen batholith that occur east of the Pinchi Fault and are part of the Quesnel terrane. It is possible that the Topley suite and associated Takla rocks are actually a northwardly displaced fragment of Quesnel terrane that has been positioned west of the Cache Creek Terrane by dextral strike slip fault motion.

## Cache Creek Terrane

### *Sitlika Assemblage*

The term Sitlika assemblage was assigned by Paterson (1974) to greenschist facies metavolcanic and metasedimentary rocks on the east side of Takla Lake that had previously been included in the Cache Creek and Takla Groups by Armstrong (1949). Schiarizza and Payie (1997) re-examined that area and described these rocks in more detail, and Schiarizza *et al.* (1998) traced the assemblage southward to about 10 km north of the Tochcha Lake map area. This Sitlika belt, which is bounded by the Cache Creek Group to the east, and Stikine Terrane to the west, is apparently truncated by a major northeast-striking fault that follows the valleys of Gloyazikut and Bivouac creeks near the south end of the 93N/4 map sheet. Rocks tentatively identified as the offset southern extension of the belt within the Tochcha Lake map area underlie a narrow north to northwesterly trending zone along the east side of Gloyazikut Creek (Figure 3-2).

Rocks assigned to the Sitlika assemblage in the Tochcha Lake map area include sandstone, siltstone, slate and limestone. These rocks are correlated with the Triassic and/or Jurassic eastern clastic unit of Schiarizza and Payie (1997) and Schiarizza *et al.* (1998) which, in the type area, stratigraphically overlies Permo-Triassic bimodal tholeiitic volcanic rocks of the assemblage. The succession along Gloyazikut Creek is inferred to be a fault-bounded panel juxtaposed against the Cache Creek Group to the east and the Takla Group and Topley Intrusive suite to the west. It faces to the east, as determined from grading and cleavage/bedding intersections in the sandstone and slate units, and can be divided into three units, based on the dominant rock type. These are, stratigraphically upward from west to east: sandstone, slate and limestone.

Westernmost exposures of the Sitlika eastern clastic unit are dominated by brown and grey-weathering, grey sandstone. It occurs as massive beds, 3 to 15 centimetre thick, that consist primarily of quartz and chert grains (0.25-1.0 millimetre). The sandstone beds are separated by interbeds of slate and siltstone; locally these are more prevalent than the sandstone.

To the east of the sandstone are exposures of slate and siltstone with minor amounts of limestone. The slate is banded in various shades of grey on a centimetre scale and breaks in thin sheets parallel to cleavage. Siltstone forms thin interbeds in portions of the slate sequence, and

limestone forms widely spaced 20 to 70 centimetre beds, with sharp contacts with the slate. The limestone is light grey weathering, dark grey to grey, finely crystalline and permeated with calcite veinlets.

The upper part of the exposed Sitlika succession is dominated by light grey weathering dark grey to grey limestone and minor light grey weathering white sugary textured dolostone. The carbonates are bioclastic, locally with 2-15 millimetre, well preserved crinoid stem fragments. Depositional features have mostly been destroyed or are obscured by a shear fabric that strikes 350 degrees and dips steeply to the east. Subcrop of dark grey slate overlies the limestone to the east.

### *Cache Creek Group*

The Cache Creek Terrane is represented mainly by the Late Paleozoic to mid-Mesozoic Cache Creek Group, which includes structurally imbricated carbonate, chert, argillite, basalt, gabbro and alpine ultramafic rocks. This assemblage of deformed oceanic rocks is generally interpreted to represent remnants of subduction complexes and dismembered ophiolite successions. The terrane is a prominent component of the Intermontane Belt over most of the Canadian Cordillera, where it occurs between the coeval arc terranes of Stikinia to the west and Quesnellia to the east. These terranes were amalgamated and juxtaposed against the western margin of North America in early to mid-Mesozoic time.

The Cache Creek Group in central British Columbia (Stuart Lake belt of Armstrong, 1949) includes polydeformed chert, siliceous argillite, limestone, phyllite, slate, siltstone, sandstone, and mafic metavolcanic and meta-intrusive rocks. Thick limestone units contain fusulinids, corals, brachiopods, bryozoans, gastropods and conodonts that are Pennsylvanian and Permian in age (Armstrong, 1949; Thompson, 1965; Orchard and Struik, 1996); radiolarian chert and cherty mudstone range from Early Permian to earliest Jurassic in age (Cordey and Struik, 1996a,b). Ultramafic rocks within the Stuart Lake belt were referred to as the Trembleur intrusions by Armstrong, who interpreted them to be intrusive bodies cutting the Cache Creek sedimentary and volcanic rocks. These rocks are now included within the Cache Creek Group, and interpreted to be the tectonically emplaced upper mantle and lower crustal portions of dismembered ophiolite sequences (Paterson, 1977; Ross, 1977; Whittaker, 1983; Ash and Macdonald, 1993; Struik *et al.*, 1996).

The Cache Creek Group rocks in the northeast corner of the Tochcha map area include ultramafic rocks, greenstone, amphibolite, limestone, phyllite and quartzite. The latter two lithologies were largely derived from metamorphosed ribbon chert. These rocks are interlayered throughout the area and appear to be fault bounded slivers in a highly imbricated or translated sequence. This contrasts with the Cache Creek Group farther to the north, where ultramafic rocks are restricted to a single belt that separates the metasedimentary part of the Cache Creek Group on the east from the Sitlika assemblage to the west.

Most of the ultramafic rocks are moderately to highly serpentinized. The serpentinite has a well developed

foliation in places, but elsewhere is massive. Protolith compositions are generally not apparent, but massive, blocky, reddish-brown weathered harzburgite, with local dunite pods, outcrops on the east flank of Tsitsutl Mountain. Elsewhere, the protolith apparently includes partially serpentinized pyroxenite or harzburgite. Serpentinite foliations are defined by distended, broken and flattened pyroxenes and chromite, and aligned serpentine. In places, strongly foliated serpentinite, locally grading to magnesite-serpentine-talc schist, contains knockers, from a few metres to tens of metres in size, of greenstone, amphibolite, limestone, and cherty metasedimentary rocks. On the map scale, the ultramafite is largely distributed as distinct, north-northwest trending linear zones that are separated from each other by amphibolite and greenstone similar to the rocks from the knockers. Lenses of listwanite border some of the serpentinite bodies. Where contacts are seen or can be inferred, the serpentinite has a shear fabric, and each of the contacts is inferred to be a fault.

The greenstone is everywhere well foliated. It is dark grey and variably olive to dun weathering. It can be massive and finely crystalline or appear fragmental with augen (2-15 millimetre) of more darkly coloured greenstone. The finely crystalline variety generally has a phyllitic texture. The greenstone is locally interlayered with amphibolite and gabbro. The gabbro is orange to dark grey weathering and has 2 to 8 millimetre amphibole crystals. The amphibolite weathers dark green-grey and is dark grey on fresh surfaces. It consists mainly of 0.2 to 4 millimetre acicular and blocky hornblende or orthoamphibole, and has very little plagioclase.

Metasedimentary rocks occur mainly within eastern exposures of the Cache Creek Group, where they are commonly intercalated with greenstone, that is in part derived from pillowed metabasalt. Metasedimentary intervals are dominated by light to dark grey platy quartz phyllites and quartzites, comprising plates and lenses of fine-grained recrystallized granular quartz, typically a centimetre or less thick, separated by phyllitic, mica-rich partings. Locally these platy rocks grade into less siliceous and more homogeneous medium to dark grey phyllites, or into light to medium grey thin-bedded chert. Less common, are light to dark grey recrystallized limestone intervals ranging in thickness from a few metres to a few tens of metres that occur within the siliceous metasedimentary successions.

## Late Jurassic to Early Cretaceous (?)

### Intrusions

The northeast corner of the Tochcha Lake map sheet is underlain by a large pluton of biotite granodiorite. This pluton, which extends northward to Takla lake in the 93N/4 map sheet is unnamed. We propose the name Pyramid Peak pluton because it is well exposed at this locality. This pluton intrudes intensely deformed rocks of the Cache Creek Group. Emplacement appears to have been passive with little thermal metamorphism of the surrounding rocks. Although not observed in the current map area, further to the north, near Takla Lake, rafts of

Cache Creek rocks are found in a coarse-grained, leucocratic, biotite granite border phase of the pluton.

Most of the Pyramid Peak pluton is monotonous, massive, blocky, grey to pink weathering, coarse-grained equigranular biotite  $\pm$  hornblende granodiorite. In places the biotite is arranged in clusters which give the rock a spotted appearance. This phase tends to break down to pinkish coloured sand comprised mainly of feldspar and quartz. The early, coarse grained granodiorite phase is cut by a younger, subporphyritic to crowded porphyritic biotite-hornblende granodiorite or quartz monzonite phase. The younger phase is more quartz rich and white to light grey weathering. Locally, both phases of the pluton are cut by porphyritic andesite dikes comprised of 10-15 percent, 2-3 millimetre feldspar and less than 1 millimetre hornblende needles in a dense, dark grey groundmass. These dikes have well-developed chill margins and were clearly emplaced after crystallization and cooling of the main granodiorite body. The youngest dikes are fine-grained pink aplite and grey feldspar phyric rhyolite to rhyodacite.

The age of the Pyramid Peak pluton is not known at this time but it resembles other plutons in the area which have been mapped as the latest Jurassic (c.a. 145-147 Ma) Francois Lake Suite. Samples were collected from the pluton for U-Pb and Ar-Ar radiometric dating.

Small stocks of quartz-biotite-hornblende feldspar porphyritic granodiorite to quartz-feldspar porphyritic rhyodacite crop out on the peak southeast of Tsitsutl Mountain and at the Mac porphyry molybdenum property near Tilledesley Creek (Figure 3-2). The Tsitsutl mountain stock intrudes ductilely deformed, greenschist facies, Cache Creek metavolcanic and metasedimentary rocks. There is a zone of disseminated pyrite enclosing the stock and in places the Cache Creek rocks appear to be hornfelsed. The porphyry is a white to pink weathering, light to medium grey, siliceous rock with 10-15 percent, 1-2 millimetre quartz eyes and in places, up to 20 percent, 10 millimetre feldspar phenocrysts.

At the Mac property, small stocks and dikes of quartz  $\pm$  biotite  $\pm$  hornblende-feldspar porphyry intrude Cache Creek metasedimentary and metavolcanic rocks and have associated molybdenum mineralization. Biotite from the stock in the Camp zone gave a  $142.5 \pm 1.4$  Ma (earliest Cretaceous) Ar-Ar isotopic age (MacIntyre *et al.*, 1997). This age is slightly younger than those of the Francois Lake suite (145-147 Ma) and suggest the porphyries and associated molybdenum mineralization at Mac may be the latest phase of the Francois Lake intrusive suite. Some of the late dikes in the Pyramid Peak pluton may also have similar ages to the porphyries at Mac and Tsitsutl Mountain.

### Tertiary Overlap Assemblages

Tertiary volcanic rocks crop out along the southern margin of the Tochcha Lake map sheet where they overlie Late Triassic to Early Jurassic Topley intrusions and Late Triassic volcanic rocks of the Takla Group. The Tertiary succession is divided into three map units. These are;

- fragmental volcanic rocks and flows containing clasts of Topley Intrusions exposed at Wright Bay on Babine Lake
- hornblende and biotite phyric rhyodacitic ash flows and tuffs that are correlated with the Eocene Ootsa Lake Group
- vesicular and amygdaloidal basalt flows, flow breccias, tuffs and epiclastic rocks that are correlated with the Eocene Endako Group

### **Wright Bay volcanic rocks**

The Wright Bay volcanic rocks, which were previously mapped as Jurassic Hazelton Group, appear to sit directly on pink weathering monzonite of the Late Triassic to Early Jurassic Topley intrusions. The volcanic rocks, which are flat-lying to gently dipping, are comprised of lapilli tuff, volcanic breccia, lahar and basaltic flows. In places the lapilli tuffs are welded and may be ash flows. The lapilli tuffs and breccias contain 1 to 5 centimetre, subrounded to angular clasts of the underlying Topley intrusions plus white weathering rhyolite clasts in a greenish grey crystal-ash matrix. In places these rocks resemble the Nose Bay Intrusive breccia which is located east of Wright Bay. This breccia, which was described in a previous report (MacIntyre *et al.*, 1996), may have been a feeder vent for the Wright Bay volcanic rocks. Similar breccias containing Topley clasts crop out south of Tachek Creek on the west side of Babine Lake, and these too may be related to the Wright Bay volcanic rocks. The latter were mapped as the Tachek Group by Armstrong and were thought to be Jurassic. Because of the relationships observed at Wright Bay, we feel these breccias are more likely Tertiary in age and may in part be correlative with the Ootsa Lake or Endako Groups.

### **Ootsa Lake Group**

Grey to pinkish grey weathering, hornblende-biotite-feldspar phyric to aphyric rhyodacitic ash flows, with lesser, thin, andesite and brown weathering basalt flows crop out as a series of knolls along the southern edge of the Tochcha Lake map sheet. The ash flows locally contain 5-10 percent hornblende and biotite phenocrysts that are up to one centimetre in diameter. Granitic inclusions are also common in some cooling units. The lower contact of the ash flow succession, which appears to be flat lying, was not seen but it is likely they sit unconformably on either Topley intrusions or Takla volcanic rocks. The ash flows are overlain by vesicular basalts which are tentatively correlated with the Endako Group. A sample of ash flow with fresh hornblende and biotite was collected for Ar-Ar isotopic dating.

### **Endako Group**

Brown weathering, flat-lying, vesicular to amygdaloidal basaltic flows cap a northwest trending ridge along the southern margin of the Tochcha Lake map sheet. Locally, the flows contain small crystals of pyroxene. The

vesicles range from 1 to 10 millimetres in diameter and comprise 20 to 35 percent of the rock. Vesicles and amygdules are often flattened parallel to the flow direction. Similar rocks are exposed in road cuts in the broad valley south of the ridge. On the ridge crest the flows are well exposed as a series of near vertical cliffs which may be fault scarps. Here, individual flows, separated by thin interbeds of volcanoclastic material, are 5 to 15 metres thick and sit unconformably on Takla volcanic rocks or Topley intrusive rocks. These rocks are correlated with the Eocene Endako Group based on lithologic similarity.

## **STRUCTURE**

The structure of the Tochcha lake area reflects the effects of at least four major tectonic events. The oldest event included Jurassic (?) ductile deformation and metamorphism during southwest directed thrust imbrication of Cache Creek Group with Sitlika Assemblage and then emplacement above Stikine Terrane (Monger *et al.*, 1978) This was followed in mid Cretaceous time by a contractional event that produced northwest-trending folds and northeast directed thrust faults in Stikinia. Crustal extension and development of north trending grabens and horsts took place in Late Eocene or younger time as both the Babine intrusions and Newman volcanic rocks have been truncated and displaced by movement on faults bounding the grabens. The latest event, which may be as young as Miocene, involved tilting of fault blocks to the southeast along northeast trending faults. In general, because of the Eocene and younger movement of fault blocks, younger rocks typically occur at lower elevations within north trending valleys while older rocks are found at higher elevations on the ridges bounding the valleys. In the southern part of the Tochcha Lake map area Tertiary volcanic rocks cap a northwest trending ridge. The same volcanic rocks are exposed in road cuts in the broad valley south of the ridge. This suggests that the Tertiary volcanic rocks, which are probably Eocene Endako Group, were displaced and possibly rotated several hundred metres downward to the south across a west to northwest trending fault. Similar displacements of Eocene volcanic rocks were noted in the Babine Lake area (MacIntyre *et al.*, 1996).

## **MINERAL OCCURRENCES**

The most important mineral occurrence in the Tochcha Lake area is the Mac porphyry molybdenum deposit which is actively being explored by Spokane Resources. Other occurrences consist of chromium, tin and copper showings in Cache Creek rocks (Table 3-1). Only the Mac property is discussed here.

### **Mac (Minfile 93K 097)**

The Mac porphyry molybdenum prospect, which has recently been described by Cope and Spence (1996), is

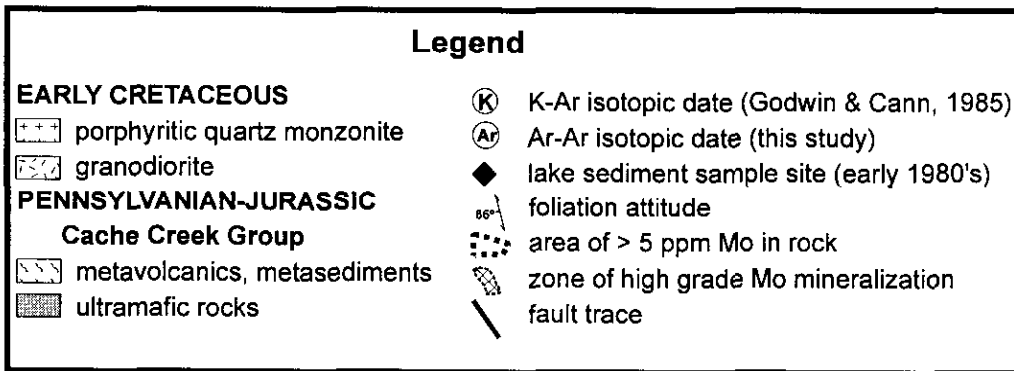
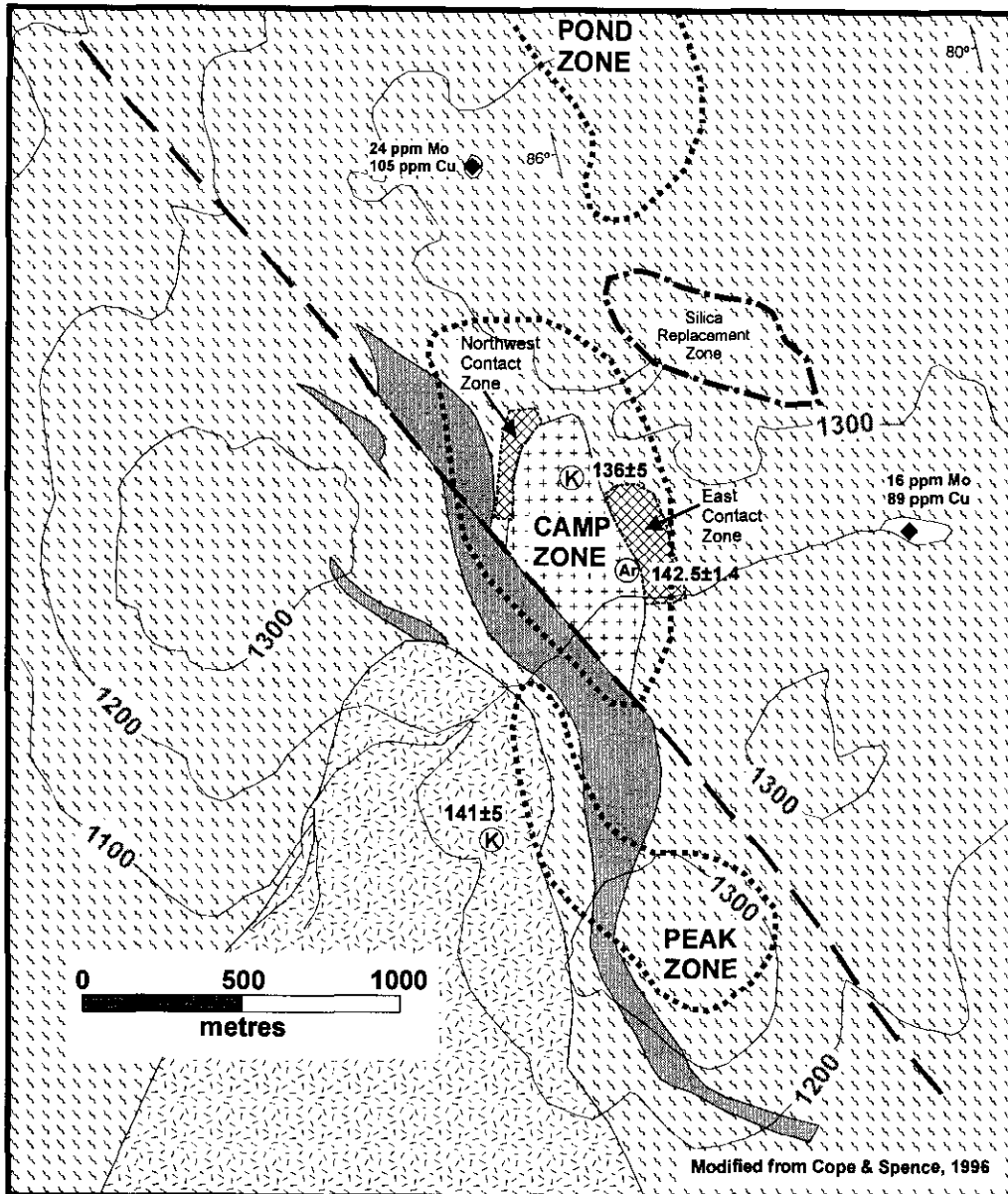


Figure 3-4. Geology of the Mac porphyry molybdenum property. Modified from Cope and Spence, 1996.

**Table 3-1. Mineral Occurrences, 93K/13**

| No.. | Property Name              | Metals                     | Hosts       |
|------|----------------------------|----------------------------|-------------|
| 37   | Tsitsutl Mountain Chromium | Cr                         | Cache Creek |
| 38   | Tilldesley Creek           | Cr                         | Cache Creek |
| 42   | Tsitsutl Mountain Tin      | Sn, Mn, Va, Co, Zn, Ro, Gs | Cache Creek |
| 63   | Tsitsutl Mountain          | Cu                         | Cache Creek |
| 67   | Diane                      | Cu                         | Cache Creek |
| 75   | Mary Ann                   | Cu                         | Ootsa Lake  |
| 97   | Mac                        | Mo, Cu                     | Cache Creek |

located on the crest of the ridge north of Tilldesley Creek (Figure 3-2). The area was first explored in the early 1980's by Rio Algom Exploration Inc. (then Riocanex Inc.). They staked the property in 1982 after boulders of granitic rock with molybdenite mineralization were located in an area that also had anomalous Mo, Cu and Ag metal values in lake and soil samples. Additional soil sampling, geophysical surveys and trenching were done in 1983 and 1984. No further work was done until 1989, when 12 diamond drill holes totaling 1489 metres were completed. Although results were encouraging, Riocanex did no additional work and in early 1995 the property was acquired by Spokane Resources. In late 1995 and early 1996, they contracted Fox Geological Services to do more geological mapping, prospecting and induced polarization surveys. This was followed by 3600 metres of drilling in 19 holes. Based on drilling to date, indicated reserves are 52.4 million tonnes with an average equivalent grade of 0.12 percent MoS<sub>2</sub> using a 0.040 Mo cutoff. There is an additional inferred resource of 47.5 million tonnes of similar grade (Spokane Resources Ltd. News Release, April 23, 1997).

The Mac property is underlain by metavolcanic, metasedimentary and serpentized ultramafic rocks of the Pennsylvanian to Jurassic Cache Creek Group. The Cache Creek rocks have a strong, regional foliation that trends 130 to 160 degrees and dips steeply to the southwest. These rocks are intruded by stocks of biotite granodiorite to porphyritic quartz monzonite that are part of the latest Jurassic to earliest Cretaceous Francois Lake intrusive suite. These intrusions also host the Endako porphyry molybdenum deposit in the Fraser Lake area, approximately 90 kilometres south-southeast of the Mac. As at Endako, molybdenum mineralization at Mac is associated with these intrusions and occurs in three areas - the Peak, Camp and Pond zones (Figure 3-4). Drilling to date has mainly focused on the Camp zone. Here, a 300 by 500 metre, northerly elongate stock of porphyritic quartz monzonite intrudes metavolcanic and metasedimentary rocks of the Cache Creek Group. The southern end of the stock is truncated and possibly offset southeastward by a northwest trending, high angle, sinistral strike-slip fault. The intrusion is medium-grained, leucocratic, and porphyritic to equigranular with 15 percent, 1-3 millimetre

feldspar, 25 percent, 1-2 millimetre quartz and 35-45 percent, 1-4 millimetre K-feldspar and up to 5 percent biotite, muscovite and hornblende (Cope and Spence, 1996).

As part of the current study, a  $142.5 \pm 1.4$  Ma (earliest Cretaceous) Ar-Ar isotopic age (MacIntyre *et al.*, 1997) was determined on biotite from the Camp zone stock. This is older than the previous  $136 \pm 5$  Ma K-Ar age obtained by Godwin and Cann (1985) from the same stock but close to the  $141 \pm 5$  Ma K-Ar age they determined for an unmineralized stock of biotite granodiorite that crops out on the south facing slope below the Camp and Peak zones (Figure 3-4). As mentioned above, the 142.5 Ma age is slightly younger than the new Ar-Ar isotopic ages determined for the Francois Lake suite (145-147 Ma) (Mike Villeneuve, personal communication, 1997). This suggests that the Camp zone stock may be a late, porphyritic phase of the Francois Lake intrusions.

Molybdenum mineralization at Mac occurs as molybdenite on fractures, as disseminations and in quartz veinlet stockworks peripheral to and within the porphyritic quartz monzonite or granite stock. Where the quartz monzonite stock is exposed on surface it is leached and has only minor ferrimolybdenite staining on fractures. Disseminated chalcopyrite also occurs in the mineralized zones at Mac. Drill results indicate that the best molybdenum grades occur in 50 metre wide zone of biotite bearing, hornfelsed rocks along the east, north and west contacts of the stock. One of the best drill intersections from this zone was 90 metres grading 0.308 percent MoS<sub>2</sub> and 0.256 percent Cu. A pyritic halo also encloses the stock and is roughly coincident with the biotite hornfels zone. Limited drilling in the Peak and Pond zones has intersected similar styles of mineralization. These zones are still relatively untested.

## ACKNOWLEDGMENTS

The authors acknowledge the excellent assistance provided by geological field assistants Rynne Metcalf, Stephen Munzar, Deanne Tackaberry, Michele Lepitre, Mike Hruddy, Crystal Huscroft, and Andrew Blair. Their enthusiasm and positive attitude even under less than ideal working conditions were exceptional. In addition, the authors acknowledge the excellent service provided by Pacific Western Helicopters, in particular pilot Bob Wellington from their base at Lovell Cove.

## REFERENCES

- Anderson, R., L'Heureux, R., Wetherup, S. and Letwin, J.M. (1997): Geology of the Hallet Lake map area, central British Columbia: Triassic, Jurassic, Cretaceous, and Eocene? plutonic rocks; *in* Current Research 1997-A; *Geological Survey of Canada*, pages 107-116.
- Armstrong, J.E. (1946): Takla, Cassiar District, British Columbia; *Geological Survey of Canada*, Map 844A.
- Armstrong, J.E. (1949): Fort St. James map-area, Cassiar

- and Coast Districts, British Columbia; *Geological Survey of Canada*, Memoir 252, 210 pages.
- Ash, C.H. and Macdonald, R.W.J. (1993): Geology, Mineralization and Litho geochemistry of the Stuart Lake Area, Central British Columbia (Parts of 93K/7, 8, 10 and 11); in *Geological Fieldwork 1992*, B.C. Ministry of Energy, Mines and Petroleum Resources, Paper 1993-1, pages 69-86.
- Carr, J.M. (1965): The Geology of the Endako Area; in *Lode Metals in British Columbia 1965*, B.C. Ministry of Energy, Mines and Petroleum Resources, pages 114-135.
- Carter, N.C. (1981): Porphyry Copper and Molybdenum Deposits West Central British Columbia; B.C. Ministry of Energy, Mines and Petroleum Resources, Bulletin 64.
- Church, B.N. (1974): Geology of the Sustut area; Geology, Exploration and Mining in British Columbia in 1973, B.C. Dept. of Mines and Petroleum Resources, pages 411-455.
- Cope, G.R. and Spence, C.D., (1996): Mac porphyry molybdenum prospect, north-central British Columbia; in *Porphyry Deposits of the Northwestern Cordillera of North America*, Schroeter, T.G., Editor, *Canadian Institute of Mining, Metallurgy and Petroleum*, Special Volume 46, pages 757-763.
- Cordey, F. And Struik, L.C., (1996a): Scope and Preliminary Results of Radiolarian Biostratigraphic Studies, Fort Fraser and Prince George Map Areas, Central British Columbia; in *Current Research 1996-A*; *Geological Survey of Canada*, pages 83-90.
- Cordey, F. and Struik, L.C., (1996b): Radiolarian Biostratigraphy and Implications, Cache Creek Group of Fort Fraser and Prince George map area, central British Columbia; in *Current Research 1996-E*; *Geological Survey of Canada*, pages 7-18.
- Godwin, C.I. and Cann, R.M., (1985): The MAC porphyry molybdenite property, central British Columbia, in *Geological Fieldwork 1984*, B.C. Ministry of Energy, Mines and Petroleum Resources, Paper 1985-1, pages 443-449.
- Kimura, E.T., Bysouth, G.D. and Drummond, A.D. (1976): Endako; in *Porphyry Deposits of the Canadian Cordillera*, Sutherland Brown, A., Editor, *Canadian Institute of Mining and Metallurgy*, Special Volume 15, pages 444-454.
- Lord, C.S. (1948): McConnell Creek Map-area, Cassiar District, British Columbia; *Geological Survey of Canada*, Memoir 251, 72 pages.
- McMillan, W.J., Thompson, J.F.H., Hart, C.J.R. and Johnston, S.T., (1995): Regional geological and tectonic setting of porphyry deposits in British Columbia and Yukon Territory. In *Porphyry Deposits of the Northwestern Cordillera of North America*. Edited by T.G. Schroeter. *Canadian Institute of Mining, Metallurgy and Petroleum*, Special Volume 46, p. 46-57.
- Monger, J.W.H. (1976): Lower Mesozoic rocks in McConnell Creek map-area (94D), British Columbia, *Geological Survey of Canada*, Paper 76-1a, pages 51-55.
- Monger, J.W.H. and Church, B.N. (1977): Revised stratigraphy of the Takla Group, north-central British Columbia; *Canadian Journal of Earth Sciences*, Volume 14, pages 318-326.
- Monger, J.W.H., Richards, T.A. and Paterson, I.A. (1978): The Hinterland Belt of the Canadian Cordillera: New Data from Northern and Central British Columbia; *Canadian Journal of Earth Sciences*, Volume 15, pages 823-830.
- Monger, J.W.H., Wheeler, J.O., Tipper, H.W., Gabrielse, H., Harms, T., Struik, L.C., Campbell, R.B., Dodds, R.B., Gehrels, G.E. and O'Brien, H., (1991): Part B. Cordilleran terranes, Upper Devonian to Middle Jurassic assemblages, Chapter 8 of *Geology of the Cordilleran Orogen in Canada*; in *Geology of Canada*, No. 4, Edited by H. Gabrielse and C.J. Yorath, p. 281-327.
- Orchard, M.J., and Struik, L.C. (1996): Conodont biostratigraphy, lithostratigraphy and correlation of the Cache Creek Group near Fort St. James, central British Columbia; in *Current Research 1996-A*; *Geological Survey of Canada*.
- Paterson, I.A. (1974): Geology of Cache Creek Group and Mesozoic Rocks at the northern end of the Stuart Lake Belt, Central British Columbia; in *Report of Activities, Part B*, *Geological Survey of Canada*, Paper 74-1, Part B, pages 31-42.
- Paterson, I.A. (1977): The Geology and Evolution of the Pinchi Fault Zone at Pinchi Lake, Central British Columbia; *Canadian Journal of Earth Sciences*, Volume 14, pages 1324-1342.
- Ross, J.V. (1977): The Internal Fabric of an Alpine Peridotite near Pinchi Lake, Central British Columbia; *Canadian Journal of Earth Sciences*, Volume 14, pages 32-44.
- Schiarizza, P. and Payie, G. (1997): Geology of the Sitlika Assemblage in the Kenny Creek - Mount Olsen Area (93N/12, 13); in *Geological Fieldwork 1996*, B.C. Ministry of Employment and Investment, Paper 1997-1.
- Schiarizza, P., Massey, N.W.D and MacIntyre, D.G. (1998): Geology of the Sitlika assemblage in the Takla Lake area (93N/3,4,5,6,12); in *Geological Fieldwork 1997*, B.C. Ministry of Employment and Investment, Paper 1998-1 (this volume).
- Struik, L.C., Floriet, C., and Cordey, F. 1996: Geology near Fort St. James, central British Columbia; in *Current Research 1996-A*; *Geological Survey of Canada*, pages 71-76.
- Thompson, M.L. (1965): Pennsylvanian and Early Permian Fusulinids from Fort St. James Area, British Columbia, Canada; *Journal of Paleontology*, Volume 39, pages 224-234.
- Wanless, R.K. (1974): Age Determinations and Geological Studies, K-Ar Isotopic Ages; *Geological Survey of Canada*, Report 11, Paper 73-2, pages 22-23.
- Whittaker, P.J. (1983): Geology and Petrogenesis of Chromite and Chrome Spinel in Alpine-type Peridotites of the Cache Creek Group, British Columbia; unpublished Ph.D. Thesis, *Carleton University*, 339 pages.



## GEOLOGY OF THE SITLIKA ASSEMBLAGE IN THE TAKLA LAKE AREA (93N/3, 4, 5, 6, 12), CENTRAL BRITISH COLUMBIA

By Paul Schiarizza, Nick Massey and Don MacIntyre

(British Columbia Geological Survey Branch contribution to the Nechako NATMAP Project)

**KEYWORDS:** Sitlika assemblage, Cache Creek Group, Takla Group, Sustut Group, Takla fault, chromite, copper

### INTRODUCTION

The Sitlika bedrock mapping program was initiated as part of the Nechako Natmap project in 1996 (Schiarizza and Payie, 1997; Childe and Schiarizza, 1997; Schiarizza *et al.*, 1997). Its purpose is to update the geologic database for the western Manson River map area and, in particular, to determine the stratigraphy and structure of the Sitlika assemblage (Paterson, 1974), the validity of its correlation with the Kutcho assemblage of northern British Columbia (Monger *et al.*, 1978; Gabrielse, 1985), and its potential to host volcanogenic massive sulphide mineralization similar to the Kutcho Creek deposit (Bridge *et al.*, 1986; Childe and Thompson, 1995; Thompson *et al.*, 1995). The 1996 mapping program covered most of the Sitlika assemblage where it was originally defined by Paterson (1974). This resulted in an improved understanding of the composition, distribution and mutual relationships of Paterson's three divisions of the assemblage, and an improved understanding of the structural relationships between the Sitlika assemblage and terranes to the east and west. Furthermore, this mapping and associated radiometric dating and geochemical analyses established that the volcanic rocks of the Sitlika assemblage are readily correlated with metavolcanic rocks of the Kutcho

Formation on the basis of lithology (mafic and felsic volcanics with associated intrusions), Permo-Triassic age, and primitive tholeiitic geochemistry (Schiarizza and Payie, 1997; Childe and Schiarizza, 1997).

This report summarizes the findings from the second year of regional mapping within and adjacent to the Sitlika belt, carried out from late June to the end of August, 1997. This mapping extends the Sitlika assemblage southward from where it was originally defined by Paterson (1974) to the south end of Takla Lake, where rocks now included within the assemblage had been assigned to the Cache Creek and Takla groups by Armstrong (1949). It is planned to continue mapping southward along the Sitlika belt in the 1998 field season, and to establish the relationships between the Sitlika and Cache Creek belts mapped as part of this project with the Cache Creek units studied by the Geological Survey of Canada's Nechako Natmap team to the southeast (*see* MacIntyre and Struik, 1997, 1998).

The 1997 map area is situated mainly within the Hogen Ranges (including the Takla and Mitchell ranges) of the western Omineca Mountains, and encompasses the southern two-thirds of Takla Lake, including most of the northwest arm of the lake (Figure 4-2). The lowlands bordering Takla Lake in the northwestern corner of the area comprise part of the northern end of the Nechako Plateau. The only permanent residences are along Takla Lake, at the village of Takla Landing in the northwest corner of the area, and at Takla Narrows in the south-central part of the area. A network of logging and Forest Service roads that originates at Fort St. James, 125 kilometres southeast of Takla Narrows, provides access to much of the southern, eastern and northern parts of the map area. Boat ramps at Takla Narrows and Takla Landing provide access to excellent bedrock exposures along much of Takla Lake, as does the BC Railroad line along the east shore of the lake. Access to the interior part of the Mitchell and Takla ranges, east and west of the main arm of Takla Lake, respectively, was by helicopter. This was facilitated by a seasonal base established by Pacific Western Helicopters at Rustad Limited's Lovell Cove logging camp, near the north end of Takla Lake.

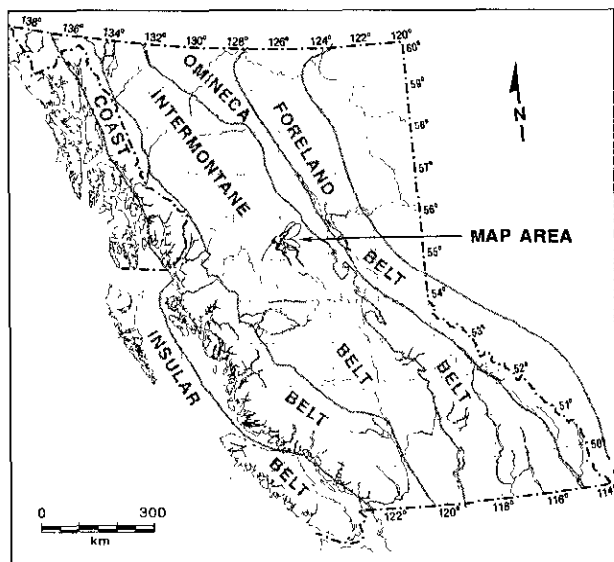


Figure 4-1. Location of the Sitlika Project Area.

### REGIONAL GEOLOGIC SETTING

The Takla Lake map area is situated within the eastern to central part of the Intermontane Belt, which includes a number of tectonostratigraphic terranes that were amalgamated and tied to the western margin of

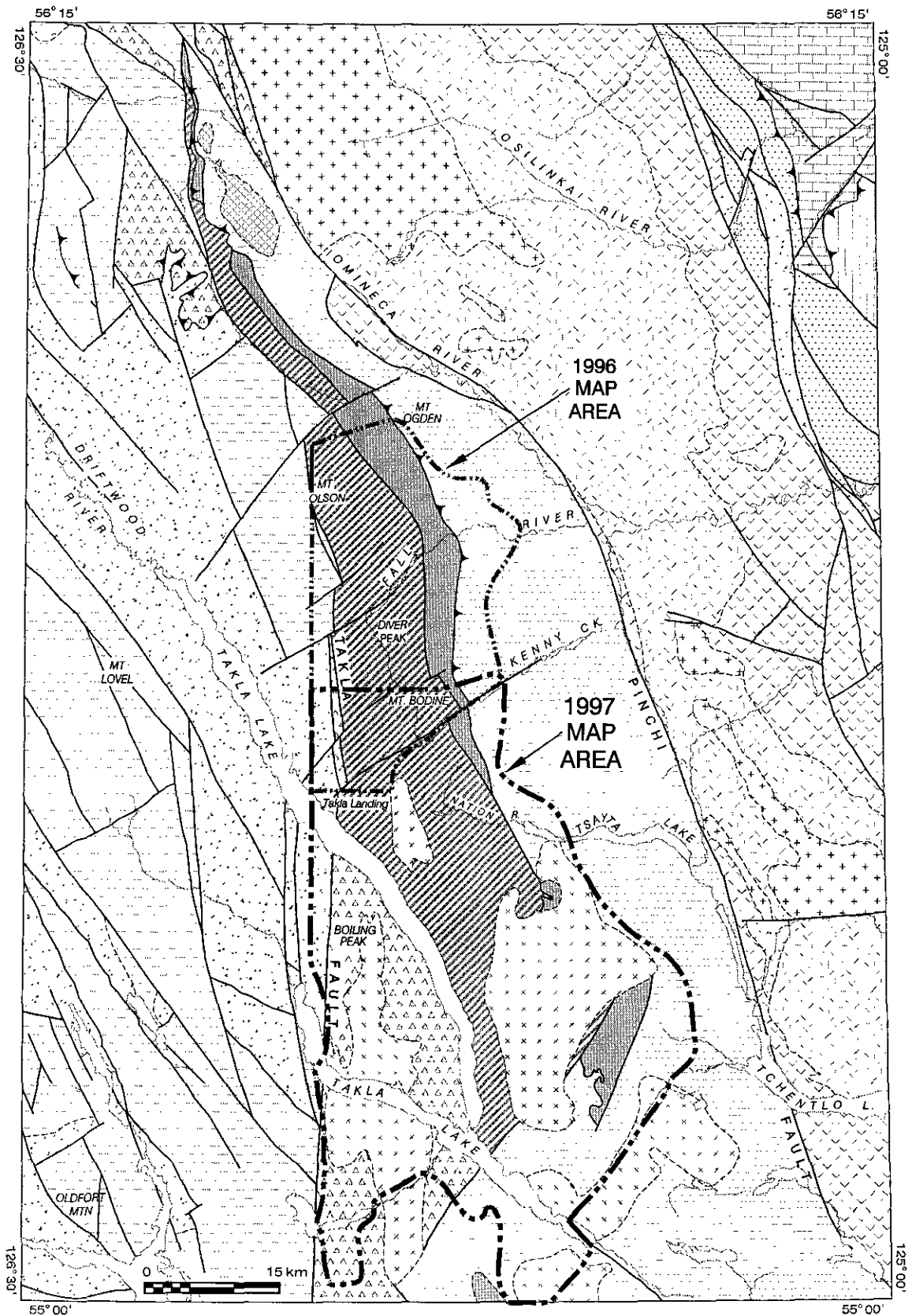


Figure 4-2. Geologic Setting of the Takla Lake map area. Modified from compilations by MacIntyre *et al.* (1994, 1995) and Bellefontaine *et al.* (1995). Note that the geology in and around the 1997 map area has not been modified to reflect this new mapping.

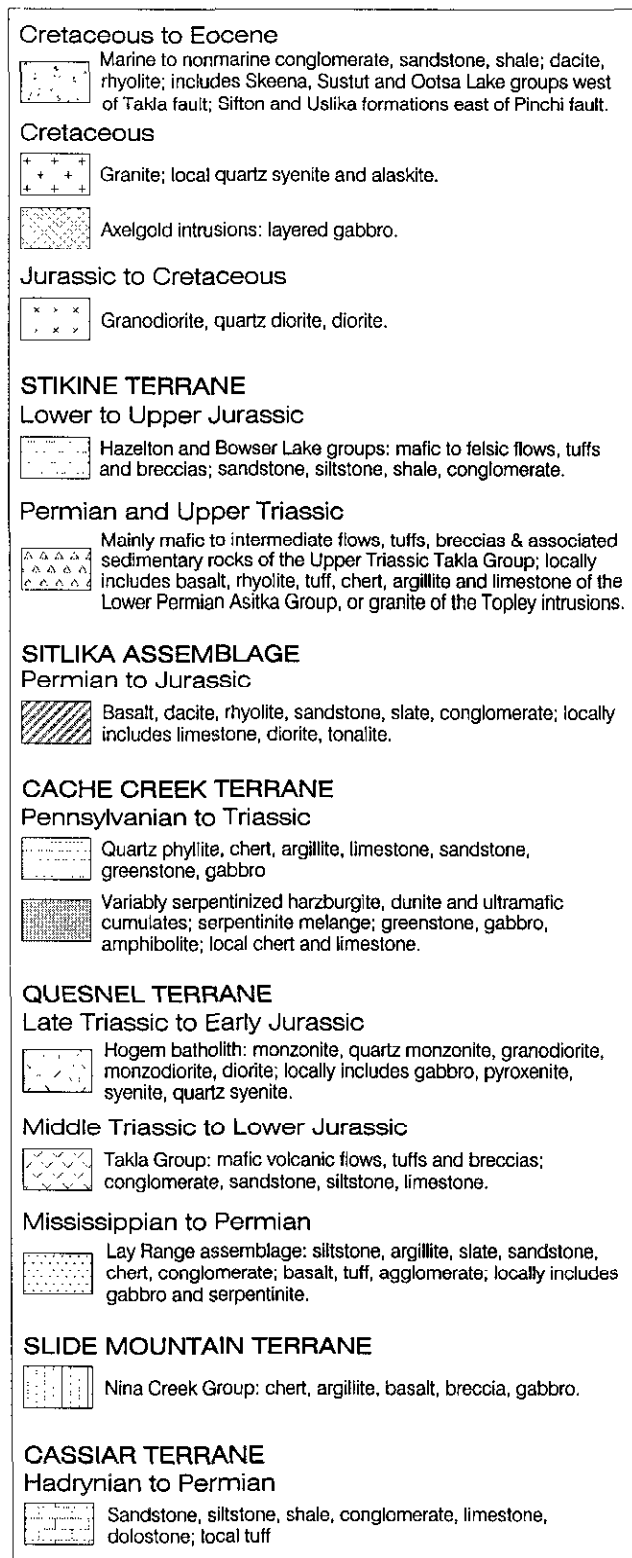
North America by Middle Jurassic time (Monger *et al.*, 1982). At this latitude the eastern Intermontane Belt includes early to mid-Mesozoic arc volcanic and plutonic rocks of the Quesnel Terrane flanked to the west by late Paleozoic and early Mesozoic oceanic rocks of the Cache Creek Terrane (Figure 4-2). The two terranes are in large

part separated by the Pinchi fault zone, which also includes slivers of deformed and altered sedimentary rocks of probable Late Cretaceous to Paleocene age. Latest movement is therefore inferred to be Tertiary, and may have been linked to a system of dextral strike-slip faults that was active over much of the length of the Canadian Cordillera during this time period (Gabrielse, 1985; Struik, 1993; Umhoefer and Schiarizza, 1996). Late Triassic blueschist-facies rocks are exposed along the fault zone at Pinchi Lake, suggesting that, at least locally, the Pinchi fault zone coincides with the early Mesozoic plate boundary between the Cache Creek accretionary wedge and the Quesnel Terrane magmatic arc (Paterson, 1977; Ghent *et al.*, 1996).

The Cache Creek Terrane is represented mainly by the Late Paleozoic to mid-Mesozoic Cache Creek Group, which includes structurally imbricated carbonate, chert, argillite, basalt, gabbro and alpine ultramafic rocks. Faulted against the Cache Creek Group to the west is a belt of metavolcanic and metasedimentary rocks that are assigned to the Sitlika assemblage (Paterson, 1974). These rocks, which are the focus of the present study, record primitive Permo-Triassic bimodal magmatism and subsequent clastic sedimentation within or adjacent to Cache Creek Terrane (Childe and Schiarizza, 1997; Schiarizza and Payie, 1997). They are apparently part of a much more extensive tract that is also recognized in northern and southern British Columbia (Childe *et al.*, 1996).

The Sitlika assemblage and Cache Creek Group are faulted to the west against the Stikine Terrane, which includes three successive assemblages of arc-derived volcanic, sedimentary and plutonic rocks that are assigned to the Lower Permian Asitka Group, the Upper Triassic Takla Group and the Lower to Middle Jurassic Hazelton Group (Tipper and Richards, 1976; Monger, 1977a; MacIntyre *et al.*, 1996). These arc successions are overlain by predominantly marine clastic sedimentary rocks of the upper Middle Jurassic to Lower Cretaceous Bowser Lake and Skeena groups, which in turn are overlapped by Upper Cretaceous to Eocene nonmarine clastic sedimentary rocks of the Sustut Group or age-equivalent continental arc volcanic rocks of the Kasalka and Ootsa Lake groups. Stikine Terrane and overlying clastic basin and continental arc assemblages cover the western two-thirds of the Intermontane Belt at the latitude of the study area, extending westward to the Coast Mountains.

The earliest deformation documented within Cache Creek Terrane in central British Columbia is related to subduction, probably beneath adjacent magmatic arc rocks of Quesnel Terrane, as indicated by blueschist facies rocks along the Pinchi fault that yield Late Triassic K-Ar and Ar-Ar cooling dates (Paterson and Harakal, 1974; Paterson, 1977; Ghent *et al.*, 1996). Subsequent uplift of Cache Creek Terrane is recorded by chert-rich clastic detritus that was shed westward into the basal part of the Bowser Lake Group in late Middle Jurassic to Late Jurassic time. This uplift may relate to the early stages of a deformational episode that generated greenschist facies metamorphism and penetrative deformation within the Cache Creek Terrane and the Sitlika assemblage, and



Legend to accompany Figure 4-2.

ultimately resulted in Cache Creek Terrane being thrust westward over Stikine Terrane (Monger *et al.*, 1978). Monger *et al.* suggest that the final stages of this contractional episode occurred in latest Jurassic to earliest Cretaceous time, based on the involvement of Oxfordian strata in west-directed thrusting to the northwest of the present study area, and a  $110 \pm 4$  Ma K-Ar date on synkinematic metamorphic biotite from a sample of the Sitlika assemblage collected in Ominicetla Creek. Younger deformation in the region involved Late Cretaceous(?) to early Tertiary dextral strike-slip and related extension, in part along major structures such as the Pinchi and Takla faults (Monger *et al.*, 1978; Gabrielse, 1985; Struik, 1993; Wetherup and Struik, 1996).

## LITHOLOGIC UNITS

### Sitlika Assemblage

The Sitlika assemblage was named by Paterson (1974) for greenschist facies metavolcanic and metasedimentary rocks on the east side of Takla Lake that had previously been included in the Cache Creek and Takla groups by Armstrong (1949). Paterson noted that they were structurally and lithologically distinct from the Cache Creek Group, and were separated from the main belt of Cache Creek rocks to the east by a zone of serpentinite melange. He did not establish the age of the assemblage, but suggested that it might correlate with Upper Triassic and Jurassic rocks that were assigned to the Takla Group in the McConnell Creek area to the northwest (Lord, 1948; Monger and Paterson, 1974). The Sitlika assemblage was subsequently traced northwestward as a narrow belt that extends through the northeastern corner of the Hazelton map area (Richards, 1990) and into the southern McConnell Creek map area (Monger, 1977a; Monger *et al.*, 1978), where it was inferred to correlate with a stratigraphic succession that included Lower Permian, Upper Triassic and Lower Jurassic rocks of the Asitka, Takla and Hazelton groups. Monger *et al.* (1978) also recognized a strong lithologic and structural similarity between the Sitlika assemblage and the Kutcho Formation, which occurs in the eastern part of the King Salmon allochthon in northern British Columbia. They suggested that the King Salmon allochthon and structurally overlying Cache Creek Group had been displaced northward from the Sitlika assemblage and adjacent Cache Creek rocks, on Late Cretaceous or early Tertiary dextral strike-slip faults.

Recent studies of the Kutcho Formation, which previously had also been correlated with either the Lower Permian Asitka Group (Panteleyev and Pearson, 1977b; Monger, 1977b) or the Upper Triassic Takla Group (Thorstad and Gabrielse, 1986), have established that the volcanic and intrusive rocks are of Permo-Triassic age and primitive tholeiitic nature (Childe and Thompson, 1995; Thompson *et al.*, 1995). Schiarizza and Payie (1997) confirmed that the Sitlika assemblage resembles the Kutcho Formation and overlying metasedimentary rocks (Sinwa and Inklin formations) in general lithology and stratigraphy, while Childe and Schiarizza (1997)

documented that the two assemblages are also similar in age, geochemistry and Nd isotopic signature. Furthermore, Childe *et al.* (1997) and Schiarizza and Payie (1997) suggest that Kutcho-Sitlika-correlatives also occur in at least two places in southern British Columbia. It appears, therefore, that the Sitlika assemblage may be part of an extensive tract within or adjacent to Cache Creek Terrane that occurs over most of the length of the Canadian Cordillera.

Paterson (1974) subdivided the Sitlika assemblage into three divisions. Schiarizza and Payie (1997) adopted this scheme and informally referred to the subdivisions as the volcanic unit (equivalent to Paterson's volcanic division), the eastern clastic unit (equivalent to Paterson's greywacke division) and the western clastic unit (equivalent to Paterson's argillite division). They established that the eastern clastic unit rests positionally above the Permo-Triassic volcanic unit, but suggested that the western clastic unit, which is structurally beneath the volcanic unit, might be a fault-bounded panel of younger rocks. During the 1997 field season, these same three units of the Sitlika assemblage were traced southward an additional 50 km to the south end of Takla Lake. This work confirms the stratigraphic relationship between the volcanic and eastern clastic units. The age and structural/stratigraphic relationships of the western clastic unit remain uncertain.

### Volcanic Unit

The Sitlika volcanic unit was traced continuously from Hagem Pass, at the south end of the belt mapped by Schiarizza and Payie (1997), to the southwest side of Takla Lake (Figure 4-3). The northern part of this belt, represented by excellent exposures along the east shore of Takla Lake, includes rocks that were assigned to the Sitlika volcanic division when it was originally defined by Paterson (1974). Southward from there, the unit crops out along the west side of Takla Lake, from Dominion Point to Takla Narrows, and includes rocks mapped by Armstrong (1949) as Cache Creek volcanics (as were correlative volcanics to the north, prior to their inclusion in the Sitlika assemblage by Paterson). The volcanic unit is not well exposed southward from there, but extends for at least 10 km south of Takla Narrows, where it includes rocks that Armstrong assigned to the Takla and Cache Creek groups on the southwest side of Takla Lake.

The volcanic unit in the Takla Lake area is dominated by a monotonous sequence of actinolite-epidote-chlorite schists and semischists derived from mafic volcanic rocks. Plagioclase, and less common pyroxene, are widespread as relict phenocrysts. Pillow structures, in places outlined by concentric zones of epidote amygdules, are commonly preserved, and locally grade into monolithic mafic fragmental schists that probably represent pillow breccias. Fragmental schists containing feldspar crystals and light grey to pale green felsic volcanic fragments also occur, typically as intervals several metres to tens of metres thick interleaved with mafic volcanics. In the Maclaing Creek area, however, schists containing felsic fragments dominate an interval about 1000 m thick, with a strike

length of about 10 km, near the base of the unit. These rocks include sericite-chlorite schists and quartz-chlorite-sericite schists containing variable proportions of feldspar, quartz and pyroxene crystals, together with mafic to felsic volcanic-lithic fragments and, locally, dioritic to tonalitic plutonic fragments. The fragmental schists are generally not conspicuously stratified, but are locally intercalated with narrow intervals, up to 5 m thick, of thin-bedded tuff or volcanic sandstone and siltstone.

Metasedimentary rocks are a very minor component of the volcanic unit, but are intercalated with the volcanics at a number of widely scattered localities within the Takla Lake area, and locally form intervals approaching 100 metres in thickness. They are most common in the vicinity of Maclaing Creek, where they occur directly above the felsic fragmental schist unit, and as intercalations within pillowed basalts that overlie the fragmental schists. The metasedimentary rocks are mainly dark grey, rusty weathered, thin-bedded slates and slaty siltstones, with local intercalations of fine to coarse grained sandstone and granule conglomerate containing feldspar, quartz, and flattened volcanic or sedimentary lithic grains. Also present are narrow intervals of black argillite interbedded with pyritic chlorite-sericite phyllite, and thin-bedded, dark grey to pale green chert, cherty argillite and slate.

Volcanic and sedimentary rocks within the Sitlika volcanic unit are intruded by a variety of mafic to felsic sills and dikes that are inferred to be broadly contemporaneous with the volcanics. They include fine to medium-grained feldspar-chlorite schists to semischists, chloritized hornblende-feldspar porphyries, and pyroxene porphyries, of intermediate to mafic composition. Felsic rocks are less abundant, but dikes of variably foliated quartz-feldspar porphyry and tonalite occur locally. These resemble tonalite of the Maclaing Creek pluton (described later), which also includes an older phase of metadiorite that resembles some of the intermediate dikes and sills. The most mafic intrusive rock observed within the unit, possibly derived from a clinopyroxenite or wehrlite, comprises relict clinopyroxene crystals interleaved with foliated phyllosilicate-like material that may include chlorite, serpentine and talc. This rock, together with associated microdiorite, forms a series of sill-like bodies that intrude clastic metasedimentary rocks and pillowed metabasalt 4 km south of the Maclaing Creek pluton.

As reported by Childe and Schiarizza (1997) the age of the Sitlika volcanic unit is in part constrained by a U-Pb date of  $258 \pm 10/-1$  Ma on zircons from a weakly foliated quartz-plagioclase-phyric rhyolite north of Mount Bodine. This Permian date is corroborated by Permian radiolarians (*Latentibifistula* sp.) extracted from a narrow chert interval intercalated with the volcanic rocks south of Mount Olson (Fabrice Cordey, written communication, 1997). A U-Pb zircon date of  $241 \pm 1$  Ma from a tonalite plug that intrudes the Sitlika volcanic unit east of Diver Lake indicates that magmatism continued into the Triassic (Childe and Schiarizza, 1997). Additional samples were submitted for both microfossil extraction and U-Pb dating following the 1997 field season, in an attempt to further constrain the age of the volcanic unit.

### *Maclaing Creek Pluton*

A composite stock of metadiorite and tonalite intrudes the Sitlika volcanic unit across the middle reaches of Maclaing Creek, about 6 km east of Takla Landing (Figure 4-3). It measures about 12 km long, parallel to the strike of the volcanic unit, and up to 4 km wide. The western and northern parts of the stock consist of moderately to weakly foliated, fine to medium-grained epidote-chlorite-feldspar schist and semischist, locally grading to weakly foliated chloritized hornblende diorite and hornblende-feldspar porphyry. Dikes and sills of similar metadiorite are common within the volcanic rocks peripheral to the stock, and also occur elsewhere within the volcanic unit. The southeastern part of the Maclaing Creek pluton consists of light grey, massive to weakly foliated chlorite-epidote-altered tonalite, characterized by a medium to coarse grained, equigranular to slightly quartz-porphyrific texture. The tonalite intrudes metadiorite to the west and northwest, and apparently cuts the upper part of the volcanic unit to the east, although this contact was not observed. The tonalite was included by Armstrong (1949) in his Late Jurassic to Early Cretaceous Omineca Intrusions, but is here included in the Sitlika assemblage due to its lithologic similarity to the Early Triassic Diver Lake pluton (Childe and Schiarizza, 1997). This correlation is currently being tested by U-Pb dating of zircons extracted from a sample of the Maclaing Creek tonalite.

### *Eastern Clastic Unit*

The Sitlika eastern clastic unit occupies a wide outcrop belt that extends continuously from Kenny Creek to the south end of Takla Lake (Figure 4-3). It rests stratigraphically above the volcanic unit to the west, and is faulted against the Cache Creek ultramafic unit to the east, although the latter contact is in part truncated by the Mitchell batholith. The eastern clastic unit is well exposed on ridges adjacent to the upper Nation River, on the east-west ridge system north of Klowkut Peak, and along the eastern shore of Takla Lake, between 5 and 15 km north of Takla Narrows. Armstrong (1949) included the metasedimentary rocks throughout this belt in his ribbon chert lithologic division of the Cache Creek Group.

Schiarizza and Payie (1997) established that the eastern clastic unit rests stratigraphically above the volcanic unit, based on unfaulted sections southeast of Mount Olson and west of Mount Bodine. There, the contact is marked by a basal conglomerate containing felsic volcanic clasts, together with clasts of limestone, mafic volcanic rocks, felsic plutonic rocks and phyllitic rocks of possible sedimentary origin. The conglomerates pass up-section into green chloritic phyllite containing layers and lenses of buff to rusty dolomitic marble, which in turn pass up-section into grey phyllite containing lenses and layers of grey marble and silty calcarenite. This calcareous interval is several tens of metres thick in the Mount Olson area, where it is overlain by predominantly thin-bedded sandstone and dark-grey slate, typical of rocks found throughout the higher stratigraphic levels of the eastern clastic unit.

In the Takla Lake area, the base of the eastern clastic unit was observed only along the east shore of Takla Lake, about 15 km north of Takla Narrows. There is no basal conglomerate developed, but the lower part of the unit

includes abundant carbonate and green chloritic phyllite, which resemble rocks found within the calcareous interval that lies directly above the basal conglomerate seen to the north. The actual contact is marked by about 2 m of pale

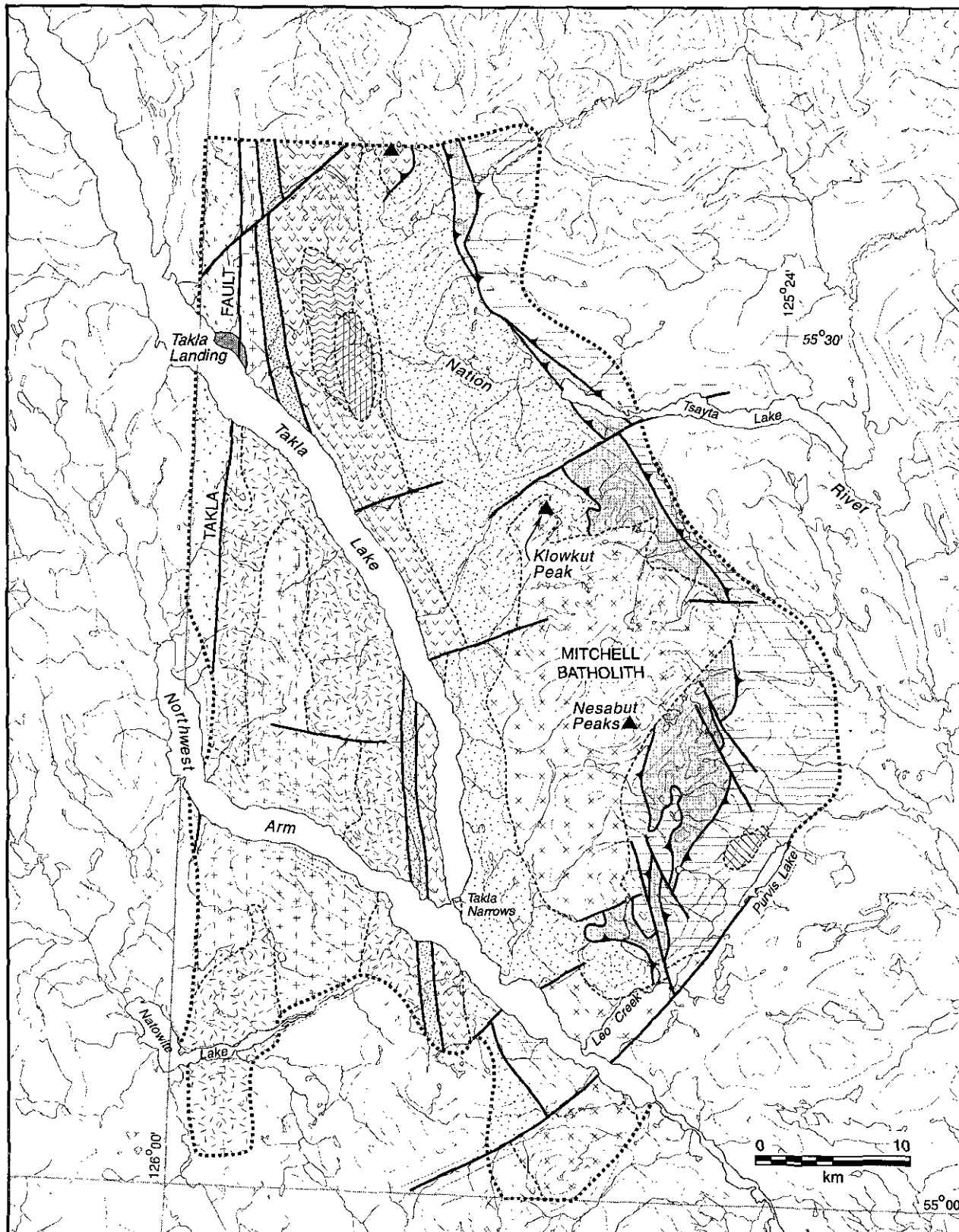


Figure 4-3. Generalized geology of the Takla Lake map area.

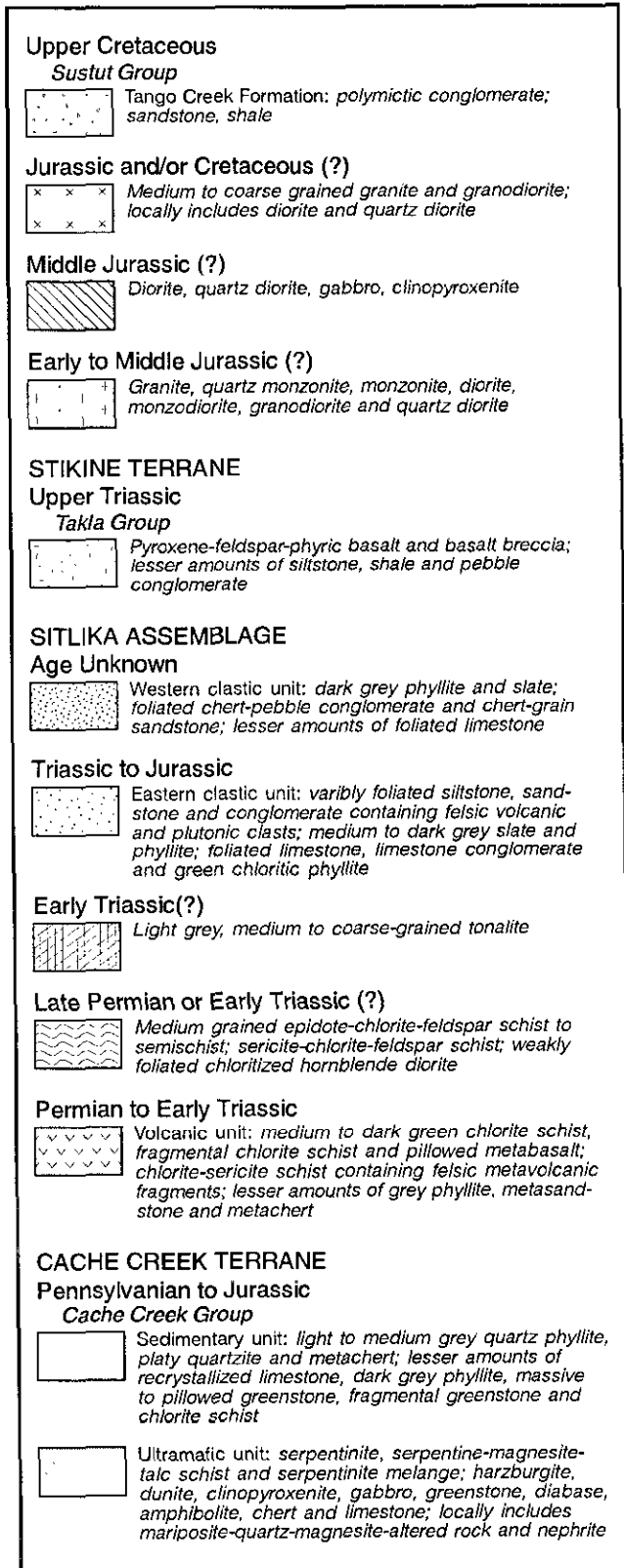
silvery-green calcareous sericite-chlorite schist with abundant stringers and lenses of carbonate. These rocks, which are included in the eastern clastic unit, are in abrupt contact with medium green, tuffaceous(?) chlorite schist of the volcanic unit, which passes down section into pillowed

metabasalt. The basal 2 m of the sedimentary section is overlain by about 10 m of grey slate containing narrow limestone interbeds, which in turn is overlain by several tens of metres of alternating grey slate and green chloritic phyllite units, each containing lenses of carbonate. Whereas grey slate, commonly containing interbeds of siltstone, sandstone or limestone, continues to be abundant higher in the section, the green chloritic phyllite with carbonate (commonly dolomitic) lenses is characteristic of the basal part of the unit.

Above the calcareous chloritic phyllites at the base, most of the eastern clastic unit consists of dark grey slate intercalated with thin beds of siltstone and slaty siltstone. Intercalations of sandstone, calcarenite, limestone and conglomerate are common, but their stratigraphic distribution is not well understood as the unit is not well exposed through much of the area, its top is nowhere exposed, and it is deformed by numerous folds and faults where exposure is good. Fine to coarse-grained sandstone and granule conglomerate occur as thin to thick, massive to graded beds intercalated with thinner interbeds of slate or siltstone. The sandstones range from schistose wackes, containing quartz, feldspar and volcanic(?) lithic clastic grains, to quartz-rich wackes and arenites. Locally the sandstone-rich intervals include beds of conglomerate or schistose conglomeratic sandstone, ranging from tens of centimetres to several metres thick. The conglomerates contain pebbles and small cobbles of felsic volcanic rock, with or without quartz and feldspar phenocrysts, along with mafic volcanics, phyllite, siltstone and limestone.

Calcareous rocks, including layers and lenses of calcareous sandstone, calcarenite, calcareous phyllite and medium to dark grey marble, are scattered throughout the eastern clastic unit, and locally dominate intervals many tens of metres thick. One such calcareous interval, 4 km northwest of Klowkut Peak, includes two or more units of light-grey weathered marble-matrix conglomerate or breccia, containing flattened pebbles and cobbles of felsic volcanic rock, as well as pebbles, cobbles and angular blocks of grey marble similar to the matrix. One of these conglomeratic marble intervals, which contains blocks of marble up to 1 m across, is about 20 m thick and was traced for more than a kilometre. Similar conglomeratic carbonate intervals are exposed on the ridge 3.5 kilometres northeast of Mount Olson, and are described by Schiarizza and Payie (1997).

The eastern clastic unit is not dated. It appears to be structurally concordant with the underlying volcanic unit, but the contact is abrupt, and the clastic rocks contain volcanic and plutonic detritus that was probably derived from the underlying unit. This suggests that the contact might be a disconformity or an unconformity. In any case, the eastern clastic unit apparently postdates the Permian to Early Triassic magmatism recorded in the underlying volcanic unit, and is therefore Middle Triassic and/or younger. The stratigraphic top of the unit is not exposed, but it is intruded by the Mitchell pluton, of suspected Late Jurassic or Early Cretaceous age. Therefore, the eastern clastic unit was most likely deposited sometime in the Middle Triassic through Middle Jurassic time interval. Limestone and chert samples analysed for microfossils



Legend to accompany Figure 4-3.

after the 1996 field season were not productive, but additional samples were collected in 1997 and are currently being processed. In addition, a sample of medium to coarse-grained sandstone from the unit was sampled for detrital zircon analysis. This may help constrain the age of the unit and provide additional insight into its provenance.

### **Western Clastic Unit**

The western clastic unit of the Sitlika assemblage consists of dark grey slate, with local intercalations of sandstone, limestone and chert-pebble conglomerate. It apparently forms a narrow continuous belt from Takla Landing to south of Takla Narrows, although it is not exposed for a length of 15 km where it follows the main arm of Takla Lake (Figure 4-3). These rocks were assigned to a sedimentary interval within the Takla Group by Armstrong (1949). Only the northern part of the belt was mapped by Paterson (1974), who assigned it to his argillite division of the Sitlika assemblage. Schiarizza and Payie (1997) traced the unit northward from near Takla Landing to the west flank of Mount Olson. They referred to these rocks as the western clastic unit, and suggested that they might be in fault contact with, and younger than, the structurally overlying volcanic unit.

Within the Takla Lake area the western clastic unit is dominated by dark grey slate and pyritic slaty argillite, with thin beds or laminae of slaty siltstone or fine-grained sandstone. Coarser grained sandstone occurs locally as medium to thick, massive or graded beds that may contain rip-up clasts and flute casts along their bases. Pebble conglomerate dominated by clasts of chert and limestone also occurs, as do rare lenses of dark grey, finely recrystallized limestone and phyllitic limestone.

The age of the western clastic unit is unknown. No macrofossils were found in the unit, and limestone samples submitted for microfossil analysis in 1996 were not productive; additional samples were collected during the 1997 field season and are currently being processed. Because it separates the generally east-facing Permian volcanic unit from Triassic rocks of Stikine Terrane to the west, one or both contacts of the intervening western clastic unit must be faults. The western contact was not observed, but the lithologic similarity between the western clastic unit and Upper Triassic sedimentary rocks within and beneath the Takla Group volcanics suggests a possible correlation. The eastern contact, between the western clastic unit and the Sitlika volcanic unit, is exposed along the railway tracks about 7 km southeast of Takla Landing. There, massive to weakly foliated feldspar-phyrlic metabasalt of the volcanic unit passes abruptly down-section into several metres of strongly foliated, green chlorite schist (possibly derived from the same basalt protolith) containing abundant veins and pods of quartz. These schistose rocks are in sharp contact with underlying dark grey slates of the western clastic unit. The contact dips steeply east, and is concordant to schistosity in both the western clastic unit and the overlying volcanic unit. The contact between the volcanic and western clastic units has a similar character where seen near Mount Olson, 40

km to the north. There, it was interpreted as a reverse fault by Schiarizza and Payie (1997). It is not clear, however, if it is actually a significant fault (in which case the age of the western clastic unit is unconstrained), or if it is a slightly sheared stratigraphic contact (in which case the western clastic unit is Permian or older).

### **Correlation of the Sitlika Assemblage**

#### **Volcanic Unit**

Correlation of the Sitlika volcanic unit with volcanic and plutonic rocks of the Kutcho Formation (Thorstad and Gabrielse, 1986; Childe and Thompson, 1995), as proposed by Monger *et al.* (1978), is strongly supported by the present study. The correlation is based on lithologic and geochemical similarity (bimodal tholeiitic volcanic and plutonic rocks), similar Permo-Triassic age of magmatism, and similar primitive REE and Nd isotopic signatures (Childe and Schiarizza, 1997).

Correlative rocks also occur to the northwest of the Kutcho Formation, in rocks of northern Cache Creek Terrane, where felsic volcanic rocks occur locally within the predominantly mafic volcanic succession assigned to the French Range Formation (Monger, 1969, 1975). Rhyodacite in the French Range is Upper Permian, as it occurs within a stratigraphic succession that includes underlying and overlying fossiliferous strata of Early and Late Guadalupian age, respectively (Monger, 1969; Mihalynuk and Cordey, 1997). It has recently yielded a U-Pb zircon date of  $263.1 \pm 1.0/-1.4$  Ma (M. Mihalynuk, personal communication, 1997) which is, within error, the same as the U-Pb date of  $258 \pm 10/-1$  Ma for the Sitlika rhyolite near Mount Bodine.

The volcanic unit of the Sitlika assemblage may also correlate with an assemblage of rocks that lies with thrust contact beneath the Cache Creek Group in the northeastern part of the Taseko Lakes map area, 400 km south of Takla Lake. There, Read (1992, 1993) documented a succession of Upper Permian metadacite flows and tuffs that is overlain by meta-andesite and metabasalt flows and intruded by a Late Permian leucoquartz monzonite pluton. The dacitic volcanics yielded a U-Pb date of  $259 \pm 2$  Ma (Read, 1993), almost identical to the date from the Sitlika rhyolite north of Mount Bodine, and the associated leucoquartz monzonite pluton has been dated at  $254 \pm 1.2$  Ma. Correlation of this succession with the Sitlika volcanic unit is based on similarities in age, general lithologic character (mafic and felsic metavolcanic rocks plus comagmatic intrusions) and structural position along the western margin of the Cache Creek Group.

Childe *et al.* (1996, 1997) suggest that the Kutcho and Sitlika successions may also correlate with one or more fault-bounded panels of felsic and mafic volcanic rocks that are juxtaposed against the Cache Creek Group in the Ashcroft map area, south of the town of Cache Creek. They report that a tonalitic body that intrudes volcanic rocks in one of these panels yielded a preliminary U-Pb zircon age of  $242 \pm 2$  Ma, which correlates with the age of magmatism in the Kutcho Formation, and with the dated tonalite body in the Sitlika assemblage.

### ***Eastern Clastic Unit***

The eastern clastic unit is undated, but is known to rest stratigraphically above the Permian to Lower Triassic volcanic unit. It is provisionally correlated with lithologically similar sedimentary rocks that overlie the Kutcho volcanics in northern British Columbia. The latter include undated conglomerates that are included in the upper part of the Kutcho Formation, as well as rocks that have been included in the Upper Triassic Sinwa and Lower Jurassic Inklin formations (Pearson and Panteleyev, 1975; Panteleyev and Pearson, 1977a,b; Thorstad and Gabrielse, 1986). Points of similarity include the presence of a basal conglomerate unit containing clasts derived from the underlying volcanic rocks; an overlying limestone unit gradational with the conglomerates (Sinwa Formation); and an upper interval of slate, siltstone and calcareous greywacke with local conglomerate intervals (Inklin Formation). Correlative sedimentary rocks may also occur in the northeastern Taseko Lakes map area, where they are represented by Lower Jurassic siltstone and sandstone assigned to Unit IJs by Read (1993). These rocks rest positionally(?) above the Upper Permian volcanic succession that is correlated with the Sitlika volcanics and, like the eastern clastic unit, contain felsic volcanic detritus that is inferred to have been derived from the underlying volcanics.

### ***Western Clastic Unit***

The age of the western clastic unit is unknown. As discussed previously, if its contact with the structurally overlying volcanic unit is a slightly sheared stratigraphic contact then the western clastic unit is Late Permian and/or older. Although this interpretation cannot be entirely dismissed, it is not presently favoured, in part because there are no sills or dikes of the overlying volcanic unit present in the metasedimentary rocks, despite the fact that mafic to felsic intrusive phases are common throughout the volcanic unit itself. Furthermore, Schiarizza and Payie (1997) suggest that there is a gradual truncation of the volcanic unit along its contact with the western clastic unit in the central part of the Kenny Creek - Mount Olson area. The contact between the western clastic unit and the volcanic unit may therefore be a significant fault, in which case the age of the western clastic unit is unconstrained, and the most likely correlation is with Upper Triassic sedimentary rocks of the Takla Group, as suggested by Armstrong (1949). Alternatively, the western clastic unit may be a fault-bounded panel of younger rocks, perhaps correlative with the Middle to Upper Jurassic Ashman Formation of the Bowser Lake Group (Schiarizza and Payie, 1997).

### **Cache Creek Group**

The Cache Creek Group within and adjacent to the Takla Lake map area was referred to as the Stuart Lake Belt by Armstrong (1949) in order to distinguish it from a separate belt of rocks that he also included in the Cache Creek Group farther to the east. The latter, which he

referred to as the Manson Creek belt, includes rocks that are presently assigned to the Cassiar, Slide Mountain and Quesnel terranes (Ferri and Melville, 1994). The Stuart Lake belt can be traced southward for 400 kilometres into the type area of the Cache Creek Group in southern British Columbia (Wheeler and McFeely, 1991). It is truncated by the Takla-Ingenika fault system about 60 km north of Takla Lake, along which it is separated by about 300 km from a belt of Cache Creek rocks exposed in northern British Columbia (Gabrielse, 1985).

The Cache Creek Group includes polydeformed chert, siliceous argillite, limestone, phyllite, slate, siltstone, sandstone, and mafic metavolcanic and meta-intrusive rocks. Thick limestone units contain fusulinids, corals, brachiopods, bryozoans, gastropods and conodonts that are Pennsylvanian and Permian in age (Armstrong, 1949; Thompson, 1965; Orchard and Struik, 1996); radiolarian chert and cherty mudstone range from Early Permian to earliest Jurassic age (Cordey and Struik, 1996a,b). Ultramafic rocks within the Stuart Lake belt were referred to as the Trembleur intrusions by Armstrong, who interpreted them to be intrusive bodies cutting the Cache Creek sedimentary and volcanic rocks. These rocks are now included within the Cache Creek Group, and interpreted to be tectonically emplaced upper mantle and lower crustal portions of dismembered ophiolite sequences (Paterson, 1977; Ross, 1977; Whittaker, 1983; Ash and Macdonald, 1993; Struik *et al.*, 1996).

In the Takla Lake map area the Cache Creek Group is subdivided into an ultramafic unit and a sedimentary unit. These units are continuous with the same subdivisions of Schiarizza and Payie (1997) to the north.

### ***Ultramafic Unit***

Paterson (1974) identified a belt of ultramafic rocks and serpentinite melange that separates metasedimentary and metavolcanic rocks of the Cache Creek Group from the Sitlika assemblage to the west. This belt was mapped in more detail by Schiarizza *et al.* (1997) who assigned it to the ultramafic unit of the Cache Creek Group. During the 1997 field season this unit was traced as a more or less continuous belt to the southern end of the Takla Lake map area. It is separated from the underlying Sitlika assemblage and the overlying Cache Creek sedimentary unit by systems of easterly-dipping thrust faults. This belt includes rocks that were mapped as Trembleur intrusions by Armstrong (1949), and later studied in more detail by Elliot (1975) and Whittaker (1983), who interpreted them to be structurally emplaced alpine-type peridotites.

The ultramafic unit comprises a relatively narrow, possibly discontinuous belt in the northern part of the map area, between Kenny Creek and Tsayta Lake. There, it consists of serpentinite, talc-magnesite schist, and serpentinite melange, as described by Schiarizza and Payie (1997) for the area along strike to the north. Knockers and lenses in the serpentinite melange include serpentinitized ultramafite of uncertain protolith, greenstone, amphibolite, gabbro and a variety of metasedimentary rocks. Silicified argillite, slate, metachert and marble are the dominant metasedimentary lithologies encountered. A sedimentary

lens exposed on the south shore of Tsayta Lake, however, includes foliated pebble conglomerate, bioclastic limestone and fossiliferous quartzose sandstone. A previous fossil collection from this lens included *Pustula* sp. and a large striated brachiopod suggestive of *Meekella kueichowensis* Huang, indicating a probable Permian age (A.E. Wilson in Armstrong, 1949, page 46). These rocks were resampled for both macrofossils and microfossils during the present study.

The ultramafic unit is considerably wider in the eastern Mitchell Range, although it is in part truncated by the Mitchell batholith (Figure 4-3). This part of the belt includes foliated serpentinite and serpentinite melange, similar to that in the northern part of the belt, but also includes large areas of more coherent ultramafic and mafic rock, which probably represent a sampling of both mantle and crustal elements of a dismembered ophiolite suite. The dominant ultramafic rock is variably serpentinitized harzburgite, which commonly contains irregular pods and lenses of dunite. Locally the harzburgite displays a penetrative foliation that may represent a mantle tectonite fabric (Whittaker, 1983). Clinopyroxenite was observed in several areas east of Klowkut Peak, where it is separated from harzburgite by narrow faults or wider zones of serpentinite melange. Relatively large blocks of layered to isotropic gabbros are likewise separated from harzburgite by faults. Gabbro and microgabbro also occur as boudinaged dike-like bodies, partially altered to rodingite, within harzburgite, clinopyroxenite and layered gabbro.

### **Sedimentary Unit**

The sedimentary unit of the Cache Creek Group is dominated by grey platy quartz phyllites, but also includes metachert, cherty argillite, slate, limestone, greenstone and chlorite schist. It crops out mainly along the eastern edge of the Takla Lake map area, and similar rocks apparently dominate the Cache Creek Group eastward all the way to the Pinchi fault (Armstrong, 1949). These rocks are juxtaposed against the ultramafic unit to the west. The contact is not well exposed anywhere in the Takla Lake area, but is inferred to be a system of predominantly east-dipping faults based on relationships seen to the north (Schiarizza and Payie, 1997). A panel of similar metasedimentary rocks that is enclosed by ultramafic rocks south of Nesabut Peaks is interpreted as a structural repeat of the sedimentary unit, exposed in the core of a synform along the southeastern margin of the Mitchell batholith. The sedimentary unit is also represented by exposures on the southwest side of southern Takla Lake. There it is faulted against the Sitlika eastern clastic unit to the west, and intruded(?) by the Purvis Lake stock and Pyramid Peak pluton to the east (Figure 4-3).

The sedimentary unit consists mainly of light to dark grey platy quartz phyllites, comprising plates and lenses of fine-grained recrystallized granular quartz, typically a centimetre or less thick, separated by phyllitic mica-rich partings. Locally these platy rocks grade into less siliceous and more homogeneous medium to dark grey phyllites. Less commonly they include intervals of light to medium

grey or green chert that occurs as beds and lenses, from 1 to 5 centimetres thick, separated by phyllitic partings.

Light to dark grey recrystallized limestone is locally intercalated with the siliceous metasedimentary rocks, and occurs as units ranging from a few metres to more than 100 metres thick. It is most common in the synformal lens on the southeast flank of the Mitchell batholith, and in a potentially correlative interval west of Purvis Lake. Armstrong (1949) included these rocks in a limestone unit that extends southeastward to Mount Copley, north of Trembleur Lake, where it contains Middle Permian fusulinids. None of the limestones encountered in the Takla Lake map area contain well-preserved macrofossils, but samples were collected and are currently being processed for microfossils.

Mafic metavolcanic rocks, including chlorite schist, pillowed greenstone and fragmental greenstone, occur as intervals ranging from a few metres to several tens of metres thick within the sedimentary unit. These are widespread, but are not volumetrically a major component of the unit. The mafic metavolcanic rocks typically form lenses parallel to the synmetamorphic foliation and transposed compositional layering in surrounding metasedimentary intervals. Locally they are associated with weakly foliated, fine-grained chlorite-feldspar semischists that were probably derived from mafic dikes or sills.

## **Stikine Terrane**

### **Takla Group**

Armstrong (1949) used the name Takla Group for occurrences of Upper Triassic and Jurassic volcanic and sedimentary rocks exposed west and southwest of the main arm of Takla Lake. In addition to the exposures around Takla Lake, he also included in the Group a more extensive belt to the east of the Pinchi fault, which extended from Pinchi Lake north-northwestward to beyond Germansen Lake. Subsequent revisions to the nomenclature of the western belt, based largely on excellent exposures in the McConnell Creek map area to the northwest, restricted the name Takla Group to Triassic rocks, and included the overlying Lower to Middle Jurassic volcanic-sedimentary succession in the Hazelton Group (Tipper and Richards, 1976; Monger, 1977a; Monger and Church, 1977). Likewise in the eastern belt, Nelson and Bellefontaine (1996) restrict the name Takla Group to Triassic rocks and assign the disconformably overlying Lower Jurassic volcanic and sedimentary rocks to several informal successions. As noted by Nelson *et al.* (1991) the two belts of Takla rocks are lithologically and stratigraphically similar, although the eastern belt is part of Quesnel Terrane and the western belt is part of Stikine Terrane.

The Takla Group is exposed on the southwest side of Takla Lake, from the shoreline south of Takla Landing to the southern boundary of the map area. This belt is bounded by the western clastic unit of the Sitlika assemblage to the east and, at least in part, by the Takla

fault to the west. Within this belt, the volcanic and sedimentary rocks of the Takla Group are intruded by Jurassic? diorite, granodiorite and quartz monzonite of the large, composite Northwest Arm pluton, and also by the smaller Takla Landing pluton.

The Takla Group is dominated by basaltic flows and associated breccias that occur in dark shades of green, grey and maroon. The volcanics typically contain phenocrysts of plagioclase and pyroxene, but may be aphyric. They lack the penetrative foliation that characterizes the volcanic rocks within the adjacent Sitlika assemblage, but commonly display varying degrees of chlorite-epidote alteration. Sedimentary rocks occur locally within the volcanics, as intervals ranging from a few metres to more than 100 metres thick. These intervals are dominated by thin-bedded siltstone, slate and cherty argillite, but also include pebble to cobble conglomerates containing clasts of chert and limestone. In contrast to the massive volcanic rocks, the sedimentary rocks are typically foliated, and are lithologically similar to rocks within the adjacent western clastic unit of the Sitlika assemblage.

The Takla rocks exposed in the Takla Lake area are correlated with the upper Carnian to lower Norian Savage Mountain Formation of Monger and Church (1977). As discussed previously, the western clastic unit of the Sitlika assemblage may be a fault-bounded(?) panel of the Dewar Formation, which underlies and interfingers with the Savage Mountain Formation in the McConnell Creek map area.

### ***Sustut Group***

The Sustut Group (Lord, 1948; Eisbacher, 1974) consists of Upper Cretaceous to Eocene nonmarine clastic sedimentary rocks and intercalated tuffs that were deposited above Stikine Terrane and overlying Bowser Lake Group in central and northern British Columbia. The group is represented by exposures along the western boundary of the Takla Lake map area, west of the Takla fault. These rocks extend westward into the Hazelton map area (Richards, 1990; MacIntyre, 1998), at the south end of a belt that extends northwestward to the type area of the group along the Sustut River in the McConnell Creek map area (Lord, 1948).

The Sustut Group in the Takla Lake map area is entirely sedimentary, and has yielded collections of Cenomanian plant fossils (Armstrong, 1949). These rocks are therefore assigned to the basal unit of the group, the Tango Creek Formation, as defined by Eisbacher (1974). Most exposures are dominated by light brownish-weathering, well-indurated conglomerate containing clasts of chert, vein quartz, quartz tectonite, mafic to felsic volcanic rock, and a wide variety of plutonic clasts, including granite, granodiorite and monzonite. The conglomerates are generally poorly to moderately sorted, with rounded to subrounded cobbles and pebbles in a gritty sandstone matrix of similar composition. They occur as medium to very thick beds, locally intercalated with thinner beds of medium to coarse-grained sandstone and gritty sandstone. In some intervals conglomerate is absent and coarse sandstone occurs as thick to thin, planar to

lenticular beds that commonly contain abundant woody material. Both conglomerate and coarse sandstone-dominated intervals are interspersed with finer-grained rocks, at least in part as distinct fining-upwards sequences. The fine-grained rocks comprise thin beds of grey to green concretionary mudstone, siltstone and fine-grained sandstone, commonly containing fossil plant remains.

## **Jurassic and Cretaceous Plutonic Rocks**

### ***Northwest Arm Pluton***

The Northwest Arm pluton is a large, composite intrusion that cuts the Takla Group in the western part of the map area. It is well exposed along both shorelines of the Northwest Arm of Takla Lake, and also in the Takla Range to the north. Less extensive exposures are scattered through the area of more subdued topography south of the arm, north of Natowite Lake and the Sakeniche River.

The northern and western portions of the Northwest Arm pluton consist mainly of pink to red weathering, medium to coarse-grained quartz monzonite and monzogranite. These rocks typically comprise equigranular intergrowths of pink K-feldspar and lesser amounts of grey-green saussuritic plagioclase, together with 10 to 20 per cent quartz and 5 to 10 percent chloritized mafic grains. Grey, medium-grained hornblende diorite constitutes an older phase that occurs as screens within the quartz monzonite and locally forms an eastern border phase in the central part of the pluton. Similar diorite, together with monzodiorite and monzonite, forms much of the southeastern part of the pluton, in the area north of the Sakeniche River. Grey biotite  $\pm$ hornblende granodiorite is a third important phase that outcrops in the central part of the pluton on both shores of the Northwest Arm. It is in contact with quartz monzonite to the west, north and northeast, and with diorite and monzodiorite to the southeast, but its chronological relationship to these phases was not established.

Westernmost exposures of plutonic rock on the south shore of the Northwest Arm comprise diorite and microdiorite that are in contact with quartz monzonite to the east. These dioritic rocks are in part heavily fractured and pervaded by quartz stockwork veins. They may be a western border phase of the Northwest Arm pluton, or might be part of a different plutonic body that is juxtaposed against the Northwest Arm pluton across the southern continuation of the Takla fault (Figure 4-3).

The age of the Northwest Arm pluton is presently unknown, but U-Pb isotopic dating of samples collected during the 1997 field season is in progress. It is suspected that these plutonic rocks correlate with either the Late Triassic-Early Jurassic Topley intrusive suite, or the Middle Jurassic Tachek suite described by MacIntyre *et al.* (1998).

### ***Takla Landing Pluton***

Sparse exposures of pink-weathering monzogranite and quartz-feldspar porphyry directly east of Takla Landing comprise part of a narrow wedge that has been

traced for almost 20 km to the north (Scharizza and Payie, 1997; Figure 4-3). The plutonic rocks within this wedge are juxtaposed against the Sustut Group to the west, across the Takla fault, and are in contact with the Sitlika western clastic unit to the east. Pink-weathering monzogranite that outcrops on the south side of Takla Lake, directly south of Takla Landing, is presumed to be part of the same plutonic body (Figure 4-3). These rocks are also truncated by the Takla fault to the west, but are in presumed intrusive contact with Takla Group volcanics to the east. They are lithologically very similar to the northern and western portions of the Northwest Arm pluton, and contain xenoliths of diorite and monzonite that likewise resemble older phases of the larger pluton to the south. A sample of monzogranite from the Takla Landing pluton, collected about 11 km north of Takla Landing in 1996, has yielded a U-Pb zircon date of 169.1 ± 1.0/-4.8 Ma (R. Friedman, written communication, 1997). This late Middle Jurassic date is somewhat younger than U-Pb and Ar-Ar ages reported for the lithologically similar Tachek intrusions, which cut the Takla Group to the south in the vicinity of Babine and Tochcha lakes (MacIntyre *et al.*, 1998).

### **Purvis Lake Stock**

A small intermediate to mafic stock, measuring about 3.5 km by 1.5 km, intrudes the Cache Creek metasedimentary unit a short distance northwest of Purvis Lake. It consists mainly of medium-grained, equigranular hornblende diorite to quartz diorite. Older phases include clinopyroxenite and gabbro, which are locally common as xenoliths and screens within the diorite. Younger phases are represented mainly by dikes, and include microdiorite, monzonite and tonalite. The Purvis Lake stock is undated, but is suspected to be Middle Jurassic based on tentative correlation with the Stag Lake - Twentysix Mile Lake plutonic suite described from the Fort Fraser and Hallet Lake map areas to the south (Whalen and Struik, 1997; Anderson *et al.* 1997).

### **Mitchell Batholith**

Granitic rocks of the Mitchell batholith underlie the core of the Mitchell Range, and intrude both the Cache Creek Group and the Sitlika assemblage. The batholith is about 25 km long, north to south, and up to 15 km wide. The northern part is dominated by light grey, massive, coarse-grained, ±hornblende-biotite monzogranite, commonly with potassium feldspar phenocrysts up to 1.5 cm in size. An earlier phase, consisting of fine to medium grained, mafic-rich biotite-hornblende quartz diorite to diorite, is common along the east-central and northwestern margins of the pluton. The southern part of the batholith, south of Nesabut Peaks, consists mainly of massive, equigranular, medium to coarse-grained biotite granodiorite, locally with conspicuous muscovite flakes. This phase, which is thought to be younger than the K-feldspar megacrystic monzogranite that dominates the northern part of the pluton, is locally intruded by thick dikes of quartz-feldspar porphyry.

The western part of the Mitchell batholith intrudes the eastern clastic unit of the Sitlika assemblage, while to the

east it intrudes both the ultramafic and sedimentary units of the Cache Creek Group. The thrust contact between the Cache Creek ultramafic unit and structurally underlying Sitlika metasedimentary rocks is truncated by the batholith 3 km southeast of Klowkut Peak. This same contact abuts the southern end of the pluton 10 km east of Takla Narrows, but there the contact is defined by a relatively young northeast-striking fault. Contact metamorphic effects of the batholith were studied in the Cache Creek ultramafic unit east of Nesabut Peaks by Elliot (1975). He found that serpentinite changed to talc-olivine rock within 2.5 to 3 km of the batholith contact, which in turn progressed to an olivine-enstatite-anthophyllite zone about 1.5 km from the contact. Contact metamorphic effects on the Sitlika eastern clastic unit are generally conspicuous for about a kilometre from the batholith contact, where semi-pelitic rocks become biotite-quartz hornfels and calcareous intervals are characterized by calc-silicate hornfels and marble, locally with small garnets.

The Mitchell batholith is not yet dated, but is suspected to be Late Jurassic or Early Cretaceous based on its lithological similarity to the Francois Lake plutonic suite which outcrops extensively near Fraser Lake, 130 km to the south-southeast (Whalen and Struik, 1997; Anderson *et al.*, 1997). A sample of K-feldspar megacrystic monzogranite, collected from the northeastern part of the pluton, has been submitted for U-Pb dating of zircons. This will establish the age of the main phase of the Mitchell batholith, and will provide a minimum date for west-directed thrusting of the Cache Creek ultramafic unit above the Sitlika eastern clastic unit.

### **Leo Creek Stock**

The Leo Creek stock consists of medium to coarse-grained ±muscovite-biotite granodiorite that is exposed along the lower reaches of Leo Creek, on the northeast side of southern Takla Lake (Figure 4-3). It resembles granodiorite that comprises the southern part of the Mitchell batholith, just 3 km to the north, and is presumed to be the same age. The Leo Creek stock intrudes the Sitlika eastern clastic unit to the north. It is apparently in contact with the Cache Creek sedimentary unit to the southwest, but the nature of this contact is obscured by Takla Lake.

### **Pyramid Peak Pluton**

Biotite granodiorite exposed on the southwest side of southern Takla Lake is part of a large pluton that extends southward into the Tochcha Lake map area, where it is referred to as the Pyramid Peak pluton by MacIntyre *et al.* (1998). The granodiorite intrudes hornfelsed argillite just west of the southern tip of Takla Lake, and locally contains screens and pendants of similar hornfelsed argillite, together with calc-silicate rock and marble. These rocks are tentatively assigned to the eastern clastic unit of the Sitlika assemblage. To the west, however, the pluton is in contact with the sedimentary unit of the Cache Creek Group. This contact is not exposed in the Takla Lake area, but is locally well-defined in the Tochcha Lake area, where

it is interpreted as an intrusive contact (MacIntyre *et al.*, 1998).

The age of the Pyramid Peak pluton is presently unknown, but samples have been submitted for U-Pb and Ar-Ar radiometric dating. It is lithologically similar to the Leo Creek stock, and is likewise thought to be Late Jurassic or Early Cretaceous. Furthermore, like the Leo Creek stock it intrudes the Sitlika eastern clastic unit to the east, and is in contact with the Cache Creek sedimentary unit to the west. The two intrusive bodies are therefore suspected to be offset portions of a single pluton, presently separated from one another by about 8 km of apparent dextral displacement along the northeast-striking Purvis Lake fault.

## STRUCTURE

### Mesoscopic Fabrics

All three units of the Sitlika assemblage are characterized by a single penetrative cleavage or schistosity defined by the preferred orientation of greenschist facies metamorphic minerals and variably flattened clastic grains or volcanic fragments. The cleavage dips steeply to the east or east-northeast through most of the Sitlika belt, although steep westerly dips prevail locally. It is axial planar to upright folds of bedding, most commonly observed in the well-bedded eastern clastic unit, with axes that plunge north-northwest or south-southeast. Younger folds and crenulations with similarly oriented axes deform the cleavage locally, as do rare east or west plunging kink folds and crenulations.

Volcanic flows and breccias of the Takla Group do not generally display a tectonic foliation. Associated fine-grained sedimentary rocks, however, commonly contain a moderately to strongly developed slaty cleavage, and intercalated conglomerates contain clasts that are variably flattened in the plane of this cleavage. Although their metamorphic mineralogy has not been studied, these clastic sedimentary rocks do not appear to differ significantly from metasedimentary rocks within the western clastic unit of the Sitlika assemblage.

The Cache Creek Group comprises greenschist facies rocks that are of comparable metamorphic grade to the Sitlika assemblage, but contrast markedly in structural style (Paterson, 1974; Schiarizza and Payie, 1997; Wright, 1997). Mesoscopic structures are best displayed in the sedimentary unit, where compositional layering has been transposed into parallelism with a prominent metamorphic foliation. In the main belt of Cache Creek rocks, along the eastern margin of the map area, this schistosity most commonly dips at moderate angles to the east or northeast, and may be related to east-dipping thrust(?) faults that separate the Cache Creek ultramafic unit from the overlying sedimentary unit and the underlying Sitlika eastern clastic unit (*see* later section). In detail, however, the schistosity and compositional layering are variable in orientation, largely due to reorientation by later structures. These younger structures are represented mainly by a set

of east-verging folds with moderately west-dipping axial surfaces, generally marked by a crenulation or fracture cleavage. The axes of these folds, along with associated crenulation lineations, plunge gently north to north-northwest through most of the area, but display southerly plunges in the south. Metamorphic minerals that define the first generation schistosity are, at least in part, bent and kinked by these younger structures, indicating that these folds postdated most of the metamorphism.

### Macroscopic Structure of the Sitlika Assemblage

The volcanic and eastern clastic units of the Sitlika assemblage are folded through a southerly-plunging anticline/syncline pair in the vicinity of Mount Bodine (Schiarizza and Payie, 1997; Figure 4-3). The volcanic unit on the western limb of the syncline extends southward for more than 50 km through the Takla Lake area as a simple homocline. Schistosity dips steeply east to northeast through most of the belt, but locally fans through the vertical to attain steep westerly dips in the eastern part of the unit. Bedding was observed only locally within the belt; it dips at moderate to steep angles eastward, typically with shallower dips than the associated schistosity.

The eastern clastic unit forms a relatively wide outcrop belt to the east of the volcanic unit. Where observed, west of Mount Bodine and on the shore of Takla Lake, the base of the unit is an east-dipping stratigraphic contact with the underlying volcanic unit. The eastern contact of the unit is an east-dipping thrust fault at the base of the Cache Creek ultramafic unit. Internally, the eastern clastic unit is folded through numerous north-northwest to south-southeast plunging synmetamorphic folds, although none of these structures has been mapped out in detail.

The western clastic unit forms a continuous narrow belt west of the volcanic unit. It is characterized by steeply east-dipping schistosity and subparallel to more gently east-dipping bedding. Where observed, on the railway tracks southeast of Takla Landing, the eastern contact dips steeply east, and is concordant to schistosity in both the western clastic unit and the overlying volcanic unit. As discussed previously, there is some evidence for shearing along this contact, but it is not clear whether or not it is a major fault. To the west, the western clastic unit is in contact with Takla Group volcanics southeast of Takla Lake, and with plutonic rocks of the Takla Landing pluton to the north. These contacts were not observed, but are suspected to be faults.

### East-dipping Thrust Faults along the Sitlika - Cache Creek Contact

Monger *et al.* (1978) referred to the contact between the Cache Creek Group and Sitlika assemblage as the Vital fault, which they described as "a zone of imbricated alpine-type peridotite and basalt up to 3 kilometres wide with fault planes dipping easterly at about 50 degrees". This fault zone corresponds to the Cache Creek ultramafic

unit of this report. Observations made during the 1996 and 1997 field seasons confirm that the Cache Creek ultramafic unit is, at least in part, bounded by east-dipping faults. Locally however, such as along the northerly-trending fault segment east of Diver Peak (Figure 4-2), the Sitlika - Cache Creek contact is marked by a system of dextral strike-slip faults (Schiarizza and Payie, 1997). These dextral faults are inferred to be relatively young structures, perhaps contemporaneous with the Tertiary Takla and Pinchi fault systems, which postdate the east to northeast-dipping fault that marks the contact elsewhere.

Structural relationships between the mappable units of the Cache Creek Group are best exposed in the Kenny Creek - Mount Olson area, where east-dipping faults, parallel to the penetrative east-dipping foliation, were observed at the contact between the ultramafic unit and overlying sedimentary and volcanic rocks in several places (Schiarizza and Payie, 1997). Kinematic indicators were observed at only one locality, east of Mount Bodine, where asymmetric fabrics within east-dipping shear zones indicate west-directed thrust movement along the fault that separates the sedimentary unit from the underlying ultramafic unit. This same fault contact has been traced southward for more than 50 km through the eastern part of the Takla Lake map area (Figure 4-3). The actual contact was not observed along this segment, but the predominantly easterly-dipping foliation is consistent with the interpretation that the sedimentary unit is structurally above the ultramafic unit throughout most of the belt. A narrow panel of metasedimentary rocks that outcrops to the west of the ultramafic unit, south of Nesabut Peaks, is interpreted as an outlier of the sedimentary unit, repeated by a synformal structure along the southeast margin of the Mitchell batholith.

The contact between the ultramafic unit and the Sitlika eastern clastic unit is fairly well constrained in the northern part of the Takla Lake map area, between Kenny Creek and the Mitchell Range, but was actually seen only to the east of Klowkut Peak (Figure 4-3). There, the ultramafic unit rests above the eastern clastic unit across a gently to moderately-dipping fault that is folded through an antiform/synform pair just north of its truncation by the Mitchell batholith. No kinematic indicators were observed along this segment of the fault. Just to the north however, south of Tsayta Lake, easternmost exposures of the eastern clastic unit contain east-northeast dipping thrust faults that are sub-parallel to foliation. These mesoscopic faults are inferred to be parallel, and related to, the contact with the immediately adjacent ultramafic rocks. The Cache Creek - Sitlika contact is obscured by the Mitchell batholith in most of the Mitchell Range, but was also mapped over a limited area south of the pluton. The contact was not observed in this area, but is mapped as a northeast-dipping thrust fault based on relationships to the north.

The northeast-dipping faults discussed above are apparently part of an extensive west-directed thrust system that places the Cache Creek Group above the Sitlika assemblage and its correlatives. This thrust system has been mapped in the western Axelgold Range at the north end of the Stuart Lake belt (Monger, 1977a; Monger *et al.*, 1978); in northern British Columbia where it separates the

Cache Creek Group from the Sitlika-correlative King Salmon allochthon (Nahlin fault: Monger *et al.*, 1978; Thorstad and Gabrielse, 1986); and in southern British Columbia where it separates the Cache Creek Group from Sitlika-correlative rocks in the northeastern Taseko Lakes map area (Read, 1992, 1993). The timing of thrusting is not well constrained in central British Columbia, but may be Late Jurassic or younger based on the involvement of Oxfordian strata in west-directed thrusting northwest of the present study area (Monger *et al.*, 1978). The pending U-Pb date from the Mitchell batholith may further constrain the timing of this deformation, as the batholith truncates the east-dipping fault that juxtaposes the Cache Creek ultramafic unit above the Sitlika eastern clastic unit.

## Contact Between the Sitlika Assemblage and the Takla Group

The contact between the Sitlika assemblage and the Takla Group is interpreted as a fault because the Permian volcanic unit faces east, but is juxtaposed against the younger Takla Group to the west. The western clastic unit is the general locus of this fault but, as discussed previously, it is not clear if the main fault is located at the eastern, western or both contacts. The presently preferred interpretation is that the western clastic unit correlates with Triassic sedimentary rocks of the Takla Group, and the main fault separates these rocks from the structurally overlying Sitlika volcanic unit. The 80-kilometre-long strike-length of the narrow western clastic unit suggests that these relatively weak sedimentary rocks might correspond to a flat within a westerly-directed thrust system, possibly related to the system that imbricates the Cache Creek Group and juxtaposes it above the Sitlika eastern clastic unit at higher structural levels to the east. This is consistent with relationships farther to the north, where westerly-directed thrust faults imbricate Stikine Terrane and Bowser basin strata, as well as structurally overlying Sitlika and Cache Creek rocks (Monger *et al.*, 1978). The steep dip of this fault system in the Takla Lake area may relate to rotation during translation and gradual northward truncation of the footwall along the younger Takla fault system (Figure 4-3).

## Takla Fault

The Takla fault (Armstrong, 1949) is interpreted as one component of a Late Cretaceous to early Tertiary dextral strike-slip fault system that may have a cumulative displacement of about 300 kilometres (Monger *et al.*, 1978; Gabrielse, 1985). It is not exposed, but its north-striking trace is fairly well defined near the western edge of the Takla Lake map area, where it separates the Upper Cretaceous Sustut Group from the Takla Group and associated plutonic rocks of the Northwest Arm and Takla Landing plutons. South of Takla Landing, monzogranite of the Takla Landing pluton adjacent to the inferred trace of the fault is cut by numerous northerly-striking faults containing gently-plunging slickensides and mineral fibres, some with accretion steps indicating dextral movement.

Northeast-trending folds mapped within the Sustut Group directly west of the fault (Schiarizza *et al.*, 1997) and in the Takla Group directly east of the fault (Armstrong, 1949) are of an appropriate orientation to be related to dextral movement on the Takla fault (Wilcox *et al.*, 1973).

### Northeast Striking Faults

Northeast striking faults, commonly along prominent topographic lineaments, correspond to apparent dextral displacements of the northwest trending stratigraphic and structural contacts at several places within the Takla Lake map area (Figure 4-3). These include a four-kilometre-offset of the thrust contact between the Cache Creek Group and Sitlika assemblage east of Tsayta Lake, and an eight-kilometre-offset of plutonic rocks and adjacent Cache Creek and Sitlika rocks along the Purvis Lake - Bivouac Creek - Gloyazikut Creek lineament near the southern boundary of the map area. These northeast striking faults are relatively young features, as they offset the Takla fault and related structures (Schiarizza *et al.*, 1997) which are probably of Tertiary age. They might be broadly related to strike-slip faulting on the Takla system, or might reflect a discrete younger event.

## MINERAL OCCURRENCES

### Chromite Occurrences within the Cache Creek Ultramafic Unit

Cache Creek ultramafic rocks in the Stuart Lake belt host a number of chromite occurrences, many of which were discovered in the early 1940s during regional mapping of the Fort St. James map area by the Geological Survey of Canada (Armstrong, 1949). A large proportion of these occurrences are in the present map area, mainly in the wide belt of ultramafic rocks that borders the eastern margin of the Mitchell batholith, east of Nesabut Peaks (Figure 4-4). These occurrences were studied in detail by Whittaker (1982, 1983; Whittaker and Watkinson, 1984), who identified 17 separate chromite concentrations. Some of these have been combined for the purposes of MINFILE, which lists 8 chromite occurrences in this area (093N 033, 034, 035, 036, 037, 038, 039, 129). Other chromite occurrences in the map area, identified by Armstrong but not included in Whittaker's study, are the Leo Creek showing (093N 040) directly south of the Mitchell batholith, and the Cyprus showing (093N 016), about 3.5 km east-southeast of Klowkut Peak, directly north of the batholith.

The Simpson prospect (093N 033), southeast of Nesabut Peaks, was staked by Hunter Simpson and Associates in 1941, but no work was recorded and the claims were allowed to lapse (Armstrong, 1949). The area of the Cyprus occurrence (093N 016), which had previously been staked by the Magnum Corporation, was restaked by Imperial Metals Corporation in 1986 and evaluated by a program of soil sampling, geological mapping and lithochemical analyses (Taylor, 1987). However, no

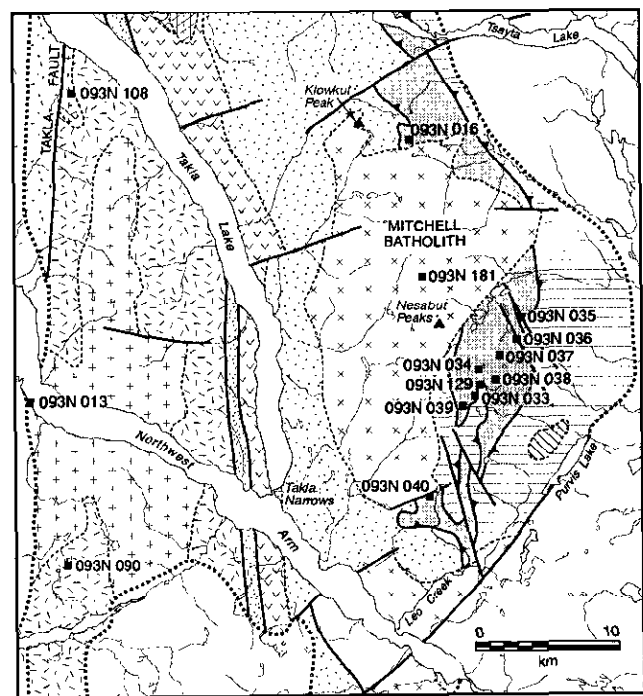


Figure 4-4. Locations of MINFILE occurrences in the Takla Lake map area. For legend see Figure 4-3.

anomalous metal targets thought to be worthy of follow-up were defined, and the claims were allowed to lapse. No other exploration work has been recorded on the ultramafic rocks in the Mitchell Range (Hancock, 1991).

The chromite occurrences in the Mitchell Range comprise discontinuous layers and pods of massive (more than 95%) to heavily disseminated (more than 75%) chromite (Whittaker, 1983; Whittaker and Watkinson, 1984). The host rocks are mainly tectonized harzburgite, although one layer of heavily disseminated chromite at the Bob prospect (MINFILE 093N 034) is hosted by dunite. Some chromite layers and pods are in sharp contact with harzburgite, while others are separated from the harzburgite by a thin dunitic selvage. Individual layers and pods range from a few centimetres to a few metres in longest dimension, are typically aligned with the harzburgite foliation, and display a range of deformational features, including schlieren structure, pinch-and-swell, boundinage and folding. Whittaker and Watkinson (1984) suggest that the Mitchell Range occurrences were derived from a chromitiferous zone in refractory harzburgite of upper mantle origin, which became extended and deformed during upper mantle tectonism and also during later obduction of the ultramafic rocks.

Ultramafic rocks in the vicinity of the Cyprus occurrence (093N 016), southeast of Klowkut Peak, locally display discontinuous zones of listwanite or quartz-carbonate alteration. Taylor (1987) reports that a sample taken from a copper-stained quartz-carbonate fracture-filling, 150 m east of the fault contact with the Sitlika eastern clastic unit, yielded 345 ppb Au. Veins and listwanite-altered zones containing anomalous gold concentrations are also known from the Cache Creek ultramafic unit east and northeast of Mount Bodine, 25 to

30 km north-northeast of the Cyprus occurrence (Schiarizza and Payie, 1997).

### Copper Occurrences within Stikine Terrane

Chalcopyrite mineralization has been reported from three separate areas within Stikine Terrane near the western edge of the Takla Lake map area (Figure 4-4). The northernmost is the Bol occurrence (MINFILE 093N 108), located on the southwest side of Takla Lake about 8 km south of Takla Landing. This area was explored by Helicon Explorations Limited and Magnum Consolidated Mining Co. Ltd. in 1966 and 1967 (Annual Report of the Minister of Mines for 1966, page 119; Annual Report of the Minister of Mines for 1967, page 119). The mineralization apparently comprises chalcopyrite within intrusive rocks along the eastern margin of the Takla Landing pluton. However, no detailed descriptions of the mineralization or exploration work are available.

The Adda occurrence (MINFILE 093N 013) is near the south shore of the Northwest Arm of Takla Lake, 18 km west-northwest of Takla Narrows, where several narrow veins of chalcopyrite were reported to occur within andestitic volcanics (Annual Report of the Minister of Mines for 1930, page A149). There has been no recent work on this showing, and it was not located during the present study. Outcrops along the shoreline near the poorly constrained MINFILE location are of fractured diorite containing quartz stockwork and quartz-calcite-chlorite veins. These rocks may be a western border phase of the Northwest Arm pluton, or may represent a separate unit, juxtaposed against the Northwest Arm pluton across an important splay of the Takla fault.

The Lucy occurrence (MINFILE 093N 090) is 4 km north of Natowite Lake and 15 km west-southwest of Takla Narrows. It is hosted by volcanic rocks of the Takla Group which are partially enclosed by two different phases of the Northwest Arm pluton; granite on the northwest and diorite to monzonite on the east. The showing was first described in 1968, as minor pyrite and chalcopyrite in small quartz veins and shears cutting intermediate volcanic rock, following a program of geological mapping and soil sampling conducted over the Lucy claims by Texas Gulf Sulphur Company (Annual Report of the Minister of Mines and Petroleum Resources for 1968, page 148). However, no assessment report was filed and the claims were allowed to lapse. The area was restaked as the Nato claims by Rio Algom Exploration Inc. in 1991, after anomalous copper values were discovered during a regional lake sediment survey. A program of reconnaissance soil sampling, rock sampling, geological mapping and prospecting was conducted over these claims in 1992, and rocks in the vicinity of the showing were described as andesites showing moderate chloritization, silicification and epidote-calcite veining, with up to 5% pyrite and traces of chalcopyrite and magnetite (Casselman and Campbell, 1992). There has been no subsequent work reported, and the Nato claims lapsed in 1993.

### Don Molybdenum Occurrence

The Don occurrence (MINFILE 093N 181) is within the east-central part of the Mitchell batholith, about 4 km north of Nesabut Peaks (Figure 4-4). Quartz-molybdenite veinlets, 1 mm to 2 cm thick, form a stockwork across several widely spaced, weakly kaolinized zones within a medium-grained, equigranular, biotite quartz monzonite stock that intrudes coarse-grained porphyritic monzogranite that forms the dominant phase of the pluton (Kimura, 1978). The Endako Mines Division of Placer Development Limited explored the area with soil geochemical surveys in 1978 and two short drill holes in 1980. One of the drill holes intersected a quartz vein containing a small clot of molybdenite, chalcopyrite and pyrite (Buckley, 1980), but the results did not encourage further work and the claims were allowed to lapse.

### Gold Nation Occurrence

The Gold Nation occurrence consists of gold-bearing quartz veins within syenite dikes that cut the Sitlika eastern clastic unit, 4.5 km due west of the west end of Tsayta Lake. The main showing is accessed by a short spur road that branches westward from the Driftwood Forest Service road near the 54 kilometre marker. The mineralization was discovered by prospector Efreem Specogna in July 1992, and staked as the Julio 1-16 mineral claims. Huntington Resources Inc. expanded the property with the addition of the Gold Nation 1-5 claims in the fall of 1983, and carried out a geological, geochemical and geophysical exploration program in the summer of 1994 (Gruenwald and Montgomery, 1994). No further assessment work was recorded, however, and the claims have lapsed.

The Gold Nation property is underlain mainly by medium to dark grey phyllite, recrystallized limestone and sandstone of the Sitlika eastern clastic unit. The metasedimentary rocks are cut by a system of fine-grained syenitic dikes, ranging from 0.5 m to almost 3 m in width. Dike rocks commonly contain finely disseminated pyrite, and locally are heavily veined with milky quartz containing pyrite and traces of chalcopyrite and altaite (PbTe). Gold values reportedly range up to .280 oz/ton at the Main showing, and .667 oz/ton at the Creek showing, 1 km to the south (Gruenwald and Montgomery, 1994). A sample of vein material collected from the main showing during this year's mapping program contained 434 ppb Au.

### ACKNOWLEDGMENTS

We thank Sheldon Modeland, Michelle Lepitre, Stephen Munzar, Ryanne Metcalf and Deanne Tackeberry for their cheerful and capable contributions to our field program. We also thank Bert Struik and his crew, of the Geological Survey of Canada, for informative discussions, field trips and joint fieldwork. We are grateful to Bob Wellington of Pacific Western Helicopters Ltd. for providing safe and reliable helicopter transportation, and

thank Carol, Dieter and Mary Ann Berg for their hospitality during our stay at Takla Rainbow Lodge. We acknowledge Verna Vilkos for the time and care she put into preparing the figures for this report, and Bill McMillan for editing the manuscript and suggesting improvements.

## REFERENCES CITED

- Anderson, R.G., L'Heureux, R., Wetherup, S. and Letwin, J.M. (1997): Geology of the Hallett Lake Map Area, Central British Columbia: Triassic, Jurassic, Cretaceous, and Eocene? Plutonic Rocks; in Current Research 1997-A, *Geological Survey of Canada*, pages 107-116.
- Armstrong, J.E. (1949): Fort St. James Map-Area, Cassiar and Coast Districts, British Columbia; *Geological Survey of Canada*, Memoir 252, 210 pages.
- Ash, C.H. and Macdonald, R.W.J. (1993): Geology, Mineralization and Litho-geochemistry of the Stuart Lake Area, Central British Columbia (Parts of 93K/7, 8, 10 and 11); in Geological Fieldwork 1992, *B.C. Ministry of Energy, Mines and Petroleum Resources*, Paper 1993-1, pages 69-86.
- Bellefontaine, K.A., Legun, A., Massey, N.W.D. and Desjardins, P. (1995): Mineral Potential Project - Northeast B.C., Southern Half; *B.C. Ministry of Energy, Mines and Petroleum Resources*, Open File 1995-24.
- Bridge, D.A., Marr, J.M., Hashimoto, K., Obara, M. and Suzuki, R. (1986): Geology of the Kutcho Creek Volcanogenic Massive Sulphide Deposits, Northern British Columbia; in Mineral Deposits of Northern Cordillera, Morin, J.A., editor, *The Canadian Institute of Mining and Metallurgy*, Special Volume 37, pages 115-128.
- Buckley, P. (1980): Diamond Drilling Report for Don 1 Mineral Claim, Omineca Mining Division; *B.C. Ministry of Energy, Mines and Petroleum Resources*, Assessment Report 8357.
- Casselman, S.G. and Campbell, E.A. (1992): Nato Claims, NTS 93N/4, Geology and Geochemistry; *B.C. Ministry of Energy, Mines and Petroleum Resources*, Assessment Report 22 645.
- Childe, F. and Thompson, J.F.H. (1995): U-Pb Age Constraints and Pb Isotopic Signature of the Kutcho VMS Deposit: Implications for the Terrane Affiliation of the Kutcho Formation, North-Central British Columbia; *Geological Association of Canada - Mineralogical Association of Canada*, Annual Meeting, Victoria, B.C., Program and Abstracts, Volume 20, page A-17.
- Childe, F.C., Thompson, J.F.H., Mortensen, J.K., Schiarizza, P., Bellefontaine, K. and Marr, J. (1996): Primitive Permo-Triassic Volcanism in the Canadian Cordillera: Terrane Implications; *Geological Society of America*, 1996 Annual Meeting, Abstracts with Program, page A312.
- Childe, F.C., Friedman, R.M., Mortensen, J.K. and Thompson, J.F.H. (1997): Evidence for Early Triassic Felsic Magmatism in the Ashcroft (92I) Map Area, British Columbia; in Geological Fieldwork 1996, *B.C. Ministry of Employment and Investment*, Paper 1997-1, pages 117-123.
- Childe, F.C. and Schiarizza, P. (1997): U-Pb Geochronology, Geochemistry and Nd Isotopic Systematics of the Sitlika Assemblage, Central British Columbia; in Geological Fieldwork 1996, *B.C. Ministry of Employment and Investment*, Paper 1997-1, pages 69-77.
- Cordey, F. and Struik, L.C. (1996a): Scope and Preliminary Results of Radiolarian Biostratigraphic Studies, Fort Fraser and Prince George Map Areas, Central British Columbia; in Current Research 1996-A, *Geological Survey of Canada*, pages 83-90.
- Cordey, F. and Struik, L.C. (1996b): Radiolarian Biostratigraphy and Implications, Cache Creek Group of Fort Fraser and Prince George Map Areas, Central British Columbia; in Current Research 1996-E, *Geological Survey of Canada*, pages 7-18.
- Eisbacher, G.H. (1974): Sedimentary History and Tectonic Evolution of the Sustut and Sifton Basins, North-Central British Columbia; *Geological Survey of Canada*, Paper 73-31, 57 pages.
- Elliot, A.J.M. (1975): Geology and Metamorphism of the Mitchell Mountains Ultramafite, Fort St. James Map Area, British Columbia; unpublished M.Sc. thesis, *University of British Columbia*, 113 pages.
- Ferri, F. and Melville, D.M. (1994): Bedrock Geology of the Germansen Landing - Manson Creek Area, British Columbia (94N/9, 10, 15; 94C/2); *B.C. Ministry of Energy, Mines and Petroleum Resources*, Bulletin 91, 147 pages.
- Gabrielse, H. (1985): Major Dextral Transcurrent Displacements along the Northern Rocky Mountain Trench and Related Lineaments in North-central British Columbia; *Geological Society of America*, Bulletin, Volume 96, pages 1-14.
- Ghent, E.D., Erdmer, P., Archibald, D.A. and Stout, M.Z. (1996): Pressure - Temperature and Tectonic Evolution of Triassic Lawsonite - Aragonite Blueschists from Pinchi Lake, British Columbia; *Canadian Journal of Earth Sciences*, Volume 33, pages 800-810.
- Gruenwald, W. and Montgomery, R. (1994): Geochemical and Geophysical Report on the Gold Nation Property, Omineca Mining Division; *B.C. Ministry of Energy, Mines and Petroleum Resources*, Assessment Report 23 502.
- Hancock, K.D. (1991): Ultramafic Associated Chromite and Nickel Occurrences in British Columbia; *B.C. Ministry of Energy, Mines and Petroleum Resources*, Open File 1990-27.
- Kimura, E.T. (1978): Geochemical Report, Don and John Mineral Claims, Omineca Mining Division; *B.C. Ministry of Energy, Mines and Petroleum Resources*, Assessment Report 6814.
- Lord, C.S. (1948): McConnell Creek Map-Area, Cassiar District, British Columbia; *Geological Survey of Canada*, Memoir 251, 72 pages.

- MacIntyre, D.G. (1998): Babine Porphyry Belt Project: Bedrock Geology of the Nakinilerak Lake Map Sheet (93M/8), British Columbia; in Geological Fieldwork 1997, *B.C. Ministry of Employment and Investment*, Paper 1998-1, this volume.
- MacIntyre, D.G. and Struik, L.C. (1997): Nechako Natmap Project - 1996 Overview; in Geological Fieldwork 1996, *B.C. Ministry of Employment and Investment*, Paper 1997-1, pages 39-45.
- MacIntyre, D.G. and Struik, L.C. (1998): Nechako Natmap Project - 1997 Overview; in Geological Fieldwork 1997, *B.C. Ministry of Employment and Investment*, Paper 1998-1, this volume.
- MacIntyre, D.G., Ash, C. and Britton, J. (1994): Mineral Potential - Skeena-Nass Area; *B.C. Ministry of Energy, Mines and Petroleum Resources*, Open File 1994-14.
- MacIntyre, D.G., Legun, A., Bellefontaine, K.S. and Massey, N.W.D. (1995): Mineral Potential Project - Northeast B.C., Northern Half; *B.C. Ministry of Energy, Mines and Petroleum Resources*, Open File 1995-6.
- MacIntyre, D.G., Schiarizza, P. and Struik, L.C. (1998): Preliminary Bedrock Geology of the Tochcha Lake Map Sheet (93K/13), British Columbia; in Geological Fieldwork 1997, *B.C. Ministry of Employment and Investment*, Paper 1998-1, this volume.
- MacIntyre, D.G., Webster, I.C.L. and Bellefontaine, K.A. (1996): Babine Porphyry Belt Project: Bedrock Geology of the Fulton Lake Map Area (93L/16), British Columbia; in Geological Fieldwork 1995, Grant, B. and Newell, J.M., editors, *B.C. Ministry of Energy, Mines and Petroleum Resources*, Paper 1996-1, pages 11-35.
- Mihalynuk, M.G. and Cordey, F. (1997): Potential for Kutcho Creek Volcanogenic Massive Sulphide Mineralization in the Northern Cache Creek Terrain: A Progress Report; in Geological Fieldwork 1996, *B.C. Ministry of Employment and Investment*, Paper 1997-1, pages 157-170.
- Monger, J.W.H. (1969): Stratigraphy and Structure of Upper Paleozoic Rocks, Northeast Dease Lake Map-Area, British Columbia (104J); *Geological Survey of Canada*, Paper 68-48.
- Monger, J.W.H. (1975): Upper Paleozoic Rocks of the Atlin Terrane, Northwestern British Columbia and South-central Yukon; *Geological Survey of Canada*, Paper 74-47.
- Monger, J.W.H. (1977a): The Triassic Takla Group in McConnell Creek Map-Area, North-Central British Columbia; *Geological Survey of Canada*, Paper 76-29, 45 pages.
- Monger, J.W.H. (1977b): Upper Paleozoic Rocks of Northwestern British Columbia; in Report of Activities, Part A, *Geological Survey of Canada*, Paper 77-1A, pages 255-262.
- Monger, J.W.H. and Church, B.N. (1977): Revised Stratigraphy of the Takla Group, North-Central British Columbia; *Canadian Journal of Earth Sciences*, Volume 14, pages 318-326.
- Monger, J.W.H. and Paterson, I.A. (1974): Upper Paleozoic and Lower Mesozoic Rocks of the Omineca Mountains; in Report of Activities, Part A, *Geological Survey of Canada*, Paper 74-1A, pages 19-20.
- Monger, J.W.H., Price, R.A. and Tempelman-Kluit, D.J. (1982): Tectonic Accretion and the Origin of the Two Major Metamorphic and Plutonic Belts in the Canadian Cordillera; *Geology*, Volume 10, pages 70-75.
- Monger, J.W.H., Richards, T.A. and Paterson, I.A. (1978): The Hinterland Belt of the Canadian Cordillera: New Data from Northern and Central British Columbia; *Canadian Journal of Earth Sciences*, Volume 15, pages 823-830.
- Nelson, J.L. and Bellefontaine, K.A. (1996): The Geology and Mineral Deposits of North-Central Quesnellia; Tezzeron Lake to Discovery Creek, Central British Columbia; *B.C. Ministry of Energy, Mines and Petroleum Resources*, Bulletin 99, 112 pages.
- Nelson, J., Bellefontaine, K., Green, M. and MacLean, M. (1991): Regional Geological Mapping near the Mount Milligan Copper-Gold Deposit (93K/16, 93N/1); in Geological Fieldwork 1990, *B.C. Ministry of Energy, Mines and Petroleum Resources*, Paper 1991-1, pages 89-109.
- Orchard, M.J. and Struik, L.C. (1996): Conodont Biostratigraphy, Lithostratigraphy and Correlation of the Cache Creek Group near Fort St. James, British Columbia; in Current Research 1996-A, *Geological Survey of Canada*, pages 77-82.
- Panteleyev, A. and Pearson, D.E. (1977a): Kutcho Creek Map-Area (104I/1W); in Geology in British Columbia 1975; *B.C. Ministry of Energy, Mines and Petroleum Resources*, pages G87-G93.
- Panteleyev, A. and Pearson, D.E. (1977b): Kutcho Creek Map-Area (104I/1W); in Geological Fieldwork 1976, *B.C. Ministry of Energy, Mines and Petroleum Resources*, pages 74-76.
- Paterson, I.A. (1974): Geology of Cache Creek Group and Mesozoic Rocks at the Northern End of the Stuart Lake Belt, Central British Columbia; in Report of Activities, Part B, *Geological Survey of Canada*, Paper 74-1, Part B, pages 31-42.
- Paterson, I.A. (1977): The Geology and Evolution of the Pinchi Fault Zone at Pinchi Lake, Central British Columbia; *Canadian Journal of Earth Sciences*, Volume 14, pages 1324-1342.
- Paterson, I.A. and Harakal, J.E. (1974): Potassium-Argon Dating of Blueschists from Pinchi Lake, Central British Columbia; *Canadian Journal of Earth Sciences*, Volume 11, pages 1007-1011.
- Pearson, D.E. and Panteleyev, A. (1975): Cupriferous Iron Sulphide Deposits, Kutcho Creek Map-Area (104I/1W); in Geological Fieldwork 1975, *B.C. Ministry of Energy, Mines and Petroleum Resources*, pages 86-92.
- Read, P.B. (1992): Geology of Parts of Riske Creek and Alkali Lake Areas, British Columbia; in Current Research, Part A, *Geological Survey of Canada*, Paper 92-1A, pages 105-112.

- Read, P.B. (1993): Geology of Northeast Taseko Lakes Map Area, Southwestern British Columbia; in Current Research, Part A, *Geological Survey of Canada*, Paper 93-1A, pages 159-166.
- Richards, T. A. (1990): Geology of Hazelton Map Area (93M); *Geological Survey of Canada*, Open File 2322.
- Ross, J.V. (1977): The Internal Fabric of an Alpine Peridotite near Pinchi Lake, Central British Columbia; *Canadian Journal of Earth Sciences*, Volume 14, pages 32-44.
- Schiarizza, P. and Payie, G. (1997): Geology of the Sitlika Assemblage in the Kenny Creek - Mount Olson Area (93N/12, 13), Central British Columbia; in Geological Fieldwork 1996, *British Columbia Ministry of Employment and Investment*, Paper 1997-1, pages 79-100.
- Schiarizza, P., Payie, G., Holunga, S., and Wright, D. (1997): Geology, Mineral Occurrences and Geochemistry of the Kenny Creek - Mount Olson Area (93N/12, 13), British Columbia; *British Columbia Ministry of Employment and Investment*, Open File 1997-2.
- Struik, L.C. (1993): Intersecting Intracontinental Tertiary Transform Fault Systems in the North American Cordillera; *Canadian Journal of Earth Sciences*, Volume 30, pages 1262-1274.
- Struik, L.C., Floriet, C. and Cordey, F. (1996): Geology Near Fort St. James, Central British Columbia; in Current Research 1996-A, *Geological Survey of Canada*, pages 71-76.
- Taylor, A.B. (1987): Geology and Geochemistry of the Cyprus Claims, Mitchell Range; *B.C. Ministry of Energy, Mines and Petroleum Resources*, Assessment Report 16 095.
- Thompson, J.F.H., Barrett, T.J., Sherlock, R.L. and Holbek, P. (1995): The Kutcho VMS Deposit, British Columbia: A Felsic Volcanic-Hosted Deposit in a Tholeiitic Bimodal Sequence; *Geological Association of Canada - Mineralogical Association of Canada*, Annual Meeting, Victoria, B.C., Program and Abstracts, Volume 20, page A-104.
- Thompson, M.L. (1965): Pennsylvanian and Early Permian Fusulinids From Fort St. James Area, British Columbia, Canada; *Journal of Paleontology*, Volume 39, pages 224-234.
- Thorstad, L.E. and Gabrielse, H. (1986): The Upper Triassic Kutcho Formation, Cassiar Mountains, North-Central British Columbia; *Geological Survey of Canada*, Paper 86-16, 53 pages.
- Tipper, H.W. and Richards, T.A. (1976): Jurassic Stratigraphy and History of North-Central British Columbia; *Geological Survey of Canada*, Bulletin 270, 73 pages.
- Umhoefer, P.J. and Schiarizza, P. (1996): Latest Cretaceous to Early Tertiary Dextral Strike-slip Faulting on the Southeastern Yalakom Fault System, Southeastern Coast Belt, British Columbia; *Geological Society of America*, Bulletin, Volume 108, pages 768-785.
- Whalen, J.B. and Struik, L.C. (1997): Plutonic Rocks of Southeast Fort Fraser Map Area, Central British Columbia; in Current Research 1997-A, *Geological Survey of Canada*, pages 77-84.
- Wetherup, S. and Struik, L.C. (1996): Vanderhoof Metamorphic Complex and Surrounding Rocks, Central British Columbia; in Current Research 1996-A, *Geological Survey of Canada*, pages 63-70.
- Wheeler, J.O. and McFeely, P. (1991): Tectonic Assemblage Map of the Canadian Cordillera and Adjacent Parts of the United States of America; *Geological Survey of Canada*, Map 1712A, scale 1:2 000 000.
- Whittaker, P.J. (1982): Chromite Occurrences in Mitchell Range Ultramafic Rocks of the Stuart Lake Belt, Cache Creek Group (93N) in Geological Fieldwork 1981, *B.C. Ministry of Energy, Mines and Petroleum Resources*, pages 234-243.
- Whittaker, P.J. (1983): Geology and Petrogenesis of Chromite and Chrome Spinel in Alpine-type Peridotites of the Cache Creek Group, British Columbia; unpublished Ph.D. thesis, *Carleton University*, 339 pages.
- Whittaker, P.J. and Watkinson, D.H. (1984): Genesis of Chromitite from the Mitchell Range, Central British Columbia; *Canadian Mineralogist*, Volume 22, pages 161-172.
- Wilcox, R.E., Harding, T.P. and Seely, D.R. (1973): Basic Wrench Tectonics; *American Association of Petroleum Geologists*, Bulletin, Volume 57, pages 74-96.
- Wright, D.M. (1997): Metamorphic Geology of the Kenny Creek - Mount Olson Map Area: Implications for the Relationship Between the Sitlika Assemblage and Cache Creek Group, Central British Columbia; unpublished B.Sc. thesis, *University of Victoria*, 75 pages.





## QUATERNARY GEOLOGY AND ICE-FLOW STUDIES IN THE SMITHERS AND HAZELTON MAP AREAS (93 L AND M): IMPLICATIONS FOR EXPLORATION

By Victor M. Levson, B.C. Geological Survey, Andrew J. Stumpf, University of New  
Brunswick, and Andrew J. Stuart, University of Waterloo

**KEYWORDS:** Applied geochemistry, ice-flow history, glaciation, mineral exploration, surficial geology, Quaternary stratigraphy

published as part of this work throughout the study area (Figure 5-1). Regional geochemical surveys conducted in the province in 1997 are discussed by Jackaman *et al.* (1998).

### INTRODUCTION

This paper provides an overview of surficial geology, ice flow history, Quaternary stratigraphy and preliminary till geochemistry studies conducted in the Smithers and Hazelton map areas (NTS 93 L and M) by the British Columbia Geological Survey in 1997. These studies are part of the Nechako National Mapping (NATMAP) Project, coordinated by the Geological Survey of Canada and the British Columbia Geological Survey. A summary of results of associated surficial geology mapping and regional till geochemistry surveys previously conducted in parts of the Anahim, Nechako, Smithers and Hazelton map areas (93 C, F, L and M, respectively) was provided by Levson and Giles (1997).

The main objectives of these surficial geology studies are to understand and map the distribution of Quaternary deposits, decipher the glacial history and ice-flow patterns, and locate areas most suitable for conducting drift exploration programs. Stratigraphic and sedimentologic studies of Quaternary deposits are conducted in order to define the glacial history and aid in interpreting till geochemical data.

### RELATED STUDIES

Reconnaissance (1:250 000-scale) mapping of Quaternary deposits in the Interior Plateau was conducted by Tipper (1971). Wittneben (1981) completed 1:50 000 scale terrain mapping in parts of the Hazelton map sheet (NTS 93 M/NW, NE, SW). More recently, Plouffe (1994, 1996) completed several 1:100 000-scale surficial geology maps in the central part of the Nechako Plateau. The surficial geology of the Babine region (93L/16, M/1, M/8) was described by Levson *et al.* (1997a). A summary of 1:50,000 scale surficial geology mapping, conducted as part of the NATMAP and Interior Plateau programs, was provided by Levson and Giles (1997). Nine regional (1:50 000-scale) surficial geology maps have been

### FIELD PROCEDURES

Procedures used in these surficial geology studies included compilation of existing terrain-mapping data, interpretation of air photographs, field checking, and stratigraphic and sedimentologic investigations of Quaternary exposures in the study areas. Ice-flow history was largely deciphered from measurement of the orientation of crag-and-tail features, flutings, drumlins and striae. Reconnaissance ice flow studies were conducted in the Smithers (93 L) and Hazelton (93 M) map areas, and to a lesser extent in the Terrace (103 I) and Whitesail (93 E) map areas.

### PHYSIOGRAPHY AND LANDFORMS

The study area is largely within the Nechako Plateau, an area of low relief, flanked by the Hazelton Mountains to the west, the Skeena Mountains to the north and the Omineca Mountains to the east. Surface elevations generally range from about 1200 to 1500 metres in the Nechako Plateau. Flat lying or gently dipping Tertiary lava flows, locally forming steep escarpments, cover older rocks throughout much of the plateau. Glacial drift is extensive and often as little as 5 per cent of the bedrock is exposed.

Well developed flutings and drumlinoid ridges are dominant landform features on the plateau. Stagnant ice topography, large esker complexes, glaciofluvial deposits and meltwater channels that developed during deglaciation are also present in many areas. Much of the variation in topography and differences in surficial geology in the plateau are due to these features. Extensive belts of glaciolacustrine sediments occur in low-lying regions, generally below 950 metres elevation, in valleys such as those now occupied by Nechako River, Babine Lake, and Nechako Reservoir. Topography in these areas is subdued and older glacial landforms are often difficult to identify.

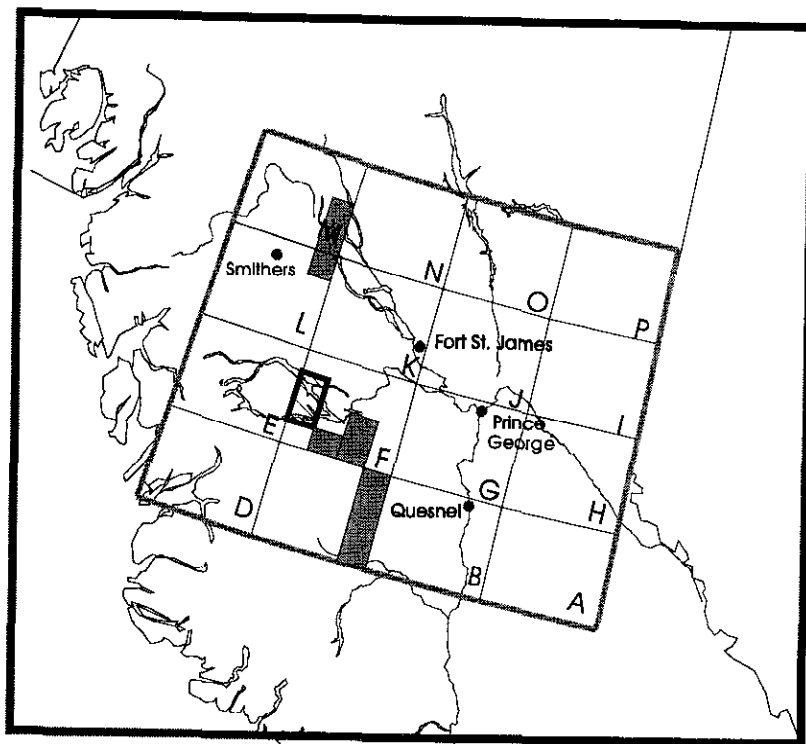


Figure 5-1. Location map of the study region. Outline shows area of surficial geology mapping conducted in 1997 (93F/5, 12); shaded blocks are previously mapped 1:50,000 scale map areas.

## 1997 TILL GEOCHEMISTRY SURVEYS

The primary objectives of till geochemical studies conducted in the region were to identify geochemically anomalous sites that might reflect areas of buried mineralization and to investigate patterns of glacial dispersal. Several regional till geochemistry surveys have been conducted in the Nechako Plateau for this purpose (Levson and Giles, 1997; Levson *et al.*, 1997b). Regional till geochemical sampling in 1997 was initiated on the Tetachuck Lake (93 F/5) and Marilla (93 F/12) 1:50,000 map sheets (Figure 5-1) where over 100 samples were collected. The 1997 regional program was combined with preliminary surficial geology mapping. Descriptions of the sampling medium, sampling methods used, types of data collected, laboratory analyses and quality control methods are provided by Levson *et al.* (1997b).

## QUATERNARY STRATIGRAPHY

The Quaternary stratigraphy of the study area has been reconstructed from a number of exposures in the region. Quaternary sediments underlying till are rarely exposed in the region. The most complete stratigraphic sections encountered mainly occur in the vicinity of the Nechako Reservoir (Levson and Giles, 1997). The stratigraphic record of pre-Late Wisconsinan events

elsewhere in the area was largely removed during the last glaciation.

Morainal sediments in the Nechako Plateau region were assigned by Tipper (1971) to the Fraser glaciation which is dated in several parts of British Columbia as Late Wisconsinan (Ryder and Clague, 1989). A Late Wisconsinan age for the last glaciation in the region is also indicated by radiocarbon dates on wood and mammoth bones recovered from lacustrine deposits under till at the Bell Copper mine (NTS 93 L/16) on Babine Lake. Single fragments of spruce (*Picea* sp.) and fir (*Abies* sp.), yielding dates of  $42\,900 \pm 1860$  years B.P. (GSC-1657) and  $43\,800 \pm 1830$  years B.P. (GSC-1687), and a date of  $34\,000 \pm 690$  years B.P. (GSC-1754) on mammoth bone collagen from the interglacial sediments (Harrington *et al.*, 1974), indicate that the overlying till was deposited during the Late Wisconsinan glaciation.

The Quaternary stratigraphy of the Nechako Reservoir area was described by Levson and Giles (1997) and is summarized here. A widespread, massive diamicton unit, interpreted as a till, is stratigraphically underlain both by stratified sands and gravels, of inferred fluvial and glaciofluvial origin, and by horizontally bedded sand, silt and clay sequences, interpreted to be advance-phase glaciolacustrine sediments. The upper part of the older glaciofluvial sequence locally contains sand wedges and dikes that may be relict permafrost features formed in cold environments just prior to the last glaciation. Advance-

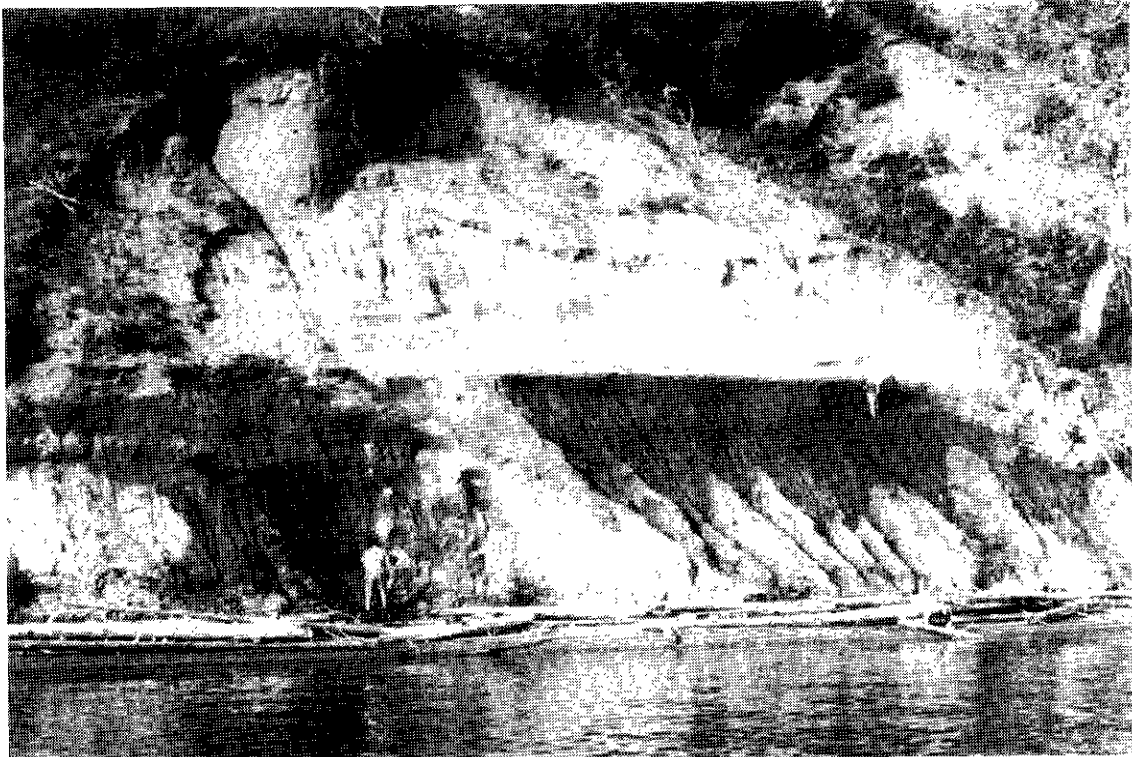


Photo 5-1. Interstadial site on Chelasie Arm of Tetachuck Lake. Organic-bearing lacustrine silts and clays in the lower part of the section (dark unit) are overlain by glaciofluvial sands and gravels (light unit) and capped by a thin till (1-2 m thick at section top). Rare fragments of wood occur in the sand and gravel sequence (see text for discussion).

phase glaciolacustrine deposits are rarely seen, but they are locally well preserved and include well bedded fine sands and silts with dropstones. Compressive deformation structures, such as shear planes, occur near the base of the till, and overturned folds and thrust faults, interpreted as glaciotectonic structures, are locally present in the upper part of the underlying sediments.

Loose, massive to stratified, sandy diamictons of inferred debris-flow origin are commonly interbedded with gravels and sands that both underlie and overlie till. They often have loaded or gradational contacts with the interbedded sediments. These deposits indicate that debris-flow deposition occurred during both the advance and retreat phases of the last glaciation in both subaerial glaciofluvial and subaqueous glaciolacustrine environments.

A new interstadial site discovered on the shores of Chelasie Arm on the Nechako Reservoir, reveals a thick sequence of lacustrine, glaciolacustrine and glaciofluvial deposits (Photo 5-1) that are overlain by till deposited during the last glaciation. These deposits are locally capped by post-glacial gravels and sands. The lowest exposed unit consists of well stratified, locally deformed, dense, fine sands, silts and clays. These sediments are interpreted as lacustrine and glaciolacustrine deposits. The lacustrine deposits near the middle of the lower unit (Photo 5-1) contain fine organic detritus that yielded a radiocarbon date of  $27,790 \pm 200$  BP (Beta-101017).

A thick unit of gravels and sands (Photo 5-1) that overlies the lacustrine and glaciolacustrine deposits is

interpreted as a glaciofluvial sequence that was deposited during the advance phase of the last glaciation in the region. The sand and gravel sequence is sharply overlain by a massive, matrix supported, dense, silty diamicton, interpreted as till. The upper part of the diamicton is less dense, has a gravelly-sand matrix and locally is crudely bedded. This unit probably was deposited as a series of debris flows during deglaciation.

## ICE-FLOW HISTORY

During Late Wisconsinan glaciation, ice moved east and northeast into the Nechako Plateau from the Coast and Hazelton mountains and southeast from the Skeena Mountains, before flowing easterly and northeasterly towards the Rocky Mountains (Tipper, 1971, Levson and Giles, 1997). In the eastern Nechako Plateau, results of ice-flow studies indicate that in most areas there was one dominant flow direction during the Late Wisconsinan glaciation, that shifted from southeast, in the north part of the plateau (Babine Lake region), to east in the central part (Francois Lake area) and east-northeast in the south (Nechako Reservoir area; Levson and Giles, 1997). However, in the western Nechako Plateau and in the adjoining Babine Range and Hazelton Mountains, anomalous westerly ice-flow indicators are present and indicate a regional, west to southwest flow event, extending over much of west central British Columbia (Figure 5-2; Levson *et al.*, 1997a). Results suggest this

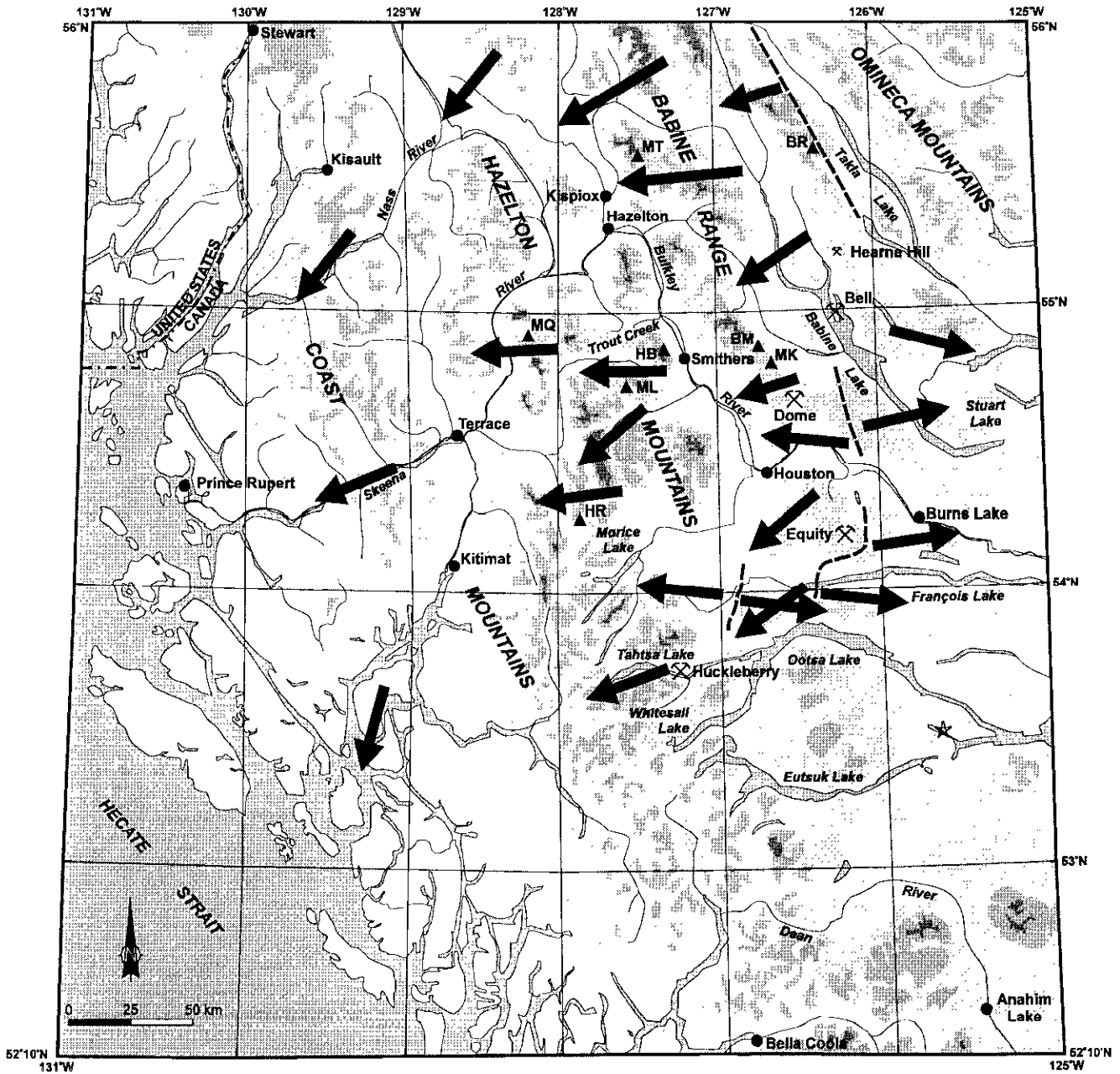


Figure 5-2: Inferred ice flow directions in west central British Columbia at the last glacial maximum. Paleoflow directions shown in the Nass River valley, and west of Terrace and Kitimat are from McCuaig (1997) and Claguc (1984), respectively. Dashed lines represent the easternmost position of ice divides inferred from available data. Ice divides may have extended further east at the glacial maximum and, during late glacial times, they locally shifted further west. Shaded contour intervals are 1000, 1500 and 2000 m above sea level. Star in lower right shows location of section in Photo 5-1.

was a more recent and widespread event than previously thought (Stumpf *et al.*, in prep). This new data is significant for drift exploration programs in central British Columbia and may be useful for modelling ice sheet dynamics and climate change.

Indications of this westerly ice-flow event include well developed *roche-moutonnée*, drumlinoids and rat-tails (Photos 5-1 and 5-2) that indicate ice-flow toward the west over the Babine Range and Hazelton Mountains. In many areas this westerly flow was independent of topography as indicated, for example, by upslope flows in the Dome Mountain area (Figure 5-2, see also Levson *et al.*, 1997a, Photo 9). Similar westerly ice-flow indicators were previously reported in the Babine Range and in the vicinity of the Equity Silver mine (Tipper, 1994). This study has extended their distribution further to the south, west and east and new evidence on the timing of this event has important implications for the Quaternary history of the region. West ice flow extends across the area bounded to the north by the Skeena Mountains, to the northeast by the Omineca Mountains, and to the southeast by François and Ootsa lakes. The northwest and southern limits of this anomalous westerly flow have not yet been defined.

At the Late Wisconsinan glacial maximum, ice covered all but the highest peaks in the region and movement appears to have been relatively unaffected by topography. In the Bait Range for example, the ice surface was in excess of 1950 metres as indicated by glacial erratics and regionally trending striae and flutings on top of Frypan Peak (elevation 1931 m, Levson *et al.*, 1997a). At the height of the last glaciation, ice flowed from ice domes/divides located to the east of the Babine Lake valley toward the Coast. Ice overtopped most mountain peaks with elevations up to at least 2200 m (upper limit of ice defined by striae at sites on Hudson Bay Mountain (HB) at 2212 m or 7300 feet; Southern Babine Mountains (BM) at 2239 m or 7390 feet; Howson Range (HR) at 2206 m or 7280 feet, Figure 5-2). Preserved evidence of west flow is not restricted to elevations above 2000 m but occurs at lower elevations on mountains such as Mount McKendrick (1742 m) and Mount Leach (1822 m, sites MK and ML, respectively on Figure 5-2), and also is present locally along valley bottoms such as the Babine Lake valley, especially in the lee of topographic obstructions, where it was preserved from later valley-parallel flow. Cross-cutting striae observed at several locations suggest that the westward event occurred at the maximum of the Late Wisconsinan glaciation, after glacier advance along valleys and prior to late-stage, retreat-phase flow that was topographically controlled in some areas. Topographic control of ice flow in a few areas in the Nechako Plateau during early glacial phases is indicated by local, valley-parallel striae on bedrock surfaces that are buried by thick till sequences (Levson and Giles, 1997).

Westerly ice flow in this region appears to have continued into the later stages of the last glaciation as indicated by stratigraphic, lithologic and geomorphic criteria (Levson *et al.*, 1997a). This includes the presence of westerly ice-flow indicators at the surface in areas where preservation from later ice erosion would not likely

occur (*e.g.* in stoss-side positions). For example, westerly ice-flow indicators in the Dome Mountain area (Figure 5-2) are preserved on the top of the mountain as well as on the east side at relatively low elevations. During the last glaciation, ice flowed along the east side of the mountain from the Babine Lake area and would have eroded or at least partially obscured the exposed features on the east side of the mountain. In addition, investigations of glacial dispersal in surface tills in these areas indicate westerly dispersal. Tracing of erratics with distinctive lithologies and known source areas in the Babine Mountains, for example, has shown substantial westerly and upslope transport of the erratics from their source areas. At sites northwest of Mount Thomlinson and northeast of Mount Quinlan (MT and MQ, respectively, on Figure 5-2), indicator lithologies were identified which have sources to the northeast. Similarly, previous studies in the vicinities of the Bell (Stumpf *et al.*, 1997) and Equity Silver mines (Ney *et al.*, 1972) have identified southwest directed transport of material in till and soil from mineralized bedrock.

Tipper (1994) postulated that westerly ice flow patterns in the southern Babine Mountains and in the Equity Silver area (Figure 5-2) represented a relict flow pattern from an earlier glaciation or possibly from an early phase of the last glaciation when movement of ice towards the Coast Mountains occurred as the result of the development of an ice dome in the central part of the Interior Plateau. Levson *et al.* (1997a), however, inferred that the westerly ice-flow features that they observed in 1996 formed during the later part of the Late Wisconsinan glaciation. The main evidence of this is the preservation of westerly trending paleoflow indicators at low elevations in the Babine and Bulkley valleys at sites that would not have been protected from later valley-parallel (southeasterly) flow. Levson *et al.* (1997a) suggested that rapid calving of tidewater glaciers in large valleys on the west side of the Coast Mountains, such as the Skeena River valley, may have resulted in a draw-down of ice in that area. Rapid calving and significant lowering of the ice surface in these valleys may have resulted in the eastern migration of ice divides, the 'capture' of glacial ice from east of the Coast Mountains and reversal of ice flow into valleys such as the Skeena and its tributaries. This hypothesis is consistent with the development of westerly ice flow indicators late in the last glaciation and with their relatively limited extent. However, the full extent, timing and duration of this westerly ice flow event and its influence on glacial dispersal was the subject of further research in 1997 and it is now known that the westerly ice-flow event was more extensive than previously thought. Evidence for late westerly flow was found not only in the southern Babine Mountains but also in the central and northern Babine Range and over a large area in the Hazelton Mountains (Figure 5-2). In addition, westerly ice flow indicators were found at a number of low elevation sites in east-trending valleys such as the Morice Lake and Trout Creek valleys (Figure 5-2). The main exception to this was found in a few valleys with headwaters in high mountain areas, such as the Telkwa River valley, where indicators of late-stage, down-valley (easterly) flows were observed. These

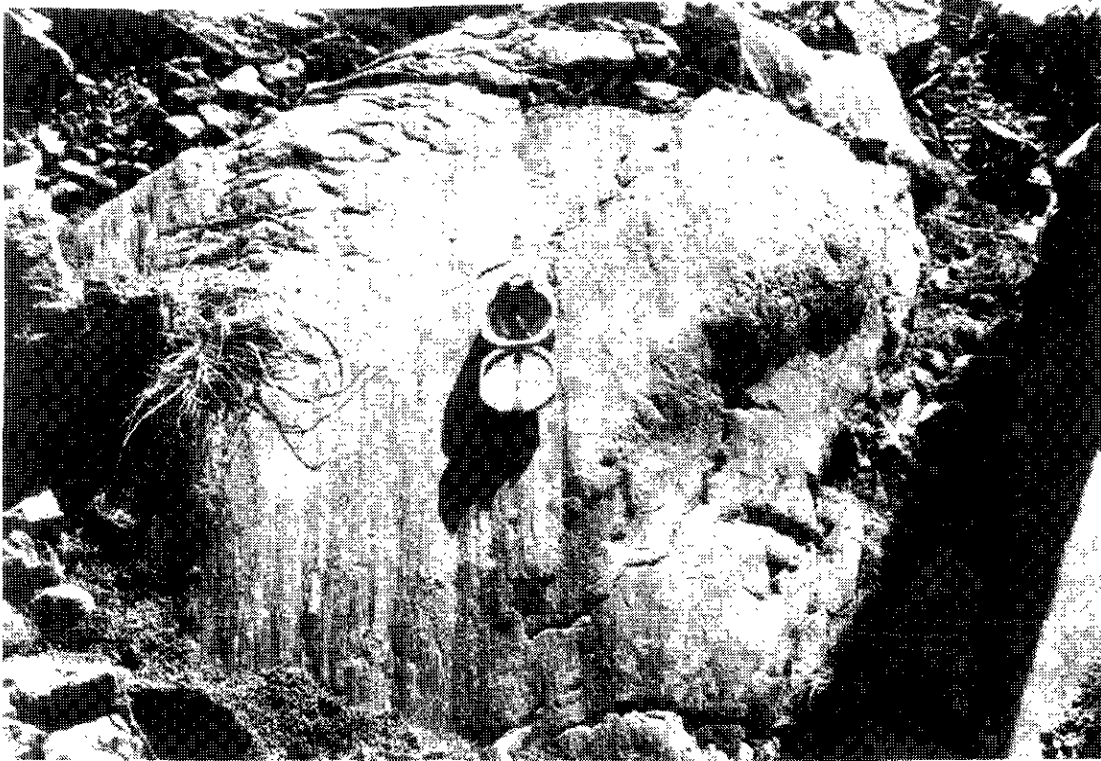


Photo 5-2. Striae with directional indicators on bedrock in the Bait Range (site BR on Figure 5-2).



Photo 5-3. Fluted ridges and drumlinoid forms on a unnamed mountain top northwest of Smithers in the Hazelton Mountains (near site MQ on Figure 5-2). Palaeoflow is left to right (west) at this site.

observations have led to the expansion of our hypothesis for the westerly event. We now propose a working model suggesting that an extensive, maximum phase, ice divide, or series of smaller divides, formed in the central part of the Nechako Plateau (east of the Babine Mountains). This ice divide persisted until near the end of the Late Wisconsinan and was not modified by late-stage, topographically-controlled, ice flow except in areas of strong alpine glaciation. Valleys in the Hazelton Mountains such as the Morice Lake and Skeena River valleys and their tributaries, that have low elevation passes that open westward into Pacific Ocean drainages, did not experience late-stage flow reversals, unlike more constricted valleys fed by high mountain alpine glaciers such as the Telkwa River valley.

During deglaciation, ice flow was increasingly controlled by topography as the glaciers thinned. Striae and other ice-flow indicators that locally diverge from the regional trend reflect this topographically influenced ice-flow during waning stages of glaciation. A more complex local ice-flow history is indicated by highly variable striae trends at a few sites. Topographic control of ice flow during the latter phases is also apparent in many areas of high relief. In these areas, ice flow is clearly indicated by the presence of well developed cirque basins on the north and east facing sides of large mountains. During deglaciation, ice flow was increasingly controlled by topography as the glaciers thinned. Cirque glacier activity dominated during the later phases of the last glaciation and this activity may have extended into the Holocene.

## SUMMARY

Results of ice-flow studies indicate that for most areas in the eastern part of the Nechako Plateau, the dominant flow-direction was easterly. Glacial dispersal patterns appear to be dominated by this regional ice-flow direction. However, in the Babine and Hazelton Mountains and in the northwest part of the Nechako Plateau, a regionally anomalous, westerly ice-flow event occurred and dispersal directions are much more complex. Westerly ice flow in this region appears to have occurred at the last glacial maximum when ice centers over the Hazelton and Coast mountains migrated eastward into the interior plateau areas. The full extent and timing of this event and its effects on dispersal are currently being investigated (Stumpf *et al.*, in prep.). Evidence for west flow is most readily found west of the Babine Lake valley and diminishes eastward suggesting that the Babine valley was near the eastward limit of the divide or that ice-center migration east of that area was not long-lived. Consequently, westward flow apparently did not influence glacial dispersal to any great extent in valleys such as the Babine Lake valley but it did have a significant effect further west.

Westerly ice-flow locally extended to the end of the last glaciation, especially in valleys with large passes opening westward to the Pacific Ocean, such as the Skeena and Morice valleys. A postulated mechanism for maintenance of an interior ice-divide late into the last glaciation, is due to the rapid calving of tide-water

glaciers fed by ice in the interior. This may have allowed for significant lowering of glaciers in those valleys relative to ice in the interior and inhibition of topographically controlled, ice-flow reversals. Late glacial ice-flow, back to the east from the Hazelton Mountains, did occur in valleys with high or relatively restricted mountain passes such as the Telkwa River valley. Further east in the Babine Lake valley, late-glacial topographically controlled, eastward flow also occurred. However, since evidence for westward flow is preserved in the Babine Lake area and in other valleys at unprotected, low elevation sites, the erosional effects of the later, topographically-controlled flows must have been minimal. These observations suggest that the maximum buildup of interior ice extended late into the last glaciation and that a topographically controlled, late-glacial, ice-flow phase was short-lived in this part of the Nechako Plateau. In the Babine and Hazelton mountains, late-phase glaciers flowing down valleys that presently drain eastward, were probably restricted to alpine cirques and to valleys with relatively confined, high mountain passes. In other east-draining river valleys with wide passes to the Pacific, upslope westward flow apparently continued to the end of the last glaciation.

## ACKNOWLEDGMENTS

Quaternary stratigraphy and ice-flow studies in the area were conducted in collaboration with Alain Plouffe from the Geological Survey of Canada. The cooperation of Bert Struik and Alain Plouffe through the NATMAP program is much appreciated. Information in this paper pertaining ice flow studies in west central British Columbia are an integral part of Andrew Stumpf's Ph.D. dissertation research at the University of New Brunswick. Analytical assistance and quality control on all laboratory analyses were provided by Ray Lett. Sample preparation was completed by Rossbacher Laboratory Limited. Helicopter support was capably provided Karl Desjarlais of Highland Helicopters Limited.

## REFERENCES

- Clague, J.J. (1984): Quaternary geology and geomorphology, Smithers-Terrace-Prince Rupert area, British Columbia; *Geological Survey of Canada*, Memoir 413, 71 pages.
- Harrington, C.R., Tipper, H.W. and Mott, R.J. (1974): Mammoth from Babine Lake, British Columbia; *Canadian Journal of Earth Sciences*, Volume 11, pages 285 - 303.
- Jackaman, W., Cook, S.J. and Lett, R. (1998): Regional Geochemical Survey Program: Review of 1997 Activities; in *Geological Fieldwork 1996*, Lefebure, D.V. and McMillan, W.J. Editors, *British Columbia Geological Survey*, Paper 1998-1, this volume.

- Levson, V.M. and Giles, T.R. (1997): Quaternary Geology and Till Geochemistry Studies in the Nechako and Fraser Plateaus, Central British Columbia; in Interior Plateau Geoscience Project: Summary of Geological, Geochemical and Geophysical Studies, Diakow, L.J., and Newell, J.M., Editors, *Geological Survey of Canada Open File 3448 and British Columbia Geological Survey, Paper 1997-2*, pages 121-145.
- Levson, V.M., Stumpf, A.J., Meldrum, D.G., O'Brien, E.K., and Broster, B.E. (1997a): Quaternary geology and Ice Flow History of the Babine Lake Region: (NTS 93 L/16, M/1, M/8); in *Geological Fieldwork 1996*, Lefebure, D.V., McMillan, W.J. and McArthur, J.G, Editors, *British Columbia Geological Survey, Paper 1997-1*, pages 427-438.
- Levson, V.M., Meldrum, D.G., Cook, S.J., Stumpf, A.J., O'Brien, E.K., Churchill, C., Broster, B.E. and Coneys, A.M. (1997b): Till Geochemical Studies in the Babine Porphyry Belt: Regional Surveys and Deposit-Scale Studies (NTS 93 L/16, M/1, M/8); in *Geological Fieldwork 1996*, Lefebure, D.V., McMillan, W.J. and McArthur, J.G, Editors, *British Columbia Geological Survey, Paper 1997-1*, pages 457-466.
- McCuaig, S.J. (1997): Quaternary geology of the Nass River region, British Columbia: in *Current Research 1997-A*, *Geological Survey of Canada*, pages 183-189.
- Ney, C.S., Anderson, J.M. and Panteleyev, A. (1972): Discovery, geologic setting and style of mineralization, Sam Goosly deposit, B.C.; *Canadian Institute of Mining and Metallurgy Bulletin*: 7, pages 53-64.
- Plouffe, A. (1994): Surficial Geology, Chuchi Lake (93N/SE) and Tezzeron Lake (93K/NE), British Columbia; *Geological Survey of Canada, Open Files 2842 and 2846* (1:100 000 maps).
- Plouffe, A. (1996): Surficial Geology, Tsayta Lake (93N/SW), Fraser Lake (93K/SE), Cunningham Lake (93K/NW), Burns Lake (93K/SW), Manson Creek (93N/NE) and Old Hogem (93N/NW); *Geological Survey of Canada, Open Files 3071, 3182, 3183, 3184, 3312, and 3313* (1:100 000 maps).
- Ryder, J.M. and Clague, J.J. (1989): British Columbia Quaternary Stratigraphy and History, Cordilleran Ice Sheet; in *Quaternary Geology of Canada and Greenland*, Fulton, R.J., Editor, *Geological Survey of Canada, Geology of Canada, Number 1*, pages 48-58.
- Stumpf, A.J., Broster, B.E. and Levson, V.M. (1997): Evaluating the Use of Till Geochemistry to Define Buried Mineral Targets: A Case Study from the Bell Mine Property, (93 L/16, M/1) West-Central British Columbia; in *Geological Fieldwork 1996*, Lefebure, D.V., McMillan, W.J. and McArthur, J.G, Editors, *British Columbia Geological Survey, Paper 1997-1*, pages 439-456.
- Stumpf, A.J., Broster, B.E. and Levson, V.M. (in prep.): Interior Ice Domes and Divides, West-Central British Columbia, Canada; submitted to *Geology*.
- Tipper, H.W. (1971): Glacial Geomorphology and Pleistocene History of Central British Columbia; *Geological Survey of Canada, Bulletin 196*, 89 pages.
- Tipper, H.W., (1994): Preliminary Interpretation of Glacial Features and Quaternary Information from the Smithers Map Area (93 L), British Columbia; *Geological Survey of Canada, Open File 2837, Report with Map*, (scale 1:250,000).
- Witneben, U. (1981): Terrain Maps for the Hazelton Map Area (NTS 93 M/NW, NE, SE); *B.C. Ministry of Environment, Lands and Parks*, unpublished 1:50,000 scale maps.



## REGIONAL GEOLOGY AND MINERALIZATION OF THE BIG SALMON COMPLEX (104N NE AND 104O NW)

By Mitchell G. Mihalynuk, JoAnne Nelson and Richard M. Friedman

**KEYWORDS:** Big Salmon Complex, volcanogenic massive sulphide, regional geology, mineralization, Nisutlin Assemblage, Yukon-Tanana Terrane, Kootenay Terrane, Atlin, Jennings River

### INTRODUCTION

Reconnaissance mapping in the Big Salmon Complex in northwestern British Columbia (104N NE and 104O NW, Figure 1a) was initiated in 1997 to test long-standing correlations (e.g. Mulligan, 1963) with rocks of the Yukon-Tanana Terrane (formerly Yukon Group) in southern Yukon (Figure 1b). Such correlations are especially important from an economic standpoint (e.g. Nelson, 1997) because of the recently recognized potential for volcanogenic massive sulphide deposits in these rocks following discovery of the Kudz Ze Kayah, Wolverine and Fyre Lake deposits in the Yukon. A single traverse of the Big Salmon Complex by Nelson (1997) served to highlight similarities between stratigraphic elements in northern British Columbia and those at the Wolverine deposit. This report provides details on the stratigraphic and structural setting of the Big Salmon Complex, as well as mineral potential in light of strengthened correlations with Yukon-Tanana Terrane (YTT) in the Yukon.

Mapping was conducted over a six week period in July and early August. More than 90% of the region is below treeline in broad fluvially-modified glacial valleys occupied by the lower Swift River and its tributaries (Plate 1). Although fluvial and glacial deposits are tens to (?)hundreds of metres thick in the main Swift River valley, above an elevation of about 900 m, there is only a thin veneer of alluvium, colluvium or organic debris and bedrock exposures are common. Outcrop is much more abundant than indicated on previous maps. Most road construction, unless following valley bottoms or perched glacial terraces, exposes semi-continuous outcrop at elevations above 900m. Thus the deep roadwork along the new Alaska Highway Route and burrow pits (circa 1988) and access roads to mineral properties both north and south of the highway, provide good sections through stratigraphy. Logtung and Pure Silver access roads are washed out at 6.5 km and 5 km respectively and the Arsenault road is washed out at the Swift River, but all are passable by foot.

### TECTONIC FRAMEWORK

In British Columbia, protoliths of the Big Salmon Complex are composed primarily of quartz-rich sediments, mafic to felsic volcanic rocks and diorite, tonalite and

leucogranite intrusions; all are polydeformed and metamorphosed to grades ranging from greenschist to lower amphibolite facies. Previous work in the Big Salmon Complex of British Columbia show them to underlie a roughly triangular area bounded to the west by Teslin Lake (Teslin fault) in the Atlin area (Aitken, 1959) and to the southeast by the Simpson Peak batholith and other plutons in the Jennings River area (Gabielse, 1969). Both Aitken (1959) and Gabielse (1969) separated thick sections of crystalline limestone from the remainder of the Big Salmon Complex, and both considered the Big Salmon Complex to be at least partly correlative with the Sylvester Group. Prior to our 1997 mapping program, further regional subdivision and correlations had not been attempted in British Columbia.

Tempelman Kluit (1979) interpreted the Yukon rocks as a subduction/collisional complex (Teslin suture zone) comprised of dismembered ophiolite of the Anvil allochthon and siliceous cataclasite of the Nisutlin allochthon. Discovery of high pressure eclogite (Erdmer and Helmstaedt, 1983; Erdmer, 1985) supported the collisional concept and work along the western part of the Big Salmon Complex (Hansen, 1989, 1992a, 1992b; Hansen et al. 1989, 1991) appeared to outline a fossil Permo-Triassic subduction zone with offscraped sediments affected by tectonic backflow. Most recently, work by Stevens (1992, 1994), Stevens and Erdmer (1993), Stevens and Harms (1995) and Stevens et al. (1996) shows that the Teslin "suture zone" is comprised not of disparate offscraped oceanic sediments, but of continental margin strata (Creaser et al., 1995) with relatively coherent stratigraphic relationships that correlate with Lower to Middle Units (*sensu* Mortensen, 1992) of the Yukon-Tanana Terrane farther north. These workers have accordingly renamed the Teslin Suture zone as the Teslin Tectonic zone. In an even more extreme departure from the subduction zone interpretation, DeKeijzer and Williams (1997) subsequently remapped part of the Teslin Tectonic zone as a polydeformed nappe.

Strata of the YTT Lower and Middle Units do appear to extend south into British Columbia where they underlie most of what was formerly mapped as the Big Salmon Complex. Despite polyphase deformation and metamorphism, a good, persistent stratigraphy is preserved across the area and direct correlations can be made with the Lower and Middle units farther north (Figures 2, 3 and 4). Thus, rocks of the Big Salmon Complex in British Columbia are at least partly equivalent to those in the Finlayson Lake area which host the newly discovered deposits mentioned above. Our mapping does not support assignment of the Big Salmon Complex in British Columbia to the Slide Mountain Terrane as suggested by Wheeler and McFeely (1987), but would be more consistent with inclusion in their Kootenay Terrane

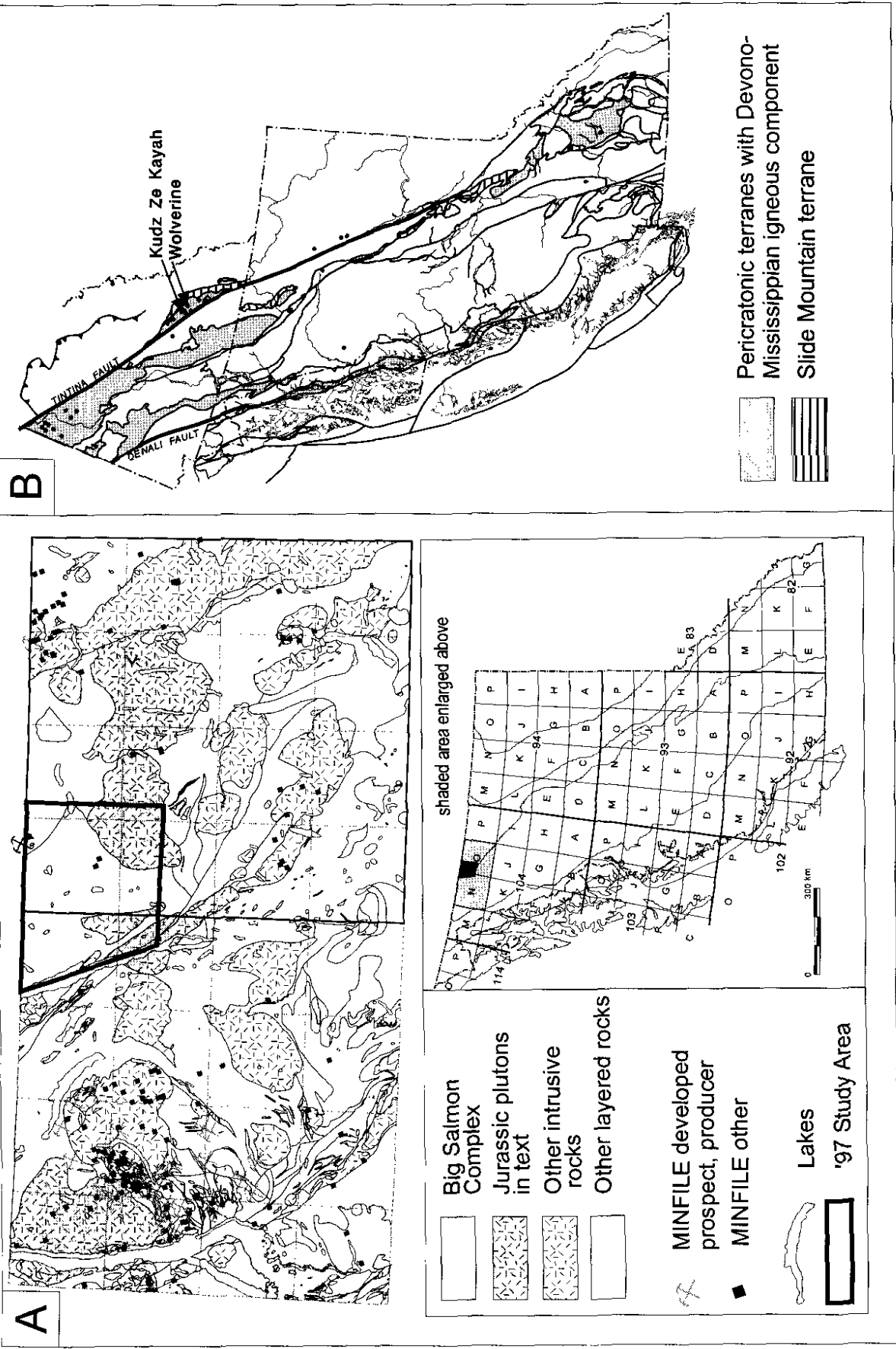


Figure 1A. Location map showing the regional geological setting of the Big Salmon Complex in British Columbia (after Mihalynuk et al., 1996). The area of Figure 2 is shown by the heavy outline. (B) map area in relation to Yukon-Tanana Terrane. Massive sulphide occurrences are shown by the black dots. Mineral deposits referred to in the text are labelled for reference.



(terminology also used by Gordey, 1995) which would include the Lower and Middle Units of the Yukon-Tanana as used by Mortensen (1992). A thick greenstone unit and overlying clastic strata within the Big Salmon Complex of British Columbia have no obvious correlatives within the Yukon-Tanana Terrane and may be considerably younger.

## GENERAL GEOLOGY

First order geological features in the Big Salmon Complex are a northwest-trending lower amphibolite grade "core zone" where protolith textures are mostly destroyed, flanked by greenschist grade rocks to both the southwest and northeast where relict protolith textures are relatively well preserved (Figure 2b). Mountain scale, southwest-verging folds and parasitic folds exert a fundamental control on the distribution of different units, but this distribution is complicated by both older and younger folding (see below). An early, nearly layer-parallel fabric is folded by the large scale folds and is commonly overprinted by a second schistosity imparted during the folding. Metamorphosed tonalite, lesser diorite and minor leucogranite, herein called the Hazel orthogneiss, dominate the north-central part of the core zone.

In general, lower, deeper parts of the stratigraphy have been more strongly deformed than presumably younger strata. No age data exists for layered rocks in the map area, but the youngest, weakly foliated and moderately lineated strata include conglomerates with phyllitic clasts that are probably derived from the underlying, previously metamorphosed units, implying at least some unconformable relationships.

## STRATIGRAPHIC FRAMEWORK

Stratigraphic associations that are well preserved and exposed on the less deformed flanks of the Big Salmon Complex can be traced into the higher grade interior. A sequence of four distinctive and contrasting units, locally displaying gradational contacts, provide the foundation for correlating from one area to another. From oldest to youngest they are: 30-150 m of buff to grey weathering limestone with metre-thick tuffaceous and thin quartzite layers; 20-50 m of thinly bedded, finely laminated manganeseiferous chert/quartzite with muscovite partings; 1200 m of tuffite-dominated greenstone; and a more than 150m thickness of sub-greenschist grade, brown to tan wacke, stretched quartzite-pebble and granule conglomerate and slate (Figure 4). Excellent preservation of protolith textures on the flanks of the Big Salmon Complex, including way-up indicators, permits moderately confident relative age assignment. Underlying this four-fold sequence is a lithologically variable succession, dominated by quartz-rich clastics with minor grey-weathering carbonate layers 1-10m thick and quartz-phyric volcanic tuff layers up to 40m thick, in which units in this variable package can be correlated only locally. More detailed lithologic descriptions, from oldest to youngest, are given below.



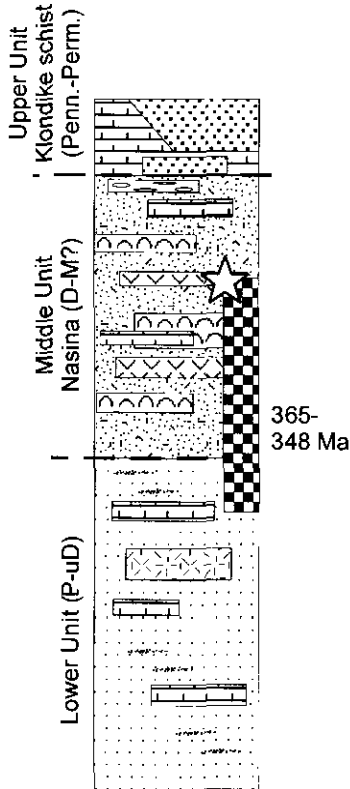
Plate 1. A view to the south from Mount Hazel towards the Swift River valley and low, tree-covered mountains beyond.

### **Graphitic quartz granule conglomerate - phyllite (>135m stratigraphic, 900m structural)**

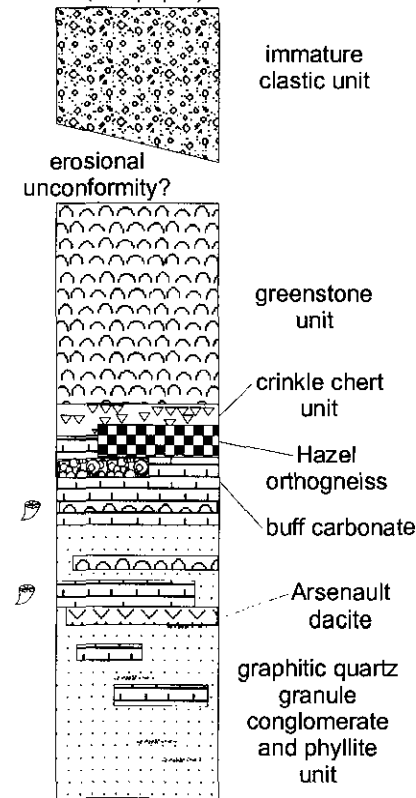
Bimodal black to silver grey, quartz-rich clastics dominate the lower part of the unit and persist in subequal amounts with combined chlorite phyllite (tuff?), carbonate and lineated quartzite in its upper parts. Protolith textures are best displayed in a borrow pit near the junction of Highway 97 and the Logtung property access road, but relict textures do occur intermittently throughout the map area. Coarse grit to granule conglomerates characterize the unit. These contain very clear to lesser milky blue quartz grains up to 4 mm in diameter which commonly comprise 4% of the rock, but are up to 40% of some layers that range from 0.5 to a few metres thick. Rounded to subangular quartz grains (50-80%) are supported by a phyllitic and schistose matrix of graphitic muscovite + feldspar. Argillite "granules" are preserved as pea-sized phyllitic smears. Dark grey graphitic phyllite forms decimetre thick interbeds which apparently increase in abundance down(?)section. Commonly the phyllite contains up to 5% pyrrhotite porphyroblasts that are consistently elongated at a small angle to the phyllitic fabric. Where these rocks are oxidized they become bleached silvery grey and commonly display the yellow coloration typical of jarosite. Where calcareous, the graphitic argillite lacks a good phyllitic fabric. A bright green mineral (chrome mica?) comprises up to several percent of one calcareous argillite(?) layer in the borrow pit. Carbonate layers are not abundant, but do occur near the base of the unit where they comprise abundantly calcite veined, dark grey recrystallized fetid limestone up to several metres thick. Carbonate also occurs near the top of the unit as hackly-weathering decimetre-thick layers associated with tuffaceous chloritic phyllite. Also near the top of the unit, a 10m thick dolomitic limestone layer, together with a 2-3m thick tuffaceous layer, sandwiched within lineated quartzite and a more than 2m thick silicified limestone/quartzite layer that contains 5% pyrite in anastomosing bands up to 2 cm thick (exposed along



**Yukon-Tanana Terrane  
Southern Yukon**  
(modified from Mortensen, 1992)



**Big Salmon Complex  
in British Columbia**  
(this paper)



**Slide Mountain Terrane  
north-central  
British Columbia**  
(modified from Ferri, 1997)

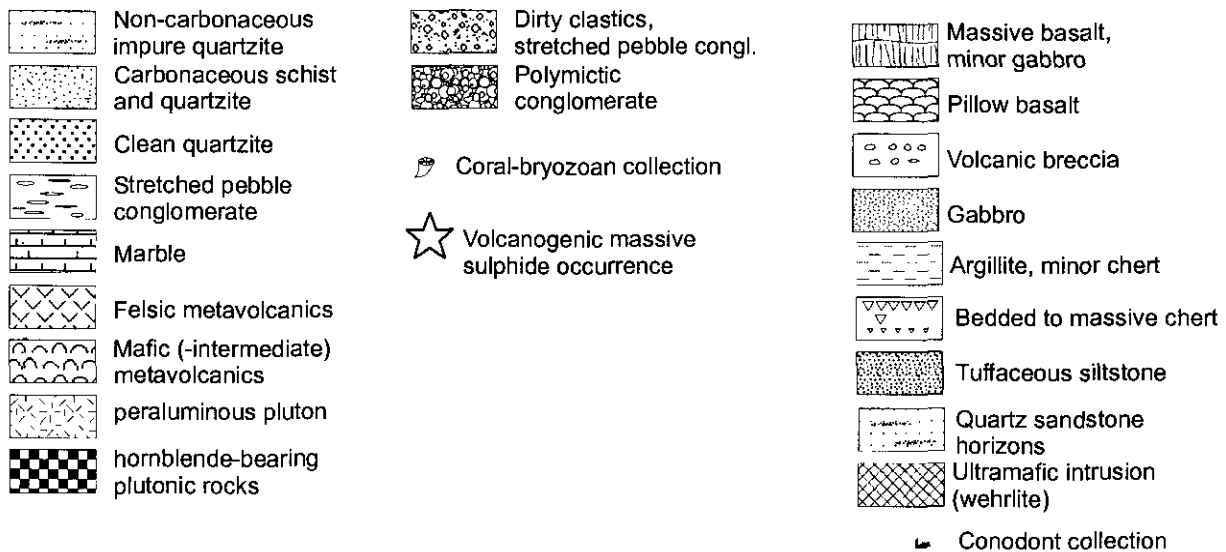
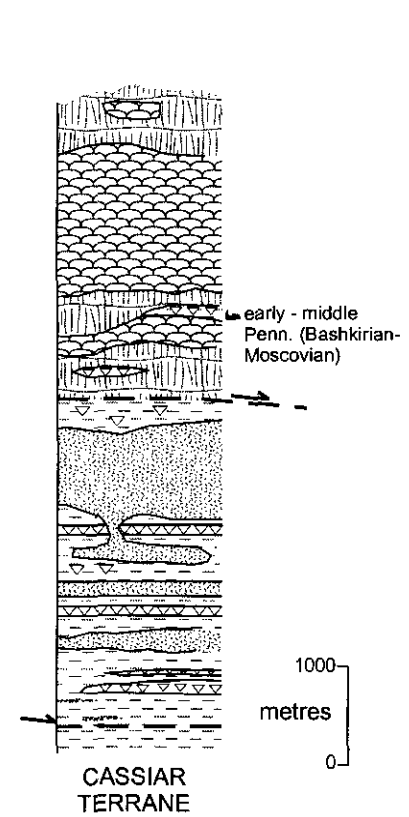


Figure 4. Comparative stratigraphy of southern Yukon-Tanana terrane (generalization of 2 columns from Figure 2 in Mortensen, 1992) with type sections of Slide Mountain Terrane (adapted from Figure 6 in Ferri, 1995) and Big Salmon Complex in British Columbia (this study).

the new Highway 97 roadcut). Similar, although not commonly dolomitic, limestone occurs at several localities near Mount Francis where it is interlayered (bedded?) with dacitic tuff and/or epiclastics similar to the Arsenault dacite (Plate 2).



Plate 2. Grey limestone with interbedded 0.2 m thick tuff bands.

### ***Orange felsic lapilli ash tuff (25m, 5m, 2m)***

Several layers of bright orange-weathering, sparsely-quartz phyric tuff occur within the structurally lowest parts of the quartz granule conglomerate unit. Flattened, white sericitic fragments ranging in size from coarse ash to fine lapilli (up to 2 cm), float in a fine, foliated ash and dust matrix. Quartz phenocrysts are fine-grained and rare. Fine pyrite is widely disseminated (1%+).

Widespread, strongly pyritic, feldspathic quartzite on the ridges northwest of Two Lakes may be a more highly metamorphosed equivalent of this tuff.

### ***Arsenault dacite tuff (to 60M or more)***

Conspicuous, coarse, blue quartz-eye dacite is best exposed at the Arsenault showing (2.5 km west southwest of Mount Francis) where it is coarsest and attains maximum thickness of about 60m. It forms a white to green-grey-weathering marker horizon that can be traced for several kilometres, helping to outline major folds. Medium grey ash with fine-grained feldspar fragments fill

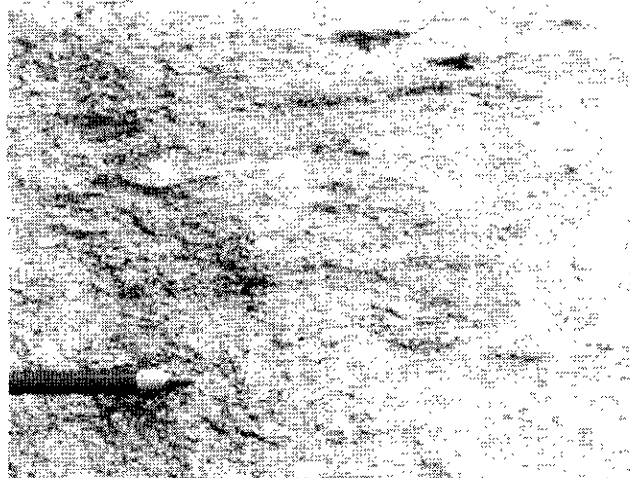


Plate 3. Arsenault dacite displaying flattened clasts and coarse quartz-eyes.

interstices between flattened, grey to cream-coloured, coarse lapilli and breccia clasts (up to 10 cm diameter and 2 cm thick, Plate 3). Quartz eyes, which comprise about 6% of the rock, are generally 3 to 5 mm diameter but range up to 2 cm in both matrix and clasts. Locally the unit contains up to 5% rounded magnetite porphyroblasts, typically 2-5 mm in diameter. Sparse accidental quartzite clasts occur near the base (?) of the unit. Structurally underlying the unit at one locality is a distinctive pure quartzite conglomerate comprised exclusively of pale pink or cream-coloured, rounded quartzite pebbles.

### **Buff carbonate (70-300m with interbeds of tuff and conglomerate)**

Buff coloured carbonate is grey to white on fresh surfaces. Along Highway 97 it has a continuously exposed structural thickness of 70m and another 70m that is discontinuously exposed. Along the Logtung road it has a discontinuously exposed structural thickness of 160m, and on the Arsenault property its structural thickness is 180 to 270m, but there it has been thickened, perhaps more than doubled, by folding.

Along Highway 97, the upper 70m of the carbonate is massive, except for two bedding surfaces outlined by poorly preserved, silicified bryozoans, coralites and possible bivalve fossils (Plate 4). These are the only macrofossils recovered from this unit. The lower 70+m section contains at least four 0.5 to 2m thick, bright green chloritic/tuffaceous beds that grade upwards into carbonate. Recrystallization is locally extreme with some irregular calcite crystals reaching decimeters across. Disseminated fine-grained pyrite glomerocrysts are relatively equant with no evidence of stretching. Similar massive and tuffaceous units occur along the Logtung Road, nearly 2 km along strike to the northwest.



Plate 4. Silicified coral and bryozoan fossil debris outlining bedding in otherwise massive buff limestone.

### ***Polymictic boulder conglomerate (5-10M)***

One 3 by 6m outcrop of flattened intrusive and volcanic cobble and small boulder conglomerate, located 1.8 km up the Logtung Road, is between layers of buff carbonate, each greater than 20m thick. Clast types include

(in approximate order of abundance): greasy grey dacite tuff with purple-blue quartz eyes up to 1.5 cm diameter; green to grey, aphanitic to sparsely feldspar porphyritic basalt; porphyritic granite with purple-blue or rose-coloured quartz eyes; yellow-orange quartzite; grey phyllite; and green phyllite. Clast flattening ratios are about 3:1 to 8:1 with slight elongation.

Basalt, pink quartzite, bleached quartz diorite and carbonate are the dominate clasts in a debris flow unit near the stratigraphic top of a strongly recrystallized carbonate 3.5 km northwest of Mount Francis. Blocks of medium to coarse plagioclase porphyritic basalt up to 0.5m diameter and mainly cobble-sized diorite clasts are subangular to subrounded, whereas quartzite clasts are typically about 5 cm diameter and angular. The blocks are cemented by a dirty carbonate matrix. All lithologies in the unit have been partly replaced by moderate to strong propylitic alteration.

### Crinkled chert (25-60m)

White to pink-weathering, thinly bedded to laminated and contorted recrystallized chert forms a distinctive, photogenic marker horizon throughout the map area (Plate 5). Where least recrystallized, beds are generally less than 2 cm thick, but range up to 10 cm thick, and display a grey to greenish-coloured fresh surface. Locally the weakly metamorphosed unit displays pinkish streaks or a pale pinkish cast. The beds are comprised of silica, lesser argillite and minor, very fine tuff(?).

Where it is strongly recrystallized, the unit displays centimetre to decimetre thick layering of micaceous quartzite with millimetre to centimetre thick interlayers of white mica. Idiomorphic garnet, specular hematite and staurolite can be observed optically. Locally it is strongly coloured pink to red due to the prograde development of piemontite (Mn-epidote). Piemontite is sporadically developed along an intermittently exposed 12 km strike length between Mt. Francis and Swift Lake. Some of the best piemontite occurrences are approximately 1 km northwest of the summit of Mount Hazel (Plates 6a, b).

Two samples of crinkle chert were analyzed by inductively coupled plasma emission spectroscopy for total barium content. They are highly anomalous (average 2254

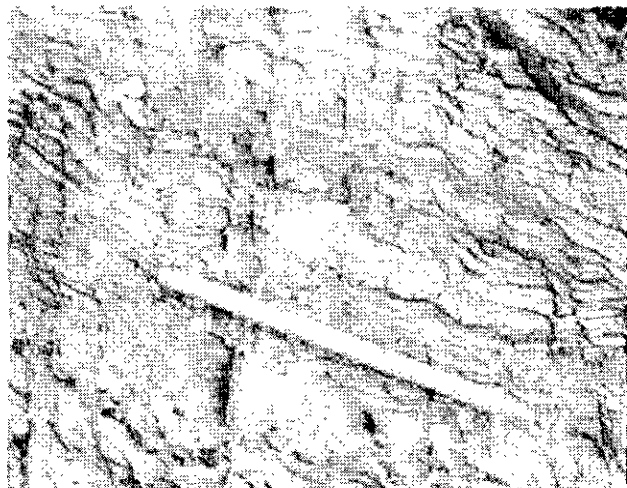


Plate 5. Typical weathering of finely laminated crinkle chert.

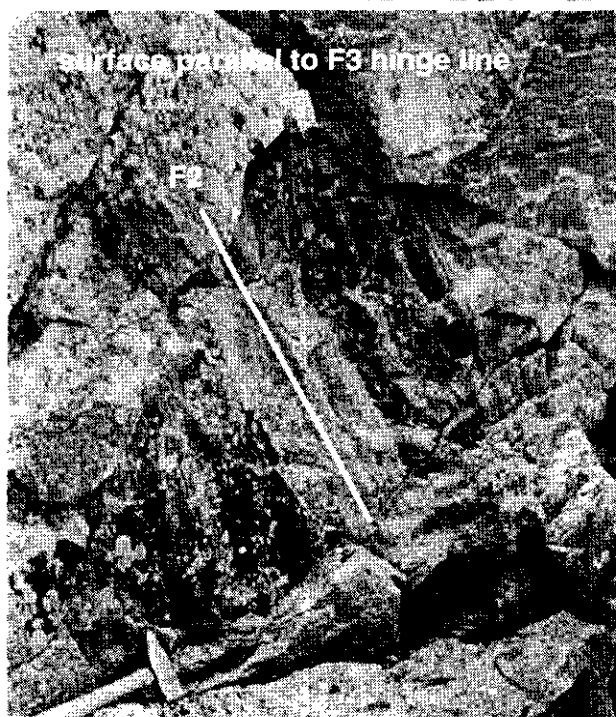
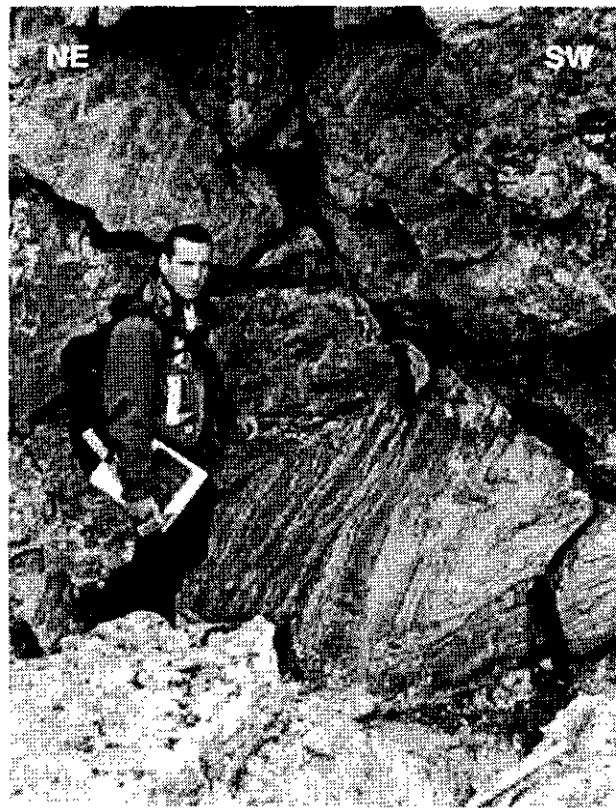


Plate 6 (a) A view to the southeast of F3 parasitic southwest-verging folds within Mount Hazel orthogneiss. (b) flattened F2 fold hinges are outlined on an F3 limb by the preservation of a strong, folded mineral lineation (mainly piemontite and garnet formed at peak P1) parallel with the F2 axial trace.

ppm) with respect to the other 28 samples analyzed (average 59 ppm; Figure 5). Samples analyzed do not represent the full range of lithologies present in the map area, but the values obtained are consistent with published



is 90% chloritized. Medium-grained quartz and albite are intergrown to weakly porphyritic, and 1-2% fine-grained epidote is generally present. Volumetrically, minor quartz porphyry occurs as layers a few metres to, rarely, tens of metres thick. These are light to dark green muscovite-chlorite-quartz-feldspar schist containing 1 to 20% conspicuous milky blue quartz eyes (to 3 mm). Porphyritic zones appear to be concentrated near the margins of the body; for example, at Mount Hazel where orthogneiss is in contact with piedmontite schist of the crinkle chert unit, and are infolded with the greenstone unit

### Pink Granite orthogneiss

About 1 km east of Teslin Lake, near the Yukon border, a northwest trending body of chloritized granitoid is at least 20m thick and can be traced for more than half a kilometre. It is medium-grained to slightly porphyritic, pink to light green-weathering and moderately to strongly foliated. Although compositionally variable, quartz and feldspar comprise approximately 25 and 50% of the rock respectively. Presumably the original mafic minerals are chloritized and smeared out into the foliated matrix. Host rocks are quartzite and tuffaceous chlorite schist. The granitoid may represent a volcanic feeder, but the nearest potential coarse proximal units are pyritic quartz sericite schists on the shore of Teslin Lake.

### Tonalite sill

A foliated tonalitic sill that is at least 5m thick intrudes greenstone about six kilometres southeast of southern Four Mile Lake. It is light green weathering and strongly foliated. Contacts have been affected by two phases of deformation (Plate 8); no crosscutting relationships are preserved. Porphyritic margins on the tonalitic body and indurated greenstone at the contact support an originally intrusive relationship.

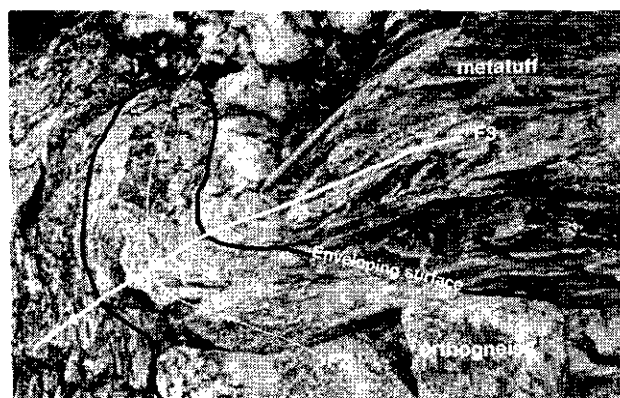


Plate 8. Foliated tonalite in the core of a flattened F2 fold refolded about F3 (view to the south).

## PLUTONIC ROCKS

### Slaughterhouse quartz diorite

Dark grey to red-weathering quartz diorite underlies Southern Teslin Lake. It is weakly to moderately foliated with rare strongly foliated zones. It is comprised of green hornblende (25%), biotite (10%), sphene (up to 1%), plagioclase (60%) and quartz (10%). Hornblende commonly displays cores of pyroxene, and biotite may occur as single grains or many clustered subgrains. Medium-grained sphene occurs as idiomorphic grains comprising up to 1% of some samples. Plagioclase is turbid due to alteration to white mica, prehnite and epidote. Plagioclase crystals occur as interlocking elongated lozenges that are moderately well aligned in foliated samples.

Alignment of plagioclase may indicate either subsolidus flow foliation or syntectonic intrusion. However, polygonized, quartz grains broken into domains with undulatory extinction and mortar-textured quartz at feldspar borders represent textures formed at subsolidus temperatures. Such deformation textures are supportive of late syntectonic emplacement.

### Age and Implications

Sample crushing, mineral separation, and isotopic analysis of weakly foliated Slaughterhouse diorite collected from west of southern Teslin Lake (MMI96-2-11, Table 1) were performed at the Geochronological Laboratory at the University of British Columbia. High quality clear, pale pink, prismatic (stubby to elongate and multifaceted) and tabular zircon, and also clear pale yellow, broken fragments of euhedral titanite grains were recovered. Six analysed fractions (four zircons and two titanites, Table 1, Figure 6) plot on or near concordia at about 170 Ma. Three of the zircon fractions are slightly discordant, suggesting the presence of inherited zircon components, and superimposed Pb loss for fraction C. Fine elongate zircon fraction D is concordant at about 170 Ma. Both titanite analyses are concordant; fraction T1 is relatively imprecise but is in agreement with zircon fraction D, while T2 is slightly older at about 171 Ma. The  $170.2 \pm 1.2$  Ma age suggested for this sample is a good conservative estimate based on the average  $^{206}\text{Pb}/^{238}\text{U}$  age of concordant fractions D and T2, with associated precision derived from the total range of overlap of these analyses with the concordia curve. Note the possibility of minor Pb loss for fractions D and T1, which would render the older portion of the error envelope, based on T2, as the most likely age for this rock.

Pyroxene cored hornblende is characteristic of both the Slaughterhouse pluton and various phases of the circa 172 Ma (Mihalynuk et al., 1992) Fourth of July batholith near Atlin (part of the more regional Three Sisters plutonic suite of Woodsworth and Anderson, 1991). The new U-Pb isotopic age determination from a sample of weakly foliated Slaughterhouse diorite performed at, is  $170.2 \pm 1.2$  Ma, confirming the Fourth of July suite association. Preliminary U-Pb age determinations from a sample collected at the south end of Teslin Lake suggest an age of 168 to 175 Ma.

TABLE 1. U-Pb ANALYTICAL DATA

| Fraction <sup>1</sup>           | Wt<br>mg | U <sup>2</sup><br>ppm | Pb* <sup>3</sup><br>ppm | <sup>206</sup> Pb <sup>4</sup><br><sup>204</sup> Pb | Pb <sup>5</sup><br>pg | <sup>208</sup> Pb <sup>6</sup><br>% | Isotopic ratios (1σ,%) <sup>7</sup> |                                     |                                      | Apparent ages (2σ, Ma) <sup>7</sup> |                                      |
|---------------------------------|----------|-----------------------|-------------------------|-----------------------------------------------------|-----------------------|-------------------------------------|-------------------------------------|-------------------------------------|--------------------------------------|-------------------------------------|--------------------------------------|
|                                 |          |                       |                         |                                                     |                       |                                     | <sup>206</sup> Pb/ <sup>238</sup> U | <sup>207</sup> Pb/ <sup>235</sup> U | <sup>207</sup> Pb/ <sup>206</sup> Pb | <sup>206</sup> Pb/ <sup>238</sup> U | <sup>207</sup> Pb/ <sup>206</sup> Pb |
| <b>MMI96-2-11 TTZ Granitoid</b> |          |                       |                         |                                                     |                       |                                     |                                     |                                     |                                      |                                     |                                      |
| A cc,N2,p,s                     | 0.228    | 292                   | 8.0                     | 5599                                                | 20                    | 12.1                                | 0.02668 (0.10)                      | 0.1825 (0.17)                       | 0.04961 (0.09)                       | 169.8 (0.3)                         | 176.8 (4.4)                          |
| B c,N2,p,e                      | 0.148    | 259                   | 7.1                     | 1162                                                | 56                    | 12.4                                | 0.02678 (0.12)                      | 0.1835 (0.26)                       | 0.04968 (0.18)                       | 170.4 (0.4)                         | 180.3 (8.4)                          |
| C m,N2,p,e                      | 0.196    | 300                   | 8.2                     | 4727                                                | 21                    | 12.4                                | 0.02645 (0.11)                      | 0.1811 (0.18)                       | 0.04966 (0.10)                       | 168.3 (0.4)                         | 179.3 (4.8)                          |
| D f,N2,p,e                      | 0.115    | 266                   | 7.3                     | 3732                                                | 14                    | 12.4                                | 0.02662 (0.11)                      | 0.1815 (0.18)                       | 0.04946 (0.11)                       | 169.4 (0.4)                         | 169.9 (4.9)                          |
| T1 cc,N2,b                      | 0.465    | 403                   | 10                      | 383                                                 | 851                   | 3.3                                 | 0.02656 (0.41)                      | 0.1819 (1.07)                       | 0.04967 (0.81)                       | 169.0 (1.4)                         | 179 (38)                             |
| T1 cc,N2,b                      | 0.470    | 422                   | 11                      | 416                                                 | 834                   | 3.0                                 | 0.02687 (0.15)                      | 0.1833 (0.50)                       | 0.04950 (0.41)                       | 170.9 (0.5)                         | 171 (19)                             |

Notes: Analytical techniques are listed in Mortensen et al. (1995).

<sup>1</sup> Upper case letter = fraction identifier; All zircon fractions air abraded; Grain size, intermediate dimension: cc=<180 μm and >134μm, c=<134μm and >104μm, m=<104μm and >74μm, f=74μm. Magnetic codes: Franz magnetic separator sideslope at which grains are nonmagnetic (N) or Magnetic (M); e.g., N1=nonmagnetic at 1°; Field strength for all fractions =1.8A; Front slope for all fractions=20°; Grain character codes: b= broken fragments, e=elongate, eq=equant, p=prismatic, s=stubby, t=tabular, ti=tips.

<sup>2</sup> U blank correction of 1-3pg ± 20%; U fractionation corrections were measured for each run with a double <sup>233</sup>U-<sup>235</sup>U spike (about 0.005/amu).

<sup>3</sup> Radiogenic Pb

<sup>4</sup> Measured ratio corrected for spike and Pb fractionation of 0.0043/amu ± 20% (Daly collector) and 0.0012/amu ± 7% and laboratory blank Pb of 10 pg ± 20%. Laboratory blank Pb concentrations and isotopic compositions based on total procedural blanks analysed throughout the duration of this study.

<sup>5</sup> Total common Pb in analysis based on blank isotopic composition

<sup>6</sup> Radiogenic Pb

<sup>7</sup> Corrected for blank Pb, U and common Pb. Common Pb corrections based on Stacey Kramers model (Stacey and Kramers, 1975) at the age of the rock or the <sup>207</sup>Pb/<sup>206</sup>Pb age of the fraction.

### Simpson Peak batholith

Simpson Peak batholith marks the southeastern limit of the Big Salmon Complex. Potassium feldspar porphyritic granite is typical, although marginal phases are compositionally heterogeneous, ranging from dark, hornblende-rich diorite to granodiorite. Near Simpson Peak the body is weakly foliated and strongly jointed. It is white to grey-weathering with a greenish or pinkish cast. Idiomorphic pink potassium feldspar crystals are conspicuous as they are up to 3 centimetres in diameter. These crystals are micropertthitic and, together with medium to fine-grained potassium feldspar, comprise about 30% of the rock. Plagioclase (30%), polygonized quartz (25%) and chloritized patches of biotite (10%) are other major constituents. Subidiomorphic sphene comprises about 1%. Epidote (2%) is the dominant alteration mineral.

Although the Simpson Peak batholith is generally weakly deformed, and well foliated at its northern margin, it clearly postdates deformation of the Big Salmon Complex, cutting across fold axes, skarning deformed limestone, and hornfelsing other Big Salmon Complex lithologies. Published K-Ar age determinations for the Simpson Peak Batholith (Wanless et al., 1970) are recalculated using modern decay constants as 185 ± 14 (hornblende) and 169 ± 8 (biotite, reset). Recalculated ages from the adjacent Nome Lake batholith are essentially concordant at 187 ± 9 (both hornblende and biotite; *ibid.*)

### Midshore granite

Coarse tan to pink granite crops out along 2.5 km of the eastern shore of Teslin Lake, midway between its southern end and the Yukon border. It is comprised of 30% coarse perthitic potassium feldspar, 25% smoky grey quartz with undulatory extinction, 35% strongly zoned plagioclase, 10% biotite and accessory tourmaline and zircon (100 microns in diameter). Alteration minerals

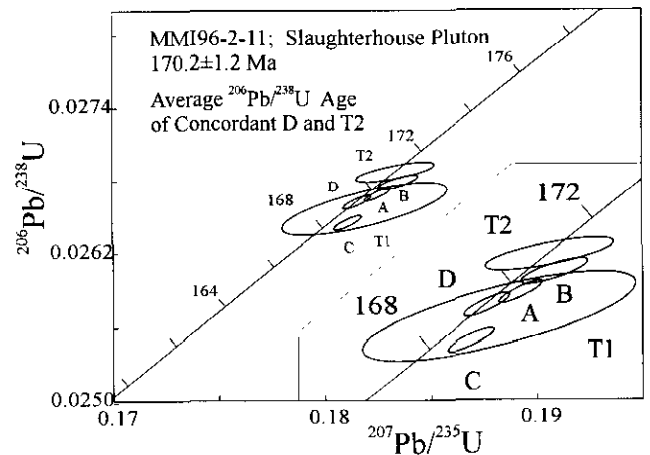


Figure 6. Concordia plot showing isotopic ratios with error estimates for four zircon (A to D) and two titanite (T1, T2) mineral fractions from the Slaughterhouse pluton.

include chlorite after biotite and white mica, prehnite and calcite after feldspars.

## Two Ladder Tonalite

Fine to medium-grained dark grey weathering hornblende tonalite forms a series of northwest-elongate, kilometre-long bodies on the ridges above Two Ladder Creek. Locally the bodies are sparsely hornblende porphyritic (up to 5 mm diameter), but are more typically equigranular. Near their margins they may display a weak foliation; although they are discordant with respect to the enclosing strata, which are hornfelsed. Away from their contacts, the bodies are not foliated.

## Coconino Tonalite

Foliated hornblende-biotite tonalite, lithologically and petrographically indistinguishable from parts of the Slaughterhouse pluton, underlies the low ridges east and south of Coconino Lake, extending 15km south of the Swift River. It forms a roughly equidimensional body with a northwestern apophysis that may have been drawn into the Teslin Fault with dextral shear. A sample collected from within a few hundred metres of its northern contact displays chill textures with idiomorphic feldspars (up to 2cm, 50%), sphene (up to 0.1cm, 2%) and minor idiomorphic apatite rimmed with interstitial quartz (20%). Weakly-oriented, fine-grained biotite forms elongated clots (20%) up to 1cm long after original biotite. Some of the biotite clots are cored with epidote, probably replacing hornblende. Most plagioclase is strongly replaced by epidote and muscovite.

A new, unpublished U-Pb age date indicates that the Coconino tonalite is about 25m.y. older than the Slaughterhouse pluton; perhaps age equivalent to the Simpson Peak and related plutons ( $185 \pm 14$  to  $187 \pm 9$  Ma; K-Ar hornblende ages recalculated from Wanless et al., 1970), but only at the oldest limit of the K-Ar error.

## STRUCTURE AND METAMORPHISM

In general, the Big Salmon Complex consists of a northwest-trending "amphibolite" grade core zone, in which protolith textures are destroyed, flanked by greenschist grade rocks in which protolith textures are moderately to well preserved. Upper greenschist to transitional greenschist-amphibolite facies conditions are recorded in the dominant stable regional metamorphic mineral assemblages throughout the area. However, in the core zone, relicts of staurolite, andalusite, and possibly kyanite, point to an amphibolite grade, early peak metamorphic event (F2, Plates 9 and 10). Amphibolite grade peak metamorphic mineral assemblages are typically retrograded to epidote, chlorite, muscovite, and calcite.

A strong, nearly layer parallel schistose or phyllitic fabric dominates the Big Salmon Complex. Evidence of at least two phases of deformation is everywhere present, and in the higher grade core zone an additional distinct, noncoaxial fold set is developed. Third phase folds are

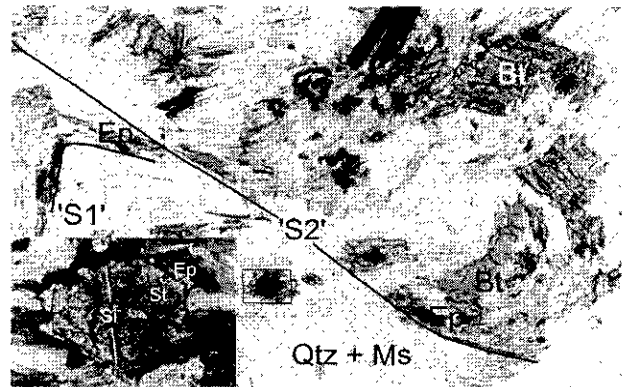


Plate 9. Earliest schistosity is recorded by inclusion trails in idiomorphic staurolite porphyroblasts (Si in inset) that are mantled by epidote. S1 is folded by S2 crenulation cleavage. Greenschist grade minerals: epidote and chlorite grow along the S2 planes. Mineral abbreviations are those recommended by Kretz (1983). Long dimension of photomicrograph is 4mm.

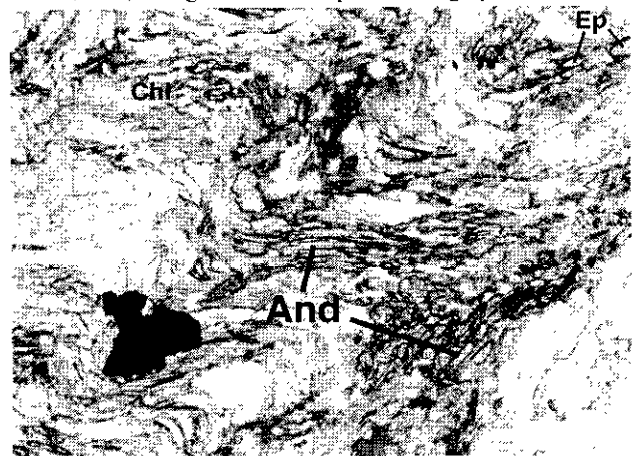


Plate 10. Viridine? (Mn andalusite (And)) in S1, is folded about S2 crenulation. This mineral is strongly sericitized along cleavage planes (photomicrograph long dimension represents 4mm).

further modified by local kinking and warping, especially in the high grade core region. At least one other deformational event can be recognized petrographically. It is cryptic, expressed mainly as deformed pre-regional S1 inclusion trails within quartz, feldspar, garnet and staurolite crystals (Plates 9, 11). So far, the extent and overall effects of this earliest event are largely unknown.

A rigorous domain by domain structural analysis of the Big Salmon Complex is beyond the scope of this paper. Nevertheless, a generalized deformational history is offered here (Figure 7). It is important to note that this interpretation is biased by the areas of best exposure, and may be inaccurate at the domain level.

Earliest deformation, here designated as D0, is only sporadically recorded in the highest grade core zone rocks as deformed inclusion trails of metamorphic minerals within porphyroblasts (Plates 9, 10). It has not been recognized in rocks younger than the Crinkle Chert unit. Preservation of D0 may be controlled by a number of factors: sufficiently argillaceous protoliths to produce schistosity, bulk rock composition suitable for porphyroblast growth, conditions permitting physical



Plate 11. Crenulated schistosity preserved as inclusion trails in subidioblastic garnet (Grt).



Plate 12. An intrafolial isocline in slate of the upper dirty elastic succession (photomicrograph long dimension represents 4mm).

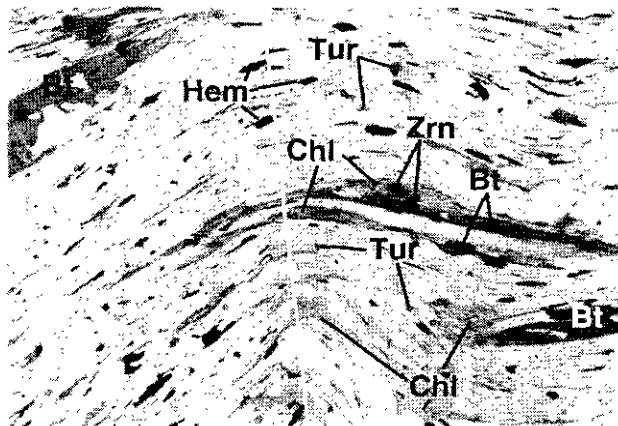


Plate 13. Crinkle chert displaying well developed S1 outlined by biotite (Bt), hematite (Hem) and and muscovite. Along incipient S2 surfaces biotite is replaced by chlorite (Chl). Note that tourmaline (Tur, metamorphic?) and zircon (Zrn, detrital?) are common but volumetrically minor (photomicrograph long dimension represents 4mm).

preservation of porphyroblasts, and others. It is possible that coeval structures are present in Big Salmon Complex superstructure, but are not recognized due to lower PT conditions and consequent lack of porphyroblast development at such high structural levels. However, the predominance of quartzite pebbles and sparse crenulated phyllite clasts in the upper dirty elastic succession is most simply explained by derivation from the lower Big Salmon Complex following a deformational event that predates deposition of the upper succession. The fabric associated with D0 is here termed S<sub>i</sub> (internal schistosity).

D1 deformation produced the first regionally recognizable set of folds and related schistosity and it is the first event that appears to have affected all units of the Big Salmon Complex, including Hazel orthogneiss and the dirty elastic succession. Thus, the folds and schistosity are designated F1 and S1 respectively. In most places D1 is manifested as a schistosity or phyllitic fabric that is within 10 degrees and commonly within 2 degrees of the bedding orientations. Such widespread near bedding parallel foliation is either due to original high amplitude and isoclinal folding (in which enveloping surfaces are not generally involved) or widespread subsequent transposition, or both. At the highest structural and stratigraphic levels, the dirty elastic succession also displays persistent very low angle bedding-cleavage relationships that support the existence of high amplitude folds, and on a microscopic scale, intrafolial isoclines within the same succession (Plate 12) indicate strong transposition. F1 fold hinges are most commonly preserved in the superstructure domains flanking the Big Salmon Complex core zone. They are open to close, upright to recumbent, subhorizontal to steeply plunging (Figure 8). Elongation lineation orientations, mainly stretched pebbles and lapilli, generally fall into one of two populations (Figure 7); both are at high angles to the S0-S1 intersection lineation. Thus, they are probably the product of flexural slip folding and formed subparallel to the D1 tectonic transport direction. Non-coaxial transposition of upper and lower limb lineations could have produced the bimodal pattern observed (Figure 7). Within most of the Big Salmon Complex, D1 produced S1, the dominant schistose fabric.

F2 folds are ubiquitous and are synchronous with peak D2 metamorphism (Plate 6a). They are outlined by deformation of the S1 fabric into parabolic to nearly chevron shapes that are open to tight, gently inclined to upright, subhorizontal to, less commonly, steeply plunging (Figure 8). However, where transposed, they are nearly recumbent and tight to isoclinal. F2 folds are most commonly observed with wavelengths and amplitudes in the range of 1 to 10 metres. Although larger F2 folds undoubtedly exist, as suggested by regional outcrop patterns, none have been traced out on the ground. Despite the peak metamorphic grades that are attained during D2, a regional coeval schistosity is NOT developed. However, axial parallel schistosity is locally formed in the core zones of these folds (designated here as S2). Well-developed shallow southeast-plunging mineral elongation lineations (Figure 7) are parallel to F2 hinge lines. Contoured poles to S1 show a bimodal distribution of relatively-lying flat limbs (Figure 8), reflecting the variable southwest and northeast vergence displayed by these folds, their tendency towards straight limbs and transposition by F3 folds (e.g. Plates 6b and 7).

F3 folds are close to isoclinal, subhorizontal, inclined to overturned and west southwest-verging (Figure 8). They

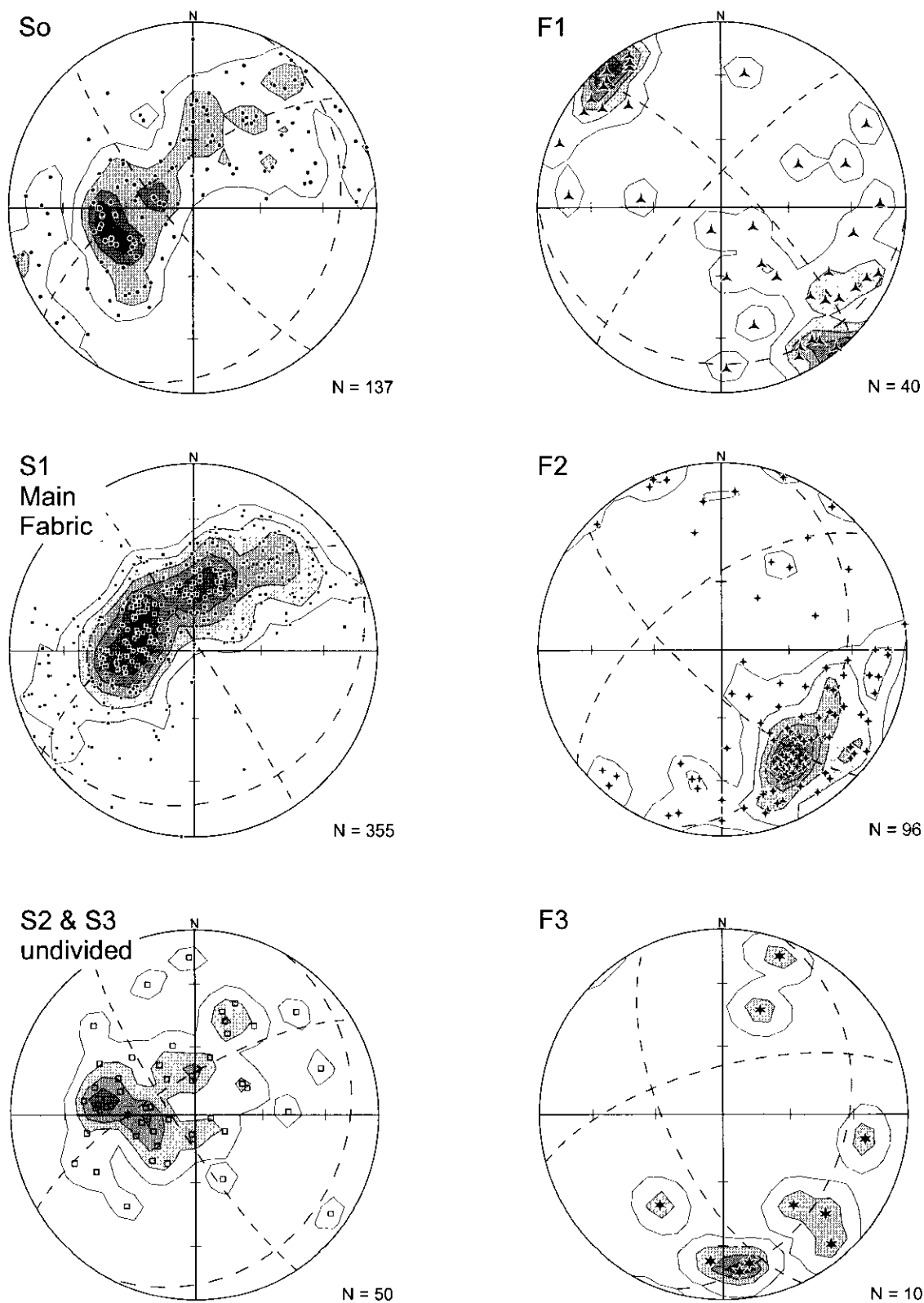


Figure 8. Stereonet plots of poles to bedding (So), first regional schistosity (S1), second schistosity (S2), first phase folds (F1), second phase folds (F2) and third phase folds (F3). Data are contoured by Gaussian counting using a weighting function equivalent to a fractional counting area of 0.01. Contour intervals are 2, 4, 6, 8, 10, 12 and 14 sigma.

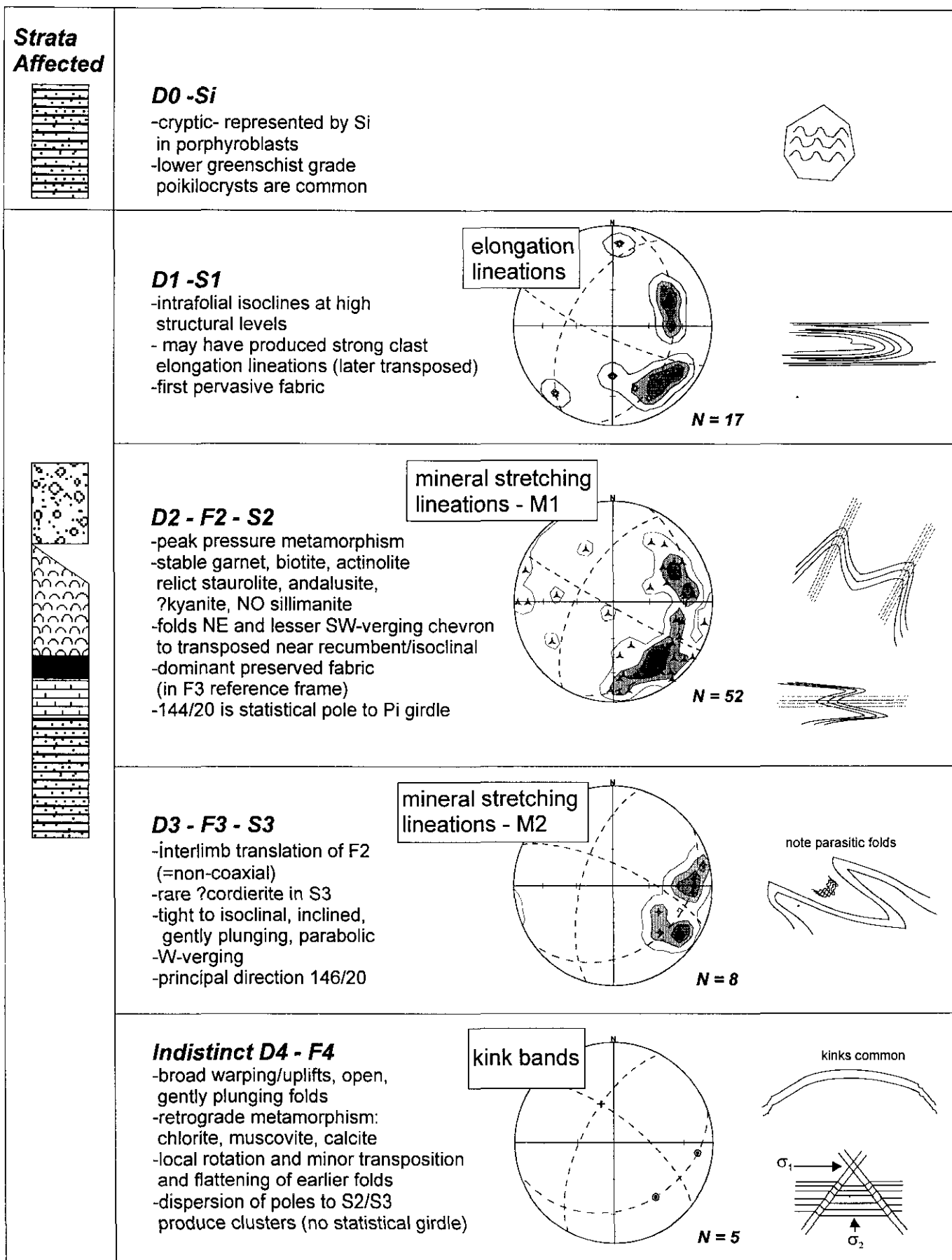


Figure 7. Deformational history. Note that lithologic patterns are consistent with those in Figure 4. Contoured stereonet plots of elongation lineations (E1) and mineral lineations (M1, M2) follow the methodology used for structural plots in Figure 8 (see also text for discussion). Mineral abbreviations are those recommended by Kretz (1983).

are semi-elliptical to parabolic in shape with high amplitudes and relatively straight limbs. Parasitic folds and an axial planar fabric are commonly developed and can be recognized in mountain scale F3 folds. However, unless fold-fabric relationships can be established at the outcrop, it is not always possible to distinguish F2 and F3 schistosity, even though they are here designated as S2, and S3 respectively. S3 can be recognized petrographically because it formed during retrograde D3 and is commonly outlined by the growth of chlorite (Plate 13), muscovite, calcite + epidote (Plate 9). In some cases chlorite-lined S3 surfaces can be distinguished in outcrop. The dispersion of poles to S2 shown in Figure 8 is the result of inclusion of S2 with S3 data, and a concentration of measurements from domains most strongly affected by F4 warping.

F4 folds are broad warps with little preferred orientation. They appear unrelated to a distinct deformational event, but probably reflect the combined effects of tectonic exhumation and stress transmitted from large bounding strike slip faults, like motion on the Teslin lineament. One large, northwest-trending warp may be responsible for uplift of the Big Salmon Complex core zone as indicated from outcrop distribution in Figures 3 and 4. Local strong development of kink bands in chlorite and muscovite schist (retrograde S3) formed during this late warping. While kink bands are relatively common, conjugate kink band sets are not widely developed within the map area. In this study, only one set was measured near Four Mile Lake. In controlled experiments, conjugate kink bands are oriented such that the obtuse and acute angles between the two kink band arrays face the shortening and stretching directions, which are approximately parallel to the major and minor principal stress directions respectively at that site. Figure 7 shows the maximum and minimum principal stresses orientations that might have existed at the time of the kink band formation. Interestingly, the maximum and minimum principal stresses are orogen parallel and orogen normal respectively.

### Age of deformation

Like the protoliths within the Big Salmon Complex of British Columbia, there are currently no concrete constraints on the age of deformational events within the Big Salmon Complex. K-Ar (muscovite) cooling ages have been reported from similar rocks immediately north of the Yukon border: 222 (Mulligan, 1963; no uncertainty quoted; from Mile 778 (about 1.5 km west of Morley River), 214 ±25 (R.K. Wanless in Mulligan, 1963; no location reported) and from British Columbia in the northwestern corner of 1040: 194 ±15Ma (Leech et al., 1963; GSC Paper 44-25). The reliability of all these ages must be considered suspect since <sup>36</sup>Ar was not determined.

Regional fabrics are cut by the Early Jurassic Simpson Peak batholith (K-Ar hornblende is 185 ±14 Ma, recalculated from Wanless et al., 1970). It intrudes, skarns and hornfelses previously deformed and metamorphosed rocks of the Big Salmon Complex and thus provides a minimum age constraint on the ductile fabrics. However, the batholith locally displays a weak tectonic foliation

indicating that the latest deformation outlasted its intrusion. Weak to rarely moderately strong foliation is also developed in the Middle Jurassic (170 Ma, Figure 6) Slaughterhouse pluton at the south end of Teslin Lake. However, the body where it has been dated cannot be shown to cut the Big Salmon Complex.

### MINERALIZATION

Within the entire Big Salmon Complex in British Columbia, the only base metal mineral occurrences recorded in MINFILE are those on the Arsenault and adjacent claims about 14 km south of the Smart and Swift River confluence. Copper mineralization was discovered on the Arsenault property by Wilf McKinnon of Hudson's Bay Mining and Smelting in the 1940's (Sawyer, 1979). Geological and geochemical work performed in 1967 included the excavation of 16 trenches; 0.10 oz/t Au over 3 metres was reported from one trench (Sawyer, 1967). Between 1970 and 1972 a major exploration program was conducted by Bolivar Mining Corporation (subsidiary of Cyprus Mines Corp. Ltd.) that included construction of an access road, airborne EM, magnetometer, induced polarization and geochemical surveys, geological mapping and 1080 metres diamond drilling on the four best anomalies. A further 440m of diamond drilling was conducted in 1979 and 235.5m in 1981 by Rebel Developments Ltd. (Sawyer, 1979; Phendler, 1982).

Mineralization exposed at surface is dominated by chalcopyrite and pyrite with associated epidote, garnet, actinolite, magnetite (Plate 14) and wollastonite (Plate 15) in quartz-rich strata at their contact with carbonate. Mineral textures preserved suggest static crystallization. Traces of bornite, molybdenite, piemontite (Mn-epidote) and spessartine (Mn-garnet) have also been reported (Sawyer, 1979). Tourmaline is common in both the quartzite and tuff.

Although the quartz-carbonate association and calc-silicate mineralogy and textures are suggestive of skarn, no causative intrusion has been found. Pink quartz-feldspar porphyry dikes, one within 200m of two mineralized trenches, others up to a kilometre away, cut the succession but they clearly post-date deformation that has affected the calc-silicate mineralogy. Furthermore, there is no correlation between soil geochemical Cu anomalies and the location of the closest dike (Sawyer, 1979). If Arsenault is a skarn, then the best candidate for an associated pluton is the dioritic complex that crops out over 2 km away, in the north face of Mount Francis, but the diorite is strongly foliated and folded, whereas calc-silicate mineralization at the Arsenault appears to have developed under mainly static conditions. Alternatively, if calc-silicate development is a product of regional metamorphism, the source of copper remains in question. Clearly, metamorphic grade and reactive lithologies alone do not form copper-rich calc-silicate zones.

The only quartzite-carbonate contacts within the area with associated chalcopyrite are those adjacent to the Arsenault dacite. Such occurrences extend from the western Arsenault showings to the east flank of Mount

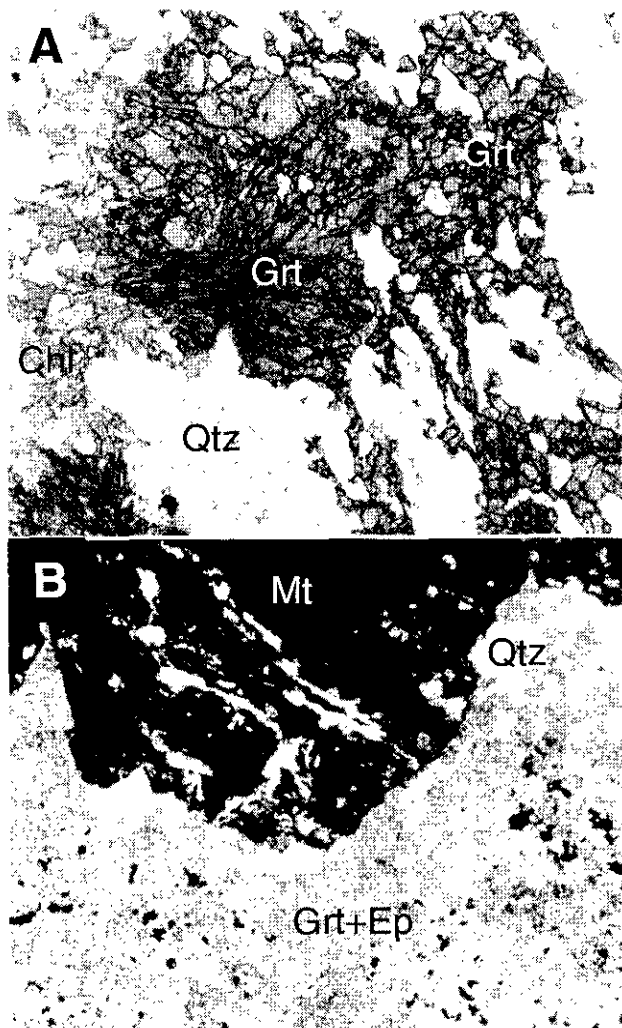


Plate 14. (a) apparent static growth of garnet (Grt) and quartz, and (b) static growth of mixed garnet (Grt), epidote (Ep) and idiomorphic magnetite (Mt) looks like a skarn texture (long dimension of photomicrographs represents 4mm).

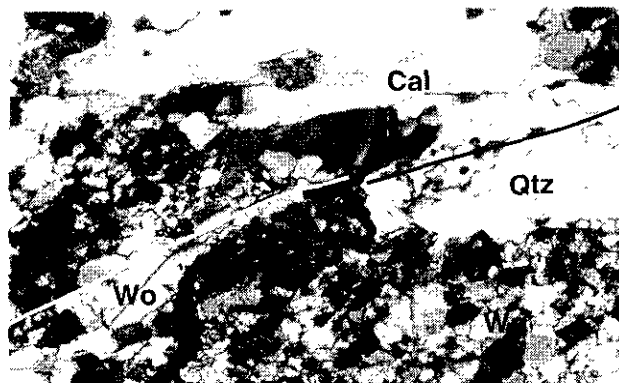


Plate 15. Stubby wollastonite crystals are aligned parallel to zones of cataclasis in adjacent quartz layers indicating a late synkinematic origin (photomicrograph long dimension represents 4mm).

Francis, a distance of 2.5 km. Chalcopyrite also occurs as disseminations and veinlets within the Arsenault dacite, both in the eastern trenches and where it crops out about 0.5 km farther to the south-southeast. This rather widespread and consistent lithological association suggests

a syngenetic origin for the copper mineralization, as originally proposed by Sawyer (1979). In support of this interpretation is the association of Mn-bearing minerals, as well as tourmaline, with the mineralized horizon. Once a clearer understanding of protolith ages within the Big Salmon Complex emerges, it should be possible to determine whether the Arsenault mineralization Pb signature (in progress) is syngenetic or a product of a cryptic, younger magmatic-related event.

### New occurrences

Four previously unrecorded mineral occurrences were encountered during the course of mapping. The first two of these are interpreted to occur in roughly the same 100m stratigraphic interval as the Arsenault, and each display some evidence of having been previously sampled. Samples collected from the new occurrences were analyzed by aqua regia digestion and inductively coupled plasma emission spectroscopy. Note that the digestion method is incomplete for most elements, particularly those marked with an asterisk. Some of the outstanding results are listed below, and the complete data set may be viewed or downloaded from our web site at <http://www.ei.gov.bc.ca/geosmin/fieldpgm/97-98/6br-dm.htm>.

#### *Arsenault east*

On the east flank of Mount Francis, near the eastern limit of the now lapsed Arsenault I claim, is a moderately steeply east-dipping, strongly deformed section of decimetre thick interbeds(?) of limestone and tuff. These are infolded with clean quartzite. Within the carbonate, near the quartzite contact, is a well developed vein replacement zone of garnet-epidote-quartz-calcite-magnetite-actinolite-chalcopyrite. The zone is 2.5 m wide and is exposed for 10 m along strike. Chalcopyrite is concentrated in the northern third of the zone in pods and irregular veins up to 4 cm wide and as much as 30 cm long. Mineralized chips collected across the 2.5m wide zone yielded 4.6% Cu, 0.3% Zn\*, 9.5 ppm Ag, 322 ppm Co\*, 26 ppm Cd and 115 ppm Bi.

#### *Teslin Lake border area*

Along east shore of northern Teslin Lake, 2 km south of the Yukon border, a series of mafic to felsic tuffaceous rocks, quartz-sericite schists and siltstones are exposed along a kilometre-long section of lakeshore. All are phyllitic to schistose and relict textures are rare. Several zones display widespread pyrite and traces of chalcopyrite. For example, at the south end of the outcrop belt a 20 m thickness of locally strongly pyritic felsic metatuff is sandwiched between mafic metatuff. The gossanous layers are up to 30 cm thick and typically contain 10% or more pyrite. Chalcopyrite occurs as sparse cm-sized clots and irregular stringers. It is evident at several localities that the zone has been previously sampled. Analysis of a single grab sample yielded 2.2% Cu and 28 ppm Ag.

## *Copper in the Crinkle Quartzite*

Two occurrences of minor sulphide mineralization and copper staining include consist of chalcocite and specularite at the peak of Mount Hazel, and chalcopyrite on the west end of the low ridge containing the Arsenault showing. At the first locality, deformed chalcocite and specularite occur as fist-sized patches in a 0.9 m thick bull quartz vein on the southeast side of Mount Hazel near the contact between crinkle quartzite and tuffaceous rocks of the greenstone unit. A similarly mineralized vein occurs on the northwest side of the peak, although it could be an along-strike continuation of the southeast vein. The second locality is below tree line about 2 km west of the old exploration camp where a few chalcopyrite veins up to a centimetre thick occur within the upper third of a 10 m cliff exposure of crinkle quartzite. No signs of prior sampling are evident.

### *Highway 97*

Extensive upgrading and straightening of Highway 97 in 1988 resulted in a number of new roadcut exposures and some extensive outcrop in burrow pits. In one new exposure, about 3.5 km west of Swan Lake, a 3 m wide gossanous zone occurs within the greenstone unit. Several north-northwest trending quartz-chlorite-magnetite-pyrite-chalcopyrite veins cut the zone. The veins attain a maximum thickness of 30 cm. There is no sign of this zone having been previously sampled. Mineralized chips collected across a 1.5m true thickness that is 80% vein material returned 0.2% Cu, 165 ppm Co\*, 210 ppm As and 45 ppm W\*.

## **SUMMARY**

Mapping along the British Columbia-Yukon border leaves little doubt that the Big Salmon Complex extends into the Yukon as suggested by earlier workers (Mulligan, 1963), and must extend into rocks recently mapping by Gordey (1995) who includes them in the Kootenay Terrane. Rocks assigned to the Kootenay Terrane in Yukon are considered to be part of the Yukon-Tanana Terrane, but the Kootenay Terrane in southeastern British Columbia is a separate tectonic entity that has demonstrable stratigraphic ties to North America (e.g. Colpron and Price, 1995). It is clear that the Big Salmon Complex bears little resemblance to classical Slide Mountain terrane (e.g. Ferri, 1995), and the assignment of Big Salmon Complex to Slide Mountain Terrane (Wheeler et al., 1991) is here considered incorrect. However, on the basis of lithological comparison alone it is not possible to unequivocally assign the Big Salmon Complex to the Yukon Tanana Terrane. Certainly the lower quartz-rich succession, Mount Hazel orthogneiss and felsic volcanic strata are lithologically similar to parts of the Yukon Tanana Terrane, but until some age control on these units is available, such correlations are speculative.

New age data from the Slaughterhouse diorite show that it is temporally equivalent to the Three Sisters plutonic suite.

Two stratigraphic intervals appear most prospective for base metal sulphide exploration: (1) porphyritic blue quartz-eye dacite tuff with interlayered limestone/quartzite that are stratigraphically equivalent to rocks that host the Arsenault occurrence and (2) barium-manganese-rich rocks of the crinkle chert unit. An exhalative origin for piedmontite schist of the crinkle chert unit was suggested by Nelson (1997). The elevated barium contents in samples from this unit supports its exhalative origin, but it also contains fine dark zircons of probable detrital origin. Scattered copper mineralization within the unit is a further indication of the importance of this unit as a potential pathway to base metal sulphide deposits.

Despite strong development of calc-silicate minerals and skarn textures with copper mineralization at the Arsenault occurrence, its classification is equivocal. Copper mineralization occurs locally over an area of about 10 km<sup>2</sup> and, if correlation with strata along Teslin Lake is correct, the copper-rich nature of this horizon is regional in extent. This suggests a syngenetic control and potential for volcanogenic massive sulphide mineralization. Blue quartz eyes are conspicuous not only in the Arsenault dacite, but interestingly also occur in graphitic quartz-granule conglomerate as well as porphyritic phases of the Hazel orthogneiss. It is possible that the Arsenault dacite and Mount Hazel orthogneiss are comagmatic and provide a detrital or pyroclastic source of blue quartz eyes for the quartz granule conglomerate. However, the simplest structural interpretation (the one preferred here) places the blue quartz-eye clastic rocks stratigraphically below the Arsenault dacite.

## **ACKNOWLEDGMENTS**

The Big Salmon Project would not have been possible if not for logistical cost sharing by Fairfield Minerals. Thanks also to Ed Balon who also shared his bottomless knowledge of Big Salmon Complex rocks. Tom Gleeson was a source of unextinguishable good cheer, excellent field assistance and interesting cuisine. Superb field support was also provided by Molly and Kim Wahl. Field discussions with Jean Pautler and Lyn Crexton of Teck Corp. were regionally illuminating. With steady nerves and expert collective, Troy Kirwan of Discovery Helicopters punctually extracted us from snag-ridden swamps that we wish never to revisit. Our base camp hosts, Russ and Tina Cummings of Jennings River Outfitters were exceptionally accommodating and generous, true ambassadors of the hospitable north. Fil Ferri gave freely his knowledge of the Slide Mountain Terrane and the stratigraphic column in Figure 4. Paul Sawyer who took time from his busy schedule to discuss the Arsenault occurrence. Statistical analysis of structural data was aided by the use of SpheriStat™2 by Pangaea Scientific.

## REFERENCES CITED

- Aitken, J.D. (1959): Atlin Map-area, British Columbia; *Geological Survey of Canada*, Memoir 307.
- Creaser, R.A., Erdmer, P., Grant, S.L. and Stevens, R.A. (1995): Tectonic Identity of Metasedimentary Strata from the Teslin Tectonic Zone, SE Yukon: Geochemical and Nd Isotopic Constraints; in Lithoprobe, Slave-Northern Cordillera Lithospheric Evolution (SNORCLE), Report of 1995 Transect Meeting, April 8-9, 1995, Lithoprobe Report No. 44, pages 51-55.
- Colpron, M. and Price, R.A. (1995): Tectonic Significance of the Kootenay Terrane, Southeastern Canadian Cordillera: an Alternative Model; *Geology*, Volume 23, pages 25-28.
- Erdmer, P. (1985): An Examination of Cataclastic Fabrics and Structures of Parts of Nisutlin, Anvil and Simpson Allochthons, Central Yukon: Test of the Arc-Continent Collision Model; *Journal of Structural Geology*, Volume 7, pages 57-72.
- Erdmer, P. and Helmstaedt, H. (1983): Eclogite from Central Yukon: a Record of Subduction at the Western Margin of Ancient North America; *Canadian Journal of Earth Sciences*, Volume 20, pages 1389-1408.
- Ferri, F. (1997): Nina Creek Group and Lay Range Assemblage, North-Central British Columbia: Remnants of Late Paleozoic Oceanic and Arc Terranes; *Canadian Journal of Earth Sciences*, Volume 34, pages 853-874.
- Gabrielse, H. (1969): Geology of the Jennings River Map-Area, British Columbia (104-O); *Geological Survey of Canada*, Paper 68-55.
- Gordey, S.P. (1995): Structure and Terrane Relationships of Cassiar and Kootenay (Yukon-Tanana) Terranes, Teslin Map Area, Southern Yukon Territory; in Current Research 1995-A; *Geological Survey of Canada*, pages 135-140.
- Gordey, S.P. and Stevens, R.A. (1994): Preliminary Interpretation of Bedrock Geology of the Teslin Area (105C), Southern Yukon; *Geological Survey of Canada*, Open File 2886.
- Hansen, V.L. (1989): Structural and Kinematic Evolution of the Teslin Suture Zone, Yukon: Record of an Ancient Transpressional Margin; *Journal of Structural Geology*, Volume 11, pages 717-733.
- Hansen, V.L., (1992a): P-T Evolution of the Teslin Suture Zone and Cassiar Tectonites, Yukon, Canada: Evidence for A- and B-type Subduction; *Journal of Metamorphic Geology*, Volume 10, pages 239-263.
- Hansen, V.L. (1992b): Backflow and Margin-parallel Shear Within an Ancient Subduction Complex; *Geology*, Volume 20, pages 71-74.
- Hansen, V.L., J.K. Mortensen, and Armstrong, R.L. (1989): U-Pb, Rb-Sr, and K-Ar isotopic constraints for ductile deformation and related metamorphism in the Teslin suture zone, Yukon-Tanana terrane, south-central Yukon; *Canadian Journal of Earth Sciences*, Volume 26, pages 2224-2235.
- Hansen, V.L., M.T. Heilzer, and Harrison, T.M. (1991): Mesozoic Thermal Evolution of the Yukon-Tanana Composite Terrane: New Evidence from  $^{40}\text{Ar}/^{39}\text{Ar}$  Data; *Tectonics*, Volume 10, pages 51-76.
- De Keijzer, M. and Williams, P.F. (1997): A New View of the Structural Framework of the Teslin Zone, South-central Yukon; in Lithoprobe, Slave-Northern Cordillera Lithospheric Evolution (SNORCLE), Report of 1997 Combined Meeting, March 7-9, 1997, Lithoprobe Report No. 56, pages 96-102.
- Kretz, R. (1983): Symbols for Rock-forming Minerals; *American Mineralogist*, Volume 68, pages 277-279.
- Leech et al. 1963. Age Determinations and Geological Studies; *Geological Survey of Canada*, Paper 63-17.
- Levinson, A.A. (1980): Introduction to Exploration Geochemistry; *Applied Publishing Ltd.*, Wilmette, Illinois, 924 pages.
- Mihalynuk, M.G., M.T. Smith, J.E. Gabites, D. Runkle, and Lefebvre, D. (1992): Age of Emplacement and Basement Character of the Cache Creek Terrane Constrained by New Geochemical Data; *Canadian Journal of Earth Sciences*, Volume 29, pages 2463-2477.
- Mihalynuk, M.G., Bellefontaine, K.A., Brown, D.A., Logan, J.M., Nelson, J.L., Legun, A.S. and Diakow, L.J. (1996): Geological Compilation, Northwest British Columbia (NTS 94E, L, M; 104F, G, H, I, J, K, L, M, N, O, P; 114J, O, P); *B.C. Ministry of Energy, Mines and Petroleum Resources*, Open File 1996-11.
- Monger, J.W.H., Wheeler, J.O. Tipper, H.W. Gabrielse, H. Harms, T. Struik L.C., Campbell, R.B. Dodds, C.J. Gehrels, G.E. and O'Brien, J. (1991): Cordilleran terranes; in Geology of the Cordilleran Orogen in Canada, Geology of Canada, Volume 4, edited by H. Gabrielse and C.J. Yorath, Chapter 8, pages 281-327, *Geological Survey of Canada*, Ottawa, Ont..
- Mortensen, J.K. (1992): Pre-mid-Mesozoic Tectonic Evolution of the Yukon-Tanana terrane, Yukon and Alaska; *Tectonics*, 11, pages 836-853.
- Mortensen, J. K., Ghosh, D.K. and Ferri, F. (1995): U-Pb Geochronology of Intrusive Rocks Associated with Copper-Gold Porphyry Deposits in the Canadian Cordillera; in Porphyry Deposits of the Northwestern Cordillera of North America, Schroeter, T.G., Editor, *Canadian Institute of Mining, Metallurgy and Petroleum*; Special Volume 46, pages 142-158.
- Mulligan, R. (1963): Geology of the Teslin Map-Area, Yukon Territory; *Geological Survey of Canada*, Memoir 326, 96 pages.
- Nelson, J. (1997): Last Seen Heading South: Extensions of the Yukon-Tanana Terrane into Northern British Columbia; in Geological Fieldwork 1996, *B.C. Ministry of Employment and Investment*, Paper 1997-1, pages 145-156.
- Phendler, R.W. (1982): Report on Assessment Work (Diamond Drilling) on the Arsenault #1, #2 and #3 Claims, Jennings River Area, Atlin Mining Division,



## EXTENSIONS AND AFFILIATES OF THE YUKON-TANANA TERRANE IN NORTHERN BRITISH COLUMBIA

By JoAnne Nelson, B.C. Geological Survey, Tekla Harms, Department of Geology,  
Amherst College, and James Mortensen, Department of Earth and Ocean  
Sciences, University of British Columbia

---

KEYWORDS: Mississippian, Dorsey Terrane, Yukon  
Tanana Terrane, Northern British Columbia

### INTRODUCTION

Kudz Ze Kayah (KZK) and Wolverine are volcanogenic massive sulphide deposits hosted by Early Mississippian meta-rhyolites, marine metasedimentary rocks and intermediate to mafic metatuffs of the Yukon Tanana Terrane in the Finlayson Lake area, southern Yukon (Figure 1). This area became a focus of intense exploration in late 1994, following Cominco's discovery of significant massive sulphides associated with metarhyolites in the ABM zone, at what later became their Kudz Ze Kayah project. Reserves at Kudz Ze Kayah now stand at 11.3 million tonnes of 6% Zn, 1% Cu, 1.3% Pb, 125 g/tonne Ag and 1.3 g Au. In 1996, reserves at Westmin-Atna Resources' Wolverine deposit were 5.3 million tonnes of 1.8 g/tonne Au, 360 g/tonne Ag, 13% Zn, 1.4% Cu and 1.5% Pb; new discoveries in 1997 will upgrade this figure. Columbia Gold's Fyre Lake deposit, located in the Finlayson Lake district 50 km south of Kudz Ze Kayah, contains a significant copper-cobalt-gold resource within a complex series of massive sulphide lenses enclosed by a mafic metavolcanic host (Blanchflower *et al.*, 1997).

This project aims to pinpoint, within central northern B.C., stratigraphy favorable to the formation of Early Mississippian volcanogenic massive sulphide deposits similar to Kudz Ze Kayah, Wolverine, and (?)Fyre Lake. In 1996, six widely scattered target areas were mapped and evaluated for this potential (Nelson, 1997). In 1997 the focus was narrowed to two areas and systematic, detailed geological mapping was begun (Figure 2). Most of the work was done on the Big Salmon Complex in northwestern Jennings River (104O) and northeastern Atlin (104N) map areas, the direct strike continuation of Yukon Tanana rocks from the Teslin map area of southern Yukon into northern B.C. It is the subject of a companion paper (Mihalynuk *et al.*, this volume). This paper describes the results of preliminary mapping in the structurally lower part of the Dorsey Terrane in central Jennings River map area (104O).

### REGIONAL CORRELATIONS AND CONTEXT

Besides the crucial Early Mississippian rocks that host the volcanogenic massive sulphide deposits, the Yukon Tanana terrane is characterised by pre-Mississippian continentally-derived siliciclastic metasediments, Early Mississippian intrusions that are coeval and probably cogenetic with the volcanic stratigraphy, Pennsylvanian and Permian limestone, Permian volcanic and plutonic rocks, and cross-cutting Early Jurassic plutons (Mortensen, 1992). This capsule geologic history provides a "thumbprint" of the terrane that can be used to help identify its correlatives.

The Dorsey Terrane has been divided into several assemblages (Harms and Stevens, 1996). The lower Dorsey Terrane in the southern Yukon comprises the Ram Creek and Dorsey assemblages. The structurally lowest Ram Creek Assemblage is a suite of mafic and intermediate to felsic metavolcanic rocks with lesser quartzite, marble and metaplutonic bodies. The overlying Dorsey Assemblage consists of quartzose, pelitic, mafic (to possibly felsic, muscovite-quartzite?) metavolcanic and intermediate metaplutonic rocks, which underwent high-temperature, high-pressure metamorphism (609-732°C, 7.7-14.1 kilobars) prior to emplacement of the mid-Permian Ram Stock (Stevens, 1996). The Dorsey Assemblage is overlain structurally by the Klinkit and Swift River assemblages, which show lower metamorphic grades and less penetrative deformation (Stevens and Harms, 1995, Harms and Stevens, 1996). Fossil ages in these upper assemblages of the Dorsey Terrane range from late Mississippian to Triassic (Harms and Stevens 1996). Limestones at different structural levels contain Pennsylvanian conodonts (Abbott, 1981): this may indicate fault and/or fold repetition.

The lower part of the Dorsey Terrane shares a number of common elements with the Yukon Tanana Terrane (Stevens, 1996). Near the Little Rancheria River, pyrite-bearing, felsic metatuffs are interbedded with intermediate metatuffs and a limestone that contains early Mississippian conodonts (Nelson, 1996). A highly deformed porphyritic tonalite, collected in 1996 from near the base of the terrane west of the Cottonwood River (Figure 3), returned an early

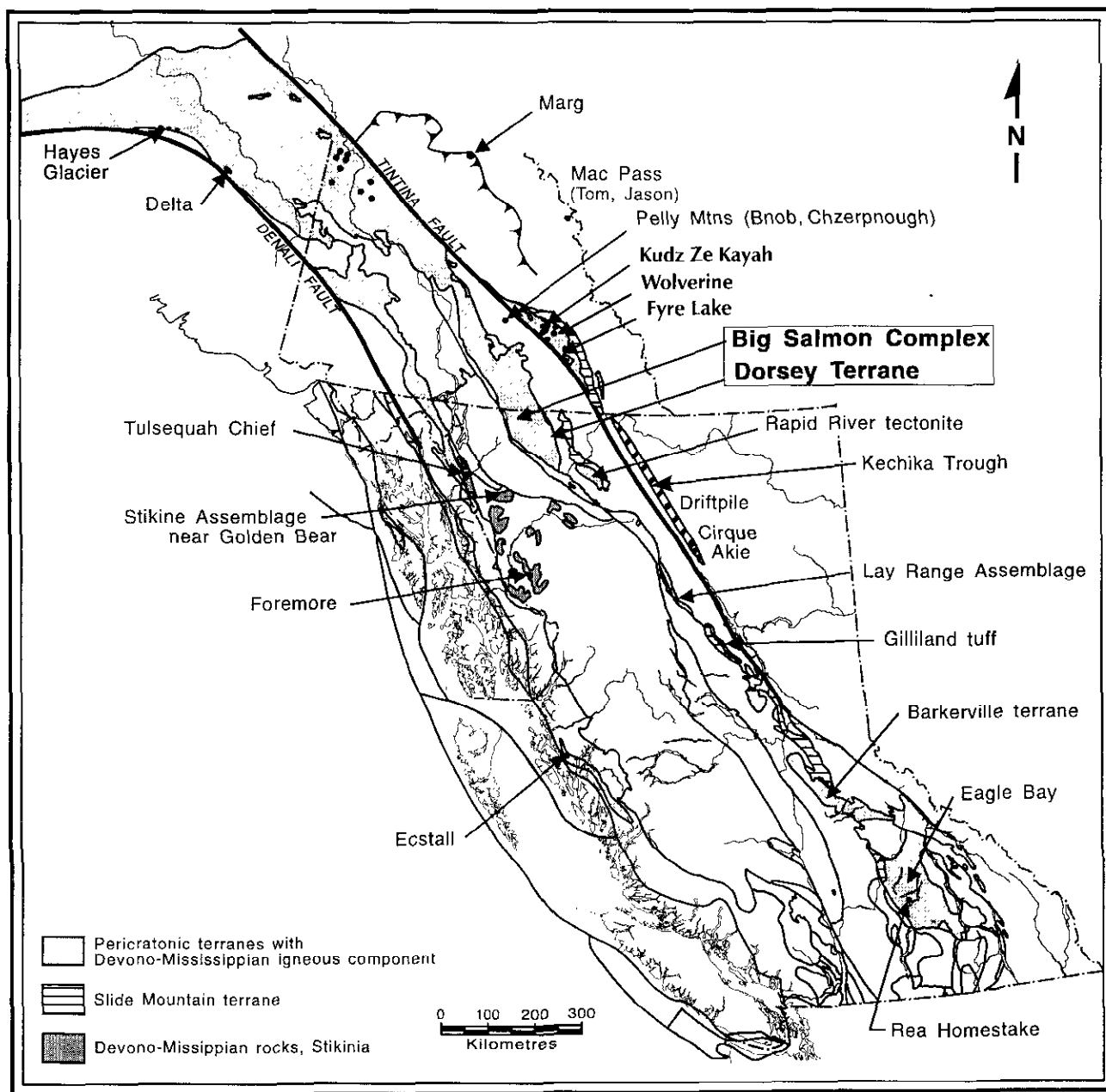


Figure 1. Location of this project (Dorsey Terrane) and Big Salmon Complex in the context of Devonian-Mississippian tectonics and metallogeny of the Canadian Cordillera  
Terrane outlines modified from Wheeler *et al.*(1991)

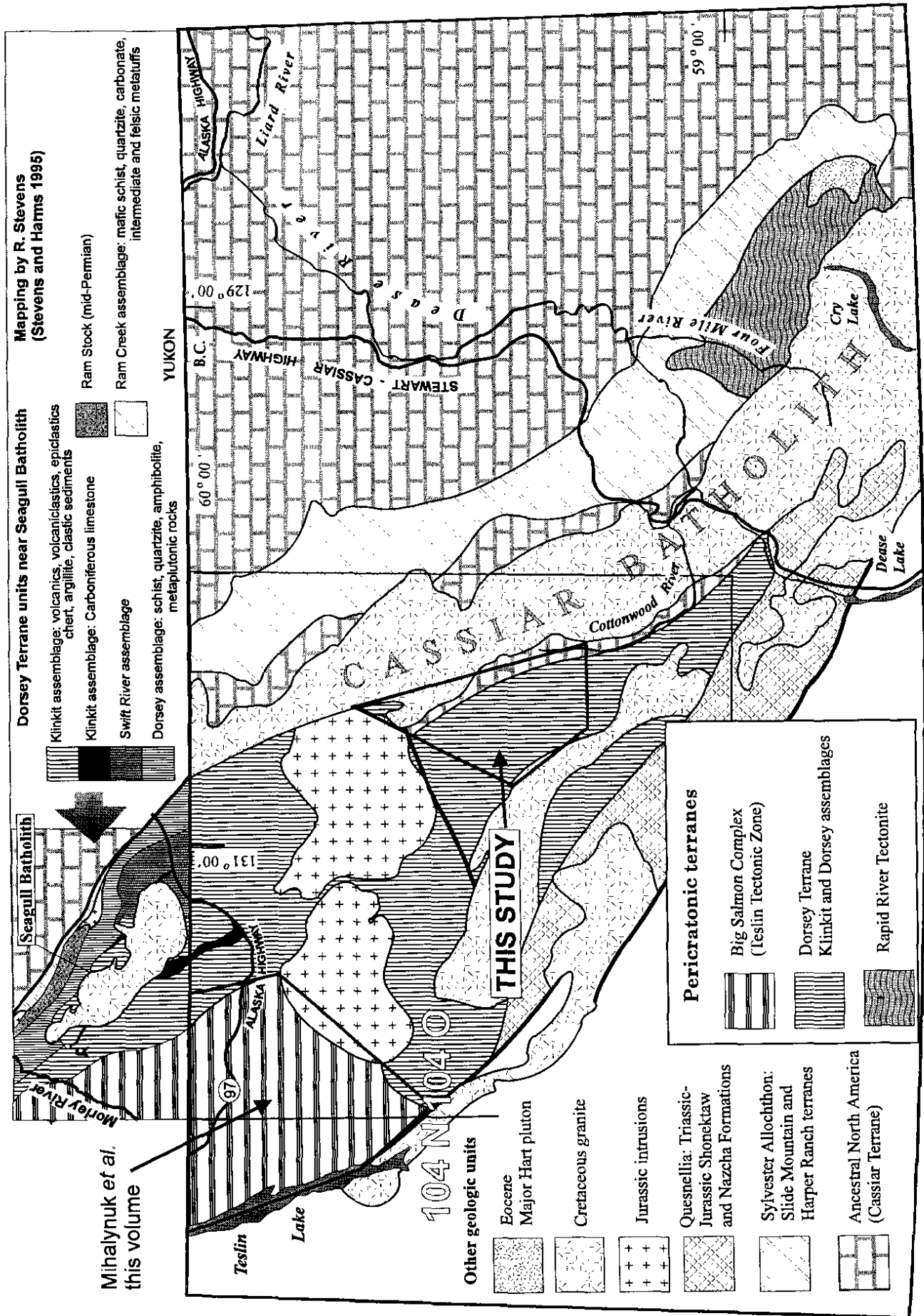


Figure 2. Tectonic location map for this project in the Dorsey Terrane and Mihalynuk et al. project in the Big Salmon Complex. Geology from Gabrielse (1963, 1969, 1994); Stevens and Harms (1995)

Mississippian U-Pb zircon age (Table 1, Figure 4 and discussion below). This age and the lack of Precambrian inheritance compare closely with the Simpson Range plutonic suite in the Finlayson Lake area (Mortensen and Jilson, 1985; Mortensen, 1992). Mid-Permian and Early Jurassic(?) intrusions cut the lower Dorsey Terrane near the Seagull Batholith in southern Yukon (Stevens, 1995).

On the eastern side of the Dorsey Terrane, the Klinkit and Swift River assemblages lie structurally above the Dorsey Assemblage in a southwesterly dipping structural stack (Stevens and Harms, 1995; Stevens, 1996). There is regional dip reversal within the Klinkit Assemblage, such that northeast-dipping low-grade chert, quartz sand-stone, slate and tuff in its western extent lie structurally above metamorphic rocks of the Big Salmon Complex (unpublished data, this project; see also structural data of Gabrielse, 1969 and Abbott, 1981). The Big Salmon Complex of Gabrielse (1969) was the subject of a detailed study during this project (Mihalynuk *et al.*, this volume). It consists of a sequence of stratified rocks cut by a highly deformed pluton, the Hazel orthogneiss. All of the units, including the Hazel orthogneiss, have been metamorphosed at grades ranging from greenschist to amphibolite, and all have undergone several episodes of folding. From lowest to highest, the stratified units in it are: siliciclastic rocks and interbedded felsic tuffs, limestone, chert that is locally highly manganiferous, a thick greenstone unit that includes both flows and pyroclastic material, and chert-quartz greywacke. The Big Salmon Complex was assigned to the Slide Mountain Terrane by Wheeler *et al.* (1991); Harms and Stevens (1996) termed it the Hazel assemblage and suggested a correlation with the Yukon-Tanana Terrane, with which it lies directly along strike. Mihalynuk *et al.* (this volume) document this correlation. Although no age is yet available for the Hazel orthogneiss, it may be equivalent to Early Mississippian tonalites that intrude the Yukon Tanana Terrane (Kootenay Terrane) in Teslin map-area (Gordey and Stevens, 1994).

The actual contact between the Klinkit Assemblage and the underlying Big Salmon Complex has not been observed; however near this contact north of the Alaska Highway and east of Logjam Creek, the westernmost Klinkit rocks are deformed into major recumbent, southwest-verging folds, like the D3 folds that have affected the rocks of the Big Salmon Complex to the west (Mihalynuk *et al.*, this volume). This suggests that the Klinkit Assemblage and Big Salmon Complex were deformed together, and thus were adjacent to each other at least by the time of this deformation. The Early Jurassic Simpson Peak and Nome Lake batholiths intrude the Dorsey Assemblage near the Little Rancheria River (Nelson, 1997), the Klinkit Assemblage in the headwaters of Hook Creek and elsewhere (Gabrielse, 1969), and the Big Salmon Complex southeast of Mt. Francis (Mihalynuk *et al.*, this volume); therefore all three were contiguous by Early Jurassic time at the latest.

The possibility of an early connection between the Dorsey assemblage and the Big Salmon Complex raises interesting questions. Although the well-developed stratigraphy of the Big Salmon Complex is not seen in the Dorsey Assemblage, they do share a number of common elements, such as orthoquartzites, mafic metavolcanics, highly deformed Early Mississippian intrusive bodies, metamorphism up to amphibolite grade and recumbent folding. Do they represent originally adjacent but strongly contrasting facies belts? What are the ages of the units involved, and what timelines are present to constrain correlations? These will only be answered in further geological and geochronological studies.

## LOCAL GEOLOGY

In the central Jennings River map area, the structurally lower part of the Dorsey Terrane is represented by four distinct lithologic packages in two or more separate thrust panels. They rest structurally on metamorphosed basinal strata that resemble rocks of the Kechika Trough and are assumed to represent the outer fringes of the Cassiar Terrane, the western edge of the North American passive continental margin. Near the headwaters of the Cottonwood River the basal contact of the allochthons over presumed continental margin strata is a dramatic juxtaposition of green rocks above black rocks, exposed in cirque walls and mountainsides over tens of kilometres.

Field mapping in 1997 identified three separate units in the lower Dorsey Terrane (Figure 3). From structurally lowest to highest they are the following:

1. "Greenstone-intrusive unit": Greenschist-grade intermediate to mafic metatuff, pyritic felsic metatuff, and tonalite/quartz diorite

2. "Metasediment-amphibolite unit": This unit consists of a lower, amphibolite-dominated part (2L on Figure 3) and an upper metasedimentary part (2U on Figure 3). The contact between the two, albeit tectonised, appears to be gradational. The lower part consists of amphibolite and garnet amphibolite, interlayered (interbedded?) with metatuffs, fine grained quartzite, biotite-muscovite±graphite schist, and quartzofeldspathic schist (metamorphosed chert, argillite and orthoquartzite, respectively), and marble. The upper part consists of thinly layered impure quartzite with biotite-muscovite partings (meta-argillite), thin bedded limestone, dark grey meta-chert; and interlayered chlorite±muscovite±garnet schist and quartz-muscovite schist that probably represent intermediate to felsic tuff protoliths. Both the upper and lower parts of this unit are intruded by pods of deformed tonalite, diorite and gabbro. Ultramafic pods are restricted to the lower, amphibolite-dominated unit.

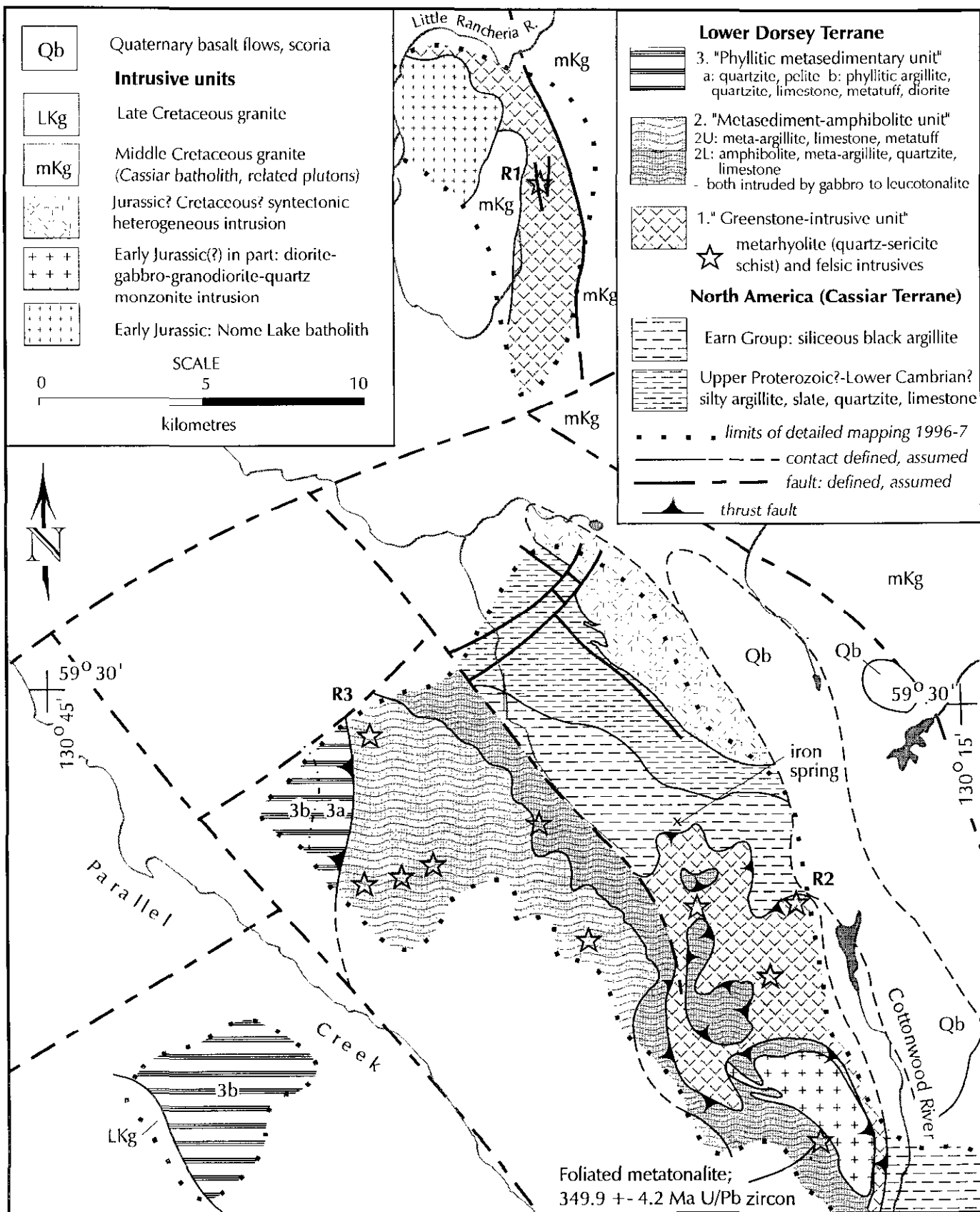


Figure 3. Geology of the area between headwaters of the Cottonwood River and Parallel Creek. Based on 1997 mapping by T. Harms, J. Nelson and M. Mihalynuk, 1996 mapping by J. Nelson and regional mapping by Gabrielse (1969)

3. "Phyllitic metasedimentary unit": Phyllitic argillite, metaquartzite, limestone, metatuff, and diorite.

### North American marginal strata

Dark grey to black slate to argillite are exposed extensively in the mountains north of the headwaters of the Cottonwood River (Figure 3). These rocks form a homoclinally southwest-dipping succession. At the base, a thick section of blocky to slabby-weathering slate and silty slate contains sparse beds of buff quartzite and white limestone. The siliciclastic rocks in this sequence are dark grey to black. They form rugged cliff outcrops and slabby to platy talus. Dark iron stains coat weathered surfaces. Muscovite is present on some bedding planes. In a few localities, large-scale current ripples are preserved on the bedding surfaces of thick-bedded silty slates. These features suggest correlation with the upper Proterozoic-Cambrian basinal rocks of the central Kechika Trough (for description see Ferri *et al.*, 1996). This unit is overlain by a few metres of black calcareous argillite, and then by a thick, monotonous unit of black, rusty-weathering, platy, carbonaceous, siliceous slaty argillite, black porcellanite, and at one locality, siltstone with graded beds. These two upper units closely resemble, respectively, the Ordovician-Lower Devonian Road River Group and the Devonian-Mississippian Earn Group of the central Kechika Trough. More locally, they are probably correlative with exposures of siliceous, pyritic black argillite, pyritic and baritic chert, and limestone on the COT claims 15 kilometres to the south (Nelson, 1997).

A strongly foliated and lineated, highly heterogeneous pluton intrudes the base of the sequence, roughly following bedding and cleavage. It ranges from diorite to tourmaline-bearing granitic pegmatite. Fairly homogeneous granodiorite with plagioclase and/or orthoclase phenocrysts is interspersed with areas of gneissic, compositionally banded intrusive. The margins of the pluton are extensive sill complexes.

Structurally, the metasedimentary sequence is characterised by a ubiquitous, moderately southwest-dipping cleavage. Bedding parallels this cleavage, as shown in their general parallel attitudes in outcrop and in Figure 5, and microscopically by the limbs of isoclinal folds. An earlier crinkled cleavage, not parallel to the dominant cleavage, is seen only in thin section, preserved in the cores of andalusite porphyroblasts. Minor to mesoscopic, northeasterly-verging folds (F2) fold earlier tight to isoclinal folds in a few outcrops. These folds and also crenulations parallel the west-northwesterly regional strike (Figure 5). The youngest (F3) chevron-style folds, which re-fold F2 at a few localities, have southwesterly plunging axes with northwesterly vergence. Perhaps related to these, top-to-the-northwest shear, determined from C and S fabrics and asymmetrical pressure shadows around relict

plagioclase phenocrysts, was noted at in granite at one locality along the margin of the pluton. Sills and dikes related to the pluton are involved in F2 and F3 folds, and foliation in the pluton is parallel to that in the surrounding rocks (Figure 5), indicating that it had been emplaced prior to much of the deformation.

Metamorphic andalusite and cordierite are widespread throughout the metasedimentary sequence. Their distribution bears no spatial relationship to the pluton. In some cases elongate andalusite porphyroblasts up to several centimetres in length show very little or no preferred orientation. Andalusite cores, however, contain a crinkled cleavage that is not parallel to the dominant rock fabric. Their later growth follows crenulations, and the crenulations themselves are deflected around the porphyroblasts. These textural relationships indicate that andalusite growth occurred throughout a sequence of progressive deformation, and even outlasted it in some localities.

A set of multielement stream sediment anomalies was determined in this area by the Regional Geochemical Survey (Geological Survey of Canada, 1978). During follow-up geochemical work, several strong northwest-trending soil anomalies were defined (Smith and Gillan, 1980). An iron spring occurs in the Earn Group a few hundred metres below the base of the allochthons (Figure 3). Our prospecting work did not locate any specific sedimentary-exhalative occurrences, although wispy pyrite and/or pyrrhotite laminae are very common in the metamorphosed black shales. In some samples, the stringers form tiny rootless isoclinal, and follow the earliest recognized cleavage. For the most part this cleavage is parallel to bedding; however in one petrographic section, both the cleavage and the sulphide stringers clearly cut across bedding in isoclinal fold hinges, indicating that the sulphide stringers are not bedding-parallel laminae, but rather the result of sulphide migration into a solution cleavage.

### "Greenstone-intrusive unit"

The "greenstone-intrusive unit" forms the lowest of the allochthons in the Cottonwood River area (Unit 1 on Figure 3), resting directly above inferred Earn Group-equivalent strata on a surface that is very gently dipping over tens of square kilometres and truncates steeper cleavage and bedding in the autochthonous rocks below. It consists of two lithologic suites: a supracrustal, metavolcanic suite, and a suite of heterogeneous intrusions. The metavolcanic suite consists primarily of quartz-sericite schist (meta-rhyolite tuff) in places. Some of the felsic metatuffs contain recognizable primary quartz and/or plagioclase phenocrysts. Quartz-sericite schist localities are shown on Figure 2 by stars. Sedimentary components of the "greenstone-intrusive unit" include volumetrically minor grey argillite and grey to sea-green chert. The metavolcanic-metasedimentary suite is intruded by deformed plutonic bodies. They range from gabbro and diorite to tonalite

and quartz diorite. Foliation in them is variably developed. It ranges from weak to protomylonitic, particularly near the base of the allochthon.

The “greenstone-intrusive unit” resembles the quartz-sericite schist-intermediate metatuff-limestone-chert sequence mapped near the headwaters of the Little Rancheria River (Nelson 1997). They are correlated on Figure 3, although the Little Rancheria sequence is isolated by Quaternary cover and Mesozoic plutons, and may be separated from the Cottonwood River allochthons by a major normal(?) fault. Similarities include: predominance of metatuffs and cogenetic high-level pre-tectonic intrusions, presence of pyritic quartz-sericite schist with plagioclase and less abundant quartz phenocrysts, and greenschist grade metamorphism with widespread biotite, chlorite, epidote and sericite. The Little Rancheria sequence contains a Mississippian limestone (Nelson, 1997).

### “Metasediment-amphibolite unit”

This unit overlies the “greenstone-intrusive unit” above a sharp, nearly flat contact (Figure 3), and is distinguished from it by strong contrasts in metamorphic grade and lithologic components. The “metasediment-amphibolite unit” is divided into a lower part and an upper part (Units 2L and 2U on Figure 3). The lower part contains thick, dark green tabular amphibolite bodies and small pods of ultramafic rock, both of which are absent in the upper part. Both upper and lower parts contain very siliceous metasedimentary rocks and marble interbeds. Chlorite phyllite (metamorphosed intermediate tuff?) and quartz-sericite schist (felsic metatuff?) commonly occur together in the upper part. The contact between the upper and lower parts is gradational, and is mapped at the top of the highest amphibolite body.

Thick bands of amphibolite and garnet amphibolite form prominent cliffside and knob exposures in the lower part of the unit (unit 2L). In petrographic section, the amphibolites consist of lepidoblastic aggregates of forest green hornblende with interstitial albite and in some cases large splotchy garnet poikiloblasts; trains of rutile and ilmenite-magnetite are heavily overgrown by retrograde sphene. The amphibolites are interlayered with quartz-rich to pelitic metasediments, some of which display protolith textures that identify them as meta-argillites, metacherts, and quartz sandstones. Small amounts of thin-bedded marble are also present, interlayered with either meta-argillite or mafic (tuffaceous) rocks. A few thin units of quartz-muscovite schist within the amphibolite are may be meta-rhyolite tuffs, although there are no relict primary textures to support this assertion. Pods and slivers of ultramafic rock occur in the lower part of unit 2. Except for one fairly intact serpentinized harzburgite tectonite near its base, these have been metamorphosed along with their

enclosing rocks. Original textures are generally obliterated and they appear as coarse aggregates of actinolite/tremolite and talc.

The relatively high metamorphic grade of the lower part of the unit is indicated by hornblende ( $\pm$ garnet $\pm$ epidote)-plagioclase-quartz-rutile in metabasites, and assemblages of coarse biotite-muscovite-quartz-feldspar in pelitic rocks. In thin sections of the mafic rocks, trains of rutile and (?)ilmenite of the peak metamorphic assemblage are heavily mantled by retrograde sphene.

The upper part of the “metasedimentary-amphibolite unit” overlies the amphibolite-bearing lower part along a lithologically gradational contact that is also a zone of comparatively strong deformation. This may be due to remobilization of an original depositional contact. Above the contact, siliceous schists are the most abundant rock type, and amphibolite and ultramafites are rare. Three rock types dominate the upper part of the unit: siliceous, platey-layered semipelites, which are probably meta-argillites and metacherts; thin-bedded limestone; and chlorite schist with quartz-sericite schist, which reflect a metamorphosed intermediate to felsic tuffaceous protolith. These components repeat across strike, probably because of fold and/or fault repetition; however without “way up” indicators and spotty exposure the exact mechanism of the thickening is not clear.

The metamorphic grade in the upper part of the unit is somewhat lower than in the lower part: chlorite-biotite $\pm$ garnet $\pm$ actinolite assemblages pre-dominate in metamorphosed intermediate tuffs, although this appears to be in part due to strong retrograde metamorphism in which garnet and biotite have partly reverted to chlorite.

Both the upper and lower parts of the unit are intruded by small mafic to tonalitic pods and sills, typically coarse grained diorites, gabbros, and white leucotonalite and granite (leucosome?), which themselves are strongly foliated, folded and refolded. A highly foliated and deformed tonalite to diorite pluton, mapped in 1996 (Nelson, 1997), intrudes rocks that are considered to be within the lower part of the unit (Figure 3). This body returned a U/Pb zircon age of  $349.9 \pm 4.2$  Ma (Table 1, Figure 4).

The base of unit 2 exhibits widespread crystalloblastic textures and fabrics typical of metamorphic rocks, including coarse-grained, schistose, mica-rich rocks; compositionally banded orthogneiss; and foliated and lineated amphibolite. The rest of the unit, including rocks of both the lower amphibolite-rich and the upper siliceous parts, is characterized by very fine grain size and a fabric of paper-thin, laterally continuous compositional bands and rodding typical of a zone of high shear strain.

**TABLE 1**

**96JN-32-6- Dorsey Assemblage metatonalite**

Three fractions of clear colourless zircon define an array characteristic of Pb loss with no evidence for inheritance. The best age estimate for this rock is  $349.9 \pm 4.2$  Ma, based on the weighted average of the three  $^{207}\text{Pb}/^{206}\text{Pb}$  ages.

**U-Pb ANALYTICAL DATA**

| Fraction <sup>1</sup>                 | Wt<br>mg | U <sup>2</sup><br>ppm | Pb* <sup>3</sup><br>ppm | <sup>206</sup> Pb <sup>4</sup><br><sup>204</sup> Pb | Pb <sup>5</sup><br>pg | <sup>208</sup> Pb <sup>6</sup><br>% | Isotopic ratios (1σ,%) <sup>7</sup> |                                     |                                      | Apparent ages (2σ, Ma) <sup>7</sup> |                                      |             |
|---------------------------------------|----------|-----------------------|-------------------------|-----------------------------------------------------|-----------------------|-------------------------------------|-------------------------------------|-------------------------------------|--------------------------------------|-------------------------------------|--------------------------------------|-------------|
|                                       |          |                       |                         |                                                     |                       |                                     | <sup>206</sup> Pb/ <sup>238</sup> U | <sup>207</sup> Pb/ <sup>235</sup> U | <sup>207</sup> Pb/ <sup>206</sup> Pb | <sup>206</sup> Pb/ <sup>238</sup> U | <sup>207</sup> Pb/ <sup>206</sup> Pb |             |
| <b>Dorsey Assemblage metatonalite</b> |          |                       |                         |                                                     |                       |                                     |                                     |                                     |                                      |                                     |                                      |             |
| A                                     | c,N5,p,s | 0.036                 | 284                     | 16                                                  | 1161                  | 30                                  | 14.1                                | 0.05492 (0.11)                      | 0.4052 (0.25)                        | 0.05351 (0.18)                      | 344.6 (0.7)                          | 350.7 (8.1) |
| B                                     | c,N5,p,s | 0.032                 | 333                     | 19                                                  | 1117                  | 33                                  | 14.1                                | 0.05466 (0.13)                      | 0.4032 (0.29)                        | 0.05350 (0.22)                      | 343.1 (0.9)                          | 350.2 (9.9) |
| E                                     | m,N5,p,s | 0.144                 | 279                     | 16                                                  | 1553                  | 87                                  | 14.1                                | 0.05321 (0.36)                      | 0.3924 (0.42)                        | 0.05348 (0.13)                      | 334.2 (2.3)                          | 349.4 (5.9) |

Notes: Analytical techniques are listed in Mortensen et al. (1995).

<sup>1</sup> Upper case letter = fraction identifier; All zircon fractions air abraded; Grain size, intermediate dimension: c = < 149µm and > 105µm and m = < 105µm and > 74µm; Magnetic codes: Franz magnetic separator sideslope at which grains are nonmagnetic (N) or Magnetic (M); e.g., N1 = nonmagnetic at 1°; Field strength for all fractions = 1.8A; Front slope for all fractions = 20°; Grain character codes: b = broken fragments, e = elongate, eq = equant, p = prismatic, s = stubby, t = tabular, ti = tips.

<sup>2</sup> U blank correction of 1pg ± 20%; U fractionation corrections were measured for each run with a double <sup>233</sup>U-<sup>235</sup>U spike (about 0.005/amu).

<sup>3</sup> Radiogenic Pb

<sup>4</sup> Measured ratio corrected for spike and Pb fractionation of 0.0035/amu ± 20% (Daly collector) and 0.001/amu ± 7% and laboratory blank Pb of 10pg ± 20%. Laboratory blank Pb concentrations and isotopic compositions based on total procedural blanks analysed throughout the duration of this study.

<sup>5</sup> Total common Pb in analysis based on blank isotopic composition

<sup>6</sup> Radiogenic Pb

<sup>7</sup> Corrected for blank Pb, U and common Pb. Common Pb corrections based on Stacey Kramers model (Stacey and Kramers, 1975) at the age of the rock or the <sup>207</sup>Pb/<sup>206</sup>Pb age of the fraction.

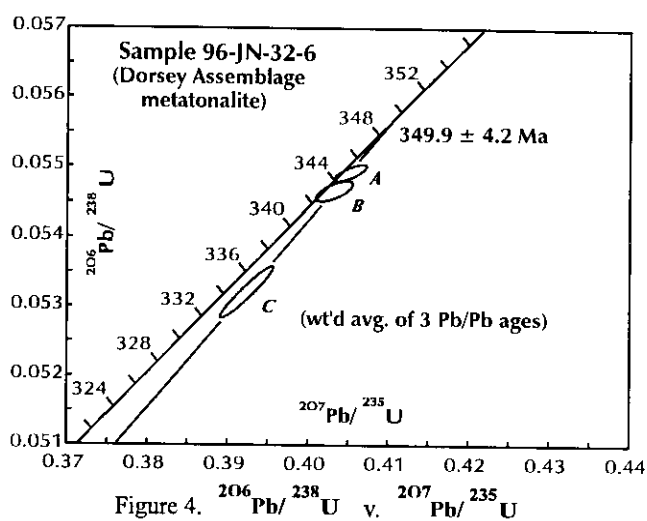


Figure 4.  $^{206}\text{Pb}/^{238}\text{U}$  v.  $^{207}\text{Pb}/^{235}\text{U}$  concordia diagram for sample 96-JN-32-6. Fractions as in Table 1.

Large, mountainside-scale recumbent folds occur within this unit, particularly in cliff exposures of the lower part, where compositional layering in amphibolite bodies outlines the noses of recumbent isoclinal folds. Mesoscopic northeasterly-verging chevron folds with gently northwest-plunging axes also occur (Figure 5). On Figure 5, the axes of small-scale isoclinal, intrafolial folds and also mineral lineations form a diffuse girdle ranging from gently northwest-plunging to steeply southwest-plunging.

**“Phyllitic metasedimentary unit”**

This structurally highest unit overlies the upper part of the “metasediment-amphibolite unit” across a covered contact. In the northern part of the mapped area, where the two units are seen in closest proximity, bedding attitudes above and below the contact show some angular discordance: possibly they lie in faulted contact. The base of the “phyllitic metasedimentary unit” there (subunit “3a” on Figure 3) consists of medium to thick bedded buff-coloured micaceous orthoquartzites with interbedded grey slate and silty slate, a section typical of Early Cambrian siliciclastics of the miogeocline. A

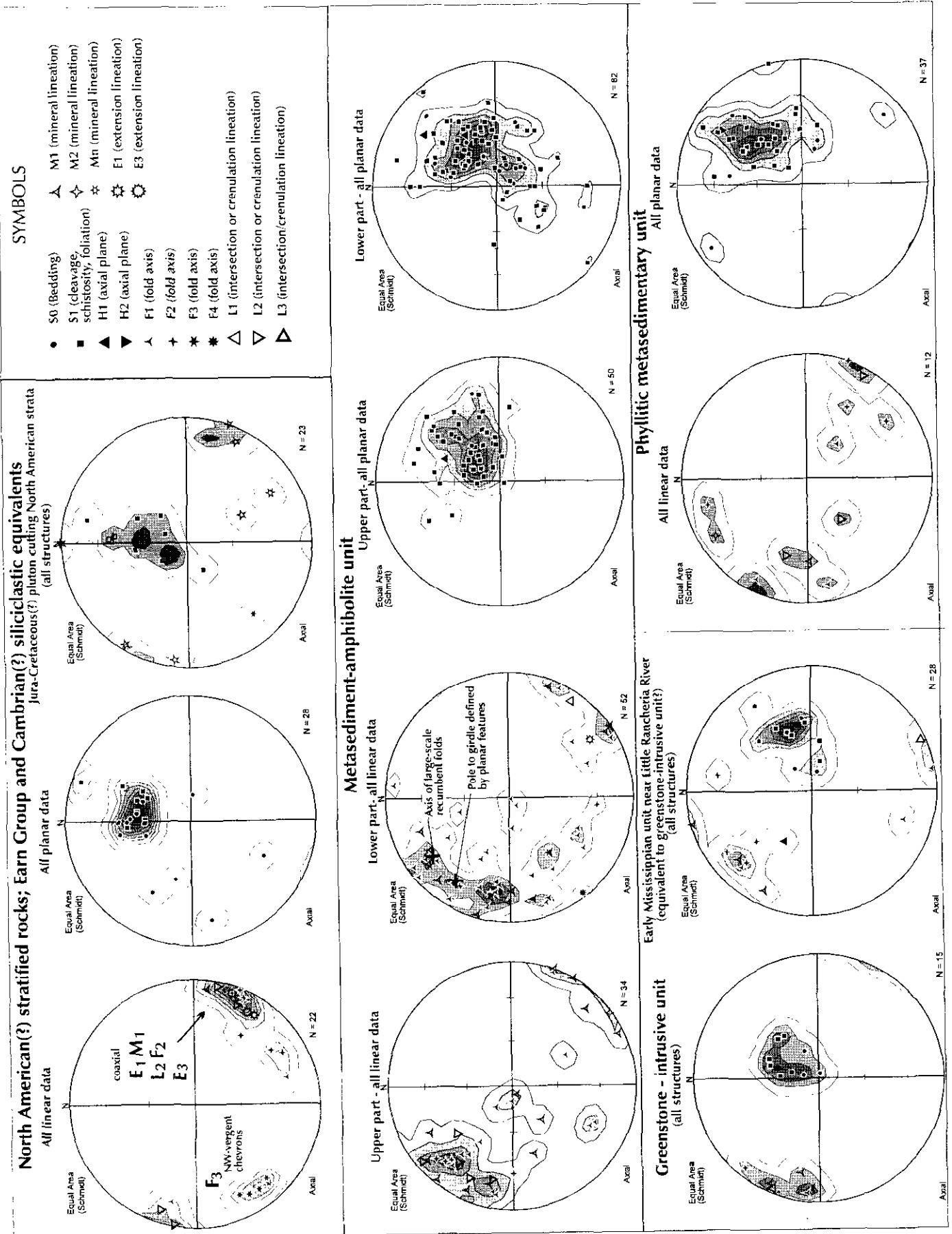


Figure 5. Structural data for the area shown on Figure 3.

minor but notable feature of this section is one dismembered bed, 0.5 to 1 metre thick, of coarse quartz-feldspar grit that forms slump blocks in impure carbonate. Towards the southwest in continuous ridge exposure, the quartzite-pelite section passes gradationally upward into finer metasedimentary strata including grey phyllite and chert (subunit "b" on Figure 3).

The main exposures of the "phyllitic meta-sedimentary unit" are southwest of Parallel Creek. There, the unit is dominated by grey, black and light green phyllitic argillite with subordinate buff, dark grey, or white quartz grit and sandstone, and thin-bedded pale green to grey chert. A few prominent bands of recrystallized limestone are present. In one continuous layer, meta-diorite grades into amphibolite and metatuff.

The "phyllitic metasedimentary unit" shows less development of metamorphic minerals and textures than the underlying "metasediment-amphibolite unit". Garnet is not seen, except in the lowermost exposures of unit 3a northeast of Parallel Creek. The structural style of this upper unit reflects deformation at a higher crustal level than the lower units. Outcrop-scale concentric folds with axial planar cleavage are common, and multiple tiny crenulations typify the phyllitic argillites.

### **Structural style of the allochthonous units**

Prevailing dips of bedding, compositional layering, cleavage and schistosity throughout the allochthonous units are moderately to the southwest (Figure 5). Ridge- and outcrop-scale isoclinal folds, common within the "metasediment-amphibolite unit", suggest that this uniformity results, at least in part, from isoclinal folding and accompanying axial planar fabric development. Axes of outcrop-scale isoclinal, intrafolial F1 folds and mineral elongation lineations throughout all of the allochthonous units have dominantly shallow west-northwest plunges but are variably dispersed about that trend within the plane of foliation (Figure 5). This pattern is consistent with the observed isoclinal folding. More open to chevron-type, in many cases northeasterly-verging minor folds re-fold the earlier cleavage and mineral lineations: they are designated F2. Their axes, which plunge gently to the northwest, do not coincide with the second-phase, northeasterly vergent minor folds in the North American sequence, which plunge gently to the southeast (Figure 5). On the other hand, the consistency of orientation of fabric elements throughout the allochthons in the study area suggests that all of them underwent a uniform orientation, if not degree, of deformation.

### **Correlations and relationships between units**

Each of the three units of the lower Dorsey Terrane described here differs from the others in lithologic

makeup and metamorphic grade. One possible common element is the early Mississippian age of the tuff-limestone sequence near the Little Rancheria River and of the felsic pluton that cuts the "amphibolite-quartzite unit" west of the Cottonwood River. Perhaps the "metasediment-amphibolite unit" was originally basement to the "greenstone-intrusive unit", but now lies structurally above it. Another "common theme" between different thrust slices is the presence of metamorphosed tuffs, including quartz-sericite schists, in both the "greenstone-intrusive" unit and in the upper part of the "metasediment-amphibolite" unit. Planned U/Pb dating will hopefully clarify inter-allochthon relationships.

### **Correlations with other allochthonous assemblages in southern Yukon and far northern B.C.**

The "greenstone-intrusive unit", the lowest of the allochthons in central Jennings River area, occupies an equivalent structural position to the Ram Creek Assemblage, which lies immediately above the Earn Group along the Swift River in southern Yukon (Stevens and Harms, 1995; Harms and Stevens, 1996). They are lithologically similar as well: both are dominated by mafic to intermediate metatuffs and intrusive rocks. Quartz-sericite schist, exposed a few metres west of the Lucy prospect on the Swift River property of Birch Mountain Resources, may be a metamorphosed felsic tuff like those in the "greenstone-intrusive unit".

The "metasediment-amphibolite unit" resembles the Dorsey Assemblage in metamorphic grade. They share a lithologic suite of pelitic schist, quartzite and metaplutonic rocks, amphibolites and garnet amphibolite. The gross distribution of rock types in it, with mafic protoliths more abundant in its lower part, is a further point of similarity with the Dorsey Assemblage (Stevens and Harms, 1995). Stevens (1996) reports high temperatures and pressures for pre-Permian metamorphism of the Dorsey Assemblage in the southern Yukon. Garnet-bearing amphibolites texturally and mineralogically very similar to those in unit 2L occur within the "Anvil allochthon" of the St. Cyr klippe (Fallas, 1997) and within the Rapid River Tectonite in the Sylvester Allochthon (Figure 2; Nelson, 1997). Contact relationships both here and in the Rapid River Tectonite show clearly that the metabasites are interbedded with metamorphosed siliciclastic rocks and very aluminous, mica-rich pelites as well as argillite, chert and limestone. This overall protolith differs very markedly from the Slide Mountain Terrane in its classic exposures. The oldest rocks known in the Slide Mountain Terrane are latest Devonian-Early Mississippian basalts interbedded with cherts and argillites, and the bulk of the microfossil ages in the terrane are Early Mississippian to Late Triassic (Nelson and Bradford, 1993). The "metasediment-amphibolite unit" is intruded by an Early Mississippian pluton: thus it is reasonably Devonian or older, and predates the Slide Mountain Terrane. Its age and tectonic setting are

problematic. The timing of the metamorphic event that this sequence experienced is also so far unknown. Is it indeed correlative with pre-mid Permian metamorphism and major deformation in the Dorsey Assemblage, or is it younger, for instance, Jurassic? Future work will address these questions.

The "phyllitic metasedimentary unit" west of Parallel Creek, correlates in lithologies and style and degree of deformation and metamorphism with the Swift River Assemblage as defined by Harms and Stevens (1996).

## Mineral potential

Quartz-sericite schists, considered to be metamorphosed rhyolite tuffs, have been identified at numerous localities within the allochthons in the central Jennings River area. Several examples are found in the "greenstone-intrusive" unit, as shown by the Little Rancheria locality (R1 on Figure 3; Nelson, 1997) and a new discovery 2 kilometres northwest of the lake that forms the headwaters of the Cottonwood River (R2, Figure 3). Quartz-sericite schists also occur at scattered localities in the upper part of the "metasediment-amphibolite unit". The most extensive exposure in this unit consists of a set of small outcrops and subcrops spread over a 400 by 150 metre area on a hillside 5 kilometres northeast of Parallel Creek (R3 on Figure 3). The exposures consist of white, rusty-weathering finely laminated siliceous exhalite(?) with pyrite stringers. So far the age of the presumed felsic metatuffs is constrained by a single early Mississippian conodont collection near R1 (Nelson 1997). Those in the "metasediment-amphibolite unit" are not dated, and their relationship to those in the "greenstone-intrusive" allochthon is not known.

## ACKNOWLEDGMENTS

Mitch Mihalynuk improved the paper with a thorough review. Kim and Molly Wahl and Amanda Ash provided excellent field assistance.

## REFERENCES

- Abbott, J.G. (1981): Geology of the Seagull Tin District; in *Yukon Geology and Exploration 1979-1980, Indian and Northern Affairs Canada*, pp. 32-44.
- Blanchflower, D., Deighton, J. and Foreman, I. (1997): Fyre Lake Deposit: A New Copper-Cobalt-Gold VMS Discovery; in *Yukon Exploration and Geology 1996, Exploration and Geological Services Division, Yukon, Indian and Northern Affairs Canada*, pp. 46-52.
- Fallas, K.M. (1997): Preliminary Constraints on the Structural and Metamorphic Evolution of the St. Cyr Klippe, South-Central Yukon; Slave-Northern Cordillera Lithospheric Evolution (SNORCLE) and Cordilleran Tectonics Workshop, Report of the 1997 Combined Meeting, pages 90-95.
- Ferri, F., Rees, C., and Nelson, J.L. (1996): Geology and Mineralization of the Gataga River Area, Northern Rocky Mountains (94L/10, 11, 14 and 15); in *Geological Fieldwork 1995*, B. Grant and J. Newell, editors, *B. C. Ministry of Energy, Mines and Petroleum Resources*; Paper 1996-1, pp. 137-154.
- Gabrielse, H. (1963): McDame Map Area, Cassiar District, British Columbia; *Geological Survey of Canada*, Memoir 319.
- Gabrielse, H. (1969): Geology of Jennings River Map Area, British Columbia (104/O); *Geological Survey of Canada*, Paper 68-55.
- Gabrielse, H. (1994): Geology of Cry Lake (104I) and Dease Lake (104J/E) Map Areas, North Central British Columbia; *Geological Survey of Canada*; Open File Map 2779.
- Geological Survey of Canada (1978): Regional Geochemical Survey of the Jennings River (104/O) Map Area, Northern British Columbia; Open File 561.
- Gordey, S.P. and Stevens, R.A. (1994): Tectonic Framework of the Teslin Region, southern Yukon Territory; in *Current Research, Geological Survey of Canada Paper 1994A*, pp. 11-18.
- Harms, T.A. and Stevens, R.A. (1996): Assemblage Analysis of the Dorsey Terrane; Slave-Northern Cordillera Lithospheric Evolution (SNORCLE) and Cordilleran Tectonics Workshop, Report of the 1996 Combined Meeting; pages 199-201
- Mihalynuk, M. Nelson, J.L. and Friedman, R.M. (this volume): Regional Geology and Mineralization of the Big Salmon Complex (104N NE and 104O NW), in *Geological Fieldwork 1997, B.C. Ministry of Employment and Investment, Geological Survey Branch*, Paper 1998-1.
- Mortensen, J.K. (1992): Pre-Mid-Mesozoic Tectonic Evolution of the Yukon-Tanana Terrane, Yukon and Alaska; *Tectonics*, Volume 11, pp.836-853.
- Mortensen, J.K. and Jilson, G.A. (1985): Evolution of the Yukon Tanana Terrane: Evidence from Southeastern Yukon Territory; *Geology*, Volume 13, pages 806-810.
- Nelson, J.L. (1997): Last Seen Heading South: Extensions of the Yukon-Tanana Terrane into Northern British Columbia; in *Geological Fieldwork 1996*, D.V. Lefebure, W.J. McMillan and J.G. McArthur, editors, *B.C. Ministry of Employment and Investment, Geological Survey Branch*, Paper 1997-1 pp. 145-156.
- Nelson, J.L. and Bradford, J. (1993): Geology of the Midway-Cassiar Area, Northern British Columbia; *B. C. Ministry of Energy, Mines and Petroleum Resources Bulletin 87*.
- Smith, L. and Gillan, J. (1980): Geological Mapping Survey and Geochemical Survey of the Bull Claims Project, Bull Claims 1-8, NTS 104O/8; *B.C. Ministry of Energy, Mines and Petroleum Resources*, Assessment Report 8365.

- Stevens, R.A. (1996): Dorsey Assemblage: Pre-Mid-Permian High Temperature and Pressure Metamorphic Rocks in the Dorsey Range, Southern Yukon Territory; Slave-Northern Cordillera Lithospheric Evolution (SNORCLE) and Cordilleran Tectonics Workshop, Report of the 1996 Combined Meeting, pages 70-75.
- Stevens, R.A. and Harms, T.A. (1995): Investigations in the Dorsey Terrane, Part I: Stratigraphy, Structure and Metamorphism in the Dorsey Range, Southern Yukon Territory and Northern British Columbia; *in Current Research, Geological Survey of Canada Paper 1995A*, pages 117-127.
- Wheeler, J.O., Brookfield, A.J., Gabrielse, H., Monger, J.W.H., Tipper, H.W. and Woodsworth, G.J. (1991): Terrane Map of the Canadian Cordillera; *Geological Survey of Canada Map 1713A*, Scale 1:2,000,000.



**TOODOGGONE - McCONNELL PROJECT:**

**GEOLOGY OF THE McCONNELL RANGE - SERRATED PEAK TO JENSEN CREEK, PARTS OF NTS 94E/2 AND 94D/15**

By L.J. Diakow and C. Rogers

**KEYWORDS:** Asitka Group, Takla Group, Black Lake intrusive suite, copper-gold porphyry, Kemess Mine, McConnell Range

## INTRODUCTION

The Toodoggone-McConnell Project was initiated in 1996 to map and evaluate a tract of Early Jurassic plutons and surrounding arc volcanic successions of Paleozoic to Jurassic age for base and precious metal mineralization.

Bedrock mapping during the first year of the program focussed on a region south of the Finlay River and east of Thutade Lake, documenting local geology near known copper-gold porphyry targets - the Kemess South deposit and Kemess North and Pine prospects (Diakow and Metcalfe, 1997). The current 1:20000 scale mapping program expands this geology to the east and south into the McConnell Range, between latitudes 57°06' and 56°39' north, and longitudes 126°39' and 126°25' east (Figure 1).

The McConnell Range was divided into two contiguous map areas along the drainage line of Jensen and Thorne creeks. The northern map segment, described in this report, ties into geological work completed in 1996 in the vicinity of the Kemess South mine. It illustrates the extent of older, Paleozoic strata as far south as Jensen Creek, and also provides a glimpse of strata low in the overlying Upper Triassic succession. Geology in the southern map segment of the McConnell Range between Jensen and Johanson creeks is reported by Legun (1998). The southern region is underlain by Upper Triassic strata that are progressively younger towards the south, which affords stratigraphic comparison to correlative rocks that host important stratabound copper deposits in the Upper Triassic Takla Group in the type-area to the west.

Staging for this program was the Kemess South minesite. It is situated along the northwestern periphery of the study area, and requires only a short helicopter ferry into the McConnell Range.

## LITHOSTRATIGRAPHY

The McConnell Range was previously mapped in regional programs undertaken by the Geological Survey of Canada (Lord, 1948; Richards, 1976). Present detailed mapping and subdivision of Paleozoic and Mesozoic units build upon this excellent earlier work. Local geology of the McConnell Range and outlying areas is summarized in

Figure 2 with representative stratigraphic sections illustrated in Figure 3.

The oldest layered rocks in the McConnell Range are assigned to the upper Paleozoic Asitka Group based on lithologies and paleontology similar to those described by Lord (1948) and Monger (1977) in the adjoining region to the west. Upper Triassic strata belonging to the Takla Group unconformably overlie the Asitka Group. Volcanic rocks of the Lower Jurassic Toodoggone formation unconformably overlie probable Upper Triassic strata at the northernmost part of the study area, just south of the tailings impoundment at the Kemess South mine. Farther to the south, in the McConnell Range, these distinctive Lower Jurassic volcanic rocks are absent. It is possible that volcanic rocks of the Toodoggone formation once overlay older strata in the McConnell Range, but have been removed by subsequent erosion that has cut down, exposing the tops of comagmatic epizonal granitic rocks. The youngest strata exposed is a continental clastic assemblage assigned to the Upper Cretaceous Sustut Group. Several small exposures of these rocks are found along the lower west side of the McConnell Range in fault contact with, and possibly unconformable on older strata.

## Mid-Pennsylvanian to Early Permian - Asitka Group

The Asitka Group was originally named for a sequence of interbedded silica bimodal volcanic rocks, chert, limestone and argillaceous strata exposed mainly between the Asitka and Niven rivers in northeast McConnell Creek map area (Lord, 1948). Monger (1977) remapped part of this area and although emphasis was on the overlying Triassic stratigraphy, he introduced a three-fold division for the Asitka Group, comprising a middle unit dominated by rhyolite, and some breccia and feldspar porphyry, which grade into underlying basaltic rocks. Basalts are also common in the uppermost and lowermost units, accompanied by limestone, in places tuffaceous and chert. Argillite is present in the lower unit.

New fossil and U-Pb isotopic data confirm that Paleozoic rocks are considerably more widely distributed than previously mapped in the southern Toodoggone River map area (Gabrielse, 1977). They underlie a broad region that extends from the northwestern side of Thutade Lake, southeastward across Duncan Ridge, through the Kemess mine area, and as far east as Serrated Peak. Near Serrated Peak they are folded and involved in west-directed thrust faulting. Southward from Serrated Peak, into the McConnell Creek map area, Paleozoic strata are uplifted

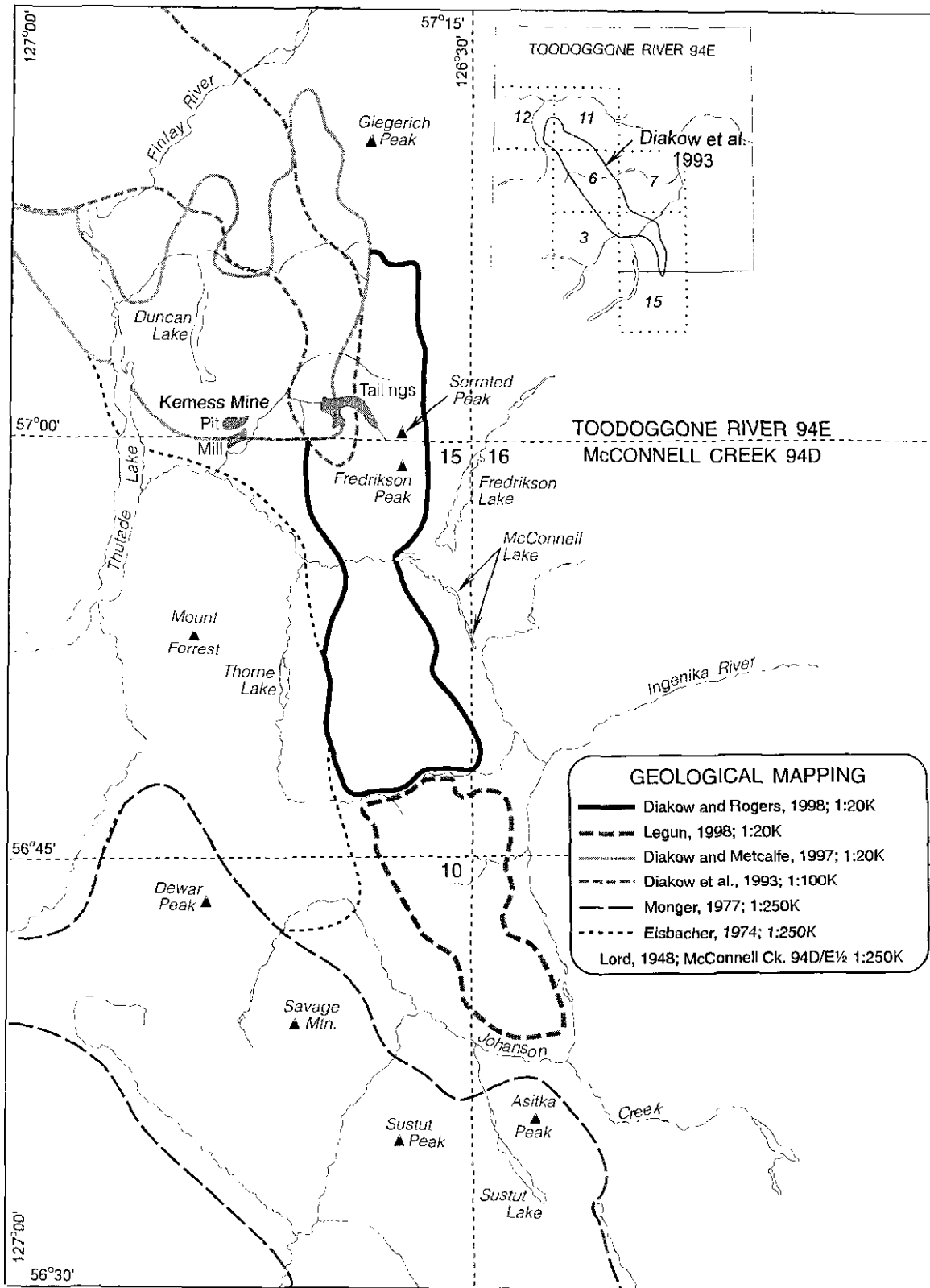


Figure 8.1. Location of recent and previous mapping in the southern Toodoggone River (94E) and northeastern McConnell Creek (94D) map areas.

and exposed mainly along the west side of the Fredrikson pluton where they are affected both by thermal contact metamorphism and numerous steep faults. The most southerly exposures are scattered along a creek that marks the trace of a major north-trending fault located immediately north of a drainage divide separating Thorne Creek from Jensen Creek.

The thickness of the Paleozoic sequence is not known since the base has not been observed. Chert and lesser argillite comprise the youngest unit of the Paleozoic sequence. The upper contact is placed at the first occurrence of grey-black platy weathering limestone containing the distinctive Late Triassic fauna, *Halobia*. These fossiliferous beds are observed at four widely spaced localities, where they are either faulted against or stratigraphically overlying the Paleozoic succession. However, the upper contact may be an unconformity. This is indicated where there are local folds in immediately underlying Paleozoic strata but planar beds in overlying Triassic strata.

Paleozoic stratigraphy south of Serrated Peak is informally subdivided into two units that have a consistent relative stratigraphic position and are in gradational contact. The lower unit is dominated by basaltic flows, lesser andesite, both as flows and as fragmental deposits, and rare rhyolite was exposed in a single section. Sedimentary rocks may occur in intervals up to 100 metres thick within this predominantly mafic succession. The upper unit consists of a varied sedimentary assemblage that includes: chert, limestone, siliceous and pyritic black shale, and tuffaceous siltstone and sandstone.

### ***Lower Volcanic Unit***

The volcanic unit is typified by dark green basalt and basaltic andesite flows that form massive sections devoid of obvious layering. Flows representative of this unit are best observed outside the map area on the southwest-facing slope immediately to the north of a small lake adjacent to the lower camp at Kemess Mine. Most flows are aphanitic, imparting a massive appearance. Subordinate varieties may contain several percent pyroxene phenocrysts, fine plagioclase phenocrysts, and rare amygdaloidal members. The latter have elliptical chlorite and lesser silica-filled amygdules. Due to their massive nature, these flows sustain an irregular pattern of fractures that may be lined with epidote and a chalky mixture of silica and carbonate.

Fragmental and felsic rocks constitute a volumetrically minor component within the mafic flow unit. A 50-metre-thick pyroclastic unit bounded by flows is well exposed on a ridge located 3.7 kilometres at 287° azimuth from Fredrikson Peak (section D in Figure 3). The base of this section comprises aphanitic basalt overlain by bedded and laminated andesitic to dacitic meta-tuffs. The tuffs are composed mainly of layers of mixed ash and crystals that pass upwards into predominantly lapilli-rich layers containing finer grained, graded interbeds. Flattening of pyroclasts along a narrow horizon suggest incipient welding, possibly as a result of compaction of hot subaerial fallout. Above a sharp, conformable contact with the tuffs is rhyolite about 60 metres thick; it is grey and aphanitic with thin, faint flow laminae. A sample of this rock has

been collected for U-Pb geochronometry. Conglomerate composed of matrix-supported cobbles derived from the underlying rhyolite marks the base of an overlying recessive 30-metre-thick sedimentary interval. Rusty pyritic black mudstone dominates the sedimentary unit but there are subordinate interbeds composed of well sorted feldspathic sandstone immediately above the conglomerate, and grey-black limestone lenses containing solitary corals, near the top of the sequence. More than 150 metres of aphanitic basalts, not unlike those found beneath the pyroclastic unit, stratigraphically overlie the sediments.

Sedimentary rocks also occur within the basaltic flow unit at a lower stratigraphic level. This sedimentary section consists of alternating light and dark metasedimentary layers that occupy an interval between 15 and 75 metres thick traceable for more than 3 kilometres along a west-facing cliff dominated by basalt. This banded section consists of recrystallized siltstone and fine-grained sandstone interbedded with more distinctive laminated black mudstone that contains some feldspathic sandstone.

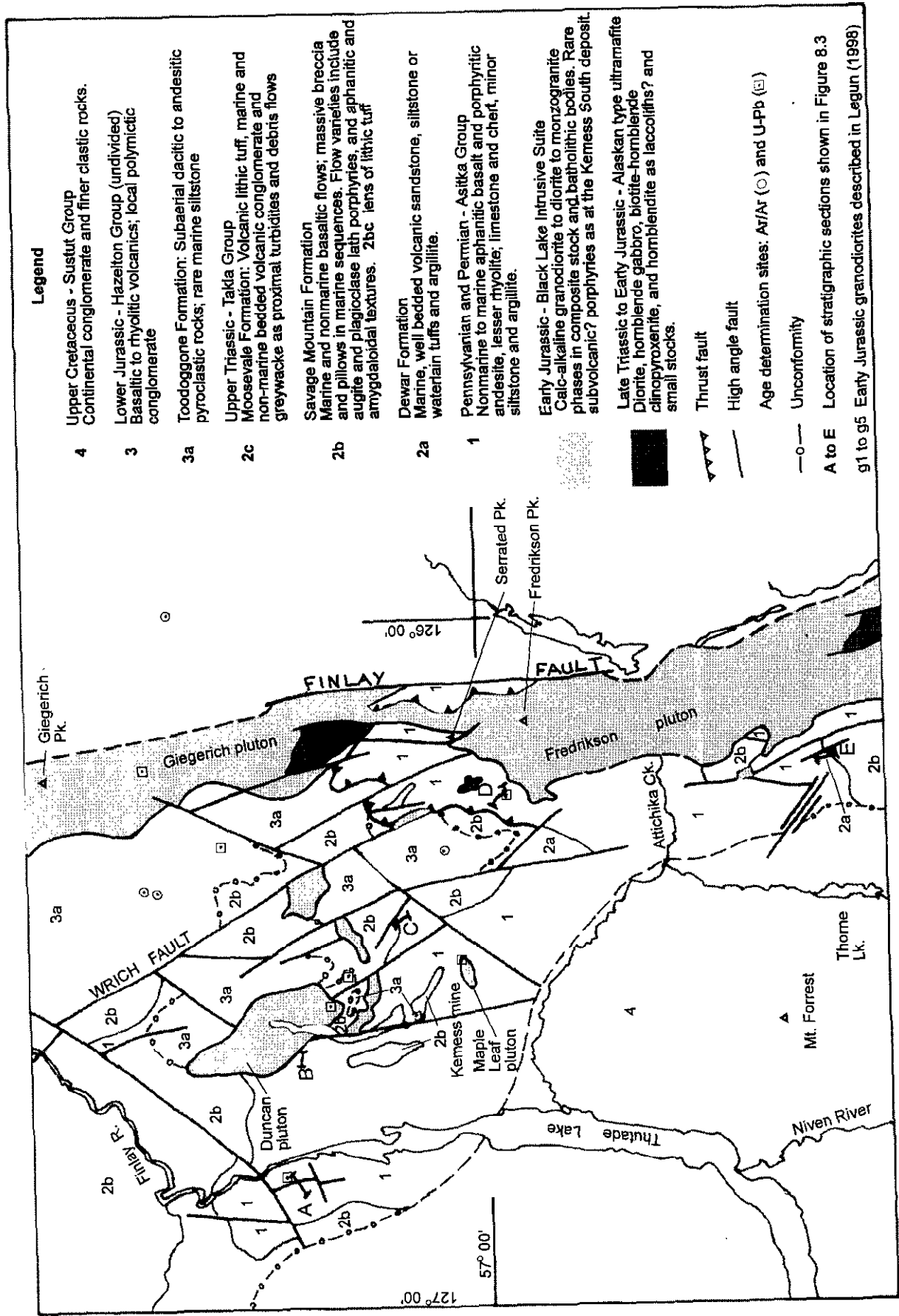
The top of the volcanic unit is placed where bedded sedimentary rocks predominate. The change from underlying volcanic to overlying sedimentary units is typically abrupt with the exception of several localities where limestone interbeds in basalt mark a gradational upper contact.

### ***Upper Sedimentary Unit***

The upper sedimentary unit of the Asitka Group is characterized by thinly bedded chert and diagnostic massive limestone. Limestone, which generally occurs nearest the base, is locally interleaved with basalt. This passes upsection into cherts with or without thin limestone, tuffaceous siltstone and sandstone interbeds, then finally into an uppermost sequence dominated by black chert and siliceous mudstone. Various combinations of these lithologies are present in the northern McConnell Range, where they are generally tilted and complicated by steeply dipping faults. Possibly the most complete sequence is a composite section reconstructed from outcrops exposed sporadically along the north slope of an unnamed mountain in the central part of the study area (see section E in Figure 3). At this locality, the lower contact of the sedimentary unit consists of limestone found both as lenses within, and beds depositionally overlying, aphanitic basalts. The upper contact of the sedimentary unit is between locally folded siliceous mudstone and interbedded black chert, representative of the uppermost Paleozoic stratigraphy, and grey-black micritic limestone containing Upper Triassic macrofossils.

### ***Limestone Facies***

Limestone occupying the lower part of section E is about 5 metres thick and consists of tan and grey beds 5 to 20 centimetres thick. Along strike they are interlayered with subordinate calcareous green siltstone and medium grained sandstone that locally rest directly on aphanitic basalt. This differs from the more typical limestone of the sedimentary unit observed in isolated structural blocks throughout the northern McConnell Range. The typical



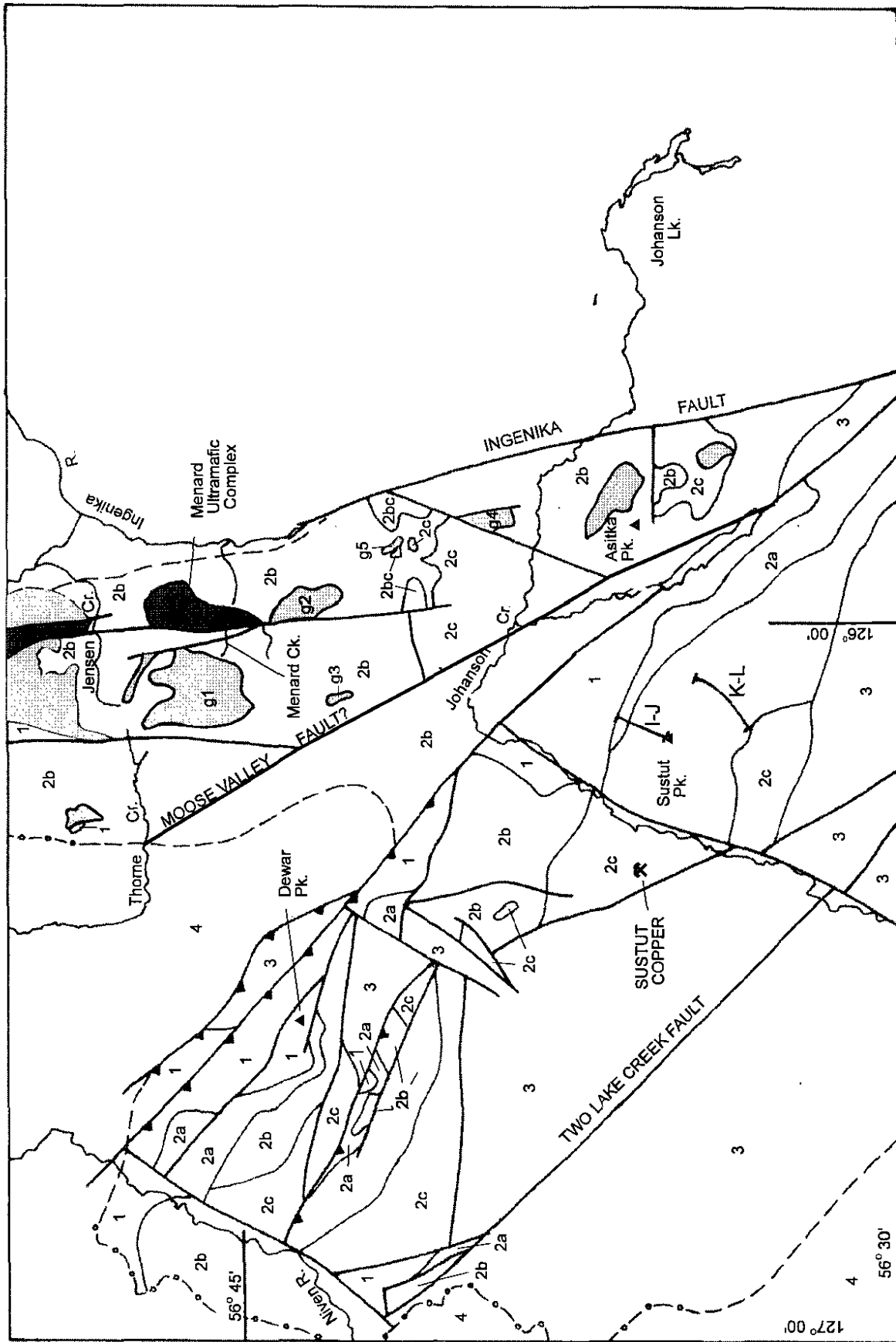


Figure 8.2 Geology of the McConnell Range showing major lithostratigraphic divisions and plutonic rocks. Geology in outlying regions to the south, northwest and west by Legun (1998), Diakow and Metcalfe (1997) and Monger (1976) respectively, are incorporated.

limestone is massive, weathers light grey or streaky grey-white, and is recrystallized. Fossils in the limestone include solitary corals, bryozoans and shell debris usually too recrystallized for specific identification. Underlying opposing slopes of a mountain immediately to the south of Attichika Creek, this limestone forms a distinctive band that is locally interlayered with aphanitic basalt. At this site massive grey, recrystallized limestone comprises several lenticular bodies; the thickest is estimated at more than 100 metres. It is either overlain by (?) or passes laterally into a distinctly laminated and bedded section about 25 metres thick which is composed of light green limestone that weathers grey with protruding siliceous laminae. Elsewhere, particularly east of Serrated Peak, strongly-folded massive grey limestone, presumed to be quite thick, is repeated in a series of imbricated thrust panels.

### **Chert Facies**

Regionally, a chert dominant succession containing variable quantities of fine-grained clastic beds gradationally overlies carbonate rocks. The transition is seen where chert layers form scarce interbeds in massive limestone then pass into sections dominated by chert containing lenses and thin beds of carbonate. In several areas, limestone is missing and chert beds directly overlie basalt. At section E, bedded siliceous mudstone, siltstone and medium to coarse-grained feldspathic sandstone are interlayered with the chert. In general, clastic rocks diminish upsection where only scarce mudstone or light green siltstone interbeds occur within the chert. Chert is mainly light grey-green or clear and translucent. However, local ribbon jasper causes colorful alternating green, red and maroon layers. Individual chert layers are typically between 1 and 15 centimetres thick. Near the top of the chert subunit, black mudstone predominates. Mud combines with silica forming siliceous mudstone which contains scarce lenses and thin layers of black micritic limestone. Pyrite disseminated throughout these black beds oxidizes to produce rusty exposures readily distinguished from a distance.

### **Age and Correlation**

A representative locality of the Asitka Group is located along the northeastern side of Duncan Ridge, an informal name given to the flat ridge bounding Duncan Lake in the west (section B in Figure 3). This locality contains massive grey limestone originally interpreted to be overlain by interbedded limestone, calcareous ash tuff and lapilli tuff stratigraphically above a base of aphanitic basalt (page 104 in Diakow and Metcalfe, 1997). Based on field relationships in the McConnell Range, this bedded sequence probably underlies the massive grey limestone and represents stratigraphy low in the upper, sedimentary subdivision of the Asitka Group. Solitary, rugose corals collected from the lowest bedded interval above basalt suggest that the stratigraphic lowest carbonates recognized in the study area are probably Early Permian; Asselian or early Sakamarian (Collections GSC C-143728, 143729, 143732 and 143734; E.W. Bamber, internal report 1-EWB-1997). Associated fusulinaceans identified as *Schwageina*

sp. ex. gr. *S. sustutensis* (Ross) confirm an Early Permian age; Sakamarian or early Artinskian [Collection GSC C-143733 (corresponds with coral collection GSC C-143732); L.Rui, internal report 1-Rui-1997]. Identical fusulineans are reported from limestone north of Sustut Peak (Ross and Monger, 1978) that was assigned to Monger's (1977) lowest stratigraphic subdivision of the Asitka Group. The age of basaltic flows dominating the lower subdivision of the Asitka Group in the McConnell Range is presently unknown. However, a sample of the aphanitic rhyolite from west of Fredrikson Peak, which interfingers similar basaltic flow members, has been collected for U-Pb geochronometry.

Outside of the current map area, west of Thutade Lake, a locally prominent fragmental member composed of rhyolitic ash-flow tuff underlies an andesite-basalt flow member (section A in Figure 3). It also includes sporadic exposures of intermediate variegated maroon and green ash tuff, lapilli tuff and rare accretionary tuff. Lithic-rich ash-flow tuff dated by U-Pb on zircons at  $308.4 \pm 0.7$  Ma [(mid-Pennsylvanian to Moscovian); R.M. Friedman, U.B.C. Geochronology Laboratory, written communication, 1997] indicate this felsic interval represents the oldest known strata of the Asitka Group. The bottom of this sequence has not been recognized, implying that older stratigraphic components of the Asitka Group may exist.

In summary, the oldest rocks assigned to the Asitka Group are felsic volcanics of mid-Pennsylvanian age. The contact of these rocks with overlying porphyritic andesite is apparently stratigraphic, but this is not proven. The andesites west of Thutade Lake extend toward the east into the McConnell Range where they have been included in a predominantly basaltic volcanic succession which also contains volumetrically minor rhyolite flows and pyroclastic rocks that are designated as the lower volcanic unit. Sedimentary rocks in this succession are not common but clearly occupy several intervals. An upper sedimentary sequence composed mainly of chemical sedimentary rocks gradationally overlies the volcanic unit. Limestones near the base of the sedimentary succession contain Early Permian fauna; they pass upsection into chert which is capped by a stratiform, rusty pyritic zone.

### **Environment of Deposition**

Earliest strata of the Asitka Group record Pennsylvanian felsic and intermediate volcanic activity during an explosive subaerial event. Subsequently, the buildup of monotonous basaltic lavas, at times interrupted by deposition of comparatively thin shale, siltstone and sandstone, took place in a shallow marine basin. As mafic volcanism waned, carbonate rocks, locally accompanied by influx of fine-grained clastic rocks dominated. Limestone appears to have accumulated in small patch reefs upon a low-relief volcanic platform. Carbonate deposition was supplanted by chert and by periodic influxes of fine grained clastic rocks in response to increasing sea level or basin subsidence. Anoxic conditions led to deposits of black pyritic siliceous mudstone and chert near the top of the Early Permian sequence.



## Upper Triassic-Takla Group

Upper Triassic strata overlie Permian stratigraphy in the McConnell Range. In general, the Triassic strata pass from lowest to highest stratigraphic levels in a north to south transect along the axis of the range. Starting south of Attichika Creek to the Thorne Creek-Jensen Creek divide, recessive micritic limestone, representing the lowest stratigraphic member, is recognized at three localities where it is either faulted against or depositionally overlies locally deformed black pyritic siliceous mudstone and chert of the Asitka Group. The contact may be unconformable. This lower sedimentary unit is in turn abruptly overlain by a middle unit characterized by a massive accumulation of basaltic flows containing subordinate pyroclastic and volcanic epiclastic rocks. South of the Thorne Creek-Jensen Creek divide, where the geology is described in a separate report (Legun, 1998), the middle, mainly mafic succession apparently thickens and changes with the principal addition of coarse feldspar phyric mafic volcanic members and increased reddish oxidation of the volcanic pile. Near the southern limit of mapping, north of Johanson Creek, the mafic succession is conformably overlain by a volcanoclastic succession composed mainly of red oxidized tuffs interspersed with sedimentary rocks. These strata are tentatively designated as the topmost unit of the Upper Triassic sequence.

### *Marine Sedimentary Rocks*

Marine, dark grey to black micritic limestone that weathers to platy angular fragments comprises the base of Upper Triassic succession. At four localities where these rocks crop out, the closest underlying strata are rusty weathering black siliceous mudstone and black chert from the uppermost Asitka Group. Distribution of these rocks ranges from the most northerly exposure on a ridge crest immediately above the open pit at Kemess Mine to a cluster of sites in the south, four to seven kilometres due east of Thorne Lake. These rocks weather recessively and appear to be relatively thin, probably less than 20 metres. In section E, these rocks directly overlie Permian strata composed of thinly bedded black chert layered with pyritic and siliceous mudstone which outline tight Z-style folds. A similar unconformable relationship between identical rock units also exists about 2 kilometres to the southeast of section E. Upslope, and slightly obscured by scree, is a pod of black limestone surrounded by black, friable mudstone which passes upsection over about 4 metres into a one-half-metre thick bed of undeformed platy black micritic limestone. This limestone contains the diagnostic Late Triassic bivalve *Halobia* and associated scarce belemnite and ammonoid fragments.

### *Augite Phyric Basalt and Associated Epiclastic Rocks*

The Takla Group is characterized by pyroxene-bearing basalt flows and associated epiclastic and volcanoclastic deposits that form castellated physiography where thickest. The predominant volcanic component typically weathers

dark green in fractured blocky exposures that rarely reveal clear indications of layering or significant compositional variability. Consequently, subdivision of the unit and reliable thickness determination are difficult. In the southwestern part of the map area, north of Thorne Creek, massifs are underlain almost entirely by lavas, estimated to be at least 400 metres thick, a calculation estimated from a rough measure of maximum relief, and assuming nearly flat layering in a presumably unfaulted section. The actual lower contact of the volcanic rocks has not been observed. However, an abrupt topographic rise corresponds with a change from the underlying recessive limestone, described above, into overlying competent volcanic sections. This probably reflects a conformable stratigraphic relationship.

Massive lava flows dominate the volcanic sequence. They are composed for the most part of distinctive basaltic porphyries with blocky augite phenocrysts. Augite phenocrysts range in size from several millimeters to sub-equant grains up to 5 millimetres in diameter in concentrations varying from a few sparse grains to 25 volume percent. Usually basalt flows containing only augite have a very dark green color which becomes lighter as randomly oriented, slender feldspar phenocrysts increase in abundance in rocks that are designated augite-plagioclase porphyry. A distinctive variety of porphyritic basalt containing plagioclase laths as long as 2 centimetres in a dark green or maroon aphanitic groundmass have been observed in a few places. These may represent thin flow members or sills and dikes. They become a significant mappable unit in the region south of Thorne Creek (Legun, 1998). Epidote, quartz, calcite and laumontite line fractures that cut the basalts.

Significant accumulations of pyroclastic rocks are notably absent in the Triassic volcanic sequence north of the Thorne Creek-Jensen Creek divide. Where present, they consist of aphanitic basaltic lapilli in a dark green groundmass.

Erosion of the volcanic pile occurred throughout volcanism resulting in scattered epiclastic interbeds. At one locality, more than 160 metres of sandstone and siltstone apparently rest on chert of the Asitka Group. Elsewhere, similar sedimentary rocks occur at a higher stratigraphic level within the basaltic volcanic sequence. There they range from individual beds a few metres thick to sequences over 100 metres thick. Everywhere they are immature and dominated by broken pyroxene and plagioclase grains in alternating dark and medium green layers 1 to 10 centimetres thick. The beds characteristically display parallel lamination and internal grading from sandstone to siltstone, with delicate cross laminations in the finer, upper parts of beds. Conglomerates are more restricted, but are well exposed in large talus blocks spalling from cliffs immediately north of the headwaters of Jensen Creek. The conglomeratic deposits locally occupy discontinuous layers up to 20 metres thick bounded stratigraphically by massive augite phyric basalts. Rounded clasts up to one-half metre in diameter and composed exclusively of pyroxene phyric basalt are suspended in a matrix of similar, smaller clasts and pyroxene-bearing sandstone.

## ***Environment of Deposition***

The preponderance of angular pyroxene and plagioclase detritus comprising the sedimentary rocks indicates derivation from the proximal basaltic volcanic sequence. Lithologic features and structure in the sediments resemble those of volcanic wackes and possibly represent mass flow turbiditic re-sedimentation.

Interpretation of the environment of deposition for volcanic and associated sedimentary rocks in the northern McConnell Range is conjectural. Shallow marine conditions prevailed prior to the outpouring of volcanic rocks. These are represented by fossiliferous mudstone and limestone that locally mark the basal unit of the Upper Triassic succession. In the overlying basalts, features that are common in submarine mafic sequences do not occur; for example, pillow lavas and pillow fragment breccias. In some marine sequences, massive lava flows have been documented which represent proximal facies that pass laterally to more distal facies dominated by pillows (McPhie *et al.*, 1993). However, because the basaltic rocks in the study area lack submarine features and locally contain interbeds of fluviatile conglomerate and finer clastic rocks, the mafic sequence is therefore interpreted to be deposited mainly in a subaerial setting. Contemporaneous erosion of the flows is indicated by sections of well sorted, immature pyroxene-bearing clastic rocks. Consequently, these sediments could record deposition in either shallow marine or lacustrine environments. However, there is an absence of marine fauna.

## ***Correlation***

Upper Triassic rocks in the northern McConnell Range are represented by two lithostratigraphic divisions - marine sediments conformably overlain by subaerial basaltic volcanic and associated sedimentary rocks. They are equivalent in age and lithologic character to the Dewar and Savage Mountain formations of the Upper Triassic Takla Group (see Takla Group stratotype in Figure 3). The Dewar Formation is a time stratigraphic equivalent of the Savage Mountain Formation. They are interpreted as a distal, sediment-dominated facies and volcanic-dominated facies, respectively (Monger, 1977). Stratigraphic relationships are well documented in a series of representative sections between Sustut Peak and Dewar Peak, about 6 kilometres west-southwest of the McConnell Range (columnar sections in pocket of Monger, 1977). Evidently, both marine and subaerial facies of the Takla Group are traceable outside the type area, underlying a broad area towards the north and northeast between the Kemess South minesite and the northern McConnell Range. Farther north in the Toodoggone River map area, similar facies have been mapped at Castle Mountain, west of the Baker Mine (Diakow *et al.*, 1993). Regional distribution of the marine facies is not well defined. It may be more extensive than presently known, but is overshadowed by the more resistant and easily recognized subaerial mafic volcanic unit.

## **Upper Cretaceous-Sustut Group**

Sedimentary rocks of the Sustut Group are exposed at two localities along the lower west slope of the McConnell Range, marking the present erosional edge of conglomerates and sandstones deposited in the Sustut Basin (Eisbacher, 1974; Lord, 1948). At the latitude of the study area, they possibly extended farther toward the east, blanketing older rocks, as indicated by outliers mapped to the north in Toodoggone River map area (Gabrielse *et al.*, 1977; Diakow *et al.*, 1993). The Sustut Group underlies much of Moose Valley, west of the McConnell Range, where it is largely concealed by cover but exposed along incised creeks. Exposure improves to the west toward Mount Forrest where westerly-inclined, uniformly-bedded sedimentary rocks hundreds of metres thick comprise east-facing cliffs.

Three kilometres east of Thorne Lake, conglomerate and sandstone beds are nearly horizontal in several creek exposures near treeline on the lower mountain slope at about 1500 metres elevation. The contact separating topographically lower Upper Cretaceous sediments from Upper Triassic volcanics upslope is concealed by a vegetated interval several hundred metres wide. The contact relationship might be an angular discordance or a major fault. At the same elevation on a southwest facing slope several kilometres to the north, flat-lying Sustut Group are clearly faulted against the Asitka Group. However, because this fault zone is oblique (*i.e.* 140° azimuth) to the general northerly trend of faults that are prominent in the McConnell Range, it is highly unlikely that an extension can be projected southward to account for distribution of the Sustut Group adjacent to Upper Triassic strata.

From a distance, the conglomerates appear to be relatively well bedded. However, up close they are typically crudely-layered aggregates composed of rounded cobbles and randomly distributed boulders, present both as a supporting closed framework or suspended largely in a finer clastic matrix. The clasts, particularly augite porphyry, chert and granitic rocks, closely resemble locally exposed map units. White vein quartz is also an abundant clast type. Coarse sandstone cemented by calcium dominates the matrix in conglomerates and occupies thinly-bedded, sometimes graded intervals between conglomeratic beds.

## **PLUTONIC ROCKS**

Plutons in the McConnell Creek map area were originally assigned to a single batholithic body comprising part of the Omineca intrusions (Lord, 1948). Woodsworth (1976) subdivided granitic rocks mainly in the Swannell Ranges north of the Hagem batholith, but also examined in reconnaissance fashion the continuation of this plutonic belt westward into the northern McConnell Range at Fredrikson Peak.

Two intrusive suites have been mapped in the McConnell Range. They include: a composite body of probable Early Jurassic age composed of unfoliated

monzogranite, coextensive and probably comagmatic with a dominantly quartz monzodiorite phase; and smaller, Alaskan-type diorite-gabbro-ultramafic complexes that locally intrude Upper Triassic volcanic strata and are faulted against the intermediate plutons.

### Early Jurassic - Intermediate Plutons

The Fredrikson pluton is named for a north-south elongated body, exposed the length of the current map area from approximately Serrated Peak in the north to Jensen Creek in the south. Between Jensen and Johanson creeks, a number of similar but smaller stocks and plug-sized bodies coincide with a characteristically strong aeromagnetic response, similar to that over the main body to the north. These smaller granitic bodies may represent apophyses of a southward-plunging extension of the Fredrikson pluton, which may be concealed by Upper Triassic strata. The Fredrikson pluton possibly extends well into the Toodoggone River map area to the north, where granitic rocks, informally named the Giegerich pluton (Diakow and Metcalfe, 1997), appear to be similar, suggesting they are part of a homogenous batholithic body stretching from at least the Finlay River in the north to Johanson Creek in the south. The best estimate of the age of the Giegerich pluton is  $197.5 \pm 2.0$  Ma based on a concordant titanite fraction from a sample collected near Giegerich Peak (R.M. Friedman, U.B.C. Geochronology Laboratory, written communication, 1997). A sample of monzogranite from the vicinity of Fredrikson Peak has been collected for U-Pb geochronology.

Monzogranite is the dominant phase of the Fredrikson pluton. The main body crops out over an area more than 23 kilometres long by 4 kilometres wide between Jensen Creek and Serrated Peak. In general, the monzogranite forms a more differentiated quartz-rich core zone that passes outward into a more mafic-rich, probable comagmatic, quartz monzodiorite phase. East of Serrated Peak and north along the eastern side of the range, a number of parallel, north trending steep faults have been mapped and coincide with a change from dominantly monzogranite on the west to quartz monzodiorite in the east. The contact between phases, which tends for the most part to be near vertical and abrupt, is traceable for kilometres between a series of ridge transects. Some contacts are clearly faults with polished surfaces. However, many are simply abrupt changes in lithology with no evidence of chilled or faulted margins. Parallelism of these abrupt lithological boundaries with demonstrable high-angle faults suggests that emplacement of these intrusive phases was controlled to a large degree by these structures.

Where monzogranite and quartz monzodiorite phases are both found in the same outcrop, the contact is typically abrupt with no clear indication of temporal relationship. However, north of Serrated Peak, narrow, isolated bodies of monzogranite are faulted against and, in places, cut quartz monzodiorite. If this relationship holds regionally, then monzogranite represents the slightly younger phase, although textural evidence indicates that both were hot when they were juxtaposed.

The contact of the monzogranite intrusive into Upper Triassic and older rocks is steep and traceable along most western and southern exposures of the pluton. Alteration of country rocks adjacent to the intrusive margin is restricted to a zone tens of metres wide, in which mafic country rocks may be weakly bleached and are contact metamorphosed to a uniformly fine-grained hard hornfels. At several localities, where limestone is exposed near the pluton, skarn alteration produced garnetiferous marble. The intrusive contact is particularly well exposed along a ridge about 3.4 kilometres due west of Fredrikson Peak, where pendants and smaller xenoliths of dioritized mafic country rocks are included in the monzogranite. Dikes composed mainly of light pink aplite and lesser pegmatite commonly project outward into the hornfelsed country rocks. Immediately north of Jensen Creek, narrow diabasic dikes, not seen elsewhere, comprise a north-northeast trending set cutting monzogranite. Contact features of the monzogranite suggest epizonal emplacement. An exception may be rare biotite-garnet schist adjacent to the pluton that may represent a deeper zone of the pluton emplaced into a probable sedimentary protolith.

Monzogranite of the Fredrikson pluton is texturally and compositionally uniform. Light pink, coarse grained and equigranular, it is composed of between 25 and 30 percent quartz, nearly equal amounts of potassium and plagioclase feldspar, and between 10 and 15 percent mafic minerals. Fresh hornblende generally exceeds the modal abundance of biotite by a factor of two to three times. Titanite and apatite are ubiquitous as minute prisms. In contrast, quartz monzodiorite is typically off-white weathering, medium grained and composed of less than 10 percent quartz, 50 to 60 percent plagioclase, less than 10 percent potassium feldspar and between 20 and 30 percent mafics. Hornblende is the dominant mafic mineral and is present as relatively unaltered grains, unlike biotite that is commonly replaced in part by chlorite. Like monzogranite, titanite and apatite are common accessory minerals.

### Late Triassic to Early Jurassic - Alaskan-type Mafic-ultramafic Complexes

Four small mafic-ultramafic intrusions have been mapped along the eastern margin of the study area in the McConnell Creek and Toodoggone River map areas. These bodies extend the distribution of Alaskan-type complexes more than 30 kilometres northward from the Menard Creek complex, which is part of a belt that extends farther southeast into the Mesilinka River map area (94C). There, many of the larger complexes have been studied in varying detail and evaluated for their potential to contain platinum group elements (Irvine, 1976; Nixon *et al.*, 1997).

In the study area, the size of the intrusions ranges from roughly four to less than one square kilometre in area. Except for one body that is a flat-lying sill or laccolith, the bodies are elongated and bounded for the most part by steep faults which are part of the north-northwest regional structural fabric. Lithologies comprising these bodies have not been mapped in detail although certain features are common to all. Diorite-gabbro is volumetrically dominant, containing hornblende and abundant magnetite. Diorite-

gabbro pass imperceptibly into less voluminous clinopyroxenite, with or without biotite and hornblende. However, it is uncertain whether this is part of a regular internal zonation. At the largest body in the north, late differentiates, rich in prismatic hornblende and feldspar, are locally associated with magnetite-rich layers. These form pegmatitic segregations in hornblende gabbro and also late dikes. Fine-grained felsite and feldspar porphyry comprise the youngest dikes cutting the northernmost body.

Regionally, Alaskan-type complexes have a close spatial association with mainly volcanic rocks of Upper Triassic age. Irvine (1976) postulated a genetic relationship with at least some compositionally similar Upper Triassic volcanic rocks. This hypothesis is supported in part by age determinations for some of the major Alaskan-type complexes in British Columbia (Nixon, 1997). Alaskan-type complexes have a broad range of ages in the Canadian Cordillera, varying from the oldest, Lunar Creek complex, at  $237 \pm 2$  Ma to the youngest, Polaris complex, at  $186 \pm 2$  Ma. No emplacement ages for the small bodies in the study area have been determined. The age and distribution of these complexes in Toodoggone River, McConnell Creek and Mesilinka River map areas is intriguing. They comprise a unique suite of similar intrusions distributed in a continuous belt that straddles adjacent tectonostratigraphic terranes (*i.e.* Quesnellia and Stikinia), and is apparently little affected by postulated dextral motion (Gabrielse, 1985) along the Ingenika-Finlay interterrane fault.

## STRUCTURE

The structural fabric of the McConnell Range is broadly similar to that documented to the north in adjacent southern Toodoggone River map area (Diakow and Metcalfe, 1997). The pattern is dominated by north trending, high angle brittle faults. Unlike the area to the north, conjugate subsidiary faults that trend northeast were not recognized in the central and northern McConnell Range. Farther to the southwest, across Moose Valley, significant facies and thickness trends in Upper Triassic strata presently coincide with major northeast trending valleys that may approximate the location of early syndepositional faults. One such fault is presumed to parallel the Sustut River between Sustut Peak and Savage Mountain (Monger, 1977); it may extend to the northeast across Moose Valley, cutting obliquely across the southern McConnell Range, north of Johanson Creek. Interestingly, in the southern McConnell Range, the youngest depositional unit of the Upper Triassic sequence is exposed only in the massif immediately south of this assumed northeasterly structure.

Several major north-northwest faults, parallel to the western margin of the Fredrikson pluton, are mapped between Attichika and Thorne creeks. These structures are nearly vertical and defined by a series of interconnected fault segments that juxtapose Paleozoic and Upper Triassic stratigraphic units. As distinctive bedded rocks of the Asitka Group are traced into fault zones comprised of one

or more en echelon structures, the beds typically become tilted to near vertical, folded and locally overturned by drag. Surprisingly, the brittle chert is generally not granulated along major faults planes. Typically, zones of breccia and gouge are rare along these structures, and seldomly more than a few centimetres wide.

The Moosevale fault or Moose Valley fault is a regional-scale structure that was proposed to delimit the McConnell Range in the west (Monger, 1977; Richards, 1976). No field evidence was found to support such a structure along the lower slope of the northern part of the range. In the south, sparse outcrops of a granitic plug are flanked on the west by a small area underlain by recrystallized Paleozoic limestone. Although the contact is buried, absence of deformation argues against a major fault. Projection of a hypothetical fault from this site toward the north is also unlikely, since exposures along strike consist of Upper Cretaceous strata which appear to unconformably overlie Upper Triassic rocks. Still farther north, correlative Upper Cretaceous sediments have clearly been faulted against Paleozoic limestone along a fault zone with azimuth about  $140^\circ$ , that presumably post dates regional north-trending faults. Finally, there is no indication of a major fault extension north beyond Attichika Creek into the Toodoggone River map area where recent detailed mapping was conducted between Thutade Lake and the Kemess South minesite (Diakow and Metcalfe, 1997).

A series of northerly trending, steeply dipping faults, similar to structures west of the Fredrikson pluton, also mark much of the eastern border of the pluton. The faults locally juxtapose Alaskan-type mafic-ultramafic complex lithologies against phases of the Fredrikson pluton. For example, parallel high-angle faults north of Jensen Creek bound a probable extension of the Menard Creek ultramafic complex in a narrow band of diorite-gabbro and lesser pyroxenite that is less than 1 kilometre wide and 4 kilometres long. To the north, steep faults also separate the Fredrikson pluton from other ultramafic bodies.

Along the lower slope east of Serrated and Fredrikson peaks, Paleozoic and Upper Triassic strata are folded and the stratigraphy repeated and inverted by a series of west-verging thrust panels. Deformation is most prevalent in a thick greyish white carbonate, part of a bedded Paleozoic succession with chert and aphanitic basalt. The carbonate layers locally outline large amplitude isoclines and other tightly appressed folds. These contractional structures are in turn cut by high-angle brittle faults that place the deformed rocks against unstrained monzodiorite of the Fredrikson pluton. A similar style of deformation is recognized west and northwest of Serrated Peak where deformed Paleozoic sequences occur in west-directed thrusts that are segmented by later high-angle faults.

The timing of the contractional deformation is unknown. However, west of Serrated Peak, basal strata of the Toodoggone formation, presumed to be around 200 million years old, apparently occupy the footwall to a thrust fault carrying overriding Paleozoic rocks (Diakow and Metcalfe, 1997). This relationship is equivocal since, although the Paleozoic rocks are in faulted contact with the

Toodoggone formation, it is not certain that they overlie the younger rocks.

The McConnell Range passes immediately to the east into a broad U-shaped valley oriented roughly north-south. This valley supposedly marks the trace of the major dextral Ingenika-Finlay fault which corresponds with separation of the tectonostratigraphic terranes Stikinia and Quesnellia (Wheeler and McFeely, 1991). Except for the odd traverse along the west side of this valley, an objective comparison of adjacent terranes and an evaluation of their common boundary requires further mapping and analysis.

## MINERAL POTENTIAL

Early Jurassic magmatism manifest in stocks and smaller hypabyssal plutons of the Black Lake calc-alkaline suite and comagmatic volcanic rocks of the Toodoggone formation are important host rocks for both copper-gold porphyry and epithermal precious metal deposits in the Toodoggone mining district (Diakow *et al.*, 1993). The Kemess South gold-copper porphyry deposit is near the southern end of this district. Based on a limited view of the deposit in a test pit that exposes hypogene ore, the host rocks bear a striking resemblance to crystal-rich dacitic volcanic rocks of the Toodoggone formation. Pervasive replacement of plagioclase by fine-grained potassium feldspar accompanies disseminations of pyrite and chalcopyrite and cross-cutting quartz-pyrite-chalcopyrite veins in hypogene ore. A sample of this rock, returned a U-Pb date of  $199.6 \pm 0.6$  Ma (R.M. Friedman, U.B.C. Geochronology Laboratory, written communication, 1997), dating crystallization of the host rock, but not necessarily the age of hypogene mineralization. Nearby volcanic rocks of the Toodoggone formation yield equivalent U-Pb dates of  $199.1 \pm 0.3$  Ma and  $200.4 \pm 0.3$  Ma (R.M. Friedman, U.B.C. Geochronology Laboratory, written communication, 1997). The equivalence of these dates implies that either mineralized rocks sampled at the Kemess South deposit are strongly altered and mineralized country rock in the aureole of the main pluton or the sampled material is an evolved crowded porphyritic subvolcanic intrusion.

Recent mapping of the Fredrikson pluton showed that it is like biotite-hornblende bearing intermediate epizonal plutons typical of the Early Jurassic Black Lake suite found elsewhere in the Toodoggone River map area. It is composed of differentiated monzogranite and quartz monzodiorite phases that probably represent the southern segment of a larger batholithic body that includes granitic rocks mapped farther north near Giegerich Peak (Diakow and Metcalfe, 1997). Contact alteration, with sporadic narrow rusty zones containing minor pyrite as well as quartz veinlets that may contain malachite is localized near the margin of the intrusion. This, coupled with the notable absence of hydrothermal alteration, diminishes the likelihood of associated economic mineralization in the Fredrikson pluton. This is supported by typically low copper and gold stream sediment geochemistry from watersheds sourced in the main granitic body (*Cf.* B.C. Regional Geochemical Survey; Jackaman, 1997). West of

the intrusion, samples from several watersheds draining mainly Paleozoic and lesser Upper Triassic rocks display multielement base metal and several gold anomalies. These anomalies were not followed up during the course of mapping.

## ACKNOWLEDGMENTS

We are exceedingly grateful to Royal Oaks Mines and particularly staff at the Kemess South mine who have, in the midst of their own busy schedules, always offered tremendous support to this program. It was also a pleasure to fly once again with Canadian Helicopters and their professional, courteous pilots. This manuscript has benefitted from the editorial comments of W.J. McMillan and A. Legun.

## REFERENCES

- Diakow, L. J., Panteleyev, A. and Schroeter, T.G. (1993): Geology of the Early Jurassic Toodoggone Formation and Gold-Silver Deposits in the Toodoggone River Map Area, Northern British Columbia; *B.C. Ministry of Energy, Mines and Petroleum Resources*, Bulletin 86, 72 pages.
- Diakow, L.J. and Metcalfe, P. (1997): Geology of the Swannell Ranges in the Vicinity of the Kemess Copper-Gold Porphyry Deposit, Attycelley Creek (NTS 94E/2), Toodoggone River Map Area; *in* Geological Fieldwork 1996, *B.C. Ministry of Employment and Investment*, Paper 1997-1, pages 101-116.
- Eisbacher, G.H. (1974): Sedimentary History and Tectonic Evolution of the Sustut and Sifton Basins, North-Central British Columbia; *Geological Survey of Canada*, Paper 73-31, 57 pages.
- Gabrielse, H. (1985): Major Dextral Transcurrent Displacements Along the Northern Rocky Mountain Trench and Related Lineaments in North-central British Columbia; *Geological Society of America Bulletin*, Volume 96, pages 1-14.
- Gabrielse, H., Dodds, C.J., Mansy, J.L. and Eisbacher, G. H. (1977): Geology of the Toodoggone River (94E) and Ware West-Half (94F); *Geological Survey of Canada*, Open File 483.
- Irvine, T.N. (1976): Alaskan-Type Ultramafic-Gabbroic Bodies in the Aiken Lake, McConnell Creek, and Toodoggone Map-Areas; *in* Report of Activities, Part A, *Geological Survey of Canada*, Paper 76-1A, pages 76-81.
- Jackaman, W. (1997): British Columbia Regional Geochemical Survey, NTS 94D-McConnell Creek; *B.C. Ministry of Employment and Investment*, BCRGS 45.
- Legun, A.S. (1998): Toodoggone-McConnell Project: Geology of the McConnell Range - Jensen Creek to Johanson Creek, Parts of NTS 94D/9,10,15,16; *in* Geological Fieldwork 1997, *B.C. Ministry of*

- Employment and Investment*, Paper 1998-1, this volume.
- Lord, C.S. (1948): McConnell Creek Map-Area, Cassiar District, British Columbia; *Geological Survey of Canada*, Memoir 251, 72 pages.
- McPhie, J., Doyle, M. and Allen, R. (1993): Volcanic Textures: A Guide to the Interpretation of Textures in Volcanic Rocks; Centre for Ore Deposit and Exploration Studies, *University of Tasmania*, 196 pages.
- Nixon, G.T., Hammack, J.L., Ash, C.H., Cabri, L.J., Case, G., Connelly, J.N., Heaman, L.M., Laflamme, J.H.G., Nuttall, C., Paterson, W.P.E. and Wong, R.H. (1997): Geology and Platinum-Group-Element Mineralization of Alaskan-Type Ultramafic-Mafic Complexes in British Columbia; *B.C. Ministry of Employment and Investment*, Bulletin 93, 142 pages.
- Monger, J.W.H. (1977): The Triassic Takla Group in McConnell Creek Map-Area, North-Central British Columbia; *Geological Survey of Canada*, Paper 76-29, 45 pages.
- Richards, T.A. (1976): Takla Project: McConnell Creek Map-Area (94D, East Half) British Columbia; in Report of Activities, Part A, *Geological Survey of Canada*, Paper 76-1A, pages 43-50.
- Ross, C.A. and Monger, J.W.H. (1978): Carboniferous and Permian Fusulinaceans from the Ominica Mountains, British Columbia; in Contributions to Canadian Paleontology, *Geological Survey of Canada*, Bulletin 267, pages 43-55.
- Wheeler, J.O. and McFeely, P. (1991): Tectonic Assemblage Map of the Canadian Cordillera and Adjacent Parts of the United States; *Geological Survey of Canada*, Map 1713A.
- Woodsworth, G.J. (1976): Plutonic Rocks of McConnell Creek (94D East Half and Aiken Lake 94C West Half) Map-Areas, British Columbia; in Report of Activities, Part A, *Geological Survey of Canada*, Paper 76-1A, pages 69-73.





## TOODOGGONE-McCONNELL PROJECT

### GEOLOGY OF THE McCONNELL RANGE

#### JENSEN CREEK TO JOHANSON CREEK, PARTS OF NTS 94D/9, 10, 15, 16

By A.S. Legun, B.C. Geological Survey

**KEYWORDS:** Volcanic redbed copper, Moosevale Formation, Menard ultramafic, Omineca intrusions, Savage Mountain Formation, Takla Group.

### INTRODUCTION

The southern McConnell Range program is part of the Toodoggone-McConnell mapping project, initiated in 1996. The area is about 20 km. south of the rapidly developing Kemess mine site of Royal Oak Mines Inc.

The McConnell Range is within the northern Omineca Mountains, at about 56 45 north latitude and 126 30 west longitude in north-central B.C. The range lies parallel to the Omineca Mining access road where it follows the Moose valley at about kilometre 425. The Omineca Mining access road is a continuation of the Finlay Forest Service Road which originates near Windy Point on Highway 97, 155 kilometres north of Prince George.

The project area is between Jensen Creek in the north, Johanson Creek in the south, the Ingenika valley to the east and the Moose Valley to the west (Figure 8.1). The area comprises about 125 square kilometres overlapping portions of NTS 94D/9, D/10, D/15 and D/16.

Parts of the range may be reached by access road. At km 421 on the Omineca road a side 4X4 road (the McConnell Creek access road) follows a deep glacial valley eastward and then swings north up the Ingenika valley to parallel the range on the east side.

The range is well dissected and back to back headwall retreat of watersheds has formed numerous sharp ridges. These are traversable with some exceptions. Elevations range from 1200 metres to 2100 metres with the treeline at about 1650 metres.

The writer assisted by Brian Untereiner completed about 35 traverses, with mostly good weather. The work involved mostly fly camps coordinated with Larry Diakow.

### PREVIOUS WORK

The area was covered by 1:250 000 mapping by the Geological Survey of Canada during the mid 1940's (Lord, 1948). A number of copper rich vein showings (eg. Marmot) were located during this effort. Sporadic work followed over the next two decades. In the late 1960's significant exploration activity focused on porphyry

copper and molybdenum mineralization. A large gossan was discovered in 1966 at the present site of the Kemess North prospect and led to similar exploration on nearby ground. Southwest of the McConnell Range In 1971 Falconbridge Nickel discovered a malachite stained bed that was traceable for over 2500 feet during a reconnaissance helicopter flight. The area is just north of the Sustut River southwest of the McConnell Range. Subsequent assessment revealed a replacement copper deposit in volcanoclastic rocks in the upper part of the Takla Group. Numerous junior and major resource companies acquired ground in the area looking for either volcanic redbed copper mineralization in porous volcanoclastics or copper and molybdenum porphyries. Detailed mapping with minor drilling was conducted in the southern McConnell Range during this period. In 1973 the B.C. Geological Survey conducted a mineral deposit study of the Sustut copper area (Church, 1974a). The Geological Survey of Canada returned to pursue detailed studies within the McConnell sheet (Monger, 1977; Richards, 1976). In the north, follow up of a gold-copper-molybdenum soil geochemical anomaly led to the discovery of the Kemess South porphyry deposit in 1983.

In 1996 a regional geochemical survey of the McConnell mapsheet included sampling of watersheds in the McConnell Range. Results indicated multielement precious and base metal anomalies within the general project area (Jackaman, 1997).

The setting of the McConnell Range between major deposits at Kemess to the north and Sustut copper to southwest, and its proximity to developing infrastructure, suggested that mapping at a 1:20000 scale work was appropriate.

### GEOLOGIC SETTING

The McConnell Range is bounded by the Ingenika fault to the east and a splay of that fault, the Moosevale fault, to the west. This fault wedge lies at the edge of the Intermontane Belt and the tectonostratigraphic Stikine Terrane. The Ingenika fault is a dextral strike slip fault, part of a prominent strike-slip system in north-central British Columbia (Gabrielse 1985). Gabrielse suggested cumulative movement of about 300 kilometres along the Kutcho, Finlay, Ingenika, and Takla faults. The volcanic sequences east and west of the fault are thus considered to be laterally offset some 300 kilometres. In spite of this the rocks are of the same age with similar trace element

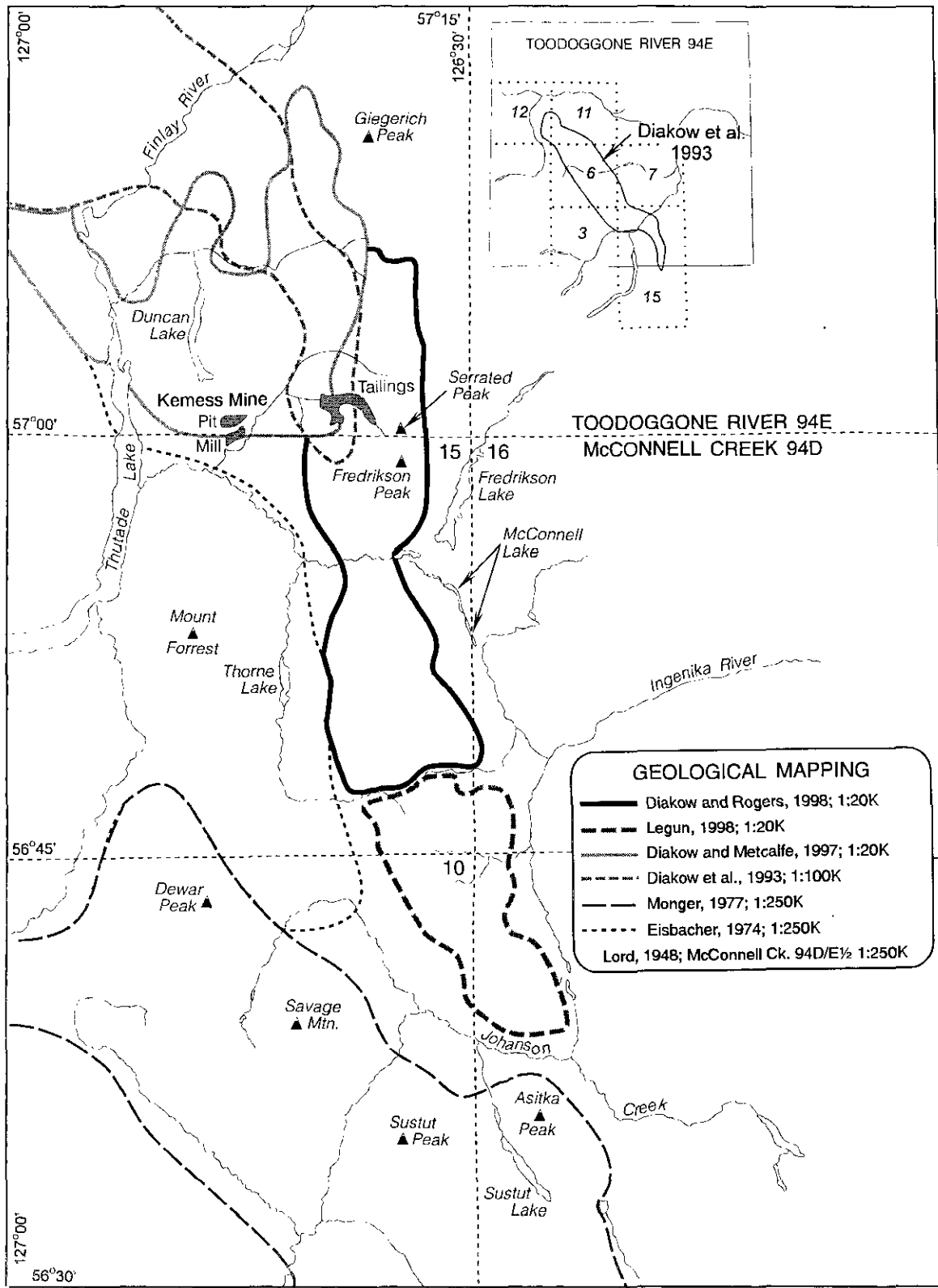


Figure 8.1. Location of recent and previous mapping in the southern Toodoggone River (94E) and northeastern McConnell Creek (94D) map areas.

geochemistry (Gale, 1996). The problem of fortuitous juxtaposition of grossly similar rocks across terrane boundaries is outside the scope of this paper. Suffice to say that the volcanic sequence in the McConnell Range can be related to a well studied sequence to the southwest in Stikinia while the stratigraphy east of the fault is not readily correlated (Zhang and Hynes 1991, Richards, 1976).

The stratigraphic sequence in the vicinity of Sustut copper deposit has been the focus of detailed stratigraphic study (Monger and Church 1976). The Takla Group in the vicinity of Mount Savage is about 3400 metres thick and subdivided into the Dewar, Savage Mountain and Moosevale formations. The Dewar formation is relatively thin ( $\leq 300$  m.), and the remaining thickness is about equally divided between the Savage Mountain and Moosevale formations.

Correlative strata of the Dewar Formation apparently thin towards the northern part of the McConnell Range (Diakow 1998). The Savage Mountain and Moosevale formations are present; the former may be reduced in thickness. Other rocks mapped include the cogenetic Menard mafic-ultramafic complex and granitic stocks and plugs of probable early Jurassic age.

Strata of the Takla Group are in the zeolite (prehnite-pumpellyite) facies of regional metamorphism. This contrasts with generally higher greenschist to amphibolite grades found east of the Ingenika fault.

The Sustut Copper deposit, immediately west of Sustut Peak contains reserves of 43.5 million tonnes grading 0.82 per cent copper (Harper 1977). The deposit consists of fine grains of hematite, pyrite, chalcocite, bornite, chalcopyrite and native copper in decreasing abundance dispersed in matrix and clasts of volcanoclastic rocks in the Moosevale formation. Gangue minerals include epidote, quartz, prehnite and carbonates. The mineralized zone is partially concordant with bedding, and lies just below the transition from green to red volcanoclastics, high in the Moosevale Formation (Harper, 1977).

The Kemess South deposit located north northwest of the McConnell Range near Kemess Creek is hosted by a flat-lying, porphyritic quartz monzodiorite intrusion that is underlain by Takla Group volcanic rocks (Rebagliati *et al.* 1995.). In contrast Diakow (1998) interprets the 'intrusion' as altered Toodogone volcanic rocks. Pyrite, the dominant sulfide accompanies quartz stringers. Chalcopyrite occurs as disseminated grains and in quartz stockworks. Reserves are approximately 220 million tons grading 0.22% copper and 0.18 ounces per ton of gold (1995 Annual Report, Royal Oak Mines).

## MAPPING ACCOMPLISHMENTS

### Takla Group

The Geological Survey of Canada mapped the Savage Mountain Formation of the Takla Group and the Toodogone Formation of the Hazelton Group in the southern McConnell Range. However the author concludes

that the southward Savage Mountain Formation passes conformably and stratigraphically into the Moosevale Formation of the Takla Group.

To the north, in the vicinity of Jensen Creek, structural attitudes are difficult to discern. Dips vary from subvertical to shallow. The steep dips are at the margins of Early Jurassic intrusions and in the vicinity of the Menard ultramafic complex. Stratigraphic elements are overprinted by hornfelsing and alteration. No cumulate thickness can be calculated. To the south a simpler structural style is evident in gentle to flat dips and block faults. Stratigraphic elements of the upper Savage Mountain Formation and Moosevale Formation can be recognized and traced.

### Jensen Creek to Menard Creek

Takla Group rocks include feldspar lath and augite porphyries, fine grained basalt, and minor tuff breccias in the Jensen Creek area. All subtypes are basaltic and with the exception of the lath porphyries, carry augite. Any subtype may be amygdaloidal. Amygdule fillings include epidote, chlorite, calcite, zeolites and albite.

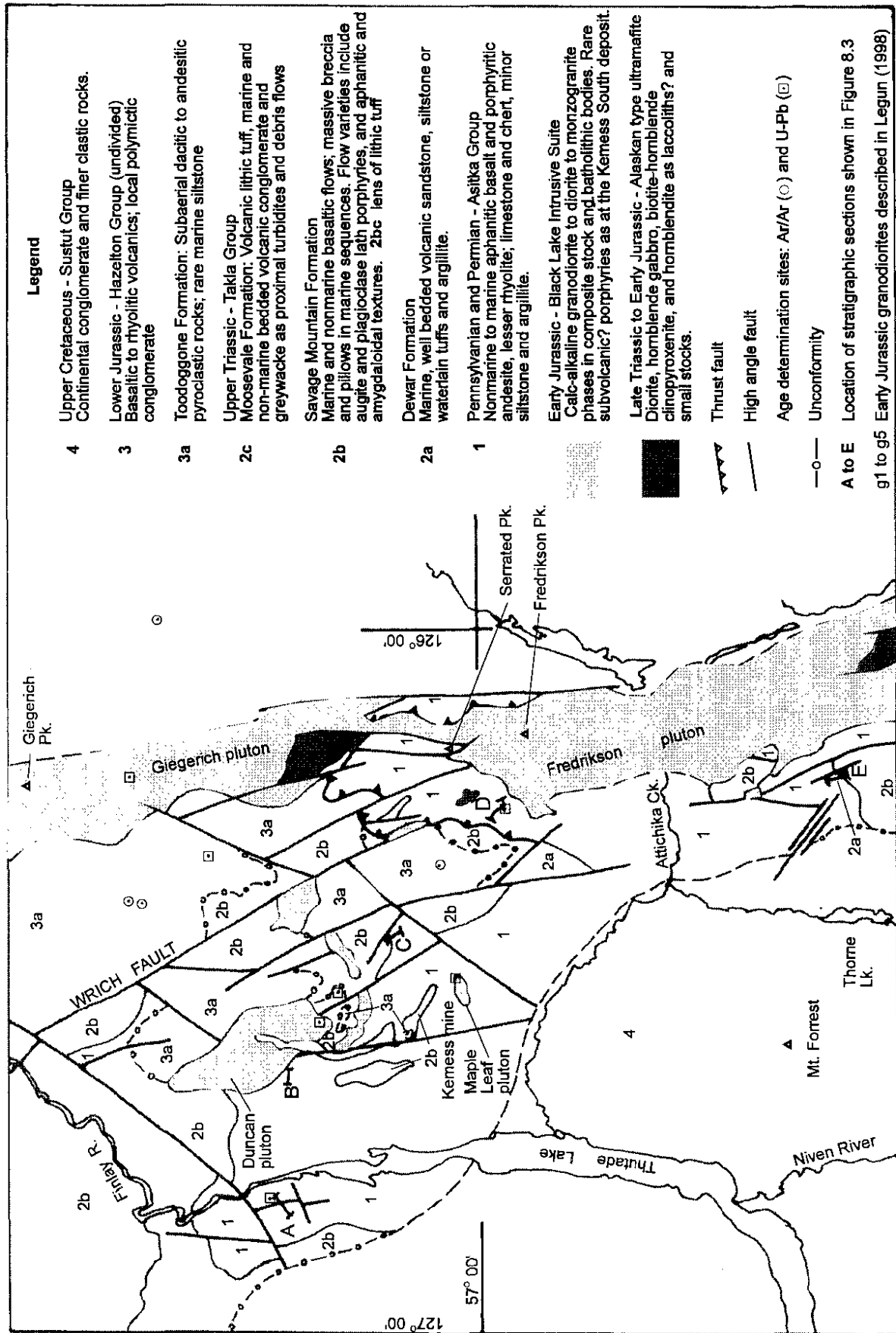
The subtypes are closely associated with each other and individually do not form mappable units. Some trends however can be discerned. On the western slopes of the Marmot area lath porphyries dominate. Amygdaloidal phases are common west of the Menard complex but were not observed north and east of the complex.

Gale (1996) described the variation in petrographic composition of various basaltic subtypes. Phyric flows display varying proportions of phenocrysts of clinopyroxene, plagioclase, and pseudomorphs of olivine within a holocrystalline groundmass.

South of Menard Creek the volcanics are variably hematized. They are occasionally knobby textured, rich in fragments and densely amygdaloidal. Fragments are coarsely to finely vesiculated fragments, or may be vesicle (amygdule) free clasts in a fluidal textured matrix defined by swirls of amygdules and aligned feldspar laths. Knobby texture in part is due to concentric hematitic bands about a dark amygdule core. Bands, lenses and irregular masses of massive red aphanitic material were also noted. These oxidized and hematized porphyries are interpreted to be distal ends of blocky and scoracious subaerial flows, possibly intermixed with fine red tuff or baked mud. Although there is no discernible bedding of sedimentary origin, contacts between amygdule rich layers suggests the volcanics are shallow dipping. A few amygdule rich dikes are present.

### Menard Creek to Johanson Creek

South of the Menard Cr. watershed a southern highland is isolated from the interconnected ridges to the north. In contrast to the adjacent segment volcanic stratigraphy is mappable on this highland. The Savage Mountain Formation, dominated by coarse lath porphyry flows, passes upward into the Moosevale Formation, dominated by lithic tuffs. There is one significant interval of well bedded waterlain sediments at the conformable contact. These waterlain sediments may correspond to unit 3a of Harper (1977) in the vicinity of Sustut Copper.



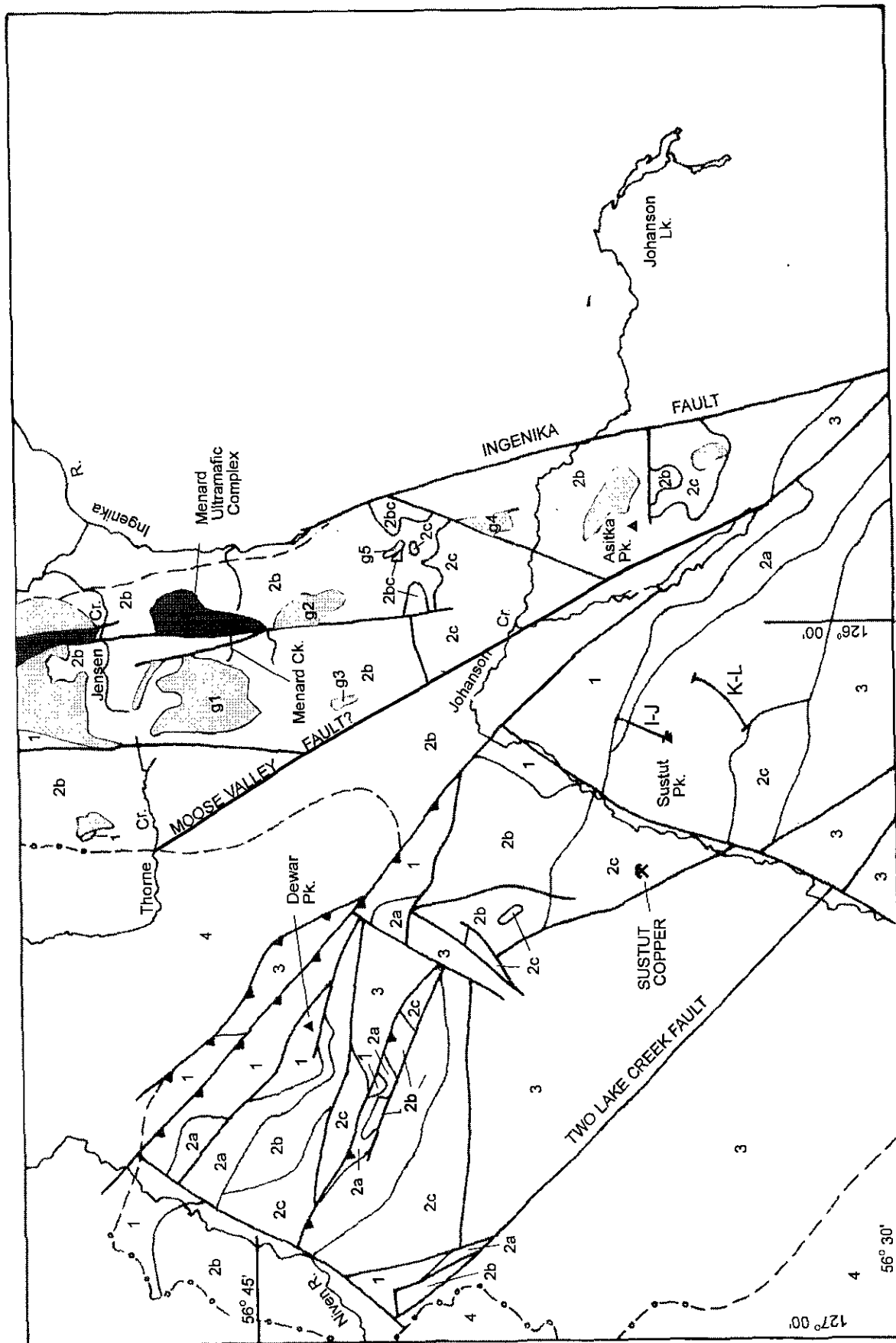


Figure 8.2 Geology of the McConnell Range showing major lithostratigraphic divisions and plutonic rocks. Geology in outlying regions to the south, northwest and west by Legun (1998), Diakow and Metcalfe (1997) and Monger (1976) respectively, are incorporated.

Discontinuous sedimentary beds are found throughout the lithic tuffs of the Moosevale Formation.

### ***Savage Mountain Formation***

In this area the Savage Mountain Formation is a composite unit of lath porphyry flows and some interbeds of lithic tuffs. Contacts and sedimentary bedding suggest the Savage Mountain Formation is flat lying to undulating on the northern flank of the highland. A pyroxene bearing phase is exposed on the lower northern slopes and believed to be at a low stratigraphic position. It is similar to phases found in the main part of the range and described as basalt porphyry or augite-feldspar porphyry.

Thickness calculations from base to ridge top in the northeast indicate at least 400 metres of lath porphyry flows are present. To the southwest calculations indicate the flow sequence has thinned to about 200 metres. There it is underlain by a wedge of lithic tuff which is absent in the north.

A tuff breccia unit of rather unusual geometry and lithic composition occurs in the north. Its mapped trace extends from the ridge top near a small granitoid dike (body g-5 in Figure 8.2) westward to the valley floor as an elongate body. The southern contact of this elongated body is steep, judging by its straight transect with closely spaced contours. Contacts of flow rocks measured about 300 metres to the east and southwest of this area indicate flat to gentle dips. The southern contact may thus be crosscutting, perhaps a small fault. Near the northern contact within the tuff breccia a coarse grained diorite mass, a few metres across (base not exposed), is exposed in a gully wall. Above it there are fragments of diorite within the tuff breccia. Other clast types include augite porphyry, lath porphyry, green laminated siltstone, dark to maroon tuff?, white chert, microdiorite, and pale sericitized fragments. No diorite, white chert, and fine pale sericitized clasts were seen in other tuff breccias. The distribution of clast types is not uniform. For example lath porphyry clasts are abundant near the margin but uncommon elsewhere. Most clasts are very angular but a few are rounded. One round chert clast has a dark alteration rim.

Further work is needed to determine the true nature of this unit. Any interpretation must explain the origin of the coarse diorite. Possibly this tuff breccia represents a vent breccia or diatrema.

### ***Moosevale Formation***

As mentioned above the Savage Mountain formation passes stratigraphically upward into the Moosevale Formation on the southern highland, and that contact is marked by a locally developed well bedded sequence. The contact is exposed in the central area of the highland. The top of the Savage Mountain Formation is reddish and amygdaloidal lath porphyry. Nearby drilling (diamond drillhole ZD 76-1, Bates 1976) indicates that the top of the lath porphyry consists of several successive flows, which are reddened at the top and include flow fragments. The base of the overlying sequence is represented by tuff and tuff intercalated with siltstone.

The well bedded sequence does not persist laterally for more than a few hundred metres. The sequence comprises thick beds of calcareous tuffaceous sandstones (with crossbeds and mudchips), lithic tuffs with sandy intervals, horizontally laminated grit, clast supported conglomerate, thin to very thin beds of red and green siltstones, banded tuff, argillaceous limestone and laminated chert. Minor detrital quartz occurs in the sandstones. The clast supported conglomerate has rounded clasts to 20 cm and is weakly stratified with grit lenses.

The stratified and "water washed" sediments which are about 50 metres thick, are overlain by at least 800 metres of lithic tuffs, massive tuffs and tuffaceous breccias cut by occasional sills of augite porphyry. In tuffaceous breccias clasts are not easily discernible from matrix. The matrix typically has a lower density of crystals and these are finer and broken.

Sedimentary intervals within the lithic tuff of the Moosevale include locally developed graded beds, channel forms, and matrix and clast supported conglomerates.

Some matrix supported clastic units with angular clasts contain siltstone rip-ups together with crystal fragments. Reddish siltstones mantle beds with coarse clasts to boulder size. The origin of these siltstones is uncertain. They may represent suspension drapes, sheet wash deposits, or reworking of the tops of debris flows. Discontinuous siltstone beds may also occur as elongate tilted slabs within these beds. These slabs must have been at least partially lithified to remain coherent. Conglomeratic masses also were observed to project through siltstone bands as if they were injected. These features suggest slumping to the writer. An association with graded beds indicates a submarine rather than subaerial environment. Resedimentation in the context of a slumping slope facies is clear in either case. Blunt nosed and spindle shaped volcanic clasts were noted associated with graded beds rich in rip ups. These clasts are interpreted to be air sculptured volcanic bombs though they could conceivably represent disaggregated remnants of pillowed lava.

### ***Alteration***

Propylitic alteration is widespread within the volcanic sequence. Epidote is the most conspicuous mineral of this assemblage that includes carbonate and hematite. In some cases epidote zones can be related to shear zones, contacts or other discontinuities. However there are many instances where lenses of massive epidote rock is within a homogenous unit such as massive lath porphyry.

Propylitic alteration also is well developed in small intrusive or subvolcanic bodies of dacite porphyry to microdiorite. The microdiorites are characterized by epidotized and sericitized feldspar phenocrysts in a fine microcrystalline to fine blocky lath matrix. Chloritized mafics are common together with calcite, opaques and granular epidote.

## Menard Ultramafic complex

The Menard ultramafic complex was studied recently by Nixon *et al.* (1989) who focused on its petrology and relationship to other Alaskan-type bodies in the region. The body is teardrop shaped in plan and elongated northward (Figure 8.2).

The following units were mapped by the writer:

- 1) clinopyroxenite
- 2) clinopyroxenite and (olivine) gabbro
- 3) gabbro with minor banded diorite
- 4) layers of pyroxenite, gabbro and basalt.

Clinopyroxenite forms a north trending lens on the west margin of the complex. Massive pyroxenite passes northeast and southeast to pyroxenite and gabbro. The transition is marked by north trending interlayering of gabbro and coarse pyroxenite. Eastward massive pyroxenite passes abruptly to gabbro. The gabbro is an oval plug-like mass whose long axis swings from north to northeast giving it an arcuate shape.

A panel of interlayered bands of pyroxenite, basalt, gabbro and lath porphyry lies on the northeast flank of the complex in uncertain contact relationship with the eastern margin of the gabbro "plug", and gabbro with pyroxenite. The contact relationship is obscured by diorite dikes and magnetite rich zones. Layers trend at about 335 degrees. The conformable interlayering of these units suggests the coarser grained rocks are sills and part of the Takla assemblage. The interlayered sills appear to pass stratigraphically eastward into Takla volcanics. The volcanic package consists of massive basalts and weakly porphyritic basalts with scattered small phenocrysts of feldspar and pyroxene. The panel of sills also appears to pass laterally into Takla volcanics to the northwest, perhaps by pinching out of sills or fining of textures.

In one location the lath porphyry shows pilotaxitic texture at its contact with the pyroxenite indicating it is a younger phase of sill intrusion.

The ultramafic complex apparently tapers southward, the southward extension being inferred from ground magnetometer data (Meyer and Overstall 1973). Exposure on the south side of Menard valley is poor and restricted to a creek gully. Here serpentinized gabbro and pyroxenite (high magnetic susceptibility) are present near a fault structure that disappears northward into the complex (approximately in line with the gabbro/pyroxenite contact).

The gabbro "plug" in its northeastern terminus comprises massive diorite and banded hornblende diorite. The banding, defined by mineral layers rich in hornblende, trends east across the overall northerly trending regional structures.

According to Irvine (1976) the intrusive phases of Alaskan type bodies develop by crystallization differentiation. The pyroxenite body appears to represent a crystal cumulate. Its form suggests the complex may have originally formed as a laccolith. Irvine suggested the juxtaposition of intrusive phases in such bodies is a result of diapiric re-emplacment. The gabbro plug-like gabbro mass may represent such a re-emplacment. Nixon noted

sharp linear contacts along phases (such as the gabbro) and suggested some fault control.

Late in its history the intrusive complex may have undergone deformation and metamorphism as suggested by the foliation of the banded diorite and the swing of the gabbroic body to the northeast along this trend.

More work is required to understand the fundamental geometry of the intrusive suite and the juxtaposition of its phases.

## Jurassic Intrusions

Several Jurassic intrusive bodies were delineated. The largest occupies the northwest portion of the upper Menard Creek valley. The intrusives are part of a 20 kilometre wide belt of scattered plutons that extend north from the Hogem batholith and continue through the southern and northern McConnell Range.

### *Marmot Intrusive (g-1 in figure 8.2)*

The Marmot intrusion is slightly elongate in a north-south direction. A penetrating lobe of hornfelsed volcanic rock on the north margin suggests there may have been two centres of igneous intrusion. Overburden in the Menard valley obscures the trace of the contact in the south. However on its northwest margin the contact is marked by transition to an igneous stockwork of dikes within the Takla. Elsewhere contacts are sharp or include volcanic rafts near the margin. A satellite body to the north arcs east to west. The western limit of this satellitic "ring dike" is obscured by cover in the topographic saddle between the Jensen Creek and Thorne creek watersheds.

White granodiorite to quartz diorite dominates the main intrusive mass. Near its western boundary (Marmot claims) Church (1974b) reports the intrusive consists of mostly tabular plagioclase and subhedral quartz with interstitial orthoclase, some euhedral prisms of hornblende, a few chloritized biotite books, and scattered accessories such as magnetite, sphene, and apatite. Woodsworth (1976) considered the intrusion to be more mafic and finer than others to the north. He described it as a massive quartz diorite to quartz monzodiorite with hornblende more abundant than biotite. The writer also noted a biotite dominant phase and considerable variation in quartz content (from 5 to over 20%).

Other intrusive phases include a pinkish quartz poor subhorizontal mass along a ridge on the western border, and a quartz rich porphyritic phase near the northern margin and within the satellite dike. The porphyritic phase consists of feldspar phenocrysts in a fine quartz rich matrix. Associated with this feldspar porphyry are minor silica flooded pyrite zones in the wallrock. The best example is at the east margin of the hornfelsed lobe of volcanic rock described above.

### *Marmot Southeast (g-2 in figure 8.2)*

A granodioritic body on the south side of the Menard valley contains abundant suspended blocks of volcanics. Numerous dikes and sills project outward from its border. A similar but smaller body lies immediately to the east.

Both igneous masses and associated stockworks trend north northwest and are truncated by a fault (see STRUCTURE).

### ***Marmot Southwest Intrusive (g-3 in figure 8.2)***

A third intrusion on the south side of Menard valley is poorly defined because exposure decreases below treeline. On its north margin there is a silicic and pyritic gossan where it is in contact with a chloritized felsitic porphyry. Church (1974b) described the body as hypidiomorphic granular granodiorite composed of 23% quartz, 22% orthoclase, and 44% plagioclase, with accessory biotite, hornblende and magnetite.

### ***Johanson Creek Intrusive (g-4 in figure 8.2)***

A fourth truncated body outcrops at the south end of the mapped area facing Johanson Creek. Like the intrusions on the south side of Menard valley one margin of the body is sharp and at an acute angle to the long axis of the intrusion. This sharp contact is traceable along gullies that align on either side of a ridge divide. In the north the intrusion is thin and dike-like and shearing is evident along the contact.

## **STRUCTURE**

A north trending line of intrusives and connecting faults transect the southern end of the McConnell Range. The elongate Menard complex is the major intrusive body. North of Jensen Creek another elongate mafic intrusion is colinear with the Menard complex (Diakow, 1998). South of the complex a north trending fault extends across the Menard valley (Figure 8.2). There in a creek valley altered granitic rocks, serpentized pyroxenite, chloritized volcanics are exposed. The fault truncates the Marmot Southeast intrusives, whose long axes are at an acute angle to the fault.

The fault can be traced to the Johanson highland. On the west side of the highland the fault is marked by altered volcanic wallrock, a subvertical mass of lath porphyry, and a resistant band of quartz stockwork within hematized agglomerate and tuff. A lath porphyry flow, present immediately east of the fault, is absent west of the fault.

A second fault on the Johanson highland trends northeast and lies east of the one described above. Related to it is an elongate intrusion (g-4). The strata east of the fault are tilted to the east and a sequence of Savage Mountain pyroxene bearing lavas that is overlain by lath porphyry similar to that found in the north is exposed. It appears that igneous intrusion exploited a fracture and subsequently beds were tilted as a block when the fracture was reactivated.

## **PROSPECTING RESULTS**

A weak skarn that was found this summer in the Northern McConnell Range is described separately under Regional Mineral Potential.

In the area mapped by the writer there are numerous small copper showings. Mineralization occurs as:

- Fracture veinlets, single or in sets related to small shears, narrow carbonate breccias, lithologic contacts, or zones of massive epidote alteration.
- Banded quartz-epidote-calcite veins up to a metre wide but discontinuous. Examples of these include Marmot and Menard Pass. Drusy quartz ribbons suggest this is a late fissure type mineralization.
- Widely spaced fracture zones in intrusive and adjacent wallrock.

These types of copper mineralization appear to be related through alteration mineralogy and sulfide minerals. The minerals include variations of malachite, azurite, chalcocite, native copper and bornite. Accessory minerals include quartz, calcite, specular hematite, and epidote. Native copper and bornite occur but are relatively uncommon.

A comparison of showings with the record in assessment reports and Minfile maps indicates that the following showings are not documented. While individually not significant, they may have some relevance in association with a review of ground geochemical and other data.

The South side of Menard valley, ridge furthest to the east (2 km ESE of Minfile 94D 090):

On the ridge top, fracture coatings of malachite and azurite are found in massive epidote rock over several square metres. The UTM coordinates are 654934E, 6291361N. Nearby is a silicified shear zone with disseminated pyrite (but no signs of copper). Traces of copper stain occur further south along the ridge.

### ***Near Menard Pass (Minfile 094D 049):***

The Menard Pass showing is on the southwest side of the Menard valley on a ridge top. Just below the ridge top on the east side is an oval patch of epidotized rock about 10 metres by 3 with abundant staining. The UTM coordinates are 649405E, 6290249N. This is within 100 metres of the Menard Pass fissure vein and within the bounds of a copper anomaly noted in Church 1974, figure 41, pg. 434. No indication of mineralization is noted on assessment report maps.

## **REGIONAL MINERAL POTENTIAL**

The McConnell Range is near the developing infrastructure related to the Kemess mine. Claims cover about one-third of the area mapped by the writer.

### **Volcanic Redbed Copper**

The Moosevale formation is prospective for volcanic redbed copper. The Sustut Copper deposit lies for example 900 metres above the base of the volcanoclastic sequence in the stratigraphic framework of Harper (1977). The nearby Willow prospect (094D 082) lies closer to the lower contact and is comparable to the stratigraphic interval mapped at the southern end of the McConnell

Range. Stratigraphic position in a volcanoclastic sequence may not be critical. The presence of porous beds near a redox boundary, a structural trap for fluid flow, the presence of either metamorphic metasomatic or hydrothermal fluids and copper source beds are more important.

In the McConnell Range there is a clear increase in the number of small copper showings from Jensen Creek to Johanson Creek. This appears to correspond to the increase in reddish oxidized volcanics and the presence of the Moosevale Formation. Such showings continue to Asitka Peak, where Moosevale Formation is inferred to be present from descriptions in assessment reports.

In spite of extensive prospecting no examples of Sustut-type mineralization have been demonstrated in the southern McConnell Range. At best there is an allusion to incipient mineralization of this kind by Mustard and Bates (assessment report 5256). In this report an exception to "shear-zone mineralization" is described as disseminated and microfracture filling bornite and chalcocite over an area of 10 by 20 feet in a green tuff adjacent to bladed feldspar porphyry. Several holes were drilled in nearby areas. These intersected lithic tuff-lath flow contacts. Diamond drillhole ZD#1 intersected 0.34% copper over 3 metres in epidote altered tuff (Mustard and Bates, 1975).

In the southern McConnell Range there is potential for a small blind stratiform orebody to be present. A halo of weak silicification and pyrite that might point to underlying Sustut-type mineralization is absent.

The presence and distribution of Moosevale Formation east of the Ingenika fault is not known.

Stratiform copper may be found in non-clastic units. The Red or Sping prospect (Minfile 094D 104) suggests stratabound potential within carbonates. The Red consists of disseminated copper within a locally developed dolomite that is up to 230 feet thick within the Hazelton Group. The dolomite is part of a larger sequence of intravolcanic sediments deposited in a small basin southwest of dominantly volcanic terrain. Some affinity to volcanic redbed copper and the copper bearing carbonate facies of Kupferschiefer mineralization (Zechstein limestone) is speculated. This also is compatible with Kipushi type mineralization, presently being documented as a deposit type for British Columbia (Trueman, in press). In that model copper-zinc-lead mineralization is deposited in karstic features within a carbonate to dolomite host under rather low temperature diagenetic conditions. Nearby basalts may provide copper and deposits are an integral part of basin evolution and burial.

Some assessment of calcareous units within Takla Group and Toodoggone Formation is merited, particularly where local facies suggest the possibility of closed structural-lithologic basins.

## Porphyry

Jurassic intrusive bodies are present in the mapped area but do not show evidence of extensive hydrothermal alteration or brecciation. Only insignificant quartz veining and a narrow secondary K-feldspar or biotite aureole is developed in contrast to the widespread alteration

associated with the Maple Leaf intrusion at the Kemess South orebody. Also absent in the McConnell Range are any persistent pyritic zones, either within or bordering the intrusions; only local minor zones are present. The bodies within the map area do not appear to be good candidates for porphyry mineralization.

A small monzonitic or granodioritic intrusion on the northeast arm of the southern highland (g-5 in figure 8.2) may merit re-examination. The body has widely spaced (a few metres apart) epidotized fracture surfaces with malachite and azurite. The malachite and azurite are also present in shears and fractures within Takla wallrocks. Originally reported in Lord (1948, pg. 61) the mineralization assayed a few per cent copper in the intrusion and wallrock fractures, with minor silver and trace gold. A number of assessment reports refer to this intrusion, which is not well delineated. The dike-like intrusion is difficult to trace as it cuts across steep slopes, but it is clearly elongate on a northwest trend. The interesting point is that though the wallrock mineralization is fracture controlled it appears to be spatially related to the intrusion. On the eastern arm along the trend but separated by a kilometre another small intrusive is noted in assessment reports. Possibly these dike bodies represent the spire of a larger, yet unroofed body. The eastern watershed of the ridge is shown as anomalous in stream sediment copper by the RGS anomaly.

## Skarn

Work in the McConnell Range suggests regional potential for skarn mineralization. Suitable host rocks though not extensive, are present. Limestone beds and calcareous beds (tuffs etc.) occur locally in the Dewar Formation, Asitka Group, undivided Takla (east of the Ingenika fault) and Moosevale Formation.

A weak skarn found this summer in a well prospected area gives some encouragement for this target. The skarn was found on the western spur of Frederickson peak at the head of a small creek that drains into Attichika creek. The skarn is developed in a drag fold at the faulted margin of the Frederickson pluton. A roof pendant of Takla volcanics is nearby. A prominent gossan is developed over the drag fold on steep difficult slopes. The gossan is developed from siliceous pyritic skarn where accessed. Very thin calc silicate bands and fine biotite? create a weak locally contorted banding. The skarn protolith is not known and granite outcrops within the zone. Either this skarn or a dacitic body further downstream may be responsible for an RGS gold anomaly in this drainage.

## ACKNOWLEDGEMENTS

Brian Untereiner provided excellent assistance in the field. Introduction to the geology of the area by Larry Diakow was much appreciated together with his example of dedication. Considerable hospitality was shown by Royal Oak Mines in use of office and dining facilities at their busy Kemess mine site. The manuscript benefitted

considerably from review by Larry Diakow and Neil Church.

## REFERENCES

- Bates, C.D.S. (1976): Drilling Report on the Asitka North Property, Z Mineral claims; *B.C. Ministry of Energy, Mines and Petroleum Resources*, Mineral assessment report 5662.
- Church, B.N. (1974a): Sustut Copper; in *Geology, Exploration and Mining in British Columbia, 1973*, *B.C. Ministry of Energy, Mines and Petroleum Resources*, pages 417-432.
- Church, B.N. (1974b): Marmot; in *Geology, Exploration and Mining in British Columbia 1973*, *B.C. Ministry of Energy, Mines and Petroleum Resources*, pages 435-443.
- Diakow, L.J. (1998): Toadoggone-McConnell Project: Geology of the McConnell Range-Serrated Peak to Jensen Creek, Parts of NTS 94E/2 and 94D/15; in *Geological Fieldwork 1997*, B.C. Ministry of Employment and Investment, Paper 1998-1, this volume.
- Gabrielse, H. (1985): Major Dextral Transcurrent Displacements along the Northern Rocky Mountain Trench and Related Lineaments in North-central British Columbia; *Geological Society of America, Bulletin*, Volume 96, pages 1-14.
- Gale, V. (1996): Paleotectonic Setting of the Takla Group Volcano-Sedimentary Assemblage, Stikine Terrane, McConnell Creek Map Area, North Central British Columbia; *Dalhousie University*, Unpublished B.Sc. thesis, 108 pages.
- Harper, G. (1977): Geology of the Sustut Copper Deposit in B.C.; *The Canadian Institute of Mining and Metallurgy Bulletin*, Volume 70, Number 777, pages 97-104.
- Irvine, T.N. (1976): Alaskan-type Ultramafic-gabbroic Bodies in the Aiken Lake, McConnell Creek and Toadoggone Map Areas; in *Report of Activities Part A, Geological Survey of Canada*, Paper 76-1A, pages 76-81.
- Jackaman, W.J. (1997): British Columbia Regional Geochemical Survey, NTS 94D - McConnell Creek; *B.C. Ministry of Employment and Investment*, BCRGS 45.
- Lord, C.S. (1948): McConnell Creek Map-Area, Cassiar District, British Columbia; *Geological Survey of Canada*, Memoir 251, 72 pages.
- Meyer, W. and Overstall, R. (1973): Geological, Geochemical and Geophysical Survey on the ARD Claims, McConnell Creek Area, Omineca Mining Division; *B.C. Ministry of Energy, Mines and Petroleum Resources*, Assessment Report 4707.
- Monger, J.W.H. (1977): The Triassic Takla Group in McConnell Creek Map-Area, North-Central British Columbia; *Geological Survey of Canada*, Paper 76-29, 45 pages.
- Monger, J.W.H. and Church, B.N. (1976): Revised Stratigraphy of the Takla Group, North-Central British Columbia; *Canadian Journal of Earth Sciences*, Volume 14, pages 318-326.
- Mustard, D.K. and Bates, C.D. (1974): Geological-Geochemical-Geophysical Report on the Z-Mineral claims, Nos. 1-60, B.C.; *B.C. Ministry of Energy, Mines and Petroleum Resources*, Assessment report 5256.
- Mustard, D.K. and Bates, C.D. (1975): Drilling Report Asitka North Property, Z Mineral Claims Z #1 to Z #40 B.C.; *B.C. Ministry of Energy, Mines and Petroleum Resources*, Assessment report 5662.
- Nixon, G.T., Ash, C.H., Connelly, J.N., Case, G. (1989): Alaskan-Type Mafic-Ultramafic Rocks in British Columbia: The Gnat Lakes, Hickman and Menard complexes; in *Geological Fieldwork 1988 B.C.*, *Ministry of Energy, Mines & Petroleum Resources*, Paper 1989-1, pages 429-442.
- Rebagliati, C.M., Bowen, B.K., Copeland, D.J., and Niosi, D.W.A. (1995): Kemess South and Kemess North Porphyry Gold-Copper Deposits, Northern British Columbia; in *Porphyry Deposits of the Northwestern Cordillera of North America*, Edited by T.G. Schroeter, *Canadian Institute of Mining and Metallurgy*, Special Volume 46, pages 377-396.
- Richards, T.A. (1976): McConnell Creek map-area (94D east-half), British Columbia; *Geological Survey of Canada*, Open File 342.
- Trueman, E.G. (in press): Carbonate hosted Cu-Pb-Zn in Selected British Columbia Mineral Deposit Profiles, Volume 3 - Metallic Deposits and Industrial Mineral; *B.C. Ministry of Employment and Investment*, Open File 1997-
- Woodsworth, G.J. (1976): Plutonic rocks of McConnell Creek (94D East Half) and Aiken Lake (94C West half) Map-areas, British Columbia; in *Report of Activities, Part A, Geological Survey of Canada*, Paper 76-1A, pages 69-73.
- Zhang, G. and Hynes, A. (1991): Structure of the Takla Group East of the Finlay-Ingenika fault, McConnell Creek Area, North-Central B.C.; in *Geological Fieldwork 1990*, *B.C. Ministry of Energy, Mines & Petroleum Resources*, Paper 1991-1, pages 121-129.



**THE MOYIE INDUSTRIAL PARTNERSHIP PROJECT:  
GEOLOGY AND MINERALIZATION OF THE YAHK-MOYIE LAKE AREA,  
SOUTHEASTERN BRITISH COLUMBIA  
(82F/01E, 82G/04W, 82F/08E, 82G/05W)**

By D. A. Brown, B.C. Geological Survey Branch, and  
R.D. Woodfill, Abitibi Mining Corp and SEDEX Mining Corp

**KEYWORDS:** Regional geology, Proterozoic, Purcell Supergroup, Aldridge Formation, Moyie sills, peperites, SEDEX deposits, tourmalinite, fragmentals, mineralization, aeromagnetic data.

**INTRODUCTION**

This article summarizes results of the Moyie Industrial Partnership Project after completion of two months of fieldwork in the Yahk, Grassy Mountain, Yahk River, and Moyie Lake map areas (82F/1, 8; 82G/4, 5) in 1997. The primary focus of this project is to provide updated compilation maps for the Aldridge Formation. The project will provide new 1:50 000-scale Open File geologic maps based on compilation at 1:20 000-scale. These maps draw extensively from Cominco Ltd.'s geological maps, recent work by Abitibi Mining Corp. in the Yahk area; and Kennecott Canada

Exploration Inc., SEDEX Mining Corp., Höy and Diakow (1982), and Höy (1993) in the Moyie Lake area. Generous financial, technical and logistical support by these companies allowed for the success of this project. New drill hole, tourmalinite and fragmental databases are another contribution of the Moyie Project.

Access to the map area is provided from Cranbrook via Highway 3 and by a network of logging roads that range from well maintained to overgrown. Mapping focused on two areas that are dominated by the Aldridge Formation, the core of the Moyie anticline, and the structural panel between the Moyie and Old Baldy faults (Figure 1). Geological features pertaining to each area

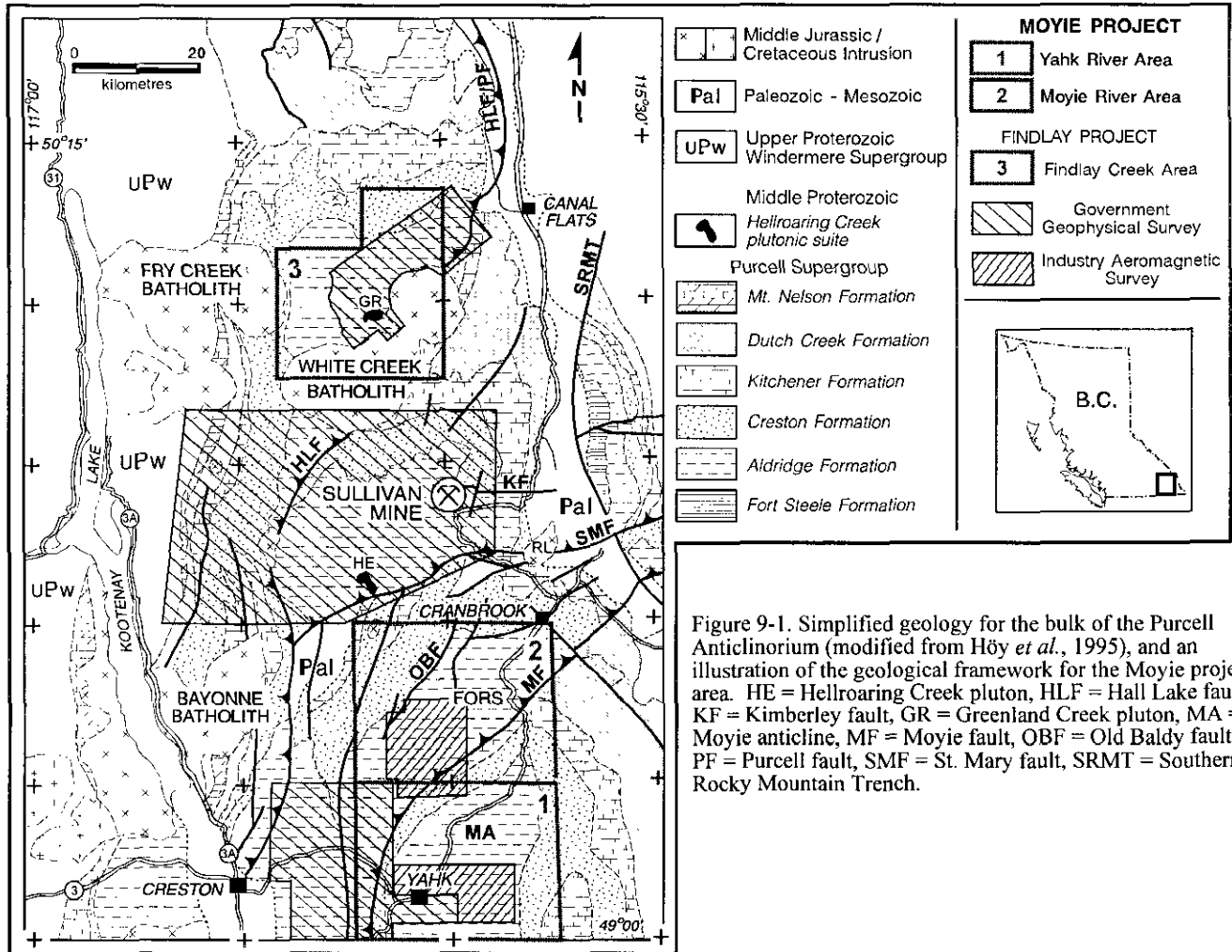


Figure 9-1. Simplified geology for the bulk of the Purcell Anticlinorium (modified from Höy *et al.*, 1995), and an illustration of the geological framework for the Moyie project area. HE = Hellroaring Creek pluton, HLF = Hall Lake fault, KF = Kimberley fault, GR = Greenland Creek pluton, MA = Moyie anticline, MF = Moyie fault, OBF = Old Baldy fault, PF = Purcell fault, SMF = St. Mary fault, SRMT = Southern Rocky Mountain Trench.

are discussed after a brief review of the regional stratigraphy, intrusive rocks, structure and metamorphism.

Physiographically, most of the map area consists of broad valleys and rounded mountains. The highest and lowest features in the Yahk area correspond to an unnamed peak 6 km south of Yahk (2057 m elevation) and Kingsgate (823 m); and in the Moyie area, Grassy Mountain (2491 m) and Elizabeth Lake (930 m). Relief is subdued with extensive glacial, alluvial and colluvial cover southwest of Mt. Olsen throughout the broad Hawkins Creek/Meadow Lake valley. The area northwest of Moyie Lake is dominated by two major northeast-trending, structurally-controlled valleys, occupied by the Moyie River and Lamb Creek. Moyie Lake lies in a north-trending, U-shaped valley but has no known structural control. The region is blanketed by locally dissected glacial and glaciofluvial deposits of variable thickness. An example of this is the drainage system from Kiakho Lakes to Palmer Bar Creek and Moyie River where a series of prominent incised valleys, visible on airphotographs and Landsat images, are interpreted to represent meltwater channels.

## Previous Geological Mapping

Geological mapping in the Nelson East Half map area was completed by Rice (1941), and in the Fernie West Half by Daly (1912a), Schofield (1915) and Rice (1937), and later, Leech (1960; Figure 2). Recent 1:100 000-scale mapping has been published by Höy (1993) and Reesor (1996). South of the international boundary, 1:250 000 scale maps were produced by Harrison *et al.* (1992), and Aadland and Bennett (1979; Figure 2). Höy *et al.* (1995a) produced a 1:250 000-scale coloured compilation map of the entire British Columbian Purcell anticlinorium. More detailed mapping adjoining and including part of the project area includes work by Brown *et al.* (1995a and c), Doughty *et al.* (1997), Burmester (1985), Höy and Diakow (1981, 1982), and Reesor (1981; Figure 2).

## Geological Setting

The project area lies in the center of the Purcell anticlinorium, a broad, gently north-plunging structural culmination cored by the Proterozoic Purcell Supergroup (Figure 1). The supergroup comprises a siliciclastic and lesser carbonate sequence at least 12 kilometres thick, that initially accumulated in an intracratonic rift basin. The strata are preserved in an area 750 kilometres long and 550 kilometres wide, that extends from southeastern British Columbia to eastern Washington, Idaho and western Montana. The original extent and geometry of the basin is poorly known, partly because the western and northwestern limits are poorly exposed, and partly due to Laramide contractional deformation.

The project area is underlain primarily by the lower strata of the Purcell Supergroup; the conformable succession of Aldridge, Creston and Kitchener

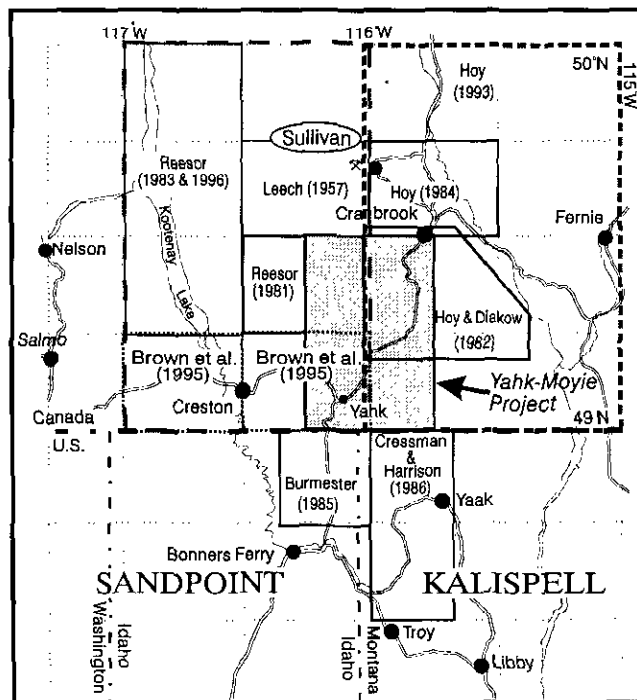


Figure 9-2. Location of Moyie project area (shaded rectangle) relative to areas of previously published geologic maps. The 1:250 000 to 1:100 000-scale map coverage includes: Fernie West-half (82G/west) -- Leech (1958, 1960), Höy (1993); Nelson East-half (82F/east) -- Rice (1941), Reesor (1996); Sandpoint -- Aadland and Bennett (1979); Kalispell -- Harrison *et al.* (1992). The 1:50 000, and 1:48 000-scale maps in the immediate vicinity of the Yahk-Moyie Lake map area include: Brown *et al.* (1995c), Burmester (1985), Cressman and Harrison (1986), Höy and Diakow (1982), and Reesor (1981).

formations. These units have been discussed by Höy (1993) for the Fernie west half, and by Brown *et al.* (1994) and Brown and Stinson (1995) for the Yahk map area. Therefore, synoptic lithological descriptions are presented here, followed by key geological features, mineral occurrences and exploration activity highlights.

## PROJECT AREA STRATIGRAPHY

### Aldridge Formation (Pa)

The Aldridge Formation is over 3000 m thick in the project area and was the focus of the mapping (Figures 1 and 3). It is divided into lower, middle and upper members in the Sullivan Mine area (Höy, 1993). However, distinction of lower and middle members becomes ambiguous to the southwest of the mine (i.e. in the Moyie project area). This is due to the absence of the distinctive, thin-bedded rusty weathering quartz wacke of the lower Aldridge that is evident in the Sullivan area.

## Lower Aldridge Formation (*Pa1*)

Lower Aldridge Formation exposures occur in two parts of the project area; along Rabbit Foot Creek (Høy and Diakow, 1982); and along Hawkins Creek, where the strata are included in the Rampart Facies, a siliceous, thicker-bedded western facies of the Lower Aldridge proper (see Brown *et al.*, 1995). The former is more typical of the lower Aldridge as seen in the Sullivan area, 45 km to the north. Outcrops along the Rabbit Foot road are uniformly rusty brown weathering fine-grained quartz wacke. This thin bedded to laminated unit contains a thick bedded quartzite over 15 m thick that could be equivalent to the Footwall Quartzite at Sullivan. The facies change from typical lower Aldridge to the Ramparts Facies remains poorly defined but must lie between Marysville and the South Moyie River area.

## Middle Aldridge Formation (*Pa2*)

The middle Aldridge underlies most of the map area and comprises a medium- to thick-bedded sequence of fine siliciclastic turbidites, dominantly planar-bedded, fine-grained quartzofeldspathic wacke to quartz wacke, with lesser argillite. It contains less pyrrhotite and hence is not as rusty brown weathering as the lower Aldridge Formation. Uncommon medium-grained units occur, and rare coarse-grained quartz arenite; for example, as exposed near Sundown Creek. Based on estimates from map distribution, the total thickness of the middle Aldridge is at least 3000-4000 metres. In the Cranbrook area it is about 2500 metres thick and farther north near the Sullivan mine area, only 2100 metres thick (Høy, 1993). This apparent thinning of the section is compatible with north to northeast-directed paleocurrents and the interpretation of a southwest source feeding northeast-prograding, submarine turbidite fans.

An atypical middle Aldridge argillaceous facies is poorly exposed along a new logging road 10.5 km southeast of Cold Creek - South Hawkins Creek junction (Figure 3b). It comprises thin bedded to laminated siltstone and argillaceous siltstone with rusty fractures. Extensive trough cross-bedding (medium scale, 2-7 cm) is unique to this local facies, and suggests a higher energy, perhaps shallower-water environment.

### *Marker laminates*

Over twenty distinct laminated siltstone marker units that occur in the middle Aldridge Formation provide stratigraphic control across the Purcell (Belt) basin (Edmunds, 1977; Huebschman, 1973). Each marker unit comprises a unique sequence of alternating light and dark grey, parallel siltite laminae that can be correlated over distances up to several hundred kilometres. They are analogous to merchandise bar codes. Individual laminae consist of quartz and feldspar grains with disseminated biotite, muscovite and pyrrhotite. The marker units range from a few centimetres to over 9 metres thick and they can be

expanded by turbiditic wacke or sill intrusion. The rusty weathering markers contain anomalous amounts of Pb and Zn relative to the background turbidites. A number of new marker laminate occurrences were located and identified during the project. This information is critical for detailed correlations and accurate map projections.

The origin of the marker units is a subject of debate as reviewed in Brown *et al.* (1994). Episodic sedimentation of terrigenous material from dust storms as recorded in the Gulf of California (Turner *et al.*, 1992) appears to be one of the better potential modern analogues. The duration required to deposit these units is unknown.

## Upper Aldridge Formation (*Pa3*)

Good exposures of the upper Aldridge Formation occur along the trace of the Moyie anticline, east of St. Eugene Mine, and west of Moyie Lake along Etna Road (Figure 3a). The upper Aldridge is a distinctly dark rusty brown weathering, thinly bedded to laminated argillaceous siltstone unit. It is planar bedded with a platy to fissile cleavage. The absence or rare occurrence (<5%) of thicker bedded (>10 cm) quartzofeldspathic wacke turbidite beds distinguish upper from middle Aldridge.

## Creston Formation (*Pc*)

The Creston Formation underlies about 20% of the map area within the Moyie anticline; exposures north of the Old Baldy Fault were not examined (Figures 1 and 3a). The Formation is divided into a lower argillaceous member (~1000 m thick), a middle quartzitic member (~1000 m thick) and an upper siltite and argillite (< 300 m thick). It represents shallow-water, reworked sediments accumulated on northward prograding deltas or fans (Hrabar, 1973). To the south, the Revett Formation, the middle Creston Formation equivalent, hosts several stratabound copper-silver deposits including Spar Lake, Montanore and Rock Creek in the western Montana copper belt.

Excellent exposures of the middle Creston Formation occur along Highway 3 east of Moyie Lake, along the shore of Moyie Lake, and along West Yahk River near the U.S. border. In the southeast, trough cross-bedded, light green fine-grained quartz arenite is interbedded with mudcracked mauve argillite. Mudchip breccia beds occur within apple green laminated to thin bedded quartz arenite. Wavy to lensoidal bedding is common. A measured section of most of the Creston Formation west of Moyie Lake was completed by Høy (1993, Section 10; location shown on Figure 3a).

The lower and middle Creston Formation produces prominent aeromagnetic anomalies in numerous areas, for example in much of the Moyie anticline (see Figure 6). This is due to fine disseminated magnetite, and quartz-magnetite veinlets and stringers. For example,

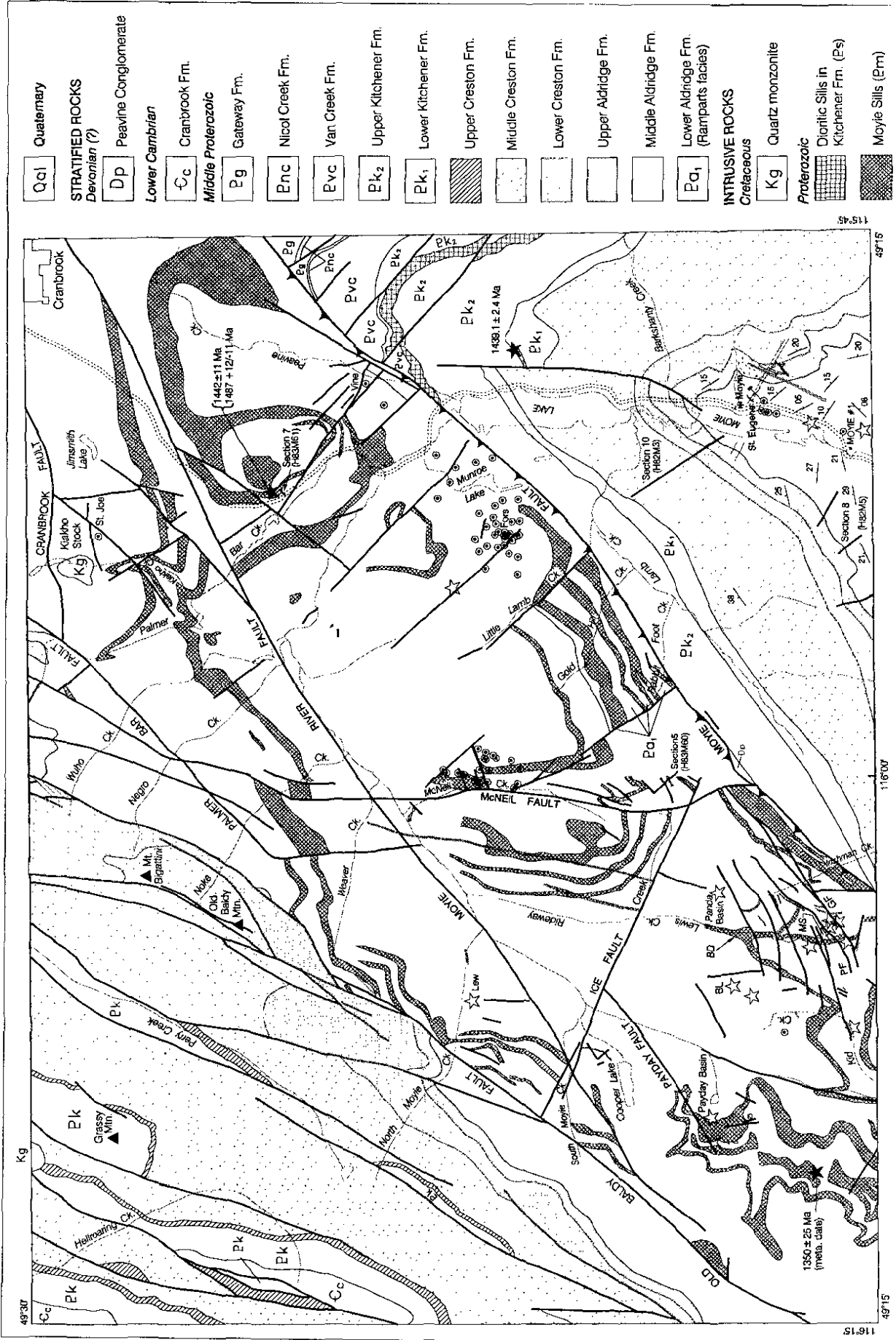


Figure 9-3(a). Simplified geology of the northern half of the Yahk-Moyie Project map area. The Moyie panel (82F/8E, 82G/05W) includes compilation from Höy (1993) and Reesor (1981, 1996) for the area northwest of the Old Baldy fault. BL = Bear Dike, BD = Big Lewis, MS = Miss Pickle, GF = Goodie fault, PF = Panda fault. Four U-Pb dates shown are from: Anderson and Davis (1995; 1487 ± 11 Ma), Höy (1993; 1442 ± 11 Ma), Ross *et al.* (1992; 1350 ± 25 Ma), and this report (1439 Ma).

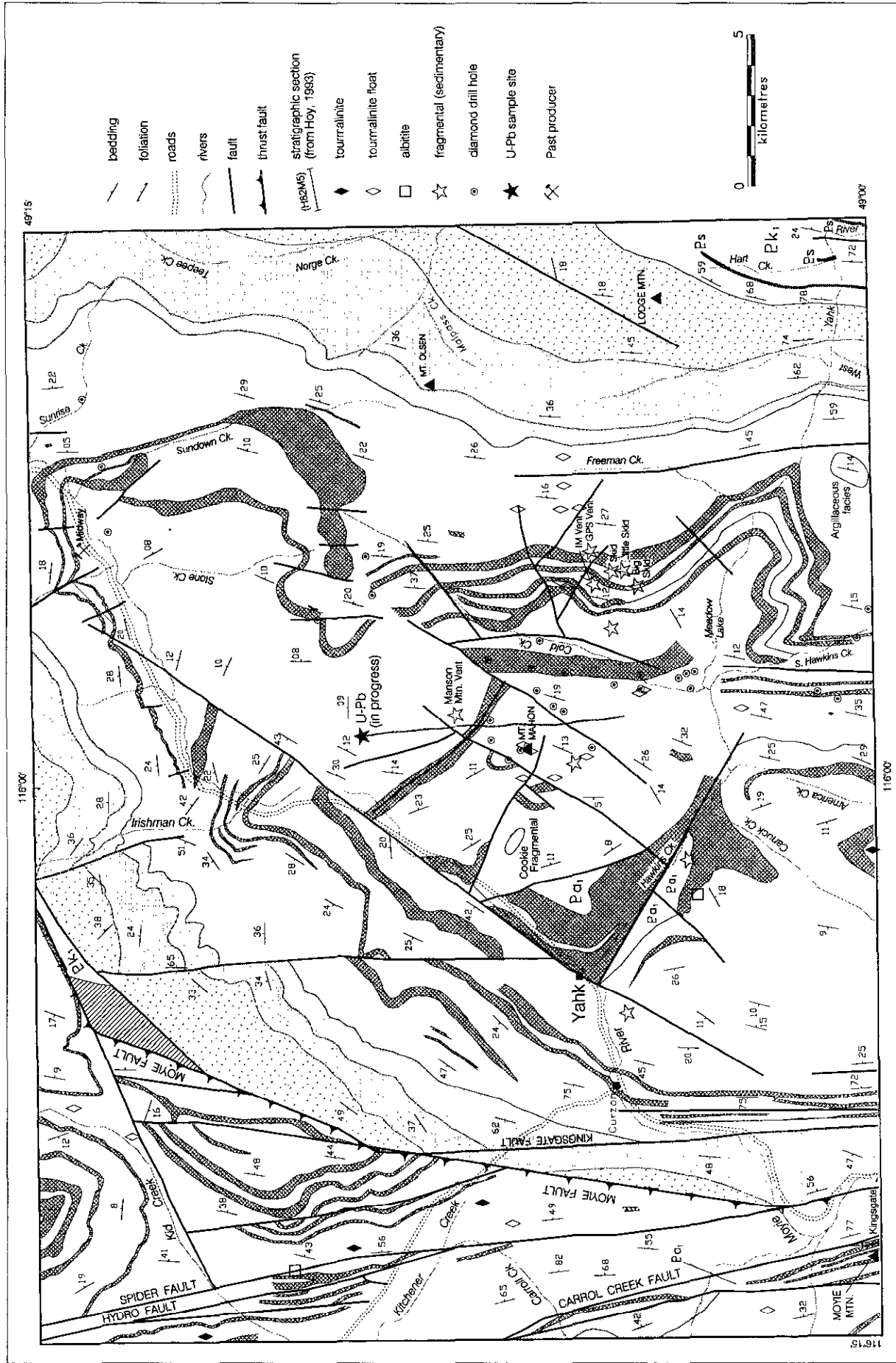


Figure 9-3(b). Simplified geology of the southern half of the Yahk-Moyie Project map area which corresponds to the core of the Moyie anticline (82F/1E, 82G/04W). The western half is taken from Brown *et al.* (1994) with minor revisions southeast of Yahk.

thin irregular fractures (< 2 mm wide) filled with black magnetite in pale green phyllitic argillite crop out in the lower Creston along Highway 95, 5.5 kilometres south of Curzon. Disseminated magnetite euhedra (<2%) occur in pale green, cross-bedded siltstone of the middle Creston at the north end of Etna Road, west of Moyie Lake.

### **Kitchener Formation (Pk)**

The Kitchener Formation overlies the Creston Formation and comprises green dolomitic siltite, argillite, carbonaceous dolomite, dolomite and limestone. It forms a succession 1600 to 1800 metres thick that is divisible into two members, a lower pale green dolomitic siltstone unit, and an upper dark grey, carbonaceous, silty dolomite and limestone unit. Typical lithologies and deposition in a shallow-water shoal environment are discussed in Höy (1993). Kitchener Formation is exposed in the footwall of the Moyie fault around Moyie Lake. Prominent but thin, brown-weathering dolomitic siltstone beds distinguish basal Kitchener Formation from uppermost Creston Formation.

Molar-tooth structures are a common feature of the formation, and are well exposed along Highway 3, 8.5 km north of Moyie. They were also noted in the southeast corner of the map area. The irregular, calcite-filled features occur in argillaceous dolomite. Their presence within small argillaceous rip-up fragments in dolomitic breccia, and as folded wedges perpendicular to bedding, indicate that they formed during diagenesis. This has led to the interpretation that they formed by gas bubble migration and expansion crack development perhaps from CO<sub>2</sub>, H<sub>2</sub>S and CH<sub>4</sub> gas generation (Furniss *et al.*, 1994). These structures are illustrated in Plate 28 of Höy (1993, p. 29).

The Wallace and Helena Formations in the United States are correlative with the Kitchener Formation. Shallowing-upward cycles, consisting of siliciclastics overlain by tan-weathering dolomite have been studied in detail by Eby (1977), Grotzinger (1986), Winston (1993) and others. Their work suggests the cycles represent repeated changes in water level such that the deeper water siliciclastics are overlain by shallower water dolomitic sediments. Whether these cycles represent lacustrine or marine transgressions and regressions continues to spark debate.

The age of the Kitchener Formation is presumed to be roughly equivalent to that determined for a bentonite horizon in the uppermost Middle Belt Carbonate, 1449 ± 10 Ma (Aleinikoff *et al.*, 1996).

### **Van Creek and younger strata (Pvc, Pnc, Pg, Cc, Dp)**

Van Creek, Nicol Creek and Gateway formations underlie a small part of the northeastern margin of the project area. Lower Cambrian Cranbrook Formation

white quartzite to pebble conglomerate occurs in the northwest corner of the map area (Reesor, 1981), and isolated, fault-bounded slivers of Devonian (?) Peavine polymictic conglomerate/breccia and carbonate lie along the hangingwall of the Moyie fault (Leech, 1962; Höy, 1993; Reesor, 1996). None of these units were examined during the course of this project.

## **INTRUSIVE ROCKS**

### **Moyie intrusions (Pm)**

Moyie intrusions, sills and rarely dikes, occur within the lower and middle Aldridge formations. The sills were first discussed by Daly (1905, 1912a) and more recently described by Höy (1989, 1993) and dated by Anderson and Davis (1995). They are commonly 50 to 100 m thick but can reach over 500 m thick, and extend laterally over tens of kilometres. The fine- to medium-grained sills range in composition from hornblende (± pyroxene) gabbro to hornblende quartz diorite and hornblendite. Mafic phenocryst contents vary up to 70%. Pyroxene is rare and due to pervasive alteration only found as relict cores surrounded by amphibole. Some of the thicker sills (>20 m) contain irregular patches of coarse pegmatitic hornblende and feldspar.

Moyie sills (meta-gabbro) are distributed throughout the project area, they reach a maximum cumulative thickness of about 800 m east of Cold Creek. In the subsurface, a 900 m thick sill within the lower Aldridge Formation was intersected south of Moyie Lake in a drill hole by Duncan Energy (Anderson, 1987; Schultze, 1988).

A model for emplacement of Moyie sills into wet, unconsolidated sediments was first proposed by Höy (1989). The zones of thickest accumulation of Moyie sills are currently considered to be closest to the feeder zones or rift axis. However, the opposite scenario is demonstrated for mafic sills in a late Carboniferous basin in northern Britain (Francis, 1982). The saucer-shaped bodies are thickest in the central part of the basin and the feeder dikes occur on the flanks, where the sills are thinnest. Therefore, more detailed observations are required to determine whether this model holds true for the Purcell Basin.

Granophyre is the term used for zones of intensely altered, biotite-rich metasediment and rare gabbro associated with the margins of meta-gabbro sills. In thin section, the rock displays a characteristic micrographic intergrowth of quartz and plagioclase (Craig Leitch, pers. comm., 1997). These granoblastic-textured rocks contain more quartz and less K-feldspar than Cretaceous intrusive rocks. Several exposures previously interpreted to be underlain by granitoid rocks, for example the small plug along America Creek (see Höy and Diakow, 1982) are currently interpreted to be zones of granophyre. For some unknown reason granophyres are restricted stratigraphically to the lower Aldridge Formation (Peter Klewchuk, pers. comm., 1997). Locally

they contain disseminated base metals and fine tourmaline needles (Craig Kennedy, per. comm., 1997).

Similar granophyre textures have been documented where mafic sills intruded wet arenaceous sediments of mid-Proterozoic age in Antarctica. Krynow *et al.* (1988) used the field term "granosediment" for partially fused and homogenized sediments along sill margins. The features they describe and illustrate in these "reconstituted sediments" are identical to macro- and microscopic textures found in the Aldridge Formation; in particular are ovoid structures and intergrowths of quartz with albite and K-feldspar. They speculate that boron or fluorine from trapped seawater may have acted as a flux to cause incipient melting in the quartz-albite-orthoclase system.

### **Sundown Creek sill-sediment contact**

Supportive evidence of the interpretation that sills were emplaced into wet, unconsolidated sediments is well exposed along Stone Creek road at Sundown Creek. The medium to thin bedded quartz wacke beds are contorted/disharmonically folded along the upper contact of the sill on the east side of Sundown Creek. The sharp, undeformed basal contact of the sill is exposed on the west side of the creek. Peperite textures described later (see Sedimentary fragmental units) also suggest syndimentary emplacement of the sills.

### **U-Pb dates**

The most accurate date for the Moyie sills, yielding a  $1467.2 \pm 1.1$  Ma age, has been obtained from two concordant single zircon grain analyses (Don Davis, written comm., 1997). The amphibolite-grade meta-gabbro sample is correlated with the Moyie sills, and was collected 10.5 km west-northwest of Creston along Highway 3 near the Summit Creek bridge (see Brown *et al.*, 1995a). Four other Moyie sill samples from the lower and middle Aldridge Formation have yielded an upper intercept U-Pb date of  $1468 \pm 3-2$  Ma (Anderson and Davis, 1995). A younger  $1445 \pm 11$  Ma zircon U-Pb age of emplacement was reported by Höy (1993) for the Lumberton sill hosted in the middle Aldridge Formation (Figure 3a). In addition, a sill collected 6.5 km southwest of Cooper Lake yielded a slightly younger titanite U-Pb date of circa 1350 Ma (Ross *et al.*, 1992; Figure 3a). This result was re-interpreted as reflecting the East Kootenay event by Anderson and Davis (1995). Previous K-Ar dates ranged from  $845 \pm 50$  to  $1585 \pm 95$  Ma (Hunt, 1962) and reflect partial resetting by younger thermal events and, less commonly, excess argon.

### **"Upper" Mafic sills and dikes**

Gabbroic to dioritic sills and rare dikes also occur in the Creston and Kitchener formations, however, they are fewer and less voluminous than the Moyie sills. A 200-300 m thick sill in the Upper Kitchener Formation underlies the hinge zone of the Moyie anticline northeast of Moyie Lake (Höy and Diakow, 1982; Figure 3a).

Another narrower (at least 75 m thick), medium-grained, massive sill with prominent joints is well exposed along new logging roads to the southwest, near the Lower-Upper Kitchener contact.

A similar 30-40 m thick, dioritic sill within the Kitchener Formation occurs in the southeast corner of the map area (Figure 3b). The dull brown weathering, pale olive green sill is fine to medium-grained, massive meta-diorite. Unlike the sills northeast of Moyie Lake, this unit has equant, white K-feldspar megacrysts (up to 2 cm) that form about 5% of the rock, in a dark green, chloritic groundmass.

Contact relationships have not been studied during this project, however, unlike the Moyie sills there have been no soft-sediment features observed (Trygve Höy, pers. comm., 1997). These sills and dikes are interpreted to be subvolcanic equivalents to the Nicol Creek lava that lies 6 km farther to the northeast.

In an effort to help constrain the age of the upper Purcell Supergroup the 75 m thick sill was sampled northeast of Moyie Lake for U-Pb dating (Figure 3a). It has yielded a  $1439.1 \pm 2.4$  Ma zircon U-Pb date (Don Davis, written comm., 1997; Figure 4). This date is interpreted to represent the age of sill emplacement and probably the age of the Nicol Creek lavas. The new 1439 Ma age is concordant with the age of  $1443 \pm 10$  Ma obtained by Aleinikoff *et al.* (1996) for the correlative Purcell Lava in Montana.

## **STRUCTURE**

The project area is naturally divided into two structural domains that comprise the footwall and hangingwall of the Moyie fault (Figure 5). The **Moyie fault** is an important transverse thrust fault that trends obliquely across the Purcell anticlinorium. It extends from the east side of the Rocky Mountain Trench, where it is called the Dibble Creek fault, southwestward through the project area and southward into northern Idaho. It is one of a family of transverse contractional faults that include the St. Mary, Hall Lake and Purcell faults (Figure 1; Benvenuto and Price, 1979). Its arcuate trace in the map area is mimicked by the Moyie-Sylvanite anticline in the footwall domain. The fault records a complex history of normal displacement that began in the Proterozoic and continued with younger reverse motion (Benvenuto and Price, 1979; Höy, 1993; McMechan, 1981). Leech (1962) believed that the fault followed a Devonian gypsum horizon that overlies the Peavine conglomerate. A portion of the fault zone in the Yahk area was examined and described by Brown and Stinson (1995).

### **Footwall Domain**

The footwall domain (equivalent to part of the "Moyie Block" of Benvenuto and Price, 1979) is represented by the **Moyie anticline**, an open, gently northeast-plunging upright parallel fold (orthogonal thickness is constant). Its southern extension, the

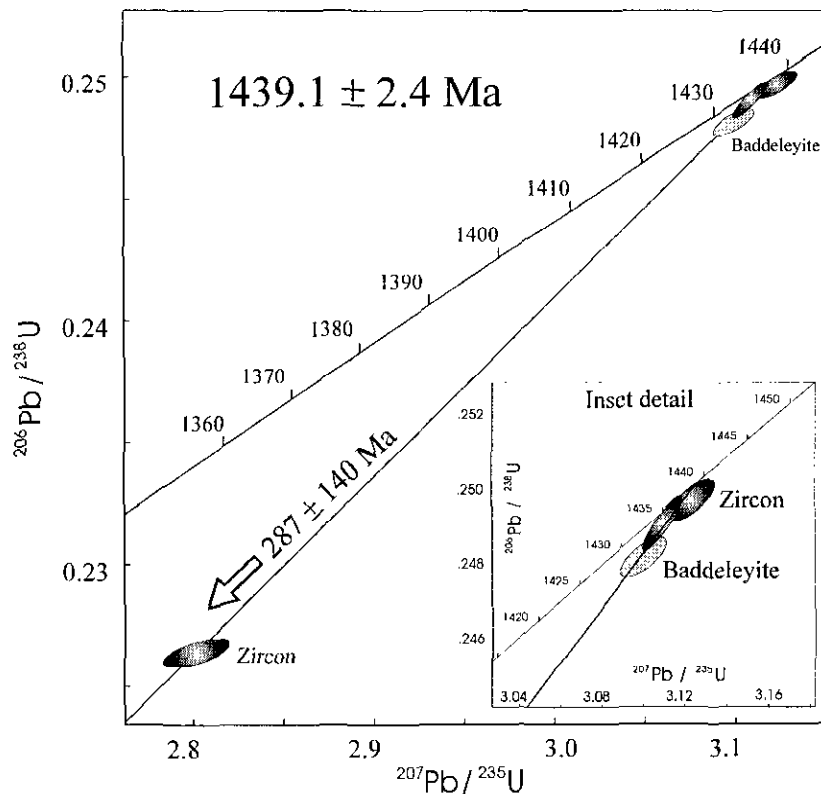


Figure 9-4. Concordia diagram showing U-Pb data points from analyses of zircon (dark shaded ellipses) and baddeleyite (light grey ellipse) in the mafic sill hosted in Kitchener Formation provided by Don Davis (Royal Ontario Museum, Nov., 1997). The regression line to all the data points is also shown.

Sylvanite anticline, plunges gently southeast and results in the overall arcuate-shaped anticline, with a hinge zone over 100 km long and about 60 km across (at surface), in the footwall of the Moyie fault. The Moyie anticline is clearly defined by the distribution of lithologic units. The oldest exposed stratigraphy within the core comprises gently-dipping lower Aldridge strata, locally called the Rampart Facies in the Hawkins Creek area. The northwest and southeast limbs of middle Aldridge strata dip moderately. However, strata steepen abruptly and bend into a north trend adjacent to the Kingsgate fault, which bounds Creston Formation in the Kingsgate graben (Brown and Stinson, 1995). The anticline is cut by numerous north-northeast, north, and northwest-trending known and inferred faults.

The Moyie anticline was investigated in 1979 by Duncan Energy Inc. as a potential hydrocarbon trap. They were searching for Paleozoic carbonates in the core of the fold, and conducted seismic and gravity surveys before drilling a 3477 m deep vertical hole south of Moyie Lake (Figure 3a; Anderson, 1987; Schultze, 1988). Cook and van der Velden (1995) combined this data with Lithoprobe seismic studies to suggest that the lower Aldridge Formation, including a series of mafic sills, was at least 8 km thick and the anticline was cored by crystalline basement.

## Hangingwall Domain

The Hangingwall domain (equivalent to a portion of the "St. Mary Block" of Benvenuto and Price, 1979) extends northwest from the trace of the Moyie fault to the Old Baldy fault, the limit of this project's mapping. The domain is dominated by gently-dipping middle Aldridge Formation (Figure 5), which form the northwest limb of a moderately northeast-plunging half anticline (*Ibid.*). In a few specific areas bedding is tightly folded and overturned, for example near the Palmer Bar fault (Höy and Diakow, 1982). The area is cut by a series of faults, at least some of which appear to have been active in the Proterozoic, an important consideration for SEDEX mineral deposit exploration.

### Northeast-trending faults

There are a series of northeast-trending faults in this domain. The Old Baldy, and Palmer Bar faults are the two most prominent after the Moyie fault. The **Old Baldy fault** is a northwest-side-down, normal fault that is well exposed on the David property south of the North Moyie River (Figure 6). It comprises a zone 8 metres wide of sheared, intensely silicified and/or albitized meta-wacke with fine disseminated pyrite and minor galena (Peter Klewchuk, written comm., 1997). Extensive quartz veins occur within the cataclastic to mylonitic shear zone. A steeply, northwest-dipping sericitic foliation (195/75 NW) developed in bleached quartz-sericite altered wacke delineates the fault. Local tight, steeply north northeast-plunging minor folds and chlorite schist zones (sheared Moyie sill gabbro) occur

along the fault zone. Dip-slip slickensides suggest normal movement late in the fault history. The **Palmer Bar fault** is a northwest-dipping fault with overturned beds in the hangingwall that suggest reverse displacement (Benvenuto and Price, 1979), however, stratigraphic offset implies normal movement. Discrete chlorite-sericite-pyrrhotite-bearing shear zones lie parallel to the northeast-trending Moyie fault in the Panda Basin area, which is at the headwaters of Lewis Creek (Figure 3a). Narrow, fine-grained, magnetic mafic dikes (ex. near Goodie fault; see below) in these zones are correlated with the Moyie intrusions and therefore suggest a Proterozoic age for some of the structures. This implies that the early and probable extensional movement on the Moyie fault could have occurred in the middle Proterozoic.

### North-trending faults

The north-trending McNeil fault is the most apparent fault of this orientation in the hangingwall domain. It corresponds to a linear airborne magnetic anomaly that extends north of the Moyie River fault without any lateral offset (Figure 7). The fault zone is poorly exposed, but includes albite-altered, iron-oxide breccia along a northeast-trending shear zone adjacent to the McNeil fault at the head of McNeil Creek (Steven Coombes, pers. comm., 1997). The breccia resembles Iron Range mineralization near Creston as described by Stinson and Brown (1995).

### Northwest-trending faults

A series of northwest-trending faults were mapped by Höy and Diakow (1982) and Cominco Ltd. east of the McNeil fault. These faults terminate at the Moyie fault but may continue on the north side of the Moyie River fault. They commonly contain gabbro dikes, for example at the Vine vein (Peter Klewchuk, per. comm., 1997), which implies some Proterozoic movement. This is supported by extensive drilling on the Fors property which indicates that the northwest faults controlled sub-basin deposition during Aldridge time, localized fragmental units and caused arching of a gabbro sill. The thick sill (up to 500 m) lies close to the lower-middle Aldridge contact and may correlate with the Mine Sill at Sullivan.

## METAMORPHISM

Much of the middle Aldridge Formation in the project area comprises meta-wacke with biotite ( $\pm$  muscovite) porphyroblasts in the bedding planes. In addition, several areas have prominent, biotite flakes aligned semi-randomly perpendicular to bedding. Locally the biotite is partially to completely retrograded to chlorite. Coarse hornblende porphyroblasts (up to 8 mm long) concentrated along calcareous layers within thin bedded to laminated meta-siltstone and wacke of the upper part of the middle Aldridge crop out near Mt. Olsen.

These biotite and hornblende porphyroblasts are being dated using the  $^{40}\text{Ar}$ - $^{39}\text{Ar}$  method in an attempt to refine age constraints on the Proterozoic burial metamorphic event. Previous dating in this region produced a biotite K-Ar date of  $720 \pm 3$  Ma (from Wanless *et al.*, 1967 but recalculated using the Steiger and Jäger (1977) decay constants). This result is interpreted to reflect partial resetting of older metamorphic minerals by younger thermal events.

It is speculated that these metamorphic minerals developed during the East Kootenay Orogeny. If correct, the Ar-Ar dates should approach the circa 1370 Ma ages obtained from metamorphic monazite in the Matthew Creek area near Sullivan (R. Parrish, unpub. data, 1996), and titanite from a Moyie sill near Cooper Lake (Figure 3a; Ross *et al.*, 1992). The East Kootenay Orogeny has recently been interpreted to involve bimodal magmatism, basin rifting, and subsidence and sedimentation (Doughty and Chamberlain, 1996).

## SULLIVAN GEOLOGICAL INDICATORS

Sullivan indicators are features associated with the Sullivan orebody. They include the obvious stratiform

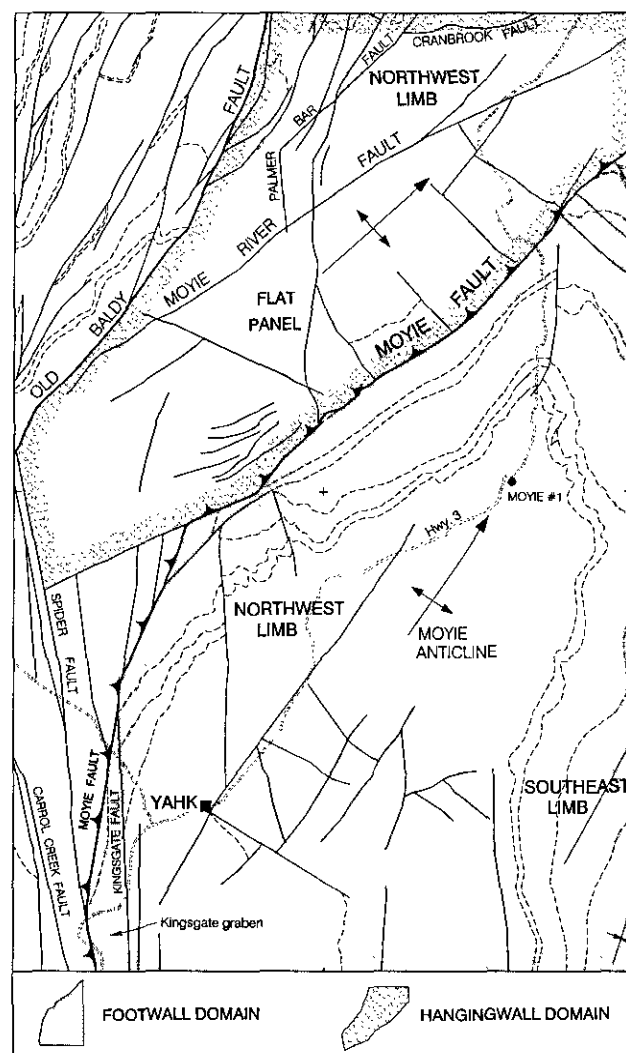


Figure 9-5 Structural domains of the Yahk-Moyie project area.

massive sulfide mineralization and less directly linked features such as structural control, sedimentary fragmental units (referred to as "conglomerates" by Höy, 1993), tourmalinite (tourmaline replaced rock), sericite, albite, and other alteration types, manganese-rich garnet horizons, syndepositional faults, and gabbro arches. Individuals have placed different values on any particular feature. When these indicators occur in combination, or are closely related in a regional context, a higher exploration significance is assigned. The goal of the Aldridge mineral explorationist is to sift through those features mentioned above to identify those related to a mineralizing system; rather than those related to background in the basin succession which are barren.

## Structural control

Structural control plays a vital role and most if not all Sullivan indicators are related to structure. Basic geologic mapping and geophysics are commonly the most valuable tools for defining favourable structures. Structural intersections, cross-structures, transfer zones and graben trends maybe identified from regional studies. The best example is the intersection of the Sullivan-North Star corridor and the Kimberley fault which are interpreted to be important Proterozoic faults. This intersection controlled the locus of the Sullivan hydrothermal system (Turner *et al.*, 1992). The Vine property area is another example of a sub-basin controlled by intersecting structures (Höy *et al.*, in prep.).

## Sedimentary fragmental units

Sedimentary fragmental units, referred to as "fragmentals" (or "conglomerates" in Höy, 1993, p. 19-20), occur sporadically in the otherwise well bedded, fine- to medium-grained, homogeneous quartz wacke Aldridge Formation. Fragments consist of sedimentary clasts that range in size up to 2 m, and in degree of roundness, from completely angular to rounded. Fragmental units fall into three basic descriptive types: (1) stratabound, (2) discordant, and (3) massive. The stratabound units are further divided into disrupted beds and biotite-rich breccia. At the Sullivan Mine there are also sulfide-matrix fragmental units. This classification scheme is modified from detailed studies around the Sullivan Mine as summarized in Turner *et al.* (in press), and in a regional synthesis by Höy *et al.* (in prep.). Some fragmental occurrences also include tourmalinite and albite alteration (flooding), albite porphyroblasts, actinolite, sericite, and manganese-rich garnet. Locally, where fragmental occurrences contain sulfide-rich clasts, clasts are interpreted to be derived from a massive sulfide horizon (ex. Vine Vein area, Dave Pighin, per. comm., 1997). Other fragmental terms include "Chaotic breccia" as found under the Sullivan orebody (Jardine, 1966), and bedded pebble fragmental. A model relating fragmental development to dewatering and sill intrusion, and demonstrating the continuum from discordant to stratabound units is presented in Höy *et al.* (in prep.).

Commonly, fragmental occurrences are poorly defined and difficult to recognize due to lack of exposure, therefore, they can not be accurately classified geometrically or genetically. However, careful mapping allows some of the fragmentals to be divided into genetic classes. For example, they can represent sedimentary fill along active, fault-bounded sub-basins as determined along the North Star corridor (Turner *et al.*, 1992). Other discordant fragmentals include dewatering structures as interpreted at the Highway 3A exposure at Moyie Lake (Figure 3a; Höy, 1993). Fluidized sediments along or near Moyie sill contacts (some examples best defined by the term peperite, see below) form another variety. An excellent example of a peperite lies near the upper contact of a sill in the Payday Basin (Figure 3a; Photo 9-1c, d, e). Irregular-shaped pods of gabbro occur in a coarse, sediment-clast dominated fragmental sheet that parallels the sill contact. The most laterally extensive fragmentals include a group of the coarsest fragmentals known that are concordant with the lower-middle Aldridge contact, for example in the Doctor Creek area (see Brown and Termuende, this volume).

Emplacement of hot mafic sills into water-saturated, unconsolidated sediments results in boiling of superheated pore water and fluidizing of the host sediment. The fragmented rock produced is known as peperite. These peperites suggest that the Aldridge basin water column was less than 3150 metres deep, assuming the basin was filled with salt water (or 2160 m if there was fresh water); the hydrostatic pressure of the water column would prevent boiling below these depths (Cas and Wright, 1987, p. 45).

## Stratabound fragmentals

Stratabound fragmentals are massive to bedded units that are parallel to the regional bedding attitudes. Turner *et al.* (in prep.) also use the term "conglomeratic siltstone" for these units. Lithic clasts dominate; commonly argillite fragments are sericite-rich.

## Disrupted beds

Disrupted beds, a variety of the stratabound fragmentals, are discontinuous zones of laminated to bedded material broken into centimetre to millimetre-scale tabular blocks. Beds above and below remain intact and undeformed. Soft-sediment deformation of argillaceous layers and slump folds occur rarely within these beds. These fragments are contorted which suggests they were ductile (unlithified) during fragmentation. Hagen (1985) used the terms "collapse" and "slump" fragments for similar units.

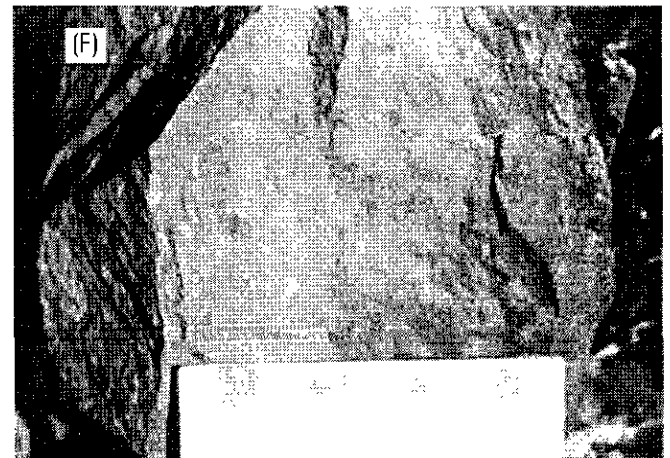
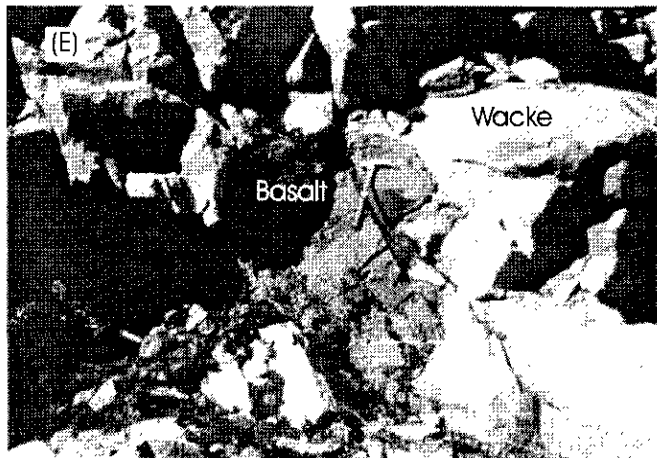
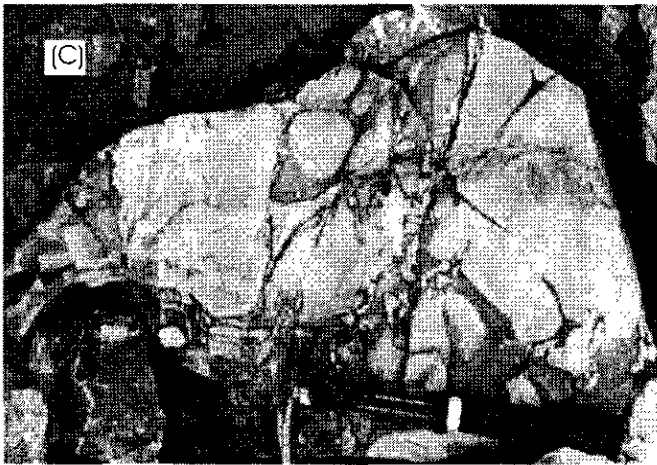
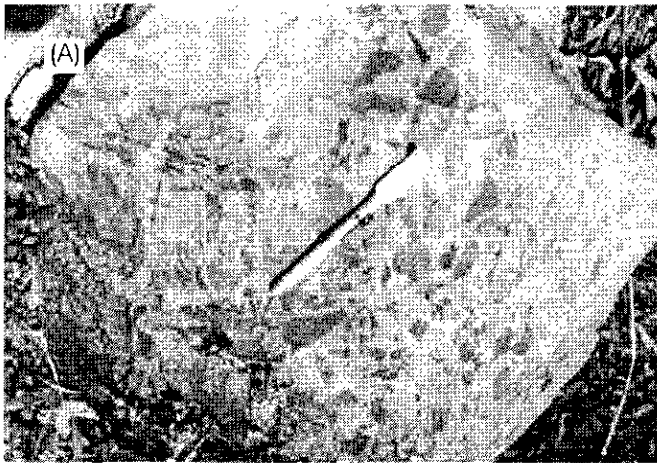


Photo 9-1. Selected examples of fragmental units in the Moyie project area: (a) Miss Pickle fragmental with matrix-supported siltstone clasts in a siltstone matrix, Panda Basin; (b) poorly size-sorted Miss Pickle fragmental; (c) sericite-altered and fragmented wacke, Payday Basin; (d) biotite-rich, large angular clasts of a stratabound fragmental in Payday Basin; (e) Bulbous amygdaloidal basalt fragment in wacke, Payday Basin; (f) massive fragmental hosted in Upper Aldridge Formation, between St. Eugene and Society Girl mines.

### ***Biotite-rich breccia/fragmental***

Clast-supported, biotite-rich, fine-grained, angular to rounded wacke clasts form a variety of fragmental that is common in the Payday Basin area, 2.75 km south of Cooper Lake (Figure 9-3a; Photos 9-1c, d, e; 9-2). They are stratabound, contain albite-altered clasts and are spatially associated with Moyie sills. It is speculated that they formed during sill emplacement.

### ***Discordant fragmentals***

Discordant fragmental occurrences cross-cut bedding at high angles. They are equivalent to clastic dikes/sandstone dikes found in shale basins except they include centimetre and smaller-scale siltstone fragments. Hagen (1985) used the term "cross-cutting" fragmentals for this type.

A well exposed discordant fragmental outcrops along Highway 3A at Moyie Lake (Figure 3a). The 10 m wide elastic dike cuts bedding at a high angle. It is massive weathering in contrast to the well bedded host strata. Diffuse, subangular siltstone and mudstone fragments (up to about 2 cm) are supported in a fine sandstone matrix. The subvertical contacts are irregular and suggest emplacement before complete lithification (see Stop 1-6 in Turner *et al.*, 1992, p. 20). This unit probably resulted from dewatering, either caused by a

seismic event or by fluidization related to sill emplacement at a lower stratigraphic level.

The discordant Goodie fragmental in the Panda Basin area lies sub-parallel to the Moyie fault and is similar to the Moyie Lake unit discussed above.

### ***Massive fragmentals***

Massive fragmentals are structureless with no internal stratification, and commonly form knobs or knolls because they lack bedding planes and therefore resist erosion. Commonly, their geometry relative to host strata is unknown due to lack of exposure. Two of the largest massive fragmental units known in the district are the Clair conglomerate in the St. Mary Lake area and the Cold Creek conglomerate exposed on the east flank on the Moyie anticline. The Clair is over 70 m thick and is exposed over 7.5 km, along a north-trending fault. The zone contains stratabound fragmentals, disrupted beds, discordant fragmentals and low-grade Pb-Zn mineralization with abundant pyrrhotite clasts. The Cold Creek fragmental is over 150 m thick and has been traced northward over 5.5 km along strike.

Massive fragmentals also occur along the St. Eugene vein system. They form at least three fragmental units, two within the St. Eugene Mine workings, and the third lies stratigraphically above the St. Eugene Mine and below the Society Girl Mine



Photo 9-2. Payday Basin area displaying flat-lying middle Aldridge strata where it is intruded by two prominent Moyie sills. View to south.

(Figure 3a; Höy *et al.*, 1995c, p. 30). This highest fragmental is unusual because it occurs near the upper Aldridge - Creston formation contact. It is not known to the authors whether these are stacked sheets or discordant bodies. The uppermost St. Eugene fragmental is massive with angular fragments up to 3 cm long supported in a fine wacke matrix (Photo 9-1f).

### **Tourmalinite alteration occurrences**

Tourmalinite alteration is significant because it is spatially and genetically associated with the Sullivan deposit (see Hamilton *et al.*, 1982, 1983; Slack, 1993), therefore, it may provide a regional exploration vector. Tourmaline occurrences are divided into two basic types: stratabound and discordant. They vary from aphanitic tourmaline to zones of tourmaline needles. Stratabound occurrences include alternating beds or laminations of aphanitic tourmalinized mudstone and fragmented zones where clasts are variably replaced by tourmaline. Black tourmaline is more common than brown but co-existing brown and black tourmalinite, considered an indication of high fluid to rock ratios (Slack, 1993), may discriminate potentially mineralized from barren tourmalinite showings. The size of tourmaline alteration zones varies.

### **Other alteration types**

Several alteration types occurring in the Sullivan Mine area are found elsewhere in the Aldridge Formation. They include sericite-chlorite alteration, albitization, biotite-chlorite alteration, actinolite/tremolite alteration, and silicification. Readers may refer to Leitch *et al.* (1991; 1995) for additional information.

### **Manganiferous garnet-rich beds**

A narrow concentration (up to 6 cm thick) of pink, manganiferous euhedral garnets in sericitic quartz wacke on the south flank of Mount Mahon and farther south across Hawkins Creek (for locations, see Brown, 1995a) may have an exhalative origin. No sulfide mineralization has yet been identified with these garnets, despite their occurrence near the stratiform Mt. Mahon tourmalinite and the presence of faults that may have been active in the Proterozoic.

### **Gabbro arch**

Moyie sills locally cut up or down section to produce arches; the best example is at the Sullivan Mine (Hamilton *et al.*, 1982). These changes in attitude indicate Proterozoic structural controls that are important in SEDEX models and mineral exploration.

## **MINERAL OCCURRENCES AND EXPLORATION**

The following discussion reviews producers, past producers, placer operations and mineral occurrences of the project area, and summarizes exploration history and activity for several properties. Sullivan-type SEDEX deposits (Hamilton, 1982; Hamilton *et al.*, 1983; Höy, 1993; Leitch *et al.*, 1991; Turner and Leitch, 1992; Leitch and Turner, 1992) are the prime exploration target throughout the Purcell Basin. Several new alteration and fragmental zones have been discovered recently and warrant further mapping and prospecting. In addition, gold-bearing shear zones and placer deposits have attracted exploration attention in this area.

The 1997 exploration programs included geological mapping, soil and litho geochemistry, detailed gravity surveys and diamond drilling. Selective results from this work are incorporated in this report. In addition, an extensive drilling program was completed by Citation Resources Inc. on the Fors Property.

### **Producers**

#### ***Swansea Ridge Ballast Quarry (Minfile 082GSW065)***

The Canadian Pacific Railway operates a ballast quarry at Swansea, about 15 km southwest of Cranbrook. The quarry extracts and crushes an estimated 400,000 tonnes of railway ballast annually to supply the CP Rail System in eastern British Columbia, southern Alberta and parts of Saskatchewan. At the facility, the moderately, northeast-dipping succession of middle Aldridge Formation rocks includes a 60 m thick Moyie diabase/gabbro (Sill D of Höy and Diakow, 1982) that is mined, crushed, stockpiled and loaded into railway cars.

### **Past producers**

#### ***St. Eugene vein system (Minfile 082GSW023, 025,027, 030)***

The St. Eugene vein system lies in the core of the Moyie anticline and its southeast-trending structure (about 110°) hosts four past producers, St. Eugene, Aurora, Society Girl and Guindon (Figure 6; Table 1). St. Eugene is the largest vein deposit to be mined in the Purcell Supergroup (excluding the Coeur d'Alène deposits in Idaho); its regional setting, the vein characteristics and mineralogy are reviewed by Höy (1993). A M. Sc. thesis study of alteration mineralogy and geochemistry, including local garnet-chlorite metamorphosed alteration assemblage, and isotope geochemistry of the vein materials is in progress by Isabelle Jonas (Département de géologie et de génie géologique, Université Laval, Québec).

The vein system extends 3.3 km laterally and 1.3 km vertically. Locally, subrounded quartz clasts (broken

quartz vein material) supported in a flow foliated sulfide matrix (*durchbewegung texture*) illustrate that there has been movement along parts of the vein system. A mafic dike exposed at surface above 1475 m elevation trends northerly, it is correlated with the Kitchener sill unit discussed above. If this dike cuts the vein then it provides strong support for Proterozoic mineralization (St. Eugene Mine plans may illustrate this).

Galena Pb isotopic signatures from ore samples at St. Eugene fall along the linear array of Proterozoic epigenetic vein deposits defined by the Coeur d'Alène deposits. Galena cores surrounded by metamorphic garnet rims along the St. Eugene vein margins yield similar Pb isotopic compositions. This suggests that the St. Eugene mineralization and alteration are pre-metamorphic, and older than the East Kootenay orogeny (circa 1370 Ma; Beaudoin, 1997).

#### **Midway Mine (Minfile 082GSW021)**

The Midway Mine is a former gold producer that was mined in the early 1930's. An east-dipping (30-50°) quartz vein cuts middle Aldridge Formation turbiditic wacke beds. The vein was developed by upper and lower adits, 381 m and 320 m long, respectively. The vein ranges up to about 2.4 m wide and contains pyrite, arsenopyrite, chalcopyrite and minor galena and sphalerite (Jim Fyles, 1974, Property File). The vein extends at least 200 m upslope from the adits but lower gold values are reported at this level (H. Sargent, 1938, Property File).

The mine produced ore for seven years in the period 1933 to 1962; yielding 1,168 tonnes averaging 7.7 gm/T Au, 73.2 gm/T Ag (Table 1). It is also the only tin producer, other than the Sullivan Mine. More information is available in the Minister of Mines Annual Reports from 1929 to 1962. Exploration and drifting were reported on the property in 1986 by Consolidated Sea Gold (George Cross Newsletter, Oct. 24, 1986).

## **Placer Operations**

### **Moyie River (Minfile 082FSE102)**

Fiorentino Bros. Contracting operate a placer deposit along the Moyie River valley. Placer gold occurs in competent gravels. The auriferous channel is about 1.8 m thick by 80 m wide as defined by drilling and seismic data. It is covered by 10 to 15 m of glacial till, gravel and clay (Leitch, 1996). Eight years of sporadic production between 1880 and 1945 yielded a reported 148 844 grams Au (Leitch, 1996). In 1988 and 1989 a total of 53,901 cubic metres were mined that produced 137 051 grams of Au (*Ibid.*). Large nuggets (sold to jewellers) and finer-grained gold are recovered; the gold is about 92% pure.

### **Weaver Creek (Minfile 082FSE084)**

The Weaver Creek placer deposit produced gold between 1874 and 1930 (Table 1). Exploration programs in 1992 and 1994 included reverse circulation drilling that outlined a glaciofluvial channel, additional drilling was recommended to define a minable resource (Clarkson, 1994).

## **Mineral Occurrences**

### **Vine Vein (Minfile 082GSW050)**

The Vine Vein occurrence lies in the hangingwall of the Moyie fault and it has been described in Höy (1993) and Höy and Pighin (1995). The vein is hosted in a 120° trending fault zone that dips 65°-75° southwest. Most of the ore is hosted in quartzite correlated with the Footwall Quartzite, and has been explored in detail in recent years. Drill indicated reserves are about 240 000 tonnes proven grading 5.20 % Pb, 2.24 % Zn, 67.23 g/t Ag and 1.92 g/t Au, and 307 000 tonnes probable grading 4.22 % Pb, 2.51 % Zn, 39.77 g/t Ag and 1.75 g/t Au (Pighin, 1991; in Höy and Pighin, 1995).

Table 9-1. Production data for mineral occurrences in the project area.

| MINFILE NO.  | NAME           | MINED (T)        | Pb (kg)            | Zn (kg)           | Cu (kg)    | Ag (gm)            | Au (gm)        | Year      |
|--------------|----------------|------------------|--------------------|-------------------|------------|--------------------|----------------|-----------|
| 082FSE084    | Weaver Creek * | unknown          | 0                  | 0                 | 0          | 0                  | 23,605         | 1880-1930 |
| 082FSE102    | Moyie River *  | 53,901           |                    |                   | 0          | 0                  | 285,895        | 1880-1989 |
| 082GSW021    | Midway         | 1,168            | 2,549              | 1,701             | 108        | 85,534             | 9,082          | 1933-62   |
| 082GSW023    | Aurora         | 3,763            | 274,307            | 512,674           | 0          | 411,463            | 0              | 1900-27   |
| 082GSW025    | St. Eugene     | 1,475,266        | 113,034,479        | 14,482,913        | 0          | 182,690,658        | 78,846         | 1899-1929 |
| 082GSW027    | Guindon        | 28               | 3,312              | 3,494             | 0          | 3,328              | 0              | 1919-27   |
| 082GSW030    | Society Girl   | 2,984            | 499,655            | 23,914            | 0          | 432,052            | 0              | 1900-52   |
| 082GSW037    | Payroll        | 16               | 0                  | 0                 | 0          | 715                | 187            | 1907      |
| <b>Total</b> |                | <b>1,537,126</b> | <b>113,814,302</b> | <b>15,024,696</b> | <b>108</b> | <b>183,623,750</b> | <b>397,615</b> |           |

Note: All production is from vein deposits except those placers marked by "\*\*\*".

**Fors (Minfile 082GSW035)**

Mineralization and alteration on the Fors Property is described by Britton and Pighin (1994, 1995). An extensive drilling program in 1996 and 1997 included 16 diamond drill holes, totaling over 12,000 metres. Citation Resources Inc. conducted the work and report that hole #2 intersected 42 m of disseminated Pb-Zn mineralization including 7 m of pyrrhotite that resembles the Concentrator Hill horizon in the Sullivan area (distal Sullivan Mine stratigraphy; Mike Leask, pers. comm., June, 1997). The property is part of a 1 by 4 km

northwest-trending corridor with several different sedimentary fragmental units, disseminated and massive sulfides, and a gabbro arch. One of the fragmental units, which is over 125 m thick and occurs at the lower-middle Aldridge contact, is restricted to a sub-basin bounded by northwest-trending faults (Gordon Leask, pers. comm., Nov., 1997). Tourmalinite replacement occurs sporadically throughout 200 metres of drill core and there is an important change from brown to black tourmalinite near the lower-middle Aldridge contact ("Sullivan time"). The Fors, located 400 m above the

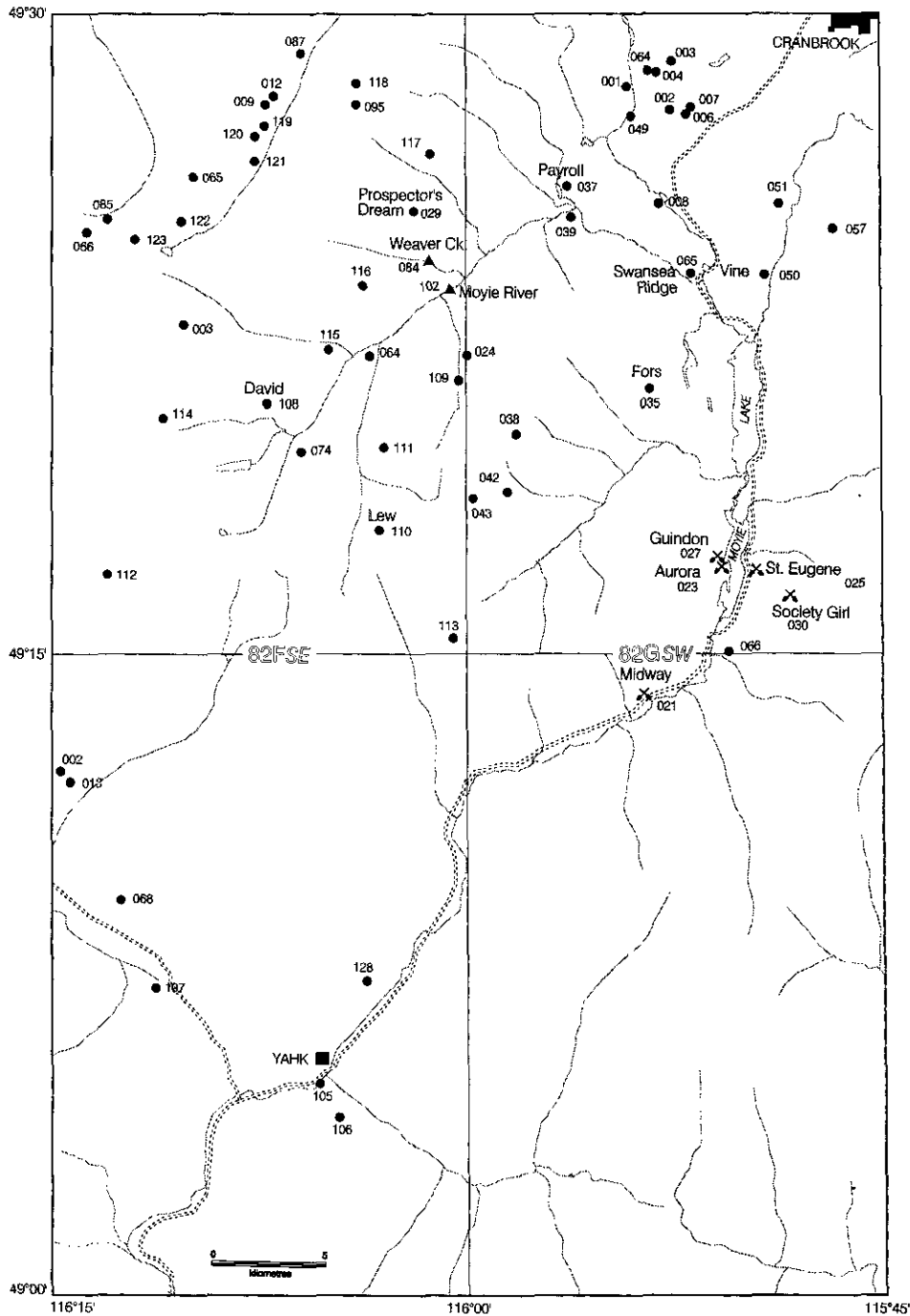


Figure 9-6 Minfile mineral occurrences of the Moyie project area. Those named on the figure are discussed in the text.

lower-middle Aldridge contact, comprises a zone of intense and varied alteration (c.f. Britton and Pighin, 1995) within a horst block. Half-grabens on the flanks of the intense alteration zone contain over 100 m of Sullivan-like black mudstone, underlain by 60 m of zinc-bearing fragmental near the lower-middle Aldridge contact (Mike Leask, pers. comm., Nov., 1997).

#### **David (Minfile 082FSE108)**

Northeast-trending, steeply northwest-dipping shears that are parallel to the Old Baldy fault host auriferous quartz-sericite alteration zones. The David property occurs 4.5 km north of Cooper Lake and was explored by Dragoon Resources Ltd. as summarized by Höy (1993; after Klewchuk, 1991) and by Leitch (1996). The alteration zones are hosted in middle Aldridge Formation and Moyie sills. Mineralization comprises pyrite, galena, chalcopyrite and sphalerite with rare visible gold. The shear zone averages about 2 m wide; mineralization has been traced for a strike length of 150 m and to a depth of more than 120 m. Drill-indicated reserves stand at 91 000 tonnes of 10 g/T Au (Mike Bapty, per. comm., 1996).

#### **Prospector's Dream (Minfile 082FSE029)**

Prospector's Dream was discovered in 1898 and at that time two declines, two shafts and numerous hand trenches were completed (Minister of Mines, Annual Report, 1898; Appendix 2, p. 1013). The workings lie between 1675 and 1800 m elevation and are hosted in

both middle Aldridge arenite and Moyie sills. Mineralization comprises pyritic quartz veins containing minor visible gold in limonitic vugs, and minor chalcopyrite and hematite. Grab samples run up to 72.99 g/T gold (O'Grady, 1991) and trench sampling results from 1991 are summarized in O'Grady (1992). The property is important because it demonstrates the potential of gold-bearing veins in the region.

#### **Pay Roll (Minfile 082GSW037)**

The Pay Roll occurrence consists of a series of narrow (< 5 cm), steeply, southwest-dipping quartz veins. They crop out on the northeast side of Negro Lake and are easily accessed via an old wagon trail at the Moyie River logging road Negro Creek junction. The veins contain pyrite, chalcopyrite, altaite (a lead telluride), and rare visible gold.

### **Exploration activity and results**

#### **Panda Basin area**

The Panda Basin is located 7 km southeast of Cooper Lake; where several fragmental and tourmalinitic occurrences were identified by prospectors Mike and Tom Kennedy. A series of fragmentals trend northwesterly and include the Miss Pickle. The Miss Pickle stratabound fragmental sheet and discordant zone lies east of the Bear Dike along the southern flank of a ridge (Photos 9-1a, b; 9-3). It weathers light grey and is



Photo 9-3. The Miss Pickle fragmental area adjacent to the Bear Dike, Panda Basin (view toward 290°).

massive at outcrop scale (i.e. no bedding evident). In this area, fine white spots (up to 2 mm across) developed in grey quartz arenite and argillite beds are believed to be albite porphyroblasts. A black, aphanitic tourmalinite occurrence lies on the southern end of the Miss Pickle fragmental sheet. It is an isolated exposure, about 2 metres across. The relationship to the fragmental is unknown.

The Bear Dike, part of a gabbro arch, comprises a medium to coarse-grained gabbro that produces a moderate to strong magnetic anomaly. Locally it hosts quartz veins with rare arsenopyrite. Another magnetic feature that lies within the Moyie fault zone comprises albite-chlorite-magnetite breccia and stringers. Between the fault zone and Bear dike the middle Aldridge wacke/arenite contains fine disseminated tourmaline needles over at least 70 m of stratigraphic thickness. Narrow (up to 2 cm) white quartz veins here contain abundant tourmaline needles with minor arsenopyrite.

Drilling in this area has intersected a sequence of bedding parallel and discordant bands of massive, coarsely crystalline sulfides consisting almost entirely of sphalerite and galena with very minor chalcopyrite and pyrrhotite (diamond drill hole K-97-03; Peter Klewchuk, per. comm., 1997). The mineralization contains no quartz which is atypical for most vein-type mineralization in the region. This intersection consists of 2.55 m of 15.47 % combined lead and zinc, including 0.65 m of massive sphalerite with minor pyrrhotite and fracture-filled chalcopyrite. The area has numerous fragmental bodies and extensive zones of albite-tourmaline-chlorite-sericite alteration with associated Zn-Pb-As anomalies.

### **Mount Mahon Property**

In 1979, St. Eugene Mining Corporation Ltd. first mapped tourmalinite occurrences on Mt. Mahon. In 1980-81 they conducted a drill program of thirteen holes (YA-1 through Y-13-81) totaling 1767 metres of core drilling. Diamond drill hole YA-6 intersected a massive sulfide zone and was the target of follow-up drilling. In 1984 Chevron Canada Resources Ltd. optioned the property and drilled two holes (MM-84-1 and MM-87-1) totaling 1084 metres to test the lower-middle Aldridge contact on Mt. Mahon for sulfide mineralization. In 1991 Minova Inc. optioned the property and drilled six holes (MM-91-1 through MM-92-06; Burge, 1991) totaling 1819 metres in search of extensions of the massive sulfide horizon intersected in YA-6.

Pink garnet-rich beds on the south flank of Mount Mahon, correlated with similar beds farther south across Hawkins Creek, were traced for over 2000 metres by prospector, Craig Kennedy. This garnet-rich horizon lies stratigraphically below stratiform tourmalinite on Mt. Mahon and is near the projected trace of the lower-middle Aldridge contact. The horizon could be a distal exhalite comprised of mixed wacke and exhalative material.

### **Cold Creek fragmentals and tourmalinite**

In 1996, Abitibi Mining Corp initiated prospecting in the Cold Creek area based on company and government airborne magnetic surveys. New tourmaline and fragmental occurrences were located and followed up by a soil survey. In 1997, Abitibi completed prospecting and mapping the area in conjunction with a regional gravity survey.

Three tourmalinite occurrences and several fragmental exposures occur in a 2 km northeast-trending belt east of Cold Creek (Van Angeren, 1997; Figure 3b). The pale brown and black aphanitic tourmalinite replaces a fragmental unit (Leitch, 1997) and locally contains disseminated galena and sphalerite. In contrast, in another part of the system, sericite alters a fragmental to produce a waxy green, soft altered rock. Another interesting feature in this area is that marker laminites occur as clasts within the one of the fragmental units.

### **AEROMAGNETIC IMAGE**

The aeromagnetic image for the project area (Figure 9-7), provided by Carmel Lowe of the Geological Survey of Canada, includes regional 1:250 000 scale and recently acquired 1:50 000 scale data as indicated. The latter data set, part of the East Kootenay Geophysical Survey, extends 13.5 km to the west toward Creston and is reviewed in Lowe *et al.* (1998). In addition, a detailed airborne magnetic survey at 200 m line spacing was completed in 1996 by the Abitibi/SEDEX joint venture. Part of their data was provided in Woodfill (1997). The main features of this image as labeled on Figure 7, and those in the industry data, are summarized below. The data allows more accurate extrapolation of contacts into covered areas and has led to modifications of previous surface mapping.

**Feature 1:** The Creston Formation in the Moyie anticline is strongly magnetic and is delineated on Figure 7. Oddly the magnetism varies from the lower to middle Creston as currently mapped. North-trending faults, for example along Irishman Creek, offset units and displace the magnetic feature. **Feature 2:** A broad magnetic anomaly is centered in the core of the Moyie anticline in an area that exposes the deepest stratigraphic levels of the Aldridge Formation, south of Yahk in the Hawkins Creek area. This area also corresponds to a thick accumulation of Moyie sills but they have no elevated magnetism at surface suggesting a buried source for the anomaly (Lowe *et al.*, 1998). **Feature 3:** An isolated magnetic high in the Panda Basin area corresponds to the Bear Dike (Figure 3a). **Feature 4:** Another isolated high 4 km north of feature 3 is a clearly defined U-shaped anomaly on the SEDEX Mining Corp. images. The feature occurs at the intersection of the Ice and Kid faults and corresponds to a buried gabbro body. Drilling in 1997 intersected a series of albite-magnetite-rich veins hosted in Moyie

gabbro and overlying Aldridge wackes. **Feature 5:** A linear, north-trending anomaly corresponds to the surface trace of the McNeil fault (Figure 3a). The anomaly terminates at the Palmer Bar fault to the north and at the Moyie fault to the south. **Feature 6:** This northeast-trending, elongate anomaly lies along the Old

Baldy fault zone. Much of the exposure in this area is unaltered middle Aldridge Formation with rare to no Moyie sills, however, locally there are magnetic sills on the David property and quartz-epidote veins and fractures along the upper contact of a Moyie sill within the middle Aldridge Formation meta-wacke.  $\Delta$

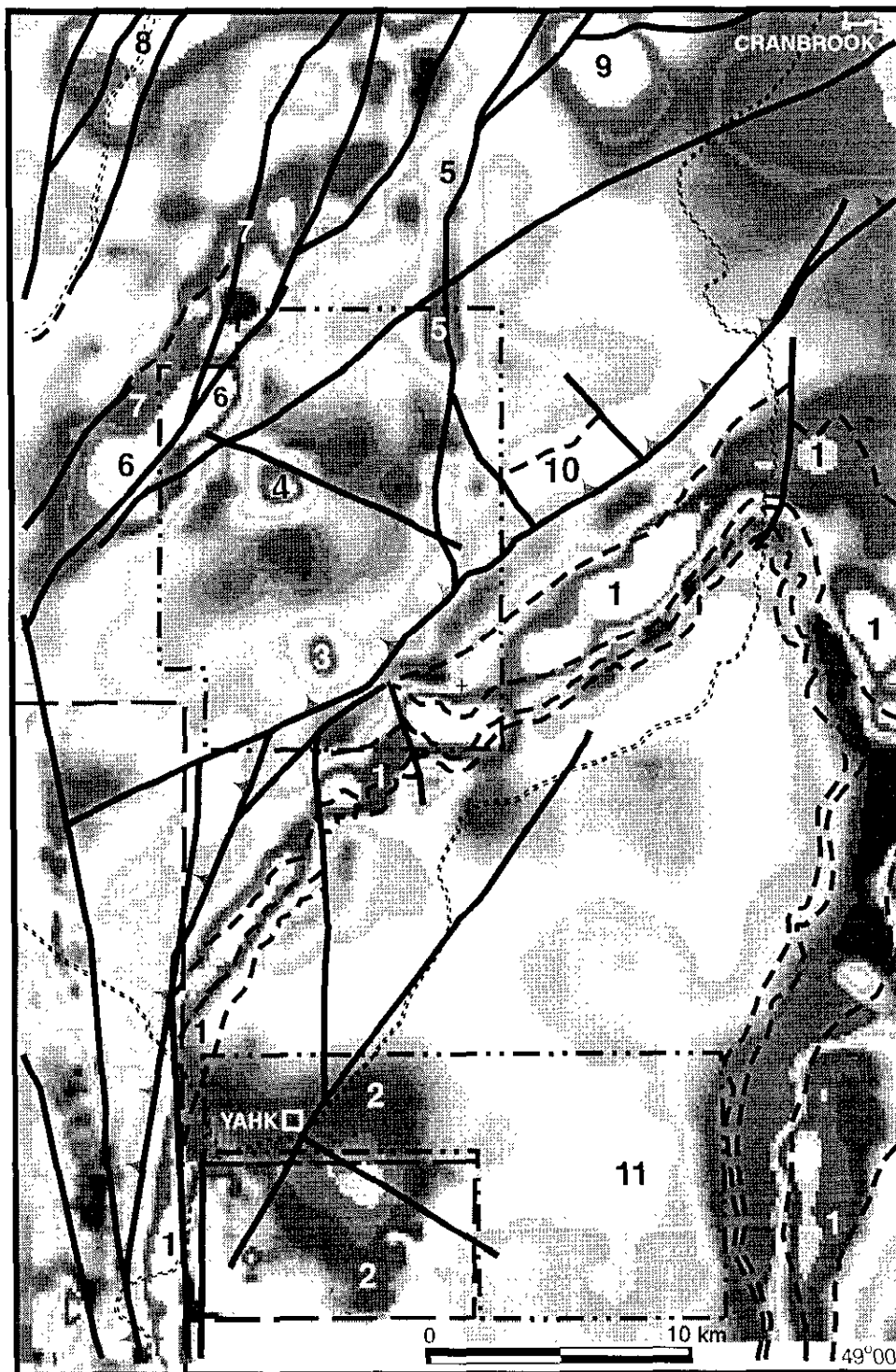


Figure 9-7 Generalized total field magnetic anomaly image for the Moyie project area incorporating regional 1:250 000 scale and recently acquired 1:50 000 scale data (available from the Geological Survey of Canada). Outline of areas where new 200 m line spaced aeromagnetic survey was acquired by industry is shown by dotted rectangles. The southern block was released in Woodfill (1997).

Cretaceous intrusion could lie at shallow depths below the present erosional surface to produce the large and intense magnetic feature. **Feature 7:** Most of the anomaly corresponds to the Creston Formation north of the Old Baldy fault and as in the Moyie anticline anomaly, it varies in intensity along strike. **Feature 8:** This feature in the northwest corner of the Figure 6 is underlain by a small Cretaceous stock that intrudes the Creston and Kitchener formations (Reesor, 1981). The magnetic anomaly extends across lithologic contacts at surface which suggest there is a magnetic halo related to the pluton. **Feature 9:** The Kiakho Pluton and surrounding host-rocks form this anomaly. The pluton is a member of the middle Cretaceous suite of plutons with magnetic phases, the most prominent magnetic anomaly on a regional scale is related to the Reade Lake pluton (Lowe *et al.*, 1997; Höy, 1993) located 15 km to the northeast. **Feature 10:** The lower Aldridge around Rabbit Foot Creek produces a weak anomaly that is believed to be related to the disseminated pyrrhotite occurring in the rusty weathering exposures of that area. **Feature 11:** The weak oval anomaly acquires a linear, north-trending geometry on the more detailed industry survey data and it correlates with the uppermost sill in the middle Aldridge Formation. The columnar jointed sill has highly magnetic parts in outcrops along Branch 17 of the Freeman Creek road.

### Other Features

A series of narrow (<10m wide) meta-gabbroic dikes produce distinct linear magnetic anomalies that are evident on the more detailed surveys of Abitibi/SEDEX but not on the regional data. One of these dikes extends northward and is exposed on the Upper Mahon road. Here, the steeply-dipping, north-trending dike cuts gently, southwest-dipping middle Aldridge quartz wacke beds. The fine-grained massive gabbro ranges from extremely to weakly magnetic. The dike in thin section comprises fine-grained unaltered plagioclase and clinopyroxene with interstitial magnetite grains. Secondary amphibole occurs in the groundmass. This dike was sampled for U-Pb dating which is in progress.

### GRAVITY DATA

A broad regional gravity anomaly encompasses the Moyie anticline and extends north to the Sullivan Mine area (Cook and Van der Velden, 1995) where it terminates against the westward projection of the northern border of the Vulcan Low (Woodfill, this volume). The source of this anomaly has been interpreted to be a basement sliver (Cook and Van der Velden, 1995) or mafic Moyie sills accumulated along the ancient Purcell rift axis (Sears, 1995; Woodfill, this volume). A secondary anomaly, part of this broad anomaly, lies along the east flank of the Moyie anticline within the study area. It is interpreted to be related to gently, east-dipping gabbro sills in the lower and middle Aldridge Formation.

## CONCLUSIONS

The Sullivan deposit projected to surface covers a 1.5 by 1.7 km area but only the old open pit area was visible mineralization at surface. Discovery of a blind deposit of similar or smaller size will require determination and utilization of all the available data for the Purcell Basin. The Moyie Project provides new map data and Sullivan indicator databases that will be utilized in continued mineral exploration in the region. Additional studies on fragmental types, their genesis and classification would be useful.

## ACKNOWLEDGMENTS

The success of this project stems from the participation, collaboration and cooperation of Cominco Ltd. (Doug Anderson, Ken Pride, Paul Ransom), Kennecott Canada Exploration Inc. (Martine Bedard, Steven Coombes, Eric Finlayson, and Jim Ryley), and Abitibi Mining Corp./SEDEX Mining Corp. (Phil Van Angeren, Brent Nassichuk, Craig, Mike and Tom Kennedy, Peter Klewchuk). Mark Smith provided able assistance during the 1997 field season and contributed greatly to the mapping effort. Crestbrook Forest Products provided updated road maps for the project area and we thank them for their assistance. Frank O'Grady provided information on the McNeil and Prospector's Dream properties. Peter Klewchuk identified several new marker samples collected during the project. The Ministry's Cranbrook regional office provided work space for the field season. Verna Vilkos produced the Website for the project and spent long hours improving many of the figures. Reviews by Steven Coombes, Eric Finlayson, Trygve Höy, Peter Klewchuk, Craig Kennedy, and Bill McMillan greatly improved the final version of this manuscript.

## REFERENCES CITED

- Aadland, R.F. and Bennett, E.H. (1979): Geologic Map of the Sandpoint Quadrangle, Idaho and Washington; *Idaho Bureau of Mines and Geology*.
- Aleinikoff, J.N., Evans, K.V., Fanning, C.M., Obradovich, J.D., Ruppel, E.T., Zeig, J.A. and Steinmetz, J.C. (1996): SHRIMP U-Pb ages of felsic igneous rocks, Belt Supergroup, western Montana; *Geological Society of America*, Abstracts With Programs, A-376.
- Anderson, D. (1987): Assessment Report on Rock Geochemistry of Well Cuttings from Well Hole Moyie d-8-c; *B.C. Ministry of Energy, Mines and Petroleum Resources*, Assessment Report 16681.
- Anderson, D. (1991): Diamond Drilling Report, Canam Property (NTS 82F/1, 82G/4); *B.C. Ministry of Energy, Mines and Petroleum Resources*, Assessment Report 21 786.
- Anderson, H.E. and Davis, D.W. (1995): U-Pb geochronology of the Moyie sills, Purcell Supergroup, southeastern

- British Columbia: implications for the Middle Proterozoic geologic history of the Purcell (Belt) basin; *Canadian Journal of Earth Sciences*, V. 32, p. 1180-1193.
- Beaudoin G., 1997: Proterozoic Pb isotope evolution in the Belt-Purcell Basin: Constraints from syngenetic and epigenetic sulfide deposits; *Economic Geology*, V. 92, p. 343-350
- Benvenuto, G.L. and Price, R.A. (1979): Structural Evolution of the Hosmer Thrust Sheet, Southeastern British Columbia; *Bulletin of Canadian Petroleum Geologists*, V. 27, p. 360-194.
- Britton, J.M. and Pighin, D.L. (1995): Fors - A Proterozoic Sedimentary Exhalative Base Metal Deposit in Middle Aldridge Formation, Southeastern British Columbia (82G/5W); in *Geological Fieldwork 1994*, Grant, B. and Newell, J.M., Editors, *B.C. Ministry of Energy, Mines, and Petroleum Resources*, Paper 1995-1, p. 99-109.
- Brown, D.A., and Termuende, T. (1998): The Findlay Industrial Partnership Project: Geology and Mineral Occurrences of the Findlay - Doctor Creek Areas, southeastern British Columbia (parts of 82F/16, 82K/1); in *Geological Fieldwork 1997*, *B.C. Ministry of Employment and Investment*, Paper 1998-1, p. 10-1 to 10-9.
- Brown, D.A., Bradford, J.A., Melville, D.M., Legun, A.S. and Anderson, D. (1994): Geology and Mineral Deposits of Purcell Supergroup in Yahk Map Area, Southeastern British Columbia (82F/1); in *Geological Fieldwork 1993*, Grant, B. and Newell, J.M., Editors, *B.C. Ministry of Energy, Mines, and Petroleum Resources*, Paper 1994-1, p. 129-151.
- Brown, D.A. and Stinson, P. (1995): Geological mapping of the Yahk map area, southeastern British Columbia: an update (82F/1); in *Geological Fieldwork 1994*, Grant, B. and Newell, J.M., Editors; *B.C. Ministry of Energy, Mines and Petroleum Resources*, Paper 1995-1, p. 111-125.
- Brown, D.A., Doughty, T. and Stinson, P. (1995a): Geology and Mineral Occurrences of the Creston map area (82F/2); *B.C. Ministry of Energy, Mines and Petroleum Resources*, Open File 1995-15.
- Brown, D.A., Stinson, P. and Doughty, T. (1995b): Preliminary Geology of the Creston Map Area, Southeastern British Columbia (82F/2); in *Geological Fieldwork 1994*, Grant, B. and Newell, J.M., Editors, *B.C. Ministry of Energy, Mines and Petroleum Resources*, Paper 1995-1, p. 135-155.
- Brown, D.A., Bradford, J.A., Melville, D.M. and Stinson, P. (1995c): Geology and Mineral Occurrences of the Yahk map area (82F/1); *B.C. Ministry of Energy, Mines and Petroleum Resources*, Open File 1995-14.
- Burge, C. (1991): Assessment Report on Diamond Drilling on the Mt. Mahon Property; *B.C. Ministry of Energy, Mines and Petroleum Resources*, Assessment Report 21 959.
- Burmester, R.F. (1985): Preliminary Geological Map of the Eastport Area, Idaho and Montana; *U.S. Geological Survey*, Open-file Report 85-0517, scale 1:48 000.
- Cas, R.A.F. and Wright, J.V. (1987): Volcanic Successions, modern and ancient; *Allen and Unwin*, 528 p.
- Clarkson, R. (1994): Weaver Creek Placer, placer drilling report; *B.C. Ministry of Energy, Mines and Petroleum Resources*, Assessment Report 24 613.
- Cook, F.A. and Van der Velden, A.J. (1995): Three-dimensional Crustal Structure of the Purcell anticlinorium in the Cordillera of Southwestern Canada; *Geological Society of America, Bulletin*, V. 107, no.6, p. 642-664.
- Cressman, E.R. and Harrison, J.E. (1986): Geologic Map of the Yaak River Area, Lincoln County, Northwestern Montana; *U.S. Geological Survey*, Miscellaneous Field Studies Map MF-1881, scale 1:48 000.
- Daly, R.A. (1905): Summary Report 1904, Part A; *Geological Survey of Canada*, p. 91-100.
- Daly, R.A. (1912): Geology of North American Cordillera at the Forty-ninth Parallel; *Geological Survey of Canada*, Memoir 38, Part 1.
- Doughty, P.T. and Chamberlain, K.R. (1996): Salmon River Arch revisited: new evidence for 1370 Ma rifting near the end of deposition in the Middle Proterozoic Belt basin; *Canadian Journal of Earth Sciences*, V. 33, p. 1037-1052.
- Doughty, T., Brown, D.A., and Archibald, D.A. (1997): Metamorphism of the Creston map area (82F/2), southeastern British Columbia; *B.C. Ministry of Employment and Investment*, Open File 1997-5.
- Eby, D.E. (1977): Sedimentation and early diagenesis within the eastern portions of the "middle Belt carbonate interval" (Helena Formation), Belt Supergroup (Precambrian- Y), western Montana; Ph.D. thesis, Stony Brook, *State University of New York*, 702 p.
- Edmunds, F.R. (1977): The Aldridge Formation, B.C., Canada; Ph.D. thesis, *Pennsylvania State University*, University Park, Pennsylvania, 368 p.
- Francis, E.H. (1982): Magma and sediment - I, Emplacement mechanism of late Carboniferous tholeiite sills in northern Britain; *J. Geol. Soc. London*, V. 139, p. 1-20.
- Furniss, G., Rittel, J.F. and Winston, D (1994): Gas bubble and expansion crack origin of "molar-tooth" calcite structures in the middle Proterozoic Belt Supergroup, western Montana; *Northwest Geology*, V. 23, p. 93-96.
- Grotzinger, J.P. (1986): Shallowing-upward cycles of the Wallace Formation, Belt Supergroup, northwestern Montana and northern Idaho; In *Belt Supergroup: A guide to Proterozoic rocks of western Montana and adjacent areas*; *Montana Bureau of Mines and Geology*, Special Publication 94, p. 143-160.

- Hagen, A. (1985): Sullivan- North Star Corridor; in Workshop on lead-zinc deposits in clastic rocks, *Cominco Ltd.* internal report.
- Hamilton, J.M., Bishop, D.T., Morris, H.C. and Owens, O.E. (1982): Geology of the Sullivan orebody, Kimberley, B.C., Canada; in Hutchinson, R.W., Spence, C.D. and Franklin, J.M., Editors, Precambrian sulfide deposits, H.S. Robinson Memorial Volume; *Geological Association of Canada*, Special Paper 25, p. 597-665.
- Hamilton, J.M., Delaney, G.D., Hauser, R.L. and Ransom, P.W. (1983): Geology of the Sullivan deposit, Kimberley, B.C.; in D.F. Sangster, Editor, Sediment-hosted stratiform lead-zinc deposits, *Mineralogical Association of Canada*, Short Course Notes, Chapter 2, p. 31-83.
- Harrison, J.E., Cressman, E.R. and Whipple, J.W. (1992): Geologic and Structure Maps of the Kalispell 1° x 2° Quadrangle, Montana, and Alberta and British Columbia; *U.S. Geological Survey*, Miscellaneous Investigations Series, Map I-2267.
- Heubschman, R.P. (1973): Correlation of fine carbonaceous bands across a Precambrian stagnant basin; *Journal of Sedimentary Petrology*, V.43, p. 688-699.
- Höy, T. (1993): Geology of the Purcell Supergroup in the Fernie West-half Map Area, Southeastern British Columbia; *B.C. Ministry of Energy, Mines and Petroleum Resources*, Bulletin 84.
- Höy, T. (1989): The age, chemistry and tectonic setting of the Middle Proterozoic Moyie sills, Purcell Supergroup, southeastern British Columbia; *Canadian Journal of Earth Sciences*, V. 29, p. 2305-2317.
- Höy, T. and Diakow L. (1981): Geology of the Proterozoic Purcell Supergroup, Moyie Lake Area; in Geological Fieldwork 1980, *B.C. Ministry of Energy, Mines and Petroleum Resources*, Paper 1981-1, p. 9-14.
- Höy, T. and Diakow L. (1982): Geology of the Moyie Lake Area; *B.C. Ministry of Energy, Mines and Petroleum Resources*, Preliminary Map 49.
- Höy, T. and Pighin, D. (1995): Vine - A Middle Proterozoic Massive Sulfide Vein, Purcell Supergroup, Southeastern British Columbia; in Geological Fieldwork 1994, Grant, B. and Newell, J.M., Editors, *B.C. Ministry of Energy, Mines and Petroleum Resources*, Paper 1995-1, p. 85-98.
- Höy, T., Pighin, D., and Ransom, P.W. (1995a): Volcanism in the Middle Aldridge Formation, Purcell Supergroup, Southeastern British Columbia; in Geological Fieldwork 1994, Grant, B. and Newell, J.M., Editors, *B.C. Ministry of Energy, Mines and Petroleum Resources*, Paper 1995-1, p. 73-83.
- Höy, T., Price, R.A., Grant, B., Legun, A., and Brown, D.A. (1995b): Purcell Supergroup, Southeastern British Columbia, Geological Compilation Map (NTS 82G, 82F/E, 82J/SW, 82K/SE); *Ministry of Energy, Mines and Petroleum Resources*, Geoscience Map 1995-1.
- Höy, T., Turner, R.J.W., Leitch, C.H.B., Anderson, D., Ransom, P.W., Pighin, D. and Brown, D. (1995c): Depositional environment, alteration and associated magmatism, Sullivan and related massive sulfide deposits, southeastern B.C.; *Geological Association of Canada, Mineralogical Association of Canada, Joint Annual Meeting 1995, Field Trip A-1, Guidebook*, 80 p.
- Höy, T., Anderson, D., Turner, R.J.W., and Leitch, C.H.B. (In prep.): Tectonic, magmatic and metallogenic history of the early synrift phase of the Purcell Basin, southeastern British Columbia; *Geological Survey of Canada*, Sullivan Volume.
- Hunt, G. (1962): Time of Purcell eruption in southeastern British Columbia and southwestern Alberta; *Journal of the Alberta Society of Petroleum Geologists*, V. 10, p. 438-442.
- Jardine, D.E. (1966): An investigation of brecciation associated with the Sullivan Mine orebody at Kimberley, B.C.; Unpublished M.Sc. thesis, *University of Manitoba*, Winnipeg, Manitoba.
- Klewchuk, P. (1991): Report on geology, geophysics, geochemistry, trenching and diamond drilling, David, Lew, Harmony and Rob claims, Fort Steele Mining Division; *B.C. Ministry of Energy, Mines and Petroleum Resources*, Assessment Report 20 873.
- Krynauw, J.R., Hunter, D.R. and Wilson, A. H. (1988): Emplacement of sills into wet sediments at Grunehogna, western Dronning Maud Island, Antarctica; *J. of the Geological Society, London*, V. 145, p. 1019-1032.
- Leech, G.B. (1957): St. Mary Lake, Kootenay District, British Columbia (82F/9); *Geological Survey of Canada*, Map 15-1957.
- Leech, G.B. (1958): Fernie Map Area, West Half, British Columbia, 82G W1/2; *Geological Survey of Canada*, Paper 58-10.
- Leech, G.B. (1960): Geology Fernie (West Half), Kootenay District, British Columbia; *Geological Survey of Canada*, Map 11-1960.
- Leech, G.B. (1962): Structure of the Bull River Valley near latitude 49°35'; *J. Alta. Soc. Petroleum Geologists*, V. 10, no. 7, p. 396-407.
- Leitch, C.H.B. (1997): Petrographic report; internal report for Abitibi Mining Corp.
- Leitch, C.H.B. (1996): MINFILE 082FSE, Creston map sheet; *B.C. Ministry Employment and Investment*.
- Leitch, C.H.B. and Turner, R.J.W. (1992): Preliminary Field and Petrographic Studies of the Sulfide-bearing Network Underlying the Western Orebody, Sullivan Stratiform Sediment-hosted Zn-Pb Deposit, British Columbia; in Current Research, Part E, *Geological Survey of Canada*, Paper 92-1E, p. 71-82.
- Leitch, C.H.B., Turner, R.J.W. and Höy, T. (1991): The District-scale Sullivan - North Star Alteration Zone,

- Sullivan Mine Area, British Columbia; in Current Research, Part E, *Geological Survey of Canada*, Paper 91-1E, p. 45-57.
- Leitch, C.H.B., Turner, R.J.W. and Ransom, P. (1995): Sullivan Deposit; in Höy, T., Turner, R.J.W., Leitch, C.H.B., Anderson, D., Ransom, P.W., Pighin, D. and Brown, D. (1995c): Depositional environment, alteration and associated magmatism, Sullivan and related massive sulfide deposits, southeastern B.C.; *Geological Association of Canada, Mineralogical Association of Canada, Joint Annual Meeting 1995, Field Trip A-1, Guidebook*, 80 p.
- Lowe, C., Brown, D.A., Best, M.E. and Shives, R.B.K. (1997): The East Kootenay Geophysical Survey, southeastern British Columbia (82F, G, K): Regional synthesis; *Geological Survey of Canada*, Current Research, Part E, Paper 97-1A, p. 167-176.
- Lowe, C., Brown, D.A., Best, M.E., Woodfill, R., Kennedy, C. (1998): New geophysical data from the Yahk map area - part of the East Kootenay multiparameter geophysical survey; in Current Research, Part E, *Geological Survey of Canada*, Paper 98-1E.
- McMechan, M.E. (1981): The Middle Proterozoic Purcell Supergroup in the Southwestern Purcell Mountains, British Columbia, and the Initiation of the Cordilleran Miogeocline, Southern Canada and adjacent United States; *Bulletin of Canadian Petroleum Geology*, V. 29, p. 583-641.
- O'Grady, F. (1987): A report on geological and geochemical surveys on the McNeil Creek Group; *B.C. Ministry of Energy, Mines and Petroleum Resources*, Assessment Report 16 606.
- O'Grady, F. (1991): Geological report on the Prospectors Dream Group; *B.C. Ministry of Energy, Mines and Petroleum Resources*, Assessment Report 19 614.
- O'Grady, F. (1992): Geological Report on trenching on the Prospectors Dream Group; *B.C. Ministry of Energy, Mines and Petroleum Resources*, Assessment Report 22 052.
- Reesor, J.E. (1981): Grassy Mountain, Kootenay Land District, British Columbia (82F/8); *Geological Survey of Canada*, Open File 820.
- Reesor, J.E. (1993): Geology, Nelson (East Half; 82F/1,2,7-10,15,11); *Geological Survey of Canada*, Open File 2721.
- Reesor, J.E. (1996): Geology of Kootenay Lake, B.C.; *Geological Survey of Canada*, Map 1864-A.
- Rice, H.M.A. (1937): Cranbrook Map-area, British Columbia; *Geological Survey of Canada*, Memoir 207.
- Rice, H.M.A. (1941): Nelson Map Area, East Half; *Geological Survey of Canada*, Memoir 228.
- Ross, G.M., Parrish, R.R. and Winston, D. (1992): Provenance and U-Pb Geochronology of the Mesoproterozoic Belt Supergroup (Northwest United States): Implications for Age of Deposition and pre-Panthalassa Plate Reconstructions; *Earth and Planetary Science Letters*, V. 113, p. 57-76.
- Schofield, S.J. (1915): Geology of the Cranbrook Map-area; *Geological Survey of Canada*, Memoir 76.
- Sears, J. (1995): Restoration model for the Lower Belt Basin, U.S and Canada; internal document prepared for Kennecott Canada Exploration Inc.
- Schultze, H.C. (1988): Assessment Report on Rock Geochemistry of Well Cuttings from Well Hole Moyie d-8-c; *B.C. Ministry of Energy, Mines and Petroleum Resources*, Assessment Report 18 128.
- Slack, J.F. (1993): Models for Tourmalinite Formation in the Middle Proterozoic Belt and Purcell Supergroups (Rocky Mountains) and their Exploration Significance; in Current Research, Part E, *Geological Survey of Canada*, Paper 93-1E, p. 33-40.
- Stoffel, K.L., Joseph, N.L., Zurenko Waggoner, S., Gulick, C.W., Korosec, M.A. and Bunning, B.B. (1991): Geologic Map of Washington -- Northeast Quadrant; *Washington Division of Geology and Earth Resources*, Geological Map GM-39.
- Turner, R.J.W., Leitch, C.H.B., Hagen, A., Höy, T., Delaney, G and Ransom, P. (in press): Sullivan-North Star corridor: geological setting, structure and mineralization; in The Sullivan deposit and its geological environment, J.W Lydon, T. Höy, M. Knapp, and J.F. Slack (editors); *Geological Survey of Canada*, Paper.
- Turner, R.J.W. and Leitch, C.H.B. (1992): Relationship of Albitic and Chloritic Alteration to Gabbro Dikes and Sills at the Sullivan Deposit and nearby Area, Southeastern British Columbia; in Current Research, Part E, *Geological Survey of Canada*, Paper 92-1E, p. 95-106.
- Turner, R.J.W., Höy, T., Leitch, C.H.B. and Anderson, D. (1992): Guide to the Tectonic, Stratigraphic and Magmatic Setting of the Middle Proterozoic Stratiform Sediment-hosted Sullivan Zn-Pb Deposit, Southeastern British Columbia; *B.C. Ministry of Energy, Mines and Petroleum Resources*, Information Circular 1992-23, 53 p.
- Wanless, R.K., Stevens, R.D., Lachance, G.R. and Edmonds, C.M. (1967): Age determinations and geological studies; K-Ar isotopic ages, Report 7; *Geological Survey of Canada*, Paper.
- Winston, D. (1993): Cycles of the Upper Helena Formation, middle Proterozoic Belt Supergroup, Montana; in Program and Abstracts, Belt Symposium III.
- Woodfill, R.D. (1998): Purcell gravity anomaly -- implications for mineral exploration; *B.C. Ministry Employment and Investment*, Paper 1998-1, this volume.
- Woodfill, R.D. (1997): Assessment report on geology, geophysics and geochemistry. Part I: Introduction and airborne magnetic survey. Part II: GPS and gravity survey. Part III: Geochemistry. Part IV: Geology and conclusions; *B.C. Ministry Employment and Investment*, Assessment report 24 652.



**THE FINDLAY INDUSTRIAL PARTNERSHIP PROJECT:  
GEOLOGY AND MINERAL OCCURRENCES OF THE FINDLAY - DOCTOR  
CREEK AREAS, SOUTHEASTERN BRITISH COLUMBIA  
(parts of 82F/16, 82K/1)**

**By D. A. Brown, B.C. Geological Survey Branch, and  
Tim Termuende, Eagle Plains and Miner River Resources Ltd.**

---

**KEYWORDS:** Proterozoic, Purcell Supergroup, Aldridge Formation, Greenland Creek stock, White Creek batholith, Sedex deposits, fragmentals.

## INTRODUCTION

This article is designed primarily to inform clients that new 1:50 000 scale maps are currently being completed for the Findlay-Doctor Creek area (Figure 10-1). A summary of preliminary results is presented for the Findlay Industrial Partnership Project after completion of three weeks of fieldwork in the Dewar and Findlay creeks map areas (82F/16, 82K/1) during 1997. The focus of the project is to provide updated 1:20 000 scale map compilations to be published at 1:50 000 scale, digital databases and prepare descriptions of mineral occurrences for the area underlain by the Aldridge Formation. In addition, a U-Pb dating and litho-geochemistry study of the Greenland Creek pluton and White Creek batholith were undertaken as part of a B.Sc. thesis (see Smith and Brown, this volume). Financial support was provided by Kennecott Canada Exploration Inc., Eagle Plains Resources Ltd. and Miner River Resources Ltd. Cominco Ltd. contributed their 1:20 000 scale geology maps. A summary of Purcell Supergroup stratigraphy can be found in Höy (1993) and Brown and Woodfill (this volume).

Access to the map area is provided by a network of gravel roads extending west from Highway 3 near Canal Flats. Several relatively new roads along Doctor Creek allow truck access to much of the project area. Partially overgrown roads/trails along Skookumchuck and Greenland creeks make it possible to get to the eastern part of Rusty Ridge on foot or by all terrain vehicle. The western and southern sections of the map area lie within the Purcell Wilderness Conservancy (Figure 10-2) and no new traverses were conducted in this region.

The physiography of the project area changes radically from northeast to southwest. The Findlay Creek valley east of Doctor Creek is a broad, open grassland area filled with glacio-fluvial outwash and silt to about 1100 m elevation. Farther west, topography is more rugged with ridges up to 2830 metres in elevation with abundant exposures in the alpine and subalpine (Doctor Peak; Figure 10-2) separated by deeply incised valleys. The largest drainages include Findlay, Skookumchuck and Doctor creeks

## Previous Work

Initial reconnaissance scale mapping in the region established the general stratigraphic framework (Rice, 1941). More detailed mapping in the early 1950's by Reesor (1958) in the Dewar Creek area (82F/16) and later, in the Lardeau east map area (82K/east, Reesor, 1973) including a portion of the current study area (Figure 10-1, 10-2), permitted subdivision of the Aldridge Formation. For example, near Dewar Creek, the Aldridge Formation was divided into lower and upper divisions, and were estimated to be over 1370 and 3350 metres thick, respectively. A quarter of the lower division comprises Moyie sills (about 330 m). The upper division, including the uppermost Argillite member, is correlated with the middle and upper Aldridge Formation as currently defined. The overlying strata consisting of Creston, Kitchener, Siyeh and Dutch Creek formations were also described by Reesor (1958) and Höy (1993).

McLaren *et al.* (1990a and b) completed a mineral potential assessment across the region and produced a 1:50 000 scale geology map that incorporated Reesor's work. A federal-provincial multiparameter airborne geophysical survey of much of the map area was undertaken in 1996, digital data and hardcopy maps are available from the Geological Survey of Canada (includes total field aeromagnetics, conductivity, potassium, thorium/potassium, and ternary radioelement maps; B.C. Ministry of Employment and Investment Open File 1996-23). The digital data set is available from the National Geophysical Data Centre in Ottawa (613-995-5326). Exploration companies have concentrated their efforts in the Rusty Ridge area, the headwaters of Doctor Creek, and the Greenland Creek areas; some of their results are incorporated in this study.

## GEOLOGICAL SETTING

The Findlay-Doctor Creek project area straddles in the central axis of the Purcell anticlinorium, a broad, gently north-plunging structural culmination cored by the Proterozoic Purcell Supergroup (Figure 10-1). The supergroup comprises a siliciclastic and lesser carbonate sequence at least 12 kilometres thick, that initially

accumulated in an intracratonic rift basin. The strata are preserved in an area 750 kilometres long and 550 kilometres wide, extending from southeastern British Columbia to eastern Washington, Idaho and western Montana. The original extent and geometry of the basin is poorly known in part because the western and northwestern margins are poorly exposed and in part due to Laramide contractional deformation.

## Stratigraphy

Most of the project area is underlain by the Aldridge Formation, the lowermost Purcell Supergroup strata, although the base is not exposed. Excellent examples of the lower and middle parts of the Aldridge Formation occur in the Rusty Ridge area between Middle Findlay Creek and the headwaters of Greenland Creek (Figure 10-2). The lower Aldridge is thin bedded to laminated and rusty brown weathering, in contrast to the medium to thick bedded, grey weathering turbidites of the middle Aldridge Formation. Middle Aldridge turbidite beds display normal grading, flame structures, load casts and rare ripples.

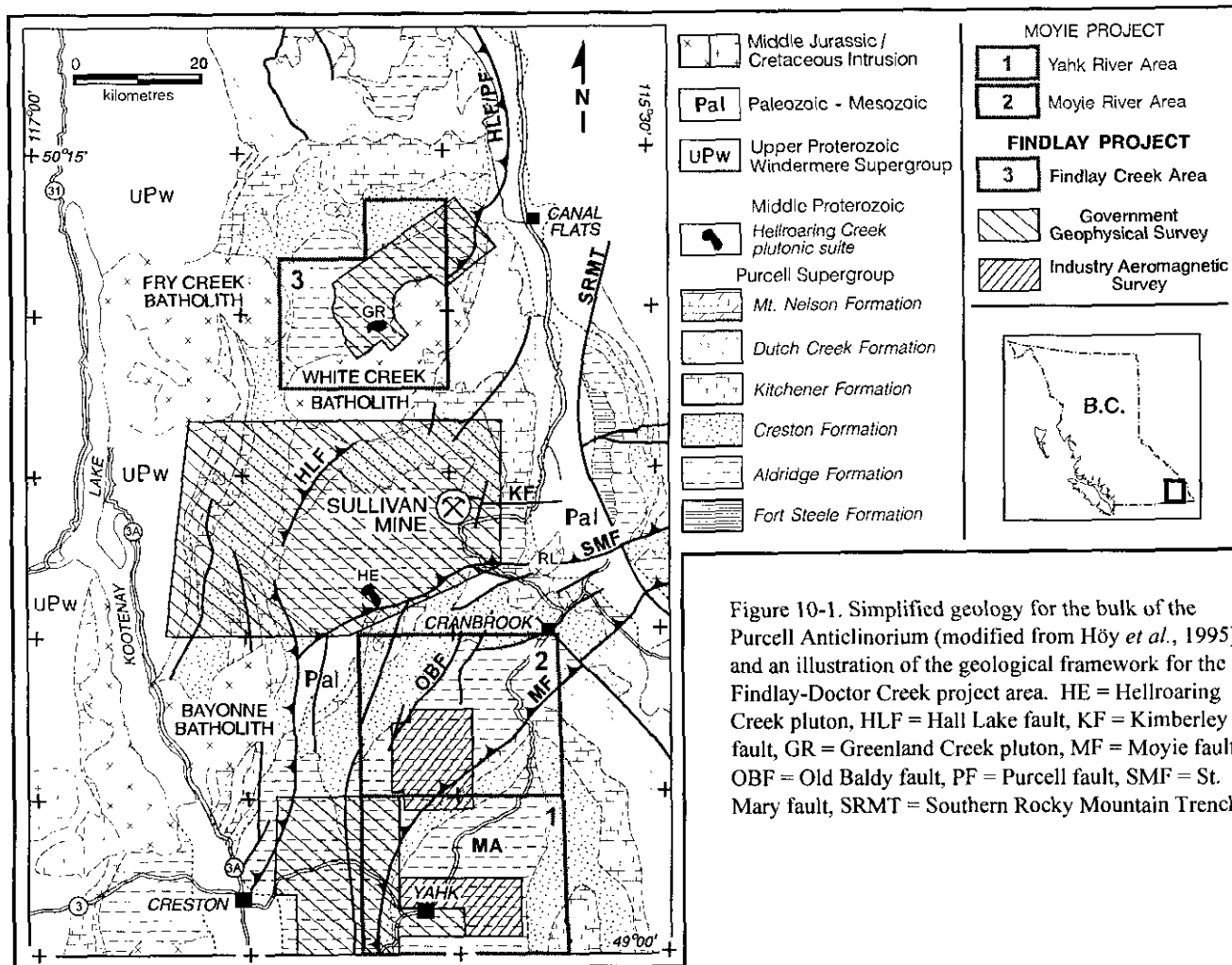
The contact between lower and middle Aldridge rocks is gradational and includes an extensive fragmental unit, here called the LMC fragmental (see

below). An important change from the more evenly bedded lower energy units of the lower Aldridge to rapidly deposited turbiditic sedimentation characteristic of the middle Aldridge suggests a fundamental change of the Purcell Basin sedimentation/tectonics at this time.

Much of the lower Aldridge succession exposed in the area is muscovite-biotite schist (meta-wacke) adjacent to the White Creek Batholith, in the vicinity of the Silver Key occurrence (Minfile 082KSE053; Figure 10-2). Minor quartz pods and lenses with black tourmaline crystals occur within the most schistose zones of this area.

The upper Aldridge comprises less than 250 m of dark grey argillaceous phyllite that weathers dark rusty brown. Tight southeast-verging minor folds and coarse crenulations are evident in outcrops along the access trail to the Alpine occurrence (Minfile 082KSE081).

The Creston Formation consists of pale grey to green argillite with interlaminated greenish siltstone, and minor pale grey quartz arenite. Lenticular and wavy bedforms, argillaceous rip-up clasts, and tectonically flattened mudcracks distinguish the Creston from the Aldridge Formation. The medium to thin bedded quartz wacke and argillite commonly displays a sericitic phyllitic foliation. The formation was only examined around the Alpine showing and west of the Doc



occurrence (Minfile 082KSE060). In these areas discrete schistose shear zones and southeast-verging minor folds are common. Narrow (<10 m thick), dark green mafic sills and dikes locally intrude the Creston Formation.

## Intrusive Rocks

Two contrasting Middle Proterozoic magmatic suites intrude the lower and middle Aldridge Formation: the laterally extensive gabbroic Moyie sills and small bodies of leucocratic pegmatite, and quartz monzonite that comprise the Greenland Creek stock. The middle Cretaceous White Creek Batholith dominates the southeastern quarter of the map area.

### *Middle Proterozoic Moyie Intrusives*

Middle Proterozoic Moyie Intrusives are the oldest magmatic rocks in the area (*cf.* Brown and Woodfill, this volume). They are massive to locally well foliated meta-diorite and amphibolitic gabbro forming dark green to brown weathering sills. Amphibole has largely replaced primary pyroxene phenocrysts (Mackenzie, 1971). The sills provide good local markers that have been clearly offset in excellent exposures along Rusty Ridge. The majority of the sills in the study area are about 10 to 100 m thick and cumulatively comprise up to 25% of the lower Aldridge section. They rarely cut up or down section to form dikes. Albite alteration along sill contacts is well developed, especially at the headwaters of Greenland Creek. U-Pb isotopic dating of the Moyie sills have returned zircon ages of 1468 Ma (Anderson and Davis, 1995; see Brown and Woodfill, this volume).

### *Middle Proterozoic Greenland Creek intrusions*

The Greenland Creek intrusions are a series of small, discordant irregularly-shaped stocks that cut Moyie sills and lower Aldridge Formation rocks (Figure 10-2; see Smith and Brown, this volume). The westernmost body displays a zoned contact; coarse-grained pegmatite grades sharply outward through a 3 m wide zone of tourmaline-quartz-rich material to aplite to a muscovite-rich selvage at the gabbro contact. Coarse-grained pegmatite contains sheets of muscovite and rare tourmaline crystals. Phyllitic to schistose fabrics developed in thin-bedded meta-wacke adjacent to the intrusive bodies suggest a narrow zone of contact metamorphism developed during emplacement of the bodies.

The geometry of scattered, isolated bodies of pegmatite and quartz monzonite hosted in Moyie sills and lower Aldridge rocks is analogous to that of the Hellroaring Creek stock and a series of smaller pegmatite bodies in the Matthew Creek area southwest of the Sullivan Mine (Figure 10-1). Compositionally, the Greenland Creek and Hellroaring Creek stocks are similar (Reesor, 1996). They also produce a similar airborne radiometric signature -- a very low Th/K ratio (see Lowe *et al.*, 1996). Therefore, they are considered part of the same Hellroaring Creek plutonic suite and are

presumed an equivalent in age, about 1370 Ma (see Smith and Brown, this volume).

### *Middle Cretaceous White Creek batholith*

The Middle Cretaceous White Creek batholith is divided into four broadly concentric phases by Reesor (1958): biotite granodiorite, hornblende-biotite granodiorite, porphyritic quartz monzonite and leuc-quartz monzonite. A fifth phase, equigranular quartz monzonite, intrudes the western two phases of the batholith. The K-feldspar megacrystic (porphyritic) quartz monzonite phase underlying the Doctor Creek area produces a strong aeromagnetic anomaly (see B.C. Ministry of Employment and Investment Open File 1996-23).

A biotite lamprophyre (minette) dike cuts the Creston Formation and probably represents the youngest intrusive rocks in the study area. The recessive weathering, dark green dike is exposed along the access road to the Alpine showing.

## STRUCTURE

The study area is dominated by broad, open folds in strata of the Aldridge and Creston formation. They plunge moderately to the west and north. However, adjacent to schistose shear zones bedding dips steepen, and tight to isoclinal minor folds with rare overturned limbs (Anderson, 1988) are present. Southeast- to east-verging minor folds are common in the Creston Formation near the Alpine showing. Local isoclinal minor folds occur near the MC showing (Minfile 82FNE107), however, it is unclear whether they are related to a discrete fault zone or a larger structural culmination. Early penetrative phyllosilicate foliation is overprinted locally by coarse crenulations or kink folds. The phyllitic to schistose shear zones locally host quartz veins and pods.

The **Hall Lake fault** is one of several right-lateral, reverse faults that cut obliquely across the northerly-trending structural grain of the Purcell anticlinorium (Figures 10-1 and 2). It puts Creston on Kitchener Formation and is truncated by the White Creek Batholith, in the Buhl Creek area (Reesor, 1996). Its northern continuation projects to where middle Aldridge Formation lies on Creston Formation (Reesor, 1973).

A reverse fault that parallels the Hall Lake fault and underlies the area near the intersection of Findlay and Doctor creeks has been mapped by Cominco Ltd., and is here called the Doctor Creek fault (Figure 10-2). It results in an apparent 6 kilometres of lateral offset of the upper Aldridge Formation. The western continuation of the fault is obscure.

A series of north-trending faults are evident between Middle Findlay and Doctor creeks, where they locally displace Moyie sills. These faults also displace the quartz vein at the Alpine showing as discussed above.

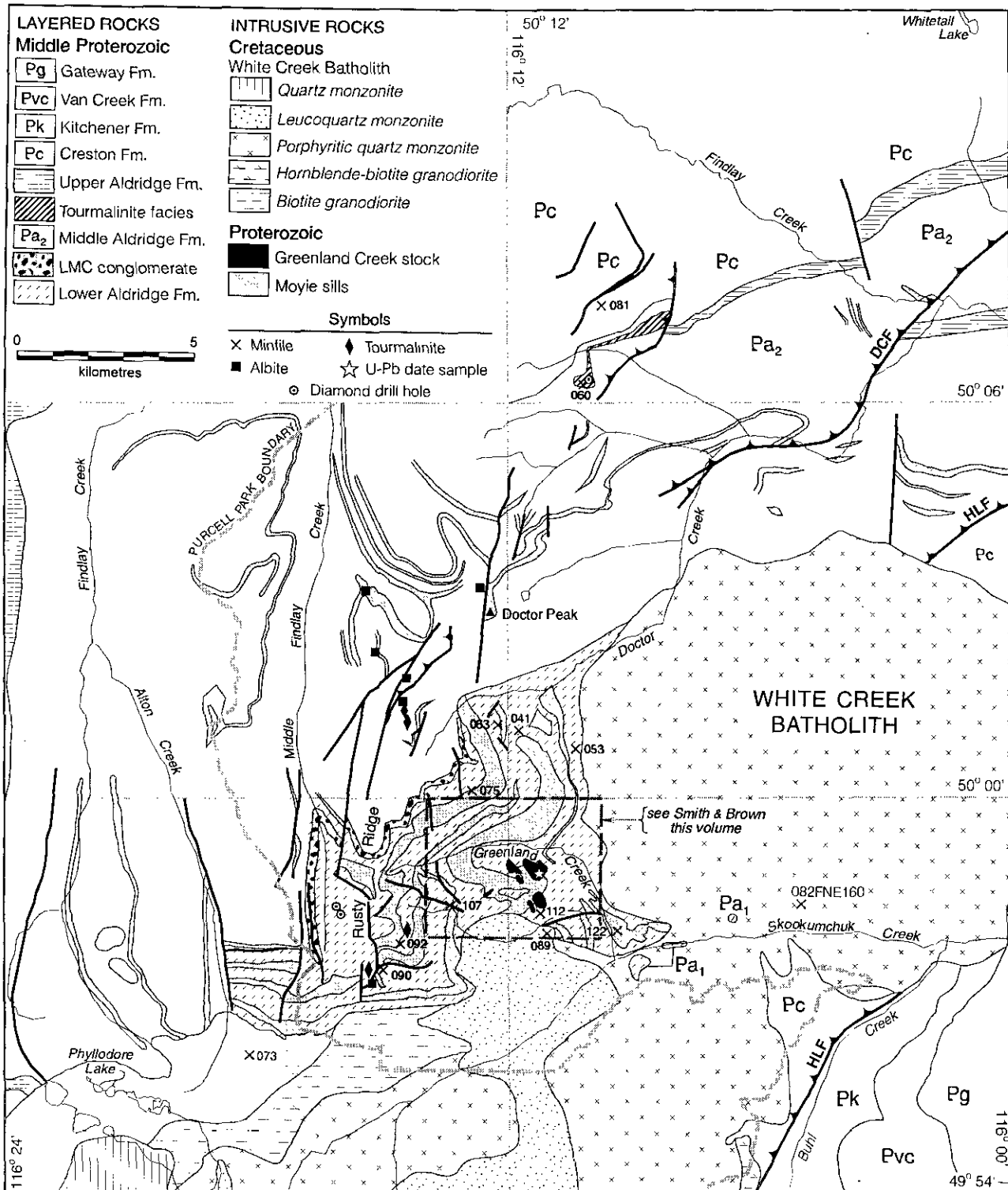


Figure 10-2. Simplified geology of the Findlay Project area modified from Reesor (1958, 1973) and Cominco Ltd. Minfile mineral occurrence locations are shown with numbers that are prefixed with 082KSE, north of 50° latitude and 082FNE to the south. DCF = Doctor Creek fault, HLF = Hall Lake fault, Purcell Wilderness Conservancy indicated as Purcell Park on this figure.

## MINERALIZED FACIES

### LMC fragmental

A stratabound fragmental unit (see Brown and Woodfill, this volume) occurs along the lower-middle Aldridge contact at the headwaters of Doctor Creek, a simplified depiction of its distribution, largely from Cominco Ltd. mapping, is shown on Figure 10-2. It extends over 6 km along strike and is up to 15 m thick. Matrix- to clast-supported units display diverse textures and rapid changes in clast size (Photo 10-1). Angular to rounded fragments include argillite, siltstone and quartz wacke; ranging in size up to about 25 cm long. Rare sulphide clasts are found within the fragmental at the headwaters of Greenland Creek (Leitch, 1997), and farther north, at the headwaters of Doctor Creek (Echo Lake area), pyrrhotite fragments are common and a boulder-size clast contains 1% Zn (Webber, 1977). Locally argillaceous siltstone fragments are aligned parallel bedding and rounded albitized wacke clasts occur locally in a fine silty matrix. A thin bedded, iron-sulphide rich meta-argillite horizon 3-4 m thick lies stratigraphically below the LMC fragmental (Webber,

1977). The fragmental body was not examined in detail but it warrants additional study and mapping. Similar stratabound fragmental units lie in the same stratigraphic position, along the lower-middle Aldridge contact, farther south at the Sullivan Mine, at the Vulcan showing (Minfile 082FNE093), and at the Clair showing (Doug Anderson, per. comm., 1996). These deposits are interpreted to herald an extensional episode within the Purcell basin by Höy *et al.* (in prep.).

### Tourmalinite Ridge

A dark grey to black silty meta-argillite facies occurs 4 km northeast of Doctor Peak (Photo 10-2). In 1996, Craig Leitch identified abundant, fine, disseminated needles in the unit as tourmaline. The facies extends over 5 km along strike and is estimated to be up to 50 m thick (1996 drilling determined it to be >18m thick; Downie, 1997). The horizon dips moderately to the north-northwest and was traced into the unnamed creek to the north of the Doc showing. The same facies crops out along the ridge between the Doc and Alpine showings. The dark grey to black argillite is fissile, silty medium to thin bedded and recessive

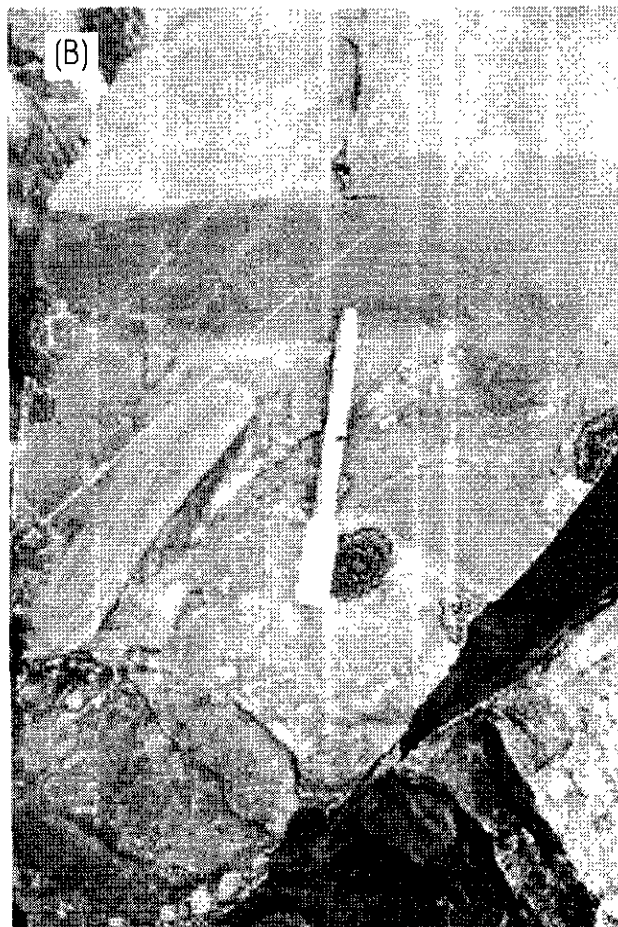


Photo 10-1. LMC fragmental, a stratabound conglomerate/fragmental unit that occurs along the lower-middle Aldridge contact at the headwaters of Doctor Creek. (a) Clast-supported, pebbly sandstone fragmental with bleached altered rims around numerous siltstone clasts; scale bar in centimetre divisions. (b) Subrounded siltstone clasts up to cobble size supported in a matrix of pebbly siltstone. The top dark grey layer immediately above the flare pen is well bedded, undisturbed siltstone.

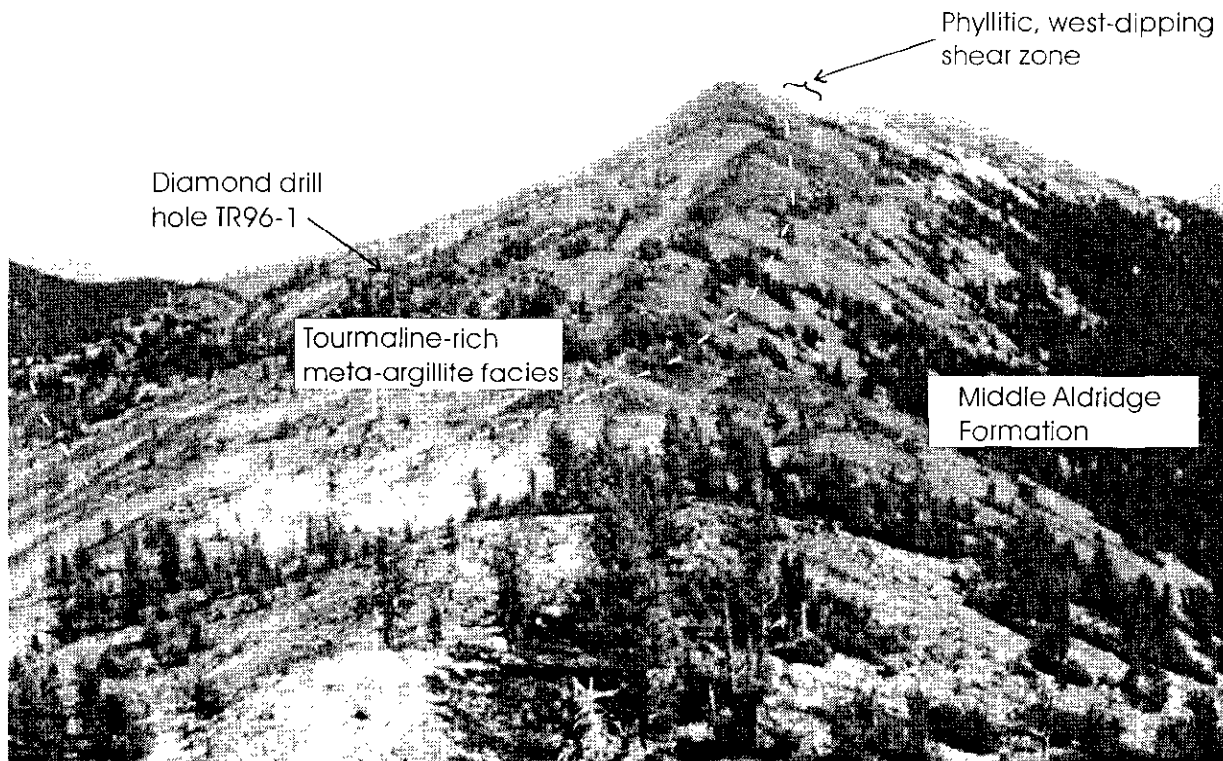


Photo 10-2. View to east of Tourmalinite Ridge, where the argillaceous siltstone facies contains abundant disseminated tourmaline-needles (up to 40%) and numerous galena-sphalerite-chalcopyrite veins.

weathering. Its stratigraphic position remains uncertain because of a shear zone (interpreted to be a reverse fault) between it and the upper Aldridge to the east (Figure 10-2). It is an important, mineralized argillaceous facies tentatively included in the upper part of the middle Aldridge Formation. This argillite unit may indicate a local, more restricted and anoxic facies of the upper middle Aldridge Formation. Alternatively, it could be a metamorphosed distal tourmaline-rich exhalative horizon. The facies is important because it is geochemically anomalous in Pb and Zn and it hosts a series of quartz veins that locally contain disseminated galena and/or tourmaline needles (see Doc Showing, Minfile 82KSE060 below).

## MINERAL OCCURRENCES

There are 13 metallic mineral occurrences in the Minfile database for the Findlay-Doctor Creek map area (Table 10-1). The Silver Key and St. Anthony are past producers (Table 10-2).

### St. Anthony past producer (Minfile 82KSE041)

The St. Anthony base metal occurrence is located in the Doctor Creek watershed. Five tonnes of material were reportedly extracted from a small pit in 1963

(Table 10-2). The occurrence consists of disseminated and veins of pyrite, pyrrhotite, magnetite, goethite, sphalerite and chalcopyrite (Mackenzie, 1971). These workings were not located in the field, however, numerous narrow, discontinuous quartz veins occur in the immediate area. The veins, containing minor pyrite, pyrrhotite and arsenopyrite, and rare galena and sphalerite, occur in sheared meta-wacke and meta-gabbro sills (Anderson, 1988).

### Silver Key past producer (Minfile 82KSE053)

The Silver Key workings lie at the headwaters of the east fork of Doctor Creek. Several adits have been driven along bedding-parallel veins within quartz wacke and Moyie sills, west of the western contact of the northern porphyritic quartz monzonite phase of the White Creek Batholith. A total of 29 tonnes of ore were mined from Silver Key (Table 10-2). Narrow quartz veins (2-5 cm wide) containing disseminated galena and pyrite occur in tightly folded and sheared country rock. At least 6 veins dip about 45° to the west. The age of mineralization is unknown but its proximity to the margin of the White Creek Batholith suggests it could be Middle Cretaceous.

## Doc Showing (Minfile 82KSE060)

The Doc showing comprises a series of white, galena-bearing quartz veins cutting the dark grey tourmalinite needle-rich meta-argillite facies of the middle Aldridge Formation, on a ridge 7 km north of Doctor Peak (Figure 10-2). It was originally explored by Kerr Addison Mines Ltd. in the 1970's when they outlined a large Pb soil geochemistry anomaly (Kerr Addison, 1972). Angular blocks of vein material occur within the argillite felsenmeer along the ridge. The northwest-and lesser northeast-trending veins are up to 100 cm wide (average 10 to 20 cm wide) and have been traced for about 100 m. Veins contain galena, lesser sphalerite and traces of chalcopyrite. Disseminated sulphides also occur in the host meta-argillite (Pautler, 1991).

## Alpine/Rocky Top Property (Minfile 82KSE081)

The Alpine, also known as the Rocky Top property is hosted in rocks correlated with the Creston Formation, based on wavy bedforms, local abundant mudcracks, interbeds of argillite and faint green colour. It has been explored by Cominco Ltd. (Mawer, 1986) and Tech Exploration Ltd. (Pautler, 1991). A moderately, northwest-dipping sericitic phyllite shear zone hosts a shallow-dipping stratabound to slightly discordant zone of alteration comprising silicified, albitized and clay-altered rocks with disseminated pyrite and lesser sphalerite and galena. A semi-concordant boudinaged quartz-ankerite vein in the shear zone with disseminated pyrite and irregular blebs of sphalerite and minor galena ranges from 20 cm to 2 m thick.

The vein is cut by a series of younger, north-trending normal faults that offset portions of it by up to about 5 m. The zone is exposed in a bulldozer trench about 6 m high and 80 m long that has been mapped in

detail by Mawer (1986). The grade of the zone is 0.5% Pb and 0.6% Zn across a 3.5 m width and over the length, with a higher grade band containing 16 gm/T Ag, 2.2% Pb and 3.7% Zn (Mawer, 1986).

## MC showing (Minfile 82FNE107)

Two old hand trenches at the MC showing have recently been re-investigated by Eagle Plains/Miner River Resources Ltd. A stratabound zone of banded and brecciated sulphides, locally with over 0.5 m of sphalerite, galena and pyrrhotite, is hosted in thin-bedded siltstone of the lower Aldridge Formation. Part of the occurrence displays "durchbewegung texture", where pyrrhotite-rich sulphide contains rounded quartz fragments. Samples of typical sulphide material returned up 130.0 g/t Ag, 9.17% Pb and 6.27% Zn over 25 cm (Miner River Resources data). Rare colourless vuggy quartz veins cut the zone and are interpreted to be younger, Mesozoic features.

The showing was drilled in late 1997 by Miner River/Eagle Plains Resources. Seven short drill holes totaling 580 metres intersected several stratabound massive sulphide intervals of variable thickness (less than 1 cm). Assay results were not available during preparation of this report.

Streams draining the showing area are in the 99<sup>th</sup> percentile for the Nelson RGS survey for the 82F map sheet (Matysek *et al.*, 1991) for the elements cesium, cobalt, copper, molybdenum, tin, tungsten, and zinc. The highest finite conductors detected for the entire Findlay Creek Area (Area 3; B.C. Ministry of Employment and Investment Open File 1996-23; 10-20 siemens; 7200 Hz, coplanar), interpreted to be narrow bedrock conductors, lie adjacent to the MC showing.

Table 10-1. Minfile mineral occurrences for the Findlay-Doctor Creek area, location are plotted on Figure 10-2.

| MINFILE   | NAME             | Commodities    | TYPE                           |
|-----------|------------------|----------------|--------------------------------|
| 082FNE073 | MOLLY            | W, Mo          | W skarn                        |
| 082FNE089 | PICO             | W, Sn, Pb, Zn  | W skarn adjacent to Moyie sill |
| 082FNE090 | VAL              | W, Sn          | W skarn                        |
| 082FNE092 | PIMACO           | Sn, W          | Sn veins and greisens          |
| 082FNE107 | MC               | Pb, Zn         | Veins Ag-Pb-Zn±Au              |
| 082FNE112 | GREENLAND CREEK  | Be             | REE pegmatite                  |
| 082FNE122 | BURNT            | Cu             | Veins Ag-Pb-Zn                 |
| 082KSE041 | ST. ANTHONY      | Ag, Pb, Zn, Cu | Veins Ag-Pb-Zn                 |
| 082KSE053 | SILVER KEY       | Ag, Zn, Pb, Cu | Veins Ag-Pb-Zn                 |
| 082KSE060 | DOC              | Ag, Pb, Zn, Cu | Veins Ag-Pb-Zn                 |
| 082KSE063 | ECHO LAKE        | W, Zn, Pb      | W veins                        |
| 082KSE075 | PICO             | W              | W veins                        |
| 082KSE081 | ALPINE/ROCKY TOP | Pb, Zn, Ag     | Veins Ag-Pb-Zn±Au              |

Table 10-2. Past production data for the Findlay-Doctor Creek area.

| MINFILE NO.  | NAME        | MINED (T) | Pb (kg)       | Zn (kg)    | Cu (kg)   | Ag (gm)        | Year      |
|--------------|-------------|-----------|---------------|------------|-----------|----------------|-----------|
| 082KSE053    | Silver Key  | 29        | 11,145        | 887        | ---       | 99,499         | 1926-1940 |
| 082KSE041    | St. Anthony | 5         | 82            | 25         | 25        | 12,006         | 1963      |
| <b>Total</b> |             | <b>34</b> | <b>11,227</b> | <b>912</b> | <b>25</b> | <b>111,505</b> |           |

## Greenland Creek Tungsten Showings

Three broad areas of scheelite-wolframite mineralization were evaluated by AMAX in the late 1970's; north and south of Greenland Creek, and at the confluence of Greenland and Skookumchuck creeks (Parry and Hodgson, 1980). Some of the showings north of Greenland Creek had been previously explored by Kerr Addison Ltd. Most showings comprise narrow quartz veins in Moyie sills, however, those near Skookumchuck Creek include quartz-garnet-diopside-scheelite skarn. A scheelite-bearing breccia dike consisting of angular fragments of phyllite, diorite, and porphyritic quartz monzonite clasts in a fine-grained pyritic matrix crops out in the latter area (*ibid.*).

Possible ages for tungsten mineralization were suggested by Parry and Hodgson (1980) as synchronous with Moyie sill intrusion, or during emplacement of the White Creek Batholith. The sill most highly mineralized with scheelite, tourmaline and cassiterite, lies near the LMC contact, which corresponds to the stratigraphic position of the Sullivan deposit, which contains those same minerals. This points to a Middle Proterozoic mineralization age. Alternatively, tungsten-bearing breccia dikes and skarns near the batholith contact support a Middle Cretaceous plutonic connection.

## CONCLUSIONS

The Findlay-Doctor Creek area Open File map is the primary product that will be generated from this project. The map area hosts a number of provocative mineral occurrences that continue to receive exploration attention, for example, the Rusty Ridge area, and Doc and Alpine occurrences. The extensive LMC fragmental unit, zones of base-metal enrichment for stream sediments and rocks illustrate that the Findlay-Doctor Creek area is a favourable SEDEX environment. Updated 1:50 000 scale mapping conducted under the auspices of this project provides a new framework for exploration.

## ACKNOWLEDGMENTS

The success of this project stems from the participation, collaboration and cooperation of Cominco Ltd. (Ken Pride and Paul Ransom), and Kennecott Canada Exploration Inc. (Eric Finlayson, Steven Coombes and Martine Bedard). Crestbrook Forest Products provided

updated road maps for the project area. The Ministry of Employment and Investment's Cranbrook regional office provided office space for the field season. Verna Vilkos patiently produced the figures. Reviews by Bill McMillan and Mitch Mihalynuk improved the final manuscript.

## REFERENCES CITED

- Anderson, D. (1988): Geological report, Echo Group, Echo 1 through 6 claims; *B.C. Ministry of Energy, Mines and Petroleum Resources*, Assessment Report 16, 925.
- Anderson, H.E. and Davis, D.W. (1995): U-Pb geochronology of the Moyie sills, Purcell Supergroup, southeastern British Columbia: implications for the Middle Proterozoic geologic history of the Purcell (Belt) basin; *Canadian Journal of Earth Sciences*, v. 32, p. 1180-1193.
- Downie, C.C. (1997): Diamond drilling report on the Eastdoc, Westdoc and Fin claim group; *B.C. Ministry of Employment and Investment*, Assessment Report 24,801.
- Höy, T. (1993): Geology of the Purcell Supergroup in the Fernie West-half Map Area, Southeastern British Columbia; *B.C. Ministry of Energy, Mines and Petroleum Resources*, Bulletin 84.
- Höy, T., Anderson, D., Turner, R.J.W., and Leitch, C.H.B. (In prep.): Tectonic, magmatic and metallogenic history of the early synrift phase of the Purcell Basin, southeastern British Columbia; *Geological Survey of Canada*, Sullivan Volume.
- Kerr Addison (1972): Report on geological and geochemical survey DOC Nos. 1-6 Mineral claims; *B.C. Ministry of Energy, Mines and Petroleum Resources*, Assessment Report 3,924.
- Leitch, C.H.B. (1997): Petrographic Report for Miner River Resources Ltd.
- Lowe, C., Brown, D.A., Best, M.E. and Shives, R.B.K. (1997): The East Kootenay Geophysical Survey, southeastern British Columbia (82F, G, K): Regional synthesis; *Geological Survey of Canada*, Current Research, Part E, Paper 97-1A, p. 167-176.

- Mackenzie, D.E. (1971): Geological survey, Ace claim group; *B.C. Ministry of Energy, Mines and Petroleum Resources*, Assessment Report 3,287.
- Matysek, P.F., Jackaman, W., Gravel, J.L., Sibbick, S.J. and Feulgen, S. (1991): British Columbia Regional Geochemical Survey, Nelson (NTS 82F); *B.C. Ministry of Energy, Mines and Petroleum Resources*, BC RGS 30.
- Mawer, A.B. (1986): Geological - soil geochemical report, Alpine Group; *B.C. Ministry of Energy, Mines and Petroleum Resources*, Assessment Report 15,195.
- McLaren, G.P., Stewart, G.G. and Lane, R.A. (1990a): Geology and Mineral Potential of the Purcell Wilderness Conservancy; *B.C. Ministry of Energy, Mines and Petroleum Resources*, Geological Fieldwork 1989, Paper 1990-1, p. 29-37.
- McLaren, G.P., Stewart, G.G. and Lane, R.A. (1990b): Geology and Mineral Occurrences of the Purcell Wilderness Study Area; *B.C. Ministry of Energy, Mines and Petroleum Resources*, Open File 1990-20.
- Parry, S.E. and Hodgson, C.J. (1980): Greenland Creek Property; Internal Company Report, AMAX.
- Pautler, J. (1991): Geological and Geochemical Assessment Report on the Doc Property; *B.C. Ministry of Energy, Mines and Petroleum Resources*, Assessment Report 21,275, 12 p.
- Reesor, J. E. (1996): Geology of Kootenay Lake, B. C.; *Geological Survey of Canada*, Map 1864-A
- Reesor, J. E. (1973): Geology of the Lardeau Map-area, east-half, British Columbia; *Geological Survey of Canada*, Memoir 369, 129 pages.
- Reesor, J. E. (1958): Dewar Creek Map-area with special emphasis on the White Creek Batholith, British Columbia; *Geological Survey of Canada*, Memoir 292, 78 pages.
- Rice, H.M.A. (1941): Nelson Map Area, East Half; *Geological Survey of Canada*, Memoir 228, 86 p.
- Smith, M. and Brown, D.A. (1998): Preliminary report on a Proterozoic (?) stock in the Purcell Supergroup and comparison to the Cretaceous White Creek Batholith, Southeastern British Columbia (82F/16, 82K/01); in *Geological Fieldwork 1997*, *B.C. Ministry of Employment and Investment*, Paper 1998-1.
- Webber, G.L. (1977): Geological report, Echo Group of 1, 2, 3 and 4 claims; *B.C. Ministry of Energy, Mines and Petroleum Resources*, Assessment Report 6,413.





**PRELIMINARY REPORT ON A PROTEROZOIC (?) STOCK IN THE  
PURCELL SUPERGROUP AND COMPARISON TO THE CRETACEOUS  
WHITE CREEK BATHOLITH, SOUTHEASTERN BRITISH COLUMBIA  
(82F/16, 82K/01)**

By Mark Smith, University of Alberta, and D. A. Brown, B.C. Geological Survey Branch

**KEYWORDS:** White Creek Batholith, Hellroaring Creek Stock, Greenland Creek Stock, Proterozoic, Purcell Supergroup, Aldridge Formation, Geochronology.

**INTRODUCTION**

In southeastern British Columbia many intrusive suites lack conclusive radiometric age dates. The purpose of this B.Sc. project is to study three of the intrusions in the Purcell Mountain Range and provide uranium-lead geochronological results on two of these to refine the igneous magmatic history of the region.

The White Creek Batholith (WCB) and the Greenland Creek Stock (GCS) are located approximately 45 km northwest of Cranbrook, B.C. The Hellroaring Creek Stock (HCS) is situated 15 km west of Cranbrook (Figure 11-1). All three intrude lower greenschist grade

regionally metamorphosed Aldridge Formation, a middle Proterozoic basin fill succession (Höy, 1993), and cut the  $1467 \pm 3$  Ma Moyie Sills (Anderson and Davis, 1995). Reesor (1958) completed previous mapping and a comprehensive study of the White Creek Batholith. Since that time, mining companies conducted a number of exploration projects searching for economic deposits of tungsten and massive sulphides. The Hellroaring Creek Stock was originally located by Rice (1941), during a regional study, and a more detailed map was published by Leech (1957). It was regarded as an intrusive of possible economic interest with exploration projects focusing in on the potential for beryllium and industrial minerals.

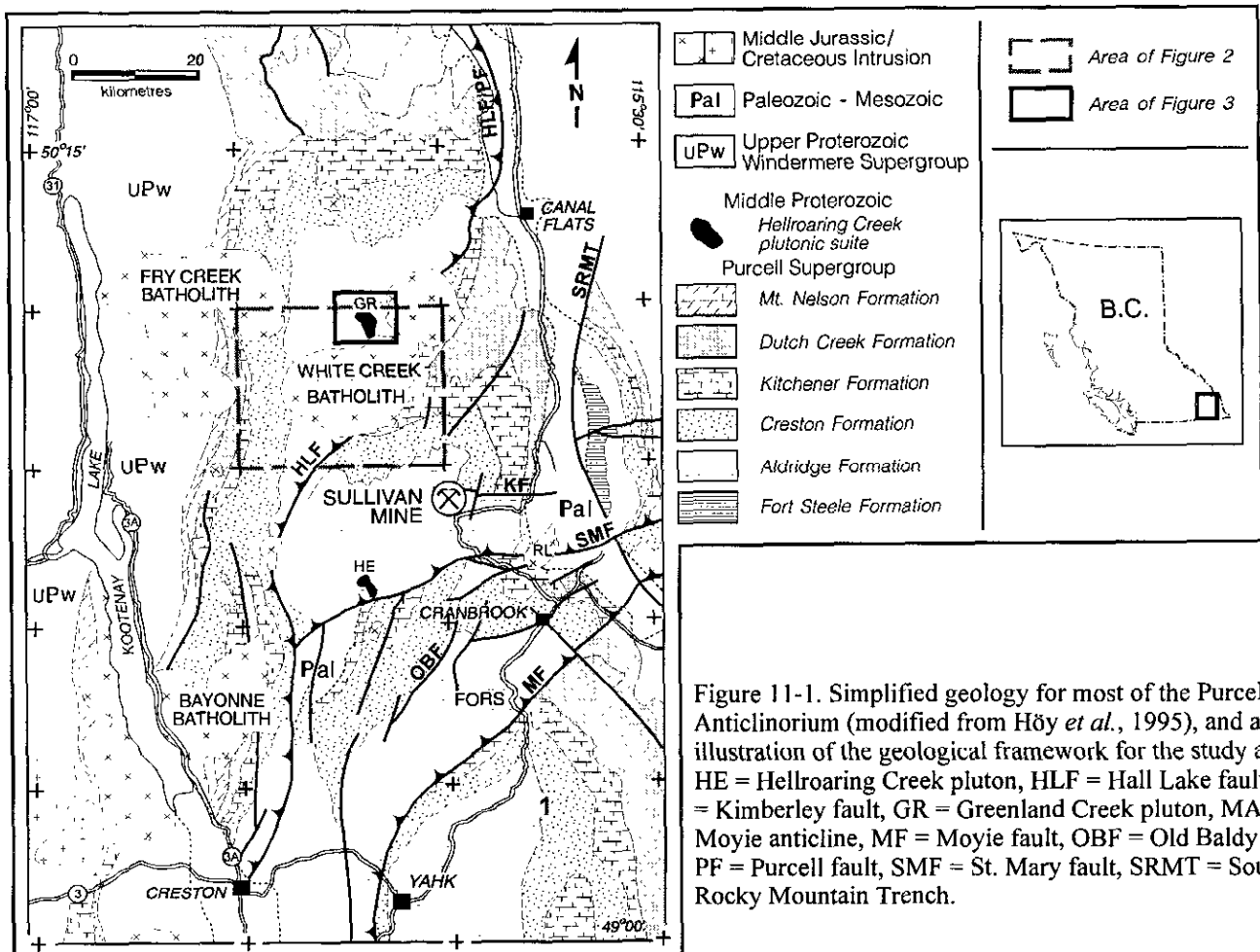


Figure 11-1. Simplified geology for most of the Purcell Anticlinorium (modified from Höy *et al.*, 1995), and an illustration of the geological framework for the study area. HE = Hellroaring Creek pluton, HLF = Hall Lake fault, KF = Kimberley fault, GR = Greenland Creek pluton, MA = Moyie anticline, MF = Moyie fault, OBF = Old Baldy fault, PF = Purcell fault, SMF = St. Mary fault, SRMT = Southern Rocky Mountain Trench.

## PROJECT COMPONENTS

The thesis project consists of three main components. The first involved mapping the Greenland Creek Stock during August 1997. The second is a petrological and geochemical study of the pegmatite intrusions, the HCS and the GCS. This aspect of the project will compare the mineralogy and abundance of major elements, trace elements, and rare earth elements to classify and determine the tectonic setting for the two stocks. The third aspect of this study is to obtain precise and accurate U-Pb ages for the Greenland Creek Stock and the White Creek Batholith. An accurate emplacement age for the GCS will link it to either the middle Proterozoic HCS suite or the middle Cretaceous WCB suite. These components will answer questions concerning the Proterozoic tectonic setting, how the intrusive suites are related in the Purcell Supergroup and lead to new constraints on the timing of igneous activity in the area.

## WHITE CREEK BATHOLITH

### Description

The White Creek Batholith was originally mapped by Reesor (1958), who published a detailed megascopic and microscopic description of the five phases. It is an oval, concentrically zoned igneous body that outcrops over an area of approximately 225 km (Figure 11-2). The oldest unit, forming a rim along the western margin, is biotite granodiorite that grades into hornblende-biotite granodiorite. Inward from these two is a large body of potassic feldspar porphyritic quartz monzonite that comprises most of the eastern half of the batholith. The inner core is a leucocratic quartz monzonite. The fifth phase is a medium grained quartz monzonite that intrudes the two older granodiorite units in the western portion of the body. Aplite and pegmatite dikes are also common in parts of the batholith, especially the porphyritic quartz monzonite phase.

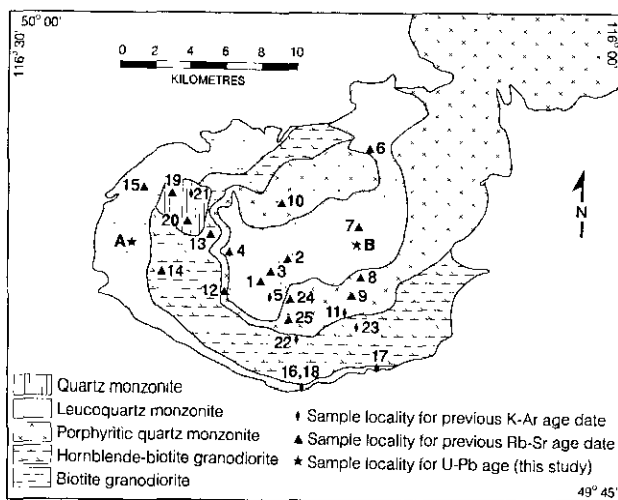


Figure 11-2. Generalized geology and sample locations within the White Creek batholith (after Reesor, 1996, 1958).

## Previous Work

The White Creek Batholith has been the focus of a number of geochronological studies summarized in Figure 11-2 and Table 11-1. The study by Wanless *et al.* (1968) emphasized mineralogy, geochemical characteristics and the geologic history of each of the phases. They document a decrease in the content of plagioclase, biotite, hornblende, epidote, and accessories and an increase in microcline, quartz, and muscovite towards the inner core. A Rb-Sr study of the WCB shows that each one of the distinct lithologic zones have different initial  $^{87}\text{Sr}/^{86}\text{Sr}$  isotopic compositions, indicating that the lithologic variations could not be produced solely by inward fractional crystallization during cooling (Wanless *et al.*, 1968).

The Rb-Sr study by Wanless *et al.* (1968) determined the first accurate emplacement age on one of the phases from an Rb-Sr whole rock isochron. They calculated the age of the leucocratic monzonite core at  $111 \pm 5$  Ma ( $^{87}\text{Rb} = 1.47 \times 10^{-11} \text{ yr}^{-1}$ ) which has since been recalculated to 115 Ma ( $^{87}\text{Rb} = 1.42 \times 10^{-11} \text{ yr}^{-1}$ ; Brandon and Lambert, 1992). Combining all the mineralogical, geochemical and geochronological data, they established four major events: emplacement of the outer margins (126 Ma), consolidation of core rocks (115 Ma), an initial thermal episode (~85 Ma), and a second thermal episode (~65 Ma).

The work of Brandon and Lambert (1992) further constrained the mid-Cretaceous episode by four Rb-Sr combined whole rock-apatite isochron ages; these were 105-115 Ma, including a  $105.9 \pm 1.2$  Ma obtained on the porphyritic granodiorite zone of the WCB. Following this paper, Brandon and Lambert (1994) conducted major element, trace element, and Sr, Nd, Pb, and O isotopic studies to determine the source for the generation of all WCB granitoids. They concluded that at least three pulses of isotopically and chemically distinct magma were present. The first was responsible for the two outer granodiorites, the second for the porphyritic phase, and the third for the monzonite core. From their results, the model calculations favored anatexis of crustal sources, with little geochemical influence of mantle-derived magma. This anatexis was interpreted to have resulted from intra-crustal melting in response to terrane accretion and collision along the western margin of North America.

## Current Research

As part of this study, samples were collected from the central and border phases, presumably the youngest and oldest intrusive units, respectively (Figure 11-2). A sample of the biotite granodiorite rim was obtained 1 km west from Price Lake and one from the leucocratic quartz monzonite core 4.5 km north of Skookumchuck Mountain. (Table 11-2) These two phases will be radiometrically dated using isotope dilution thermal ionization mass spectrometry U-Pb methods at the geochronology laboratory, University of Alberta. Concise ages documenting the duration of emplacement of the White Creek Batholith will augment the established geochemical

Table 11-1. Sample localities from studies on the White Creek Batholith after Wanless *et al.*, (1968) and Brandon and Lambert (1994). WRX = whole rock sample

| Rock Unit                       | #           | Sample      | Method | Age (Ma)                   | Reference                    |
|---------------------------------|-------------|-------------|--------|----------------------------|------------------------------|
| Quartz monzonite                | 19          | WRX         | Rb-Sr  | -                          | Wanless <i>et al.</i> (1968) |
|                                 | 20          | WRX         | Rb-Sr  | -                          | Wanless <i>et al.</i> (1968) |
|                                 | 21          | Biotite     | K-Ar   | 18                         | Lowdon (1961)                |
| Leucoquartz monzonite           | 1           | WRX         | Rb-Sr  | 115                        | Wanless <i>et al.</i> (1968) |
|                                 | 2           | WRX         | Rb-Sr  | 115                        | Wanless <i>et al.</i> (1968) |
|                                 | 3           | WRX         | Rb-Sr  | 115                        | Wanless <i>et al.</i> (1968) |
|                                 | 4           | WRX         | Rb-Sr  | 115                        | Wanless <i>et al.</i> (1968) |
|                                 | 5           | WRX         | Rb-Sr  | 115                        | Wanless <i>et al.</i> (1968) |
|                                 |             | Biotite     | K-Ar   | 82                         | Lowdon <i>et al.</i> (1962)  |
|                                 |             | Muscovite   | K-Ar   | 80                         | Lowdon <i>et al.</i> (1962)  |
|                                 | 6           | WRX         | Rb-Sr  | 115                        | Wanless <i>et al.</i> (1968) |
|                                 | 7           | WRX         | Rb-Sr  | 115                        | Wanless <i>et al.</i> (1968) |
| A                               | Zircon      | U-Pb        | N/A    | <b>Current Study</b>       |                              |
| Porphyritic quartz monzonite    | 8           | WRX         | Rb-Sr  | -                          | Wanless <i>et al.</i> (1968) |
|                                 |             | WRX-apatite | Rb-Sr  | 105.9                      | Brandon and Lambert (1992)   |
|                                 | 9           | WRX         | Rb-Sr  | -                          | Wanless <i>et al.</i> (1968) |
|                                 |             | WRX-apatite | Rb-Sr  | 105.9                      | Brandon and Lambert (1992)   |
|                                 | 10          | WRX         | Rb-Sr  | -                          | Wanless <i>et al.</i> (1968) |
|                                 | 11          | WRX         | Rb-Sr  | -                          | Wanless <i>et al.</i> (1968) |
|                                 |             | Biotite     | K-Ar   | 60                         | Lowdon (1961)                |
|                                 | 12          | WRX         | Rb-Sr  | -                          | Wanless <i>et al.</i> (1968) |
|                                 | 22          | Biotite     | K-Ar   | 29                         | Lowdon (1961)                |
| 24                              | WRX-apatite | Rb-Sr       | 105.9  | Brandon and Lambert (1992) |                              |
| 25                              | WRX-apatite | Rb-Sr       | 105.9  | Brandon and Lambert (1992) |                              |
| Hornblende-biotite granodiorite | 13          | WRX         | Rb-Sr  | -                          | Wanless <i>et al.</i> (1968) |
|                                 | 14          | WRX         | Rb-Sr  | -                          | Wanless <i>et al.</i> (1968) |
|                                 | 23          | Hornblende  | K-Ar   | 87                         | Lowdon (1961)                |
| Biotite granodiorite            | 15          | WRX         | Rb-Sr  | -                          | Wanless <i>et al.</i> (1968) |
|                                 | 16          | WRX         | Rb-Sr  | -                          | Wanless <i>et al.</i> (1968) |
|                                 |             | Biotite     | K-Ar   | 73                         | Lowdon <i>et al.</i> (1962)  |
|                                 | 17          | WRX         | Rb-Sr  | -                          | Wanless <i>et al.</i> (1968) |
|                                 |             | Biotite     | K-Ar   | 79                         | Lowdon (1961)                |
|                                 | 18          | WRX         | Rb-Sr  | -                          | Wanless <i>et al.</i> (1968) |
|                                 |             | Biotite     | K-Ar   | 56                         | Lowdon (1961)                |
| B                               | Zircon      | U-Pb        | N/A    | <b>Current Study</b>       |                              |

data by Brandon and Lambert (1994) and Wanless *et al.* (1968), constraining the magmatic evolution of the WCB.

## HELLROARING CREEK STOCK

### Description

The Hellroaring Creek Stock outcrops over an area of 10 km<sup>2</sup> and generally is composed of medium- to coarse-grained granodiorite pegmatite. Ryan and Blenkinsop (1971) recognized four phases based on differences in

composition and texture. The first was a coarse-grained albitic granodiorite that consists of feldspar, muscovite and tourmaline phenocrysts in a feldspar-quartz-muscovite groundmass. The second was a granophyre unit, the third a medium-grained tourmaline-free granodiorite. The fourth phase sampled was a medium- to coarse-grained tourmaline-rich granodiorite. Some of the phases were only locally developed and it is likely that others exist as well. For example, a fine-grained aplite unit consisting of tourmaline and garnet was observed along the contacts with the surrounding country rock.

## Previous Work

Earlier geochronological studies on the Hellroaring Creek Stock yielded imprecise ages. The first attempt at radiometric dating was using K-Ar methods on a muscovite sample. Lowdon (1961) obtained an age of 705 Ma followed by Hunt (1962), who obtained an age of 769 Ma. These ages could reflect K-Ar resetting due to a metamorphic event.

The work of Ryan and Blenkinsop (1971) contradicted the previous K-Ar dates and provided the most reasonable age until recently. Using the Rb-Sr whole rock method, they obtained an isochron of  $1260 \pm 50$  Ma. The implications from this data were significant because it indicated that the Hellroaring Creek stock was the oldest intrusion in the Purcell Supergroup. Although more recent work has produced a  $\sim 1370$  Ma U-Pb monazite age (Mortensen, written comm., 1997) Ryan and Blenkinsop's result was the first indication of a Proterozoic magmatic event in this region.

## Current Research

Due to the fact the Greenland Creek Stock may be linked to the Hellroaring Creek Stock, samples were collected from the HCS for geochemical studies. The major elements, trace elements, and rare earth elements of phases with similar mineralogy and texture will be compared to determine if the two pegmatites have similar source magmas.

## GREENLAND CREEK STOCK

### Description

The Greenland Creek Stock crops out 1 km north of the core phase of the White Creek Batholith (Figure 11-3; Photos 11-1 and 2). It is a typical granitoid pegmatite of variable texture and coarseness (0.5 mm to  $\sim 4$  cm). The dominant phase is coarse-grained with interlocking feldspars, and quartz and large sheets of muscovite. The second is a relatively equigranular unit composed of 0.5 to 1 cm grains of feldspar, quartz and muscovite. The third and fourth phases appear to occur in conjunction with each other near the contacts of surrounding lower Aldridge Formation and Moyic Sills. The chilled margins of the pluton are aplite with tourmaline needles and coarse sheets of muscovite. A coarse-grained tourmaline-rich pegmatite is associated with this phase.

Although similar in composition, there are a few differences between the HCS and the GCS that were recognized in the field. The first is the abundance of large quartz lenses in the GCS that were rare in the HCS. The second is the presence of garnet (and trace pyrite) that was common in the aplite phases of the HCS, but rarely found in the GCS. And lastly is the size of the tourmaline crystals. The crystals in HCS frequently were up to 8 cm in size but the GCS rarely had tourmaline larger than 4 cm.

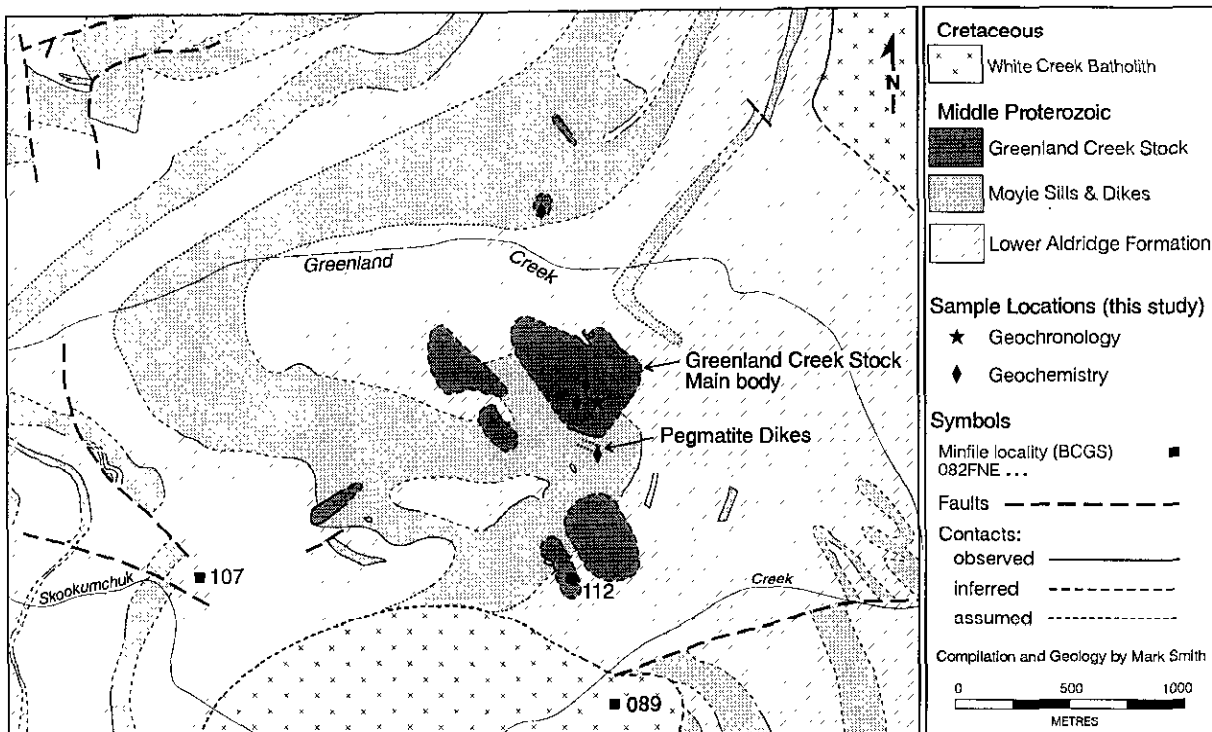


Figure 11-3. Geological compilation map for the Greenland Creek stock area.



Photo 11-1. View to 340° to the westernmost satellitic phase of the Greenland Creek stock where it intrudes lower Aldridge Formation and a Moyie sill. Contacts are sharp and intrusive with no evidence of faulting. Access trail to the Greenland Creek tungsten occurrences (see Perry and Hodgson, 1980) is evident along the right side of the photo.



Photo 11-2. View to 340° to a series of white weathering, leucocratic tourmaline-muscovite pegmatite and medium-grained quartz monzonite dikes hosted in a massive Moyie sill gabbro along the southern contact zone of the main Greenland Creek stock (see Figure 11-3 for location marked as "Pegmatite Dikes").

## Previous Work

Although originally mapped and described by Reesor (1958) as part of the mid-Cretaceous White Creek batholith, his more recent compilation map designates it as a Proterozoic intrusion (Reesor, 1996). Since his original mapping, work on and near the Greenland Creek Stock has been limited to exploration companies searching for economic deposits. A number of detailed maps were produced, most notably by AMAX (Perry and Hodgson, 1980), and were used in conjunction with this study (Figure 11-3).

In 1995 a government geophysical survey was conducted in the Purcell Mountains. One of the interesting anomalies was a Th/K low over the Greenland Creek Stock that was strikingly similar to the signature over the HCS (Lowe *et al.*, 1997). These new data, along with geological comparison, has led to speculation that the GCS is mid-Proterozoic in age, and part of the Hellroaring Creek suite rather than part of the mid-Cretaceous suite.

## Current Research

The main focus of this thesis study is to compare the Greenland Creek Stock to the Hellroaring Creek Stock and the White Creek Batholith. Geological mapping was conducted in the area, and a detailed map was compiled using earlier work done by AMAX (Perry and Hodgson, 1980). From this study, four intrusive phases were recognized and sampled in the field. These phases are mineralogically and texturally very similar to those present in the Hellroaring Creek Stock, located 45 km to the south. Each of these phases was sampled and geochemical analyses of major elements, trace elements, and rare earth elements will be performed to more accurately provide comparisons. The equigranular sample (location in Table 11-2) will be used for the U-Pb age date and determination of an epsilon Nd value. The epsilon Nd value will help measure the amount of influence mantle or crustal sources had in the formation of the magma. These will be compared to the values obtained by Brandon and Lambert (1994) for the WCB. The geochemical data will be used to classify the units and pegmatite to attempt to resolve the question of the source of the stock and its tectonic setting.

## DISCUSSION

The lack of conclusive U-Pb radiometric dates on many of the intrusive suites in southeastern British Columbia has led to a great deal of speculation about the geologic history of the region. If successful, the U-Pb ages obtained in this study on the White Creek Batholith will provide an accurate estimate of emplacement history and constrain the timing of this mid-Cretaceous magmatic event. The age date on the Greenland Creek Stock, used in conjunction with the geochemical analyses will attempt to determine its tectonic environment and link it to either the Proterozoic or Cretaceous plutonic episode.

The Proterozoic history of the Purcell Supergroup has recently been the source of debate. The collisional tectonic event associated with the HCS magmatism is known as the East Kootenay Orogeny (McMechan and Price, 1982). However, Doughty and Chamberlain (1996) concluded that an extensional event occurred in the Belt Supergroup (correlates to the Purcell Supergroup) further south in Montana. They show that the circa 1370 Ma tectonothermal event involved burial metamorphism, bimodal magmatism and partial melting of high grade metasedimentary rock. They also showed that extensional deformation was concentrated in the deeper level high grade rocks. If an extensional event caused the plutonism, then the term orogeny is incorrect.

The goal of this study is to analyze the mineralogy and geochemistry of the two pegmatites and obtain a precise and accurate age on the GCS. The U-Pb age on the GCS will resolve whether the intrusion is linked to either, the mid-Proterozoic HCS or the mid-Cretaceous WCB. Although pegmatites may not be good discriminators for a granitoids' tectonic environment, they potentially are the only evidence of Proterozoic plutonism at ~1370 Ma. The new data should help to classify the stocks, correlate the magmatic episodes in the Belt-Purcell Supergroup and lead to insights as to whether there was an East Kootenay orogenic or extensional event.

## ACKNOWLEDGMENTS

Bill McMillan reviewed and improved the final manuscript. Verna Vilkos skillfully produced the final figures.

Table 11-2. UTM coordinates for U-Pb samples collected for the current study ( $\pm 50$  m; in NAD83).

| Sample # | Rock Type                        | Easting (m) | Northing (m) |
|----------|----------------------------------|-------------|--------------|
| Green1   | Equigranular granitoid pegmatite | 558170      | 5536800      |
| WCB-A    | Biotite granodiorite             | 543250      | 5525700      |
| WCB-B    | Leucoquartz monzonite            | 543450      | 5525700      |

## REFERENCES CITED

- Anderson, H.E. and Davis, D.W. (1995): U-Pb geochronology of the Moyie sills, Purcell Supergroup, southeastern British Columbia: implications for the Middle Proterozoic geologic history of the Purcell (Belt) basin; *Canadian Journal of Earth Sciences*, v. 32, p. 1180-1193.
- Brandon, A. D. and Lambert, R. StJ. (1994): Crustal melting in the Cordilleran interior: The mid-Cretaceous White Creek Batholith in the southern Canadian Cordillera; *Journal of Petrology*, V. 35, part 1, p. 239-269.
- Brandon, A. D. and Lambert, R. StJ. (1993): Geochemical characterization of mid-Cretaceous granitoids of the Kootenay Arc in the southern Canadian Cordillera; *Canadian Journal of Earth Sciences*, V. 30, p. 1076-1090.
- Brandon, A. D. and Lambert, R. StJ. (1992): Rb-Sr geochronology of Mesozoic granitoids in the southern Canadian Cordillera; Project Lithoprobe Southern Cordillera Transect, *University of Calgary*, Alberta, Rep. 24, p. 95-104.
- Brown, D. A. and Termuende, T. (1998): The Findlay Industrial Partnership Project: Geology and Mineral Occurrences of the Findlay Creek area, southeastern British Columbia (82F/16, 82K/01); in *Geological Fieldwork 1997, B.C. Ministry of Employment and Investment*, Paper 1998-1, this volume.
- Doughty, P. T. and Chamberlain, K. R. (1996): Salmon River Arch revisited: new evidence for 1370 Ma rifting near the end of deposition in the Middle Proterozoic Belt basin; *Canadian Journal of Earth Sciences*, V. 33, p. 1037-1052.
- Höy, T. (1993): Geology of the Purcell Supergroup in the Fernie West-half Map Area, Southeastern British Columbia; *B.C. Ministry of Energy, Mines and Petroleum Resources*, Bulletin 84.
- Hunt, G. (1962): Time of Purcell eruption in southeastern British Columbia and southwestern Alberta; *Journal of Alberta Society of Petroleum Geologists*, V. 10, pages 438-442.
- Leech, G. B., Lowdon, J. A., Stockwell, C. H., and Wanless, R. K. (1963): Age determinations and geologic studies; *Geological Survey of Canada*, paper 63-17, page 30.
- Lowdon, J. A. (1961): Age determinations by the Geological Survey of Canada, Report 2, Isotope Ages; *Geological Survey of Canada*, Paper 61-17, page 6.
- Lowdon, J. A., Stockwell, C. H., Tipper, H. W., and Wanless, R. K. (1962): Age determinations by the Geological Survey of Canada; *Geological Survey of Canada*, Paper 62-17, page 17.
- Lowe, C., Brown, D.A., Best, M.E. and Shives, R.B.K. (1997): The East Kootenay Geophysical Survey, southeastern British Columbia (82F, G, K): Regional synthesis; *Geological Survey of Canada*, Current Research, Part E, Paper 97-1A, p. 167-176.
- McMechan, M. E., and Price, R. A. (1982): Superimposed low-grade metamorphism in the Mount Fisher area, southeastern British Columbia-implications for the East Kootenay orogeny; *Canadian Journal of Earth Sciences*, V. 19, pages 476-489.
- Parry, S. E. and Hodgson C. J. (1980): Greenland Creek Property, 1979 year end report; AMAX, unpublished report, 20 pages.
- Reesor, J. E. (1996): Geology of Kootenay Lake, B. C.; *Geological Survey of Canada*, Map 1864-A
- Reesor, J. E. (1958): Dewar Creek Map-area with special emphasis on the White Creek Batholith, British Columbia; *Geological Survey of Canada*, Memoir 292, 78 pages.
- Rice, H. M. A. (1941): Nelson map area, east half, British Columbia; *Geological Survey of Canada*, Memoir 228.
- Ryan, B. D. and Blenkinsop, J. (1971): Geology and geochronology of the Hellroaring Creek Stock, British Columbia; *Canadian Journal of Earth Sciences*, V. 8, p. 85-95.
- Wanless, R. K., Loveridge, W. D., and Mursky, G. (1968): A geochronological study of the White Creek Batholith, southeastern British Columbia; *Canadian Journal of Earth Sciences*, V. 5, p. 375-386.
- Wasylyshyn, R. (1984): Hellroaring Creek Group; *B. C. Ministry of Energy, Mines, and Petroleum Resources*, Assessment Report 13 415.
- White, G. V. (1988): Nelson; *B. C. Ministry of Energy, Mines and Petroleum Resources*, Exploration in British Columbia, 1987; p. B109-B116.





## PURCELL GRAVITY ANOMALY--IMPLICATIONS FOR MINERAL EXPLORATION

By Robert Woodfill, Sedex Mining Corporation,  
Cranbrook Field Office, P.O. Box 215, Main Station, Cranbrook, B.C., V1C 4H7.

**KEYWORDS:** Purcell anticlinorium, gravity anomaly, Purcell (Belt) Supergroup, Aldridge Formation, new density data, Moyie sills, Sullivan deposit, sedimentary exhalative (SEDEX) deposits.

### INTRODUCTION

This study is part of Sedex Mining Corporation's exploration program for Sullivan-type, sedimentary exhalative (SEDEX) massive sulphide deposits in southeastern British Columbia.

### PURCELL ANTICLINORIUM

The Purcell anticlinorium is a broad, gently north-plunging structure that is cored by the middle Proterozoic Purcell (Belt) Supergroup and flanked by late Proterozoic Windermere Supergroup rocks in southeastern British Columbia and northwestern United States (Price, 1981). Regionally extensive seismic reflections imaged beneath the anticline in the upper crust correlate with ca. 1468 Ma gabbroic sills (Anderson and Davis, 1995) in the Aldridge formation of the Purcell (Belt) Supergroup. The reflectors define broad folds and thrusts, and support an interpretation that the anticlinorium formed during Mesozoic contraction when imbricate thrust faults carried up to 15 km of Purcell (Belt) and Paleozoic margin sedimentary rocks, and basement in some areas, eastward over a prominent basement ramp (Cook and Van der Velden, 1995).

### PURCELL GRAVITY ANOMALY

Combined U.S. Geological Survey and Geological Survey of Canada Bouguer gravity data (no terrain correction applied) define a 50 by 300 km positive gravity anomaly with an amplitude of approximately 20 mgals in southeastern British Columbia and northwestern Montana (Figure 12-1). This anomaly is outlined by the -150 mgal Bouguer gravity contour and shows a steep gradient on the northeast side. The gravity anomaly terminates against the westward projection of the strike of the northern border of the Vulcan Low on the north and against the Lewis-Clark lineament and westward projection of the Sapegoat-Bannatyne lineament on the south (Figure 12-2). This gravity anomaly, here named the Purcell gravity anomaly, appears to core the geographical outline of the Purcell anticlinorium.

### NEW DENSITY DATA

Density determinations were made on eighty-six representative samples of rock units in the area to provide better control on the gravity interpretations. Twenty-seven of the density measurements were from core and the remainder on hand-size samples from the field. Results are summarized in Table 12-1.

### INTERPRETATION

The Purcell gravity anomaly, which cores the Purcell anticlinorium, is here interpreted to represent a buried complex consisting entirely of Moyie-type intrusions and may represent the location of the rift axis of the Purcell (Belt) basin. Isopachs of the cumulative thickness of Moyie sills and turbidites of the middle Aldridge and unit G, Prichard formation (Höy, Turner and Leitch, 1995) from data by Cressman (1989), Höy (1993) and Turner et. al. (1993), also define a sill injection axis along the core of the Purcell anticlinorium.

### IMPLICATIONS FOR MINERAL EXPLORATION

If the Purcell gravity anomaly can be interpreted to identify the location of the incipient phase of Purcell (Belt) basin rifting, the Purcell gravity anomaly may define the limits of hydrothermal systems and sedimentary exhalative (SEDEX) deposits emplaced prior to the Moyie sill event (Anderson and Davis, 1995) in the lower and middle Aldridge formations.

The Sullivan mine and other sedimentary exhalative (SEDEX) occurrences (Kootenay King, Vulcan, Fors and Panda) appear to be positioned along structures that are within or parallel to broad northeast-trending structural zones that cut the Purcell anticlinorium. Höy (1982) defined such a structural zone, which he termed a transverse zone, lying between the Hall Lake and Moyie faults. The zone contained northeast-trending structures, boron (tourmalinite) concentrations and intraformational conglomerate occurrences. The Sullivan mine is located along the central part of this transverse zone. Höy's transverse zone lies along the northern border of the western

Table 12-1. Density data for the Purcell Supergroup samples.

| Rock Type              | Host Unit | Number of measurements | Range (g/cm <sup>3</sup> ) | Mean Density |
|------------------------|-----------|------------------------|----------------------------|--------------|
| Moyie Sills            | M-A       | 14                     | 2.85-3.14                  | 2.97         |
| Moyie Sills            | L-A       | 8                      | 2.87-3.02                  | 2.96         |
| Moyie Dikes            | M-A       | 3                      | 2.98-3.02                  | 3.00         |
| All Moyie Intrusives   | M-L-A     | 25                     | 2.85-3.14                  | 2.97         |
| Quartzites             | M-A       | 5                      | 2.69-2.74                  | 2.73         |
| Quartzites             | L-A       | 12                     | 2.66-2.83                  | 2.73         |
| Argillites             | U-A       | 1                      | 2.79                       | 2.79         |
| Argillites             | M-A       | 9                      | 2.67-2.79                  | 2.74         |
| Siltstones             | M-A       | 2                      | 2.55-2.57                  | 2.56         |
| Siltstones             | L-A       | 3                      | 2.73-2.80                  | 2.76         |
| Schists                | L-A       | 7                      | 2.63-2.84                  | 2.78         |
| Fragmental Rocks       | M-A       | 5                      | 2.67-2.72                  | 2.70         |
| Laramide Intrusives    | M-A       | 3                      | 2.60-2.73                  | 2.67         |
| Cambrian Intrusives    | M-A       | 3                      | 2.57-2.62                  | 2.60         |
| Granophyres            | L-A       | 2                      | 2.66-2.71                  | 2.69         |
| Lamprophyres           | L-M-A     | 3                      | 2.91-2.94                  | 2.92         |
| Hellroaring Intrusives | M-A       | 4                      | 2.60-2.65                  | 2.63         |
| Massive Sulphide       | L-M-A     | 2                      | 4.14-4.20                  | 4.17         |

A = Aldridge Formation, L = lower, M = middle, U = upper.

projection of the Vulcan Low (Figure 12-2), as defined by Clowes et. al. (1997). By analogy, the western projection of the southern boundary should also be considered a highly prospective area for sedex-type mineralization. Are there other Vulcan Low-type continental structures that control mineralization along the Purcell (Belt) basin? Detailed gravity surveys may be a useful tool to locate and define other northeast transverse zones or rift axis offsets within the basin. Such studies may provide new exploration targets.

#### ACKNOWLEDGMENTS

The author thanks Derek Brown, Trygve Höy and Bill McMillan (B.C. Geological Survey Branch), Carmel Lowe (GSC-Sidney) and Fred Cook (U. of Calgary) for their comments. The interpretations are entirely the author's.

Figure 12-1 is a plot of 11,638 U.S. Geological Survey records and 904 Geological Survey of Canada records. The Canadian gravity data is available from the Geophysical data Centre (fdostaler@gsc,NRCan.gc.ca) at \$0.01CND/point and the USA gravity data is available from NOAA/National Geophysical Data Center (info@ngdc.noaa.gov) for approximately \$200 USD. Surfer for Windows (www.golden.com) software was

used for data reduction. Data is presented as simple Bouguer gravity values without terrain corrections.

#### REFERENCES CITED

- Anderson, H.E. and Davis, D.W. (1995): U-Pb geochronology of the Moyie sills, Purcell Supergroup, southeastern British Columbia: implications for the Mesoproterozoic geological history of the Purcell (Belt) basin, *Can. J. Earth Sci.* 32, p. 1180-1193.
- Clowes, R., Hammer, P., Mandler, H., Ross, G., Cook, F., Eaton, D. (1997): The Vulcan Low, Matzhiwin High and related domains as revealed by SALT 95 reflection data; in Ross, G.M., (compiler), *1997 Alberta Basement Transects Workshop*, Lithoprobe Report #59, Lithoprobe Secretariat, University of British Columbia, p. 15-22.
- Cook, F.A. and van der Velden, A.J. (1995): Three-dimensional crustal structure of the Purcell anticlinorium in the Cordillera of southwestern Canada; *Geological Society of America Bulletin*, v. 107, p. 642-664.

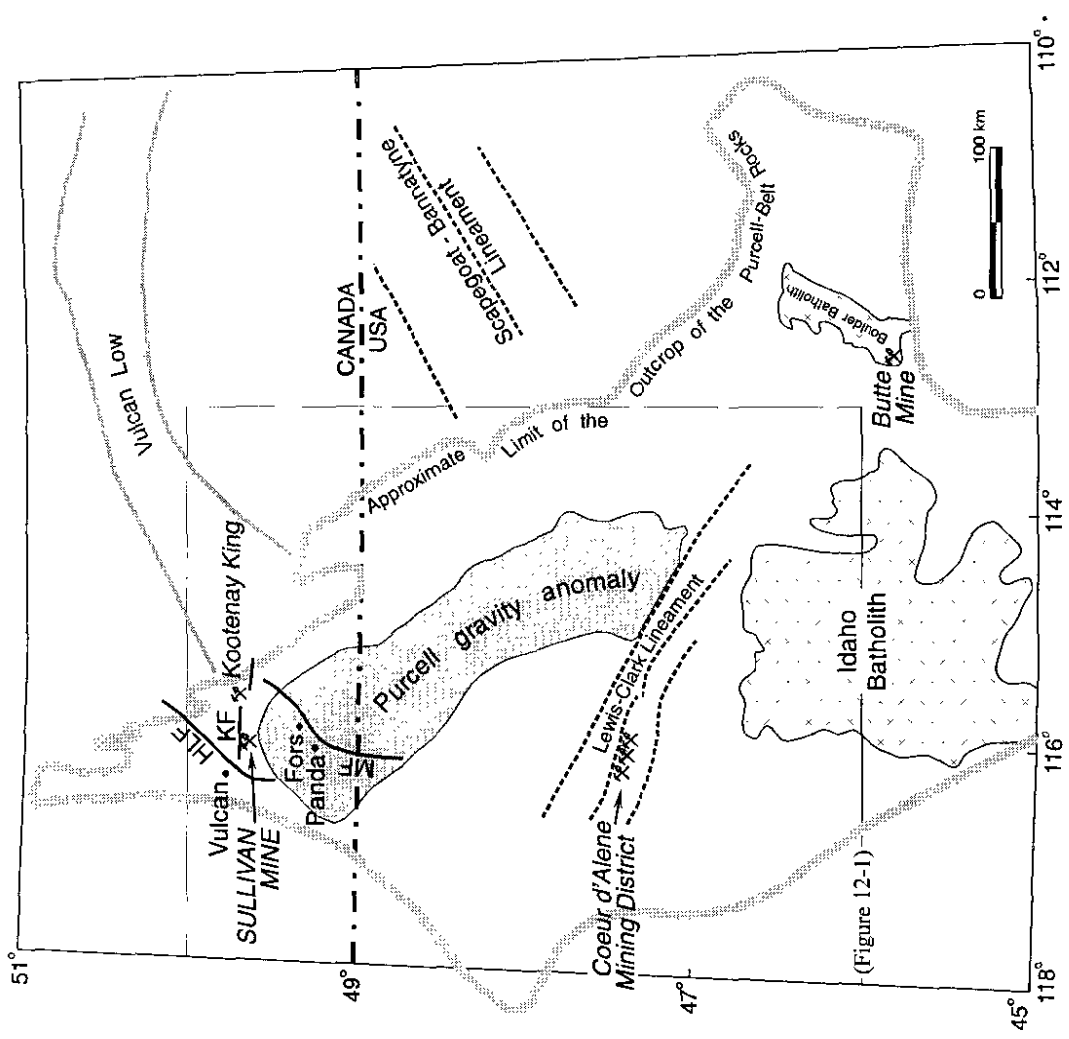


Figure 2. Map showing location of Purcell gravity anomaly and regional structures. Abbreviations are as follows: HLF, Hall Lake fault; MF, Moyie fault; and KF, Kimberley fault. The location of the Purcell gravity anomaly is outlined in grey.

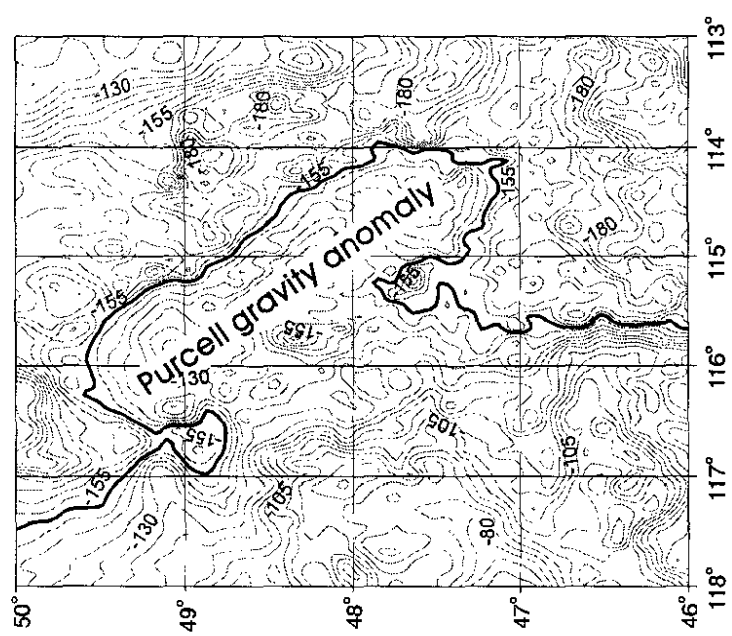


Figure 1. Simple Bouguer gravity anomaly map for part of the Purcell anticlinorium. 12,542 stations from U.S. Geological Survey and Geological Survey of Canada records.

- Cressman, E.R. (1989): Reconnaissance Stratigraphy of the Prichard Formation (Middle Proterozoic) and the Early Development of the Belt Basin, Washington, Idaho and Montana; *U.S. Geological Survey, Professional Paper* 1490.
- Höy, T. (1982a): Stratigraphic and Structural Setting of Stratabound Lead-Zinc Deposits in Southeastern B.C.; *Canadian Institute of Mining and Metallurgy, Bulletin* 75, Number 80, p. 114-134.
- Höy, T. (1982b): The Purcell Supergroup in Southern British Columbia; Sedimentation, Tectonics and Stratiform Lead-Zinc Deposits; *in Precambrian Sulphide Deposits, H.S. Robinson Memorial Volume, Hutchinson, R.W., Spence, D.D. and Franklin, J.M., Editors, Geological Association of Canada, Special Paper* 25.
- Höy, T. (1993): Geology of the Purcell Supergroup in the Fernie West-half map area, Southeastern British Columbia; *B.C. Ministry of Energy, Mines and Petroleum Resources, Bulletin* 84, 157p.
- Höy, T., Turner, R.J.W., Leitch, C.H.B., Anderson, D., Ransom, P.W., Pighin, D. and Brown, D. (1995): Depositional Environment, Alteration and Associated Magmatism, Sullivan and Related Massive Sulphide Deposits, Southeastern B.C.; A1: Field Trip Guidebook, Victoria '95, GAC/MAC Annual Meeting—May 17-19, 1995, p. 6-7.
- Price, R.A. (1981): The Cordilleran Foreland Thrust and Fold Belt in the Southern Canadian Cordillera; *in Thrust and Nappe Tectonics, McClay, K.R. and Price, N.J., Editors, Geological Society of London, Special Publication* 9, p. 427-448.
- Turner, R.W., Höy, T., Leitch, C.H.B., Anderson, D. and Ransom, P.W. (1993): Guide to the Geological Setting of the Middle Proterozoic Sullivan Sediment-hosted Pb-Zn Deposit, Southeastern British Columbia; *in Link, P.K., Editor, Geologic Guidebook to the Belt-Purcell Supergroup, Glacier National Park and Vicinity, Montana and Adjacent Canada; Belt Symposium III Fieldtrip Guidebook, Belt Association Inc., Spokane, Washington, p. 53-94.*



British Columbia Geological Survey  
Geological Fieldwork 1997

## Economic Geology

# STRATABOUND BASE METAL DEPOSITS OF THE BARKERVILLE SUBTERRANE, CENTRAL BRITISH COLUMBIA (093A/NW)

By Trygve Höy and Filippo Ferri  
B.C. Geological Survey Branch

**KEYWORDS:** Economic geology, massive sulphides, sedex, carbonate-hosted lead-zinc, gold-quartz veins, Ace, Mae, Barkerville subterrane, Snowshoe Group, Downey succession, Ramos succession.

Barkerville subterrane. This paper describes and classifies a number of known mineral occurrences and attempts to correlate stratigraphic packages in the Barkerville with other parts of the Kootenay terrane.

## INTRODUCTION

The Barkerville subterrane is part of the pericratonic Kootenay terrane, deposited along the western edge of ancestral North America. The Kootenay terrane, and possible correlative rocks of northern British Columbia and Yukon, contain numerous volcanogenic massive sulphide deposits, concentrated largely in EoCambrian to Early Cambrian and Middle Devonian to Early Mississippian times. These periods represent contrasting tectonic regimes along the continental margin, with distinct volcanic assemblages and characteristic massive sulphide deposits.

Tholeiitic and alkalic mafic volcanism in latest Precambrian through early Paleozoic time records episodic extensional tectonics along the rifted, western margin of North America. Mafic volcanics occur locally in the EoCambrian part of the Hamill Group, as Unit EBG in the Eagle Bay Assemblage and in the basal part of the Index Formation in the Goldstream area north of Revelstoke. A number of Cu-Zn Besshi-type deposits of the Goldstream camp are the best examples of volcanogenic massive sulphides in these mafic volcanic/metasedimentary successions.

Bimodal arc volcanism occurred along the preserved western margin of the Kootenay terrane in middle to late Paleozoic time, in response to eastward subduction of a paleopacific ocean. Within the Eagle Bay Assemblage, this volcanism is recorded as thick accumulations of mafic and felsic pyroclastic rocks. In the Omineca Mountains in northern British Columbia, the Gilliland tuff records similar volcanism (Ferri, 1997). Rhyolitic and rhyodacitic tuffs of Unit EBA of the Eagle Bay Assemblage contain numerous small, polymetallic massive sulphide deposits.

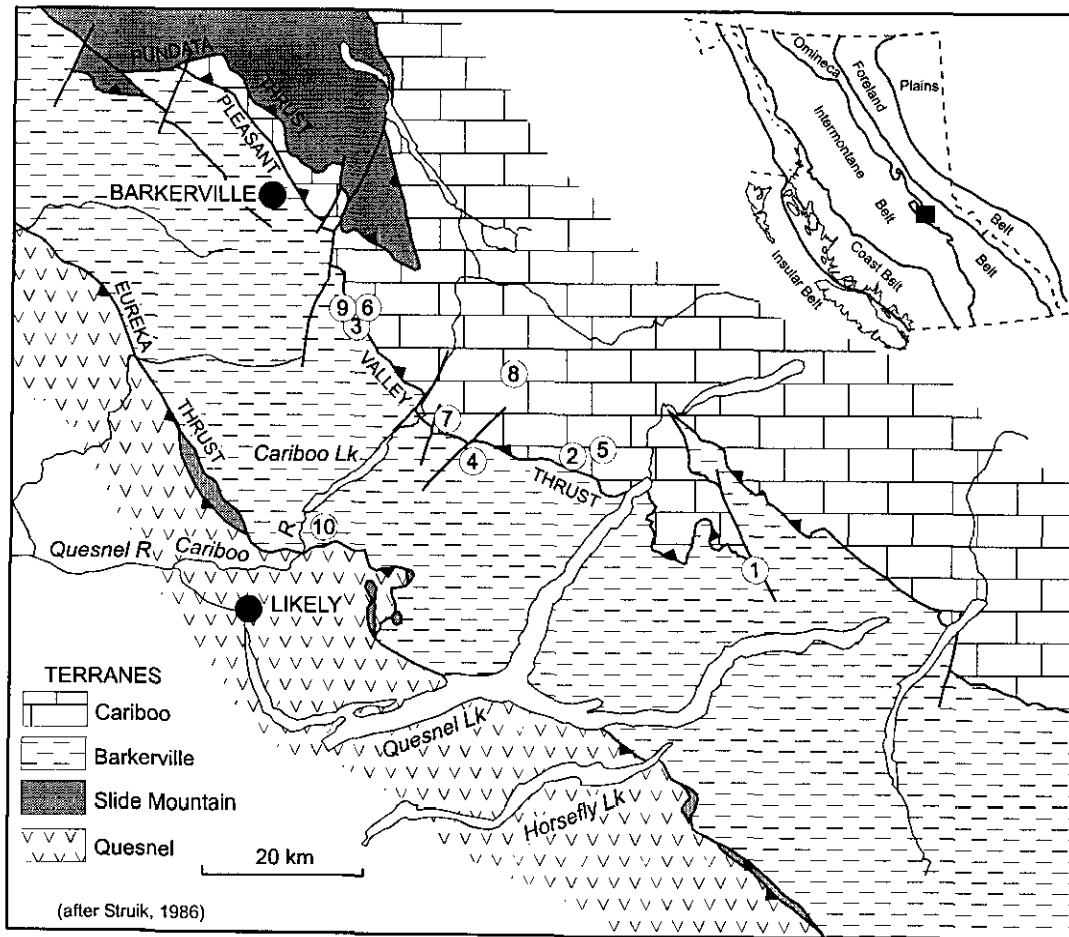
The objective of this study is to evaluate the potential for massive sulphide mineralization in the

## REGIONAL GEOLOGY

The Barkerville-Likely area is underlain by three fault-bounded geological terranes (Struik, 1988). The Barkerville subterrane is separated from more inboard rocks of the Cariboo subterrane by the west-verging Pleasant Valley thrust fault. The oceanic Slide Mountain terrane has been structurally emplaced along the western margin of the Barkerville subterrane, carried on the east-verging Eureka Thrust fault (Figure 1). It also structurally overlaps the Barkerville and Cariboo terranes along the Pundata thrust (Struik, *op. cit.*). Rocks in these terranes have been polydeformed and metamorphosed, possibly as early as middle Paleozoic time (Sutherland Brown, 1963) but certainly during the Mesozoic (Struik, 1981, 1988).

The stratigraphy of the Barkerville subterrane has been assigned, almost entirely, to the Proterozoic to Paleozoic Snowshoe Group (Struik, 1986; 1988). This package of rocks is dominated by distal, fine grained siliciclastics with lesser carbonate and volcanics. It has been subdivided into several informal units: Ramos succession, Tregillus clastics, Kee Khan marble, Keithley succession, Harveys Ridge succession, Goose Peak quartzite, Agnes conglomerate, Eaglesnest succession, Downey succession, Bralco limestone, Hardscrabble Mountain succession, unnamed carbonate, Island Mountain amphibolite and Tom succession (Figure 2).

Units of assumed Proterozoic age include the Ramos, Tregillus, Kee Khan and Keithley packages. Lithologies are dominated by feldspathic quartzite and phyllite in the Ramos and Tregillus successions and grey quartzite and phyllite of the Keithley succession. These lithologies have similarities with Windermere sequences in the Cordillera.



| Property                       | Commodities      | Host                              | Deposit type(s)               | Terrane     |
|--------------------------------|------------------|-----------------------------------|-------------------------------|-------------|
| 1. Green Ice (093A 082)        | Zn               | Snowshoe Gp limestone             | disseminated/vein             | Barkerville |
| 2. Mae (093A 083)              | Cu-Zn-Pb         | Downie calc silicate              | stratabound?                  | Barkerville |
| 3. Peter Gulch (093A 093)      | Pb-Zn            | Snowshoe Gp limestone             | vein/replacement              | Barkerville |
| 4. Ace (new) (093A 142)        | Cu-Au-Ag-Zn-(Pb) | Downie "phyllite"                 | volcanogenic massive sulphide | Barkerville |
| 5. Al (093A 065)               | Pb-Zn-(Cu)       | Cunningham limestone              | replacement Zn-Pb             | Cariboo     |
| 6. Vic (093A 070)              | Pb-Zn-barite     | Midas Fm limestone                | stratiform (sedex?)           | Cariboo     |
| 7. Maybe (093A 110)            | Pb-Zn-Ag         | Black Stuart Gp black pelite unit | replacement/vein              | Cariboo     |
| 8. Comin Throu Bear (093A 158) | Pb-Zn-barite     | Mural Fm limestone                | replacement                   | Cariboo     |
| 9. Cunningham Creek area       | Pb-Zn            | Hardscrabble Mtn limestone        | stratiform (sedex?)           | Barkerville |
| 10. Big Gulp (new) (093A 143)  | Cu-Zn-(Ag-Au)    | Downie phyllite                   | volcanogenic massive sulphide | Barkerville |

Figure 1: Regional geology of the Barkerville - Likely area showing major terrane boundaries and massive sulphide occurrences (after Struik *et al.*, 1992).

|                               |                      |                                  |
|-------------------------------|----------------------|----------------------------------|
| Upper Paleozoic               | Snowshoe Group       | Sugar limestone                  |
|                               |                      | Island Mountain amphibolite      |
|                               |                      | Hardscrabble Mountain succession |
| Paleozoic                     |                      | Bralco limestone                 |
|                               |                      | Eaglenest succession             |
|                               |                      | Downey succession                |
|                               |                      | Agnes conglomerate               |
|                               |                      | Goose Peak quartzite             |
| Late Proterozoic              |                      | Harveys Ridge succession         |
|                               |                      | Keithley succession              |
|                               | Kee Khan marble      |                                  |
|                               | Tregillus succession |                                  |
| Late Proterozoic or Paleozoic | Ramos succession     |                                  |
|                               | Tom succession       |                                  |

Figure 2: Stratigraphic chart of the Barkerville subterrane (after Struik, 1988); see text for suggested revision.

The age of the Paleozoic part of the succession is problematic as it is based primarily on a few fossil localities and correlations of several units with sections of the Eagle Bay Assemblage farther south. The Harveys Ridge succession (Figure 2), a package of black micaceous quartzite, siltite, phyllite, conglomerate, limestone and mafic metavolcanics, is correlated with Unit EBS of the Eagle Bay Assemblage (Struik, 1988; Schiarizza and Preto, 1987). The age of unit EBS is bracketed between Early Cambrian and Middle Devonian. Micaceous feldspathic quartzite, phyllite, marble and mafic metavolcanics of the Downey succession are also correlated, in part, with unit EBS. The Downey contains several microfossil localities of broadly Paleozoic age. The Bralco limestone is interpreted to sit stratigraphically above these successions. It contains Paleozoic echinoderm fragments and has been correlated with the Early Cambrian Tshinakin limestone of the Eagle Bay Assemblage (Struik, 1988; Schiarizza and Preto, 1987).

## VOLCANIC ROCKS: SNOWSHOE GROUP

Our work concentrated on examining and sampling the volcanic successions and immediate host rocks

within the Snowshoe Group in order to attempt to correlate these with volcanic rocks elsewhere within the Kootenay Terrane. Due to intense deformation and moderate to high grades of regional metamorphism, recognition and interpretation of volcanic rocks can be difficult in the area. However, two distinct successions have been identified (Struik, *op. cit.*), within the Downey and Ramos successions.

### Downey Succession

The Downey succession is "characterized from others of the Snowshoe Group by its abundant marble and tuff" (Struik, 1988, page 59). Volcanic rocks include "green chlorite phyllite", "volcanic tuff", and diorites" that may also be tuffs (Struik, *op. cit.*).

Green phyllites of the Downey succession are interlayered with marbles, calcsilicate schists, phyllites and impure quartzites. They are commonly massive, consisting mainly of quartz, muscovite and chlorite with variable but minor garnet, actinolite, carbonate, clinozoite and/or opaques. Locally, green chlorite phyllites contain prominent augens, several centimetres in length, of quartz, feldspar and chlorite. Phyllites may weather a pale brown colour due to alteration of fine iron-rich carbonate.

At higher metamorphic grades, volcanic rocks of the Downey succession are amphibolites. These were recognized at the Mae prospect (Figure 1) and as thick, competent units within phyllite and marble on Barker Mountain (Struik, 1988). Amphibolites on the Mae property are thin, massive to finely laminated layers within coarse-grained garnet-sericite-biotite schist. They are rusty weathering due to finely dispersed pyrrhotite.

Analyses of a few samples of Downey succession metavolcanics are given in Table 1. Major element analyses suggest that they are subalkaline; however, these elements can be relatively mobile during regional metamorphism and, hence, plots with less mobile trace elements are typically more reliable. On a Zr/TiO<sub>2</sub> versus Nb/Y diagram, Downey metavolcanics appear to be alkaline, with compositions ranging from alkali basalts to trachy andesites (Figure 3a), whereas on an SiO<sub>2</sub> versus Zr/TiO<sub>2</sub> diagram (Figure 3b), these same samples plot mainly in the subalkaline fields.

### Discussion

Mafic volcanic rocks are recognized in at least three separate stratigraphic levels in ancestral North American and Kootenay terrane rocks of southern and central British Columbia: (1) Late Proterozoic to Early Cambrian Hamill Group, Mohican Formation or correlative(?) EBG of the Eagle Bay Assemblage, (2) Early Paleozoic Index Formation of the Lardeau Group and mafic volcanics of EBS in the Eagle Bay, and (3) the middle (?) Paleozoic Jowett Formation of the Lardeau Group and EBM of the Eagle Bay.

TABLE 1: MAJOR AND TRACE ELEMENT ANALYSES OF SAMPLES OF METAVOLCANIC ROCKS OF THE SNOWSHOE GROUP

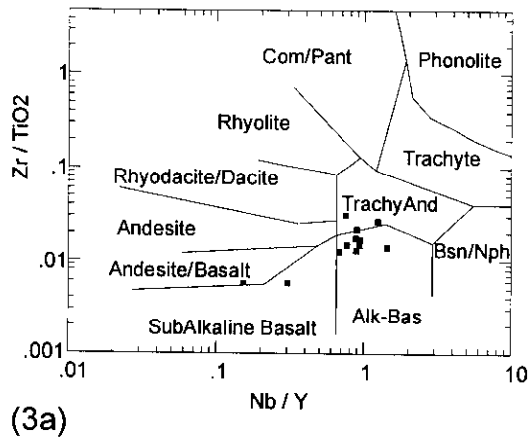
| Sample                         |     | H97    | H97    | H97   | H97   | H97    | H97    | H97   | H97    | H97    | H97   | H97   | H97    | H97    | H97    | H97   |       |
|--------------------------------|-----|--------|--------|-------|-------|--------|--------|-------|--------|--------|-------|-------|--------|--------|--------|-------|-------|
|                                |     | BC-59d | BC-60e | BC-6a | BC-6b | BC-11a | BC-11b | BC-32 | BC-34a | BC-34b | BC-36 | BC-37 | BC-43a | BC-43c | BC-43e | BC-44 | BC-45 |
| Description                    |     | ATMM   | ATMM   | BGMM  | BGMM  | GCMM   | GCMM   | HCMM  | HCMM   | HCMM   | MM    | MM    | RFV    | RFV    | RFV    | RFV   | RFV   |
| SiO <sub>2</sub>               | %   | 62.5   | 55.51  | 50.73 | 55.97 | 52.18  | 47.87  | 63.01 | 58.09  | 58.32  | 58.34 | 58.1  | 78.32  | 78.18  | 75.08  | 80.78 | 74.55 |
| TiO <sub>2</sub>               | %   | 0.77   | 0.96   | 0.58  | 0.66  | 1.01   | 0.93   | 1.07  | 1.15   | 1.16   | 0.88  | 1.16  | 0.39   | 0.39   | 0.57   | 0.35  | 0.52  |
| Al <sub>2</sub> O <sub>3</sub> | %   | 17.78  | 21.15  | 15.84 | 18.29 | 14.95  | 14.45  | 18.29 | 19.82  | 19.95  | 19.95 | 20.02 | 10.14  | 10.13  | 11.7   | 9.24  | 11.38 |
| Fe <sub>2</sub> O <sub>3</sub> | %   | 1.4    | 1.21   | 1.22  | 1.77  | 1.85   | 2.14   | 2     | 2.22   | 1.84   | 1.63  | 1.09  | 2.18   | 2.3    | 2.75   | 1.79  | 1.02  |
| FeO                            | %   | 5.6    | 6.17   | 11.73 | 3.58  | 7.85   | 9.32   | 4.8   | 5.96   | 5.89   | 5.07  | 6.4   | 1.28   | 1.7    | 1.29   | 1.13  | 3.01  |
| MnO                            | %   | 0.03   | 0.05   | 0.12  | 0.06  | 0.17   | 0.21   | 0.04  | 0.15   | 0.08   | 0.13  | 0.07  | 0.02   | 0.04   | 0.03   | 0.04  | 0.04  |
| MgO                            | %   | 2.56   | 2.36   | 7.26  | 3.44  | 7.2    | 7.44   | 1.93  | 2.22   | 2.31   | 2.41  | 2.13  | 1.01   | 1      | 1.16   | 0.65  | 1.37  |
| CaO                            | %   | 0.24   | 1.01   | 2.38  | 5.26  | 8.58   | 13.27  | 0.13  | 0.24   | 0.19   | 0.93  | 1.04  | 0.2    | 0.12   | 0.18   | 0.17  | 0.6   |
| Na <sub>2</sub> O              | %   | 0.87   | 1.37   | 2.64  | 2.92  | 3.43   | 1.1    | 0.32  | 1.53   | 1.05   | 1.67  | 2.03  | 2.24   | 1.16   | 0.73   | 1.87  | 2.45  |
| K <sub>2</sub> O               | %   | 3.6    | 4.9    | 0.03  | 2.8   | 0.13   | 0.18   | 3.85  | 3.9    | 4.23   | 4.3   | 2.91  | 1.27   | 1.79   | 3.36   | 1.97  | 2.23  |
| P <sub>2</sub> O <sub>5</sub>  | %   | 0.1    | 0.12   | 0.13  | 0.12  | 0.07   | 0.08   | 0.07  | 0.12   | 0.1    | 0.06  | 0.14  | 0.05   | 0.05   | 0.07   | 0.06  | 0.07  |
| LOI                            | %   | 4.17   | 4.65   | 7.01  | 4.37  | 2.57   | 2.26   | 4.19  | 4.26   | 4.25   | 4.16  | 3.87  | 2.6    | 2.82   | 2.64   | 1.85  | 2.24  |
| SUM                            | %   | 99.77  | 99.54  | 99.68 | 99.69 | 100    | 99.25  | 99.82 | 99.85  | 99.54  | 99.71 | 99.25 | 99.74  | 99.73  | 99.66  | 99.95 | 99.53 |
| Nb                             | ppm | 18     | 32     | 15    | 15    | 5      | 10     | 31    | 23     | 23     | 23    | 27    | 9      | 11     | 16     | 13    | 15    |
| Sr                             | ppm | 102    | 194    | 195   | 498   | 77     | 64     | 68    | 173    | 163    | 288   | 690   | 104    | 62     | 52     | 94    | 138   |
| Y                              | ppm | 24     | 36     | 17    | 16    | 33     | 33     | 25    | 26     | 34     | 30    | 29    | 15     | 8      | 13     | 17    | 19    |
| Zr                             | ppm | 235    | 206    | 100   | 111   | 58     | 53     | 282   | 149    | 146    | 131   | 171   | 181    | 181    | 261    | 238   | 249   |
| V                              | ppm | 92     | 119    | 118   | 105   | 308    | 282    | 124   | 120    | 136    | 110   | 141   | 57     | 52     | 70     | 42    | 77    |
| Ba                             | ppm | 530    | 540    | 0     | 3500  | 0      | 0      | 950   | 1200   | 1300   | 1200  | 2000  | 310    | 360    | 750    | 460   | 350   |
| Zn                             | ppm | 120    | 122    | 605   | 141   | 0      | 80     | 168   | 0      | 127    | 153   | 0     | 0      | 115    | 0      | 0     | 0     |
| Co                             | ppm | 18     | 18     | 17    | 14    | 41     | 41     | 8     | 30     | 18     | 16    | 20    | 5      | 6      | 10     | 8     | 10    |
| Cr                             | ppm | 160    | 190    | 130   | 120   | 500    | 430    | 150   | 180    | 170    | 140   | 140   | 220    | 160    | 180    | 200   | 160   |
| Cs                             | ppm | 4      | 4      | 0     | 3     | 1      | 0      | 4     | 4      | 4      | 4     | 2     | 2      | 3      | 5      | 2     | 2     |
| Hf                             | ppm | 9      | 9      | 3     | 5     | 2      | 2      | 10    | 6      | 6      | 5     | 6     | 7      | 7      | 10     | 10    | 9     |
| Na                             | ppm | 0.69   | 1.09   | 2.03  | 2.27  | 2.64   | 0.76   | 0.23  | 1.14   | 0.77   | 1.19  | 1.59  | 1.93   | 0.99   | 0.69   | 1.57  | 2.04  |
| Ni                             | ppm | 130    | 0      | 0     | 0     | 0      | 79     | 0     | 0      | 0      | 0     | 0     | 0      | 0      | 0      | 0     | 0     |
| Rb                             | ppm | 82     | 170    | 0     | 97    | 0      | 19     | 120   | 160    | 140    | 170   | 110   | 62     | 66     | 110    | 68    | 76    |
| Sc                             | ppm | 14     | 20     | 12    | 15    | 44     | 40     | 16    | 19     | 20     | 17    | 21    | 6.6    | 7.2    | 9.2    | 6.7   | 9.2   |
| Ta                             | ppm | 1.4    | 2      | 0     | 0     | 0      | 0      | 0     | 0      | 1.3    | 2.3   | 2.2   | 0      | 0      | 0      | 0     | 0     |
| Th                             | ppm | 15     | 22     | 12    | 13    | 0      | 0      | 14    | 12     | 11     | 15    | 13    | 8.4    | 11     | 13     | 15    | 12    |
| U                              | ppm | 1.7    | 4.3    | 0     | 3.3   | 0      | 0      | 3.6   | 2.5    | 2.8    | 2.7   | 0     | 2.5    | 2.4    | 2.4    | 3.3   | 2.3   |
| La                             | ppm | 51     | 86     | 28    | 51    | 1.7    | 1.8    | 35    | 50     | 58     | 58    | 49    | 15     | 8.3    | 21     | 36    | 33    |
| Ce                             | ppm | 91     | 150    | 50    | 79    | 8      | 6      | 65    | 92     | 99     | 99    | 84    | 30     | 17     | 57     | 55    | 63    |
| Nd                             | ppm | 32     | 66     | 18    | 26    | -5     | -5     | 25    | 39     | 46     | 41    | 38    | 8      | 9      | 13     | 28    | 23    |
| Sm                             | ppm | 6.4    | 10     | 2.8   | 4.4   | 1.7    | 1.6    | 4.1   | 6.2    | 7.2    | 6.5   | 6.2   | 2      | 1      | 2.6    | 3.9   | 3.8   |
| Eu                             | ppm | 1.7    | 2.6    | 1     | 1     | 0      | 0.9    | 1.3   | 1.9    | 2.3    | 1.8   | 1.2   | 0.6    | 0.4    | 0.8    | 1.1   | 1     |
| Tb                             | ppm | 0      | 1.7    | 0     | 0     | 0      | 0.8    | 0     | 1      | 0.9    | 0     | 0     | 0      | 0      | 0      | 0     | 0.8   |
| Yb                             | ppm | 3      | 5.1    | 1.1   | 1.7   | 3.4    | 3      | 3.2   | 3.3    | 4      | 3     | 3     | 1.4    | 1.1    | 1.8    | 1.6   | 2.3   |
| Lu                             | ppm | 0.45   | 0.82   | 0.18  | 0.31  | 0.57   | 0.45   | 0.51  | 0.54   | 0.69   | 0.47  | 0.51  | 0.19   | 0.2    | 0.35   | 0.31  | 0.28  |

ATMM: Ace Trench mafic metavolcanics; BGMM: Big Gulp mafic metavolcanics; GCMM: Grain Ck mafic metavolcanics; HCMM: Hailey Ck. mafic metavolcanics; MM: mafic metavolcanics; RFV: Ramos felsic volcanics. Major Oxides, Nb, Sr, Y, Zr and V analyzed by X-Ray Fluorescence at Cominco Laboratories, Vancouver, British Columbia. Remaining elements analyzed by Thermal Neutron Activation Analysis at ActLabs, Ancaster, Ontario.

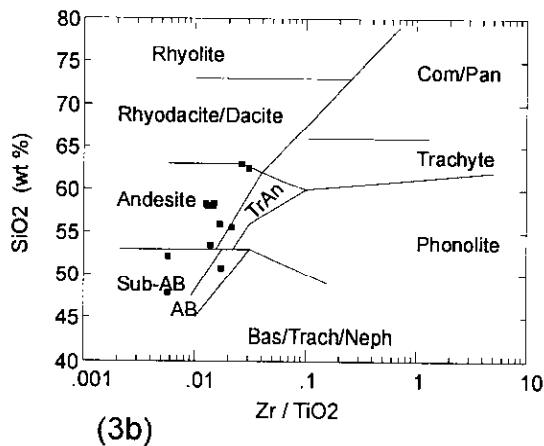
Preliminary geochemical data of Downey mafic volcanic rocks suggests they are comparable to the dominantly alkali basalts of the Late Proterozoic Hamill Group (Logan *et al.*, 1996). However, two undiagnostic fossils, collected from the Downey succession, indicate a Paleozoic (but less likely Cambrian) age (Struik, 1988, p. 60), restricting correlations to the Lardeau Group.

A correlation of Downey metavolcanics with Jowett Formation basalts near the top of the exposed Lardeau Group in both the Goldstream (Logan and Rees, 1997) and Ferguson (Fyles and Eastwood, 1962) areas is also possible. However, the close association of mafic volcanics, limestone, impure quartzite and phyllites is

most comparable to the Index Formation at the base of the Paleozoic Lardeau Group. This is supported by a stratigraphic contact with a white marble, the Bralco, which may correlate with the Early Cambrian Tshinakin limestone (Struik, *op. cit.*; Schiarizza and Preto, *op. cit.*) or Badshot (Mural) Formation. A correlation of the Bralco - Downey with the Badshot - Index implies that the Snowshoe Group is inverted and may generally young to the west. Considerable more sampling, analyses and interpretation are required to characterize Downey metavolcanics and to make comparisons with the dominantly Mid-Ocean ridge basalt (MORB) compositions of the Index Formation.



(3a)



(3b)

Figure 3: (a): Zr/TiO<sub>2</sub> versus Nb/Y and (b) SiO<sub>2</sub> versus Zr/TiO<sub>2</sub> plots of samples of metavolcanic rocks of the Downey succession; data in Table 1 (plot after Winchester and Floyd, 1977).

Correlating the Downey with the basal Lardeau has considerable implications regarding metallogeny of the Barkerville subterrane. The Index Formation contains numerous volcanogenic massive sulphide deposits, including Goldstream (Höy, 1979; Logan and Colpron, 1995), and therefore the Downey succession must be considered prospective ground for exploration of this deposit type. The restriction of most gold mineralization of the Barkerville camp to the Downey succession (Struik, 1988) may also, by analogy, point to the potential for discovery of lode gold deposits in the Index Formation to the south.

### Ramos Succession

The Ramos succession comprises micaceous quartzites, phyllite and siltstone with minor amphibolite, marble and tuffaceous units. Tuff near the top of the Ramos succession in Ramos Creek and Swift River "includes 1 to 2 metre thick beds in black and olive phyllite and fine grained quartzite. Along Keithley Creek tuff is interlayered with dark grey and

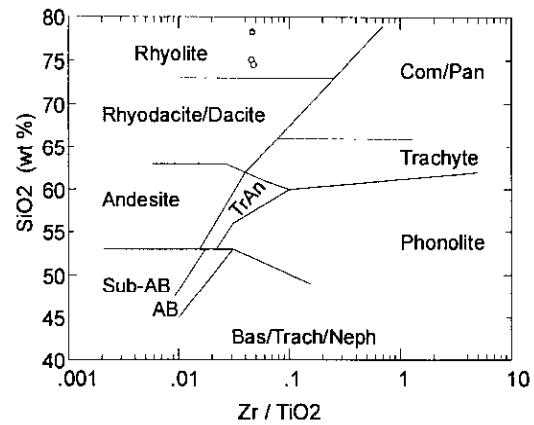
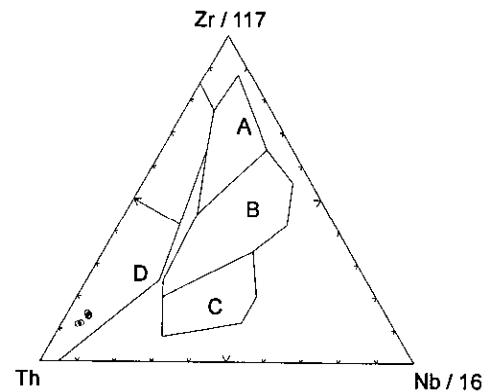
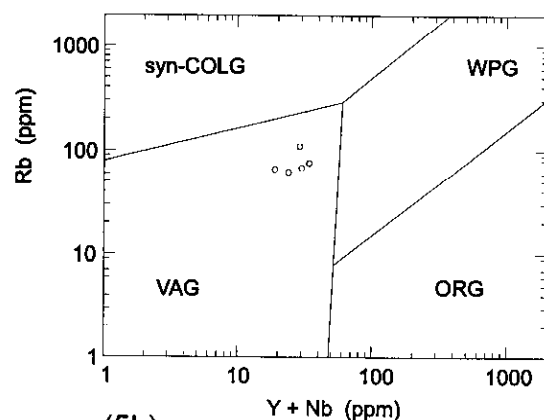


Figure 4: SiO<sub>2</sub> versus Zr/TiO<sub>2</sub> plot of samples of metavolcanic rocks of the Ramos succession; data in Table 1 (plot after Winchester and Floyd, 1977).



(5a)



(5b)

Figure 5 (a): Nb-Th-Zr plot (after Wood, 1980) and (b) Rb versus Y+Nb plot (after Pearce *et al.*, 1984) of samples of metavolcanic rocks of the Ramos succession, showing their volcanic arc affinity. A - N-type MORB; B - E-type MORB, C - alkaline within plate, D - destructive plate margin.

olive phyllite near the upper contact of the Ramos with the Harveys Ridge succession" (Struik, 1988, p. 52).

A poorly exposed section of Ramos tuffs on a logging road along the western slopes of Ramos Creek includes several tens of metres of tan to brown weathering quartz-eye sericite phyllites with minor interbeds of argillite or argillaceous phyllite. In thin section, they comprise crystals of quartz and feldspar in a matrix of sericite, biotite, quartz, feldspar and minor chlorite; other samples contain small clasts, up to a millimetre in length, of intergrown quartz and feldspar. These rocks are interpreted to be intermediate to felsic ash and crystal tuffs. However, separated zircons appear to have a detrital origin, suggesting either considerable reworking of these units or a sedimentary origin (J. Mortenson, personal communication, 1997). An attempt to date these zircons is now in progress.

Analyses of Ramos tuffs (Table 1) support felsic compositions. Analyzed samples are calcalkaline rhyolites (Figure 4). On a trace element tectonic discrimination diagram, Ramos tuffs plot in the volcanic arc field (Figure 5a) and on a Rb versus Y+Nb plot, designed for intrusive rocks, they also plot in the volcanic arc granitoid field (Figure 5b).

### Discussion

The Ramos succession has been assigned a Late Proterozoic age, based largely on structural interpretations, regional correlations and superposition of units (Struik, 1988). We suggest, however, that a Devonian age for the Ramos is possible, supporting a model that the Snowshoe Group tends to young to the west.

Arc volcanism in the Kootenay terrane was first documented in Devonian rocks of the Eagle Bay Assemblage. These comprise thick accumulations of felsic and mafic pyroclastic rocks, containing a number of Late Devonian subvolcanic plutons. It is possible that felsic arc volcanics of the Ramos succession are thin, distal correlatives of these Eagle Bay volcanics. Furthermore, the Quesnel Lake orthogneisses may be subvolcanic intrusions related to this volcanism. This is supported by the similar volcanic arc signatures of these gneisses (in preparation) and their restriction to western exposures of the Snowshoe Group.

The suggestion that Ramos tuffs are Devonian in age allows correlation with felsic arc volcanics in the Yukon-Tanana terrane, host to the Kudz Ze Kayah and Wolverine deposits, the Gilliland tuffs in the Big Creek Group, and the massive sulphide host rocks of the Eagle Bay Assemblage.

### Summary: Stratigraphic Correlations

Struik (1988), in his definitive work on the Snowshoe Group, correlates certain parts of this succession with similar lithologies in the Eagle Bay Assemblage. This includes equating the Bralco and Tshinakin limestones and the Harveys Ridge and

Downey successions with unit EBS. More precise ages on parts of the Eagle Bay Assemblage (Schiarizza and Preto, 1987), and reevaluation of volcanic successions, allow for possible reinterpretation of the stratigraphic succession of the Snowshoe Group. Schiarizza and Preto (*op. cit.*), based on the presence of archeocyathids, assigned an Early Cambrian age to the Tshinakin limestone and placed unit EBS broadly in the Early Cambrian to Middle Devonian due to its stratigraphic position above the Tshinakin and below Middle Devonian felsic volcanics.

Hence, we suggest revisions to the assigned ages of some members of the Snowshoe Group. The Devonian-Mississippian age of the Hardscrabble Mountain succession is probably correct, based on similarities of its black siltites and abundance of Pb-Zn-Ba sedex showings with Devonian-Mississippian black clastic successions (the Earn Assemblage) elsewhere in the miogeocline. The relative ages of the Ramos to Keithley successions become problematic. We suggest that the felsic tuff intercalated with gritty to phyllitic rocks of the Ramos succession may be Devonian to Mississippian in age and correlative, in part, with unit EBA of the Eagle Bay Assemblage. The Tregillus, Kee Khan and Keithley successions would then be Paleozoic in age. Finally, we suggest that the Downey may correlate with the basal part of the Lardeau Group.

## DEPOSITS

### Cunningham Creek occurrences

Numerous small, conformable lead-zinc showings occur in the Cunningham Creek valley south of Barkerville (Figure 1). These showings comprise argentiferous galena, sphalerite, pyrite +/- barite in a dark graphitic shale sequence that has been correlated with the Late Proterozoic Midas Formation (Hodgson, 1978; Longe *et al.*, 1978; Longe, 1979). Struik (1988), however, places similar occurrences on the south side of the Cunningham Creek in the Late Paleozoic Hardscrabble Mountain succession. We suggest that the nature of these deposits, similar to sediment-hosted massive sulphide deposits, and their close spatial association, argues for a common host and, hence, include all of them in Hardscrabble Mountain.

The Cunningham Creek showings were discovered between 1971 and 1976 by Coast Interior Ventures Ltd. and Riocanex Ltd. in a follow up of both stream and soil geochemical anomalies. Extensive trenching, sampling and limited drilling has recognized both the stratabound nature and the extent of mineralization in the Roundtop Mountain area.

Showings on the northeast side of Cunningham Creek are within a structurally complex succession of phyllites, sandstones, slates, dark shales and minor carbonates (Hodgson, *op. cit.*). Holland (1954) and Sutherland Brown (1963) map this succession as right way up whereas Struik (1988) interprets it to be inverted. The sulphide-barite layers are in either dark

limestone or associated black pyritic shales that locally contain minor chert.

The Vic showing (093A 070) comprises massive, fine-grained galena and sphalerite in a siliceous unit in grey banded limestone of a black graphitic shale succession (Longe *et al.*, *op. cit.*). The showing is conformable with layering, of variable width, and exposed strike length of 20 metres.

The Evening showing, located approximately 1200 metres south of Vic, is similar, with fine-grained sulphides, but is in black cherty shales. A geochemical soil anomaly suggests mineralization is more extensive than that exposed in trenching. Samples of the Vic and Evening showings, from Longe *et al.* (*op. cit.*) assayed:

|         | % Pb | % Zn | oz/t Ag | sample width |
|---------|------|------|---------|--------------|
| Vic 1   | 3.3  | 3.65 | 0.41    | 30 cm        |
| Vic 2   | 13.1 | 7.6  | 1.72    | 20 cm        |
| Evening | 0.99 | 3.25 | 0.23    | 40 cm.       |

A number of other showings in the immediate area also have similar mineralogy as Vic and are hosted in either black siliceous shales or dark limestone. Due to extensive overburden and structural complexity it is not possible to determine if these are structural repetitions or separate stratigraphic horizons. The X anomaly, 3 kilometres southeast of the Evening showing, is hosted in dark limestone and consists of minor disseminated sphalerite and galena, and some massive barite with pyrite. Drilling intersected green chloritic phyllite that may be a mafic volcanic unit, as well as some coarse, probable volcanoclastic units (Hodgson, 1978). The Bralco zinc showing comprises massive to wispy sphalerite with less galena, also in siliceous dark limestone. Grades of two grab samples averaged 5.3 % Pb, 15 % Zn and 0.9 oz/t Ag (Longe, 1977).

Showings south of Cunningham Creek (A-1, A-2 and Ten Dollar) occur in silicified dolostone or limestone that Struik (1988) correlates with the Hardscrabble Mountain succession. Detailed mapping by Hodgson (*in Longe et al.*, *op. cit.*), correlates these successions with those north of Cunningham Creek, supporting a model that all conformable sulphide deposits are in Hardscrabble Mountain.

The conformable (stratabound) nature of many of these showings, their simple mineralogy, fine grain size, host stratigraphy and lack of replacement textures suggest that they may be sedimentary exhalite deposits.

## Mae (093A 087)

### Introduction

The Mae property comprises a number of layers of stratabound Pb-Zn-Cu mineralization in a calcsilicate-amphibolite assemblage of the Downey succession. It is located north of the 8400 logging road, just west of Maeford Lake (Figure 1).

The property was initially staked in 1988, following the discovery of sulphide-bearing float and a follow-up soil geochemical survey (Pride, 1989). Subsequent soil surveys outlined three zones with coincident lead-zinc anomalies. Despite limited outcrop, mineralization was discovered in two of the anomalous zones (Pride, *op. cit.*).

The area is underlain by a northwest dipping succession of garnet schist, black phyllite, calcsilicate gneiss and minor marble and amphibolite of the Downey succession. Although interpreted to be middle Paleozoic in age (Struik, 1988), it is suggested that the Downey may correlate with the Early Paleozoic Index Formation. Immediately to the north, this succession is overlain by a thick limestone-marble unit, the Bralco limestone. Late northwest trending faults, with displacements of a few tens of metres, cut these units. The regional metamorphic grade is high, with garnets and staurolites developed in pelitic units and amphibole in calcsilicates and mafic metavolcanics.

Mineralization in the lower anomalous zone comprises dispersed sulphides in two thin, rusty-weathering, fine-grained quartz-garnet amphibolite layers. High Mn content is reflected in the abundant spessartine (+ almandine/grossular) garnets in the amphibolite (Table 2). The amphibolites are interlayered with coarse-grained garnet-biotite schist, minor calcsilicate gneiss and thin impure marble layers. Petrographic study of a piece of float from this showing contained approximately 10 percent opaques, comprising 60 % pyrite, 20 % pyrrhotite, 12 % magnetite, 5 % chalcopyrite 2 % galena and 1 % sphalerite (Pride, 1989). Pyrite (and marcasite) occurs in late veinlets and replacing pyrrhotite.

The second anomalous zone, on the slopes above the lower zone, is underlain mainly by the Bralco limestone. The only discovered mineralization is minor galena in a sparry dolomite filled fracture within the marble. It is not believed to be the source of the Zn-Pb geochemical anomaly (Pride, 1989).

These showings and host succession have similarities with Mn-rich, stratabound Pb-Zn showings of the Bend prospect (Leask, 1982; Reddy and Godwin, 1987) north of Golden. They also have similarities with volcanogenic sulphide deposits, in particular Besshi-type deposits. These include a mixed mafic volcanic(?) / metasedimentary host succession and a copper, zinc and lead metal content.

## Big Gulp (093A 143)

Big Gulp is a new discovery by Barker Minerals Ltd. It is located approximately 1.5 kilometres south of Cariboo Lake, along "C road", a spur of the 8400 logging road. Work on the property is limited, with only reconnaissance mapping, some sampling, and a soil geochemical survey.

TABLE 2: ASSAYS OF HAND SAMPLES OF MASSIVE SULPHIDE PROSPECTS IN THE SNOWSHOE GROUP,  
BARKERVILL SUBTERRANE

| Sample          | Description       | Source | Mo<br>ppm | Cu<br>ppm | Pb<br>ppm | Zn<br>ppm | Ag<br>ppm | Au<br>ppb | Ni<br>ppm | Co<br>ppm | Mn<br>ppm | Sr<br>ppm | Cd<br>ppm | Bi<br>ppm | V<br>ppm | La<br>ppm | Cr<br>ppm | Ba<br>ppm |
|-----------------|-------------------|--------|-----------|-----------|-----------|-----------|-----------|-----------|-----------|-----------|-----------|-----------|-----------|-----------|----------|-----------|-----------|-----------|
| <b>BIG GULP</b> |                   |        |           |           |           |           |           |           |           |           |           |           |           |           |          |           |           |           |
| 1197BC-6C       | py-se schist      | 1      | < 2       | 674       | 61        | 45031     | < .5      | 14        | 42        | 62        | 2343      | 457       | 171       | 19        | 58       | 15        | 98        | 125       |
| <b>ACE</b>      |                   |        |           |           |           |           |           |           |           |           |           |           |           |           |          |           |           |           |
| 1197BC-10       | po-chl schist     | 1      | 20        | 630       | 17        | 393       | 0.5       | 6         | 123       | 70        | 6055      | 158       | < .4      | < 5       | 431      | 28        | 77        | 26        |
| H97BC-1-E-1     | py-qtz schist     | 1      | 3         | 427       | 39        | 524       | 1.6       | 6         | 253       | 22        | 6537      | 279       | 1         | < 5       | 869      | 27        | 67        | 109       |
| H97BC-1-E-2     | po-qtz schist     | 1      | 2         | 673       | 58        | 131       | 1.4       | < 2       | 214       | < 2       | 17624     | 249       | 0.8       | 7         | 1336     | 41        | 84        | 86        |
| RAL 97-9        | qtz-bi schist     | 2      | 5         | 361       | 11        | 95        | < 5       | < 5       | 124       | 62        | 9182      | 216       | < 1       | 5         | 797      | 27        | 183       | 74        |
| RAL 97-10       | qtz-se schist     | 2      | 60        | 50        | 65        | 617       | < 5       | 6         | 54        | 9         | 1204      | 246       | 9         | < 5       | 144      | 22        | 117       | 812       |
| 1133            | sulphide schist   | 3      | 5         | 3249      | < 2       | 306       | 1.4       | 35        | 23        | 55        | 1590      | 24        | < 1       | < 5       | 159      | < 10      | 29        | 15        |
| 1362            | gn-qtz-chl schist | 3      | < 1       | 1281      | 10        | 35        | 3.2       | 75        | 474       | 138       | 1586      | 37        | 2         | < 5       | 107      | < 10      | 72        | 50        |
| <b>MAE</b>      |                   |        |           |           |           |           |           |           |           |           |           |           |           |           |          |           |           |           |
| 1197BC-46-2b    | po-amph schist    | 1      | < 2       | 403       | 57        | 159       | < .5      | 13        | 104       | 13        | 43955     | 22        | 1.5       | 6         | 208      | 27        | 76        | 1         |
| 1197BC-46-2c    | po-amph schist    | 1      | 6         | 772       | 30        | 112       | < .5      | 8         | 130       | 25        | 21236     | 26        | < .4      | < 5       | 144      | 36        | 76        | 3         |
| 1197BC-46-3a    | po-amph schist    | 1      | < 2       | 328       | 10        | 77        | < .5      | 132       | 45        | 7         | 28360     | 8         | < .4      | 9         | 100      | 27        | 39        | < 1       |

| Sample          | Fe<br>% | Ca<br>% | P<br>% | Ti<br>% | Na<br>% | K<br>% |
|-----------------|---------|---------|--------|---------|---------|--------|
| <b>BIG GULP</b> |         |         |        |         |         |        |
| 1197BC-6C       | 10.57   | 8.57    | 0.04   | 0.03    | 0.46    | 0.7    |
| <b>ACE</b>      |         |         |        |         |         |        |
| 1197BC-10       | 18.11   | 2.44    | 0.592  | 0.2     | 0.93    | 0.94   |
| H97BC-1-E-1     | 23.15   | 3.46    | 0.478  | 0.13    | 0.78    | 1.36   |
| H97BC-1-E-2     | 17.24   | 6.93    | 0.246  | 0.11    | 0.72    | 1.84   |
| RAL 97-9        | >10     | 5.92    |        | 0.06    | 0.32    | 1.09   |
| RAL 97-10       | 3.03    | 2.13    |        | 0.05    | 2.05    | 0.57   |
| 1133            | 9.41    | 0.39    | 0.19   | <.01    | <.04    | <.01   |
| 1362            | 26.3    | 2.04    | 0.49   | <.01    | <.01    |        |
| <b>MAE</b>      |         |         |        |         |         |        |
| 1197BC-46-2b    | 18.48   | 3.04    | 0.309  | 0.1     |         |        |
| 1197BC-46-2c    | 17.48   | 2.8     | 0.308  | 0.11    |         |        |
| 1197BC-46-3a    | 12.64   | 1.49    | 0.097  | 0.09    |         |        |

Notes: Analyses of float samples of Barker Minerals are by Echo-tech labs, Kamloops  
Analyses of samples, this report are by MIC, Acme Analytical Laboratories, Vancouver  
MIC = HClO<sub>4</sub>-HNO<sub>3</sub>-HCl-HF digestion and ICP  
FAC = Fire assay-ICP/graphite furnace finish  
data source: 1. this report; 2. R. Lane, personal communication, 1997; 3. Barker Minerals Ltd.  
arsenic: Big Gulp = 16 ppm. all other values below 10 ppm

Big Gulp is a stratabound semi-massive sulphide occurrence in the Downey succession. Immediate host rocks are pale grey to green sericite phyllite and darker chlorite phyllite; both contain abundant dispersed ankerite and variable amounts of calcite. These phyllites are interpreted to be altered mafic tuffs (samples H97BC-6a, 6b, Table 1). The phyllites overlie Quesnel Lake orthogneiss immediately to the southwest and are structurally overlain by a "chert to cherty tuff" horizon and then argillite (Roach, 1997).

Mineralization comprises a number of thin layers with dark sphalerite, and minor chalcopyrite and pyrite, dispersed in a siliceous, sericitic matrix. It is streaked parallel to a prominent west-plunging mineral lineation. Sulphides also occur in thin, discontinuous foliation-parallel quartz stringers. A grab sample assayed 4.5 % Zn and 0.06% Cu (H97BC-6a; Table 2), and a sample by Roach (1997) contained 3.17 % Zn and 0.04 % Cu.

The host succession and Zn-Cu tenor suggest similarities with Besshi-type massive sulphide mineralization. Alteration, including sericitic, silicification and "brownish-white carbonate" just northwest of the showing, is also characteristic of this deposit type.

## Ace

### Introduction

The Ace property is located on the south side of the Little River, approximately 35 km northeast of Likely (Figure 1). It is readily accessible by the Welwood 8400 logging road that cuts through the property. Exposures in the area are minimal, largely restricted to isolated outcrops along the banks of the Little River, on the higher slopes of Mount Barker, in logging roadcuts and in recent trenches. A considerable part of the property has been logged; the remainder is covered by stands of fir, spruce and pine, and by considerable thicknesses of glacial till.

High gold values in sands of the Little River as well as sulphide float boulders, first recognized by Louis Doyle, led to the acquisition of the Ace property and formation of Barker Minerals Ltd. in 1994. Subsequent detailed prospecting, line cutting and soil geochemistry outlined a sulphide boulder float train and coincidental geochemical anomalies that paralleled the regional structural trend. More recent work, during the summer of 1995, including additional prospecting, geochemistry, geophysical surveys and some geological mapping, defined more clearly exploration targets on the property. As a result of successful regional work, the property was expanded significantly in 1996, and now includes prospects such as Big Gulp and the Maybe (*see* Höy and Ferri, 1998). Work in 1997 included considerable trenching, geological mapping and sampling. The following description of the Ace property incorporates results presented in assessment reports as well as unpublished internal reports by Barker Minerals Ltd.

Two main targets are apparent on the Ace claims: massive sulphides and gold-quartz veins. Both of these were recognized in the float train and have since been discovered in trenches. Geochemical soil surveys identified coincident Zn and Pb anomalies, with threshold values of 100 and 25 ppm respectively, along the northern margin of the float train. A moderately anomalous Cu zone was identified to the south, along the lower slopes of Mount Barker; it is locally associated with high As values. The regional extent of these anomalies, their tenor and their orientation parallel to regional structural and stratigraphic trends, suggest that they may be related to massive sulphide targets. Local Bi anomalies, and erratic Au highs, may be related to vein mineralization.

### Geology

The Ace property is underlain by phyllitic rocks of the Downey succession. These have been assigned an early to middle Paleozoic age, possibly correlative, in part, with the Broadview Formation of the Lardeau Group (Struik, 1986); however, as described above, they may correlate with the Index Formation at the base of the Lardeau. The succession trends easterly, with moderate dips to the north. It has been cut by at least two prominent northeast trending faults (Struik, 1988), referred to informally as the GSC-1 and GSC-2 faults by Barker Minerals Ltd., that may define a horst in the central part of the Ace claims (Lammle, 1997).

Dominant rock types in trenches include tan to pale grey or green phyllites and dark grey graphitic phyllite, both interpreted to be fine grained metasediments. These are interlayered occasionally with impure sericite quartzites or orthoquartzites and rare dark limestone beds. Green, massive chlorite phyllites are interpreted to be mafic volcanics. At higher metamorphic grades on the northern slopes of Mount Barker, these occur as amphibolites that are referred to as "diorites" or "diorite tuffs" (Struik, 1988).

### Mineralization and alteration

The two dominant deposit types on the Ace property, semimassive sulphides and gold-quartz veins, have been found in numerous float samples, in trenches and in a few of the natural exposures.

Pyrite and pyrrhotite are commonly dispersed throughout phyllites on the Ace property. Semimassive sulphides, dominantly pyrite and pyrrhotite, are also concentrated parallel to foliation in coarse, quartzofeldspathic schists. Sulphide concentrations greater than 50 per cent are common and, therefore, the term "massive sulphide" is locally appropriate. The sulphides are deformed, along with their gangue and host succession, in a ductile manner. A crude banding is often apparent, defined by variable sulphide/silicate concentrations. Chalcopyrite and sphalerite contents are variable, but generally less than a few per cent each.

The sulphide host rock is typically a granular quartz-feldspar schist or phyllite, with grain size up to several millimetres. In the field it has been variously

referred to as an exhalite, leucocratic diorite, quartzite or siliceous alteration zone. However, as these various rock types are not all at a single stratigraphic horizon, it is possible that they represent, in part, distinct units. The schist is commonly banded due to either variable sulphide or possibly biotite content. This banding appears to be a tectonic rather than a primary fabric. The schist comprises dominantly plagioclase (andesine and albite) and quartz with varying amounts muscovite, sericite, biotite, ankerite, calcite and opaques (Payne, 1997). Several per cent apatite is common, with local concentrations greater than 20 per cent.

Petrographic work (Payne, *op.cit.*) suggests that the original rock is an intrusive leucodiorite? that has undergone various degrees of alteration, deformation and mineralization. These include albitization, producing aggregates of fine-grained, equant, non-twinned albite, silicification with introduction of quartz, and potassic (muscovite / sericite and minor K-spar) and magnesian (phlogopite) alteration. Late chlorite commonly replaces biotite. Early sulphides include both pyrrhotite and pyrite, with minor finely dispersed chalcopyrite and sphalerite. Subhedral pyrite grains appear to have formed as a replacement of pyrrhotite; chalcopyrite and pyrite are both commonly remobilized into thin discontinuous veinlets. Marcasite may occur as a late replacement of other iron sulphides.

Analyses of a number of sulphide host rock samples are listed in Table 2. Of note are the high Cu/Pb and Zn/Pb ratios and relatively high Mn values, typical of some Besshi deposits. However, Co/Ni ratios are considerably lower than those typical of Besshi deposits.

Numerous white quartz veins, locally with abundant sulphides, occur on the Ace property. Some are folded along with their host rock while others are clearly post tectonic, cutting across foliation. These may be folded during deformation that crenulates foliation. Veins contain variable amounts of quartz and pyrite, generally minor base metal sulphides and muscovite, biotite, chlorite and tourmaline. "Mineralogical studies indicate the presence of cubanite, various tellurides, cosalite, native bismuth and native gold and prismatic tourmaline. Geochemical analyses indicate presence of Fe, As, Au, Ag, Zn, Cu, Bi and Te and locally at least some Ni, Co and Cr. For the most part, the microscope studies reveal that native gold is sometimes associated with native bismuth, native tellurium and with Bi and Te minerals. In others, gold is enclosed in quartz, in sulphide minerals and along the edges of sulphide minerals" (internal Barker Minerals report, August, 1997).

Analyses of numerous quartz-sulphide float samples, collected and analyzed by Barker Minerals Ltd., indicate variable but locally appreciable gold content; 53 samples had an average gold content of 3106 ppb, with a range from 220 ppb to 28,972 ppb (Lammle, 1997).

## Summary and discussion

Semimassive to massive sulphide mineralization on the Ace claims has similarities to Besshi style volcanogenic massive sulphide deposits. Host rocks include a succession of sericite phyllites, impure quartzites, minor calcareous units and chlorite phyllites. These are interpreted to be metasediments and mafic metavolcanic units. They are similar to and may correlate with the basal Index Formation in the Goldstream area, host to a number of massive sulphide deposits.

Sulphides, dominantly pyrrhotite and pyrite with minor chalcopyrite and sphalerite, are in a granular feldspathic schist. The protolith of this unit is unknown; however, it has similarities to the siliceous alteration zone that hosts Goldstream massive sulphides (Höy, 1979) and the albite envelope around other Besshi style deposits (Slack, 1993) and is, therefore, interpreted to be largely an alteration envelope. More regional alteration includes potassic (sericite +/- K-spar), magnesium (chlorite and phlogopite), and widely dispersed pyrite and pyrrhotite.

The metal content, dominantly Cu and Zn with low Pb, is also similar to Besshi deposits. As well, anomalous concentrations of a variety of metals, including Co, Mo, Bi, As and Ni are typical of many Besshi deposits (Slack, 1993). These deposits can also contain high precious metal content, with typical grades of 5 to 20 ppm Ag and variable but locally high gold values.

The gold-quartz veins have some similarities with vein mineralization of the Barkerville-Wells camp. These deposits include both early replacement deposits and younger gold-sulphide veins. They all occur in the Downey succession, in rocks of greenschist facies regional metamorphism, and in fold hinges or along consistent fault or fracture patterns. By analogy, veins on the Ace property may have similar stratigraphic, metamorphic and structural control. Their distribution, coincident with semimassive sulphide mineralization and targets, and somewhat similar base and precious metal content, suggest that they may be, in part, remobilized from these early deposits as has been suggested for deep level veins associated with deposits in the Besshi district, Japan (*see* Slack, 1993).

## SUMMARY AND DISCUSSION

The Snowshoe Group of the Barkerville subterranean contains at least two separate and distinct packages of metavolcanic rocks. Correlation of these successions with volcanics elsewhere in the Kootenay terrane allows possible revision of the recognized Snowshoe Group succession.

We suggest that the metavolcanics of the Downey succession may correlate with tholeiitic basalts of the Lower Paleozoic Index Formation and with some of the greenstones of unit EBG of the Eagle Bay assemblage.

Furthermore, we propose that felsic volcanics of the Ramos succession correlate with Devono-Mississippian arc volcanics of the Eagle Bay Assemblage.

Revised correlation of the Snowshoe Group has considerable metallogenic implications. The Downey succession, host to numerous gold veins and replacement deposits in the Barkerville-Wells area, also has potential for Besshi-type volcanogenic massive sulphide deposits similar to those that occur in the Index Formation in the Goldstream camp. Recognition and correlation of Ramos succession tuffs with arc volcanics of the Eagle Bay and possibly Devono-Mississippian volcanics of the Yukon-Tanana terrane enhances its potential for discovery of Kuroko-type (polymetallic) massive sulphide deposits.

Recent discovery by Barker Minerals Ltd. of Cu-Zn+/-Au occurrences in the Downey, including the Ace and Big Gulp prospects, may be examples of stratabound volcanogenic deposits.

## ACKNOWLEDGEMENTS

Louis Doyle and personnel of Barker Minerals Ltd. are thanked for their support and encouragement of this project. Discussions with numerous individuals, including B. Struik, P. Schiarizza, B. Lane, L. Doyle and J. Payne are much appreciated. R. Lett is thanked for expediting samples for geochemical analyses, M. Fournier for helping prepare diagrams, and G. Light for assisting in the field. Reviews of this manuscript by D. Lefebure, P. Schiarizza and B. Struik are gratefully acknowledged.

## REFERENCES

- Ferri, F. (1997): Nina Creek Group and Lay Range Assemblage, North-central British Columbia: Remnants of Late Paleozoic Oceanic and Arc Terranes; *Canadian Journal of Earth Sciences*, Volume 34, pages 854-874.
- Fyles, J.F. and Eastwood, G.P.E. (1962): Geology of the Ferguson Area, Lardeau District, British Columbia; *B.C. Ministry of Energy, Mines and Petroleum Resources*, Bulletin 45.
- Hodgson, G.D. (1978): Geology of Cunningham Creek Claims; in Barkerville Project - 1977; Cunningham Creek Claims, *B.C. Ministry of Energy, Mines and Petroleum Resources*, Assessment Report 6545
- Holland, S.S. (1954): Geology of the Yanks Peak-Roundtop Mountain Area, Cariboo District, British Columbia; *British Columbia Department of Mines*, Bulletin 34, 102 pages.
- Höy, T. (1979): Geology of the Goldstream Area, *B.C. Ministry of Energy, Mines and Petroleum Resources*, Bulletin 71, 49 pages.
- Höy, T. and Ferri, F. (1998): Zn-Pb Deposits in the Cariboo Subterranean, Central British Columbia (93A/NW); *B.C. Ministry of Employment and Investment*, Geological Fieldwork 1997, Paper 1998-1.
- Lammle, C.A.R. (1997): Little River and Ace Properties, Cariboo Mining Division, British Columbia; internal report, *Barker Minerals Ltd.*
- Leask, J.M. (1982): Geology of the MGM Property, Big Bend District, East Central British Columbia; *B.C. Ministry of Energy, Mines and Petroleum Resources*, Assessment Report 9994.
- Logan, J.M. and Colpron, M. (1995): Northern Selkirk Project - Geology of the Goldstream River Map Area (82M/9) and Parts of 82M/10; *B.C. Ministry of Energy, Mines and Petroleum Resources*, Geological Fieldwork 1994, Paper 1995-1, pages 215-242.
- Logan, J.M., Colpron, M. and Johnson, B.J. (1996): Northern Selkirk Project - Geology of the Downie Creek Map Area (82M/8); *B.C. Ministry of Energy, Mines and Petroleum Resources*, Geological Fieldwork 1995, Paper 1996-1, pages 107-125.
- Logan, J.M. and Rees, C. (1997): Northern Selkirk Project, Geology of the Laforme Creek Area, (82M/1); *B.C. Ministry of Employment and Investment*, Geological Fieldwork 1996, Paper 1997-1, pages 25-38.
- Longe, R.V. (1977): Barkerville Project: Description of Sulphide Showings and Geochemistry of Soils; *B.C. Ministry of Energy, Mines and Petroleum Resources*, Assessment Report 6314.
- Longe, R.V. (1979): Bralco Option: 1978 Programme of Trenching and Drilling, Cariboo Mining District; *B.C. Ministry of Energy, Mines and Petroleum Resources*, Assessment Report 7106.
- Longe, R.V., Hodgson, G.D. and McCance, J. (1977): Barkerville Project - 1977; Cunningham Creek Claims; *B.C. Ministry of Energy, Mines and Petroleum Resources*, Assessment Report 6545.
- Payne, J.G. (1997): Geological Report; internal report, *Barker Minerals Ltd.*
- Pearce, T.H., Harris, N.B.W. and Tindle, A.G. (1984): Trace Element Discrimination Diagrams for the Tectonic Interpretation of Granitic Rocks; *Journal of Petrology*, Volume 25, pages 956-983.
- Pride, K.R. (1989): Assessment Report - 1989: Geology and Geochemistry of Mae Mineral Claims, Cariboo Mining District, B.C.; *B.C. Ministry of Energy, Mines and Petroleum Resources*, Assessment Report 19,327.
- Reddy, D.G. and Godwin, C.I. (1987): Geology of the Bend Zinc-lead-silver Massive Sulphide Prospect, Southeastern British Columbia; *B.C. Ministry of Energy, Mines and Petroleum Resources*, Geological Fieldwork 1986, Paper 1987-1, pages 47-52.
- Roach, S.N. (1997): Geological Mapping Surveys Conducted on the Goose Range Project Area, Cariboo Mining Division, B.C.; internal report, *Barker Minerals Ltd.*
- Schiarizza, P. and Preto, V.A. (1987): Geology of the Adams Plateau-Clearwater-Vavenby Area; *B.C.*

- Ministry of Energy, Mines and Petroleum Resources*, Paper 1987-2, 88 pages.
- Slack, J.F. (1993): Descriptive and Grade-tonnage Models for Besshi-type Massive Sulphide Deposits; in *Mineral Deposit Modelling*, Kirkham, R.V., Sinclair, W.D., Thorpe, R.I. and Duke, J.M. (Editors); *Geological Association of Canada*, Special Paper 40, pages 343-371.
- Struik, L.C. (1981): A Re-examination of the Type Area of the Devonian-Mississippian Cariboo Orogeny, Central British Columbia; *Canadian Journal of Earth Sciences*, Volume 18, pages 1767-1775
- Struik, L.C. (1986): Imbricated Terranes of the Cariboo Gold Belt with Correlations and Implications for Tectonics in Southeastern British Columbia; *Canadian Journal of Earth Sciences*, Volume 23, pages 1047-1061.
- Struik, L.C. (1988): Structural Geology of the Cariboo Gold Mining District, East-central British Columbia; *Geological Survey of Canada*, Memoir 421, 100 pages.
- Struik, L.C., Murphy, D.C. and Rees, C.J. (1992): Cariboo Mountains and Cariboo Highlands; in *Geology of the Cordilleran Orogeny in Canada*; Chapter 17, Gabrielse, H. and Yorath, C.J. (Editors), *Geological Survey of Canada*, pages 614-615.
- Sutherland Brown, A. (1963): Geology of the Cariboo River Area, British Columbia; *B.C. Ministry of Energy, Mines and Petroleum Resources*, Bulletin 47.
- Winchester, J.A. and Floyd, P.A. (1977): Geological Discrimination of Different Magma Series and their Differentiation Products Using Immobile Elements; *Chemical Geology*, Volume 20, pages 325-342.
- Wood, D.A. (1980): The Application of a Th-Hf-Ta Diagram to Problems of Tectomagmatic Classification and to Establishing the Nature of Crustal Contamination of Basaltic Lavas of the British Tertiary Volcanic Province; *Earth and Planetary Sciences Letters*, Volume 20, pages 11-30.



## Zn-Pb DEPOSITS IN THE CARIBOO SUBTERRANE, CENTRAL BRITISH COLUMBIA (93A/NW)

By Trygve Höy and Filippo Ferri  
B.C. Geological Survey Branch

**KEYWORDS:** Economic geology, massive sulphides, carbonate hosted Zn-Pb, Maybe, Comin Throu Bear, Cariboo subterrane, Barkerville subterrane, Kootenay terrane, Cassiar terrane, Cariboo Group, Black Stuart Group.

### INTRODUCTION

The Cariboo subterrane comprises dominantly Precambrian to Early Mesozoic clastic and carbonate rocks that were deposited along the western margin of North America (Struik, 1988). It correlates with parts of the Cassiar Platform and Selwyn Basin of the Yukon and northern British Columbia, and with Proterozoic and Paleozoic rocks in the Selkirk and Purcell Mountains of southern British Columbia. These rocks include both basinal and platformal sediments with demonstrated stratigraphic ties to North America. They contain numerous mineral deposits, including a variety of veins, Pb-Zn and W skarns, and carbonate and sediment-hosted massive sulphide occurrences. These massive sulphide deposits are the focus of this paper.

This paper overviews known Zn-Pb massive sulphide deposits of the Cariboo subterrane in the Likely-Barkerville area (Figure 1), focusing on the Maybe (MINFILE no. 093A 110) prospect. The paper is part of a regional study of both volcanogenic and sediment-hosted massive sulphide deposits in adjacent Kootenay terrane and correlative Yukon-Tanana terranes (Nelson *et al.*, 1997). A companion paper (Høy and Ferri, 1998) overviews the geology of the Barkerville subterrane, compares it to the other parts of the Kootenay terrane, and describes, classifies and compares contained massive sulphide deposits.

### MASSIVE SULPHIDE DEPOSITS

Massive sulphide deposits in miogeoclinal rocks correlative with those in the Cariboo subterrane include stratiform sediment hosted deposits and carbonate replacement deposits. Sediment hosted deposits (sedex deposits) are concentrated during periods of extensional tectonics, typified by marine transgressions, pronounced

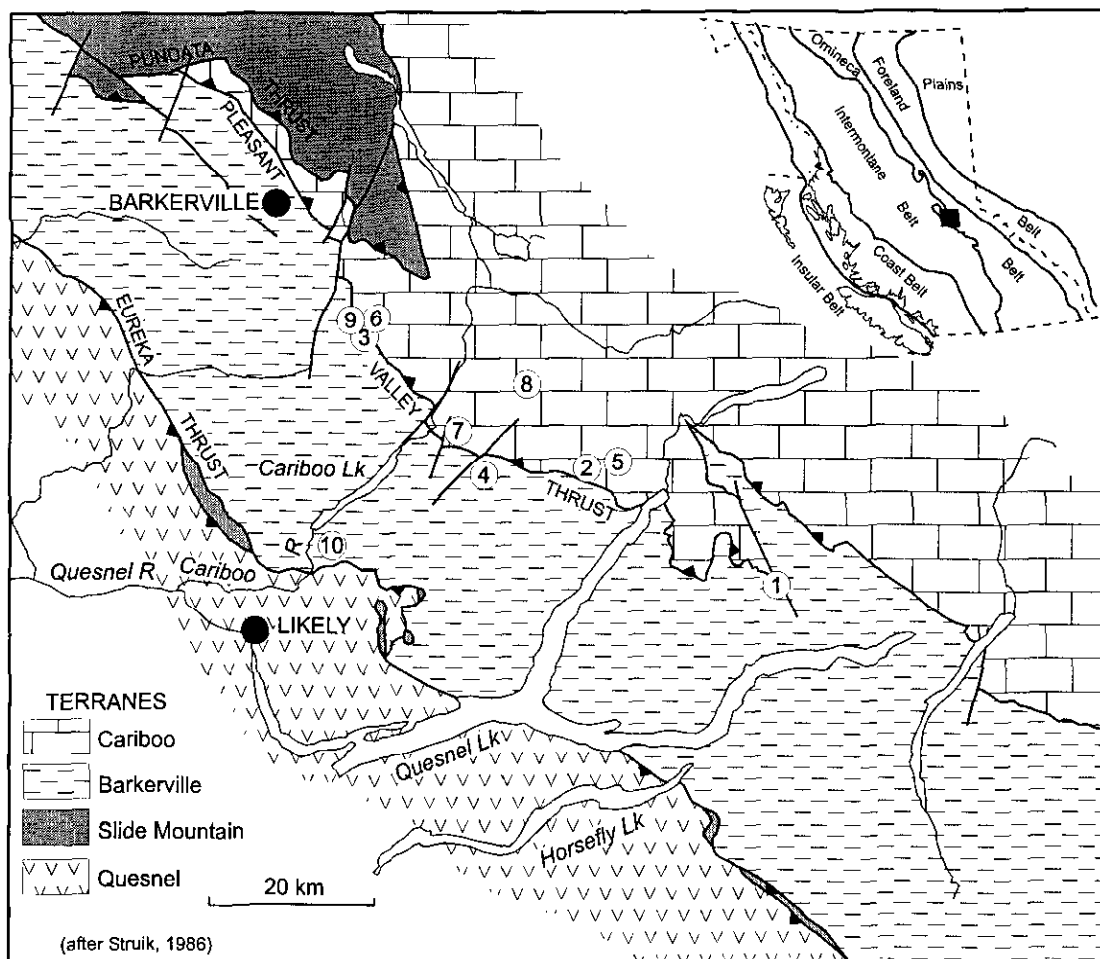
facies changes from shallow to deeper water, and locally with mafic volcanism. Carbonate-replacement deposits are also commonly controlled by tectonics, localized near regional unconformities and along major structural breaks.

EoCambrian to Early Cambrian time is marked, locally, by rifting, volcanism and submergence along the ancestral continental margin. Sedex deposits occur in a variety of rock types in British Columbia including the Bend in platformal carbonate rocks (Leask, 1982), Cottonbelt and other Shuswap deposits in high grade metamorphic rocks of the Monashee Complex (Fyles, 1970; Höy, 1987) and Lucky Coon and Mosquito King in a metasedimentary / metavolcanic succession of the Eagle Bay Assemblage (Schiarizza and Preto, 1987). As well, carbonate-replacement deposits characterize Early Cambrian platformal carbonates in the Kootenay Arc; those in Middle Cambrian rocks, including Monarch and Kicking Horse in the Rocky Mountains, occur at a platform margin.

A marine transgression in Middle Ordovician time, also marked locally by mafic volcanism, is associated with sedex deposits in Road River Group rocks of the Gataga District (McIntyre, 1991). In southern British Columbia, a few small carbonate-hosted Pb-Zn occurrences, such as Hawk Creek (082N 021), may be in Ordovician rocks.

In Middle Devonian to Early Mississippian time, opening of the Slide Mountain ocean to the west is believed to have occurred in response to arc volcanism along the distal continental margin, remnants of which are found in the Eagle Bay Assemblage of the Kootenay terrane (Ferri, 1997). Continental margin rocks are characterized by extensional tectonics, isolated rift basins, minor volcanism and major unconformities, an event referred to as the "Little Diastrophism" by Struik (1980). These rocks host numerous large sedex deposits, including Pb-Zn-barite deposits in the Ketchika trough and Selwyn basin in northern British Columbia and Yukon.

Known massive to semi-massive sulphide deposits in the Cariboo subterrane include a number of carbonate-hosted Zn-Pb deposits (Figure 1). They are in



| Property                       | Commodities      | Host                              | Deposit type(s)               | Terrane     |
|--------------------------------|------------------|-----------------------------------|-------------------------------|-------------|
| 1. Green Ice (093A 082)        | Zn               | Snowshoe Gp limestone             | disseminated/vein             | Barkerville |
| 2. Mae (093A 083)              | Cu-Zn-Pb         | Downie calc silicate              | stratabound?                  | Barkerville |
| 3. Peter Gulch (093A 093)      | Pb-Zn            | Snowshoe Gp limestone             | vein/replacement              | Barkerville |
| 4. Ace (new) (093A 142)        | Cu-Au-Ag-Zn-(Pb) | Downie "phyllite"                 | volcanogenic massive sulphide | Barkerville |
| 5. Al (093A 065)               | Pb-Zn-(Cu)       | Cunningham limestone              | replacement Zn-Pb             | Cariboo     |
| 6. Vic (093A 070)              | Pb-Zn-barite     | Midas Fm limestone                | stratiform (sedex?)           | Cariboo     |
| 7. Maybe (093A 110)            | Pb-Zn-Ag         | Black Stuart Gp black pelite unit | replacement/vein              | Cariboo     |
| 8. Comin Throu Bear (093A 158) | Pb-Zn-barite     | Mural Fm limestone                | replacement                   | Cariboo     |
| 9. Cunningham Creek area       | Pb-Zn            | Hardscrabble Mtn limestone        | stratiform (sedex?)           | Barkerville |
| 10. Big Gulp (new) (093A 143)  | Cu-Zn-(Ag-Au)    | Downie phyllite                   | volcanogenic massive sulphide | Barkerville |

Figure 1. Map of the Cariboo and Barkerville subterranean (after Struik, 1988), with location of stratabound Zn-Pb occurrences.

carbonate rocks that range in age from Late Proterozoic to Middle Devonian. The Maybe and Comin Throu Bear (093A 148) prospects are interpreted to be carbonate replacement deposits above a Late Silurian to Early Devonian unconformity. Numerous small concordant sulphide deposits in dark calcareous shales in the Cunningham Creek area have been interpreted to be in the Eocambrian Midas Formation (e.g., Longe, 1977). However, they may be in the Barkerville subterrane which hosts correlative? barite occurrences in the Devonian Hardscrabble Mountain succession (Struik, 1988).

## CARIBOO SUBTERRANE

The Cariboo subterrane includes: the Late Proterozoic Kaza Group, a succession of dominantly impure quartzites, phyllites and conglomerates; the overlying Late Proterozoic to Early Paleozoic Cariboo Group; and the Early to Late Paleozoic Black Stuart Group (Struik, 1988). Much of the Barkerville-Likely area underlain by the Cariboo subterrane has been

|                              |                    |                        |                    |
|------------------------------|--------------------|------------------------|--------------------|
| Middle Pennsylvanian         |                    | ALEX ALLEN FORMATION   |                    |
| Early Mississippian          |                    | GREENBERRY FORMATION   |                    |
| late Devonian to Early Miss. |                    | GUYET FORMATION        | ← unconformity     |
| Middle to Late Devonian      | BLACK STUART GROUP | WAVERLY FORMATION      |                    |
| Mississippian & younger      |                    | sandstone unit         |                    |
| Devonian                     |                    | black pelite unit      | * Maybe            |
| Early Dev. & Late Silurian   |                    | chert-carbonate unit   | * Comin Throu Bear |
| Upper Ordovician             |                    | black pelite unit      | ← Unconformity     |
| Early Cambrian               | CARIBOO GROUP      | DOME CREEK FORMATION   |                    |
|                              |                    | MURAL FORMATION        |                    |
|                              |                    | MIDAS FORMATION        | * Vic              |
|                              |                    | YANKS PEAK FORMATION   |                    |
|                              |                    | YANKEE BELLE FORMATION |                    |
|                              |                    | CUNNINGHAM FORMATION   | * Al               |
| PROTEROZOIC                  | KAZA GROUP         | ISAAC FORMATION        |                    |

Figure 2. Table of formations for the Cariboo and Black Stuart Group, Cariboo subterrane (after Struik, 1988), showing position of stratabound Zn-Pb occurrences.

mapped by Sutherland Brown (1963), Campbell *et al.* (1973) and Struik (*op. cit.*). Debate concerning the internal stratigraphy, paleotectonic environment and regional correlations of the Cariboo Group, as discussed in Struik (1988), is beyond the scope of this paper; as such, the most recent nomenclature of Struik is used.

The Cariboo and Black Stuart successions are illustrated in Figure 2. The Cariboo Group includes phyllite, slate, limestone and minor quartzite of the Isaac, Cunningham and Yankee Bell formations, quartzites of the Yanks Peak Formation and limestone of the Lower Cambrian Mural Formation. These correlate with the North American Windermere Group, Hamill Group and Badshot Formation respectively in southern British Columbia. Conformably overlying slate and shale of the Dome Creek Formation may correlate with similar lithologies in the Chancellor Group of the southern Rocky Mountains (see Struik, 1986) and perhaps with the base of the Index Formation of the Lardeau Group in the Kootenay terrane.

The Black Stuart Group unconformably overlies the Cariboo Group (Struik, 1986, 1988); it ranges in age from Late Ordovician to Mississippian. A discontinuous chert and dolostone breccia unit, host to Comin Throu Bear mineralization, commonly defines the base of the group. It is overlain by dark shales, slate, cherty argillite, phyllite and minor limestone of the "black pelite unit", host to the Maybe prospect. A thin succession of mafic volcanoclastics, the Waverly Formation, and a prominent Devonian-Mississippian (?) conglomeratic facies, the Guyet Formation, occur near the top of the Black Stuart Group.

## MAYBE (093A 110)

The Maybe prospect is one of a number of stratabound Zn-Pb occurrences in Early Paleozoic platform carbonates of the Cariboo subterrane. It is located 5 kilometres northeast of the confluence of the Cariboo and Little Rivers and 35 kilometres northeast of the town of Likely (Figure 1). The deposit occurs on the steep eastern slopes of the Cariboo River, at elevations ranging from just over 1000 metres to 1400 metres. Most of the area has been recently logged, and exposures of mineralization are largely restricted to logging roads. Access is provided by a road that leaves the Likely-Barkerville (8400) road at km 21.2, then crosses the Little River.

## Exploration History

Exposures of Pb-Zn mineralization, discovered in 1986 on new outcrops created by logging roads, were drilled in 1987 by Gibraltar Mines Ltd. Twenty N.Q. holes, totaling 3,044 metres, intersected "numerous" lead-zinc horizons and associated veinlets and mineralized quartz veins (Bysouth, 1988). Three main



mineralized layers were defined, with estimated geological reserves of 400 000 tonnes containing 4 percent combined lead and zinc.

Sable Resource Ltd. optioned the property in 1988 and undertook an exploration program of detailed geological mapping, trenching and limited geochemical soil surveys. This program concluded that the mineralization was dominated by fracture controlled veins, but that several of the showings were similar to "metamorphosed strata-bound lead-zinc carbonate-hosted occurrences" (Spencer, 1989).

The Maybe claim area has been acquired recently by Barker Minerals Ltd. Additional geological mapping and sampling has extended known mineralization and discovered higher grade massive sulphide zones. The recognition of anomalous values of antimony and mercury suggested to Roach (1997) that mineralization had similarities with an epithermal system. Test geophysical surveys concluded that the mineralization has a positive response to VLF-EM but no magnetic signature (Lammle, 1997).

## Stratigraphy

The Maybe deposit area has been mapped at a scale of 1:50 000 by Struik (1988). The geology is dominated by northwest plunging, tight overturned folds that are cut by steeply dipping, northwest trending faults. A more detailed map, illustrated in Figure 3, attempts to adhere to the stratigraphic nomenclature of Struik (*op. cit.*). Several mineralized horizons are recognized within dark calcareous units of the Middle Devonian (?) black pelite unit; these are interpreted to be in an overturned north dipping succession, structurally overlain by dark siltstones and quartzites of the Eocambrian Midas Formation (Struik, *op. cit.*). Spencer (1989) places a fault rather than an inferred unconformity between these successions (*see* Figure 3) and, hence, the facing direction of the mineralized succession is not known.

### *Late Proterozoic and Early Cambrian: Yankee Belle, Yanks Peak and Midas Formations*

The Yankee Belle, Yanks Peak and Midas formations are exposed south of the Maybe deposit. These units have been mapped as the northern limb of an overturned, northwest plunging fold with Midas rocks in its core and Yanks Peak and Yankee Belle formations on its limb (Struik, 1988). The discontinuous nature of orthoquartzites in this footwall succession (Figure 3) may be due to structural complexity such as interfolding between Yanks Peak and Yankee Belle formations or, less likely, to rapid lateral facies changes in Yanks Peak.

The Late Proterozoic Yankee Belle Formation (Sutherland Brown, 1963) includes phyllite, calcareous phyllite, argillite and minor limestone and quartzite. In

the Maybe deposit area, it comprises tan coloured phyllite with minor phyllitic siltstone and very minor grey to dark grey phyllite. The contact with the structurally underlying Yanks Peak is sharp, placed the base of a white orthoquartzite.

The Yanks Peak is dominated by quartzite with minor interlayered siltstone, phyllite and argillite. It is inferred to be tightly folded along the north limb of a syncline, structurally beneath the Yankee Belle Formation (Figure 3). It comprises ridge-forming, thick-bedded white to tan orthoquartzite, interlayered with thinner bedded impure quartzites and tan to medium grey phyllite and silty phyllite. A thin, discontinuous green chlorite phyllite within the Yanks Peak may be a mafic tuff unit.

The Midas Formation is exposed south of the Yanks Peak and in the structural hangingwall north of the deposit (Figure 3). The more northern exposures are dominated by dark grey phyllite, slate, and graphitic argillite, interlayered with dark, fine-grained quartzite. These quartzites may be argillaceous and are commonly cut by numerous 2-3 cm quartz veins. Sericite phyllites are less common. Rare grey to greenish phyllite units, less than a metre thick, containing dispersed ankerite and minor mariposite, may be thin mafic tuff layers.

### *Paleozoic: Black pelite unit*

The black pelite unit is interpreted by Struik (1988) to be inverted, and to unconformably overlie the Midas Formation in the deposit area. Alternatively, as suggested above, a fault may separate these units, as mineralized layers in the younger black pelite unit appear to be truncated along this contact; however, it is possible that the contact is locally fault reactivated. The Midas and black pelite unit are differentiated by the abundant limey units in the latter.

The black pelite unit comprises dark grey phyllite, fissile graphitic phyllite and interlayered limestone. The limestone is typically streaked light and dark grey, although locally a tan to pale grey limestone occurs. Minor pale green chloritic phyllite may have a volcanic origin. Lead-zinc mineralization is hosted by tan, siliceous carbonate units, interlayered with medium grey to tan calcareous and sericitic phyllite.

The black pelite unit, as defined by Struik (1988), includes both graptolitic slates of Ordovician age and dark phyllite and argillite that overlies an Early Devonian chert-carbonate unit. Its age in the deposit area is not known; however, the abundance of included dark limestone suggests a Middle Devonian or younger age rather than an Ordovician age (L.C. Struik, personal communication, 1997).

## Mineralization

The Maybe prospect comprises at least three thin, continuous layers of dominantly ankerite, dolomite and

quartz that contain streaky sphalerite, galena and minor pyrite. These layers are within dark grey limey intervals in the more typical dark phyllite of the black pelite unit. Drill intersections, illustrated in Figure 4, indicate that mineralized layers commonly have a higher grade core, up to one metre thick, of locally semimassive sphalerite and galena, with dispersed and vein mineralization extending two to three metres on either side.

Figure 5 is a detailed section through one of the mineralized intervals exposed at surface (see Figure 3). The stratigraphic top is not known, but based on regional work by Struik (1988), the section may be inverted. Two thin carbonate layers, separated by sericite phyllite, host sulphides.

The host carbonate layers comprise dominantly brown weathering, grey ankerite and quartz, with minor sericite, dolomite, calcite, trace fuchsite and locally actinolite. These minerals are typically sheared or foliated or, less commonly, brecciated with dolomite or ankerite clasts in a granular ankerite-quartz groundmass.

Sulphide minerals include dark brown sphalerite and galena, with minor pyrite and trace chalcocopyrite and pyrrhotite. Sphalerite and galena are commonly streaked parallel to layering (and foliation) and/or disseminated in the carbonate matrix. Less commonly, they occur in both early sheared quartz-carbonate veinlets and late, discontinuous, post-shearing veins. However, most of the late veins are barren or contain only pyrite.

Petrographic study (Payne, 1997) confirms that many sulphides and carbonates are foliated or strained. Sphalerite and galena are intimately intergrown and typically concentrated in thin, discontinuous lamellae that parallel foliation. They also occur as extremely fine inclusions in ankerite. Some sphalerite grains contain fine inclusions of chalcocopyrite or pyrrhotite. Galena and sphalerite may also occur as coarser, recrystallized grains with ankerite and quartz.

Galena can also occur as inclusions in pyrite, replacement of ankerite, and rarely in late veinlets that

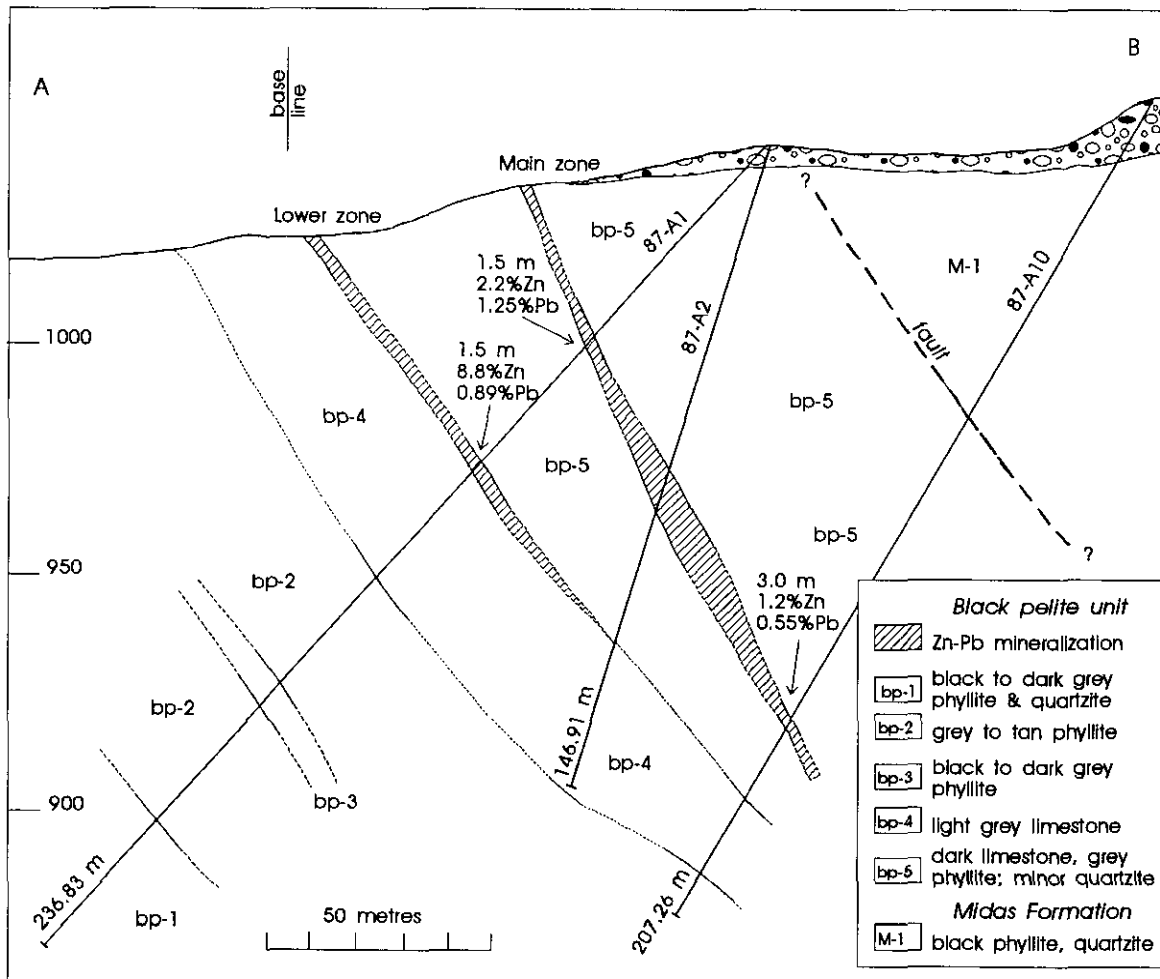


Figure 4. Vertical section through the Maybe prospect, based on drilling by Gibraltar Mines Ltd. (Bysouth, 1988); see Figure 3 for location.

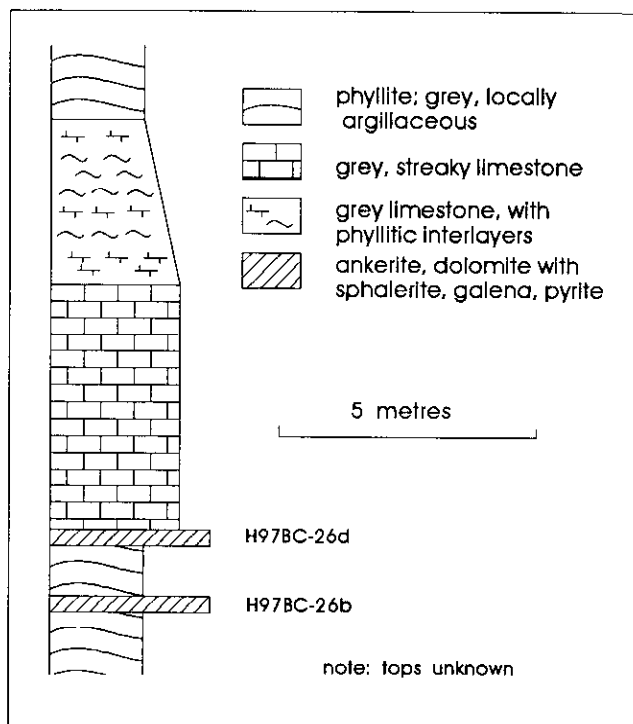


Figure 5. Schematic section through a mineralized interval of the Maybe prospect; see Figure 3 for location.

cut foliation. Pyrite is commonly late, occurring as euhedral grains and in late veins. Dendritic hematite and limonite form late veinlets and irregular alteration patches.

Analyses of a number of hand samples of the mineralized layers are given in Table 1. Lead and zinc values are highly variable, with selected massive sulphide samples containing greater than 10 per cent combined lead and zinc. Silver content is variable, but commonly 15 to 30 ppm. Gold values are low, with a maximum obtained value of 109 ppb. Roach (1997) reports anomalous mercury, with samples typically containing more than 2-3 ppm (Table 1). Antimony and selenium are also anomalous.

### Discussion

The origin of mineralization at the Maybe occurrence is difficult to determine due to metamorphism and deformation. Sulphide and gangue textures suggest a paragenetic sequence of early intergrowth of sphalerite, galena, ankerite and possibly pyrite; chalcopyrite may be due to exsolution from sphalerite. This mineralization is clearly prekinematic. Syn to post kinematic mineralization includes pyrite overgrowths, and possibly layer-parallel ankerite-sulphide veining. Late, post-kinematic mineralization includes pyrite, as well as discordant quartz-dolomite veins that contain minor pyrite and rare sphalerite and galena.

TABLE 1  
ASSAYS OF SELECTED SAMPLES OF MINERALIZED LAYERS FROM THE MAYBE PROSPECT;  
SEE FIGURES 3 AND 5 FOR LOCATIONS

| Sample     | Description                | Source | Cu<br>ppm | Pb<br>% | Zn<br>% | Ag<br>ppm | Au<br>ppb | Ni<br>ppm | Co<br>ppm | Mn<br>ppm | As<br>ppm | Sb<br>ppm | Cr<br>ppm | Se<br>ppm | Hg<br>ppb |
|------------|----------------------------|--------|-----------|---------|---------|-----------|-----------|-----------|-----------|-----------|-----------|-----------|-----------|-----------|-----------|
| 4009       | massive sulphide           | 1      | 58        | 4.64    | >10     | 22.3      | 25        | 9         | 11        | 2273      | 1.4       | 21.2      | 258       | 9.1       | 3185      |
| 4012       | calcareous chert           | 1      | 59        | 1.4     | 3.46    | 8.7       | 19        | 9         | 3         | 638       | 2.3       | 17.9      | 64        | 0.5       | 2590      |
| 4013       | calcareous chert           | 1      | 73        | 4.51    | 5.24    | 25.4      | 49        | 22        | 4         | 832       | 2.4       | 61.4      | 93        | 1.6       | 2340      |
| 4081       | massive sulphide           | 1      | 99        | 2.36    | >10     | 53        | 59        | 33        | 36        | 2213      | 3.7       | 61.2      | 192       | 24.6      | 9260      |
| 4139       | qz-carb. stockwork         | 1      | 233       | 1.25    | 4.54    | 11.6      | 12        | 28        | 6         | 3259      | 177       | 14        | 41        | 2.6       | 1060      |
| 4164       | massive sulphide           | 1      | 136       | 3.47    | >10     | 117.2     | 83        | 10        | 59        | 2266      | 8         | 154       | <1        | 0.4       | 99999     |
| H97BC-26b  | semi-massive sulphide      | 2      | 56        | 2.85    | 9.95    | 25.8      | 87        | 7         | 4         | 595       | <5        | 18        | 72        |           |           |
| H97BC-26d  | semi-massive sulphide      | 2      | 69        | 3.33    | 9.15    | 28.1      | 109       | 12        | 6         | 586       | <5        | 14        | 73        |           |           |
| H97BC-48a  | semi-massive sulphide/vei  | 2      | 78        | 1.15    | >10     | 8         | 82        | 10        | 6         | 1642      | 25        | 18        | 101       |           |           |
| H97BC-48b  | semi-massive sulphide/vei  | 2      | 140       | 3.4     | >10     | 19.9      | 44        | 11        | 10        | 1800      | 20        | 14        | 79        |           |           |
| H97BC-50   | semi-massive sulphide/vei  | 2      | 90        | 3.31    | >10     | 33.7      | 34        | 10        | 11        | 2713      | 8         | 17        | 93        |           |           |
| H97BC-71b  | brecciated sulphides/veins | 2      | 112       | 2.36    | >10     | 16.1      | 24        | 7         | 16        | 3404      | 26        | 16        | 84        |           |           |
| H97BC-84   | diss. to massive sulphide  | 2      | 37        | 0.87    | 1.21    | 4.6       |           | 38        | 12        | 2372      | 5         | <5        | 76        |           |           |
| H97BC-103a | massive sulphide           | 2      | 182       | 3.44    | >10     | 43.3      |           | 16        | 13        | 1199      | 11        | 47        | 189       |           |           |
| H97BC-103b | massive sulphide           | 2      | 24        | 0.41    | >10     | <5        |           | 6         | 8         | 1247      | 11        | <5        | 42        |           |           |
| H97BC-110  | semi-massive sulphide      | 2      | 77        | 2.54    | 4.3     | 18.6      |           | 14        | 2         | 834       | <5        | 15        | 60        |           |           |

Notes: Analyses of samples of Roach (1997) are by ICP, Acme Analytical Laboratories, Vancouver

Analyses of samples from this report are by MIC, Acme Analytical Laboratories, Vancouver

Source: 1. Roach, 1977; 2. this report

The restriction of all mineralization to specific carbonate horizons within the black pelite unit, the recognition that considerable mineralization is prekinematic, and the pseudolayered nature of this mineralization suggest a syngenetic origin. However, comparisons with other carbonate-hosted Zn-Pb deposits, the dominant ankeritic host, chemistry and abundant vein mineralization suggest that Maybe is a replacement deposit.

The metal content of the Maybe deposit, with high Zn/Pb ratios, moderate silver content, and low gold, is similar to many carbonate-hosted Zn-Pb deposits, including those in the Early Cambrian platform carbonates in the Kootenay Arc in southern British Columbia and the Irish deposits in Early Carboniferous rocks. However, in these deposits the dominant host is a fine-grained granular dolomite or, less commonly, silica in contrast to the ankeritic host of Maybe mineralization. A considerable portion of the mineralization in the Maybe occurs in sheared, foliation parallel veins; other includes later cross-cutting veins. It is possible that this vein mineralization records remobilized sulphides and gangue, as it is restricted to carbonate host.

In summary, Maybe is a carbonate-hosted Pb-Zn deposit and, as is common to many of these deposits, its origin remains enigmatic. Detailed work on the Irish deposits, often considered examples of syngenetic sulphide deposition in carbonate rocks, now suggests that they are largely structurally controlled diagenetic to epigenetic replacement mineralization (e.g., Hitzman, 1995). We suggest that mineralization of the Maybe prospect is also largely replacement/vein in origin. Its unusual characteristics are similar to some manto style deposits.

## COMIN THROU BEAR (093A 148)

The Comin Throu Bear showings comprise galena and barite replacement of a Late Silurian to Early Devonian chert-dolostone breccia in the Black Stuart Group (Figure 2). The property is located at an elevation of approximately 1800 metres on Black Stuart Mountain, approximately 18 kilometres northeast of Cariboo Lake. Past work on the property includes mapping, trenching, sampling and diamond drilling totalling 465.6 metres in 16 holes (Reed *et al.*, 1981). The property was not visited this past summer, and these descriptions are summarized from assessment reports.

The showings occur in fine grained clastic dolostone that overlies the Mural Formation. The dolostone is recessive weathering due to high pyrite content. It contains lenses of limestone and two showings of coarse-grained barite and galena. It is underlain by a grey weathering limestone of the Mural Formation, and overlain gradationally by a dolostone breccia that grades upwards to chert-dolostone breccia.

The breccia is highly variable both vertically and laterally, and records an unconformity within the basal Black Stuart Group (Struik, 1988). It is overlain by black slates of the Black Stuart Formation.

Mineralization has been located in two areas (Reed *et al.*, 1981), separated by a strike length of approximately 1200 metres. Five of eleven trenches in the eastern "Area B" expose coarse-grained barite with interstitial galena, with widths up to eight metres. Mineralization is at the contact of dolostone and overlying laminated grey limestone. Trenching at the western "Area A" exposes a similar zone 15 cm thick.

Reed *et al.* (1981) suggest that these occurrences are early (diagenetic?) carbonate replacement and possible open-space fill deposits. Alteration includes early dolomitization, concentrated in breccias and clastic units, followed by silicification, then sulphide deposition. The simple mineralogy, textures, brecciation and stratigraphic control, suggest similarities with Mississippi Valley type deposits.

## SUMMARY AND DISCUSSION

The Cariboo subterrane comprises Late Proterozoic to Paleozoic basinal to platformal successions that were deposited on the North American continental margin. Massive sulphide deposits in these and correlative rocks include both syngenetic sediment-hosted and replacement carbonate-hosted lead-zinc  $\pm$  barite mineralization. These types of mineralization are typically concentrated during periods of extensional tectonics; sedex deposits form in rift-controlled basins and carbonate replacement deposits occur along structural breaks commonly at or above unconformities or along platformal margins.

Known massive sulphide deposits in the Cariboo subterrane are within carbonate successions that immediately overlie a Late Silurian to Early Devonian unconformity, locally marked by conglomerate and breccia facies and removal of underlying stratigraphy. They include the stratabound Maybe and Comin Throu Bear prospects, both interpreted to be replacement deposits. Maybe is unusual because it has an ankeritic host and a geochemical signature that includes anomalous trace element concentrations such as mercury, antimony and selenium.

Exploration for new sulphide discoveries in the Cariboo subterrane should focus on recognized stratigraphic intervals that host deposits in correlative rocks elsewhere, such as the EoCambrian to Cambrian Midas and Mural Formations, and the Early Devonian carbonate clastic succession or black pelite unit above the Late Silurian to Early Devonian unconformity.

## ACKNOWLEDGEMENTS

We would like to thank Louis Doyle of Barker Minerals Ltd. for his hospitality and his generous sharing of both ideas and data. Reviews and edits of the manuscript by Bert Struik, Paul Schiarizza and Dave Lefebure are much appreciated. Ray Lett is thanked for expediting samples for geochemical analyses and M Fournier, for helping with drafting. Cheerful and able field assistance by Gloria Light is much appreciated.

## REFERENCES

- Bysouth, G.D. (1988): Diamond Drill Report - Maybe Group, Cariboo Mining Division; *B.C. Ministry of Energy, Mines and Petroleum Resources*, Assessment Report 17,357.
- Campbell, R.B., Mountjoy, E.W. and Young, F.G. (1973): Geology of the McBride Map Area, British Columbia; *Geological Survey of Canada*, Paper 72-35.
- Ferri, F. (1997): Nina Creek Group and Lay Range Assemblage, North-central British Columbia: Remnants of Late Paleozoic Oceanic and Arc Terranes; *Canadian Journal of Earth Sciences*, Volume 34, pages 854-874.
- Fyles, J.F. (1970): The Jordan River Area near Revelstoke, British Columbia; *B.C. Ministry of Energy, Mines and Petroleum Resources*, Bulletin 57, 64 pages.
- Høy, T. and Ferri, F. (1998): Stratabound Base Metal Deposits of the Barkerville Subterranean, Central British Columbia (93A/NW); *B.C. Ministry of Employment and Investment*, Geological Fieldwork 1997, Paper 1998-1.
- Høy, T. (1987): Geology of the Cottonbelt Lead-Zinc-Magnetite Layer, Carbonatites and Alkalic Rocks in the Mount Grace Area, Frenchman Cap Dome, Southeastern British Columbia; *B.C. Ministry of Energy, Mines and Petroleum Resources*, Bulletin 80, 99 pages.
- Hitzman, M.W. (1995): Geological Setting of the Irish Zn-Pb-(Ba-Ag) Orefield; in Irish Carbonate-hosted Zn-Pb Deposits, Anderson, K., Ashton, J., Earls, G., Hitzman, M.W. and Sears, S., Editors, *Society of Economic Geologists*, Guidebook Series, Volume 21, pages 25-61.
- Lammle, C.A.R. (1997): Little River and Ace Properties, Cariboo Mining Division, British Columbia; internal report, *Barker Minerals Ltd.*
- Leask, J.M. (1982): Geology of the MGM Property, Big Bend District, East Central British Columbia; *B.C. Ministry of Energy, Mines and Petroleum Resources*, Assessment Report 9994.
- Longe, R.V. (1977): Barkerville Project: Description of Sulphide Showings and Geochemistry of Soils; *B.C. Ministry of Energy, Mines and Petroleum Resources*, Assessment Report 6314.
- McIntyre, D.G. (1991): SEDEX - Sedimentary Exhalative Deposits; *B.C. Ministry of Energy, Mines and Petroleum Resources*, Paper 1991-4, pages 25-70.
- Nelson, J., Sibbick, S., Høy, T., Bobrowski, P. and Cathro, M. (1997): The Paleozoic Massive Sulphide Project: An Investigation of Yukon-Tanana Correlatives in British Columbia; *B.C. Ministry of Employment and Investment*, Paper 1997-1, pages 183-186.
- Payne, J.G. (1997): Geological Report; internal report, *Barker Minerals Ltd.*
- Reed, A.J., Lovang, G. and Greenwood, H.J. (1981): Assessment Report on the "Comin Throu Bear" Property, Black Stuart Mountain, B.C.; *B.C. Ministry of Energy, Mines and Petroleum Resources*, Assessment Report 9819.
- Roach, S.N. (1997): Geological Mapping Surveys Conducted on the Goose Range Project Area, Cariboo Mining Division, B.C.; internal report, *Barker Minerals Ltd.*
- Schiarizza, P. and Preto, V.A. (1987): Geology of the Adams Plateau-Clearwater-Vavenby Area; *B.C. Ministry of Energy, Mines and Petroleum Resources*, Paper 1987-2, 88 pages.
- Spencer, B.E. (1989): Report on a Geological, Geochemical and Trenching Programme on the Maybe Property; *B.C. Ministry of Energy, Mines and Petroleum Resources*, Assessment Report 19,027.
- Struik, L.C. (1980): Geology of the Barkerville-Cariboo River area, Central British Columbia; unpublished Ph.D. Thesis, *University of Calgary*.
- Struik, L.C. (1986): Imbricated Terranes of the Cariboo Gold Belt with Correlations and Implications for Tectonics in Southeastern British Columbia; *Canadian Journal of Earth Sciences*, Volume 23, pages 1047-1061.
- Struik, L.C. (1988): Structural Geology of the Cariboo Gold Mining District, East-central British Columbia; *Geological Survey of Canada*, Memoir 421, 100 pages.
- Sutherland Brown, A. (1963): Geology of the Cariboo River Area, British Columbia; *B.C. Ministry of Energy, Mines and Petroleum Resources*, Bulletin 47, 60 pages.



## GEOCHEMICAL PATHFINDERS FOR MASSIVE SULPHIDE DEPOSITS IN THE SOUTHERN KOOTENAY TERRANE

By R.E.Lett, P.Bobrowsky, M.Cathro  
and A.Yeow (University of British Columbia)

**KEYWORDS:** Kootenay Terrane, geochemistry, sulphide deposits, pathfinder elements, soil, till.

### INTRODUCTION

A variety of geochemical methods have proved effective exploration tools for base metal massive sulphide deposits. The most extensive geochemical expression from massive sulphide mineralization is characteristically shown by those elements most mobile in the near surface environment (e.g. copper, zinc, sulphate). These elements combined with changes in surface water pH may be detected by regional stream sediment, stream water or lake sediment surveys. However, massive sulphidic bodies are small compared to many other styles of mineralization and are difficult to locate especially where bedrock is covered by glacial deposits. Soil and till geochemical surveys commonly use the ore-related elements (e.g. gold, copper, lead, silver, zinc) to detect mineralization. Hydromorphic dispersion of the geochemically immobile elements (e.g. gold, lead) is limited compared to more mobile elements (e.g. copper). Immobile element soil anomalies can be the most direct indicator to the location of a concealed base metal sulphides or mineralized material in till (Cameron, 1977). However, element patterns in soil and till are typically small and therefore difficult to detect without a detailed survey. Anomaly size can be increased and the character of the sulphide mineral source better established by using pathfinder elements commonly found associated with the sulphide ore. Typical pathfinders are arsenic for gold and mercury for copper-lead-zinc sulphides.

A regional stream water survey, detailed geochemical studies, a regional till geochemical survey, surficial mapping and mineral deposit studies were carried out by the Geological Survey Branch in 1996. These projects were part of an integrated study of the Eagle Bay Assemblage within NTS sheets 82M 4 and 5 (Dixon-Warren *et al.*, 1997; Bobrowsky *et al.*, 1997; Sibbick *et al.*, 1997; Höy, 1997). Surficial mapping, mineral deposit studies and the geochemical surveys covered two 1:50,000 scale map sheets (82M 4 and 5). Strong arsenic, copper, cobalt, gold, lead and zinc geochemical dispersal plumes were revealed in till samples collected down-ice from a number of massive sulphide deposits within these map sheets. More subdued copper, zinc, sulphate

hydrogeochemical anomalies were detected by the stream water survey.

Studies of the Southern Kootenay Terrane continued during the summer of 1997. Geochemical studies included a regional till survey of the western half of two 1:50,000 NTS sheets, 92P1 and 8 (Paulen *et al.*, 1998) and detailed geochemical sampling within NTS 82M4 and 5 outlined in Figure 1.

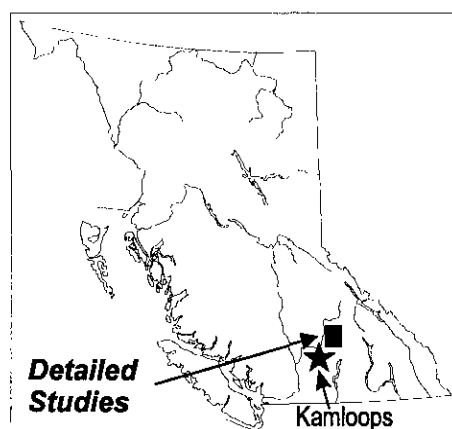


Figure 1. Location of the project area.

The aims of the detailed sampling were:

- To establish the geochemical expression in soil and till near different sulphide occurrences.
- To discriminate between different mineral sources within down-ice dispersal plumes.

Preliminary results of detailed geochemistry for three occurrences are described in this paper.

### TOPOGRAPHY AND GEOLOGY

Detailed geochemical studies were carried out at several locations on the Adams Plateau and near North Barriere Lake. The moderate to high relief of the region is typical of the Shuswap highlands. West of Adams Lake the undulating land surface is dissected by several major east-trending valleys, such as those occupied by Simax Creek and the North Barriere River. Valley sides are often steep and have extensive talus below cliff sections. A varying thickness of till, deposited by an ice advance from the northwest, covers bedrock on the more subdued plateau topography. Vegetation ranges from cottonwood stands in

valley bottoms to a western hemlock, red cedar and Douglas fir canopy on the plateau. (Rowe, 1972). Organic and gleysolic soils are common in poorly drained areas whereas luvisolic and regosolic soils are typically developed on hill slope and plateau regimes. The predominant surficial deposits are basal till, ablation till, glaciofluvial sediment, glaciolacustrine sediment, fluvial sediment, organic accumulations and colluvium (Bobrowsky *et al.*, 1997). Till, colluvium and glaciofluvial sediments are most common on the rolling plateau and hill slopes. Fluvial, glaciofluvial and glaciolacustrine deposits mantle the valley floors.

The Adams Plateau-North Barriere Lake area is underlain by Paleozoic rocks of the Eagle Bay Assemblage and Fennell Formation. The western part of the area is dominated by the Fennell Formation, a Devonian to Permian sequence of oceanic bedded cherts, gabbro, diabase, pillow basalt, sandstone, quartz-porphyrty rhyolite and conglomerate. The Fennell Formation forms part of the Slide Mountain Terrane and has a thrust contact with the Cambrian to Mississippian Eagle Bay Assemblage to the east. The Eagle Bay Assemblage is part of the Kootenay Terrane that was originally deposited along the ancestral margin of North America. Older Eagle Bay rocks range from quartzites, quartz-rich schists and limestone. These are overlain by grit, phyllite and quartz mica schist and coarse grained clastic metasediments interbedded with felsic volcanic rocks. Above the metasedimentary rocks are limestone and calcareous phyllite, calcsilicate schist and skarn, pillowed greenstone and chlorite-sericite-quartz schist of felsic origin. At the top of the sequence are slates and siltstone. The Eagle Bay Assemblage has been intruded by quartz monzonite of the Cretaceous Baldy and Raft batholiths (Schiarrizza and Preto, 1987).

## MINERAL DEPOSITS

A variety of massive sulphide deposits occur within rocks of the Eagle Bay Assemblage and Fennell Formation (Nelson *et al.*, 1997; Höy, 1991, 1996; Schiarrizza and Preto, 1987). The deposits have been a source of base and precious metals in the past and continue to be an attractive exploration target. Among the more significant sulphide deposits and occurrences are:

- Kuroko-type volcanogenic massive sulphide gold-copper-lead-zinc-barite deposits hosted by felsic volcanic rocks of the Eagle Bay Assemblage. Typical of this type are the Homestake (MINFILE 82M025), Rea Gold (MINFILE 82M191), Samatosum (MINFILE 82M244) and Harper (MINFILE 82M60).
- Besshi-type volcanogenic massive sulphide copper-zinc deposits hosted predominantly by metasediments of the Eagle Bay Assemblage. The

Mount Amour occurrence (MINFILE 92P050) is most likely an example of this type of deposit.

- Cyprus-type volcanogenic massive sulphide copper-zinc deposits in mafic volcanic rocks. The Chu Chua deposit (MINFILE 92P140) hosted by mafic flows and tuffs of the Fennell Formation is an example of this type.
- SEDEX-type lead-zinc-silver sulphide deposits hosted by metasedimentary rocks of the Eagle Bay Assemblage. An example of this type is the Spar occurrence (MINFILE 82M017).

## DETAILED GEOCHEMICAL STUDIES

Detailed geochemical orientation studies were conducted at nine locations (Figure 2). The locations were selected to include sulphide mineralization typical of the Kootenay Terrane and to include examples of gold, arsenic and copper glacial dispersal trains. The metal association of each occurrence and the types of sample collected are listed in Table 1.

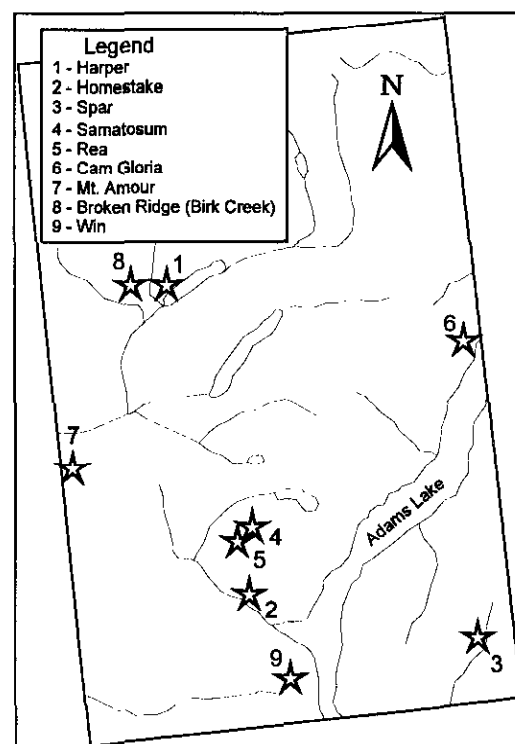


Fig 2. Location of the orientation studies.

Objectives of the orientation studies were to determine the effectiveness of various geochemical sampling media and pathfinder elements for detecting sulphide mineralization. Soil, till and bedrock samples were collected from pits or profiles excavated at intervals on lines that traversed the deposits. Vegetation samples were also collected at the Harper, Homestake and Spar deposits. The vegetation types included tree bark from Lodgepole

pine (*Pinus contorta*) and Douglas fir (*Pseudotsuga glauca*) and twigs from Subalpine fir (*Abies lasiocarpa*).

Table 1. Mineralization and Sample Types for Study Areas

| Area           | Mineralization | Sample Type                 |
|----------------|----------------|-----------------------------|
| Broken Ridge   | Cu-Pb-Zn-Ag    | Soil, Till, Rock,           |
| Cam-Gloria     | Au-Ag-Bi-Pb    | Soil, Till, Rock            |
| Harper         | Cu-Pb-Zn-Ag-Au | Soil, Till, Rock, Tree Bark |
| Homestake      | Au-Cu-Pb-Zn-Ba | Soil, Till, Rock, Tree Bark |
| Mt Amour       | Cu-Pb-Zn       | Soil, Till, Rock            |
| Samatosum -Rea | Au-Ag-Cu-Pb-Zn | Soil, Till, Rock            |
| Spar           | Au-Ag-Pb-Zn-Cu | Soil, Till, Rock, Tree Bark |
| Win            | Cu-Pb-Zn       | Soil, Till, Rock            |

Soil samples (minus 63 micron fraction) were analysed for 50 elements including gold, arsenic, barium, cobalt, copper, molybdenum, nickel, mercury and zinc by thermal neutron activation at Activation Laboratories, Ancaster Ltd., Ontario and by aqua regia digestion-inductively coupled plasma emission spectroscopy (ICP) at Acme Analytical Laboratories Ltd., Vancouver. Tree bark, leaf and twig samples were macerated and part of the sample compressed into a briquette. A second portion of the macerated material was ashed at 480°C and the ash analysed for 30 elements by aqua regia digestion-ICP at Activation Laboratories Ltd. Selected soil and till samples were analysis for up to 70 trace metals by enzyme leach-inductively coupled mass spectroscopy at Activation Laboratories Ltd. Rock samples collected in 1997 were prepared and analysed for gold by fire assay and trace metals by aqua regia digestion-ICP at Eco-Tech Laboratories Ltd., Kamloops.

Soil, till and rock samples were also analysed for molybdenum, copper, lead, zinc, silver, arsenic, cadmium, antimony, bismuth, thallium, tellurium, mercury, selenium and gallium by aqua regia digestion-solvent extraction and ultrasonic nebulizer-inductively coupled plasma emission spectroscopy at Acme Analytical. Detection limits for direct ICP and ultrasonic nebulizer ICP are compared in Table 2.

## RESULTS

Preliminary results for soil, till and rock samples from the Harper, Broken Ridge (Birk Creek) and Cam-Gloria occurrences are shown here to illustrate the typical geochemical response to base and precious metal mineralization.

### 1. Harper Property (MINFILE 82M60)

At the Harper property two northwest trending lenses of pyrrhotite, pyrite, chalcocopyrite, sphalerite and galena occur

in phyllite and schist of the Eagle Bay Assemblage. The lenses are up to 8 metres wide and can be traced for up to 210 metres along strike. The contact between the batholith and felsic metalvolcanic rocks of the Eagle Bay Assemblage lies approximately 500 metres north of the main sulphide occurrence. Bedrock is covered by a thin (1-2 metres) veneer of a light brown to grey sandy till. The overburden texture and the abundance of monzonite clasts in the till suggests that the source is mainly the Baldy batholith.

Table 2. Detection limits (DL) for elements by aqua-regia-ultrasonic nebulizer-ICP (UICP) and direct ICP

| Element    |    | DL-UICP | DL-ICP  |
|------------|----|---------|---------|
| Aluminium  | Al | 0.01%   | 0.01%   |
| Antimony   | Sb | 2 ppm   | 0.2 ppm |
| Arsenic    | As | 2 ppm   | 0.5 ppm |
| Barium     | Ba | 1 ppm   | 1 ppm   |
| Bismuth    | Bi | 2 ppm   | 0.1 ppm |
| Boron      | B  | 3 ppm   | 3 ppm   |
| Cadmium    | Cd | 0.2 ppm | 10 ppb  |
| Calcium    | Ca | 0.01%   | 0.01%   |
| Chromium   | Cr | 1 ppm   | 1 ppm   |
| Cobalt     | Co | 1 ppm   | 1 ppm   |
| Copper     | Cu | 0.2 ppm | 1 ppm   |
| Gallium    | Ga | -       | 0.5 ppm |
| Gold       | Au | 3 ppm   | 100 ppb |
| Iron       | Fe | 0.01%   | 0.01%   |
| Lanthanum  | La | 1 ppm   | 1 ppm   |
| Lead       | Pb | 3 ppm   | 0.3 ppm |
| Magnesium  | Mg | 0.01%   | 0.01%   |
| Manganese  | Mn | 1 ppm   | 1 ppm   |
| Mercury    | Hg | -       | 10 ppb  |
| Molybdenum | Mo | 1 ppm   | 0.1 ppm |
| Nickel     | Ni | 1 ppm   | 1 ppm   |
| Selenium   | Se | -       | 0.4 ppm |
| Silver     | Ag | 0.3 ppm | 30 ppb  |
| Sodium     | Na | 0.01%   | 0.01%   |
| Tellurium  | Te | -       | 0.2 ppm |
| Titanium   | Ti | 0.01%   | 0.01%   |
| Thorium    | Th | 2 ppm   | 2 ppm   |
| Tungsten   | W  | 2 ppm   | 2 ppm   |
| Strontium  | Sr | 1 ppm   | 1 ppm   |
| Thallium   | Tl | 5 ppm   | 0.2 ppm |
| Uranium    | U  | 5 ppm   | 5 ppm   |
| Vanadium   | V  | 1 ppm   | 1 ppm   |
| Zinc       | Zn | 1 ppm   | 1 ppm   |

A predominantly luvisolic soil has developed on a gentle, south facing slope. Lodgepole pine (*Pinus contorta*), Douglas fir (*Pseudotsuga glauca*), and paper Birch (*Betula papyrifera*) are the main canopy species

growing in the area. The hill side has been disturbed by trenching, excavation of a short adit and the construction of logging roads (now largely overgrown).

The rock samples were collected to help establish background element concentrations in the soil and till. Sample 97RL17R is a dark grey schist containing magnetite and pyrrhotite. Sample 97RL18R is a very rusty weathered, siliceous, light grey phyllite containing pyrite. Both taken 97RL17R and 97RL18R were taken close to the adit. Sample 97RL19R from a trench 250 metres east of the adit is a dark grey-green siliceous schist with banded pyrite and minor chalcopyrite. Element concentrations in these samples and in an oxidized till samples collected within 10 metres of 97RL17R are shown in Table 3. The highest gold detected in rock is 20 ppb whereas the till contains 179 ppb gold. Bismuth, mercury, lead and selenium are also higher in the till. The enhancement of gold and other elements in the till relative to bedrock may reflect glacial dispersal of sulphides from an up-ice source rather than the geochemistry of the underlying bedrock.

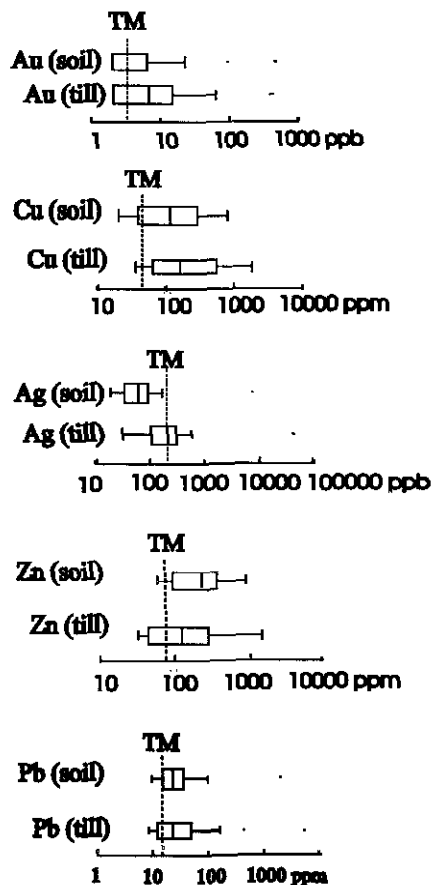


Figure 3. Median and range values for gold, silver, copper, lead and zinc in combined Harper-Broken Ridge soil and till samples. TM indicates median value for 1996 regional till survey.

Median and range gold, silver, copper, lead, zinc, arsenic, mercury, bismuth, selenium and antimony values in soil and till samples from the Harper and Birk Creek Broken Ridge (Birk Creek) occurrences are compared by box and whisker plots shown in Figures 3 and 4. Geochemical data for samples from these areas has been combined because the occurrences are less than 5

kilometres apart and occur in a similar host rock. Also shown in Figure 3 for comparison are median copper, silver, gold, zinc and lead values for the 1996 regional till survey.

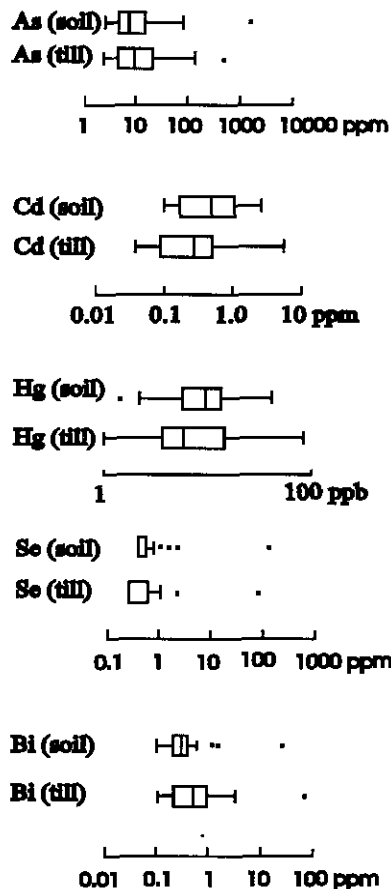


Figure 4. Median and range values for pathfinder elements in combined Harper-Broken Ridge soil and till samples.

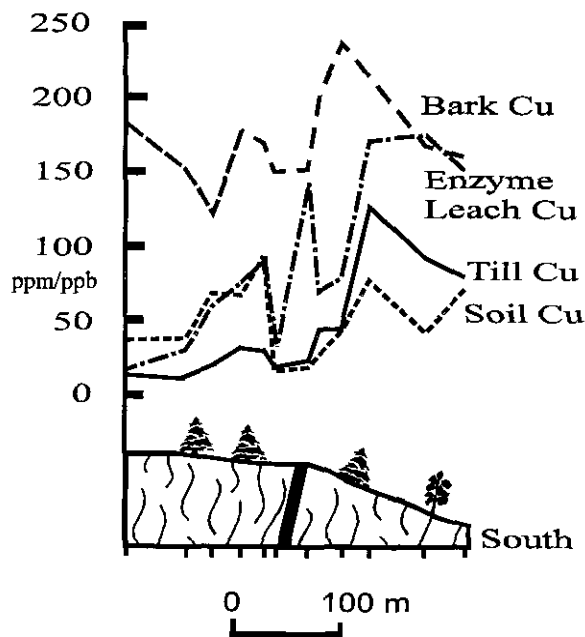


Figure 5. Copper in soil, till and tree bark, Harper occurrence.

Table 3. Geochemistry of Harper area samples. Gold by INA. Other elements by aqua regia-ICP

| Element | Till978111 | R97RL17 | R97RL18 | R97RL19 |
|---------|------------|---------|---------|---------|
| Au ppb  | 179        | 20      | 10      | 18      |
| Ag ppb  | 3170       | 596     | 633     | 1779    |
| As ppm  | 5.9        | 2.2     | 35      | 2.5     |
| Bi ppm  | 41.7       | 17.5    | 1.6     | 3.4     |
| Cd ppm  | 0.1        | 1.24    | 0.18    | 0.19    |
| Co ppm  | 0.3        | <1      | 4       | 37      |
| Cu ppm  | 286        | 870     | 282     | 1869    |
| Fe %    | 18.9       | 21.4    | 5.56    | 13.45   |
| Ga ppm  | 15.4       | 19      | 6.7     | 8.4     |
| Hg ppb  | 33         | 10      | 25      | <10     |
| Mn ppm  | 708        | 1042    | 462     | 1849    |
| Mo ppm  | 2.6        | 1.4     | 4.7     | 2.3     |
| Ni ppm  | 3          | 17      | 5       | 16      |
| Pb ppm  | 117        | 36      | 35      | 14      |
| Sb ppm  | <0.2       | <0.2    | 0.2     | <0.2    |
| Se ppm  | 21         | 7.1     | 3.2     | 7.0     |
| Te ppm  | 0.7        | 0.9     | <0.2    | <0.2    |
| Tl ppm  | <0.3       | <0.2    | <0.2    | <0.2    |
| V ppm   | 94         | 66      | 35      | 20      |
| Zn ppm  | 199        | 341     | 125     | 50      |

The distribution of copper in soil, till and tree bark along a north-south traverse crossing the strike of the most easterly sulphide lens is shown in Figure 5. Also shown in Figure 5 is the copper extracted from soil using an enzyme leach. The decrease of copper directly over the mineralization could reflect increasing mobility in the more acid soil due the weathering of the sulphides. Increased copper down-slope from the mineralization in soil and till can be most likely explained by the transition from till to colluvium that contains a larger amount of locally derived mineralized bedrock.

## 2. Broken Ridge (MINFILE 82M130)

The Broken Ridge occurrence, located north of the confluence between Birk and Harper Creeks, was selected as a detailed study area because a regional till sample collected in 1996 near the occurrence contained 3653 ppm copper. Mineralization consists of banded pyrite, pyrrhotite, chalcopyrite, minor sphalerite and galena in dark green actinolite schist of the Eagle Bay Assemblage. In Table 4 geochemical results for rock, soil and till samples taken from close to the occurrence are shown. The rock samples are respectively a banded sulphide (97RL3R) and a grey-green gneiss (97RL5R). Bedrock is partly covered by basal till and, locally, by colluvium on the steeper parts of the east facing hill slope above Harper Creek. Variation of elements down a soil-till profile close to the occurrence is illustrated by samples 978065 and 978066 in Table 4. The distribution of gold, copper, silver,

Table 4. Geochemistry of Broken Ridge samples Gold by INA. Other elements by aqua regia-ICP.Col.-Colluvium

| Element | Soil978065 | Col.978066 | Rock 97RL3 | Rock 97RL5 |
|---------|------------|------------|------------|------------|
| Au ppb  | 10         | 23         | 1          | 5          |
| Ag ppb  | 481        | 568        | 133        | 3229       |
| As ppm  | 39.6       | 139        | 1.8        | 1005.6     |
| Bi ppm  | 1.2        | 0.4        | 0.6        | 3.7        |
| Cd ppm  | 2.04       | 3.0        | 0.34       | 0.48       |
| Co ppm  | 22         | 63         | 23         | 16         |
| Cu ppm  | 252        | 1083       | 254        | 2243       |
| Fe %    | 4.37       | 10.82      | 11.29      | 20.6       |
| Ga ppm  | 11.8       | 15.4       | 21.6       | 3.6        |
| Hg ppb  | 24         | 53         | 10         | 17         |
| Mn ppm  | 740        | 2062       | 1013       | 214        |
| Mo ppm  | 1.1        | 3.5        | 3.2        | 4.3        |
| Ni ppm  | 66         | 128        | 120        | 43         |
| Pb ppm  | 234        | 117        | 3.9        | 131.7      |
| Sb ppm  | 0.3        | 0.5        | <0.2       | 3.2        |
| Se ppm  | <0.3       | 1.2        | 0.5        | 10.7       |
| Te ppm  | 0.2        | 0.8        | <0.2       | 1.4        |
| Tl ppm  | 0.3        | 0.8        | 0.2        | 0.2        |
| V ppm   | 59         | 104        | 195        | 15         |
| Zn ppm  | 852        | 957        | 279        | 76         |

arsenic, bismuth and mercury in till and colluvium is shown in Figures 6-11.

The highest gold, silver, arsenic, and selenium values occur in oxidized colluvium 50 metres to the south of the occurrence. Increased iron, copper, lead, bismuth, thallium and tellurium are also found in the colluvium at this site. Most element levels decrease to the southeast of the anomalous sample although high copper levels persist beyond the limit of the sampling. The decreased values to the southeast of the highly anomalous site can be explained by down-slope transport and dilution of mineralized rock in the colluvium.

The most anomalous copper occurs in a weakly oxidized till 800 metres to the west of the Broken Ridge occurrence. This anomaly is close to the site of a 1996 regional till sample containing over 3000 ppm copper. Other 1996 till samples collected 1 kilometres northwest and up-ice from the peak anomaly have less than 50 ppm copper. However, a till sample 400 metres southeast (down-ice) has 550 ppm copper indicating glacial dispersal of copper-mineralized rock can be up to 2 kilometres from the source.

Only weakly anomalous mercury levels were found in soil and till close to the Broken Ridge occurrence. The highest mercury (93 ppb) with enhanced bismuth occurs in basal till 1.5 kilometres southwest and this weak anomaly has no apparent sulphide source. Interpretation of soil and till geochemical patterns is complicated by the existence of other small base-metal sulphide bodies in the Birk Creek area similar to the Broken Ridge occurrence.

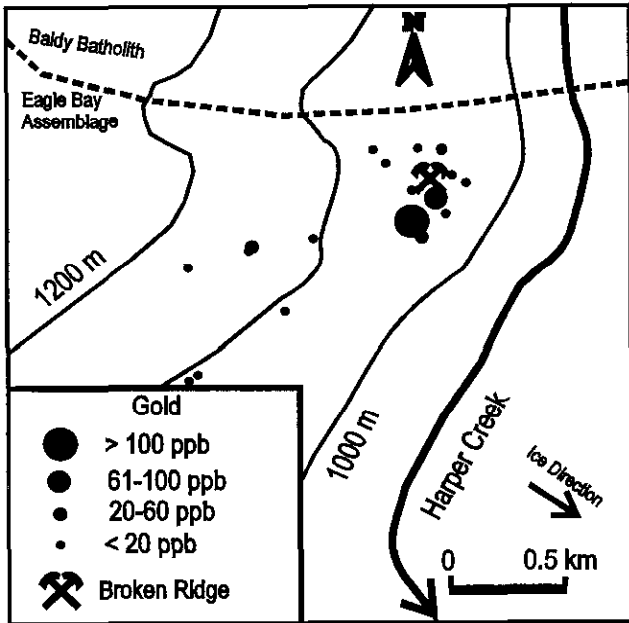


Figure 6. Gold in Till Samples, Broken Ridge Area.

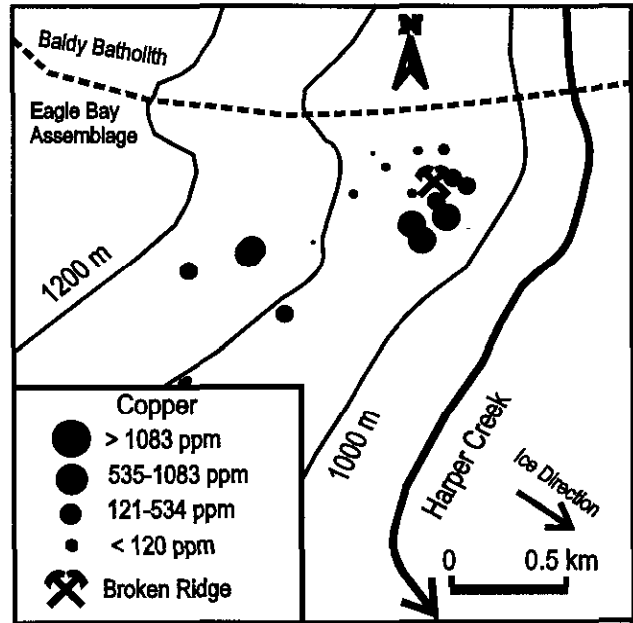


Figure 8. Copper in Till Samples, Broken Ridge Area.

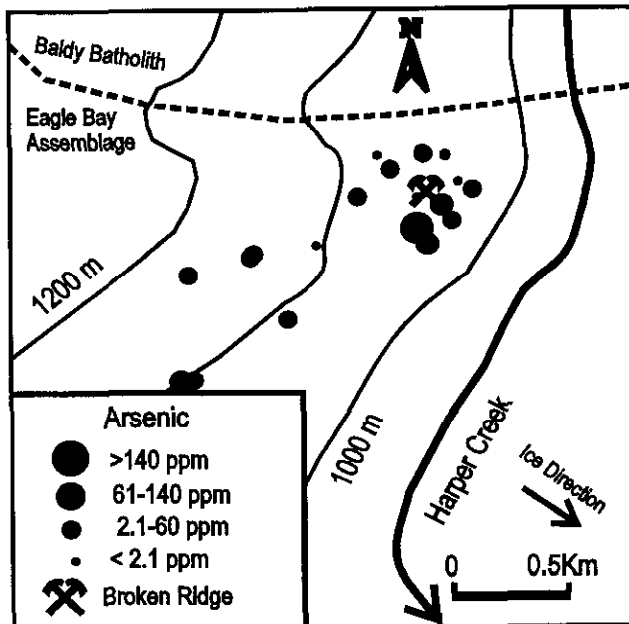


Figure 7. Arsenic in Till Samples, Broken Ridge Area.

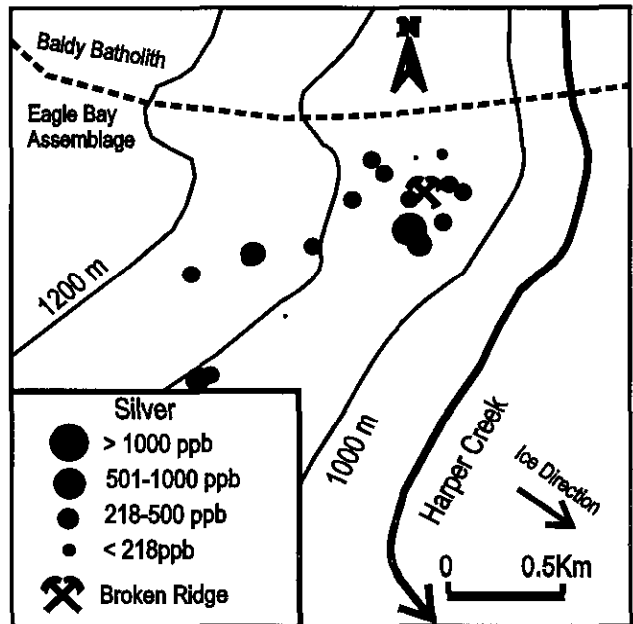


Figure 9. Silver in Till Samples, Broken Ridge Area.

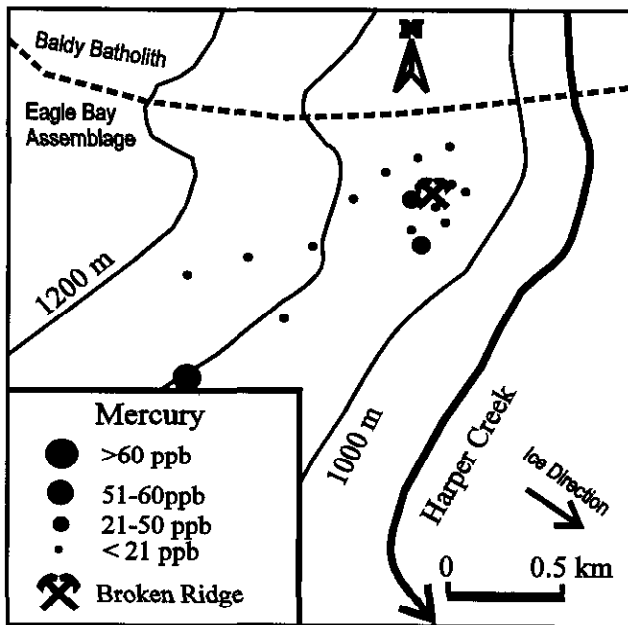


Figure 10. Mercury in Till Samples, Broken Ridge Area.

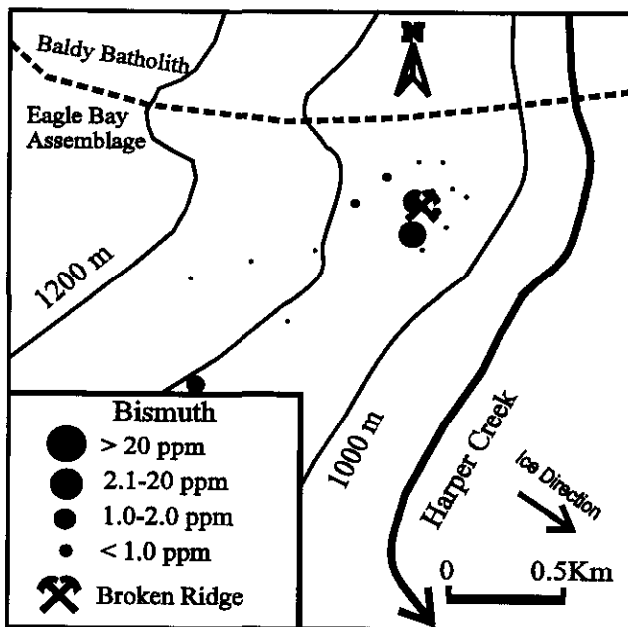


Figure 11. Bismuth in Till Samples, Broken Ridge Area.

### Cam-Gloria Property

Several new mineral occurrences have been discovered near Honeymoon Bay on Adams Lake by prospector Camille Berube through follow up of two till samples from the 1997 till release (Bobrowsky *et al.*,

1997). The till samples were strongly anomalous in gold (215 and 43 ppb), and very weakly anomalous in silver (0.6 ppm), bismuth (5 ppm), arsenic (15 ppm), molybdenum (11 ppm) and tungsten (6 ppm). Prior to Berube's work there were no MINFILE occurrences or records of previous work in this area.

The Honeymoon area is underlain by biotite quartz monzonite of the Cretaceous Baldy batholith which intrude amphibolite grade micaceous quartzite, quartz-mica schist and rare calcareous schist of the Eagle Bay Assemblage, and Devonian granitic orthogneiss (Schiarizza and Preto, 1987).

A large, rusty auriferous quartz vein (Honeymoon or "012" vein, Cam-Gloria claims) is the most interesting new mineral occurrence. It is located at about the 7 kilometre point on the north fork of the Grizzly Forest Service road, approximately 3 kilometres west of the Honeymoon Bay campsite on Adams Lake. The vein strikes at  $050^{\circ}$  and dips steeply northwest. The main body of quartz is up to 10 metres wide and approximately 200 metres in length. Other quartz outcrops and float have been found over an additional 150 metres of strike length. Concentrations of sulphide minerals occur within the vein, particularly on its southeast side and include pyrite, galena and minor chalcopryite. Grab samples of this sulphide-rich material have returned values as high as 27.4 ppm gold, 28.4 ppm silver, 120 ppm bismuth, 534 ppm lead, 427 ppm copper, 35 ppm arsenic, and 26 ppm molybdenum (Camille Berube, personal communication, 1997).

A random grab sample (97RL33R) from the whole quartz vein outcrop was taken during the detailed geochemical studies in July, 1997. The grab sample contained 1.38 ppm gold, 7.8 ppm silver, 55 ppm bismuth, 430 ppm lead, 118 ppm copper and 21 ppm molybdenum. Results for this and a second grab sample of vuggy quartz vein (CAM 1) collected by Trygve Høy are shown in Table 5. Also shown in Table 5 are results for till and soil samples collected within 2 metres from the vein. Element concentrations in a till sample (978219) reflect the rock geochemistry, but there is no increase of gold or other pathfinder metals in the B soil horizon (978220). A horizontal profile of gold, arsenic, bismuth, antimony, lead and zinc in till samples down-ice from the vein (Figure 12) reveals that most elements can be detected up to 1 kilometre to the southeast.

Approximately 1000 metres to the northeast, at the five kilometre mark on the road one of the authors (M.S. Cathro) tentatively identified pyrrhotite-bearing garnet-pyroxene skarn in float. This skarn may originate from the contact between Eagle Bay metasediments and monzonite to the northwest. In addition, roadcuts between the two areas expose several narrow (<4 centimetres wide) monzonite-hosted quartz-fluorite veins (strike  $290^{\circ}$ ; dip  $70^{\circ}$ S) and a 30 centimetre wide quartz-pyrite-pyrrhotite vein (strike  $015^{\circ}$ ; dip  $90^{\circ}$ ).

The Honeymoon prospect has broad similarities with intrusion-related mesothermal gold deposits such as those near Fairbanks, Alaska (McCoy *et al.*, 1997) and those associated with Tombstone suite intrusions in the Dawson-Mayo area of Yukon Territory (Poulsen *et al.*, 1997). The most important similarities are the gold-bismuth-

molybdenum association, the nearby occurrence of pyrrhotite-bearing skarn and fluorite-bearing veins, and the hostrock of Cretaceous monzonite intruding metamorphosed, carbonate-bearing pericratonic rocks. Honeymoon Bay appears to differ, however, in its lack of sheeted veins and its relatively low content of arsenic and antimony. Few of the Honeymoon Bay rocks have been analysed for metals such as tellurium and selenium. These elements are known to be present in the northern Cordillera deposits.

A possible analogue for the Honeymoon Bay vein may be the poorly described, but potentially economically significant, Pogo (Stoneboy) deposit near Fairbanks which is currently being explored by Sumitomo Metal Mining Arizona Inc. and Teck Corporation. There, a large, flat lying, high temperature quartz vein system is reported to be hosted by a mixed package of gneiss and Cretaceous monzonite over an 8 kilometre strike length. It carries very high gold values associated with pyrite, pyrrhotite and minor chalcopyrite, bismuthinite, arsenopyrite and stibnite (Tom Schroeter, personal communication, 1997).

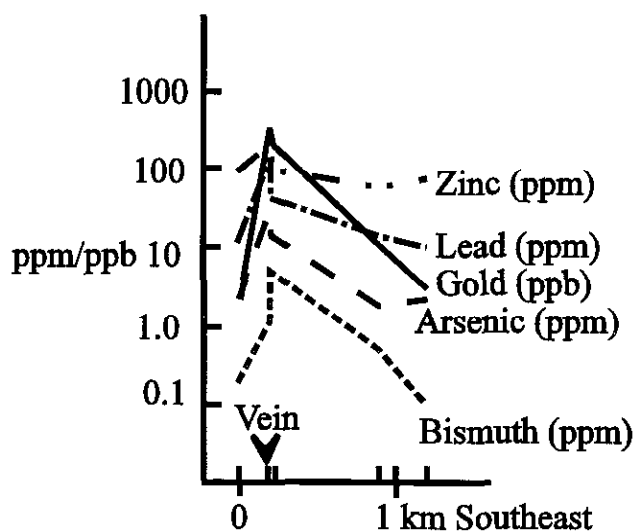


Figure 12. Geochemical Profiles for Elements in Till, Cam-Gloria Property.

## CONCLUSIONS

Element concentrations are typically higher in till and colluvium compared to levels in the B soil horizon. Comparison of geochemical patterns surrounding the Broken Ridge copper-lead-zinc-silver sulphide occurrence reveals a close spatial relationship between anomalous gold, silver, arsenic, copper and bismuth levels in till samples. The gold, silver and arsenic dispersal pattern are relatively short and most likely reflect down-slope transport of mineralized material in colluvium from the Broken Ridge occurrence. However, anomalous copper

values can be detected for up to 2 kilometres indicating a more extensive dispersal of copper mineralized bedrock in basal till. Selenium and arsenic in soil and till are geochemical pathfinders for precious-base metal mineralization typical of massive sulphide deposits in the Kootenay Terrane. However, mercury does not appear to be an effective pathfinder.

Copper anomaly contrast is not increased using tree bark as a sample type or by enzyme leach analysis.

Table 5. Cam-Gloria geochemistry. Gold by INA. Other elements by aqua regia-ICP. ND=Not Determined.

| Element | Soil97220 | Till97219 | Rock 97RL33 | CAM-1 |
|---------|-----------|-----------|-------------|-------|
| Au ppb  | 3         | 326       | 1112        | 3746  |
| Ag ppm  | 0.4       | 1.0       | 8.6         | 61.0  |
| As ppm  | 39.62     | 28.4      | 27.4        | 87    |
| Bi ppm  | 0.2       | 1.1       | 55          | 56    |
| Cd ppm  | 0.19      | 0.76      | 0.14        | <0.4  |
| Co ppm  | 4         | 7         | 3           | <2    |
| Cu ppm  | 8.5       | 24.2      | 113         | 17    |
| Fe %    | 1.38      | 3.51      | 10.78       | 1.68  |
| Ga ppm  | 6.5       | 5.1       | 3.5         | ND    |
| Hg ppb  | 32        | 24        | 29          | ND    |
| Mn ppm  | 468       | 784       | 72          | 40    |
| Mo ppm  | 0.9       | 0.5       | 11.6        | <2.0  |
| Ni ppm  | 10        | 8         | 5           | <2.0  |
| Pb ppm  | 10.4      | 127       | 420         | 191   |
| Sb ppm  | <0.2      | 0.6       | 3.7         | <5.0  |
| Se ppm  | <0.3      | <0.3      | <0.3        | ND    |
| Te ppm  | <0.2      | <0.3      | 3.5         | ND    |
| Tl ppm  | 0.2       | 0.3       | 0.7         | ND    |
| V ppm   | 22        | 34        | 7           | <2    |
| Zn ppm  | 135       | 202       | 27.1        | 18    |

Gold, bismuth, lead, arsenic and antimony can be detected in till up to 2 kilometres down-ice from the quartz-vein gold mineralization on the Cam-Gloria claims close the Honeymoon Bay on Adams Lake. However, element levels in the corresponding B-soil horizon of the till were lower or could not be detected. Anomalous bismuth also occurs in surficial material at the Broken Ridge and at the Harper Occurrence. The presence of anomalous bismuth could indicate reflect another mineralized source such as a skarn or vein associated with the Baldy batholith-Eagle Bay contact

Interpretation of data for the other study areas is in progress to identify additional geochemical pathfinders for mineralization and to compare the geochemistry of different grain size fractions of soil and till.

## ACKNOWLEDGMENTS

The authors would like to thank Steve Sibbick, now with Norecol, Dames and Moore, Inc., Vancouver, for

initiating this project and preliminary studies of the Harper, Homestake and Spar occurrences in 1996. Camille Berube is thanked for sharing his data and knowledge of the Cam-Gloria Claims. Dave Lefebure very kindly and promptly edited the first draft of this paper and his constructive suggestions are very much appreciated. The authors would also like to thank Trygve Höy for his comments on geology and mineralization of the Kootenay Terrane; Wayne Jackaman and Steve Cook for their very constructive comments on the paper.

## REFERENCES CITED

- Bobrowsky, P.T., Leboe, E.R., Dixon-Warren, A., Ledwon, A., MacDougall, D. and S.J. Sibbick (1997): Till Geochemistry of the Adams Plateau-North Barriere Lake area (82M/4 and 5); *B.C. Ministry of Employment and Investment*, Open File 1997-9.
- Bobrowsky, P.T., Leboe, E.R., Dixon-Warren, A. and Ledwon, A. (1997): Eagle Bay Project: Till Geochemistry of the Adams Plateau-North Barriere Lake area (82M/4 and 5); *in Geological Fieldwork 1996*, Lefebure, D.V., McMillan, W.J. and McArthur, G., Editors, *B.C. Ministry of Employment and Investment*, Paper 1997-1, pages 413-422.
- Cameron, E.M. (1977): Geochemical Dispersion in Mineralized Soils of a Permafrozen Environment; *Journal of Geochemical Exploration*, Volume 7, No.3, pages 301-326
- Dixon-Warren, A., Bobrowsky, P.T., Leboe, E.R. and Ledwon, A. (1997): Eagle Bay Project: Surficial Geology of the Adams Plateau (82M/4) and North Barriere Lake (82M/5) Map Areas; *in Geological Fieldwork 1996*, Lefebure, D.V., McMillan, W.J. and McArthur, G., Editors, *B.C. Ministry of Employment and Investment*, Paper 1997-1, pages 405-412.
- Höy, T. (1997): Harper Creek: A Volcanogenic Sulphide Deposit within the Eagle Bay Assemblage, Kootenay Terrane, southern British Columbia; *in Geological Fieldwork 1996*, Lefebure, D.V., McMillan, W.J. and McArthur, G., Editors, *B.C. Ministry of Employment and Investment*, Paper 1997-1, pages 199-210.
- Höy, T. (1991): Volcanogenic Massive Sulphide Deposits in British Columbia; *in Ore Deposits, Tectonics and Metallogeny in the Canadian Cordillera.*, McMillan, W.J, Editor, *B.C. Ministry of Energy, Mines and Petroleum Resources* Paper 1991-4, pages 89-199.
- Nelson, J. Sibbick, S.J. Höy, T. Bobrowsky, P. and Cathro, M. (1997): The Paleozoic Massive Sulphide Project: An investigation of the Yukon-Tanana Correlatives in British Columbia; *in Geological Fieldwork 1996*, Lefebure, D.V., McMillan, W.J. and McArthur, G., Editors, *B.C. Ministry of Employment and Investment*, Paper 1997-1, pages 183-186.
- McCoy, D. Newberry, R.J. Layer, P. DiMarchi, J.J., Bakke, A. Masterman, J.S. and Minehane, D.L. (1997): Plutonic-Related Gold Deposits of Interior Alaska, *Economic Geology*. Monograph No.9, pages. 191-241.
- Paulen, R., Bobrowsky, P.T., Little, E.C., Prebble, A.C. and Ledwon, A. (1998): Drift Exploration in the Southern Kootenay Terrane; *in Geological Fieldwork 1997*; *B.C. Ministry of Employment and Investment*, Paper 1998-1 (this volume).
- Poulsen, K.H. Mortensen, J.K. and Murphy, D.C. (1997): Styles of Intrusion Related Gold Mineralization in the Dawson-Mayo area, Yukon Territory, *in Current Research 1997A*, *Geological Survey of Canada*, pages 1-10.
- Rowe, J.S. (1972): Forest Regions of Canada; *Department of Fisheries and the Environment*, Canadian Forestry Services Publication No. 1300.
- Schiarizza, P. and Preto, V.A. (1987): Geology of the Adams Plateau-Clearwater-Vavenby Area. *B.C. Ministry of Energy, Mines and Petroleum Resources*; Paper 1987-2. 88 pages.
- Sibbick, S.J., Runnels, J.L. and Lett, R.E. (1997): Eagle Bay Project Regional Hydrogeochemical Survey and Geochemical Orientation Studies; *in Geological Fieldwork 1996*, Lefebure, D.V., McMillan, W.J. and McArthur, G., Editors, *B.C. Ministry of Employment and Investment*, Paper 1997-1, pages 423-426.



## SURFICIAL DEPOSITS IN THE LOUIS CREEK AND CHU CHUA CREEK AREA

By Roger C. Paulen, Peter T. Bobrowsky, Edward C. Little,

Amy C. Prebble and Anastasia Ledwon

B.C. Geological Survey Branch

**KEYWORDS:** Quaternary, surficial geology, terrain mapping, till, drift exploration, geochemistry, exploration, prospecting, North Thompson River, Louis Creek, Chu Chua Creek, Eagle Bay, Fennell.

### INTRODUCTION

Surficial geological mapping and drift exploration studies were undertaken in the summer of 1997 north of Kamloops in NTS map sheets 92P/1 (Louis Creek) and 92P/8 (Chu Chua Creek), as a continuation of the Eagle Bay Project initiated in the previous year (Bobrowsky *et al.*, 1997; Dixon-Warren *et al.*, 1997). The surficial component is part of an integrated regional study centred on Devonian-Mississippian rocks of the Eagle Bay Assemblage and Permian to Devonian rocks of the Fennell Formation. Massive sulphide deposits hosted in stratiform volcanogenic assemblages of the Fennell Formation at Chu Chua (MINFILE 092P 140) and syngenetic sedimentary rocks of the Eagle Bay Assemblage at Mount Armour (MINFILE 092P 051) suggest the region has considerable mineral potential. Polymetallic gold-bearing veins hosted in volcanic and volcanogenic rocks of the Fennell Formation at Windpass (MINFILE 092P 039) also suggest a high potential for gold in the area. Several placer occurrences of Au have also been recorded in the region.

Recent exploration and successful mineral discoveries in the Yukon (*i.e.* Kudz Ze Kayah and Wolverine) in correlative rocks to the Eagle Bay Assemblage provided the impetus for a Geological Survey Branch integrated project in the Kamloops district. This exploration project includes, mineral deposit studies (Höy and Ferri, 1998), detailed ice-flow dispersal studies (Lett *et al.*, 1998), till geochemistry sampling, and 1:50 000 scale surficial geology mapping. The latter two components provide vital information for mineral exploration in regions where unconsolidated sediments of variable thickness mask the underlying bedrock (Bobrowsky *et al.*, 1995).

The purpose of the drift exploration program was to map the surficial geology of the area and to document results of a reconnaissance level till geochemistry sampling survey. The goal of the surficial geology research was to map approximately 1000 square kilometres of rugged, high relief, glaciated terrain, by documenting the type and distribution of Quaternary sediments present. The surficial

maps for both 92 P/1E and 92P/8E are available at a 1:50000 scale as separate Open Files (Paulen *et al.*, 1998a; Paulen *et al.*, 1998b).

The objectives of the project were:

- to stimulate new exploration and economic activity in the area;
- to define new anomalies which may be used in the discovery of mineralization;
- to document ice-flow indicators and both local and regional ice-flow patterns which will aid drift prospecting in the area;
- to provide information that will be of use in other areas where mineral exploration has been hampered by thick glacial drift cover.

This paper describes the surficial mapping methods and preliminary results focusing on the types, distribution and character of Quaternary deposits. We also summarize the 1997 till geochemistry activities. Discussion of the ice-flow history and the Quaternary stratigraphy are provided to supplement the analytical results of the survey which will be released as a separate Open File with digital data on disc in 1998.

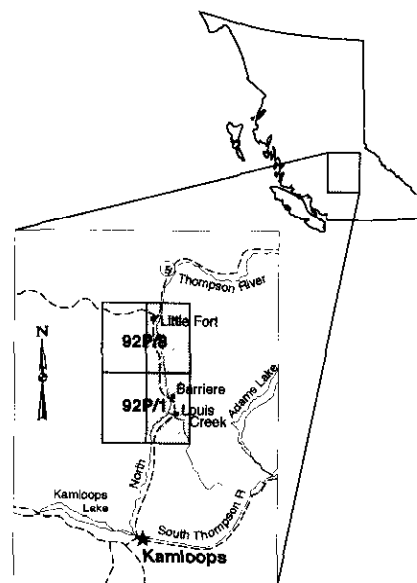


Figure 16-1. Location of the Eagle Bay drift exploration project (1997) study area in south-central British Columbia.

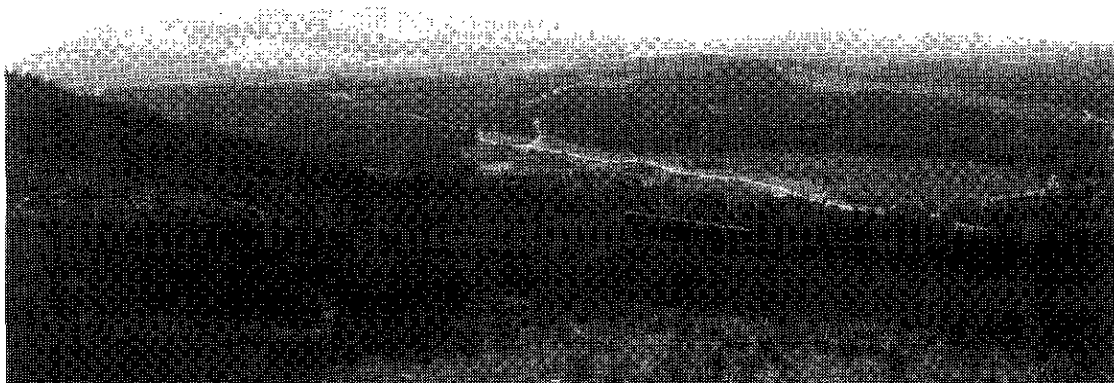


Photo 16-1. General view of topography and terrain in the Eagle Bay area. Till blanket/veneer covers prominent hills and ridges in background of photograph.

## BACKGROUND AND SETTING

Located in south-central British Columbia, the Louis Creek and Chu Chua map area (Figure 16-1) lies in the southwestern part of the Shuswap Highland and the northeastern part of the Thompson Plateau within the Interior Plateau (Holland, 1976). This region is characterized by moderate to high relief, glaciated, and fluvially dissected topography (Photo 16-1). Elevations range from 360 metres above sea level in the North Thompson River Valley in the west to about 2290 metres above sea level at Baldy Mountain in the northeast. Topography is variable with many flat areas interspersed with low to high relief. There is a relatively large plateau approximately 1300 metres above sea level which is heavily dissected by numerous prominent valleys. The largest valley, the North Thompson River occurs along the Louis Creek Fault and is the boundary between the Adams Plateau to the east and the Bonapart Hills to the west.

All streams and minor creeks drain into the North Thompson River which is characterized by a broad, braided fluvial plain. The river flows southward and joins the Thompson River at Kamloops which is a major tributary to the Fraser River system. Dunn Lake is the only other notable body of water in the study area.

Most of the area is covered by drift of mixed genesis and of variable thickness. Ground moraine (of various facies) dominates the landscape, followed in turn by colluvial, glaciofluvial, fluvial and glaciolacustrine sediments which collectively make the area extremely favorable for a till geochemistry sampling survey.

## Bedrock Geology

The area lies within a belt of structurally complex low-grade metamorphic rocks which lies along the western

margin of the Omineca Belt. This belt is flanked by high grade metamorphic rocks of the Shuswap Complex to the east and by rocks of the Intermontane Belt to the west (Schiarrizza and Preto, 1987). Lower Paleozoic to Mississippian rocks of the Eagle Bay Assemblage (Kootenay Terrane) underlie a significant part of the area. The rocks consist of calcareous phyllite, calc-silicate schist and skarn, or mafic metavolcanics overlain by felsic metavolcanic rocks, intermediate metavolcanics and clastic metasediments. To the north, the Permian to Devonian rocks of the Fennell Formation comprise imbricated oceanic rocks of the Slide Mountain Terrane. These consist of bedded cherts, gabbro, diabase, pillowed basalt and volcanogenic metasediments. To the northeast and northwest, mid-Cretaceous granodiorite and quartz monzonite intrusions of the Baldy Batholith and the late Triassic - early Jurassic monzo-granite and granodiorite of Thuya Batholith (Campbell and Tipper, 1971) underlie the area, respectively. The far northwestern margin of the map area is underlain by Upper Triassic Nicola Group (Quesnel Terrane) andesite, tuff, argillite, greywacke and limestone, generally in faulted contact with the rocks of the Fennell Formation.

A major north-trending fault within the North Thompson River valley separates the Kootenay and Slide Mountain terranes from the younger Quesnel terrane to the west. Eocene breccias occur sporadically along the western edge of the Thompson River valley and also at Skull Hill.

Polymetallic precious and base metal massive sulphides occurrences are hosted by Devonian-Mississippian felsic to intermediate metavolcanic rocks of the Eagle Bay Assemblage. Massive sulphides are hosted in oceanic basalts of the Fennell Formation; skarn mineralization and silver-lead-zinc vein mineralization occur as numerous deposits within the Fennell Formation near the Cretaceous granitic intrusions. There are a total of 19 mineral occurrences in the study area (Figure 16-2), seven occur in

the Eagle Bay Assemblage and eight occur in the Fennel Formation. There are four occurrences within the Baldy and Thuya batholiths containing Mo and Mo-Cu-Ni. In total, there are 11 gold occurrences, of which two are placer deposits.

## METHODS

Fieldwork was based from one camp at Tod Mountain. Access to the map area is excellent with Yellowhead Highway #5 bisecting both the study area. There is an extensive network of logging roads except for the steeper slopes. Only in the northeast in the higher alpine areas of Baldy and Chu Chua mountains are roads infrequent and access poor.

Fieldwork was conducted with 4-wheel drive vehicles along all major and secondary roads and trails of varying condition. In some cases, traverses were completed on foot where access was blocked or non-existent. One helicopter traverse was conducted to examine large-scale features, as well as to evaluate terrain polygons that were inaccessible otherwise.

Initial work consisted of compiling and evaluating all existing terrain information available for the area. Regional Quaternary mapping completed by the Geological Survey of Canada (Tipper, 1971) and soil and landscape maps produced by the Resource Analysis Branch of the B.C. Ministry of Environment (Gough, 1987a, 1987b) provided preliminary information on the types and distribution of the surficial sediments. Air photographic analysis contributed to the regional ice-flow history through the identification of lineations and drumlinoid forms on the plateaus. Detailed local ice-flow directions were obtained by measuring and determining the directions of striations, grooves and local roche moutonnées.

Air photographic interpretation and 'pretyping' followed the methodology of the Resources Inventory Committee (1996) and the terrain classification system of Howes and Kenk (1997). Air photographs at a scale of 1:30 000 (approx.) (flight lines 15BCC-95009, 95014, 95017) were used in the map generation. Final terrain maps were produced at a scale of 1:50 000. Preliminary terrain polygon interpretations were verified through ground-truthing. Approximately seventy-five percent of the polygons were evaluated on the ground, thereby corresponding to a Terrain Survey Intensity Level B (Resources Inventory Committee, 1996).

At each ground-truthing field station some or all of the following observations were made: GPS-verified UTM location, geographic features (*i.e.* creek, cliff, ridge, plateau, etc.), type of bedrock exposure, if present, unconsolidated surface material and expression (terrain polygon unit), general slope, orientation of striations/grooves on bedrock or of bullet-shaped boulders, large scale features of streamlined landforms, elevations of post-glacial deposits (glaciofluvial and glaciolacustrine) and active geological processes.

Bulk sediment samples (1-5 kg in size) were collected for geochemical analysis over much of the study area. Emphasis was placed on collecting basal till deposits (first derivative products according to Shilts, 1993), although

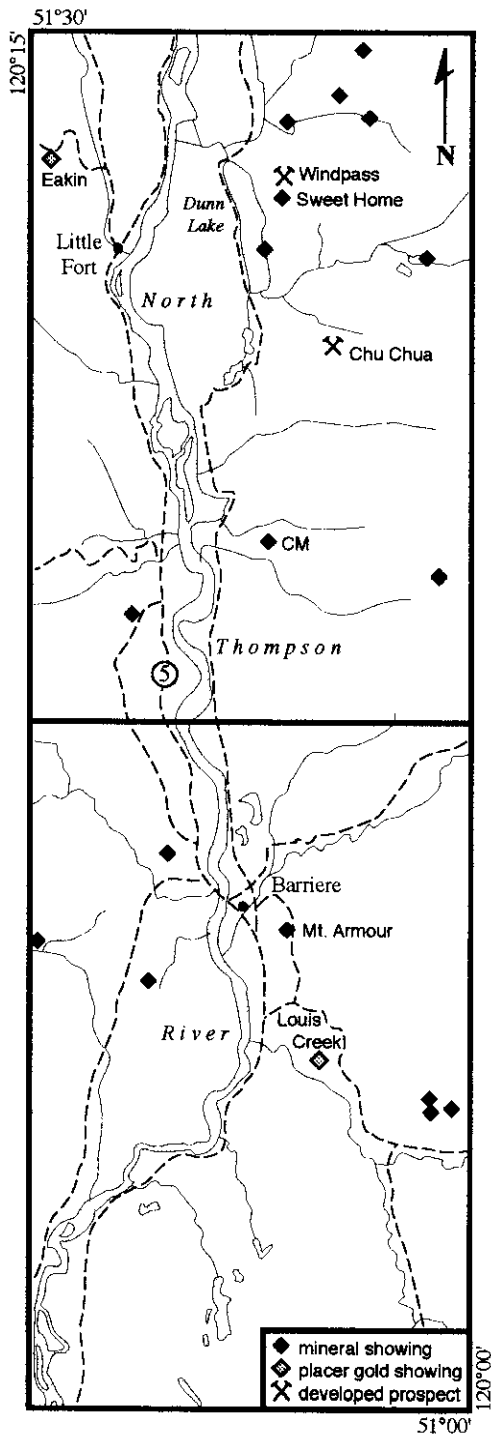


Figure 16-2. Mineral occurrence locations for NTS 92P/1E and 92P/8E from the MINFILE database.

ablation till, colluviated till and colluviated till was also collected under certain circumstances. Natural exposures and hand excavation were used to obtain samples from undisturbed, unweathered C horizon (parent material) deposits. At each sample site, the following information was recorded: type of exposure (gully, roadcut and so on), depth to sample from top of soil, thickness of A and B soil horizons, total exposed thickness of the surficial unit, stratigraphy of the exposure, clast percentage, matrix or clast supported diamicton, consolidation, matrix texture, presence or absence of structures, bedding, clast angularity (average and range), clast size (average and range), clast lithologies, and colour. The sample was evaluated as being derived from one of the four categories; basal till, ablation till, basal/ablation till derived from the Baldy Batholith, or colluviated/reworked basal till. Sediment samples were sent to Eco Tech Laboratories in Kamloops for processing. This involved air drying, splitting and sieving to <math><63 \mu\text{m}</math>. The pulps, <math><63 \mu\text{m}</math> sample and unsieved split were subsequently returned to the BCGS. The <math><63 \mu\text{m}</math> fraction of each sample was further divided into 10 and 30 gm portions. The smaller portion was sent to Acme Analytical Laboratory, Vancouver, where samples were subjected to aqua regia digestion and analysis for 30 elements by ICP (inductively coupled plasma emission spectroscopy) and for major oxides by  $\text{LiBO}_2$  fusion - ICP (11 oxides, loss on ignition and 7 minor elements). The larger portion was sent to Activation Laboratories, Ancaster, Ontario for INA (thermal neutron activation analysis) for 35 elements (Table 16-1).

**TABLE 16-1: ANALYTICAL METHODS EMPLOYED AND ELEMENTS ANALYZED FOR TILL GEOCHEMISTRY SURVEY.**

| ANALYSIS   | ELEMENTS                                                                                                                                                                                                                                                                  |
|------------|---------------------------------------------------------------------------------------------------------------------------------------------------------------------------------------------------------------------------------------------------------------------------|
| Whole Rock | $\text{SiO}_2$ , $\text{Al}_2\text{O}_3$ , $\text{Fe}_2\text{O}_3$ , $\text{CaO}$ , $\text{MgO}$ , $\text{Na}_2\text{O}$ , $\text{K}_2\text{O}$ , $\text{MnO}$ , $\text{TiO}_2$ , $\text{P}_2\text{O}_5$ , $\text{Cr}_2\text{O}_3$ , LOI, Ba, C, Ni, Nb, S, Sr, Sc, Y, Zr |
| INA        | Au, Ag, As, Ba, Br, Ca, Co, Cr, Cs, Fe, Hf, Hg, Ir, Mo, Na, Ni, Rb, Sb, Sc, Se, Sn, Sr, Ta, Th, U, W, Zn, La, Ce, Nd, Sm, Eu, Tb, Yb, Lu                                                                                                                                  |
| ICP        | Mo, Cu, Pb, Zn, Ag, Ni, Co, Mn, Fe, As, U, Au, Th, Sr, Cd, Sb, Bi, V, Ca, P, La, Cr, Mg, Ba, Ti, B, Al, Na, K, W, Tl, Hg, Se, Te, Ga                                                                                                                                      |

## RESULTS

A total of 530 field stations were examined for ground truthing during the survey. The density of the stations for the total map area is approximately one station per 1.8  $\text{km}^2$ . A total of 352 bulk sediment samples were collected for the till geochemistry study (Figure 16-3). Samples were collected at an average depth of 1.7 metres below the soil surface. Till sample density averaged one per 2.8  $\text{km}^2$  for the total survey. This level of survey and sampling provides a high level of reconnaissance information for the region.

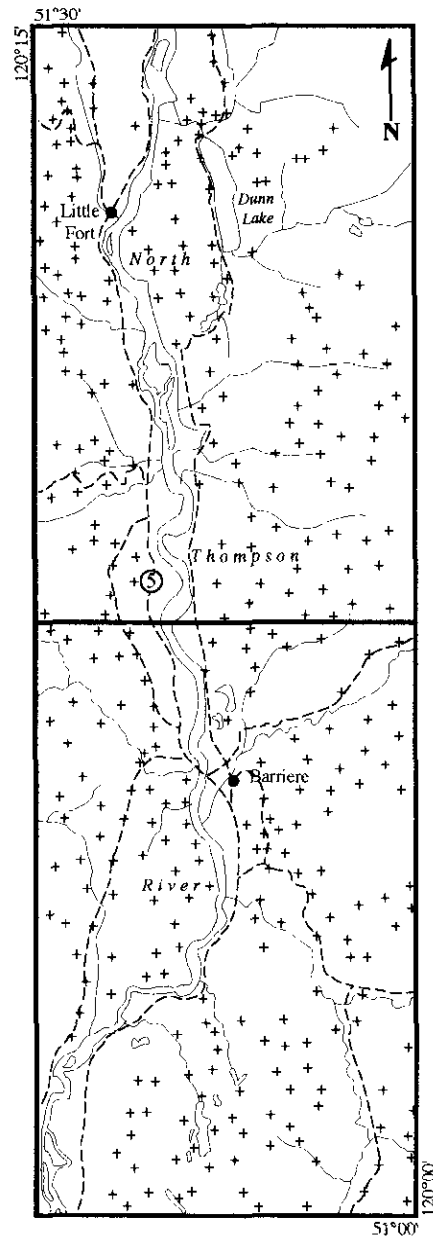


Figure 16-3. Till geochemistry 1997 survey sample sites.

Most of the samples taken for geochemical analysis were representative of basal till (M1), most likely lodgement till (Photo 16-2). Of the 352 samples, 255 or 72% represented this sediment type (Table 16-2). Ablation and basal till derived from the Baldy Batholith rocks (M3) only accounted for 2 samples or <1% of the total. Basal till which has undergone slight downslope movement was identified as colluviated till (CM). Samples of this material accounted for 9 or 3% of the total. Together these groups (76%) represent the best media to sample for drift exploration. The remaining 86 or 24% of the samples which were collected from ablation till (M2) are also valid, but more difficult to interpret. Results and interpretation of the till geochemistry survey for this study will be released elsewhere.

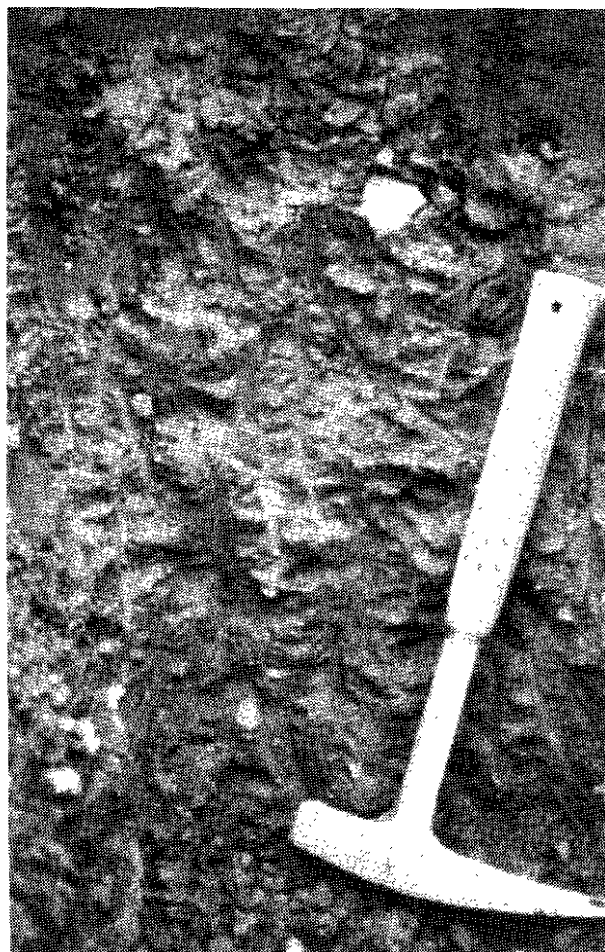


Photo 16-2. Close-up view of typical basal lodgement till commonly sampled during drift prospecting.

Previous geochemical studies in the area provide an early indication as to the style of mineralization, configuration of the anomaly plumes and regional dispersal patterns one can expect for this region. Two examples of property scale geochemical sampling from two separate occurrences, are presented here as precursors to the expected regional dispersal patterns.

At the Cedar I to VI mineral claims (MINFILE 92P 055), located eight km northwest of Little Fort and directly above Eakin Creek, soil samples taken from the C horizon illustrates two forms of geochemical dispersal patterns (Yorston and Ikona, 1985). The gold dispersal pattern shows a small, fan-shaped, down-ice dispersal pattern on the higher ground with the axis of symmetry paralleling the regional ice-flow from northwest to southeast and thus reflects a typical clastic dispersal (DiLabio, 1990). On the slopes above Eakin Creek, a secondary downslope dispersion has modified the original dispersal fan stretching the southern boundary of the anomaly. This is shown in Figure 16-4 where the gold illustrates a compound two vector configuration consisting of clastic plus hydromorphic dispersal.

**TABLE 16-2. FREQUENCY DISTRIBUTION FOR DRIFT PROSPECTING SAMPLES ACCORDING TO PRIMARY GENETIC MATERIAL.**

| UNIT         | DESCRIPTION                                                                                     | #          | %          |
|--------------|-------------------------------------------------------------------------------------------------|------------|------------|
| M1           | Basal till derived from Kootenay, Slide Mountain and Quesnel terranes                           | 255        | 72         |
| M2           | Ablation till derived from Kootenay, Slide Mountain Terranes and Cretaceous-Tertiary intrusions | 86         | 24         |
| M3           | Lodgment and ablation till derived from Baldy Batholith                                         | 2          | <1         |
| CM           | Colluviated/ reworked till                                                                      | 9          | 3          |
|              |                                                                                                 |            |            |
| <b>TOTAL</b> |                                                                                                 | <b>352</b> | <b>100</b> |

At the CM Property (MINFILE 92P 101), located 15 km north of Barriere and near the confluence of Cold and Newhykulston Creeks, soil geochemistry shows several ribbon anomalies of copper (Casselmann, 1993). The dispersal pattern parallels the local ice-flow which was directed down the North Thompson River valley in the early and late stages of the Fraser Glaciation. There is little or no indication of regional dispersal to the southeast during the peak glacial period. As in the previous case, the anomaly shows secondary downslope dispersion due to hydromorphic extension (Figure 16-5).

## GLACIAL HISTORY AND STRATIGRAPHY

According to Fulton and others (Fulton, 1975; Fulton and Smith, 1978; Ryder *et al.*, 1991), the present day landscape of south-central British Columbia is the result of two glacial cycles, one interglacial period and vigorous early-Holocene erosion and sedimentation. Only the latter

glacial deposits and the post-glacial deposits are present in the study area. Although not necessarily present in the study area, the following lithological units and their correlative geological climate units have been identified in south-central British Columbia.

the present-day surface cover of postglacial deposits. This unit consists of silt, sand, gravel and till deposited during the Fraser Glaciation (Late Wisconsinan).

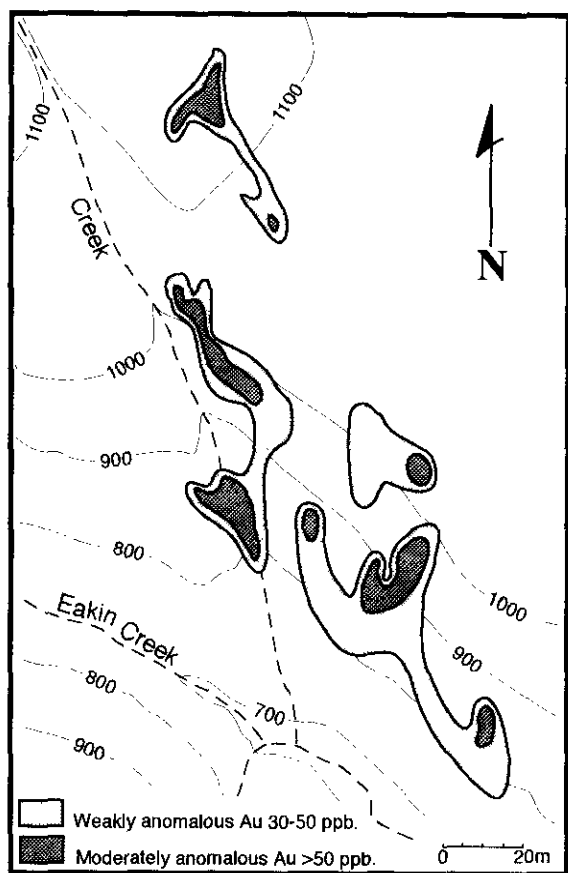


Figure 16-4. Gold soil anomaly for the Cedar I to VI mineral claims (Eakin Creek). Modified after Yortson and Ikona (1985).

Stratigraphically the oldest and identified only at two locations some 60 and 100 km to the south, are the interglacial Westwold Sediments. The deposits consist of cross-stratified gravely sand capped by marl, sand, silt, and clay, all of which are equivalent to the Highbury non-glacial interval in the Fraser Lowland (Sangamonian). Next youngest are Okanagan Centre Drift deposits, consisting of coarse, poorly stratified gravel, till and laminated silt, currently identified at Heffley Creek (20 km south of the map area), and elsewhere farther south. The sediments were deposited during the Okanagan Centre Glaciation, equivalent to the Semiahmoo Glaciation in the Fraser Lowland (early Wisconsinan). Middle Wisconsinan, Olympic Non-Glacial Bessette Sediments overlie the Okanagan Centre Drift. They consist of nonglacial silt, sand and gravel with some organic material and up to two tephra. The Kamloops Lake Drift (25.2 ka; Dyck and Fyles, 1963) overlies the Bessette sediments, and underlies

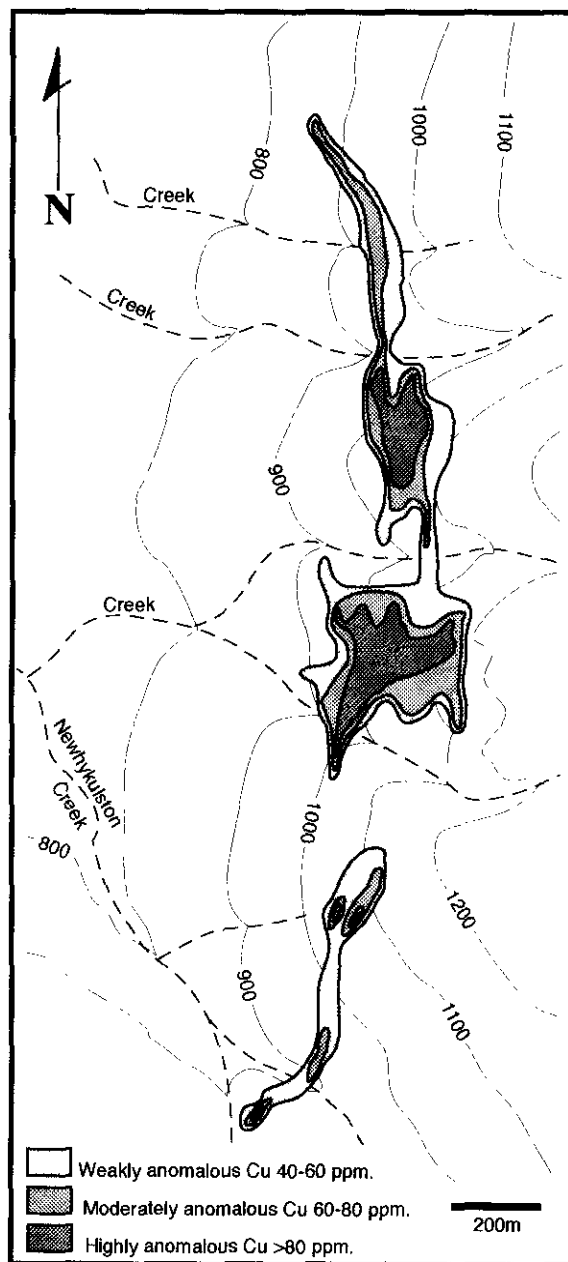


Figure 16-5. Copper soil anomaly for the CM Property (L.K.). Modified after Cassleman (1993).

An outlier of sculpted rock and erratics, possibly from the Penultimate glaciation, occurs 2500 metres above present day sea level near the northeastern margin of the map area. Rare, older striae preserved on bedrock surfaces suggest an early glacial advance from the northeast to the southwest, but there is no evidence of this in the surficial record. The surface and near-surface sediments mapped in the Louis Creek and Chu Chua Creek area directly result

from the last cycle of glaciation and deglaciation (Fraser Glaciation), as well as ensuing post-glacial activity.

### ***Fraser Glaciation***

The onset of Fraser glaciation began in the Coast, Cariboo and Monashee Mountains. Valley glaciers descended to lower elevations to form piedmont lobes in the Interior Plateau and eventually coalesced to form a mountain ice sheet (Ryder *et al.*, 1991). Ice sheet margins reached a maximum elevation between 2200 and 2400 metres along rimming mountains; the entire Shuswap Highland, except for perhaps Dunn Peak (2630 metres) and higher peaks to the north, was completely buried beneath an ice cap by approximately 19 ka. At Fraser Glaciation maximum, regional ice-flow was to the south-southeast, with deviations up to 45° (Fulton *et al.*, 1986). Ice-flow was initially diverted down the North Thompson River valley and again diverted during deglaciation. Basal till deposits, which range widely in texture with the underlying bedrock, blanketed the land surface.

Deglaciation of the Interior Plateau was rapid; the equilibrium line rose considerably, reducing the area of accumulation for the Cordilleran ice sheet, and the ice mass decayed by down-wasting. Ablation till was deposited by stagnating ice in several high-elevation portions of the region. As uplands were deglaciated prior to low benches and valleys, meltwater was channeled to valley sides, resulting in kame terraces and ice-contact sediments that mainly occur below 540 metres elevation. Valleys clear of ice above the stagnating glaciers became areas of confinement for meltwater blocked from drainage, thereby resulting in local mantles of glaciolacustrine sediments. Observations show that these ice-dammed lakes attained a minimum elevation of 425 metres (above present day sea level). Radiocarbon dates of 11.3 ka to the north at McGillivray Creek (Clague, 1980), and 10.1 and 9.84 ka on Mount Feadar Plateau (Blake, 1986) in the southeast indicate that deglaciation began about 12 ka and that the modern drainage pattern was established by 9 ka. A minor re-advance of ice from local peaks and summits to the north occurred between 11 and 6.6 ka (Duford and Osborn, 1978).

### ***Holocene Post-Glacial***

Once ice-dammed lakes were released, melt-waters carrying heavy sediment loads deposited thick units of stratified sand and gravel in valleys. As sediment loads decreased, deposition was replaced by erosion, and water courses cut down through valley fills, leaving glaciofluvial terraces abandoned on valley sides. Following the complete deglaciation of the region, unstable and non-vegetated slopes were highly susceptible to erosion. Intense mass wasting of surface deposits on oversteepened valley slopes resulted in the deposition of colluvial fans and aprons along valley bottoms. Most post-glacial

deposition occurred within the first few hundred years of deglaciation, and certainly before the eruption of Mt. Mazama, 6.6 ka, which deposited tephra near the present-day ground surface. Fluvial plain deposits and active talus slopes typify the modern sedimentation in the area.

## **SURFICIAL SEDIMENTS**

Eight types of surficial deposit associations were defined and observed in the map area including: ground moraine (basal till), ground moraine (ablation till), colluvial, fluvial, glaciofluvial, glaciolacustrine, organic, and anthropogenic. General observations suggest the plateaus and hills are mainly covered by combinations of till, colluvium and minor glaciofluvial deposits, whereas glaciolacustrine, glaciofluvial and fluvial sediments occur mainly in the valleys. Bedrock outcrops account for less than 5% of the total map area, and these are predominately found in the northeast near Baldy and Chu Chua mountains. Anthropogenic deposits are not widespread and can be found only near developed prospects and the larger communities. Organic deposits occur locally, but in minor amounts in all types of terrain.

### ***Basal Till***

Throughout the region, the bedrock topography is mantled by variable amounts of massive, very poorly sorted matrix-supported diamicton (Photo 16-3). Deposits range in thickness from thin (<1 m) veneers to thick (>10 m) blankets. Characteristics of this diamicton suggest that it is most likely a lodgement depositional environment (Dreimanis, 1988). Basal till facies were variable with respect to the underlying bedrock, but not areally extensive enough to be subdivided into mappable units.

In general, basal till (lodgement till) deposits are primarily massive to poorly-stratified, light to dark olive grey, moderately to highly consolidated and derived from greenstone metavolcanics and metasediments of the Eagle Bay Assemblage and Fennell Formation. The matrix is fissile and has a clayey silt to a silty sand texture. Deposits are dense, compact, cohesive with irregular jointing patterns. Clast content ranges from 15-35%, usually averaging about 25%, and clasts range in size from granules to boulders (over 2 metres) averaging 1-2 centimetres. The clasts are mainly subrounded to subangular in shape and consist of various lithologies of local and exotic source. A number of clasts have striated and faceted surfaces.

To the west and northwest, basal till in the vicinity of the Thuya River Batholith is characteristically sandier in texture and the clasts reflect the nature of the source material. Modal grain size is much higher than basal till derived from the finer-grained greenstone rocks of the Eagle Bay Assemblage and the Fennell Formation and is a result of the coarse crystals of the monzonite intrusion.



Photo 16-3. View of basal till overlying glaciolacustrine sediments.

Clast content ranges from 25-45%, usually averaging 35%, and clasts range in size from granules to very large boulders (over 4 metres) averaging 2-4 centimetres. The clasts are mainly rounded to subangular in shape and due to the nature of the source rock, are rarely striated or faceted.

#### *Ablation Till*

Massive to crudely stratified, clast-supported diamicton (Photo 16-4) occurs frequently throughout the study area. Most commonly, deposits of ablation till occur as a thin mantle overlying basal till and/or bedrock on the higher plateaus. Deposits also occur in areas of hummocky terrain where evidence of recessional ice and mass-wasting occurred during deglaciation. In contrast to the basal tills, these diamictons are light to medium grey, moderately compact and cohesive. The sandy matrix is poorly consolidated usually contains less than 5% silt and clay.

Clast content ranges from 30-60% and average clast size is 2-5 centimetres. Clast lithology is variable but often deposits are monolithologic, primarily granodiorites and monzonite derived from the Thuya River, Baldy and Raft Batholiths. Only till derived from the Baldy Batholith (M3) is considered areally extensive enough to be mapped as a separate till facies. This

feature is common to the west and northeast but mixed lithologies increase in abundance gradually to the south. These diamictons are interpreted as supraglacial or ablation till deposits, resulting from deposition by stagnating glacier ice (Dreimanis, 1988).

#### *Glaciofluvial Sediments*

Deposits of massive to stratified sand, gravel and silt occur in upland valleys and as terraces in the North Thompson River valley. Deposit characteristics vary considerably from kame terraces to meltwater channels or large deltaic sequences in the lower valleys. The large glaciofluvial terraces in the North Thompson River valley primarily occur below 540 metres elevation and provide a near-maximum elevation for the northern extent of the glaciolacustrine lake that existed in the Kamloops area at the close of the Fraser Glaciation (Fulton, 1965). The coarse gravel beds range from open framework clast-supported beds to very well-stratified beds with normal, reverse or no grading exhibited. Pebble imbrication, cross-stratified beds, ripples and other structures provide evidence for paleo-stream flow. These are often interstratified with finer beds of silty sand, to coarse pebbly sand occasionally with cross-bedding. They likely represent ice-proximal to ice-distal facies deposited during deglaciation. In rare cases, eskers

were observed directly east of the Bonapart Hills. These tend to be only a few metres in height and no more than 10 metres in width and trending southeasterly for a few hundred metres.

### ***Glaciolacustrine Sediments***

Along the North Thompson River, large sections of glaciolacustrine sediments form terraces above the modern day floodplain. The terraces occur below 425 metres above sea level, providing a minimum elevation of a large post-glacial lake in the valley. The exposures

consist of rhythmically laminated, horizontal, tabular beds of massive to normally graded beds of fine sand, silt and clay. Ripple laminations, ball and pillow structures, and flame structures are common. Ice-rafted stones are common and the surrounding sediments exhibit penetrative structures. Individual rhythmites have sharp basal contacts and vary in thickness from a few millimetres to several tens of centimetres. Variations in deposit characteristics indicate differing proximity to the retreating ice front.



Photo 16-4. General view of coarse textured ablation till.

### ***Fluvial Sediments***

Intensive Holocene erosion has resulted in extensive fluvial deposits. Abandoned stream channels and large fluvial fans commonly occur at the edges of the North Thompson River valley. The islands and modern floodplain of this river valley comprise the majority of the fluvial deposits in the region. The entire community of Barriere is built upon a post-glacial fluvial fan. Deposits consist of clean, well-sorted and stratified sand and gravel. Clasts are well-rounded and reflect both local bedrock and older drift provenance. Fluvial deposits are mainly restricted to the lower elevations,

occurring as terraced landforms or discontinuous sediment veneers over modern day floodplains.

### ***Colluvium***

The intense erosion of the Holocene and the high relief topography of the region has produced significant amounts of colluvial debris. Deposition and accumulation of colluvial sediments is a result of gravity-induced downslope movement of fractured bedrock and/or unconsolidated sediments. The source material contributing to the deposit strongly influences its character. As a result, colluvium varies from massive

to crudely stratified, poorly-sorted to moderately-sorted, matrix to clast-supported, and monolithologic to polyolithic. Deposits of colluvium in the region vary from a thin veneer to several metres thick and overlie all other types of surficial sediments and bedrock. Clast size ranges from granules to boulders and shape ranges from subrounded to angular, depending on source provenance. Deposits can occur as massive cones on bedrock slopes, to broad stratified fans, to a thin veneer on steep till slopes.

### ***Organic Deposits***

Organic deposits occur locally in areas of poor drainage. Deposits occur in the established islands and in abandoned oxbow channels in the North Thompson

River. Organic deposits are also common around major meltwater channels, where modern day drainage is very poor. On the high plateaus, organic deposits are formed in-between the drumlinoid landforms and roche moutonnées where the bedrock topography traps surface water and forms small highland bogs (Photo 16-5).

### ***Anthropogenic Deposits***

Anthropogenic deposits consist of materials modified by human activities to the extent that their initial physical properties and surface expression are drastically altered. Such deposits occur in the mine dumps of the Windpass and Sweet Home developed prospects and within the town of Barriere as fill.

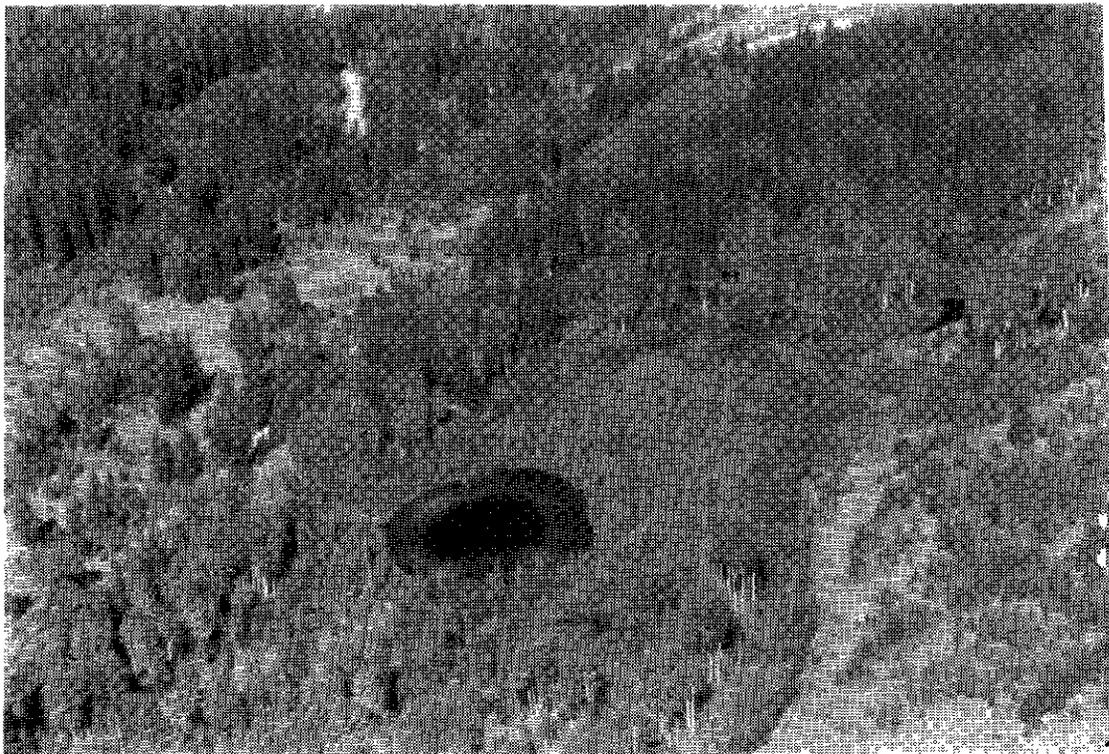


Photo 16-5. Oblique view of upland bog terrain found in lowlying areas between fluted ridges.

## **DRIFT EXPLORATION IMPLICATIONS**

The thin drift mantling the upland plateaus and the defined valley systems provides an excellent landscape for drift prospecting. The lower-lying areas above the terraces of the North Thompson River valley have thin veneers of colluvium that are usually derived from local basal till. Basal tills in this region directly overlie the bedrock and are representative of the last glaciation to have affected the region. No sediments that predate this event were observed in the area. Thin deposits of basal tills, like that observed on the upland plateaus, usually

reflect a more proximal source area for the sediments (Bobrowsky *et al.*, 1995). Basal tills are the dominate sediment type and this media has been recognized as the most ideal sampling media for drift prospecting (Shilts, 1993). If there are no complications related to multiple ice-flow directions, then a dispersal plume should reflect the last glacial event. Finally, the ice-flow direction is generally east-southeast to south-southeast over the plateau and may vary from south to southwest in the North Thompson River valley. Such characteristics provide ideal conditions for both reconnaissance and property scale drift prospecting.

Reported geochemical anomalies from known mineral occurrences indicate that the dispersal plumes conform to classic down-ice shapes, usually proximal to the source bedrock. It is expected that clastic dispersal patterns associated with any anomalous values detected from this reconnaissance survey will most likely parallel ice-flow, but may be imprinted with minor fluctuations from hydromorphic downslope dispersal. Given the nature of the sediment genesis and deposit characteristics, it is further expected that these anomalies will occur within a 100 metres from source rock. Particular care must be observed when working in the North Thompson River valley because evidence suggests ice-flow was locally diverted during the onset and retreat of the Fraser Glaciation.

## CONCLUSION

A drift exploration program was initiated and completed during the summer of 1997 focusing on surficial geology mapping and till geochemistry over potentially polymetallic rocks of the Eagle Bay Assemblage and base metal and gold-bearing rocks of the Fennell Formation north of Kamloops. Two 1:50 000 scale terrain geology maps have been completed for the area, showing the type and distribution of surficial sediments present. A total of 352 samples were collected for the till geochemistry survey and subjected to ICP, INA and whole rock analysis. A total of 26 mineralized float and gossan samples were collected for analysis as well.

The landscape of the Louis Creek - Chu Chua Creek region is the product of a well-documented glacial and postglacial geological history. Although the region has experienced several glaciations, it is only the effects of the final glaciation during the Late Wisconsinan coupled with extensive modification during the Holocene that has had the most significant impact on the type and distribution of the surficial sediments in the area. Much of the area is covered by ground moraine, often veneers or thin blankets of basal till and veneers and hummocks of supraglacial till. Colluvium is the next most abundant and areally extensive surficial material. It most commonly occurs as a thin (<25 centimetres) veneer on moderate to steep till slopes and occasionally occurs as a thick colluvial fan deposit at the base of a slope and hanging valleys. Stratified outwash deposits are found in small valleys at higher elevations and as kame deltas and glaciofluvial deltas from paleo-streams that once flowed into an ice-dammed lake in the present Thompson River valley. These deltas now form terraces at a common elevation along the length of the North Thompson River and this could be useful for potential aggregate source material. Glaciolacustrine sediments are found in small areas of ponding in some of the smaller valleys and as

thick deposits in the North Thompson River valley. Finally, in flat-lying areas of poor drainage, organic deposits are commonly found.

The type, character, thickness and distribution of the surficial sediments is an important element in any regional and local exploration program. The lack of bedrock exposure in some areas implies that the proper genetic interpretation of glacial overburden is essential in delimiting and understanding potential areas of mineralization. Knowledge of ice-flow history is very critical for a drift exploration program and known geochemical anomalies that exhibit classic down-ice dispersal patterns follow the regional ice flow patterns. This indicates that the local terrain is highly suitable for drift exploration studies. Local and regional ice flow patterns are readily determined in the field at the site level. The recorded showings of placer gold also warrant investigation of unknown source rock material. Integration of the surficial geology maps and this reconnaissance till survey should now be pursued at the property scale of exploration to locate potential sites of buried mineralized zones.

## ACKNOWLEDGMENTS

This work was completed as part of the B.C. Geological Survey Branch Kootenay Terrane Project. Thanks to Ray Lett for managing sample preparation and analysis of all the geochemistry samples. We extend our thanks to the Kamloops office of the Ministry of Employment and Investment for providing logistical services and especially to Mike Cathro for providing insight on the bedrock geology and some of the local mineral deposits. Field accommodation was provided by Sun Peaks Resort. Al Gilmore provided supportive field logistics and equipment. Ayisha Yeow assisted with the till sampling.

## REFERENCES CITED

- Blake, W., Jr. (1986): Geological Survey of Canada Radiocarbon Dates XXV; *Geological Survey of Canada*, Paper 85-7, 32 p.
- Bobrowsky, P.T., Sibbick, S.J., Matysek, P.F. and Newell, J. (1995): Drift Exploration in the Canadian Cordillera, *B.C. Ministry of Energy, Mines and Petroleum Resources*, Paper 1995-2, 303 pages.
- Bobrowsky, P.T., Leboe, E.R., Dixon-Warren, A. and Ledwon, A. (1997): Eagle Bay Project: Till Geochemistry of the Adams Plateau (82 M/4) and North Barriere Lake (82M/5) map areas; *in Geological Fieldwork 1996*, Lefebure, D.V., McMillan, W.J. and McArthur, G., Editors, *B.C. Ministry of Employment and Investment*, Paper 1997-1, pages 413-421.

- Campbell, R.B. and Tipper, H.W. (1971): Geology of Bonapart Lake map area, British Columbia; *Geological Survey of Canada*, Memoir 363.
- Casselman, S. (1993): 1993 Geochemical and Litho-geochemical report on the CM Property, Barriere, B.C.; *B.C. Ministry of Energy, Mines and Petroleum Resources*, Assessment Report 23155.
- Clague J.J. (1980): Late Quaternary geology and geochronology of British Columbia, Part 1: Radiocarbon Dates; *Geological Survey of Canada*, Paper 80-13, 28 pages.
- DiLabio, R.N.W. (1990): Glacial Dispersal Trains; in *Glacial Indicator Tracing*, Kujansuu, R. and Saarnisto, M., Editors, *A.A. Balkema*, Rotterdam, pages 109-122.
- Dixon-Warren, A., Bobrowsky, P.T., Leboe, E.R. and Ledwon, A. (1997): Eagle Bay Project: Surficial Geology of the Adams Plateau (82 M/4) and North Barriere Lake (82M/5) map areas; in *Geological Fieldwork 1996*, Lefebure, D.V., McMillan, W.J., and McArthur, G., Editors, *B.C. Ministry of Employment and Investment*, Paper 1997-1, pages 405-411.
- Dreimanis, A. (1988): Till: Their Genetic Terminology and Classification; in *Genetic Classification of Glacigenic Deposits*, R.P. Goldthwait and C.L. Matsch, Editor, *Balkema*, pages 17-67.
- Duford, J.M. and Osborn, G.D. (1973): Holocene and Latest Pleistocene Cirque Glaciations in the Shuswap Highland, British Columbia; *Canadian Journal of Earth Sciences*, Volume 15, pages 865-873.
- Dyck, W. and Fyles, J.G. (1963): Geological Survey of Canada Radiocarbon Dates I and II; *Geological Survey of Canada*, Paper 63-21, 31 pages.
- Fulton, R.J. (1965): Silt deposition in late-glacial lakes of Southern British Columbia; *American Journal of Science*, Volume 263, pages 553-570.
- Fulton, R.J. (1975): Quaternary stratigraphy in south-central British Columbia; in *The Last Glaciation*, D.J. Easterbrook, Editor; IUGS-UNESCO International Geological Correlation Program, Project 73-1-24, Guidebook for Field Conference (Western Washington University, Bellingham, Washington), pages 98-124.
- Fulton, R.J. and Smith, G.W. (1978): Late Pleistocene Stratigraphy of South-central British Columbia; *Canadian Journal of Earth Sciences*, Volume 15, pages 971-980.
- Fulton, R.J., Alley, N.F. and Achard, R.A. (1986): Surficial Geology, Seymour Arm, British Columbia; *Geological Survey of Canada*, Map 1609A, 1:250 000.
- Gough, N. (1987a): Terrain Map (soils and surficial geology) Louis Creek; *B.C. Ministry of Environment*, Resource Analysis Branch, 1:50 000.
- Gough, N. (1987b): Terrain Map (soils and surficial geology) Chu Chua Creek; *B.C. Ministry of Environment*, Resource Analysis Branch, 1:50 000.
- Holland, S.S. (1976): Landforms of British Columbia, a Physiographic Outline; *B.C. Ministry of Energy, Mines and Petroleum Resources*, Bulletin 48.
- Howes, D.E. and Kenk, E. (1997): Terrain classification System for British Columbia (Version 2); *B.C. Ministry of Environment, Land and Parks, Survey and Resource Mapping Branch*, MOE Manual 10, 102 pages.
- Höy, T. and Ferri, F. (1998): Massive Sulphide Potential of the Kootenay Terrane, British Columbia; in *Geological Fieldwork 1997*, Lefebure, D.V. and McMillan, W.J. Editors, *B.C. Ministry of Employment and Investment*, Paper 1997-1.
- Lett, R.E., Bobrowsky, P. and Yeow, A. (1998): South Kootenay Project: Geochemical Pathfinders for Massive Sulphide Deposits (82M/4 and 5); in *Geological Fieldwork 1997*, Lefebure, D.V. and McMillan, W.J., Editors, *B.C. Ministry of Employment and Investment*, Paper 1998-1, pages 15-1 - 15-6.
- Paulen, R.C., Bobrowsky, P.T., Little, E.C., Prebble, A.C., and Ledwon, A. (1998a): Terrain geology of the Louis Creek area, NTS 92P/1E, scale 1:50 000; *B.C. Ministry of Employment and Investment*, Open File 1998-2.
- Paulen, R.C., Bobrowsky, P.T., Little, E.C., Prebble, A.C., and Ledwon, A. (1998b): Terrain geology of the Chu Chua Creek area, NTS 92P/1E, scale 1:50 000; *B.C. Ministry of Employment and Investment*, Open File 1998-3.
- Resources Inventory Committee (1996): Guidelines and Standards to Terrain Mapping in British Columbia. Surficial Geology Task Group, Earth Sciences Task Force, British Columbia, Resources Inventory Committee, Publication #12, 216 pages.
- Ryder, J.M., Fulton, R.J. and Clague, J.J. (1991): The Cordilleran Ice Sheet and the Glacial Geomorphology of Southern and Central British Columbia; *Géographie Physique et Quaternaire*, Volume 45, pages 365-377.
- Tipper, H. (1971): Surficial Geology, Bonapart Lake, British Columbia; *Geological Survey of Canada*, Map 1278A, 1:250 000.
- Schiarizza, P. and Preto, V.A. (1987): Geology of the Adams Plateau-Clearwater-Vavenby area; *B.C. Ministry of Energy, Mines and Petroleum Resources*, Paper 1987-2, 88 pages.
- Shilts, W.W. (1993): Geological Survey of Canada's Contributions to Understanding the Composition of Glacial Sediments; *Canadian Journal of Earth Sciences*, Volume 30, p. 333-353.
- Yorston, R. and Ikona, C.K. (1985): Geological Report on the Cedar I to VI mineral claims; *B.C. Ministry of Energy, Mines and Petroleum Resources*, Assessment Report #13519.



## THE NIZI PROPERTY: A CLASSIC (EOCENE?) EPITHERMAL GOLD SYSTEM IN FAR NORTHERN BRITISH COLUMBIA

By Heather Plint, Shear Quality Consulting Ltd.,  
William J. McMillan and JoAnne Nelson, B.C. Geological Survey Branch,  
and Andre Panteleyev, XDM Consultants Ltd.

*Keywords:* Nizi, epithermal gold, northern British Columbia, Rapid River tectonite.

### INTRODUCTION

The Nizi property is located 80 kilometres northeast of Dease Lake, British Columbia and 60 kilometres southeast of Cassiar (Figure 1). The Nizi hosts gold-bearing epithermal-type veins associated with felsic volcanic rocks (Cavey and Chapman, 1992; Paul Wodjak, personal communication 1995). The Nizi lies within a poorly understood, highly metamorphosed geologic unit, the Rapid River tectonite (Gabrielse, 1994), which, like the Yukon Tanana Terrane (Mortensen, 1992), is intruded by early Mississippian plutons (Gabrielse *et al.*, 1993). The presence of felsic volcanic rocks within the Rapid River tectonite suggested a comparison with the volcanogenic massive sulphide systems of Kudz Ze Kayah and Wolverine (Nelson, 1997).

This paper is based on a field examination of the property by Nelson and McMillan in 1996 and on more thorough geological study by Plint in 1997 as part of a major exploration program conducted by Madrona Mining Limited. Panteleyev's overview of the epithermal system is based field observations and interactions with Plint during a brief visit to the property in 1997. The overall result of our work is to show that the Nizi mineralization, along with the volcanic rocks that host it, post-date the early Mississippian metamorphic and mid-Permian plutonic bodies that enclose them. The system may be as young as Eocene. It presents a type of mineralization, comparable to Mt. Skukum and the epithermal systems associated with the Carmacks Group in the Yukon, that was not previously known in this area. Consideration of this model may shed light on the source of some multi-element geochemical anomalies defined in the recent Cry Lake RGS release (Jackaman, 1996).

### PROPERTY HISTORY

J. Atenbury first staked claims on the Nizi property in 1969. The claims covered a gossanous zone of polymetallic mineralization hosted by quartz veins in "shear" zones. In 1970, a soil-geochemistry survey (84

samples) and reconnaissance geological mapping was conducted. Anomalous concentrations of lead and zinc were discovered associated with a gossanous area immediately northwest of Zinc Lake and with north-trending topographic lineaments near the northwest end of the property (Zimmerman, 1970). The property was optioned to Sumac Mines Limited in 1972 who explored for a porphyry-style copper deposit by systematic geological mapping and soil/silt geochemical surveys. Although several silver-zinc anomalies and a gold anomaly were identified (Rodgers, 1972), the claims were allowed to lapse in 1973.

Regional Resources Limited re-staked the area in 1979. Detailed geological mapping (1:5 000 scale) and geochemical surveys were carried out to assess the precious metal potential. Several gold and silver-bearing veins were outlined during this program (Rowe, 1980). In 1982, Regional Resources conducted a prospecting and rock sampling program in geochemically anomalous areas and reported that the highest gold values were obtained from massive galena-sphalerite-pyrite vein material.

The claims were allowed to lapse. The property was re-staked in 1987 by Izumi Exploration Limited (later renamed Gold Giant Minerals Incorporated). A 36.4 kilometre grid was established. Geological prospecting, geochemical and geophysical surveys were undertaken to re-define known anomalies and veins and to locate new ones. Six main zones of mineralization were identified and named Zones A through F. Precious and base metal mineralization in quartz and quartz-carbonate-sulphide veins associated with north to northwest-trending faults was reported. Additional exploration in 1991 outlined quartz vein stockworks termed the "G Zone" and later the "Discovery Vein" (Figure 2a). Assay values up to 41.0 g/t Au and 764.6 g/t Ag over 1.5 metres were obtained for this area (Cavey and Chapman, 1992; McIntosh and Scott, 1991). A VLF-EM conductor was interpreted to reflect pyritization associated with the quartz stockworks (Cavey and Chapman, 1992).

An airborne geophysical survey was completed in the spring of 1992 (Woolham, 1992) followed by soil sampling, geological mapping and diamond drilling during the 1992 field season. Base and precious metal mineralization associated with minor faults and fractures was reported. The highest assay values were obtained from an area of quartz veining in silicified rhyolite in the

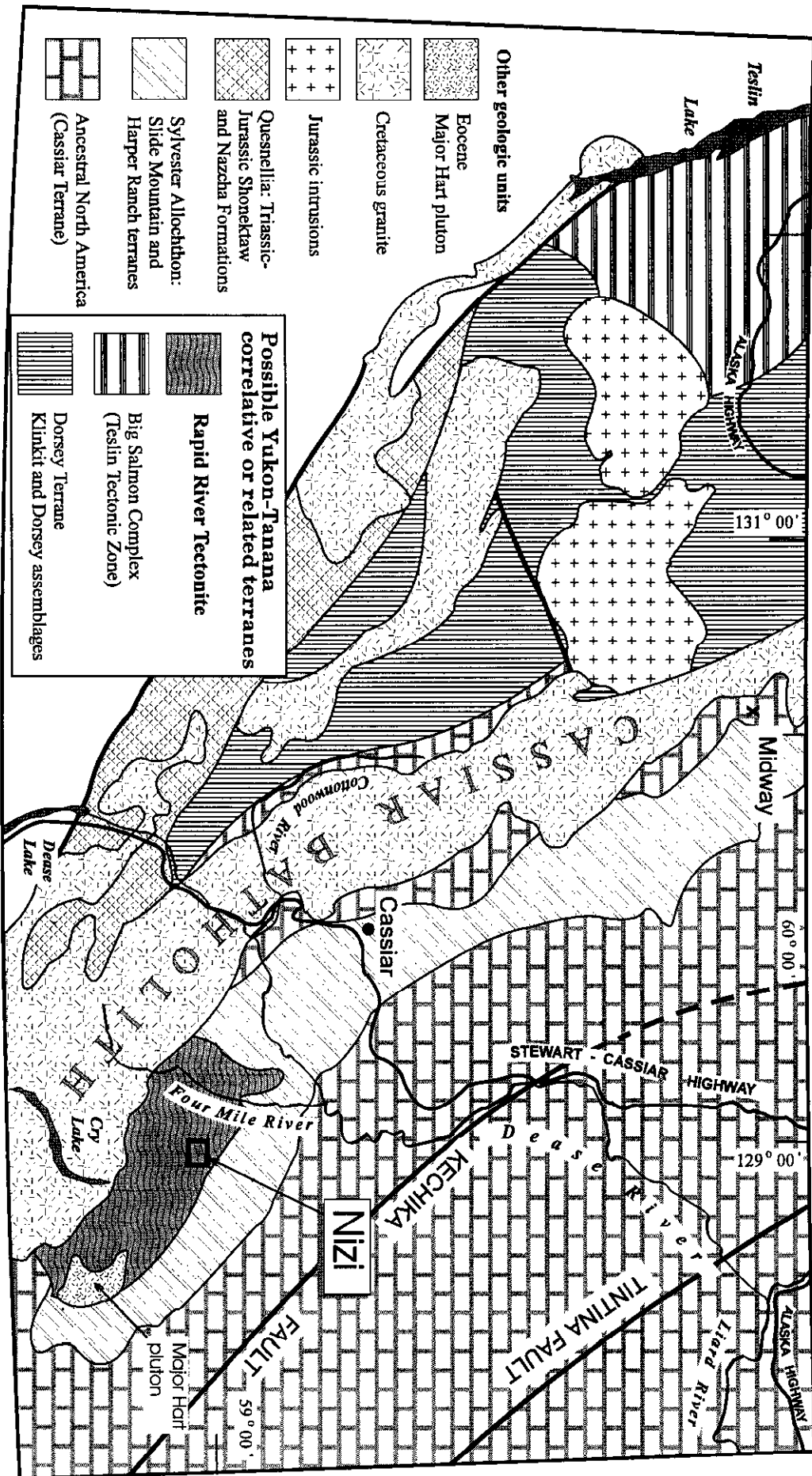


Figure 1. Geological location map of the Nizi property

Discovery Vein area and the nearby, newly identified Surprise Vein (Figure 2). The most significant surface soil gold anomaly coincided with the Discovery Vein. Five drill holes, with a total length of 957.38 metres were drilled. Two holes (NZ92-1, 2) tested the Discovery Vein/Surprise Vein area. The remaining three holes (NZ92-3, 4,5) tested the H Zone, Grizzly Ridge Vein and Gully A Zone, respectively. Three additional holes were drilled in the Discovery Vein area by Gold Giant Minerals Incorporated. Drilling indicated the continuity of gold-bearing structures. Significant gold assays were reported from intervals of smoky blue/grey quartz veins, from grey to black, quartz-flooded rhyolite cut by quartz-carbonate-sulphide veins, and from adjacent fault zones. Since gold assays from drill core were generally lower than surface values (Bond, 1993), the claims were allowed to lapse.

In 1994, claims were re-staked in the Nizi area by Lawrence Barry of Hunter Explorations. The property was optioned by Oro Grande Resources Inc. in 1995. Madrona Mining Limited entered into an agreement with Oro Grande Resources in July 1996. In September 1996, six diamond drill holes with a total length of 921.1 metres were drilled by Madrona Mining in joint venture with Oro Grande Resources. Five holes were drilled in the vicinity of the Discovery and Surprise Veins. One hole was drilled to test the southeastern extension of the Zinc Lake Zone (Zone E of Augsten, 1987 and Bond, 1993). Significant gold mineralization was encountered in holes NZ96-9, 10 and 12. Base-metal mineralization (sphalerite and galena) was encountered in holes NZ96-10, 12 and 13 in a steeply-dipping, northwest-striking zone of fault breccia. The breccia is characterized by the presence of sphalerite-galena-rich and carbon clasts.

In 1997, Madrona Mining undertook further exploration on the property. Plint remapped and relogged preexisting core prior to a 3000-foot drill program that was completed in September.

## REGIONAL GEOLOGY

The Nizi property lies within the Sylvester Allochthon, a set of thrust-bounded terranes that lies on top of the Cassiar Terrane (Figure 1). The structurally lowest terrane, the Slide Mountain (Mississippian to Permian ocean basin or marginal basin), is overlain on a major thrust fault by Harper Ranch Terrane (Mississippian to Permian island arc) (Nelson, 1991). Highest in the stack is the Rapid River Tectonite (Gabrielse, 1994; Harms, 1990, 1993), which occupies the southeastern portion of the Sylvester Allochthon and surrounds the Nizi claims (Figure 1). It is an assemblage of amphibolite grade, intercalated mylonitic tectonites and intrusive rocks. Rock types include amphibolite, serpentinitized ultramafic rock, marble, garnet-muscovite-zoisite and garnet-biotite-staurolite schists, and quartzite, intruded by plutons of quartz diorite, monzodiorite, diorite and gabbro. Metamorphism and mylonitization predate Late Devonian to Early Mississippian synkinematic quartz diorite (362 to 350 Ma); mid-

Permian plutons are also present (Gabrielse *et al.*, 1993). The Rapid River tectonite may have correlatives in the allochthonous terranes west of the Cassiar Batholith (Nelson, this volume).

## PROPERTY GEOLOGY

The geology of the Nizi property (Figure 2a) is divided into four major map units. In order of oldest to youngest they are:

1. the Rapid River tectonite: a pre-Mississippian metamorphic sequence of metasedimentary and metavolcanic schist and gneiss, orthogneiss, and ultramafites,
2. an Early Permian(?) intrusive unit of fine- to coarse-grained, non-foliated granodiorite, quartz diorite and diorite,
3. a sequence of felsic to mafic volcanic flows and pyroclastic rocks (hereafter the "Nizi volcanic sequence"), and
4. kaolinitized megacrystic orthoclase-quartz-(biotite) porphyry dikes.

Diorite dikes of unit 2 intrude the metamorphic sequence, and dikes resembling the Nizi volcanic sequence intrude the diorite. The volcanic sequence is thus considered younger than the diorite. Geophysical data and field observations indicate that subsequent faulting (*see below*) has modified the diorite-volcanic contacts. The timing of intrusion of the kaolinitized K-feldspar-quartz porphyry relative to the Nizi volcanic sequence is unknown. However, it apparently occupies much of the fault zone between the volcanic sequence and quartz diorite to the northeast. As the porphyry is not tectonized, it is likely a late intrusion into the fault zone and therefore younger than all other map units.

### Unit 1: Metamorphic Sequence (Rapid River Tectonite)

The metamorphic sequence includes quartzite, quartz-feldspar-hornblende-biotite tectonite and orthogneiss, amphibolite, metacarbonate and calc-silicate rock, massive to fish-scale-textured serpentinite and minor muscovite-biotite schist. Compositional layering in the metamorphic sequence varies in scale from one millimetre to several metres. Foliation is moderately well-developed and defined by hornblende, micas, and/or compositional variation between quartz-feldspar-rich and hornblende-rich lamellae and layers. Locally, the foliation is accentuated by white to grey quartz lenses up to 2 centimetre thick and quartz veins up to 10

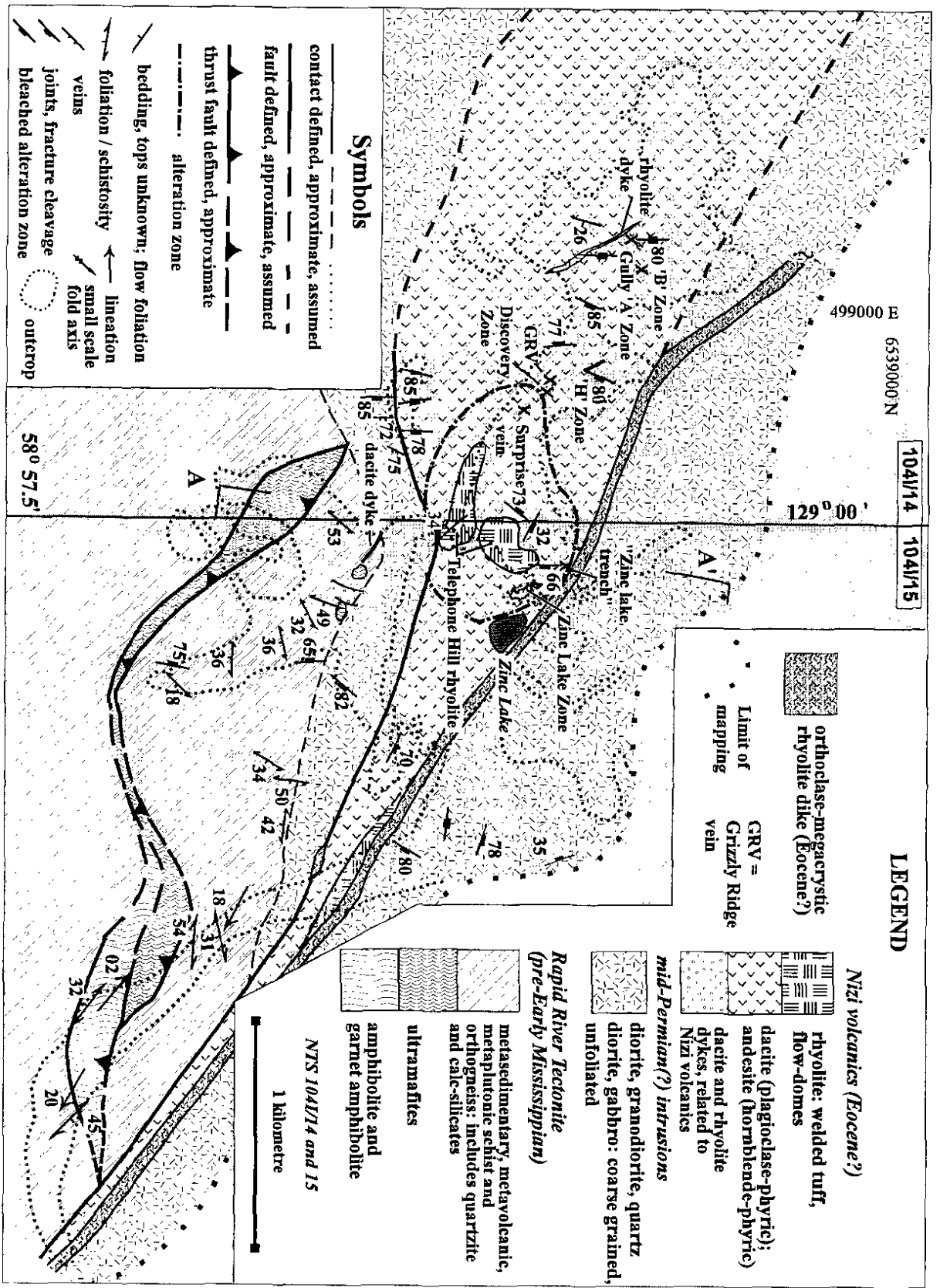


Figure 2a. Geology of the Nizi Claims area. Cross section on Figure 2b.

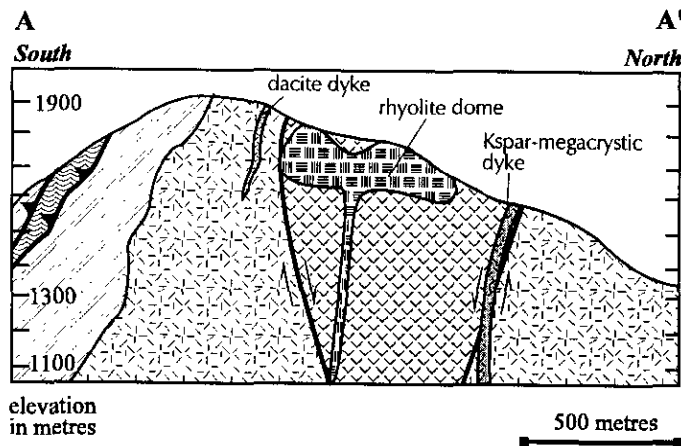


Figure 2b. Cross section A-A' across the "Telephone Hill" area. Legend as for Figure 2a.

centimetres thick. The latter also cut the foliation. In some areas, granitic layers or diffuse lensoidal patches in quartz-feldspar-hornblende tectonite, oriented broadly parallel to the foliation, give the rock a migmatitic appearance. The metamorphic sequence is intruded by metre-scale dikes of granodiorite to diorite of Unit 2 and by dikes of fine-grained, feldspar-quartz porphyry dacite that are probably related to the Nizi volcanic sequence.

The contact between serpentinite and other metamorphic rocks in the sequence is assumed to be faulted due to the extreme compositional difference of their protoliths, the lens-shaped map pattern of the serpentinite and the presence of numerous slickensided surfaces in serpentinite.

The strike of foliation in the Rapid River tectonite varies from northwest to west to, less commonly, northeast; dips are predominantly to the south and southwest. Rootless centimetre-scale folds with axial surfaces parallel to the foliation were observed in boulders of quartz-feldspar-amphibolite orthogneiss, and at one location, a closed fold with a moderately southeasterly plunging axis and a steeply southwest dipping axial plane is exposed in quartz-feldspar-amphibole tectonite. These observations indicate that the foliation in the metamorphic sequence is at least a second generation feature.

## Unit 2: Diorite, Quartz Diorite, Granodiorite

Diorite is exposed to the northeast and southwest of the Nizi volcanic sequence (Figures 2a, 2b). To the southwest, the diorite is massive, fine- to coarse-grained with pyroxene and minor amphibole or biotite. Trace amounts of disseminated pyrite are common. To the northeast, the unit consists of white to beige weathering, medium- to coarse-grained quartz diorite to granodiorite with randomly oriented, acicular amphibole crystals. Biotite, commonly chloritized, is present locally. Grain size and compositional variations at the outcrop scale are common in the diorite unit. Inclusions of fine-grained

diorite in coarse-grained diorite and quartz diorite, very coarse-grained patches in otherwise medium-grained diorite, and small dikes of granodiorite cutting diorite are common. A fine-grained quartz diorite phase is present along the contact with the Nizi volcanic sequence in outcrop south of Zinc Lake and in creek exposures in the northwestern part of the map area.

In outcrop immediately northeast of Zinc Lake and along the north-northwesterly trending ridge north of Zinc Lake, the quartz diorite is cut by fine grained to aphanitic, feldspar-phyric mafic dikes and by rusty to dirty green weathering, pale green to pale green-grey, feldspar-quartz porphyry dykes. Phenocrysts in the mafic dikes and porphyry are subhedral and generally less than 5 millimetres long. The mafic dikes locally enclose angular clasts of the quartz diorite. In outcrop immediately northeast of Zinc Lake, a mafic dike grades into the feldspar-quartz porphyry suggesting that both rock types are part of the same intrusive event. These dikes are interpreted to be part of the Nizi volcanic sequence. On the mountain southwest of Zinc Lake, dacitic and rhyolitic dikes related to the Nizi volcanic sequence intrude diorite.

Dikes of Unit 2 intrude the Rapid River tectonite and thus are younger than the Late Devonian to Early Mississippian deformation in the tectonite. Permian diorite is common in the Rapid River Tectonite. Bodies of mid-Permian foliated hornblende diorite ( $266 \pm 1.5$  Ma) and massive diorite to granodiorite ( $262 \pm 0.5$  to  $270 \pm 4$  Ma) are exposed to the northwest and west of the Nizi property (Gabielse and Harms, 1989). Therefore, Unit 2 is interpreted to be mid-Permian.

## Unit 3: Nizi Volcanic Sequence

The Nizi volcanic sequence crops out in a west-northwest trending, wedge-shaped belt that widens to the northwest and pinches out to the southeast (Figure 2a). The sequence is composed of approximately 80% intermediate to mafic feldspar phyric and amygdaloidal volcanic flows, 10% intermediate lapilli-crystal tuffs and 10% rhyolite flows and dikes. These rocks, in contrast to the Rapid River tectonite, are unmetamorphosed and unfoliated; although in part they are affected by very intense, texture-obliterating silicification.

Rhyolitic volcanic flows and minor tuffs are exposed in an irregular map pattern along the easterly-trending ridge immediately northwest of Zinc Lake (Figure 2a). This occurrence is referred to informally in this report as the Telephone Hill rhyolite. A second discrete rhyolite body hosts mineralization in the Zinc Lake Zone. Northwest, north and northeast-trending, subvertical rhyolitic dikes cut the volcanic sequence. They are commonly less than 5 metres, but locally up to 30 metres, wide. Rhyolite weathers rusty yellow to white or pale pinkish orange. It is pale grey, pale green or white on the fresh surface and typically aphanitic with conchoidal, angular or blocky fracture patterns. Disseminated pyrite, generally less than 3%, is common. Rhyolite flows typically contain blocky and minor lath-

shaped feldspar phenocrysts or glomerophenocrysts, heavily altered to microcrystalline quartz, and subhedral quartz phenocrysts. Phenocrysts are typically less than 0.5 millimetres in the largest dimension and comprise approximately 15% of the rock. They define a flow foliation in the Telephone Hill rhyolite. The strike of the flow layering is highly variable, but dip angles are consistent at about 40 to 50 degrees.

Intermediate, polyolithic, lapilli-crystal tuff and very minor ash tuff underlies the Telephone Hill rhyolite. Lapilli are typically less than 5 millimetres long but locally range up to 2 centimetres and constitute about 15% of the rock. At one locality, a crystal-lithic lapilli tuff contains large tabular, subrounded feldspar crystals up to 1.5 centimetres diameter, angular microcrystalline quartz fragments, rounded fine-grained, dark green volcanic fragments, rhyolite fragments with flow foliation and rare, rounded igneous fragments composed of medium-grained quartz, feldspar and biotite. Angular, cusped fragments altered to dark green chloritic material in tuff are interpreted to be glass shards on the basis of their shape.

The intermediate (? dacitic) volcanic flows weather rusty orange to a brownish olive green. They range from green-grey to pale green on the fresh surface. Feldspar phenocrysts are interpreted to be plagioclase and K-feldspar based on their lath-like and blocky outlines, respectively, and on polysynthetic twinning in plagioclase. Feldspar phenocrysts, generally <1.0 millimetre in their longest dimension, are replaced by milky white or grey microcrystalline quartz and/or altered to dark green chloritic material. In thin section, sericitic alteration of feldspars and microcrystalline quartz pseudomorphs after feldspar are observed. Rare anhedral clots of quartz observed in thin section may be amygdules or partly resorbed and pseudomorphed feldspar phenocrysts.

Intermediate (andesitic?), amygdaloidal, plagioclase hornblende, and locally augite-phyric volcanic flows are most common in the northwest corner of the map area, where they apparently grade vertically and laterally into intermediate (dacitic?) flows and tuffs. Intermediate flows are also exposed along the base of the ridge northwest of the Discovery Vein area. The flows weather a dark grey to maroon color and are grey-maroon to green-grey on the fresh surface. Although generally aphanitic, they locally contain plagioclase phenocrysts (<5%) less than 0.5 millimetres in diameter, and amygdules filled with dark green chlorite and milky white, microcrystalline quartz. The plagioclase phenocrysts define a flow foliation that strikes northeast and dips gently to moderately southeast. They are typically altered to a mixture of carbonate, sericite, pyrite and chlorite.

A general volcanic stratigraphy for the Discovery Vein area is evident in drill core. The stratigraphic sequence (from the base) consists of:

(a) mafic (andesitic), green, amygdaloidal, plagioclase-phyric flows and minor intercalated lithic lapilli tuffs,

(b) intermediate (dacitic), grey-green to grey, lithic-crystal lapilli tuffs,

(c) intermediate to mafic, grey to green-grey (dacitic to andesitic) amygdaloidal-feldspar-phyric flow, which is commonly hematized and limonitized.

Contacts range from sharp and irregular to gradational over 5 to 10 centimetres. Flow foliation is uncommon in flows of units (a) and (c). Measurement of the angle between flow foliation and the core axis, together with flow foliation attitudes observed in outcrop, indicate that the volcanic stratigraphy is moderately dipping (average about 40°). Not all units are present in each drill hole. Lithic lapilli tuff is encountered only in holes NZ96-11, 12 and 13. In addition to the volcanic units, a near-vertical grey, feldspar-phyric rhyolite dyke is present in all but drill hole NZ96-11, between units (b) and (c).

The Nizi volcanic sequence is younger than the quartz diorite that it intrudes, although no absolute age determinations exist for the sequence. No zircons were recovered from a sample of Zinc Lake Zone rhyolite collected in 1996.

#### **Unit 4: Kaolinitized Quartz-K-Feldspar Porphyry**

A buff to locally maroon weathering quartz-K-feldspar porphyry is exposed in isolated outcrops along the northeastern contact of the Nizi volcanic sequence with the quartz diorite. K-feldspar phenocrysts are subhedral and range from 5 millimetres to 2 centimetres in diameter, averaging 1 centimetre. The K-feldspar phenocrysts are entirely altered to kaolinite in most exposures and commonly only subhedral pits remain on the weathered surface. Quartz phenocrysts are clear, vitreous, subhedral to anhedral and from 1 to 5 millimetres in diameter. Minor biotite phenocrysts are observed locally. The matrix is pale pink to buff weathering, slightly greenish beige on the fresh surface and aphanitic.

The contacts of the kaolinitized porphyry are not exposed, however its extrapolated map pattern on Figure 2a shows that it is a dike. Along most of its length it separates the Nizi volcanic sequence to the west from the acicular amphibole quartz diorite to the east. However, at its northern end it is enclosed within the quartz diorite, and probably intrudes it. The absence of a tectonic fabric in the porphyry and its coincidence with the regional strike-slip fault identified from apparent resistivity contours (*see below*), suggest that it intruded along the fault after motion ceased. It is thus younger than the Nizi volcanic sequence. However, if faulting was largely synchronous with the extrusion of the Nizi volcanic sequence, the porphyry may be a late

subvolcanic intrusion related to the Nizi volcanic sequence. Considering that rhyolite dikes intrude the Nizi volcanic sequence, the latter interpretation is plausible. Gabrielse (1994) mapped the kaolinitized feldspar-quartz porphyry as belonging to the same intrusive suite as the Early Eocene Major Hart pluton, which is exposed about 20 kilometres to the southeast of the Nizi property (Figure 1).

## Depositional setting of the Nizi volcanic sequence

The Nizi volcanic sequence consists of amygdaloidal and porphyritic flows and lapilli, lithic and crystal tuffs. No pillowed flows, pillow breccias or intercalated clastic sedimentary rocks are present. These observations suggest that the Nizi volcanic sequence was erupted subaerially. The map pattern of the rhyolite exposed at Telephone Hill and the wide variation in flow foliation attitude supports the interpretation that the rhyolite is a flow dome (Figure 2b). The presence of lithic and ash tuff, locally showing planar layers ("beds") underlying the rhyolite probably represent explosive pyroclastic activity that predated extrusion of the rhyolite. The Zinc Lake Zone rhyolite lacks flow foliation and is spatially associated with the Telephone Hill rhyolite. It may be a small feeder dike related to the Telephone Hill rhyolite.

## Structural geology

The Nizi volcanic suite lies within a southeasterly-tapering graben bounded on both sides by steeply-dipping faults with normal sense of stratigraphic separation, as indicated by the outcrop patterns on Figure 2a and illustrated in the cross section in Figure 2b. Wherever contacts between the Nizi volcanics and adjacent plutonic bodies are seen, they are faulted, with zones of shearing, chloritic fractures, and slickensides. Analysis of apparent resistivity contour maps indicates that northwest-trending fault zones and sets of northeast-trending and north-trending fractures or faults dissect the Nizi property (McGowan, 1997). Comparison of the resistivity contours with field data suggests that the northeastern contact of the Nizi volcanic sequence with the quartz diorite is a regional, dextral strike-slip fault. The fault dextrally offsets three, northeast-trending, negative resistivity anomalies by 300 to 400 metres.

Jointing in and near the Nizi volcanics probably formed in response to several processes, such as igneous cooling in magmatic and volcanic rocks, hydrothermal fracturing and subsequent tectonism. Compilation of joint orientations from Bond (1993) and data collected during the 1997 field season shows a wide variety of strike orientations of both joints and fracture cleavage, with moderate to vertical dips predominating. In the mineralized areas north, northwest and northeast-striking, steeply dipping to vertical joints and fracture cleavage are well developed.

Centimetre-scale, strike-slip offset of mineralized quartz veins indicates that at least some of the joints and fracture cleavage are related to faulting. Commonly, motion along the northwest-striking faults is dextral whereas along northeast-striking faults it is sinistral. This is best illustrated in the Discovery Vein area. There, a northwest-striking, vertical, dextral strike-slip fault offsets a contact between an intermediate flow to tuff and a rhyolite dike by 27.5 metres. The fault also offsets and has brecciated the Discovery Vein. Smaller scale, northeast-striking, subvertical to vertical, sinistral faults offset the Discovery Vein on the order of 50 centimetres or less. All the faults are marked by fracture cleavage. The dextral and sinistral strike-slip faults are interpreted to be largely coeval as no offset of either fault is observed where they intersect.

Bond (1993) reported northwest-trending, dextral strike-slip faults and northeast-striking, sinistral strike-slip faults in the H Zone area. A brief examination of the H Zone by Plint confirmed that it is a north-northeast-trending, recessive weathering, fault zone of uncertain displacement, offset dextrally by northwest-trending faults.

Most of the northeast-trending faults/fractures occur to the southwest of the regional, northwest-striking, dextral strike-slip fault that bounds the Nizi volcanic sequence to the northeast (McGowan, 1997). This observation suggests that the northeast system is either older than, or controlled by the regional northwest-striking fault zone. This interpretation is consistent with laboratory analyses of strike-slip systems. Models show that deformation is taken up along synthetic and antithetic shears ("Riedel" shears) *prior* to motion along the principal fault zone, although motion on the Riedel shears may continue after motion along the principal fault (e.g. Sylvester, 1988). Antithetic shears develop at angles of 60 to 75 degrees to the principal fault zone and synthetic shears at an angle of 15 to 20 degrees to the principal fault zone. Therefore, the northeast-striking faults are probably antithetic shears (R shears) to the more through-going, northwesterly-striking dextral strike-slip fault.

Fault motion along zones of north-trending, subvertical to vertical fracture cleavage and joints has not been unequivocally documented in the field. At one outcrop in the Gully A Zone, brecciation and steeply plunging slickensides are developed in a 3 metre wide zone of vertical, north-striking fractures. This observation suggests that some fault motion has occurred. In a northwest-striking, dextral strike-slip fault system, north-trending normal (extensional) faults are expected to develop. Therefore, it is probable that any fault motion along the north-trending fracture/fault system is normal. The northerly-striking H Zone may also be a normal fault.

We conclude that the Nizi volcanic sequence records deformation related to regional strike-slip faulting. The northwest, north and northeast-trending fracture cleavage and joints that dominate in mineralized areas are interpreted to reflect this faulting, although

documentation of displacement is hindered by the lack of marker beds.

## **Mineralization and alteration**

Mineralization on the Nizi property is a vein-stockwork system with associated hydrothermal brecciation. Two distinct styles are present: sulphide-poor, gold-silver-quartz veins and stockworks associated with pervasive silicification, and sulphide-rich iron carbonate-sphalerite-galena veins associated with pervasive carbonate alteration.

There are six main mineralized areas outlined to date on the Nizi property: Zinc Lake Zone, Discovery Vein/Surprise Vein, Grizzly Ridge Vein, H Zone, Gully A Zone and B Zone. In addition, the Hill Zone is introduced here as an area of interest on the basis of 1997 mapping and assays reported by Gold Giant (Bond, 1993).

### ***Gold-Silver-Quartz Mineralization***

#### ***Discovery Vein/Surprise Vein area***

The Discovery /Surprise Vein area is characterised by multistage, microcrystalline quartz-carbon-sulphide barite stockworks. The Discovery Vein is the largest surface expression of the mineralization, although small areas to the southeast (Surprise Vein) and to the northwest ("DV2" of Bond, 1993) are also exposed. The Discovery Vein is actually a stockwork zone which is most evident only at the northwestern and southeastern ends of the "vein". The stockworks trend west-northwest and are steep to vertical. The zone pinches and swells along strike and reaches a maximum true width of 2.5 metres. It cuts across a contact between a rhyolite dike and an intermediate volcanic tuff or flow. Very fine-grained pyrite, galena, sphalerite, chalcopyrite, tetrahedrite and acanthite are disseminated or follow microfractures in the quartz stockworks. Pyrite also occurs in fine veinlets up to 5 millimetres wide.

In 1997 drill core, sulphide-carbonate veins are seen to crosscut the gold-quartz veins (holes NZ-97-16 at 17-18 metres and NZ-97-18 at 115-118 metres). This relationship shows that gold-enriched quartz veining preceded the sulphide-carbonate style of mineralization.

Channel samples of the Discovery vein have returned the following selected high-grade values: 27.09 g/t Au and 1220.6 g/t Ag over 2.0 metres; 15.09 g/t Au, 1073.2 g/t Ag over 3.5 m; 8.91 g/t Au, 596.6 g/t Ag over 1.0 metres, 1.54 g/t Au, 190.3 g/t Ag over 1.0 metres. Channel samples from the Surprise Vein area ran 6.5 g/t Au over 1.3 m, 462.9 g/t Ag over 0.8 m and 2.16 g/t Au, 496.8 g/t Ag over 1.0 metre (Bond, 1993). The Discovery Vein area represents the best exploration target identified to date on the Nizi Property. Of the fourteen drill holes have been completed in the area, assays in all but two have confirmed the presence of

significant gold-silver mineralization in microcrystalline quartz-carbon-pyrite-barite veins and stockworks, although the values are erratic and on the whole somewhat lower than the best surface results, with notable exceptions such as 3.54 g/t Au, 49.1 g/t Ag over 6.1 metres in DDH NZ-96-9 and 1.44 g/t Au, 27.21 g/t Ag over 6.88 metres in DDH NZ-96-10 (Day, 1996).

#### ***Zinc Lake Zone***

The Zinc Lake Zone is hosted by white to pale grey to green, quartz phyric, silicified rhyolite, cut by north and northwest-striking, steep to vertical joints. Zones of fracture cleavage, generally less than 1 metre wide are developed parallel to the north-striking joint set. The rhyolite is silicified and locally pyritized with 1 – 10% disseminated pyrite along the fracture cleavage zones. Minor iron carbonate veins occur along some zones of fracture cleavage. Steep to vertical lenses of white to grey microcrystalline quartz, carbon and pyrite trend parallel to the joints. The lenses, typically less than 20 centimetres wide, pinch out along strike and are confined to an area of intense iron-staining in the rhyolite.

The largest quartz lens is approximately 3 metres wide by 10 metres long in outcrop. It is composed of microcrystalline quartz cut by randomly oriented, carbon-filled, hairline fractures that are in turn cut by a network of irregular pyrite veinlets. Two grab samples from the main quartz lens, collected by Madrona Mining Limited, returned values up to 3.14 g/t Au and 950.0 g/t Ag. Microcrystalline quartz-barite stockworks enclose angular centimetre-scale clasts of bleached rhyolite. They broadly follow northeast-striking, vertical fractures. Grab samples returned values of 0.39 g/t Au and 1.3 g/t Au. One hole (NZ96-14) has been drilled in the area of Zinc Lake Zone. It intersected a sequence of intermediate, heterolithic lapilli tuffs and minor silicified amygdaloidal to massive flows. The failure of this hole to intersect rhyolite may reflect the steeply inclined contacts of a subvolcanic intrusion.

#### ***Grizzly Ridge Vein***

The Grizzly Ridge vein was examined briefly by Plint and Panteleyev. It is a northerly-trending quartz vein exposed in two small outcrops and in felsenmeer over a distance of 125 metres, located on the ridge top 100 metres south of the Discovery vein. The Grizzly Ridge vein consists of white, massive, fine-grained quartz cut by minor carbon-filled hairline fractures. In talus surrounding the vein, the rock is strongly altered to a pale yellow/chalky white material cut by fine, microcrystalline quartz veinlets, up to 3 metres from the vein. This alteration was previously reported to be "sericitic" although no sericite was observed in hand sample. Similar alteration envelopes less than a metre wide are present along nearby northeast-striking, subvertical, fracture cleavage zones. Unlike other gold-

bearing veins on the property, it formed as a single stage vein containing little carbon or sulphides and no barite. A 2.5 m chip sample assayed 0.270 g/t Au; all other samples ran less than 0.1 g/t (Bond 1993).

### **Hill Zone**

Bond (1993) reported quartz veins that crop out 150 m south of the Gully A Zone. Mapping in 1997 identified northerly-trending quartz-barite-pyrite stockworks cut by carbon-filled hairline fractures in a strongly silicified host rock and an east-striking, 40 centimetres wide, quartz-barite-pyrite-chalcopyrite vein in a mafic, plagioclase-phyric flow. Grab samples of quartz vein returned low values of 3.58 g/t, 0.86 g/t, and 204 ppb Au (Madrona Mining Ltd., unpublished data).

### **Iron Carbonate-Sphalerite-Galena Mineralization**

#### **H Zone**

Sheer cliffs make much of the H zone inaccessible. It is interpreted to be a northerly-trending fault zone marked by well developed planar, subvertical joints that strike north-northwest to north-northeast. A banded carbonate-quartz-sphalerite-galena-pyrite vein with an exposed true width of 2 metres occupies part of the fault zone. The vein orientation is parallel to planar joints in the host rock. Within 50 centimetres of the vein the host rock is altered to a pinkish beige, granular material cut by randomly oriented limonitic fractures. In general, gold values are low although a 1.8 metre chip sample of sphalerite-galena-pyrite-carbonate-rhyolite breccia returned values of 2.26 g/t Au, 278.1 g/t Ag, 1900 ppm Pb and 32.1% Zn (Bond, 1993).

#### **Gully A Zone and B Zone**

The main showings of both the Gully A and B zones are iron carbonate-microcrystalline quartz-rhodochrosite-sphalerite-galena-pyrite veins controlled by north-striking subvertical fractures. Both exhibit a pinkish-beige, granular alteration of the host rock identical to that observed in the H Zone. The alteration contains disseminated blebs of pyrite and trace galena and is cut by numerous, randomly oriented limonitic fractures. The mineralized interval at the Gully A showing is a 20 centimetre wide zone of hydrothermal breccia. It consists of angular clasts of sulphide (sphalerite, pyrite and minor galena) and of host rock in an iron carbonate matrix. The host rock to the zone is silicified green-grey, plagioclase-phyric mafic volcanic flow which is altered within 2 metres of the eastern margin of the breccia. The best assays for Gully A Zone were 11.38 g/t Au and 22.4 g/t Ag (Bond 1993).

Zone B consists of a vertical, north-trending, banded carbonate-sphalerite-quartz vein exposed over 0.5 metres. Host rocks to the vein are intermediate to

mafic volcanic flows. The host rocks within 1.5 metres of the vein show the same granular alteration as those at the Gully A and H zones. Carbonate alteration that is subparallel to a vertical, east-striking, 2 m wide zone of fracture cleavage cuts the host rock and the alteration. Bond (1993) reports grab sample assays of 1.2 to 3.63 g/t Au and 3308.6 to 5485.8 g/t Ag for B Zone veins.

### **Alteration**

Rocks underlying the Nizi property are weakly to moderately altered over a wide area. Some of the alteration appears to be aligned along the contact of the mid-Permian(?) intrusion that bounds the Nizi volcanic sequence on the northeast (Fig. 2a). Moderate to intense silicification and microscopically visible sericitic alteration is best developed in the area of the Discovery Zone and related showings, and carbonate alteration and veining occurs with varying intensity throughout the area sampled. An area of patchy to pervasive silicification, sericite alteration and destruction of primary igneous textures encloses the main area of rhyolite domes, quartz stockwork mineralization and precious metal mineralization. To the west, mineralization includes more base metals and is related to carbonate veining and alteration. As a generalization, there seems to be a zoning outward from intense silicification near the rhyolites, through sericitic alteration to a fringe of carbonate alteration. This corresponds to the metal zoning pattern from precious metal-enriched quartz veins and stockworks, outward to lower precious metal contents in sulphide-carbonate veins. In the outer part of the zone, chlorite occurs as an alteration product after feldspars, fills amygdules and forms fractures and veinlets with carbonate. Epidote is present locally as veinlets, with or without carbonate. Epidote alteration is particularly strong adjacent to the faulted contacts between the Nizi volcanic sequence and the surrounding plutonic rocks. Conclusive evidence is lacking, but the sericitized and silicified zones may be overprinted on an earlier propylitic assemblage that could be of regional metamorphic origin, or be intrusion-related. The carbonate alteration event or events are more widespread and spanned the development of the other alteration assemblages.

### **Summary of vein types and distribution**

Gold and silver-bearing quartz veins and stockworks consist of microcrystalline to very fine-grained white to grey quartz and carbon, commonly with white subhedral to euhedral barite, finely disseminated veinlet pyrite, and minor iron carbonate. They occur in the Zinc Lake Zone, the Discovery Vein/Surprise Vein, and in the Hill Zone. In these low-sulphide veins (total sulphides less than 5%), disseminations of sphalerite, galena, acanthite, tetrahedrite and rare chalcopyrite are identifiable in polished section and rarely in hand sample. Gold and silver are in electrum, which forms tiny grains intergrown with the sulphides and sulphosalts, or included within them. The gold and silver-bearing quartz veins show minor quartz comb

texture, visible with a hand lens or in thin section, and rare vugs, but otherwise exhibit few void-fill textures.

Sphalerite-galena, gold-bearing, iron carbonate-quartz veins are present in the Gully Zone, B Zone and H Zone. These veins, with total sulphides from 20 to 40%, commonly exhibit colloform banding, crustification, cockscomb textures and multistage, hydrothermal breccia textures. On the basis of textures and mineralogy, mineralization on the Nizi Property is best described as low sulphidation (or "adularia-sericite"), sulphide-poor, epithermal mineralization.

The key result of the 1997 exploration program is recognition that significant gold mineralization is consistently associated with discrete zones of microcrystalline quartz-carbon-pyrite-barite-carbonate silicification (e.g. Zinc Lake Zone, Surprise Vein, Discovery Vein, Hill Zone) rather than pervasive quartz flooding. Carbon, previously reported as tourmaline, is present in both the gold-bearing quartz and in the host rocks, commonly spatially associated with pyrite. It occurs as disseminations or along fine, dark grey, hairline fractures that may be planar and parallel to jointing, oriented perpendicular to vein walls, or in random networks. Gold grades appear to be independent of the amount of pyrite and immediate host rock type. However, the areas of strongest gold-quartz mineralization cluster near the Zinc Lake and Telephone Hill rhyolite bodies (Figure 2a). In outcrop, the silicified zones are discontinuous, commonly lensoid and consist predominantly of quartz stockworks with lesser quartz matrix in hydrothermal breccias and silica replacement ("quartz-flooding") of wallrock. The iron carbonate-sulphide-quartz veins and hydrothermal breccias are apparently late-forming features, compared to the silicification and gold-(silver)-quartz mineralization. "Massive sulphide clasts" identified by Day (1996) are part of a multistage, epithermal carbonate-sulphide-quartz breccia and do not reflect a volcanic massive sulphide system at depth.

### *Physical Controls on Mineralization*

Epithermal deposits vary widely in form because of the low pressure, hydrostatic conditions under which they form (Sillitoe, 1993). Rock permeability and rheology control the sites of fluid flow and metal deposition. Rock permeability may be controlled lithologically, hydrothermally and/or structurally (Sillitoe, 1993, 1997). Typical structural controls are steeply-dipping faults, ring fractures in calderas or fractures in rhyolite flow domes. Overpressured hydrothermal fluids result in hydrothermal brecciation, particularly in highly competent rocks. The hydrothermal fluid, if highly acidic, may also dissolve the host rock. Contrasting rock types may focus fluids by providing a system of aquifers and aquitards.

The presence of carbonate-sulphide-quartz veins, pyritization and bleaching alteration along fractures in the Gully A and B zones and "sericite" alteration along NE striking fractures north of the Discovery Vein,

indicates that pre-existing structures have influenced hydrothermal fluid flow in the Nizi volcanic sequence. This influence is most apparent in the carbonate-sulphide-rich mineralization. In one core intersection, NZ96-9, carbon-bearing chalcedonic quartz occurs in tension gashes related to a small-scale fault. In several instances, strike-slip faults offset and brecciate the gold-bearing quartz veins and stockworks, so at least some of the faulting postdated the mineralization.

The gold-bearing quartz veins and stockworks are invariably microcrystalline, multistage, and locally brecciate and/or incorporate fragments of the host rock. Texturally, they show little evidence of open space filling. Locally, carbon-filled black hairline fractures are oriented normal to vein walls indicating extensional opening of fractures after growth of the quartz. More commonly, however, carbon-filled fractures are planar with no preferred orientation or form branching irregular networks in veins or quartz flooded zones. The gold-bearing quartz veins and stockworks are not restricted to a specific rock type. In the subsurface, they concentrate in rhyolite, but also occur in lithic-crystal lapilli tuff and in amygdaloidal, feldspar phyric intermediate to mafic (?) flows. The only consistent correlation is between gold-bearing quartz veins and rhyolite dikes, which at least near the Gully A Zone occupy the same structures (Figure 2a). The migration of gold-bearing fluids may have been controlled largely by dilation presumably caused by overpressured, hydrothermal fluids, rather than filling of pre-existing open spaces.

### *Age of mineralization*

Galena was collected from the H Zone in 1996 for lead isotopic analysis. Its lead-lead isotopic signature (Figure 3) plots above, and near the very young end of the shale curve defined by Godwin and Sinclair (1982). It is similar to lead from veins and skarns near the Seagull Batholith, the Cassiar gold-quartz veins, Midway, Butler Mountain and other Cretaceous-Early Tertiary epigenetic deposits in the Cassiar area (Bradford, 1988). The Midway manto system is associated with a cryptic granite; alteration there is about 70 Ma by K/Ar methods. Butler Mountain is associated with 50-Ma quartz porphyry dikes. Both are hosted by carbonate strata of the continental Cassiar Terrane. By contrast, the Early Cretaceous Table Mountain veins and Seagull Batholith deposits occur in isotopically more primitive, allochthonous, non-cratonic host rocks. This difference in host rocks may contribute more to their less evolved lead signatures than do the small difference in ages of epigenetic mineralization. Similarly, the slightly less radiogenic nature of the Nizi lead than Midway and Butler Mountain may well be due, not to an older age, but to the more primitive nature of the rocks in the Sylvester Allochthon, as opposed to the Cassiar Terrane.

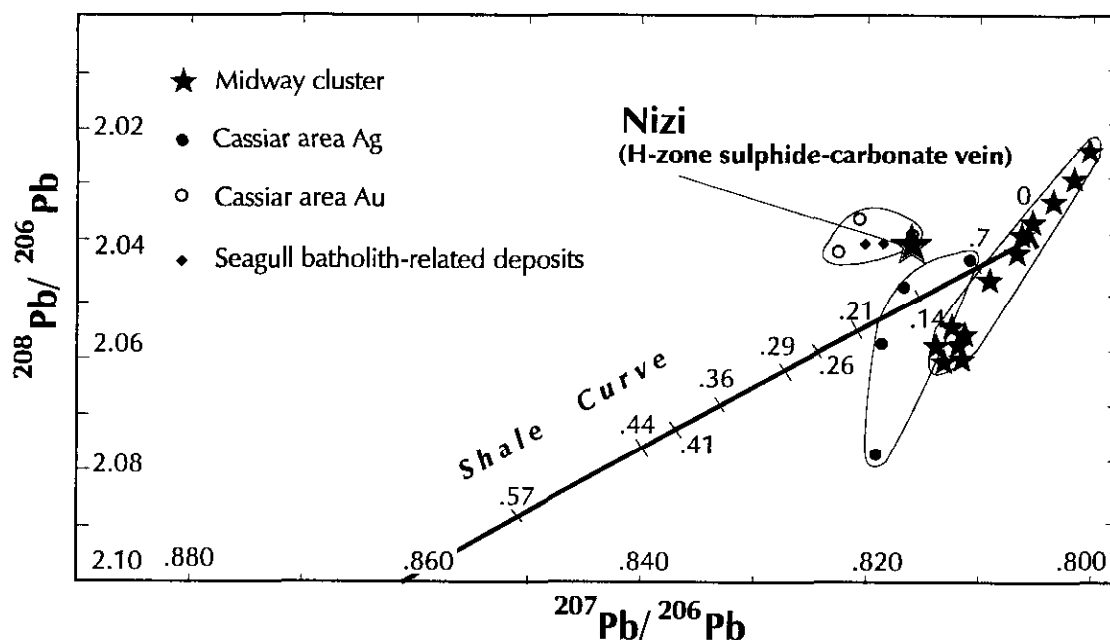


Figure 3. Lead isotopic signature for galena from Nizi sulphide-carbonate vein: comparison with other Cassiar area epigenetic deposits.

## CONCLUSIONS

The Nizi vein system has many points of affinity with classic epithermal systems. It is a set of gold-bearing chalcedonic quartz-bladed barite vein-stockworks and sulphide-carbonate vein, developed within an intermediate to felsic volcanic sequence in a structural regime of strike-slip and related faulting. The highest grade vein-stockworks are associated with rhyolite flow domes and a zone of intense silicification and pyritization. They are sinuous, lensoid, multi-stage chalcedonic vein swarms, in places with breccia textures involving wall rock fragments. Sulphide-carbonate veins occur peripheral to the central gold-quartz stockwork zone. Sulphide-carbonate also occurs as a late phase within the Discovery Vein in the central zone, crosscutting the gold-bearing chalcedonic quartz. It probably signifies cooling of the hydrothermal system.

The very young inferred lead isotopic age of the sulphide carbonate veins suggests that the mineralized system is Cretaceous-Tertiary in age. The coincident centering of the alteration halo and the gold-quartz veins around the rhyolites near Zinc Lake strongly favors cogenesis between Nizi volcanic activity and the epithermal event. If this inference is correct, then the Nizi volcanics are, like the veins, Cretaceous-Tertiary in age. The association of this system with northwest-trending dextral strike slip faults is certainly consistent with regional tectonics in Cretaceous-Tertiary time, when northern British Columbia was slivered and dextrally shuffled along such major northwesterly faults as the Kechika, the Cassiar and the Tintina (Figure 1; Gabrielse 1985).

The nearest known body of this age is the Major Hart pluton (Figure 1), described by Gabrielse (1994) as partly miarolitic granite. Gabrielse assigned the kaolinized quartz-Kspars porphyry on the Nizi property to the Eocene suite, although in large-scale mapping he did not have the opportunity to trace out its remarkable strike length: on sheet 104I/15 it appears as a small blob. The spatial association of the porphyry dike with the Nizi volcanic suite suggests that it was a late phase of the sequence. We therefore tentatively assign the entire Nizi volcanic sequence to the Eocene. By this we also infer an igneous-epithermal system that potentially extends from the Major Hart pluton as far north as the Four Mile River.

This suite correlates with other post-orogenic, mid-Cretaceous to Eocene, mafic to felsic volcanic suites in the northern Cordillera. The post-orogenic volcanism clusters into three age groups: mid-Cretaceous (e.g. Mt. Nansen Group, 105 Ma), Late Cretaceous (e.g. Carmacks Group, 70 Ma) and Eocene (e.g. Sloko Group, Skukum Group and unnamed bimodal volcanic rocks along the Tintina dextral strike-slip fault system). Gold-silver epithermal mineralization is associated with all of these units (e.g. Christie *et al.*, 1992).

A strong multi-element stream geochemical anomaly is associated with the Nizi (Jackaman, 1996). Other multi-element anomalies identified by the Cry Lake regional geochemical survey and not associated with known bedrock showings, particularly those on the northwest trend defined by the Nizi and the Major Hart pluton, may also be attributable to epithermal-type mineralization.

## ACKNOWLEDGEMENTS

We are grateful to M. Marchand of Madrona Mining Limited for permission to publish this paper. Janet Gabites of The University of British Columbia Geochronology Laboratory kindly provided the lead isotopic data. Dave Lefebure's review added clarity to the text.

## REFERENCES

- Augsten, B.E.K. (1987): Report on the Nizi Project, Liard Mining Division, British Columbia; Report for Izumi Exploration Limited. *B.C. Ministry of Energy, Mines and Petroleum Resources Assessment Report 17334*.
- Bond, W.D. (1993): Geological, Geochemical and Diamond Drill Report on the Nizi Mineral Claims, Gold Fields Canadian Mining Ltd. *B.C. Ministry of Energy, Mines and Petroleum Resources, Assessment Report 22840*.
- Bradford, J.A., (1988): Geology and Genesis of the Midway Silver-Lead-Zinc Deposit, North-Central British Columbia; unpublished M.Sc. Thesis, *The University of British Columbia*, 280 pages.
- Cavey, G. and Chapman, J. (1992): Report on the Nizi Project for Gold Giant Minerals Inc., Liard Mining Division, British Columbia, NTS 104I/14,15 and 104P2,3.
- Christie, A.B., Duke, J.L. and Rushton, R. (1992): Grew Creek Epithermal Gold-Silver Deposit; in: Yukon Geology Volume 3, Exploration and Geological Services Division, Yukon, *Indian and Northern Affairs Canada*, pages 223-259.
- Day, W.C. (1996): Diamond Drill Report on the Nizi Claims, Liard Mining Division; Private Report for Madrona Mining Limited.
- Gabrielse, H. (1985): Major Dextral Transcurrent Displacements along the Northern Rocky Mountain Trench and Related Lineaments in North-Central British Columbia; *Geological Society of America Bulletin*, Volume 96, pages 1-14.
- Gabrielse, H. (1994): Geology of Cry Lake (104I) and Dease Lake (104J/E) Map Areas, North Central British Columbia; *Geological Survey of Canada*, Open File Map 2779.
- Gabrielse, H. and Harms, T.A. (1989): Permian and Devonian Plutonic Rocks in the Sylvester Allochthon, Cry Lake and McDame map areas, Northern British Columbia; in Current Research, Part E. *Geological Survey of Canada Paper 89-1E*, pages 1-4.
- Gabrielse, H., Mortensen, J.K., Parrish, R.R., Harms, T.A., Nelson, J.L., and van der Heyden, P. (1993): Late Paleozoic Plutons in the Sylvester Allochthon, Northern British Columbia; in Radiogenic Age and Isotopic Studies, Report 7, *Geological Survey of Canada*, Paper 93-1, pages 107-118.
- Harms, T.A. (1990): Complex Tectonite Suites in the Sylvester Allochthon; *Geological Association of Canada*, Program with Abstracts, Volume 15, page A54.
- Harms, T.A. (1993): Devonian Tectonism, Metamorphism and Sialic Plutonism Preserved in the Oceanic Sylvester Allochthon; *Geological Association of Canada*, Program with Abstracts, Annual Meeting 1993, p A-40.
- Jackaman, W. (1996): British Columbia Regional Geochemical Survey: NTS 104/I - Cry Lake; Stream Sediment and Water Geochemical Data; B.C. RGS 44; *B.C. Ministry of Employment and Investment Open File B.C. RGS 44*.
- McGowan, E. (1997): Geophysical Interpretations for the Nizi Property Area; Madrona Mining Limited, Internal Company Report.
- McIntosh, R. and Scott, G. (1991): Report on the Cry Lake Project for Omega Gold Corporation, Liard Mining Division, British Columbia, NTS 104I; Internal Company Report.
- Mortensen, J.K. (1992): Pre-mid-Mesozoic Tectonic Evolution of the Yukon-Tanana Terrane, Yukon and Alaska; *Tectonics*, Volume 11, pages 836-853.
- Nelson, J.L. (1993): The Sylvester Allochthon: Upper Paleozoic Marginal Basin and Island-Arc Terranes in Northern British Columbia; *Canadian Journal of Earth Sciences*, Volume 30, pages 631-643.
- Rodgers, T. (1972): Report on the Geology and Geochemistry of the Nizi Group (Nizi 1 - 40 Claims), Liard Mining Division; Sumac Mines Limited; *B.C. Ministry of Energy, Mines and Petroleum Resources*, Assessment Report 4096.
- Rowe, J.D. (1980): Geological and Geochemical Report on the Beale Group (Beale # 1-4), Liard Mining Division, British Columbia. Report for Regional Resources Limited. *B.C. Ministry of Energy, Mines and Petroleum Resources*, Assessment Report 7818.
- Sillitoe, R.H. (1997): Characteristics and Controls of the Largest Porphyry Copper-Gold and Epithermal Gold Deposits in the Circum-Pacific Region, *Australian Journal of Earth Science*, Volume 44, pages 373-388.
- Sillitoe, R.H. (1993): Epithermal models: Genetic Types, Geometrical Controls and Shallow Features; in: Mineral Deposit Modelling, Kirkham, R.V., Sinclair, W.D., Thorpe, R.I. and Duke, J.M., editors; *Geological Association of Canada*, Special Paper 40, pages 403-417.
- Sylvester, A.G. (1988): Strike-Slip Faults; *Geological Society of America Bulletin*, Volume 100, pages 1666-1703.
- Woolham, R.W. (1992): Report on a Combined Helicopter-borne Magnetic, Electromagnetic and VLF-EM Survey, Nizi/Rapid Property, Cassiar

Area, British Columbia; *B.C. Ministry of Energy, Mines and Petroleum Resources*, Assessment Report 22840.

Zimmerman, C.E. (1970): Geological and Geochemical Report on the Nizi Group of Mineral Claims; *B.C. Ministry of Energy, Mines and Petroleum Resources*, Assessment Report 2789.



## NI-CU SULFIDE MINERALIZATION IN THE TURNAGAIN ALASKAN-TYPE COMPLEX: A UNIQUE MAGMATIC ENVIRONMENT

By G. T. Nixon, B. C. Geological Survey

**KEYWORDS:** Ni-Cu sulfides, magmatic sulfides, Alaskan-type, Turnagain complex

### INTRODUCTION

Nickel is a scarce commodity in the Canadian Cordillera, and there are currently no active nickel mines in British Columbia. The most notable past producer was the Giant Mascot (Pacific Nickel or Pride of Emory) mine (1958-1974) near Hope which processed some 4.2 million tonnes of sulfide ore averaging 0.77 wt. % Ni, 0.33 wt. % Cu, 0.68 g/t Au and 0.34 g/t PGE (platinum-group elements). The ore resided in an ultramafic phase of the Spuzzum pluton (*see* Nixon and Hammack, 1991).

The Turnagain ultramafic complex (Figure 1) hosts one of the few magmatic nickel occurrences of economic potential in British Columbia (Hancock, 1990; Nixon and Hammack, 1991). The geological setting of the sulfide mineralization is unusual in that it is hosted by an Alaskan-type complex, a magmatic environment that is not generally noted for its sulfide potential. In the case of the Turnagain complex, it appears that a unique set of genetic circumstances were responsible for the precipitation of substantial Fe-Ni-Cu sulfides from the parental magmas. The principal factors that appear to have promoted sulfide saturation in the Alaskan-type environment are considered below. It is suggested that the most important control on the formation of magmatic sulfides may ultimately derive

from the rocks that host the intrusion, and hence have fundamental significance for exploration.

### GEOLOGICAL ENVIRONMENTS FOR MAGMATIC SULFIDE DEPOSITS

Magmatic sulfide ores hosted by mafic and ultramafic rocks have historically been the principal source of world nickel production. Considering the recent discovery of high-grade Ni-Cu-Co deposits at Voisey's Bay, Labrador, such sulfides seem destined to remain the dominant producer of nickel in the foreseeable future. However, with the advent of innovative leaching and electrorefining techniques for metal extraction in recent years, low-grade, bulk-tonnage operations are now feasible for low-cost recovery of nickel and associated base and precious metals in sulfide ores. Owing to these developments, there are several prospective environments for mafic-ultramafic-hosted nickeliferous sulfide deposits in the Cordillera that warrant further attention. The most significant mafic-ultramafic rock packages occur in the oceanic (ophiolitic) and volcanic-arc terranes that were accreted to the margin of North America in the Early Mesozoic.

The geological environments of magmatic sulfide deposits may be classified according to tectonic and petrochemical affiliations. The vast majority of the world's magmatic nickel deposits are hosted by tholeiitic to komatiitic extrusive rocks and their intrusive equivalents (reviewed by Naldrett, 1989). These include important occurrences in Archean greenstone belts (*e.g.* Kambalda, Western Australia), rift-related settings (*e.g.* Thompson Nickel Belt, Manitoba), intrusions related to flood basalts (*e.g.* Noril'sk-Talnakh, Siberia), and large stratiform intrusions (*e.g.* Bushveld Complex, South Africa and Sudbury, Ontario). Among the environments traditionally regarded as least favourable for significant magmatic Ni-Cu sulfide deposits are those associated with ophiolites, kimberlites, carbonatites and other alkaline associations, and Alaskan-type complexes.

In this respect, it is interesting to note that the anorthositic Voisey's Bay intrusive suite was also formerly categorized as an unfavourable exploration environment for important Ni-Cu sulfide deposits. Yet, if predicted reserves are accurate, the Voisey's Bay troctolite body hosts one of the richest Ni-Cu sulfide deposits in the world. The lesson from Voisey's Bay is that, given apparently favourable genetic circumstances, even traditionally unimportant environments for magmatic Ni-Cu sulfide deposits, like that of the Alaskan-type Turnagain complex, may contain economically important sulfide mineralization. The impact of specific geologic variables

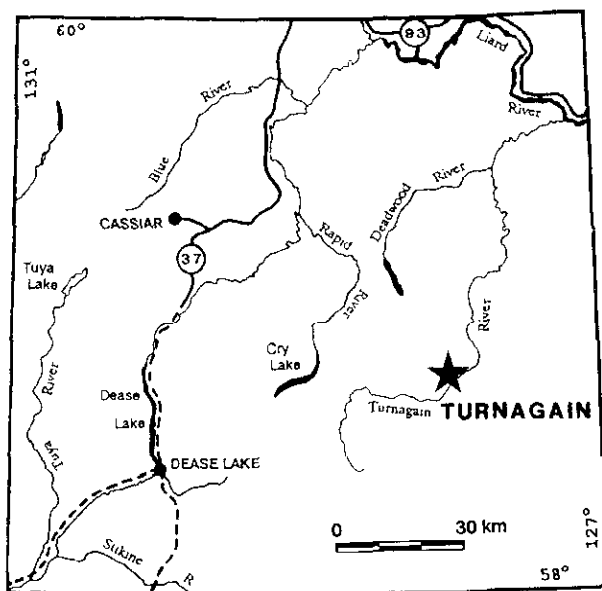


Figure 18-1. Location of the Turnagain Alaskan-type complex.

conducive to sulfide saturation in Alaskan-type parental magmas are considered below following a review of the exploration history and geology of the Turnagain complex.

## EXPLORATION HISTORY OF THE TURNAGAIN COMPLEX

Fe-Ni-Cu sulfides in the Turnagain complex were first discovered in 1956 at a showing on the banks of the Turnagain River. Little work was done until 1966 when Falconbridge Nickel Mines Limited acquired the claims. Between 1966 and 1973 extensive geological and geophysical surveys identified a number of sulfide showings (MINFILE 104I 014, 038, 051, 117-120 and references therein) that were subsequently tested by a program of short diamond drill holes (McDougall and Clark, 1972; Clark and McDougall, 1973). Many mineralized outcrops were tested only by packsack drilling and some important semi-massive sulfide zones, such as the "Discovery" showing on the Turnagain River, were apparently never drilled successfully. The geological studies initiated by Falconbridge culminated in a Ph.D. dissertation by Clark (1975) and resulting publications (Clark, 1978, 1980). Interest in the PGE potential of the Turnagain complex in the mid to late 1980's led to additional geochemical sampling and geological mapping (Page, 1986; Nixon *et al.*, 1989). Maximum PGE values for the sulfide showings were reported as 461 ppb Pt and 1455 ppb Pd (Page, 1986). Renewed interest in the property began in 1996 when Bren-Mar Resources Limited initiated geophysical and geological work, including diamond drilling to more adequately test mineralized areas. To date, some 2500m of drilling have identified narrow (1m) intersections of semi-massive sulfides grading up to 1.4 wt. % Ni and 0.07 wt. % Co within much broader zones of disseminated mineralization (Livgard, 1996). Chalcopyrite-rich grab samples from the Discovery showing have yielded maximum grades of 1.6 wt. % Cu. From both the recent drilling and surface sampling, it is clear that disseminated sulfide mineralization in the Turnagain complex is more widespread than previously indicated.

## REGIONAL SETTING

The regional geological setting of the Turnagain complex is somewhat enigmatic (Figure 2). In the most recent revision of the Cry Lake map sheet (Gabrielse, *in press* and personal communication, 1997), which builds upon earlier work (Gabrielse, 1985, 1991), the Turnagain complex is shown to be hosted by a westward-facing, folded and faulted, Cambrian to Mississippian metasedimentary succession that defines the miogeoclinal margin of Ancestral North America (Figure 2A). The wallrocks of the Turnagain complex, in part, are taken as equivalents of the fine-grained clastics of the Road River and Earn Groups. These rocks are overlain in turn by Upper Paleozoic to Triassic metavolcanic and metasedimentary sequences of unknown terrane affinity.

The Kutcho Fault separates the latter rocks from the Early Jurassic Eaglehead pluton that forms part of Quesnellia, and oceanic accretionary complexes of the Cache Creek Terrane. Mid-Cretaceous plutons of the Cassiar Batholith intrude Lower Paleozoic and older strata of the miogeocline.

This interpretation of the regional geology implies that the Turnagain body, and an associated ultramafic to dioritic "ring complex" to the south that has a well-defined metamorphic aureole (Clark, 1975), have intruded rocks of the miogeocline. In all other cases (in British Columbia at least), Alaskan-type complexes are confined to the accretionary arc terranes of Quesnellia and Stikinia, and these terranes are faulted against Ancestral North America. Thus, a supra-subduction zone setting is required for the North American margin at the time of intrusion of the Turnagain complex. The age of the Turnagain complex potentially places constraints on this interpretation and is currently being investigated using  $^{40}\text{Ar}$ - $^{39}\text{Ar}$  dating techniques.

An alternative interpretation of the regional geology proposed in Figure 2B, places the Turnagain complex within an imbricated sequence of rocks thrust eastward onto the miogeoclinal margin of North America. This interpretation is possible because stratigraphic assignments are based largely on lithological similarities, and the contentious units (discussed below) have no age control. The rocks next to the Kutcho Fault that are designated as Upper Paleozoic to Triassic comprise a tightly folded package of interbedded felsic ("quartz-eye") to intermediate volcanic rocks, shale, siltstone, chert, volcanic greywacke and conglomerate, and minor carbonate (Clark, 1975; Gabrielse, *in press*). Their lithological mix and structural style strongly resemble rocks found further south that form the Lay Range Assemblage (Mississippian to Permian), widely regarded as the basement of Quesnellia (Monger, 1973; Ferri *et al.*, 1993), and this correlation is favoured here. However, another possibility (not shown in Figure 2) is that these rocks are atypically deformed and metamorphosed volcanic-sedimentary assemblages of the Upper Triassic Nicola-Takla arc.

The wallrocks of the Turnagain complex are black carbonaceous slates and grey graphitic phyllites. In Figure 2B, these rocks are considered to be correlative with the Middle to Late Triassic "black phyllite" unit which occurs near the base of the Nicola Group in the Quesnel Lake area (Bloodgood, 1987, 1988; Bailey, 1988; Panteleyev *et al.*, 1996). This interpretation, therefore, requires a fault (thrust?) between the Cambro-Ordovician Kechika Group and Triassic slate and phyllite. The exact location of this inferred fault is unknown and has been arbitrarily placed at the top of the Kechika Group where it delineates the easternmost limit of Quesnellia.

The eastern margin of the Turnagain complex is marked by a reverse fault; shear-bands observed in footwall slates indicate an eastward direction of motion. The nature of the southwestern contact of the Turnagain complex, observed only in drill core and inferred from aeromagnetic data, is uncertain (Clark, 1975). However,

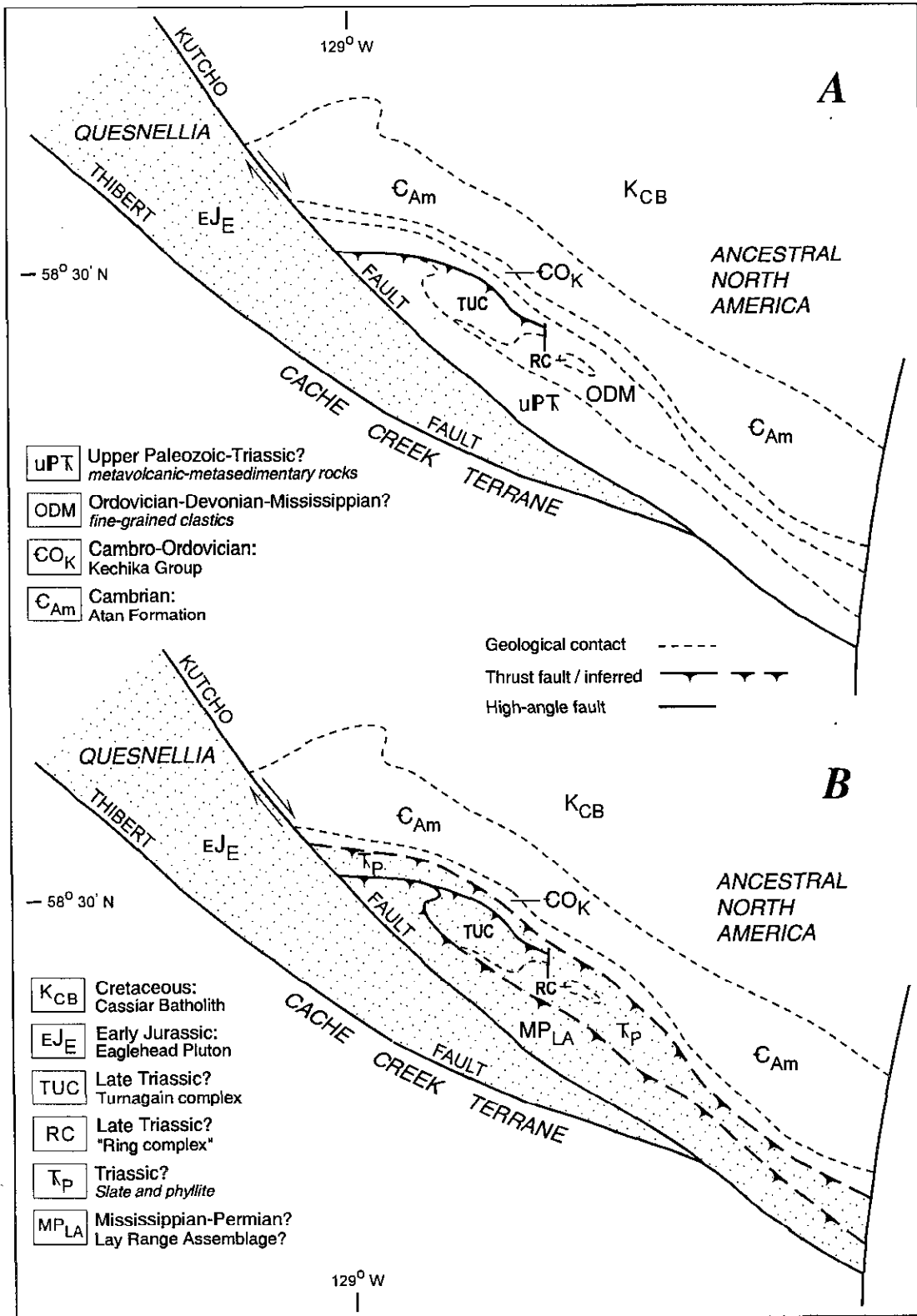


Figure 18-2. Regional geology of the Turnagain Alaskan-type complex according to A. Gabrielse (*in press*); B. this study.

the northwestern contact of the complex is interpreted herein as a thrust fault that places Lay Range Assemblage on ultramafic rocks. Strongly laminated metasedimentary and metavolcanic rocks in the hangingwall of this fault contain garnet, amphibole and oligoclase-andesine, indicating a metamorphic grade of uppermost greenschist to lowermost amphibolite facies. Similar lithologies also containing amphibole-bearing assemblages were mapped south of the Turnagain River by Clark (1975), and allow this fault to be extended along strike where it separates these higher grade rocks from underlying slate and phyllite of lower to middle greenschist facies. The inferred geometry of this fault plane at the northwestern extremity of the ultramafic complex, and difference in metamorphic grade, is consistent with an easterly directed thrust fault. It is noteworthy that the Polaris Alaskan-type complex, which intrudes similar lithologies further south in the Lay Range, is also involved in an eastward-verging deformation (*ca.* 186 Ma) at the leading edge of Quesnellia that reflects the earliest stages of accretion (Nixon *et al.*, 1997).

### IS THE SULFIDE-RICH TURNAGAIN INTRUSION REALLY AN ALASKAN-TYPE COMPLEX?

As indicated above, the Turnagain intrusion is unusually well-endowed in sulfides for a Alaskan-type complex. The only other sulfide deposit of presumed Alaskan-type affinity known to the author is found in the Early Paleozoic Salt Chuck intrusion, Prince of Wales Island, southeastern Alaska. In contrast to the Turnagain Ni-Cu sulfides, the Salt Chuck ore is Ni-poor and Cu-rich [ $Cu/(Cu+Ni) = 0.99$ ] and hosted by biotite-bearing magnetite clinopyroxenite and gabbro (Gault, 1945; Loney and Himmelberg, 1992). During its intermittent mining history, the Salt Chuck mine (1905-1941) produced some 0.3 million tonnes of sulfide ore with an estimated grade of 0.95 wt. % Cu, 1 ppm Au, 5 ppm Ag and 2 ppm Pd (Holt *et al.*, 1948). The principal ore minerals are bornite and lesser chalcopyrite. Minor platinum-group minerals (PGM) identified by Watkinson and Melling (1992) include kotulskite (PdTe), temagamite ( $Pd_3HgTe_3$ ), sopcheite ( $Pd_3Ag_4Te_4$ ) and auriferous sperrylite ( $PtAs_2$ ). Although the Cu-rich nature of the ore and origin of the PGM have been related to hydrothermal remobilization of magmatic sulfides, the mechanism for concentrating the copper and precious metals is debatable: Loney and Himmelberg (1992) advocated a magmatic process (fractional crystallization) whereas Watkinson and Melling (1992) favoured a hydrothermal origin.

The classification of mafic-ultramafic complexes as Alaskan-type is *not* based on the presence or nature of sulfides or PGM but rather on silicate mineralogy, as outlined by Taylor (1967) and Irvine (1974). The IUGS classification scheme for ultramafic rocks is shown in Figure 3. Cumulate silicate assemblages that characterize the Alaskan-type association lie along the olivine-clinopyroxene join and comprise dunite, wehrlite, olivine

clinopyroxenite and clinopyroxenite; orthopyroxene is characteristically lacking. The only other common silicate to appear in ultramafic lithologies is amphibole, which forms hornblende clinopyroxenite, clinopyroxene hornblendite and minor hornblendite. Plagioclase may be found in minor amounts in olivine-poor ultramafic lithologies and becomes a dominant constituent in associated mafic rocks (hornblende- or clinopyroxene-bearing gabbro and diorite). Accessory phases commonly include mica (phlogopite-biotite), apatite, and spinel (chromite in olivine-rich rocks; magnetite in amphibole- or clinopyroxene-rich rocks); primary sphene, ilmenite and rare zircon and quartz may appear in feldspar-rich cumulates and/or late-stage segregation veins. Magnetite may locally become a dominant cumulate phase and an economically viable commodity (*e.g.* Tulameen complex, Findlay, 1969; Nixon *et al.*, 1997).

### CLASSIFICATION OF ULTRAMAFIC ROCKS

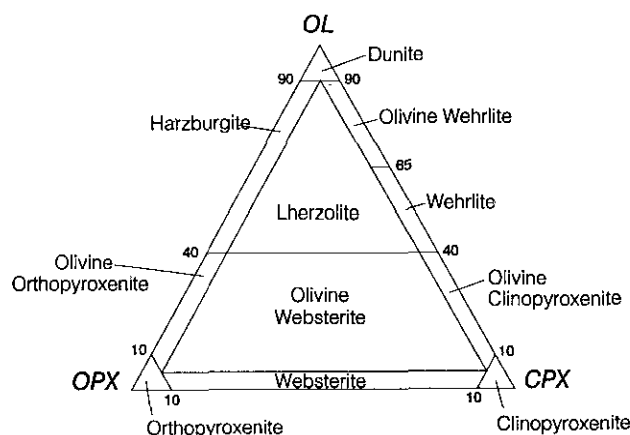


Figure 18-3. Classification of ultramafic rocks (modified after Le Maitre, 1989).

Other features typical of Alaskan-type complexes include a crude internal zonation of ultramafic and mafic lithologies (hence the common reference to zoned complexes in the literature), a general lack of layering in outcrop (Duke Island is a notable exception) which is so typical of stratiform complexes, an absence of high-temperature tectonite fabrics like those that pervade obducted ophiolitic mantle, the common occurrence of fault-bounded contacts, and, where intrusive contacts have been established, thermal aureoles of hornblende hornfels (or amphibolite-grade regional metamorphism where deformation occurred while the intrusion was still hot, *e.g.* Polaris complex, Nixon *et al.*, 1997).

The key features of Alaskan-type complexes portrayed by the Turnagain intrusion include the following:

- ultramafic cumulates are restricted to mixtures of olivine and clinopyroxene with minor chromite, rare amphibole and trace phlogopite; orthopyroxene is absent
- centimetre-scale layering is comparatively rare
- localized chromitite layers (<1m in length) in the dunite have been entirely remobilized to form

schlieren and syndepositional folds, features that are characteristic of all Alaskan-type occurrences in British Columbia

- clinopyroxene compositions are diopsidic (Clark, 1975, 1978) and comparable to other Alaskan-type intrusions

Taken together, these features are sufficient to warrant the Alaskan-type classification for the Turnagain complex.

## GEOLOGY OF THE TURNAGAIN COMPLEX: A SYNOPSIS

The generalized geology of the Turnagain complex is shown in Figure 4. The body is elongate (8km x 3km) and broadly conformable to the northwesterly-trending structural grain. The principal lithologies comprise dunite, wehrlite and olivine clinopyroxenite and represent crystal cumulate sequences. Minor hornblende clinopyroxenite and hornblendite appear restricted to the northwestern and

southwestern parts of the complex, and clinopyroxenite commonly forms dikes. Unlike many other Alaskan-type complexes, gabbroic to dioritic members of the intrusive suite are lacking. Common accessory minerals include chromite in dunite, and trace amounts of phlogopite, especially in clinopyroxene-rich rocks. Among the oxide phases, cumulus or intercumulus magnetite is conspicuously absent, except for grains intergrown with primary sulfides, and primary ilmenite has only been identified in hornblende-rich rocks (Clark, 1975, 1978).

Dunite occupies the eastern and central portions of the body and is flanked by wehrlite and olivine clinopyroxenite. The ultramafic rocks are generally fresh to mildly serpentinized; however, more intense serpentinization and talc-carbonate alteration are common along faults and restricted zones within the complex. The central part of the ultramafic body is intruded by granodiorite to diorite, and hornblende±clinopyroxene-plagioclase porphyry dikes and sills. The latter are documented in drill core near the southwestern contact of the complex (Clark, 1975).

Primary layering in clinopyroxene-rich cumulates, reflecting variations in the modal abundance of olivine and pyroxene, is comparatively well-developed in outcrop, and at a larger scale, at the northwestern end of the complex (Figure 4). The layering has moderate to steep dips and is truncated by the faulted eastern boundary of the complex. Millimetre- to centimetre-scale layering in the dunite core is evident locally where concentrations of chromite crystals have accumulated. These chromite horizons are discontinuous and commonly remobilized and intruded by thin dunite dikes. Despite localized zones of well-developed layering, way up criteria are inconclusive and the internal structure of the Turnagain complex is poorly understood.

Contacts between dunite and surrounding clinopyroxene-rich rocks are gradational to sharp. The latter relationship, observed at the northwestern margin of the dunite, was interpreted as evidence for intrusion of

wehrlite-clinopyroxenite cumulates by the dunite (Clark, 1975). Such relationships, however, may be of local significance only, and confined to a narrow time interval when dunite and pyroxenite were being deposited penecontemporaneously in different parts of the complex. Another possibility is that the dunite at this contact is a discordant metasomatic body formed locally by replacement of pre-existing cumulates, as documented in other Alaskan-type complexes (e.g. Duke Island, Irvine, 1974). In general, the gradational contacts observed elsewhere, the occurrence of interlayered dunite and wehrlite, and the wehrlite-clinopyroxenite dikes so prevalent throughout the main dunite mass are consistent with deposition of clinopyroxene-rich cumulates after the dunite was formed. In this regard, it is also worth noting that olivine compositions determined by Clark (1975) in the dunite are generally more magnesian (Fo>88 mol. %) and more enriched in nickel than those in pyroxenitic cumulates (Fo<88 mol. %), as would be expected during the normal course of fractional crystallization. It was also shown by Clark (*ibid.*) that olivines coexisting with primary sulfides are more depleted in nickel than olivines in sulfide-free rocks due to the preferential partitioning of nickel into the sulfide phase.

## SULFIDE MINERALIZATION

The main occurrences of massive to semi-massive Fe-Ni-Cu sulfide mineralization are shown in Figure 4. In addition to these prospects, disseminated primary sulfides are widespread in pyroxenitic rocks. With few exceptions, economically interesting sulfide concentrations are largely hosted by wehrlite, olivine clinopyroxenite and clinopyroxenite. Dunite is practically devoid of significant sulfide mineralization. However, sulfides in the Discovery and Cliff showings, in particular, are hosted by serpentinite that may originally have been dunite. In the case of the Davis #2 showing at the northwestern end of the complex, primary sulfides are hosted by clinopyroxene hornblendite and hornblendite.

Primary sulfides, in decreasing order of abundance, comprise pyrrhotite, pentlandite, chalcopyrite and trace bornite (Clark, 1975). Their textures are diagnostic of the precipitation of an immiscible sulfide melt from a silicate liquid: intercumulus and blebby sulfides in disseminated zones coalesce to form continuous networks enclosing cumulate silicate grains, and these net-textured sulfides locally occlude silicates altogether to form massive accumulations. In coarse-grained rocks, spheroidal to amoeboid sulfide globules are poikilitically enclosed in clinopyroxene or hornblende. Drill intersections reveal centimetre-scale layering of massive and semi-massive sulfide concentrations in zones up to one metre wide, and these concentrations yield the highest assays (>1 wt. % Ni). Locally, there is evidence in drill core for limited remobilization of primary sulfides along fractures and veins, correlated with a general increase in the pyrrhotite/pentlandite ratio (Clark, 1975). Thus, remobilized sulfide appears to be comparatively Ni-poor but may be relatively Cu-rich.

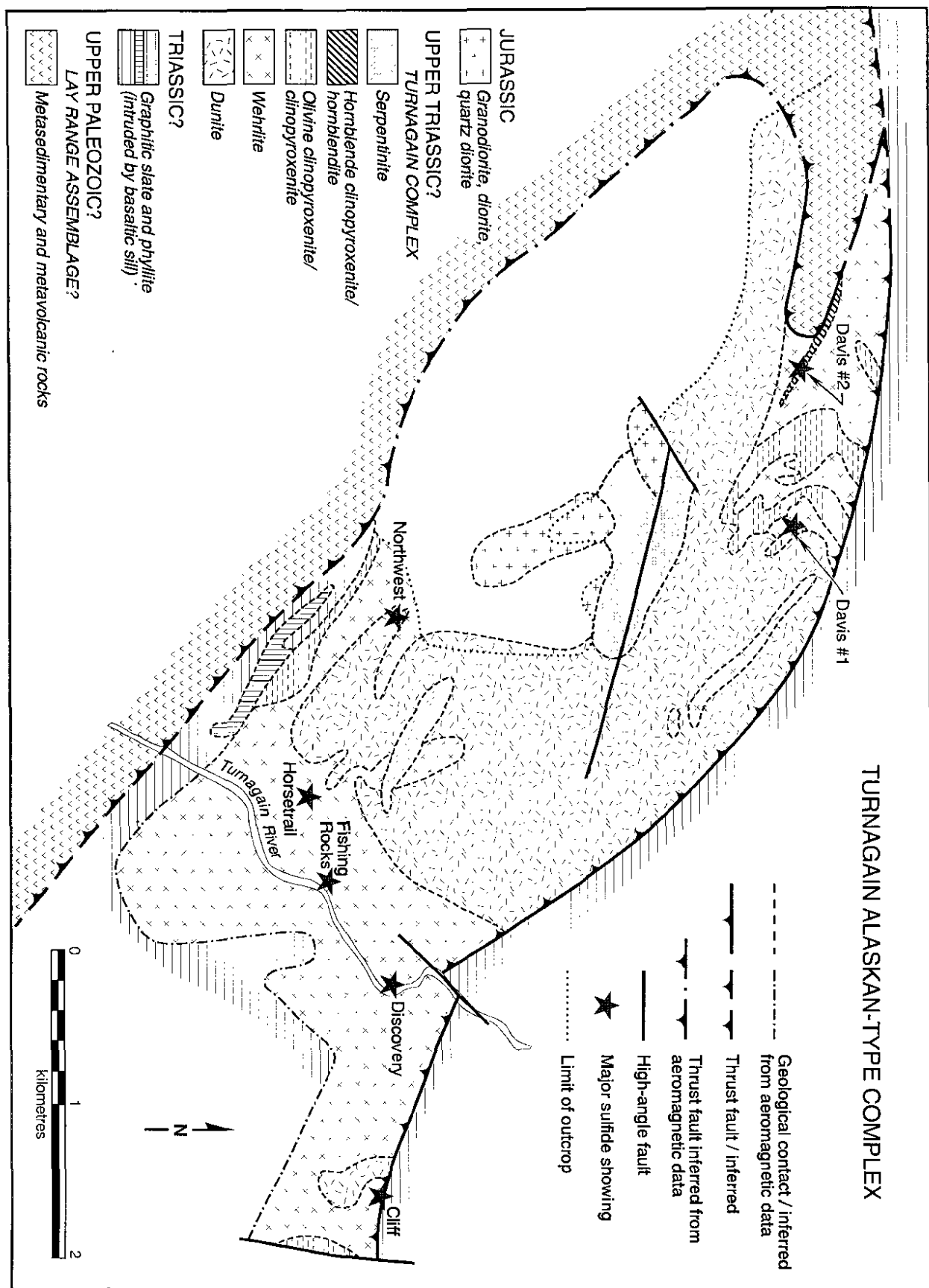


Figure 18-4. Simplified geology of the Turnagain ultramafic complex showing major occurrences of sulfide mineralization (modified after Clark, 1975).

Secondary sulfides include violarite ( $\text{FeNi}_2\text{S}_4$ ), valleriite  $4(\text{Fe,Cu})\text{S}\cdot 3(\text{Mg,Al})(\text{OH})_2$ , pyrrhotite, pyrite, rare molybdenite and possibly mackinawite  $[(\text{Fe,Ni})_9\text{S}_8]$  (Clark, 1975). These minerals are widely distributed as fine disseminations of irregular grains in variably serpentinized rocks, or concentrated in veins and fractures. Clark related their origin to precipitation from hydrous fluids during serpentinization.

It is noteworthy that both primary and secondary sulfides in the Turnagain complex are associated with graphite. The fact that graphite preferentially occurs in serpentinized zones with fine-grained secondary sulfides, forms halos around sulfide veins, and commonly coats fractures and faults, led Clark (1975) to suggest that the graphite was introduced from an external source by  $\text{CO}_2$ -rich aqueous solutions that became reduced and deposited graphite during the serpentinization process. A viable source of carbon is the graphitic sediments that host the intrusion. Although most of the textural evidence points to a hydrothermal origin for the graphite, the inclusion of graphite flakes in semi-massive to massive primary sulfides, albeit in partially serpentinized host rocks, suggests that some of the carbon may have been introduced at the magmatic stage. This may have been effected by incorporation of xenoliths and/or screens of fine-grained graphitic wallrocks which have been encountered in recent drilling (B. Downing, personal communication, 1997). As indicated below, contamination by carbon-rich wallrocks may be a key mechanism whereby magmas of Alaskan-type affinity precipitate economically significant quantities of primary Fe-Ni-Cu sulfides.

## ORIGIN OF MAGMATIC SULFIDES IN ALASKAN-TYPE MAGMAS: PROBLEMS AND POSSIBILITIES

On the basis of the sulfide mineralogy and textural evidence summarized above, it is clear that the main concentrations of Fe-Ni-Cu sulfides in the Turnagain complex are of magmatic origin, and conform to the products predicted to form during fractional crystallization of both silicate and sulfide melts. Clark (1975, 1980) concluded that the key factor responsible for unusual concentrations of sulfides in the Turnagain intrusion was a high initial content of sulfur in the primitive magma(s), reflecting extensive melting of a sulfide-enriched region of the upper mantle.

The bulk composition and oxidation state of a magma have been shown to be important factors, among others, governing the separation of an immiscible sulfide liquid from a silicate melt (e.g. Naldrett, 1989). It is suggested below that:

- the extremely high MgO content previously proposed for primitive Turnagain magma(s) may be seriously overestimated
- external factors may have played a crucial role in determining the oxidation state of the melt, and thereby promoting conditions conducive to the

formation of sulfide deposits in Alaskan-type magmas with nominal amounts of dissolved sulfur

## Primitive Alaskan-type magmas

The primitive magmas that produced Alaskan-type complexes are generally considered to be highly magnesian [in terms of the ratio  $100\text{Mg}/(\text{Mg}+\Sigma\text{Fe}^{2+})$  or Mg#] with high MgO contents (ultrabasic), and mildly alkalic and hydrous (e.g. Findlay, 1969; Irvine, 1974; Clark, 1980). These compositional attributes have to be deduced from crystal compositions since no direct samples of primitive Alaskan-type magmas have been identified, and few volcanic equivalents have been proposed (e.g. Irvine, 1973). It is therefore extremely important to distinguish cumulus from post-cumulus (i.e. intercumulus) minerals, since only the former potentially yield compositional information that is directly pertinent to initial liquid compositions, assuming subsolidus re-equilibration of such phases is insignificant. The composition of primitive magma deduced for the Turnagain complex is easily the most magnesian (Mg# $\geq 85$ ) and MgO-rich (32 wt. %; Clark, 1980) of any parental liquid composition inferred for Alaskan-type complexes. In fact, these particular attributes match those of komatiitic melts.

The hydrous and alkali-rich character postulated for primitive Turnagain magmas seems reasonable in view of the occurrence of phlogopite and hornblende in olivine-rich rocks. In the case of the Turnagain complex, however, these phases appear to be exclusively *intercumulus* in nature and thus yield information that is only directly relevant to pore fluids within the cumulate pile rather than presumably more primitive melt in the main magma chamber. The author has observed trace amounts of rare euhedral phlogopite enclosed by olivine in the dunites of both the Tulameen and Polaris Alaskan-type complexes. In these cases, at least, the alkalic (potassic) nature of their primitive magmas is firmly established. Another facet commonly regarded as evidence for an alkaline affinity is the diopsidic nature of clinopyroxene, which usually occurs as both an intercumulus and cumulus phase. Pyroxenes of this composition, however, are not restricted to alkaline magmas. For example, recent experimental work has shown that diopsidic clinopyroxenes similar to those found in Alaskan-type complexes may crystallize from *subalkaline* melts under high water pressures (Gaetani *et al.*, 1993). From these considerations, the hydrous nature of primitive Alaskan-type magmas appears to be well established, and it is probably necessary to consider a range of alkali contents appropriate to both alkali-rich subalkaline and mildly alkaline magmas.

The interpretation that the primitive liquid for the Turnagain complex was komatiitic rests exclusively on the composition of the most Mg-rich olivine in dunite (reported as ~95 mol. % Fo; Clark, 1980). For comparison, the most Mg-rich olivines in other complexes are ~91 mol. % Fo (e.g. Duke Island, Irvine, 1974; Tulameen complex, Findlay, 1969). Although the Turnagain olivine is indeed a

cumulus phase, such an Mg-rich composition is not necessarily representative of the liquid from which it crystallized. The total range of olivine compositions in dunite varies from 87 to ~96.5 mol. % Fo. Clark showed that the most Mg-rich olivine compositions (~95-96.5 mol. % Fo) were the result of *subsolidus* cooling and Fe-Mg exchange between olivine and chromite in chromite-enriched dunite, with the result that olivine within and adjacent to chromite layers became markedly more Mg-rich. This process has also been documented in the Tulameen complex where olivine in chromite layers changed composition from ~ 91 to 95 mol. % Fo (Nixon *et al.*, 1990). Excluding chromite-enriched samples, only two dunites in the Turnagain complex, both with normal proportions of chromite (1-2 vol. %), have olivine compositions in the range 93-94 mol. % Fo, whereas 11 dunites have olivines in the range 90-92 mol. % Fo. With one exception, the more Mg-rich olivines ( $\geq$ ~92 mol. % Fo) lie within the central part of the Turnagain dunite where there is abundant evidence for disturbance of chromite layers, reflecting gravitational collapse and transport of cumulates previously deposited on the walls of the magma chamber. It is therefore likely that such processes have redistributed Mg-rich olivine grains that were formerly equilibrated with chromite layers during *subsolidus* cooling. Such cryptic Mg-rich olivine accumulations would be expected to be localized and relatively thin (centimetre-scale). Also, for such olivines to preserve their heritage, sedimentation and cooling at the site of deposition must have been fairly rapid so as to effectively expel pore fluid and prevent re-equilibration with more Fe-rich olivine in surrounding cumulates. The fact that these cryptic olivine xenocrysts are less magnesian than olivines in chromites implies either that *subsolidus* re-equilibration with chromite was incomplete, or that they have partially re-equilibrated to their new chromite-poor environment. Thus, the composition of olivine that crystallized from primitive magmas may have been significantly less Mg-rich than Fo<sub>95</sub>. Small differences in olivine composition are extremely important because they translate into extremely large differences in the estimated MgO content of coexisting melt. For example, all things being equal, an olivine composition of 91 mol. % Fo would be expected to crystallize from a primary mantle-derived melt containing about 12-15 wt. % MgO (i.e. basaltic to picrobasaltic composition; *cf.* Irvine, 1973) as compared to the komatiitic values of 32 wt. % MgO that have been proposed. There is therefore no compelling evidence to support the proposition that unusually high-MgO liquids were responsible for the deposition of sulfides in the Turnagain complex. The question as to whether these magmas were anomalously enriched in sulfur, as suggested by Clark, cannot be addressed with the data presently available. However, other factors that control sulfide precipitation, such as oxidation state, are explored below.

## Oxidation State and Sulfide Precipitation

It has been shown that the oxidation state of a magma, as reflected, for example, by the Fe<sup>+3</sup>/Fe<sup>+2</sup> ratio of the melt,

strongly influences the speciation of sulfur in the melt, which in turn governs the precipitation of magmatic sulfides (reviewed by Wallace and Carmichael, 1992). It has been shown in recent years that certain types of magmas are intrinsically more oxidized than others, and that the oxidation state of the upper mantle is heterogeneous (*e.g.* Carmichael, 1991). In general, tholeiitic magmas and their differentiation products, such as the large stratiform intrusions associated with major magmatic Ni-Cu deposits, have relatively low oxidation states, near or significantly below the synthetic quartz-fayalite-magnetite (QFM) oxygen buffer. In comparison, volcanic arc magmas typically have higher oxidation states appropriate to that of the nickel-nickel oxide (NNO) buffer or higher, and strongly alkaline magmas are inherently the most oxidized, commonly extending well above NNO to the magnetite-hematite (MH) buffer. Observations from natural magmatic systems indicate that the *relative* redox states of parental magmas are generally maintained over the course of crystallization, and over the high-temperature part of the *subsolidus* cooling interval.

The dissolution of sulfur in a given melt composition is sensitive to the redox state of the melt. At redox conditions near the NNO buffer, there is a marked solubility minimum for sulfur in silicate melts. Under reducing conditions below this transition point, the main dissolved sulfur species is sulfide (S<sup>2-</sup>) whereas in melts more oxidized than the transition point, the dominant species is sulfate (SO<sub>4</sub><sup>2-</sup>). Experimental studies have shown that the fugacity of oxygen exerts the dominant control on sulfur speciation, the effects of temperature, pressure and melt composition being relatively minor (*e.g.* Carroll and Rutherford, 1988). For tholeiitic magmas crystallizing at or below the QFM buffer, for example, the dominant sulfur species at magmatic temperatures will be sulfide (>80%ΣS), and sulfur saturation will produce an immiscible Fe-Ni-Cu sulfide liquid phase. It is important to note that immiscible monosulfide solution may dissolve appreciable amounts of oxygen (largely controlled by fO<sub>2</sub>), and that on cooling, such melts crystallize Fe-Ni-Cu minerals accompanied by a small quantity of magnetite (<4 wt. %; Doyle and Naldrett, 1987). The amount of magnetite exsolved is directly dependent upon ambient redox conditions.

At progressively higher oxidation states, the capacity of the same melt composition to produce immiscible sulfides on cooling is dramatically impaired. In extreme cases, such as the sulfur-rich trachyandesite magmas erupted in 1982 from El Chichon, Mexico, and dacitic pumice ejected in 1991 from Mt. Pinatubo, Philippines, highly oxidizing conditions (near the MH buffer) induced the crystallization of primary anhydrite. Thus, other things being equal, the oxidation state of the magma may play a deterministic role in the ability of silicate melts to produce magmatic sulfide deposits.

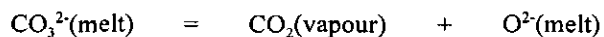
In the case of Alaskan-type complexes, the oxidation state of their primitive magmas is poorly known. From their hydrous and relatively alkali-rich nature inferred above, and supra-subduction zone environment (valid for complexes in British Columbia, at least), they would be expected to have oxidation states appropriate to NNO or

higher. This would, of course, explain to some degree why such complexes are generally devoid of magmatic sulfide deposits.

Some indication of the oxidation state of Alaskan-type magmas appears to be reflected in the composition of chrome spinel. Irvine (1974) showed that chromites in Alaskan-type complexes have moderately high Cr/(Cr+Al) ratios, similar to those of the major stratiform intrusions, but that their ferric iron contents expressed as  $Fe^{+3}/(Cr+Al+Fe^{+3})$  are distinctly higher, which he related to an intrinsic property of the parental magma. Irvine also noted that one such property that could account for chromites enriched in ferric iron was the oxidation state of the melt. Thus, the compositions of early formed chromite in many Alaskan-type complexes is compatible with inferences made above concerning the oxidation state of their primitive melts.

The compositions of early crystallizing chrome spinels in the Turnagain complex appear anomalous in that they have higher Cr/(Cr+Al) ratios and lower ferric iron contents than other Alaskan-type complexes (Clark, 1978). In particular, their  $Fe^{+3}/(Cr+Al+Fe^{+3})$  ratios are comparable to the chromites of stratiform intrusions. Following Irvine (1974), Clark cautioned against interpreting these spinel compositions solely in terms of a lower oxidation state for primitive Turnagain magmas, but noted that such an explanation would be consistent with the unusual absence of magnetite in crystal cumulates and the low proportion of magnetite (1-2 vol. %) exsolved during the cooling of primary immiscible sulfide ores. From the available data, therefore, it appears that an anomalously low oxidation state for Turnagain magmas relative to other Alaskan-type complexes is a tenable hypothesis. The higher chrome contents of Turnagain spinels may reflect a *slightly* more magnesian parental magma composition.

Given the general proposition that primitive Alaskan-type magmas are relatively oxidized (at or above the NNO buffer), either the Turnagain magma represents partial melting of an anomalously reduced upper mantle source region, or some process operating after melts left their source served to reduce their oxidation state to levels more appropriate for sulfide-enriched mafic magmas. The latter possibility is particularly intriguing since the wallrocks of the Turnagain complex are slates and phyllites enriched in graphite, and significant contamination by wallrocks appears to be a likely mechanism. As noted earlier, evidence that graphitic wallrocks were in fact incorporated into the Turnagain magma chamber has been observed in drill core. Since it has been found that carbon dissolves in mafic melts primarily as carbonate ( $CO_3^{2-}$ ) species (Fine and Stolper, 1985), it could promote the reduction of formerly more oxidized melts. For example, addition of carbon at magmatic temperatures may induce the formation of a vapour phase because of the extremely low solubility of carbon dioxide in basaltic melts at shallow crustal pressures. The composition of the initial vapour will be rich in carbon species ( $CO-CO_2$ ) and relatively poor in water (Mathez, 1989). In the case of a relatively oxidized magma (e.g. NNO buffer), the dominant species in the vapour phase will be  $CO_2$  (Mathez, *ibid.*) and degassing reactions of the type:



would lead to net loss of oxygen from the magma chamber. Moreover, processes that tend to change the oxidation state of a melt will have more impact on the potential for sulfide saturation if the original oxidation state of the magma was near the sulfide-sulfate transition point. As pointed out above, this redox condition (i.e. near the NNO buffer) seems appropriate for the primitive magmas associated with Alaskan-type complexes. If the intimate intergrowths of graphite and sulfides noted earlier in olivine-rich cumulates of the Turnagain complex were formed at magmatic temperatures, this could place rigorous constraints on the maximum oxidation state of the graphite-sulfide-silicate melt system. If the inferences drawn above are correct, then clearly other types of mafic magma that are not normally associated with significant sulfide deposits could be emplaced in environments that induce economic mineralization.

## ACKNOWLEDGMENTS

Bren-Mar Resources Limited kindly provided accommodation and logistical support from their camp at Boulder City on the Turnagain River. Bruce Downing generously made time for geological discussions in his hectic drilling schedule and freely shared his observations. Jim Reed, helicopter pilot extraordinaire, made the trip safe and enjoyable, and many thanks are extended to the crew at Boulder City for their hospitality. Verna Vilkos kindly drafted the better figures (18-2 and 18-4).

## REFERENCES CITED

- Bailey, D.G. (1988): Geology of the Central Quesnel Belt, Hydraulic, South-central British Columbia (93A/12); in *Geological Fieldwork 1987 B.C. Ministry of Energy, Mines and Petroleum Resources*, Paper 1988-1, pages 147-153.
- Bloodgood, M.A. (1987): Geology of the Triassic Black Phyllite in the Eureka Peak Area, Central British Columbia (93A/7); in *Geological Fieldwork 1986, B.C. Ministry of Energy, Mines and Petroleum Resources*, Paper 1987-1, pages 135-142.
- Bloodgood, M.A. (1988): Geology of the Quesnel Terrane in the Spanish Peaks Area, Central British Columbia (93A/11); in *Geological Fieldwork 1987, B.C. Ministry of Energy, Mines and Petroleum Resources*, Paper 1988-1, pages 139-145.
- Carmichael, I.S.E. (1991): The Redox States of Basic and Silicic Magmas: a Reflection of Their Source Regions?; *Contributions to Mineralogy and Petrology*, Volume 106, pages 129-141.
- Carroll, M.R. and Rutherford, M.J. (1988): Sulfur Speciation in Hydrous Experimental Glasses of Varying Oxidation State: Results From Measured Wavelength Shifts of Sulfur X-rays; *American Mineralogist*, Volume 73, pages 845-849.

- Clark, T. (1975): Geology of an Ultramafic Complex on the Turnagain River, Northwestern British Columbia; unpublished Ph.D. thesis, *Queen's University*, 453 pages.
- Clark, T. (1978): Oxide Minerals in the Turnagain Ultramafic Complex, Northwestern British Columbia; *Canadian Journal of Earth Sciences*, Volume 15, pages 1893-1903.
- Clark, T. (1980): Petrology of the Turnagain Ultramafic Complex, Northwestern British Columbia; *Canadian Journal of Earth Sciences*, Volume 17, pages 744-757.
- Clark, T. and McDougall, J.J. (1973): Geological Report on North Group Mineral Claims, Turnagain River, B.C.; *B.C. Ministry of Energy, Mines and Petroleum Resources*, Assessment Report 4097.
- Doyle, C.D. and Naldrett, A.J. (1987): The Oxygen Content of 'Sulfide' Magma and Its Effect on the Partitioning of Nickel Between Coexisting Olivine and Molten Ores; *Economic Geology*, Volume 82, pages 208-211.
- Findlay, D.C. (1969): Origin of the Tulameen Ultramafic-Gabbro Complex, Southern British Columbia; *Canadian Journal of Earth Sciences*, Volume 6, pages 399-425.
- Fine, G.J. and Stolper, E. (1985): Dissolved Carbon Dioxide in Basaltic Glasses: Concentrations and Speciation; *Earth and Planetary Science Letters*, Volume 76, pages 263-278.
- Ferri, F. Dudka, S., Rees, C. and Meldrum, D. (1993): Geology of the Aiken Lake and Osilinka River Areas, Northern Quesnel Trough (94C/2, 3, 5, 6, 12); in *Geological Fieldwork 1992*, B.C. Ministry of Energy, Mines and Petroleum Resources, Paper 1993-1, pages 109-134.
- Gabrielse, H. (1985): Major Dextral Transcurrent Displacements Along the Northern Rocky Mountain Trench and Related Lineaments in North-central British Columbia; *Geological Society of America*, Volume 96, pages 1-14.
- Gabrielse, H. (1991): Late Paleozoic and Mesozoic Terrane Interactions in North-central British Columbia; *Canadian Journal of Earth Sciences*, Volume 28, pages 947-957.
- Gabrielse, H. (in press): Geology of the Dease Lake (104J) and Cry Lake (104I) Map Areas, North-central British Columbia; *Geological Survey of Canada*, Bulletin 504.
- Gaetani, G. A., Grove, T.L. and Bryan, W. B. (1993): The Influence of Water on the Petrogenesis of Subduction-related Igneous Rocks; *Nature*, Volume 365, pages 332-334.
- Gault, H.R. (1945): The Salt Chuck Copper-Palladium Mine, Prince of Wales Island, Southeastern Alaska; *U.S. Geological Survey*, Open File Report 19, 18 pages.
- Hancock, K.D. (1990): Ultramafic-associated Chromite and Nickel Occurrences in British Columbia; *B.C. Ministry of Energy, Mines and Petroleum Resources*, Open File 1990-27, 62 pages.
- Holt, S.P., Shepard, J.G., Thorne, R.L., Tolonen, A.W. and Fosse, E.L. (1948): Investigation of the Salt Chuck Copper Mine, Prince of Wales Island, Southeastern Alaska; *U.S. Bureau of Mines*, Report of Investigations 4358, 16 pages.
- Irvine, T.N. (1973): Bridget Cove Volcanics, Juneau Area, Alaska: Possible Parental Magma of Alaskan-type Ultramafic Complexes; *Carnegie Institution of Washington*, Yearbook 72, pages 478-491.
- Irvine, T.N. (1974): Petrology of the Duke Island Ultramafic Complex, Southeastern Alaska; *Geological Society of America*, Memoir 138, 240 pages.
- Le Maitre, R.W., Editor (1989): A Classification of Igneous Rocks and Glossary of Terms; *Blackwell Scientific Publications*, Oxford, 193 pages.
- Livgard, E. (1996): Exploration 1996 Cub Claims: Turnagain Ultramafic Complex; *B.C. Ministry of Employment and Investment*, Assessment Report 24911.
- Loney, R.A. and Himmelberg, G.R. (1992): Petrogenesis of the Pd-rich Intrusion at Salt Chuck, Prince of Wales Island: An Early Paleozoic Alaskan-type Ultramafic Body; *Canadian Mineralogist*, Volume 30, pages 1005-1022.
- Mathez, E. A. (1989): Vapor Associated with Mafic Magma and Controls on Its Composition; in *Ore Deposition Associated with Mafic Magmas*, Whitney, J.A. and Naldrett, A.J., Editors, *Reviews in Economic Geology*, Volume 4, pages 21-31.
- McDougall, J.J. and Clark, T. (1972): Geological Report on South Group Mineral Claims, Turnagain River, B.C.; *B.C. Ministry of Energy, Mines and Petroleum Resources*, Assessment Report 3735.
- Monger, J.W.H. (1973): Upper Paleozoic Rocks of the Western Canadian Cordillera; *Geological Survey of Canada*, Paper 73-1A, pages 27-28.
- Naldrett, A.J. (1989): Magmatic Sulfide Deposits; *Oxford University Press*, New York, 186 pages.
- Nixon, G.T. and Hammack, J.L. (1991): Metallogeny of Mafic-Ultramafic Rocks in British Columbia with Emphasis on Platinum-group Elements; in *Ore Deposits, Tectonics and Metallogeny in the Canadian Cordillera*, B.C. Ministry of Energy, Mines and Petroleum Resources, Paper 1991-4, pages 125-161.
- Nixon, G.T., Cabri, L.J. and LaFlamme J.H.G. (1990): Platinum-group Element Mineralization in Lode and Placer Deposits Associated with the Tulameen Alaskan-type Complex, British Columbia; *Canadian Mineralogist*, Volume 28, pages 503-535.
- Nixon, G.T., Ash, C.H., Connelly, J.N., and Case, G., (1989): Geology and Noble Metal Geochemistry of the Turnagain Ultramafic Complex, Northern British Columbia; *B.C. Ministry of Energy, Mines and Petroleum Resources*, Open File 1989-18.
- Nixon, G.T., Hammack, J.L. Ash, C.H., Cabri, L.J., Case, G., Connelly, J.N., Heaman, L.M., LaFlamme J.H.G., Nuttall, C., Paterson, W.P.E. and Wong, R.H. (1997): Geology and Platinum-group Element Mineralization of Alaskan-type Ultramafic-mafic

- Complexes in British Columbia; *B.C. Ministry of Employment and Investment*, Bulletin 93, 142 pages.
- Page, J.W. (1986): Report on a Geochemical Survey of the Turnagain Property Consisting of the Turn 1-20 Claim, Again 21-40 Claim, Davis Claim; *B.C. Ministry of Energy, Mines and Petroleum Resources*, Assessment Report 15994.
- Panteleyev, A., Bailey, D.G., Bloodgood, M.A. and Hancock, K.D. (1996): Geology and Mineral Deposits of the Quesnel River - Horsefly Map Area, Central Quesnel Trough, British Columbia; *B.C. Ministry of Energy, Mines and Petroleum Resources*, Bulletin 97, 156 pages.
- Taylor, H.P. Jr. (1967): The Zoned Ultramafic Complexes of Southeastern Alaska; in *Ultramafic and Related Rocks*, P. J. Wyllie, Editor, *John Wiley and Sons Inc.*, New York, pages 97-121.
- Wallace, P. and Carmichael, I.S.E. (1992): Sulfur in Basaltic Magmas; *Geochimica Cosmochimica Acta*, Volume 56, pages 1863-1874.
- Watkinson, D.H. and Melling, D.R. (1992): Hydrothermal Origin of Platinum-group Mineralization in Low-temperature, Copper Sulfide-rich Assemblages, Salt Chuck Intrusion, Alaska; *Economic Geology*, Volume 87, pages 175-184.





# EPITHERMAL GOLD DEPOSITS OF THE QUEEN CHARLOTTE ISLANDS

By David V. Lefebure, B.C. Geological Survey

**KEYWORDS:** Queen Charlotte Islands, Tertiary magmatism, gold, mineral deposits, epithermal veins, hot spring deposits.

## INTRODUCTION

The Queen Charlotte Islands (QCI), located off the west coast of British Columbia (Figure 1), host a variety of mineral deposit types including skarns, precious metal veins, hot spring gold, perlite, bentonite, alluvial sands and coal. Since the 1970s most of the mineral exploration effort has been directed towards finding gold-rich deposits on the Islands. Descriptions of many of the mineral occurrences are documented in company assessment reports and have been incorporated into MINFILE, the provincial mineral occurrence database. This information is used in this article, in conjunction with the wealth of geological and geochronological data produced by the Frontier Geoscience Program of the Geological Survey of Canada (Woodsworth, 1991), to reassess the setting and potential of the gold and silver-bearing mineral occurrences.

The structural controls, host rocks and age dates associated with the precious metal occurrences on the Queen Charlotte Islands are interpreted to link almost all of them to Tertiary volcanic and intrusive rocks. This relationship can be used to explain many of their characteristics and to model the different styles of mineralization. There is considerable potential to discover new precious metal deposits on the QCI, particularly if the prospective areas with relatively limited outcrop and dense vegetation cover are reevaluated.

## REGIONAL GEOLOGY

The Queen Charlotte Islands are located along the margin of the North American plate which is bounded to the west by the Queen Charlotte dextral transform fault and the Pacific plate (Irving, Souther and Baker, 1992). The oldest reported rocks on the islands are Permian sediments (Hesthammer *et al.*, 1991) which are very restricted in extent. Volcanic rocks of the Late Triassic Karmutsen Formation are a widespread succession of tholeiitic pillow basalts and breccias that are approximately 4 000 metres thick (Sutherland Brown, 1968). Overlying the Karmutsen Formation are Triassic to Early Jurassic sediments and limestones of the Kunga Group, Early Jurassic sediments of the Maude Group and Middle Jurassic sedimentary and volcanic rocks belonging to the

Yakoun Group; all these units are regionally extensive. On the other hand, the Early Cretaceous clastic sediments of the Longarm Formation and Cretaceous Queen Charlotte Group sediments and minor mafic volcanic rocks are more restricted in extent. Unnamed Tertiary volcanic and sedimentary rocks occur throughout the Queen Charlotte Islands (Figure 2, Lewis *et al.*, 1991). Tertiary Skonun Formation sediments and the mainly Miocene Masset Formation volcanic flows and pyroclastic rocks are restricted to the northern half of the archipelago. Cenozoic sedimentary rocks are present throughout the Queen Charlotte Basin (Figure 1) that is interpreted to be a Tertiary extensional basin which is now largely below sea level (Yorath and Chase, 1981, Irving, Souther and Baker, 1992). The reader is referred to summary volume for the Frontier Geoscience Program (Woodsworth and Tercier, 1991) for up-to-date descriptions and interpretations of many of the units described above.

The Cretaceous and older rocks are variably deformed and can be subdivided into discrete structural domains separated by major faults. The older rocks are cut by Tertiary plutons and dike swarms and overlain unconformably by Tertiary volcanics and sediments and/or Quaternary sediments (Sutherland Brown, 1968; Hickson, 1991).

The stratigraphy is intruded by the Middle Jurassic San Christoval and Burnaby Island plutonic suites and the Tertiary Kano Plutonic Suite and dikes (Anderson and Reichenbach, 1991). The Burnaby Island Plutonic Suite, which is commonly intensely fractured and hydrothermally altered, is believed to be the source of fluids that formed the numerous iron and base metal skarns that are found proximal to these intrusions (Anderson, 1988). Various company reports show that some Tertiary dikes and intrusions are strongly altered to disseminated pyrite and other minerals and can have zones with anomalous gold, or rarely, copper concentrations.

The Tertiary volcanic rocks and related intrusive rocks formed from Eocene to Miocene time. The analysis of a suite of Tertiary igneous samples using U-Pb isotopic dating by Anderson *et al.* (1995) has distinguished four pulses of Tertiary magmatism - Middle Eocene, Late Eocene, Early Oligocene and Late Oligocene. The age dates show that the locus of magmatism generally migrated northwesterly over time, a point first made by Young (1981). Therefore, erosion has generally exposed increasingly deeper stratigraphic levels and more intrusive rocks in the southern islands of the QCI archipelago.

The Late Tertiary Skonun Formation consists of marine and non-marine sand, sandstone, shale and conglomerate (Sutherland Brown, 1968). In some locations

it overlies volcanic rocks of the Masset Formation; however, the deeper, older units are believed to be coeval (Lewis *et al.*, 1991).

## TERTIARY MAGMATIC SUITE

### Tertiary Intrusive Suite

#### *Kano Plutonic Suite*

The Kano Plutonic Suite (KPS), a series of small monzodiorite, diorite and granite stocks, crop out on the east and west coasts of Moresby Island and the west coast of Graham Island (Figure 3). These Late Eocene to Oligocene epizonal plutons are seriate to porphyritic, homogeneous, and commonly contain miarolitic cavities (Anderson and Reichenbach, 1991). Some KPS intrusions exhibit hypabyssal textures and intrude Tertiary volcanic rocks, both characteristics of a relatively high level of emplacement.

#### *Tertiary Dike Swarms*

Numerous Tertiary dikes are found throughout the QCI (Sutherland-Brown, 1968); they are typically steeply dipping to vertical, vary from less than a metre to 20 metres in thickness, and can form composite dikes up to 100 metres wide (Souther and Jessop, 1991). Columnar jointing perpendicular to flow contacts occurs in many dikes while others exhibit marginal flow banding. The dikes are often concentrated in broad regional swarms that are from 10-20 kilometres across and up to 40 kilometres long. Within a swarm, the dikes display a dominant trend with relatively minor variation. Souther and Jessop (1991) identified seven major swarms called informally the Rennell Sound, Selwyn Inlet, Tasu Sound, Lyell Island, Bigsby Inlet, Burnaby Island and Carpenter Bay dike swarms. New mapping indicates a north-northwesterly trending sheeted dike swarm near Redtop Mountain, that cuts across the east-trending Selwyn Inlet dike swarm, is related to the Tasu Dike swarm (Anderson *et al.*, 1995). Towards the centre of some swarms, dikes coalesce into sheeted complexes with associated KPS plutons. The best examples of these "central igneous complexes" are at Carpenter Bay, Lyell Island and southern Louise Island (Souther and Jessop, 1991).

The dikes are frequently aphanitic to weakly phyrlic. Most are basaltic to andesitic in composition, but there are some dacites and rhyolites. Detailed mapping by Souther and Jessop (1991) established that the dikes comprise from 1 to 7% of the rock exposed across a transect of a particular dike swarm. The dikes have experienced relatively little deformation - minor offsets on faults or possibly minor post-emplacement tilting. The dike swarms formed during periods of extension and strike north, northwesterly, northeasterly and easterly. Souther and Jessop (1991) describe alteration associated with dikes in the Renell Sound, Bigsby Inlet, Selwyn, Lyell Island, Burnaby Island and Carpenter Bay swarms. Some dikes

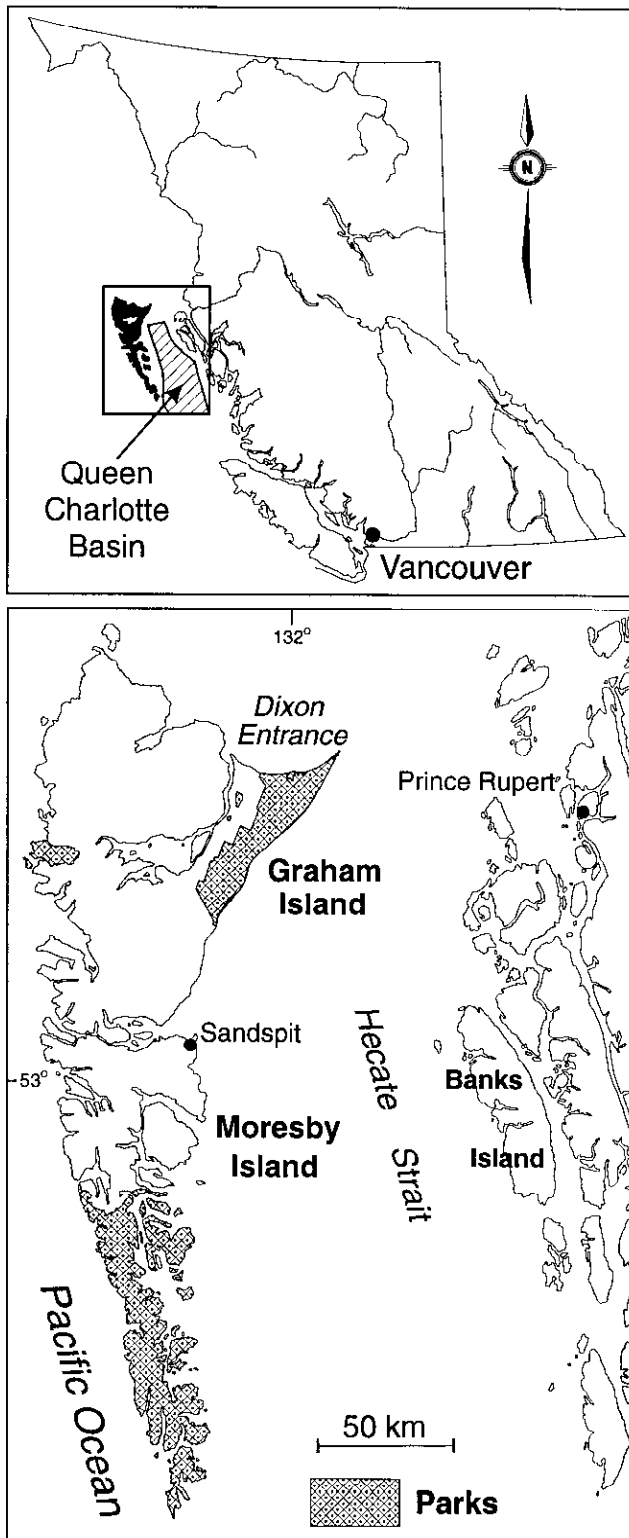


Figure 1. Location of Queen Charlotte Islands.

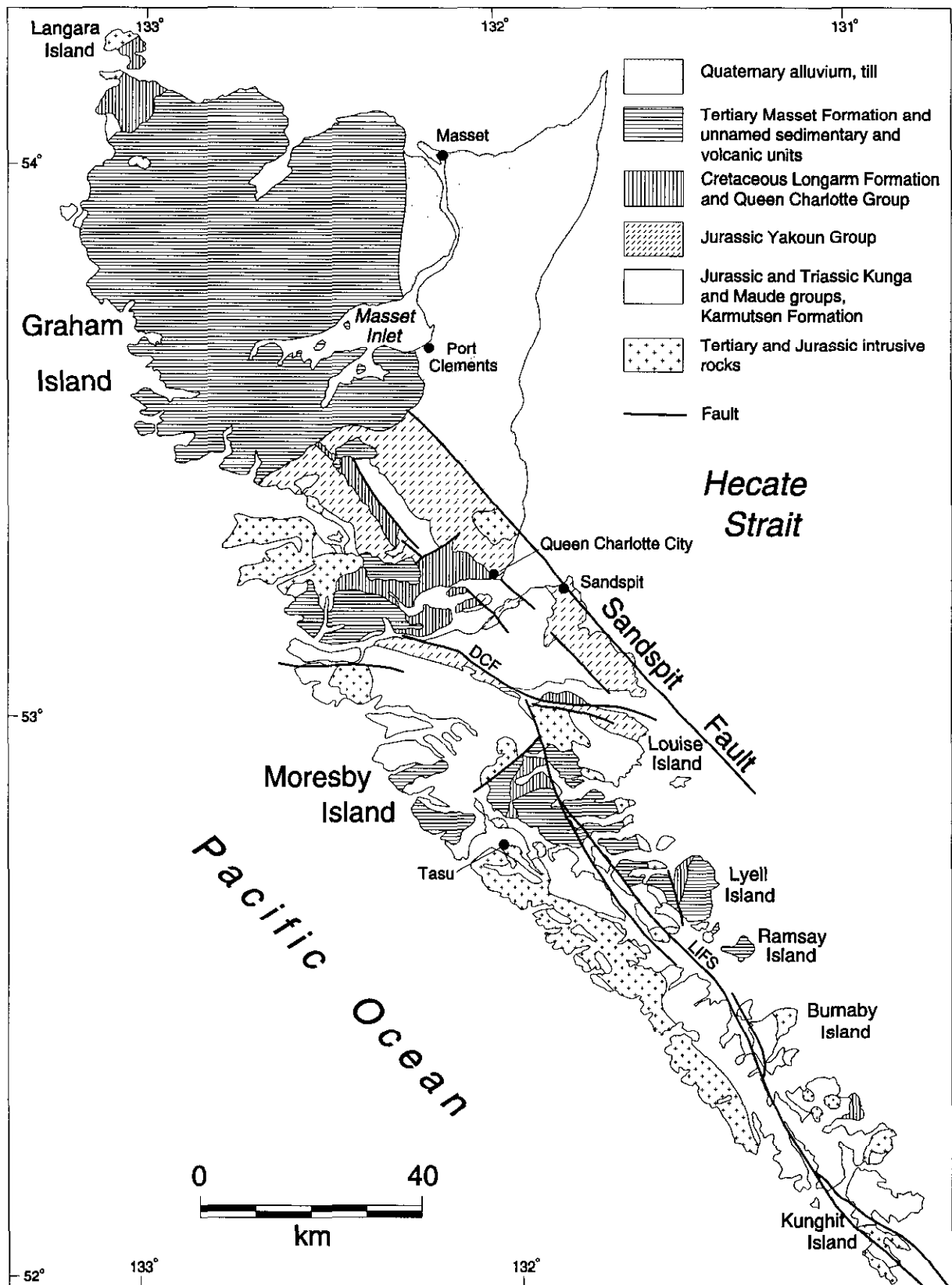
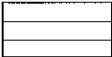
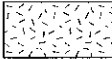


Figure 2. Simplified geology map of the Queen Charlotte Islands, from Lewis *et al.* (1991). DCF- Dawson Cove fault, LIFS - Louscoone Inlet fault system.

-  Masset Formation
-  Tertiary sediments
-  Eocene and Oligocene volcanic rocks
-  Tertiary dykes and subvolcanic intrusions
-  Kano Plutonic Suite Intrusions

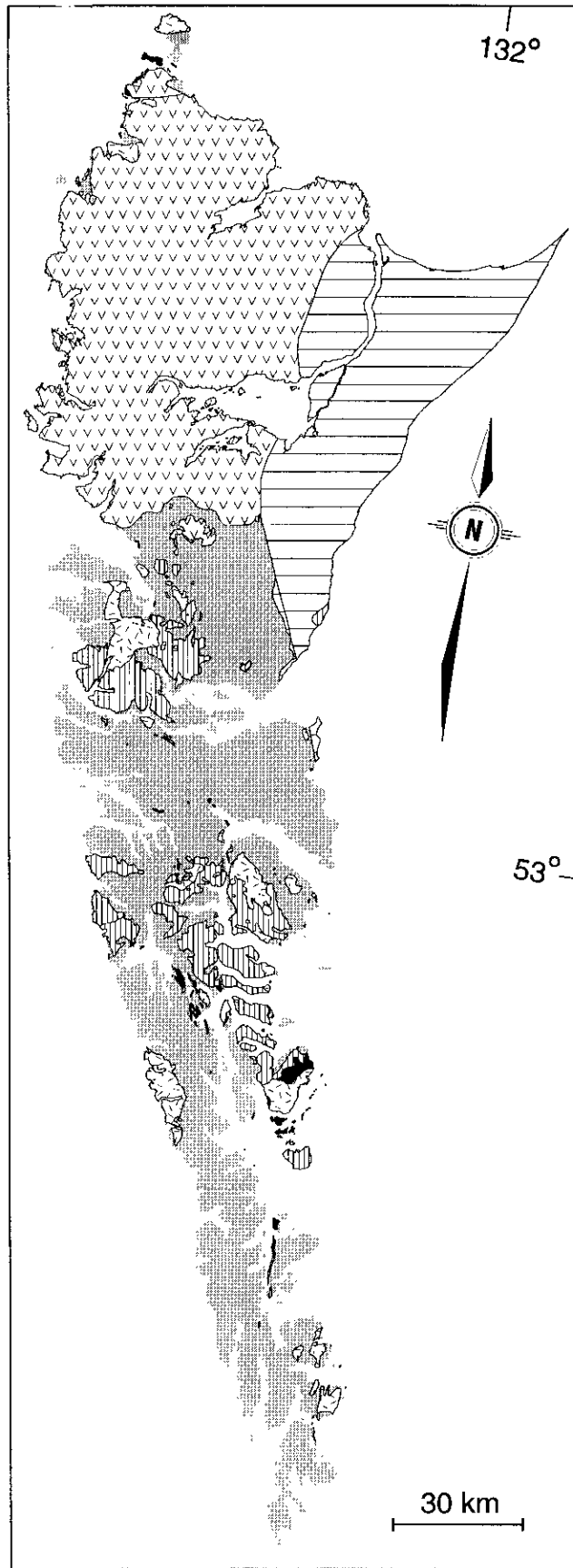


Figure 3. Tertiary Geology of the Queen Charlotte Islands.

are altered to a variety of minerals including disseminated pyrite, quartz, zeolites and carbonates.

The composition and spatial distribution, as well as a number of age dates link the dike swarms to Tertiary volcanism and the KPS (Anderson and Reichenbach, 1991; Souther and Jessop, 1991). As such, the KPS stocks and, in some cases, dikes represent the subvolcanic intrusions which lay beneath Tertiary volcanic accumulations that have been largely eroded.

## Tertiary Volcanic Rocks

A mixed suite of Tertiary mafic and felsic volcanics occurs throughout the northern two-thirds of the Queen Charlotte Islands, with the greatest volume on Graham Island (Sutherland Brown, 1968). These volcanic rocks consist of columnar basalt flows, mafic breccias, felsic lava flows and pyroclastic rocks and are cut by intimately related hypabyssal intrusions (Sutherland Brown, 1968; Souther, 1991, 1993). The volcanics are predominantly subaerial in character; submarine textures have only been noted locally. The flows are subhorizontal and believed to be largely undeformed, although some post-emplacment tilting may have taken place (Hickson, 1991). While Sutherland Brown identified three different facies, a regional Tertiary volcanic stratigraphy has not been developed due to numerous local variations (Souther, 1993; Hickson, personal communication, 1997).

Earlier workers included all the Tertiary volcanic rocks in the Masset Formation (Sutherland-Brown, 1968 and Cameron and Hamilton, 1988). More recently Hickson (1991) restricted the Masset Formation to aphyric to sparsely phyrlic, calc-alkaline volcanics and associated epiclastic sediments found on Graham Island. These volcanics are estimated to be about 3 000 metres thick. K-Ar and a few U-Pb age dates indicate that older Tertiary volcanic rocks are essentially coeval with the KPS and dike swarms (Anderson *et al.*, 1995). The Masset Formation, as defined by Hickson, is currently interpreted to be Miocene in age (25 to 20 Ma) based on a large number of K-Ar dates.

Within the pre-Tertiary rocks of the Queen Charlotte Islands, only the western part of Moresby Island south of Bigsby Inlet is relatively free of Tertiary dikes and intrusions (Souther and Jessop, 1991). This suggests that the Tertiary volcanic rocks were originally considerably more extensive on Moresby Island than at present. Hickson (1991) believes that a significant portion of the western Masset Formation has been displaced north along the Queen Charlotte Fault to Alaska. Mafic volcanic rocks cropping out on islands on the eastern side of Hecate Strait have been equated by some with QCI Tertiary volcanic rocks because they are an equivalent age and have similar geochemistry and composition (Woodsworth, 1991). Possible Tertiary volcanic rocks have also been identified in drilling in Hecate Strait (Hyndman and Hamilton, 1991).

Several styles of volcanism are interpreted for the Tertiary volcanic units of the QCI based on their morphology, textures, distribution, relationship to

structures and geochemistry. Jessop and Souther (1991) envisioned central volcanoes along a continental margin arc, like the Cascades, spaced approximately 30-50 kilometres apart. In an interesting extension to their model, Jessop and Souther (1991) integrated the dike swarms and "central intrusive complexes" into a three-dimensional model which suggested that the dikes extended possibly ten times as far laterally as vertically. In contrast, based on mapping on Graham Island, Hickson (1991) suggests that Masset volcanic centres were large, low profile shield volcanoes on the order of 20-30 kilometres in diameter and almost contiguous.

## Tertiary Magmatic Suite Geochemistry

Initial petrographic and geochemical work on the Tertiary volcanic rocks by Sutherland Brown (1968) identified alkali basalts and sodic rhyolites. More recent work has identified a mixed parentage for the Tertiary igneous suite, which appears to be the product of both calc-alkaline and tholeiitic magmatism (Souther and Jessop, 1991). The Masset Formation has an orogenic, calc-alkaline to tholeiitic signature according to Hickson (1991). On the other hand, Hamilton and Dostal (1993) examined analyses from all the Tertiary rocks on the QCI and suggested the basalts are depleted oceanic tholeiites to variably enriched tholeiites which are often found in rifted continental margins and within-plate settings. They believe the dacites and rhyolites formed by fractional crystallization.

## TERTIARY TECTONIC SETTING

During the Eocene to Miocene period in the Queen Charlotte Islands region, western North America was converging with the Farallon Plate to the west. Some workers believe the Tertiary magmatic rocks formed in a volcanic arc related to this convergence (Souther, 1991), possibly as part of the Pemberton Volcanic belt which extends from the Chilliwack Batholith in southern British Columbia to the QCI (Souther and Yorath, 1991). This arc is now represented by widely spaced epizonal plutons and deeply eroded volcanic piles.

A more complex interpretation of plate movements during the Eocene to Miocene period is tied to migration of the Farallon-Pacific-North American plate triple junction, which was close to the QCI during that time. One possibility is that the triple junction was north of the QCI until Early Miocene. This would result in back arc extension in the QCI Basin and an eastward shift in the Farallon-Pacific spreading axis with production of tholeiitic igneous rocks (Souther and Jessop, 1991). Alternatively, Hyndman and Hamilton (1991) suggested the Tertiary volcanism could result from oblique plate extension which would produce transcurrent movement along the continent margin and orthogonal extension inland.

## QCI MINERAL OCCURENCES

More than 140 mineral occurrences are documented in the Queen Charlotte Islands in the provincial MINFILE database, including skarns, precious metal veins, perlite, bentonite, alluvial sands and coal. Iron and copper skarns containing magnetite, chalcopyrite, pyrite and pyrrhotite are the most abundant mineral deposit type (Figure 4). The skarns are hosted mainly by Kunga Formation limestones and Karmutsen Formation mafic volcanics (Sutherland Brown, 1968; Ray and Webster, 1997). They are related, and found proximal, to intrusions of the Late Jurassic Burnaby Island Plutonic Suite (Anderson, 1988). The only major mineral production in the QCI has been from these skarns. Between 1914 and 1983 the Tasu mine produced 20.8 Mt containing 12.2 Mt of iron, 59 866 tonnes of copper, 50 394 kilograms of silver and 1 339 kilograms of gold, while the Jessie deposit produced 3.9 Mt containing 2.1 Mt of iron (MINFILE). The skarns have attracted little exploration attention in recent years.

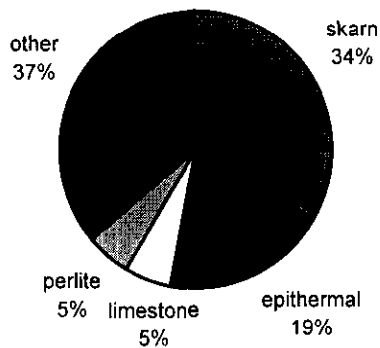


Figure 4. Relative abundances of the more common deposit types on the Queen Charlotte Islands.

A variety of epithermal precious metal occurrences, commonly associated with faults and/or Tertiary dikes, are the next most abundant style of mineralization on the QCI. Most of them have been found in the last thirty years. Higher grade mineralization is typically confined to quartz veinlets, veins and stockworks, while some alteration zones contain approximately one or more grams per tonne gold over tens of metres. Disseminations and occasional veinlets of fine grained pyrite and arsenopyrite are found in almost all the veins and often occur in the associated wallrock alteration zones. Many occurrences have associated broad zones of silicification and/or clay alteration with geochemically anomalous gold and arsenic values.

These precious metal occurrences are both epithermal hot springs and veins. The differences between these two styles of mineralization relate primarily to the original depth of emplacement in the earth's crust. Hot spring gold occurrences formed near, or at the surface, while epithermal gold-silver veins formed at up to a kilometre below the surface (Panteleyev, 1991). Epithermal and hot spring deposits can generally be distinguished from each other by their mineralogy, form, alteration, geochemistry and Au:Ag ratios. These precious metal deposit types continue to attract exploration attention and are discussed in more detail below.

There are a number of other mineral deposit types on the QCI (Table 1), including possible mesothermal gold-bearing quartz veins, volcanic redbed copper (basaltic copper) occurrences hosted by Triassic volcanic rocks, placer gold and heavy mineral accumulations, coal and a variety of industrial mineral deposits (Sutherland Brown, 1968). The Early Bird was the first lode mine in British Columbia and produced 171 tonnes grading 51 g/t gold and 7.3 g/t silver. Along with the Haida Gold and Highgrade occurrences, the Early Bird is interpreted to be a mesothermal gold-bearing quartz vein. These veins may

Table 1. Number of occurrences of different deposit types in the MINFILE database for the Queen Charlotte Islands.

| <u>Deposit Type</u>               | <u>No. of Deposits</u> | <u>Deposit Type</u>                        | <u>No. of Deposits</u> |
|-----------------------------------|------------------------|--------------------------------------------|------------------------|
| iron skarn                        | 25                     | porphyry (?)                               | 2                      |
| copper skarn                      | 23                     | polymetallic veins Ag-Pb-porphyry Cu±Mo±Au | 1                      |
| garnet skarn                      | 1                      | carbonate-hosted disseminated              | 1                      |
| epithermal hot spring Au-Ag       | 17                     | oil shale                                  | 2                      |
| epithermal Au-Ag: low             | 7                      | bitumen, tar seeps                         | 2                      |
| epithermal Au-Ag - unassigned     | 4                      | peat                                       | 1                      |
| epithermal manganese              | 1                      | bentonite                                  | 1                      |
| limestone                         | 8                      | sedimentary kaolin                         | 1                      |
| perlite                           | 8                      | diatomite                                  | 1                      |
| coal                              | 7                      | agate                                      | 1                      |
| volcanic redbed copper (basaltic) | 5                      | hot spring                                 | 1                      |
| marine placer                     | 5                      | unclassified                               | 16                     |
| gold-quartz veins                 | 2                      |                                            |                        |

Table 2. MINFILE occurrences of the Queen Charlotte Islands of presumed Tertiary age. The status of the occurrence is classified as follows: S - showing, P - prospect, DP - developed prospect and PP - past producer. Some host lithologies could not be determined and this is indicated by the abbreviation N/D.

|    | <u>Name</u>          | <u>MINFILE No.</u> | <u>Status</u> | <u>Deposit Type</u>    | <u>Host Lithology</u>               |
|----|----------------------|--------------------|---------------|------------------------|-------------------------------------|
| 1  | April                | 103B 064           | P             | hot spring Au-Ag       | Tertiary volcanics                  |
| 2  | Gumbo                | 103F 001           | S             | hot spring Au-Ag       | Yakoun Group                        |
| 3  | Point                | 103F 002           | S             | hot spring Au-Ag       | Tertiary Masset, rhyolite tuffs     |
| 4  | Courte               | 103F 003           | S             | hot spring Au-Ag       | Yakoun volcanics                    |
| 5  | Needles              | 103F 006           | S             | hot spring Au-Ag       | Yakoun volcanics and sediments      |
| 6  | Stib                 | 103F 009           | S             | hot spring Au-Ag       | Yakoun volcanics and sediments      |
| 7  | Marie Lake           | 103F 010           | S             | hot spring Au-Ag       | Kano intrusives                     |
| 8  | Marie Lake           | 103F 011           | S             | hot spring Au-Ag       | Tertiary Masset felsic pyroclastics |
| 9  | Dome                 | 103F 027           | S             | hot spring Au-Ag       | Masset Formation                    |
| 10 | Specogna (Cinola)    | 103F 034           | DP            | hot spring Au-Ag       | Skonun and Skidegate Formation      |
| 11 | Inconspicuous 4      | 103F 043           | S             | hot spring Au-Ag       | Masset - andesite and               |
| 12 | Inconspicuous 6      | 103F 044           | S             | hot spring Au-Ag       | Masset Formation                    |
| 13 | Bateaux (B & D)      | 103F 049           | S             | hot spring Au-Ag       | Tertiary volcanics?                 |
| 14 | Marino               | 103G 008           | S             | hot spring Au-Ag       | N/D                                 |
| 15 | Bella                | 103G 028           | S             | hot spring Au-Ag       | Tertiary volcanics?                 |
| 16 | SHG                  | 103C 007           | S             | hot spring Au-Ag?      | Kunga limestone                     |
| 17 | Ellen                | 103B 012           | PP            | hot spring Au-Ag?      | Karmutsen Formation                 |
| 18 | Carpenter            | 103B 056           | S             | epithermal Au-Ag       | Yakoun Group                        |
| 19 | Crescent             | 103B 062           | S             | epithermal Au-Ag       | Yakoun volcanics                    |
| 20 | Colinear Creek       | 103B 068           | S             | epithermal Au-Ag       | N/D                                 |
| 21 | Security (AB)        | 103F 028           | S             | epithermal Au-Ag       | Karmutsen Formation                 |
| 22 | Security (Overproof) | 103F 029           | S             | epithermal Au-Ag       | Yakoun Group, Karmutsen             |
| 23 | Security (B)         | 103F 033           | S             | epithermal Au-Ag       | fault breccia                       |
| 24 | Seven                | 103F 045           | S             | epithermal Au-Ag       | Yakoun volcanics                    |
| 25 | Cumshewa (L.1223)    | 103G 009           | S             | epithermal Au-Ag       | Yakoun Group                        |
| 26 | Locke                | 103B 066           | S             | unassigned epithermal  | Kunga Group, Karmutsen              |
| 27 | Bateaux (C)          | 103F 042           | S             | unassigned epithermal  | Karmutsen volcanics                 |
| 28 | Bateaux (A)          | 103F 050           | S             | unassigned epithermal  | N/D                                 |
| 29 | Baxter Creek (Snow)  | 103G 005           | S             | unassigned epithermal? | N/D                                 |
| 30 | Shag Rock            | 103K 001           | P             | epithermal Mn          | Masset Formation                    |
| 31 | Alder Gold           | 103B 007           | S             | carbonate-hosted Au-Ag | Kunga, Yakoun, Kartmutsen           |
| 32 | Brendar              | 103F 032           | S             | porphyry               | West Kano pluton                    |
| 33 | Raspberry Cove       | 103B 055           | S             | porphyry Cu±Mo±Au      | Kano Pluton                         |
| 34 | Blackwater Creek     | 103F 024           | S             | bentonite              | Tertiary Masset, rhyolite           |
| 35 | Yakoun River         | 103F 025           | S             | diatomite              | Skonun sediments                    |
| 36 | Cape Ball            | 103G 003           | S             | agate                  | N/D                                 |
| 37 | Ironside Mountain    | 103F 019           | S             | perlite                | Tertiary Masset, rhyolite           |
| 38 | Coates Creek         | 103F 020           | S             | perlite                | Tertiary Masset, rhyolite           |
| 39 | Skelu Bay            | 103F 021           | S             | perlite                | Tertiary Masset, rhyolite           |
| 40 | Blackwater Perlite   | 103F 022           | S             | perlite                | Tertiary Masset, rhyolite           |
| 41 | Canoe Creek          | 103F 023           | S             | perlite                | Tertiary Masset, rhyolite           |
| 42 | Ship Kieta Island    | 103F 036           | S             | perlite                | Tertiary Masset volcanics           |
| 43 | Juskatla Inlet       | 103F 037           | S             | perlite                | Tertiary Masset volcanics           |
| 44 | Florence Creek       | 103F 053           | S             | perlite                | Tertiary Masset volcanics           |
| 45 | Skonum Point         | 103K 002           | P             | coal                   | N/D                                 |
| 46 | Ramsay Island        | 103B 005           | S             | bitumen                | Tertiary volcanics                  |
| 47 | Tian Point           | 103F 048           | S             | bitumen                | N/D                                 |

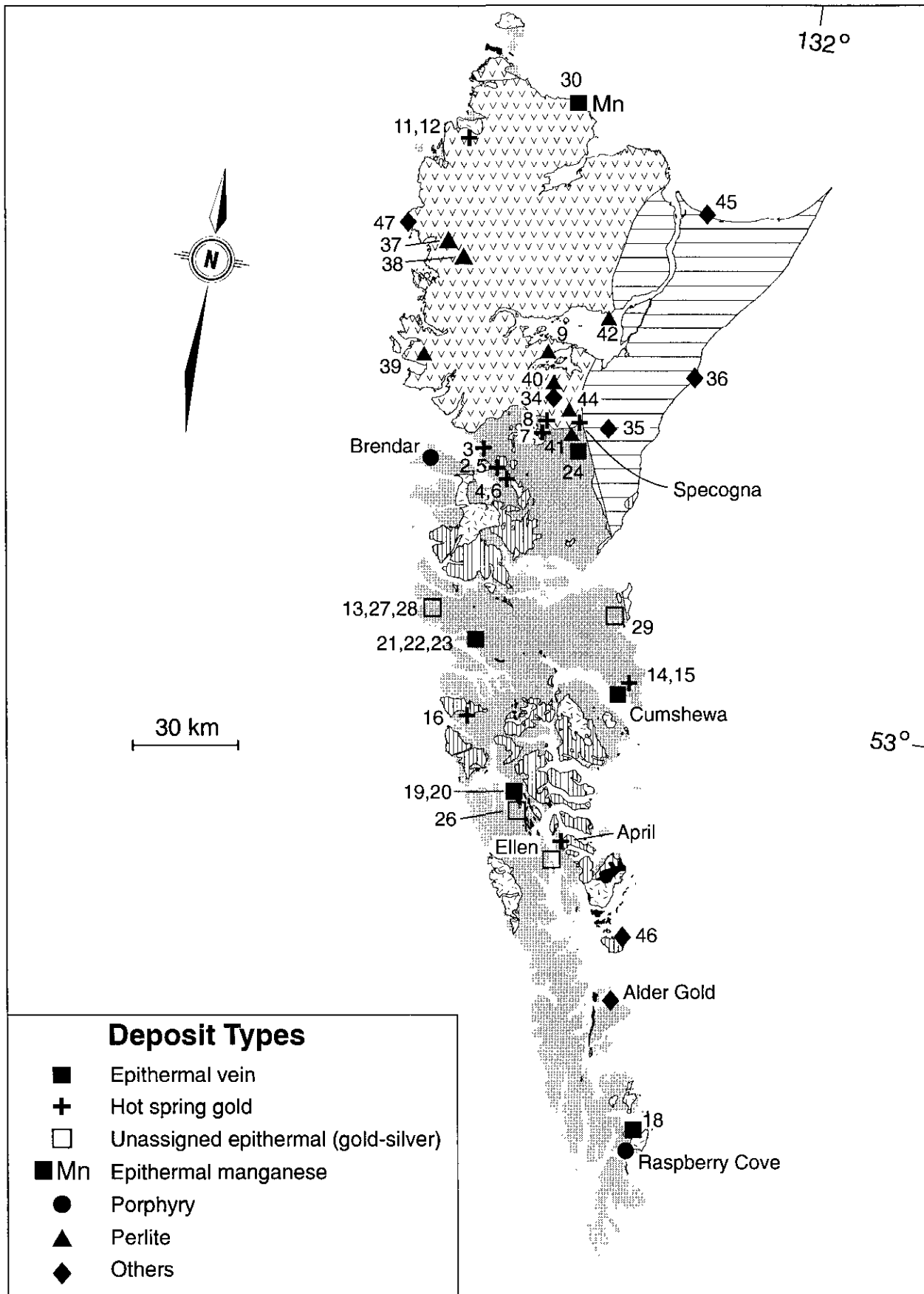


Figure 5. Tertiary Mineral Occurrences on the Queen Charlotte Islands. See Figure 3 for geological legend. See Table 2 for names of numbered mineral occurrences.

be Tertiary or older. Although polymetallic veins constitute more than 20% of the known mineral occurrences in British Columbia, the QCI has only one known example, the Southeaster. It was developed with underground workings in the 1920s and 1930s and produced 459 tonnes grading 2.8 g/t gold and 1.8 g/t silver with minor copper and lead (MINFILE).

## TERTIARY MINERAL OCCURRENCES

Over 40 mineral occurrences on the Queen Charlotte Islands are interpreted to be have formed at the same time as the Tertiary volcanism (Table 2, Figure 5). Their ages are inferred from the geology of the occurrences, the age of the host rock, the association with Tertiary structures and the absence of any younger igneous events. Champigny and Sinclair (1982) obtained two K-Ar age dates of 14 Ma for silicified and sericitized porphyritic rhyolite from the Specogna (also called Cinola or Babe) deposit. They interpret the dates as the minimum age of the emplacement of the rhyolite and the timing of the mineralization. Since there are no other published dates from mineral occurrences, it is fortunate that there are numerous dates on the associated Tertiary magmatic suite that provide quantitative constraints on the age of mineralization. The following discussion focuses on the precious metal occurrences, but includes a brief discussion of several porphyry occurrences.

Information concerning the Tertiary precious metal occurrences are available in company reports filed with the provincial government for assessment credits and distributed on microfiche. Several articles and one thesis have been published on the Specogna deposit which provide more complete descriptions of this deposit (Champigny and Sinclair, 1980; Champigny, 1981; Christie; 1988; Tolbert and Froc, 1988). It is worth noting that many of the occurrences have high Au:Ag ratios, hence exploration geologists frequently reported only the gold values from bedrock samples described in these reports.

### Hot Spring Au Occurrences

The following description of hot spring precious metal deposits is drawn largely from work by Panteleyev (1991, 1996). For more information, the reader is referred to articles by Sillitoe (1993), White (1981) and Lehrman (1986). Hot spring deposits consist of chalcedonic silica and fine-grained quartz in veins, stockworks and breccias which commonly show evidence of multiple periods of fracturing and deposition. The mineralization is gold or electrum, often microscopic, which occurs with very fine grained, disseminated pyrite and marcasite. Stibnite, realgar and/or cinnabar can occur with the mineralization. The wallrocks are commonly strongly silicified with argillic or, less commonly, advanced argillic assemblages. Propylitic alteration occurs distal from, or deeper than the argillic assemblage. Hot spring deposits have relatively Hedenquist and Reid (1985) used Au:Ag ratios of more

than 1 to 10 to separate hot spring deposits from epithermal veins.

Hot spring deposits form at the top of epithermal systems due to boiling of hydrothermal fluids at shallow depths and in hot springs at surface. The hydrothermal fluids tend to follow faults or fractures, hydrothermal breccias and permeable stratigraphic units. The deeper hydrothermal fluid systems can be developed along active, high-angle faults and volcanic and subvolcanic intrusion-related structures. While individual veins can contain high grade, bonanza gold over narrow widths, these deposits are currently more attractive as lower grade, bulk tonnage targets which typically contain more than 10 Mt grading 1 to 2 g/t gold.

The Point, Courte, Stib, Marie Lake (Rockhound and Prospector showings), Specogna, Inconspicuous (4 and 6), Bateau (B & D), Marino, Bella, April and Dome can be classified as hot spring occurrences (Figure 5, Table 2). The majority of these occurrences are located on Graham Island and a few are found at the northern end of Moresby Island. The April mineralization is located on northern Lyell Island and inside South Moresby National Park. It is hosted by Tertiary pyroclastic rocks and significantly farther south than the other hot spring occurrences.

The Specogna is the only hot spring gold deposit on the QCI with calculated reserves. Current reserves are 31 Mt grading 2.05 g/t gold with a 1.2 g/t gold cut-off (News Release, May 12, 1997, Misty Mountain Gold Limited). Exploration in the late 1980s and early 1990s defined reserves of 40.7 Mt grading 1.65 g/t Au with a cutoff of 1.1 g/t Au (Tolbert and Froc, 1988). A bulk sample weighing 2.4 t shipped to the Tacoma smelter in 1975 contained 116.5 g/t gold, 52.1 g/t silver, trace quantities of copper lead and zinc and anomalous amounts of arsenic and bismuth (MINFILE). Within the larger deposit there are some veins which grade over 10 g/t gold. For descriptions of this deposit the reader is referred to Christie (1988) and Tolbert and Froc (1988).

A number of the hot spring occurrences are hosted by Tertiary volcanic or intrusive rocks and the Specogna deposit occurs in the Miocene to Pliocene Skonun Formation (Table 2). Given the inferred Tertiary age of the mineralization and shallow depths of emplacement required to form these deposits (usually less than a kilometre, Panteleyev, 1991), these strata are at the erosion level expected to host this style of mineralization. However, there are other hot spring gold occurrences which are hosted by Middle Jurassic Yakoun Group sediments or volcanics or the underlying Kunga Group limestone or sediments. The Bateau (B&D) occurrence is even cited as occurring in the Karmutsen Formation (Pattison, 1981), but this is likely incorrect as the company report cites felsic volcanics intercalated with the basalts. Felsic volcanics are common in the Tertiary sequence, but not found in the Karmutsen Formation (Sutherland Brown, 1968). These older host rocks could reflect the fact that the mineralization sometimes formed in areas with few or no Tertiary volcanic rocks.

The Specogna deposit and other hot spring occurrences in the QCI exhibit similarities in mineralogy,

alteration, relationship to felsic volcanic activity and chemistry to the active geothermal system at Steamboat Springs in Nevada (White, 1981). For example, at Steamboat Springs the contemporaneous felsic volcanism is spatially restricted, strongly controlled by structures, and there are no extrusive igneous rocks in direct association with the top of the hot spring system. Stibnite occurs in veinlets and cavities to depths of 45 metres at Steamboat Springs and there is an absence of base metal sulphides. Gold, arsenic, antimony, mercury and thallium are anomalous in the upper parts of the of the Nevada geothermal system (drilling was to depths of 558 metres), while silver favours middle and deeper parts. Mercury is only found within 15 metres of surface.

### Epithermal Vein Au-Ag Occurrences

The other style of precious metal mineralization on the QCI that has attracted considerable exploration interest comprises gold and silver-bearing epithermal veins, stockworks and breccias. The Carpenter, Crescent, Colinear Creek, Security (AB), Security (Overproof), Security (B), Seven and Cumshewa (L. 1223) are classified as epithermal gold-silver occurrences based on MINFILE descriptions and assessment reports (Figure 5). All except for the Seven are located on Moresby Island, extending from near the southern tip to the northwest corner. The Seven is located south of Specogna on Graham island. The Cumshewa is the only occurrence with past mining activity. It was discovered in 1907 and 1,800 feet of underground development had been completed by 1913 (Sutherland Brown, 1968). Apparently a small quantity of hand-picked ore was shipped. Five MINFILE occurrences exhibit epithermal characteristics and are judged to be Tertiary age; however, they are poorly described and have not been assigned to specific deposit type (Table 2).

The epithermal vein occurrences are hosted by Yakoun Group sediments or volcanics, Karmutsen Formation volcanics, or in one case a fault breccia with fragments of Tertiary volcanics and Karmutsen basalt.

### Porphyry Occurrences

Given the presence of relatively numerous Tertiary and Jurassic intrusions with coeval volcanic rocks, the Queen Charlotte Islands have remarkably few porphyry occurrences (Figure 5). The Brendar and Raspberry Cove occurrences are possible examples of porphyry mineralization that are hosted by Tertiary intrusions. There is also a quartz stockwork occurrence with molybdenite, pyrite and chalcopyrite, the Yakulanias, hosted by a middle Jurassic Burnaby Island Plutonic Suite intrusion.

The Tertiary igneous complexes identified by Souther and Jessop (1991) commonly have associated zones of hydrothermal alteration. They noted one such rusty brown weathering zone on southeastern Lyell Island associated with a large plagioclase quartz dacite porphyry unit which contains pyrite as disseminations and along fractures (rarely with bornite) and widespread epidote alteration (Anderson *et al.*, 1992).

The small number of Tertiary porphyry occurrences likely reflects the limited amount of erosion experienced by younger Tertiary rocks on the northern half of Moresby Island and on Graham Island. The preservation of fairly extensive Tertiary volcanic rocks in the QCI despite the relatively thin original accumulations (see below) is congruent with modest amounts of erosion since the Tertiary. As the Tertiary intrusions are small, often aphanitic to weakly porphyritic, and have been emplaced in an extensional environment, they may not have experienced much differentiation before solidification. This could also explain both the small number and limited development of the porphyry occurrences found to date.

There may be potential for intrusive-related gold deposits. For example, on the Bateau property the felsic dikes are reported to consistently carry high gold values (Lickley and Vincent, 1980). This association between anomalous gold values and Tertiary felsic intrusive rocks warrants further investigation.

### Carbonate-hosted Au-Ag Occurrences

During the first years after its discovery, Specogna was thought to be a Carlin-type gold deposit because the mineralization is hosted by sediments, has a similar geochemical signature, and is a bulk tonnage, low grade gold deposit (Richards *et al.*, 1976; Champigny and Sinclair, 1982). Subsequent studies have shown that Specogna is a classic hot spring gold deposit (Christie, 1988). However, there are at least two carbonate-hosted gold occurrences on the Queen Charlotte Islands that represent possible Carlin-type deposits. The Alder Gold occurrence has visible gold with minor sphalerite within silicified Kunga Group limestone (Shearer, 1980), while the Locke showing, near Crescent Inlet, has anomalous gold in a jasperoid zone with disseminated pyrite and arsenopyrite. These small occurrences have not been well explored.

The style of mineralization appears to be disseminated pyrite within silicified Mesozoic sediments, primarily limestones, associated with regional and/or local faults. The most common host rocks are flaggy black limestone and limy argillites in the upper part of Kunga Group. These rocks are similar lithologies to the Roberts Mountain Formation, the main host of the Carlin-type deposits in Nevada (Teal and Jackson, 1997). There are other carbonate units in the Mesozoic sequence which could also be attractive host rocks for this style of mineralization (Lewis *et al.*, 1991).

## EXPLORATION MODELS

During the 1970s and into the 1980s a number of major companies, including Chevron, City Resources, Energy Reserves, Placer, Noranda, Quintana Minerals and UMEX, and a variety of junior companies and prospectors carried out exploration programs for gold on the Queen Charlotte Islands. The geologists involved in these

exploration plays were often using deposit models and exploration methodologies developed in the United States and/or the southwest Pacific to explore for Tertiary epithermal deposits. They were successful in identifying new occurrences (Richards *et al.*, 1979); unfortunately, very little information about the conceptual models employed by these prospectors and geologists was published.

Frederick Felder and geologists at UMEX had developed a model for gold mineralization related to Tertiary dikes. They recognized the importance of a variety of features, including altered hypabyssal dike swarms intruding variably altered Yakoun Formation rocks (referred to by Wilson *et al.*, 1986). The recognition of the importance of this relationship led to one of the exploration projects being called the Golden Dike property (Wilson *et al.*, 1986). Virtually all the companies were using anomalous gold, arsenic, antimony, mercury and silver values in stream sediments and soils to target areas of interest. As well, geologists were searching for silicification and clay alteration.

More recently, information from the Frontier Geoscience Program provides support for the correlation between felsic Tertiary intrusions and gold mineralization. Souther and Jessop (1991) analysed seven major dike swarms to determine a variety of characteristics, including the percentage of felsic dikes. The Carpenter Bay and Burnaby Island swarms contain 7 % felsic dikes, while the Lyell Island, Tasu Sound and Renell Sound swarms contain 8%, 15% and 19% respectively. In contrast the Selwyn Inlet swarm is mostly andesite and the Bigsby Inlet swarm contains only mafic dikes. The two dike swarms with no felsic dikes have no known gold occurrences, while all the other swarms, except Burnaby Inlet, have associated precious metal occurrences. Furthermore, Souther noted during his mapping that the felsic dikes were much more likely to be altered than the mafic dikes (personal communication, 1997).

The association between gold mineralization and felsic intrusions is perhaps the most important key to understanding the setting of these epithermal deposits. Sillitoe (1989) argues for a magmatic connection for gold deposits hosted by volcanic arcs in the western Pacific, which could explain the relationship. On the other hand the association could reflect only a common structural control for the igneous intrusions and precious metal mineralization. A simple schematic model for the epithermal mineralization in the QCI emphasizes the connection to Tertiary magmatism (Figure 6). It is similar to an unpublished conceptual section for the Specogna deposit prepared independently by Misty Mountain Gold Limited (1996).

## TERTIARY METALLOGENY

Epithermal gold occurrences are found throughout the QCI and many are intimately related to Tertiary magmatism. This close spatial association suggests they formed at the same time. Descriptions of the deposits

clearly demonstrate that many are related to felsic intrusive rocks, a relationship that was identified by exploration geologists in the 1970s and 1980s. Epithermal gold mineralization occurs in hot spring and vein environments and these grade into each other. Minor base metal mineralization occurs with the epithermal veins and several porphyry-style copper occurrences are hosted by the Tertiary Kano Plutonic Suite. The limited number of Tertiary porphyry occurrences in the QCI is believed to reflect both the limited depth of erosion and the style of magmatic activity. Given the anomalous levels of gold in some felsic aphanitic to phyrlic dikes, the KPS stocks may represent targets for low grade, bulk tonnage, intrusion-related gold deposits.

Since epithermal precious metal occurrences are found throughout the QCI and are related to Eocene to Miocene magmatism, it appears that conditions favourable for this style of mineralization existed for tens of millions of years. The mineralization and alteration are associated with the more differentiated, felsic Tertiary igneous rocks. Therefore, there could be a link between precious metal mineralization and more evolved igneous activity during this extended period, although not all these rocks are mineralized.

In contrast to many epithermal deposits which are hosted by roughly coeval volcanic rocks, the hot spring and vein occurrences on the QCI are often hosted by much older Jurassic rocks. This suggests that any Tertiary volcanic cover rocks in the immediate area of the occurrences must have been less than a kilometre thick at the time of mineralization. In fact, the lengthy dike swarms may have extended beyond the associated extrusive rocks, as suggested by Souther and Jessop (1991). Therefore, epithermal mineralization related to these dykes would be hosted by the Tertiary Skonun Formation sediments, like the Specogna deposit, or Cretaceous and older units. Since the Cretaceous rocks are not widely distributed in the QCI, this could explain the abundance of epithermal occurrences hosted by Jurassic rocks.

Geological criteria that can be used to identify prospective areas for hot spring deposits in the QCI are:

- permeable and/or porous host rocks
- Kunga Group or younger host rocks
- proximity to Tertiary structures
- existence of Tertiary intrusive rocks at depth
- large zones of silicification, extensive breccias or quartz stockworks which can form areas of positive relief
- gold occurrences with gold to silver ratios greater than 1:10
- presence of fine-grained pyrite  $\pm$  marcasite and stibnite
- advanced argillic alteration
- anomalous mercury in rock, soil or stream sediment samples

Prospective areas for epithermal veins are likely to have some of the following characteristics:

- Cretaceous or older host rocks, typically the Jurassic Yakoun Group
- proximity to Tertiary structures
- evidence of Tertiary intrusive activity, particularly felsic dikes directly associated with mineralization
- envelopes of silicification, propylite and other alteration assemblages
- precious metal occurrences with gold to silver ratios of less than 1:10
- pyrite, arsenopyrite and minor base metal sulphides
- presence of quartz veins, veinlets and stockworks

As has been noted, both types of deposits share some characteristics and grade into one another. For example, stibnite occurs in both types, although it is more common in the hot spring gold deposits.

## CONCLUSIONS

Tertiary intrusions and related volcanics in the Queen Charlotte Islands formed in an extensional environment which resulted in numerous dike swarms, small stocks and shield volcanoes. In some cases the magmatic suites evolved to felsic end members. Associated with some of the Tertiary magmatic events, particularly those with felsic dikes, are epithermal hot spring and vein gold-silver occurrences and porphyry-style mineralization. The relationships between these styles of mineralization are particularly well displayed in the QCI because the volcanic and intrusive rocks generally become older and more deeply eroded from north to south.

Using a combination of mineral occurrence descriptions and recently published geological data, it has been possible to construct a metallogenic model for the Tertiary gold mineralization on the Queen Charlotte Islands. In addition, there is interesting potential for carbonate-hosted gold deposits of the Carlin-type.

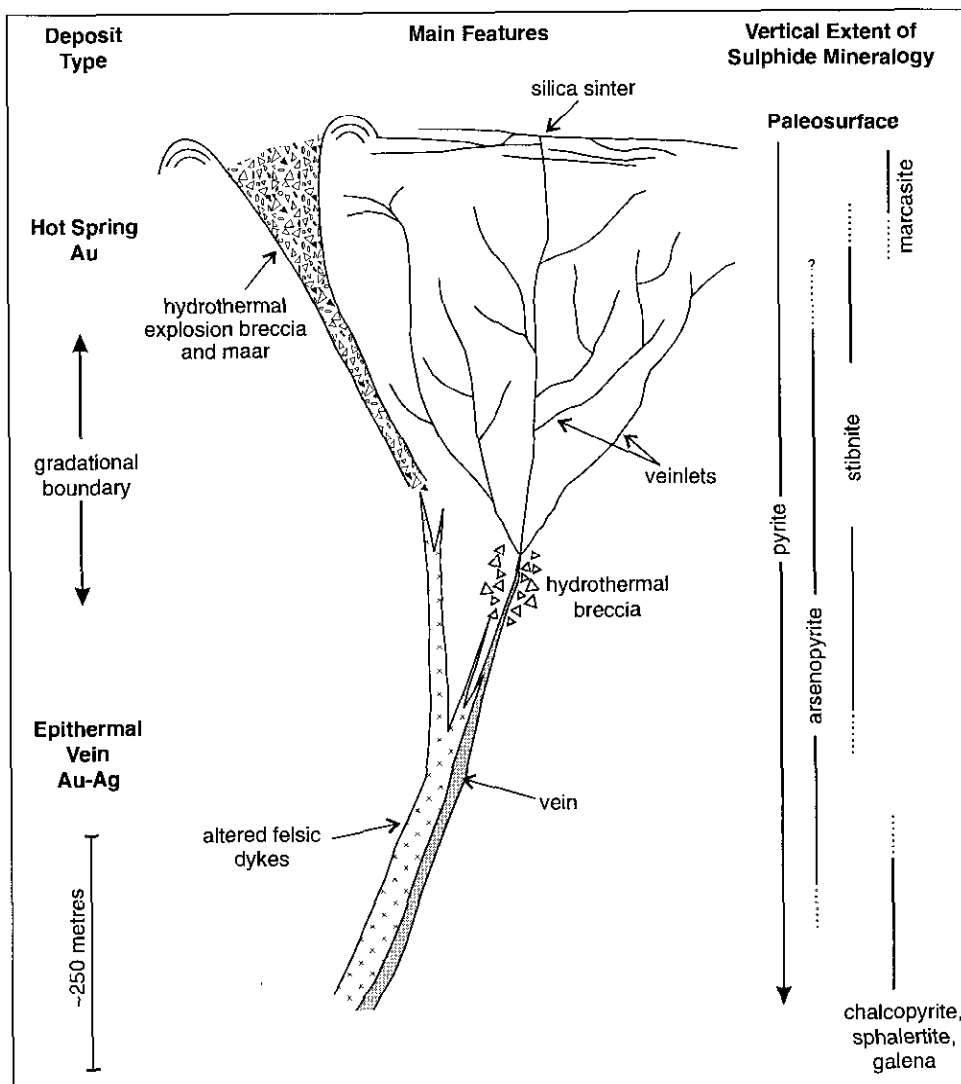


Figure 6. Schematic model of the epithermal precious metal mineralization on the Queen Charlotte Islands. More than one type of mineralization will not necessarily be present at a single locality. Figure modified from Berger and Simon (1983).

## ACKNOWLEDGEMENTS

The author's personal knowledge of the Queen Charlotte Islands is limited to visits to the Specogna deposit and Cimodora occurrence. For this reason, discussions with geologists who have worked for industry and government on the QCI proved invaluable in writing this article. Bob Anderson of the Geological Survey of Canada (GSC) provided an insightful overview of the geology of the QCI and details of the plutonic rocks and their ages. Other members of the GSC, Tark Hamilton, Cathie Hickson and Jack Souther, shared their knowledge of the Tertiary volcanic rocks and tectonic setting of the QCI. A number of industry geologists shared their knowledge of specific mineral occurrences on the QCI, including James Christie, Frederick Felder, Barry Price and Joe Shearer.

Mike Fournier drafted the figures and worked to his usual high standards. Special filters provided by Ward Kilby for the digital geology and MINFILE databases expedited the research. The article benefited from reviews by Bob Anderson, Trygve Höy, Bill McMillan and Gerry Ray.

## REFERENCES

- Anderson, R. G. (1988): Plutonic Rocks and Skarn Deposits on the Queen Charlotte Islands; *Mining Review*, March issue, pages 19-24.
- Anderson, R.G., Gunning, M.H. and Porter, S. (1992): Progress in Mapping of Jurassic and Tertiary Plutonic Styles, Queen Charlotte Islands, British Columbia; in *Current Research, Geological Survey of Canada*, Paper 92-1E, pages 117-123.
- Anderson, R.G., McNicoll, V.J., Souther, J.G. and Haggart, J.W. (1995): Extensional and Transtensional Eocene and Oligocene Magmatism in Southern Queen Charlotte Islands; Abstract, *Geological Association of Canada - Mineralogical Association of Canada*, Program with Abstracts, Volume 20, page A2.
- Anderson, R.G. and Reichenbach, I. (1991): U-Pb and K-Ar Framework for Middle to Late Jurassic (172- $\geq$ 158 Ma) and Tertiary (46-27 Ma) Plutons in Queen Charlotte Islands, British Columbia; in *Evolution and Hydrocarbon Potential of the Queen Charlotte Basin, British Columbia, Geological Survey of Canada*, Paper 90-10, pages 59-87.
- Berger, B.R. and Eimon, P.I. (1983): Conceptual Models of Epithermal Precious Metal Deposits; in *Cameron Volume on Unconventional Mineral Deposits*, Shanks, W.C., Editor, American Institute of Mining, Metallurgy and Petroleum Engineers, pages 191-205.
- Cameron, B.E.B. and Hamilton, T.S. (1988): Contributions to the Stratigraphy and Tectonics of the Queen Charlotte Basin, British Columbia; in *Current Research, Part E, Geological Survey of Canada*, Paper 88-1E, pages 221-227.
- Champigny, N. (1981): A Geological Evaluation of the Cinola (Specogna) Gold Deposit, Queen Charlotte Islands, B.C.; *University of British Columbia, M.Sc. thesis*, 199 pages.
- Champigny, N. and Sinclair, A.J. (1980): Progress Report on the Geology of the Specogna (Babe) Gold Deposit; in *Geological Fieldwork 1980, British Columbia Ministry of Energy, Mines and Petroleum Resources*, Paper 1981-1, pages 159-171.
- Champigny, N. and Sinclair, A.J. (1982): The Cinola Gold Deposit, Queen Charlotte Islands, British Columbia; in *Geology of Canadian Gold Deposits, Proceedings of the CIM Gold Symposium, September, 1980*, Hodder, R.W. and Petruk, W. Editors, *Canadian Institute of Mining and Metallurgy*, Special Volume 24, pages 243-254.
- Christie, A.B. (1988): Cinola Gold Deposit, Queen Charlotte Islands (103F/9E); in *Geological Fieldwork, 1980, British Columbia Ministry of Energy, Mines and Petroleum Resources*, Paper 1989-1, pages 423-428.
- Hamilton, T.S. and Dostal, J. (1993): Geology, Geochemistry and Petrogenesis of Middle Tertiary Volcanic Rocks of the Queen Charlotte Islands, British Columbia (Canada); *Journal of Volcanology and Geothermal Research*, Volume 59, pages 77-99.
- Hedenquist, J.W. and Reid, F. (1985): Epithermal Gold; Earth Resources Foundation, *University of Sydney*, 311 pages.
- Hesthammer, J., Indrelid, J., Lewis, P.D. and Orchard, M.J. (1991): Permian Strata on the Queen Charlotte Islands, British Columbia; in *Current Research, Part A, Geological Survey of Canada*, Paper 91-1A, pages 321-329.
- Hickson, C.J. (1991): The Masset Formation on Graham Island, Queen Charlotte Islands, British Columbia; in *Evolution and Hydrocarbon Potential of the Queen Charlotte Basin, British Columbia, Geological Survey of Canada*, Paper 90-10, pages 305-324.
- Hyndman, R.D. and Hamilton, T.S. (1991): Cenozoic Relative Plate Motions Along the Northeastern Pacific Margin and their Association with Queen Charlotte Area Tectonics and Volcanism; in *Evolution and Hydrocarbon Potential of the Queen Charlotte Basin, British Columbia, Geological Survey of Canada*, Paper 90-10, pages 107-126.
- Irving, E., Souther, J.G. and Baker, J. (1992): Tertiary Extension and Tilting in the Queen Charlotte Islands, Evidence from Dyke Swarms and their Paleomagnetism; *Canadian Journal of Earth Science*, Volume 29, pages 1878-1898.
- Lehrman, N.J. (1986): The McLaughlin Mine, Napa and Yolo Counties, California; *Nevada Bureau of Mines and Geology*, Report 41, pages 85-89.

- Lewis, P.D., Haggart, J.W., Anderson, R.G., Hickson, C.J., Thompson, R.I., Dietrich, J.R. and Rohr, K.M.M. (1991): Triassic to Neogene Geological Evolution of the Queen Charlotte Island Region; *Canadian Journal of Earth Sciences*, Volume 28, pages 854-869.
- Lickley, P. and Vincent, J.S. (1980): Bateaux Group, Report on Geology and Geochemistry; *British Columbia Ministry of Energy, Mines and Petroleum Resources*, Assessment Report 8519, 17 pages.
- Panteleyev, A. (1991): Gold in the Canadian Cordillera - a Focus on Epithermal and Deeper Environments; in *Ore, Deposits, Tectonics and Metallogeny in the Canadian Cordillera*, B.C. Ministry of Energy, Mines and Petroleum Resources, Paper 1991-4, pages 163-212.
- Panteleyev, A. (1996): Hot Spring Au-Ag; in *Selected British Columbia Mineral Deposit Profiles*, Volume 2, More Metallics, Lefebvre, D.V. and Höy, T., Editors, *British Columbia Ministry of Employment and Investment*, Open File 1996-13, pages 33-35.
- Pattison, E.F. (1981): Bateaux/Aura Claims Option Report on Geology and Geochemistry Kitgaro Inlet, N.W. Moresby Island, Queen Charlotte Islands; *British Columbia Ministry of Energy, Mines and Petroleum Resources*, Assessment Report 10255, 9 pages.
- Ray, G.E. and Webster, I.C.L. (1997): Skarns in British Columbia; *British Columbia Ministry of Employment and Investment*, Bulletin 101, pages 260.
- Richards, G.G., Christie, J.S. and Livingstone, K.W. (1979): Some Gold Deposits of the Queen Charlotte Islands; Abstract, *Canadian Institute of Mining and Metallurgy*, Volume 72, Number 809, page 64.
- Richards, G.G., Christie, J.S. and Wolfhard, M.R. (1976): Specogna: a Carlin-type Gold Deposit, Queen Charlotte Islands, British Columbia; Abstract, *Canadian Institute of Mining and Metallurgy*, Volume 69, Number 733, page 64.
- Shearer, J.T. (1980): Geological and Geochemical Report on Alder Group One, Two and Three; *British Columbia Ministry of Energy, Mines and Petroleum Resources*, Assessment Report 8094, 30 pages.
- Sillitoe, R.H. (1989): Gold Deposits in Western Pacific Island Arcs: the Magmatic Connection; *Society of Economic Geologists*, Monograph Number 6, pages 274-291.
- Sillitoe, R.H. (1993): Epithermal Models: Genetic Types, Geometric Controls and Shallow Features; in *Ore Deposits Modeling*, *Geological Association of Canada*, Special Volume 40, pages 403-417.
- Souther, J.G. (1991): Volcanic Regimes; in *Geology of the Cordilleran Orogen in Canada*, Gabrielse, H. and Yorath, C.J., Editors, *Geological Survey of Canada*, Number 4, pages 457-490.
- Souther, J.G. and Yorath, C.J. (1991): Neogene Assemblages; in *Geology of the Cordilleran Orogen in Canada*, Gabrielse, H. and Yorath, C.J., Editors, *Geological Survey of Canada*, Number 4, pages 373-401.
- Souther, J.G. (1993): Tertiary Volcanic and Subvolcanic Rocks of the central Moresby and Talunkwan Islands; in *Current Research*, *Geological Survey of Canada*, Paper 93-1A, pages 129-137.
- Souther, J.G. and Jessop, A.M. (1991): Dyke Swarms in the Queen Charlotte Islands, British Columbia, and Implications for Hydrocarbon Exploration; in *Evolution and Hydrocarbon Potential of the Queen Charlotte Basin*, British Columbia, *Geological Survey of Canada*, Paper 90-10, pages 465-487.
- Sutherland-Brown, A. (1968): Geology of the Queen Charlotte Islands, British Columbia; *Ministry of Energy, Mines and Petroleum Resources*, Bulletin 54, 226 pages.
- Teal, L. and Jackson, M. (1997): Geologic Overview of the Carlin Trend Gold Deposits and Descriptions of Recent Deep Discoveries; *Society of Economic Geologists*, Newsletter Number 31, pages 1 and 13-25.
- Tolbert, R.S. and Froc, N.V. (1988): Geology of the Cinola Gold Deposit, Queen Charlotte Islands, B.C., Canada; in *Major Gold-Silver Deposits of the Northern Canadian Cordillera*, *Society of Economic Geologists*, Field Trip Note Book, pages 15-63.
- White, D.E. (1981): Active Geothermal Systems and Hydrothermal Ore Deposits; *Economic Geology*, 75th Anniversary Volume, pages 392-423.
- Wilson, R.G., Britton, J.M. and Bradish, L.C. (1986): Report on the Geological, Geochemical, Geophysical Surveys on the Golden Dyke Joint Venture; *British Columbia Ministry of Energy, Mines and Petroleum Resources*, Assessment Report 15325, 42 pages.
- Woodsworth, G.J. (1991): Neogene to Recent Volcanism along the East Side of Hecate Strait, British Columbia; *Geological Survey of Canada*, Paper 90-10, pages 325-355.
- Woodsworth, G.J. and Tercier, P.E. (1991): Evolution of the Stratigraphic Nomenclature of the Queen Charlotte Islands, British Columbia; *Geological Survey of Canada*, Paper 90-10, pages 151-162.
- Yorath, C.J. and Chase, R.G. (1981): Tectonic History of the Queen Charlotte Islands and Adjacent Areas - a Model; *Canadian Journal of Earth Sciences*, Volume 18, pages 1717-1739.
- Young, I.F. (1981): Structure of the Western Margin of the Queen Charlotte Basin, British Columbia; unpublished M.Sc. Thesis, *University of British Columbia*, 380 pages.



## GEOLOGY OF THE NIFTY Zn-Pb-Ba PROSPECT, BELLA COOLA DISTRICT, BRITISH COLUMBIA

By G.E. Ray, B.C. Geological Survey  
J.A. Brown, 21385 121<sup>st</sup> Ave., Maple Ridge, B.C. V2X 3S5  
R.M. Friedman, University of British Columbia, and  
S.B. Cornelius, Washington State University

**KEYWORDS:** Economic geology, Bella Coola, tholeiitic, calc-alkaline bimodal volcanics, Hazelton Group, Zn-Pb-Ag-Ba exhalite deposit, barite, jasper, Nifty, Keen, Jamtart, Malachite Cliff mineral occurrences, Middle Jurassic dikes, Eskay Creek deposit.

### INTRODUCTION

The Nifty Zn-Pb-Ag-Ba prospect is located in the headwaters of the Noosegulch River valley, approximately 23 kilometres north-east of Hagensborg in west-central British Columbia (Figure 1). The area lies within the Stikine Terrane of the Coast Belt and is mostly underlain by various packages of mafic to felsic volcanic, volcanoclastic and sedimentary rocks (Figure 1). Many of these packages are of uncertain age and they are intruded by, and form roof pendants within, plutons of the Coast Belt. The volcanic rocks host several mineral occurrences, of which the Nifty prospect (B.C. Minfile number 093D) 006 is the most important and best explored. Other occurrences in the area include the Jamtart, Bella Coola Chief and Malachite Cliff occurrences as well as the Keen soil geochemical anomaly (Figure 1).

Despite exploration and drilling by various mining companies, the origin and age of the Nifty prospect have remained uncertain, and little has been reported about the chemistry of either the hostrocks or the mineralization. This paper describes the geology of the Nifty prospect. It also presents chemical data on the hosting volcanic rocks, the mineralization and its associated alteration halo, as well as some other intrusive and volcanic rocks elsewhere in the district. U-Pb data for zircons from a suite of quartz porphyry dikes that cuts the Nifty mineralization is also presented. The character and chemistry of the Nifty mineralization and its hostrocks suggest it represents a volcanogenic disseminated sulphide exhalite deposit, although an epigenetic origin has been also suggested (Morton and Birkland, 1993).

### FIELD PROGRAM

The following was accomplished during the 1996 summer field program:

- (1) Assay samples were collected of mineralized and altered rocks from the Nifty, Keen and Jamtart

occurrences (Figure 1), and other sulphide-rich outcrops in the district.

- (2) In order to determine the composition of the rocks hosting the mineral occurrences, samples of the unaltered volcanic, volcanoclastics and intrusive rocks were collected for major and trace element analyses. The bulk of this sampling effort was concentrated over the Nifty prospect.
- (3) Two samples each of the felsic volcanics and quartz porphyry dikes at the Nifty prospect were collected to attempt age determination by U-Pb methods on zircons.
- (4) A previously unrecorded copper showing named the Malachite Cliff occurrence, was discovered at 3500 feet elevation on the western slopes of the Noosegulch River valley at UTM 5816950N; 677070E.
- (5) An area of rock slide potential was noted in cliffs high on the western flanks of the Noosegulch River canyon at UTM 5827200N; 674250E, close to the Jamtart mineral occurrence. The hazardous area is at an elevation of 1400m and comprises a number of high, unstable cliffs that lie above a scree slope which stretches down to the river. A large area of bedrock (400 m by 500 m) immediately above the cliffs shows evidence of chaotic subsidence and is cut by a series of wide, crevasse-like fissures. These tension fissures trend parallel to a northerly trending fault passing along Noosegulch River; they reach up to 1m wide and are estimated to be hundreds of metres deep. A landslide in this area could temporarily dam the Noosegulch River and lead to damage downstream.

### PREVIOUS WORK

The Nifty claims were first staked and explored in 1929-1930 (Mandy, 1931) after prospectors working for Consolidated Mining Smelting Co. (now Cominco Ltd.) were attracted to the extensively rust-stained cliffs on the east side of the Noosegulch River. Trenching revealed a zone of sphalerite-galena-barite mineralization and, subsequently, a 9 metre-long adit was driven beneath this zone (Figure 2).

Baer (1973) geologically mapped the region at a scale of 1:250 000 and considered the volcanic rocks hosting the Nifty prospect to be part of the Middle Jurassic Hazelton Group, as defined by Tipper (1963).

**LEGEND FOR FIGURE 1**  
(numbers in brackets represent rock units of Baer, 1973)

CENOZOIC



Olivine basalt (18)



Intrusive rocks-granite, syenite, granodiorite (13,14,16)  
and dacitic volcanics (11)

CRETACEOUS



Andesitic volcanics; minor black slates (12)

CRETACEOUS AND/OR JURASSIC



Andesitic volcanics and tuffs; minor sediments  
and dacitic volcanics (11)



Black slate and argillite (10)

TRIASSIC OR OLDER



Schistose metasediments (8)



Greenstone and chlorite schist (7)



Granodiorite, commonly foliated (5,6)



Diorite and quartz diorite, commonly foliated (3,4)



Ortho and paragneiss (1,2)

--- Fault

$\frac{45}{\text{---}}$  Strike and dip of sedimentary bedding or volcanic layering

△ Mountain or peak

■ Mineral occurrence

N=Nifty

K=Keen

MC=Malachite cliff

BC=Bella Coola Chief

J=Jamtart

★ Middle Jurassic (mid Bajocian) fossils  
(Baer, 1973)

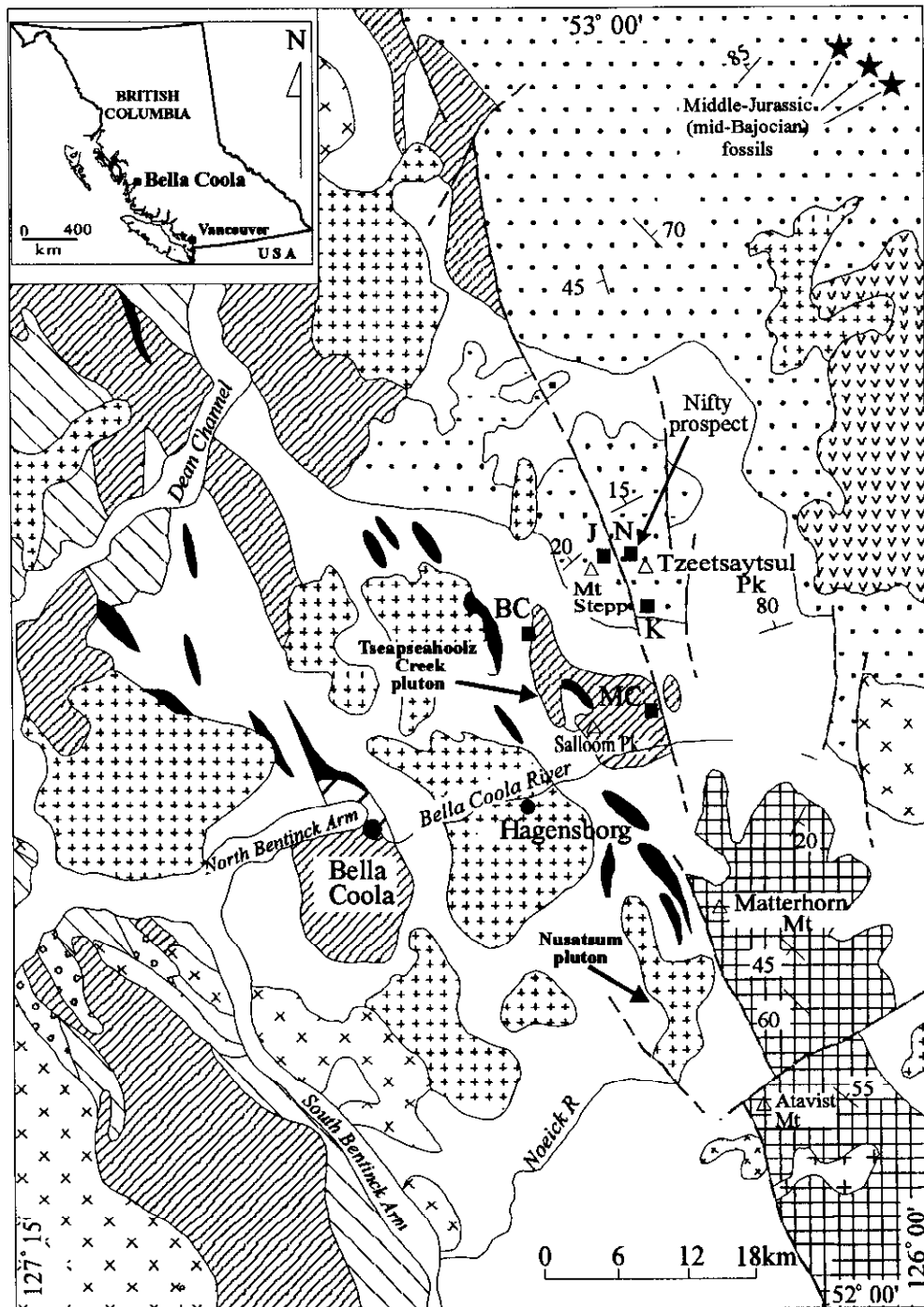
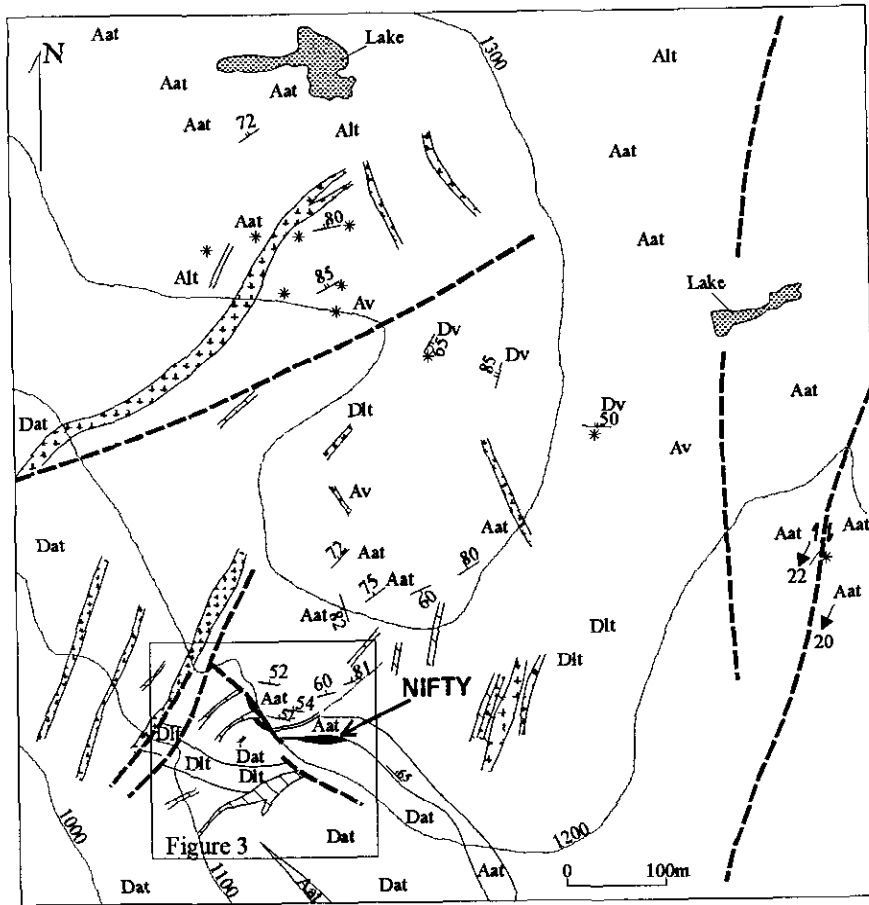


Figure 1. Regional geology of the Bella Coola district showing locations of the Nifty and other mineral occurrences. Adapted after Baer (1973).



Aat = Andesitic ash tuffs; massive to bedded  
 Alt = Andesitic lapilli tuffs; massive  
 Av = Andesitic volcanics; massive to flow banded  
 Dlt = Dacitic lapilli tuffs; massive  
 Dv = Dacitic volcanics; massive to flow banded to spherulitic  
 \* = Veins and pods of red jasper

**Intrusive rocks**

 Andesite dikes  
 Quartz porphyry dikes (c. 164 Ma)

 Barite, massive to bedded, commonly sheared  
 Dat = altered dacitic to andesitic ash tuffs, minor lapilli tuff and possible volcanic flows  
 Dlt = altered dacitic to andesitic lapilli tuffs, minor ash tuff and possible volcanic flows

 Fault  
 Geological contact  
 60 Strike and dip of bedding  
 85 Strike and dip of volcanic flow  
 22 Plunge of slickensiding  
 Direction of lateral fault movement  
 Nifty adit  
 Contour are in metres

Figure 2. Generalized geology in the vicinity of the Nifty prospect, Bella Coola. Adapted largely from Bailes and McArthur (1978, 1979) and observations of the authors.

However, Glen Woodsworth of the Geological Survey of Canada, in a talk presented in 1980, suggested that the rocks belong to the Early Cretaceous Gambier Group. In southern British Columbia the Gambier hosts the Britannia volcanogenic massive sulphide deposit (McCull, 1987). This latter correlation was accepted by many company geologists who subsequently explored the area. However, U-Pb dating presented in this paper demonstrates a pre-164 Ma (Middle Jurassic) age for the rocks hosting the Nifty prospect; this age is supported by the recent discovery of Jurassic marine fossils in the vicinity of Compass Lake, approximately 4 kilometres northeast of the Nifty prospect (Glenn Woodsworth, personal communication, 1997).

In the late 1970's, Pan Ocean Oil Ltd. mapped and soil sampled an extensive area around the Nifty prospect and the immediate vicinity of the prospect was mapped at a scale of 1:100 by J.R. Woodcock (Figure 3; Bailes, 1977). The company completed five drill holes, collared in hangingwall rocks, in an attempt to intersect downdip extensions of the sphalerite-galena-barite zone (Figure 3). The results of that work have been summarized by Lewis (1979, 1981). Although this drilling did not intersect economic mineralization at Nifty (Bailes, 1977; Bailes and McArthur, 1978), reconnaissance work resulted in the discovery of another small Pb-Zn showing (later called the Jamtart or West Side occurrence) situated west of Noosegulch Creek, approximately 2.4 kilometres south-west of Nifty (Figure 1). In addition, Pan Ocean discovered a Zn-Pb geochemical anomaly in soils about 6 kilometres south of the Nifty which is called the Keen occurrence (Figure 1; Bailes and McArthur, 1979).

In 1980 and 1981, Rio Tinto Canadian Exploration Ltd. conducted an exploration program over the Nifty and Keen properties (Holby and Campbell, 1980; Lohman, 1981). The work included drilling in hangingwall rocks to test for downdip extensions of the Nifty mineralization. The first hole was abandoned at 175 metres due to ground problems; a second parallel hole drilled immediately nearby reached a depth of 495 metres. Both holes intersected sequences of andesitic and dacitic ash and lapilli tuffs with lesser amounts of intrusive rocks, but no economic mineralization was encountered.

Imperial Metals Corporation completed some soil, rock and stream sediment sampling on the Keen and Nifty properties in 1984 and 1989 respectively (Morton, 1984; Taylor 1989). It is believed that Imperial Metals drilled into altered footwall rocks immediately east of the Nifty adit but the results of this program are not available. In 1985, Cominco Ltd. once again completed a large program of mapping and sampling over the Nifty and Keen properties without economic success (Anonymous, 1985; Blackwell, 1985). The most recent exploration activity was in 1992 when the area was restaked and a geological and geochemical program was completed for Inco Exploration and Technical Services Inc., and Eastfield Resources Ltd. (Morton and Birkeland, 1993).

## DISTRICT GEOLOGY

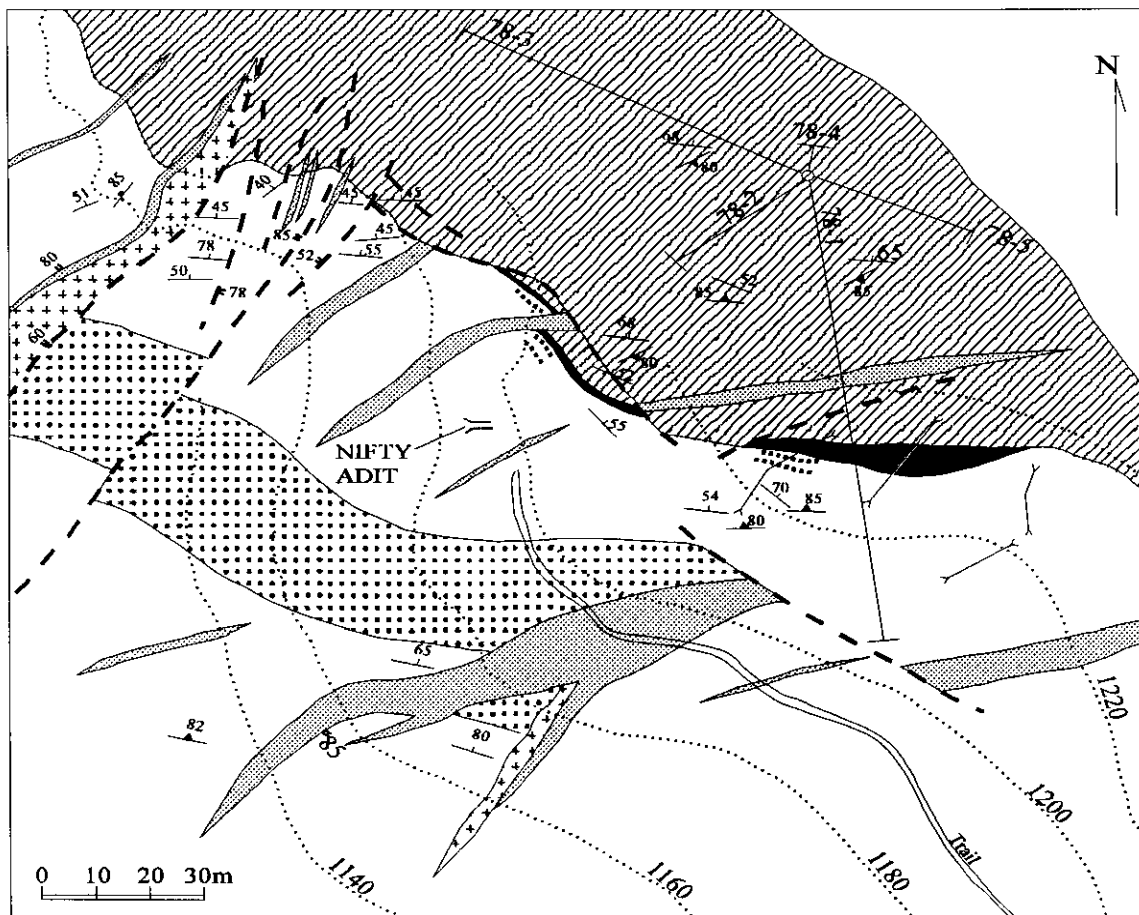
The geology of the Bella Coola area, adapted after Baer (1973) is presented in Figure 1. The area is underlain by varied packages of volcanic and lesser sedimentary rocks that generally form north to northwesterly trending pendants within intrusions of the Coast Plutonic Complex. The stratigraphic and structural relationships of these packages to one another are poorly understood and their ages range from Cenozoic to Triassic or older. The volcanic rocks are mostly of basaltic-andesitic composition but those hosting the Nifty prospect are distinct in containing some felsic lavas and tuffs (Figure 4). The sedimentary rocks include small, generally highly deformed units of black slate, argillite and greywackes. Some greywackes in the northeastern part of the Bella Coola mapsheet (Figure 1) contain fossils of middle Jurassic age (Tipper, 1963; Baer, 1973).

The roof pendant country rocks are intruded by, and in some instances thermally overprinted by, numerous plutons and small stocks of the Coast Plutonic Complex. These are largely of diorite-granodiorite composition and vary from massive rocks to intensely foliated orthogneisses. There is a westerly increase in both the regional metamorphic grade and structural deformation across the district. Consequently, in the southwestern part of the area (Figure 1), the country rocks and some of the older intrusions have been converted to schists and gneisses. North to north-westerly trending horizons of strongly foliated rock are interpreted to be ductile shear zones.

Our geological investigations and sampling were concentrated in four separate areas in the district. Most of the detailed work and sampling were conducted in and around the Nifty prospect (Figures 2 and 3) although some time was spent examining and sampling the rocks hosting both the Jamtart occurrence further west and the Keen Pb-Zn soil geochemical anomaly further south. In addition, some mafic volcanics and hornfelsed metasediments close to the Nusatsum pluton, south-west of Matterhorn Mountain (Figure 1) were also sampled. The analytical data for the rocks are presented in Table 1. Chemical plots indicate that the volcanic rocks adjacent to the Nusatsum pluton and those hosting the Jamtart and Keen properties are largely subalkaline, calcalkaline basalts and andesites that have a medium to high K<sub>2</sub>O content (Figure 4).

## GEOLOGY AND CHEMISTRY OF THE ROCKS HOSTING THE NIFTY PROSPECT

The geology of the Nifty area, compiled from the work of Bailes and McArthur (1978, 1979),



**Hangingwall rocks (commonly epidote-altered)**

-  Andesitic ash tuffs and tuffaceous sediments, commonly epidote-altered
-  Altered dacitic-andesitic ash tuffs, minor lapilli tuff and possible volcanic flows

**Footwall rocks (commonly silicified and pyritic)**

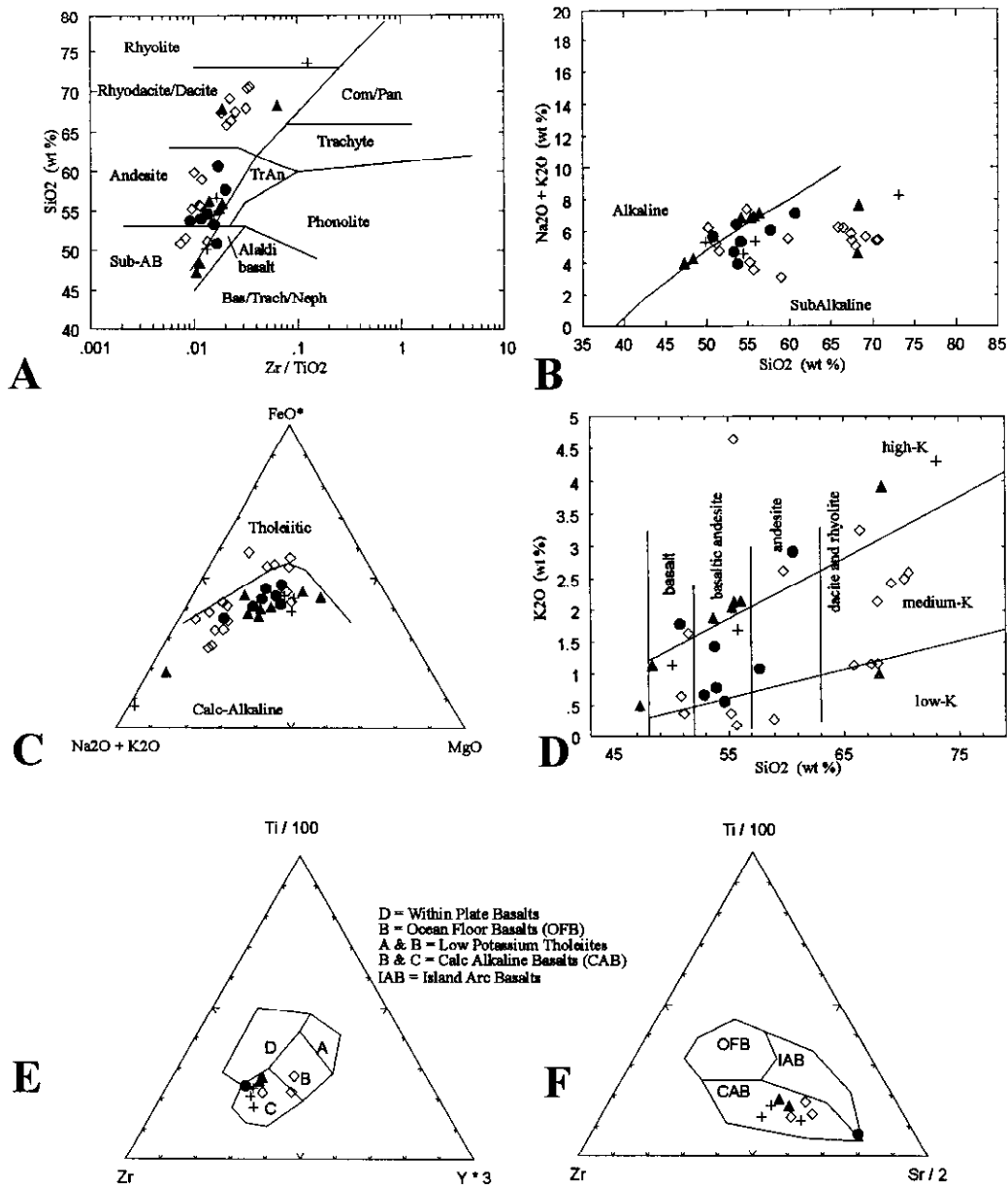
-  Barite, massive to bedded, commonly sheared
-  Altered dacitic tuffs with galena-sphalerite-barite mineralization
-  Altered dacitic-andesitic ash tuffs, minor lapilli tuff and possible volcanic flows
-  Altered dacitic-andesitic lapilli tuffs, minor ash tuff and possible volcanic flows

**Intrusive rocks**

-  Andesite dikes
-  Quartz porphyry dikes (c. 164 Ma)

-  52 Fault with dip
-  Geological contact
-  54 Strike and dip of bedding
-  85 Strike and dip of slaty cleavage
-  80 Dip of dike contact
-  Adit
-  Trench
-  Drillhole with drill number
-  Contour in metres

Figure 3. Geology of the Nifty prospect, Bella Coola. Adapted from the mapping of J.R. Woodcock (Bailes, 1977) and the authors. Note: distribution of the silicified and pyritic footwall rocks is shown in Figure 5.



- ◇ Volcanics & tuffs stratigraphically overlying the Nifty Prospect
- Volcanics & tuffs south of the Keen occurrence
- ▲ Volcanic rocks in the vicinity of the Jamtart occurrence
- + Hornfelsed volcanics adjacent to the Nasatsum pluton

Figure 4. Geochemical plots of some volcanic rocks in the Bella Coola district:  
 (A) SiO<sub>2</sub> versus log (Zr/TiO<sub>2</sub>) plot (after Winchester and Floyd, 1977).  
 (B) Alkali versus silica plot (after Irvine and Baragar 1971).  
 (C) Triangular Na<sub>2</sub>O + K<sub>2</sub>O - FeO - MgO plot (after Irvine and Baragar 1971).  
 (D) K<sub>2</sub>O versus SiO<sub>2</sub> plot (after Le Maitre, 1989).  
 (E) Triangular Zr - Ti/100 - Y x 3 plot (after Pearce and Cann, 1973).  
 (F) Triangular Zr - Ti/100 - Sr/2 plot (after Pearce and Cann, 1973).

TABLE 1  
MAJOR AND TRACE ELEMENT ANALYSES OF VOLCANIC ROCKS HOSTING THE JAMTART AND KEEN  
Pb-Zn OCCURRENCES AND INTRUDED BY THE NUSATSUM PLUTON, BELLA COOLA DISTRICT

| Volcanic rocks hosting the Jamtart occurrence. |         |         |         |         |         |          |         |         |  |  |  |  |
|------------------------------------------------|---------|---------|---------|---------|---------|----------|---------|---------|--|--|--|--|
|                                                | GR96-85 | GR96-88 | GR96-89 | GR96-90 | GR96-91 | GR96-91R | GR96-92 | GR96-93 |  |  |  |  |
| SiO <sub>2</sub>                               | 47.27   | 67.89   | 48.36   | 53.65   | 55.28   | 55.53    | 55.52   | 68.32   |  |  |  |  |
| Al <sub>2</sub> O <sub>3</sub>                 | 16.41   | 13.21   | 17.25   | 16.78   | 16.79   | 16.84    | 16.92   | 16.40   |  |  |  |  |
| MgO                                            | 7.58    | 1.94    | 5.61    | 4.27    | 3.46    | 3.41     | 3.40    | 0.49    |  |  |  |  |
| Na <sub>2</sub> O                              | 3.47    | 3.89    | 3.14    | 4.81    | 4.75    | 4.85     | 4.67    | 3.69    |  |  |  |  |
| MnO                                            | 0.16    | 0.19    | 0.16    | 0.13    | 0.14    | 0.15     | 0.14    | 0.06    |  |  |  |  |
| Fe <sub>2</sub> O <sub>3</sub>                 | 9.97    | 5.96    | 9.18    | 8.06    | 7.78    | 7.71     | 7.78    | 2.09    |  |  |  |  |
| TiO <sub>2</sub>                               | 1.22    | 0.70    | 1.22    | 0.91    | 0.93    | 0.94     | 0.92    | 0.29    |  |  |  |  |
| P <sub>2</sub> O <sub>5</sub>                  | 0.33    | 0.29    | 0.32    | 0.43    | 0.55    | 0.57     | 0.57    | 0.08    |  |  |  |  |
| CaO                                            | 8.63    | 1.77    | 8.54    | 5.13    | 4.82    | 4.84     | 4.98    | 3.16    |  |  |  |  |
| K <sub>2</sub> O                               | 0.50    | 1.07    | 1.13    | 1.88    | 2.05    | 2.06     | 2.14    | 3.92    |  |  |  |  |
| Cr <sub>2</sub> O <sub>3</sub>                 | 0.03    | 0.01    | 0.02    | 0.01    | 0.01    | 0.01     | 0.01    | 0.01    |  |  |  |  |
| LOI                                            | 4.03    | 2.85    | 4.96    | 3.72    | 3.02    | 2.91     | 2.76    | 1.20    |  |  |  |  |
| Total                                          | 99.60   | 99.77   | 99.89   | 99.78   | 99.58   | 99.82    | 99.81   | 99.71   |  |  |  |  |
| Ba                                             | 240     | 322     | 623     | 915     | 989     | 983      | 945     | 1302    |  |  |  |  |
| Y                                              | 23      | 38      | 24      | 23      | 31      | 27       | 29      | 17      |  |  |  |  |
| Sr                                             | 373     | 55      | 459     | 390     | 521     | 522      | 558     | 1688    |  |  |  |  |
| Zr                                             | 127     | 132     | 138     | 136     | 163     | 164      | 168     | 184     |  |  |  |  |
| Nb                                             | 12      | 13      | 12      | 13      | 13      | 15       | 13      | 17      |  |  |  |  |
| Ce                                             | 24      | 40      | 18      | 43      | 46      | 43       | 40      | 32      |  |  |  |  |
| V                                              | 194     | 53      | 203     | 177     | 167     | 173      | 161     | 34      |  |  |  |  |

| Volcanic rocks hosting the Keen soil geochemical anomaly. |        |        |        |        |        |         |         | Hornfelsed volcanic rocks adjacent to the Nasatsum Pluton. |         |         |         |          |
|-----------------------------------------------------------|--------|--------|--------|--------|--------|---------|---------|------------------------------------------------------------|---------|---------|---------|----------|
|                                                           | GR96-5 | GR96-6 | GR96-7 | GR96-8 | GR96-9 | GR96-12 | GR96-16 | GR96-94                                                    | GR96-97 | GR96-98 | GR96-99 | GR96-100 |
| SiO <sub>2</sub>                                          | 54.25  | 50.77  | 53.92  | 53.57  | 53.24  | 57.68   | 60.64   | 65.75                                                      | 54.46   | 50.08   | 55.86   | 73.11    |
| Al <sub>2</sub> O <sub>3</sub>                            | 17.96  | 19.79  | 18.56  | 17.40  | 19.54  | 17.44   | 16.12   | 15.65                                                      | 17.29   | 18.42   | 16.79   | 13.99    |
| MgO                                                       | 3.68   | 3.35   | 3.85   | 3.51   | 3.95   | 2.91    | 1.95    | 1.28                                                       | 4.92    | 4.76    | 5.47    | 0.14     |
| Na <sub>2</sub> O                                         | 3.55   | 3.88   | 4.35   | 5.12   | 3.98   | 4.94    | 4.19    | 3.94                                                       | 3.24    | 4.17    | 3.63    | 3.93     |
| MnO                                                       | 0.13   | 0.14   | 0.10   | 0.14   | 0.10   | 0.14    | 0.30    | 0.23                                                       | 0.11    | 0.28    | 0.18    | 0.04     |
| Fe <sub>2</sub> O <sub>3</sub>                            | 7.54   | 8.70   | 7.88   | 7.74   | 7.32   | 6.65    | 5.75    | 4.33                                                       | 8.00    | 8.82    | 7.56    | 0.76     |
| TiO <sub>2</sub>                                          | 0.71   | 0.67   | 0.77   | 0.68   | 0.71   | 0.58    | 0.65    | 0.54                                                       | 0.90    | 1.42    | 0.82    | 0.06     |
| P <sub>2</sub> O <sub>5</sub>                             | 0.31   | 0.32   | 0.34   | 0.29   | 0.33   | 0.29    | 0.21    | 0.18                                                       | 0.34    | 0.54    | 0.30    | 0.03     |
| CaO                                                       | 7.61   | 5.84   | 5.63   | 5.02   | 5.85   | 4.69    | 3.55    | 3.82                                                       | 7.48    | 6.92    | 6.29    | 1.46     |
| K <sub>2</sub> O                                          | 0.54   | 1.78   | 0.79   | 1.30   | 0.70   | 1.08    | 2.92    | 2.23                                                       | 1.30    | 1.14    | 1.69    | 4.30     |
| Cr <sub>2</sub> O <sub>3</sub>                            | 0.01   | 0.01   | 0.01   | 0.01   | 0.01   | 0.01    | 0.01    | 0.01                                                       | 0.02    | 0.02    | 0.01    | 0.01     |
| LOI                                                       | 3.17   | 4.38   | 3.64   | 5.19   | 3.72   | 3.22    | 2.51    | 1.57                                                       | 1.69    | 2.81    | 0.61    | 1.68     |
| Total                                                     | 99.46  | 99.63  | 99.84  | 99.97  | 99.45  | 99.63   | 98.80   | 99.53                                                      | 99.75   | 99.38   | 99.21   | 99.51    |
| Ba                                                        | 383    | 734    | 436    | 435    | 429    | 496     | 1653    | 980                                                        | 499     | 634     | 1100    | 869      |
| Y                                                         | 13     | 20     | 18     | 17     | 19     | 17      | 25      | 26                                                         | 22      | 30      | 27      | <5       |
| Sr                                                        | 886    | 1028   | 818    | 410    | 1032   | 914     | 252     | 351                                                        | 538     | 486     | 354     | 329      |
| Zr                                                        | 94     | 105    | 93     | 87     | 111    | 116     | 111     | 133                                                        | 140     | 188     | 157     | 75       |
| Nb                                                        | 11     | 11     | 8      | 10     | 10     | 13      | 13      | 13                                                         | 14      | 15      | 14      | 11       |
| Ce                                                        | 32     | 10     | 41     | 20     | 26     | 16      | 9       | 20                                                         | 30      | 21      | 23      | 7        |
| V                                                         | 138    | 177    | 142    | 125    | 147    | 117     | 122     | 61                                                         | 189     | 221     | 182     | <5       |

Analyses completed at the Cominco Research Laboratory, 1486 East Pender St., Vancouver, B.C. using steel mill grinding.

Major element oxides in percent; trace elements in ppm.

Fe<sub>2</sub>O<sub>3</sub> = total iron as Fe<sub>2</sub>O<sub>3</sub>

For analytical methods see Table 2.

1 = Fused Disc - X-ray fluorescence

2 = Pressed pellet - X-ray fluorescence

3 = LOI calculated after heating predried samples to 1100<sup>o</sup> for 4 hours.

Ba = Fused disc analysis for XRF calibration.

TABLE 1 CONTINUED

**Sample descriptions**Volcanic rocks in the vicinity of the Jamtart occurrence, west of the Noosegulch River and Nifty Prospect

|          |                                                                                 |
|----------|---------------------------------------------------------------------------------|
| GR96-85  | Grey, weakly layered, fine grained ash tuff with trace pyrite                   |
| GR96-88  | Green, silicious, fine grained vesicular lava flow or sill                      |
| GR96-89  | Dark green, fine grained vesicular lava flow or sill                            |
| GR96-90  | Grey, massive, fine grained volcanic rock. Minor epidote and pyrite             |
| GR96-91  | Grey, massive volcanic rock with feldspar phenocrysts. Minor epidote and pyrite |
| GR96-91R | Grey, massive volcanic rock with feldspar phenocrysts. Minor epidote and pyrite |
| GR96-92  | Grey, massive volcanic rock with feldspar phenocrysts. Minor epidote and pyrite |
| GR96-93  | Pale grey, fine grained, flow banded felsic volcanic                            |

Volcanic rocks south and southwest of the Keen soil geochemical anomaly, east of the Noosegulch River.

|         |                                                                                          |
|---------|------------------------------------------------------------------------------------------|
| GR96-5  | Dark green, massive volcanic with feldspar phenocrysts up to 4 mm. Minor epidote         |
| GR96-6  | Dark green, massive volcanic with minor lapilli fragments                                |
| GR96-7  | Dark green, massive volcanic with feldspar phenocrysts up to 4 mm. Minor epidote         |
| GR96-8  | Dark green, massive volcanic with feldspar phenocrysts up to 2 mm.                       |
| GR96-9  | Dark green, massive volcanic with feldspar and hornblende phenocrysts up to 4 mm.        |
| GR96-12 | Dark green, massive to weakly layered ash tuff with clasts and crystals up to 4 mm.      |
| GR96-16 | Pale grey-green, massive, fine grained volcanic. Trace pyrite.                           |
| GR96-94 | Silicified, pervasively altered volcanic with 1 to 3 percent finely disseminated pyrite. |

Hornfelsed volcanic rocks adjacent to the Nasatsum pluton, SE of Hagensborg

|          |                                                                             |
|----------|-----------------------------------------------------------------------------|
| GR96-97  | Dark, fine grained and massive, hornfelsed silicious meta-volcanic          |
| GR96-98  | Dark, fine grained and massive, hornfelsed silicious meta-volcanic          |
| GR96-99  | Dark, fine grained, massive, weakly hornfelsed, amygdaloidal mafic volcanic |
| GR96-100 | Pink, fine grained, felsic volcanic or sill                                 |

Blackwell (1985) and our own observations is illustrated in Figures 2 and 3. The area is underlain by a moderate to steep northerly dipping and east to northeast striking package of dust, ash and lapilli tuffs with subordinate amounts of volcanic flows, volcanic breccias and tuffaceous sediments. No sedimentary younging indicators have been recognized. However, based largely on the orientation of the interpreted footwall and hangingwall alteration at Nifty, the stratigraphy is believed to face northwards with no significant structural repetition.

A general stratigraphic succession is recognized. The lowest part of the succession occurs immediately south and south-west of the Nifty property. Due to the pervasive alteration related to the Nifty hydrothermal system, the original lithologies and composition of the rocks in the lower footwall sequence are uncertain. However, they are believed to include massive to well bedded lapilli, ash and dust tuffs of rhyodacite-dacite to basalt composition, as well as some rare, thin units of fine-grained, possibly silty or argillaceous sediments.

The lower sequence is overlain by a thin barite unit (Figure 3) which also forms a caprock to the mineralization. This in turn passes up to a 500 to 600 metre-thick hangingwall sequence of mafic tuffs with minor mafic flows and rare, thin units of rhyodacitic-dacitic flows, tuffs and volcanic breccias. At the base of this hangingwall package, the mafic tuffs tend to be well layered, epidote-altered rocks that are dark to medium green in colour. Further north however, and higher in the sequence, the mafic rocks include maroon colored units that are commonly more massive; this change suggests that they were deposited in an

emerging basin and that the environment altered from shallow submarine to subaerial and highly oxidized.

Most of the tuffs in the area are massive, but well preserved layering and sedimentary bedding are seen locally, particularly in the lower part of the sequence, in the immediate hanging and footwall rocks of the Nifty prospect. Tuffs form dark green to maroon colored rocks with angular to well-rounded clasts that are generally less than 10 centimetres in diameter. Coarser varieties of volcanic tuff breccia contain fragments exceeding 0.3 metres in size. The volcanic and tuffaceous clasts are generally matrix supported and vary from monomictic to polymictic. In the latter, clasts vary considerably in texture, colour and composition; grey, pink, red, green and black porphyritic and non porphyritic fragments are present. They are mainly massive to flow banded mafic volcanics and ash and lapilli tuffs with lesser amounts of leucocratic and felsic material of presumed rhyodacitic-dacitic composition. Where felsic clasts are abundant in the tuffs, broken quartz crystals are also common. Many of the massive and bedded mafic tuffs are characterized by epidote alteration.

The mafic volcanic flows are mostly massive and fine-grained. They locally contain random to well orientated feldspar phenocrysts up to 4 millimetres in length. Rarely, well rounded quartz phenocrysts up to 2 millimetres in length are present, and pervasive epidote alteration is a common feature. The felsic flows generally form thin (< 10 metres thick) units ranging from pink to grey to greenish brown in colour. They comprise fine grained siliceous rocks that vary from massive to flow banded and from equigranular to porphyritic; the latter varieties contain phenocrysts of feldspar as well as rounded crystals of quartz. Some

felsic volcanic units are characterized by deformed spherulites as well as hollow lithophysae up to 1 centimetres in diameter.

Pods, disrupted layers and cross-cutting veins of red jasper, up to 30 centimetres thick, occur locally throughout the volcanic sequence. They are most common approximately 500 metres north of the Nifty prospect (Figure 2) and are believed to represent distal products of exhalite activity. In rare instances, the jasper has replaced the original fine grained matrix in the coarser lapilli tuffs. The jasper contains minor amounts of disseminated coarse pyrite, white quartz, and veinlets of specular hematite; some veins are rimmed with epidote. However, assays show no anomalous quantities of metals in the jaspers.

Major and trace element analytical results on the less altered volcanic and tuffaceous rocks that overlie the Nifty prospect are presented in Table 2. Geochemical plots (Figure 4) suggest these rocks are bimodal; they include a calc-alkaline suite of rhyodacite-dacite composition as well as some tholeiitic basalts and andesites. Most of the Nifty volcanic rocks have a low to medium potassium content (Figure 4D), and tectonic discrimination plots indicate the mafic volcanics are calcalkaline basalts (Figs. 4E and F).

## MINERALIZATION AND GEOCHEMISTRY OF THE NIFTY PROSPECT

Three distinct zones of alteration are recognized at the Nifty property: (1) an upper stratabound barite cap, (2) an underlying zone containing sporadic amounts of pyrite, sphalerite, galena and barite, and (3) a lower extensive and discordant zone of pervasive silicification and fine-grained pyrite that is barren of economic mineralization. The uppermost capping unit consist predominantly of white, massive to sheared barite. It locally exceeds 10 metres in thickness and has a strike length of at least 130 metres (Figure 3). It is sharply overlain by a thick sequence of well layered, epidote-altered mafic ash tuffs.

The barite horizon is underlain by a zone of altered tuffs that contains some barite and sporadic veins, masses and disseminations of sulphides. This sulphide-bearing zone is less than 10 metres thick and is discontinuously traceable along strike for approximately 90 metres (Figure 3). Sulphides include abundant massive pyrite with lesser amounts of brown to black sphalerite and galena, and trace amounts of tetrahedrite-tennantite and some other Ag or Pb-bearing minerals, including polybasite ( $9Ag_2S.Sb_2S_3$ ).

The mineralized zone passes gradationally down into massive to well bedded lapilli, ash and dust tuffs that are believed to have originally been largely of rhyodacitic composition. These rocks are highly altered and are interpreted to represent a footwall alteration zone related to the hydrothermal feeder

system responsible for the overlying Nifty barite and Pb-Zn-Ag mineralization. The footwall alteration forms a discontinuous, rust-weathered, 120 by 220 metres zone, that extends south-west and west of the Nifty Zn-Pb-Ba showing (Figure 5). The rocks in this zone are intensely bleached, silicified and contain between 1 and 5 percent by volume finely disseminated pyrite.

To determine any vertical and lateral geochemical variations in the hydrothermal system, a number of lithochemical samples were collected on two traverse lines across the prospect. One line trended southwest and passed vertically down through the barite cap, the underlying mineralized zone and the footwall alteration; the other line was run in a northwest direction, subparallel to the topographic contours, and passed laterally through the barren footwall alteration zone. Figures 6A and B illustrate the vertical and lateral chemical changes in the Nifty host rocks noted from sampling these two lines. Assay results of selected grab samples from the capping barite unit, the Zn-Pb-Ba-bearing zone and the underlying siliceous-pyritic footwall zone are presented in Table 3. Gold and copper values are extremely low, but parts of the barite cap rocks and the underlying sphalerite-galena-bearing zone contain anomalous quantities of Ba, Zn, Pb, Ag, Cd, Sb, Sr, As and Hg. Increased values of  $K_2O$  in the sphalerite-galena zone and in parts of the underlying footwall mark areas of potassic-feldspar alteration. Generally, the extensive zone of silicified and pyritic footwall rocks is not enriched in economic base metals. However, higher  $Na_2O$  values at the top of the footwall zone suggests the sphalerite-galena mineralization is immediately underlain by a unit of possible albitic alteration (Figure 6A). The samples collected laterally across the footwall alteration show a progressive increase in  $MgO$  (up to 2 per cent) towards the north-western margin of the zone, suggesting a corresponding increase in chloritic alteration.

## STRUCTURE IN THE NIFTY PROSPECT AREA

One major episode of post-ore deformation is recognized, and the related small-scale asymmetric open to tight folds indicate that the Nifty area lies on a steeply-dipping, northern limb of a large anticline of unknown age. The small-scale folds have steeply dipping axial planes and, in some of the finer grained tuffaceous sedimentary rocks, a pronounced easterly trending fracture cleavage is developed (Figure 3). Bedding-cleavage intersection measurements indicate that the fold axes plunge 15 to 25 degrees in a east to south-east direction.

Several phases of brittle faulting are identified. One of the earliest phases strikes southeast and appears to have accompanied local shearing along the Nifty barite horizon. Several later phases strike northerly to east north-east. Moderately plunging slickenslides on a northerly trending fault situated approximately 600

TABLE 2  
MAJOR AND TRACE ELEMENT ANALYSES OF VOLCANIC ROCKS STRATIGRAPHICALLY  
OVERLYING THE NIFTY PROSPECT, BELLA COOLA DISTRICT

|                                | Sample | GR96-19 | GR96-20 | GR96-26 | GR96-52 | GR96-52R | GR96-53 | GR96-54 | GR96-57 | GR96-58 | GR96-59 |
|--------------------------------|--------|---------|---------|---------|---------|----------|---------|---------|---------|---------|---------|
|                                | Method |         |         |         |         |          |         |         |         |         |         |
| SiO <sub>2</sub>               | 1      | 50.86   | 51.51   | 51.10   | 70.64   | 70.40    | 67.36   | 67.47   | 55.53   | 55.22   | 55.68   |
| Al <sub>2</sub> O <sub>3</sub> | 1      | 16.89   | 18.57   | 16.60   | 14.77   | 14.67    | 15.40   | 15.34   | 21.73   | 17.02   | 16.24   |
| MgO                            | 1      | 5.58    | 2.65    | 5.36    | 1.19    | 1.27     | 1.28    | 1.48    | 1.44    | 2.75    | 3.48    |
| Na <sub>2</sub> O              | 1      | 5.29    | 3.08    | 4.84    | 2.83    | 2.84     | 4.65    | 4.23    | 2.45    | 3.67    | 3.38    |
| MnO                            | 1      | 0.18    | 0.31    | 0.15    | 0.07    | 0.07     | 0.09    | 0.09    | 0.08    | 0.22    | 0.21    |
| Fe <sub>2</sub> O <sub>3</sub> | 1      | 10.71   | 9.62    | 8.54    | 2.69    | 2.81     | 3.80    | 3.74    | 6.85    | 9.07    | 9.13    |
| TiO <sub>2</sub>               | 1      | 0.95    | 0.87    | 1.02    | 0.38    | 0.39     | 0.51    | 0.51    | 0.87    | 0.87    | 0.82    |
| P <sub>2</sub> O <sub>5</sub>  | 1      | 0.28    | 0.19    | 0.34    | 0.09    | 0.08     | 0.11    | 0.13    | 0.28    | 0.21    | 0.23    |
| CaO                            | 1      | 3.72    | 7.41    | 6.07    | 2.34    | 2.38     | 3.34    | 3.45    | 2.09    | 6.66    | 6.93    |
| K <sub>2</sub> O               | 1      | 0.65    | 1.64    | 0.37    | 2.60    | 2.55     | 1.16    | 1.17    | 4.65    | 0.37    | 0.19    |
| Cr <sub>2</sub> O <sub>3</sub> | 1      | 0.01    | 0.02    | 0.02    | 0.01    | 0.01     | 0.01    | 0.01    | 0.01    | 0.01    | 0.01    |
| LOI                            | 3      | 4.60    | 3.79    | 5.10    | 2.16    | 2.22     | 1.68    | 1.44    | 3.85    | 3.46    | 3.34    |
| Total                          |        | 99.72   | 99.66   | 99.51   | 99.77   | 99.69    | 99.39   | 99.06   | 99.83   | 99.53   | 99.64   |
| Ba                             | 1      | 343     | 742     | 497     | 779     | 772      | 413     | 463     | 967     | 305     | 271     |
| Y                              | 2      | 28      | 22      | 26      | 23      | 29       | 25      | 26      | 24      | 26      | 27      |
| Sr                             | 2      | 414     | 321     | 487     | 230     | 228      | 321     | 285     | 157     | 353     | 426     |
| Zr                             | 2      | 70      | 72      | 138     | 132     | 128      | 94      | 128     | 100     | 83      | 92      |
| Nb                             | 2      | 8       | 13      | 15      | 13      | 15       | 10      | 11      | 13      | 10      | 12      |
| Ce                             | 2      | 14      | 14      | 12      | 26      | 16       | 12      | 29      | <5      | 9       | 15      |
| V                              | 2      | 272     | 191     | 174     | 55      | 63       | 103     | 77      | 232     | 197     | 209     |

|                                |        | GR96-70 | GR96-71 | GR96-72 | GR96-73 | GR96-74 | GR96-103 |
|--------------------------------|--------|---------|---------|---------|---------|---------|----------|
|                                | Method |         |         |         |         |         |          |
| SiO <sub>2</sub>               | 1      | 66.44   | 65.86   | 59.82   | 67.92   | 58.94   | 69.14    |
| Al <sub>2</sub> O <sub>3</sub> | 1      | 14.74   | 15.36   | 16.29   | 15.07   | 15.08   | 13.85    |
| MgO                            | 1      | 0.52    | 1.53    | 1.55    | 1.46    | 3.16    | 0.76     |
| Na <sub>2</sub> O              | 1      | 2.93    | 5.09    | 2.91    | 2.93    | 2.82    | 3.21     |
| MnO                            | 1      | 0.08    | 0.12    | 0.12    | 0.12    | 0.19    | 0.08     |
| Fe <sub>2</sub> O <sub>3</sub> | 1      | 4.23    | 5.92    | 11.15   | 4.01    | 9.18    | 4.51     |
| TiO <sub>2</sub>               | 1      | 0.67    | 0.82    | 0.97    | 0.42    | 0.79    | 0.70     |
| P <sub>2</sub> O <sub>5</sub>  | 1      | 0.25    | 0.29    | 0.20    | 0.16    | 0.21    | 0.22     |
| CaO                            | 1      | 3.11    | 1.63    | 1.07    | 2.51    | 6.61    | 2.06     |
| K <sub>2</sub> O               | 1      | 3.25    | 1.14    | 2.62    | 2.14    | 0.28    | 2.43     |
| Cr <sub>2</sub> O <sub>3</sub> | 1      | 0.01    | 0.01    | 0.01    | 0.01    | 0.01    | 0.01     |
| LOI                            | 3      | 3.69    | 2.14    | 3.04    | 2.41    | 2.74    | 2.78     |
| Total                          |        | 99.92   | 99.91   | 99.75   | 99.16   | 100.01  | 99.75    |
| Ba                             | 1      | 524     | 365     | 596     | 864     | 141     | 568      |
| Y                              | 2      | 41      | 37      | 15      | 23      | 25      | 40       |
| Sr                             | 2      | 96      | 170     | 54      | 290     | 387     | 118      |
| Zr                             | 2      | 152     | 169     | 98      | 134     | 94      | 155      |
| Nb                             | 2      | 13      | 15      | 11      | 11      | 15      | 15       |
| Ce                             | 2      | 32      | 37      | <5      | 23      | 27      | 32       |
| V                              | 2      | 51      | 52      | 180     | 78      | 195     | 52       |

Analyses completed at the Cominco Research Laboratory, 1486 East Pender St., Vancouver, B.C. using steel mill grinding.

Major element oxides in percent; trace elements in ppm.

Fe<sub>2</sub>O<sub>3</sub> = total iron as Fe<sub>2</sub>O<sub>3</sub>

Methods

1 = Fused Disc - X-ray fluorescence

2 = Pressed pellet - X-ray fluorescence

3 = LOI calculated after heating predried samples to 1100° for 4 hours.

Ba = Fused disc analysis for XRF calibration.

TABLE 2 CONTINUED

**Sample descriptions**

|          |                                                                                                            |
|----------|------------------------------------------------------------------------------------------------------------|
| GR96-19  | Grey-green, massive, fine grained, equigranular volcanic                                                   |
| GR96-20  | Dark grey, massive volcanic with feldspar phenocrysts up to 3 mm.                                          |
| GR96-26  | Grey-green, weakly layered ash tuff with epidote veinlets                                                  |
| GR96-52  | Core sample of dark brown lapilli tuff.                                                                    |
| GR96-52R | Core sample of dark brown lapilli tuff.                                                                    |
| GR96-53  | Core sample of dark brown ash tuff.                                                                        |
| GR96-54  | Core sample of dark brown lapilli tuff.                                                                    |
| GR96-57  | Maroon coloured tuff with feldspathic lapilli and quartz fragments                                         |
| GR96-58  | Light grey to maroon coloured, massive, equigranular crystal tuff                                          |
| GR96-59  | Maroon coloured, fine grained and massive crystal tuff                                                     |
| GR96-70  | Pale grey to pink, fine grained, flow banded felsic volcanic with feldspar and quartz crystals up to 2 mm. |
| GR96-71  | Pale grey to pink, fine grained, flow banded felsic volcanic with spherulites up to 1 cm.                  |
| GR96-72  | Dark, fine grained, mafic crystal tuff                                                                     |
| GR96-73  | Grey, cherty dust tuff                                                                                     |
| GR96-74  | Pale grey, fine grained, flow banded volcanic                                                              |
| GR96-103 | Light grey, fine grained, flow banded felsic volcanic                                                      |

metres east of the Nifty prospect (Figure 2) indicate late dextral transverse movement. Some north-east trending faults are relatively old and have controlled the emplacement of the quartz porphyry and andesitic dikes, although post-intrusion reactivation of these fractures is commonly seen along the dike margins. Some north-east striking faults and dikes that cut the Nifty footwall rocks are believed to have followed precursor fractures that were conduits to the hydrothermal system.

Many of the late faults, particularly those along dike margins, are associated with sets of shallow and steeply dipping milky white quartz veins up to 10 centimetres thick. Irregular, sigmoidal tension gash veins are present, as well as regular, parallel vein sets spaced between 1 to 5 centimetres apart. They contain minor epidote and pink potassic feldspar but no sulphides were identified. An epidote-rich alteration halo is present around some veins. They occur both in the Nifty area and in the vicinity of the Keen soil geochemical anomaly approximately 6 kilometres further south.

## MICROPROBE ANALYSES OF THE NIFTY MINERALIZATION

Two samples of strongly altered and mineralized tuff (GR96-38 and GR96-95) containing sphalerite and galena in a gangue of quartz, pyrite, barite and feldspar were subjected to microprobe analysis, and the data are presented in Tables 4A to 4E. The sphalerite has low quantities of iron and cadmium (<1.5 weight per cent and <0.6 weight per cent, respectively), and the galena contains less than 0.17 per cent silver (Tables 4A and 4B). Some sphalerites contain exsolution blebs of chalcopyrite up to 30 microns in diameter. Rarely, galena is cut by microfractures containing various unidentified silver and/or lead-bearing minerals, some of which are believed to be late oxides and sulphates. Small, micron-sized grains of tetrahedrite-tennantite,

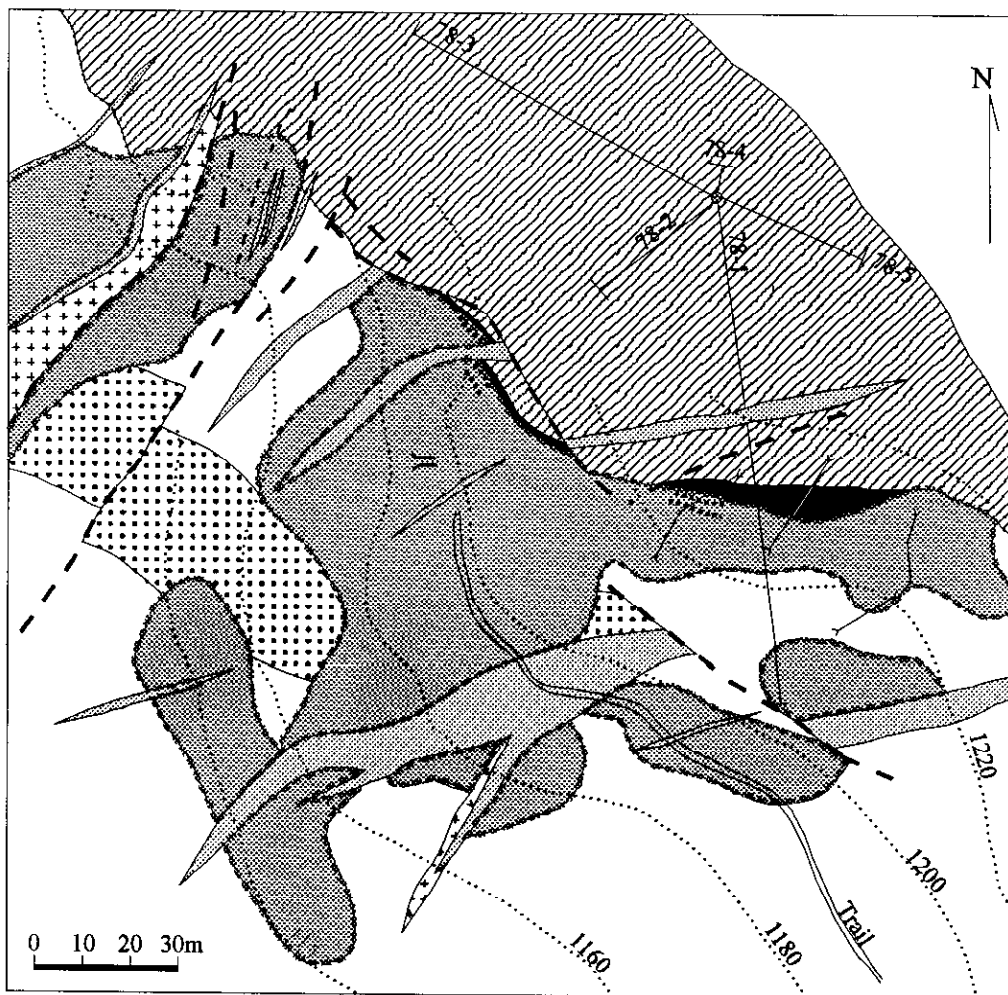
polybasite-pearcite ( $9Ag_2S.Sb_2S_3$ ) and some other unidentified minerals were also detected and analysed (Table 4C).

The barite crystals in the gangue contain up to 2.67 weight per cent SrO. One crystal containing 0.5 per cent PbO was detected, but in most of the barite analysed, the CaO and PbO values were extremely low or undetectable (Table 4D). The gangue also includes feldspars containing up to 16.6 weight per cent  $K_2O$  and 9.6 weight per cent BaO (Table 4E). Within individual feldspar crystals, the barium content exhibits extreme variations on a micron scale.

## U-Pb GEOCHRONOLOGY OF THE IGNEOUS ROCKS

Two felsic volcanic flows in the hangingwall sequence together with a post-ore quartz porphyry felsic dike at the Nifty prospect were sampled for U-Pb geochronology. Unfortunately, both samples of the felsic flows yielded insufficient zircons for dating. However, the 30 kilogram sample of quartz-feldspar porphyry dike yielded an abundant amount of good quality, clear, colourless, stubby prismatic zircon crystals. Mineral separation and U-Pb analytical techniques are described by Mortensen *et al.* (1995). All mineral separation and analytical work was carried out at the Geochronology Laboratory at the University of British Columbia.

U-Pb data are listed in Table 5 and plotted on Figure 7. Five of the strongly abraded zircon fractions are concordant or slight discordant, the latter having apparently lost a minor proportion of their radiogenic lead. Furthermore, the data suggests there are no older inherited zircon components within the analyses fractions. The weighted average  $^{207}Pb/^{206}Pb$  age of  $164.3 \pm 4.4$  Ma provides a good age estimate, but the overlap of concordant ellipses A and C with concordia provides the best age estimate at  $164.2 +1.2/-0.9$  Ma (Figure 7). These data indicate that the Nifty



**Post-ore intrusive rocks**

-  Andesite dikes
-  Quartz porphyry dikes

**Hangingwall rocks (commonly epidote-altered)**

-  Andesitic ash tuffs and tuffaceous sediments, commonly epidote-altered
-  Altered dacitic-andesitic ash tuffs, minor lapilli tuff and possible volcanic flows

**Footwall rocks (commonly silicified and pyritic)**

-  Barite, massive to bedded, commonly sheared
-  Altered dacitic tuffs with galena-sphalerite-barite mineralization
-  Altered dacitic-andesitic ash tuffs, minor lapilli tuff and possible volcanic flows
-  Altered dacitic-andesitic lapilli tuffs, minor ash tuff and possible volcanic flows

-  Fault
-  Geological contact
-  54 Strike and dip of bedding
-  85 Strike and dip of slaty cleavage
-  80 Dip of dike contact
-  Adit
-  Trench
-  Drillhole with drill number
-  Contour in metres
-  Silicification and pyritic alteration

Figure 5. Geology of the Nifty area showing distribution of the silicified and pyritic footwall rocks.

**TABLE 3**  
**MAJOR AND TRACE ELEMENT ANALYSES OF SELECTED MINERALIZED GRAB SAMPLES**  
**FROM THE NIFTY PROSPECT, BELLA COOLA DISTRICT**

|                                    |        | GR96-35 | GR96-36 | GR96-37 | GR96-38 | GR96-39 | GR96-40 | GR96-41 | GR96-42 | GR96-43 | GR96-44 | GR96-45 |
|------------------------------------|--------|---------|---------|---------|---------|---------|---------|---------|---------|---------|---------|---------|
|                                    | Method |         |         |         |         |         |         |         |         |         |         |         |
| SiO <sub>2</sub>                   | 1      | 13.05   | 52.15   | 18.85   | 45.88   | 77.86   | 75.97   | 70.71   | 67.93   | 73.74   | 74.94   | 78.44   |
| Al <sub>2</sub> O <sub>3</sub>     | 1      | 4.69    | 5.53    | 5.70    | 14.33   | 8.01    | 9.35    | 13.18   | 15.24   | 12.30   | 9.10    | 9.45    |
| MgO                                | 1      | 1.37    | 0.79    | 1.25    | 0.64    | 0.20    | 0.27    | 1.57    | 1.66    | 0.73    | 0.55    | 0.79    |
| Na <sub>2</sub> O                  | 1      | 4.21    | 1.57    | 3.48    | 1.10    | 0.41    | 0.39    | 3.33    | 3.43    | 0.69    | 0.16    | 0.27    |
| MnO                                | 1      | 0.01    | 0.03    | 0.02    | 0.05    | 0.02    | 0.01    | 0.13    | 0.09    | 0.02    | 0.04    | 0.03    |
| Fe <sub>2</sub> O <sub>3</sub>     | 1      | 0.63    | 0.98    | 3.06    | 7.51    | 1.04    | 1.15    | 5.05    | 3.69    | 2.63    | 3.30    | 1.95    |
| TiO <sub>2</sub>                   | 1      | 0.36    | 0.36    | 0.40    | 0.84    | 0.39    | 0.45    | 0.43    | 0.49    | 0.52    | 0.42    | 0.38    |
| P <sub>2</sub> O <sub>5</sub>      | 1      | 0.34    | 0.10    | 0.13    | 0.21    | 0.12    | 0.14    | 0.10    | 0.15    | 0.13    | 0.15    | 0.12    |
| CaO                                | 1      | 0.65    | 0.31    | 0.44    | 0.51    | 0.83    | 0.48    | 1.79    | 2.68    | 0.33    | 1.57    | 0.63    |
| K <sub>2</sub> O                   | 1      | 0.63    | 3.38    | 1.14    | 6.58    | 5.56    | 6.47    | 1.29    | 1.81    | 6.26    | 5.50    | 5.48    |
| LOI                                | 3      | 1.93    | 1.87    | 5.00    | 8.58    | 1.39    | 1.38    | 1.94    | 2.09    | 2.02    | 2.38    | 1.69    |
| Total                              |        | 27.87   | 67.07   | 39.47   | 86.23   | 95.83   | 96.06   | 99.52   | 99.26   | 99.37   | 98.11   | 99.23   |
| K <sub>2</sub> O/Na <sub>2</sub> O |        | 0.15    | 2.15    | 0.33    | 5.98    | 13.56   | 16.59   | 0.39    | 0.53    | 9.07    | 34.38   | 20.30   |
| Ba                                 | 1      | 391640  | 177348  | 336822  | 21196   | 13264   | 14037   | 950     | 634     | 3510    | 1744    | 1888    |
| Y                                  | 2      | <5      | <5      | <5      | <5      | 16      | 9       | 27      | 26      | 12      | 12      | 22      |
| Sr                                 | 2      | 6845    | 2708    | 5168    | 245     | 93      | 100     | 221     | 242     | 87      | 152     | 45      |
| Zr                                 | 2      | 97      | 70      | 92      | 73      | 57      | 60      | 137     | 137     | 93      | 75      | 126     |
| Nb                                 | 2      | 9       | 8       | 9       | 6       | 10      | 9       | 10      | 13      | 12      | 9       | 14      |
| Ce                                 | 2      | <5      | <5      | <5      | <5      | <5      | <5      | 19      | 13      | <5      | <5      | <5      |
| V                                  | 2      | 36      | <5      | <5      | 420     | 32      | 55      | 82      | 75      | 93      | 52      | 26      |
| Au (ppb)                           | 4      | <2      | 9       | 7       | <2      | 11      | 7       | <2      | <2      | 5       | 5       | <2      |
| As                                 | 4      | 54      | 87      | 300     | 350     | 59      | 59      | 13      | 22      | 25      | 12      | 11      |
| As                                 | 5      | 19      | 75      | 119     | 57      | 33      | 28      | <5      | NA      | 9       | <5      | <5      |
| Co                                 | 4      | 4       | 7       | 7       | 23      | 5       | 3       | 7       | 8       | 4       | 10      | 6       |
| Hg                                 | 4      | <1      | 5       | 2       | 15      | <1      | <1      | <1      | <1      | <1      | <1      | <1      |
| Mo                                 | 4      | 23      | 7       | 24      | 250     | 9       | <1      | <1      | <1      | 12      | 5       | 7       |
| Sb                                 | 4      | 39      | 34      | 54      | 90      | 10      | 9.8     | 2.4     | 5.2     | 2.6     | 2.3     | 1.1     |
| Sb                                 | 5      | 79      | 31      | 83      | 120     | 20      | 13      | <5      | NA      | 6       | <5      | <5      |
| Th                                 | 4      | 1.2     | <0.5    | <0.5    | <0.5    | 1.1     | 1.9     | 4       | 2.4     | 2.2     | 1.9     | 3.3     |
| W                                  | 4      | <1      | <1      | 27      | 15      | 7       | 13      | <1      | <1      | <1      | <1      | <1      |
| Cu                                 | 5      | 87      | 34      | 48      | 274     | 174     | 12      | 7       | NA      | 7       | 40      | 6       |
| Pb                                 | 5      | 1059    | 203     | 622     | 32404   | 10850   | 335     | 27      | NA      | 30      | 33      | 28      |
| Zn                                 | 5      | 22742   | 3342    | 6006    | 99999   | 8947    | 5726    | 121     | NA      | 36      | 1651    | 42      |
| Ag                                 | 5      | 132.2   | 26.6    | 176.7   | 181.9   | 10.4    | 3.5     | 0.25    | NA      | 0.25    | 0.25    | 0.25    |
| Cd                                 | 5      | 45.4    | 17.2    | 19.9    | 596.6   | 70.3    | 35.7    | 0.4     | NA      | <.4     | 7.4     | 0.4     |
| Zn/Zn+Pb                           |        | 0.96    | 0.94    | 0.91    | 0.76    | 0.45    | 0.94    | 0.82    | NA      | 0.55    | 0.98    | 0.60    |
| Zn/Pb                              |        | 21.47   | 16.46   | 9.66    | 3.09    | 0.82    | 17.09   | 4.48    | NA      | 1.20    | 50.03   | 1.50    |
| Pb/Ag                              |        | 8       | 8       | 4       | 178     | 1043    | 96      | 108     | NA      | 120     | 132     | 112     |

Analyses completed at the Cominco Research Laboratory, 1486 East Pender St., Vancouver, B.C. and Activation Labs., Ancaster, Ontario.  
 Major element oxides in percent; trace elements in ppm except Au in ppb. NA = element not analysed.  
 Fe<sub>2</sub>O<sub>3</sub> = total iron as Fe<sub>2</sub>O<sub>3</sub>

**Methods**

- 1 = Fused Disc - X-ray fluorescence
- 2 = Pressed pellet - X-ray fluorescence
- 3 = LOI calculated after heating predried samples to 11000 for 4 hours.
- 4 = Thermal neutron activation analysis
- 5 = ICP
- Ba = Fused disc analysis for XRF calibration.

**Sample descriptions**

- GR96-35 Massive barite from barite cap.
- GR96-36 Massive barite from barite cap.
- GR96-37 Massive barite from barite cap.
- GR96-38 Sphalerite-galena-barite mineralization
- GR96-39 Sphalerite-galena-barite mineralization
- GR96-40 Barite alteration with minor sphalerite
- GR96-41 Silicious, pyritic footwall dust-tuffs
- GR96-42 Silicious, pyritic footwall lapilli tuffs
- GR96-43 Bleached, pyritic footwall rocks
- GR96-44 Silicious, pyritic footwall tuffs
- GR96-45 Silicious, pyritic footwall tuffs

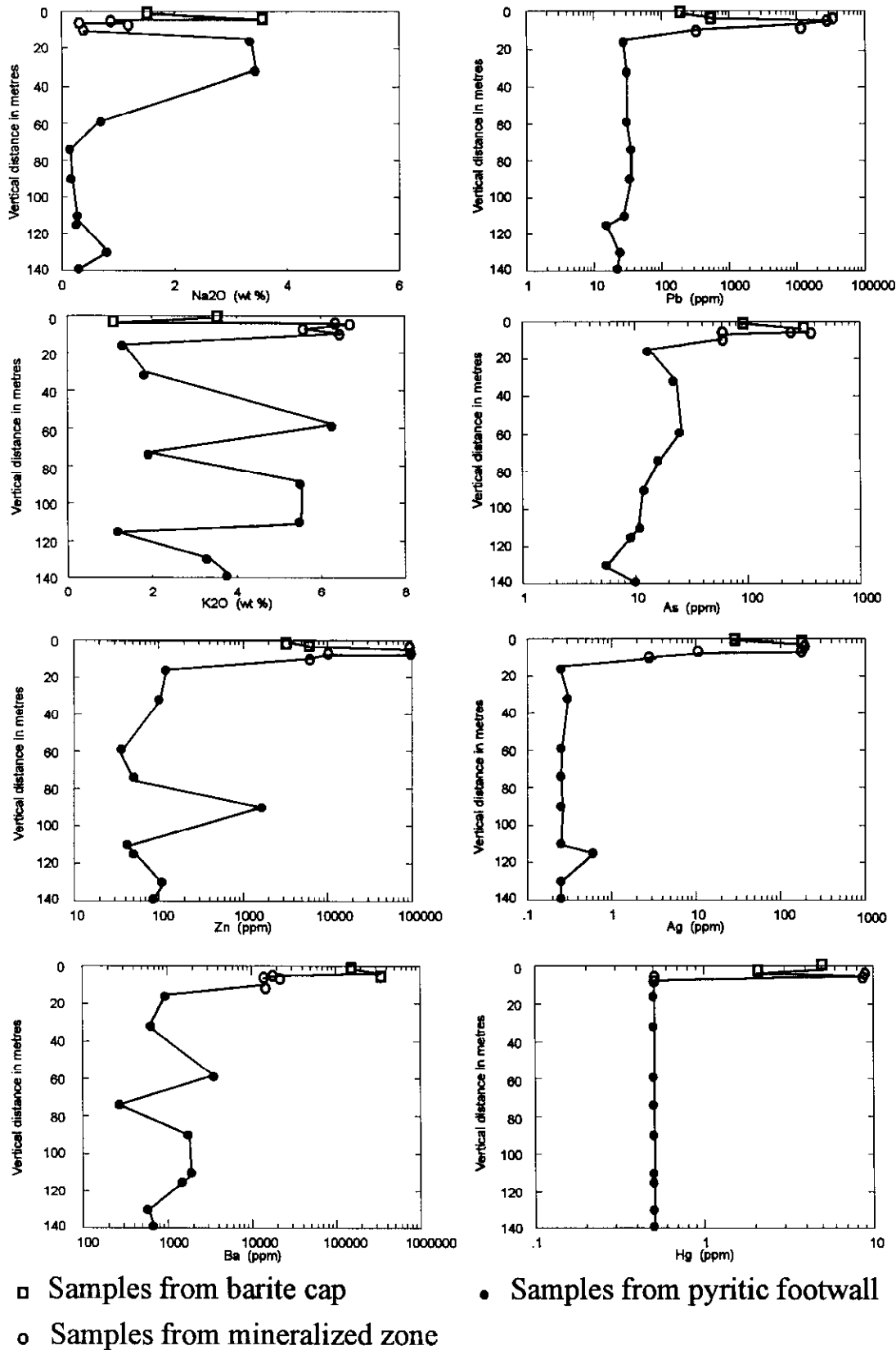


Figure 6. Chemical changes noted in the Nifty Prospect:  
 A. Vertical chemical variations from the barite cap down into the footwall alteration.

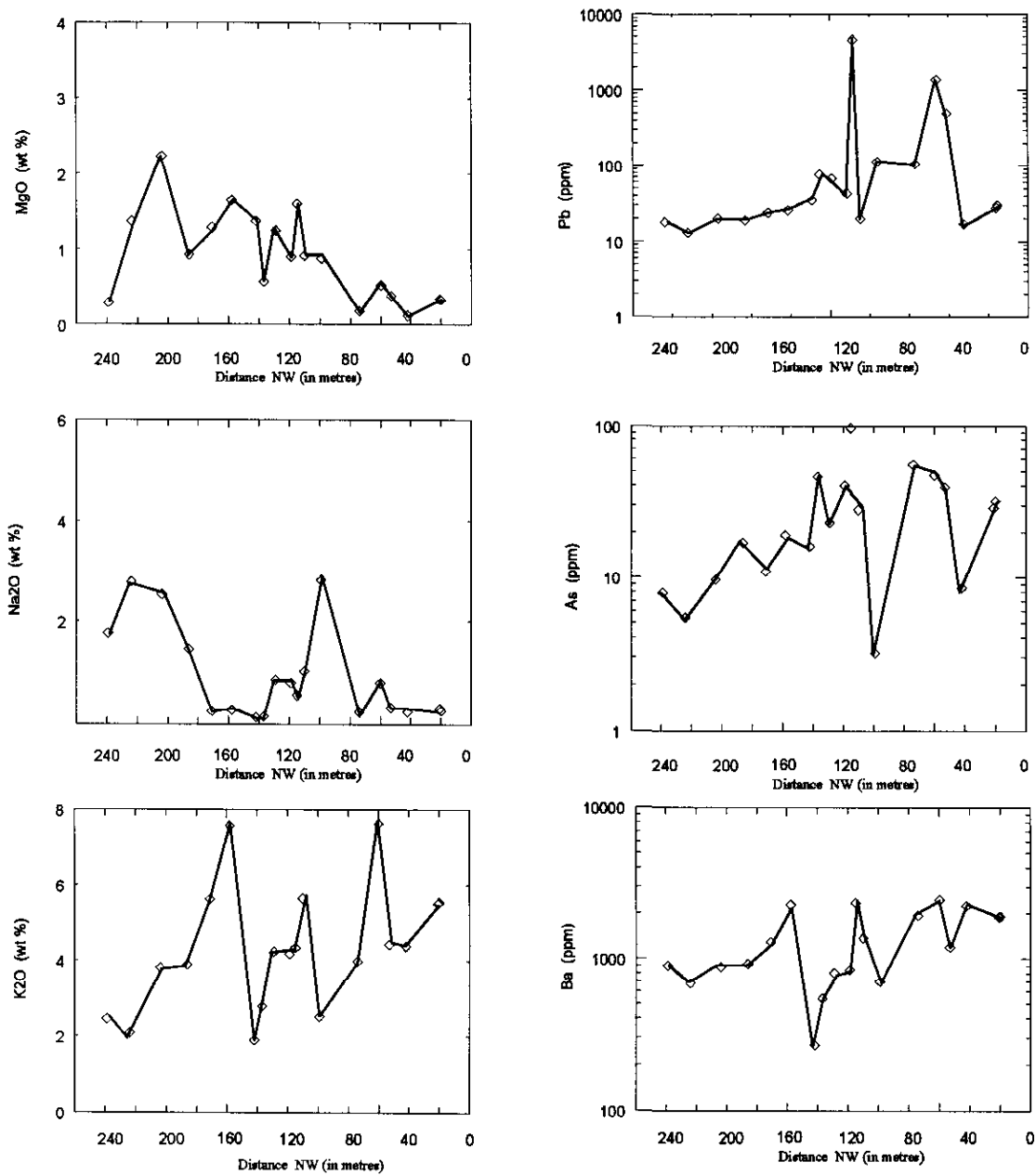


Figure 6. Chemical changes noted in the Nifty Prospect:  
 B. Lateral chemical variations through the footwall silicified and pyritic alteration zone.

TABLE 4A  
 REPRESENTATIVE MICROPROBE ANALYSES OF SPHALERITE AT THE  
 NIFTY PROSPECT, BELLA COOLA DISTRICT, B.C.

| Crystal Point Description | Sample GR96-38   |                  |                  |                   |                   | Sample GR96-95    |                   |                   |                   |                   |
|---------------------------|------------------|------------------|------------------|-------------------|-------------------|-------------------|-------------------|-------------------|-------------------|-------------------|
|                           | 401/056<br>605-1 | 338/040<br>605-4 | 324/033<br>605-5 | 408/342<br>605-11 | 468/082<br>605-13 | 407/037<br>605-14 | 417/368<br>605-16 | 426/246<br>605-19 | 420/068<br>605-24 | 420/068<br>605-25 |
|                           | 1                | 1                | 1                | 2                 | 3                 | 1                 | 1                 | 4                 | 5                 | 6                 |
| Zn                        | 67.00            | 66.48            | 66.56            | 64.97             | 65.32             | 66.58             | 66.08             | 64.90             | 63.35             | 65.43             |
| Cd                        | 0.33             | 0.35             | 0.28             | 0.40              | 0.33              | 0.27              | 0.61              | 0.46              | 0.44              | 0.59              |
| Fe                        | 0.10             | 0.13             | 0.18             | 0.48              | 0.88              | 0.14              | 0.19              | 0.93              | 1.43              | 0.44              |
| Mn                        | 0.00             | 0.00             | 0.03             | 0.02              | 0.03              | 0.02              | 0.03              | 0.00              | 0.02              | 0.01              |
| Ag                        | 0.00             | 0.00             | 0.00             | 0.00              | 0.00              | 0.02              | 0.00              | 0.00              | 0.09              | 0.03              |
| Sb                        | 0.00             | 0.00             | 0.00             | 0.04              | 0.00              | 0.04              | 0.03              | 0.01              | 0.06              | 0.04              |
| As                        | 0.02             | 0.01             | 0.00             | 0.00              | 0.00              | 0.00              | 0.05              | 0.00              | 0.00              | 0.04              |
| S                         | 32.86            | 32.81            | 32.78            | 33.00             | 32.92             | 32.37             | 32.85             | 32.52             | 32.63             | 33.27             |
| Total                     | 100.31           | 99.78            | 99.83            | 98.90             | 99.48             | 99.43             | 99.82             | 98.81             | 98.02             | 99.87             |

Data in weight percent.

Description:

- 1 = massive sphalerite
- 2 = 30 $\mu$  sphalerite grain.
- 3 = 60 $\mu$  sphalerite grain with pyrite inclusions.
- 4 = massive sphalerite with minute chalcopyrite inclusions.
- 5 = 100 $\mu$  sphalerite grain with minute chalcopyrite inclusions.
- 6 = 60 $\mu$  sphalerite grain.

TABLE 4B  
 REPRESENTATIVE MICROPROBE ANALYSES OF GALENA AT THE NIFTY PROSPECT,  
 BELLA COOLA DISTRICT, B.C.

| Crystal Point Description | Sample 96GR-38   |                  |                  |                  |                   | Sample 96GR-95    |                   |                   |                   |                  |
|---------------------------|------------------|------------------|------------------|------------------|-------------------|-------------------|-------------------|-------------------|-------------------|------------------|
|                           | 412/346<br>606-1 | 385/336<br>606-4 | 358/319<br>606-6 | 417/286<br>606-9 | 404/090<br>606-14 | 388/105<br>606-18 | 391/160<br>606-19 | 473/237<br>606-20 | 472/311<br>606-21 | 418/063<br>607-1 |
|                           | 1                | 2                | 3                | 4                | 5                 | 6                 | 2                 | 2                 | 7                 | 8                |
| As                        | 0.00             | 0.00             | 0.00             | 0.00             | 0.03              | 0.01              | 0.00              | 0.05              | 0.05              | 0.17             |
| Zn                        | 0.02             | 0.14             | 0.08             | 0.00             | 0.53              | 0.24              | 0.01              | 0.10              | 0.00              | 0.00             |
| Mn                        | 0.03             | 0.00             | 0.01             | 0.00             | 0.00              | 0.05              | 0.00              | 0.02              | 0.00              | 0.00             |
| S                         | 13.41            | 13.35            | 13.47            | 13.37            | 13.39             | 13.27             | 13.53             | 13.63             | 13.51             | 13.40            |
| Cu                        | 0.01             | 0.00             | 0.05             | 0.03             | 0.06              | 0.00              | 0.00              | 0.04              | 0.01              | 0.08             |
| Sb                        | 0.02             | 0.00             | 0.10             | 0.06             | 0.05              | 0.00              | 0.00              | 0.02              | 0.00              | 0.01             |
| Pb                        | 85.92            | 85.85            | 84.99            | 86.74            | 85.61             | 86.94             | 85.66             | 85.80             | 85.53             | 86.68            |
| Fe                        | 0.06             | 0.04             | 0.09             | 0.01             | 0.00              | 0.00              | 0.09              | 0.03              | 0.00              | 0.00             |
| Cd                        | 0.16             | 0.04             | 0.06             | 0.01             | 0.08              | 0.06              | 0.00              | 0.02              | 0.07              | 0.01             |
| Ag                        | 0.16             | 0.13             | 0.03             | 0.04             | 0.13              | 0.00              | 0.02              | 0.01              | 0.04              | 0.15             |
| Total                     | 99.79            | 99.56            | 98.88            | 100.26           | 99.88             | 100.57            | 99.31             | 99.72             | 99.21             | 100.49           |

Data in weight percent.

Description

- 1 = 20 $\mu$  grain
- 2 = 50 $\mu$  grain
- 3 = 15 $\mu$  grain
- 4 = 25 $\mu$  grain
- 5 = 150 $\mu$  grain
- 6 = 100 $\mu$  grain
- 7 = 200 $\mu$  grain
- 8 = massive galena

TABLE 4C  
 REPRESENTATIVE MICROPROBE ANALYSES OF Ag-BEARING SULPHIDES AT THE  
 NIFTY PROSPECT, BELLA COOLA DISTRICT, B.C.

| Point<br>Description | Sample<br>GR96-38 |       |       |       |        |        | Sample<br>GR96-95 |       |       |
|----------------------|-------------------|-------|-------|-------|--------|--------|-------------------|-------|-------|
|                      | 606-2             | 606-3 | 606-5 | 606-7 | 606-12 | 606-15 | 606-24            | 607-5 | 607-6 |
|                      | 1                 | 1     | 2     | 3     | 4      | 5      | 6                 | 7     | 7     |
| Cu                   | 35.65             | 34.28 | 32.44 | 35.27 | 0.28   | 8.47   | 17.66             | 3.05  | 2.73  |
| Fe                   | 0.81              | 0.69  | 0.73  | 0.67  | 0.23   | 0.13   | 1.30              | 0.03  | 0.06  |
| Ag                   | 6.44              | 6.96  | 5.69  | 6.49  | 64.79  | 59.48  | 10.14             | 65.12 | 64.96 |
| Zn                   | 6.98              | 6.79  | 6.64  | 7.06  | 0.16   | 0.04   | 3.55              | 0.07  | 0.06  |
| Mn                   | 0.01              | 0.00  | 0.00  | 0.00  | 0.01   | 0.01   | 0.00              | 0.00  | 0.03  |
| Pb                   | 0.00              | 0.00  | 0.00  | 0.00  | 15.29  | 4.61   | 29.17             | 1.98  | 0.88  |
| Cd                   | 0.20              | 0.24  | 0.17  | 0.26  | 4.93   | 0.08   | 0.78              | 0.04  | 0.19  |
| Sb                   | 11.34             | 12.32 | 11.12 | 11.80 | 0.70   | 3.21   | 14.48             | 11.07 | 12.52 |
| As                   | 12.89             | 11.96 | 11.95 | 12.74 | 3.12   | 4.84   | 2.97              | 0.88  | 0.65  |
| S                    | 25.11             | 25.41 | 24.11 | 25.38 | 11.88  | 15.73  | 18.93             | 15.93 | 16.46 |
| Total                | 99.43             | 98.64 | 92.84 | 99.66 | 101.40 | 96.60  | 98.98             | 98.17 | 98.53 |

Data in weight percent.

|                                               |                                                                                                                  |
|-----------------------------------------------|------------------------------------------------------------------------------------------------------------------|
| Description                                   | 4 = 2 $\mu$ grain of unknown mineral. Approx. (Ag,M) <sub>2</sub> S where M is a metal                           |
| 1 = 20 $\mu$ grain of tetrahedrite-tennantite | 5 = Polybasite-pearceite? Approx. 9Ag <sub>2</sub> S.Sb <sub>2</sub> S <sub>3</sub>                              |
| 2 = 10 $\mu$ grain of tetrahedrite-tennantite | 6 = Unknown mineral. Approx. (Cu,Fe) <sub>2</sub> (Pb,Ag,Zn,Cd) <sub>2</sub> (Sb,As) <sub>4</sub> S <sub>4</sub> |
| 3 = 15 $\mu$ grain of tetrahedrite-tennantite | 7 = Unknown mineral. Approx. (Ag,Cu)(Sb,S)                                                                       |

TABLE 4D  
 REPRESENTATIVE MICROPROBE ANALYSES OF BARITE GANGUE,  
 THE NIFTY PROSPECT, BELLA COOLA DISTRICT, B.C.

| Crystal<br>Point | Sample<br>GR96-38 |          |          |          | Sample<br>GR96-95 |           |           |           |           |
|------------------|-------------------|----------|----------|----------|-------------------|-----------|-----------|-----------|-----------|
|                  | 468/225           | 469/223  | 478/225  | 467/224  | 401/230           | 394/197   | 399/195   | 424/295   | 425/122   |
|                  | 97-608-1          | 97-608-4 | 97-608-5 | 97-608-7 | 97-608-9          | 97-608-10 | 97-608-11 | 97-608-12 | 97-608-15 |
| BaO              | 62.68             | 62.70    | 61.64    | 62.15    | 63.76             | 64.18     | 64.71     | 64.05     | 63.53     |
| SrO              | 1.95              | 1.96     | 2.44     | 2.67     | 1.31              | 1.23      | 1.18      | 1.33      | 1.14      |
| CaO              | 0.11              | 0.00     | 0.02     | 0.03     | 0.00              | 0.02      | 0.00      | 0.01      | 0.01      |
| PbO              | 0.00              | 0.00     | 0.00     | 0.00     | 0.00              | 0.00      | 0.00      | 0.00      | 0.53      |
| SO <sub>3</sub>  | 34.19             | 34.49    | 34.41    | 33.84    | 34.54             | 34.21     | 34.84     | 34.76     | 34.81     |
| Total            | 98.94             | 99.14    | 98.51    | 98.68    | 99.60             | 99.63     | 100.73    | 100.15    | 100.03    |

Data in weight percent

TABLE 4E  
 REPRESENTATIVE MICROPROBE ANALYSES OF FELDSPAR GANGUE  
 THE NIFTY PROSPECT, BELLA COOLA DISTRICT, B.C.

| Crystal Pt.                    | Sample GR96-38 |         |         |         |         |         | Sample 96GR-95 |         |         |         |         |         |
|--------------------------------|----------------|---------|---------|---------|---------|---------|----------------|---------|---------|---------|---------|---------|
|                                | 410/074        | 415/125 | 416/175 | 440/200 | 443/236 | 428/257 | 411/144        | 413/106 | 418/084 | 419/267 | 418/270 | 454/245 |
|                                | 11             | 13      | 14      | 15      | 17      | 18      | 2              | 4       | 5       | 8       | 9       | 10      |
| Na <sub>2</sub> O              | 0.19           | 0.20    | 0.21    | 0.29    | 0.25    | 0.30    | 0.22           | 0.26    | 0.27    | 0.28    | 0.29    | 0.23    |
| K <sub>2</sub> O               | 16.59          | 15.60   | 12.34   | 14.24   | 15.59   | 12.16   | 14.47          | 12.77   | 12.48   | 14.07   | 13.52   | 16.39   |
| Fe <sub>2</sub> O <sub>3</sub> | 0.05           | 0.14    | 0.04    | 0.03    | 0.05    | 0.26    | 0.02           | 0.03    | 0.05    | 0.01    | 0.03    | 0.04    |
| BaO                            | 0.09           | 0.99    | 1.34    | 4.41    | 1.46    | 9.59    | 3.90           | 8.00    | 8.74    | 5.57    | 6.83    | 0.08    |
| CaO                            | 0.00           | 0.00    | 0.00    | 0.00    | 0.01    | 0.05    | 0.00           | 0.00    | 0.00    | 0.01    | 0.01    | 0.00    |
| Al <sub>2</sub> O <sub>3</sub> | 18.71          | 18.73   | 13.99   | 19.82   | 18.43   | 21.45   | 19.33          | 20.51   | 20.01   | 20.10   | 20.19   | 18.24   |
| SiO <sub>2</sub>               | 64.53          | 64.64   | 72.01   | 60.21   | 64.17   | 57.65   | 63.53          | 59.67   | 56.68   | 60.14   | 58.34   | 64.90   |
| Total                          | 100.16         | 100.30  | 99.94   | 99.00   | 99.97   | 101.46  | 101.47         | 101.24  | 98.24   | 100.18  | 99.22   | 99.88   |

Data in weight percent

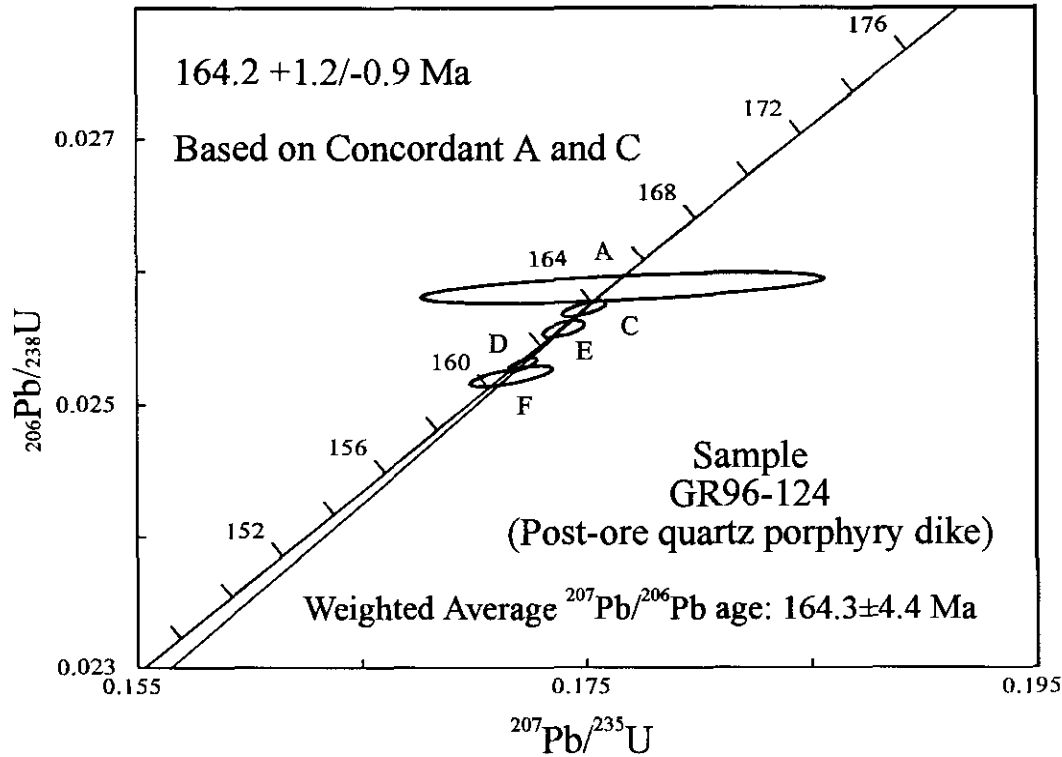


Figure 7. Concordia diagram for a quartz porphyry dike at the Nifty prospect.

TABLE 5  
U-Pb ANALYTICAL DATA OF QUARTZ PORPHYRY DIKE,  
NIFTY PROSPECT, BELLA COOLA DISTRICT

| Fraction <sup>1</sup> | Wt<br>mg | U <sup>2</sup><br>ppm | Pb <sup>3</sup><br>ppm | <sup>206</sup> Pb <sup>4</sup><br><sup>204</sup> Pb | Pb <sup>5</sup><br>pg | <sup>208</sup> Pb <sup>6</sup><br>% | Isotopic ratios (1s,%) <sup>7</sup> |                                     |                                      | Apparent ages (2s, Ma) <sup>7</sup> |                                      |
|-----------------------|----------|-----------------------|------------------------|-----------------------------------------------------|-----------------------|-------------------------------------|-------------------------------------|-------------------------------------|--------------------------------------|-------------------------------------|--------------------------------------|
|                       |          |                       |                        |                                                     |                       |                                     | <sup>206</sup> Pb/ <sup>238</sup> U | <sup>207</sup> Pb/ <sup>235</sup> U | <sup>207</sup> Pb/ <sup>206</sup> Pb | <sup>206</sup> Pb/ <sup>238</sup> U | <sup>207</sup> Pb/ <sup>206</sup> Pb |
| A c,N5,p,s            | 0.005    | 112                   | 3.0                    | 131                                                 | 8                     | 13.9                                | 0.02588 (0.22)                      | 0.1766 (2.5)                        | 0.04951 (2.4)                        | 164.7 (0.7)                         | 172 (113)                            |
| C c,N5,p,s            | 0.063    | 194                   | 5.2                    | 1129                                                | 18                    | 13.0                                | 0.02572 (0.11)                      | 0.1749 (0.29)                       | 0.04933 (0.22)                       | 163.7 (0.4)                         | 163 (10)                             |
| D m,N5,p              | 0.080    | 332                   | 8.8                    | 3581                                                | 12                    | 14.2                                | 0.02531 (0.10)                      | 0.1722 (0.19)                       | 0.04934 (0.13)                       | 161.1 (0.3)                         | 164.2 (6.0)                          |
| E m,N5,p,s            | 0.020    | 336                   | 9.1                    | 2135                                                | 5                     | 14.6                                | 0.02557 (0.12)                      | 0.1740 (0.27)                       | 0.04936 (0.22)                       | 162.8 (0.4)                         | 165 (10)                             |
| F m,N5,p,s            | 0.030    | 239                   | 6.3                    | 381                                                 | 31                    | 13.7                                | 0.02522 (0.16)                      | 0.1717 (0.54)                       | 0.04938 (0.44)                       | 160.6 (0.5)                         | 166 (21)                             |

Description and location of sample No. GR96-124: Fine grained felsic dike, approximately 2m thick, containing phenocrysts of feldspar and rounded, glassy quartz up 4 mm in diameter. Dike intrudes hangingwall andesitic tuffs and volcanics approximately 100 m east-northeast of the Nifty Prospect at UTM 675150E; 5828850N.

Notes: Analytical techniques are listed in Mortensen et al. (1995).

<sup>1</sup> Upper case letter = fraction identifier; All zircon fractions air abraded; Grain size, intermediate dimension: cc=>134mm, c=>134 mm and >104mm, m=<104mm and >74mm, f=<74mm; Magnetic codes: Franz magnetic separator sideslope at which grains are nonmagnetic (N) or Magnetic (M); e.g., N1=nonmagnetic at 1°; Field strength for all fractions =1.8A; Front slope for all fractions=20°; Grain character codes: p=prismatic, s=stubby.

<sup>2</sup> U blank correction of 1pg ± 20%; U fractionation corrections were measured for each run with a double <sup>233</sup>U-<sup>235</sup>U spike (about 0.004/amu).

<sup>3</sup>Radiogenic Pb

<sup>4</sup>Measured ratio corrected for spike and Pb fractionation of 0.0035/amu ± 20% (Daly collector) and 0.0012/amu ± 7% and laboratory blank Pb of 3-5pg ± 20%. Laboratory blank Pb concentrations and isotopic compositions based on total procedural blanks analysed throughout the duration of this study.

<sup>5</sup>Total common Pb in analysis based on blank isotopic composition

<sup>6</sup>Radiogenic Pb

<sup>7</sup>Corrected for blank Pb, U and common Pb. Common Pb corrections based on Stacey Kramers model (Stacey and Kramers, 1975) at the age of the rock or the <sup>207</sup>Pb/<sup>206</sup>Pb age of the fraction.

mineralization and its hostrocks are pre-164 Ma (Middle Jurassic) in age.

## INTRUSIVE ROCKS

Four suites of intrusive rocks in the district were examined and geochemically sampled. Two of these represent minor intrusions comprising post-ore dikes of quartz porphyry and andesite which are well developed around the Nifty prospect (Figure 2). The other two suites occur as larger plutons, one of which is informally named the Tseapseahoolz Creek pluton (Figure 1) and hosts the Malachite Cliff Cu occurrence. The other, informally named Nusatsum pluton, intrudes a package of mafic calc-alkaline basalts (Figure 4) and minor metasediments that outcrop south of the Bella Coola River (Figure 1) but is not associated with any known mineral occurrences.

## MINOR INTRUSIONS

The volcanic and volcanoclastic package hosting the Nifty prospect are cut by two contrasting suites of minor intrusions, both of which post-date the mineralization and hydrothermal alteration. The oldest suite is a pale grey weathering quartz ± feldspar porphyry that forms dike swarms and isolated bodies generally less than 25 metres thick (Figures 2 and 3); U-Pb dating on zircons reveals the suite to be Middle Jurassic in age. These leucocratic, fine to medium grained rocks are characterized by euhedral to subhedral phenocrysts of feldspar and rounded crystals of glassy quartz up to 5 millimetres in width; quartz crystals are more common in the central portions of the dikes. Most of these rocks are massive but a thin-layered flow foliation is seen in some dikes, and angular xenoliths of country rock are present locally. Fine grained, chilled margins are seen on the edges of

some dikes, and many bodies are cut by tension gash veins of milky quartz. The country rocks immediately adjacent to some quartz porphyry dikes are silicified.

Analytical results of unaltered samples of quartz porphyry are presented in Table 6. This suite is subalkaline and calcalkaline and the rocks are peraluminous granodiorites (Figure 8A, B, C and D). Trace element plots (Figure 8E and F) show that the quartz porphyry dikes represent "volcanic arc" intrusions as defined by Pearce *et al.* (1984).

Younger mafic dikes, up to 15 metres in width, are also extremely common and widespread on the Nifty claims (Figures 2 and 3); in many cases these intrusions have been controlled by, and have followed, the margins of the older quartz porphyry dikes. They are dark grey to green coloured, massive to well flow banded and fine to medium-grained rocks that vary from equigranular to porphyritic; the latter contain plagioclase phenocrysts up to 4 millimetres long. Some dikes also have spherical to elongate vesicles up to 1 centimetres in length. Where feldspar phenocrysts and vesicles are present in the same dike, it is common for the vesicles to be more abundant in the centre of the body while the phenocrysts tend to be better developed closer to the dike margins. Many dikes are cut by veins of milky quartz similar to those cutting the quartz porphyry dikes or younger veins of epidote. These rocks are subalkaline, calcalkaline and metaluminous (Table 6; Figure 8A, B and D). Most range in composition from gabbro to quartz diorite and tonalite and trace element plots show them to be "volcanic arc" intrusions as defined by Pearce *et al.* (1984) (Figure 8C, E and F).

## MAJOR INTRUSIONS

### *TSEAPSEAHOOZ CREEK PLUTON* (Unit 4 of Baer, 1973)

This body lies about 10 kilometres north-east of Hagensborg and is exposed in the southern part of Tseapseahoolz Creek valley and on the slopes of Salloom Peak (Figure 1). It forms an elongate, north-west trending pluton that includes rocks described by Baer (1973) as "foliated, chloritized quartz diorite" with lesser amounts of granodiorite and diorite. Our work establishes that the north-eastern margin of the pluton west of Noosegulch River extends considerably further northwards than is shown by Baer (1973); in this area it hosts the Malachite Cliff Cu occurrence (Figure 1).

In exposures along logging roads up the east side of Tseapseahoolz Creek the rocks in the pluton are generally coarse grained, massive and highly epidotized. They vary from a biotite-bearing granodiorite with less than 5 percent mafic minerals to a dark colored diorite-quartz diorite with more than 20 percent biotite and amphibole. Some rocks in this area are cut by pink veins of coarse grained potassium

feldspar and quartz, as well as late, narrow dike of fine grained andesite.

Three lithochemical samples were collected from the east side of Tseapseahoolz Creek; plots indicate these rocks are subalkaline and calcalkaline (Table 6; Figure 8A and B). Two of the leucocratic, biotite-bearing samples have a granodiorite composition and are peraluminous whereas a more mafic, hornblende-bearing sample is a metaluminous quartz diorite (Figure 8C and D). Trace element plots show all samples fall within the "volcanic arc" field as defined by Pearce *et al.* (1984) (Figure 8E and F).

### *NUSATSUM PLUTON (Unit 13 of Baer, 1973)*

This northerly trending, elongate body, which Baer (1973) believed to be of Eocene or Palaeocene age, lies about 20 kilometres south-south-east of Hagensborg and 7 kilometres south-west of Matterhorn Mountain (Figure 1). The central parts of the body comprise massive, coarse grained and equigranular biotite-hornblende-bearing rocks containing 5 to 8 percent mafic minerals. These rocks are subalkaline, calcalkaline, peraluminous granodiorites (Table 6; Figure 8A, B, C and D) that are volcanic arc-related (Figure 8E and F), similar to the other intrusions sampled in the district.

The marginal rocks in the Nusatsum pluton are considerably more mafic than those in the main body; they contain up to 20 percent hornblende and biotite, and are believed to be of diorite-quartz diorite composition. The mafic volcanic and metasedimentary country rocks adjacent to the pluton have been converted to a biotite hornfels that locally contains fine disseminated pyrite and some rare garnet. The thermal aureole contains irregular dikes of mafic diorite that probably originated from the adjacent pluton.

## GEOLOGY OF THE MALACHITE CLIFF OCCURRENCE

Whilst flying by helicopter, the senior author noted malachite staining on some cliffs high on the western slopes of the Noosegulch River valley. The cliffs are located at an elevation of 3500 feet at UTM 5816950N; 677070E (Figure 1). This copper occurrence, which was previously unreported, has been named the "Malachite Cliff" occurrence. A field traverse down to the occurrence from the overlying ridge-top passed over massive, coarse grained pinkish grey, leucocratic and equigranular granodiorites of the Tseapseahoolz Creek pluton. These rocks are generally unaltered and contain between 4 and 6 percent mafic minerals comprising coarse biotite with minor hornblende. In the vicinity of the occurrence, the pluton locally contains abundant xenoliths and large screens of hornfelsed metasediments and greenstone. The pluton is also cut by numerous dikes of fine-

TABLE 6  
MAJOR AND TRACE ELEMENT ANALYSES OF INTRUSIVE ROCKS,  
BELLA COOLA DISTRICT

| Andesite dikes at the Nifty Prospect |         |         |         |         |         |         |         |         |         |         |         |
|--------------------------------------|---------|---------|---------|---------|---------|---------|---------|---------|---------|---------|---------|
|                                      | GR96-28 | GR96-34 | GR96-46 | GR96-50 | GR96-51 | GR96-55 | GR96-56 | GR96-66 | GR96-67 | GR96-68 | GR96-69 |
| SiO <sub>2</sub>                     | 52.45   | 56.89   | 63.34   | 53.84   | 53.97   | 55.00   | 54.65   | 50.59   | 51.73   | 55.82   | 57.66   |
| Al <sub>2</sub> O <sub>3</sub>       | 15.75   | 14.87   | 15.40   | 16.73   | 16.85   | 14.17   | 16.17   | 17.89   | 17.18   | 14.29   | 14.76   |
| MgO                                  | 3.65    | 3.45    | 2.13    | 4.60    | 4.54    | 2.87    | 4.23    | 4.31    | 4.88    | 2.89    | 3.15    |
| Na <sub>2</sub> O                    | 3.43    | 4.32    | 3.51    | 3.64    | 2.49    | 3.00    | 2.41    | 3.56    | 5.73    | 4.21    | 4.40    |
| MnO                                  | 0.19    | 0.18    | 0.13    | 0.17    | 0.15    | 0.21    | 0.14    | 0.16    | 0.18    | 0.19    | 0.18    |
| Fe <sub>2</sub> O <sub>3</sub>       | 9.13    | 9.72    | 6.97    | 8.22    | 8.47    | 9.29    | 8.00    | 9.78    | 9.99    | 9.50    | 9.57    |
| TiO <sub>2</sub>                     | 1.35    | 1.03    | 0.68    | 0.73    | 0.73    | 1.00    | 0.70    | 0.90    | 0.86    | 1.01    | 1.04    |
| P <sub>2</sub> O <sub>5</sub>        | 0.48    | 0.29    | 0.20    | 0.28    | 0.27    | 0.27    | 0.25    | 0.17    | 0.24    | 0.27    | 0.29    |
| CaO                                  | 5.99    | 4.07    | 2.56    | 5.30    | 6.28    | 5.98    | 7.42    | 7.27    | 5.33    | 5.49    | 4.08    |
| K <sub>2</sub> O                     | 1.23    | 0.70    | 1.77    | 1.54    | 2.11    | 1.16    | 1.78    | 1.16    | 0.50    | 0.45    | 0.29    |
| Cr <sub>2</sub> O <sub>3</sub>       | 0.01    | 0.01    | 0.01    | 0.01    | 0.01    | 0.01    | 0.01    | 0.01    | 0.01    | 0.01    | 0.01    |
| LOI                                  | 5.59    | 4.07    | 3.15    | 4.12    | 3.35    | 6.78    | 3.64    | 3.83    | 2.94    | 5.49    | 4.42    |
| Total                                | 99.25   | 99.60   | 99.85   | 99.18   | 99.22   | 99.74   | 99.40   | 99.63   | 99.57   | 99.62   | 99.85   |
| Ba                                   | 1569    | 891     | 532     | 757     | 865     | 380     | 622     | 750     | 486     | 1002    | 298     |
| Y                                    | 32      | 22      | 24      | 21      | 19      | 27      | 20      | 23      | 20      | 26      | 26      |
| Sr                                   | 379     | 243     | 175     | 566     | 536     | 193     | 546     | 569     | 465     | 382     | 389     |
| Zr                                   | 143     | 90      | 89      | 88      | 88      | 85      | 87      | 72      | 72      | 91      | 94      |
| Nb                                   | 16      | 11      | 12      | 12      | 12      | 11      | 12      | 9       | 13      | 9       | 11      |
| Ce                                   | <5      | <5      | 21      | 18      | 12      | 35      | 8       | <5      | 5       | <5      | 12      |
| V                                    | 250     | 241     | 126     | 178     | 187     | 206     | 148     | 235     | 249     | 191     | 211     |
| Rb                                   | 7.5     | 7.5     | 40      | 7.5     | 55      | 31      | 38      | 7.5     | 7.5     | 7.5     | 7.5     |

|                                | Quartz porphyry dikes at the Nifty Prospect |         |         |         |          | Tseapseahoolz Creek pluton |         |         | Nusatsum pluton |         |
|--------------------------------|---------------------------------------------|---------|---------|---------|----------|----------------------------|---------|---------|-----------------|---------|
|                                | GR96-27                                     | GR96-33 | GR96-64 | GR96-65 | GR96-124 | GR96-75                    | GR96-76 | GR96-77 | GR96-101        | R96-102 |
| SiO <sub>2</sub>               | 71.17                                       | 72.61   | 69.69   | 70.32   | 74.43    | 72.33                      | 71.97   | 56.46   | 72.96           | 72.79   |
| Al <sub>2</sub> O <sub>3</sub> | 13.90                                       | 13.64   | 13.38   | 13.30   | 12.93    | 14.48                      | 14.58   | 17.08   | 14.73           | 14.64   |
| MgO                            | 0.87                                        | 0.73    | 1.05    | 0.87    | 0.58     | 0.67                       | 0.58    | 3.70    | 0.44            | 0.40    |
| Na <sub>2</sub> O              | 2.72                                        | 3.22    | 2.79    | 3.48    | 3.13     | 4.56                       | 4.46    | 3.32    | 4.67            | 4.62    |
| MnO                            | 0.07                                        | 0.06    | 0.10    | 0.07    | 0.05     | 0.07                       | 0.07    | 0.13    | 0.07            | 0.07    |
| Fe <sub>2</sub> O <sub>3</sub> | 2.63                                        | 2.47    | 3.29    | 3.42    | 2.25     | 2.02                       | 2.06    | 7.67    | 1.60            | 1.55    |
| TiO <sub>2</sub>               | 0.28                                        | 0.26    | 0.30    | 0.32    | 0.22     | 0.21                       | 0.21    | 0.69    | 0.19            | 0.18    |
| P <sub>2</sub> O <sub>5</sub>  | 0.10                                        | 0.08    | 0.08    | 0.08    | 0.07     | 0.09                       | 0.10    | 0.18    | 0.09            | 0.09    |
| CaO                            | 2.13                                        | 1.70    | 2.95    | 2.45    | 1.66     | 1.99                       | 1.93    | 6.98    | 1.87            | 1.83    |
| K <sub>2</sub> O               | 2.69                                        | 2.45    | 2.54    | 2.16    | 2.34     | 2.43                       | 2.59    | 1.72    | 2.70            | 2.71    |
| Cr <sub>2</sub> O <sub>3</sub> | 0.01                                        | 0.01    | 0.01    | 0.01    | 0.01     | 0.01                       | 0.01    | 0.01    | 0.01            | 0.02    |
| LOI                            | 3.00                                        | 2.56    | 3.68    | 3.26    | 2.06     | 0.82                       | 0.94    | 1.83    | 0.46            | 0.70    |
| Total                          | 99.57                                       | 99.79   | 99.86   | 99.74   | 99.73    | 99.68                      | 99.50   | 99.77   | 99.79           | 99.60   |
| Ba                             | 959                                         | 949     | 807     | 1263    | 1169     | 908                        | 947     | 515     | 1076            | 1071    |
| Y                              | 21                                          | 23      | 21      | 18      | 26       | 12                         | 15      | 15      | 6               | 10      |
| Sr                             | 108                                         | 163     | 125     | 120     | 209      | 290                        | 296     | 535     | 396             | 389     |
| Zr                             | 141                                         | 144     | 118     | 128     | 129      | 106                        | 108     | 98      | 82              | 79      |
| Nb                             | 11                                          | 11      | 15      | 10      | 12       | 11                         | 10      | 11      | 15              | 11      |
| Ce                             | 8                                           | 18      | 17      | <5      | 24       | 9                          | <5      | 11      | <5              | <5      |
| V                              | 37                                          | 30      | 54      | 38      | 27       | 20                         | 27      | 191     | 15              | 26      |
| Rb                             | 62                                          | 57      | 58      | 33      | 7.5      | 50                         | 7.5     | 42      | 7.5             | 7.5     |

Major element oxides in percent; trace elements in ppm.

Rb = Thermal neutron activation analysis completed at Activation Labs., Ancastor, Ontario.

For analytical methods of other elements and oxides see Table 2.

## TABLE 6 CONTINUED

### **Sample descriptions**

#### Andesite dikes at the Nifty Prospect.

- GR96-28 Grey, massive, fine grained and equigranular rock with 1 percent disseminated pyrite.  
GR96-34 Grey-green, massive, fine grained, equigranular and visicular dike with rare, small xenoliths.  
GR96-46 Grey-green, massive, fine grained, equigranular dike with some feldspar veinlets.  
GR96-50 Grey-green, fine grained, weakly flow banded dike with feldspar phenocrysts up to 3 mm.  
GR96-51 Grey-green, fine grained, weakly flow banded dike with feldspar phenocrysts up to 3 mm.  
GR96-55 Grey-green, fine grained, visicular dike  
GR96-56 Grey-green, fine grained, visicular dike  
GR96-66 Dark green, massive, fine grained, visicular dike  
GR96-67 Dark green, massive, visicular dike  
GR96-68 Dark green, massive, visicular dike  
GR96-69 Dark green, massive, visicular dike

#### Quartz porphyry dikes at the Nifty Prospect.

- GR96-27 White to grey, massive dike with quartz phenocrysts up to 4 mm.  
GR96-33 White to grey, massive dike with quartz phenocrysts up to 2 mm. Slightly weathered.  
GR96-64 White to grey, massive dike with quartz phenocrysts up to 3 mm.  
GR96-65 White to grey, massive dike with quartz phenocrysts up to 5 mm.  
GR96-124 White to grey, massive dike with quartz phenocrysts up to 4 mm.

#### Tseapseahoolz Creek Pluton

- GR96-75 Grey, massive, coarse grained, equigranular granodiorite with 5 percent biotite  
GR96-76 Grey, massive, coarse grained, equigranular granodiorite with 5 percent biotite  
GR96-77 Mafic, massive, coarse grained quartz diorite with 15 to 20 percent biotite and hornblende

#### Nusatsum Pluton

- GR96-101 Pale grey, massive, coarse grained, equigranular granodiorite with 8 to 10 percent biotite  
GR96-102 Pale grey, massive, coarse grained, equigranular granodiorite with 5 to 8 percent biotite

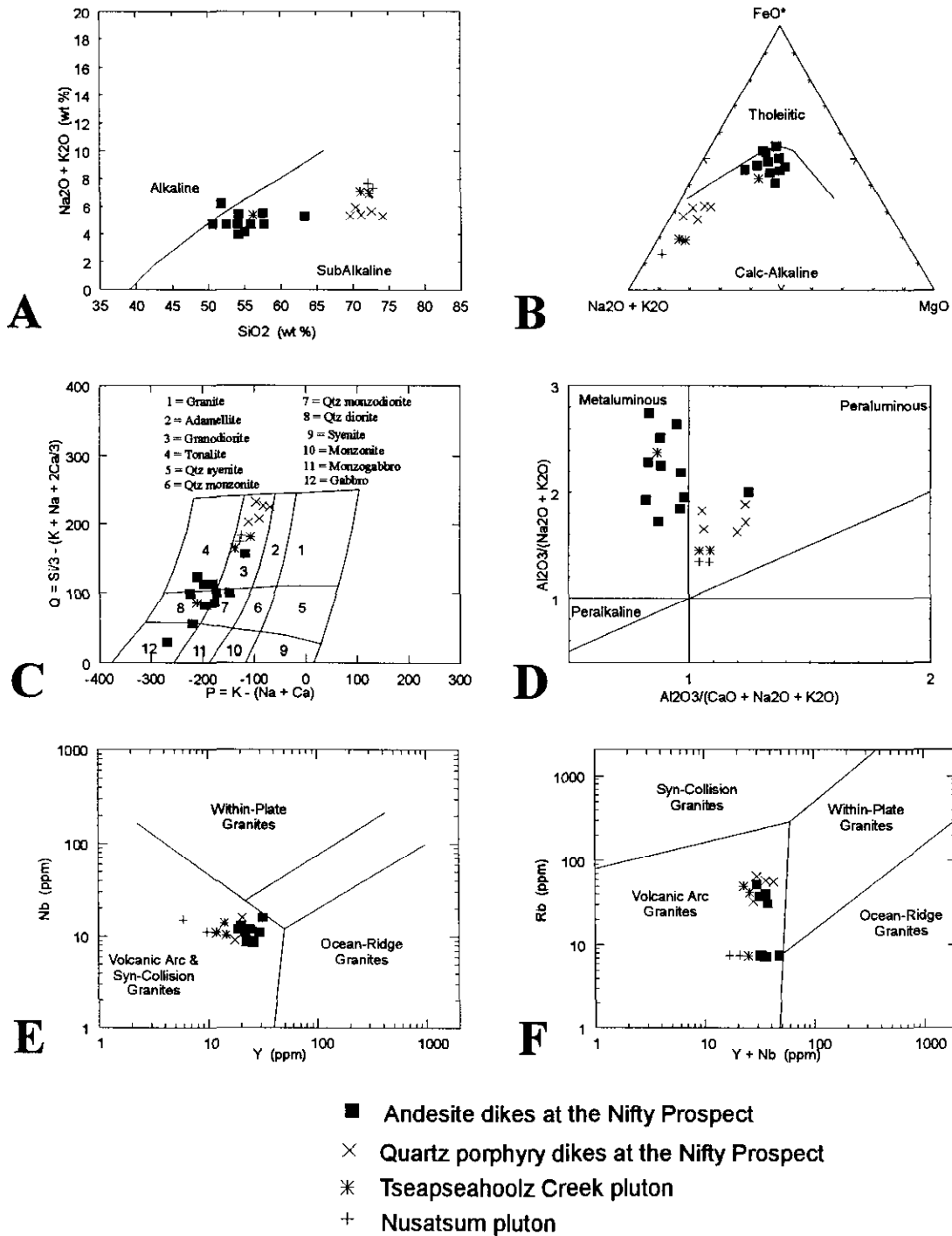


Figure 8. Geochemical plots of some major and minor intrusive rocks in the Bella Coola district:  
 (A) Alkali versus silica plot (after Irvine and Baragar 1971).  
 (B) Triangular Na<sub>2</sub>O + K<sub>2</sub>O - FeO - MgO plot (after Irvine and Baragar 1971).  
 (C) Plot (after Debon and Le Fort, 1983) illustrating intrusive rock compositions.  
 (D) Plot (after Maniar and Piccoli, 1989) differentiating metaluminous and peraluminous intrusive rocks.  
 (E) Triangular Zr - Ti/100 - Y x 3 plot (after Pearce and Cann, 1973).  
 (F) Triangular Zr - Ti/100 - Sr/2 plot (after Pearce and Cann, 1973)

grained andesite which are generally less than 1 metre wide.

At the occurrence, there is an estimated 30 to 40 metre high cliff of leucocratic granodiorite. The plutonic rocks are cut by a subvertical set of narrow shear fractures and joints that trend north, subparallel to the cliff-face. These fractures have controlled some narrow (5 centimetre to 1 metre) dikes of greenstone that show no chilled margins or thermal haloes. The source of the malachite staining occurs approximately 20 metres up the cliff face, and is inaccessible. However, malachite-stained float at the base of the cliff comprises granodiorite cut by thin (< 1 centimetre) shear fractures filled with euhedral quartz, minor pyrite and traces of chalcopyrite. Two grab samples of granodiorite with quartz-sulphide veinlets gave maximum assays of 530 ppm copper, 1.1 ppm silver, 32 ppm molybdenum and 10 ppb gold. Mineralization at the Malachite Cliff occurrence is probably related to a northerly-striking fault set, and it may be similar in origin to the Bella Coola Chief copper occurrence (Day, 1987), situated further northwest (Figure 1). It probably has little economic potential, but suggests that the north trending faults visible in air photographs along the Noosegulch valley have a potential for hosting copper-bearing veins.

## CONCLUSIONS

The Nifty Zn-Pb-Ag-Ba prospect represents a shallow-marine, low temperature volcanogenic massive sulphide system that is characterized by disseminated mineralization with an atypical VMS metal tenure. An exhalative origin is indicated by: (1) the stratiform and conformable nature of the barite cap which probably represents a chemical sedimentary unit; and (2) the sporadic occurrence of pyritic, red jasper pods and veins in the hosting sequence (particularly in the hangingwall rocks).

The prospect is hosted by a package of bimodal (basalt-andesite and rhyodacite-dacite) volcanic rocks that contains both tholeiitic and calc-alkaline signatures. Variations in the colour and character of the stratigraphic section suggest the hostrocks were deposited in an oxidized, emerging basin environment that progressively changed from shallow marine to subaerial.

A U-Pb date of 164 Ma on zircons from a suite of post-ore quartz porphyry dikes demonstrates that the Nifty mineralization and its hosting package are Middle Jurassic or older. This radiometric age date, the bimodal chemistry of the volcanics, and the presence of Jurassic fossils at Compass Lake, four kilometres north-east (Glen Woodsworth, personal communication, 1997) and in another roof-pendant approximately 50 kilometres to the north-northeast (Figure 1), supports Baer's (1973) view that the package hosting the Nifty prospect belongs to the Middle Jurassic Hazelton Group.

The Nifty prospect comprises a caprock of massive barite which passes down into a zone of strongly altered tuffs containing sporadic sphalerite, galena and pyrite in a gangue dominated by quartz, barite and feldspar. This mineralization is underlain by a thick and extensive zone of barren silicification that contains disseminated, fine-grained pyrite. This zone probably represents footwall alteration developed adjacent to the original hydrothermal conduits responsible for the overlying Zn-Pb-Ag-Ba mineralization. These conduits are now probably occupied by younger, post-ore dikes.

Microprobe analyses show that the barite in both the barite cap and in the underlying mineralized zone contains moderate amounts of SrO (up to 2.67 weight per cent). The ore minerals consist primarily of sphalerite and galena with trace amounts of tetrahedrite-tennantite, polybasite ( $9\text{Ag}_2\text{S}\cdot\text{Sb}_2\text{S}_3$ ), chalcopyrite and some other unidentified Ag or Pb-rich sulphides, oxides and sulphates. The chalcopyrite occurs as small (<30 microns) inclusions in other sulphides whereas the other trace minerals form either minute and discrete grains in the gangue or late microscopic veinlets. Sphalerite has a low Fe and Cd content and some crystals contain minute exsolution blebs of chalcopyrite. Galena is Ag-poor and is cut rarely by microfractures containing various unidentified Ag or Pb-rich minerals. The gangue includes potassium and barium-rich feldspars which may indicate that the hydrothermal fluids were highly saline.

As well as having anomalous quantities of Ba, Zn and Pb, Ag and Cd, the mineralization is weakly enriched in As, Hg and Sb. The very low values of Au and Cu, and anomalous amounts of Hg (up to 15 ppm) suggests that the Nifty formed in a relatively low temperature hydrothermal system. No Hg-bearing minerals were detected. However, tetrahedrite-tennantite and sphalerite can contain Hg in their crystal lattice and this may account for the moderate Hg anomalies in the mineralization at the Nifty prospect. The distribution of  $\text{Na}_2\text{O}$ ,  $\text{MgO}$  and  $\text{K}_2\text{O}$  in the footwall rocks indicates the existence of various vertically and laterally distributed alteration zones rich in either albite, chlorite or K-feldspar.

The massive, non-bedded nature of the barite cap, which lacks sedimentary reworking, suggests it precipitated in sea water above a hydrothermal vent or vents. Both the barite and the sulphides were possibly deposited in narrow, fault-controlled topographic depressions on the sea floor, resulting in elongate ore zones (Figure 9). The presence of red jasper veins and pods in the hangingwall succession (Figure 2) shows that hydrothermal activity continued in the area well after the formation of the Nifty mineralization.

A postulated model for the Nifty prospect involves oxidised, saline and low temperature hydrothermal fluids rising to the shallow sea floor along conduits that cut tuffs and tuffaceous sediments (Figure 9). Later, these conduits were reactivated by northeast-trending faults which subsequently controlled

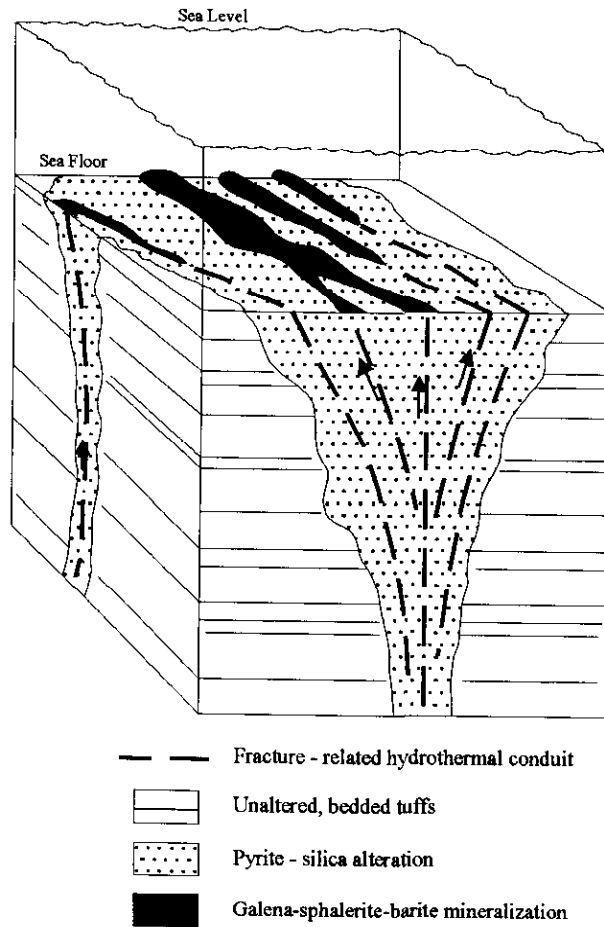


Figure 9. Postulated model for the Nifty Prospect: Volcanogenic hydrothermal fluids rising to the sea-floor along fractures. Precipitation of barite cap in elongate, structurally controlled seafloor depressions, accompanied by deposition of disseminated Pb-Zn-Fe sulphides immediately under the cap and development of an extensive barren footwall alteration zone. The conduits later controlled the emplacement of various post-ore intrusions, including a 164 Ma (Middle Jurassic) suite of quartz porphyry dikes.

the emplacement of the quartz porphyry and younger andesitic dikes.

The Nifty rocks have been folded and deformed; they currently lie on the northern, steeply dipping limb of a major anticline. Small-scale fold measurements demonstrate that the major fold has gently (15 to 25 degrees), east to south-east plunging axes. Although the exposed mineralization is relatively minor, blind and elongate orebodies could be present. The plunge of these postulated linear orebodies would be partly controlled by: (1) the strike of the faults marking the original hydrothermal conduits, (2) the orientation of the original sea floor surface, and (3) the easterly trending fold axes. Consequently, detailed geological mapping to determine the geometry of the fold structures, to outline the mineral alteration zones and locate the original hydrothermal conduits are essential prerequisites to any future drilling at the prospect.

The age, bimodal tholeiitic and calc-alkaline chemistry and oxidized, shallow-marine depositional environment of the Nifty hostrocks are similar to the Hazelton Group package hosting the Eskay Creek deposit in northwestern British Columbia (Alldrick, 1993; Roth, 1993; MacDonald *et al.*, 1996), and a correlation is possible. Thus, the volcanic roof pendants in the Bella Coola area and those elsewhere along the Coast Belt should be re-evaluated as potential hostrocks for Eskay Creek-type VMS deposits. Furthermore, because the volcanic rocks that stratigraphically overlie the Nifty prospect show local evidence of hydrothermal activity in the form of jasper veins, it suggests that the subaerial rocks in the package warrant exploration for epithermal targets.

## ACKNOWLEDGEMENTS

We thank the following: L. J. Diakow, who originally suggested this project; pilot R.E. Skelly, of Vancouver Helicopters Ltd., for his assistance in the field; T. Hoy, D.V. Lefebure and R.H. Pinsent for discussions concerning volcanogenic massive sulphide and exhalite deposits and their environment of formation; R. Lett for his logistical help with the commercial laboratories that analysed the rock and assay samples; D.M. Johnson and other members of the geoanalytical laboratory, Department of Geology, Washington State University, for their assistance with the microprobe analyses which were conducted using a Cameca MBX instrument.

## REFERENCES

- Alldrick, D.J. (1993): Geology and Metallogeny of the Stewart Mining Camp, northwestern British Columbia; *B.C. Ministry of Energy Mines and Petroleum Resources*, Bulletin 85, 105 pages.
- Anonymous (1985): Geology and Geochemistry of the Nifty, Nifty 2, 3, 4, 5, 6, 7, 8, 9, 10, 11, 12 and 14 and Keen, Keen 2, 3 Mineral Claims; Unpublished Report for Cominco Ltd. *B.C. Ministry of Energy Mines and Petroleum Resources*, Assessment Report 14115.
- Baer, A.J. (1973): Bella Coola - Laredo Sound Map-Areas, British Columbia; *Geological Survey of Canada*, Memoir 372, 119 pages.
- Bailes, R.J. (1977): Geology and Geochemistry of a Portion of the Nifty 2 and Nifty 5 Claims, Skeena Mining Division; Report for Pan Ocean Oil Ltd. *B.C. Ministry of Energy, Mines and Petroleum Resources*, Assessment Report 6735
- Bailes, R.J., and McArthur, G.F. (1978): Geology and Geochemistry Nifty 2, 3, 4, 5 Mineral Claims, Skeena Mining Division; Report for Pan Ocean Oil Ltd. *B.C. Ministry of Energy Mines and Petroleum Resources*, Assessment Report 6836.
- Bailes, R.J., and McArthur, G.F. (1979): Geology, Geophysics and Geochemistry of a Portion of the Keen 1 and 2 Mineral Claims, Skeena Mining Division; Report for Pan Ocean Oil Ltd. *B.C. Ministry of Energy, Mines and Petroleum Resources*, Assessment Report 7216.
- Blackwell, J.D. (1985): Geology and Geochemistry of the Nifty, Nifty 2, 3, 4, 5, 6, 7, 8, 9, 10, 11, 12 and 14 and Keen, Keen 2,3 Mineral Claims; Report for Cominco Ltd. *B.C. Ministry of Energy, Mines and Petroleum Resources*, Assessment Report 14115.
- Day, W.C. (1987): Report on the Bella Coola Chief Group of Claims; Unpublished report for Green Lake Resources Ltd. *B.C. Ministry of Energy, Mines and Petroleum Resources*, Assessment Report 15867.
- Debon, F., and Le Fort, P. (1983): A Chemical-mineralogical Classification of Common Plutonic Rocks and Associations; *Royal Society of Edinburgh Transactions*, Earth Sciences, Volume 73, pages 135-149.
- Holtby, M.H., and Campbell, C.J. (1980): Geological Report on the Nifty 2, Nifty 5, Keen 1 and Keen 2 Mineral Claims. Report for Rio Tinto Canadian Exploration Ltd. *B.C. Ministry of Energy Mines and Petroleum Resources*, Assessment Report 8528.
- Irvine, T.N., and Baragar, W.R.A. 1971. A Guide to the Chemical Classification of the Common Volcanic Rocks. *Canadian Journal of Earth Sciences*, Volume 8, pages 523-547.
- Le Maitre, R.W. (1989): A Classification of Igneous Rocks and Glossary of Terms; *Blackwell Publishing*, Oxford, 193 pages.
- Lewis, T.D. (1979): Nifty (93D/9W); in *Geological Fieldwork 1978*, *B.C. Ministry of Energy, Mines and Petroleum Resources*, Paper 1979-1, pages 94-96.
- Lewis, T.D. (1981): 1978 - Nifty Deposit (93D/9W); in *Geology in British Columbia 1977-1981*, *B.C. Ministry of Energy, Mines and Petroleum Resources*, pages 103-107.

- Lohman, G. (1981): Nifty 8 Mineral Claim, Skeena Mining Division, Drilling and Geophysics 1981; Report for Rio Tinto Canadian Exploration Ltd.
- Mandy, J.T. (1931): North-Western Mineral Survey District (No. 1): Nifty; Annual Report of the B.C. Ministry of Mines for 1930, *British Columbia Ministry of Mines*, pages A55 and A61.
- Macdonald, A.J., Lewis, P.D., Thompson, J.F.H., Nadaraju, G., Bartsch, R.D., Bridge, D.J., Rhys, D.A., Roth, T., Kaip, A., Godwin, C.I. and Sinclair, A.J. (1996): Metallogeny of an Early to Middle Jurassic Arc, Iskut River Area, northwestern British Columbia; *Economic Geology*, Volume 91, pages 1098-1114.
- Maniar, P.D. and Piccoli, P.M. (1989): Tectonic Discrimination of Granitoids; *Geological Society of America Bulletin*, Volume 101, pages 635-643.
- McCull, K.M. (1987): Geology of Britannia Ridge, East Section, Southwest British Columbia; Unpublished M.Sc. thesis, *The University of British Columbia*.
- Mortensen, J. K., Ghosh, D.K. and Ferri, F. (1995): U-Pb Geochronology of Intrusive Rocks Associated with Copper-Gold Porphyry Deposits in the Canadian Cordillera; in, Porphyry Deposits of the Northwestern Cordillera of North America, Schroeter, T.G., Editor, *Canadian Institute of Mining, Metallurgy and Petroleum*, Special Volume 46, pages 142-158.
- Morton, J.W. (1984): Grid Establishment and Geochemical Survey Keen Grid Nifty Property; Report for Imperial Metals Corporation, *B.C. Ministry of Energy, Mines and Petroleum Resources*, Assessment Report 12747.
- Morton, J.W. and Birkland, A.O. (1993): Geochemical and Geological Reconnaissance Report on the B.C. Ministry of Energy Mines and Petroleum Resources, Assessment Report 10409.
- Cutfinger Claims; Report for Eastfield Resources Ltd., and Inco Exploration, *B.C. Ministry of Energy, Mines and Petroleum Resources*, Assessment Report 23031.
- Pearce, J.A. and Cann, J.R. (1973): Tectonic Setting of Basic Volcanic Rocks Determined Using Trace Element Analyses; *Earth and Planetary Science Letters*, Volume 19, pages 290-300.
- Pearce, J.A., Harris, N.B.W., and Tindle, A.G. (1984): Trace Element Discrimination Diagrams for the Tectonic Interpretation of Granitic Rocks; *Journal of Petrology*, Volume 25, pages 956-983.
- Roth, T. (1993): Surface Geology of the 21A Zone, Eskay Creek, British Columbia (104B/9W); *B.C. Ministry of Energy, Mines and Petroleum Resources*, Geological Fieldwork 1992, Paper 1993-1, pages 325-330.
- Stacey, J.S. and Kramers, J.D. (1975): Approximation of Terrestrial Lead Isotope Evolution by a Two-Stage Model; *Earth and Planetary Science Letters*, Volume 26, pages 207-221.
- Taylor, A.B. (1989): Geochemical Survey on the Western Nifty Group; Report for Imperial Metals Corporation, *B.C. Ministry of Energy, Mines and Petroleum Resources*, Assessment Report 19201.
- Tipper, H.W. (1963): Nechacko River Map-Area, British Columbia. *Geological Survey of Canada*, Memoir 324.
- Winchester, J.A. and Floyd, P.A. (1977): Geological Discrimination of Different Magma Series and their Differentiation Products Using Immobile Elements; *Chemical Geology*, Volume 20, pages 325-343.



**EPITHERMAL MINERALIZATION  
ON THE WATSON BAR PROPERTY (92/01E),  
CLINTON MINING DIVISION, SOUTHERN B.C.**

By M.S. Cathro, B.C. Mines Branch, R.M. Dürfeld, Stirrup Creek Gold Ltd.  
and G.E. Ray, B.C. Geological Survey

**KEYWORDS:** Watson Bar, Second-Ulcer claims, Zone V, low sulphidation, epithermal, gold, silver, arsenic, mercury, antimony, lead, zinc, Jackass Mountain Group, porphyry sills and dikes, thrust faults.

## INTRODUCTION

This paper describes low-sulphidation epithermal gold-silver-base-metal mineralization at Zone V on the Watson Bar property (Second-Ulcer claims, Second prospect; MINFILE number 092O 051). Zone V is located south of Watson Bar Creek in the Camelsfoot Range on the west side of the Fraser River, approximately 40 kilometres north-northwest of Lillooet (Figure 1). The area is reached by following the all-weather Slok Creek (West Pavilion) logging road north from Lillooet to the 71 kilometre mark. An alternate access route is from Clinton via logging roads and the Big Bar ferry.

Mineralization at Zone V is hosted by a shallow southwest-dipping thrust fault which cuts feldspathic and volcanic lithic arenites of the Early Cretaceous Jackass Mountain Group. Drilling since 1989 has outlined a zone up to 35 metres thick which contains a stacked series of auriferous quartz-sulphide veins and carbonaceous shear zones. Zone V was estimated to contain a geological reserve of 136 962 tonnes grading 14.33 ppm gold at a 6.86 ppm cut-off, or 306 143 tonnes grading 8.13 ppm gold at a 1.71 ppm cut-off (J. Casey, private report for Stirrup Creek Gold Ltd., July, 1997). The thrust is marked by a two kilometre long, moderate to strong, induced polarization chargeability anomaly. At Zone I, located 800 metres to the south, similar Au-As mineralization has been intersected at the inferred down dip extension of the Zone V thrust fault, suggesting that these two zones may be part of the same structure.

## Watson Bar Gold Belt

Although only Zone V was studied in detail for this paper, a review of regional geology and mineral occurrence maps indicates there is a pronounced southeast alignment of mineral prospects and geologic features which we call the Watson Bar gold belt. The Zone V prospect occurs near the southern end of this 25 kilometre long trend, which also includes the Mad (MINFILE number 092O 092), Buster (92O 055), Astonisher (92O 054), GB (92O 060) and several new or unnamed prospects (Figure 1). These structurally controlled mineral

occurrences are all hosted by the Jackass Mountain Group on the southwest side of the Slok Creek fault, and are spatially associated with a series of porphyry bodies. At least five different styles of mineralization are recognized:

1. Iron carbonate-silica alteration zones. These occur as wide (>500 metres) and extensive (>1000 metres long) reddish-brown weathering zones that are marked by pervasive iron carbonate alteration, local chalcedonic silica, sericitic and clay alteration, sporadic to widespread As, Sb and Hg enrichment and spotty anomalous gold values. Examples include Zone IV and the rusty weathering cliffs in lower Madsen Creek and Watson Bar Creek.

2. Thrust-hosted quartz-sulphide mineralization. At Zone V, this consists of tectonic clasts and boudins of mineralized and unmineralized wallrock and auriferous quartz-sulphide veins surrounded by a highly deformed, carbonaceous fault gouge matrix. The Mad (Adit) occurrence (Lisle, 1988) may be analogous.

3. Intrusion-hosted quartz-sulphide veins. At Zone I, gold-bearing, quartz-sulphide veins, breccias and stockworks cut silicified and sericitized quartz-feldspar porphyry sills and adjacent sandstone containing carbonaceous shears. This mineralization may be a deeper, more proximal style of mineralization, perhaps the upper part of a buried porphyry system.

4. High-angle quartz-sulphide veins and stockworks. These occur as narrow (<1.5 metres) veins of quartz, quartz breccia and chalcedonic silica that carry gold with variable amounts of pyrite, arsenopyrite and other sulphides. The veins have sharp margins and thin envelopes of bleaching in adjacent wallrocks. They crosscut the bedding in the hosting sedimentary wallrocks at a high angle.

5. Weakly to moderately auriferous conformable zones. Sulphides occur in conformable veins, siliceous replacements and as disseminations in sandstone beds (Lisle, 1988).

## History

The first recorded mineral discovery in the Watson Bar area was made in 1886 when two prospectors reported finding "some very heavy, lead-coloured rock" 11 kilometres up Watson Bar Creek on its south side. Assays showed that the rock contained no Au or Ag but a very large percentage of As (Minister of Mines Annual Report, 1886, p. 209). This occurrence probably corresponds to

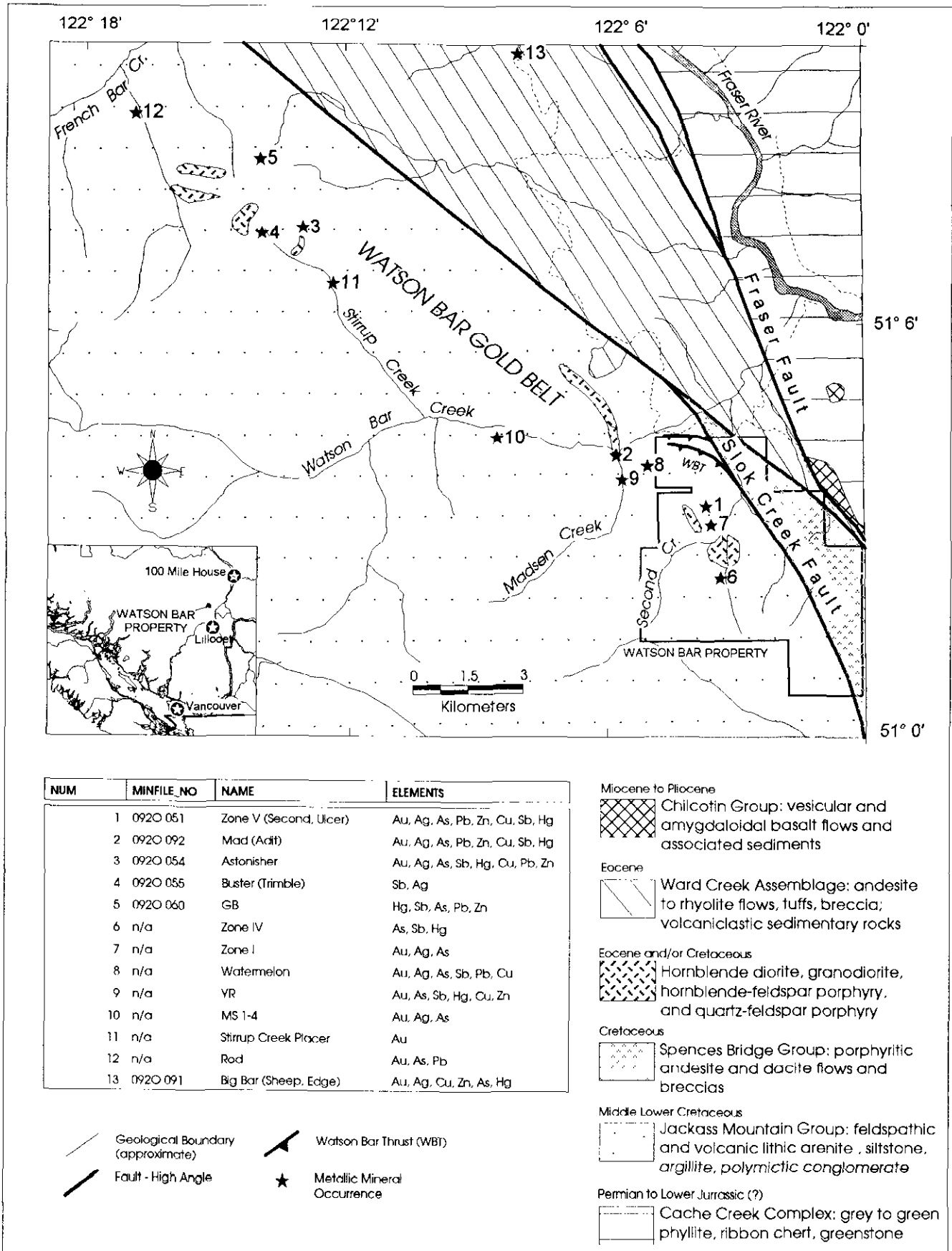


Figure 1. Generalized geology map of the Watson Bar gold belt (after Tipper, 1978, and Hickson *et al.*, 1994) showing precious metal occurrences and the location of the Watson Bar Property.

one of several arsenopyrite showings on the current Mad claims (Figure 1).

Placer gold was discovered on Stirrup Creek at the north end of the belt during World War I, and although exact production figures are unknown, Warren (1982) estimated that approximately 3000 to 5000 ounces of gold was produced by about 1940. Old placer workings in Watson Bar Creek probably correspond to this period also, and small scale placer mining continues to the present day. Since 1924, prospecting for the bedrock source of the gold in the headwaters of Stirrup Creek has resulted in the discovery of the Buster (Sb, Ag), Astonisher (Au, Sb, As, Hg, Cu), GB (Hg, Sb, Pb, Zn) and several other minor showings (Lisle and McAllister, 1989).

In May 1980, E & B Explorations Inc., staked the Carolyn 1-8 claims over the Madsen and Second Creeks area and identified several large alteration zones of silica and carbonate, with sporadic stibnite, arsenopyrite, pyrite, cinnabar and other sulphides (Price *et al.*, 1981; Livingston, 1982). Follow-up work outlined numerous As, Hg and Au soil anomalies including one over the Zone V area. Following a 1982 release of government stream sediment survey data which showed anomalous Cu, As, Au and Hg in the area, Utah Mines Ltd. staked the Mad I-11 claims to the west of the Carolyn group. The Carolyn claims later lapsed and the ground was restaked in 1986-87 as the Second-Ulcer claims (Watson Bar property) by R.M. Dürfeld and J.A. McClintock, and as extensions to the Mad property by Utah Mines Ltd.

The Watson Bar property was optioned by Cyprus Gold (Canada) Ltd. in 1987 which conducted soil sampling, geological mapping and induced polarization surveys to define 14 targets. In 1988, test pitting and trenching of gold-arsenic soil anomalies at Zone V discovered a shallow dipping zone of quartz veins containing visible gold (McClintock and Dürfeld, 1988). The first drill hole, WB-89-1 intersected the vein zone 20 metres down dip of the trench and assayed 4 metres grading 24.5 ppm Au and 67 ppm Ag, as well as several deeper zones of lower grade mineralization (Dürfeld, 1990). Cyprus Gold (Canada) Ltd. further explored Zone V and other targets with trenching and drilling before relinquishing the property in 1992. A 91 tonne bulk sample grading 39.74 ppm Au was mined from the Zone V trench and processed at Westmin Resources' Premier Mill at Stewart in 1993-94.

The current operator, Stirrup Creek Gold Ltd., optioned the property and drilled 14 holes at Zone V in 1996 (Dürfeld, 1996). A further 11 holes were drilled on Zones I, V, X and XI in 1997 and exploration is continuing.

## REGIONAL GEOLOGICAL SETTING

The Watson Bar gold belt is hosted by clastic sedimentary rocks of the Early Cretaceous Jackass Mountain Group (JMG) which forms part of the accreted Methow terrane. The belt occurs southwest of the Slok Creek fault (SCF), a southeast-trending structure that

merges with the Fraser Fault near Lillooet (Figure 1). To the northeast of the SCF are andesites and dacites of the Cretaceous Spences Bridge Group and andesite flows and tuffs and bentonitic sediments of the Eocene Ward Creek Assemblage (Trettin, 1961, Hickson *et al.*, 1994).

The JMG is a shallow to moderately southwest-dipping package of volcanoclastic sedimentary rocks which is at least 5000 metres thick. It was probably deposited in a submarine fan setting on the margin of the Tyaughton Basin, a 150 kilometre long, southward-narrowing synclinorium (Trettin, 1961; Kleinspehn, 1985; Hickson *et al.*, 1994). The Watson Bar gold belt is mainly underlain by the informally named "Member 3" of Hickson *et al.* (1994) which comprises thick-bedded to massive, medium to coarse-grained feldspathic and volcanic lithic arenite with intercalated pebble conglomerate, siltstone and argillite.

Coincident with the gold belt is a southeast trending belt of small stocks, dikes and sills which intrude the JMG (Figure 1). These intrusions range in composition from diorite to rhyodacite and are most commonly granodiorite. They are commonly porphyritic but are locally medium-grained and equigranular in texture. Phenocrysts are generally hornblende and/or plagioclase, and less commonly quartz. The intrusions are locally deformed and weakly altered. On the Watson Bar property the largest stock is about 1 kilometre in diameter. The intrusions have not been radiometrically dated but field relationships suggest they are post-Early Cretaceous and pre-Eocene in age.

The SCF has been interpreted to be a high-angle splay of the Fraser Fault with latest motion being strike slip (Hickson *et al.*, 1994). The paucity of Eocene strata west of the fault suggests that at least some of the movement was post-Eocene with a minimum, east-side-down displacement of 1000 metres. To the northwest, near French Bar Creek, the SCF disappears under Tertiary volcanic rocks (Tipper, 1978).

South of Watson Bar Creek, the SCF cuts the Watson Bar thrust (WBT), an imbricate zone of south southwest-dipping thrust faults mapped by Hickson *et al.* (1994). The WBT is described as a highly disrupted, iron stained zone, approximately 500 metres thick. It is exposed between the 72 and 75 kilometre marks on the West Pavillion road, where it consists of boudinaged sandstone blocks surrounded by sheared and contorted carbonaceous material (Figure 2). Here, the WBT strongly resembles the mineralized thrust at Zone V. Tectonic indicators suggest north or northeasterly directed movement on the structure. To the west, near Madsen Creek, the sheared carbonaceous material is uncommon and it appears the WBT either dies out, is covered by overburden, or is focused into a few narrow thrust planes which have not yet been identified. The easterly orientation of the WBT suggests that it may be an accommodation structure associated with movement on the Fraser fault system (J.M. Journeay, personal communication, 1993, cited in Hickson *et al.*, 1994).

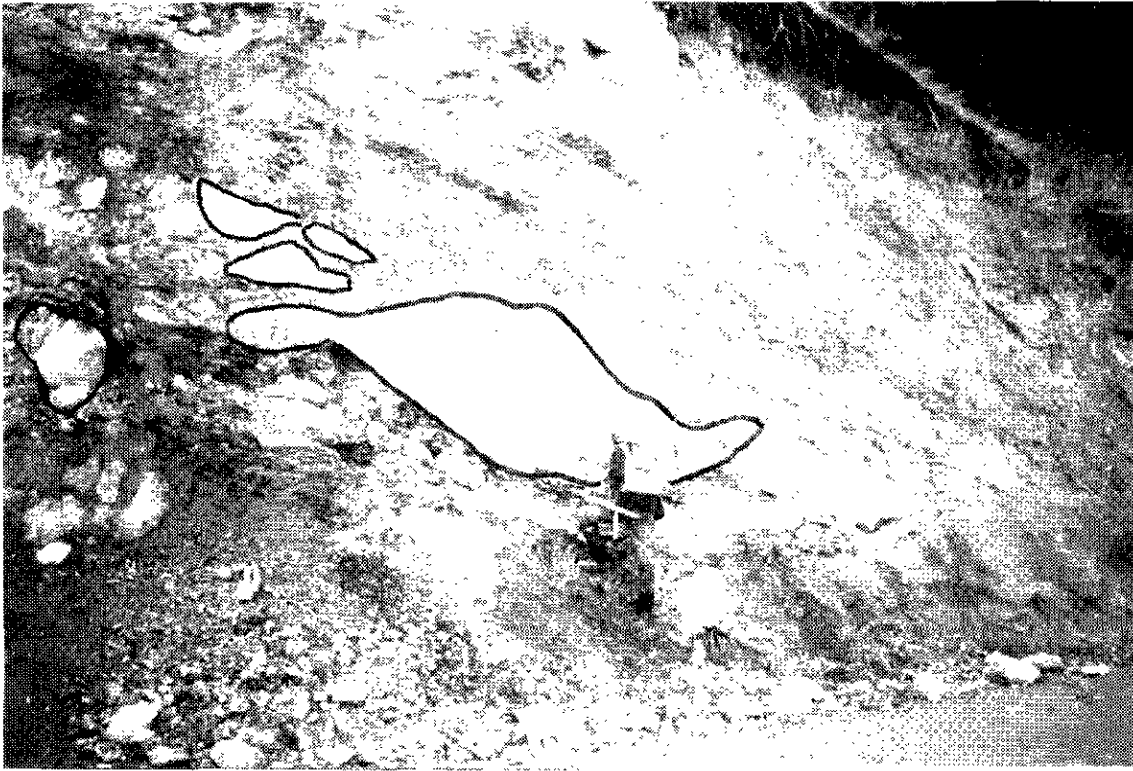


Figure 2. Photograph of Watson Bar thrust fault showing blocks of sandstone (white) surrounded by contorted carbonaceous gouge (grey). Roadcut at 72.5 kilometres, West Pavilion road.

## GEOLOGY OF WATSON BAR PROPERTY

The Watson Bar (Second) property has been mapped at a scale of 1:5000 by Dürfeld and McClintock (1987), McClintock and Dürfeld (1988), Dürfeld and Jackson (1990), Dürfeld (1990, 1992) and Read (unpublished data). All petrographic descriptions presented here are summarized from unpublished thin and polished thin-section reports done by J. G. Payne for Cyprus Gold (Canada) Ltd. or by R. C. Wells and J.F. Harris for Stirrup Creek Gold Ltd. X-ray diffraction (XRD) results for four samples were provided by M. Chaudry (personal communication, 1997). The following description refers to the immediate area of Zones V, IV and I.

### Structure and Lithologies

Bedding in the JMG at the property strikes southeasterly (130 degrees) and dips shallowly (15-30 degrees) to the southwest. In the vicinity of Zone V, the JMG consists mainly of thick-bedded to massive, grey to greyish-green, fine- to medium-grained, altered feldspathic arenite, siltstone and minor argillite and conglomerate. Peripheral to Zone V, many of the sandstone/siltstone units contain calcite veins and/or secondary carbonate in the matrix.

In thin-section, the arenites are seen to be grain-supported and composed mainly of 0.1-1.0 millimetre detrital grains of feldspar, lesser quartz, biotite, and lithic fragments in a secondary matrix of calcite, ankerite, sericite, biotite and chlorite. Conglomerates are matrix supported and polymictic with intrusive and volcanic clasts up to 10 centimetres in diameter.

At least six sills and several small dikes intrude the sandstone succession at the Zone V occurrence (Figure 3). The intrusions are porphyritic, containing phenocrysts up to five millimetres in length of plagioclase and/or hornblende. Quartz phenocrysts are locally present. The sills range in thickness from 2 to 15 metres and have a similar strike and dip to the mineralized zone. Dikes in the area are steeply dipping with strikes trending roughly north or east to southeasterly. The dikes and sills are fresh to weakly altered; altered varieties are mottled, greenish-grey, weakly to moderately sericitized and chloritized, and weakly calcareous. Plagioclase is altered to fine sericite, clay and carbonate and hornblende is partially replaced by chlorite, carbonate and fine opaques. At Zone I, quartz-feldspar porphyry sills have been intersected by drillholes at about the same stratigraphic level as the Zone V thrust. Here they are moderately sericitized, silicified and locally mineralized with weakly auriferous (500-2440 ppb Au) quartz-arsenopyrite-pyrite veins. At Zone IV, a porphyry border phase of the stock has iron carbonate alteration and fine calcite veins cutting it.

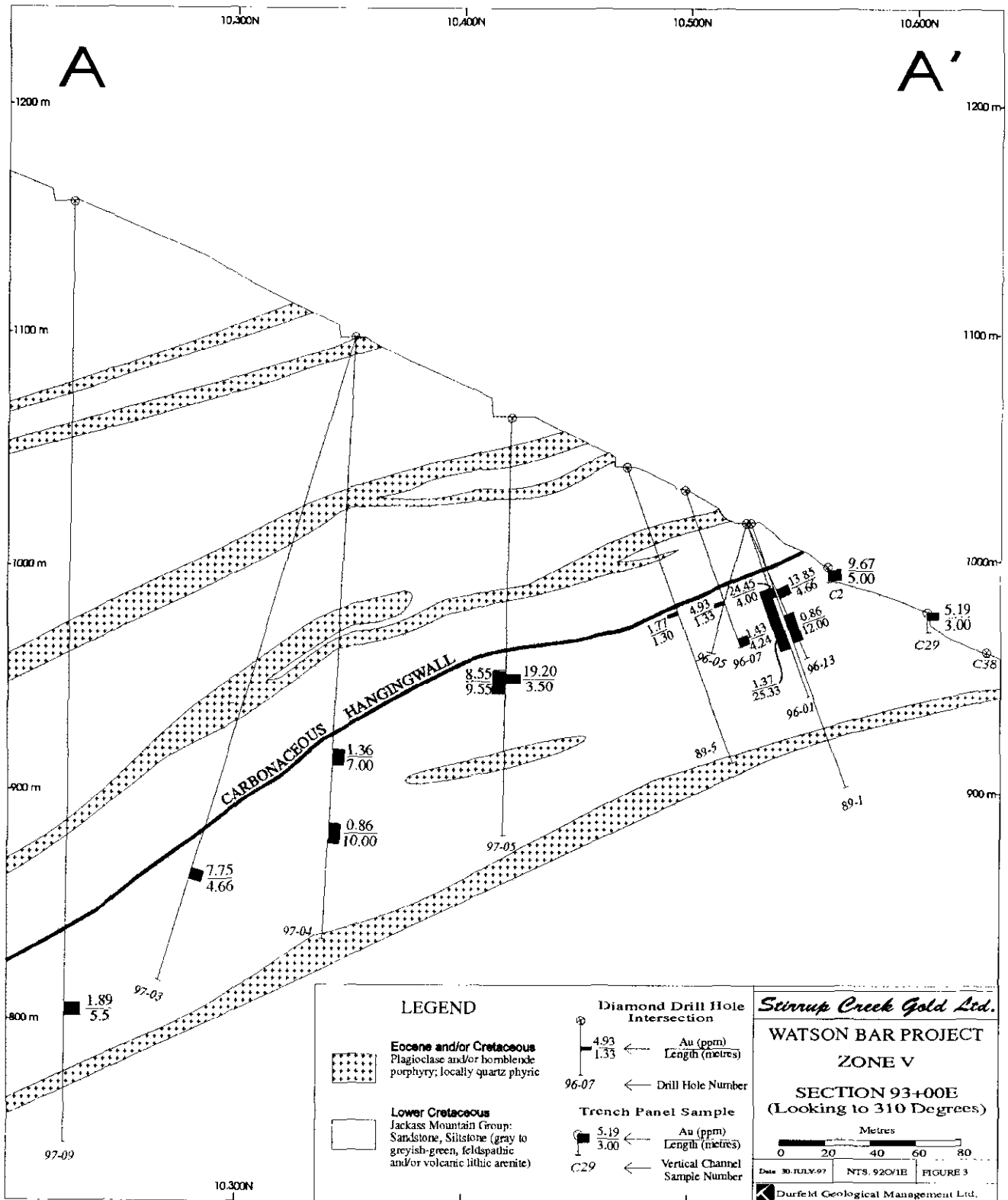


Figure 3. Cross-section 93+00E through Zone V (looking northwest).

## Alteration

Wallrock alteration at the Watson Bar property includes locally developed pervasive zones of carbonate, sericite-pyrite and silica alteration, together with some biotite, argillic and propylitic alteration. The identification of these alteration types has been aided by x-ray diffraction analyses (XRD) and by whole rock analyses presented in Table 1.

### Carbonate Alteration

At Zones I and IV, large areas (>500 metres wide) of the sandstone are brown weathering due to pervasive iron carbonate and/or dolomite alteration, and calcite is common on fractures. Similar, extensive zone of iron carbonate alteration are also seen in the Madsen Creek and Watson Bar drainages to the northwest. Although calcite or dolomite may be present as a minor constituent of quartz veins at Zone V, wallrock directly adjacent to these veins is generally not carbonate-rich, probably due to later overprinting by more advanced alteration types. Above and below the mineralized zone, however, strong pervasive calcite-iron carbonate alteration is present. Thin-section examination of drill core specimens indicates that feldspar grains and matrix are altered to fine carbonate, sericite, chlorite, and possibly clay.

### Silicification

In addition to the auriferous quartz-sulphide veins and stockworks described above, there is local pervasive replacement by massive chalcedonic quartz. At Zone IV, small zones (up to a few metres wide) of chalcedonic silica with quartz-calcite-realgar-arsenopyrite-stibnite veins and weakly anomalous gold values are present, and occur within a broad iron carbonate alteration zone. Whole rock analysis shows this rock to be mainly composed of silica, aluminum, iron, magnesium and calcium, a composition which is consistent with quartz, dolomite, iron carbonate and mica minerals (sample GR97-44, Table 1).

### Sericite-Pyrite Alteration

Sericite-pyrite alteration occurs as selvages adjacent to auriferous quartz-carbonate-sulphide veins. It generally lacks carbonate minerals, suggesting it has overprinted and replaced the earlier, more widespread carbonate alteration. Muscovite has been identified by XRD in black carbonaceous material, and in light grey "clay" alteration. In thin-section, sericite is seen replacing both detrital grains and matrix in the sandstones, and pyrite occurs as subhedral to euhedral grains up to 0.3 millimetres in size. In general, intrusive rocks at Zone V show only weak sericite-chlorite-carbonate alteration, however, porphyry sills mineralized with quartz-arsenopyrite-pyrite veins in the deeper part of Zone I to the south show pervasive quartz-sericite-pyrite alteration and are locally silicified.

### Argillic Alteration

Zones of pervasive argillic alteration of sandstone have been identified in the main trench at Zone V. Pale grey to white, mineralized sandstone adjacent to cockscomb quartz veins is rich in silica, aluminum and potassium (samples GR97-48, 49, Table 1). An XRD analysis of sample GR97-48 indicates that illite/muscovite, quartz, scorodite, and kaolinite-smectite are present. In addition, an unweathered, clay-altered sample, taken from DDH 97-05, contains muscovite/illite, kaolinite and pseudorutile. Small patches of similar argillic alteration are exposed in road cuts at Zones I and IV. These contain white clay or kaolinite alteration adjacent to silicified zones within larger zones of pervasive iron carbonate alteration. A sample of clay-altered rock from Zone IV is high in  $Al_2O_3$  and  $SiO_2$  (sample GR97-43, Table 1) and XRD analyses indicates that the minerals quartz, kaolinite, scorodite and chlorite are present. Some of the kaolinite in surface exposures was probably formed by weathering rather than hypogene processes.

### Biotite Alteration

At Zone V, minor brown biotite occurs as both detrital grains and in the sandstone matrix. However, it is not clear if the biotite in the matrix represents minute detritus, is a hydrothermal alteration related to the nearby mineralization, or is a weak hornfels related to the porphyry sills and dikes.

## Mineralization

### Geometry and Structure

Zone V consists of an assemblage of bedding-parallel shears, brecciated quartz-sulphide vein material, gouge, carbonaceous material and altered and unaltered sandstone blocks. It varies from a few metres to as much as 35 metres in thickness, strikes southeasterly and dips shallowly southwest, conformable with the local strike and dip of the sandstone bedding.

The upper plane of the zone is marked by sheared, pyritic, carbonaceous material and is undulating in cross-section (Figure 3), ranging in dip angle from 15 to 35 degrees but averaging 20-25 degrees. To date the zone has been defined by trenching and drilling over a strike length of 150 metres and a dip length of 350 metres. In the main trench (Figure 4), the zone consists of a numerous tectonized blocks of quartz-sulphide vein material, altered and mineralized wallrock and unmineralized sandstone country rock, all surrounded by contorted and sheared carbonaceous material and gouge. Individual unaltered sandstone blocks are locally boudinaged and show rounding, milling and rotation (Figure 4). Most blocks are ellipsoid and have an apparent northerly elongation.

Table 1. Whole rock geochemical data, Zones I, IV and Watson Bar Property.

| Element | Units | Method | Sample #<br>Zone<br>Lab. | GR97-43 | GR97-44 | GR97-46 | GR97-47 | GR97-48 | GR97-49 | GR97-53 | GR97-54 |
|---------|-------|--------|--------------------------|---------|---------|---------|---------|---------|---------|---------|---------|
|         |       |        |                          | IV      | IV      | V       | V       | V       | V       | I       | I       |
| SiO2    | %     | XRF1   | COM                      | 67.97   | 53.61   | 81.92   | 83.69   | 69.08   | 66.72   | 46.35   | 58.35   |
| TiO2    | %     | XRF1   | COM                      | 1.21    | 0.18    | 0.02    | 0.02    | 0.51    | 0.97    | 0.82    | 0.89    |
| Al2O3   | %     | XRF1   | COM                      | 20.72   | 4.65    | 0.95    | 0.84    | 16.18   | 17.83   | 17.48   | 19.21   |
| Fe2O3   | %     | XRF1   | COM                      | 0.43    | 6.03    | 5.53    | 4.37    | 2.05    | 1.95    | 5.66    | 7.85    |
| MnO     | %     | XRF1   | COM                      | 0.01    | 0.16    | 0.03    | 0.02    | 0.01    | 0.01    | 0.09    | 0.11    |
| MgO     | %     | XRF1   | COM                      | 0.16    | 4.73    | 1.31    | 0.68    | 1.24    | 1.24    | 3.5     | 0.11    |
| CaO     | %     | XRF1   | COM                      | 0.15    | 11.78   | 0.17    | 0.19    | 0.19    | 0.22    | 7.26    | 2.03    |
| Na2O    | %     | XRF1   | COM                      | 0.01    | 0.01    | 0.02    | 0.02    | 0.15    | 0.08    | 0.02    | 0.04    |
| K2O     | %     | XRF1   | COM                      | 0.28    | 0.31    | 0.11    | 0.06    | 4.33    | 4.71    | 0.09    | 0.16    |
| P2O5    | %     | XRF1   | COM                      | 0.11    | 0.05    | 0.02    | 0.02    | 0.03    | 0.13    | 0.24    | 0.28    |
| Ba      | %     | XRF1   | COM                      | 0.01    | 0.04    | 0.01    | 0.01    | 0.04    | 0.05    | 0.01    | 0.02    |
| LOI     | %     | FUS    | COM                      | 8.89    | 17.48   | 5.32    | 4.9     | 4.48    | 5.12    | 18.39   | 10.78   |
| Total   | %     | SUM    | COM                      | 99.95   | 99.03   | 95.41   | 94.82   | 98.29   | 99.03   | 99.91   | 99.83   |

Notes:

Steel mill grinding @ GSB  
 XRF1 = Fused Disc - X-ray fluorescence  
 Ba\* = Fused disc analysis for XRF calibration (use with CAUTION)  
 COM = Cominco  
 FUS = Fusion

Sample descriptions:

GR97-43 Trench grab - white clay  
 GR97-44 Trench grab - silicification+realgar+arsenopyrite+pyrite veins  
 GR97-46 Trench grab - bladed quartz vein  
 GR97-47 Trench grab - bladed quartz vein  
 GR97-48 Trench grab - grey, clay-altered wallrock  
 GR97-49 Trench grab - grey, clay-altered wallrock  
 GR97-53 Surface grab - limonite-weathered grey-green rock  
 GR97-54 Surface grab - limonite stained arkosic sandstone

Table 2. Trace element geochemical data, Zones I, IV and V, Watson Bar Property.

| Element | Units | Method | Lab.     | Sample #<br>Zone<br>Detection | GR97-43 | GR97-44 | GR97-45 | GR97-46 | GR97-47 | GR97-48 | GR97-49 | GR97-50 | GR97-52 | GR97-53 | GR97-54 | GR97-55 | GR97-56 | GR97-57 |
|---------|-------|--------|----------|-------------------------------|---------|---------|---------|---------|---------|---------|---------|---------|---------|---------|---------|---------|---------|---------|
|         |       |        |          |                               | IV      | IV      | IV      | V       | V       | V       | V       | V       | V       | I       | I       | V       | V       | V       |
| Au      | PPB   | INA    | ACT 2    |                               | <2      | <2      | 44      | 42300   | 39400   | 3000    | 3570    | 71200   | 52100   | 88      | 62      | 3900    | 10400   | 10700   |
| Ag      | PPM   | TICP   | ACM 0.5  |                               | 0.6     | <.5     | 1.2     | 54.2    | 77.5    | 2.1     | 3.3     | 26.8    | 103.5   | <.5     | 9.3     | 1       | 11.9    |         |
| Al      | %     | TICP   | ACM 0.01 |                               | 10.27   | 2.33    | 1.45    | 0.32    | 0.22    | 7.7     | 8.83    | 0.88    | 0.45    | 9.11    | 9.69    | 5.25    | 7.11    | 0.49    |
| As      | PPM   | INA    | ACT 0.5  |                               | 2200    | 2400    | 6100    | 39000   | 30000   | 11000   | 9500    | 100000  | 45000   | 210     | 110     | 32000   | 61000   | 40600   |
| Ba      | PPM   | TICP   | ACM 1    |                               | 65      | 395     | 24      | 35      | 10      | 357     | 486     | 61      | 26      | 94      | 116     | 314     | 55      | 23      |
| Bi      | PPM   | TICP   | ACM 5    |                               | <.5     | <.5     | <.5     | 84      | 76      | <.5     | 5       | 29      | 121     | <.5     | <.5     | 27      | <.5     | 20      |
| Ca      | %     | TICP   | ACM 0.01 |                               | 0.11    | 7.35    | 8.75    | 0.02    | 0.02    | 0.09    | 0.12    | 0.14    | 0.02    | 4.85    | 1.41    | 2.08    | 4.77    | 0.04    |
| Cd      | PPM   | TICP   | ACM 0.4  |                               | <.4     | 0.4     | <.4     | 5.2     | 3.5     | 2.2     | 1.3     | 5.5     | 8       | 0.4     | <.4     | 6.3     | <.4     | 2.8     |
| Co      | PPM   | INA    | ACT 1    |                               | <1      | 3       | 3       | <1      | 2       | <1      | <1      | <1      | 8       | 25      | 22      | 8       | 11      | 1       |
| Cu      | PPM   | TICP   | ACM 2    |                               | 11      | 59      | 54      | 434     | 482     | 96      | 27      | 824     | 518     | 45      | 40      | 127     | 14      | 6       |
| Fe      | %     | INA    | ACT 0.01 |                               | 0.36    | 4.07    | 3.76    | 3.65    | 2.9     | 1.33    | 1.46    | 17.2    | 4.48    | 3.72    | 5.21    | 4.11    | 7.95    | 4.46    |
| Hg      | PPB   | FLA    | ACM 10   |                               | 12465   | 4095    | 10440   | 855     | 1360    | 160     | 225     | 3735    | 1175    | 1135    | 1065    | 1005    | 225     | 265     |
| K       | %     | TICP   | ACM 0.01 |                               | 0.24    | 0.25    | 0.22    | 0.08    | 0.06    | 3.29    | 3.8     | 0.41    | 0.13    | 0.08    | 0.13    | 1.71    | 2.63    | 0.16    |
| Mg      | %     | TICP   | ACM 0.01 |                               | 0.04    | 2.62    | 3.67    | 0.01    | 0.01    | 0.39    | 0.48    | 0.06    | 0.02    | 2.12    | 0.1     | 0.68    | 1.08    | 0.04    |
| Mn      | PPM   | TICP   | ACM 5    |                               | 56      | 1164    | 832     | 20      | 19      | 36      | 51      | 8       | 13      | 686     | 870     | 363     | 982     | 18      |
| Mo      | PPM   | INA    | ACT 1    |                               | <2      | <2      | <2      | <17     | <9      | <1      | <1      | <1      | <1      | <1      | <1      | <11     | <24     | <19     |
| Na      | %     | INA    | ACT 0.01 |                               | 0.07    | 0.06    | 0.07    | 0.03    | <0.01   | 0.1     | 0.13    | 0.11    | 0.12    | 0.08    | 0.08    | <0.01   | <0.02   | <0.01   |
| Ni      | PPM   | TICP   | ACM 2    |                               | <2      | 6       | 5       | 3       | 4       | 2       | 2       | <2      | 4       | 29      | 28      | 18      | 21      | 4       |
| P       | %     | TICP   | ACM 0.01 |                               | 0.059   | 0.017   | 0.015   | 0.01    | 0.008   | 0.018   | 0.066   | 0.066   | 0.013   | 0.113   | 0.124   | 0.051   | 0.071   | 0.003   |
| Pb      | PPM   | TICP   | ACM 5    |                               | <.5     | 23      | 266     | 6213    | 23184   | 519     | 288     | 14440   | 15574   | 15      | 8       | 494     | 52      | 1042    |
| Sb      | PPM   | INA    | ACT 0.1  |                               | 220     | 380     | 250     | 78      | 70      | 14      | 20      | 240     | 82      | 4.6     | 2.5     | 29      | 62      | 46      |
| Se      | PPM   | INA    | ACT 3    |                               | <3      | <3      | <3      | 13      | 17      | <3      | <3      | 20      | 11      | <3      | 4       | 6       | <3      | 5       |
| Se      | PPM   | UTIC   | ACM 3    |                               | n/a     | n/a     | n/a     | 15.5    | 20.4    | <3      | n/a     | 28.2    | 25.4    | n/a     | n/a     | 14.3    | <3      | 13.6    |
| Tl      | %     | TICP   | ACM 0.01 |                               | 0.73    | 0.1     | 0.05    | <.01    | <.01    | 0.21    | 0.56    | 0.01    | <.01    | 0.49    | 0.52    | 0.18    | 0.2     | 0.01    |
| Tl      | PPM   | UTIC   | ACM 2    |                               | n/a     | n/a     | n/a     | 10.7    | 7.6     | 3.3     | n/a     | 10.9    | 17.9    | n/a     | n/a     | 15.1    | <2      | 13.1    |
| V       | PPM   | TICP   | ACM 2    |                               | 206     | 65      | 41      | 7       | 5       | 82      | 191     | 30      | 10      | 202     | 234     | 82      | 127     | 8       |
| W       | PPM   | INA    | ACT 1    |                               | 18      | <2      | <1      | <1      | <4      | <1      | <5      | <1      | <1      | <1      | <1      | <1      | <1      | <1      |
| Zn      | PPM   | TICP   | ACM 2    |                               | 6       | 70      | 135     | 149     | 89      | 41      | 38      | 271     | 243     | 86      | 66      | 491     | 28      | 312     |

Notes:

Fe\*, Cr = Possible Fe & Cr contamination from grinding  
 INA = Thermal neutron activation analysis  
 TICP = HClO4-HNO3-HCl-HF digestion - inductively coupled plasma emission spectroscopy  
 UTIC = Aqua regia digestion - ultratrace inductively coupled plasma emission spectroscopy  
 FLA = Flameless AAS  
 ACT = Act.Labs, Ancaster, Ontario  
 ACM = ACME Analytical

Sample descriptions:

GR97-43 Trench grab - white clay  
 GR97-44 Trench grab - silicification+realgar+arsenopyrite+pyrite veins  
 GR97-45 Trench grab - chalcadonic silica+scorodite  
 GR97-46 Trench grab - bladed quartz vein  
 GR97-47 Trench grab - bladed quartz vein  
 GR97-48 Trench grab - grey, clay-altered wallrock  
 GR97-49 Trench grab - grey, clay-altered wallrock  
 GR97-50 Trench grab - gouge+grey-altered wallrock - high Au (3.4 oz/ton)  
 GR97-52 Trench grab - bladed quartz+scorodite+galena+arsenopyrite  
 GR97-53 Surface grab - limonite-weathered grey-green rock  
 GR97-54 Surface grab - limonite stained arkosic sandstone  
 GR97-55 Drill hole grab, DDH97-06@186.5 m, quartz vein+graphitic rock  
 GR97-56 Drill hole grab, DDH 97-03@244.33 m, graphitic sheared rock+massive arsenopyrite+cubic pyrite  
 GR97-57 Drillhole grab, DDH 97-06, 113.5 m, quartz vein and white (clay) wallrock

Locally, gently south-dipping, coarsely bladed cockscomb quartz-sulphide veins are separated by thin gouge layers (Figure 5). These veins appear to be sigmoidal tension veins, however, it is unclear whether the veins are pre-shear in age or whether they developed in dilational zones during the thrusting movement. In other places, greyish-white clay-altered sandstone is cut by a stockwork of coarsely bladed, cockscomb, auriferous quartz veins (Figure 6). Overall, this zone of shearing and brecciation is interpreted to be a north or northeast-directed thrust fault, and could represent the upper plane of the Watson Bar thrust.

Drill hole cross-sections also suggest, in a larger sense, that the carbonaceous/quartz-sulphide zone is an undulating, anastomosing series of parallel, conformable thrusts (Figure 3). However, there are typically two distinct mineralized zones that locally merge to form one thick zone up to 35 metres thick (Figure 3). The upper zone is typically richer in Au and is situated from five to ten metres below the carbonaceous hangingwall and is less than ten metres in thickness. The top of the lower zone lies from 20 to 30 metres beneath the upper plane and it can be as much as fifteen metres thick.

A contoured plan of Au grade times thickness in drill intersections shows that there are two or three trends of gold enrichment and/or thickening of the mineralized zone (Figure 7). These trends have northerly, easterly, and southeasterly azimuths. These enriched zones may be due to smearing and/or elongation of the gold mineralization due to the north or

northeasterly directed shearing. Alternatively, they may represent unrecognized cross faults which could have acted as channelways for mineralizing fluids.

### Mineralogy

Gold at the Zone V trench occur in the following settings: (1) in deformed, fractured, coarse-bladed, drusy, cockscomb quartz-carbonate-sulphide veins, (2) in black carbonaceous gouge material which contains broken-up quartz-sulphide veins, and (3) less commonly, in bleached, clay-altered sandstone which locally forms wallrock to the quartz veins. Analyses for gold and other metals are presented in Table 2.

Visible gold is seen locally in the quartz veins, and free gold can be panned from scorodite-rich quartz vein material taken from the main trench (Figures 5, 6). The quartz veins grade up to 233.8 ppm Au in grab samples (Dürfeld, 1996). Individual veins are generally less than 20 centimetres in width and consist of bladed, cockscomb quartz crystals up to 5 centimetres in length and interstitial carbonate and sulphides. The quartz is commonly deformed and brecciated and contains abundant coarse-grained euhedral arsenopyrite, pyrite and lesser galena, sphalerite and chalcopyrite (samples GR97-46, 47, 57, Table 2). Gangue minerals are predominantly quartz with lesser calcite and/or dolomite. The bladed habit of the quartz crystals suggest that they are pseudomorphs after early formed calcite and this is one feature suggesting it developed in an epithermal environment.

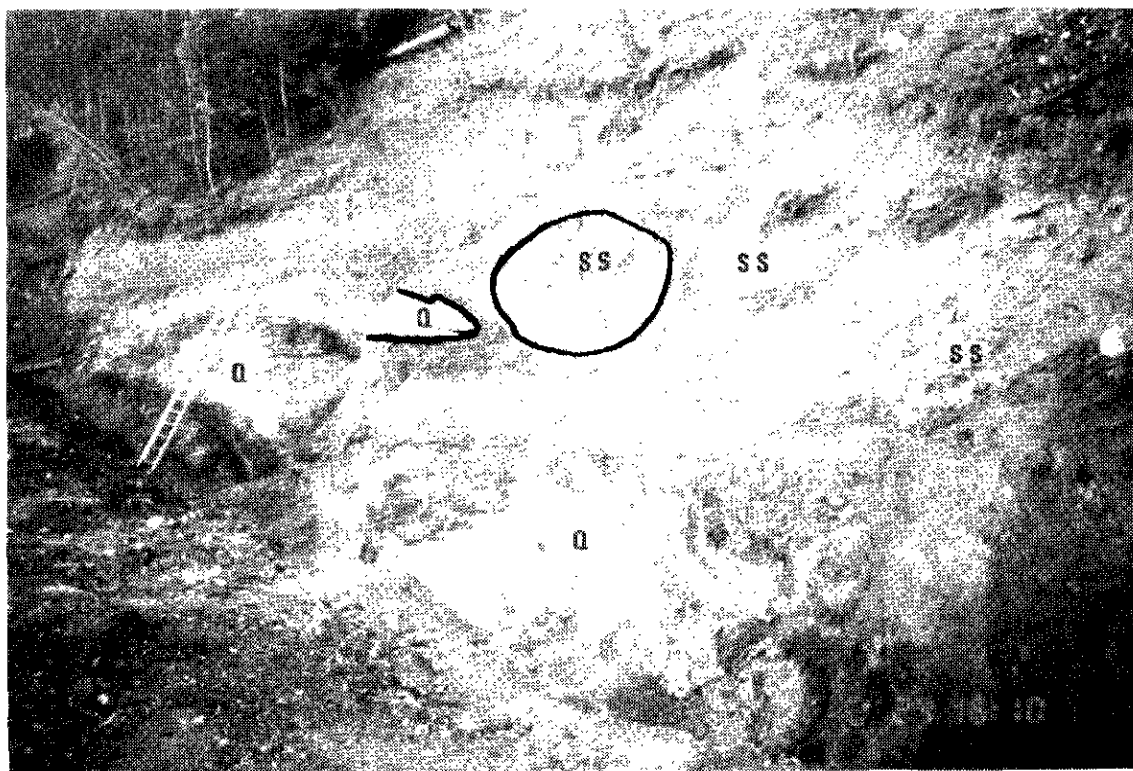


Figure 4. Zone V trench, looking south. Note rounded, milled blocks and boudinaged beds of unaltered sandstone (SS) and quartz-veined and clay-altered sandstone (Q) surrounded by sheared carbonaceous material (black).

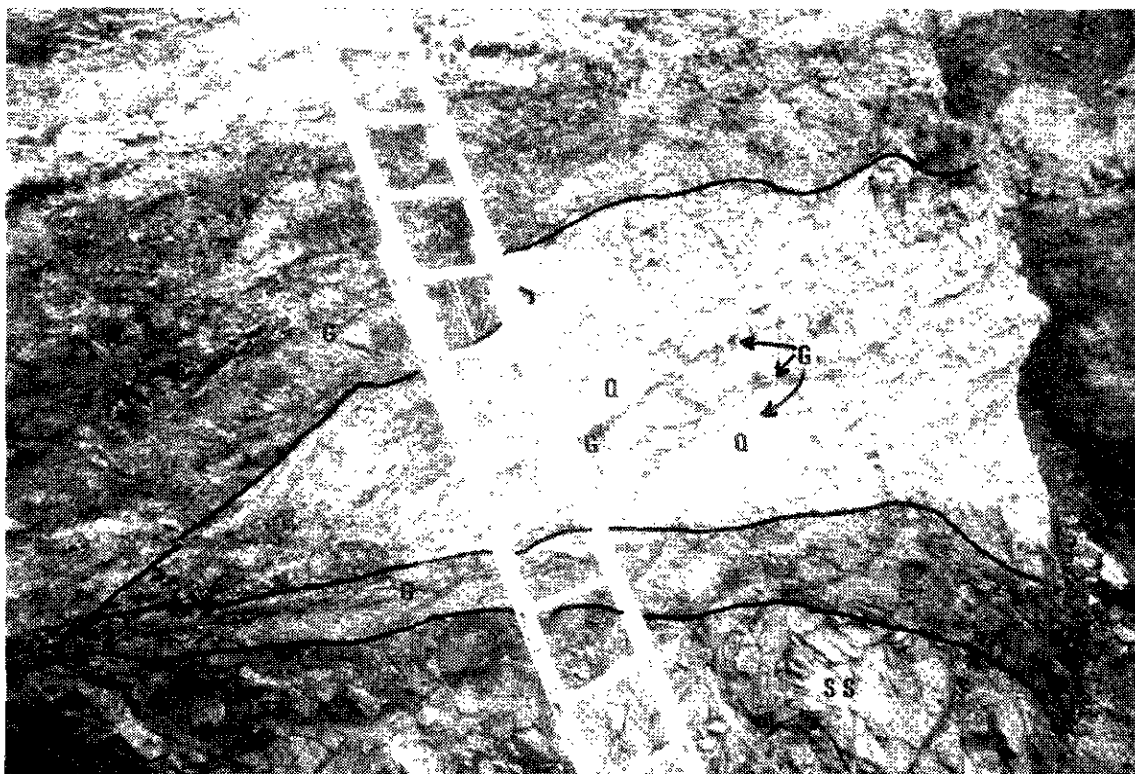


Figure 5. Zone V trench, looking southwest. Note coarsely bladed, cockscomb, auriferous quartz-sulphide veins (Q) separated by dark grey, contorted carbonaceous gouge (G). Lower bed is relatively unaltered sandstone (SS).

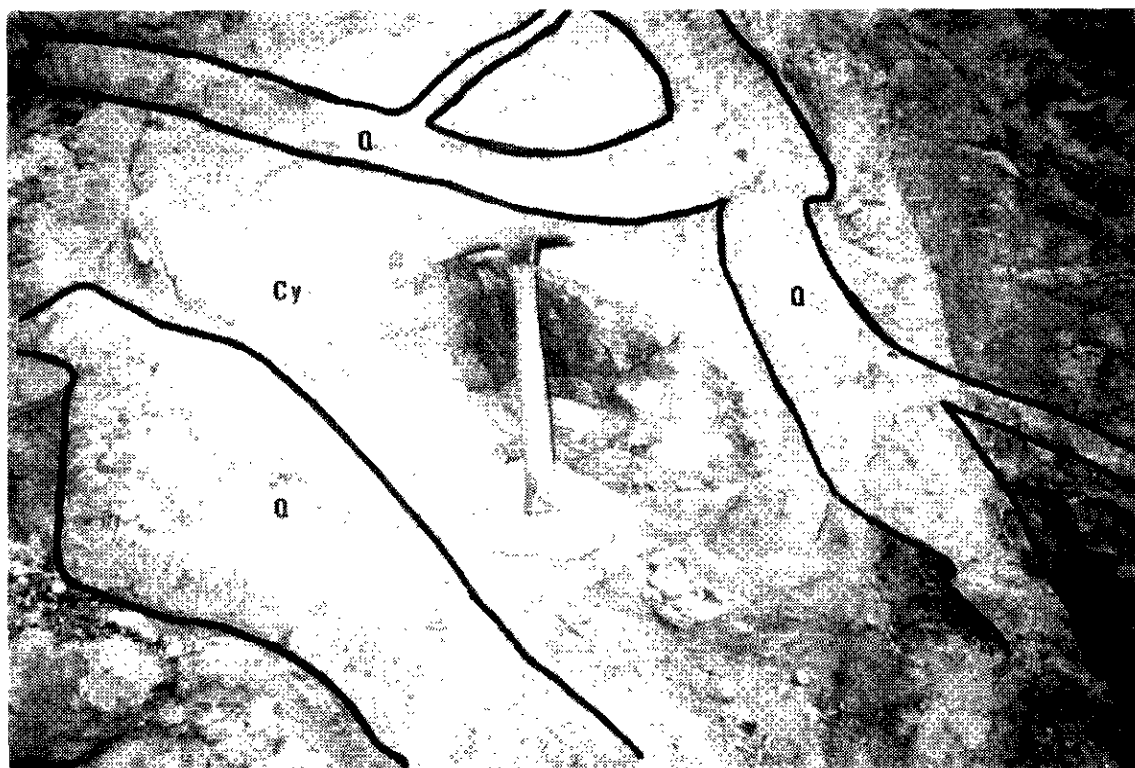


Figure 6. Zone V trench, looking southwest. Note stockwork of auriferous cockscomb quartz-sulphide veins (Q) cutting bleached, clay-altered sandstone (Cy).

Ore-grade gold values also occur in various types of gouge including black, foliated carbonaceous material that often contain fragments of fractured quartz-sulphide vein together with disseminated fine grained pyrite and arsenopyrite (sample GR97-56, Table 2). An XRD analysis from DDH 97-08 indicates that graphite, muscovite, chlorite, and quartz are present, with possibly some realgar and ankerite.

Gold values also occur in the greyish-white, clay-altered sandstone wallrock lying adjacent to quartz veins (samples GR97-48 and 49, Tables 1 and 2; Figure 6). Whole rock data show these rocks to contain abundant  $\text{SiO}_2$ ,  $\text{Al}_2\text{O}_3$ ,  $\text{Fe}_2\text{O}_3$ , and  $\text{K}_2\text{O}$ . This is consistent with XRD analyses indicating the presence of illite/muscovite, quartz, scorodite, kaolinite-smectite and pseudorutile.

## LITHOGEOCHEMISTRY

Most drill core from the Second-Ulcer property has been subjected to comprehensive fire assays and multi-element ICP analyses and these results are presented by Dürfeld (1992, 1996). A review of these data shows that in addition to gold, the mineralization at Zone V contains high quantities of silver (to >200 ppm), arsenic (to >10000 ppm) and lead (to >1%). Locally, the gold-rich zones may be moderately to highly enriched in bismuth (to 329 ppm), cadmium (to >100 ppm), copper (to 3216 ppm), antimony (to 225 ppm), zinc (to >1%), and tungsten (to 61 ppm). The Ag/Au ratio at Zone V is variable, ranging between 0.1 and 25.3 but averages 2.0, based on 47 fire assays from drill core.

The highest gold, silver and associated metal values in Zone V correlate with the quartz-carbonate-sulphide veins, carbonaceous material and gouge. In general, the content of all metals increase sharply below the hangingwall of the uppermost, thick, brecciated, quartz and sulphide-bearing, carbonaceous thrust fault zone in each hole. In most holes there are upper and lower mineralized zones separated by up to 20 metres of barren, weakly to unaltered sandstone. In some holes, consistently anomalous gold values (>500 ppb) extend for as much as 35 metres, across the entire thrust zone.

As part of this study, a small number of multi-element geochemical analyses were completed on mineralized, weakly mineralized and unmineralized samples collected from Zones V, I and IV (Table 2). Mineralization at Zone V is highly enriched in Au, Ag, As and Pb, and moderately enriched in Sb, Cu, Zn, Cd, Bi, Se, Tl and Hg.

By contrast, the altered rocks from Zone IV contain high levels of Sb and Hg but only weak to moderate amounts of As, Pb and Zn and background values in Au, Ag and Cu. The high Sb and Hg values and the presence of chalcedonic silica and kaolinite alteration suggest that Zone IV formed part of an epithermal hot spring system, and perhaps lay above the level where an enrichment in Au-Ag-Cu-Pb-Zn values could be expected.

Intrusive sills in Zone V are generally devoid of anomalous metal values, although 800 metres to the south,

at Zone I, drillholes have intersected mineralized sills at the same stratigraphic position as Zone V. These sills are sericitized and silicified quartz-feldspar porphyries and are cut by auriferous quartz-arsenopyrite-pyrite veins and carbonaceous material.

## DISCUSSION

The Zone V gold-silver-base metal occurrence is a structurally controlled, low sulphidation, epithermal deposit similar to those described by White and Hedenquist (1995). Evidence for this origin include (1) the predominant occurrence of gold in coarsely bladed, cockscomb, cavity-filled quartz-carbonate-sulphide veins, (2) the association with sericite-pyrite and local clay (illite, smectite, kaolinite) wallrock alteration, and (3) the consistent association of Au-Ag-As-Pb with local zones of moderate to highly anomalous Bi, Cd, Cu, Hg, Sb, Se, Tl, W, and Zn values. The deposit is unusual in its occurrence in a thrust fault zone, its feldspathic arenite host rocks, and the abundance of carbonaceous material. In addition, its Ag/Au ratio of about two is anomalously low for epithermal deposits which are generally more silver-rich.

The timing of mineralization in relation to intrusion of porphyry sills, thrust faulting and alteration is so far poorly constrained. In the Watson Bar gold belt regionally extensive iron carbonate alteration is spatially, and possibly temporally, associated with a belt of small porphyry bodies. Sills at Zone V are unmineralized, only weakly altered, and exhibit no obvious association with the gold mineralization. However, at Zone I, to the south, similar quartz-feldspar porphyry sills are silicified, sericitized and cut by auriferous quartz-sulphide veins. Therefore, we believe that the main phase of Au mineralization in the area is genetically related to the sills.

The thrusting event at Zone V is probably in part older or coeval with, and in part younger than the mineralization. Some of the veins have the appearance of sigmoidal tension veins which have grown in place during movement on the thrust (Figure 5). These veins dip shallowly south, are oblique to the thrust surface, and consist of cockscomb quartz-carbonate-sulphide veins separated by thin gouge layers. The cockscomb quartz veins are delicate and it seems unlikely that blocks of this material could have remained intact during extensive thrusting. Other evidence, however, suggests that some of the thrust movement took place after mineralization, such as the presence of (1) brecciated vein material in sheared carbonaceous gouge, and (2) large, rounded and milled blocks of unaltered sandstone intermixed with blocks of altered and mineralized rock (Figures 5, 6). Although the amount of movement is unknown, the upper plate of the thrust apparently moved in a northerly or northeasterly direction. Thus, the source of the mineralized blocks was probably to the south or southwest of the current Zone V drilling.

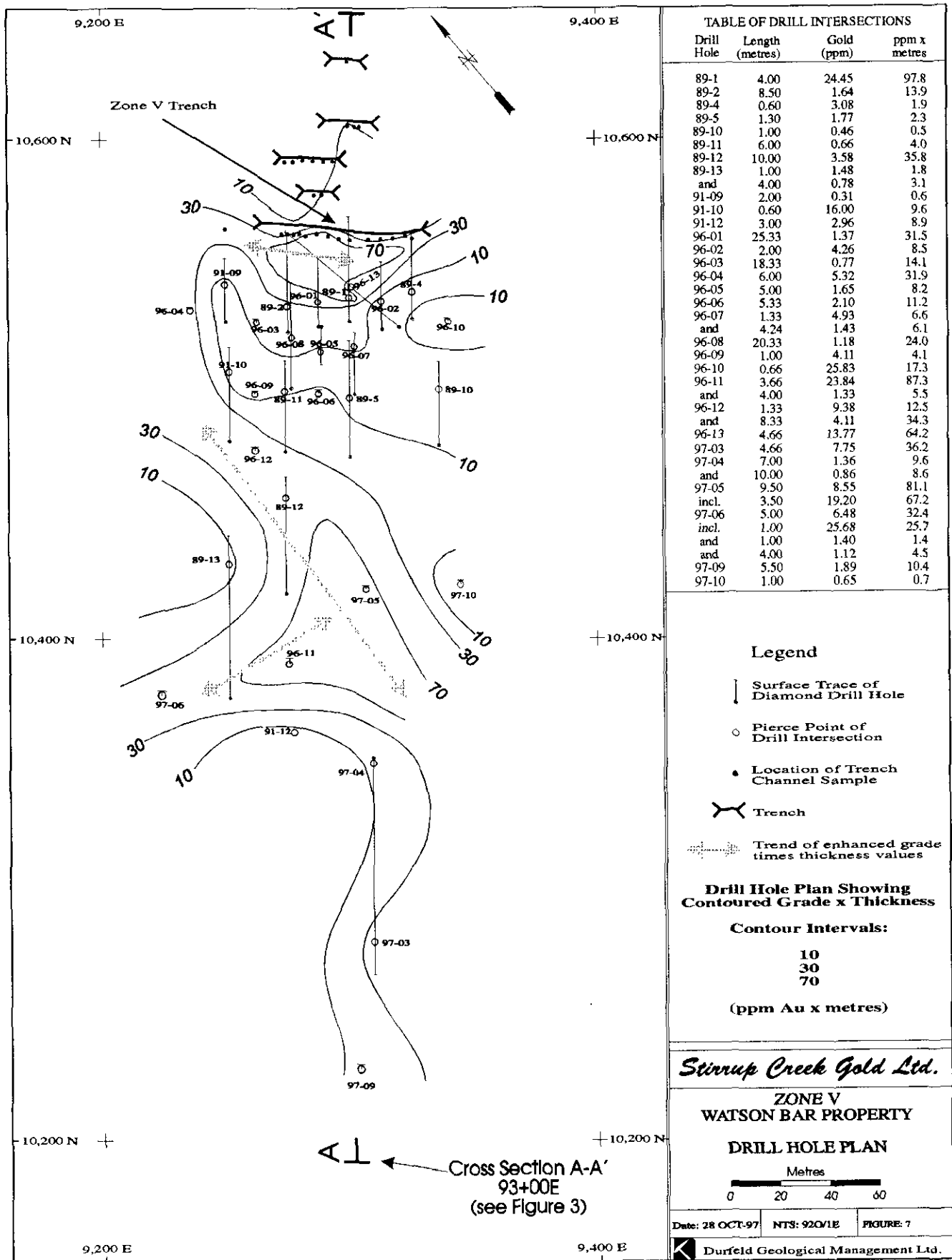


Figure 7. Grade times thickness plot of drill hole pierce points in Zone V showing northerly, easterly and southeasterly enrichments.

## CONCLUSIONS

This study has the following implications for exploration at Zone V and the Watson Bar gold belt:

- Low sulphidation, epithermal precious-metal mineralization, comprising the Watson Bar gold belt, occurs over a 25 kilometres long area. Regionally, the occurrences are spatially associated with small intrusive bodies and widespread iron carbonate alteration. On a local scale, however, some occurrences such as the Zone V mineralization, are associated with sporadic sericite-pyrite and clay alteration which overprints the older iron carbonate alteration. These more advanced alterations are a better guide to gold mineralization.

- The mineralization discovered at Zone V indicates that thrust faults are an excellent structural host for mineralization in the Watson Bar gold belt. The Watson Bar thrust and other low angle structures in the belt have the potential for similar mineralization.

- A strong association exists between the auriferous quartz-sulphide veins and sheared carbonaceous material at Zone V. It is possible that the carbon has acted as a chemical trap for gold and other metals. This carbonaceous material may represent sheared argillaceous sedimentary rocks, or alternatively, it may have formed through hydrothermal transportation and re-deposition of carbon during or prior to gold mineralization.

- Barren silicification and kaolinite alteration with anomalous Hg, Sb and As at Zone IV may represent epithermal mineralization formed at a very high level. Blind epithermal deposits containing Au, Ag, Cu, Pb, and Zn may underlie these barren alteration zones.

- Mineralization discovered at Zone V provides evidence that the Watson Bar gold belt has the potential for hosting both high-grade, bonanza veins, as well as bulk tonnage gold deposits.

## ACKNOWLEDGEMENTS

We would like to thank Larry Reaugh of Stirrup Creek Gold Ltd. for permission to publish the results of this study. Ron Britton, John Harrop and Peter Bradshaw of First Point Minerals Corp. provided a useful tour and helpful discussions regarding mineralization on the Mad claims. Bruce Madu is thanked for his assistance in computer drafting of Figure 1.

## REFERENCES

- Duffell, S. and McTaggart, K.C. (1952): Ashcroft Map-Area, British Columbia; *Geological Survey of Canada*, Memoir 262, 122 pages.
- Dürfeld, R.M. (1990): Report on Diamond Drilling, Watson Bar Project; *B.C. Ministry of Energy, Mines and Petroleum Resources*, Assessment Report 19777.
- Dürfeld, R.M. (1992): Report on Trenching and Diamond Drilling, Watson Bar Property; *B.C. Ministry of Energy, Mines and Petroleum Resources*, Assessment Report 22497.
- Dürfeld, R.M. (1996): Drilling and Trenching Report on the Watson Bar Mineral Project; *B.C. Ministry of Energy, Mines and Petroleum Resources*, Assessment Report 24676.
- Dürfeld, R.M. and Jackson, A.W. (1990) Report on Geology, Geochemistry, Trenching, Induced Polarization and Diamond Drilling, Watson Bar Project; *Unpublished Internal Report for Cyprus Gold (Canada) Ltd.*
- Dürfeld, R.M. and McClintock, J.A. (1987) Geological and Geochemical Report on the Second Claim Group; *B.C. Ministry of Energy, Mines and Petroleum Resources*, Assessment Report 16879.
- Girling, C.A., Peterson, P.J., and Warren, H.V. (1979): Plants as Indicators of Gold Mineralization at Watson Bar, B.C.; *Economic Geology*, Volume 74, pages 902-907.
- Hickson, C.J., Mahoney, J.B. and Read, P. (1994): Geology of Big Bar Map area, B.C.; in *Current Research 1994A, Geological Survey of Canada*, pages 143-150.
- Kleinspehn, K.L. (1985): Cretaceous Sedimentation and Tectonics, Tyaughton-Methow Basin, Southwestern B.C.; *Canadian Journal of Earth Sciences*, Volume 22, pages 154-174.
- Lisle, T.E. (1988): Report on the Drilling and Prospecting Program on the Mad Claim Group; *B.C. Ministry of Energy, Mines and Petroleum Resources*, Assessment Report 17781.
- Lisle, T.E. and McAllister, S.G. (1989): Geological, Geophysical and Diamond Drilling Report on the Watson Project (M584), Warren Option; *B.C. Ministry of Energy, Mines and Petroleum Resources*, Assessment Report 18352.
- Livingston, K.W. (1982): Geological and Geochemical Report, Watson Bar Prospect; *B.C. Ministry of Energy, Mines and Petroleum Resources*, Assessment Report 10381.
- McClintock, J.A. and Dürfeld, R.M. (1988) Geological and Geochemical Report on the Second Claim Group; *B.C. Ministry of Energy, Mines and Petroleum Resources*, Assessment Report 17473.
- Price, B.J., Livingston, K.W. and Howell, W.A. (1981): Watson Bar, Geological and Geochemical Report; *B.C. Ministry of Energy, Mines and Petroleum Resources*, Assessment Report 9462.
- Trettin, H.P. (1961): Geology of the Fraser River between Lillooet and Big Bar Creek; *B.C. Ministry of Energy, Mines and Petroleum Resources*, Bulletin 44, 109 pages.
- Tipper, H.W. (1978): Taseko Lakes (920) Map-Area; *Geological Survey of Canada*, Open File 534.

Warren, H.V. (1982): The Significance of a Discovery of Gold Crystals in Overburden; in Precious Metals in the Northern Cordillera; Levinson, A.A. editor, *The Association of Exploration Geochemists*, pages 45-51.

Warren, H.V. and Hajek, J.H., 1973, An Attempt to Discover a "Carlin-Cortez" type of gold deposit in B.C., *Western Miner*, Number 46, pages 124-134.  
White, N.C. and Hedenquist, J.W. (1995), Epithermal Gold Deposits: Styles, Characteristics and Exploration; *Society of Economic Geologists Newsletter*, Number 23, pages 1, 9-13.





## METALLOGENY OF THE SLOCAN CITY MINING CAMP (82F11/14)

By B.N. Church (P.Eng.), B.C. Geological Survey

**KEYWORDS:** Slocan veins, silver-lead-zinc, Nelson batholith, Kootenay Arc.

### INTRODUCTION

The Slocan area has had a long and illustrious mining history which has fluctuated from periods of intense exploration to inactivity (Figure 1). Prospecting in the West Kootenays dates back to the 1820's when the Bluebell deposit near Riondel on Kootenay Lake was discovered. Active exploration began around 1865. In 1883 Thomas Hammil located the Lulu and Spring claims at Ainsworth and Jim Brennan, a prospector working west of Ainsworth in the late 1880's, collected some high grade silver samples which attracted considerable attention to this new and virtually unexplored area. After initial interest at Sandon, prospectors extended their range of exploration to the south and west, discovering several deposits containing appreciable gold on Memphis Creek and locating the Dayton claim near Slocan City in 1893.

During this period, sustained mining throughout the Slocan area provided the incentive for the Canadian Pacific Railway to extend their line south and east from Nakusp to Kaslo and Cody in 1895, and connect Slocan City with the Nelson line in 1897. Slocan soon became one of the most productive mining camp in the province. The ore was shipped to smelters at Trail and Nelson from numerous local concentrating mills. Peak production in the Slocan was attained in 1918.

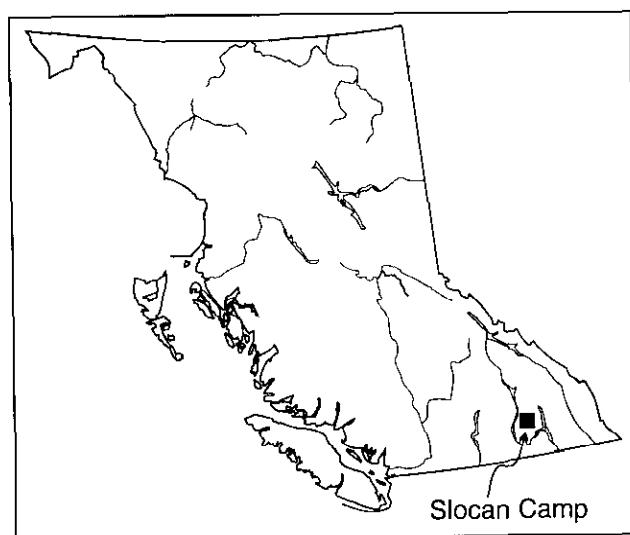


Figure 1. Location map, Slocan City mining camp.

### GEOLOGICAL SETTING

The geology of the Slocan area (82FNW) comprises diverse lithological elements belonging to several tectonic terranes (Figure 2). On a regional scale, the Slocan Mining Camp is within the Kootenay Arc which lies between the Precambrian Purcell anticlinorium on the east and the Monashee and Valhalla metamorphic complexes to the west and northwest (Reesor, 1965).

The Kootenay arc is a 400 km long curving belt of early Paleozoic to Mesozoic sedimentary, volcanic and crystalline metamorphic rocks trending northeast for 160 kilometres across Washington state into British Columbia, then north along Kootenay Lake and northwest into the Revelstoke area.

In the Kootenay Lake area, the arc succession comprises the Hamill, Lardeau, Milford, Kaslo, Slocan and Rossland groups. The Hamill and Lardeau constitute the early Paleozoic pericratonic Kootenay terrane; the Milford and Kaslo belong to the accreted late Paleozoic Slide Mountain terrane. The Hamill is mostly quartzite; the Lardeau has a lower calcareous section overlain by a thick succession of schists and quartzites with lenticular masses of volcanic rock. The Milford and Kaslo groups are late Paleozoic oceanic assemblages that include phyllites, thinly bedded calc-silicate metasedimentary rocks, chert beds, basic volcanic rocks and serpentinites (Fyles, 1967).

The Mesozoic formations constitute the Quesnel terrane that lies along the western side and within the curvature of the Kootenay arc. The Rossland volcanics (Hoy and Dunne, 1997) and the Slocan argillite, slate and limestones are important units in this terrane and contain significant mineral deposits such as found in the Slocan silver-lead-zinc camp.

Granitic plutons including several small batholiths, many stocks and sill-like masses, interrupt the continuity of the older deformed stratigraphic succession throughout the Kootenay Arc. These include the Nelson batholith and many smaller stocks and sill-like masses. They are predominantly granite and granodiorite although the compositions range widely. The Nelson plutonic rocks are generally considered to be Upper Jurassic or Lower Cretaceous (Sevigny and Parrish, 1993).

The Nelson batholith and many of the granitic stocks have local zones of intense deformation around their margins. On the north and western edge of the Nelson batholith older strata are buckled downward within 1 kilometre or so of exposed granitic rock. Regional structures are deflected into near parallelism with the margins of the intrusion. It may be that the warps

preceded and controlled the emplacement of the granitic masses or, possibly, forceful intrusion deformed the wallrocks accompanied, or followed by, marginal zones of faulting.

Small Tertiary intrusions are common in the southern part of the arc and west of it. These include stocks of fresh granite and augite-biotite syenite and monzonite.

All the rocks are cut by lamprophyre dikes which follow fractures, faults or prominent foliation planes and range from small discontinuous masses to bodies a few tens of metres wide and a few thousand metres long. They are dark greenish grey or brownish rocks commonly with subhedral phenocrysts of biotite, feldspar, hornblende or augite. These dikes are undeformed and mainly Tertiary age (Beaudoin, 1991).

## Nelson Plutonic Rocks

The Nelson batholith underlies much of the western part of the Kootenay district where it is a complex of intrusives rocks differing in structure, texture and composition. It was first examined by Dawson (1890), and named the "Nelson granite" by McConnell and Brock (1904). The batholith is the principal rock type within the Slocan City camp and in this area it is subdivided into three phases (Cairnes, 1934) - granitic porphyry, crushed porphyry, and massive equigranular granite and granodiorite (Figure 2).

The granitic porphyry is the predominant phase and hosts most of the ore deposits (Photo 1). It is characteristically coarse-grained and distinguished by rectangular phenocrysts (megacrysts) of K-spar, commonly several centimetres long and comprising up to 50 per cent of the rock. The K-spar megacrysts are simple or Carlsbad twins of perthitic orthoclase replaced locally by microcline. Exposed surfaces of the rock are light grey with a flesh-colour hue due to weathering of the K-spar. The megacrysts are set in a coarse grained groundmass comprising subhedral plagioclase ( $An_{30-50}$ ), anhedral quartz, irregular clots of amphibole and biotite, interstitial microcline, and minor amounts of apatite, sphene, magnetite and sulphides. Thin sections and chemical analyses indicate that the rock is a silica-poor granite verging to monzonite composition, having roughly equal amounts of alkali feldspar and plagioclase and an alkali/lime index greater than 1 (Table 1). The granite facies, such as found at the Meteor, Arlington and Enterprise mines, is light coloured (colour index 5-8 per cent), compared to the monzonite facies at the Little Tim, Ottawa and Westmont mines, where the rock typically has less than 20 per cent quartz and a colour index of 9-15 per cent. Pegmatitic facies are confined to small, irregular masses in the porphyritic granite, fragments of which are seen in outcrops, the rock dumps and core samples from the Ottawa, Arlington and Chapleau mines.

The crushed porphyry forms a 100-300 metre wide band adjacent to the Slocan Lake fault along the west margin of the Nelson batholith. It is the same composition as the normal granite/monzonite porphyry and is believed to be the result of deformation caused by orogenic forces such as the intrusion of the Nelson batholith (Columbian) or detachment faulting (Laramide) associated with the development of the Valhalla metamorphic complex west of the batholith (Carr et al., 1987). The rock is commonly rust coloured as a result of alteration of ferromagnesian constituents by hydrothermal solutions moving along numerous fractures and shear planes (Parrish, 1984).

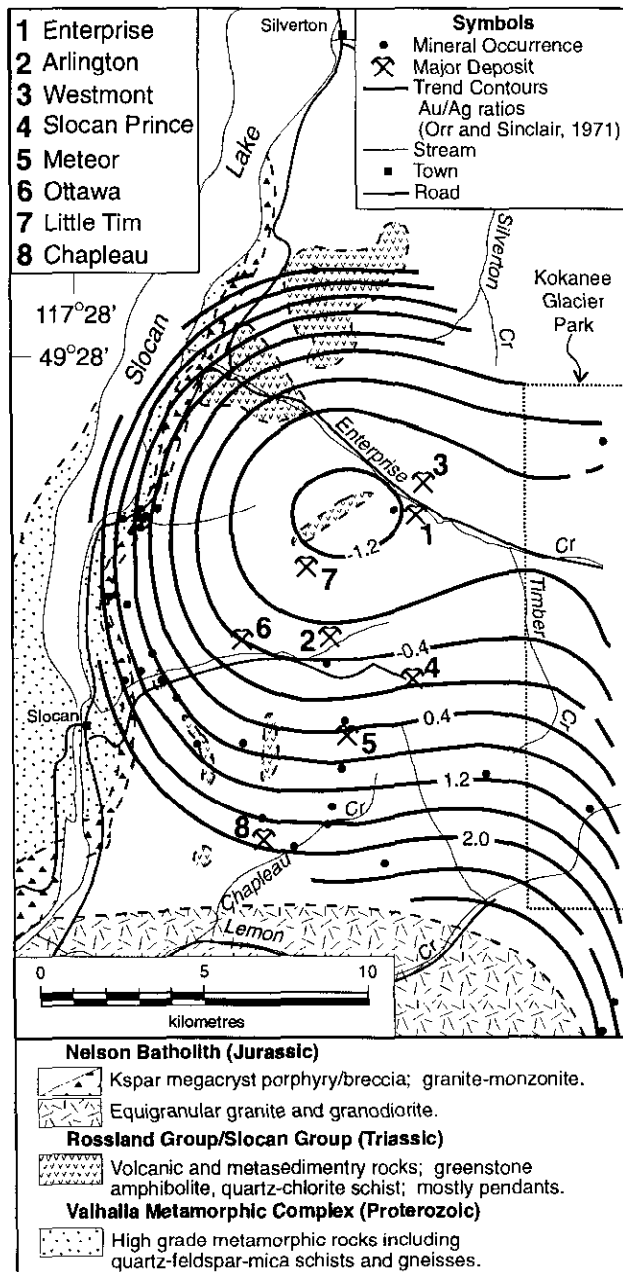


Figure 2. Geology of the Slocan City area (after Cairnes, 1934; Little, 1960); contours are 3<sup>rd</sup> order polynomial fit of Au/Ag ratios (Orr and Sinclair, 1971).



Photo 1. Nelson granitic porphyry.

Non-porphyrific facies of the Nelson batholith occur as dark coloured diorite and amphibolitic border facies and as xenoliths within the porphyry facies. Also, a large equigranular granite - granodiorite body underlies Lemon Creek and the area to the south. The dark coloured facies, containing as much as 50 per cent amphibole, may represent wholly or partially digested walls (Slocan or Rossland rocks?) of the batholith. The Lemon Creek granitic rocks may be slightly older or younger than the Nelson porphyry.

### Structural Geology

The Slocan Lake fault is a 100 kilometre long, linear detachment structure exposed above the east shore of Slocan Lake (Figure 2). It dips moderately to the east and juxtaposes a ductilely deformed 'lower plate' of retrograded gneissic rocks of the Valhalla complex with an 'upper plate' of brecciated, fractured and hydrothermally altered granitic rocks of the Nelson batholith (Parrish, 1984). The lack of penetrative fabric distinguishes plutonic rocks of the Nelson batholith from the gneisses of the lower plate. Fabrics in the shear zone associated with the fault indicate easterly down dip displacement of the upper plate. Geochronological data suggest that some ductile strain exhibited in the gneisses and faulting is early Tertiary age and superimposed on considerably older deformation structures possibly related to the original emplacement of the Nelson batholith.

The fracture frequency pattern displayed by the Nelson batholith in the Slocan City area has three principal directions based on 318 measurements. These are (1)  $030^{\circ}/70^{\circ}\text{SE}$ ; (2)  $105^{\circ}/80^{\circ}\text{S}$  and (3)  $160^{\circ}/85^{\circ}\text{SW}$  (Figure 3). Fracture sets (1) and (2) are cross joints, steeply inclined to the gently dipping Slocan Lake fault and footwall gneiss complex. The northeast-striking fracture set (1) is the main direction, similar in strike and dip to the veins at the Enterprise, Arlington and Little Tim mines (Table 2). Subsidiary fractures (2) trend easterly similar to the veins at the Meteor and Chapleau mines. Fracture set (3) coincides with a sinistral fault that cuts the main vein at the Enterprise mine. It may also be related to the listric movement associated with footwall complex as shown in Figure 4.

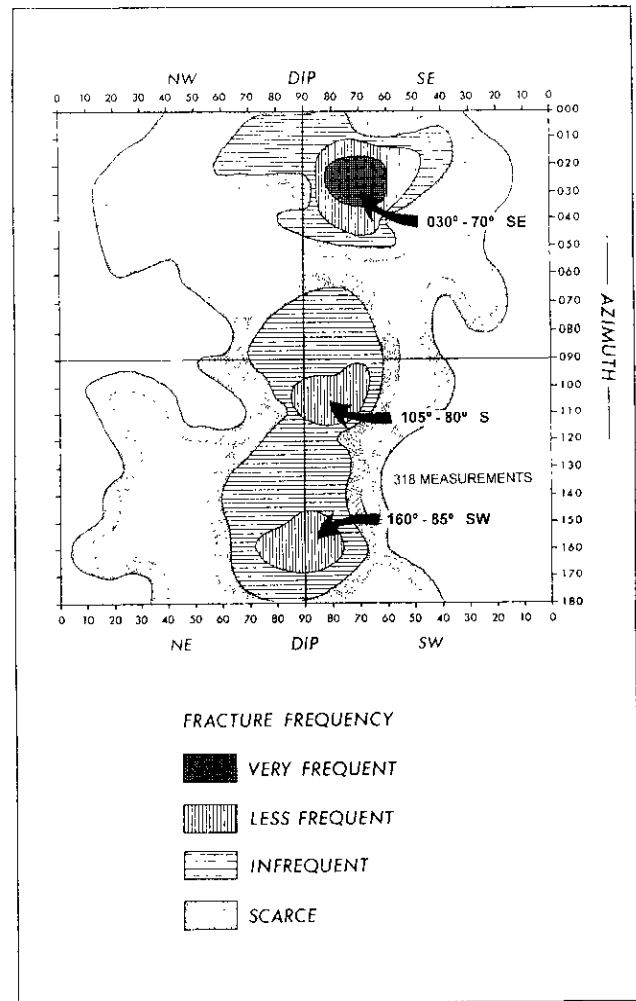


Figure 3. Fracture frequency plot.

Parrish (1984) and Carr (1985) have explained the mechanism of listric normal detachment faulting as related to the Valhalla metamorphic core complex and the overlying westerly lobe of the Nelson batholith. According to these authors, the uplift of the core complex in the early Tertiary resulted in detachment of the batholith along the lower contact of the intrusion to form the Slocan Lake fault, resulting in downward movement of the granite slab

to the east. In this listric process, the gently east-dipping Slocan Lake fault was associated with the development of steeply dipping cross fractures (normal faults) in the hanging wall due to the extension of the overlying granite slab. The combination of the Slocan Lake fault and the accompanying crushed zone (brecciation and shearing) and the cross fractures, provided a channelway system for hydrothermal solutions.

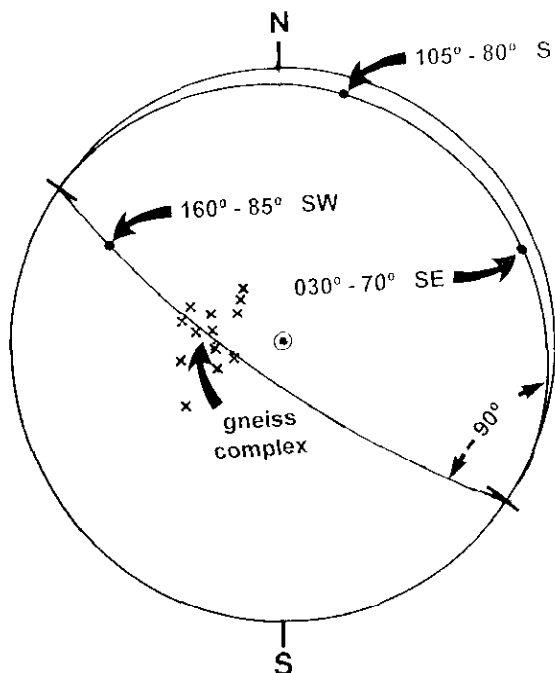


Figure 4. Stereographic projection of (lower hemisphere) of the main fracture directions related to the Nelson Batholith and adjacent gneiss complex.

It is assumed that shallow dipping contact of the Nelson batholith with the underlying Valhalla metamorphic rocks is the result of an outward and upward (ramping) movement of magma at the time of intrusion in the Jurassic. The crushed zone of granite that conforms more or less closely with the boundaries of the intrusion is probably due in part to deformation of the margins of the batholith before batholith was completely solid (Cairnes, 1934).

## MINERAL DEPOSITS

The Slocan is one of the few areas in British Columbia where small scale mining remained viable for many years because of the richness of the ores. This camp and the surrounding area includes 125 documented mineral deposits of which more than half are mineral producers - 13 mines have produced more than 1 million grams of silver. The Enterprise, Arlington and Ottawa mines have

each produced more than 30 million grams of silver plus significant amounts of lead and zinc.

Comprehensive descriptions of the mineral deposits of the region are by Cairnes (1934), Maconachie (1940), Little (1960) and Brown and Logan (1989). Specific details of the history and geology of the various properties are recorded in the numerous B.C. Minister of Mines reports and assessment reports covering the camp.

The following descriptions, arranged in order of production, are based on MINFILE reports and recent brief visits to the principal mines by the author. Where access to the old workings was limited, sampling of mine dumps proved successful and locations were checked by GPS equipment.

### *Enterprise (L. 1014; MINFILE 082FNW148)*

The Enterprise mine is foremost in the quantity and total value of ore produced in the Slocan City mining camp. The property consists of the Enterprise, Slocan Queen, Rambow, Iron Horse, Sunset, Millsite, Montezuma and Sunrise Crown granted claims and fractions. The mine is on the south side of the valley (elevation ~ 670 metres) near the confluence of Enterprise and Neepawa creeks, 11 kilometres northeast of Slocan (Photo 2). Access to the mine from the Slocan highway is via the Enterprise Creek road.



Photo 2. The headframe of No. 1 shaft, Enterprise mine.

The main vein was discovered in 1894 and mined by Enterprise (B.C.) Mines Co. Ltd. until 1901 and then by lessees. In 1928 the property was purchased by Yankee Girl Consolidated Mines Ltd. which was obliged to close operations in 1930. From 1941 to 1943 the property was leased, during which time the mine tailings and dump were re-worked. In 1944 Western Exploration Co. Ltd. purchased the property and operated it until 1953. Subsequently, until 1977, there has been intermittent production from a number of mining and salvage operations. Production from the property began in 1896 and 10,687 tonnes of ore were mined by 1977 yielding 32,676,718 g of silver, 1,674 tonnes of lead, 1,068 tonnes of zinc and ancillary gold, cadmium and copper.

The Enterprise lode has been developed by nine adits, several intermediate levels and two shafts. One shaft was sunk on the lode about 15 metres above and 90 metres southwest of the uppermost adit, and the other shaft from a point about 10 metres below and a short distance northeast of the lowest adit - the difference in elevation between the collar of the upper shaft and the bottom of the lower shaft being about 335 metres.

The rock underlying the property is a light coloured, coarse grained porphyritic granite of the Nelson batholith (Table 1, Number 2). More basic phases of the batholith, found locally in the mine workings, form irregular bodies of varying size that appear to be either digested inclusions or differentiates of the granitic magma. The Nelson rocks are intruded by a few small, hornblende porphyry and olivine-pyroxene lamprophyre dikes. Some of these dikes cut across the Enterprise lode whereas others are pre-mineral and disrupted by the same faults that cut the vein.

The main vein, averaging less than 0.3 metres wide, is continuous for more than 600 metres striking 050°, dipping 70° to 85° southeast (Table 2). On the upper levels of the mine the vein is filled with varying proportions of quartz and ore minerals, especially galena and tetrahedrite. On the lower levels, siderite and other carbonate gangue minerals are more abundant than quartz, and sphalerite is the predominant ore mineral. Most of the silver is believed to be contained in tetrahedrite and ruby silver (Photo 3).

The vein is interrupted by a major fault, or fault zone, and several minor faults and slips. The major fault intercepts the vein nearly at right angles about midway between the two shafts. The zone of faulting is 6 to 9 metres wide, strikes 160° and dips 90° to 75° northeast. The apparent displacement of the vein is about 30 metres to the left.

Aside from the extensive developments on the main Enterprise lode, some work has been done on a second lode outcropping 115 metres to the west. In 1927 it had been drifted on for about 45 metres. It is a wide shear zone composed mostly of crushed granitic rock partly cemented by quartz gangue with some calcite. It strikes 040° and dips 70° southeast. In character and width, this lode bears some resemblance to a vein developed at the Arlington mine which may be on part of a continuous structure. It seems that both lodes at the Enterprise mine and those on adjoining properties are within a single, wide zone of

fissuring, shearing and brecciation, and that to the southwest this zone passes through the Arlington, Speculator and intervening properties.



Photo 3. Sulphides and quartz filling, Enterprise vein (solid circle = 1 cm.).

#### *Arlington (L. 3648; MINFILE 082FNW152)*

The Arlington property comprises the Arlington, Burlington No. 2 and Stephanite Crown granted claims and fractions situated on the north slope of the valley near the confluence of Speculator and Springer creeks, 8 kilometres east-northeast of Slocan. Access to the property from the Slocan highway is via the Spinger Creek road.

The Arlington mine was worked extensively from 1899 through 1903, then intermittently until 1971. In 1969 and 1970 Arlington Silver Mines Ltd. stoped and shipped ore, which was mainly salvaged from the old workings, and what appears to be the northern extension of the vein system was explored by diamond drilling.

The mine was developed by eight adits over a vertical range of about 200 metres. In the early years the bulk of the ore was taken from the fifth to seventh levels and from the original discovery at surface near the shaft. In the latter years, underground work was confined to the lowest two levels.

The Arlington lode is a mineralized shear zone, about 20 metres wide, in coarse-grained hornblende granite of the Nelson batholith with basic monzonite inclusions

(Table 1, Numbers 3 and 13). The zone includes a number of parallel fissures and maintains a uniform strike of 040°, dipping 60° to 70° southeast (Table 2).

The ore is largely replacement of the country rock occurring as thin sulphide lenses on continuous fractures. The chief ore minerals are coarse to medium grained galena and sphalerite associated disseminated pyrite, chalcopyrite, stephanite, tetrahedrite and native silver (Photo 4).



Photo 4. Replacement sulphides in shear, Arlington mine (solid circle = 1 cm.).

#### ***Westmont (L. 8929; MINFILE 082FNW145)***

The Westmont property, comprising the Westmont (L. 8929), Eastmont (L. 8924), Oddfellow, White Cloud, Lily G., Yankee Girl and Clipper Crown granted claims and fractions, is situated on the north slope of the valley of Enterprise Creek, 12.5 kilometres northeast of Slocan. Access to the property is from the Slocan highway via the main Enterprise Creek road. The 0.8 kilometres of old road between the main road and the mine was reopened in 1958 and a bridge was constructed over Westmont Creek.

Development work on the Westmont property began in the 1890s although production started in 1907 and continued until 1914. The property was worked continuously. Subsequent mining until 1971, mainly by leases, was intermittent. The mine workings consist of at least four adits, located east of Westmont Creek, ranging in

elevation from 150 to 400 metres above the main road along Enterprise Creek. In 1958, the No. 4 adit was retimbered from the entry to the intersection of the main vein, a distance of 60 metres. At this time caved ground was cleared west of the intersection, for about 300 metres, to provide sufficient access to the bottom of the old stope area to re-establish natural ventilation. East of the intersection, 30 metres of drifting was done on the main vein and about 400 tonnes of ore was removed from the stope above the drift. Production from the mine to 1980 totals 3,211 tonnes of ore that yielded 11,084,830 grams of silver plus 2,058 grams of gold, 199,781 kilograms lead and 65,920 kilograms of zinc.



Photo 5. Tetrahedrite-rich ore, Westmont mine (solid circle = 1 cm.).

The property is underlain chiefly by coarse grained, porphyritic Nelson monzonite (Table 1, Number 9). The granite is traversed by basic dikes along which some renewed faulting has occurred. Faulting follows two principal directions, one striking northeast and steeply dipping, the other striking northwest and dipping steeply northeast.

The main lode, as exposed in the lower No. 3 and No. 4 adits, is mostly a steeply dipping fault-fissure zone that strikes northeast, however, at about 120 metres from the portal of these two adits the lode swings to a more easterly strike and dips 70° north (Table 2). It varies up to 2.4 metres in width and averages 1.2 metres wide. The lode is composed of broken and crushed rock partly cemented by

quartz which also forms veins and lenses 0.5 metres or more thick. The quartz is banded and also shows some comb structure. It carries disseminations, pockets and streaks of galena, sphalerite, pyrite, tetrahedrite, ruby silver, and native silver intimately associated with one another in varying proportions (Photo 5). The richest ore was found between No. 2 and No. 3 levels. In some places high silver is associated with galena but elsewhere combinations of tetrahedrite, sphalerite and native silver yield the best silver values.

### ***Slocan Prince (L. 582); (MINFILE 082FNW140):***

The Slocan Prince property, comprising the Slocan Prince (L. 582), Two Friends (L. 1020), Black Prince (L. 584), Bank of England (L. 2214) and Moonraker (L. 8939) Crown granted claims and fractions, is situated at the head of Crusader Creek, 10 kilometres east of Slocan. Access to the property from the Slocan highway is via the Lemon Creek and Crusader Creek roads.

This property was among the first staked in the Slocan City mining division and much work was done on it prior to 1900. The first production recorded was in 1896 from the Two Friends claim and this consisted of 36 tonnes of ore averaging 10,000 g/t silver and 50 per cent lead. The Slocan Prince and Black Prince had greater output, especially in the years 1901, 1905 and 1906 when ore shipments from these claims ranged to several hundred tonnes. Total ore production from the property up to 1970 amounts to 1,754 tonnes containing 7,045,304 grams of silver plus 128,781 kilograms of lead and 11,852 kilograms of zinc.

The property is underlain by coarse grained, porphyritic phases of the Nelson batholith. Granite and monzonite are the most common rocks but locally more basic phases of this intrusion are present (Table 1, Number 12). These granitic rocks are traversed by a few acid and basic dikes and many faults and shear zones, along which mineralization has occurred.

The workings comprise seven or more crosscut adits driven northerly to northwesterly and distributed from west to east across the claim group. The workings develop, principally, two fissure-vein systems referred to as the North and South lodes. The North lode outcrops on both the Bank of England and the Two Friends claims and has been traced for about 450 metres in an easterly direction almost parallel with the north and south boundaries of these claims. The north lode is intercepted by two adits on the Bank of England claim and, farther east, by two or three adits on the Two Friends claim. The lode strikes 060° to 070° and dips steeply northwest. In the Bank of England workings the mineralization is about 0.5 metre wide, nearly continuous for about a hundred metres, and consists of quartz with some calcite carrying galena, sphalerite and probably high-grade silver minerals. The lode intersects and slightly displaces a small basic dike. The Two Friends adits are situated about 135 metres to the east of the Bank of England workings by the west boundary of the claim. These adits are crosscuts to the North lode that is 1 to 3 metres wide containing a well defined galena-sphalerite

rich ore body, varying in width from a narrow streak to 35 centimetres.

The South lode is exposed in the workings on the easterly claims of the group. A crosscut adit driven 130 metres on the Slocan Prince claim intercepts this lode which strikes 020° to 030° and dips 60° northwest. The lode, which is about 6 metres wide, has been drifted on for more than 120 metres. The ore occurs on both walls but mainly along the footwall. A second adit on Black Prince ground is a crosscut for 39 metres, beyond which it follows the lode for about 120 metres. The lode is a strongly crushed zone as much as 10 metres wide. Abundant quartz partly cements and replaces the crushed rock and forms veins in places. Ore minerals occur both as disseminations and concentrations included in and associated with quartz, some siderite, and a little calcite. They comprise argentiferous galena, sphalerite, tetrahedrite, pyrite, some native silver and possibly other silver-rich minerals. No appreciable gold occurs in the ore.

### ***Meteor (L. 2893; MINFILE 082FNW137)***

The Meteor property, comprising the Meteor, Ottawa and Cultus claims and fractions, is situated at the head of Tobin Creek on the northwesterly slope of the divide between Lemon and Springer creeks, 8 kilometres east of Slocan. Access to the property from the Slocan highway is via the Lemon Creek and Chapleau Creek roads.

The Meteor Crown granted claim was staked in 1895. The initial production of ore, amounting to about 70 tonnes, was shipped in 1897 yielding 1182 grams of gold and 466,500 grams of silver. Since this time mining continued intermittently, until 1967, achieving greatest production of 1,715 tonnes of ore in 1964. Total production from the Meteor mine is 2,659 tonnes of ore yielding 4,724,994 grams of silver, 13,177 grams of gold and a small amount of lead and zinc.

The rocks underlying the property are a light coloured, coarse-grained granite porphyry phase of the Nelson batholith (Table 1, Number 1). The granite is sheared and altered near the mine workings and intruded by felsic and basic dikes. Faults, shears and joints are oriented north and north-northeast with moderate to steep dips.

The workings of the Meteor mine consist of six adits that intersect a 5-50 centimetre wide vein that strikes 105° and dips 35° north. Vein mineralization is associated with the sheared upper contact of a 3 metre wide dike and narrow off-shoot fissures.

The vein is largely quartz carrying some sphalerite, galena, tetrahedrite, stephanite, argentite and native silver (Photo 6). Pyrite and chalcopyrite are also present and associated with significant gold values. The dike, containing up to 2 per cent disseminated pyrite, is pervasively sericitized in vicinity of the vein. Both the vein and dike are dislocated by faulting that shows dip slip downward movement to the south.

Scheelite was discovered on the Nos. 2 and 4 levels as small solitary lens-shaped bodies on the Meteor vein and on No. 6 level as disseminated grains in the granitic host rocks on a well developed fracture system striking 105°

dipping 35° northerly and 140°, dipping 80° northeast (Table 2). Also, molybdenite was discovered in a fragment of quartz stockwork hosted by sericitized granite from the Meteor mine dump.

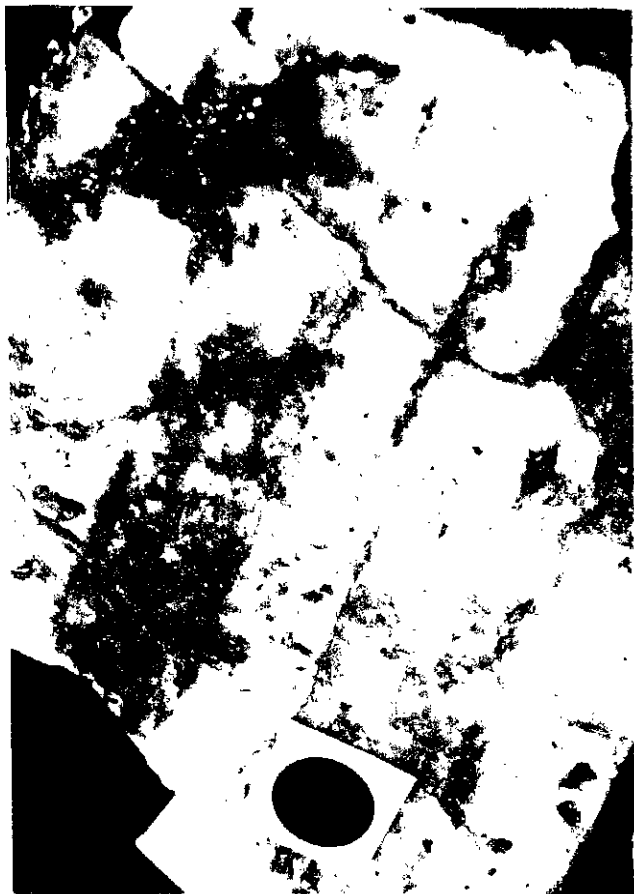


Photo 6. Sulphides in banded quartz, Meteor mine (solid circle = 1 cm.).

#### ***Ottawa (L. 4968); (MINFILE 082FNW155):***

The Ottawa mine is centred on a group of about 20 Crown granted claims and fractions on the north slope of the valley of Springer Creek (elev. ~ 1500 metres), 5 kilometres northeast of Slocan. Access to the mine site is from the Slocan highway via the Springer Creek road.

The history of the Ottawa mine dates back to 1896 when the Ottawa claim (L. 4968) was located, however, it was not until 1902 that major development work was attempted. The production of high grade silver-lead ore followed in 1903 and continued steadily through 1909. In 1913 the mine was purchased by Consolidated Mining and Smelting Co. Ltd. and in 1920 a 50-ton per day mill was constructed. In 1935 the property was obtained by the Ottawa Silver Mining and Milling Co. Ltd. who, in 1937, built a 100-ton per day flotation plant. Much of the work after 1938 was done under lease or option. In 1950 and 1951, options were held by Violamac Mines (B.C.) Ltd. and subsequently by Harrison Drilling and Exploration Co. Ltd. Total recorded production between 1903 and 1984 amounts to 22,438 tonnes mined yielding 55,940,682

grams of silver plus significant amounts of gold, lead and zinc.

The property is developed on nine levels, five of which are serviced by adits driven at vertical intervals of about 30 metres. These workings explore a broad shear/breccia zone in coarse-grained, porphyritic, Nelson quartz monzonite (Table 1, Number 8) cut by felsic and lamprophyre dikes. The zone trends nearly north and dips easterly from 25° to 45° (Table 2). The zone comprises two rather well defined lodes known as the West or Noble and East or Ottawa veins, respectively. Mining at the surface and underground indicates that these lodes are not exactly parallel, but approach each other towards the south and may join. On the No.5 level the lodes are about 10 metres apart. Most of the work has been done on the East lode that is 0.6 to 6 metres wide, composed of crushed and broken granite, gouge and vein material - the latter having been stoped in places across a width of as much as 2.4 metres. The West lode is as much as 15 metres wide in places and it is reported to have produced some good ore in the uppermost workings. On No. 8 level, the stoped vein on the West lode, strikes 025° to 040° and dips 20° southeast. The vein is up to 0.3 metres wide and bounded by a sharply defined gouge-filled slip along the footwall and an irregular hanging wall. The East lode on the No. 8 level is strong and composed of about 1 metre of gouge and beccia cemented by quartz. It strikes 170° and dips 30° to 40° east.

The ore minerals consist mostly of mixture of galena, pyrite, sphalerite and a little chalcopyrite, native silver, argentite and tetrahedrite disseminations in quartz gangue. In some high grade ore, barite is reported to be predominant gangue mineral. Beryl (aquamarine) in fragments of pink pegmatitic host rock has been found on the Ottawa mine dump.

#### ***Little Tim (MINFILE 082FNW157)***

The Little Tim mine is situated east of Ottawa Hill at the head of Little Tim Creek (elev. ~2070 metres), 8 kilometres northeast of Slocan. Access is from the Slocan highway via the Springer Creek logging road system on the Memphis Creek - Ottawa Hill branch leading to the Little Tim Creek mine road.

The Little Tim claim was staked in 1918 and worked intermittently until 1947 by the owner. Hardex Mines Ltd. held an option on the property from 1951 to 1953, during which time considerable drifting and diamond drilling was done. Several individuals have held leases since the early 1950's and all shipments from the property consist of hand sorted ore. Approximately 300 metres of drifts, crosscuts and raises were developed in the original mine and by 1981 a total of 339 metres of new drifts and crosscuts were added.

The property is underlain by coarse grained porphyritic quartz monzonite of the Nelson batholith (Table 1, Number 4). These rocks are traversed by two, nearly parallel fissure vein lodes, on which considerable work has been done. The lodes are 90 metres apart and strike 055° to 070° northeast, and dip 45° to 70° southeast (Table 2).

The mine, located just southwest and downslope from an unnamed summit, is comprised of a shaft and three adits on the northwest lode, and three adits and an intermediate level on the southeast lode - the shaft being the lowest working at an elevation of approximately 2040 metres. The shaft is reported to have followed a vein to a depth of about 15 metres. The vein, about 0.3 metres wide, consists of vuggy quartz containing disseminated, galena, sphalerite, pyrite and tetrahedrite. The same vein is heavily stoped to a point about 90 metres above the shaft. On the southeast lode, the main adit is 75 metres long and follows a fissure which is well developed at the face but not mineralized. The orebody on this level, about 8 metres long, was stoped through to an intermediate level 12 metres above, where the ore was exposed for a length of 15 metres and width ranging from 10 to 30 centimetres. This ore forms a streak of nearly solid galena, sphalerite, conspicuous tetrahedrite and a little chalcopyrite. The gangue is principally quartz but some calcite and barite are also present. Some of the quartz appears to be chalcedonic. The veins are commonly flanked by a chloritic alteration envelope up to 1.2 metres wide grading into the granite.

#### **Chapleau (L. 4963); (MINFILE 082FNW130):**

The Chapleau property comprises the Chapleau and Chapleau Consolidated fraction and several other Crown granted claims centred 6 kilometres southeast of Slocan City. The Chapleau mine may be reached by a short access road about 1.5 kilometres long connected to the main road at a point about 13 kilometres from the Slocan highway.

Chapleau was one of the first properties in Lemon Creek area to receive attention. In 1896 the initial shipment of ore yielded 435 grams of gold and 11788 grams of silver. Until 1900, development was rapid and an aerial tramway and stamp mill were erected. However, in 1904 the mine was closed as a result of decreasing value of the ore and difficulties were encountered because of faulting of the vein. Until 1941 ore was shipped intermittently by lessees. In 1946 and 1947 the workings were rehabilitated and a new road was constructed to the property, but there were no shipments of ore.

The country rock is porphyritic Nelson quartz monzonite (Table 1, Number 5) bounded a short distance to the north and northwest by a large pendant and other inclusions of argillaceous quartzite. These rocks are cut by small dikes of fine grained granite, pegmatite, and aplite. The phenocrysts of orthoclase and microcline in the porphyritic granite are up to a centimetre long. Larger feldspar phenocrysts, up to 7 centimetres in length, occur in the pegmatite dikes, elongated parallel to the walls. Some pegmatites contain small crystals of garnet and magnetite but no mica or ferromagnesian minerals.

The vein strikes 110° and dips 25° northeast (Table 2). Its width ranges from 7 centimetres to 1.2 metres. The gangue is quartz that in places forms drusy cavities. Pyrite is the most abundant metallic mineral followed by sphalerite and galena. Minor chalcopyrite, free gold and ruby silver (?) are also reported.

## **Style of Mineralization**

As can be seen from the preceding descriptions, silver-lead-zinc ores predominate in the Slocan City camp. The ore minerals are mainly galena and sphalerite. There is a small amount of pyrite, chalcopyrite, and pyrrhotite. Silver is the most important commodity occurring in argentiferous tetrahedrite, galena and less commonly as native silver and sporadically in argentite, polybasite, ruby silver, stephanite and electrum. Gold is present in small quantities and rarely seen as native gold or electrum. Quartz is the dominant gangue mineral, but carbonates such as siderite, calcite and/or dolomite are significant gangue components in some deposits. Fluorite and barite are less common. The deposits are characterized by open-space filling, with minor evidence of replacement. In a few deposits, where replacement of wall rock has been extensive, carbonate gangue is relatively abundant.

Cairnes (1934) recognized several types of veins, the most common of which are the so-called "wet ore" composed of massive galena-sphalerite with some siderite, quartz or calcite gangue, such as found at the Enterprise mine, and "dry ore" comprising veins of quartz with galena, sphalerite and tetrahedrite, characterized by high silver values, (quartz greatly exceeded the abundance of sulphides), such as found at the Little Tim, Meteor and Ottawa mines. The "dry ores" are mostly confined to the Nelson intrusion.

## **Discussion**

Combined field and laboratory evidence indicates that the Slocan City mineral deposits formed over a long period. The mineralizing process began at time of the intrusion of the Nelson batholith dated mid-Jurassic (Armstrong, 1988). This effected the adjacent country rocks such as on Mount Alywin, where the Willa gold-silver-copper deposit (dated 165 - 184 Ma) is hosted in skarnified Rossland Group rocks (Ray and Webster, 1997; Hoy and Dunne, 1997). The mineralizing events continued during cooling of the intrusion and resulted in the development of veins within the batholith.

The Ag-Pb-Zn vein and replacement deposits of the Slocan area have long been thought to be genetically related to the Nelson batholith (Cairnes, 1934; Little, 1960). More recent work by Orr and Sinclair (1971) using Au/Ag ratios from 43 mineral occurrences in the camp supports this interpretation. Relatively high silver values are in ores hosted by a K-spar porphyry lobe of the Nelson granite at the centre of the camp, and the highest relative gold values are associated with ores from the distal parts of the porphyry and outer boundaries of the camp between Mount Alywin and Slocan City (Figure 2). This suggests that the hydrothermal plumbing system is geographically related to the granitic body.

LeCouteur (1973) also noted a concentric zonal pattern in his study of lead isotope ratios ( $Pb^{206}/Pb^{240}$ ) from the Slocan region. He attributed this pattern to leaching of lead from country rocks by rising ore fluids. Apparently the original isotope composition of lead in the fluid was

progressively changed en route to depositional sites, depending on the proportions of the original and leached components. The amount of leachable lead is related simply to the volume of the rock traversed, and thus to distance from the centre of the circulation system. Accordingly, the difference in metal values (Ag-Pb-Zn, Ag-Au, Au-Ag) in the Slocan City camp (Cairnes, 1934; Little, 1960) may be the result of different proportions of the elements being scavenged by a single wide-spread ore fluid. The model is not unique, however, and other models relating compositional changes to time or to decreasing availability of leachable lead have been proposed (Austin and Slawon, 1961; and Sinclair and Walcott, 1966).

Indeed, detailed lead isotope investigations indicate that the lead in the Kootenay arc ores went through several stages of redistribution beginning with the introduction of uranium and thorium in the upper crust 1,700 million years ago (Sinclair, 1964; LeCoutier, 1973; Bevier, 1987).

Beaudoin (1991) shows that some hydrothermal activity is coeval with the Paleocene-Eocene crustal extension in the region. At this time the Valhalla metamorphic core complex was rapidly uplifted along the Slocan Lake fault - (an east dipping 'transcrustal' listric normal fault zone). Accordingly, "Pb isotopic ratios from veins display regional zonation revealing fluid flow paths of a large, fossil hydrothermal system. Regional isotopic zonation is controlled by deep fracture zones, such as the Slocan Lake fault, which channelled lower crustal and mantle Pb, and mantle CO<sub>2</sub> to higher crustal levels where mixing occurred with upper crustal fluids which had leached local sulphur and upper crustal Pb."

Analyses of the Nelson granitic porphyry (Table 1) shows a range of relatively low lead (2 to 22 ppm), zinc (80 to 142 ppm) and only moderate levels of barium (0.06 to 0.16 per cent). These levels appear to preclude the Nelson intrusion as a source of these elements in the Slocan City camp. However, Sangster and Vaillencourt (1990) show that trace amounts of lead, zinc, barium and iron can be leached by meteoric waters from weathered and altered granitic rocks and redistributed to form ore bodies. Fractured and crushed granitic rocks in the Slocan Lake fault zone could provide a source. The continued passage of meteoric waters through the clastic granite could result in K-spar alteration to clay releasing lead and barium from the feldspar lattice, and zinc and iron from hornblende. These elements combine with sulphur to produce pyrite, galena, spalerite and barite. (Pb and Ba are ionically substituted for K in feldspar, and Zn with Fe<sup>+2</sup> in hornblende). Silica, released by the same breakdown of feldspar, may precipitate as quartz gangue.

Figure 5 shows hypothetical cross-sections of the Slocan City camp during (A) intrusion of the Nelson batholith and (B) the development of the Slocan Lake fault zone. By this model, the west margin of the Nelson batholith was broken and crushed during the process of intrusion and again during listric-normal detachment faulting/facturing associated with crustal extension. Prolonged movement in the crushed contact zone of the batholith is believed to have sustained a channelway for hydrothermal solutions.

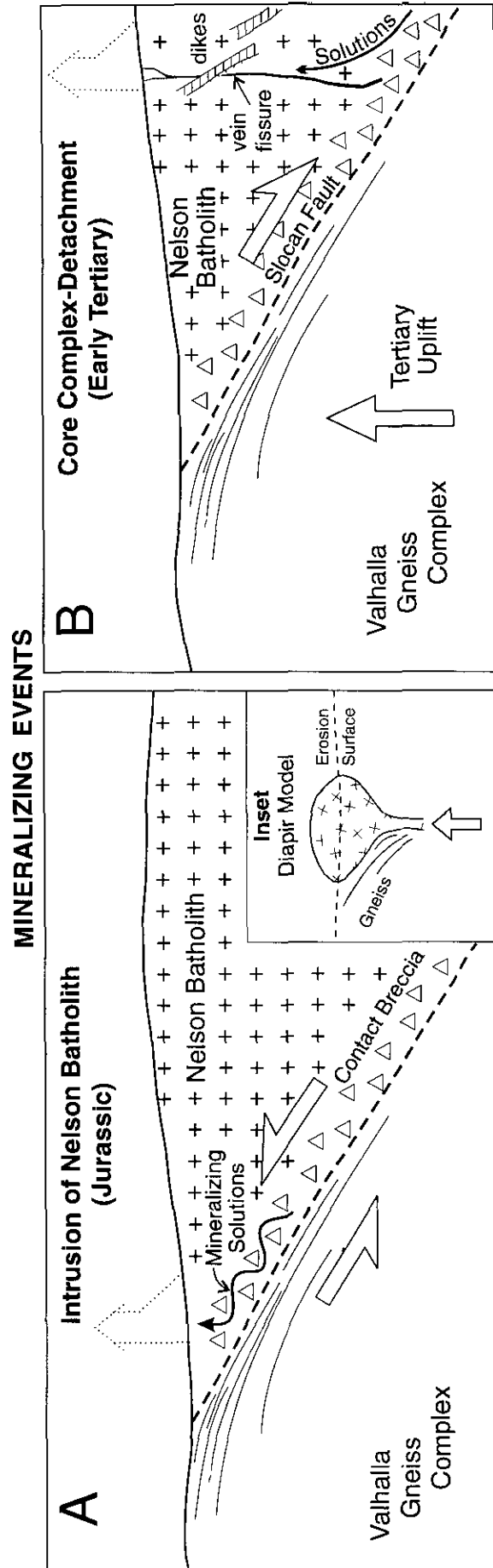


Figure 5. Hypothetical cross-sections of the Slocan City camp.

## CONCLUSIONS

The silver-lead-zinc veins of the Slocan City camp are characterized by mineralogy, metal ratios and structural setting. The veins, consisting mostly of galena and sphalerite in a quartz-carbonate gangue, are hosted in the Nelson batholith. Early workers regarded these granitic rocks as the singular magmatic - hydrothermal source of lead-zinc mineralization, however, recent studies suggest a more complicated genesis. Lead isotope investigations indicate that the lead of the Kootenay arc ores went through several stages of redistribution beginning in the Proterozoic through Jurassic to early Tertiary.

The veins formed at about the time of the Nelson intrusion and subsequently. The veins are fillings and replacements in fractures that appear to be related to the Slocan Lake fault that occurs at the west boundary of the batholith. Prolonged movement on the Slocan Lake fault is believed to have sustained a channelway for hydrothermal solutions, which are the result of commingling of metamorphic and magmatic fluids and meteoric water. The main source of zinc and sulphur in the ores is believed to be the local country rocks (Nelson batholith) but, based on isotope data, a significant amount of lead in some deposits is derived from the lower crust and older rocks.

## ACKNOWLEDGEMENTS

The writer is much obliged to David Lefebure of the Geological Survey Branch for suggesting the project and for numerous improvements to this report, and to David Barclay of Slocan City for his advice in the field. Thanks are also owing Larry Jones, Mike Fournier and George Owsiak of the Branch for their assistance in the preparation of tables, figures and photographs and to Dorthe Jakobsen for final editing duties.

## REFERENCES CITED

- Armstrong, R.L. (1988): Mesozoic and Early Cenozoic magmatic evolution of the Canadian Cordillera; *Geological Society of America*, Special Paper 218, pages 55-91.
- Austin, C.F. and Slawson, W.F. (1961): Isotopic Analyses of Single Galena Crystals: a Clue to History of Deposition; *American Mineralogist*, Volume 46, pages 1132-1140.
- Beaudoin, G. (1991): The Silver-Lead-Zinc Veins of the Kokanee Range, British Columbia; unpublished Ph.D. Thesis, *University of Ottawa*, 168 pages.
- Bevier, M. (1987): A Pb Isotope Study of the Valhalla Complex and its Surrounding Rocks, Southeastern British Columbia: Preliminary Interpretations; Radiogenic Age and Isotopic Studies, Report 1; *Geological Survey of Canada*, Paper 87-2, pages 13-20.
- Brown, D.A. and Logan, J.M. (1989): Geology and Mineral Evaluation of Kokanee Glacier Provincial Park, Southeastern British Columbia (82F/11,14); *British Columbia Ministry of Energy, Mines and Petroleum Resources*, Paper 1989-5, 47 pages.
- Carr, S.D. (1985): Ductile Shearing and Brittle Faulting in Valhalla Gneiss Complex, southeastern British Columbia; in Current Research, Part A, *Geological Survey of Canada*, Paper 85-1A, pages 89-96.
- Carr, S.D., Parrish, R.R. and Brown, R.L. (1987): Eocene Structural Development of the Valhalla Complex, southeastern British Columbia; *Tectonics*, Volume 6, Number 2, pages 175-196.
- Cairnes, C.E. (1934): Slocan Mining Camp, British Columbia, *Geological Survey of Canada*, Memoir 173, 137 pages.
- Dawson, G.M. (1890): On a Portion of the West Kootenay District, British Columbia; *Geological Survey of Canada*, Annual Report 1888-879, Volume 4, pages 7A-12A, 5B-66B.
- Fyles, J.T. (1967): Geology of the Ainsworth-Kaslo Area, British Columbia; *British Columbia Department of Mines and Petroleum Resources*, Bulletin 53, 125 pages.
- Hoy, T. and Dunne, K.P.E. (1997): Early Jurassic Rossland Group, southern British Columbia, Part 1 - Stratigraphy and Tectonics; *British Columbia Ministry of Employment and Investment*, Bulletin 102, 124 pages.
- LeCouteur, P.C. (1973): A Study of Lead Isotopes from Mineral Deposits in southeastern British Columbia and in the Anvil Range, Yukon Territory; Unpublished Ph.D. thesis, *University of British Columbia*, 142 pages.
- Little, H.W. (1960): Nelson Map-area, west half British Columbia (82F west half), *Geological Survey of Canada*, Memoir 308, 205 pages.
- Maconachie, R.J. (1940): Lode-Gold Deposits, Upper Lemon Creek Area and Lyle Creek - Whitewater Creek Area, Kootenay District; *British Columbia Department of Mines*, Bulletin 7, 50 pages.
- McConnell, R.G. and Brock, R.W. (1904): West Kootenay Sheet, British Columbia; *Geological Survey of Canada*, Map 792.
- Orr, J.F.W. and Sinclair, A.J. (1971): Mineral Deposits in the Slocan and Slocan City Area of British Columbia; *Western Miner*, pages 22-33.
- Parrish, R., (1984): Slocan Lake Fault - a Low Angle Fault Zone Bounding the Valhalla Gneiss Complex, Nelson map-area, southern British Columbia; in Current research, Part A, *Geological Survey of Canada*, Paper 84-1A, pages 323-330.
- Ray, G.E. and Webster, I.C.L. (1997): Skarns in British Columbia; *B. C. Ministry of Employment and Investment*, Bulletin 101, 260 pages.
- Reesor, J.E. (1965): Structural Evolution and Plutonism in Valhalla Gneiss Complex, British Columbia; *Geological Survey of Canada*, Bulletin 129, 128 pages.

- Sangster, D.F. and Vaillancourt, P.D. (1990): Geology of the Yava Sanstone-Lead Deposit, Cape Breton Island, Nova Scotia, Canada; in Mineral Deposit Studies in Nova Scotia, Volume 1, Sangster, A.L., Editor, *Geological Survey of Canada*, Paper 90-8, pages 203-244.
- Sevigny, J.H. and Parrish, R.R. (1993): Age and origin of Late Jurassic and Paleocene granitoids, Nelson Batholith, southern British Columbia; *Canadian Journal of Earth Sciences*, Volume 30, pages 2305-2314.
- Sinclair, A.J. (1964): A Lead Isotope Study of Mineral Deposits in the Kootenay Arc; Unpublished Ph.D. thesis, *University of British Columbia*, 257 pages.
- Sinclair, A.J. and Walcott, R.I. (1966): The Significance of Th/U Ratios Calculated from west-central New Mexico Multistage Lead Data; *Earth and Planetary Science Letters*, Volume 1, pages 38-41.

**Table 1 Chemical Analyses of Nelson Granitic Rocks**

| Sample | SiO <sub>2</sub><br>% | TiO <sub>2</sub><br>% | Al <sub>2</sub> O <sub>3</sub><br>% | Fe <sub>2</sub> O <sub>3</sub><br>% | MnO<br>% | MgO<br>% | CaO<br>% | Na <sub>2</sub> O<br>% | K <sub>2</sub> O<br>% | P <sub>2</sub> O <sub>5</sub><br>% | Ba<br>% | LOI<br>% | SUM<br>% | Pb<br>ppm | Zn<br>ppm | Ag<br>ppm |
|--------|-----------------------|-----------------------|-------------------------------------|-------------------------------------|----------|----------|----------|------------------------|-----------------------|------------------------------------|---------|----------|----------|-----------|-----------|-----------|
| 1      | 68.4                  | 0.31                  | 15.11                               | 2.59                                | 0.05     | 0.68     | 2.68     | 3.64                   | 4.46                  | 0.11                               | 0.11    | 1.27     | 99.38    | 16        | 80        | <0.4      |
| 2      | 68.3                  | 0.40                  | 15.0                                | 3.18                                | 0.06     | 0.95     | 2.28     | 3.00                   | 5.50                  | 0.19                               | 0.09    | 0.84     | 99.75    | 22        | 142       | <0.4      |
| 3      | 67.4                  | 0.43                  | 14.74                               | 3.68                                | 0.06     | 1.07     | 3.25     | 3.66                   | 3.54                  | 0.18                               | 0.08    | 1.25     | 99.29    | 6         | 86        | <0.4      |
| 4      | 65.0                  | 0.47                  | 16.08                               | 3.84                                | 0.08     | 1.22     | 3.14     | 3.63                   | 5.03                  | 0.26                               | 0.16    | 0.96     | 99.83    | 16        | 84        | <0.4      |
| 5      | 63.6                  | 0.61                  | 16.54                               | 4.86                                | 0.06     | 1.37     | 3.92     | 3.54                   | 3.75                  | 0.23                               | 0.12    | 0.81     | 99.41    | 12        | 108       | <0.4      |
| 6      | 62.9                  | 0.56                  | 16.12                               | 4.63                                | 0.08     | 1.60     | 4.11     | 3.61                   | 3.36                  | 0.23                               | 0.13    | 1.94     | 99.29    | 8         | 104       | <0.4      |
| 7      | 63.5                  | 0.55                  | 16.23                               | 4.64                                | 0.10     | 1.57     | 4.09     | 3.75                   | 3.66                  | 0.27                               | 0.13    | 1.16     | 99.68    | 12        | 108       | <0.4      |
| 8      | 61.6                  | 0.66                  | 16.43                               | 5.31                                | 0.09     | 1.73     | 4.44     | 3.68                   | 3.53                  | 0.34                               | 0.16    | 1.60     | 99.57    | 10        | 102       | <0.4      |
| 9      | 62.1                  | 0.61                  | 16.4                                | 5.15                                | 0.10     | 1.69     | 4.09     | 3.59                   | 3.77                  | 0.32                               | 0.15    | 1.35     | 99.32    | 10        | 118       | <0.4      |
| 10     | 61.3                  | 0.65                  | 16.82                               | 5.47                                | 0.11     | 1.85     | 4.53     | 3.81                   | 3.63                  | 0.34                               | 0.14    | 1.03     | 99.63    | 12        | 122       | <0.4      |
| 11     | 62.0                  | 0.65                  | 16.67                               | 5.56                                | 0.09     | 1.79     | 4.36     | 3.99                   | 3.70                  | 0.32                               | 0.14    | 0.61     | 99.87    | 16        | 104       | <0.4      |
| 12     | 61.2                  | 0.88                  | 16.94                               | 6.52                                | 0.10     | 2.09     | 4.69     | 3.17                   | 2.60                  | 0.32                               | 0.08    | 1.07     | 99.62    | 2         | 128       | <0.4      |
| 13     | 57.0                  | 0.88                  | 17.45                               | 7.68                                | 0.13     | 2.72     | 5.69     | 4.57                   | 2.20                  | 0.44                               | 0.06    | 0.91     | 99.75    | 6         | 142       | <0.4      |

**Table 2 Principal Vein Attitudes at Mines and Prospects**

| Occurrences<br>(MINFILE No.) | Location  |            | Vein Attitudes         |
|------------------------------|-----------|------------|------------------------|
|                              | Lat.      | Long.      |                        |
| Chapleau (130)               | 49° 44.0' | 117° 23.5' | 110°/25°NE             |
| Kilo (131)                   | 49° 44.0' | 117° 22.7' | 145°/35°NE             |
| Hollinger (132)              | 49° 43.7' | 117° 22.2' | 180°/15°NE             |
| Goldstream (134)             | 49° 44.4' | 117° 22.2' | 075°/20°NW             |
| Tailholt (135)               | 49° 44.9' | 117° 21.7' | 135°/20°NE             |
| Meteor (137)                 | 49° 45.6' | 117° 21.3' | 105°/35°NE, 140°/80°NE |
| Elk (138)                    | 49° 45.9' | 117° 21.1' | 115°/30°SW             |
| Alice (139)                  | 49°46.4'  | 117° 21.1' | 095°/70°SW             |
| Slocan Prince (140)          | 49° 46.7' | 117° 19.8' | 065°/60°NW             |
| B&R (142)                    | 49° 47.3' | 117° 19.6' | 065°/45°NW             |
| Westmont (145)               | 49° 49.7' | 117° 19.6' | 045°/70°SE             |
| Dalhousie (146)              | 49° 45.0' | 117° 15.0' | 070°/45°SE             |
| Neepawa (147)                | 49° 49.3' | 117° 19.9' | 030°/65°SE             |
| Enterprise (148)             | 49°49.3'  | 117° 19.5' | 053°/70°SE, 040°/85°SE |
| Mabou (149)                  | 49° 48.9' | 117° 20.2' | 055°/75°SE             |
| Bondholder (150)             | 49° 48.7' | 117° 21.4' | 065°/58°SE             |
| Speculator (151)             | 49° 48.0' | 117° 21.2' | 030°/65°SE             |
| Arlington (152)              | 49° 47.4' | 117° 21.7' | 040°/58°SE, 034°/70°SE |
| Lily B (153)                 | 49° 46.9' | 117° 21.4' | 075°/55°SE, 105°/50°SW |
| Ottawa (155)                 | 49° 47.1' | 117° 23.7' | 030°/20°SE, 170°/35°NE |
| Tamarak (156)                | 49° 47.3' | 117° 24.5' | 030°/25°SE             |
| Little Tim (157)             | 48° 48.4' | 117° 22.0' | 055°/70°NE, 073°/45°SE |
| Molly (158)                  | 49° 48.6' | 117° 23.1' | 050°/80°SE             |
| Myrtle (159)                 | 49° 48.6' | 117° 24.7' | 047°/38°SE             |
| Coronation (162)             | 49° 49.2' | 117° 25.4' | 090°/65°N              |
| Whitehope (165)              | 49°49.4'  | 117°26.6'  | 140°/50°SW             |
| Lakeview (172)               | 49° 46.2' | 117° 26.7' | 167°/80°NE             |
| Smeralda (231)               | 49° 45.7' | 117° 25.0' | 024°/43°SE             |





## THE ALLIN PROPERTY AND EQUITY-TYPE MINERALIZATION, CENTRAL BRITISH COLUMBIA

B.N. Church, Ph.D., B.C. Geological Survey Branch, and G.H. Klein P.Eng., Consultant

**KEYWORDS:** Equity-type mineralization, Houston area, copper, silver, gold, drift prospecting.

Development Co. Ltd. in 1996/97 and is the focus of continuing exploration (Wojdak, 1997).

### INTRODUCTION

The Allin discovery is approximately 4.5 kilometres east of the Equity Silver mine and 38 kilometres southeast of Houston (Figure 1) in central British Columbia (Latitude 54°11.3', Longitude 126°11.5'). Access to the area is by an all-weather gravel road from the town of Houston and seasonal logging roads from the village of Colleymount on the north shore of Francois Lake.

This report outlines evidence of additional Equity-type replacement mineralization related to the Goosly syenomonzonite-gabbro stock. The study is based on drift sampling guided by a thorough knowledge of the local geology. The discovery of high grade boulders in drift on the Allin property represents a success for the British Columbia Prospectors Assistance '94/95 Program which provided funds for prospecting.

### ALLIN PROPERTY

The alteration on the east side of the Goosly intrusion above Allin Creek has been known since 1964 when Summit Oil Limited first staked the area. In 1969 Kencco Exploration Limited cut lines to test the alteration zone, however, a thick till cover hampered investigations (Ney *et al.*, 1972). The property was restaked by Kengold Mines Limited in 1986 as the DEV and GO claims, then the property was optioned to Normine Resources Limited. In 1987 work was commissioned to Westview Resources Limited and subsequently several programs were completed including geochemical, resistivity and magnetometer surveys and diamond drilling. The drilling revealed that the same Mesozoic-age rocks hosting the Equity ore bodies west of the Goosly stock also occur east of the stock on the Allin property, although with a somewhat greater ratio of lava flows to clastic rocks (Garagan, 1988). Additional drilling in 1993, by Equity Silver Mines Limited, traced a zone of pyritization and propylitic alteration eastward onto the Allin claims (Wall, 1993). Recent logging in the Allin Creek area has facilitated access to the property and has led to the discovery of well mineralized float, similar to Equity ore, associated with a silver soil anomaly. The discovery encouraged further work on the Allin property by the second author supported by the British Columbia Prospectors Assistance Program in 1994/95. The property was optioned to Hudson Bay Exploration and

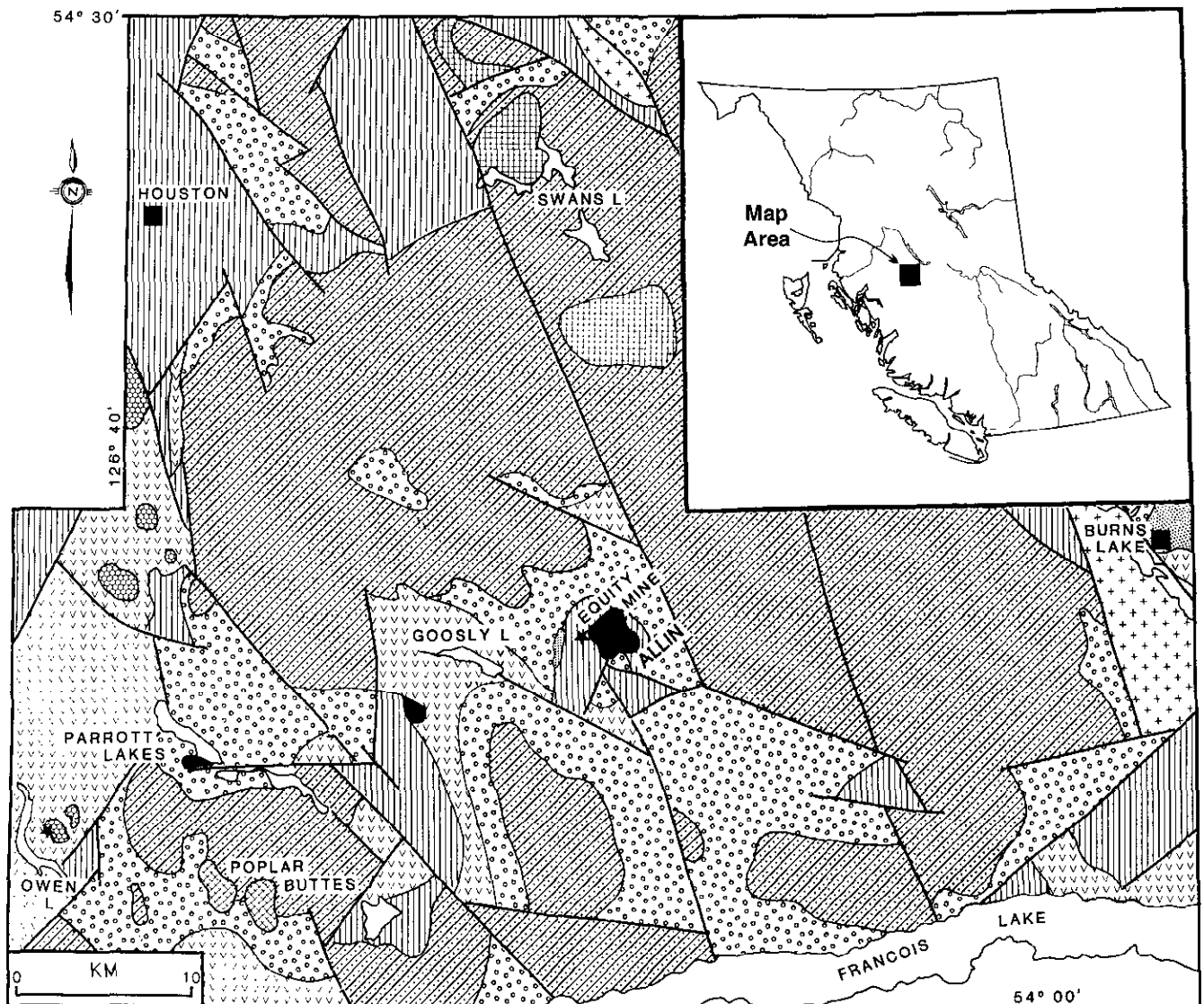
### Mineralization

Mineralization on the Allin property is not well defined because of thick forest cover and overburden. Westview Resources was able to outline a silver anomaly covering a south-trending elongated area (~1 kilometre by 200 metres) of glacial drift having a local source (Figure 2). Drilling on the Allin property intersected moderately to intensely altered volcanic rocks (quartz-sericite and quartz-chlorite alteration) containing up to 15 per cent pyrite (Wall, 1993), which are similar to clasts in the overlying glacial drift and the host rocks at the Equity deposit. Pyrite occurs as fracture fillings and disseminations throughout the host rocks accompanied by pyrrhotite and minor amounts of sphalerite, chalcopyrite, arsenopyrite, galena and tetrahedrite.

The Allin property covers part of the alteration halo adjacent to the Goosly stock east of the Equity Silver Mines property (Kowalchuck *et al.*, 1984). The Equity and Allin mineralization / alteration occurs in a lithochemical halo that surrounds the Goosly stock (Church and Barakso, 1990). The halo is believed to be the result of activation of hydrothermal solutions during intrusion of the stock.

Recent drift prospecting in the Allin Creek area (Klein, 1994 and 1995) found numerous subangular fragments similar in mineralogy and chemical composition to the Equity ore (Photos 1, 2 and 3; Tables 1 and 2). For example, drift sample no. 5 (Table 1, this report) assays 0.48 ppm gold, 54 ppm silver, 1.23 per cent copper, 123 ppm lead, 1137 ppm zinc and 571 ppm arsenic. This is similar to sample SG-67A collected from the discovery exposure at the Equity deposit which yielded 0.28 ppm gold, 50 ppm silver, 1.36 per cent copper, 280 ppm lead, 450 ppm zinc and 684 ppm arsenic (Church and Barakso, 1990). In general, the ore samples from the Equity mine are similar to drift clasts from the Allin area (Tables 1 and 2, Figure 5).

The drift samples are typically enriched in sulphides with replacement textures, have relatively minor gangue minerals and average 1.6 ppm gold, 125 ppm silver and 1.8 per cent copper. The rocks hosting the sulphides in these samples are generally similar to the fine grained sericitized and chloritized Jurassic volcanic rocks that occur immediately east and west of the Goosly intrusion and host the Equity ore deposit.



**LEGEND**

| BEDDED ROCKS                               | INTRUSIONS | SYMBOLS |
|--------------------------------------------|------------|---------|
| Chilcotin Group                            |            |         |
| Poplar Buttes F.                           |            | Fault   |
| Francois Lake Group                        |            | Mine    |
| Swans Lake Volcs.                          |            |         |
| Buck Creek F.                              | Goosly     |         |
| Goosly Lake F.                             | Nanika     |         |
| Burns Lake F.                              | Bulkley    |         |
| Tip Top Hill F.                            |            |         |
| Undivided Mesozoic Units                   |            |         |
| Hazelton Volcs. etc.   + + +   Topley etc. |            |         |

Figure 1. Geological map of the Buck Creek basin, Houston area, Central British Columbia.

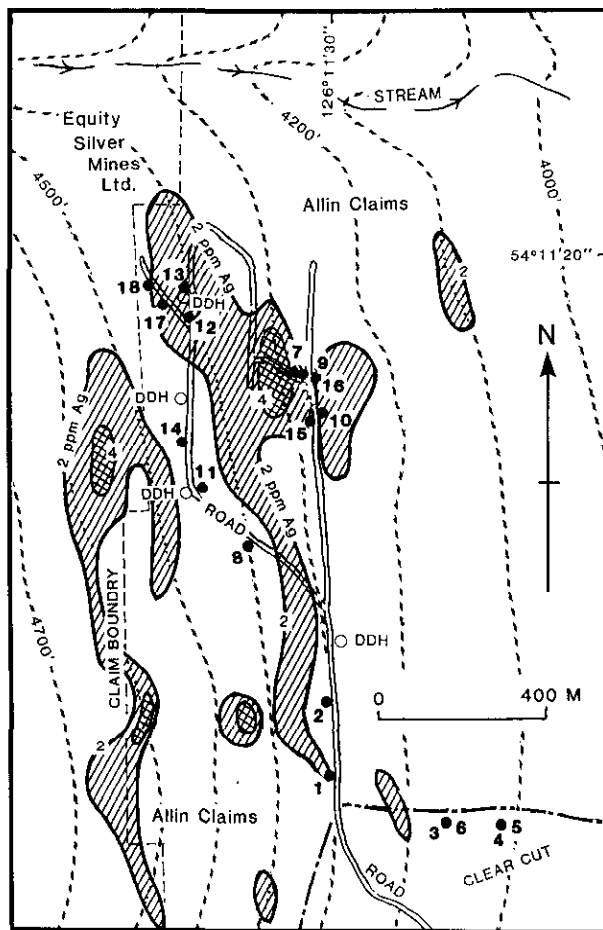


Figure 2. Anomalous silver-soil geochemistry and location of mineralized drift samples (dots - bold numbers correspond to assays in Table 1) Allin prospect.

The source of the drift samples was originally thought to be the Equity ore body. This is consistent with interpretations that the Fraser pulse of Pleistocene regional glaciation moved easterly across the area scraping the bedrock exposures west of the Allin property (Church and Barakso, 1990; Fulton, 1995). However, the authors found no entrained mineralized boulders extending eastward from the Equity deposit. Furthermore this direction of ice movement does not explain the south-trending silver soil anomaly with which the drift samples on the Allin property are associated.

There is evidence of a second glacial event in vicinity of the Equity ore deposit (formerly the Sam Goosly prospect) where glacial erratics appear to have moved southerly (Church, 1970). Ney *et al.* (1972) concluded that the silver soil anomalies in this area were for the most part ice-transported, and a very close correspondence was obtained between the up-ice cutoff in soil sample values on the northeast and the projected surface trace of the ore deposit. According to Tipper (1994) a second pre- or post-Fraser glaciation event from an ice dome may be responsible for apparent glacial reversals in the area as noted by previous authors. This scenario could also explain the dispersion of mineralized drift on the Allin property where local glaciation may have eroded bedrock from an

altered and mineralized zone located east of the Goosly intrusion and deposited the debris in south-trending alignments.

## EQUITY DEPOSIT

The Equity deposit is similar to the Allin Creek mineralization located 4 kilometres to the east. The Equity deposit was a significant gold, silver and copper producer for 13 years. The Equity Silver mine began production in 1980 on what was originally known as the Sam Goosly prospect. Early exploration in the 1960's was centred mostly on a small granitic body that hosts low grade porphyry-style mineralization. By 1969 attention was refocussed on an area located about a kilometre to the east near the Goosly syenomonzonite-gabbro stock (Figure 1; Dostal *et al.*, 1998). The area adjacent to the Goosly stock subsequently became the site of the Main, Waterline, Southern Tail and Northern ore zones of the Equity deposit (Figure 3). Mining of these zones was completed in 1993. Production from the Equity mine is summarized in Table 3.

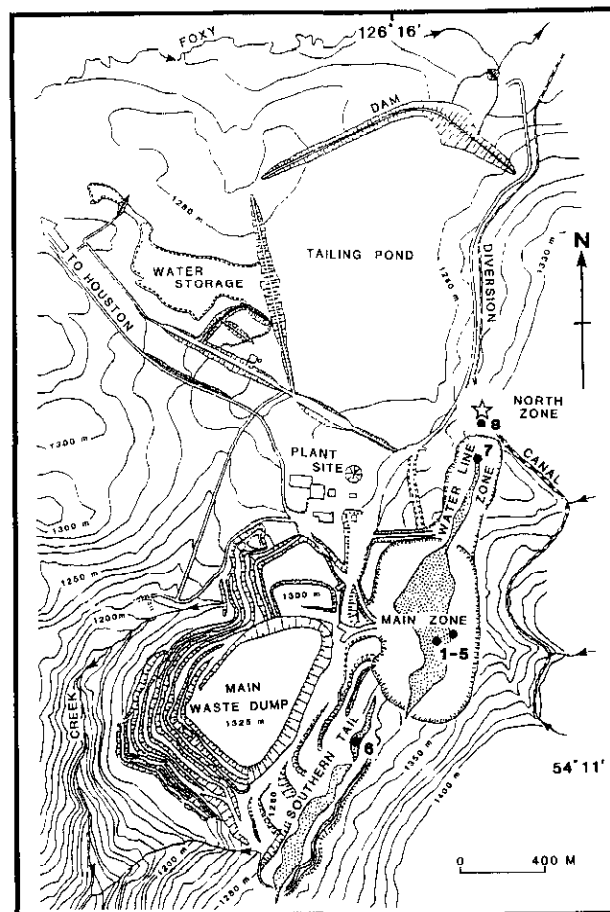


Figure 3. Plan view of the Equity Silver mine showing the ore zones (stippled) and sampling stations (dots - bold numbers correspond to assays in Table 2).

TABLE 1  
ANALYTICAL RESULTS OF DRIFT SAMPLING, ALLIN PROPERTY

| Lab. No. | Au ppm | Ag ppm | Cu %  | Pb ppm | Zn ppm | Ni ppm | Co ppm | As ppm |
|----------|--------|--------|-------|--------|--------|--------|--------|--------|
| 1        | 0.78   | 145    | 1.78  | 484    | 2,138  | 40     | 46     | 1,158  |
| 2        | 5.09   | 505    | 10.00 | 59     | 13,175 | 44     | 16     | 575    |
| 3        | 0.51   | 79     | 1.15  | 329    | 387    | 148    | 19     | 3,653  |
| 4        | 1.56   | 136    | 0.63  | 400    | 14,755 | 85     | 15     | 592    |
| 5        | 0.48   | 54     | 1.23  | 123    | 1,137  | 60     | 17     | 571    |
| 6        | 2.61   | 257    | 1.26  | 512    | 240    | 35     | 27     | 1,200  |
| 7        | 1.24   | 23     | 0.48  | 48     | 137    | 57     | 24     | 510    |
| 8        | 2.05   | 119    | 2.36  | 179    | 30,136 | 33     | 11     | 1,657  |
| 9        | 2.62   | 210    | 2.08  | 752    | 558    | 19     | 9      | 265    |
| 10       | 0.25   | 19     | 0.96  | 34     | 5,226  | 17     | 11     | 1,032  |
| 11       | 0.17   | 4      | 0.99  | 24     | 53     | 17     | 8      | 15     |
| 12       | 0.97   | 55     | 1.89  | 43     | 1,505  | 38     | 13     | 732    |
| 13       | 1.38   | 85     | 1.34  | 363    | 5,071  | 16     | 6      | 918    |
| 14       | 3.89   | 77     | 0.37  | 1,324  | 1,158  | 90     | 17     | 989    |
| 15       | 0.69   | 40     | 5.93  | 18     | 9,205  | 8      | 2      | 354    |
| 16       | 0.49   | 229    | 5.11  | 103    | 9,761  | 22     | 17     | 2,460  |
| 17       | 0.18   | 2      | 0.64  | 17     | 53     | 89     | 113    | 16     |
| 18       | 12.42  | 395    | 8.16  | 846    | 1,152  | 38     | 11     | 2,999  |

(Samples collected by G.H. Klein; results from unpublished reports by Klein 1994, 1995)

TABLE 2  
ANALYSES OF ORE SAMPLES, EQUITY MINE

| No. | Au ppm | Ag ppm | Cu % | Pb ppm | Zn ppm | Ni ppm | Co ppm | As ppm |
|-----|--------|--------|------|--------|--------|--------|--------|--------|
| 1   | 0.96   | 178    | 7.30 | 83     | 4,500  | 119    | 20     | 1,800  |
| 2   | 2.14   | 157    | 3.59 | 48     | 1,500  | 164    | 65     | 1,300  |
| 3   | 7.09   | 103    | 3.47 | 65     | 9,900  | 28     | 11     | 410    |
| 4   | 3.06   | 211    | 0.28 | 734    | 120    | 24     | 9      | 1,400  |
| 5   | 4.04   | 203    | 0.36 | 396    | 140    | 20     | 8      | 910    |
| 6   | 6.69   | 203    | 4.50 | 69     | 5,700  | 38     | 17     | 450    |
| 7   | 2.44   | 114    | 1.67 | 105    | 690    | 138    | 155    | 850    |
| 8   | 16.10  | 164    | 7.60 | 87     | 11,809 | 49     | 25     | 199    |
| 9   | 0.28   | 50     | 1.36 | 280    | 450    | 300    | 96     | 684    |

(Samples collected by B.N. Church; Nos. 1-6 from Church and Barakso, 1990; Nos. 7-8, this report)

TABLE 3  
PRODUCTION STATISTICS (Company Data)

| Ore Zones | Tonnes     | Au<br>g/t | Ag<br>g/t | Cu<br>% | Pit Area    |
|-----------|------------|-----------|-----------|---------|-------------|
| Southern  | 6 860 000  | 1.3       | 121.8     | 0.42    | 750 x 250m  |
| Main      | 24 205 000 | 0.9       | 96.5      | 0.32    | 850 x 500m  |
| Waterline | 2 614 000  | 1.2       | 86.9      | 0.33    | 450 x 200m  |
| Northern  | 226 600    | 4.2       | 147.8     | 0.46    | underground |
| Waste Tip | 76 000 000 | tonnes    |           |         |             |

## Mineralization

The Equity mine is located in a window of Mesozoic age rocks in a small uplifted area near the centre of the Buck Creek basin. The elliptical or elongated ore zones at the mine are aligned north-northeast (025°) subparallel to the steep westerly dipping strata. The total strike length of the deposit is approximately 2 kilometres (Figure 3). The Main zone, at the centre of the Equity deposit, is in contact with the Goosly stock that is also the locus of a major magnetic anomaly (Figure 4 this report; Church and Pettipas, 1990). The Equity ore occurs in a brecciated tongue of dust-tuff within a succession of dacitic volcanic breccia and conglomerate beds containing chert pebbles. Similar units are exposed southeast of the mine on the north shore of Francois Lake and contain fragments of Weyla fossils of Jurassic age. Brecciation of the Jurassic age pyroclastic rocks caused by the intrusion of the Goosly stock, has provided channelways for metalliferous hydrothermal solutions that caused the alteration and formed fracture filling and replacement-type ore (Church and Barakso, 1990).

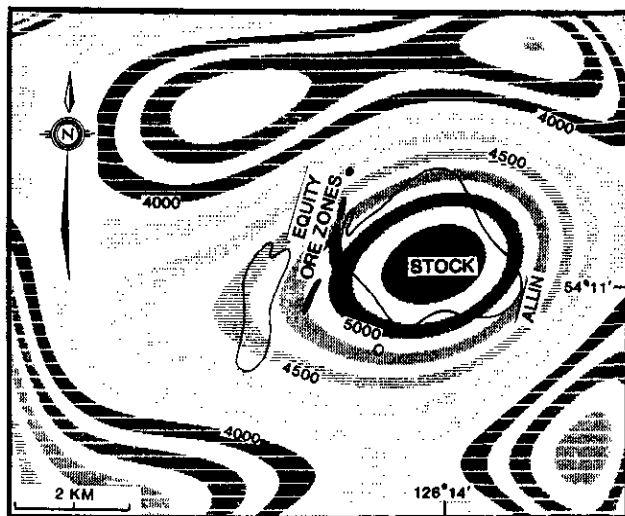


Figure 4. The Goosly stock and mineralized zones projected onto aeromagnetic contours (contours are nanateslas on a 6<sup>th</sup> order polynomial surface - based on data from Church and Pettipas, 1990).

The age of mineralization is similar to the age range of Goosly stock and adjacent altered rocks -  $48.3 \pm 1.7$  to  $54.3 \pm 2.2$  Ma based on K/Ar analyses of micaeous and whole rock samples (Church, 1970; Ney *et al.*, 1972;

Church and Barakso, 1990). However, the country rocks contain multiple generations of sericite inherited from repeated cycles of metamorphism/alteration at the distal extremities of the Southern Tail zone beyond the main mineralization and thermal halo of the Goosly stock (Wodjak and Sinclair, 1984). In this area, the Southern Tail zone is a narrow vein-like body that formed at relatively cool temperatures of  $< 200^{\circ}\text{C}$  - below the temperature of formation of some muscovite/sericite (Deer *et al.*, 1962). Consequently, the K/Ar 'age' of sericitized host rocks in the area, reported to be  $58 \pm 2$  Ma by Cyr *et al.* (1984), is probably an average age of multiple metamorphic and mineralizing events including the age of the nearby granitic intrusion that ranges from  $56 \pm 2.3$  to  $61.1$  Ma (Church, 1970; Ney *et al.*, 1972). It may be incorrect, therefore, to accept this as the age of mineralization for the Equity deposit as suggested by Cyr *et al.* (1984).

The Equity Silver orebodies consist of discordant lenses of massive sulphides which range from a few to several metres thick within the alteration envelope. In the Main zone the massive sulphide lenses consist mostly of coarse to medium-grained pyrite, pyrrhotite and chalcopyrite filling fissures, and replacement ore comprised of the same minerals together with minor amounts of sphalerite, tetrahedrite, arsenopyrite and locally magnetite. The alteration envelope is an aluminous assemblage several hundred metres wide composed of medium to high-temperature minerals that include andalusite, scorzalite, pyrophyllite, corundum, tourmaline, sericite and clay minerals; silicification is minor. Fine-grained disseminated pyrite, chalcopyrite and tetrahedrite occur throughout the zone of alteration. Mineralization temperatures, determined from fluid inclusions, decrease markedly from  $625^{\circ}\text{C}$  in the Main zone to  $200^{\circ}\text{C}$  in the Southern Tail zone (Wojdak and Sinclair, 1984). The Southern Tail zone is a narrow orebody with sharp contacts and a relatively thin alteration envelope of sericitic and chloritic metavolcanic rocks. Fragments of brecciated host rock are rimmed and replaced by arsenopyrite. The Waterline zone is a narrow extension of the Main zone ore body and has a similar mineralogy but contains somewhat higher gold values. The North zone was discovered and delineated by several drilling programs between 1983 to 1987 in the area 900 metres northeast of the Equity mill site (Figure 3). The North zone strikes northward from the Waterline zone where it is accessed by a 300-metre drift adit driven into the floor of the open pit in October 1992. The North orebody is 15 metres wide, dips steeply to the west and plunges north. As in the Main and Waterline zones, the massive sulphide ore of the North zone consists mostly of coarse- to medium-grained pyrite, pyrrhotite and chalcopyrite replacing dacitic tuff and tuff breccia (Photo 4). A well mineralized grab sample from near the portal of the lower adit returned the following assay result: 2.44 ppm gold, 114 ppm silver, 1.67% copper, 105 ppm lead, 690 ppm zinc, 39.4% iron, 850 ppm arsenic, 33 ppm antimony, 155 ppm cobalt and 138 ppm nickel. A second sample taken midway between the portal and face assayed 16.1 ppm gold, 164 ppm silver, 7.6% copper, 87 ppm lead, 1809 ppm zinc, 26% iron, 199 ppm arsenic, 163 ppm antimony, 25 ppm cobalt and 49 ppm

nickel. These new assay values are added to the previously published data for the Equity mine shown in Table 2; sample locations are plotted on Figure 3.

## CHEMICAL SIGNATURE OF EQUITY-TYPE MINERALIZATION

The chemical signature of the Equity mineralization can be investigated by using a correlation matrix for the ore forming and pathfinder elements. As well, multiple regression of element variables can be performed using methods adapted from Sinclair (1982), Matysek *et al.* (1982) and Church (1987). The product moment correlation matrix is determined (Table 4) using log transformed values for gold, silver, copper, lead, zinc, arsenic, cobalt and nickel from the assay data in this report and Church and Barakso (1990). Of the 28 pairs of elements generated by this procedure Cu-Zn, Ag-Pb and Co-Ni are among the pairs that show a good positive correlation. There is also a three-way positive correlation between As-Ag-Pb. These correlations reflect common associations of the principal ore-forming chalcophile elements. The low Pb-Ni correlation is explained by the usual occurrence of nickel with high temperature sulphide deposits and the usual association of lead with low temperature ores. Some of the other low and negative correlations, especially Zn-Pb and Cu-Pb, and may be a feature of the Equity-type in common with some high temperature pyrometamorphic deposits that also show strong negative Cu-Pb correlations (Ray *et al.*, 1988).

TABLE 4  
CORRELATION MATRIX (r<sup>2</sup>)

|    | Au   | Ag   | Cu   | Pb    | Zn    | As   | Co    | Ni    |
|----|------|------|------|-------|-------|------|-------|-------|
| Au | 1.00 | 0.73 | 0.31 | 0.44  | 0.18  | 0.31 | -0.05 | -0.06 |
| Ag |      | 1.00 | 0.41 | 0.58  | 0.38  | 0.72 | -0.10 | 0.05  |
| Cu |      |      | 1.00 | -0.29 | 0.59  | 0.15 | -0.06 | -0.04 |
| Pb |      |      |      | 1.00  | -0.10 | 0.53 | -0.09 | 0.06  |
| Zn |      |      |      |       | 1.00  | 0.34 | -0.26 | -0.13 |
| As |      |      |      |       |       | 1.00 | -0.08 | 0.16  |
| Co |      |      |      |       |       |      | 1.00  | 0.77  |
| Ni |      |      |      |       |       |      |       | 1.00  |

The mineralization can be characterized by multiple regression analysis (Ostle, 1960, page 202). This is expressed in terms of the ore forming and important ancillary elements by the following equation based on 26 assays from Tables 1 and 2:

$$\text{Log (Au)} = -5.54 + 1.00\text{Log(Ag)} - 0.0386 \text{Log(Cu)} + 0.0623\text{Log(Pb)} - 0.449\text{Log(As)}$$

where Au, Ag and Pb are given in terms of ppm and Cu and As are reported in per cent.

Coef. of Determination = 0.637 (Ostle, p. 180)  
 Coef. of Multiple Correlation = 0.799 (Ostle, p. 223)  
 Standard Error of Estimate = 0.801 (Ostle, p. 215)

An evaluation of the samples solely from the Equity deposit (Table 2 and SG-67A) yields a somewhat different equation:

$$\text{Log(Au)} = -7.5 + 1.79 \text{Log(Ag)} - 0.563 \text{Log(Cu)} - 0.7 \text{Log(Pb)} - 1.355 \text{Log(As)}$$

which is similar to that for selected samples from the Allin Creek area (Table 1; nos. 2, 3, 5, 6, 12, 13, 14, 15 and 16):

$$\text{Log (Au)} = -7.06 + 0.82 \text{Log(Ag)} - 0.226 \text{Log(Cu)} + 0.286 \text{Log(Pb)} - 0.919 \text{Log(As)}$$

The first equation, based on the most comprehensive collection of samples obtained from the area by the authors, is believed to best represent the Equity-type deposit profile.

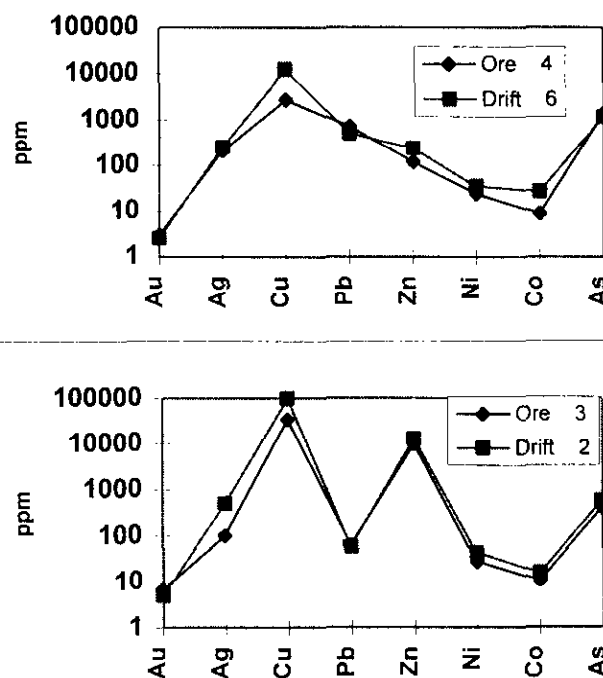


Figure 5. Comparison of Equity ore samples (diamonds) and Allin drift samples (squares).

## GENESIS OF THE EQUITY DEPOSIT

The various theories on the origin of the Equity ore deposit were outlined by Ney *et al.* (1972), Wojdak and Sinclair (1984), Cyr *et al.* (1984), Church and Barakso (1990).

Cyr *et al.* (1984) adopted the hypothesis, first suggested very early in exploration, that the mineralization on the Equity Silver property occurs as part of a porphyry system related to a small late Cretaceous / early Tertiary-age granitic stock near the west boundary of the property. Schroeter and Panteleyev (1988) amplified this line of argument and classified the deposit as 'Transitional' between porphyry copper and epithermal systems (also, see Cox and Singer, 1996; Panteleyev, 1995).

However, this model and classification is in sharp contrast to the earlier view of Ney, Anderson and Panteleyev (1972). They suggested that the mineral deposition had volcanogenic affiliations related to the Jurassic-age volcanic pile hosting the deposit (no black ores but Kuroko-like in geological setting and style of mineralization). With the beginning of mining in 1980, new exposures showed that the ore was comprised mostly replacement sulphides and discordant fissure fillings and was clearly not syngenetic. Textures and structures of the Equity deposit give strong evidence of metasomatism in keeping with Lindgren's metasomatic classification and Gilbert and Parks (1996) description of replacement ores.

This was more consistent with an intrusion-related, porphyry style of mineralization, however, the Main ore zone is more than a kilometre from the proposed 'source' granite body and the mineralization and alteration bears little similarity to that in porphyry copper environments Nielson (1969).

Wojdak and Sinclair (1984) propose that the principal ore mineralization represents a late high temperature hydrothermal mineralizing episode that resulted in widespread wall-rock alteration. Wojdak and Sinclair imply that no direct link need exist between the weak early phyllic alteration related to the porphyry mineralization associated with the granitic body and the strong acid leaching alteration associated with the silver-copper-gold-arsenic deposition in the Jurassic volcanic rocks. Salinity and temperature data from fluid inclusions suggest that circulating meteoric waters were involved in the ore mineralization. The convective hydrothermal system apparently developed subsequent to fracturing and brecciation induced by shallow igneous intrusions. Nielson (1969) favours the Eocene-age Goosly stock as the thermal engine and concentrating agent for the mineralizing solutions. The breccia zone at the Equity deposit, which bears a geometrical relationship to the margin of the intrusion, is believed to be the principal control for ore emplacement.

The sequence of events leading to mineralization on the Equity Silver property, summarized by Church and Barakso (1990), combines the main elements of the epigenetic theories. Initially a small granitic stock intruded Jurassic volcanic and metasedimentary rocks resulting in weak porphyry copper mineralization in the immediate vicinity of the stock (no associated volcanism). Several million years later the larger Goosly syenomonzonite-gabbro intrusion, with several phases and many offshoot dikes, was emplaced a few kilometres east of the granite, brecciating the adjacent host rocks. Outward movement of hydrothermal solutions from the Goosly stock produced a broad aureole of alteration and sulphide dissemination, replacement and fracture filling. A late stage hydrothermal event followed accompanied by a resurgence of igneous activity that intruded earlier formed parts of the mineral deposit. These events produced silver, copper and arsenic lithogeochemical halos about the Equity deposit and Goosly intrusion.

## CONCLUSIONS

Drift prospecting combined with geochemical methods and a knowledge of local geology and glacial history has been successful in delineating a new exploration target for Equity-type mineralization in the Allin Creek area, southeast of Houston B.C..

A large southerly-trending silver-soil geochemical anomaly, east of the Goosly stock near Allin Creek, appears to be caused by a zone of mineralization similar to the Equity deposit. Diamond drilling on the Allin property intersected Jurassic dacitic breccia and dust tuff formations similar to the rocks hosting the ore at the Equity mine. Drift samples from the area of the soil anomaly on the Allin property include many subangular clasts with sulphide disseminations, replacements and fracture fillings characteristic of the Equity mineralization.

To aid in the search for similar deposits, a description of Equity-type mineralization is presented in this report which includes a chemical signature expressed in terms of a correlation matrix and multiple regression analysis of available assay results.

## ACKNOWLEDGMENTS

The Prospectors Assistance Program of the B.C. Ministry of Energy, Mines and Petroleum Resources contributed to the funding of this project in response to the proposals 1994/95-P39 and 1995/96-P36 of G.H. Klein (co-author of this report). Appreciation is owing R. Player for lapidary and photography, D. V. Lefebure for editorial work and V.A. Preto, PA Program Manager, for his support and V. Levson for his review of an early draft of this manuscript. Chemical analyses for this study were completed by ACME Analytical Laboratories Limited of Vancouver.

## REFERENCES CITED

- Church, B.N. (1970): SG (Sam Goosly); *B.C. Department of Mines and Petroleum Resources, Geology, Mining and Exploration in British Columbia 1969*, pages 142-148.
- Church, B.N. (1987): Lithogeochemistry of the Gold-Silver Veins and Country Rocks in the Blackdome Mine Area; in *B.C. Ministry of Energy, Mines and Petroleum Resources, Exploration in British Columbia, 1986*, pages B41-B49.
- Church, B.N. and Barakso, J.J. (1990): Geology, Lithogeochemistry and Mineralization in the Buck Creek Area, British Columbia; *B.C. Ministry of Energy, Mines and Petroleum Resources, Paper 1990-2*, 95 pages.
- Church, B.N. and Pettipas, A.R. (1990): Interpretation of the Second Derivative of Aeromagnetic Maps at the Silver Queen and Equity Silver mines, Houston, B.C.; *Canadian Institute of Mining and Metallurgy, Bulletin Volume 83, Number 934*, pages 69-76.

- Church, B.N. (1993): The North Zone, Equity Silver Mine (93L/1); *B.C. Ministry of Energy, Mines and Petroleum Resources*, unpublished report.
- Cox, D.P. and Singer, D.A. (1986): Mineral Deposit Models; *U.S. Geological Survey, Bulletin 1693*, 379 pages.
- Cyr, J.B., Pease, R.B. and Schroeter, T.G. (1984): Geology and Mineralization at the Equity Silver Mine; *Economic Geology*, Volume 79, pages 947-968.
- Deer, W.A., Howie, R.A. and Zussman, J. (1962): Rock-Forming Minerals, Volume 3 Sheet Silicates; Longmans, London, 270 pages.
- Dostal, J., Robichaud, D.A., Church, B.N. and Reynolds, P.H. (1998): Eocene Volcanism in Central British Columbia: An Example from the Buck Creek Basin; *Canadian Journal of Earth Sciences*, (in press).
- Fulton, R.J. (1995): Surficial Materials of Canada; Geological Survey of Canada, Map 1880A, 1:5 000 000.
- Garagan, T. (1988): Report on the 1987 Exploration Activities on the DEV Project, Goosly Lake Area; *B.C. Ministry of Energy, Mines and Petroleum Resources*; Assessment Report Number 17680, 15 pages.
- Gilbert, J.M. and Parks, C.F. (1986): The Geology of Ore Deposits; W.H. Freeman and Company, New York, 985 pages.
- Klein, G.H., (1994): The Allin Project; *B.C. Ministry of Energy, Mines and Petroleum Resources*, Prospectors Assistance Program, Reference Number '94 -95-P39.
- Klein, G.H., (1995): The Allin Project; *B.C. Ministry of Energy, Mines and Petroleum Resources*, Prospectors Assistance Program, Reference Number '95 -96-P36.
- Kowalchuck, J.M., Church, B.N., Bradshaw, P.M.D. and Barakso, J.J. (1984): Litho-geochemistry at the Equity Silver Mine; *Western Miner*, Volume 57, Number 4, pages 50-54.
- Matysek, P., Sinclair, A.J. and Fletcher, W.K. (1982): Rapid Anomaly Recognition and Ranking for Multi-Element Regional Stream Sediment Surveys; *B.C. Ministry of Energy, Mines and Petroleum Resources*, Geological Fieldwork 1981, Paper 1982-1, pages 176-186.
- Nielsen, R.L. (1969): Progress Report on the Mineralogic Studies of Drill Core from the Sam Goosly Prospect, British Columbia; Kennecott Exploration Inc., Research Division, (unpublished report).
- Ney, C.S., Anderson, J.M. and Panteleyev, A. (1972): Discovery, Geological Setting and Style of Mineralization, Sam Goosly Deposit, British Columbia; *Canadian Institute of Mining and Metallurgy*, Bulletin, Volume 65, Number 723, pages 53-64.
- Ostle, B. (1960): Statistics in Research, Basic Concepts and Techniques for the Research Workers; *The Iowa State University Press*, 487 pages.
- Panteleyev, A. (1995): Subvolcanic Cu-Au-Ag (Ag-Sb) in Selected British Columbia Mineral Deposit Profiles, Volume I-Metallics and Coal; *B.C. Ministry of Energy, Mines and Petroleum Resources*, Open File 1995-20, pp. 79-82.
- Ray, G.E., Dawson, G.L. and Simpson, R. (1988): Geology, Geochemistry and Metallogenic Zoning in the Hedley Gold Skarn Camp; *B.C. Ministry of Energy, Mines and Petroleum Resources*, Geological Fieldwork 1987, Paper 1988-1, pages 59-80.
- Schroeter, T. and Panteleyev, A. (1987): Lode Gold-Silver Deposits in Northwestern British Columbia, in Mineral Deposits of the Northern Cordillera; *Canadian Institute of Mining and Metallurgy*, Special Volume 37, pages 178-190.
- Sinclair, A.J. (1982): Multivariate Models for Relative Mineral Potential, Slocan Silver- Lead- Zinc- Gold-Camp; *B.C. Ministry of Energy, Mines and Petroleum Resources*, Geological Fieldwork 1981, Paper 1982-1, pages 167-175.
- Tipper, H.W. (1994): Preliminary Interpretation of Glacial and Geomorphic Features of Smithers Map-Area (93L), British Columbia; *Geological Survey of Canada*, Open File 2837, 7 pages.
- Wall, T.J. (1993): Assessment Report on the Allin Property, Omenica Mining Division, British Columbia; *B.C. Ministry of Energy, Mines and Petroleum Resources*, Assessment Report Number 23132, 12 pages.
- Wojdak, P.J. and Sinclair, A.J. (1984): Equity Silver-Copper- Gold Deposit, Alteration and Fluid Inclusion Studies; *Economic Geology*, Volume 79, pages 969-990.
- Wojdak, P.J. (1997): Mine and Exploration Highlights, Northwest British Columbia 1996, *B.C. Ministry of Employment and Investment*, Exploration in British Columbia 1996, pages B1-B15.

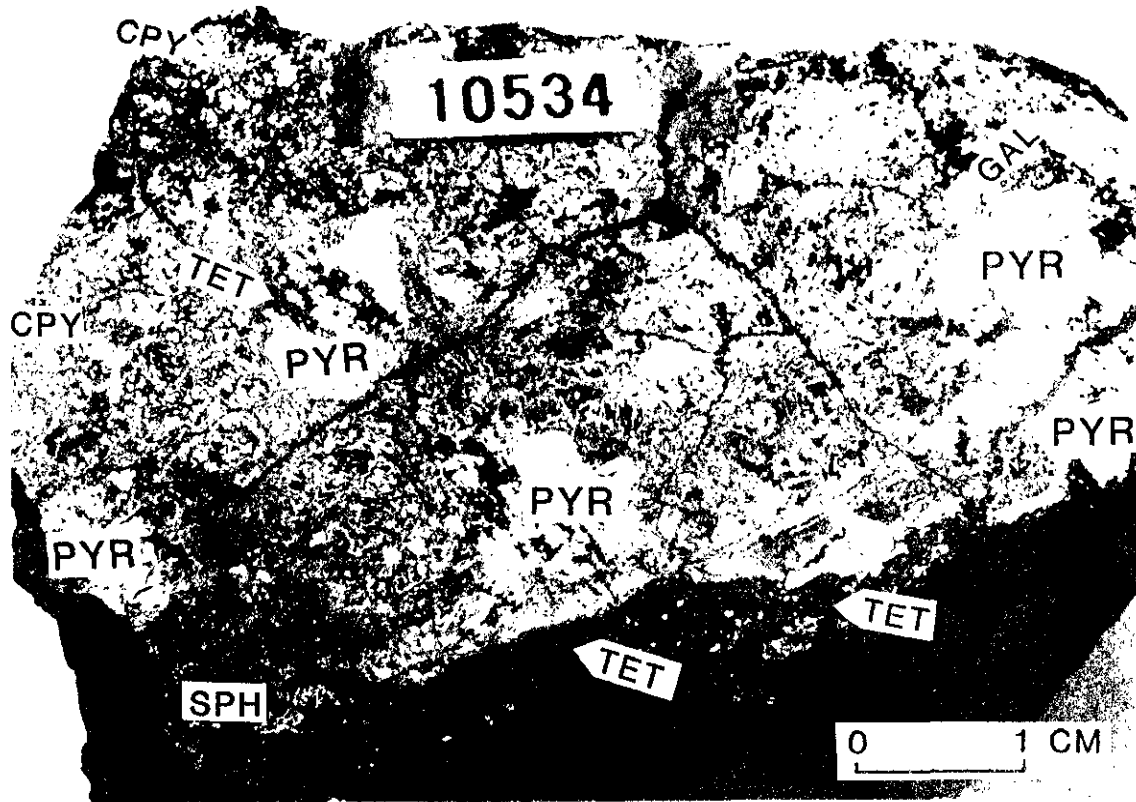


Photo 1 Mineralized float from Allin prospect; pyrite megacrysts in matrix of fine grained mixed sulphides of pyrite, chalcopyrite, sphalerite, tetrahedrite and galena, replacing tuff breccia.

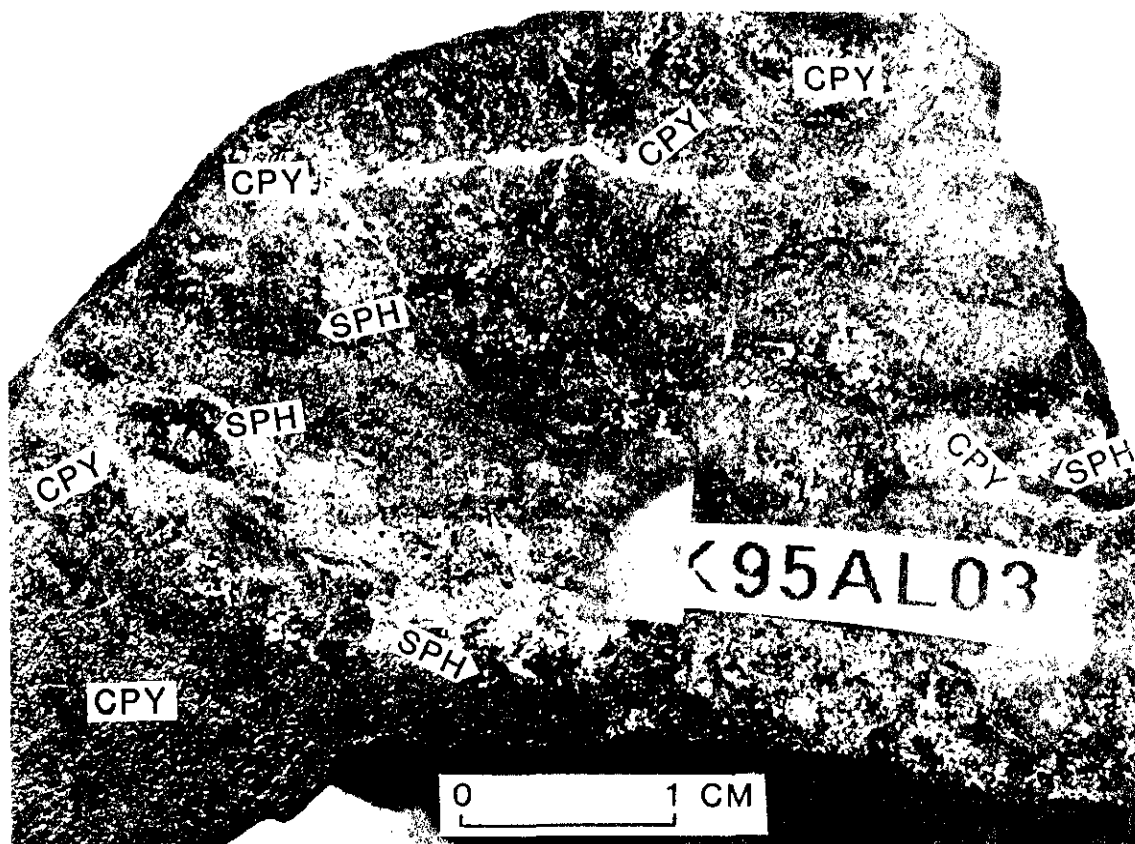


Photo 2 Mineralized float from Allin prospect; chalcopyrite, pyrite and sphalerite dissemination.

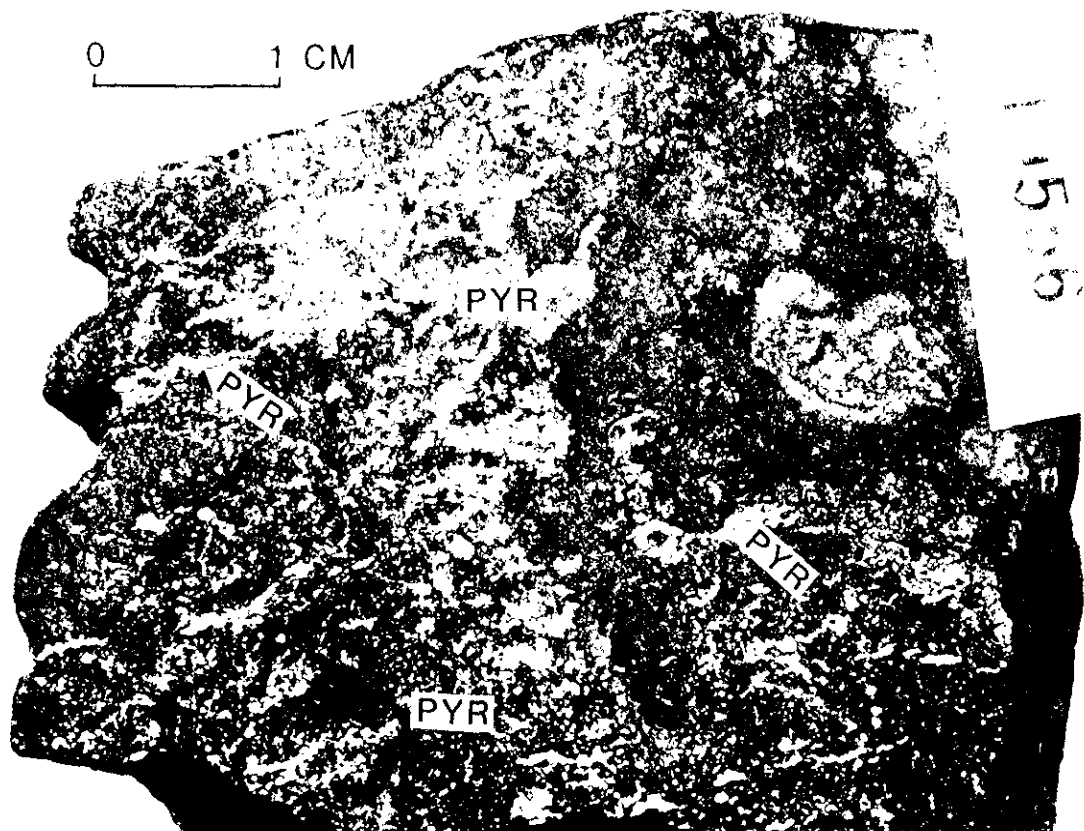


Photo 3. Mineralized float from Allin property; auriferous pyrite dissemination and filling in tuff breccia.

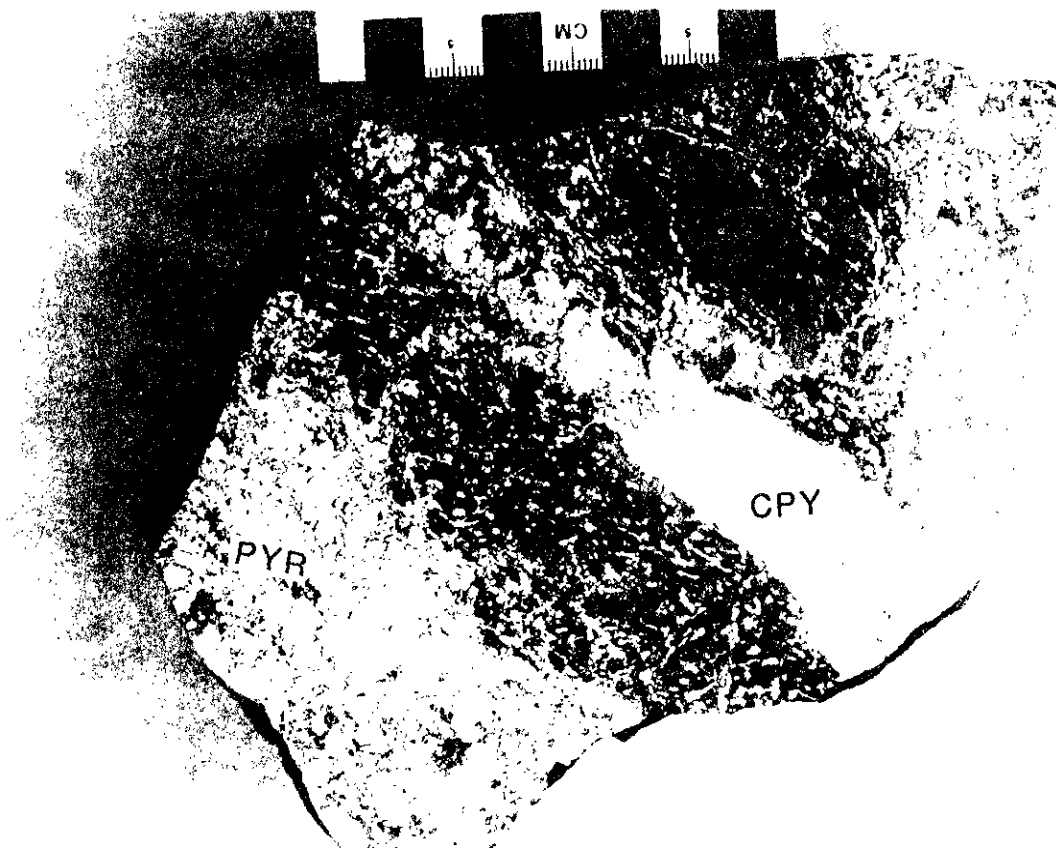


Photo 4. Sulphide replacement and fracture filling of dacitic tuff breccia; medium to coarse grained pyrite (grey), pyrrhotite and chalcopyrite (bright); sample from North zone, Equity mine.



British Columbia Geological Survey  
Geological Fieldwork 1997

## Selected Mineral Deposit Profiles

# BRITISH COLUMBIA MINERAL DEPOSIT PROFILES

By David V. Lefebure, B. C. Geological Survey

**KEYWORDS:** Deposit models, deposit profiles, Cordillera, resource data.

## INTRODUCTION

Seventeen deposit profiles are included in this volume (see following articles), bringing the total number of descriptive models completed by the British Columbia Geological Survey to 76. These profiles provide a concise introduction to deposit types that are found in Cordilleran environments.

The initial 60 profiles were published in two Open File publications (Lefebure and Ray, 1995, Lefebure and Höy, 1996) and have also been posted to the following British Columbia Geological Survey web site under the Economic Geology section.

<http://www.ei.gov.bc.ca/geology/>

Survey staff are continuing to work towards completing approximately 50 more deposit models. This is being done in conjunction with geologists from industry, government and academia. The BCGS welcomes any criticisms of the deposit profiles which will be used to improve future versions.

## B.C. DEPOSIT PROFILES

The British Columbia Geological Survey (BCGS) started a provincial mineral potential assessment in 1992. A fundamental part of this process was the compilation of information concerning British Columbia's mineral deposits, including descriptions, classification and resource data. A large number of in-house models were developed for deposit types found in the Cordillera of North and South America. These are called 'deposit profiles' to distinguish them from other published descriptions, such as the United States Geological Survey (USGS) 'deposit models' (Cox and Singer, 1986). They have a standard format (Lefebure and Ray, 1995) intended to make them useful to geologists, prospectors and students, as well as land use planners.

Several indexes for the deposit profiles have been published and posted to the BCGS web site. A listing of all the profiles by lithological affinity is particularly pertinent to mineral potential assessments (Lefebure and Ray, 1995; Table 4). A commodity index of profiles was included in the second Open File (Lefebure and Höy, 1996; Table 23). A third index is organized by deposit group (Lefebure and Höy, 1996; Table 22).

The BCGS has compiled grade and tonnage data for 21 profiles, based largely on British Columbia deposits (Lefebure and Höy, 1996, page 121). For more comprehensive resource figures, the reader is referred to a number of USGS publications listed in the bibliography, including Cox and Singer (1986).

## ACKNOWLEDGMENTS

For many of the profiles, geologists from other government agencies, industry and academia have helped write a profile or provided useful criticism. We thank all of them for their assistance.

## SELECTED BIBLIOGRAPHY

- Cox, D. P. (1993): Mineral Deposit Models, Their Use and Misuse - A Forum Review; *Society of Economic Geologists*, Newsletter No. 14, pages 12-13.
- Cox, D.P. and Singer, D.A., Editors (1986): Mineral Deposit Models; *United States Geological Survey*, Bulletin 1693, 379 pages.
- du Bray, Edward A. (1995): Preliminary Compilation of Descriptive Geoenvironmental Mineral Deposit Models; *United States Geological Survey*, Open File 95-831, 272 pages.
- Eckstrand, O.R., Editor (1984): Canadian Mineral Deposit Types: A Geological Synopsis; *Geological Survey of Canada*, Economic Geology Report 36, 86 pages.
- Eckstrand, O.R., Sinclair, W.D. and Thorpe, R.I, Editors (1995): Geology of Canadian Mineral Deposit Types; Geological Survey of Canada, *Geology of Canada*, Number 8, 640 pages.
- Grunsky, E.C., Kilby, W.E. and Massey, N.W.D. (1994): Resource Assessment in British Columbia; *Nonrenewable Resources*, Volume 3, No. 4, pages 271-283.
- Grunsky, E.C (1995): Grade-Tonnage Data for Mineral Deposit Models in British Columbia; in Geological Fieldwork 1994, Grant, B. and Newell, J.M., Editors, *British Columbia Ministry of Energy, Mines and Petroleum Resources*, Paper 1995-1, pages 417-423.
- Hodgson, C.J. (1993): Uses (and Abuses) of Ore Deposit Models in Mineral Exploration; *Geoscience Canada*, Reprint Series 6, pages 1-11.
- Kilby, W. (1995): Mineral Potential Project -Overview; in Geological Fieldwork 1994, Grant, B. and Newell, J.M., Editors, *British Columbia Ministry of Energy, Mines and Petroleum Resources*, Paper 1995-1, 411-416.

- Kilby, W. (1996): Mineral Potential Assessment Projects - An Update; in Geological Fieldwork 1995, Grant, B. and Newell, J.M., Editors, *British Columbia Ministry of Energy, Mines and Petroleum Resources*, Paper 1996-1, pages 301-308.
- Kirkham, R.V., Sinclair, W.D., Thorpe, R.I., and Duke, J.M. (1993): Mineral Deposit Modelling; *Geological Association of Canada*, Special Paper 40, 770 pages.
- Laznicka, P. (1985): Empirical Metallogeny - Depositional Environments, Lithologic Associations and Metallic Ores, Vol. 1: Phanerozoic Environments, Associations and Deposits; *Elsevier*, New York, 1758 pages.
- Lefebure, D.V., Alldrick, D.J., Simandl, G.J. and Ray G.E. (1995a): British Columbia Mineral Deposit Profiles; in Geological Fieldwork 1994, Grant, B. and Newell, J.M., Editors, *British Columbia Ministry of Energy, Mines and Petroleum Resources*, Paper 1995-1, pages 469-490.
- Lefebure, D.V., Alldrick, D.J. and Simandl, G.J., (1995b): Mineral Deposit Profile Tables - Listed by Deposit Group and Lithological Affinities; *British Columbia Ministry of Energy, Mines and Petroleum Resources*, Open File 1995-8.
- Lefebure, D.V. and Höy, T. (1996): Selected British Columbia Mineral Deposit Profiles, Volume II - More Metallic Deposits; *British Columbia Ministry of Employment and Investment*, Open File 1996-13, 172 pages.
- Lefebure, D.V. and Ray, G.E. (1995): Selected British Columbia Mineral Deposit Profiles, Volume I - Metallics and Coal; *British Columbia Ministry of Energy, Mines and Petroleum Resources*, Open File 1995-20, 136 pages.
- McMillan, W.J., Höy, T., MacIntyre, D.G., Nelson, J.L., Nixon, G.T., Hammock, J.L., Panteleyev, A., Ray, G.E. and Webster, I.C.L. (1991): Ore Deposits, Tectonics and Metallogeny of the Canadian Cordillera; *British Columbia Ministry of Energy, Mines and Petroleum Resources*, Paper 1991-4, 276 pages.
- Peters, W. C. (1978): Exploration and Mining Geology; *John Wiley & Sons, Inc.*, New York, 696 pages.
- Orris, G.J. and Bliss, J.D. (1991): Some Industrial Mineral Deposit Models - Descriptive Deposit Models; UNITED STATES Geological Survey; Open-File Report 91-11A, 73 pages.
- Orris, G.J. and Bliss, J.D. (1992): Industrial Mineral Deposit Models: Grade and Tonnage Models; *United States Geological Survey*; Open-File Report 92-437, 84 pages.
- Rogers, M.C., Thurston, P.C., Fyon, J.A., Kelly, R.I. and Breaks, F.W. (1995): Descriptive Mineral Deposit Models of Metallic and Industrial Deposit Types and Related Mineral Potential Assessment Criteria; *Ontario Geological Survey*, Open File Report 5916, 241 pages.
- Rytuba, J. J. and Cox, D. P. (1991): Porphyry Gold: A Supplement to U. S. Geological Survey Bulletin 1693; *United States Geological Survey*, Open File Report 91-116, 7 pages?.
- Singer, D.A., (1993): Development of Grade and Tonnage Models for Different Deposit Types; in Kirkham, R.V., Sinclair, W.D., Thorpe, R.I. and Duke, J.M., Editors, Mineral Deposit Modeling, *Geological Association of Canada*, Special Paper 40, pages 21-30.
- Singer, D.A. (1993): Basic Concepts in Three-part Quantitative Assessments of Undiscovered Mineral Resources; *Nonrenewable Resources*, Volume 2, pages 69-81.
- Singer, D.A. (1995): World Class Base and Precious Metal Deposits: a Quantitative Analysis; *Economic Geology*, Volume 90, pages 88-104.
- Singer, D.A., Menzie, W.D., DeYoung, J.H., Jr., Sander, M. and Lott, A. (1980): Grade and Tonnage Data Used to Construct Models for the Regional Alaskan Mineral Resource Assessment Program; *United States Geological Survey*, Open-File Report 80-799, 58 pages.
- Singer, D.A., Mosier, D.L. and Menzie, W.D. (1993): Digital Grade and Tonnage Data for 50 Types of Mineral Deposits; *United States Geological Survey*, Open File 93-280, digital file.



## CARBONATE HOSTED $\text{Cu}\pm\text{Pb}\pm\text{Zn}$

EO2

by E.A.G. (Ted) Trueman<sup>1</sup>



### IDENTIFICATION

SYNONYMS: Tsumeb or Kipushi type.

COMMODITIES (BYPRODUCTS): Cu, Pb, Zn, Ge (Ag, Ga, As, Cd).

EXAMPLES (British Columbia - Canada/International): Blue (Minfile 94F005); *Grinnell and Kanuyak Island (Northwest Territories, Canada), Kennecott, Ruby Creek and Omar (Alaska, USA), Apex (Utah, USA), Gortdrum (Ireland), Tsumeb and Kombat (Namibia), Kipushi (Zaire), M'Passa (Congo), Timna (Israel), Nifty (Australia), and portions of Dongchuan deposits (China).*

### GEOLOGICAL CHARACTERISTICS

CAPSULE DESCRIPTION: Irregular, discordant bodies of Cu sulphides (bornite, chalcopyrite, chalcocite, tennantite), sometimes with significant galena and sphalerite, form massive pods, breccia/fracture fillings and stockworks in carbonate or calcareous sediments. Igneous rocks are absent or unrelated to the deposition of metals.

TECTONIC SETTING: Intracratonic platform and rifted continental margin sedimentary sequences; typically gently folded and locally faulted.

DEPOSITIONAL ENVIRONMENT / GEOLOGICAL SETTING: Host carbonate sediments were deposited in shallow marine, inter-tidal, sabkha, lagoonal or lacustrine environments and are often overlain disconformably by oxidized sandstone-siltstone-shale units. Largest deposits are within thick sedimentary sequences.

AGE OF MINERALIZATION: Hosts rocks are Middle Proterozoic to Triassic; the largest deposits are in Upper Proterozoic rocks. Mineralization is at least slightly younger than host lithologies and may have spanned a large time interval.

HOST / ASSOCIATED ROCK TYPES: Dolomite or limestone, often stromatolitic or arenaceous, hosts the mineralization within a sequence which typically includes fine to coarse grained clastic sediments and evaporite. Occasionally basalt flows are nearby or part of sequence. Intrusive rocks are absent or different age than mineralization.

DEPOSIT FORM: The pipe-like to tabular deposits are irregular, discordant and often elongated in one direction up to 2 000 m or more. In cross section, deposits can be up to 100 by 200 m or 60 by 500 m in size. Sometimes Zn-Pb rich mantos project from the main zone of mineralization as replacement bodies parallel to bedding.

---

<sup>1</sup> Trueman Consulting Ltd., Denman Island, British Columbia.

# CARBONATE HOSTED CU±Pb±Zn

E02

**TEXTURE / STRUCTURE:** Massive, stringer/stockwork and disseminated mineralization styles occur and grade into one another; clots of sulphides are common. Features characteristic of a karst environment, including collapse breccias, are typical. Two or more breccia types may be present as a result of karst dissolution and hydrothermal fracturing. Open spaces within deposits are common. Narrow bodies or irregular masses of arenaceous sediment may occur within deposit. These clastics may have developed as a result of dissolution of an arenaceous carbonate host, with accumulation of clastic lag sediments, or by clastic sedimentation into karst openings as a result of submergence.

**ORE MINERALOGY (Principal and subordinate):** Chalcopyrite, bornite, chalcocite, tennantite (*tetrahedrite*), galena, sphalerite, pyrite, enargite, *renierite*, *germanite*, *arsenopyrite*, *marcasite*, *magnetite*, *gallite*, *Co-Ni arsenides*, *carrollite*, *molybdenite* and *others*. Deposits contain low to moderate Fe; pyrite may be common or virtually absent. Cu is sometimes crudely zoned vertically in deposits relative to Fe with the Cu-rich phases closer to surface. Cu may also be spatially partitioned with respect to Pb-Zn.

**GANGUE MINERALOGY (Principal and subordinate):** Dolomite, quartz, calcite, barite, fluorite, clay minerals, sericite, hematite, siderite and minor *pyrobitumen*.

**ALTERATION MINERALOGY:** Dolomite, silica, calcite and argillic alteration. Deposits are usually coincident with a zone of dolomitization. Dolomitization may be pre-, syn- and/or post-mineralization, and may extend 100's of metres beyond mineralization. Vuggy openings are often lined with calcite or baroque dolomite.

**WEATHERING:** Wide variety of secondary products form especially limonite, goethite, Cu minerals (malachite, azurite, diopside), cerussite and smithsonite. Some deposits are deeply oxidized (Kennecott, Tsumeb, Apex) as a result of fluid circulation through/along solution cavities, faults/fractures and bedding planes. Oxidation is typically developed at surface but there may also be an oxidized profile at considerable depth (>1,000m) as a result of continuation/reactivation of fluid flow along bedding planes aquifers.

**ORE CONTROLS:** The openings in carbonate rocks are created by brecciation, karsting, faulting, and/or alteration. Deposits form in proximity to a redox boundary between reduced carbonates and oxidized clastic sediments or occasionally oxidized basalt. Evaporites in the sedimentary sequences may have enhanced brine salinity and contributed sulphur.

**GENETIC MODEL:** Pre-mineralization plumbing systems were created by karsting, collapse zones, faulting/fracturing, collapse related to evaporite removal, and/or bedding plane aquifers and were enhanced by volume reduction during dolomitization, ongoing carbonate dissolution and hydrothermal alteration. Oxidized, diagenetic fluids scavenged metals from clastic sediments and their source area, with deposition in open spaces in reduced carbonates, often immediately below an unconformity. In a few examples, nearby basalts could have provided Cu. Fluid inclusion data indicate mineralizing solutions were saline and generally low temperature, in the 100-240°C range. Mineralization may have been initiated soon after host sediments became indurated and was likely a prolonged event, possibly continuing intermittently over 100's of millions of years in larger deposits. Deposits are basically formed through diagenetic processes and are an integral part of basin evolution. In some deposits, different fluids could have prevailed within oxidized and reduced strata leading to different metal sources - this could explain why only some deposits have a significant Zn-Pb-Ge component.

# CARBONATE HOSTED $Cu\pm Pb\pm Zn$

**E02**

**ASSOCIATED DEPOSIT TYPES:** Genetic processes which form carbonate-hosted  $Cu\pm Pb\pm Zn$  may be analogous to stratiform Cu (E04), carbonate hosted Zn-Pb (E12), unconformity U (I16) and sandstone U (D05) deposit types. Carbonate hosted  $Cu\pm Pb\pm Zn$  deposits have many similarities with carbonate hosted Zn-Pb deposits (E12), and are possibly a link between these deposits and stratiform Cu (E04).

**COMMENTS:** Deposits often occur in the same basin as stratiform Cu or carbonate-hosted Zn-Pb deposits. Other possible candidates for this type include: Mount Isa Cu, Kilgour, Yah Yah and Cooley (Australia), Nite and Ellesmere (Northwest Territories, Canada), Lord Aylmer and Acton Vale (Quebec, Canada).

## ***EXPLORATION GUIDES***

**GEOCHEMICAL SIGNATURE:** Dominantly elevated Cu but Zn, Pb, As, Ag and Ge are key indicators in rock samples; subtle Cu-stream silt geochemical anomalies occur in proximity to some deposits. Other elements which may be useful pathfinders are Co, Ga, Bi, Cd, V, Mo and Ba.

**GEOPHYSICAL SIGNATURE:** Resistivity, IP and gravity could be useful but there are no definitive tools.

**OTHER EXPLORATION GUIDES:** Tectonically disturbed zones and karsted areas within carbonate/oxidized clastic couplets of major basins are regional targets. Dolomitized zones should be carefully examined. Deposits often occur in clusters and/or in proximity to associated deposit types. Deposits oxidize readily forming gossans with secondary Cu and Fe minerals; many other secondary products and malachite-coated nuggets of copper sulphides may be present. Thermal maturation anomalies and clay mineral zoning, as applied to carbonate hosted Zn-Pb and unconformity uranium deposits, may be useful tools.

## ***ECONOMIC FACTORS***

**TYPICAL GRADE AND TONNAGE:** Tsumeb produced ~30 million tonnes at 4.0% Cu, 9.0% Pb and 3.2% Zn. Production plus reserves at Kipushi are believed to be about 70 million tonnes at 4.8% Cu, 8.8% Zn and 0.5% Pb. Kennecott production was 4.4 million tonnes at 12.4% Cu and 95 g/t Ag. These three deposits are the most significant producers and also reflect the highest average grades for Cu (Kennecott), Pb (Tsumeb) and Zn (Kipushi). The Ruby Creek resource is 90 million tonnes grading 1.2% Cu. Ge and Ga were produced at Tsumeb, Kipushi(?) and Apex; Apex grades were in the order of 0.06% Ge and 0.03% Ga.

**ECONOMIC LIMITATIONS:** Although several deposits have been partially mined by open pit methods, the elongate morphology usually requires underground mining. The complex suite of metallic minerals in some deposits could complicate metallurgy.

**IMPORTANCE:** Gross and unit metal values can be very high. Few significant deposits are recognized; however, the type is poorly understood and exploration efforts have been minimal.

## ***SELECTED BIBLIOGRAPHY***

**ACKNOWLEDGEMENTS:** Work leading to this summary was supported by BHP Minerals Canada Ltd. and their Canadian Exploration Manager, Neil le Nobel. Numerous other geologists have enhanced my understanding of this deposit type, including Tom Pollock, Murray Hitzman, Rod Kirkham, Hans Trettin and Arno Günzel. Dave Lefebure and Trygve Höy reviewed drafts and significantly improved this profile.

- Bateman, A.M. and D.H. McLaughlin (1920): Geology of the Ore Deposits of Kennecott, Alaska; *Economic Geology*, Volume 15, pages 1-80.
- Bernstein, L.R. (1986): Geology and Mineralogy of the Apex Germanium-Gallium Mine, Washington County, Utah; *U.S. Geological Survey, Bulletin 1577*, 9 pages.
- Bernstein, L.R. and D.P. Cox (1986): Geology and Sulfide Mineralogy of the Number One Orebody, Ruby Creek Copper Deposit, Alaska; *Economic Geology*, Volume 81, pages 1675-1689.
- Blockley, J.G. and J.S. Myers (1990): Proterozoic Rocks of the Western Australian Shield - Geology and Mineralisation; in *Geology of the Mineral Deposits of Australia and Papua New Guinea*, F.E. Hughes, Editor, *Australian Institute of Mining and Metallurgy, Monograph 14*, pages 607-615.
- British Columbia Department of Mines and Petroleum Resources (1971): Blue; in *Geology, Exploration and Mining in B.C.*, pages 72-75.
- Buffet, G., Amosse, J., Mouzita, D. and Giraud, P. (1997): Geochemistry of the M'Passa Pb-Zn Deposit, Niari syncline, People's Republic of the Congo - Arguments in Favor of a Hydrothermal Origin; *Mineralium Deposita*, Volume 22, pages 64-77.
- Chabu, M. (1990): Metamorphism of the Kipushi Carbonate Hosted Zn-Pb-Cu deposit, Shaba, Zaire; in *Regional Metamorphism of Ore Deposits*, P.G. Spry and L.T. Bryndzia, Editors, *Proceedings of 28th International Geological Conference, VSP*, pages 27-47.
- Cox, D.P. and L.R. Bernstein (1986): Descriptive Model of Kipushi Cu-Pb-Zn; in *Mineral Deposit Models*, D.P. Cox and D.A. Singer, Editors, *U.S. Geological Survey, Bulletin 1693*, 227 pages.
- Deane, J.G. (1995): The Structural Evolution of the Kombat Deposits, Otavi Mountainland, Namibia; *Communications, Geological Survey of Namibia*, Volume 10, pages 99-107.
- De Magnee, I. and A. Francois (1988): The Origin of the Kipushi (Cu, Zn, Pb) Deposit in Direct Relation with a Proterozoic Salt Diapir, Copperbelt of Central Africa, Shaba, Republic of Zaire; in *Base Metal Sulphide Deposits*, G.H. Friedrich and P.M. Herzig, Editors, *Springer-Verlag*, pages 74-93.
- Folger, P.F. and J.M. Schmidt (1986): Geology of the Carbonate-hosted Omar Copper Prospect, Baird Mountains, Alaska; *Economic Geology*, Volume 81, pages 1690-1695.
- Hitzman, M.W. (1986): Geology of the Ruby Creek Copper Deposit, Southwestern Brooks Range, Alaska; *Economic Geology*, Volume 81, pages 1644-1674.
- Hoeve, J. and D. Quirt (1989): A Common Diagenetic-hydrothermal Origin for Unconformity-type Uranium and Stratiform Copper Deposits?; in *Sediment-hosted Stratiform Copper Deposits*, R.W. Boyle *et al.*, Editors, *Geological Association of Canada, Special Paper 36*, pages 151-172.
- Innes, J. and R.C. Chaplin (1986): Ore Bodies of the Kombat Mine, South West Africa/Namibia; in *Mineral Deposits of Southern Africa*, C.R. Anhaeusser and S. Maske, Editors, *Geological Society of South Africa*, pages 1789-1805.
- Lhoest, J.J. (1995): The Kipushi Mine, Zaire; *Mineralogical Record*, Volume 26, Number 3, pages 163-192.
- Lombaard, A.F., Günzel, A., Innes, J. and Kruger, T.L. (1986): The Tsumeb Lead-copper-zinc-silver Deposit, South West Africa/Namibia; in *Mineral Deposits of Southern Africa*, C.R. Anhaeusser and S. Maske, Editors, *Geological Society of South Africa*, pages 1761-1787.
- Ran, C. (1989): Dongchuan-type Stratabound Copper Deposits, China - a Genetic Model; in *Sediment-hosted Stratiform Copper Deposits*, R.W. Boyle *et al.*, Editors, *Geological Association of Canada, Special Paper 36*, pages 667-677.
- Ruan, H., R. Hua and D.P. Cox (1991): Copper Deposition by Fluid Mixing in Deformed Strata Adjacent to a Salt Diapir, Dongchuan Area, Yunnan Province, China; *Economic Geology*, Volume 86, pages 1539-1545.
- Sagev, A. (1992): Remobilization of Uranium and Associated Metals through Karstification Processes - a Case Study from the Timna Formation (Cambrian), Southern Israel; *Ore Geology Reviews*, Volume 7, pages 135-148.
- Steed, G.M. (1986): The Geology and Genesis of the Gortdrum Cu-Ag-Hg Orebody; in *Geology and Genesis of Mineral Deposits in Ireland*, C.J. Andrew, *et al.*, Editors, *Irish Association, Economic Geology*, pages 481-499. Draft 3b, December 18, 1997



## BENTONITE

E06

by Z.D. Hora



### IDENTIFICATION

**SYNONYMS:** Sodium and calcium montmorillonites, montmorillonite clay, smectite clay, volcanic clay, soap clay, mineral soap. Other terms for sodium montmorillonites are sodium bentonite, swelling bentonite, Wyoming or Western bentonite, while calcium montmorillonites are referred to as calcium bentonites, non-swelling bentonite, Southern bentonite or fuller's earth, sub-bentonite.

**COMMODITY:** Bentonite (many different grades for a variety of applications and end uses).

**EXAMPLES (British Columbia (MINFILE #)- Canada/International):** Hat Creek (0921NW084), Princeton (092HSE151), Quilchena (0921SE138), French Bar (0920099); *Rosalind (Alberta, Canada), Truax (Saskatchewan, Canada) Morden (Manitoba, Canada), Black Hills District, Big Horn Basin (Wyoming, USA), Gonzales and Lafayette Counties (Texas, USA), Iwambaand and Monroe Counties (Mississippi, USA), Milos (Greece), Landshut (Germany), Sardinia (Italy), Annalka (Japan), Campina Grande (Brazil).*

### GEOLOGICAL CHARACTERISTICS

**CAPSULE DESCRIPTION:** Montmorillonite-rich clay beds intercalated with shales, sandstones and marls which are part of shallow marine or lacustrine environment deposits.

**TECTONIC SETTINGS:** Virtually all continental or continental platform settings; also common in island arcs.

**DEPOSITIONAL ENVIRONMENT / GEOLOGICAL SETTING:** Bentonite deposits form when volcanic ash is deposited in a variety of freshwater (sometimes alkaline lakes) and marine basins characterized by low energy depositional environments and temperate climatic conditions.

**AGE OF MINERALIZATION:** Mostly Cretaceous to Miocene age, but are known to be as old as Jurassic and as recent as Pleistocene.

**HOST/ASSOCIATED ROCK TYPES:** Bentonites are hosted by and associated with argillite, mudstone, siltstone, sandstone, tuff, agglomerate, ignimbrites, marl, shale, zeolite beds and coal.

**DEPOSIT FORM:** Beds range in thickness from several centimeters to tens of meters and can extend hundreds of kilometres. In island arc environment, bentonite can also occur as lens-shaped bodies with a limited lateral extent.

**TEXTURE/STRUCTURE:** Bentonite is bedded, with a soapy texture and waxy appearance. It ranges in colour from white to yellow to olive green to brown to blue. In outcrop, bentonite has a distinctive "popcorn" texture.

**ORE MINERALOGY [Principal and subordinate]:** Montmorillonite, *beidellite, illite.*

**GANGUE MINERALOGY [Principal and subordinate]:** Mica, feldspar, quartz, calcite, zeolites, gypsum, *opaline silica, cristobalite, unaltered volcanic glass.* These minerals rarely constitute more than 10% of a commercially viable deposit.

**ALTERATION MINERALOGY:** Alteration consists of devitrification of the volcanic ash with hydration and crystallization of the smectite mineral. In some instances there is evidence of a loss of alkalis during the alteration. Also, silicification of beds underlying some bentonites indicates downward migration of silica. There is also sometimes an increase in magnesium content compared to parent material. Besides smectite minerals, other alteration products in the volcanic ash include cristobalite, opaline silica, zeolites, calcite, selenite and various iron sulphate minerals.

# BENTONITE

E06

**WEATHERING:** Yellow colouration (the result of oxidized iron ions) may improve the colloidal properties of bentonite. Also, weathering may decrease exchangeable calcium and increase exchangeable sodium. Some soluble impurities like calcite, iron sulphates or selenite may be removed by weathering process.

**ORE CONTROLS:** The regional extent of bentonite deposits is controlled by the limit of the regional deposition environment, paleogeography and distribution of the volcanic pyroclastic unit. Porosity of the host rocks may be important for the alteration process. Deposits in the continental and continental platform settings are the largest.

**GENETIC MODELS:** Volcanic pyroclastic material is ejected and deposited in shallow marine or lacustrine setting. Bentonite is a product of alteration of the glass component of ashes and agglomerates. Alteration of the glassy pyroclastic material possibly starts when the ash contacts the water or may occur soon after the ash reaches the seafloor or lake bottom. Wyoming bentonites, however, were altered after burial by reaction with diagenetic seawater pore fluids

**ASSOCIATED DEPOSIT TYPES:** Other clays, zeolite (D01, D02), lignite coal (A02), sepiolite, palygorskite (F05).

## *EXPLORATION GUIDES*

**GEOCHEMICAL SIGNATURE:** Nil

**GEOPHYSICAL SIGNATURE:** Apparent resistivity and refraction seismic survey may help to interpret the lithology.

**OTHER EXPLORATION GUIDES:** Sedimentary basins with volcanic ash layers. In some locations bentonite layers can form a plane of weakness that results in landslides. Montmorillonite displays popcorn texture on the dry surface.

## *ECONOMIC FACTORS*

**TYPICAL GRADE AND TONNAGE:** Montmorillonite content is usually more than 80%. Other properties depend on specifications for particular applications. Published data on individual deposits are very scarce. Typically, commercial beds in Wyoming are 0.9 to 1.5 metres thick. Individual bentonite beds are continuous for several kilometres. The Wilcox mine in Saskatchewan has three bentonite seams - 61, 46 and 30 centimetres thick within a 6 metre thick sequence of shale. In Manitoba, another mine has 6 beds which have a cumulative thickness of about 76 centimetres within a 1 meter sequence.

**ECONOMIC LIMITATIONS:** Value of the product depends on the type of impurities, colour, size of clay particles, cation exchange capability, rheological properties and structures of the clay. Sodium bentonites are of more interest because of swelling properties and in general higher cation exchange capacity. Calcium bentonites are frequently activated by acids or soda ash to provide better performing product. Economic viability is often determined by the thickness of the overlying strata and overburden. The Wyoming deposits are mined with up to 12 metres of overburden. The 1997 quoted price for Wyoming bentonite is from US\$25 to 40 a short ton.

**END USES:** Main uses for bentonite are in foundry sands, drilling muds, iron ore pelletizing and absorbents. Important applications are also in civil engineering for a variety of composite liners and as a food additive for poultry and domestic animals. (Special uses include filtration in food processing, cosmetics and pharmaceuticals.)

**IMPORTANCE:** Bentonite is an important industrial mineral; about 6 million tonnes are produced annually in North America. Declining markets in drilling mud and pelletizing will likely be easily offset by increasing use in environmental applications like liners and sealers.

*SELECTED BIBLIOGRAPHY*

- Elzea, J. and Murray, H.H. (1994): Bentonite; in *Industrial Minerals and Rocks*, D.D. Carr, Editor, *Society for Mining, Metallurgy, and Exploration, Inc.*, Littleton, Colorado, pages 233-246.
- Grim, R.E. and Güven, N. (1978): Bentonites: Geology, Mineralogy, Properties and Uses; *Developments in Sedimentology 24*, *Elsevier Publishing Company*, New York, 256 pages.
- Guillet, G.R. and Martin, W. Editors (1984): The Geology of Industrial Minerals in Canada; Special Volume 29, *The Canadian Institute of Mining and Metallurgy*, 350 pages.
- Güven, N. (1989): Smectites; in *Hydrous Phyllosilicates*, Bailey, S.W., Editor, *Reviews in Mineralogy*, Volume 19, *Mineralogical Society of America*, pages 497-560.
- Harben, P.W. and Bates, R.L. (1990): *Industrial Minerals and World Deposits*; *Metal Bulletin*, London, 312 pages.
- Robertson, R.H.S. (1986): Fuller's Earth - a History of Calcium Montmorillonite; *Mineralogical Society*, Occasional Publication, Volturna Press, 412 pages.

Draft #3a December 15, 1997





## SEDIMENTARY KAOLIN

E07

by Z.D. Hora

### IDENTIFICATION



**SYNONYMS:** Secondary kaolin deposits, fireclay, underclays, high-alumina clay, china clay.

**COMMODITIES (BYPRODUCTS)** Kaolin (many different grades for specific applications), ceramic clay, ball clay, refractory clay (cement rock, bauxite, silica sand).

**EXAMPLES** (British Columbia (MINFILE #) - *Canada/International*): Sumas Mountain (92GSE004, 92GSE024), Blue Mountain (92GSE028), Lang Bay (92F137), Quinsam (92F319), Giscoe Rapids (93J020); *Cypress Hills (Alberta, Canada), Eastend, Wood Mountain, Ravenscrag (Saskatchewan, Canada), Moose River Basin (Ontario, Canada), Shubenacadie Valley (Nova Scotia, Canada), Aiken (South Carolina, USA), Wrens, Sandersville, Macon-Gordon, Andersonville (Georgia, USA), Eufaula (Alabama, USA), Weipa (Queensland, Australia), Jari, Capim (Brazil).*

### GEOLOGICAL CHARACTERISTICS

**CAPSULE DESCRIPTION:** Beds, lenses and saucer-shaped bodies of kaolinitic claystones hosted by clastic sedimentary rocks, with or without coaly layers or coal seams. They usually occur in freshwater basins filled with sediments derived from deeply weathered, crystalline feldspathic rocks.

**TECTONIC SETTINGS:** Low-lying coastal plains at continental edge; extension basins in orogenic belts; stable continental basins; back arc basins.

**DEPOSITIONAL ENVIRONMENT / GEOLOGICAL SETTING:** Clay beds are generally deposited in low energy environments within freshwater basins. Temperate to tropical climatic conditions can produce intensive kaolinitic weathering of feldspathic rocks of granitic composition. The kaolin is then eroded and transported to estuaries, lagoons, oxbow lakes and ponds.

**AGE OF MINERALIZATION:** Most of the world class deposits are Upper Cretaceous to Eocene age. Some "fireclay" and "underclay" deposits are Late Carboniferous.

**HOST/ASSOCIATED ROCK TYPES:** Kaolin beds are associated with variably kaolinitic, micaceous sandstones within mudstone, siltstone, sandstone and conglomerate sequences which often are cross-bedded. Coal (sub-bituminous and lignite) may be associated with kaolin beds. Diatomite may also be present.

**DEPOSIT FORM:** Beds exhibit variable thickness, usually a few metres; sometimes multiple beds have an aggregate thickness of approximately 20 metres. Deposits commonly extend over areas of at least several square kilometers.

**TEXTURE/STRUCTURE:** Kaolin is soft and exhibits conchoidal or semiconchoidal fracture; it can be bedded or massive. Most kaolins will slake in water, but some "flint" varieties break into smaller angular fragments only. Depending on kaolin particle size and presence of organic matter, some clays may be very plastic when moist and are usually called "ball clays".

**ORE MINERALOGY [Principal and subordinate]:** Kaolinite, halloysite, quartz, dickite, nacrite, diaspor, boehmite, gibbsite.

**GANGUE MINERALOGY [Principal and subordinate]:** Quartz, limonite, goethite, feldspar, mica, siderite, pyrite, illmenite, leucoxene, anatase.

**WEATHERING:** The kaolin forms by weathering which results in decomposition of feldspars and other aluminosilicates and removal of fluxing components like alkalis or iron. Post depositional weathering and leaching can produce gibbsitic bauxite. In some deposits, post depositional weathering may improve crystallinity of kaolin particles and increase the size of crystal aggregates.

# SEDIMENTARY KAOLIN

E07

**ORE CONTROLS:** The formation and localization of clay is controlled by the location of the sedimentary basin and the presence of weathered, granitic rocks adjacent to the basin, particularly rapidly eroding paleotopographic highs.

**GENETIC MODELS:** Ideal conditions to produce kaolinitic chemical weathering are high rainfall, warm temperatures, lush vegetation, low relief and high groundwater table. The kaolin is eroded and transported by streams to a quiet, fresh or brackish, water environment. Post-depositional leaching, oxidation, and diagenesis can significantly modify the original clay mineralogy with improvement of kaolin quality.

**ASSOCIATED DEPOSIT TYPES:** Peat (A01), coal seams (A02, A03, A04), paleoplacers (CO4), some bentonites (EO6), lacustrine diatomite (FO6).

## *EXPLORATION GUIDES*

**GEOCHEMICAL SIGNATURE:** None. Enrichment in Al does not provide sufficient contrast with host sediments.

**GEOPHYSICAL SIGNATURE:** Apparent resistivity and refraction seismic surveys can be used in exploration for fireclay beds.

**OTHER EXPLORATION GUIDES:** Most readily ascertainable regional attribute is sedimentary basins with Upper Cretaceous and Eocene unconformities. Within these basins kaolin occurs with sediments, including coal seams, deposited in low energy environments.

## *ECONOMIC FACTORS*

**TYPICAL GRADE AND TONNAGE:** Published data on individual deposits are very scarce. Deposits in Georgia, USA contain 90 to 95% kaolinite. Individual Cretaceous beds are reported to be up to 12 m thick and extend more than 2 km while those in the Tertiary sequence are 10 to 25 m thick and up to 18 km along strike. The Weipa deposit in Australia is 8 to 12 m thick and contains 40 to 70% kaolinite. The Jari deposit in Brazil is reported to contain more than 250 Mt of "good, commercial grade kaolin". Over 200 Mt of reserves "have been proven" at Capim deposit in Brazil. Ball clay deposits in Tennessee and Kentucky consist of kaolin with from 5 to 30% silica; individual deposits may be more than 9 m thick and extend over areas from 100 to 800 m long and up to 300 m wide.

**ECONOMIC LIMITATIONS:** Physical and chemical properties affect end use. Physical properties include brightness, particle size distribution, particle shape and rheology. Limonite staining is a negative feature. The high level of processing required to meet industry specifications and minimize transportation cost to the end user are the main limiting factors for kaolin use. While local sources compete for low value markets, high quality products may be shipped to users several thousand km from the plant. Most production is from open pits; good quality fireclay seams more than 2 meters thick are sometimes mined underground. Typically, paper coating grade sells for up to US\$120, filler grade for up to US\$92 and sanitary ceramics grade for \$US55 to \$65 per short ton (Industrial Minerals, 1997). Refractory and ball clay prices are within the same range.

**END USES:** The most important use for kaolin is in the paper industry, both as a filler and coating pigment. A variety of industrial filler applications (rubber, paints, plastics, etc.) are another major end use. Kaolin's traditional use in ceramic products is holding steady, but the refractory use has declined substantially in the last two decades because of replacement by other high performance products.

**IMPORTANCE:** One of the most important industrial minerals in North America. Over 11 Mt is produced annually and production is on a steady increase.

*SELECTED BIBLIOGRAPHY*

- Bristow, C.M. (1987): World Kaolins - Genesis, Exploitation and Application, *Industrial Minerals*, No. 238, pages 45-59.
- Guillet, G.R. and Martin, W., Editors (1984): The Geology of Industrial Minerals in Canada, Special Volume 29, *The Canadian Institute of Mining and Metallurgy*, 350 pages.
- Harben, P.W. and Bates, R.L. (1990): Industrial Minerals and World Deposits, *Metal Bulletin*, London, 312 pages.
- Mařkovsky, M. and Vachtl, J., Editors (1969): Kaolin Deposits of the World, A-Europe, B-Overseas Countries; Proceedings of Symposium 1, *23rd International Geological Congress*, Prague, 1968, 460 pages.
- Malkovsky, M. and Vachtl, J., Editors (1969): Genesis of the Kaolin Deposits; Proceedings of the Symposium 1, *23rd International Geological Congress*, Prague, 1968, 135 pages.
- Murray, H.H. (1989): Kaolin Minerals: Their Genesis and Occurrences, Hydrous Phyllosilicates, in Reviews in Mineralogy, Bailey, S.W., Editor, *Mineralogical Society of America*, Volume 19, pages 67-89.
- Murray, H.H., Bundy, W.M. and Harvey, C.C., Editors (1993): Kaolin Genesis and Utilization, *The Clay Minerals Society*, Boulder, Colorado, 341 pages.
- Patterson, S.H. and Murray, H.H. (1984): Kaolin, Refractory Clay, Ball Clay and Halloysite in North America, Hawaii, and the Caribbean Region; *U.S. Geological Survey*, Professional Paper 1306, 56 pages.

Draft # 3a December 15, 1997





## SPARRY MAGNESITE

E09

by G.J. Simandl and K. Hancock

### IDENTIFICATION



SYNONYMS: Veitsch-type, carbonate-hosted magnesite, crystalline magnesite.

COMMODITY: Magnesite.

EXAMPLES (British Columbia (MINFILE) - *Canada/International*): Mount Brussilof (082JNW001), Marysville (082GNW005), Brisco area and Driftwood Creek (082KNE068); *Veitsch, Entachen Alm, Hochfilzen, Radenthein and Breitenau (Austria), Eugui (Navarra Province, Spain), deposits of Ashan area, Liaoning Province (China), Satka deposit (Russia).*

### GEOLOGICAL CHARACTERISTICS

CAPSULE DESCRIPTION: Stratabound and typically stratiform, lens-shaped zones of coarse-grained magnesite mainly occurring in carbonates but also observed in sandstones or other clastic sediments. Magnesite exhibits characteristic sparry texture.

TECTONIC SETTING: Typically continental margin or marine platform, possibly continental settings, occur in belts.

DEPOSITIONAL ENVIRONMENT / GEOLOGICAL SETTING: The host sediments are deposited in a shallow marine environment adjacent to paleobathymetric highs or a lacustrine evaporitic environment.

AGE OF MINERALIZATION: Proterozoic or Paleozoic.

HOST/ASSOCIATED ROCK TYPES: Magnesite rock, dolostone, limestones, shales, chert. Associated with sandstone, conglomerate and volcanics and their metamorphic equivalents.

DEPOSIT FORM: Commonly strata, lenses or rarely irregular masses, typically few hundred metres to several kilometres in strike length. Shortest dimension of the orebody (metres to tens of metres) is commonly normal to the bedding planes.

TEXTURE/STRUCTURE: The magnesite-bearing rocks exhibit sparry, pinolitic, zebra-like, or xenotopic (anhedral) textures on the fresh surface. Magnesite or dolomite pseudomorphs after sulphates. "Box-textures", rosettes, monopolar and antipolar growths are locally present.

ORE MINERALOGY: Magnesite.

GANGUE MINERALOGY (Principal and *subordinate*): Dolomite  $\pm$  quartz  $\pm$  chert  $\pm$  talc  $\pm$  chlorite  $\pm$  sulphides  $\pm$  sulphosalts,  $\pm$  calcite,  $\pm$  mica,  $\pm$  palygorskite,  $\pm$  aragonite,  $\pm$  clay (as veinlets), organic material. In highly metamorphosed terrains, metamorphic minerals derived from above precursors will be present.

ALTERATION MINERALOGY: Talc may form on quartz-magnesite boundaries due to low temperature metamorphism.

WEATHERING: Surface exposures are typically beige or pale brown and characterized by "granola-like" appearance. Most sulphides are altered into oxides in near surface environment.

ORE CONTROLS: Deposits are stratabound, commonly associated with unconformities. They are typically located in basins characterized by shallow marine depositional environments. Lenses may be located at various stratigraphic levels within magnesite-hosting formation.

# SPARRY MAGNESITE

E09

GENETIC MODELS: There are two preferred theories regarding the origin of sparry magnesite deposits:

- 1) Replacement of dolomitized, permeable carbonates by magnesite due to interaction with a metasomatic fluid.
- 2) Diagenetic recrystallization of a magnesia-rich protolith deposited as chemical sediments in marine or lacustrine settings. The sediments would have consisted of fine-grained magnesite, hydromagnesite, huntite or other low temperature magnesia-bearing minerals. The main difference between these hypotheses is the source of magnesia; external for metasomatic replacement and in situ in the case of diagenetic recrystallization. Temperatures of homogenization of fluid inclusions constrain the temperature of magnesite formation or recrystallization to 110 to 240°C. In British Columbia the diagenetic recrystallization theory may best explain the stratigraphic association with gypsum and halite casts, correlation with paleotopographic highs and unconformities, and shallow marine depositional features of the deposits. A number of recent cryptocrystalline sedimentary magnesite deposits, such as Salda Lake in Turkey and the Kunwarara deposit in Queensland, Australia, huntite-magnesite-hydromagnesite deposits of Kozani Basin, Northern Greece, and the magnesite- or hydromagnesite-bearing evaporitic occurrences from Sebkhah el Melah in Tunisia may be recent analogs to the pre-diagenetic protoliths for British Columbia sparry magnesite deposits.

ASSOCIATED DEPOSIT TYPES: Sediment-hosted talc deposits (E08) and Mississippi Valley-type deposits (E12) are geographically, but not genetically, associated with sparry magnesite in British Columbia. The magnesite appears older than cross-cutting sparry dolomite that is commonly associated with MVT deposits.

COMMENTS: Magnesite deposits can survive even in high grade metamorphic environments because of their nearly monomineralic nature.

## *EXPLORATION GUIDES*

GEOCHEMICAL SIGNATURE: Tracing of magnesite boulders and blocks with pinolitic texture. Magnesite grains in stream sediments.

GEOPHYSICAL SIGNATURE: N/A.

OTHER EXPLORATION GUIDES: Surface exposures are beige, pale brown or pale gray. White fine-grained marker horizons are useful in southwest British Columbia. "Granola-like" weathering texture is a useful prospecting indicator. Magnesite may be identified in the field using heavy-liquids. In British Columbia the deposits are often associated with unconformities, paleotopographic highs within particular stratigraphic horizons.

## *ECONOMIC FACTORS*

TYPICAL GRADE AND TONNAGE: Grades range from 90 to 95% MgCO<sub>3</sub> with the resources ranging from several to hundreds of million tonnes. British Columbia deposits are characterized by lower iron content than most of the European deposits.

ECONOMIC LIMITATIONS: There is large but very competitive market for magnesia-based products. China is the largest exporter of magnesite. Quality of primary raw materials, cost of energy, cost of transportation to markets, availability of existing infrastructure, and the quality of finished product are major factors achieving a successful operation.

END USES: Magnesite is used to produce magnesium metal and caustic, dead-burned and fused magnesia. Caustic magnesia, and derived tertiary products are used in chemical and industrial applications, construction, animal foodstuffs and environmental rehabilitation. Fused and dead-burned magnesia are used in high-performance refractories. Magnesium metal has wide range of end uses, mostly in the aerospace and automotive industries. The automotive market for magnesium metal is expected to expand rapidly with current efforts to reduce the weight of vehicles to improve fuel economy and reduce harmful emissions.

# SPARRY MAGNESITE

E09

IMPORTANCE: Sparry magnesite deposits account for 80% of the world production. Significant quantities of magnesite are also produced from ultramafic-hosted deposits and fine grained or nodular deposits.

## SELECTED BIBLIOGRAPHY

ACKNOWLEDGEMENTS: The manuscript benefited from discussion with I. Knuckey and C. Pilarski of Baymag Mines Co. Ltd. Review by D.V. Lefebure is appreciated.

- Chevalier, P. (1995): Magnesium; in 1994 Canadian Mineral Yearbook, *Natural Resources Canada*, pages 29.1-29.13.
- Grant, B. (1987): Magnesite, Brucite and Hydromagnesite Occurrences in British Columbia; *B.C. Ministry of Energy, Mines and Petroleum Resources*, Open File 1987-13, 80 pages.
- Hancock, K.D. and Simandl, G.J. (1992). Geology of the Marysville Magnesite Deposit, Southeastern British Columbia; *B.C. Ministry of Energy, Mines and Petroleum Resources*, Exploration in British Columbia, Part B, pages 71-80.
- Harben, P.W. and Bates, R.L. 1990. Industrial Minerals, Geology and World Deposits. Industrial Minerals Division, *Metal Bulletin PLC*, London, 312 pages.
- Kendall, T. (1996): Dead-burned Magnesite, *Industrial Minerals*, Number 341, pages 25-51.
- Möller, P. (1989): Magnesite; Monograph Series on Mineral Deposits, Number 28, *Gebrüder Borntraeger*, pages 105-113.
- Morteani, G. (1989): Mg-metasomatic Type Sparry Magnesites of Entachen Alm, Hochfilzen/Bürglkopf and Spiessnagel (Austria); in Magnesite; Monograph Series on Mineral Deposits, Number 28, *Gebrüder Borntraeger*, 300 pages.
- Niashihara, H. (1956): Origin of bedded Magnesite Deposits of Manchuria; *Economic Geology*, Volume 51, pages 25-53.
- O'Driscoll, M. (1994): Caustic Magnesia Markets; *Industrial Minerals*, Volume 20, pages 23-45.
- O'Driscoll, M. (1996): Fused Magnesia; *Industrial Minerals*, Number 340, pages 19-27.
- Simandl, G.J. and Hancock K.D. (1996): Magnesite in British Columbia, Canada: A Neglected Resource; *Mineral Industry International*, Number 1030, pages 33-44.
- Simandl, G.J., Simandl, J., Hancock, K.D. and Duncan, L. (1996): Magnesite deposits in B.C. - Economic Potential; *Industrial Minerals*, Number 343, pages 125-132.
- Simandl, G.J., Hancock, K.D., Paradis, S. and Simandl, J. (1993). Field identification of Magnesite-bearing rocks Using Sodium Polytungstate; *CIM Bulletin*, Volume 966, pages 68-72.
- Simandl, G.J. and Hancock, K.D., 1992. Geology of the Dolomite-hosted Magnesite Deposits of Brisco and Driftwood Creek areas, British Columbia; in: Fieldwork 1991, *B.C. Ministry of Mines and Petroleum Resources*, Paper 1992-1, pages 461-478.

Draft #4a December 15, 1997





## SEDIMENTARY-HOSTED, STRATIFORM BARITE E17

by S. Paradis<sup>1</sup>, G.J. Simandl, D. MacIntyre and G.J. Orris<sup>2</sup>



### IDENTIFICATION

SYNONYM: Bedded barite.

COMMODITIES (*BYPRODUCTS*): Barite (possibly Zn, Pb,  $\pm$  Ag).

EXAMPLES (British Columbia (MINFILE #)- *Canada/International*): Kwadacha (094F020), Gin (094F017), Gnome (094F02E); *Tea, Tyrala, Hess, Walt and Cathy (Yukon, Canada), Walton (Nova Scotia, Canada), Fancy Hill (Arkansas, USA), Mountain Springs, Greystone (Nevada, USA), Jixi and Liulin (China), Fig Tree and Mabiligwe (South Africa).*

### GEOLOGICAL CHARACTERISTICS

CAPSULE DESCRIPTION: Sedimentary-hosted, stratiform or lens-shaped barite bodies, that may reach over ten metres in thickness and several kilometres in strike length. Barite-rich rocks (baritites) are commonly lateral distal equivalents of shale-hosted Pb-Zn (SEDEX) deposits. Some barite deposits are not associated with shale-hosted Zn-Pb deposits.

TECTONIC SETTINGS: Intracratonic or continental margin-type fault-controlled marine basins or half-grabens of second or third order and peripheral foreland (distal to the continental margin) basins.

DEPOSITIONAL ENVIRONMENT / GEOLOGICAL SETTING: Deep, starved marine basins to shallow water shelves. The barite-rich rocks (baritites) were deposited on the seafloor and commonly grade laterally into either shale-hosted Pb-Zn (SEDEX) deposits which formed closer to the submarine hydrothermal vents, or the more distal cherts, hematite-chert iron formations, silica and manganese-enriched sediments.

AGE OF MINERALIZATION: Deposits are hosted by rocks of Archean to Mesozoic ages but are most common in rocks of Phanerozoic, especially in the mid to late Paleozoic age.

HOST/ASSOCIATED ROCK TYPES: Major rock types hosting barite are carbonaceous and siliceous shales, siltstones, cherts, argillites, turbidites, sandstones, dolomites and limestones.

DEPOSIT FORM: Stratiform or lens-shaped deposits are commonly metres thick, but their thickness may exceed 50 metres. Their lateral extent may be over several square kilometres.

TEXTURE/STRUCTURE: The barite ore is commonly laminated, layered or massive. Barite may form rosettes, randomly oriented laths or nodules. Some of the barite deposits display breccias and slump structures. In metamorphosed areas, barite may be remobilized (forming veinlets) and/or recrystallized.

ORE MINERALOGY [Principal and *subordinate*]: Barite.

GANGUE MINERALOGY [Principal and *subordinate*]: Quartz, clay, organic material, celsian, hyalophane, cymrite, barytocalcite, calcite, dolomite, pyrite, *marcasite, sphalerite, galena, and in some cases witherite.*

ALTERATION MINERALOGY: None in most cases. Secondary barite veining. Weak to moderate sericitization reported in, or near, some deposits in Nevada.

WEATHERING: Barite-rich exposures sometimes create vegetation "kill zones".

<sup>1</sup> Geological Survey of Canada, Sidney, British Columbia.

<sup>2</sup> U.S. Geological Survey, Tuscon, Arizona.

# SEDIMENTARY-HOSTED, STRATIFORM BARITE E17

**ORE CONTROLS:** Sedimentary depositional environment is mainly half-grabens and basins of second or third order. While Zn-Pb-barite (SEDEX) deposits may require euxinic environment to stabilize sulphides, more oxidized depositional environment may be the key for deposition of high-grade (nearly sulphide-free) barite deposits. Syndepositional faults are extremely important for SEDEX deposits that are commonly proximal to the vents, but may not be essential for all sediment-hosted stratabound barite deposits.

**GENETIC MODEL:** Some stratiform barite deposits form from hydrothermal fluids that exhaled on the seafloor and precipitated barite and other minerals (sulphides, chert, etc.) as chemical sediments. The chemical sediments change composition with distance from the vent reflecting changes in temperature and other parameters of the hydrothermal fluid as it mixed with seawater. Barite-rich sediments can reflect hydrothermal fluids deficient in metals (lack of base metals in the source rock or insufficient temperature or unfavorable physical-chemical fluid conditions to carry base metals) or discharge of hydrothermal fluids in a shallow marine environment that does not favor precipitation of sulphides. Some of the sedimentary-hosted barite deposits are interpreted as chemical sediments related to inversion of stratified basin resulting in oxygenation of reduced waters. Others formed by erosion and reworking of sub-economic chemical sediments (Heinrichs and Reimer, 1977) or of semi-consolidated clays containing barite concretions (Reimer, 1986), resulting in selective concentration of barite.

**ASSOCIATED DEPOSIT TYPES:** Shale-hosted Zn-Pb deposits (E14), Irish-type massive sulphide deposits (E13), sedimentary manganese deposits (F01) and vein barite deposits (I10). In oxygen-starved basins, barite deposits may be stratigraphically associated with black shales enriched in phosphates (F08), vanadium, REE and uranium mineralization and possibly shale-hosted Ni-Mo-PGE (E16) deposits.

**COMMENTS:** There is a complete spectrum from sulphide-rich to barite-rich SEDEX deposits. The Cirque deposit in British Columbia, represents the middle of this spectrum and consists of interlaminated barite, sphalerite, galena and pyrite. Its reserves are in excess of 38.5 million tonnes averaging 8% Zn, 2.2% Pb, 47.2 g/tonne of Ag and 45-50% barite. Witherite, a barium carbonate, occurs as an accessory mineral in some barite deposits and rarely forms a deposit on its own. There has been no commercial witherite production in the western world since the mines in Northumberland, England closed. Recently, the Chengkou and Ziyang witherite deposits have been discovered in China (Wang and Chu, 1994). Witherite deposits may form due to severe depletion of seawater in  $\text{SO}_4^{2-}$  and enrichment in Ba (Maynard and Okita, 1991). Alternatively, these deposits could have formed by high temperature replacement of barite by witherite (Turner and Goodfellow, 1990).

## EXPLORATION GUIDES

**GEOCHEMICAL SIGNATURE:** Barium enrichment on the scale of the basin and other indicators of shale-hosted Zn-Pb deposits, such as high values of Zn, Pb, Mn, Cu and Sr, in rock and stream sediment samples. Strongly anomalous Ba values in stream sediments and heavy sediments are only found in close proximity to barite mineralization because barite abrades rapidly during stream sediment transportation. The difference between  $^{87}\text{Sr}/^{86}\text{Sr}$  ratios of barite and coeval seawater may be used to distinguish between cratonic rift (potentially SEDEX-related) barite occurrences and those of peripheral foreland basins (Maynard *et al.*, 1995).

**GEOPHYSICAL SIGNATURE:** Deposit may correspond to a gravity-high.

**OTHER EXPLORATION GUIDES:** Appropriate tectonic and depositional setting. Proximity to known occurrences of barite, shale-hosted SEDEX or Irish-type massive sulphide occurrences, exhalative chert, hematite-chert iron formations and regional Mn marker beds. Vegetation "kill zones" coincide with some barite occurrences.

## ECONOMIC FACTORS

**TYPICAL GRADE AND TONNAGE:** Deposits range from less than 1 to more than 25 million tonnes grading 30% to over 95% barite with a median size of 1.24 million tonnes containing 87.7 %  $\text{BaSO}_4$  (Orris, 1992). Portions of some deposits may be direct shipping ore. The Magcobar mine in the Silvermines district of Ireland produced 4.6 Mt of 85%  $\text{BaSO}_4$  lump. Barite is produced at some metal mines, including the Ramelsburg and Meggen (8.9 Mt) mines in Germany.

## SEDIMENTARY-HOSTED, STRATIFORM BARITE E17

**ECONOMIC LIMITATIONS:** Several modern applications require high brightness and whiteness values and high-purity products. There are different requirements for specific applications. Abrasivity, grade of concentrate, color, whiteness, density and type of impurities, oil index, water index, refractive index and base metal content are commonly reported for commercially available concentrates. Transportation cost, specific gravity and content of water-soluble alkaline earth metals, iron oxides and sulphides are important factors for barite used in drilling applications. Currently sulphide-free barite deposits are preferred by the barite producers. Some of the barite on the market is sold without complex upgrading. Selective mining and/or hand sorting, jigging, flotation and bleaching are commonly required. It is possible that in the future, due to technological progress, a substantial portion of barite on the market will originate as by-product of metal mining.

**END USES:** Barite is used mainly in drill muds, also as heavy aggregate, marine ballast, a source of chemicals, a component in ceramics, steel hardening, glass, fluxes, papers, specialized plastics and radiation shields, in sound proofing and in friction and pharmaceutical applications. Witherite is a desirable source of barium chemicals because it is soluble in acid, but it is not suitable for applications where inertness in acid environments is important.

**IMPORTANCE:** Competes for market with vein-type barite deposits. Celestite, ilmenite, iron oxides can replace barite in specific drilling applications. However the impact of these substitutes is minimized by relatively low barite prices.

### SELECTED BIBLIOGRAPHY

**ACKNOWLEDGMENTS:** Reviews of the manuscript by Dr. John Lydon of the Geological Survey of Canada and Dr. D.V. Lefebvre of the B.C. Geological Survey are appreciated.

- Brobst, D.A. (1994): Barium Minerals; in *Industrial Minerals and Rocks*, 6th edition, D.D. Carr, Senior Editor, *Society for Mining, Metallurgy and Exploration, Inc.*, Littleton, Colorado, pages 125-134.
- Clark, S. and Orris, G.J. (1991): Sedimentary Exhalative Barite; in *Some Industrial Mineral Deposit Models: Descriptive Deposit Models*, Orris, G.J. and Bliss, J.D., Editors, *U.S. Geological Survey*, Open-File Report 91-11A, pages 21-22.
- Heinrichs, T.K and Reimer, T.O. (1977): A Sedimentary Barite Deposit from the Archean Fig Tree Group of the Barberton Mountain Land (South Africa), *Economic Geology*, Volume 73, pages 1426-1441.
- Large, D.E. (1981): Sediment-hosted Submarine Exhalative Sulphide Deposits - a Review of their Geological Characteristics and Genesis; in *Handbook of Stratiform and Stratiform Ore Deposits*; Wolfe, K.E., Editor, *Geological Association of Canada*, Volume 9, pages 459-507.
- Lydon, J.W (1995): Sedimentary Exhalative Sulphides (SEDEX); in *Geology of Canadian Mineral Deposit Types*, Eckstrand, O.R., Sinclair, W.D. and Thorpe, R.I., Editors, *Geological Survey of Canada*, *Geology of Canada*, no. 8, pages 130-152.
- Lydon, J.W., Lancaster, R.D. and Karkkainen, P. (1979): Genetic Controls of Selwyn Basin Stratiform Barite/Sphalerite/Galena Deposits: An Investigation of the Dominant Barium Mineralogy of the TEA Deposit, Yukon; in *Current Research, Part B*; *Geological Survey of Canada*, Paper 79-1B, pages 223-229.
- MacIntyre, D.E. (1991): Sedex-Sedimentary-exhalative Deposits; in *Ore Deposits, Tectonics and Metallogeny in the Canadian Cordillera*, McMillan, W.J., Coordinator; *B.C. Ministry of Energy Mines and Petroleum Resources*, Paper 1991-4, pages 25-69.
- Maynard, J.B. and Okita, P.M. (1991): Bedded Barite Deposits in the United States, Canada, Germany, and China: Two Major Types Based on Tectonic Setting; *Economic Geology*, volume 86, pages 364-376.
- Maynard, J.B. and Okita, P.M. (1992): Bedded Barite Deposits in the United States, Canada, Germany, and China: Two Major Types Based on Tectonic Setting - A Reply; *Economic Geology*, volume 87, pages 200-201.
- Orris, G.J. (1992): Grade and Tonnage Model of Bedded Barite; in *Industrial Minerals Deposit Models: Grade and Tonnage Models*; Orris, G.J. and Bliss J.D., Editors, *U.S. Geological Survey*, Open-File Report 92-437, pages 40-42.

## SEDIMENTARY-HOSTED, STRATIFORM BARITE E17

- Reimer, T.O. (1986): Phanerozoic Barite Deposits of South Africa and Zimbabwe; *in* Mineral Deposits of South Africa, Volume; Enhauser, C.R. and Maske, S., Editors, The Geological Society of South Africa, pages 2167-2172.
- Turner, R.J.W. (1992): Bedded Barite Deposits in the United States, Canada, Germany, and China: Two Major Types Based on Tectonic Setting- A Discussion; *Economic Geology*, Volume 87, pages 198-199.
- Turner, R.J.W. and Goodfellow, W.D. (1990): Barium Carbonate Bodies Associated with the Walt Stratiform Barite Deposit, Selwyn Basin, Yukon: a Possible Vent Complex Associated with a Middle Devonian Sedimentary Exhalative Barite Deposit; *in* Current Research, Part E, Geological Survey of Canada, Paper 90-1E, pages 309-319.
- Wang, Z.-C. and Chu, X.-L. (1994): Strontium Isotopic Composition of the Early Cambrian Barite and Witherite Deposits; *Chinese Science Bulletin*, Volume 39, pages 52-59.
- Wang, Z. and Li, G. (1991): Barite and Witherite in Lower Cambrian Shales of South China: Stratigraphic Distribution and Chemical Characterization; *Economic Geology*, Volume 86, pages 354-363.

Draft #3a      December 16, 1997



# UNCONFORMITY-ASSOCIATED U

I16

by R.H. McMillan<sup>1</sup>



## IDENTIFICATION

SYNONYMS: Unconformity-veins, unconformity-type uranium, unconformity U.

COMMODITIES (BYPRODUCTS): U (Au, Ni).

EXAMPLES (British Columbia - Canada/International): None in British Columbia; *Rabbit Lake, Key Lake, Cluff Lake, Midwest Lake, McClean Lake, McArthur River, Cigar Lake and Maurice Bay in the Athabasca uranium district (Saskatchewan, Canada), Lone Gull (Kiggavik) and Boomerang Lake, Thelon Basin district (Northwest Territories, Canada), Jabiluka, Ranger, Koongarra and Nabarlek, Alligator River district (Northern Territory, Australia).*

## GEOLOGICAL CHARACTERISTICS

CAPSULE DESCRIPTION: Uranium minerals, generally pitchblende and coffinite, occur as fracture and breccia fillings and disseminations in elongate, prismatic-shaped or tabular zones hosted by sedimentary/metasedimentary rocks located below, above or across a major continental unconformity.

TECTONIC SETTING: Intracratonic sedimentary basins.

GEOLOGICAL SETTING/DEPOSITIONAL ENVIRONMENT: Structurally-prepared and porous zones within chemically favourable reduced or otherwise reactive strata.

AGE OF MINERALIZATION: Mid-Proterozoic, however, there is potential for younger deposits.

HOST/ ASSOCIATED ROCK TYPES: Shelf facies metasedimentary (amphibolite or granulite facies) rocks of Early Proterozoic age (graphitic or sulphide-rich metapelites, calcsilicate rocks and metapsammites), regolith and overlying continental sandstones of Middle Proterozoic age. The Early Proterozoic hostrocks in many cases are retrograded amphibolite-facies metamorphic rocks on the flanks of Archean gneiss domes. The overlying continental sandstones are well sorted fluvial quartz-rich psammites; generally with a clay or siliceous matrix and red or pale in colour. Dikes and sills, commonly diabases and lamprophyres, occur in some districts.

DEPOSIT FORM: Orebodies may be tabular, pencil shaped or irregular in shape extending up to few kilometres in length. Most deposits have a limited depth potential below the unconformity of less than a 100 m, however, the Jabiluka and Eagle Point deposits are concordant within the Lower Proterozoic host rocks and extend for several hundred metres below the unconformity.

TEXTURE/STRUCTURE: Most deposits fill pore space or voids in breccias and vein stockworks. Some Saskatchewan deposits are exceptionally rich with areas of "massive" pitchblende/coffinite. Features such as drusy textures, crustification banding, colloform, botryoidal and dendritic textures are present in some deposits.

<sup>1</sup> Consulting Geologist, Victoria, British Columbia.

ORE MINERALOGY (Principal and *subordinate*): Pitchblende (Th-poor uraninite), coffinite, uranophane, thucolite, brannerite, iron sulphides, *native gold*, *Co-Ni arsenides and sulpharsenides*, *selenides*, *tellurides*, *vanadinates*, *jordesite (amorphous molybdenite)*, *vanadates*, *chalcopyrite*, *galena*, *sphalerite*, *native Ag and PGE*. Some deposits are “simple” with only pitchblende and coffinite, while others are “complex” and contain Co-Ni arsenides and other metallic minerals.

GANGUE MINERALOGY: Carbonates (calcite, dolomite, magnesite and siderite), chalcedonic quartz, sericite (illite) chlorite and dravite (tourmaline).

ALTERATION: Chloritization, hematization, kaolinization, illitization and silicification. In most cases hematization is due to oxidation of ferrous iron bearing minerals in the wallrocks caused by oxidizing mineralizing fluids, however, the intense brick-red hematite adjacent to some high grade uranium ores is probably due to loss of electrons during radioactive disintegration of U and its daughter products. An interesting feature of the clay alteration zone is the presence of pseudomorphs of high grade metamorphic minerals, such as cordierite and garnet, in the retrograded basement wallrock.

WEATHERING: Uranium is highly soluble in the +6 valence state above the water table. It will re-precipitate as uraninite and coffinite below the water table in the +4 valence state in the presence of a reducing agents such as humic material or carbonaceous “trash”. Some U phosphates, vanadates, sulphates, silicates and arsenates are semi-stable under oxidizing conditions, consequently autunite, torbernite, carnotite, zippeite, uranophane, uranospinite and numerous other secondary minerals may be found in the near-surface zone of oxidation, particularly in arid environments.

ORE CONTROLS: A pronounced control related to a mid-Proterozoic unconformity and to favourable stratigraphic horizons within Lower Proterozoic hostrocks - these strata are commonly graphitic. Local and regional fault zones that intersect the unconformity may be important features. Generally found close to basement granitic rocks with a high U clark.

GENETIC MODEL: The exceptionally rich ore grades which characterize this type of deposit point to a complex and probably polygenetic origin.

- Some form of very early pre-concentration of U in the Archean basement rocks seems to have been important.
- The hostrocks are commonly Lower Proterozoic in age, and are comprised of metamorphosed rocks derived from marginal marine and near-shore facies sedimentary rocks which may have concentrated U by syngenetic and diagenetic processes.
- Although the behaviour of U under metamorphic and ultrametamorphic conditions is poorly known, it is possible that U could have been mobilized in the vicinity of Archean gneiss domes and anatectic granites and precipitated in pegmatites and stratabound deposits as non-refractory, soluble uraninite.
- Supergene enrichment in paleo regoliths, that now underlie the unconformity, may have been an important process in the additional concentration of U.
- Typically the overlying quartz-rich fluvial sandstones have undergone little deformation, but are affected by normal and reverse faults that are probably re-activated basement faults. In Saskatchewan, these faults carry ore in several deposits and in others appear to have facilitated the transport of U within the cover sandstones.
- Hydrothermal/diagenetic concentration of U through mixing of oxidized basinal and reduced basement fluids appear to have resulted in exceptional concentrations of U and Ni. There is a possibility that radiogenic heat developed in these extremely rich deposits may have been instrumental in heating formation fluids and in remobilizing the metals upwards above the deposit.

- Diabase dikes occur in faults near some deposits and some researchers have suggested that the dikes might have provided the thermal energy that remobilized and further upgraded U concentrations. Recent age dates of the Mackenzie dikes in the Athabasca district do not support this interpretation.

ASSOCIATED DEPOSIT TYPES: Sandstone-hosted U deposits (D05) are found in associated supracrustal quartz-rich arenites. Stratabound disseminated or skarn deposits, such as the Dudderidge Lake and Burbidge Lake deposits (Saskatchewan) and pegmatitic occurrences are commonly present in the metamorphosed basement rocks. In arid or semi-arid environments surficial deposits may be present in the overburden. The deposits have affinities to "Classical" U veins (I15).

COMMENTS: Virtually all the known unconformity-associated uranium deposits are found in the Athabasca Basin, Alligator River district and Thelon Basin. In British Columbia favourable target areas for this style of mineralization might be found within strongly metamorphosed shelf-facies Proterozoic strata near gneiss domes, particularly in plateau areas near the Cretaceous-Tertiary paleosurface. The Midnite mine, located 100 km south of Osoyoos, British Columbia, may be an unconformity-associated U deposit. The ore comprises fracture-controlled and disseminated U and alteration minerals (pitchblende, coffinite as well as autunite and other secondary minerals) within metamorphosed shelf-facies pelitic and calcareous rocks of the Precambrian Togo Formation. Production and reserves prior to closing at the Midnite mine are estimated at approximately 3.9 Mt grading 0.12% U.

## *EXPLORATION GUIDES*

GEOCHEMICAL SIGNATURE: U, Ni, Co, As, Pb and Cu are good pathfinder elements which can be utilized in standard stream silt, lake bottom sediment and soil surveys. Stream and lake bottom water samples can be analyzed for U and Ra. In addition, the inert gases He and Ra can often be detected above a U-rich source in soil and soil gas surveys, as well as in groundwater and springs. In Saskatchewan, lithogeochemical signatures have been documented in Athabasca Group quartz arenites for several hundred metres directly above the deposits and in glacially dispersed boulders located "down ice" - the signature includes boron (dravite) and low, but anomalous U as well as K and/or Mg clay mineral alteration (illite and chlorite).

GEOPHYSICAL SIGNATURE: During early phases of exploration of the Athabasca Basin, airborne and ground radiometric surveys detected near surface uranium deposits and their glacial dispersions. Currently, deeply penetrating ground and airborne electromagnetic surveys are used to map the graphitic argillites associated with most deposits. The complete spectrum of modern techniques (gravity, magnetic, magneto-telluric, electromagnetic, VLF-EM, induced polarization, resistivity) can be utilized to map various aspects of structure as well as hostrock and alteration mineral assemblages in the search for deep targets.

OTHER EXPLORATION GUIDES: Standard techniques using sensitive gamma ray scintillometers to detect mineralization directly in bedrock or in float trains in glacial till, frost boils, talus or other debris derived from U mineralization remain the most effective prospecting methods.

*ECONOMIC FACTORS*

**TYPICAL GRADE AND TONNAGE:** Individual deposits are generally small, but can be exceedingly high-grade, up to several percent U. The median size for 36 Saskatchewan and Australian deposits is 260 000 t grading 0.42% U (Grauch and Mosier, 1986). Some deposits are exceptionally high grade such as the Key Lake Gaertner-Deilmann deposits (2.5 Mt @ 2.3% U), Cigar Lake deposits (900 000 t @ 12.2% U) and McArthur River (1.4 Mt @12.7% U).

**ECONOMIC LIMITATIONS:** Since the early 1980s, average ore grades have generally risen to exceed 0.25% U. Problems related to the pervasively clay-altered wallrocks and presence of radon gas and other potentially dangerous elements associated with some high-grade uranium deposits in Saskatchewan have resulted in exceptionally high mining costs in some cases.

**IMPORTANCE:** The Rabbit Lake mine, opened in 1975, was the first major producer of unconformity-type ore. Since then the proportion of the world's production to come from unconformity-type deposits has increased to 33% and is expected to rise in the future.

*SELECTED BIBLIOGRAPHY*

**ACKNOWLEDGMENTS:** Nirankar Prasad and Sunil Gandhi of the Geological Survey of Canada, Larry Jones of the British Columbia Geological Survey and Jim Murphy of Uranerz Exploration reviewed the profile and provided many constructive comments.

- Cady, J.W. and Fox, K.F. Jr. (1984): Geophysical Interpretation of the Gneiss Terrane of Northern Washington and Southern British Columbia, and its Implication for Uranium Exploration; *U.S. Geological Survey, Professional Paper 1260*, 29 pages.
- Farstad, J. and Ayers, D.E. (1986): Midwest Uranium Deposit, Northern Saskatchewan, in Uranium Deposits of Canada, Evans, E.I., Editor, *Canadian Institute of Mining and Metallurgy, Special Volume 33*, pages 178-183.
- Fogwill, W.D. (1985): Canadian and Saskatchewan Uranium Deposits: Compilation, Metallogeny, Models Exploration; in *Geology of Uranium Deposits*, Sibbald T.I.I. and Petruk W. Editors, *Canadian Institute of Mining and Metallurgy, Special Volume 32*, pages 3-19.
- Jones, L. D. (1990): Uranium and Thorium Occurrences in British Columbia; *B.C. Ministry of Energy, Mines and Petroleum Resources, Open File 1990-32*, 78 pages.
- Grauch, R. I. and Mosier, Dan L. (1986): Descriptive Model of Unconformity U-Au; in *Mineral Deposit Models*, Cox, D. P. and Singer, D. A., Editors, *United States Geological Survey, Bulletin 1693*, pages 248-250.
- Milne, P.C. (1979): Uranium in Washington State: Proven Deposits and Exploration Targets; *The Canadian Institute of Mining and Metallurgy, Bulletin, Volume 72*, pages 95-101.
- Nash, J.T., Granger, H.C. and Adams, S.S. (1981): Geology and Concepts of Genesis of Important Types of Uranium Deposits; in *Economic Geology, 75th Anniversary Volume*, pages 63-116.
- Ruzicka, Vlad (1986): Uranium deposits of the Rabbit Lake -Collins Bay area, Saskatchewan; in *Uranium Deposits of Canada*, Evans, E.I., Editor, *Canadian Institute of Mining and Metallurgy, Special Volume 33*, pages 144-154.
- Tremblay, L.P. and Ruzicka, V. (1984): Unconformity-associated Uranium; in *Canadian Mineral Deposit Types: A Geological Synopsis*, Eckstrand, O.R., Editor, *Geological Survey of Canada, Economic Geology Report 36*, page 61.
- Wallis, R.H., Saracoglu, N., Brummer, J.J., and Golightly, J.P. (1986): The Geology of the McClean Uranium Deposits, Northern Saskatchewan; in *Uranium Deposits of Canada*, Evans, E.I., Editor, *Canadian Institute of Mining and Metallurgy, Special Volume 33*, pages 193-217.

December 8, 1997 Draft # 6



## Au SKARNS

K04

by Gerald E. Ray

Revised 1997



### IDENTIFICATION

SYNONYMS: Pyrometamorphic, tactite, or contact metasomatic Au deposits.

COMMODITIES (BYPRODUCTS): Au (Cu, Ag).

EXAMPLES (British Columbia - Canada/International): Nickel Plate (092HSE038), French (092HSE059), Canty (092HSE 064), Good Hope (092HSE060), QR - Quesnel River (093A121); *Fortitude, McCoy and Tomboy-Minnie (Nevada, USA), Buckhorn Mountain (Washington, USA), Diamond Hill, New World district and Butte Highlands (Montana, USA), Nixon Fork (Alaska, USA), Thanksgiving (Philippines), Browns Creek and Junction Reefs-Sheahan-Grants (New South Wales, Australia), Mount Biggenden (Queensland, Australia), Savage Lode, Coogee (Western Australia, Australia), Nambija (Ecuador), Wabu (Irian Jaya, Indonesia).*

### GEOLOGICAL CHARACTERISTICS

CAPSULE DESCRIPTION: Gold-dominant mineralization genetically associated with a skarn gangue consisting of Ca - Fe - Mg silicates, such as clinopyroxene, garnet and epidote. Gold is often intimately associated with Bi or Au-tellurides, and commonly occurs as minute blebs (<40 microns) that lie within or on sulphide grains. The vast majority of Au skarns are hosted by calcareous rocks (calcic subtype). The much rarer magnesian subtype is hosted by dolomites or Mg-rich volcanics. On the basis of gangue mineralogy, the calcic Au skarns can be separated into either pyroxene-rich, garnet-rich or epidote-rich types; these contrasting mineral assemblages reflect differences in the hostrock lithologies as well as the oxidation and sulphidation conditions in which the skarns developed.

TECTONIC SETTINGS: Most Au skarns form in orogenic belts at convergent plate margins. They tend to be associated with syn to late island arc intrusions emplaced into calcareous sequences in arc or back-arc environments.

DEPOSITIONAL ENVIRONMENT / GEOLOGICAL SETTING: Most deposits are related to plutonism associated with the development of oceanic island arcs or back arcs, such as the Late Triassic to Early Jurassic Nicola Group in British Columbia.

AGE OF MINERALIZATION: Phanerozoic (mostly Cenozoic and Mesozoic); in British Columbia Au skarns are mainly of Early to Middle-Jurassic age. The unusual magnesian Au skarns of Western Australia are Archean.

HOST/ASSOCIATED ROCK TYPES: Gold skarns are hosted by sedimentary carbonates, calcareous clastics, volcanoclastics or (rarely) volcanic flows. They are commonly related to high to intermediate level stocks, sills and dikes of gabbro, diorite, quartz diorite or granodiorite composition. Economic mineralization is rarely developed in the endoskarn. The I-type intrusions are commonly porphyritic, undifferentiated, Fe-rich and calc-alkaline. However, the *Nambija, Wabu* and *QR* Au skarns are associated with alkalic intrusions.

DEPOSIT FORM: Variable from irregular lenses and veins to tabular or stratiform orebodies with lengths ranging up to many hundreds of metres. Rarely, can occur as vertical pipe-like bodies along permeable structures.

TEXTURE/STRUCTURE: Igneous textures in endoskarn. Coarse to fine-grained, massive granoblastic to layered textures in exoskarn. Some hornfelsic textures. Fractures, sill-dike margins and fold hinges can be an important loci for mineralization.

# Au SKARNS

K04

**ORE MINERALOGY (Principal and subordinate):** The gold is commonly present as micron-sized inclusions in sulphides, or at sulphide grain boundaries. To the naked eye, ore is generally indistinguishable from waste rock. Due to the poor correlation between Au and Cu in some Au skarns, the economic potential of a prospect can be overlooked if Cu-sulphide-rich outcrops are preferentially sampled and other sulphide-bearing or sulphide-lean assemblages are ignored. The ore in pyroxene-rich and garnet-rich skarns tends to have low Cu: Au (<2000:1), Zn: Au (<100:1) and Ag: Au (<1:1) ratios, and the gold is commonly associated with Bi minerals (particularly Bi tellurides).

**Magnesian subtype:** Native gold ± pyrrhotite ± chalcopyrite ± pyrite ± magnetite ± galena ± tetrahedrite.

**Calcic subtype:**

**Pyroxene-rich Au skarns:** Native gold ± pyrrhotite ± arsenopyrite ± chalcopyrite ± tellurides (e.g. *hedleyite*, *tetradymite*, *altaite* and *hessite*) ± bismuthinite ± cobaltite ± native bismuth ± pyrite ± sphalerite ± maldonite. They generally have a high sulphide content and high pyrrhotite:pyrite ratios. Mineral and metal zoning is common in the skarn envelope. At Nickel Plate for example, this comprises a narrow proximal zone of coarse-grained, garnet skarn containing high Cu: Au ratios, and a wider, distal zone of finer grained pyroxene skarn containing low Cu: Au ratios and the Au-sulphide orebodies.

**Garnet-rich Au skarns:** Native gold ± chalcopyrite ± pyrite ± arsenopyrite ± sphalerite ± magnetite ± hematite ± pyrrhotite ± galena ± tellurides ± bismuthinite. They generally have a low to moderate sulphide content and low pyrrhotite:pyrite ratios.

**Epidote-rich Au skarn:** Native gold ± chalcopyrite ± pyrite ± arsenopyrite ± hematite ± magnetite ± pyrrhotite ± galena ± sphalerite ± tellurides. They generally have a moderate to high sulphide content with low pyrrhotite:pyrite ratios.

**EXOSKARN MINERALOGY (GANGUE):**

**Magnesian subtype:** Olivine, clinopyroxene (Hd2-50), garnet (Ad7-30), chondrodite and monticellite. Retrograde minerals include serpentine, epidote, vesuvianite, tremolite-actinolite, phlogopite, talc, K-feldspar and chlorite.

**Calcic subtype:**

**Pyroxene-rich Au skarns:** Extensive exoskarn, generally with high pyroxene:garnet ratios. Prograde minerals include diopsidic to hedenbergitic clinopyroxene (Hd 20-100), K-feldspar, Fe-rich biotite, low Mn grandite garnet (Ad 10-100), wollastonite and vesuvianite. Other less common minerals include rutile, axinite and sphene. Late or retrograde minerals include epidote, chlorite, clinozoisite, vesuvianite, scapolite, tremolite-actinolite, sericite and prehnite.

**Garnet-rich Au skarns:** Extensive exoskarn, generally with low pyroxene:garnet ratios. Prograde minerals include low Mn grandite garnet (Ad 10-100), K-feldspar, wollastonite, diopsidic clinopyroxene (Hd 0-60), epidote, vesuvianite, sphene and apatite. Late or retrograde minerals include epidote, chlorite, clinozoisite, vesuvianite, tremolite-actinolite, sericite, dolomite, siderite and prehnite.

**Epidote-rich Au skarns:** Abundant epidote and lesser chlorite, tremolite-actinolite, quartz, K-feldspar, garnet, vesuvianite, biotite, clinopyroxene and late carbonate. At the *QR* deposit, epidote-pyrite and carbonate-pyrite veinlets and coarse aggregates are common, and the best ore occurs in the outer part of the alteration envelope, within 50 m of the epidote skarn front.

**ENDOSKARN MINERALOGY (GANGUE):** Moderate endoskarn development with K-feldspar, biotite, Mg-pyroxene (Hd 5-30) and garnet. Endoskarn at the epidote-rich *QR* deposit is characterized by calcite, epidote, clinozoisite and tremolite whereas at the *Butte Highlands* Mg skarn it contains argillic and propylitic alteration with garnet, clinopyroxene and epidote.

**WEATHERING:** In temperate and wet tropical climates, skarns often form topographic features with positive relief.

**ORE CONTROLS:** The ore exhibits strong stratigraphic and structural controls. Orebodies form along sill-dike intersections, sill-fault contacts, bedding-fault intersections, fold axes and permeable faults or tension zones. In the pyroxene-rich and epidote-rich types, ore commonly develops in the more distal portions of the alteration envelopes. In some districts, specific suites of reduced, Fe-rich intrusions are spatially related to Au skarn mineralization. Ore bodies in the garnet-rich Au skarns tend to lie more proximal to the intrusions.

## Au SKARNS

K04

**GENETIC MODEL:** Many Au skarns are related to plutons formed during oceanic plate subduction. There is a worldwide spatial, temporal and genetic association between porphyry Cu provinces and calcic Au skarns. Pyroxene-rich Au skarns tend to be hosted by siltstone-dominant packages and form in hydrothermal systems that are sulphur-rich and relatively reduced. Garnet-rich Au skarns tend to be hosted by carbonate-dominant packages and develop in more oxidising and/or more sulphur-poor hydrothermal systems.

**ASSOCIATED DEPOSIT TYPES:** Au placers (C01,C02), calcic Cu skarns (K01), porphyry Cu deposits (L04) and Au-bearing quartz and/or sulphide veins (I01, I02). Magnesian subtype can be associated with porphyry Mo deposits (L05) and possibly W skarns (K05). In British Columbia there is a negative spatial association between Au and Fe skarns at regional scales, even though both classes are related to arc plutonism. Fe skarns are concentrated in the Wrangellia Terrane whereas most Au skarn occurrences and all the economic deposits lie in Quesnellia.

**COMMENTS:** Most Au skarns throughout the world are calcic and are associated with island arc plutonism. However, the *Savage Lode* magnesian Au skarn occurs in the Archean greenstones of Western Australia and the *Butte Highlands* magnesian Au skarn in Montana is hosted by Cambrian platform dolomites. Note: although the Nickel Plate deposit lies distal to the Toronto stock in the pyroxene-dominant part of the skarn envelope, the higher grade ore zones commonly lie adjacent to sills and dikes where the exoskarn contains appreciable amounts of garnet with the clinopyroxene.

### EXPLORATION GUIDES

**GEOCHEMICAL SIGNATURE:** Au, As, Bi, Te, Co, Cu, Zn or Ni soil, stream sediment and rock anomalies, as well as some geochemical zoning patterns throughout the skarn envelope (notably in Cu/Au, Ag/Au and Zn/Au ratios). Calcic Au skarns (whether garnet-rich or pyroxene-rich) tend to have lower Zn/Au, Cu/Au and Ag/Au ratios than any other skarn class. The intrusions related to Au skarns may be relatively enriched in the compatible elements Cr, Sc and V, and depleted in lithophile incompatible elements (Rb, Zr, Ce, Nb and La), compared to intrusions associated with most other skarn types.

**GEOPHYSICAL SIGNATURE:** Airborne magnetic or gravity surveys to locate plutons. Induced polarization and ground magnetic follow-up surveys can outline some deposits.

**OTHER EXPLORATION GUIDES:** Placer Au. Any carbonates, calcareous tuffs or calcareous volcanic flows intruded by arc-related plutons have a potential for hosting Au skarns. Favorable features in a skarn envelope include the presence of: (a) proximal Cu-bearing garnet skarn and extensive zones of distal pyroxene skarn which may carry micron Au, (b) hedenbergitic pyroxene (although diopsidic pyroxene may predominate overall), (c) sporadic As-Bi-Te geochemical anomalies, and, (d) undifferentiated, Fe-rich intrusions with low Fe<sub>2</sub>O<sub>3</sub>/FeO ratios. Any permeable calcareous volcanics intruded by high-level porphyry systems (particularly alkalic plutons) have a potential for hosting epidote-rich skarns with micron Au. During exploration, skarns of all types should be routinely sampled and assayed for Au, even if they are lean in sulphides.

### ECONOMIC IMPORTANCE

**TYPICAL GRADE AND TONNAGE:** These deposits range from 0.4 to 13 Mt and from 2 to 15 g/t Au.

Theodore *et al.* (1991) report median grades and tonnage of 8.6 g/t Au, 5.0 g/t Ag and 213 000 t. *Nickel Plate* produced over 71 tonnes of Au from 13.4 Mt of ore (grading 5.3 g/t Au). The 10.3 Mt *Fortitude* (Nevada) deposit graded 6.9 g/t Au whereas the 13.2 Mt *McCoy* skarn (Nevada) graded 1.5 g/t Au. The *QR* epidote-rich Au skarn has reserves exceeding 1.3 Mt grading 4.7 g/t Au.

**IMPORTANCE:** Recently, there have been some significant Au skarn deposits discovered around the world (e.g. *Buckhorn Mountain*, *Wabu*, *Fortitude*). Nevertheless, total historic production of Au from skarn (more than 1 000 t of metal) is minute compared to production from other deposit types. The *Nickel Plate* deposit (Hedley, British Columbia) was probably one of the earliest major Au skarns in the world to be mined. Skarns have accounted for about 16 % of British Columbia's Au production, although nearly half of this was derived as a byproduct from Cu and Fe skarns

## REFERENCES

- Billingsley, P. and Hume, C.B. (1941): The Ore Deposits of Nickel Plate Mountain, Hedley, British Columbia; *Canadian Institute of Mining and Metallurgy*, Bulletin, Volume 44, pages 524-590.
- Brookes, J.W., Meinert, L.D., Kuyper, B.A. and Lane, M.L. (1990): Petrology and Geochemistry of the McCoy Gold Skarn, Lander County, Nevada; in *Geology and Ore Deposits of the Great Basin*, Symposium Proceedings, *Geological Society of Nevada*, April 1990.
- Ettlinger, A.D. and Ray, G.E. (1989a): Precious Metal Enriched Skarns in British Columbia: An Overview and Geological Study; *B. C. Ministry of Energy, Mines and Petroleum Resources*, Paper 1989-3, 128 pages.
- Ettlinger, A.D., Albers, D., Fredericks, R. and Urbisnov, S. (1995): The Butte Highlands Project, Silver Bow County, Montana; An Olivine-rich Magnesian Gold Skarn; in *Symposium Proceedings of Geology and Ore Deposits of American Cordillera*, *Geological Society of Nevada, U.S. Geological Survey* and *Geological Society of Chile*, April 10-13, 1995, Reno, Nevada.
- Fox, P.E., and Cameron, R.S. (1995): Geology of the QR Gold Deposit, Quesnel River Area, British Columbia; in *Porphyry Deposits of the Northwest Cordillera of North America*, (editor) T.G. Schroeter. *Canadian Institute of Mining, Metallurgy and Petroleum*, Special Volume 46, Paper 66, pages 829-837.
- Hammarstrom, J.M., Orris, G.J., Bliss, J.D., and Theodore, T.G. (1989): A Deposit Model for Gold-Bearing Skarns; Fifth Annual V.E. McKelvey Forum on Mineral and Energy Resources, *U.S. Geological Survey*, Circular 1035, pages 27-28.
- McKelvey, G.E., and Hammarstrom, J.M. (1991): A Reconnaissance Study of Gold Mineralization Associated with Garnet Skarn at Nambija, Zamora Province, Ecuador, in *USGS Research on Mineral Resources - 1991*, Program and Abstracts. Editors E.J. Good, J.F. Slack and R.K. Kotra, U.S. Geological Survey, Circular 1062, page 55.
- Meinert, L.D. (1989): Gold Skarn Deposits - Geology and Exploration Criteria; in *The Geology of Gold Deposits; The Perspective in 1988*; *Economic Geology*; Monograph 6, pages 537-552.
- Mueller, A.G. (1991): The Savage Lode Magnesian Skarn in the Marvel Loch Gold-Silver Mine, Southern Cross Greenstone Belt, Western Australia; Part I. Structural Setting, Petrography and Geochemistry; *Canadian Journal of Earth Sciences*, Volume 28, Number 5, pages 659-685.
- Orris, G.J., Bliss, J.D., Hammarstrom, J.M. and Theodore, T.G. (1987): Description and Grades and Tonnages of Gold-bearing Skarns; *U. S. Geological Survey*, Open File Report 87-273, 50 pages.
- Ray, G.E. and Dawson, G.L. (1994): The Geology and Mineral Deposits of the Hedley Gold Skarn District, Southern British Columbia; *B.C. Ministry of Energy, Mines and Petroleum Resources*, Bulletin 87, 156 pages.
- Ray, G.E. and Webster, I.C.L. (1997): Skarns in British Columbia; *B.C. Ministry of Energy, Mines and Petroleum Resources*, Bulletin 101, 260 pages.
- Ray, G.E., Ettlinger, A.D. and Meinert, L.D. (1990): Gold Skarns: Their Distribution, Characteristics and Problems in Classification; in *Geological Fieldwork 1989*, *B.C. Ministry of Energy, Mines and Petroleum Resources*, Paper 1990-1, pages 237-246.
- Theodore, T.G., Orris, G.J., Hammarstrom, J.M. and Bliss, J.D. (1991): Gold Bearing Skarns; *U. S. Geological Survey*; Bulletin 1930, 61 pages.



## GARNET SKARNS

K08

by Gerald E. Ray



### IDENTIFICATION

SYNONYM: Pyrometasomatic or contact metasomatic garnet deposits.

COMMODITIES (*BYPRODUCTS*): Garnet (wollastonite, magnetite).

EXAMPLES (*British Columbia - Canada/International*): Mount Riordan (Crystal Peak, 082ESW102); *San Pedro (New Mexico, USA)*.

### GEOLOGICAL CHARACTERISTICS

CAPSULE DESCRIPTION: Garnet-dominant skarn hosted by calcareous rocks generally near an intrusive contact.

TECTONIC SETTINGS: Virtually any setting.

AGE OF DEPOSIT: May be any age.

HOST/ASSOCIATED ROCK TYPES: Garnet is hosted by carbonate or altered calcareous mafic volcanic sequences that are intruded by relatively oxidized plutons.

DEPOSIT FORM: Irregular zones of massive garnet developed in exoskarn close to plutonic contacts. The shape of the deposit may be controlled partly by the morphology of the original conformable units.

TEXTURES: Coarse grained, massive granoblastic textures in exoskarn.

ORE MINERALOGY (Principal and *subordinate*): Abundant and massive, coarse grained garnet (grossular-andradite)  $\pm$  wollastonite  $\pm$  magnetite.

ALTERATION MINERALOGY (Principal and *subordinate*): Garnet, *clinopyroxene*, quartz, feldspar, calcite, sphene, apatite, axinite, vesuvianite and sericite.

OPAQUE MINERALOGY: Economically viable garnet deposits typically have very little or no sulphides.

ORE CONTROLS: Plutonic contacts and oxidized carbonate host rocks. The Mount Riordan garnet skarn lies proximal to the intrusion.

ASSOCIATED DEPOSIT TYPES: Cu, Fe, Au and wollastonite skarns (K01, K03, K04 and K09).

COMMENTS: The best industrial garnets (due to higher specific gravity and hardness) are almandine-pyrope composition. These generally occur in high grade metamorphic rocks and require secondary concentration in beach or stream placers to be mined economically. Examples include the Emerald Creek deposit located in Idaho, USA, and a 6 Mt beach-sand deposit situated near Geraldton, Western Australia that grades 35 per cent garnet. The Mount Riordan deposit is one of the largest and highest grade garnet skarns yet identified; its garnet is suitable for the production of sandblasting and other abrasive products that require high angularity and a wide range of grain sizes. In British Columbia, there have been intermittent attempts to process the garnet-rich tailings from the Iron Hill-Argonaut Fe skarn (092F075).

## *EXPLORATION GUIDES*

GEOCHEMICAL SIGNATURE: May get very weak W, Mo, Zn and Cu geochemical anomalies.

GEOPHYSICAL SIGNATURE: Gravity and possible magnetic anomalies.

## *ECONOMIC FACTORS*

GRADE AND TONNAGE: To be economic, garnet skarn deposits should be large tonnage (>20 Mt) and high grade (> 70% garnet). The Mount Riordan (Crystal Peak) deposit contains reserves of 40 Mt grading 78% garnet and San Pedro is a 22 to 30 Mt deposit with 85% andraditic garnet.

ECONOMIC LIMITATIONS: The garnet should be free of inclusions, possess a relatively high specific gravity and high angularity, and be present as discrete grains that can be processed easily by conventional beneficiation techniques. Economic concentrations of clean and industrially suitable grossularite-andradite garnet in skarn are rare. This is because skarn garnets tend to be relative soft and many contain fine-grained carbonate inclusions. Easy access, low cost transportation and a ready and reliable market for the product are essential features controlling the economic viability of a deposit.

END USES: Sandblasting, water-jet equipment and abrasives, such as sandpaper. Grossular-andradite garnets have more restricted uses than almandine.

IMPORTANCE: World production in 1995 of industrial garnet was approximately 110 000 tonnes, of which just under half (valued at \$US 11 million) was produced in the U.S. Worldwide, most garnet is obtained from placer deposits or as a byproduct during hard rock mining of other commodities. The demand in North America for industrial garnet is growing; skarns are expected to be an important future source for the mineral.

## *SELECTED BIBLIOGRAPHY*

- Austin, G.T. (1991): Garnet (Industrial); in Mineral Commodity Summaries 1991, *Department of the Interior, United States Bureau of Mines*, pages 58-59.
- Grond, H.C., Wolfe, R., Montgomery, J.H. and Giroux, G.H. (1991): A Massive Skarn-hosted Andradite Deposit near Penticton, British Columbia; in *Industrial Minerals of Alberta and British Columbia, Canada, B.C. Ministry of Energy, Mines and Petroleum Resources*, Open File 1991-23, pages 131-133.
- Harben, P.W. and Bates, R.L. (1990): Garnet; in *Industrial Minerals, Geology and World Deposits, Industrial Minerals Division, Metal Bulletin Plc.*, London, pages 120-12.
- Hight, R.P. (1983): Abrasives; in *Industrial Minerals and Rocks*, 5th edition, *American Institute of Mining, Metallurgy and Petroleum Engineers*, Lefond, S.J., Editor, New York, pages 11-32.
- Smoak, J.F. (1985): Garnet; *United States Bureau of Mines*, Bulletin 675, pages 297-304.
- Ray, G.E., Grond, H.C., Dawson, G.L. and Webster, I.C.L. (1992): The Mount Riordan (Crystal Peak) Garnet Skarn, Hedley District, Southern British Columbia; *Economic Geology*, Volume 87, pages 1862-1876.

DRAFT #: 7b

December 19, 1997



## MAGMATIC Ti-Fe±V OXIDE DEPOSITS

MO4

By G.A. Gross<sup>1</sup>, C. F. Gower<sup>2</sup> and D.V. Lefebure



### IDENTIFICATION

SYNONYMS: Mafic intrusion-hosted titanium-iron deposits.

COMMODITIES (BYPRODUCTS): Ti, Fe

EXAMPLES (British Columbia - Canada/International): None in B.C.; *Methuen, Unfravile, Matthews-Chaffrey, Kingston Harbour (Ontario, Canada); Lac-du-Pin-Rouge, Lac Tio, Magpie (Quebec, Canada), Sanford Lake (New York, USA), Tellnes, Egersund (Norway), Smaalands-Taberg, Ulvno (Sweden).*

### GEOLOGICAL CHARACTERISTICS

CAPSULE DESCRIPTION: Ilmenite, hemo-ilmenite or titaniferous magnetite accumulations as cross-cutting lenses or dike-like bodies, layers or disseminations within anorthositic/gabbroic/noritic rocks. These deposits can be subdivided into an ilmenite subtype (anorthosite-hosted titanium-iron) and a titaniferous magnetite subtype (gabbro-anorthosite-hosted iron-titanium).

TECTONIC SETTING: Commonly associated with anorthosite-gabbro-norite-monzonite (mangerite)-charnockite granite (AMCG) suites that are conventionally interpreted to be anorogenic and/or extensional. Some of the iron-titanium deposits occur at continental margins related to island arc magmatism followed by an episode of orogenic compression.

DEPOSITIONAL ENVIRONMENT / GEOLOGICAL SETTING: Deposits occur in intrusive complexes which typically are emplaced at deeper levels in the crust. Progressive differentiation of liquids residual from anorthosite-norite magmas leads to late stage intrusions enriched in Fe and Ti oxides and apatite.

AGE OF MINERALIZATION: Mainly Mesoproterozoic (1.65 to 0.90 Ga) for the ilmenite deposits, but this may be a consequence of a particular combination of tectonic circumstances, rather than any a priori temporal control. The Fe-Ti deposits with titaniferous magnetite do not appear to be restricted in time.

HOST/ASSOCIATED ROCKS: Hosted by massive, layered or zoned intrusive complexes - anorthosite, norite, gabbro, diorite, diabase, quartz monzonite and hornblende pyroxenite. The anorthosites are commonly emplaced in granitoid gneiss, granulite, schist, amphibolite and quartzite. Some deposits associated with lower grade rocks.

DEPOSIT FORM: Lensoid, dike-like or sill-like bodies of massive ore, or disseminated in mafic host rocks. Some ore is disseminated as layers in layered intrusions. Typically the massive material has sharp, cross-cutting contacts with its anorthositic hosts, forming lenses tens to hundreds of metres wide and several hundred metres long. The massive ore may have apophyses cutting the host rock, be associated with intrusive breccias and contain anorthositic xenoliths. In layered deposits individual layers range in thickness from centimetres to metres and may be followed up to several thousand metres. Lean (disseminated) ore grades into unmineralized host rock. Lac Tio and Tellnes ore bodies are very large examples of the ilmenite subtype. Lac Tio is an irregular, tabular intrusive mass, 1100 m long and 1000 m wide. The Tellnes ore body, which is 400 m thick and 2.5 km long, is part of a 14 km long dike.

<sup>1</sup> Geological Survey of Canada, Ottawa.

<sup>2</sup> Newfoundland Department of Mines and Energy, St. John's, Newfoundland

# MAGMATIC Ti-Fe±V OXIDE DEPOSITS

MO4

**TEXTURE/STRUCTURE:** Massive, disseminated or locally in layers. No zoning of ore minerals, but there may be variation in modal proportions of associated silicates. Medium or coarse grained, primary magmatic textures. Exsolution intergrowths of either ilmenite and hemo-ilmenite, or titanomagnetite, titaniferous magnetite or ilmenite in magnetite. Locally the massive ore, particularly near contacts with host rock, contains abundant xenoliths and xenocrysts derived from the associated intrusive.

**ORE MINERALOGY (Principal and subordinate):** Ilmenite, hemo-ilmenite, titaniferous magnetite and magnetite. Proportions of ilmenite and magnetite generally correlate with host rock petrology. Fe-sulphides such as *pyrrhotite*, *pentlandite* and *chalcopyrite*.

**GANGUE MINERALOGY (Principal and subordinate):** Silicate minerals, especially plagioclase, orthopyroxene, clinopyroxene and olivine, with apatite, minor *zircon* and *pleonaste spinel*. Orthopyroxene is rare to absent in the island arc-related titaniferous magnetite deposits.

**ALTERATION MINERALOGY:** Not normally altered.

**WEATHERING:** Rarely residual enrichment may occur in weathering zone.

**ORE CONTROLS:** The key control is the development of a late, separate Ti and Fe-rich liquid from a fractionating magma under stable conditions. Many deposits occur in elongate belts of intrusive complexes emplaced along deep-seated faults and fractures. Ilmenite deposits are associated with lower magnesian phases of anorthositic intrusions. Titaniferous magnetite deposits are commonly associated with magnesian, labradorite phases of anorthositic intrusions or gabbroic phases near the margins of the stock. In layered intrusions the titaniferous magnetite seams are commonly within the upper stratigraphic levels and in marginal zones of complex intrusive bodies.

**GENETIC MODELS:** Progressive differentiation of liquids residual from anorthosite-norite magmas leads to late enrichment in Fe and Ti. Typically plagioclase crystallization results in concentration of Fe and Ti in residual magmas which typically crystallize to form ferrodiorites and ferrogabbros. Layers form by crystal settling and accumulation on the floors of magma chambers and the disseminated deposits are believed to have formed in-situ. The origin of the discordant deposits, primarily associated with the Proterozoic anorthosites, is not well understood. Two genetic models have been suggested - remobilization of the crystal cumulates into cracks or fractures or emplacement as a Fe-Ti-oxide-rich immiscible melt with little silica.

**ASSOCIATED DEPOSIT TYPES:** Ni-Cu-Co magmatic sulphide deposits (M02), chromite deposits (e.g. Bushveld Complex), platinum group deposits (e.g. Stillwater Complex, Bushveld Complex), and placer ilmenite, magnetite, rutile and zircon (C01, C02).

**COMMENTS:** Titaniferous magnetite deposits associated with zoned ultramafic complexes in Alaska and British Columbia, such as Lodestone Mountain (092HSE034) and Tanglewood Hill (092HSE035), are included with Alaskan-type deposits (M05). Some authors would include them with magmatic Fe-Ti±V oxide deposits. In California in the San Gabriel Range occurrences of the ilmenite-subtype are hosted by anorthosite and ferrodiorite intrusions within a metamorphic complex composed of gneisses.

## EXPLORATION GUIDES

**GEOCHEMICAL SIGNATURE:** Ti, Fe, V, Cr, Ni, Cu, Co geochemical anomalies.

**GEOPHYSICAL SIGNATURE:** Magnetic or EM response, although if the deposit is particularly ilmenite-rich it may exhibit either a subdued or a strong negative anomaly. Sometimes the subdued response displays characteristic irregular patterns of negative and positive anomalies that show broad smooth profiles or patterns.

**OTHER EXPLORATION GUIDES:** Heavy mineral concentrations of ilmenite and titaniferous magnetite in placer deposits. Abundant apatite in some deposits. Association with anorthosite and gabbro intrusive complexes along deep fracture and fault zones.

*ECONOMIC FACTORS*

**GRADE AND TONNAGE:** Both grade and tonnage vary considerably. The ilmenite deposits are up to several hundreds of millions of tonnes with from 10 to 75% TiO<sub>2</sub>, 32 to 45% Fe and less than 0.2% V. The Tellnes deposit comprises 300 Mt averaging 18% TiO<sub>2</sub>. The Lac Tio deposit, largest of 6 deposits at Allard Lake, contains more than 125 mt of ore averaging 32% TiO<sub>2</sub> and 36% FeO. Titaniferous magnetite deposits can be considerably larger, ranging up to a billion tonnes with grades between 20 to 45% Fe, 2 to 20% TiO<sub>2</sub> and less than 7% apatite with V contents averaging 0.25%.

**ECONOMIC LIMITATIONS:** The economic deposits are typically coarse, equigranular aggregates which are amenable to processing depending on the composition and kinds of exsolution textures of the Fe-Ti-oxide minerals.

**USES:** Titanium dioxide is a non-toxic, powdered white pigment used in paint, plastics, rubber, and paper. Titanium metal is resistant to corrosion and has a high strength-to-weight ratio and is used in the manufacturing of aircraft, marine and spacecraft equipment.

**IMPORTANCE:** Apart from placers, this type of deposit is the major source of TiO<sub>2</sub>. These deposits were an important source of iron (pig iron) in the former Soviet Union. They have been mined for Fe in Canada, however, the grades are generally lower than those in iron formations and iron laterites. The only current iron production is as a coproduct with TiO<sub>2</sub> in pyrometallurgical processing of ilmenite ore.

*SELECTED BIBLIOGRAPHY*

- Ashwal, L.D. (1993): Anorthosites; *Springer-Verlag*, Berlin, 422 pages.
- Force, Eric R. (1986): Descriptive Model of Anorthosite Ti; in *Mineral Deposit Models*, Cox, Denis P. and Singer, D.A., Editors, *U.S. Geological Survey*, Bulletin 1693, pages 32-33.
- Force, E.R. (1991): Geology of Titanium-mineral Deposits; *Geological Society of America*, Special Paper 259, 113 pages.
- Gross, G.A. (1965): General Geology and Evaluation of Iron Deposits; Volume I, in *Geology of Iron Deposits in Canada*, *Geological Survey of Canada*, Economic Geology Report 22, 111 pages.
- Gross, G.A. and Rose, E.R. (1984): Mafic Intrusion-hosted Titanium-Iron; in *Canadian Mineral Deposit Types: A Geological Synopsis*; Geological Survey of Canada, Economic Geology Report 36, Eckstrand, O.R., Editor, page 46.
- Gross, G.A. (1995): Mafic Intrusion-hosted Titanium-iron; in *Geology of Canadian Mineral Deposit Types*, Eckstrand, O.R., Sinclair, W.D. and Thorpe, R.I. (Editors), Geological Survey of Canada, *Geology of Canada*, Number 8, pages 573-582.
- Hammond, P. (1952): Allard Lake Ilmenite Deposits; *Economic Geology*, Volume 47, pages 634-649.
- Hancock, K.D. (1988): Magnetite Occurrences in British Columbia, Open File 1988-28, B.C. Ministry of Energy, Minerals and Petroleum Resources, 153 pages.
- Korneliussen, A., Geis, H.P., Gierth, E., Krause, H., Robins, B. and Schott, W. (1985): Titanium Ores: an Introduction to a Review of Titaniferous Magnetite, Ilmenite and Rutile deposits in Norway; *Norges Geologiske Undersøkelse Bulletin*, volume 402, pages 7-23.
- Lister, G.F. (1966): The Composition and Origin of Selected Iron-titanium Deposits; *Economic Geology*, volume 61, pages 275-310.
- Reynolds, I.M. (1985): The Nature and Origin of Titaniferous Magnetite-rich Layers in the Upper Zone of the Bushveld Complex: a Review and Synthesis; *Economic Geology*, volume 80, pages 1089-1108.
- Rose, E.R. (1969): Geology of Titanium and Titaniferous Deposits of Canada; *Geological Survey of Canada*, Economic Geology Report 25, 177 pages.
- Wilmart, E., Demaiffe, D. and Duchesne, J.C. (1989): Geochemical Constraints on the Genesis of the Tellnes Ilmenite Deposit, Southwest Norway; *Economic Geology*, Volume 84, pages 1047-1056.

Draft #3b January 14, 1997





## ULTRAMAFIC-HOSTED CHRYSOTILE ASBESTOS M06

by Z.D. Hora



### IDENTIFICATION

SYNONYMS: Quebec-type asbestos, serpentine-hosted asbestos, ultramafic-intrusion hosted asbestos.

COMMODITIES (BYPRODUCTS): Chrysotile asbestos (nephrite jade at Cassiar).

EXAMPLES (British Columbia (MINFILE #) - *Canadian/International*): Cassiar (104P005), McDame (104P084), Letain (104I006), Ace (104K025), Asbestos (082 KNW075); *Thetford Mines, Black Lake, Asbestos (Quebec, Canada), Belvidere Mine (Vermont, USA), Coalinga (California, USA), Cana Brava (Brazil), Pano Amiandes (Cyprus), Bazhenovo (Russia), Barraba (New South Wales, Australia), Barberton (Transvaal, South Africa)*.

### GEOLOGICAL CHARACTERISTICS

CAPSULE DESCRIPTION: Chrysotile asbestos occurs as cross fibre and/or slip fibre stockworks, or as less common agglomerates of finely matted chrysotile fibre, in serpentinized ultramafic rocks. Serpentinites may be part of ophiolite sequence in orogenic belts or synvolcanic intrusions of Archean greenstone belts.

TECTONIC SETTINGS: Chrysotile deposits occur in accreted oceanic terranes, usually part of an ophiolite sequence, or within Alpine - type ultramafic rocks. They are also found in synvolcanic ultramafic intrusions of komatiitic affinity in Archean greenstone belts. In British Columbia the significant occurrences are found in the Slide Mountain, Cache Creek and Kootenay terranes.

DEPOSITIONAL ENVIRONMENT / GEOLOGICAL SETTING: The serpentine host must have a nonfoliated texture and must be situated near a fault that is active during a change in the orientation of the regional stress from dip-slip to strike-slip fault motion. The serpentinite must be in the stability field of chrysotile when the change in orientation occurs. Subsequent deformation or temperature increase may destroy the fibre and result in a different mineralogy.

AGE OF MINERALIZATION: Precambrian to Tertiary. Deposits in British Columbia are considered Upper Cretaceous, deposits in southeastern Quebec formed during a relatively late stage of Taconic orogeny (late Ordovician to early Silurian), deposits in Ungava and Ontario are Precambrian. Chrysotile asbestos deposits are generally considered to be syntectonic and to form during the later stages of deformation.

HOST/ASSOCIATED ROCK TYPES: Serpentinite, dunite, peridotite, wehrlite, harzburgite, pyroxenite. Associated rocks are rodingite and steatite.

DEPOSIT FORM: In plan orebodies are equidimensional to somewhat oblate zones from 100 to 1000 metres in diameter within masses of serpentinized ultramafic rock. The vertical distribution of mineralized zones may be in the order of several hundreds of metres.

TEXTURE/STRUCTURE: Asbestos veins fill tension fractures in serpentinized ultramafic rocks or form a matrix of crushed and brecciated body of serpentinite. Usually, the orebodies grade from numerous stockwork veins in the centre to a lower number of crosscutting veins on the fringes. Cross-fibre veins, where the chrysotile fibres are at a high angle to the vein walls, are more abundant than slip fibre veins which parallel the vein walls. Individual veins are up to several metres in length and for the most part less than 1 cm thick, but may be up to 10 cm thick. In some deposits, powdery agglomerates of finely matted chrysotile form the matrix for blocks and fragments of serpentinite rock.

ORE MINERALOGY [Principal and *subordinate*]: Chrysotile.

# ULTRAMAFIC-HOSTED CHRYSOTILE ASBESTOS M06

**GANGUE MINERALOGY** [Principal and *subordinate*]: Gangue minerals in chrysotile veinlets are brucite and magnetite. Antigorite and lizardite may also be present in association with chrysotile veining.

**ALTERATION MINERALOGY**: Chrysotile and associated minerals are alteration products of ultramafic rocks. This process which starts as serpentinization, may be pervasive, but also fracture controlled and incomplete with serpentine surrounding peridotite (or other rock) cores. In relationship to changes in temperature, pressure and the fluid chemistry a variety of minerals from lizardite to talc and antigorite, or tremolite can be produced. Since the serpentinization of ultramafic rocks is frequently a multiple stage process, which can be either prograde or retrograde, many deposits contain minerals which do not form in the same stability field. Therefore, the alteration and gangue mineralogy are practically identical.

**WEATHERING**: In northern climates, only physical weathering of chrysotile and the serpentinized host rock takes place. Brucite and carbonates may be removed in solution and precipitated as hydromagnesite elsewhere. Lateritic soils should be expected in tropical climates.

**ORE CONTROLS**: Chrysotile veinlets are often best developed in massive serpentinite bodies with no schistose fabric. Chrysotile stability field; proximity to a fault that is active during change in the orientation of stress field; limited subsequent deformation and no subsequent medium to high grade metamorphism after the asbestos formation. Asbestos veins fill tension fractures in serpentinized ultramafic rocks or form a matrix of crushed and brecciated body of serpentinite.

**GENETIC MODELS**: Chrysotile asbestos deposits develop in nonfoliated, brittle ultramafic rocks under low grade metamorphic conditions with temperatures of  $300 \pm 50^\circ\text{C}$  and water pressures less than 1 kbar. The chrysotile forms as the result of fluid flow accompanied by deformation where water gains access to partly or wholly serpentinized ultramafics along fault and shear zones.

**ASSOCIATED DEPOSIT TYPES**: Spatial association (but no genetic relationship) with podiform chromite deposits (M03) and jade (Q01) in ophiolitic sequences. Cryptocrystalline magnesite veins (I17), ultramafic-hosted talc-magnesite (M07) and anthophyllite asbestos deposits may be genetically related.

**COMMENTS**: Anthophyllite, a variety of amphibole, is another asbestiform mineral. Production of anthophyllite has been limited; Green Mountain mine in North Carolina is the only North American past producer.

## ***EXPLORATION GUIDES***

**GEOCHEMICAL SIGNATURE**: None.

**GEOPHYSICAL SIGNATURE**: Magnetite, which is a product of both serpentinization and the formation of chrysotile, can produce well defined, magnetic anomalies. Gravity surveys can distinguish serpentinite from the more dense (~20%) peridotite.

**OTHER EXPLORATION GUIDES**: Asbestos fibres found in soils. Massive, brittle and unsheared ultramafic bodies which are partly or fully serpentinized in proximity to faults and shears.

## ***ECONOMIC FACTORS***

**TYPICAL GRADE AND TONNAGE**: Total fibre content of commercial deposits is between 3 and 10%, the tonnage is between 500 000 to 150 million tons (in the asbestos industry fibre length is a critical parameter as well). In British Columbia, company reports indicate the Cassiar mine produced 31 Mt grading 7 to 10% fibre. There are however 25 Mt of tailings with 4.2% recoverable short fibre. Another 7.3 Mt geological reserves was left in the pit. The adjacent McDame deposit has measured reserves of 20 Mt @ 6.21% fibre and estimated geological reserves of 63 Mt. In the Yukon Clinton Creek produced 15 Mt @ 6.3% fibre. The following figures are from Duke (1996) and include past production plus reserves: Jeffrey, Quebec: 800 Mt @ 6% fibre, Bell-Wing-Beaver, Quebec: 250 Mt @ 6% fibre, British Canadian, Quebec: 150 Mt @ 6% fibre, Advocate, Newfoundland: 60 Mt @ 3% fibre. A relatively few deposits have been developed to mine agglomerates of finely matted chrysotile fibre which have much higher grades.

# ULTRAMAFIC-HOSTED CHRYSOTILE ASBESTOS M06

## *ECONOMIC FACTORS*

**TYPICAL GRADE AND TONNAGE** (continued): The very large Coalinga deposit in California has reported short fibre recoveries in the order of 35 to 74%. The Stragari mine in Serbia is recovering 50-60% fibre.

**ECONOMIC LIMITATIONS:** Fibre lengths may vary significantly within and between deposits; stockwork mineralization is typically more economically attractive if the proportion of longer fibres is higher. Typically, the fibre value starts at CDN\$180/ton for the shortest grade and reaches CDN\$1750 for the longest (Industrial Minerals, 1997).

**END USES:** Asbestos-cement products; filler in plastics; break lining and clutch facings; asbestos textiles; gaskets; acoustic and electric and heat insulation.

**IMPORTANCE:** Ultramafic-hosted chrysotile is the only source of asbestos in North America and considered the least hazardous of commercial asbestos minerals. During the 1980s the market for asbestos in many countries declined due to health hazard concerns.

## *SELECTED BIBLIOGRAPHY*

- Cogulu, E. and Laurent R. (1984): Mineralogical and Chemical Variations in Chrysotile Veins and Peridotite Host - Rocks from the Asbestos Belt of Southern Quebec; *Canadian Mineralogist*, volume 22, pages, 173-183.
- Duke, J.M. (1995): Ultramafic-hosted Asbestos; in *Geology of Canadian Mineral Deposit Types*, Eckstrand, O.R., Sinclair, W.D. and Thorpe, R.I., Editors, *Geological Survey of Canada*, Geology of Canada, Number 8, pages 263-268.
- Harvey-Kelly, F.E.L. (1995): Asbestos Occurrences in British Columbia; *British Columbia Ministry of Employment and Investment*, Open File 1995 - 25, 102 pages.
- Hemley, J.J., Montoya, J.W., Christ, C.L. and Hosletter, P.B. (1977): Mineral Equilibria in the MgO-SiO<sub>2</sub>-H<sub>2</sub>O System: I Talc-Chrysotile-Forsterite-Brucite Stability Relations; *American Journal of Science*, Volume 277, pages 322-351.
- Hemley, J.J., Montoya, J.W., Shaw, D.R. and Luce, R.W. (1977): Mineral Equilibria in the MgO-SiO<sub>2</sub>-H<sub>2</sub>O System: II Talc-Antigorite-Forsterite-Anthophyllite-Enstatite Stability Relations and Some Geological Implications in the System; *American Journal of Science*, Volume 277, pages 353-383.
- Hewett, F.G. (1984): Cassiar Asbestos Mine, Cassiar, British Columbia; in *The Geology of Industrial Minerals of Canada*, Guillet, G.R. and Martin W., Editors, *Canadian Institute of Mining and Metallurgy*, Montreal, Quebec, pages 258-262.
- Mumpton, F.A. and Thompson, C.S. (1975): Mineralogy and Origin of the Coalinga Asbestos Deposit; *Clays and Clay Minerals*, Volume 23, pages 131-143.
- Nelson, J.L. and Bradford, J.A., (1989): Geology and Mineral Deposits of the Cassiar and McDame Map Areas, British Columbia; *B.C. Ministry of Energy, Mines and Petroleum Resources*, Paper 1989-1, pages 323-338.
- O'Hanley, D.S. (1987): The Origin of the Chrysotile Asbestos Veins in Southeastern Quebec; *Canadian Journal of Earth Sciences*, Volume 24, pages 1-9.
- O'Hanley, D.S. (1988): The Origin of the Alpine Peridotite-Hosted, Cross Fibre, Chrysotile Asbestos Deposits; *Economic Geology*, Volume 83, pages 256-265
- O'Hanley, D.S. (1991): Fault Related Phenomena Associated With Hydration and Serpentine Recrystallization During Serpentinization; *Canadian Mineralogist*, Volume 29, pages 21-35.
- O'Hanley, D.S. (1992): Solution to the Volume Problem in Serpentinization; *Geology*, Volume 20, pages 705-708.
- O'Hanley, D.S., Chernosky, J.U. Jr. and Wicks, F.J. (1989): The Stability of Lizardite and Chrysotile; *Canadian Mineralogist*, Volume 27, pages 483-493.

# ULTRAMAFIC-HOSTED CHRYSOTILE ASBESTOS M06

- O'Hanley, D.S., and Offler, R. (1992): Characterization of Multiple Serpentinization, Woodsreef, New South Wales; *Canadian Mineralogist*, Volume 30, pages 1113-1126.
- O' Hanley, D.S., Schandl, E.S. and Wicks, F.J. (1992): The Origin of Rodingites from Cassiar, British Columbia, and their use to Estimate T and P(H<sub>2</sub>O) during Serpentinization; *Geochimica et Cosmochimica Acta*, Volume 56, pages 97-108.
- Page, N.J., (1986): Descriptive Model of Serpentine-Hosted Asbestos; in Mineral Deposit Models, Cox, D.P. and Singer, D.A., Editors, *U.S. Geological Survey, Bulletin 1693*, pages 46-48.
- Riordan, P.H., Editor (1981): Geology of Asbestos Deposits; *American Institute of Mining and Metallurgical Engineers*, New York, 118 Pages.
- Virta, R.L. and Mann, E.L. (1994): Asbestos; in Industrial Minerals and Rocks, Carr, D.D., Editor, *Society for Mining, Metallurgy and Exploration, Inc.*, Littleton, Colorado, pages 97-124.
- Wicks, F.J. (1984): Deformation Histories as Recorded by Serpentinites. I. Deformation Prior to Serpentinization; *Canadian Mineralogist*, Volume 22, pages 185-195.
- Wicks, F.J. (1984): Deformation Histories as Recorded by Serpentinites. II Deformation during the after Serpentinization; *Canadian Mineralogist*, Volume 22, pages 197-203.
- Wicks, F.J. (1984): Deformation Histories as Recorded by Serpentinites: III. Fracture Patterns Development Prior to Serpentinization; *Canadian Mineralogist*, Volume 22, pages 205-209.
- Wicks, F.J. and O'Hanley, D.S. (1988): Serpentine Minerals: Structures and Petrology; in Hydrous Phyllosilicates, Bailey, S.W., Editor, *Reviews in Mineralogy, Mineralogical Society of America*, Volume 19, pages 91-167.
- Wicks, F.J. and Whittaker, E.J.W. (1977): Serpentine Textures and Serpentinization; *Canadian Mineralogist*, Volume 15, pages 459-488.

DRAFT #: 3a Dec. 15, 1997



## KIMBERLITE-HOSTED DIAMONDS

N02

by Jennifer Pell<sup>1</sup>



### IDENTIFICATION

**SYNONYMS:** Diamond-bearing kimberlite pipes, diamond pipes, group 1 kimberlites.

**COMMODITIES (BYPRODUCTS):** Diamonds (some gemstones produced in Russia from pyrope garnets and olivine).

**EXAMPLES (British Columbia - Canada/International):** No B.C. deposits, see comments below for prospects; *Koala, Panda, Sable, Fox and Misery (Northwest Territories, Canada), Mir, International, Udachnaya, Aikhal and Yubilenaya (Sakha, Russia), Kimberly, Premier and Venetia (South Africa), Orapa and Jwaneng (Botswana), River Ranch (Zimbabwe).*

### GEOLOGICAL CHARACTERISTICS

**CAPSULE DESCRIPTION:** Diamonds in kimberlites occur as sparse xenocrysts and within diamondiferous xenoliths hosted by intrusives emplaced as subvertical pipes or resedimented volcanoclastic and pyroclastic rocks deposited in craters. Kimberlites are volatile-rich, potassic ultrabasic rocks with macrocrysts (and sometimes megacrysts and xenoliths) set in a fine grained matrix. Economic concentrations of diamonds occur in approximately 1% of the kimberlites throughout the world.

**TECTONIC SETTING:** Predominantly regions underlain by stable Archean cratons.

**DEPOSITIONAL ENVIRONMENT / GEOLOGICAL SETTING:** The kimberlites rise quickly from the mantle and are emplaced as multi-stage, high-level diatremes, tuff-cones and rings, hypabyssal dikes and sills.

**AGE OF MINERALIZATION:** Any age except Archean for host intrusions. Economic deposits occur in kimberlites from Proterozoic to Tertiary in age. The diamonds vary from early Archean to as young as 990 Ma.

**HOST/ASSOCIATED ROCK TYPES:** The kimberlite host rocks are small hypabyssal intrusions which grade upwards into diatreme breccias near surface and pyroclastic rocks in the crater facies at surface. Kimberlites are volatile-rich, potassic ultrabasic rocks that commonly exhibit a distinctive inequigranular texture resulting from the presence of macrocrysts (and sometimes megacrysts and xenoliths) set in a fine grained matrix. The megacryst and macrocryst assemblage in kimberlites includes anhedral crystals of olivine, magnesian ilmenite, pyrope garnet, phlogopite, Ti-poor chromite, diopside and enstatite. Some of these phases may be xenocrystic in origin. Matrix minerals include microphenocrysts of olivine and one or more of: monticellite, perovskite, spinel, phlogopite, apatite, and primary carbonate and serpentine. Kimberlites crosscut all types of rocks.

**DEPOSIT FORM:** Kimberlites commonly occur in steep-sided, downward tapering, cone-shaped diatremes which may have complex root zones with multiple dikes and "blows". Diatreme contacts are sharp. Surface exposures of diamond-bearing pipes range from less than 2 up to 146 hectares (Mwadui). In some diatremes the associated crater and tuff ring may be preserved. Kimberlite craters and tuff cones may also form without associated diatremes (e.g. Saskatchewan); the bedded units can be shallowly-dipping. Hypabyssal kimberlites commonly form dikes and sills.

**TEXTURE/STRUCTURE:** Diamonds occur as discrete grains of xenocrystic origin and tend to be randomly distributed within kimberlite diatremes. In complex root zones and multiphase intrusions, each phase is characterized by unique diamond content (e.g. Wesselton, South Africa). Some crater-facies kimberlites are enriched in diamonds relative to their associated diatreme (e.g. Mwadui, Tanzania) due to winnowing of fines. Kimberlite dikes may display a dominant linear trend which is parallel to joints, dikes or other structures.

---

<sup>1</sup> Consulting Geologist, Ottawa, Canada.

# KIMBERLITE-HOSTED DIAMONDS

N02

ORE MINERALOGY: Diamond.

GANGUE MINERALOGY (Principal and *subordinate*): Olivine, phlogopite, pyrope and eclogitic garnet, chrome diopside, magnesian ilmenite, enstatite, chromite, carbonate, serpentine; *monticellite, perovskite, spinel, apatite. Magma contaminated by crustal xenoliths can crystallize minerals that are atypical of kimberlites.*

ALTERATION MINERALOGY: Serpentinization in many deposits; silicification or bleaching along contacts. Secondary calcite, quartz and zeolites can occur on fractures. Diamonds can undergo graphitization or resorption.

WEATHERING: In tropical climates, kimberlite weathers quite readily and deeply to "yellowground" which is predominantly comprised of clays. In temperate climates, weathering is less pronounced, but clays are still the predominant weathering product. Diatreme and crater facies tend to form topographic depressions while hypabyssal dikes may be more resistant.

ORE CONTROLS: Kimberlites typically occur in fields comprising up to 100 individual intrusions which often group in clusters. Each field can exhibit considerable diversity with respect to the petrology, mineralogy, mantle xenolith and diamond content of individual kimberlites. Economically diamondiferous and barren kimberlites can occur in close proximity. Controls on the differences in diamond content between kimberlites are not completely understood. They may be due to: depths of origin of the kimberlite magmas (above or below the diamond stability field); differences in the diamond content of the mantle sampled by the kimberlitic magma; degree of resorption of diamonds during transport; flow differentiation, batch mixing or, some combination of these factors.

GENETIC MODEL: Kimberlites form from a small amount of partial melting in the asthenospheric mantle at depths generally in excess of 150 km. The magma ascends rapidly to the surface, entraining fragments of the mantle and crust, en route. Macroscopic diamonds do not crystallize from the kimberlitic magma. They are derived from harzburgitic peridotites and eclogites within regions of the sub-cratonic lithospheric mantle where the pressure, temperature and oxygen fugacity allow them to form. If a kimberlite magma passes through diamondiferous portions of the mantle, it may sample and bring diamonds to the surface provided they are not resorbed during ascent. The rapid degassing of carbon dioxide from the magma near surface produce fluidized intrusive breccias (diatremes) and explosive volcanic eruptions.

ASSOCIATED DEPOSIT TYPES: Diamonds can be concentrated by weathering to produce residual concentrations or within placer deposits (C01, C02, C03). Lamproite-hosted diamond deposits (N03) form in a similar manner, but the magmas are of different origin.

COMMENTS: In British Columbia the Cross kimberlite diatreme and adjacent Ram diatremes (MINFILE # - 082JSE019) are found near Elkford, east of the Rocky Mountain Trench. Several diamond fragments and one diamond are reported from the Ram pipes.

## EXPLORATION GUIDES

GEOCHEMICAL SIGNATURE: Kimberlites commonly have high Ti, Cr, Ni, Mg, Ba and Nb values in overlying residual soils. However, caution must be exercised as other alkaline rocks can give similar geochemical signatures. Mineral chemistry is used extensively to help determine whether the kimberlite source is diamondiferous or barren (see other exploration guides). Diamond-bearing kimberlites can contain high-Cr, low-Ca pyrope garnets (G10 garnets), sodium-enriched eclogitic garnets, high chrome chromites with moderate to high Mg contents and magnesian ilmenites.

GEOPHYSICAL SIGNATURE: Geophysical techniques are used to locate kimberlites, but give no indication as to their diamond content. Ground and airborne magnetometer surveys are commonly used; kimberlites can show as either magnetic highs or lows. In equatorial regions the anomalies are characterized by a magnetic dipolar signature in contrast to the "bulls-eye" pattern in higher latitudes. Some kimberlites, however, have no magnetic contrast with surrounding rocks. Some pipes can be detected using electrical methods (EM, VLF, resistivity) in airborne or ground surveys. These techniques are particularly useful where the weathered, clay-rich, upper portions of pipes are developed and preserved since they are conductive and may contrast sufficiently with the host rocks to be detected. Ground

# KIMBERLITE-HOSTED DIAMONDS

N02

based gravity surveys can be useful in detecting kimberlites that have no other geophysical signature and in delineating pipes. Deeply weathered kimberlites or those with a thick sequence of crater sediments generally give negative responses and where fresh kimberlite is found at surface, a positive gravity anomaly may be obtained.

OTHER EXPLORATION GUIDES: Indicator minerals are used extensively in the search for kimberlites and are one of the most important tools, other than bulk sampling, to assess the diamond content of a particular pipe. Pyrope and eclogitic garnet, chrome diopside, microilmene, chromite and, to a lesser extent, olivine in surficial materials (tills, stream sediments, loam, etc.) indicate a kimberlitic source. Diamonds are also usually indicative of a kimberlitic or lamproitic source; however, due to their extremely low concentration in the source, they are rarely encountered in surficial sediments. Weathered kimberlite produces a local variation in soil type that can be reflected in vegetation.

## *ECONOMIC FACTORS*

TYPICAL GRADE AND TONNAGE: When assessing diamond deposits, grade, tonnage and the average value (\$/carat) of the diamonds must be considered. Diamonds, unlike commodities such as gold, do not have a set value. They can be worth from a few \$/carat to thousands of \$/carat depending on their quality (evaluated on the size, colour and clarity of the stone). Also, the diamond business is very secretive and it is often difficult to acquire accurate data on producing mines. Some deposits have higher grades at surface due to residual concentration. Some estimates for African producers is as follows:

| <u>Pipe</u> | <u>Tonnage (Mt)</u> | <u>Grade (carats*/100 tonne)</u> |
|-------------|---------------------|----------------------------------|
| Orapa       | 117.8               | 68                               |
| Jwaneng     | 44.3                | 140                              |
| Venetia     | 66                  | 120                              |
| Premier     | 339                 | 40                               |

\* one carat of diamonds weighs 0.2 grams

ECONOMIC LIMITATIONS: Most kimberlites are mined initially as open pit operations; therefore, stripping ratios are an important aspect of economic assessments. Serpentinized and altered kimberlites are more friable and easier to process.

END USES: Gemstones; industrial uses such as abrasives.

IMPORTANCE: In terms of number of producers and value of production, kimberlites are the most important primary source of diamonds. Synthetic diamonds have become increasingly important as alternate source for abrasives.

## *SELECTED BIBLIOGRAPHY*

- Atkinson, W.J. (1988): Diamond Exploration Philosophy, Practice, and Promises: a Review; *in* Proceedings of the Fourth International Kimberlite Conference, Kimberlites and related rocks, V.2, Their Mantle/crust Setting, Diamonds and Diamond Exploration, J. Ross, editor, *Geological Society of Australia*, Special Publication 14, pages 1075-1107.
- Cox, D.P. (1986): Descriptive Model of Diamond Pipes; *in* Mineral Deposit Models, Cox, D.P. and Singer, D.A., Editors (1986), *U.S. Geological Survey*, Bulletin 1693, 379 pages.
- Fipke, C.E., Gurney, J.J. and Moore, R.O. (1995): Diamond Exploration Techniques Emphasizing Indicator Mineral Geochemistry and Canadian Examples; *Geological Survey of Canada*, Bulletin 423, 86 pages.

- Griffin, W.L. and Ryan, C.G. (1995): Trace Elements in Indicator Minerals: Area Selection and Target Evaluation in Diamond Exploration; *Journal of Geochemical Exploration*, Volume 53, pages 311-337.
- Gurney, J.J. (1989): Diamonds; in J. Ross, A.L. Jacques, J. Ferguson, D.H. Green, S.Y. O'Reilly, R.V. Danchin, and A.J.A. Janse, Editors, Kimberlites and Related Rocks, Proceedings of the Fourth International Kimberlite Conference, *Geological Society of Australia*, Special Publication Number 14, Volume 2, pages 935-965.
- Haggerty, S.E. (1986): Diamond Genesis in a Multiply-constrained Model; *Nature*, Volume 320, pages 34-37.
- Helmstaedt, H.H. (1995): "Primary" Diamond Deposits What Controls Their Size, Grade and Location?; in Giant Ore Deposits, B.H. Whiting, C.J. Hodgson and R. Mason, Editors, Society of Economic Geologists, Special Publication Number 2, pages 13-80.
- Janse, A.J.A. and Sheahan, P.A. (1995): Catalogue of World Wide Diamond and Kimberlite Occurrences: a Selective Annotative Approach; *Journal of Geochemical Exploration*, Volume 53, pages 73-111.
- Jennings, C.M.H. (1995): The Exploration Context for Diamonds; *Journal of Geochemical Exploration*, Volume 53, pages 113-124.
- Kirkley, M.B., Gurney, J.G. and Levinson, A.A. (1991) Age, Origin and Emplacement of Diamonds: Scientific Advances of the Last Decade; *Gems and Gemmology*, volume 72, Number 1, pages 2-25.
- Kjarsgaard, B.A. (1996): Kimberlite-hosted Diamond; in *Geology of Canadian Mineral Deposit Types*, O.R. Eckstrand, W.D. Sinclair and R.I. Thorpe, editors, *Geological Survey of Canada*, Geology of Canada, Number 8, pages 561-568.
- Levinson, A.A., Gurney, J.G. and Kirkley, M.B. (1992): Diamond Sources and Production: Past, Present, and Future; *Gems and Gemmology*, Volume 28, Number 4, pages 234-254.
- Macnae, J. (1995): Applications of Geophysics for the Detection and Exploration of Kimberlites and Lamproites; *Journal of Geochemical Exploration*, Volume 53, pages 213-243.
- Michalski, T.C. and Modreski, P.J. (1991) Descriptive Model of Diamond-bearing Kimberlite Pipes; in *Some Industrial Mineral Deposit Models: Descriptive Deposit Models*, editors, Orris, G.J and Bliss, J.D., U.S. Geological Survey, Open-File Report 91-11a, pages 1-4.
- Mitchell, R.H. (1991): Kimberlites and Lamproites: Primary Sources of Diamond; *Geoscience Canada*, Volume 18, Number 1, pages 1-16.
- Nixon, P.H. (1995): The Morphology and Nature of Primary Diamondiferous Occurrences; *Journal of Geochemical Exploration*, Volume 53, pages 41-71.
- Pell, J.A. (1997): Kimberlites in the Slave Craton, Northwest Territories, Canada; *Geoscience Canada*, Volume 24, Number 2, pages 77-96.
- Scott Smith, B.H. (1996): Kimberlites; in *Undersaturated Alkaline Rocks: Mineralogy, Petrogenesis and Economic Potential*, R.H. Mitchell, editor, *Mineralogical Association of Canada*, Short Course 24, pages 217-243.
- Scott Smith, B.H. (1992): Contrasting Kimberlites and Lamproites; *Exploration and Mining Geology*, Volume 1, Number 4, pages 371-381.

Draft #2a December 17, 1997



## LAMPROITE-HOSTED DIAMONDS

N03

by Jennifer Pell<sup>1</sup>



### IDENTIFICATION

SYNONYMS: None.

COMMODITY: Diamonds.

EXAMPLES (British Columbia (MINFILE #) - *Canada/International*): No B.C. examples; *Argyle, Ellendale (Western Australia), Prairie Creek (Crater of Diamonds, Arkansas, USA), Bobi (Côte d'Ivoire), Kapamba (Zambia), Majhgawan (India).*

### GEOLOGICAL CHARACTERISTICS

**CAPSULE DESCRIPTION:** Diamonds occur as sparse xenocrysts and in mantle xenoliths within olivine lamproite pyroclastic rocks and dikes. Many deposits are found within funnel-shaped volcanic vents or craters. Lamproites are ultrapotassic mafic rocks characterized by the presence of olivine, leucite, richterite, diopside or sanidine.

**TECTONIC SETTING:** Most olivine lamproites are post-tectonic and occur close to the margins of Archean cratons, either within the craton or in adjacent accreted Proterozoic mobile belts.

**DEPOSITIONAL ENVIRONMENT / GEOLOGICAL SETTING:** Olivine lamproites are derived from metasomatized lithospheric mantle. They are generally emplaced in high-level, shallow "maar-type" craters crosscutting crustal rocks of all types.

**AGE OF MINERALIZATION:** Any age except Archean. Diamondiferous lamproites range from Proterozoic to Miocene in age.

**HOST/ASSOCIATED ROCK TYPES:** Olivine lamproite pyroclastic rocks and dikes commonly host mineralization while lava flows sampled to date are barren. Diamonds are rarely found in the magmatic equivalents. Lamproites are peralkaline and typically ultrapotassic (6 to 8% K<sub>2</sub>O). They are characterized by the presence of one or more of the following primary phenocryst and/or groundmass constituents: forsteritic olivine; Ti-rich, Al-poor phlogopite and tetraferriphlogopite; Fe-rich leucite; Ti, K-rich richterite; diopside; and Fe-rich sanidine. Minor and accessory phases include priderite, apatite, wadeite, perovskite, spinel, ilmenite, armalcolite, shcherbakovite and jeppeite. Glass and mantle derived xenocrysts of olivine, pyrope garnet and chromite may also be present.

**DEPOSIT FORM:** Most lamproites occur in craters which are irregular, asymmetric, and generally rather shallow (often the shape of a champagne glass), often less than 300 metres in depth. Crater diameters range from a few hundred metres to 1500 metres. Diamond concentrations vary between lamproite phases, and as such, ore zones will reflect the shape of the unit (can be pipes or funnel-shaped). The volcanoclastic rocks in many, but not all, lamproite craters are intruded by a magmatic phase that forms lava lakes or domes.

**TEXTURE/STRUCTURE:** Diamonds occur as discrete grains of xenocrystic origin that are sparsely and randomly distributed in the matrix of lamproites and some mantle xenoliths.

**ORE MINERALOGY:** Diamond.

**GANGUE MINERALOGY (Principal and subordinate):** Olivine, phlogopite, richterite, diopside, sanidine; *priderite, wadeite, ilmenite, chromite, perovskite, spinel, apatite, pyrope garnet.*

---

<sup>1</sup> Consulting Geologist, Ottawa, Canada.

# LAMPROITE-HOSTED DIAMONDS

N03

**ALTERATION MINERALOGY:** Alteration to talc  $\pm$  carbonate  $\pm$  sulphide or serpentine -septechlorite + magnetite has been described from Argyle (Jacques *et al.*, 1986). According Scott Smith (1996), alteration to analcime, barite, quartz, zeolite, carbonate and other minerals may also occur. Diamonds can undergo graphitization or resorption.

**WEATHERING:** Clays, predominantly smectite, are the predominant weathering product of lamproites.

**ORE CONTROLS:** Lamproites are small-volume magmas which are confined to continental regions. There are relatively few lamproites known world wide, less than 20 geological provinces, of which only seven are diamondiferous. Only olivine lamproites are diamondiferous, other varieties, such as leucite lamproites presumably did not originate deep enough in the mantle to contain diamonds. Even within the olivine lamproites, few contain diamonds in economic concentrations. Controls on the differences in diamond content between intrusions are not completely understood. They may be due to: different depths of origin of the magmas (above or below the diamond stability field); differences in the diamond content of the mantle sampled by the lamproite magma; differences in degrees of resorption of diamonds during transport; or some combination of these factors.

**GENETIC MODEL:** Lamproites form from a small amount of partial melting in metasomatized lithospheric mantle at depths generally in excess of 150 km (i.e., within or beneath the diamond stability field). The magma ascends rapidly to the surface, entraining fragments of the mantle and crust en route. Diamonds do not crystallize from the lamproite magma. They are derived from harzburgitic peridotites and eclogites within regions of the sub-cratonic lithospheric mantle where the pressure, temperature and oxygen fugacity allow them to form in situ. If a lamproite magma passes through diamondiferous portions of the mantle, it may sample them and bring diamonds to the surface provided they are not resorbed during ascent.

**ASSOCIATED DEPOSIT TYPES:** Diamonds can be concentrated by weathering to produce residual concentrations or by erosion and transport to create placer deposits (C01, C02, C03). Kimberlite-hosted diamond deposits (N02) form in a similar manner, but the magmas are of different origin.

## EXPLORATION GUIDES

**GEOCHEMICAL SIGNATURE:** Lamproites can have associated Ni, Co, Ba and Nb anomalies in overlying residual soils. However, these may be restricted in extent since lamproites weather readily and commonly occur in depressions and dispersion is limited. Caution must be exercised as other alkaline rocks can give similar geochemical signatures.

**GEOPHYSICAL SIGNATURE:** Geophysical techniques are used to locate lamproites, but give no indication as to their diamond content. Ground and airborne magnetometer surveys are commonly used; weathered or crater-facies lamproites commonly form negative magnetic anomalies or dipole anomalies. Some lamproites, however, have no magnetic contrast with surrounding rocks. Various electrical methods (EM, VLF, resistivity) in airborne or ground surveys are excellent tools for detecting lamproites, given the correct weathering environment and contrasts with country rocks. In general, clays, particularly smectite, produced during the weathering of lamproites are conductive; and hence, produce strong negative resistivity anomalies.

**OTHER EXPLORATION GUIDES:** Heavy indicator minerals are used in the search for diamondiferous lamproites, although they are usually not as abundant as with kimberlites. Commonly, chromite is the most useful heavy indicator because it is the most common species and has distinctive chemistry. To a lesser extent, diamond, pyrope and eclogitic garnet, chrome spinel, Ti-rich phlogopite, K-Ti-richrichterite, low-Al diopside, forsterite and perovskite can be used as lamproite indicator minerals. Priderite, wadeite and shcherbakovite are also highly diagnostic of lamproites, although very rare.

*ECONOMIC FACTORS*

**TYPICAL GRADE AND TONNAGE:** When assessing diamond deposits, grade, tonnage and the average value (\$/carat) of the diamonds must be considered. Diamonds, unlike commodities such as gold, do not have a set value. They can be worth from a few to thousands of \$/carat depending on their quality (evaluated on the size, colour and clarity of the stone). Argyle is currently the only major lamproite-hosted diamond mine. It contains at least 75 million tonnes, grading between 6 and 7 carats of diamonds per tonne (1.2 to 1.4 grams/tonne). The Prairie Creek mine produced approximately 100 000 carats and graded 0.13 c/t. Typical reported grades for diamond-bearing lamproites of <0.01 to .3 carats per tonne are not economic (Kjarsgaard, 1995). The average value of the diamonds at Argyle is approximately \$US 7/carat; therefore, the average value of a tonne of ore is approximately \$US 45.50 and the value of total reserves in the ground is in excess of \$US 3.4 billion.

**END USES:** Gemstones; industrial uses such as abrasives.

**IMPORTANCE:** Olivine lamproites have only been recognized as diamond host rocks for approximately the last 20 years as they were previously classified as kimberlites based solely on the presence of diamonds. Most diamonds are still produced from kimberlites; however, the Argyle pipe produces more carats per annum (approximately 38,000 in 1995), by far, than any other single primary diamond source. Approximately 5% of the diamonds are good quality gemstones.

*SELECTED BIBLIOGRAPHY*

- Atkinson, W.J. (1988): Diamond Exploration Philosophy, Practice, and Promises: a Review; *in Proceedings of the Fourth International Kimberlite Conference, Kimberlites and Related Rocks, Volume 2, Their Mantle/Crust Setting, Diamonds and Diamond Exploration*, J. Ross, Editor, *Geological Society of Australia*, Special Publication 14, pages 1075-1107.
- Bergman, S.C. (1987): Lamproites and other Potassium-rich Igneous Rocks: a Review of their Occurrence, Mineralogy and Geochemistry; *in Alkaline Igneous Rocks*, J.G. Fitton and B. Upton, Editors, *Geological Society of London*, Special Publication 30, pages 103-190.
- Fipke, C.E., Gurney, J.J. and Moore, R.O. (1995): Diamond Exploration Techniques Emphasizing Indicator Mineral Geochemistry and Canadian Examples; *Geological Survey of Canada*, Bulletin 423, 86 pages.
- Griffin, W.L. and Ryan, C.G. (1995): Trace Elements in Indicator Minerals: Area Selection and Target Evaluation in Diamond Exploration; *Journal of Geochemical Exploration*, Volume 53, pages 311-337.
- Haggerty, S.E. (1986): Diamond Genesis in a Multiply-constrained Model; *Nature*, Volume 320, pages 34-37.
- Helmstaedt, H.H. (1995): "Primary" Diamond Deposits What Controls their Size, Grade and Location?; *in Giant Ore Deposits*, B.H. Whiting, C.J. Hodgson and R. Mason, Editors, Society of Economic Geologists, Special Publication Number 2, pages 13-80.
- Jacques, A.L., Boxer, G., Lucas, H. and Haggerty, S.E. (1986): Mineralogy and Petrology of the Argyle Lamproite Pipe, Western Australia; *in Fourth International Kimberlite Conference, Perth, Western Australia*, Extended Abstracts, pages 48-50.
- Jennings, C.M.H. (1995): The Exploration Context for Diamonds; *Journal of Geochemical Exploration*, Volume 53, pages 113-124.
- Kjarsgaard, B.A. (1996): Lamproite-hosted Diamond; *in Geology of Canadian Mineral Deposit Types*, O.R. Eckstrand, W.D. Sinclair and R.I. Thorpe, Editors, *Geological Survey of Canada*, Geology of Canada, Number 8, pages 568-572.
- Levinson, A.A., Gurney, J.G. and Kirkley, M.B. (1992): Diamond Sources and Production: Past, Present, and Future; *Gems and Gemmology*, Volume 28, Number 4, pages 234-254.
- Macnae, J. (1995): Applications of Geophysics for the Detection and Exploration of Kimberlites and Lamproites; *Journal of Geochemical Exploration*, Volume 53, pages 213-243.

# LAMPROITE-HOSTED DIAMONDS

N03

- Mitchell, R.H. (1991): Kimberlites and Lamproites: Primary Sources of Diamond; *Geoscience Canada*, Volume 18, Number 1, pages 1-16.
- Mitchell, R.H. and Bergman, S.C. (1991): Petrology of Lamproites; *Plenum Press*, New York, 447 pages.
- Nixon, P.H. (1995): The Morphology and Nature of Primary Diamondiferous Occurrences; *Journal of Geochemical Exploration*, Volume 53, pages 41-71.
- Scott Smith, B.H. (1992): Contrasting Kimberlites and Lamproites; *Exploration and Mining Geology*, Volume 1, Number 4, pages 371-381.
- Scott Smith, B.H. (1996): Lamproites; in *Undersaturated Alkaline Rocks: Mineralogy, Petrogenesis and Economic Potential*, R.H. Mitchell, Editor, *Mineralogical Association of Canada*, Short Course 24, pages 259-270.
- Scott Smith, B.H. and Skinner, E.M.W. (1984): Diamondiferous Lamproites; *Journal of Geology*, Volume 92, pages 433-438.

Draft # 2a

Dec. 15 1997



## ANDALUSITE HORNFELS

PO1

By Z.D. Hora



### IDENTIFICATION

SYNONYM: Chialstolite hornfels.

COMMODITIES (BY PRODUCTS): Andalusite (staurolite, garnet).

EXAMPLES [BRITISH COLUMBIA (MINFILE #) - *Canada/International*]: Kootenay (082FSE099), Kwoiek Needle (092ISW052), Atna Peak (103H040); *Kiglapait (Labrador, Canada), Canso (Nova Scotia, Canada), McGerrigle Pluton (Quebec, Canada), Groot Marico-Zeerust, Thamazimbi, Lydenburg (Transvaal, South Africa), Glomel (France), Tomduff (Ireland), Spargoville (Western Australia), Aktash (Uzbekistan).*

### GEOLOGICAL CHARACTERISTICS

CAPSULE DESCRIPTION: Andalusite occurs in metamorphosed rocks of originally clay-rich composition (usually pelitic) in thermal aureoles formed in the proximity of igneous intrusions. Andalusite is formed under conditions of high temperature and low pressure.

TECTONIC SETTINGS: Mostly in orogenic belts, but also may occur in a platformal environment. Orogenic plutonism intruding pelitic sedimentary sequence.

DEPOSITIONAL ENVIRONMENT/GEOLOGICAL SETTING: Andalusite hornfels is a product of thermal recrystallization of rocks with high alumina and low calcium contents. The protolith is usually argillaceous sediment, but may also be hydrothermally altered volcanic or volcanoclastic rock. The whole spectrum of granitic to gabbroic igneous rocks can act as a source of heat may cover the whole spectrum from granitic to gabbroic composition. Metamorphic zonation of the contact aureole is characterized by distinct mineral assemblages and textural features, where andalusite may be major or minor component, fine grained or as crystal porphyroblasts several millimetres or even centimetres in size.

AGE OF MINERALIZATION: Precambrian to Tertiary. The largest producing deposits are related to intrusion of the Bushveld Igneous Complex (South Africa) about 1.95 billion years old. The deposit in France, the second largest producer in the world is related to granite of Hercynian age. The occurrences in British Columbia are Cretaceous and Eocene in age.

HOST/ASSOCIATED ROCK TYPES: The host rocks are chialstolite metapelite. The associated rocks are spotted slates, andalusite-cordierite hornfels, staurolite hornfels, spinel-corundum hornfels, silimanite hornfels, skarns and a variety of igneous intrusions.

DEPOSIT FORM: Large intrusions into pelitic sedimentary units may produce tabular deposits 20 to 60 metres wide and up to 6 kilometres long. Majority of occurrences are small and irregular in shape. Primary deposits may be associated with alluvial and eluvial accumulations.

TEXTURE/STRUCTURE: Andalusite forms euhedral crystals as porphyroblasts in a fine grained matrix. Individual crystals may reach the size of 60 millimetres in length. Randomly oriented minerals are characteristic of decussate texture. The chialstolitic rocks are characterized by fairly homogenous distribution and size of the andalusite crystals.

# ANDALUSITE HORNFELS

PO1

ORE MINERALOGY: (Principle and *subordinate*): Andalusite, *staurolite*, *garnet*.

GANGUE MINERALOGY (Principle and *subordinate*): Fine grained hornfels matrix - usually cordierite, biotite, muscovite, chlorite and quartz.

ALTERATION MINERALOGY: Retrograde metamorphism results in andalusite being altered to mica and staurolite or mica and chlorite. Such alteration (even partial) may render the andalusite unusable for industrial applications.

WEATHERING: Andalusite is not highly susceptible to chemical weathering and as such, may accumulate in alluvial sediments or as a residual deposit.

ORE CONTROLS: Andalusite development is a factor of the composition of the protolith and the high temperature/low pressure conditions adjacent to an igneous intrusion. The chemical nature and thickness of the original sedimentary layers and their respective distance from the intrusive contact are the main controls on the formation of andalusite hornfels orebodies. Although the metamorphic aureole may extend a large distance, typically only a few areas within the aureole satisfy the conditions necessary to produce economic accumulations of andalusite.

GENETIC MODELS: Andalusite deposits develop in pelitic rocks with high alumina and low calcium contents at temperatures of 550° to 600°C and low pressures of about two kilobars. Such conditions usually develop within the contact aureole of an intrusive. At higher temperatures, sillimanite or corundum and spinel would form at the expense of andalusite.

ASSOCIATED DEPOSIT TYPES: Wollastonite (K09) and garnet (K08) skarns form under similar circumstances from calcium-rich protoliths. Andalusite hornfels deposits can be the source for placer andalusite (C01, C02). Microcrystalline graphite (P03) and gem corundum (Q09) are also found in contact aureoles of igneous rocks.

COMMENTS: Under special conditions, regional, low pressure metamorphism can result in crystallization of sufficient andalusite to be a commercial grade. Some contact aureoles of large intrusive complexes, like the Bushveld Complex, are so extensive that they have features similar to regional low-pressure metamorphism.

## ***EXPLORATION GUIDES***

GEOCHEMICAL SIGNATURE: None.

GEOPHYSICAL SIGNATURE: None.

OTHER EXPLORATION GUIDES: Andalusite, corundum and spinel in alluvial deposits; geological contacts of pelitic sediments with plutonic rocks; sedimentary roof pendants in large plutonic complexes. Most deposits are found within one km of the related igneous intrusion. Economic deposits are more likely in prospective regions with well developed weathering profiles.

## *ECONOMIC FACTORS*

**TYPICAL GRADE AND TONNAGE:** South African deposits contain approximately 35 Mt of economically recoverable reserves. The Andafrax deposit is a 60 m thick zone with 5 to 20% andalusite crystals and with production of about 36 ktpy. The Grootfontein mine contains 15% andalusite with annual production capacity estimated at 140 kt. The Krugerspost deposit has an average width of 20 m with andalusite content 8 to 12% and annual mine production about 30 kt. The Havercroft mine has a 50 m thick hornfels ore zone with 7 to 8% andalusite and annual mine capacity about 50 kt. The Hoogenoeg mine ore contains between 8 and 12% andalusite; production capacity is 35 kt per year. The Kerphales deposit in France contains 15% andalusite crystals and is about 400 m thick. It has proven and possible reserves of 10 Mt and produces 65 kt per year.

**ECONOMIC LIMITATIONS:** Andalusite concentrate should contain from 57 to 61%  $\text{Al}_2\text{O}_3$  and 0.6 to 0.9%  $\text{Fe}_2\text{O}_3$  and is priced between US\$180 and US\$140 per tonne (Industrial Minerals, 1997). Because of extreme hardness, some fresh andalusite hornfels are uneconomic to process in spite of high andalusite content and only the weathered zones are mined (Hoogenoeg mine, South Africa). Andalusite recovery generally ranges from 50 to 60%, some production from primary deposits is supplemented from adjacent alluvial accumulations.

**END USES:** The most important use of andalusite is in monolithic refractories and unfired bricks for blast and glass furnaces, cement kilns and combustion chambers. Smaller quantities are used in specialty ceramics, like spark plugs, acoustic tiles, etc.

**IMPORTANCE:** Andalusite is a high quality, raw material for high-alumina refractory products. It can be substituted by synthetic mullite, kyanite and sillimanite.

## *SELECTED BIBLIOGRAPHY*

- Grobbelaar, A.P. (1994): Andalusite, in *Industrial Minerals and Rocks*, Carr, D.D. Senior Editor, *Society for Mining, Metallurgy and Exploration*, Inc. Littleton, Colorado, pages 913-920.
- Harben, P.W. and Bates, R.L. (1990): *Industrial Minerals and World Deposits*, *Metal Bulletin*, London, 312 pages.
- Kerrick, D.M. (1990): The  $\text{Al}_2\text{SiO}_5$  Polymorphs; *Reviews in Mineralogy*, Volume 22, *Mineralogical Society of America*, Washington, D.C., 406 pages.
- Kerrick, D.M. (1993): Contact Metamorphism, *Reviews in Mineralogy*, Volume 26. *Mineralogical Society of America*, Washington, D.C., 821 pages.
- Pell, J. (1988): The Industrial Mineral Potential of Kyanite and Garnet in British Columbia, *British Columbia Ministry of Energy, Mines and Petroleum Resources*, Open File 1988-26, 43 pages.
- Simandl, G.J., Hancock, K.D., Church, B.N. and Woodsworth, G.J. (1995): Andalusite in British Columbia - New Exploration Targets, in *Geological Fieldwork 1994*, *British Columbia Ministry of Energy, Mines and Petroleum Resources*, Paper 1995-1, pages 385-394.

Draft #2 October 26, 1997





## MICROCRYSTALLINE GRAPHITE

P03

G.J. Simandl and W.M. Kenan<sup>1</sup>

### IDENTIFICATION



SYNONYM: "Amorphous graphite" is a technically incorrect but commonly used commercial term for the same product.

COMMODITY: Microcrystalline graphite.

EXAMPLES (British Columbia (MINFILE #) - *Canada/International*): *Kellog Mine in Moradillos (State of Sonora, Mexico), Kaiserberg, Styria region (Austria) and Velké Vrbno-Konstantin (Czech Republic)*.

### GEOLOGICAL CHARACTERISTICS

CAPSULE DESCRIPTION: Most amorphous graphite deposits are formed by contact or regional metamorphism of coal beds or other highly carbonaceous sedimentary rocks. Deposits may consist of several beds or lenses, each a few metres thick and up to several kilometres in length. Typical host rocks are quartzites, phyllites, schists and metagraywackes.

TECTONIC SETTINGS: Continental margin or intracratonic basins.

DEPOSITIONAL ENVIRONMENT / GEOLOGICAL SETTING: Near shore sedimentary rocks with intercalated coal seams, or other highly carbonaceous sedimentary beds, that are metamorphosed by nearby igneous intrusions or affected by regional metamorphism.

AGE OF MINERALIZATION: Most of the deposits are Mississippian to Cretaceous in age or younger.

HOST/ASSOCIATED ROCK TYPES: The host rocks are coal seams or other highly carbon-rich rock types and their low to medium grade metamorphic equivalents. Amorphous graphite deposits occur within sequences of chlorite and muscovite schists, phyllites, quartzites, metagraywackes, limestones, sandstones and conglomerates which may be cut by diabasic or granitic intrusions with associated andalusite-bearing hornfels.

DEPOSIT FORM: Stratiform or lens-shaped; beds may be deformed and/or repeated by folding and faulting. Pinching and swelling of beds is common. Deposits may consist of several beds, each one to few metres thick. They may be exposed for hundreds of metres to several kilometres in strike length.

TEXTURE/STRUCTURE: Graphite-bearing beds may contain lenses of hangingwall or footwall host rocks and are characterised by abundant slickensides. Graphite ore is schistose or massive.

ORE MINERALOGY [Principal and *subordinate*]: Microcrystalline graphite

GANGUE MINERALOGY [Principal and *subordinate*]: *Meta-anthracite ± anthracite ± quartz ± mica ± coke ± clay ± pyrite and other sulphides ± apatite ± gypsum.*

ALTERATION MINERALOGY: N/A.

WEATHERING: Weathered outcrops of microcrystalline graphite are typically dull, porous and dark-gray to black.

---

<sup>1</sup> Asbury Graphite Mills Inc., Asbury, New Jersey.

# MICROCRYSTALLINE GRAPHITE

P03

**ORE CONTROLS:** Coal beds invaded by intrusive rocks or sedimentary sequences with coal seams or other carbon-rich rocks metamorphosed typically to greenschist facies. Size, grade and mineral impurities of the graphite deposit depend on the characteristics of the original coal seams and carbon-bearing or carbonaceous sediments. Degree of metamorphism controls the degree of graphitization. Graphite may grade into coal with increasing distance from the heat source. Temperatures required for graphitization are lower under shear conditions. Faults and folds may control the thickness or repetition of graphite beds.

**GENETIC MODELS:** Graphitization can be described as an extreme case of coal maturation. Coal maturation involves the following sequence: peat - lignite - bituminous coal - semi-anthracite - anthracite - meta-anthracite - microcrystalline graphite. Source of heat in contact-metamorphic environment may be plutons, dikes or sills adjacent to coal beds.

**ASSOCIATED DEPOSIT TYPES:** Coal deposits, (A03, A04, A05). Some coal beds may be only partially converted into graphite. Expanding shale (R02) and bentonite deposits (E06) are commonly associated with coal. Andalusite deposits (P01) may be present in cases where graphite is formed by contact metamorphism.

**COMMENTS:** Although several areas appear favorable for the formation of amorphous graphite there are no known deposits in British Columbia. Meta-anthracite is reported at Guess Creek near Smithers and Flint Creek near Hazelton.

## *EXPLORATION GUIDES*

**GEOCHEMICAL SIGNATURE:** Graphite may be present in residual soils. Positive vanadium and nickel anomalies and negative boron anomalies associated with graphite beds were reported by Tichy and Turnovec (1978). This enrichment is probably related to the trace element content of the protolith, therefore, each deposit may have its own geochemical characteristics. It is unlikely that the chemical signature could be used effectively in grassroots mineral exploration

**GEOPHYSICAL SIGNATURE:** Graphite deposits have been located using induced polarization (IP), resistivity, ground and airborne electromagnetic (EM), spontaneous potential (SP) and audiomagnetotelluric (AMT) surveys. Outcrops may have associated radioactivity because of trace amounts of uranium.

**OTHER EXPLORATION GUIDES:** The most important regional exploration guides for high-grade amorphous deposits are: 1) coal beds invaded by igneous rocks or 2) coal seams traced across regional metamorphic isograds into low to medium-grade metamorphic areas.

## *ECONOMIC FACTORS*

**TYPICAL GRADE AND TONNAGE:** The mean size of the deposits reported by Bliss and Sutphin (1992) is 4 900 000 tonnes. Major active mines contain over 80 per cent carbon, but the average grade of some of the European deposits may be as low as 55%. Some beds may be only partly graphitized.

**ECONOMIC LIMITATIONS:** Mines are mainly open pit, however underground mining is possible depending on the thickness and orientation of the ore. Prices of amorphous graphite are substantially lower than the prices of the crystalline flake graphite. The ore is commonly hand-sorted. Quantity and type of impurities and ash content are major concerns. The degree of graphitization varies from one deposit to another and as a result, proportions of microcrystalline graphite to carbon also varies.

**END USES:** Microcrystalline graphite is used in brake linings, foundry applications, lubricants, pencils, refractories, and steel making. The graphite may contain several percent volatile material. In fact, some meta-anthracite from South Korea is marketed as microcrystalline graphite, but it may be due largely to export restrictions on energy exports from Korea.

**IMPORTANCE:** Metamorphosed coal beds are the main source of microcrystalline graphite. For most applications, synthetic graphite and crystalline graphite may be substituted for amorphous graphite but at increased cost.

## *SELECTED BIBLIOGRAPHY*

- Bliss, J.D. and Sutphin, D.M. (1992): Grade and Tonnage Model of Amorphous Graphite: Model 18k; in G.J. Orris and J.D. Bliss, Editors, *U.S. Geological Survey*, Open File Report 92-437, pages 23-25.
- Harben, P.W. and Bates, R.L. (1990): *Industrial Minerals - Geology and World Deposits*; Metal Bulletin Plc., London, 312 pages.
- Graffin, G.D. (1975): Graphite; in *Industrial Minerals and Rocks*, 4th Edition; *American Institute of Mining, Metallurgical, and Petroleum Engineers, Inc.*, pages 691-705.
- Krauss, U.H., Schmitt, H.W., Taylor, H.A., Jr. and Sutphin, D.M. (1988): International Strategic Minerals Inventory Summary Report - Natural Graphite; *U.S. Geological Survey*, Circular 930-H, 29 pages.
- Kuzvart, M. (1984): *Industrial Minerals and Rocks*; Elsevier; New York, 454 pages
- Riddle III, H.M. and Kenan, W.M. (1995): Natural and Synthetic Graphite Powders; *Industrial Minerals*, Number 338, pages 61-65.
- Tichy, L. and Turnovec, I. (1978): On possible Geochemical Identification of Graphite in South Bohemia (In Czech); *Geologicky Pruzkum*, Volume 20, pages 73-75.
- Weis, P.L. and Salas, G.A. (1978): Estimating Reserves of Amorphous Graphite in Sonora, Mexico; *Engineering and Mining Journal*, volume 179, Number 10, pages 123 - 128.

DRAFT #: 3a December 15, 1997





## CRYSTALLINE FLAKE GRAPHITE

P04

by G.J. Simandl, and W.M. Kenan<sup>1</sup>

### IDENTIFICATION



SYNONYM: Disseminated flake graphite deposits.

COMMODITY: Crystalline flake graphite and crystalline graphite powder.

EXAMPLES (British Columbia (MINFILE #) - *Canada/International*): AA prospect (092M 017), Black Crystal (82FNW260), Mon (093N 203); *Lac Knife deposit, Asbury Graphite mine and Peerless Mine (Quebec, Canada), Graphite Lake and Black Donald mines (Ontario, Canada); American Graphite Company mine (New York State, USA).*

### GEOLOGICAL CHARACTERISTICS

CAPSULE DESCRIPTION: Disseminated flakes graphite deposits are commonly hosted by porphyroblastic and granoblastic marbles, paragneisses and quartzites. Alumina-rich paragneisses and marbles in upper amphibolite or granulite grade metamorphic terrains are the most favourable host rocks. Highest grades are commonly associated with rocks located at the contacts between marbles and paragneisses and deposits are thickest within fold crests. Minor feldspathic intrusions, pegmatites and iron formations also contain disseminated flake graphite.

TECTONIC SETTINGS: May be found in any setting with favourable paleo-environment for accumulation and preservation of organic materials, such as intracratonic or continental margin-type basins.

DEPOSITIONAL ENVIRONMENT / GEOLOGICAL SETTING: Metasedimentary belts of granulite or upper amphibolite facies invaded by igneous rocks.

AGE OF MINERALIZATION: Known deposits are mostly of Precambrian age, but could be of any age.

HOST/ASSOCIATED ROCK TYPES: Marbles, paragneisses, quartzites, magnetite-graphite iron formations, clinopyroxenites, amphibolites and pegmatites can host flake graphite deposits. Associated lithologies are orthogneisses, charnockites, orthopyroxenites, amphibolites, granulites and variety of intrusive rocks.

DEPOSIT FORM: Stratiform lens-shaped or saddle-shaped. Individual, economically significant deposits are several metres to tens of metres thick and hundreds of metres in strike length.

TEXTURE/STRUCTURE: Strong foliation, schistosity and lepidoblastic texture for paragneiss and schists. Granoblastic, equigranular or porphyroblastic textures in marbles.

ORE MINERALOGY [Principal and *subordinate*]: Crystalline flake graphite  $\pm$  *microcrystalline graphite*.

GANGUE MINERALOGY [Principal and *subordinate*]: In carbonate-hosted graphite deposits: calcite, clinopyroxene, pyrite and other sulphides  $\pm$  *dolomite*  $\pm$  *anorthite*  $\pm$  *chlorite*  $\pm$  *clinozoisite*  $\pm$  *zoisite*  $\pm$  *garnet*. In paragneiss-hosted graphite deposits: feldspar, quartz, biotite,  $\pm$  clinopyroxene  $\pm$  garnet  $\pm$  sillimanite  $\pm$  kyanite  $\pm$  sulphides  $\pm$  *clinozoisite*  $\pm$  scapolite  $\pm$  *secondary gypsum*.

ALTERATION MINERALOGY: Chlorite, prehnite, zoisite and clinozoisite are common retrograde minerals in porphyroblastic marbles.

WEATHERING: Jarosite is a common weathering product of disseminated pyrite-bearing, gneiss-hosted graphite deposits.

<sup>1</sup> Asbury Graphite Mills Inc., Asbury, New Jersey

# CRYSTALLINE FLAKE GRAPHITE

P04

**ORE CONTROLS:** Low grade, large tonnage deposits are hosted mainly by paragneisses and are stratabound. Higher grade portions of these deposits are commonly located in fold crests; along paragneiss-marble, quartzite-marble and quartzite-paragneiss contacts; or along other zones that acted as channels for retrograde metamorphic fluids.

**GENETIC MODELS:** Low-grade, stratabound and stratiform deposits are believed to be a product of graphitization of the organic material within pre-metamorphic protolith (carbonates and shales). The crystallinity of graphite is linked to the degree of metamorphism. Higher grade portions of these deposits are usually structurally controlled, and were probably enriched during the retrograde phase of the regional or contact metamorphism. Late graphite precipitation (enrichment) may have been triggered by internal or external buffering or fluid mixing.

**ASSOCIATED DEPOSIT TYPES:** Commonly associated with vein-graphite deposits (P05).

**COMMENTS:** Can be spatially associated with kyanite, sillimanite, mica and garnet (P02), dimension stone (R03), wollastonite skarn (K09) and abyssal (ceramic) pegmatite (Q04) deposits.

## *EXPLORATION GUIDES*

**GEOCHEMICAL SIGNATURE:** Graphite concentrations in residual soils and stream beds. Geochemical trace element methods were pioneered in USSR although these methods do not rival with geophysical methods in effectiveness.

**GEOPHYSICAL SIGNATURE:** Effective methods for detecting high grade mineralization (where at least locally the individual flakes are touching) are airborne EM, ground VLF and other EM methods. Induced polarisation, applied potential and self potential are also used, although IP is considered relatively expensive and in many cases too sensitive.

**OTHER EXPLORATION GUIDES:** Graphite deposits commonly form clusters. Overall quality of graphite flake increases with the intensity of regional metamorphism. Metasedimentary rocks of upper amphibolite or granulite facies represent the best exploration ground. Traces of graphite within a metasedimentary sequence indicate that the oxidation-reduction conditions were favourable for the preservation of graphite deposits. High-grade ores are associated with fold crests and contacts between adjacent lithological units. In some regions, blue quartz is found in close spatial association with crystalline-flake graphite deposits and could be considered as an empirical indirect indicator of favourable environment for graphite exploration.

## *ECONOMIC FACTORS*

**TYPICAL GRADE AND TONNAGE:** Grade and tonnage of producing mines and developed prospects varies substantially. The median grade and size is 9.0% and 2 400 000 tonnes respectively (Bliss and Sutphin, 1992). Depending on market conditions, large deposits containing high proportions of coarse flakes, which can be easily liberated, may be economic with grades as low as 4%.

**ECONOMIC LIMITATIONS:** Price of the commercial concentrate is determined by flake size, degree of crystallinity (toughness), graphitic carbon content, ash content and type of the impurities. Crystalline flake graphite is commonly chemically-and heat-treated to enhance its properties. Depending on the applications, the most common limiting technical parameters are the carbon content, the diameter of the graphite flakes, the degree of crystallinity (which is related to the flake toughness), the type of impurities and the ash content. Metallurgical and consumer tests are therefore required to market flake graphite.

**END USES:** Main uses are in refractors, lubricants, brake linings, foundry moulds and dressings, crucibles, electrodes, pencils and others. Graphite use in non-traditional applications, such as expanded graphite and graphite foils, is increasing, while the demand for use in refractors is highly cyclical.

**IMPORTANCE:** Flake graphite can be substituted for in most of its applications, however substitute materials are more expensive and do not perform as well.

*SELECTED BIBLIOGRAPHY*

- Krauss, U.H., Schmitt, H.W., Taylor, H.A., Jr. and Sutphin, D.M. (1988): International Strategic Minerals Inventory Summary Report- Natural Graphite; *U.S. Geological Survey*, Circular 930-H, 29 pages.
- Marchildon, N., Simandl, G.J. and Hancock, K.D. (1992): The AA Graphite Deposit, Bella Coola Area, British Columbia: Exploration Implications for the Coast Plutonic Complex; in: *Geological Fieldwork 1992*, Grant, B. and Newell, J.M., Editors, *B.C. Ministry of Energy, Mines and Petroleum Resources*, Paper 1993-1, pages 389-397.
- Riddle III, H.M. and Kenan, W.M. (1995): Natural and Synthetic Graphite Powders; *Industrial Minerals*, Number 338, pages 61-65.
- Rogers, R.S. (1995): Graphite; in *Descriptive Mineral Deposit Models of Metallic and Industrial Mineral Deposit Types and Related Mineral Potential Assessment Criteria*; M.C. Rogers, P.C. Thurston, J.A. Fyon, R.I. Kelly and, F.W. Breaks, Editors, Open File Report 5916, *Ontario Geological Survey*, pages 167-171
- Simandl, G.J., Paradis S., Valiquette, G., and Jacob, H.-L. (1995): Crystalline Graphite Deposits, Classification and Economic Potential, Lachute-Hull-Mont Laurier Area, Quebec; in *Proceedings of 28th Forum on the Geology of Industrial Minerals*, Martinsburg, West Virginia, May 3-8, 1992, pages 167-174.
- Simandl, G.J. (1992): Gîtes de Graphite de la Région de la Gatineau, Québec; Unpublished Ph.D. Thesis, *Ecole Polytechnique*, Montréal (in French), 383 pages.
- Sutphin, D.M. (1991): Descriptive Model of Disseminated Flake Graphite; in *Some Industrial Mineral Deposit Models; Descriptive Deposit Models*, G.J. Orris and J.D. Bliss, Editors, *U.S. Geological Survey*, Open File Report 91-11A, pages 49-51
- Bliss, J.D. and Sutphin, D.M. (1992): Grade and Tonnage Model of Disseminated Flake Graphite: Model 371; in G.J. Orris and J.D. Bliss, Editors; *U.S. Geological Survey*, Open File Report 92-437, pages 67-70.

DRAFT # 3a - December 15, 1997





## VEIN GRAPHITE IN METAMORPHIC TERRAINS

P05

by G.J. Simandl and W.M. Kenan<sup>1</sup>



### IDENTIFICATION

SYNONYMS: Lump and chip graphite, epigenetic graphite.

COMMODITY: Crystalline lump and chip graphite.

EXAMPLES (British Columbia (MINFILE #) - Canada/International): *Calumet, Clot, Walker and Miller mines and St. Sauveur occurrences (Quebec, Canada), Dillon (Montana, USA), Bogala Mine (Sri Lanka), deposits of South Kerala (India).*

### GEOLOGICAL CHARACTERISTICS

CAPSULE DESCRIPTION: Graphite veins currently mined are from few centimetres to a metre thick. Typically they cut amphibolite to granulite grade metamorphic rocks and/or associated intrusive rocks.

TECTONIC SETTING(S): Katazone (relatively deep, high-grade metamorphic environments associated with igneous activity; conditions that are common in the shield areas).

DEPOSITIONAL ENVIRONMENT / GEOLOGICAL SETTING: Veins form in high-grade, dynamothermal metamorphic environment where metasedimentary belts are invaded by igneous rocks.

AGE OF MINERALIZATION: Any age; most commonly Precambrian.

HOST/ASSOCIATED ROCK TYPES: Hosted by paragneisses, quartzites, clinopyroxenites, wollastonite-rich rocks, pegmatites. Other associated rocks are charnockites, granitic and intermediate intrusive rocks, quartz-mica schists, granulites, aplites, marbles, amphibolites, magnetite-graphite iron formations and anorthosites.

DEPOSIT FORM: Veins are from a few millimetres to over a metre thick in places, although usually less than 0.3 meter thick. Individual veins display a variety of forms, including saddle-, pod- or lens-shaped, tabular or irregular bodies; frequently forming anastomosing or stockwork patterns. The mines in Sri Lanka are from 30 metres to 400 metres deep; individual veins rarely extend more than tens of metres. TEXTURE/STRUCTURE: Rosettes, coarse flakes, "fibers" or "needles" oblique or perpendicular to wall rock, or in some cases schistosity subparallel to the vein walls.

ORE MINERALOGY [Principal and *subordinate*]: Crystalline and microcrystalline graphite.

GANGUE MINERALOGY [Principal and *subordinate*]: Depends largely on the host-rock.

In marble or skarn: calcite  $\pm$  wollastonite  $\pm$  hedenbergite  $\pm$  zoisite  $\pm$  clinozoisite  $\pm$  prehnite  $\pm$  quartz  $\pm$  titanite  $\pm$  sulphides  $\pm$  diopside  $\pm$  scapolite  $\pm$  prehnite.

In most of other rocks: feldspar  $\pm$  apatite  $\pm$  garnet  $\pm$  scapolite  $\pm$  biotite  $\pm$  sillimanite  $\pm$  secondary iron oxides.

ALTERATION MINERALOGY: Most veins are not surrounded by macroscopically distinguishable alteration halos, while some veins have narrow (< 1cm thick) alteration halos that are not well documented. Sillimanite, graphite-sillimanite or graphite-tourmaline alteration is reported adjacent to the veins in Sri Lanka and New Hampshire. In Quebec, some of the veins cut rocks with contact metamorphic or skarn characteristics. Sillimanite, graphite-sillimanite or graphite-tourmaline alteration is reported adjacent to the veins in Sri Lanka and New Hampshire.

<sup>1</sup> Asbury Graphite Mills Inc., Asbury, New Jersey

# VEIN GRAPHITE IN METAMORPHIC TERRAINS

P05

**WEATHERING:** In the near surface environments, graphite grades are enhanced by weathering out of gangue minerals.

**ORE CONTROLS:** Veins form along joints, breccia zones, crests of folds, decollements along geological contacts and foliations. Joints in brittle lithologies (such as hornfels or skarns in contact metamorphic aureoles associated with deep seated intrusive rocks) are particularly favourable. Relatively reducing conditions (within the graphite stability field).

**GENETIC MODELS:** The origin of graphite veins is controversial. The ultimate source of carbon may vary from one deposit to other. Although most of the veins are hosted by high grade metamorphic rocks, the graphite precipitation may take place during the retrograde phase of the regional or contact metamorphism. This is suggested by coexistence of low temperature minerals such as prehnite with vein-graphite. Depending on the occurrence, the interaction of fluid with the host rock (internal or external buffering), such as oxidation of CH<sub>4</sub>-bearing fluids by wall rock, cooling of a hot fluid nearly saturated with respect to graphite, or fluid mixing are the most probable causes of vein formation.

**ASSOCIATED DEPOSIT TYPES:** Commonly associated with disseminated crystalline flake graphite deposits (P04) and in some cases with wollastonite deposits (K09) and abyssal (ceramic) pegmatites (O04).

**COMMENTS:** 1) Crystalline graphite veins hosted by ultramafic rocks are relatively uncommon and are not covered by this profile.  
2) Portions of the AA crystalline flake graphite deposit, located near the southern tip of Bentick Arm, British Columbia, contain microscopic graphite veinlets, suggesting that graphite veins may also occur in the metasedimentary roof pendants of the Coast Plutonic Complex.

## *EXPLORATION GUIDES*

**GEOCHEMICAL SIGNATURE:** Veins may have in some cases narrow (< 1cm thick) alteration halos that are not well documented and are too thin to be of use in exploration. The chemical composition of ore is influenced mainly by the composition of gangue minerals.

**GEOPHYSICAL SIGNATURE:** Ground electromagnetic methods (VLF in initial exploration stage, horizontal or vertical loupe at later stages) and resistivity are the most appropriate methods to locate large graphite veins. "Mise a la masse" is useful in vein delineation.

**OTHER EXPLORATION GUIDES:** Graphite veins are most common in highly metamorphosed terrains and in several cases are associated with crystalline flake graphite deposits. Because graphite is inert in the weathering environment, boulder tracing and use of electromagnetic mats may be effective.

## *ECONOMIC FACTORS*

**TYPICAL GRADE AND TONNAGE:** Veins contain 40 to 90% graphitic carbon before hand sorting. No reliable data is available on the tonnages for individual veins.

**ECONOMIC LIMITATIONS:** Since the deposits are relatively narrow veins, the mines are typically small scale, labour intensive and underground. The ore is hand sorted, washed and screened. Where possible, consumers substitute the less expensive and readily available crystalline flake graphite for vein graphite. The main technical parameter of the vein-graphite concentrate is its ability to mould to any shape and flow when exposed to extreme pressures.

**END USES:** Graphite from veins is used mainly in: powder metals, special refractories, copper graphite and carbon graphite brushes for electrical applications.

**IMPORTANCE:** The only current source of crystalline lump graphite is Sri Lanka; it is exported world-wide. British Columbia has no documented vein graphite occurrences.

*SELECTED BIBLIOGRAPHY*

- Cirkel, F. (1907): Graphite, its Properties, Occurrences, Refining and Uses: *Canada Department of Mines, Mines Branch, Ottawa, Number 202, 263 pages.*
- Dobner, A., Graf, W., Hahn-Winheimer, P., and Hirner, A. (1978): Stable Carbon Isotopes of Graphite from Bogala Mine, Sri Lanka; *Lithos*, volume 11, pages 251-255.
- Harben, P.W. and Bates, R.L. (1990): Industrial Minerals - Geology and World Deposits, London, *Metal Bulletin Plc.*, 312 pages.
- Frost, B.R. (1979): Mineral Equilibria Involving Mixed Volatiles in a C-O-H Fluid Phase: The Stabilities of Graphite and Siderite; *American Journal of Science*, volume 279, pages 1033-1059.
- Krauss, U.H., Schmitt, H.W., Taylor, H.A., Jr. and Suthphin, D.M. (1988): International Strategic Minerals Inventory Summary Report- Natural Graphite; *U.S. Geological Survey, Circular 930-H, 29 pages.*
- Riddle III, H.M. and Kenan, W.M. (1995): Natural and Synthetic Graphite Powders; *Industrial Minerals, Number 338, pages 61-65.*
- Rumble III., D. and Hoering, T.C. (1986): Carbon Isotope Geochemistry of Graphite Vein Deposits from New Hampshire, U.S.A; *Geochemica and Cosmochemica Acta*; volume 50, pages 1239-1247.
- Simandl, G.J., Paradis S., Valiquete G., Jacob, H.-L. (1995): Crystalline Graphite Deposits, Classification and Economic Potential, Lachute-Hull-Mont Laurier Area, Quebec; in *Proceedings, 28th Forum on the Geology of Industrial Minerals, Martinsburg, West Virginia, May 3-8, 1992, pages 167-174.*
- Simandl, G.J. (1992): Graphite deposits in the Gatineau Area, Quebec; Unpublished Ph.D. Thesis, Ecole Polytechnique de Montreal, Montreal; (in French), 383 pages.
- Soman, K. Lobzova, R.V. and Sivadas, K.M. (1986): Geology, Genetic Types, and Origin of Graphite in South Kerala, India; *Economic Geology*, volume 81, pages 997-1002.
- Suthphin, D.M. (1991): Descriptive Model of Graphite Veins; in *Open File Report 91-11A, United States Geological Survey, pages 52-54.*

Draft# 3a December 15, 1997





British Columbia Geological Survey  
Geological Fieldwork 1997

## Industrial Minerals

# BLUE BERYL / AQUAMARINE OCCURRENCES IN THE HORSERANCH RANGE, NORTH CENTRAL BRITISH COLUMBIA (NTS 104P07, 10)

By G.J. Simandl<sup>1</sup>, G. Payie<sup>2</sup> and B. Wilson<sup>3</sup>

<sup>1</sup> B.C. Geological Survey and School of Earth and Ocean Sciences at University of Victoria, Victoria, British Columbia

<sup>2</sup> B.C. Geological Survey, Victoria, British Columbia

<sup>3</sup> Alpine Gems, Kingston, Ontario

## INTRODUCTION

This paper describes part of a reconnaissance study carried out on the MRX and Harvey Lake prospects in the Horseranch Range of north-central British Columbia. The main objective of this study was to test the potential of the area to host emerald or other gem-quality beryl deposits. The prospects are located about 70 and 85 kilometres southeast of Watson Lake, Yukon (Figure 1) and are accessible by helicopter.

Beryllium was first detected by the British Columbia Department of Mines in 1949, in the area called the MRX prospect and previously referred to as Cassiar Beryl (MINFILE # 104P 024). The first beryl crystals were discovered by prospector Einar Hagen in 1953; numerous beryl-bearing pegmatite blocks were found in talus by Holland (1956). The prospects now belong to Esmeralda Exploration International Inc. and were staked to cover ultramafic rocks described by Gabrielse (1963) and Plint (1991). The six pale-blue beryl occurrences in the Harvey Lake area described in this paper represent new discoveries.

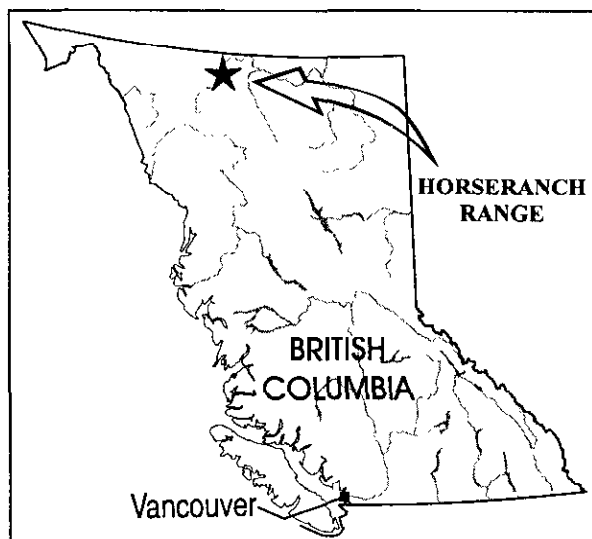


Figure 1. Location of Harvey Lake and MRX properties, Horseranch Range, north-central British Columbia.

Gem-quality beryl ( $\text{Be}_3\text{Al}_2\text{Si}_6\text{O}_{18}$ ) designations according to colour are aquamarine (light blue), heliodor (yellow-green), morganite (pink), emerald (green) and red beryl (informally known as bixbite - red). Emerald is a highly-prized, grass-green coloured variety of beryl. Only red beryl from Utah is more valuable than emerald. The green colour is caused by the substitution of trace amounts of chromium and/or vanadium for aluminum, nevertheless, only chromium-coloured, gem-quality beryls are universally accepted as emeralds. In nature, the coexistence of beryllium with chromium is not common.

Emerald mineralization is known to occur in "Colombia-type" shale hosted deposits, pegmatites and "schist-hosted" ultramafic or mafic rock hosted deposits (Simandl and Hancock, 1996). The Horseranch Range is worth investigating for either pegmatite- or schist-hosted emerald mineralization. In this area, ultramafic rocks (potential sources of chromium) are closely associated with granitic rocks or pegmatites (potential sources of beryllium).

## GEOLOGICAL SETTING

The general geology of the Horseranch Range area (Figure 2) is described by Gabrielse (1963, 1985), Plint and Erdmer (1988, 1989) and Plint (1991) and detailed geology is given by Plint (1991). The Horseranch Range is underlain by the Proterozoic and/or Cambrian Ingenika Group, Cambrian Atan Group, Cambrian and Ordovician Kechika Group and Ordovician and Silurian Sandpile Group. The Ingenika Group consists mainly of medium to high-grade schists, quartzites, marbles and minor orthogneiss. The overlying Atan Group consists mainly of quartzite. The Kechika Group is composed mainly of chloritic phyllite and schists and the Sandpile Group of dolostones and dolomitic limestones. Foliation and synchronous early Cretaceous or younger regional metamorphism was followed by mesoscopic to macroscopic, upright folding about northwest and southeast-plunging axes that define the overall structure of the range. Rapid Eocene uplift and cooling occurred during dextral, oblique-slip mylonitization along the western margin of the Range that is believed to be related to regional mid-Cretaceous to Tertiary strike-slip motion

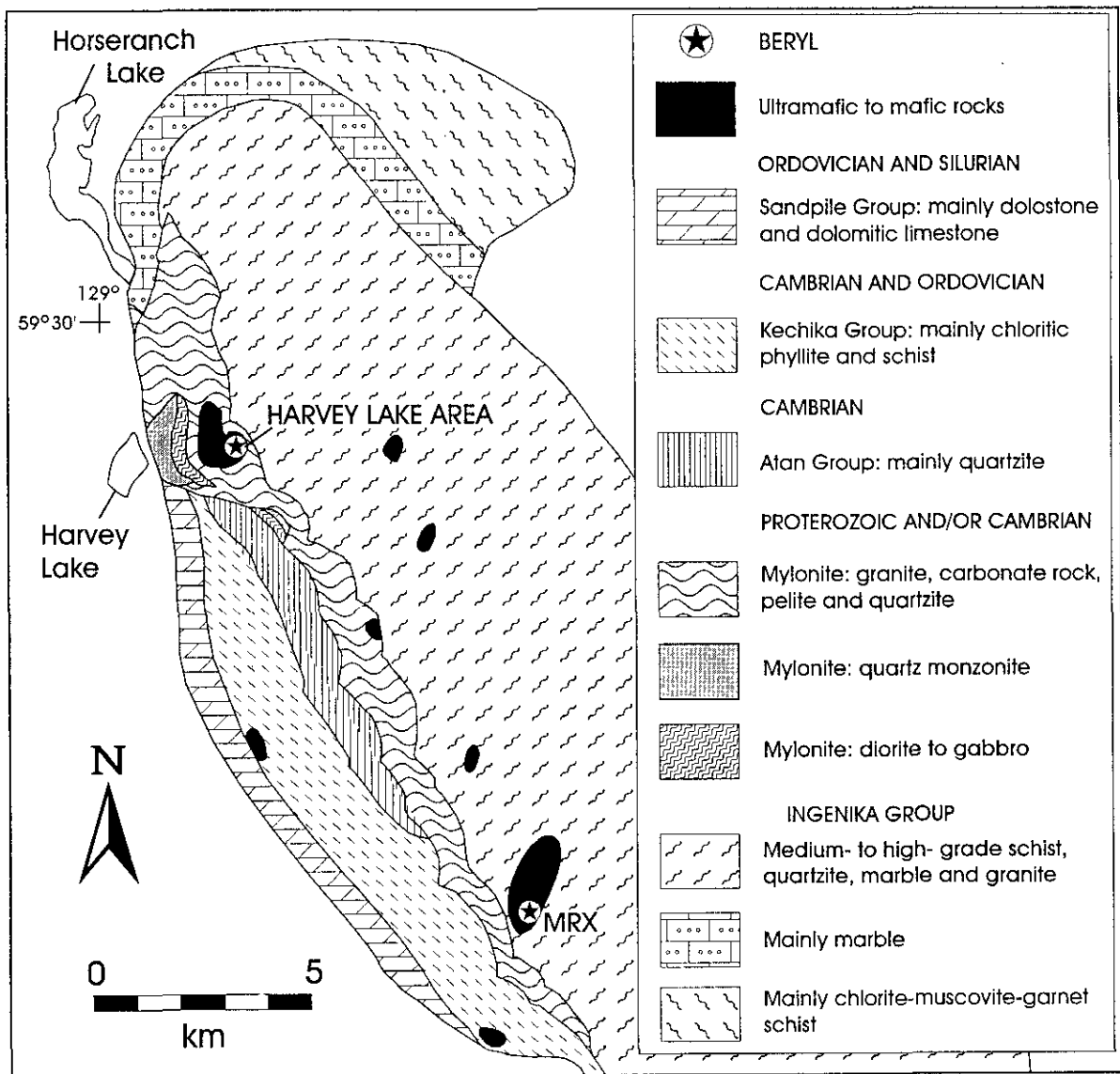


Figure 2. General geology of the northern portion of the Horseranch Range showing the MRX and Harvey Lake properties (modified from Plint, 1991).

along the nearby Kechika fault (Plint, 1991; Plint and Parish, 1994).

The igneous rocks in the Horseranch Range consist of granite dikes, pegmatites and ultramafic and mafic rocks. Granites are dated by U-Pb zircon to be mid-Cretaceous and Eocene age. These granitic dykes occur in the Ingenika Group and Eocene granite is mylonitized in the mylonite zone

Ultramafic and mafic rocks are exposed as undeformed bodies in the Ingenika and Kechika Group and mylonitized to undeformed bodies in the mylonite zone (Plint 1997, personal communication). They are undated but assigned an Eocene age (Plint, 1991) based on

their field relations with the mylonite zone. Plint(1991) reports sharp but ambiguous contacts between granite and the mafic to ultramafic rock in the MRX area. A mylonite zone, trending northwest- southeast, (Figure 2), is interpreted to be a Riedel shear or splay of the mid-Cretaceous dextral slip Ketchika fault. Radiometric and fission tracks record Eocene mylonitization and cooling (Plint, 1991; Plint and Parish, 1994). The field relationships between felsic dikes and mafic and ultramafic rocks in the Harvey Lake and MRX areas, the age of these rocks relative to mylonitization are important criteria for emerald exploration and are discussed below in light of our field observations.

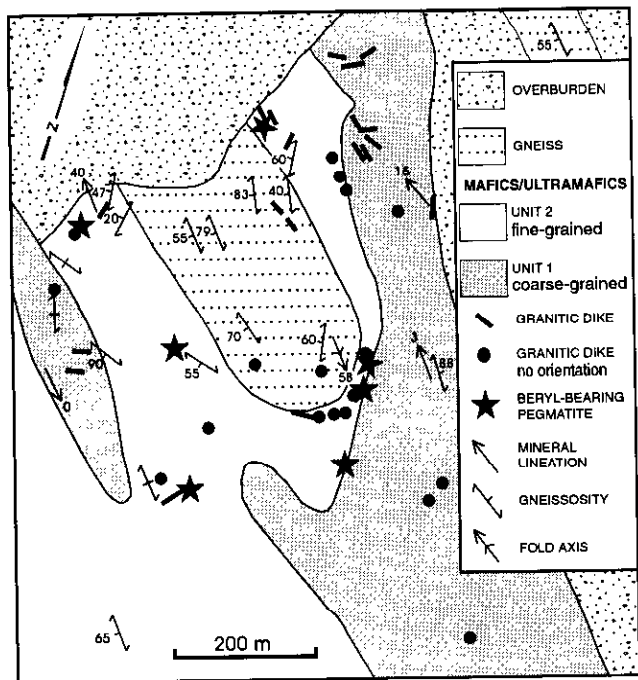


Figure 3. Geological setting of the Harvey Lake beryl showings. Note the distribution and orientation of the pegmatite and granite dikes. For location see Figure 2. For the detailed descriptions of ultramafic and mafic rocks see the text.

## ULTRAMAFIC COMPLEX

The ultramafic and mafic rocks in the Harvey Lake area were briefly described by Gabrielse (1963). Additional outcrops, southeast of Harvey Lake, were discovered during regional mapping by Plint (1991, Figure 2). It is not yet clear, if these rocks are part of a larger igneous complex connected at depth, or if they are slivers of the single body, displaced by tectonic activity. Plint (1991) describes sharp contacts between the mafic rocks and surrounding lithologies. In the Harvey Lake area, the contacts are only rarely exposed. An electromagnetic geophysical survey is scheduled to be released by the Geological Survey of Canada later this year and could be useful to clarify the situation.

Based on 1997 field observations, the Harvey Lake ultramafic/mafic zone (Figure 3) is divided into two units depending on the dominant rock textures. The first unit is a coarse-grained, phenocrystalline, commonly biotite-bearing ultramafic unit with a knobby weathered appearance. The second unit is medium-grained, nearly equigranular and dominantly mafic rock. The contacts between these two units and enclosing lithologies are poorly exposed. Where a contact is exposed, both units are commonly separated from the gneissic rocks by granitic dikes or sills having locally lepidoblastic texture and foliation. No metasomatic or contact metamorphic effects were recognised in the wallrocks adjacent to the complex,

however, this may be masked by the relatively high metamorphic grade of the surrounding lithologies.

The coarse-grained, porphyritic, biotite-bearing, ultramafic unit is weathered surfaces and a knobby appearance caused by resistance characterised by a dark brown or rusty colour on of phenocrysts to weathering. On a fresh surface they are dark green, nearly black or dark brown. The main constituents are clinopyroxene (possibly diopsidic), olivine, biotite/phlogopite, hornblende and orthopyroxene. Biotite, hornblende and clinopyroxene exhibit poikilitic textures and contain rounded olivine grains. Accessory minerals are plagioclase, titanite, apatite, sulphides and oxides. Locally, carbonate (<<0.5%) appears to fill microfractures. The  $\text{Cr}_2\text{O}_3$  content of these rocks attains 0.28 weight percent, indicating that these rocks are indeed a potential source of chromium needed for emerald formation.

The lithologies of the medium-grained unit are beige, green or brown on weathered surfaces and dark green or beige on a freshly broken surface. They have subequigranular and hypidiomorphic texture and consist mainly of feldspar (10 to 60%), pyroxene (<40%), hornblende (<25%), biotite (0 to 10%) and rounded olivine crystals (0 to 25%). Reaction rims separate olivine from plagioclase. The cores of some of the plagioclase crystals are sericitized. Minor constituents are secondary chlorite after biotite and rarely serpentine after pyroxene or olivine. Oxides, sulphides, apatite and titanite generally form less than 1% of the rock.

The rocks of these two units may be classified as amphibolites, olivine mica pyroxenites, olivine pyroxene hornblendites, pyroxene hornblendites, olivine pyroxene gabbros or possibly diorites, depending on the proportions of the mafic minerals and the composition of the feldspars. The mafic and ultramafic rocks of the Harvey Lake and MRX sites, if viewed as a single complex, have similarities with Alaskan-type intrusions, as defined by Taylor (1967) and Nixon *et al.* (1997). Both the rocks of the Horseranch Range and Alaskan-type intrusions contain olivine, member of spinel group, diopsidic (?) clinopyroxene and phlogopite mica in what may be early cumulates. Hornblende, biotite, magnetite and plagioclase dominate in mesocratic units. More detailed petrology and mineral chemistry studies are in progress in order to confirm this Alaskan-type affinity, as first proposed by Plint (1991).

## Pegmatites and Granitic Rocks

Dikes of granitic composition crop out throughout the MRX and Harvey Lake claim groups and were also described elsewhere within the northern half of the Horseranch Range by Plint (1991) and Gabrielse (1963). According to Plint, these dikes commonly cut the main foliation in all units and also the folds in the schist complex. They are also deformed in the mylonite zone.

The pegmatitic and granitic dikes, lenses and pods, in the study areas, are less than 3 metres thick and some of them are interpreted to extend along strike more than a hundred metres. Most of them, however, are less than 1 metre in thickness and outcrop less than 10 metres along

strike. These rocks are white or cream-coloured on a fresh surface and white on weathered surfaces. They weather with a positive relief and crop out along cliff faces or form knob-like features and frost-heaved block-trains in areas with moderate relief. These granitic rocks were observed to crosscut not only schists and marbles, but also mafic/ultramafic rocks. In the MRX area, they are mostly parallel to, or cut foliation at low angle. They were described to occur over an area of 750 metres by 5 kilometres (Holland, 1956). In the Harvey Lake area virtually all our work was concentrated within the ultramafic complex, where the level of rock exposure does not permit to determination of the contact orientations of many of the coarse-grained granite and pegmatite dike. The orientation of dikes (Figure 3) suggest that substantial proportion of dikes trend discordantly to the schistosity and mylonitic foliation. Some of the dikes within mafic rocks have lepidoblastic textures and display C/S ("Cisaillement" / "Schistosité") fabric as defined by Hanmer and Passchier (1991), suggesting that mafic and ultramafic rocks of the area may be older than previously interpreted. Mafic rocks may be more competent than granitic rocks, which are preferentially mylonitized. The tectonic fabric is only rarely observed in mafic rocks. Most contacts between granitic dikes and mafic/ultramafic rocks are sharp and bear no signs of interaction, however there are two exceptions. One of the pegmatites in the MRX area is separated from the mafic host by 1 centimetre thick schistose, biotite-rich zone. An other exception occurs on the Harvey Lake claim group, where in a single outcrop, the contacts of irregular pods and lens of pegmatite rocks within the more differentiated end-members of the mafic-ultramafic suite are diffuse and gradual over 10 to 20 centimetres.

Most of the granitic rocks are relatively homogeneous and fine-grained (1 to 3 millimetres), particularly those with well developed lepidoblastic texture. Granitic and pegmatitic dikes consist mainly of alkali and perthitic feldspars, plagioclase (probably albite), quartz and pale green muscovite. The muscovite may form coarse books up to 5 centimetres in diameter within pegmatites or occur as disseminated flakes in foliated or massive, fine-grained dikes. Minor black tourmaline is widespread within the dikes. It may be microscopic to over 10 centimetres in length and the size of the crystals appears to be in some cases independent of the size of matrix-forming minerals. Large tourmaline crystals are often fractured. Fine-grained, red or brown, euhedral garnet (<2mm) appears to be widespread but not universally present throughout. Where present, it forms less than one percent of the granitic rocks. Locally, in pegmatites, individual garnets may exceed 4 millimetres in diameter. Light-coloured beryls, varying in length from a few millimetres to 7 centimetres, are described below in the section on mineralization. Zircon and apatite are present in trace amounts. Some of the dikes are zoned, in terms of mineralogy, granulometry and textures.

A sketch of a zoned, beryl-bearing dyke from the Harvey Lake area is shown in Figure 4. The central zone of the pegmatite consists of randomly oriented crystals of muscovite (<1 cm, <1%), quartz (<2 cm, <5%), feldspar

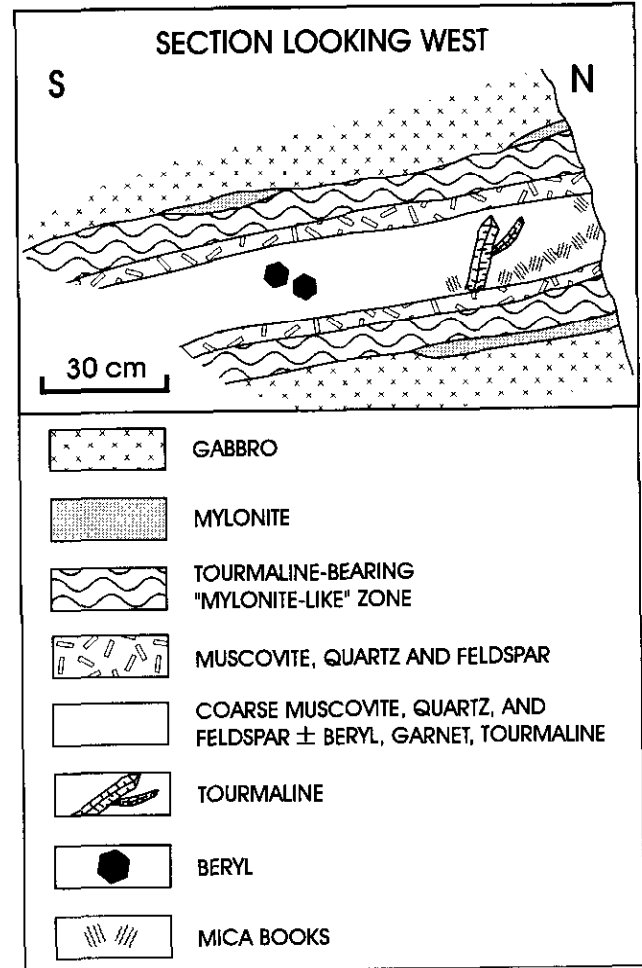


Figure 4. Sketch of a symmetrically zoned, beryl-bearing granite dike, Harvey Lake area. Vertical section looking west.

(3-4 cm, >90%), tourmaline (<15 cm, <5%), beryl (<2 cm, trace), garnet (<0.5 cm, trace). Only the coarsest tourmaline and mica books are shown at scale. The central zone is surrounded by a muscovite (<3 cm, 50%), quartz (<1 cm, 30%) feldspar (<1 cm, 20%) zone with local planar fabric, which is in turn in contact with medium-grained (2 mm) "mylonite-like" tourmaline-bearing and tourmaline-free zones. There is no readily observed planar fabric in the equigranular mafic host rock.

Figure 5 shows a zoned, beryl-bearing pegmatite with a quartz core from the Harvey Lake area, surrounded by a muscovite (<4 cm, 20%) feldspar (<3 cm, 80%), quartz (<8 mm, <10%) zone with traces of garnet (2-8 mm). Beryl was observed in the feldspar-quartz-muscovite zone. C/S fabric developed at the contact between coarse mica and feldspar zones.

Figures 6 shows a number of granitic dikes. The thickest dike has a pegmatitic core (pod). The pegmatite core consists mainly of quartz, feldspar and muscovite books 1 to 10 centimetres in diameter. Tourmaline (<1 cm) and garnet (<2 mm) are present in traces. Granitic dike consists mainly of feldspar (75-85%), quartz (10 -20%), muscovite (<2%) and garnet (<0.5%). One of the few beryl crystal found in an outcrop in the MRX

TABLE 1  
CHEMICAL COMPOSITION OF THE GRANITIC INTRUSIVE ROCKS; MRX (MRX SERIES)  
AND HARVEY LAKE (GS97 SERIES) AREAS.

| SAMPLE |     | MRX-8G | MRX-8E | MRX-8C | GS97-25 | GS97-61 | GS97-63 | GS97-58 | GS97-55 | GS97-57 |
|--------|-----|--------|--------|--------|---------|---------|---------|---------|---------|---------|
| UNITS  |     |        |        |        |         |         |         |         |         |         |
| SiO2   | %   | 74.40  | 74.00  | 74.00  | 73.60   | 76.70   | 75.30   | 76.40   | 75.10   | 75.40   |
| TiO2   | %   | 0.01   | 0.01   | 0.02   | 0.01    | 0.02    | <0.00   | 0.00    | 0.01    | 0.00    |
| Al2O3  | %   | 15.30  | 15.00  | 15.40  | 15.40   | 14.50   | 14.60   | 14.70   | 13.90   | 14.80   |
| Fe2O3  | %   | 0.63   | 1.50   | 0.44   | 0.59    | 0.91    | 0.67    | 1.02    | 0.77    | 0.67    |
| MnO    | %   | 0.09   | 0.51   | <0.01  | 0.06    | 0.07    | 0.17    | 0.15    | 0.11    | 0.05    |
| MgO    | %   | <0.01  | <0.01  | 0.02   | <0.01   | 0.07    | 0.02    | 0.03    | 0.03    | <0.01   |
| CaO    | %   | 1.67   | 0.43   | 3.21   | 0.56    | 0.90    | 0.58    | 0.74    | 0.53    | 0.47    |
| Na2O   | %   | 4.39   | 5.04   | 4.85   | 4.06    | 3.82    | 5.93    | 4.61    | 5.24    | 4.60    |
| K2O    | %   | 3.36   | 3.05   | 1.66   | 5.33    | 2.33    | 2.55    | 1.68    | 3.16    | 3.38    |
| P2O5   | %   | 0.05   | 0.07   | 0.12   | 0.11    | 0.20    | 0.11    | 0.07    | 0.13    | 0.06    |
| Cr2O3  | %   | 0.02   | 0.03   | 0.03   | 0.01    | 0.02    | 0.01    | <0.01   | 0.02    | 0.02    |
| S      | %   | <0.01  | <0.01  | 0.01   | <0.01   | <0.01   | <0.01   | <0.01   | <0.01   | 0.01    |
| LOI    | %   | 0.35   | 0.50   | 0.35   | 0.50    | 0.85    | 0.30    | 0.75    | 0.35    | 0.60    |
| SUM    | %   | 100.30 | 100.20 | 100.20 | 100.30  | 100.50  | 100.30  | 100.20  | 99.40   | 100.10  |
| Li     | ppm | 39.00  | 57.00  | 29.00  | 132.00  | 162.00  | 13.00   | 55.00   | 15.00   | 40.00   |
| Be     | ppm | 17.00  | 118.00 | 164.00 | 26.00   | 206.00  | 30.00   | 36.00   | 150.00  | 21.00   |
| B      | ppm | <10.00 | 138.00 | <10.00 | 132.00  | 767.00  | 141.00  | 593.00  | 670.00  | 197.00  |
| Sc     | ppm | 0.50   | 0.70   | 0.50   | 0.60    | 0.90    | 0.50    | 0.70    | 0.50    | 0.80    |
| V      | ppm | <10.00 | <10.00 | <10.00 | <10.00  | <10.00  | <10.00  | <10.00  | <10.00  | <10.00  |
| Co     | ppm | <1.00  | <1.00  | <1.00  | <1.00   | <1.00   | <1.00   | <1.00   | <1.00   | <1.00   |
| Ni     | ppm | 2.00   | <1.00  | 10.00  | 1.00    | 2.00    | 2.00    | <1.00   | 2.00    | 1.00    |
| Cu     | ppm | <0.50  | <0.50  | 9.30   | <0.50   | <0.50   | <0.50   | <0.50   | 1.60    | <0.50   |
| Zn     | ppm | 11.80  | 26.70  | 8.50   | 20.90   | 47.60   | 16.90   | 41.40   | 34.50   | 25.60   |
| Ge     | ppm | <10.00 | <10.00 | <10.00 | <10.00  | <10.00  | <10.00  | <10.00  | <10.00  | <10.00  |
| As     | ppm | <1.00  | <1.00  | <1.00  | <1.00   | 1.00    | <1.00   | <1.00   | <1.00   | <1.00   |
| Se     | ppm | <3.00  | <3.00  | <3.00  | <3.00   | <3.00   | <3.00   | <3.00   | <3.00   | <3.00   |
| Br     | ppm | 3.00   | 2.00   | 3.00   | 3.00    | 3.00    | 3.00    | 3.00    | 2.00    | 2.00    |
| Rb     | ppm | 273.00 | 364.00 | 105.00 | 403.00  | 383.00  | 294.00  | 290.00  | 361.00  | 454.00  |
| Sr     | ppm | 119.00 | 10.00  | 286.00 | 35.00   | 41.00   | 66.00   | 42.00   | 18.00   | 14.00   |
| Y      | ppm | <2.00  | <2.00  | <2.00  | <2.00   | <2.00   | <2.00   | <2.00   | <2.00   | <2.00   |
| Zr     | ppm | 35.00  | 47.00  | 23.00  | 17.00   | 11.00   | 30.00   | 28.00   | 20.00   | 21.00   |
| Nb     | ppm | 17.00  | 19.00  | 17.00  | 19.00   | 111.00  | 12.00   | 44.00   | 16.00   | 30.00   |
| Mo     | ppm | <1.00  | <1.00  | <1.00  | <1.00   | <1.00   | <1.00   | <1.00   | <1.00   | <1.00   |
| Pd     | ppb | n.d.   | n.d.   | n.d.   | n.d.    | n.d.    | n.d.    | n.d.    | n.d.    | n.d.    |
| Ag     | ppm | <0.20  | <0.20  | 0.20   | <0.20   | <0.20   | <0.20   | <0.20   | <0.20   | <0.20   |
| Cd     | ppm | <1.00  | <1.00  | <1.00  | <1.00   | <1.00   | <1.00   | <1.00   | <1.00   | <1.00   |
| Sn     | ppm | <10.00 | <10.00 | <10.00 | <10.00  | 135.00  | <10.00  | 50.00   | <10.00  | 58.00   |
| Sb     | ppm | <0.20  | 0.20   | <0.20  | 0.30    | 0.80    | <0.20   | 0.60    | 0.90    | 0.80    |
| Cs     | ppm | 9.00   | 12.00  | 7.00   | 20.00   | 36.00   | 7.00    | 21.00   | 32.00   | 32.00   |
| Ba     | ppm | 130.00 | 32.00  | 173.00 | 44.00   | 11.00   | 45.00   | <2.00   | 9.00    | 18.00   |
| Hf     | ppm | 3.00   | 3.00   | 2.00   | 1.00    | 1.00    | 2.00    | 1.00    | 2.00    | 1.00    |
| Ta     | ppm | 6.00   | 4.00   | 27.00  | 8.00    | 52.00   | 1.00    | 17.00   | 9.00    | 9.00    |
| W      | ppm | <3.00  | <3.00  | <3.00  | <3.00   | 5.00    | <3.00   | 3.00    | <3.00   | <3.00   |
| Pt     | ppb | n.d.   | n.d.   | n.d.   | n.d.    | n.d.    | n.d.    | n.d.    | n.d.    | n.d.    |
| Au     | ppb | n.d.   | n.d.   | n.d.   | n.d.    | n.d.    | n.d.    | n.d.    | n.d.    | n.d.    |
| Pb     | ppm | 27.00  | 18.00  | 18.00  | 38.00   | <2.00   | 20.00   | 8.00    | 23.00   | 18.00   |
| Bi     | ppm | <5.00  | <5.00  | <5.00  | <5.00   | 14.00   | <5.00   | 5.00    | <5.00   | <5.00   |
| La     | ppm | 1.70   | 3.80   | 1.30   | 2.90    | 2.40    | 1.10    | 3.10    | 1.20    | 1.70    |
| Ce     | ppm | 3.00   | 8.00   | <3.00  | 5.00    | <3.00   | <3.00   | 6.00    | <3.00   | <3.00   |
| Nd     | ppm | <5.00  | 5.00   | <5.00  | <5.00   | <5.00   | <5.00   | <5.00   | <5.00   | <5.00   |
| Sm     | ppm | 0.50   | 1.30   | 0.40   | 0.60    | 0.30    | 0.40    | 0.40    | 0.30    | 0.30    |
| Eu     | ppm | 0.30   | <0.20  | 0.30   | 0.30    | <0.20   | <0.20   | <0.20   | <0.20   | <0.20   |
| Tb     | ppm | <0.50  | <0.50  | <0.50  | <0.50   | <0.50   | <0.50   | <0.50   | <0.50   | <0.50   |
| Yb     | ppm | 0.40   | 1.20   | <0.20  | 0.70    | 0.20    | 0.80    | 0.90    | 0.40    | 0.40    |
| Lu     | ppm | 0.08   | 0.17   | <0.05  | 0.11    | <0.05   | 0.12    | 0.12    | 0.06    | 0.07    |
| Th     | ppm | 1.00   | 1.00   | <1.00  | 1.00    | 1.00    | <1.00   | 2.00    | <1.00   | 1.00    |
| U      | ppm | 17.50  | 8.90   | 7.80   | 1.20    | 16.30   | 1.30    | 4.70    | 1.20    | 2.50    |

Legend: gn = garnet, mu= muscovite, tm = tourmaline. MRX-8G - granite dike - gn >mu > tm; MRX-8c - pegmatite, local cataclastic texture, gn>mu> tm ; GS97--25 - Pegmatite, local cataclastic texture, mu>tm>gn, sericitization along fractures; GS97-61 - Pegmatite mu>>tm, local cataclastic texture, feldspar sericitized along fractures. GS97-63 - Mylonitized granite dyke, tm>gn>mu, GS97-55 - Granite dike - gn>tm>mu and GS97-57a - Homogenous granitic dike - tm>gn.

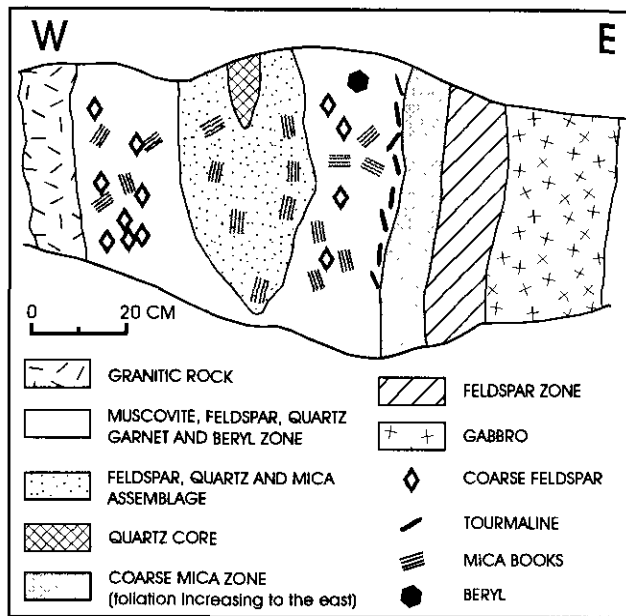


Figure 5. Sketch of a zoned, beryl-bearing pegmatite with quartz core. Vertical section looking west.

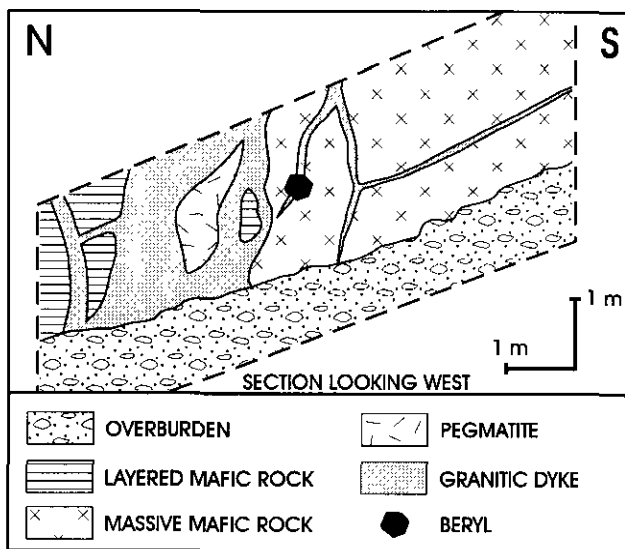


Figure 6. Granitic dike within a pegmatitic pod. One of the few in-situ aquamarine crystal found in the MRX area is within this granitic dike. Vertical section looking west.

area is in the thin granitic dikes (Figure 2). It is glassy, transparent, pale blue-green in color about 8 mm in length. It occurs within a 3 to 4 centimetre thick apophysis of a larger granite dike.

Overall, the internal structure of pegmatites in the Harvey Lake area is more complex than that of those in the MRX area. There are also more in situ beryl occurrences relative to the number of pegmatite and granite dike outcrops in the Harvey Lake area than in the MRX area. These observations suggest a possible zoning within the pegmatite field on the scale of the Horseranch Range.

Representative chemical analyses of the granitic and pegmatitic rocks are given in Table 1. Eight out of the nine dikes analyzed can be referred to as peraluminous and one as subaluminous (Figure 7).

## MINERALIZATION

Most of the beryls in the MRX area, previously described by Holland (1956), were found in the coarse-grained blocks of granite dike and pegmatite in talus slopes of the Camp Creek dike valley that were probably derived from local dikes. Eight of such talus block occurrences and few bluish beryls were found in outcrop during our reconnaissance work in 1997, but only one aquamarine crystal was found in outcrop. This contrasts markedly with the Harvey Lake area where all beryls discovered in 1997 were in outcrops. Both in the MRX and in Harvey Lake areas, pale-blue beryl is irregularly distributed in the granitic and pegmatite lithologies. Beryl was observed in zoned pegmatites, as well as in fine- to medium-grained homogeneous granitic dikes. Beryl crystals are entirely enclosed by hostrock, except where exposed on outcrop surfaces by weathering. No beryl was observed in foliated dikes. Mirolitic cavities, such as those bearing aquamarine-beryl in the famous pegmatite province of Minas Gerais in Brazil, or those bearing emerald as described in the emerald mines of Byrud, Norway (Werner, 1995), were not observed during this reconnaissance study.

Spatial distribution of beryl-bearing granitic dikes within the Harvey Lake area is shown on Figure 3. The beryl is pale blue in colour and mostly translucent, but in several cases crystals are nearly colourless and transparent. The individual crystals vary in size from a few millimetres to several centimetres in length and were not observed to form more than 0.5% of the rock on the outcrop scale. There appears to be no relationship between the colour of the beryl and the distance from a contact with ultramafic rocks. Most of the beryl crystals are translucent to subtranslucent and microfractured. Unlike tourmaline, the microfractures do not appear healed or filled-in. As a result, only small crystals or portions of some larger crystals can be cut as gemstone.

Figure 8 shows three cut stones from the MRX claims. The largest of these gems is 0.94carat. No extensive metasomatic zones, such as those described by Frantz *et al.* (1996) and Martin-Izard (1995, 1996) in the Franqueira alexandrite, emerald and phenakite occurrence in northwestern Spain, were observed in our study areas. This suggests little, or no element exchange between the granitic rocks and ultramafic rocks.

The chemical compositions of the pegmatites and beryl-bearing and beryl-free fine-grained dikes are shown in Table 1. The beryllium (Be) content ranges between 17 and 206 ppm. The latter value corresponds roughly to the minimum concentration required to form beryl in a granitic rock (0.050 weight % BeO) as described by Solodov (1971). However, the beryllium content is too low to be of interest as a source of ore for

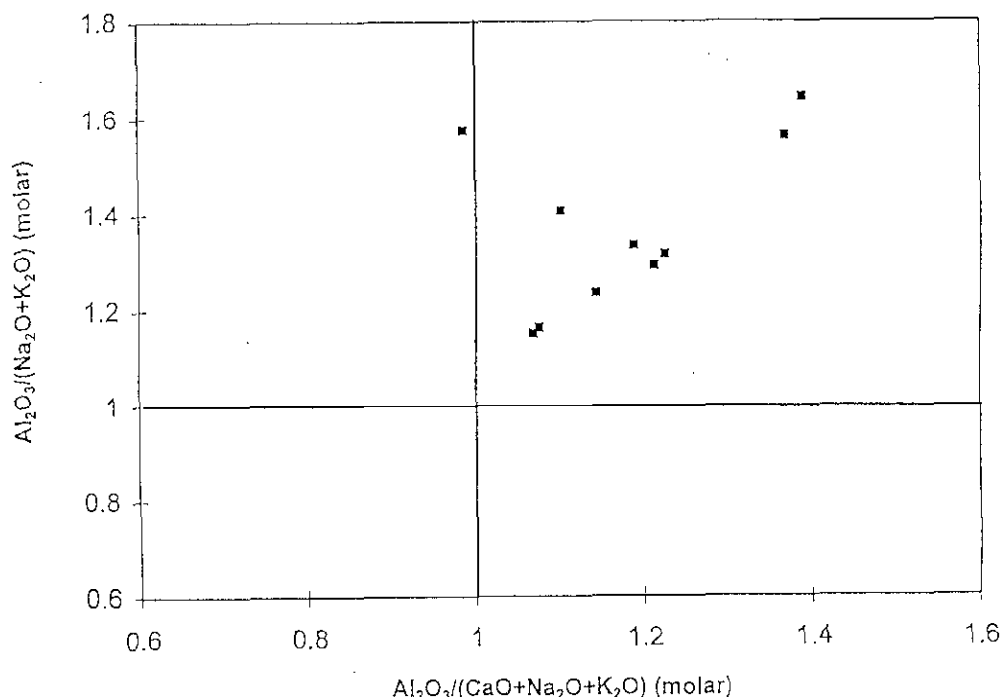


Figure 7. Shand index diagram showing granitic and pegmatitic rocks from MRX and Harvey Lake claims (modified from Maniar and Piccoli, 1980 and Cerny, 1991).

beryllium hydroxide production, which can be subsequently converted to beryllium metal alloys or oxide.

## DISCUSSION

Beryl deposits can be important for gemstones or as sources of beryllium hydroxide. Emerald deposits are known to occur in pegmatites cutting relatively unaltered mafic rocks, such as the Shelby deposit in the United States where emerald-bearing pegmatite is enclosed by olivine gabbro and hornblende gabbro (Sinkankas, 1959). However, most mafic or ultramafic rock-hosted emerald deposits are of the "schist-hosted" variety, where mafic or ultramafic rocks were transformed into talc-chlorite-carbonate schists, chlorite-serpentine-biotite schists, etc. The "schist-hosted" deposits may be associated with suture zones, such as the Pakistan deposits described by Kazmi et al. (1989), and may not be spatially associated with pegmatites.

In the Horseranch Range, the cross-cutting relationships suggest that mafic and ultramafic rocks are older than most of pegmatites and granitic dikes. If both ultramafic and granitic rocks predate or are of the same age as the mylonites, then the possibility exists that suture-related, "schist-hosted" emerald deposits could be present in the area.

Both ultramafic rocks and pegmatites are currently being dated to complement the data of Plint (1991). The

geochemistry, mineral chemistry and petrology in progress will permit the classification of the pegmatites and confirm or reject the hypothesis that the Horseranch ultramafic/mafic rocks belong to an Alaskan-type complex. Such complexes are known to be favourable hosts for platinum group element mineralization and are a source of PGE placers (Nixon *et al.*, 1997).

## SUMMARY

Several granitic dikes and pegmatites with low concentrations of pale blue beryl were discovered in the Harvey Lake and MRX claim area. The number of the beryl-bearing dikes is encouraging. Some of the small crystals are transparent and relatively fracture free. Portions of some of the large crystals could be judged near gem-quality beryl or aquamarine. No accompanying emerald mineralization was discovered. However, the properties were not adequately covered by mapping and prospecting to establish their gem beryl potential. Beryl-bearing pegmatites are not restricted to ultramafic and mafic hosts and more pale blue beryl and aquamarine-bearing pegmatites will probably be discovered in the area. The uniformity in color of the beryl throughout the area suggests that it is less likely that emerald mineralization will be encountered in pegmatites. On the other hand, if the felsic dikes and the ultramafic complex are pre- or syn- mylonitic, then there is a possibility that "suture-related" emerald mineralization will be encountered. There is also a

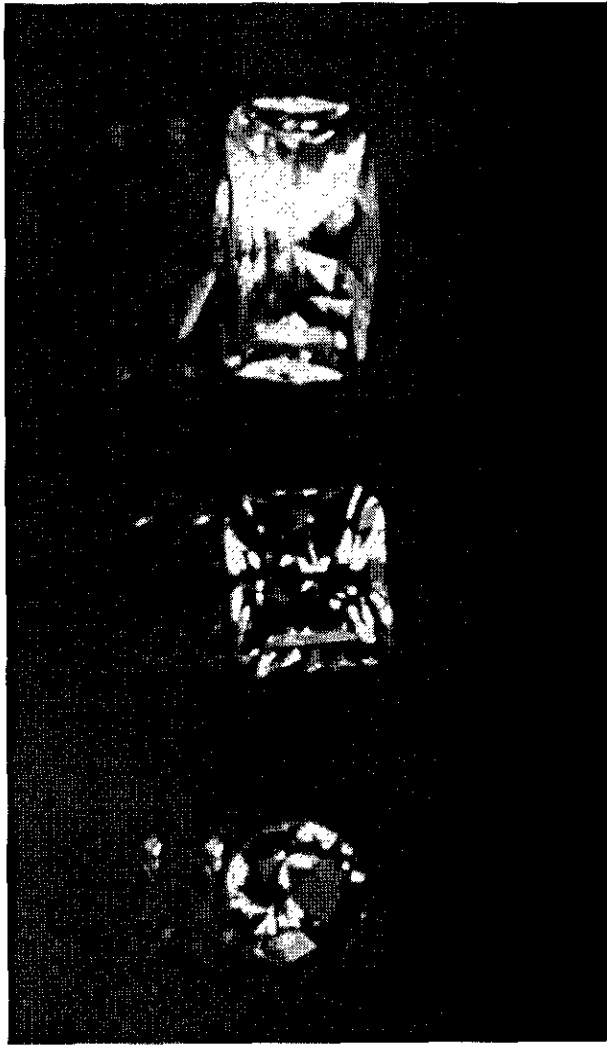


Figure 8. Cut, pale blue beryl gems, from MRX claims cut by B. Wilson. Courtesy of the Esmeralda Exploration International Inc. The largest stone weights 0.94 carat.

geological potential to discover larger beryl-bearing pegmatites that could be looked upon as potential sources of beryllium. The beryllium grades of the 9 samples that were analysed are not economic, and the visually estimated beryllium grades of pegmatites encountered to date also indicate subeconomic grades.

## ACKNOWLEDGEMENT

This study was made possible because of the financial support of Esmeralda Exploration International Inc. and was carried out in collaboration with the School of Earth and Ocean Sciences at the University of Victoria. Field assistance by Jason Tataren is also appreciated. Discussion of ultramafic and mafic lithologies with Dr. Graham Nixon of the B.C. Geological Survey helped to bring this paper to timely

conclusion. The reviews by Dr. Heather Plint of Shear Quality Consulting, Dr. David, V. Lefebvre and Dr. Neil B. Church of B.C. Geological Survey Branch improved substantially the clarity of the paper and are very appreciated.

## REFERENCES

- Cerny, P. (1991): Rare-element Granitic Pegmatites . Part 2: Regional to Global Environments and Petrogenesis: *Geoscience Canada*, Volume 18, pages 68-81.
- Cerny, P. and Simpson, F.M. (1977): The Tanco Pegmatite at Bernic Lake, Manitoba; *Canadian Mineralogist*, Volume 15, pages 489-499.
- Frantz, G., Gilg, H.A., Grundmann, G. and Morteani, G. (1996): Metasomatism at a Granitic Pegmatite - Dunite Contact in Galicia: The Franqueira Occurrence of Chrysoberyl (alexandrite), emerald, and phenakite: Discussion. *Canadian Mineralogist*, Volume 34, pages 1329-1331.
- Gabrielse, H. (1985): Major Dextral Transcurrent Displacements along the Northern Rocky Mountain Trench and related lineaments in north-central British Columbia; *Geological Society of America Bulletin*, Volume 96, pages 1-14.
- Gabrielse, H. (1963): McDame Map-area, Cassiar District, British Columbia; *Geological Survey of Canada*, Memoir 319, 139 pages.
- Hanmer, S. and Passchier, C. (1991): Shear-sense Indicators: A Review; *Geological Survey of Canada*, Paper 90-17, 72 pages.
- Holland, S.S. (1956): Cassiar Beryl; British Columbia; *British Columbia Ministry of Energy, Mines and Petroleum Resources*, Minister of Mines Annual Report - 1955, pages 9-10.
- Kazmi, A.H., Anwar, J. and Hussain, S. (1989): Emerald Deposits of Pakistan; in *Emeralds of Pakistan, Geology, Gemmology and Genesis*, A.H. Kazmi and L.W. Snee, Editors, *Van Nostrand Reinhold Co.*, New York, USA, pages 39-74.
- Maniar, P.D. and Picolli, P.M. (1989): Tectonic Discrimination of Granitoids; *Geological Society of America Bulletin*, Volume 101, pages 635-643.
- Martin-Izard, A., Paniagua A., Moreiras, D., Aceveddo, R.D. and Marcos-Pasqual, C. (1995): Metasomatism at a Granitic Pegmatite - Dunite Contact in Galicia: The Franqueira Occurrence of Chrysoberyl (alexandrite), Emerald, and Phenakite. *Canadian Mineralogist*, Volume 33, pages 775-792.
- Martin-Izard, A., Paniagua A., Moreiras, D., Aceveddo, R.D. and Marcos-Pasqual, C. (1996): Metasomatism at a Granitic Pegmatite - Dunite Contact in Galicia: The Franqueira Occurrence of Chrysoberyl (Alexandrite), Emerald, and Phenakite: Reply; *Canadian Mineralogist*, volume 34, pages 1332-1336.

- Nixon G.T., Hammack, J.L. Ash, C.H., Cabri, L.J. Case, G. Connelly, J.N., Heaman, L.M. Laflamme, J.H.G., Nuttall, C., Paterson, W.P.E. and Wong, R.H. (1997): Geology and Platinum-Group-Element Mineralization of Alaskan-type Ultramafic-mafic Complexes in British Columbia; *British Columbia Ministry of Energy, Mines and Petroleum Resources*, Bulletin 93, 142 pages.
- Plint, H.E. (1991): Metamorphism, Deformation, Uplift and their Tectonic Implications in the Horseranch Range, North-Central British Columbia; Ph.D. Thesis, *University of Alberta*, 266 pages.
- Plint, H.E. and Erdmer, P.(1988): Geological Studies in the Horseranch Range (104P/7,10); in Geological Fieldwork 1987, *British Columbia Ministry of Energy, Mines and Petroleum Resources*, Paper 1988-1, pages 255-260.
- Plint, H.E. and Erdmer, P. (1989):Metamorphism, deformation and Uplift of Proterozoic and Lower Palaeozoic Rocks in the Horseranch Range, North-central British Columbia (102P2,7,10); in Geological Fieldwork 1988, *British Columbia Ministry of Energy, Mines and Petroleum Resources*, Paper 1989-1, pages 347-351.
- Plint, H.E., Erdmer, P., Reynolds, P.H. and Grist, A.M. (1992): Eocene Tectonics in the Omineca Belt, Northern British Columbia, Canada: Field, 40Ar-39Ar, and Fission Track Data from the Horseranch Range; *Geological Society of America Bulletin*, Volume 104, pages 106-116.
- Plint, H.E. and Parrish (1994): U-Pb Geochronometry in the Horseranch Range, Northern Omineca Belt, British Columbia, Canada; *Canadian Journal of Earth Sciences*, Volume 31, pages 341-350.
- Simandl, G.I. and Hancock, K.D. (1996): Sapphires/Rubies, Emeralds, and Precious Opal Deposit Models -Possible Applications to British Columbia, Canada. 99th Annual General Meeting of CIM, Abstract. CIM Bulletin, Volume 90, page 98.
- Sinkankas, J. (1959): Gemstones of North America; *D. Van Nostrand Company Inc.*, Princeton; 75 pages.
- Solodov, N.A. (1971): Scientific Principles of Perspective Evaluation of Rare-Element Pegmatites; Nauka, Moscow (in Russian; cited by Cerny and Simpson, 1977).
- Taylor, H.P. Jr. (1967): The zoned Ultramafic Complexes of Southeastern Alaska; in Ultramafic and Related Rocks, P.J. Wyllie, Editor, *John Willey and Sons Inc.*, New York, pages 97-121.
- Werner, R. (1995): The Emerald Mines of Byrud, Norway. *Mineral News*, Volume 11, No. 6, pages 5 and 10.



## USE OF HEAVY MINERALS IN EXPLORATION FOR SAPPHIRES, EMPRESS Cu-Au-Mo DEPOSIT, BRITISH COLUMBIA

G.J. Simandl, B.C. Geological Survey, P. Jones, Carleton University,  
J.W., Osborne, Westpine Metals Ltd.,  
G. Payie, B.C. Geological Survey and J. McLeod, Cominco Ltd. Laboratory

**KEYWORDS:** Corundum, sapphire, heavy minerals, gold, base metals, exploration methodology.

### INTRODUCTION

One of the most commonly used exploration methods in regional reconnaissance is the sampling of stream sediments. In most cases, stream sediment anomalies are due to mechanical dispersion of metallic or indicator minerals, and to a lesser extent, to transport of metals in solution followed by their precipitation or adsorption on iron oxides and hydroxides, clay particles or organic material. Stream sediment anomalies are generally restricted in extent and decrease rapidly down stream due to dilution by sterile sedimentary particles (Wilhelm and Artignan, 1988). In northern environments, heavy mineral sampling amplifies anomalies that could have been missed using stream sediments. Heavy mineral surveys have become an important component in exploration for base-metals, niobium, tantalum, gold, tin (Fletcher and Loh, 1996), barite, chromite, platinum group elements (Salpeteur and Jezequel, 1992), kimberlite pipes (Fipke, 1989 and Schulze, 1994) and other mineral commodities. This paper describes a heavy-mineral survey over the Empress, a copper-gold-molybdenum porphyry deposit located 225 kilometres north of Vancouver and 50 kilometres northwest of Goldbridge and the Bralorne mining camp (Figure 1). The primary objective of the survey was to determine if corundum mineralization

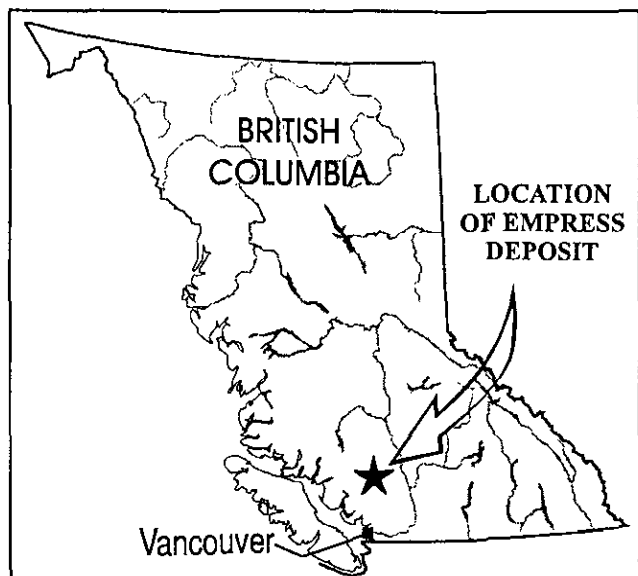


Figure 1. Location of the Empress Cu-Au-Mo deposit with an associated corundum occurrence.

described by Simandl *et al.* (1997) could be detected. A secondary objective was to test for the signature of the porphyry copper-molybdenum-gold deposit described by Osborne and Allen (1995).

Corundum is an alumina-rich mineral ( $Al_2O_3$ ) that may be of variable color due to substitution of metal ions for  $Al^{3+}$ . It is usually gray, blue-gray, brown, yellow, green or colorless. Its gemstones are known by their colors, red for ruby and blue for sapphire. The red colour is linked to  $Cr^{3+}$  content, while blue and green corundum have significant contents of  $Ti^{4+}$ ,  $Fe^{3+}$  and  $Fe^{2+}$  and in some cases  $V^{5+}$ ,  $Co^{2+}$  or  $Ni^{2+}$  (Phillips and Griffen, 1981). Gem-quality corundum was documented in variety of geological settings and lithologies such as dikes and lava flows or intrusive rocks of alkaline affinity; strongly metamorphosed, alumina-rich sediments; partially melted gneisses; desilicated dikes of pegmatitic affinity in contact with marbles and ultramafic rocks (Simandl and Hancock, 1997). Most corundum gemstones are produced from placer or residual deposits derived by weathering and reworking of primary corundum-bearing rocks.

In the Empress deposit area, corundum, in association with andalusite-pyrophyllite rock, was reported in several drill holes (Lambert, 1989, 1991a and b) located south of Taseko River and east of Granite Creek (Figure 4a). A float boulder measuring approximately 15 centimetres in diameter containing coarse corundum was found in a nearby trench in 1990. New concentrations of angular and friable boulders, containing from trace to 1% of coarse corundum (greater than 3 millimetres), were found nearby during our visit to the property in 1996. Because the Empress property is largely overburden covered, the bedrock corundum potential is difficult to assess. However, the overburden contains corundum and should also be assessed as a potential source of sapphire.

A number of corundum occurrences associated with porphyry-type deposits are reported in the literature (Gustafson and Hunt, 1975; Lowder and Dow, 1978; Brimhal, 1977; Wojdak and Sinclair, 1984, and Price, 1986). In most cases, the corundum is either very fine grained or not described in detail. Except for recent studies by Simandl *et al.* (1997), the potential for gem-corundum mineralization in porphyry-type deposits has not been described.

### GEOLOGICAL SETTING

The Empress deposit is located near the eastern margin of the Coast Plutonic Complex in rocks of the Tyaughton basin. The regional geology of the area has been described by Tipper (1978), Glover *et al.* (1986), McLaren and Rouse (1989) and Schiariazza *et al.* (1997).

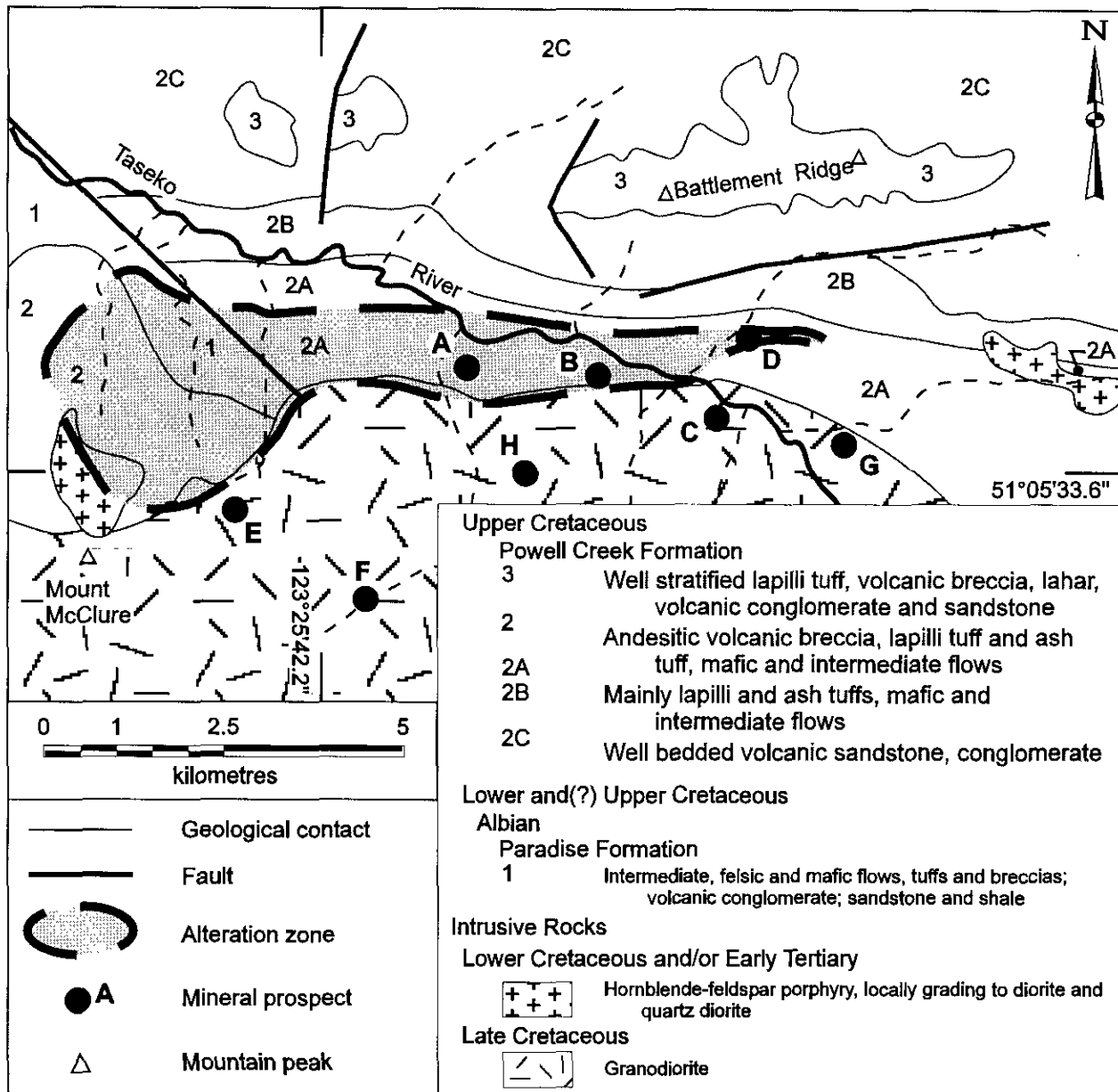


Figure 2. Geological setting of the Empress Cu-Au-Mo deposit (A) with an associated corundum occurrence; modified from Schiariazza *et al.* (1993). Other selected deposits occurring in the area are B - Bur, Minfile # 920- 039, Porphyry (Cu, Mo); C - Buzzer, Minfile # 920-038, Porphyry (Cu, Mo, Au, Ag); D - Taylor Windfall, Minfile # 920-028, Polymetallic vein (Au,Ag); E - Spokane, Minfile # 920-004, Porphyry (Cu, Au, Ag, W); F- Phair, Minfile # 920-029; G- Teek, Minfile # 920-063, (Cu); H - Mohawk, Minfile # 920-001, Porphyry (Cu, Ag, Mo);

Rocks outcropping in the deposit area belong to the Upper Cretaceous Powell Creek and Lower to Upper(?) Cretaceous Paradise formations. The deposit is located within an alteration zone that is 11 kilometres long and up to 3 kilometres wide (Figure 2). There are substantial changes in the nature and intensity of alteration within the outlined zone (McMillan, 1976; Bradford, 1985; Price, 1986). Because of the high degree of alteration of the few available outcrops, the nature of the protolith within the alteration zone in the Empress area is not well established. Large masses of Late Cretaceous granodiorite of the Coast Plutonic Complex outcrop south of the alteration zone. Smaller intrusions (Figure 2) of Early Cretaceous to Early Tertiary age consist of hornblende-feldspar porphyry which locally grades into diorite and quartz diorite.

## DEPOSIT GEOLOGY

The Empress deposit occurs in an area with very little outcrop and nearly all information was acquired from drill core. There are three copper, gold and molybdenum-bearing zones totaling 10 004 000 tonnes grading 0.61 per cent copper and 0.789 grams per tonne gold using cut-off grade of 0.4 per cent copper (Osborne and Allen, 1995). Near surface, the contact between rocks of the Powell Creek Formation and the Late Cretaceous granodiorite is nearly sub-vertical. Drilling indicates that it is sub-horizontal at depth, towards the Taseko River. Westpine Metals Ltd. geologists divide the host rocks into four alteration assemblages and one intrusive unit: quartz rock, quartz-magnetite rock, plagioclase-quartz-pyrophyllite-andalusite rock, quartz-andalusite-pyrophyllite rock and granodiorite-quartz monzonite (Osborne and Allen, 1995). These rock types are the product of hydrothermal alteration of a volcanic or volcanoclastic protolith in a porphyry system (McMillan, 1976). A brief description of these lithological units follows.

Quartz rock (QR) is typically light grey and weathers brown. It consists of quartz grains (90 to 95 per cent), minor quantities of magnetite (1 to 5 per cent) and trace amounts of pyrophyllite, clay, chlorite, carbonate, titanite, pyrite and chalcopyrite. In various areas of the property, Westpine geologists interpret QR as an altered volcanic rock, explaining relict planar textures as banded rhyolite and welded tuff (Lambert, 1988, 1989, 1991a and b).

Quartz magnetite (QM) rock consists mainly of quartz and magnetite with chlorite and hematite as minor constituents. The magnetite content varies from 5 to 70 percent by volume, but typical content varies from 10 to 20 volume percent. The distinction between the QM and QR units is based on the magnetite content.

The plagioclase-quartz-pyrophyllite-andalusite (PQSA) unit consists of several distinct alteration assemblages that are too limited in extent to be treated separately at the current scale. The most characteristic lithology of this unit is relatively coarse-grained (2 to 150 millimetres), cream-colored, grey or white albite-rich, orthoclase-bearing lenses, layers or irregular masses (Hudon *et al.*, 1996). These masses are rarely more than a few metres in apparent thickness in drill core. At surface,

large blocks of this material are several metres across. They are intimately associated with pale green, fine-grained to aphanitic zones consisting mainly of muscovite, pyrophyllite, fine sericite and andalusite-rich areas that are highly irregular in shape. The pyrophyllite-andalusite zones are bluish grey. Corundum, magnetite and chlorite are the most common accessory minerals.

Corundum typically occurs in quartz-free zones within this rock unit. Detailed examination of corundum-bearing rocks indicates that this mineral is found adjacent to a light grey or pinkish, coarse-grained feldspathic rock comprised mainly of albite and strongly zoned orthoclase. Corundum comprises trace amounts to two percent of the rock over widths of 0.6 to 21 metres, with one intersection of 34 metres, most of it within andalusite-pyrophyllite-sericite rock. Usually, corundum occurs within andalusite but a few corundum grains are encased directly in feldspar. The corundum observed in drill core is dark to light blue in color and the grains are commonly less than two millimetres in size. However, blue-black, euhedral crystals up to 3 centimetres in length with hexagonal prism or steep hexagonal dipyrnidal forms, approaching barrel-shaped crystals, occur in surface float overlying the 76 zone. A heavy mineral concentrate of overburden from the 76 zone contains dark-blue corundum and colorless corundum crystals that have commonly light blue patches or blue, hexagonal cores. Petrographic examination of corundum from the host rock indicates that most of the fine-grained crystals are microfractured or contain inclusions of pyrophyllite or diasporite. Some of the coarser crystals have relatively fracture-free zones several millimetres across that may be of gem quality. Individual corundum crystals are separated from the host by pale grey halos, 2 to 5 millimetres wide, that consist mainly of coarse muscovite. Some corundum grains within copper-gold mineralized zones are rimmed by sulphides (Simandl *et al.* 1997), others are zoned.

Quartz-andalusite-pyrophyllite (QAS) rock is equigranular with grains less than 1 millimetre in size to aphanitic. Minor mineral constituents include magnetite, clay, chlorite and gypsum. Weathered surfaces are typically yellow-stained from the weathering of pyrite and fresh surfaces are sugary and grey. This unit does not contain the coarse plagioclase observed in PQSA.

Granodiorite-quartz monzonite weathers buff and is white to bluish on fresh surface. It is medium to coarse grained and equigranular. It consists of feldspar, quartz, hornblende and biotite with minor titanite. This intrusive rock is the footwall to the deposit and forms the southern limit to the deposit.

## Heavy Sediment Sampling and Laboratory Procedure

Sediments from the several active streams draining the deposit area (Figure 2) were sampled. Sample sites were chosen in areas that favoured the deposition of heavy sediments. Naturally concentrated gravel and fines were screened to less than 6 millimetres. The standard volume of sediment sampled equaled 7.0 litres. The samples were washed, removing light minerals and leaving an

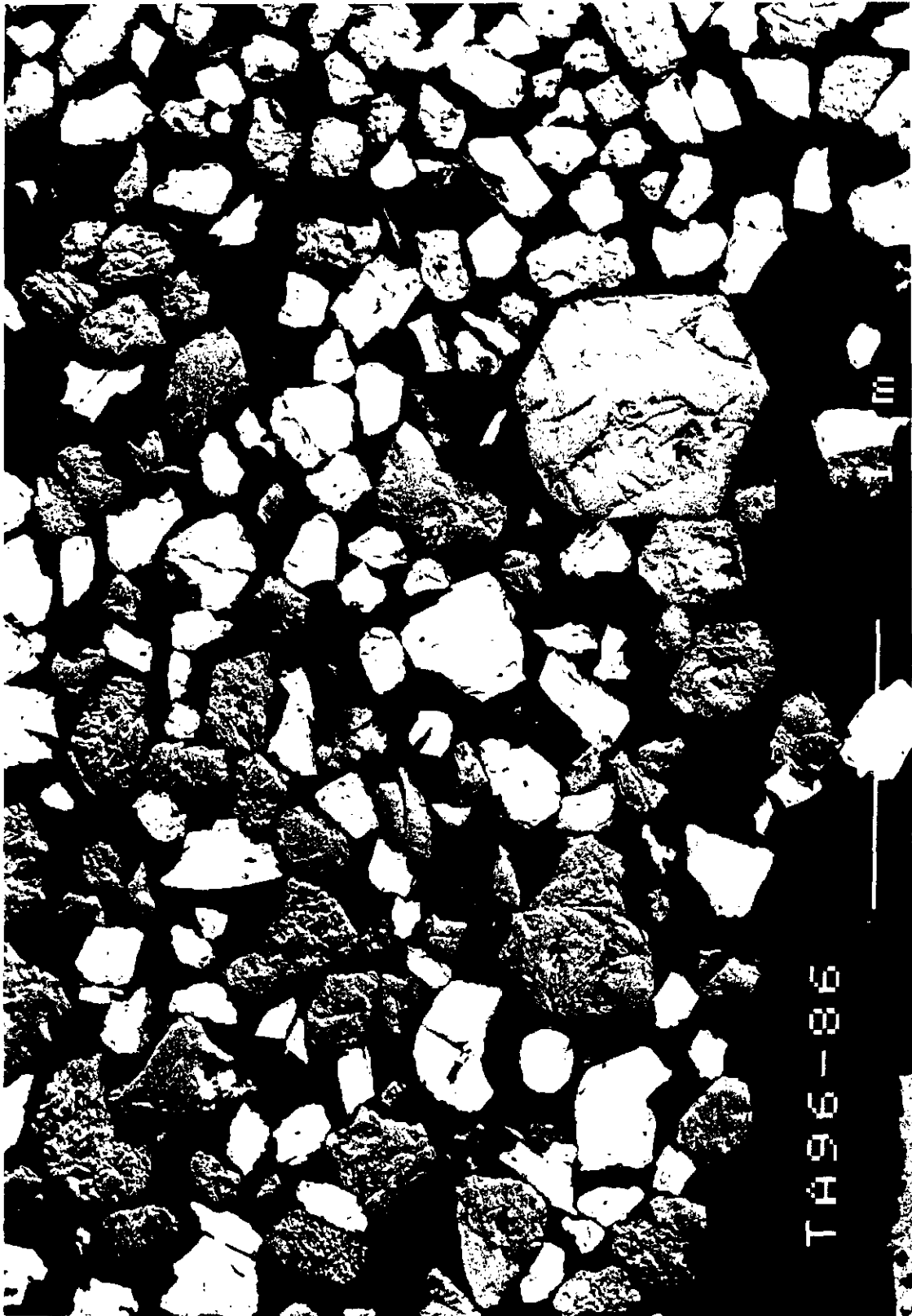


Figure 3: Backscatter microphotograph of the corundum (dark) andrutile (pale) concentrate

enriched heavy sediment concentrate; the size of the samples was reduced to approximately 1/4 of their original volume. This on site pre-concentration was necessary to permit backpacking the samples to camp, as the program was not helicopter-supported.

Samples were dried in an oven and screened into -100 mesh, +100 to -20 mesh and +20 mesh fractions. The finest fraction was analysed for major and trace elements using INA and ICP.

The +100 to -20 mesh fraction was passed through a magnetic separator. Tetrabromethane (TBE) was subsequently used to separate minerals with a density greater than 2.96 g/cm<sup>3</sup> and methylene iodine (MI) was used to separate heavy minerals with density greater than 3.32 g/cm<sup>3</sup>. The heavy liquid methodology used is similar to that described by Muller (1977). The mixture of mineral particles and appropriate heavy liquid is stirred inside a beaker to ensure complete wetting. The minerals with densities greater than heavy liquid (in our case TBE first and then with MI) sink. The float and sink are recovered and washed with acetone and all heavy liquids are recycled. Samples are dried at low temperature for 15 to 20 minutes

The heavy mineral concentrates (the sink from MI heavy liquid separation stage) were examined using a binocular microscope and transparent corundum was identified in 4 samples. Other heavy minerals readily identified include bright red-rutile, sulphides, epidote and magnetite. Selected grains were removed, placed on electrically conductive carbon tape, and coated with a 250 angstrom conductive film of carbon.

The grains were then placed in the vacuum chamber of the scanning electron microscope (SEM) and examined. Identification of smaller grains was made by examining the x-ray spectrum collected from each specimen. Corundum grains were confirmed in a number of samples by this method.

For each heavy element concentrate, a representative aliquot was selected, mixed with epoxy and glued to a standard petrographic glass slide. The epoxy was then cured on a hot plate and the slide ground to a thickness of about 40 microns. A series of polishing stages then followed to produce a polished thin section. These slides were then coated with conductive carbon and viewed in the electron microscope in back-scattered electron (BSE) mode. Minerals with a high mean atomic number reflect back more electrons than minerals with a low atomic number. These variations in brightness (grey-level) are most useful in discriminating between mineral species in polished thin sections. Within the context of this study, corundum appears dark grey when viewed in BSE mode. Rutile, Fe-oxides, and sulphides are much brighter (Figure 3).

In one mode of analysis, a digital image is collected by the X-ray analyser and the electron beam placed upon the grain or grains of interest. An X-ray spectrum is collected and the mineral identified from its spectrum. This combination of BSE imaging and X-ray analysis is effective in mapping a section and determines quantitative proportions of mineral constituents within a given sample.

Specimens were analysed on a JEOL 6400 digital scanning electron microscope interfaced to a Link Systems eXL x-ray analyser equipped with stage automation and digital beam control. Operating conditions were 20 kilovolts accelerating potential and a beam current of 2 nanometres.

A second mode of analysis employed involved automated counting and classification of grains. This included detection of grains from a digital image made by the x-ray analyser and the collection of a x-ray spectrum from each grain. A previously defined elemental window file for elements of interest is employed and the proportion of these elements of the total x-ray spectrum for each grain is determined. A series of criteria for each element as a proportion of the total x-ray spectrum collected are defined, based upon minimum and maximum values expected. A series of criteria for several elements are then used to define a mineral class. In the case of corundum, for example a criterion such as high Al (*e.g.* >70%) may be employed together with other criteria such as low Mg, Zn, and Fe. The additional criteria would block any other Al-bearing phases such as spinels from being incorrectly classed as corundum. The entire operation is controlled by the x-ray analyser computer which is interfaced to the electron microscope. It is a powerful tool for automating repetitive operations previously used to identify mineral grains.

## Results

The stream sediment samples contained between 271 and 1557 grams of non-magnetic heavy fraction in category -20 to + 100 mesh after TBE separation. After MI processing this translated to 1.2 to 40 grams of heavy minerals denser than 3.32 g/cm<sup>3</sup>.

The selected trace element composition of fine-fraction (-100 mesh) not treated by heavy liquids is presented in Table 1. The copper, molybdenum, gold and tungsten values are also displayed on Figures 4a, b, c and d. These results indicate that the metal concentrations in the Empress deposit area are high, and probably the deposit would have been detected using this methodology. Since most of the samples lie in the proximity of the deposit, and within regional-scale alteration zone (Figure 2) no background values are available. The high gold concentrations are particularly interesting, however, corresponding silver values remains below the detection limit. Follow-up work will be carried out to locate gold-bearing grains using the scanning electron microscope. Anomalous concentrations of tungsten are also of interest. Drill core was not analysed for tungsten during exploration of the Empress deposit.

Under the binocular microscope corundum occurs either as, transparent, angular grains that are grey, colorless or bluish, or as white, translucent aggregates of grains with a sugary appearance. Corundum was detected in 17 out of 26 samples (Table 2, Figure 4e) and represents 1-30 per cent of all heavy mineral particles denser than 3.32 g/cm<sup>3</sup>.

TABLE I  
TRACE ELEMENT COMPOSITION OF HEAVY MINERAL CONCENTRATES  
(PARTIALLY CONCENTRATED BY PANNING, NO HEAVY LIQUIDS USED).

| Element         | Au   | 44 As | Ba  | Co   | Cr   | Cs  | Mo   | Sb   | Cu   | Pb   | Ni   | Mn   | Fe*  | Cd   | Bi   | V    |      |
|-----------------|------|-------|-----|------|------|-----|------|------|------|------|------|------|------|------|------|------|------|
| Units           | ppm  | ppm   | ppm | ppm  | ppm  | ppm | ppm  | ppm  | ppm  | ppm  | ppm  | ppm  | %    | ppm  | ppm  | ppm  |      |
| Method          | INA  | INA   | INA | INA  | INA  | INA | INA  | INA  | TICP |      |
| Detection Limit | 2    | 5     | 0.5 | 50   | 1    | 5   | 1    | 1    | 0.1  | 2    | 5    | 2    | 5    | 0.01 | 0.4  | 5    | 2    |
| Field No.       |      |       |     |      |      |     |      |      |      |      |      |      |      |      |      |      |      |
| TA96-1          | 11   | <5    | 24  | 560  | 19   | 180 | 4    | 11   | 3.4  | 89   | 12   | 28   | 758  | 7.61 | <.4  | <5   | 243  |
| TA96-2          | <2   | <5    | 16  | 400  | 20   | 190 | 3    | <1   | 4    | 34   | <5   | 31   | 969  | 11.5 | <.4  | <5   | 422  |
| TA96-3          | 242  | <5    | 86  | 1800 | 21   | 130 | <1   | 15   | 9.2  | 103  | 47   | 28   | 548  | 11.3 | 0.4  | <5   | 294  |
| TA96-4          | 10   | <5    | 41  | 400  | 27   | 640 | <1   | <1   | 4    | 86   | 81   | 32   | 1113 | 12.1 | 2.2  | <5   | 449  |
| TA96-5          | 170  | <5    | 48  | 200  | 27   | 680 | <1   | <1   | 3.6  | 67   | 69   | 34   | 1172 | 15.1 | <.4  | <5   | 562  |
| TA96-8          | <2   | <5    | 30  | 480  | 15   | 260 | 2    | <1   | 2.9  | 78   | 40   | 27   | 941  | 9.24 | <.4  | <5   | 339  |
| TA96-10         | <2   | <5    | 31  | 290  | 17   | 210 | 2    | <1   | 3    | 68   | 38   | 20   | 823  | 5.32 | 0.8  | <5   | 183  |
| TA96-11         | 14   | <5    | 35  | 560  | 20   | 470 | <1   | 4    | 3.4  | 63   | 46   | 28   | 1041 | 12.7 | 0.5  | <5   | 476  |
| TA96-13         | 1360 | <5    | <5  | <50  | 23   | 490 | 3    | <1   | 3.5  | 77   | 60   | 33   | 1111 | 14.3 | 0.8  | <5   | 541  |
| TA96-14         | 1860 | <5    | 9.2 | 490  | 14   | 230 | <1   | 6    | 2.2  | 68   | <5   | 23   | 427  | 8.41 | <.4  | <5   | 335  |
| TA96-15         | 18   | <5    | 13  | 440  | 14   | 120 | 3    | 6    | 1.9  | 128  | 17   | 24   | 461  | 6.42 | <.4  | <5   | 233  |
| TA96-16         | 4850 | <5    | 23  | 600  | 14   | 210 | 3    | 15   | 3.1  | 122  | 18   | 23   | 484  | 7.53 | <.4  | <5   | 288  |
| TA96-17         | 1030 | <5    | 16  | 480  | 9    | 120 | 2    | <1   | 2    | 82   | 20   | 17   | 307  | 5.5  | <.4  | <5   | 249  |
| TA96-18         | 146  | <5    | 19  | 440  | 14   | 300 | 4    | <1   | 3.4  | 46   | 18   | 23   | 701  | 8.47 | <.4  | <5   | 343  |
| TA96-19         | 56   | <5    | 32  | 590  | 18   | 150 | 4    | 3    | 4.6  | 77   | 16   | 20   | 618  | 6.62 | <.4  | <5   | 197  |
| TA96-75         | 460  | <5    | 11  | 730  | 10   | 82  | 5    | <1   | 3.6  | 35   | 21   | 18   | 591  | 5.05 | 1.7  | <5   | 177  |
| TA96-76         | <2   | <5    | 15  | 450  | 13   | 140 | 2    | 9    | 3.1  | 39   | 58   | 20   | 614  | 7.07 | 1.3  | <5   | 277  |
| TA96-77         | 71   | <5    | 17  | 470  | 33   | 360 | 3    | 8    | 2.9  | 65   | <5   | 48   | 594  | 16.8 | <.4  | <5   | 662  |
| TA96-78         | 283  | <5    | 21  | 450  | 56   | 610 | 2    | 22   | 3.4  | 64   | 25   | 71   | 750  | 24.8 | <.4  | <5   | 982  |
| TA96-79         | 11   | <5    | 22  | 670  | 17   | 270 | 5    | 7    | 2.5  | 33   | 11   | 24   | 517  | 9.23 | <.4  | <5   | 348  |
| TA96-80         | 531  | <5    | 21  | 100  | 40   | 620 | 4    | 12   | 3.4  | 63   | 13   | 59   | 771  | 22.3 | 0.9  | <5   | 1004 |
| TA96-81         | 179  | <5    | 44  | 500  | 17   | 210 | 5    | 12   | 7    | 50   | 13   | 31   | 323  | 9.38 | <.4  | <5   | 286  |
| TA96-82         | 1240 | <5    | 35  | 500  | 27   | 480 | 3    | 4    | 10   | 77   | <5   | 47   | 393  | 13.6 | <.4  | <5   | 448  |
| TA96-83         | 307  | <5    | 22  | <87  | 5    | 88  | 5    | <3   | 1.5  | 53   | 7    | 5    | 116  | 42.4 | <.4  | <5   | 120  |
| TA96-84         | 108  | <5    | 37  | 820  | 57   | 480 | 3    | 22   | 4.5  | 97   | 34   | 77   | 693  | 20.8 | <.4  | <5   | 764  |
| TA96-86         | 285  | <5    | 8.2 | 890  | 13   | 330 | 6    | <1   | 4.1  | 209  | 20   | 21   | 291  | 8.03 | <.4  | <5   | 328  |
| Median          | 158  |       | 22  | 480  | 17.5 | 245 | 3    | 4    | 3.4  | 68   | 24   | 27.5 | 616  | 9.31 | 0.2  |      | 337  |
| Mean            | 509  |       | 26  | 515  | 21.5 | 310 | 2.9  | 6.25 | 3.85 | 75.9 | 26.7 | 31.2 | 659  | 12.4 | 0.47 |      | 407  |
| Std.dev         | 1012 |       | 17  | 335  | 12.8 | 188 | 1.61 | 6.7  | 2    | 36.6 | 21.9 | 16.6 | 280  | 8.08 | 0.53 |      | 231  |

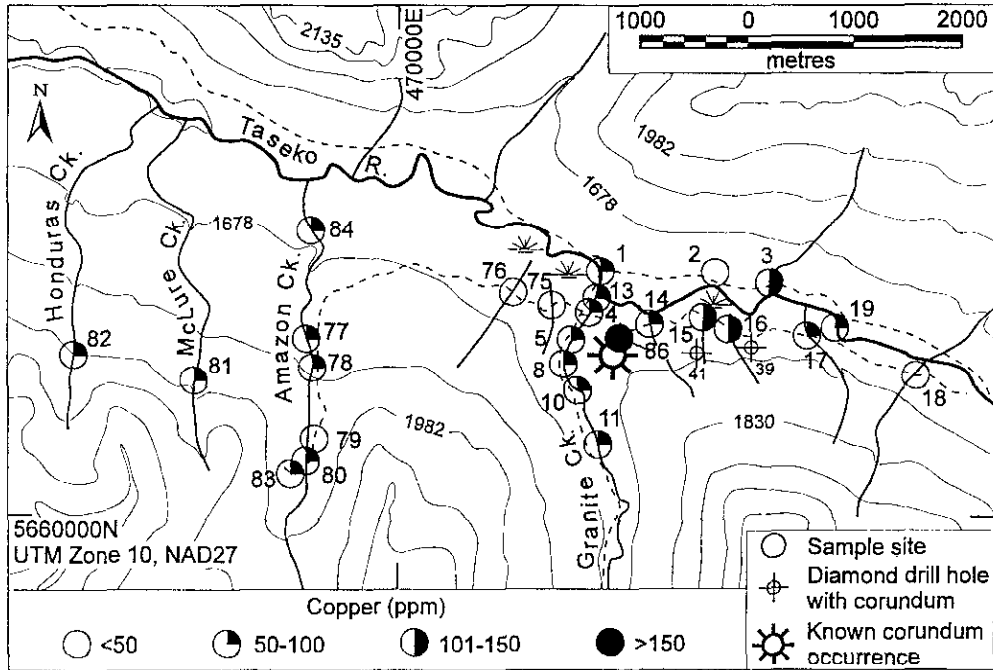


Figure 4a. Copper values in the heavy mineral fraction (-100 mesh size) from the Empress deposit area. Samples concentrated by panning.

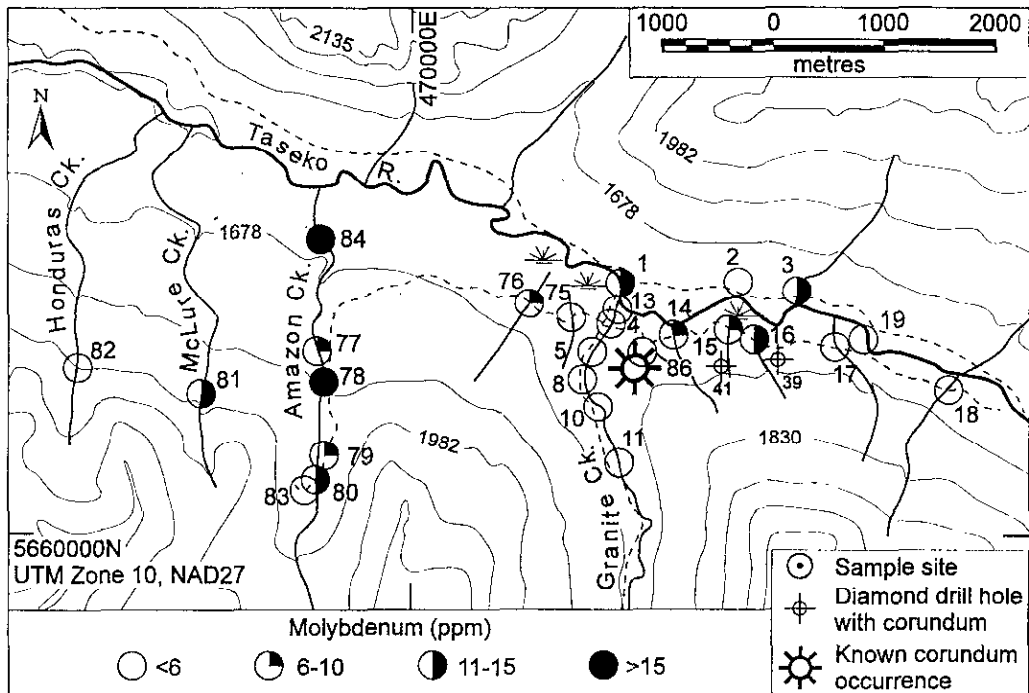


Figure 4b. Molybdenum values in the heavy mineral fraction (-100 mesh) of samples from the Empress deposit area. Samples concentrated by panning.

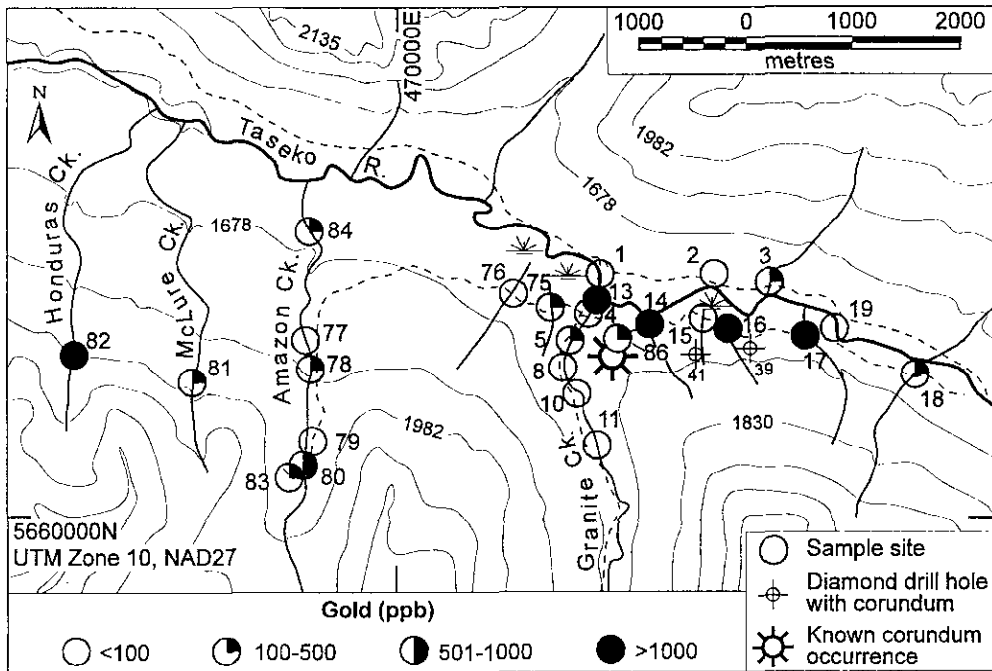


Figure 4c. Gold values in heavy mineral concentrates (-100 mesh grain size) of samples from the Empress deposit area. Samples concentrated by panning.

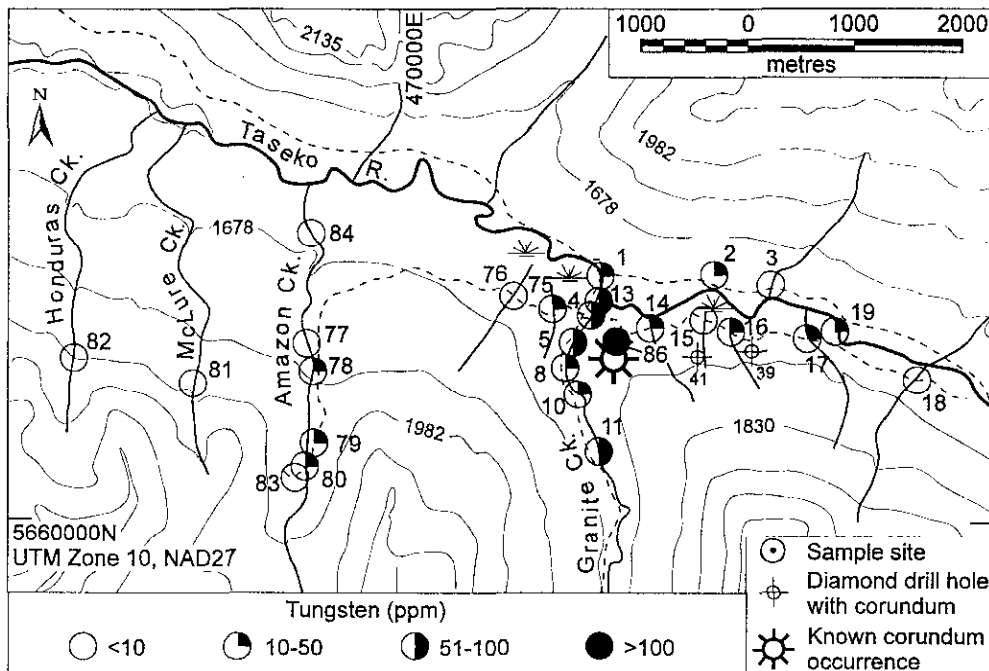


Figure 4d. Distribution of samples analysed for tungsten. Heavy mineral concentrate (-100 mesh fraction) was produced by panning only), Empress deposit area. Samples concentrated by panning.

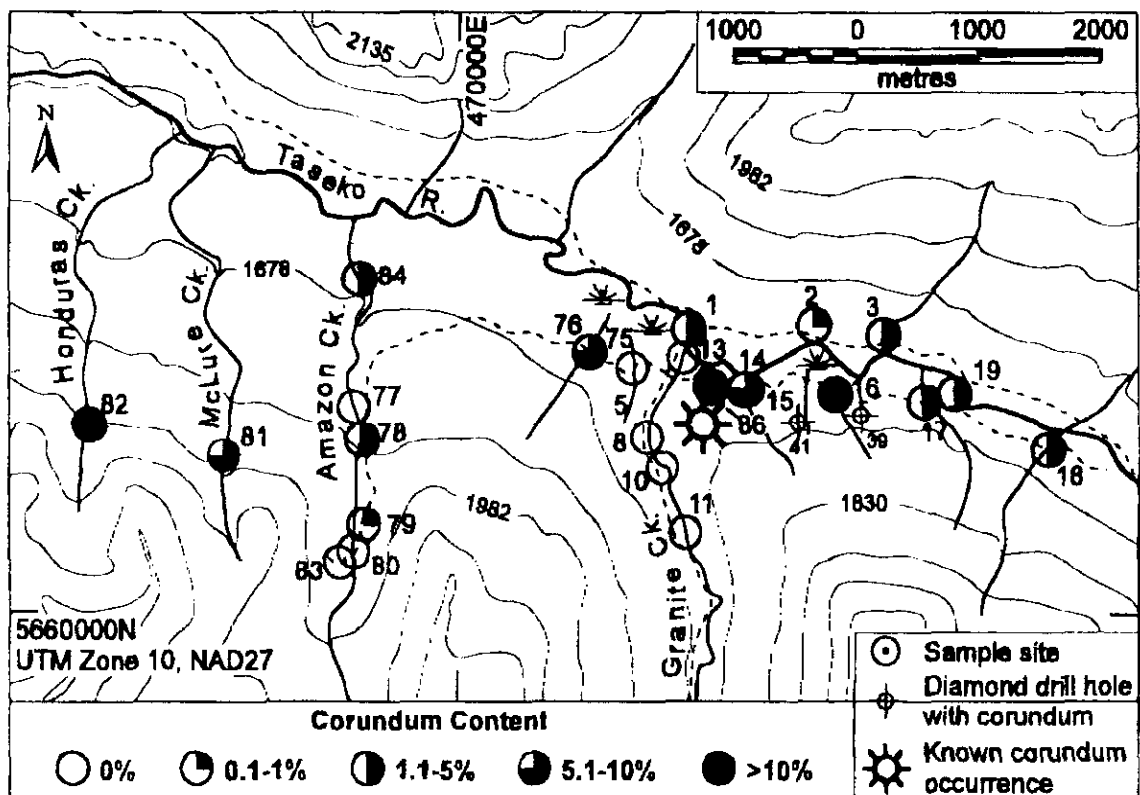


Figure 4e. Distribution of Corundum concentrations (pre-concentration by panning & heavy liquids); Empress deposit area.

Several samples contain a transparent variety of corundum, as colorless, blue or zoned (colorless with blue core) grains. The large number of composite grains and their angular shape indicate that corundum is locally derived.

The other minerals observed are yellowish and light green epidote (0 to 75 per cent), iron oxides other than magnetite (0-100 per cent), pink rutile (0 to 30 per cent), ilmenite (0-17.8 per cent), orthopyroxene (0 to 26 per cent), clinopyroxene (0 to 14 per cent), amphibole (0-7.8 per cent), titanite (0 to 7 per cent), aluminosilicate (0 to 7 per cent; kyanite and andalusite should have been removed during heavy liquid separation), barite (<1 per cent), zircon (0 to 1.8 per cent), allanite (<1 per cent) and unidentified silicate minerals. The variations in the proportion of the heavy minerals over a small area demonstrate the importance of large samples and the need for careful microscopic examination. Minerals that are characteristic of the metalliferous Empress deposit are pyrite, magnetite, chalcopyrite and pink rutile.

Of particular interest is the presence of scheelite detected in samples TA96-4, 10, 11, and 13 and coinciding with above normal tungsten contents in the fine fraction detected by chemical analysis. The sample TA96-82 is anomalous in corundum and gold. This sample was collected from the stream that drains the area of the Spokane porphyry Cu-Au-Ag-W prospect, where corundum was not previously reported.

In summary we can say that analysis of the -100 mesh fraction of panned mineral concentrate using 7 litre samples is adequate to detect corundum mineralization, if a relatively tight sampling pattern is used in the Taseko Lake area. The survey also detected the metallic signature of the Au-Cu-Mo deposit and points to areas where follow-up is warranted. However, larger samples would be necessary if the spacing between the samples was relaxed or if larger catchment areas were involved..

| Sample     | corundum | rutile | ilmenite | Fe oxides | epidote | opx  | opx  | spx  | amphibole | titanite | Al-Silicate | u. silicate | banite | scheelite | zircon | pyrite | allanite |
|------------|----------|--------|----------|-----------|---------|------|------|------|-----------|----------|-------------|-------------|--------|-----------|--------|--------|----------|
| TA96-1     | 2.1      | 3.5    | 7.8      | 21.2      | 47.5    | 2.1  | 1.4  | 1.4  | 1.4       | 1.4      | 5.6         | 0.7         | 2.1    |           |        |        |          |
| TA96-2     | 1        | 5.5    | 15       | 13.5      | 44.4    | 11.1 | 1.6  | 1.6  | 1.6       | 1.6      | 2.4         | 1.6         | 0.8    |           | 0.8    |        |          |
| TA96-3     | 1.5      | 11.6   | 17.8     | 28.7      | 3.8     | 0.7  | 14.7 | 14.7 |           |          | 2.1         | 3.1         | 5.1    | 0.7       |        |        |          |
| TA96-4     | 0.5      | 0.5    | 2.8      | 10.3      | 68.5    |      | 4.7  | 4.7  | 4.2       | 4.2      | 5.1         | 1.4         |        | 0.5       |        |        |          |
| TA96-5     |          | 1.3    | 1.9      | 18        | 60      | 0.6  | 0.6  | 0.6  | 5.1       | 5.1      | 8.4         |             |        |           | 0.6    |        | 0.6      |
| TA96-8     |          |        | 1.4      | 13.4      | 69      | 0.7  |      |      | 4.2       | 4.2      | 8.3         | 0.7         |        |           | 0.7    |        | 0.7      |
| TA96-10    |          |        | 0.5      | 6.3       | 81      | 1.1  |      |      | 5.2       | 5.2      | 3.7         | 0.5         |        | 0.2       | 0.5    |        | 0.5      |
| TA96-11    |          |        | 1.3      | 7.2       | 75.1    | 0.6  | 0.6  | 0.6  | 7.8       | 7.8      | 3.9         | 0.6         |        | 0.3       | 0.6    |        | 1.9      |
| TA96-13    |          |        | 1.6      | 7.7       | 75.2    | 0.5  | 0.8  | 0.8  | 5.5       | 5.5      | 2.2         | 0.5         |        | 0.5       |        |        | 4.4      |
| TA96-14    | 8.6      | 14.4   | 8        | 22.5      | 23.1    | 8.6  | 2.3  | 2.3  | 2         | 2        | 2.3         | 0.6         | 0.6    |           | 0.8    |        | 4.6      |
| TA96-15    | 2.8      | 9.4    | 9.4      | 28.3      | 19.8    | 13.2 | 1.9  | 1.9  | 1.9       | 1.9      | 5.7         | 0.9         | 1.8    |           |        | 4.7    | 0.9      |
| TA96-16    | 32.4     | 14     | 9.6      | 35.1      | 0.8     | 1.7  | 0.8  |      |           |          | 2.6         |             |        |           |        |        |          |
| TA96-17    | 1.8      | 30.9   | 13.6     | 37.2      | 9       | 0.9  |      |      | 0.9       | 0.9      | 2.7         | 2.7         |        |           |        |        | 2.6      |
| TA96-18    | 4.5      | 8.3    | 14.3     | 41.9      | 9.8     | 11.6 | 0.9  |      | 1.8       | 1.8      | 1.3         |             | 1.8    |           | 1.8    |        |          |
| TA96-19    | 1.8      | 3      | 7.9      | 18.3      | 44.5    | 1.2  | 7.3  | 7.3  | 3.6       | 3.6      | 4.3         | 1.2         | 3      | 0.6       |        |        | 4.8      |
| TA96-75    |          | 6.1    | 9.9      | 23.7      | 33.6    | 10.7 |      |      | 0.8       | 0.8      | 6.8         | 0.8         | 1.1    |           | 0.8    |        | 3.4      |
| TA96-76    | 8.3      | 7.6    | 17.4     | 23.5      | 20.4    | 9.8  | 0.7  | 0.7  | 0.7       | 0.7      | 6           | 2.2         |        |           |        |        | 1.5      |
| TA96-77    |          |        | 12.6     | 34.2      | 2.7     |      |      |      |           |          | 6.3         | 4.5         |        |           |        |        | 38.7     |
| TA96-78    | 1.1      | 1.1    | 4.5      | 36.4      |         | 2.2  |      |      |           |          | 3.4         | 2.2         | 0.8    |           |        |        | 48.8     |
| TA96-79    | 0.8      | 6      | 12.8     | 37.6      | 4.3     | 26.5 |      |      |           |          | 6.8         | 0.8         | 1.4    | 0.8       |        |        | 0.8      |
| TA96-80    |          | 25.3   | 6.3      | 32.4      | 2.1     | 0.7  |      |      | 0.7       | 0.7      | 4.9         | 0.7         | 2.4    |           |        |        | 21.8     |
| TA96-81    | 7.9      | 1.4    | 5        | 70.5      |         | 7.2  |      |      |           |          |             | 4.3         | 1.4    | 0.3       |        |        | 0.7      |
| TA96-82    | 11.9     | 11.1   | 8.7      | 50.8      | 3.1     |      |      |      |           |          | 3.9         | 7.1         |        |           |        |        | 2.4      |
| TA96-83    |          |        |          | 100       |         |      |      |      |           |          |             |             |        |           |        |        |          |
| TA96-84    | 2.2      | 4.5    | 6.8      | 18.9      | 5.3     |      |      |      |           |          | 2.3         | 1.5         |        |           |        |        | 57.6     |
| TA96-86    | 37.1     | 51.5   | 1.8      | 0.6       | 0.6     | 0.6  | 0.3  | 0.3  | 0.6       | 0.6      | 1.2         | 2.4         | 0.8    |           |        |        | 1.2      |
| Median     | 2.2      | 6.85   | 7.9      | 23.6      | 20.4    | 1.7  | 1.15 | 1.15 | 1.95      | 1.95     | 3.9         | 1.4         | 1.4    | 0.65      | 0.4    | 0.75   | 3        |
| Mean       | 7.43     | 10.85  | 7.95     | 28.39     | 30.59   | 5.35 | 2.76 | 2.76 | 2.90      | 2.90     | 4.26        | 1.91        | 1.78   | 0.60      | 0.38   | 0.83   | 9.80     |
| Stand Dev. | 10.66    | 12.39  | 5.29     | 21.21     | 28.86   | 6.67 | 3.94 | 3.94 | 2.21      | 2.21     | 2.12        | 1.69        | 1.23   | 0.22      | 0.15   | 0.41   | 16.54    |

Table 2: Mineral composition of heavy mineral concentrates denser than 3.32 g/cm<sup>3</sup>; u. silicate = unknown silicate, opx = orthopyroxene, cpx = clinopyroxene.

## CONCLUSIONS

Fine grains of corundum are present in most of the heavy mineral concentrates from the stream sediments collected in the Empress deposit area. Some of the corundum fragment recovered from the concentrate are transparent and colorless or blue, suggesting potential for gem-quality mineralization.

A next step in the assessment of the gem-corundum potential of the property would require collection and processing of large samples of overburden, with special attention paid to the size, shape and quality of the crystals recovered.

The methodology developed during this study can be used in exploration for gem-quality corundum in the Taseko Lake area and is well worth considering for other regions with appropriate modifications to the minimum size of the samples needed.

The source of the scheelite in the heavy mineral sediments near the Empress deposit, coinciding with the above background tungsten content in the panned samples, remains to be established.

## ACKNOWLEDGEMENT

The manuscript benefited from reviews by Dr. David Lefebvre of the B.C. Geological Survey and Dr. Suzanne Paradis of the Geological Survey of Canada. The SEM work was financed by Westpine Metals Ltd. and carried out at Carleton University, Ottawa. Kirk D. Hancock formerly with B.C. Geological Survey helped in the collection of stream sediment samples and with on site pre-concentration. Heavy liquid separation was carried out by Cominco Ltd. laboratory.

## REFERENCES

- Bradford, J.A. (1985): Geology and Alteration in the Taseko River Area, Southwestern British Columbia; unpublished B.Sc. thesis, *The University of British Columbia*.
- Brimhall, G.H. (1977): Early Fracture-controlled Disseminated Mineralization at Butte, Montana; *Economic Geology*, Volume 72, pages 37-59.
- Fipke, C. (1989): The Development of Advanced Technology to Distinguish between Diamondiferous and Barren Diatremes; *Geological Survey of Canada*, Open File 2124, Part 1, 90 pages.
- Fletcher, W.K. and Loh, C.H. Transport of Cassiterite in a Malaysian Stream: Implications for Geochemical Exploration; *Journal of Geochemical Exploration*, volume 57, pages 9-20.
- Glover, J.K., Schiarizza, P., Umhoefer, P. and Garver, J. (1986): Geology of the Warner Pass Area, British Columbia; *British Columbia Ministry of Energy, Mines and Petroleum Resources*, Open File Map, 1987-3.
- Gustafson, L.B. and Hunt, J.P. (1975): The Porphyry Copper Deposits at El Salvador, Chile; *Economic Geology*, Volume 70, pages 564-579.
- Hudon, P., Simandl, G.J. and Martignole, J. (1996): Corundum from the Empress Deposit, British Columbia, Canada. Abstrast. *GAC/MAC Annual Meeting*, Ottawa, Abstract Volume, page A-70.
- Lambert, E. (1988): Report on the 1988 Exploration Project of the Taseko Property, Alpine Exploration Group; *Alpine Exploration Group*, unpublished company report.
- Lambert, E. (1989): Geochemical and Diamond Drilling Program of the Taseko Property, Westpine Metals Ltd.; *British Columbia Ministry of Energy, Mines and Petroleum Resources*, Assessment Report 19350, 155 pages.
- Lambert, E. (1991a): 1990 Diamond Drilling Program of the Taseko Property, Westpine Metals Ltd.; *British Columbia Ministry of Energy, Mines and Petroleum Resources*, Assessment Report 20889, 206 pages.
- Lambert, E. (1991b): 1991 Diamond Drilling Program of the Taseko Property, Westpine Metals Ltd.; *British Columbia Ministry of Energy, Mines and Petroleum Resources*, Assessment Report 21985, 142 pages.
- Lowder, G.G. and Dow, J.A. (1978): Geology and Exploration for Copper Deposits in North Sulawesi, Indonesia; *Economic Geology*, Volume 73, pages 628-644.
- McLaren, G.P. and Rouse, J.N. (1989): Geology and Mineral Occurrences in the Vicinity of Taseko Lakes; in *Geological Fieldwork 1988*, *British Columbia Ministry of Energy, Mines and Petroleum Resources*, Paper 1989-1, pages 153-158.
- McMillan, W.J. (1976): Granite Creek Property, 92O/3W; in *Geology in British Columbia 1976*, *British Columbia Ministry of Energy, Mines and Petroleum Resources*, pages 67-84.
- Muller, L.D. (1977): Laboratory methods of Mineral Separation; in: J.Zussman editor, *Physical Methods in Determinative Mineralogy*, 2nd ed., *Academic Press*, London, pages 1-34.
- Osborne, W.W. and Allen, D.G. (1995): The Taseko Copper-gold-molybdenum Deposits, Central British Columbia; in *Porphyry Deposits of the Northwest Cordillera of North America*, T.G. Schroeter, Editor, *Canadian Institute of Mining, Metallurgy and Petroleum*, Special Volume 46, pages 441-450.
- Phillips, W.R. and Griffen, D.T. (1981): *Optical Mineralogy*; *W.H. Freeman and Company*, San Francisco, 677 pages.
- Price, G. (1986): Geology and Mineralization, Taylor-Windfall Gold Prospect, British Columbia, Canada; unpublished M.Sc. thesis, *Oregon State University*, 144 pages.

- Salpeteur, I. and Jezequel, J. (1992): Platinum and Palladium Stream-sediment Geochemistry Downstream from PGE-bearing Ultramafics, West Andriamena Area, Madagascar; *Journal of Geochemical Exploration*, volume 43, pages 43-65.
- Simandl, G.J. and Hancock, K.D. (1997): Sapphires/Rubies, Emeralds, and Precious Opal Deposit Models -Possible Applications to British Columbia, Canada. 99th Annual General Meeting of CIM, Abstract. *CIM Bulletin*, Volume 90, page 98.
- Simandl, G.J., Hancock, K.D., Lambert, E., Hudon, P. and Martignole, J. and Osborne, W.W. (1997): The Empress Cu-Au-Mo Deposit- Gemstone and Industrial Mineral Potential in Geological Fieldwork 1996, Lefebure, D., McMillan, W.J. and McArthur, J.G., Editors, *British Columbia Ministry of Employment and Investment*, Paper 1997-1, pages 339-346.
- Schiariazza, P., Glover, J.K., Umhoefer, P.J., Garver, J.I., Handel, D., Rapp, P., Riddell, J.M. and Gaba, R.G. (1993): Geology and Mineral Deposits of the Warner Pass Map Area (92O/3): *British Columbia Ministry of Energy, Mines and Petroleum Resources*, Geoscience Map 1993-10
- Schiariazza P., Gaba, R.G., Glover, J.K., Garver, J.I. and Umhoefer, P.J. (1997): Geology and Mineral Occurrences of the Taseko-Bridge River Area; *British Columbia Ministry of Employment and Investment*, Bulletin 100, 291 pages.
- Schulze, D.J. (1994): An Introduction to the Recognition and Significance of Kimberlite Indicator Minerals; in Kimberlites and their Indicator Minerals; short course notes, Cordilleran Section, Geological Association of Canada.
- Tipper, H.W. (1978): Taseko Lakes (92O) Map Area; *Geological Survey of Canada*, Open File Map 534.
- Wilhelm, E. and Artignan, D. (1988): L'analyse des Minéraux Lourds en Exploration Minière: Revue Critique et Propositions; *Chronique de la Recherche Minière*, Number 490, pages 47-53.
- Wojdak, P.J. and Sinclair, A.J. (1984): Equity Silver Ag-Cu-Au Deposit, Alteration and Fluid Inclusion Studies; *Economic Geology*, Volume 79, pages 969-990.



## FLUIDITY OF WESTERN CANADIAN COALS AND ITS RELATIONSHIP TO OTHER COAL AND COKE PROPERTIES

By Barry Ryan, B.C. Geological Survey  
and  
John Gransden and John Price CETC, CANMET Energy Technology Centre.

**KEYWORDS:** Fluidity, petrography, coke quality, coke textures.

### INTRODUCTION

This paper is intended to provide the reader with an understanding of Gieseler Plastometer measurements of coal fluidity and how they are influenced by other coal properties. It uses data from western Canadian coals and consequently is also a review of the fluidity of western Canadian coals (WCC). The paper introduces some new data but it also makes extensive use of data that are available in scattered and less accessible articles. One of the most important sources for data on Canadian coking coals is the Canadian Carbonization Research Association, which has advanced the understanding of the quality characteristics of WCC to the great benefit of the companies marketing metallurgical coal overseas.

In simply terms there are three types of coal differentiated by rank (maturity): thermal (low-rank steaming coal), bituminous (middle-rank metallurgical coal) and smokeless coal (anthracite rank). The bituminous coals, which cover the rank from high-volatile to low-volatile bituminous, are so called because bitumen can be obtained from them. In fact, the coke making process involves the destructive distillation of bitumen derived from coal as it is heated in a coke oven. The coal goes through a plastic phase in the coke oven as bitumen is distilled out of the coal. As the temperature continues to rise the bitumen is destroyed and the coal is finally annealed into coke at temperatures of over 1000°C. The formation of a plastic or sticky phase is critical to the formation of quality coke. One measure of coal's ability to make quality coke is fluidity is fluidity, a test which measures the rheological properties. test, which measures rheological properties.

The fluidity of bituminous coal samples is important in predicting coke quality but often its importance as one technical parameter for predicting coke quality is overshadowed by its importance as a bargaining chip in the high-stakes game of coal sales. A recent paper (Coin and Broome, 1997) de-emphasizes the importance of fluidity and suggest that its usefulness for predicting coke quality is extremely limited. They point out many problems with the various models that use coal rheology

or petrography to predict coke properties. They suggest that the two most important coal properties are rank and ash chemistry because they correlate strongly with coke strength after reaction (CSR), which they consider to be the most important coke quality parameter.

Intense efforts are underway in countries like Japan to reduce the costs of raw materials. For example, the use of pulverized coal injection (PCI) allows use of weak or soft coking coals in the coke blend to reduce the overall cost of the blend. This means that there is increased emphasis on quality control as it pertains to the coal leaving the mines and the coke made in the coke ovens. Contracts include reference to an increasing number of quality parameters, which are increasingly more rigorously defined.

One can measure the quality of coke by its performance in the blast furnace. This is too late for the coke oven operator to respond to changes in coke quality. It is better to test coke before it gets to the blast furnace. This requires making test coke and establishing tests that duplicate conditions in the blast furnace. The data are reasonably expensive to obtain but provide a good prediction of the performance of coke in the blast furnace. The least costly method is to predict the quality of coke by using data from tests on coal. Fluidity is one of the tests used to predict the quality of the coke and the blending potential of coals used to charge coke ovens.

### COAL RHEOLOGY

Many of the performance characteristics of coke, that are measured by tests on cold rather than hot coke, are heavily influenced by the coal rank and rheology (i.e. dealing with flow and deformation) of the parent coals. Consequently the three tests, described in the next paragraph, that measure the rheological properties of coal, are frequently used to predict coke properties. The coke property most often determined is the resistance of cold coke to abrasion and impact. This property is measured by tumbling sized coke in a drum under fixed conditions and then measuring the amount of material remaining on a screen. There are two frequently used variations of the test. In America the

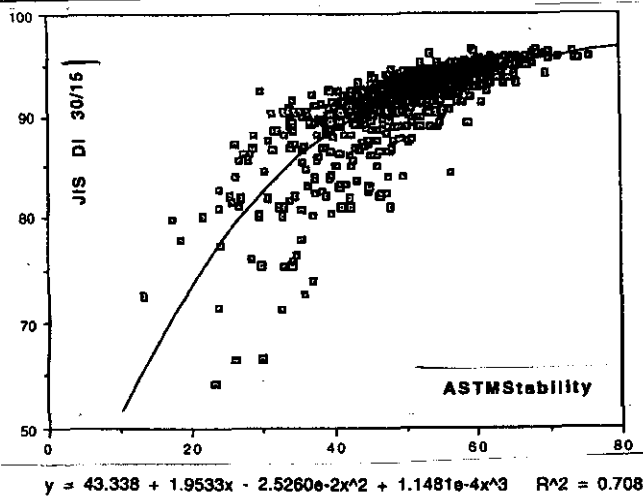


Figure 1: Comparison between ASTM Stability Factor and JIS DIN 30/15 measures of coke quality for a number of Western Canadian coals.

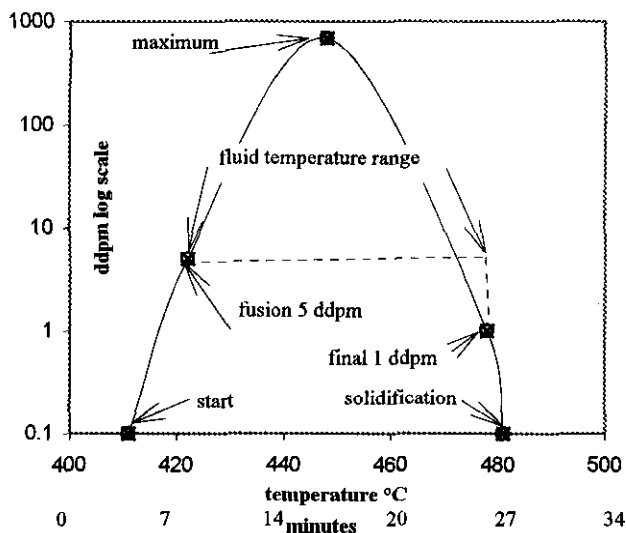


Figure 2: An example of a log fluidity ddpm versus temperature plot for data obtained from a Gieseler Plastometer.

Stability Factor (ASTM test) is measured while in Japan the JIS din 30/15 drum test is performed. Results for the two tests are compared in Figure 1; it is useful to be able to convert from the Japanese index to the ASTM index. Many diagrams exist relating cold coke tests to various coal properties. Because the two tests involve slightly different procedures there is no exact relationship between the tests as indicated by the data scatter in Figure 1.

The three tests that measure rheological properties are FSI, dilatation and fluidity. The FSI test is the oldest and most universal, though its usefulness is limited because there are only 20 possible increments to the range of FSI values. In some countries FSI is referred to as CSN (crucible swelling number). In Europe the dilatometer test, in which a small pencil of coal powder is heated through a contraction and expansion phase, is preferred as a measure of coal rheology. In North America the Gieseler Plastometer is

more widely used. In this test a sample is slowly heated and measurements made of its fluidity (viscosity) at elevated temperatures.

The most extensive investigation of the rheological properties of western Canadian coals is by Price and Gransden (1987). It indicates that dilatation is the least accurate way of predicting cold coke strengths followed by fluidity and then FSI. This means that as long as a sample has good FSI there is a good chance it will make acceptable coke. If the dilatation is low, fluidity and FSI measurements should be made to see if they contradict the initial prediction of poor coke quality.

### SIGNIFICANCE OF MAXIMUM FLUIDITY AND FLUID TEMPERATURE RANGE MEASUREMENTS USING A GIESELER PLASTOMETER

Fluidity is measured using the Gieseler Plastometer (Figure 2), which documents the changing fluidity of a coal sample in air as it is heated at a constant rate of 2° to 3°C/minute through its softening and melting temperature. The sample is 5 grams of coal crushed and screened to pass 35 mesh (0.5 mm) and loosely compacted. The heating rate is similar to that employed in commercial coke ovens. The temperature range extends from about 350°C to 550°C. The maximum fluidity is recorded as are the temperatures at which the coal reaches maximum fluidity, first starts to soften, and finally solidifies. The difference between the last two temperatures is the fluid temperature range (FTR). The fluidity is measured using a paddle, under constant torque. The paddle is inserted in the sample and as it softens the paddle starts to rotate, rotating faster as the sample becomes more fluid. Eventually at high temperatures the coal sample hardens and the paddle stops rotating. The speed of rotation is measured in dial divisions per minute (ddpm). There are 100 divisions per revolution, consequently a fluidity of 100 ddpm corresponds to a speed of 1 revolution per minute of the paddle. Most instruments can not record a rotation of more than 280 revolutions per minute, therefore, fluidities above 28 000 can not be measured and measurements over 10 000 probably are not reproducible.

Measurements of maximum fluidity (MF) and FTR are used to predict the behaviour of the plastic phase during coking. The property of "fluidity" measured by a spinning paddle is not completely analogous to the properties of softening, sticking, smearing and binding, that in loose terms describe what is happening in a coke oven. Based on the heating rate of about 3°C/minute coal is plastic for about 10 to 30 minutes (bottom scale in Figure 2) in the plastometer or in the coke oven. If the maximum fluidity is 300 ddpm, which is above average for most British Columbian coals, then the paddle is turning once in 20 seconds. Considering these conditions one can envisage a transitory phase in which the reactive macerals become soft, sticky and swell as

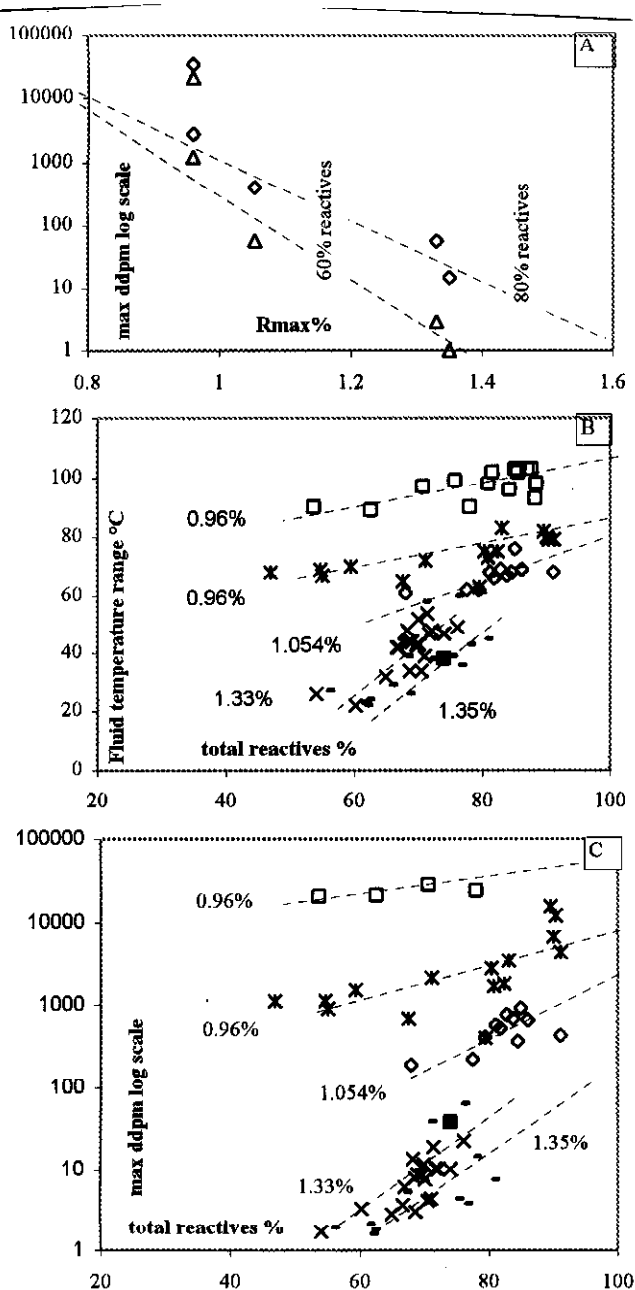


Figure 3: (a) Relationship of maximum fluidity to rank at constant total reactivity content. Data are plotted for sample suites containing 80% and 60% total reactivity and for ranks from 0.96% to 1.35%. (b) Variation of fluid temperature range with total reactivity content for coals of different rank; (c) Variation of maximum fluidity with total reactivity content for coals of different rank; Data from Canadian coals; open square and star Rmax=0.96%, diamond 1.054%, cross 1.33% dash 1.35%. The solid square is for a single low-volatile bituminous coal.

vesicles form. This phase forms a front, which moves slowly inwards towards the centre of the coke oven, leaving behind it semicoke heated to temperatures greater than the solidification temperature of the coal. The process is not one in which large volumes of coal become fluid for long durations during coke making.

The MF is an empirical and approximate measure of the minimum viscosity of the sample achieved at a

particular temperature. Unfortunately the instrument sets up shearing forces in viscous coals and in fluid coals forms froth so that the paddle stirring a mixture of coal and gas. Consequently fluidity measurements do not correlate exactly with the true viscosity of the sample and the results for highly fluid coals probably do not correlate well with coke-making processes.

There are many variations of the plastometer but they have not gained wide acceptance and do not provide a basis for comparing coals. For example, there have been attempts in France to use a constant speed variable torque version of the Gieseler Plastometer to overcome some of the problems described above.

The fluidity measurement is an attempt to provide a practical test for comparing the rheology of coals. It is important that coal samples are prepared consistently. Samples are crushed to pass 35 mesh (0.5 mm). This is much finer than the 80% minus 3.35 mm size consist used in commercial coke ovens. The finer size inhibits fluidity, samples would exhibit greater fluidity if crushed to a coarser size consist. The softer nature (higher HGI) and susceptibility to crush to fine size consists are two possible reasons why some WCC exhibit fluidities lower than expected based on rank and petrography. Values of FTR and MF are improved if the heating rate is faster. In fact the FTR can increase by as much as 20°C if the heating rate is increased from 2 °C/min to 5 °C/min (Loison *et al.*, 1988).

In general fluidity is controlled by the relative proportions of plastic components (vitrinite+liptinites) and inert components (inertinite + mineral grains). The plasticity does not survive at higher temperatures because the plastic bitumen loses hydrogen and solidifies into carbon grains that cement the sample. The instrument is therefore providing information on a number of processes.

- Generation of a plastic/fluid component that is mobile enough to move through the mixture of plastic and solid fragments and coat them so that the combination is plastic.
- The temperature range over which the sample remains plastic.
- The maximum fluidity or minimum viscosity obtained.

In the coke-making process the coal must provide a phase that also eventually acts as a cement. A hydrogen-rich material might provide very high fluidity, but after the hydrogen evolves at high temperatures there is not enough carbon cement to stick the inert grains together. For example a mixture of the hydrogen-rich hydrocarbons tar and anthracite, will not make coke. There is therefore an optimum amount of fluidity required by a coal blend to make good coke.

Coin and Broome (1997) suggest a slightly different model for coke formation, in which vitrinites swell and become sticky as the charge is heated. The swelling is caused by the development of pores. The vitrinite grains eventually partially enclose the inert fragments and stick the heterogeneous solid together. This model obviously emphasizes dilatation behaviour

rather than fluidity. There is a strong correlation between the two properties.

## CONTROLS ON MAXIMUM FLUIDITY AND FLUID TEMPERATURE RANGE

Fluidity of coal is controlled by:

- petrography and rank.
- grain size.
- chemistry.
- the amount, grain size and chemistry of ash.
- aging and oxidation.

### Petrography and rank

At constant rank, fluidity increases as the amount of total reactivities increases in a sample (Figure 3c). The rate of increase varies depending on rank, probably influenced by the hydrogen content of the vitrinite. High-volatile coals are characterized by high values of fluidity that are insensitive to changes in petrography. This may in part be due to limited amounts of in medium-volatile coals. Medium to low-volatile coals are characterized by low fluidity values, that are zero at intermediate concentrations of total reactivities and increase rapidly at higher concentrations. The approximate linear relationships of total reactivities to log MF and FTR for Canadian coals is apparent in a number of plots in Figure 3b and 3c. It should be remembered that there is no natural law, which states log MF *versus* total reactivities relationship should be linear and many exponent relationships may give a better empirical relationship. The apparent linear relationship has some very important implications for WCC, which are characterized by major variations in total reactivities within and between seams. An increase in total reactivities from 50% to 60% changes fluidity from 5 to 20 ddpmm whereas the same 10% increase from 70% to 80% reactivities changes the MF from 100 to 700 ddpmm. High-volatile coals will exhibit some fluidity even if they are rich in inertinite where as medium-volatile coals have zero fluidity if total reactivities are below about 45%. This threshold probably rises for low-volatile coals. It is very important to monitor changes in petrography of low fluidity medium-volatile coals, especially when they have high contents of inertinite.

Using the linear relationships in Figure 3c, it is possible to produce a plot of MF *versus* rank for samples with constant total reactivities content (Figure 3a). Apart from the very fluid, low rank coal data, log MF is roughly linearly related to rank of coals with similar total reactivities content. Fluidity is therefore a measure of the combined effect of petrography and rank. If a version of Figure 3a was constructed containing more tracts of coals with similar reactivities contents but varying rank, then it would be possible to estimate the fluidity of any coal. It is not clear if Figure 3a will work for a blend of samples of different rank.

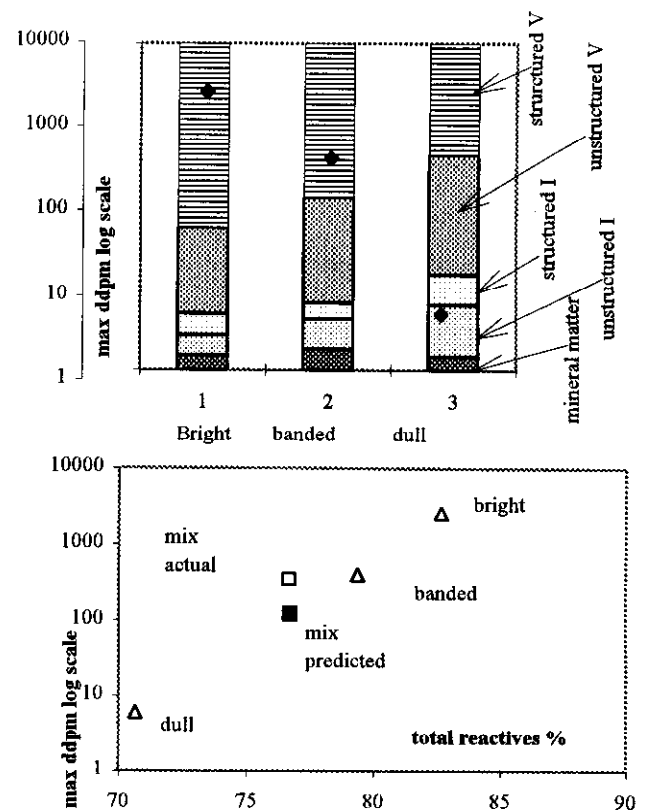


Figure 4: Maximum fluidity and petrography of bright, banded and dull lithotypes of a single medium-volatile seam. Solid diamonds are maximum fluidity of lithotypes; V = vitrinite, I=inertinite.

Three samples of a single high-volatile seam ( $R_{max} = 1.03\%$ ) representing average seam (banded lithotypes), bright lithotype bands and dull lithotype bands were collected. The bright and dull lithotype samples were also combined in equal proportions to make a mixed sample. For these samples the macerals were grouped petrographically into structured vitrinite (tellinite and telocollinite), unstructured vitrinite (desmocollinite and detrovitrinite), structured inertinite (semifusinite and fusinite) and unstructured inertinite (macrinite, inertodetrinite and micrinite). The most striking difference between the bright and dull lithotypes is the increased amount of structured vitrinite in the bright lithotype (Figure 4). The amount of inertinite increases in the dull lithotype. Fluidity is very sensitive to changes in total reactivities, more so than for other high-volatile data suites (Figure 3c). This suggests that it is the larger changes in percent structured vitrinite that are controlling the fluidity and this maceral has the highest fluidity. This may be because the cell structure of tellinite is often filled by other maceral material, such as resinite and liptinite, which have high fluidities. It appears that maximum fluidity is very sensitive to small additions of bright lithotypes, which contain high concentrations of structured vitrinite.

Cameron and Babu (1968) measured fluidity of whole coal and bright lithotype samples from a

Table 1  
Effect of particle size and SG on reactivities/inerts ratio and maximum fluidity of medium-volatile coals

| size mm    | raw(R) or 1.5 fl(F) | ash  | vitrite A | vitrite B | Semifusinite | Fusinite | Total Reactives | total inerts | Volume reactivities | Volume inerts | Volume min matter | predicted ddp <sup>m</sup> * |
|------------|---------------------|------|-----------|-----------|--------------|----------|-----------------|--------------|---------------------|---------------|-------------------|------------------------------|
| 50 x 0.0   | R                   | 22.0 | 52        | 21        | 22           | 5        | 73              | 26           | 66.1                | 23.7          | 10.1              | 53                           |
| 50 x 2.0   | R                   | 18.0 | 47        | 23        | 19           | 10       | 70              | 29           | 64.6                | 27.0          | 8.5               | 39                           |
| 50 x 2.0   | F                   | 9.9  | 31        | 32        | 25           | 12       | 63              | 37           | 60.0                | 35.1          | 4.8               | 17                           |
| 2.0 x 0.6  | R                   | 17.9 | 52        | 21        | 21           | 6        | 73              | 27           | 67.0                | 24.6          | 8.4               | 62                           |
| 2.0 x 0.6  | F                   | 5.9  | 46        | 29        | 19           | 6        | 75              | 25           | 72.8                | 24.3          | 2.9               | 181                          |
| 0.6 x 0.15 | R                   | 14.1 | 55        | 25        | 16           | 3        | 80              | 19           | 75.5                | 17.8          | 6.8               | 299                          |
| 0.6 x 0.15 | F                   | 7.2  | 47        | 35        | 14           | 3        | 81              | 17           | 79.5                | 16.9          | 3.6               | 636                          |
|            | plant               |      |           |           |              |          |                 |              |                     |               |                   |                              |
| 50 x 2.0   | W                   | 9.4  | 25        | 51        | 17           | 6        | 76              | 24           | 72.7                | 22.7          | 4.6               | 180                          |
| 2.0 x 0.6  | W                   | 7.7  | 44        | 26        | 26           | 3        | 70              | 29           | 68.1                | 28.1          | 3.8               | 76                           |
| 0.6 x 0.15 | W                   | 7.3  | 47        | 42        | 6            | 5        | 88              | 12           | 85.2                | 11.2          | 3.6               | 1847                         |

\*log fluidity = 0.081 x TR-3.636

medium-volatile seam. Generally the bright lithotypes had fluidities 2 orders of magnitude higher than the whole coal samples. Coke breeze is added to some coal blends to increase the inert content of the blend and because it is available as a waste product from the coke ovens. Their data illustrate that fluidity is decreased and the FTR shrinks symmetrically about the maximum fluid temperature as the amount of inerts increases.

Fluidity is dependent on rank, which is measured by vitrinite reflectance. But for any coal, vitrinite reflectance measurements produce a range of values. Some grains have higher than average reflectance and others lower. This range of values is composed of the V types also used to calculate the stability index (Schapiro and Gray, 1964). Probably each V type has its own characteristic fluidity with low V types having high MF, large FTR and low  $T_{max}$  temperatures and high V types having low MF, small FTR and high  $T_{max}$  temperatures. It is the mix of V types and the amount of inert material in a sample that control its fluidity. The fluidity characteristics of a particular V type vitrinite may be the same irrespective of whether it is from the upper part of a histogram from a low-rank coal or from the lower part of a histogram from a high-rank coal.

The fluid temperature range (FTR) decreases as rank increases (Figure 3b) and in general has similar relationships to rank and petrography as maximum fluidity. At a rank of medium-volatile, FTR is sensitive to changes in total reactive content whereas at lower ranks it is relatively insensitive. If coke quality is related to FTR, then the coking properties of WCC coals of medium-volatile rank may be susceptible to small changes in petrography or ash contents.

Petrographic composition can vary within a seam and there are a number of papers that document increased inertinite in the upper parts of seams (Lamberson and Bustin, 1997; Ryan, 1997). It can also be influenced by washing as illustrated by Bustin

(1982) who analyzed the petrography of a number of seams from the Fording River coal mine. The samples were subjected to float-sink analysis and individual specific gravity (SG) increments analyzed (Figure 5). The inertinite/reactives ratio on an ash-free basis reaches a maximum at intermediate SG values. Petrography is also influenced by crushing and sizing, which concentrates the inert macerals in the intermediate sizes (Table 1). The fluidity of a sample may be improved if either the intermediate sized material, or the material with SG values in the 1.4 to 1.6 range, is removed.

Fluidity is very sensitive to the amount of exinite in high-volatile coals (Figure 6). Unfortunately exinite is usually destroyed by the time the rank reaches medium to low-volatile bituminous. However for coals with  $R_{max}$  values less than 1.3%, small changes in the amount of exinite may explain unexpected variations in fluidity.

### Grain size

The grain sizes of both the maceral components within the solid coal and the fragments of coal can potentially influence fluidity. No data were located on the relative significance of maceral sizes. Macerals such as tellinite and telocollinite usually occur as large masses where as desmocollinite and detrovitrinite usually occur in small masses. Similarly within the inert macerals, micrinite and inertodetrinite form smaller fragments within the solid coal than macrinite, fusinite and semifusinite. A high proportion of inertodetrinite and low proportion of fusinite plus semifusinite in the inertinite component of a coal significantly increases the surface area of inert material that must be cemented. Changing proportions of macerals can effectively change the relative homogeneity of the coal blend without even considering particle size. The size of the maceral fragments compared to the size of coal fragments

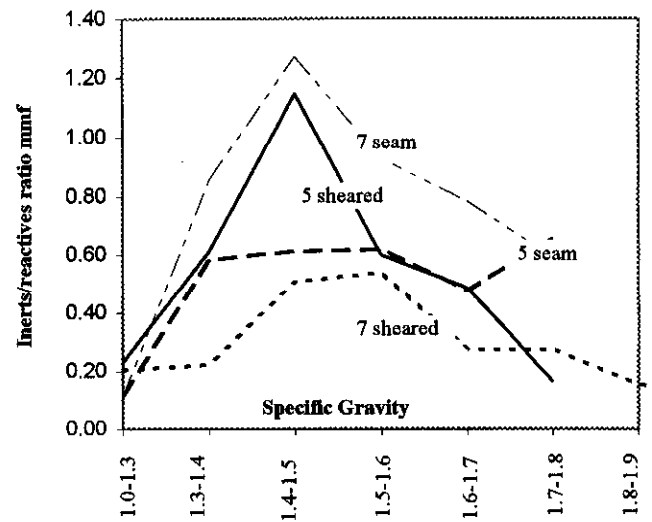


Figure 5: Variation of inerts/reactives ratio for different specific fractions. Data from Bustin (1982).

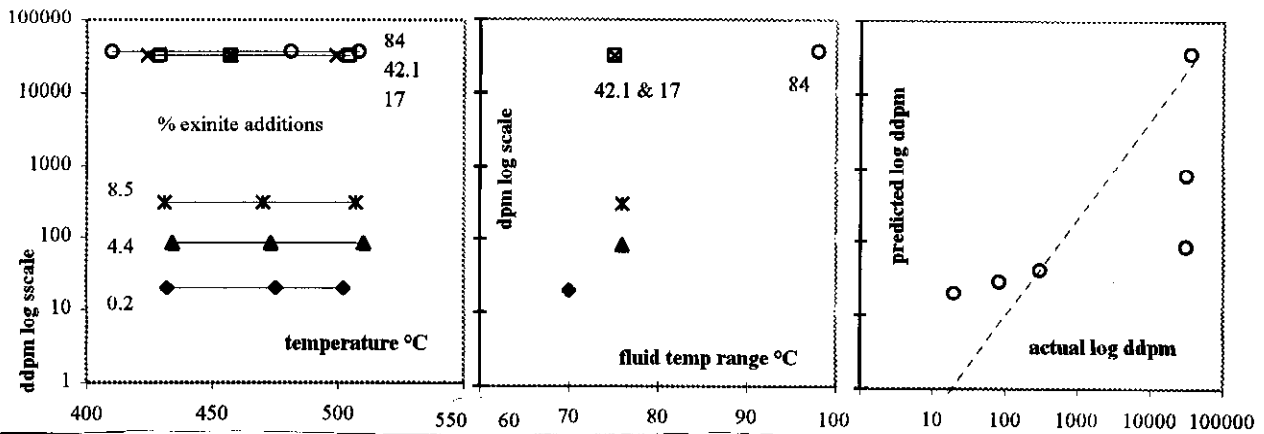


Figure 6: Maximum fluidity and fluid temperature range of blends of a medium-volatile coal and an exinite-rich cannel coal.

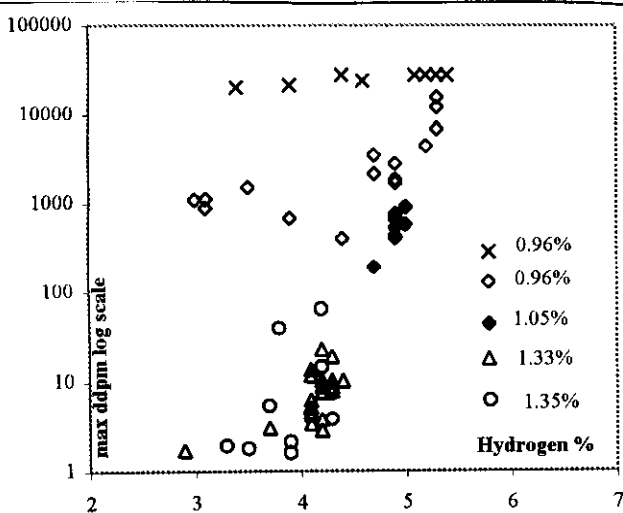


Figure 7: Relationship of hydrogen content to maximum fluidity for Canadian coals of different ranks.

probably plays an important part in aiding or inhibiting the ability of the reactive macerals to coat and cement inert fragments. Possibly the most important factor is the number of coal particles that are composed of a combination of reactive and inert maceral components. These coal particles will have much less difficulty sticking together than coal fragments composed of a single maceral. Crushing to a finer size increases the number of monomaceral coal fragments.

It is also possible that the fine fragment size speeds the distillation process, shrinks the FTR and gives the reactive components less time to coat the inert fragments. Decrease in grain size lowers fluidity and the effect is particularly pronounced in the case of dull coals (Lowry, 1963). There have been a number of studies by the CCRA in which vitrinite-rich coal from the fine circuits of wash plants has been added to the clean single coal product in an attempt to improve coke quality. The results were generally not as good as predicted by petrography, indicating, that for a single coal, fine size may have a negative effect on coal rheology, in particular fluidity and coke strength. However finer size does not lower FSI values, possibly

because of the higher heating rate (Price and Gransden, 1987).

There are data that indicate that crushing blend coals to a finer size-consist improves coke quality (Leeder *et al.*, 1997). It is not clear why this differs from the single coal data. Possible factors influencing coke quality are that these blends were crushed to an overall finer size where as additional fine coal was added to an existing size consist for the single coals. Obviously the average coal fragment separation is influenced by fragment size and size distribution.

## Hydrogen chemistry

Hydrogen is concentrated in the reactive macerals, especially the liptinites, and is less abundant in higher rank coals. Since these are coals with poorer rheology for making coke, it could theoretically provide a good indication of the fluidity of a coal. Fluidity is very sensitive to small changes in hydrogen content in medium-volatile coals but much less sensitive to changes in high-volatile coals (Figure 7). In general the hydrogen content of coals can not be used to predict fluidity or coke properties. Hydrogen can effect fluidity, if it is available to be donated to solvent species (Clemens and Matheson, 1991). The process is similar to what happens when hydrogen is introduced to help liquefy coals.

The relationship of fluidity to the general chemistry and molecular structure of coal is complex. In simple terms as rank increases coal molecules become larger and take on the form of interlocking hexagonal plates (aromatic structures), which inhibit the formation of fluidity in the coal.

## Ash

Ash contents are reported as weight percents but fluidity is probably more dependent on the relative volume of inerts in the sample. An ash content of 10% by weight is equivalent to about 6% by volume. Price and Gransden (1987) studied the effect of ash on a number of rheological and coking properties of WCC. They washed three coals (Rmax 0.91%, 1.32%, and

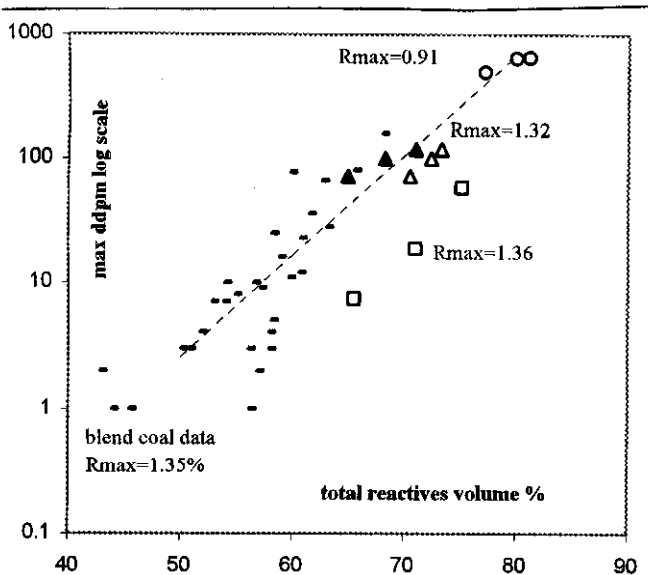


Figure 8: Maximum fluidity *versus* total reactivities for samples washed to different ash concentrations. Dash points with line are from medium-volatile data set. Ash concentrations are plotted on the diagram with the ash contribution to total inerts calculated on a weight percent basis (solid triangles) and volume percent basis (open triangles, circles and squares).

1.36%) to different specific gravities to produce different ash concentrations. Three samples of similar petrography but different ash concentrations were derived from each coal (Figure 8). The medium-volatile data set for the three coals has a similar trend to data for a number of medium-volatile samples if the ash effect is calculated on a volume percent basis, but not if it is calculated on a weight percent basis. This means that, for example, a 5% increase in volume percent inertinites is equivalent to about a 10% increase in weight percent ash; emphasizing the important influence of change in volume of reactive and inert macerals on fluidity.

Experiments indicate that minerals generally act like additional inert material, but for some compounds there also seems to be a chemical influence on fluidity (Price *et al.*, 1992). As little as one percent addition of minerals can cause maximum fluidity to decrease as much as 36%. Quartz and kaolinite caused minor increases in MF where as additions of inert compounds, such as sulphur and  $\text{Fe}_2\text{O}_3$  caused larger decreases in MF. Most of these changes in MF seem large but are similar to expected decreases based on an equivalent 1% increase in inherent ash content (Figure 9).

The mineral additions can effect fluidity in three ways. They increase the total surface area of inerts that must be incorporated into the plastic phase and in this case the size of the grains is very important. The introduced grains may have different surface tension characteristics with respect to the plastic phase. The mineral additions may react chemically with plastic components. It appears that in most cases the mineral additions mimic changes in ash content in a normal sample. The sulphur and  $\text{Fe}_2\text{O}_3$  (magnetite) additions change fluidity much more, probably indicating a

chemical reaction with the plastic components in the coal.

Minerals in the experiments were added as a fine powder and therefore mimicked natural ash occurring as finely dispersed extraneous fragments. Natural ash in washed samples can occur finely disseminated in desmocollinite, filling cells in semifusinite, or as ions forming part of the coal molecules. The mineral matter that is locked in inert coal fragments can have negligible effect on fluidity where as that dispersed in desmocollinite or external to maceral fragments can have a pronounced effect on fluidity. In this regard a sample with calcite filling cells in semifusinite may have a reasonable fluidity, but the calcium oxide will have a devastating effect on CSR at higher temperatures. The way mineral matter is dispersed in the macerals will effect the way it influences MF and other coke properties.

The main effect of mineral addition is to decrease MF and FTR in amounts comparable to normal coal ash with the exception of additions containing sulphur and iron. These substances obviously get involved in chemical reactions, which inhibit MF but do not have an equivalent effect on stability factor. In contrast the 1% additions of some minerals caused major changes in CSR illustrating the ash chemistry control on this property. Obviously fluidity will be a poor indicator of stability factor if there is a chemical reaction between the mineral matter and the plastic components in the coal. This is the case for coals with Fe-rich ash, which lowers fluidity causing an under estimation of stability factor. CSR is even more sensitive to ash chemistry than fluidity, therefore in some cases it will be over estimated if based on fluidity data.

## Aging and oxidation

Fluidity is more sensitive to oxidation than FSI, though when MF values are plotted on a log scale the effects are of the same magnitude as those experienced by FSI values. Pyrite has a moderate effect on fluidity but  $\text{Fe}_2\text{O}_3$  has a major effect (Figure 9). Obviously if pyrite oxidizes, or if magnetite is introduced by heavy medium cleaning, fluidity will be effected. Price *et al.* (1992) measured the deterioration of fluidity over 200 days (Figure 10). Log MF decreased slightly where as stability factor and CSR values were unchanged and FSI values varied from 7.5 to 8.5 with no downward trend. When plotted on an MOF diagram (Figure 10) the changes in fluidity appear insignificant. There has been a lot of emphasis on the rapid deterioration of fluidity as samples oxidize. For many coals, the changes due to oxidation are irrelevant in terms of coke quality. The initial decrease in fluidity may be associated with adsorption of oxygen, which occurs rapidly to all coals when they are brought to surface as a result of mining. This occurs long before they are used for coke making. Fluidity is probably a very sensitive, but expensive, test for oxidation. The alkali extraction test is becoming widely accepted by the coal industry because it is faster and, cheaper.

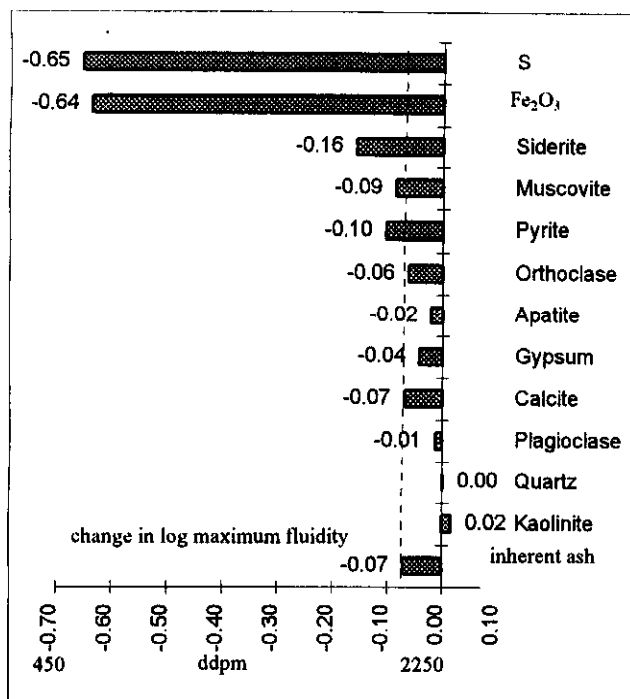


Figure 9: Effect on fluidity of 1% mineral additions to coal samples. Data from Price *et al.* (1992). The vertical line is the decrease in MF expected for a 1% increase in weight percent ash based on the data from Figure 8.

## COAL BLENDS AND THE ADDITIVE PROPERTIES OF FLUIDITY

A number of experiments aimed at calculating the fluidity of coal blends indicate that fluid properties are not additive. It is not possible to derive an average fluidity by calculating the weighted average of log fluidity values of a number of samples. In fact this process nearly always predicts average fluidities that are too low. This can be explained by the fact that fluidity is proportional to VM (daf), which has a non linear relationship to reflectance. Averaging ranks produces an intermediate rank that is higher than would be calculated from the average VM (daf) value for the mixture.

The 50/50 mix of lithotypes (open square, Figure 4) produced a noticeably greater fluidity than predicted (solid square), based on averaging the log fluidity values of samples with identical rank.

One blending experiment looked at the effect of mixing a sample containing 84% exinite (cannel or needle coal from the Elk Formation in south-eastern British Columbia) with a medium-volatile coal containing 0.2% exinite. Addition of small amounts of cannel coal produced major changes in MF that could not be predicted by adding the log MF values of the two coals (Figure 6 and 11c). In fact this process consistently predicted MF values that were too low. Additions of cannel coal in amounts of less than 1% can increase fluidity significantly. Consequently varying amounts of exinite in high-volatile coals may destroy

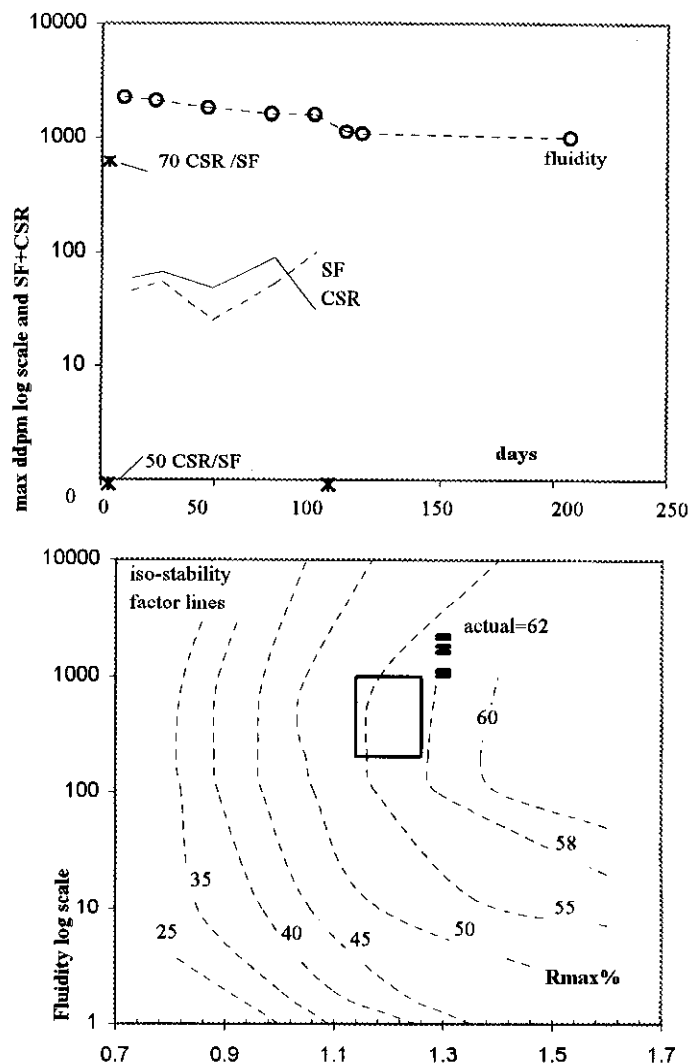


Figure 10: (a) Effect of oxidation/aging on fluidity, stability factor and coke strength after reaction for up to 200 days. (b) fluidity data plotted into an MOF diagram. Data from Price *et al.* (1992).

the linear log MF *versus* total-reactives relationship seen in medium-volatile coals. It should be noted that exinite-rich coals often have high contents of inherent ash and organic sulphur. Additions of exinite-rich cannel coal have been found to decrease coke oven pressure and coke strength (Stell, 1986).

A similar blending experiment was conducted by Fawcett and Dawson (1990; Figures 11a & b). They blended high and low-volatile coals and were unable to accurately predict MF by weighted log averages. However the errors when comparing log MF values are less significant. Plotting the results on an MOF diagram illustrates that 2 component blends do not plot on chords joining the plotted positions of the component coals.

Generally very little attention is given to the MF temperature relative to the start and final temperatures. If it is not mid way between these two temperatures then the fluidity curve is asymmetric. There is some indication that blending produces asymmetric log MF *versus* temperature plots. It is apparent in Figure 6 that

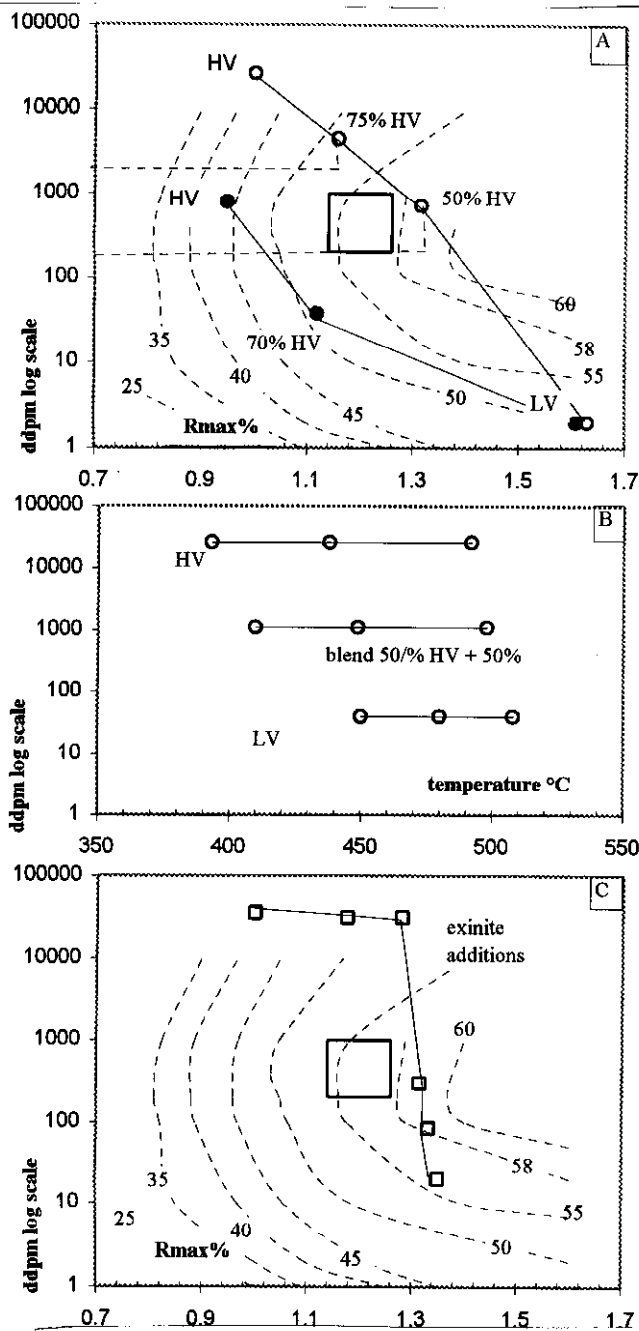


Figure 11: MOF plot of blends of coals of different ranks; HV= high-volatile, LV= low-volatile.

as the amount of exinite in the blend increases the start temperature is largely unaffected but the MF temperature decreases. Figure 11 b, illustrates the effect on MF temperature ( $T_{max}$ ) and FTR of blending the coals. The FTR of the blend is increased but not as much as the full overlap.

It is not surprising that fluidities can not be predicted by weighted averages of log values because fluidity is a measurement of the amount of plastic material in the coal sample at a particular temperature. For a single coal the amount of plastic material starts at zero at a low temperature, reaches a maximum at  $T_{max}$  and then decreases to zero as the temperature continues to increase. A second coal goes through the same

process but over a different temperature range and with a different relationship of plastic components to measured fluidity. Any attempt at predicting blend fluidity should start by summing the plastic and inert components of the individual coals in the blend over a range of temperatures. The resulting plot of proportion of plastic phase versus temperature can then be converted into a fluidity versus temperature plot and the maximum fluidity determined. Generally fluidity data are not reported on a continuous basis as the temperature increases, so that there are no data on the shape of fluidity versus temperature plots for blends of coal to use to help the modeling.

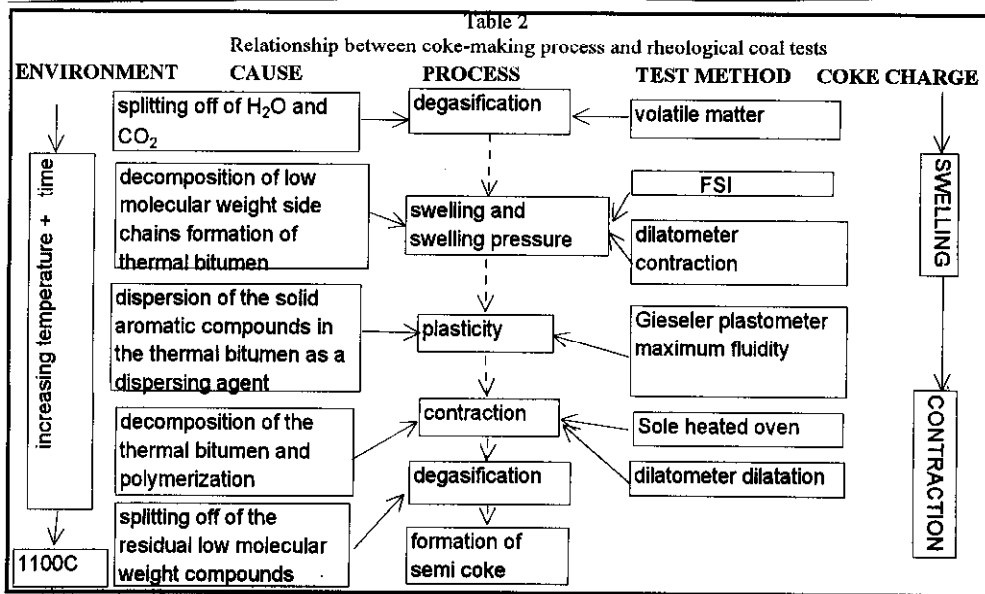
Sakurovs *et al.* (1994) modeled blend fluidity and in cases where there was no chemical interaction between components that enhanced or suppressed fluidity, the predicted results were close to experimental results.

Simple plots of Log MF versus total reactivities are approximately linear for coals of similar rank (Figure 3). This means that if the total reactivities of the component coals are known then it is possible to calculate the total reactivities of the blend. The data on a total reactivities versus log MF diagram can be used to predict the MF value for the blend. This method for predicting blend fluidity will probably only work for coals of similar rank.

The MOF diagram, which plots log MF versus mean maximum reflectance ( $R_{max}$ ) is used to predict blend fluidities for coals of different rank. It appears that blend coal values plot near the line joining the two end members based on calculating the average  $R_{max}$ . But as discussed earlier, the blends will generally plot above the line. It is therefore not possible to accurately predict MF values of blends of coals with different  $R_{max}$  values using the MOF diagram. It is also questionable if the term average rank has any significance. It does not necessarily indicate what the average petrography is in terms of the distribution of V types.

## COKE FORMATION

Coke is made by crushing coal to 80% minus 6 mesh, 1/8 inch or 3.5 mm and then charged into a slot oven. During the coking process, the coal charge goes through a number of changes over a period of 15 to 25 hours as the temperature rises to a maximum of about 1100°C. Initially at temperatures up to about 100°C, water and CO<sub>2</sub> evolve with some increase in pressure. As the temperature rises to 350°C the coal expands. At temperatures above 350°C the outer layer of the coal in the coke oven starts to form a plastic layer characterized by the distillation of bitumen, tars and oils. As the temperature increases the distillation products evaporate and the plastic layer moves inwards leaving behind, on the outer side, semi-coke, which continues to evolve gases such as CH<sub>4</sub>. The plastic layer meets in the middle of the oven, either trapping gases to form a final pressure surge (test oven) or



allowing the last gas to escape upwards (commercial oven). As the temperature increases towards 1100°C hydrogen gas is evolved, the charge usually shrinks and true coke forms.

The various rheology tests attempt to provide information about different stages in the coke forming process as indicated in Table 2, which is adapted from Lowry (1963). As the coal is transformed into coke it initially expands and then contracts. The amount of expansion is very important in terms of coke oven pressure and the amount of contraction is important in terms of ease of pushing (removing coke from oven). The balance of expansion and contraction depends on:

- porosity of the charge.
- porosity of the coke.
- weight of volatile matter lost.

Also based on the chemistry of the ash there may be a tendency of the coke to stick to the brick lining of the ovens.

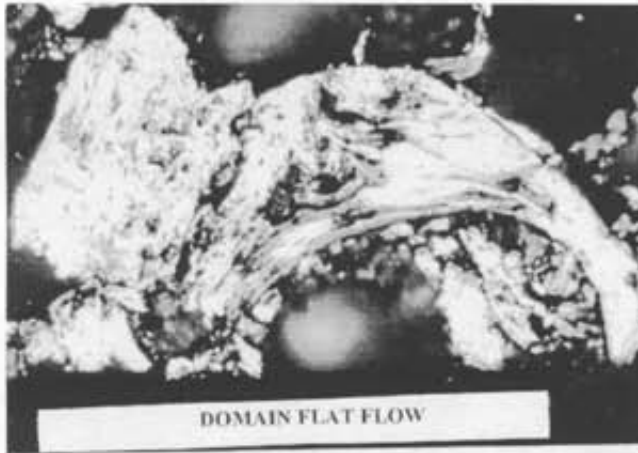
The expansion or contraction of a coke charge varies with rank. When a high-volatile coal is coked there is an increase in porosity as the plastic layer forms vesicles, but this is more than offset by the substantial loss of volatile matter. The charge will generally not generate a lot of pressure. The plastic components in higher rank coals lose less volatile matter so that there is a tendency to generate more oven pressure and to contract less in the final stages of coking.

Reactive macerals in the coal swell, soften and melt during coking and the less viscous components flow around the inert fragments eventually solidifying into a mosaic of anisotropic carbon grains that cement the inert particles together. These grains can have a number of shapes that generally indicate the amount of plastic flow that took place. A classification for coke textures is suggested by Gransden *et al.* (1991; Table 3). Vitrinite from high-rank coal (R<sub>max</sub>>2%) does not melt and forms large anisotropic grains with little change in shape from the original coal fragment. Vitrinites from low-volatile coals form large highly

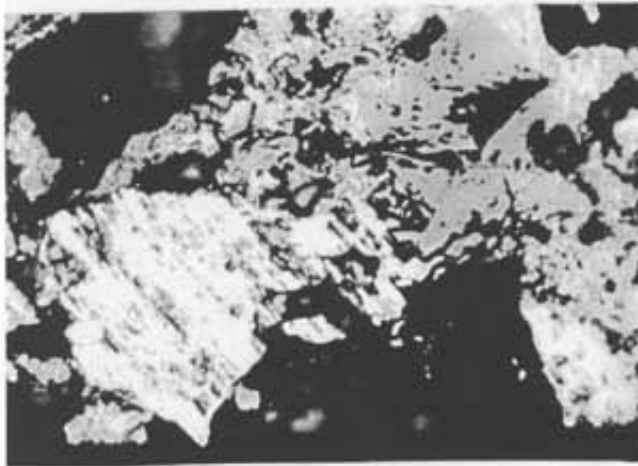
anisotropic grains described as domains; usually with length to width factors greater than 2 (Photo 1). Vitrinites from medium-volatile coals form a lot of medium-sized, anisotropic mosaic grains (Photo 2). Vitrinite from high-volatile coals forms fine anisotropic mosaic grains and isotropic areas indicating high fluidity (Photo 3). Gransden *et al.* (1991) studied the relative proportions of textures in cokes made from coals of different ranks (Figure 12).

At any rank there is a distribution of reflectance values of the vitrinite. These are the V types that are fundamental to predicting stability index using petrographic data. Generally there appears to be a reasonable correlation between vitrinite V type and coke texture it generates. For example V types of 7 to 9 will produce a lot of isotropic, very fine or fine mosaic texture whereas V types of 10 to 15 produce medium mosaic and domain textures. As the rank of a coal increases the V type distribution shifts to the higher numbers and the proportions of coke texture types changes accordingly.

The volatile content of the reactive macerals can decrease by 30% from high-volatile rank to low-volatile rank reactives which results in 30% less carbon cement left after loss of the volatile component. Strong cokes require a balance between medium and fine mosaics, domain structure and inert material. The inert macerals, fusinite and inert semifusinite, remain isotropic and undergo little change in shape. Mineral matter contained in cells in the semifusinite will have minimal effect on fluidity or coke textures, but may cause fracturing of the inert carbon grains at higher temperatures. Mineral matter that is disseminated in desmocollinite may inhibit fluidity and formation of medium mosaic structures. In fact Cameron and Botham (1964) found that the accuracy of predicted stability indexes is improved by considering desmocollinite to be a semi inert maceral. Mineral matter or inertinite fragments that are large can severely weaken the coke.



DOMAIN FLAT FLOW



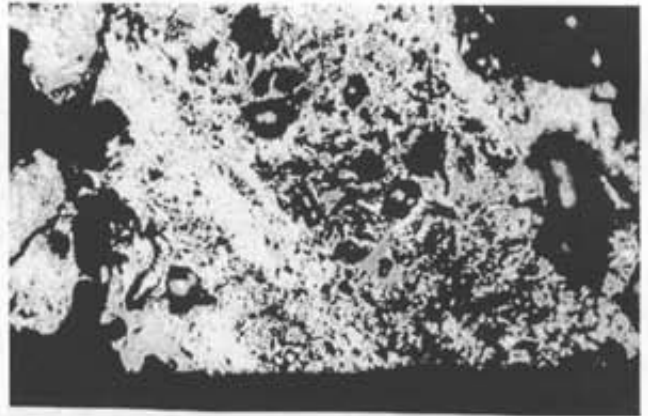
LARGE GRAIN DOMAIN UNDULATING

Photo 1: Coke from low-volatile coal with large highly anisotropic grains described as domains; usually with length to width factors greater than 2.

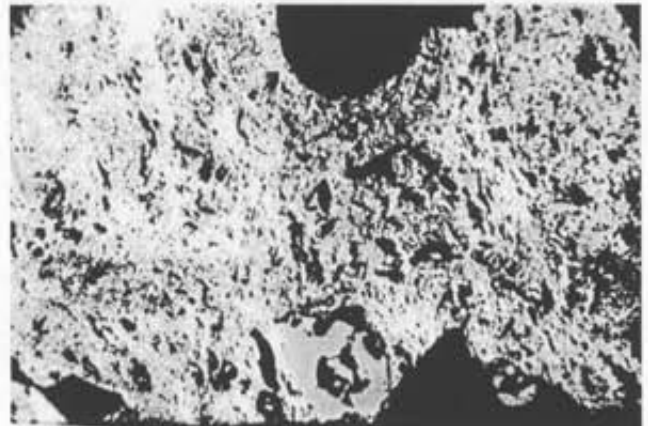
## PREDICTING COKE QUALITY USING PETROGRAPHY OR RHEOLOGY

Most models that predict cold coke strength (ASTM coke stability factor or JIS DI 30/15 index) use petrographic or rheological criteria. The petrographic methods can be made to predict accurate results for coal with high concentrations of semifusinite by empirically choosing the proportion of semifusinite that is considered reactive. This proportion is more than 1/3 but varies from one coal to another. CANMET assumes that 50% of the semifusinite is reactive when making the calculations and Pearson (1984) calculates the amount of reactive semifusinite based on the rank of the coal. Figure 13 illustrates the agreement between predicted stability index and measured stability factor for a number of western Canadian coals using the CANMET 50/50 method of assigning inerts.

Coin and Broome (1997) have recently called into question the usefulness of plots which use petrography to predict coke stability index, such as those of Schapiro and Gray (1964). The data set used by Schapiro and Gray is quite restricted and the vitrinite



MEDIUM MOSAIC AND INERTINITE FRAGMENTS



MEDIUM MOSAIC AND INERTINITE FRAGMENTS

Photo 2: Medium-sized anisotropic mosaic grains formed from a medium-volatile coal.

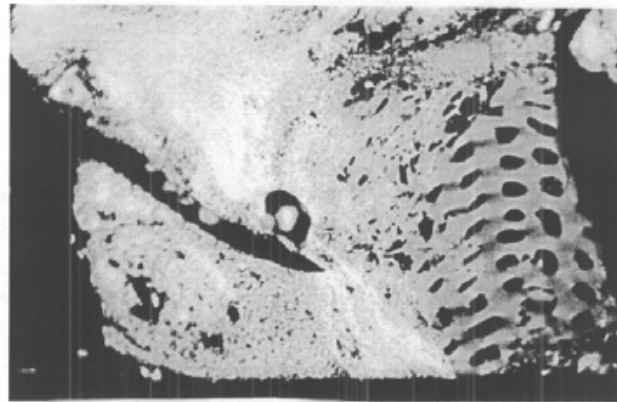
contents of the samples are strongly correlated with rank. Vitrinite contents increase from about 60% at  $R_{max}$  of 0.8% to 75% at an  $R_{max}$  of 1.8%. This trend is counter to that found in coal from the Mist Mountain Formation in south-east British, in which vitrinite contents decreases as the rank increases (Ryan and Khan, 1998). Coin and Broome suggest that, based on data from Australian coals, stability factor is almost independent of vitrinite content at constant rank (Figure 14). Experience with WCC suggests that stability factor is influenced by variation in petrography at constant rank but that the influence may be less than previously thought.

Predictive methods based on measurements of coal rheology include the MOF diagram and the FSI versus volatile matter diagram. Noticeably absent from all models for predicting cold coke strength is any consideration of ash chemistry, particle size effects and operational parameters. Ash chemistry has a major effect on CSR but has not been shown to have much effect on cold coke strength indexes. Particle size can have a major effect on coke quality as can changes in coke battery operating conditions.

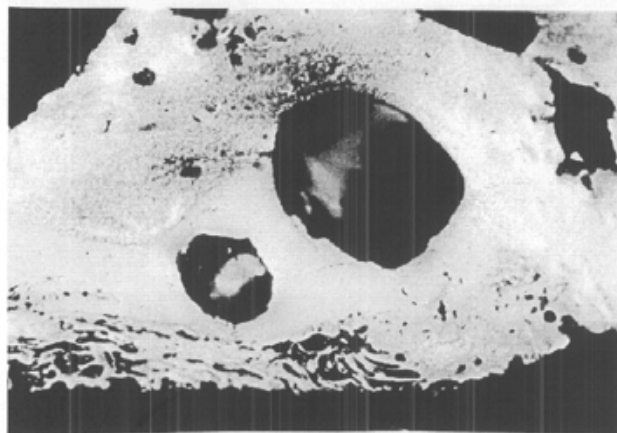
Price *et al.* (1987) have attempted to put iso-stability factor lines on the MOF diagram (Figure 10b)

Table 3  
CANMET CLASSIFICATION OF COKE TEXTURES  
TEXTURE DESCRIPTION MACERALS

| TEXTURE                                                                     | DESCRIPTION                                             | MACERALS                                                                            |
|-----------------------------------------------------------------------------|---------------------------------------------------------|-------------------------------------------------------------------------------------|
| ISOTROPIC                                                                   | no change in form                                       | fusinite                                                                            |
| WEAK ANISOTROPY                                                             | little change in form                                   | inert<br>semifusinite                                                               |
| MOSAIC<br>very fine mosaic<br>fine mosaic<br>medium mosaic<br>coarse mosaic | < 0.5UM<br><1.5>0.5 UM<br>,5>1.5 UM<br><10>5 UM         | reactive macerals including reactive<br>semifusinite anisotropy increases with rank |
| ELONGATED FLOW<br>TEXTURES<br>fine<br>medium<br>coarse                      | L = 2xW<br>W=<1.5>0.5 um<br>W=<5>1.5 um<br>W=<10>5.0 um |                                                                                     |
| DOMAIN<br>ribbon<br>creased<br>undulating<br>flat flow                      | large<br>anisotropic<br>areas                           |                                                                                     |
| BASIC ANISOTROPY                                                            | anisotropic<br>no change in<br>form                     | high<br>rank                                                                        |



INERT SEMIFUSINITE SURROUNDED BY FINE MOSAIC



SEMIFUSINITE ISOTROPIC AND FINE MOSAIC

Photo 3: Fine anisotropic mosaic grains and isotropic areas indicating high fluidity, formed from vitrinite from high-volatile coal.

so that the diagram can be used to estimate coke quality. It is unlikely that coke stability factor can be accurately and consistently predicted using only rank and a single rheology term. Coin and Broome (1997) consider that rank is the most important indication of the ability of a coal to make good coke and in this regard it should be noted that the iso-stability factor lines tend to be vertical for fluidities greater than 10 in the rank window 1% to 1.4%. This is very important, because it implies that in the rank window of  $R_{max} = 1\%$  to 1.4%, stability factor is not sensitive to changes in MF.

Price *et al.* (1987) and Pearson (1980) have both produced FSI versus VM (daf) diagrams with iso-stability factor contours (Figure 15). Pearson examined 109 British Columbia experimental cokes and Price *et al.* used the CANMET database, which includes oxidized and high ash samples. The contour patterns differ somewhat probably because of the inherent difficulty in fitting contours through the data. It is interesting to note that where as, at a medium-volatile rank, stability factor is not sensitive to changes in fluidity, based on the contour lines in Figure 15, it is sensitive to changes in FSI. There appears to be some decoupling of the relationships FSI versus VM and fluidity versus rank.

The combination of FSI versus VM (daf) may be a more sensitive indicator of coke quality than the MOF diagram. This may be in part because VM (daf) is sensitive to changes in petrography as well as rank. In fact for a sample of constant rank both FSI and VM (daf) will increase as the amount of vitrinite in the

sample increases and this explains in part the positive slope of the iso-stability factor contour lines.

One advantage of the FSI versus VM (daf) plot is that it requires less sophisticated analytical data than the fluidity versus  $R_{max}$  plot. Price *et al.* found that, for diagrams utilizing rank and a single rheology term, the FSI versus VM (daf) diagram was the most accurate for predicting stability factor.

The iso-stability factor contours on the MOF and FSI versus VM (daf) diagrams are curved and two coals of different rank with low stability factors can be mixed produce a blend with a stability factor value higher than that of either component coal. A check of a number of Canadian coals (Figure 16a, 17a) indicates that based on the iso-stability factor contours in the diagrams they both often predict low values of SF.

There is a weak tendency for the data in the plots to increase in the direction of high iso-stability factor contour lines but the general consistency between posted values and contour lines values is poor.

Coin and Bloome (1997) suggest that there is no correlation between stability factor and petrography at constant rank (Figure 14) and they also question the

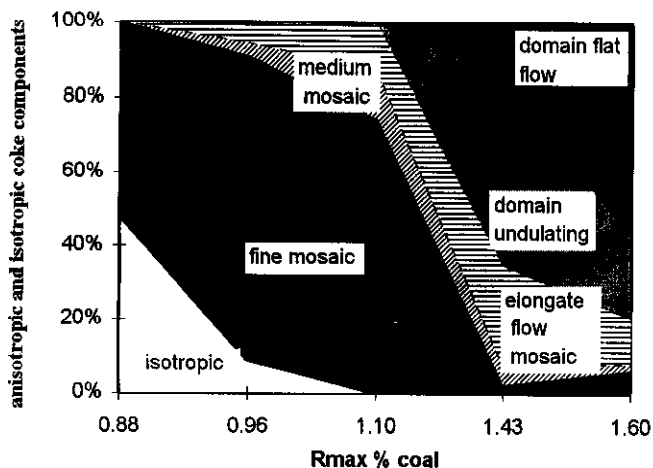


Figure 12: Relative proportion of coke textures for coals of different ranks from Gransden *et al.*, 1991.

usefulness of Gieseler Plastometer results in predicting coke quality. This is not completely born out for WCC based on the limited data in Figure 16b in which there is some tendency for stability factors to increase as maximum fluidity increases at constant rank. There is an approximate linear relationship between total reactivities and maximum fluidity at constant rank (Figure 3), implying an increase in stability factor with increasing total reactivities content. Certainly the general steepness of the iso stability factor contour lines in the MOF diagram indicates a large measure of insensitivity of stability factor values to changes in fluidity at constant rank.

Without attempting to quantify the usefulness of the MOF and VM (daf) *versus* FSI plots, it appears that the data are more consistent with the contour pattern in the FSI *versus* VM (daf) plot in agreement with the conclusion of Price *et al.* (1987). Data in Figures 16c and 17c are for blends of coals of differing ranks and in both cases the diagrams do not appear to be useful in predicting blend stability factor values.

## COMPARISONS BETWEEN EASTERN USA, AUSTRALIAN AND WESTERN CANADIAN COALS

The fluidities of Western Canadian coals (WCC) are generally less than that of eastern USA coals of similar rank. Part of the reason may be because WCC generally have less vitrinite. It has also been suggested that vitrinite from the USA coals has more hydrogen than vitrinite from WCC of similar rank (Price and Gransden, 1987). This would explain the lower fluidity of WCC because there is a moderate correlation of fluidity to hydrogen content for medium-volatile coals. The average hydrogen content of vitrinite from WCC at  $R_{max} = 1.22\%$  is approximately 5.05% and that of Appalachian coals is 5.25%. This is somewhat surprising because usually vitrinite reflectance corresponds with the hydrogen content of vitrinite. One possibility is that there are variations in hydrogen

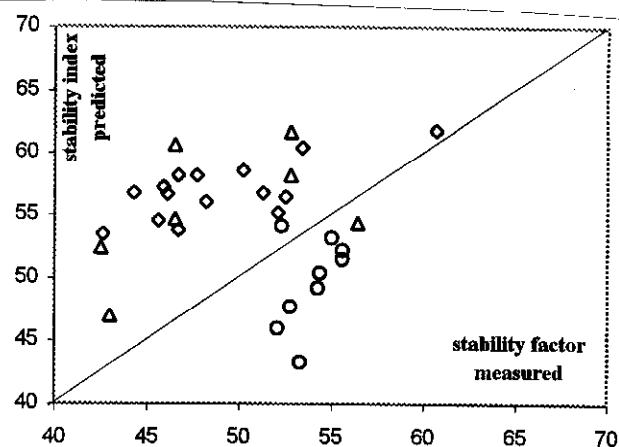


Figure 13: Comparison between predicted stability index and measured stability factor for coal from a number of areas. Samples are not all normal product coals.

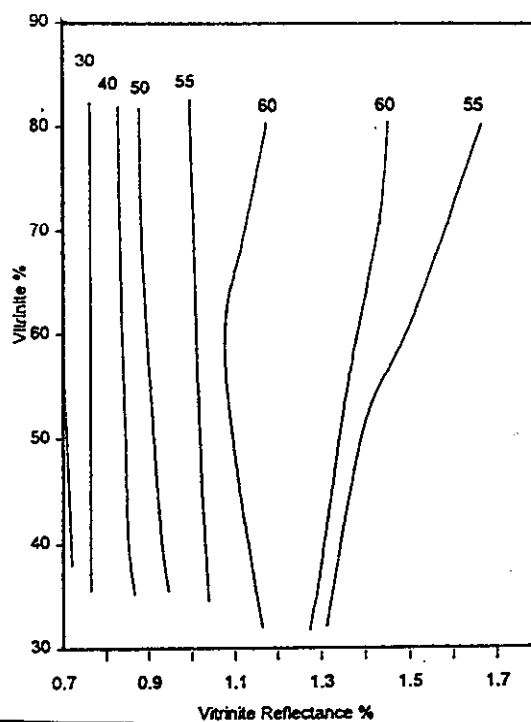


Figure 14: Relationship between stability factor, rank and vitrinite content for Australian coals; from Coin and Bloome (1997).

content of the vitrinite sub macerals. Possibly desmocolinite contains less hydrogen than telocollinite. Mastalerz and Bustin (1993) measured the hydrogen content of individual maceral grains and found no statistically significant difference (telocollinite 2.64% H and desmocolinite 2.63% H). If there is a variation in the fluidity of the sub macerals, then probably telocollinite and tellinite are more fluid than desmocolinite. Reflectance is measured on telocollinite, which may have similar hydrogen contents in both coals. If WCCs have more desmocolinite, then the overall hydrogen content of WCCs may be lower than that of Appalachian coals. Unfortunately most of the literature that provides petrography and rheology data does not differentiate the vitrinite sub macerals.

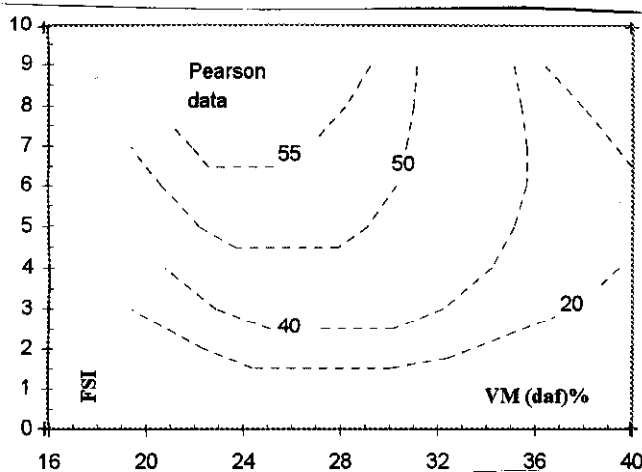


Figure 15: FSI versus VM (daf) diagram with iso-stability factor contours from Pearson (1980).

The  $R_{max}$  is rank dependent, but also tends to increase as the amount of inertinite in a sample increases (Ryan, 1997).

A partial explanation for the different hydrogen contents of the vitrinites from the two areas may be found in the biaxiality of the WCC compared to the possible uniaxial negative optical properties of vitrinite from the eastern USA coals. It is possible that the rank of the Carboniferous eastern USA high-vitrinite coals was imposed during a simple burial history and they are uniaxial negative, whereas the more complicated maturation history of WCC ensured that they are predominantly biaxial negative. Bustin *et al.* (1986) heated and deformed samples of anthracite and was able to increase the reflectance, as well as the biaxial negative component of the reflectance indicating surface. Clearly deformation does change a uniaxial negative reflectance indicating surfaces into a biaxial negative one, possibly with higher  $R_{max}$  values.

The value  $R_{max}$ % (true maximum reflectance) is greater than  $R_{mmax}$ % (mean maximum reflectance) for biaxial coals and the relationship for Mist Mountain coals (Grieve, 1991) is given by:

$$R_{max}\% = R_{mmax}\% \times 1.044.$$

Grieve suggests that the biaxiality is caused by a differential stress factor imposed upon the hydrostatic stress, which is responsible for the uniaxial component of the reflectance indicating surface. If this is the case, then coals that experienced a simple burial history will have uniaxial reflectance indicating surfaces,  $R_{mmax}$ % will equal  $R_{max}$ %, and  $R_{mmax}$ % will be a true measure of rank. However for coals whose rank was established during folding,  $R_{mmax}$ % will be an underestimate of rank and the true rank will be indicated by  $R_{max}$ %. Vitrinites from WCC have approximately 2% less volatile matter and 0.1% less hydrogen than their Appalachian counterparts. Many WCCs are biaxial negative consequently their  $R_{mmax}$ % values could have been underestimated by about 0.05%. This, based on the hydrogen versus  $R_{mmax}$ % relationship in Stach *et al.* (1982) could explain about 0.06% of the missing hydrogen. If the

true rank of the western Canadian vitrinites is used, then they may appear to be less anomalous in terms of rheology and hydrogen content.

There is some data that indicate that Australian coals of the same rank as WCC are more fluid (Leeder *et al.*, 1997). Part of this effect may be due to variations in petrography. A limited amount of fluidity and petrographic data grouped by average rank are plotted in Figure 18. It appears that at a rank of high-volatile bituminous there is a distinct difference between WCC and Australian coals, however at higher ranks the apparent difference may be due to higher concentrations of inertinite in WCC.

Gransden *et al.* (1991) studied the relative proportions of reactive coke textures in cokes made from WCC and eastern USA coals of different ranks (Figure 12). There is a strong correlation between vitrinite V type and the type of coke texture generated. They found very little difference in the proportions of textures for cokes derived from the two types of coals at similar rank. If the amount of reactive coke and the relative proportions of the textural types are important in determining the quality of the coke, then the proportions of vitrinite V types must be more important than any subtle changes in fluidity or chemistry of vitrinite. This point is very important for WCC because it means that fluidity at a particular rank is not as important in determining coke quality as petrography especially V type distribution. This conclusion is similar to that reached by Coin and Broome (1997) with regards to fluidity but there is still the implication that petrography in terms of the amount of reactives and their V type distribution are important.

## CONCLUSIONS

Fluidity is one of three primary measures of coal rheology, the other two being FSI and dilatation. The fluidity of a coal is dependent on rank and the content of reactive macerals. For medium-volatile coals there is a threshold reactive maceral content below which the coal has no fluidity. Above the threshold fluidity can increase rapidly as the content of reactive macerals increases.

Fluidity data provide information about the formation of a plastic phase during coke making. This is only one of the processes that takes place as coal is converted into coke and its usefulness in predicting coke quality has been questioned by Coin and Broome (1997). The steepness of the iso stability factor contours in the MOF diagram also indicates that coke quality is insensitive to changes in coal fluidity over a wide range of rank values.

There is no simple way of predicting the fluidity of a blend of coals. It is not possible to weight average the log values of MF, though it may be possible to derive a blend fluidity using petrographic data for the component coals. More complicated methods of adding reactives exist but they do not take into account

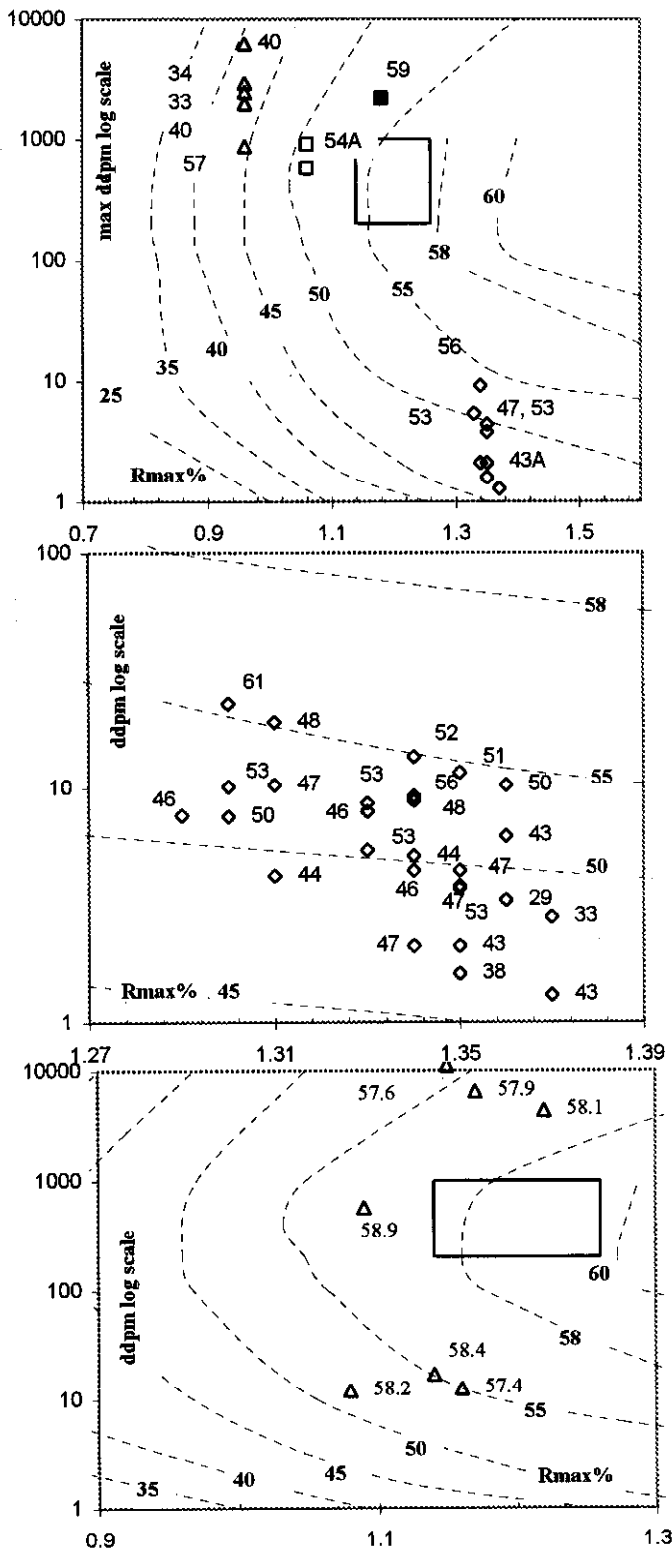


Figure 16: (a) MOF diagram with posted stability factor values for a number of WCCs and one eastern USA coal (solid symbol) with stability factor values are posted next to the data. (b) Window of (a) showing data for a number of single seam samples of similar rank. (c) data for blend samples composed of seams of different ranks. The data are for single coals but not necessarily product coals. The A following a stability factor values indicates an average value for overlapping data points.

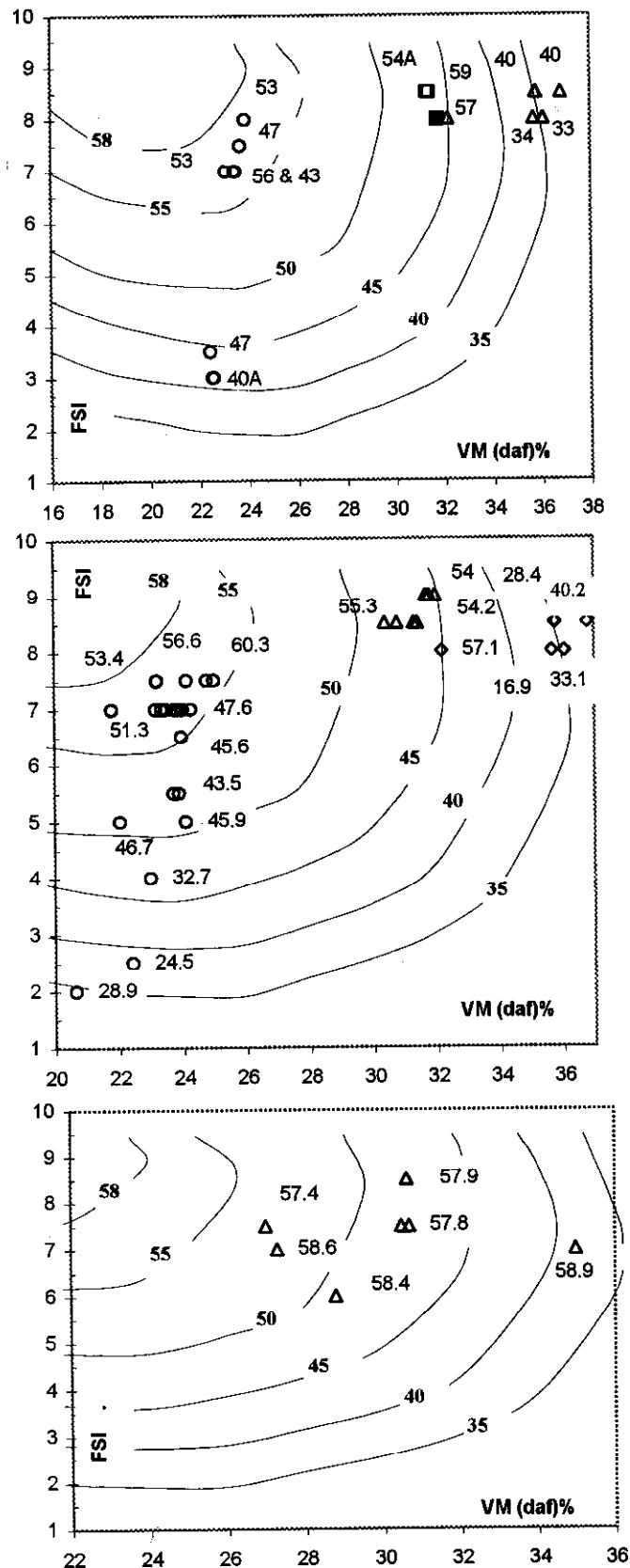


Figure 17: (a) VM (daf) versus FSI diagram with posted stability factor values for a number of Canadian coals. (b) Window of (a) showing extra data indicating some agreement between posted stability factor values and iso-stability factor contour lines. (c) Data for blend samples composed of seams of different ranks.

Western Canadian coals contain high proportions of semifusinite and as yet there is no accepted way of predicting what proportion of this material will become plastic. This introduces a level of uncertainty in petrographic techniques for predicting coke quality. Measures of coal rheology effectively take into account the semifusinite problem but the results are often inconsistent because they utilize small samples. No test approaches the quality of the data obtained from a movable wall coke oven test which links coal rheology data to industrial coke oven experience.

## ACKNOWLEDGMENTS

Thanks are extended to the Canadian Carbonization Research Association for permitting use of some of their data on Western Canadian coals. The paper benefited considerably from an editorial review by Dave Lefebure.

## REFERENCES

- Bustin, R.M. (1982): The Effect of Shearing on the Quality of some Coals in the Southeastern Canadian Cordillera; *Canadian Institute of Mining and Metallurgy Bulletin*, Volume 75, pages 76-83.
- Bustin, R.M., Ross, J.V. and Moffat, I. (1986): Vitrinite Anisotropy under Differential Stress and High Confining Pressure and Temperature: Preliminary Observations; *International Journal of Coal Geology*, Volume 17, pages 343-351.
- Cameron, A.R. and Babu, S.K. (1968): Petrology of the No. 10 (Balmer) Coal Seam in Natal Area of the Fernie Basin, British Columbia; *Geological Survey of Canada*, Paper 68-35, pages 1-25.
- Cameron, A.R. and Botham, J.C. (1964): Petrography and Carbonization Characteristics of some Western Canadian Coals; *Coal Science*, Robert F. Gould, Editor, American Chemical Society Publications, pages 564-576.
- Clemens, A.H. and Matheson, T.W. (1991): Further Studies of Gieseler Fluidity Development in New Zealand Coals; *Fuel*, pages 193-197.
- Coin, C.D.A. and Broome, A.J. (1997): Coke Quality Prediction from Pilot Scale Ovens and Plant Data; *11th International Conference on Coal Research*, Conference proceedings Calgary, September 9, pages 325-332.
- Fawcett, D.A. and Dawson, R.F. (1990): Unique Blending Properties of Smoky River Coal, *Ironmaking Proceedings*, Iron and Steel Society/American Institute of Mining, Metallurgical and Petroleum Engineers, Volume 49, pages 227-234.
- Gransden, J.F., Jorgensen, J.G., Manery, N. Price, J.T. and Ramey, N.J. (1991): Applications of Microscopy to Coke Making; *International*

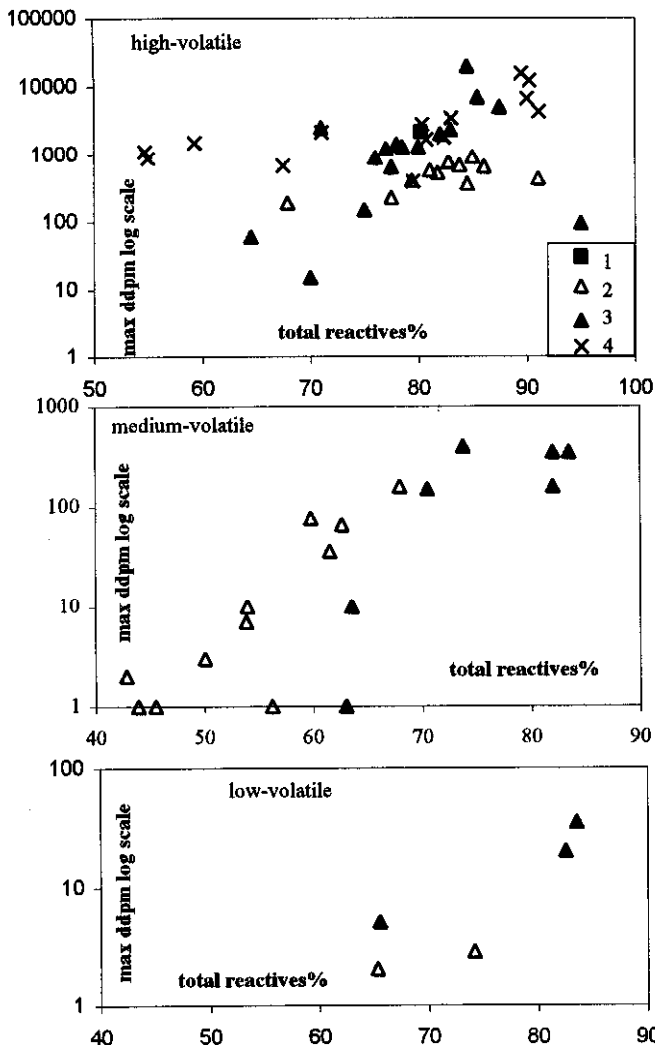


Figure 18: Fluidity versus total reactivities for Canadian and Australian coals of different ranks. 1=Appalachian. 2=WCC. 3=Australian. 4=Eastern Canadian coals.

interaction between the reactive particles from the different component coals.

As with petrography and other measures of rheology, fluidity is used to predict coke quality, in particular cold coke strength as measured by ASTM stability factor or the JIS DI 30/15 index. Coke quality is strongly dependent on coal rank and somewhat dependent on petrographic composition. It also depends on coal size consist and coke battery operational parameters. No single measure of coal rheology will consistently and accurately predict coke quality.

If a single measure of rheology suggests that a coal will make poor coke, this should not be taken at face value. Other measures of rheology should be checked for consistency. Low FSI is probably the best current coal-derived indicator of poor coking potential for a single coal. In fact the FSI versus VM (daf) diagram, can be much more useful than the MOF diagram in providing a rough estimate of coke quality. It has the added advantage that it is much cheaper.

- Journal of Coal Geology*, Volume 19, pages 77-107.
- Grieve, D.A. (1991): Biaxial Vitrinite Reflectance in Coals of the Elk Valley Coalfield, Southeastern British Columbia, Canada; *International Journal of Coal Geology*, Volume 19, pages 185-200.
- Lamberson, M., Bustin, M.R., Kalkrueth, W.D. and Pratt, K.C. (1996): The Formation of Inertinite-Rich Peats in Mid-Cretaceous Gates Formation: Implications for the Interpretation of Mid-Albian History of Paleowildfire; *Paleogeography, Palaeoclimate, Palaeoecology*, 120 pages 235-260.
- Leeder, R.W., Price, J.T. and Gransden, J.F. (1997): Western Canadian Coking Coals - Thermal Rheology and Coking Quality, *Ironmaking Proceedings*, Iron and Steel Society/American Institute of Mining, Metallurgical and Petroleum Engineers, pages 1-8.
- Loison, R., Peytavy, A., Boyer, A.F. and Grillot, R. (1963): The Plastic Properties of Coal; in *The Chemistry of Coal Utilization*, Lowry editor, John Wiley and Sons, Inc., pages 150-201.
- Mastalerz, M. and Bustin, M.R. (1993): Variation in Elemental Composition of Macerals; An Example of Application of Electron Microprobe to Coal Analysis; *International Journal of Coal Geology*, Volume 22, pages 83-99.
- Pearson, D.E. (1980): The Quality of Western Canadian Coking Coal; *Canadian Institute of Mining and Metallurgy Bulletin*, Volume 73, pages 1-15.
- Pearson, D.E. (1984): An Indirect Evaluation of the Reactivity of Inertinites in Western Canadian Coking Coals; *Canadian Centre for Mineral and Energy Technology*, CANMET Contract Report No 1SQ83-00061.
- Price, J.T. and Gransden, J.F. (1987) Metallurgical Coals in Canada: Resources, Research, and Utilization, *Canadian Centre for Mineral and Energy Technology*, Report Number 87-2E. pages 1-72.
- Price, J.T., Gransden, J.F., Khan, M A. and Ryan, B.D. (1992): Effect of Selected Minerals on High Temperature Properties of Coke. Abstract. *Ironmaking Proceedings*, Iron and Steel Society/American Institute of Mining, Metallurgical and Petroleum Engineers, 1992.
- Ryan, B.D. (1997): Coal Rank Variations in Cabinet Creek Area of the Telkwa Coalfield Central British Columbia (93L/11); in *Geological Fieldwork 1996*, B.C. Ministry of Employment and Investment, Paper 1997-1, pages 365-372.
- Ryan, B.D. (1997): Coal Quality Variations in the Gething Formation Northeast British Columbia; in *Geological Fieldwork 1996*, B.C. Ministry of Employment and Investment, Paper 1997-1, pages 373-397.
- Ryan, B.D. and Khan, M. (1998): Maceral Affinity of Phosphorus in Coal from the Elk Valley Coalfield, British Columbia; in press in *Geological Fieldwork 1997*, B.C. Ministry of Employment and Investment, Paper 1998-1.
- Sakurovs, R., Lynch, L.J and Maher, T.P. (1994): The Prediction of Fusibility of Coal Blends; *Fuel Processing Technology*, Volume 37, pages 255-269.
- Schapiro, N. and Gray, R.J. (1964): The Use of Coal Petrography in Coke Making; *Journal of the Institute of Fuel*, Volume 11, Number 30, pages 234-242.
- Stach, E., Mackowsky, M-Th, Teichmuller, M., Taylor, G.H., Chandra, D. and Teichmuller, R. (1982): Coal Petrography; *Gebruder Borntraeger*, Berlin, page 47, Table 4A.
- Stell, S. M. (1986): The Effects of Cannel Coal on Coal and Coke Quality Parameters and Blast Furnace Ironmaking Costs; *Journal of Coal Quality*, October, pages 126-129.

## MACERAL AFFINITY OF PHOSPHORUS IN COALS FROM THE ELK VALLEY COALFIELD, BRITISH COLUMBIA.

By Barry Ryan, B.C. Geological Survey and Mohammed Khan, Fording Coal Limited, Calgary

**KEYWORDS:** Elk Valley coals, phosphorus, coal macerals, seam stratigraphy

### INTRODUCTION

British Columbia exports about 25 million tonnes per year of metallurgical coal from two coalfields, which follow the Rocky Mountains along the eastern edge of the Province. In the north there are two mines in the Peace River coalfield and in the south, five mines in the east Kootenay coalfields (Figure 1). The east Kootenay coalfields are divided into the Elk Valley, Crowsnest and Flathead fields (Figure 2). Three mines are situated in the Elk Valley coalfield, the most important coal-producing area in British Columbia, and they account for about 15.7 million tonnes of export coal. All the economic seams in the Kootenay coalfields are contained in the Mist Mountain Formation of late Jurassic to early Cretaceous age.

Phosphorus in steel reduces its flexibility and is generally considered to be an undesirable element in coal. Most steel mills blend coals to achieve a phosphorus concentration in coal of less than 0.04%.

Data collected during this study are not located with respect to any particular mine and the seams sampled are identified by sequential letters from A near the base of the section through the Mist Mountain Formation to near the top. The lettering system does not correspond exactly with the seam numbering in any particular mine, but does retain the relative stratigraphic positions of all the data discussed in this paper.

### PREVIOUS WORK

The comprehensive paper by Gluskoter *et al.* (1977) used washability analysis to assign elements a coal (organic) or ash affinity. He found that phosphorus sometimes had an inorganic affinity, but in a majority of the cases followed the coal. Finkleman (1980) reviewed the existing literature and used XRD and SEM techniques to identify the modes of occurrence of many elements, including phosphorus in coal. Powell (1987) suggested that ionic potential can be used to separate elements into organic or inorganic affinities and that based on this,  $P^{3+}$  should have an organic affinity and  $P^{5+}$  an inorganic affinity.

Studies of phosphorus in British Columbia coals include Van Den Bussche and Grieve (1990), which provided information on average phosphorus

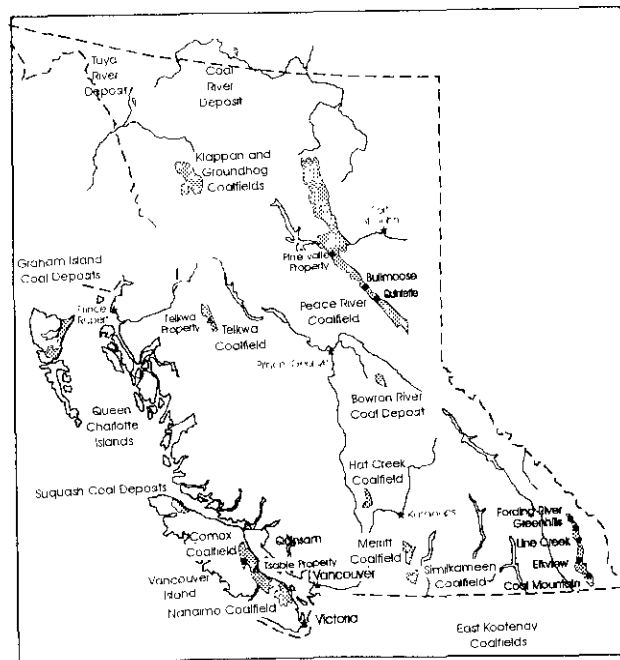


Figure 1 Location map of coalfields and coal deposits in British Columbia.

concentrations in the Gates, Gething and Mist Mountain formations; Grieve and Holuszko (1991), which provided phosphorus and trace element data and Grieve (1992), which compiled all previous data. Ryan and Grieve (1995) discussed the origin of phosphorus in coal and analyzed incremental samples through a number of seams in the Mist Mountain Formation.

A number of papers describe the distribution of elements, including phosphorus in seam sections. These include Karner *et al.* (1986) who studied the distribution of elements in a North Dakota lignite of Paleocene age and described phosphorus as having an uncertain or inorganic association. Other papers include Harris *et al.* (1981) who studied coals in eastern Tennessee and Hills (1990) who studied the Hat Creek deposit in British Columbia.

The distribution of phosphorus in Australian coals has been studied by Ward *et al.* (1996). They found a bimodal distribution of phosphorus in coals from Queensland. A bimodal distribution is not evident in coals from the Elk Valley coalfield.

## ORGANIC OR INORGANIC AFFINITY OF PHOSPHORUS

There is considerable literature on major oxides, minor and trace elements in coal. Unfortunately a lot of phosphorus data is reported as  $P_2O_5$  in ash without providing the concentration of ash in the sample, making it impossible to calculate the concentration of phosphorus in the total sample. Also it is often not clear if the samples were of raw or washed coal. In short, there is deceptively little useful published phosphorus data.

There have been a number of studies of the occurrence of phosphorous in coal but there is no direct evidence of a true organic bonding (Burchill *et al.*, 1990), though classic washability studies such as those of Gluskoter *et al.* (1977) indicate in part a coal affinity. In the classic sense organic affinity means that the element is part of the organic molecules that make up coal. In practice, elements that are difficult to remove by conventional washing methods and tend to remain with the coal are described as having an organic affinity. These elements may occur in very small mineral grains dispersed in the coal in a way not related to the amount of ash in the coal. Consequently the term organic affinity may be somewhat misleading and a better way of describing the occurrence of elements may be to simply to refer to them as elements that follow the coal, or the ash, during washing. Those following the coal will be difficult to remove and may be a problem for the purchaser. Those removed by washing may provide problems for the producer when disposing of the tails and coarse reject material.

## PHOSPHORUS CONCENTRATIONS IN VEGETATION AND COAL

The main phosphorus minerals in coal are a calcium phosphate (apatite) and the two crandallite group minerals gorceixite (barium aluminum phosphate) and goyazite (strontium aluminum phosphate). It is not always possible to differentiate between goyazite and gorceixite and they are sometimes jointly referred to as crandallite.

The average phosphorus content of world coals is estimated by Bertine and Goldberg (1971) to be about 0.05% (500 ppm). Concentrations vary around the world and through time and there is a tendency for Permian coals from India and Australia, and Cretaceous coals from Western Canada, to have higher phosphorus concentrations than Carboniferous coals from Europe and USA (Ryan and Grieve, 1995 and Ward *et al.*, 1996). These authors suggest that most of the phosphorus in coal originates from the parent vegetation.

The tendency for Cretaceous and Permian coals to have higher phosphorus contents may be because of higher concentrations in the parent vegetation, either because of different species, or because of colder climates, in which vegetation requires more phosphorus to grow. There is a distinct shift to cooler climates and more polar latitudes from the Carboniferous to Permian and younger times

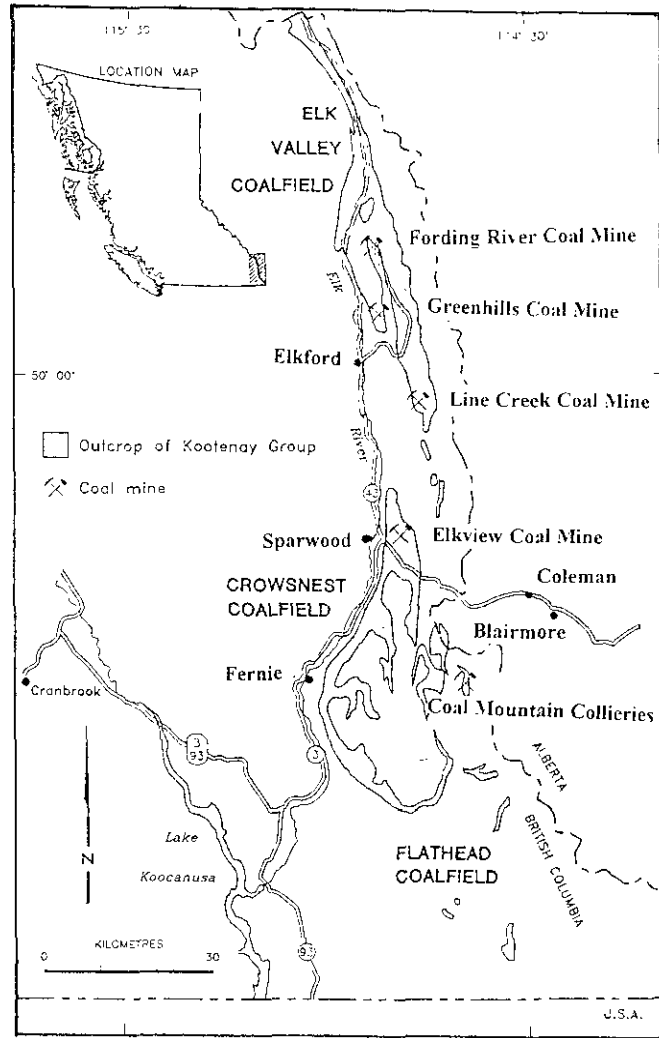


Figure 2: Coalfields and coal mines in southeastern British Columbia.

(Diessel, 1992, page 26). Alternatively the coal-forming swamp environment and maceral composition of these coals may have been less favourable for the removal of phosphorus.

Cretaceous coals could also contain phosphorous from bones, shells or guano, which generally contain more than 10%  $P_2O_5$  and would probably dissolve in an acid swamp environment allowing the phosphorus to be redistributed. Flying reptiles, which appeared in the Jurassic, are known to have populated the western shoreline of the Fernie sea, which covered much of Alberta and parts of British Columbia in the Cretaceous. It has been suggested that high-phosphorus coal seams higher in the Mist Mountain Formation were derived from more woody vegetation than seams low in the section, which are low in phosphorus. The flying reptiles were not strong fliers and would have needed tall trees to perch on and glide from. Pterosaurs, which are known to have had a wing span of up to 23 metres, could have contributed a reasonable amount of phosphorus to the coastal swamp. Based on assuming, values for body weight, amount of guano produced, population density, vegetation accumulation rate and compaction factor, they could have contributed a minor amount of phosphorus to the coal.

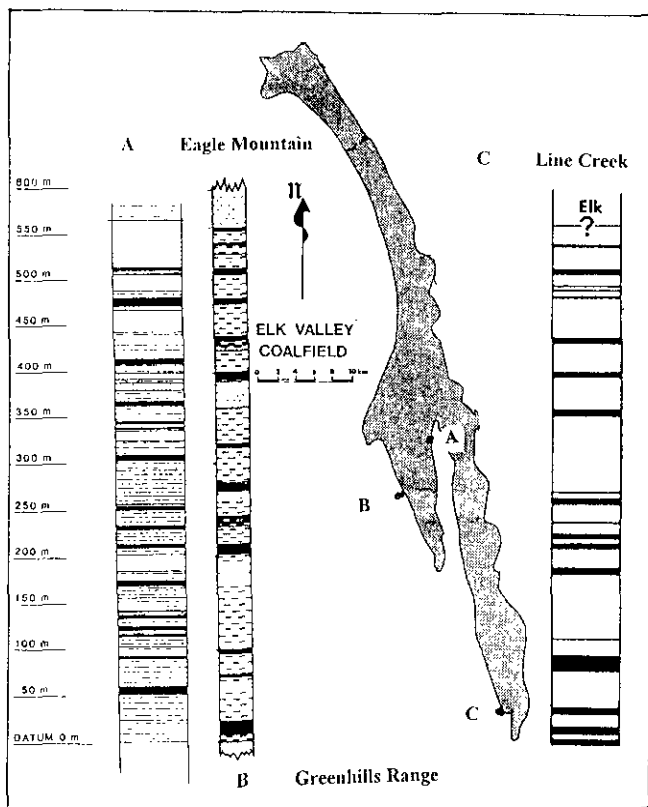


Figure 3: Mist Mountain seam sections for the Elk valley coalfield from Grieve (1993), Taplin (1976), Britch (1981) and Line Creek.

A comparison of phosphorus data for vegetation and coal indicates that concentrations in vegetation are much higher than those observed in coal. The phosphorus content of dried modern plants is estimated to be about 10 times higher than the concentration in coal (Francis, 1961). Phosphorus occurs in vegetation in low levels and is an essential nutrient. Salisbury and Ross (1969) indicate that 0.2% is the amount required in higher plants. Plants absorb phosphorus as the orthophosphate anion ( $H_2PO_4^-$  or  $H_2PO_4^{2-}$ ) or as inorganic phosphorus compounds, possibly finely dispersed varieties of apatite. The carbon content of dry conifers is about 49.6% (Ledig and Botkin, 1974) and for hard-woods varies from 50% to 53% on a dry basis (Shah *et al.*, 1992).

Grasses probably have a higher phosphorous/carbon ratio than trees (Marschner, 1986) and this implies possible phosphorous contents in coal averaging over 0.5% (5000 ppm). The phosphorus contents for a number of small plants range from 0.1% to 0.645% (daf basis) and for wheat range from 0.3% to 0.5% (Wedepohl, 1970). Generally there is more phosphorus in deciduous trees than pines, and within a single species the phosphorus is not uniformly distributed. Because it is an essential plant nutrient, it is usually found in those parts of the plant that grow most rapidly. For example, it is concentrated in bark and leaves of a number of different species (Kramer and Kozlowski, 1979).

The phosphorus to carbon ratio of woody vegetation is about 0.004 for woody vegetation. Medium-volatile bituminous coals have over 85% carbon on a dry ash-free basis, so that if all the phosphorus stays in the coal and the same phosphorous/carbon ratio is maintained, then 0.2%

phosphorus in vegetation would be equivalent to about 0.36% phosphorous in coal (daf basis) compared to a world average of about 0.05%. Either there is a process at work that removes variable amounts of phosphorus from the dead vegetation (Ward *et al.*, 1996 and Ryan and Grieve, 1995), or there may be a process of recycling the phosphorus upwards from rotting vegetation to overlying growing vegetation. In this case the amount of phosphorus required to account for all the vegetation that made a coal seam may be much less than expected.

Based on data in this study, it appears that phosphorus distribution in coal is controlled by petrographic composition. Different macerals have the potential to retain or attract phosphorus minerals. In this context it is useful to divide the vitrinite macerals into structured vitrinite (tellinite and telocollinite) and unstructured vitrinite (detrovitrinite and desmocollinite). Inertinite is divided into structured inertinite (semifusinite and fusinite) and unstructured inertinite (macrinite, micrinite and inertodetrinite). In a rough way these divisions separate maceral groups that may retain organic phosphorus (structured vitrinite) or have the phytal porosity available for secondary deposition of phosphorus minerals (structured inertinite) from those that probably lost phosphorus (unstructured vitrinite and inertinite).

## REGIONAL GEOLOGY AND STRATIGRAPHY OF THE ELK VALLEY COALFIELD

The Elk Valley coalfield is composed of a north-trending synclorium of Jura-Cretaceous rocks situated in the Front Ranges of the Rocky Mountains and over thrust by older rocks from the west. On the local scale the geology varies from broad open synclines to tight folds complicated by many thrusts, that often repeat the coal section. The Mist Mountain Formation, which ranges in thickness from 425 to 700 metres in the Elk Valley coalfield, is the main coal bearing formation (Grieve, 1993). Coal makes up approximately 10 volume % of the formation, which contains over 29 seams in the Greenhills syncline, 15 seams in the Eagle Mountain block east of the Erichson fault and a thinner section of seams in the south (Figure 3). Donald and Bustin (1987) divided the Mist Mountain Formation at Eagle Mountain into three informal units. The lowest unit contains 2 seams, which formed behind beach and dune ridge deposits, and is dominated by sandstones. Unit 2 is 200 metres thick and includes coal seams and sediments, which were deposited in a fluvial-flood plain environment. Sedimentation was dominated by three major river systems that frequently flooded coal-forming swamps causing partings in the seams. Unit 3 formed in a flood plain environment, which did not contain major rivers in the area studied.

Table 1  
FULL SEAM ANALYTICAL DATA

| seam              | Sple No | ADM         | VM          | Ash         | FC          | P%          | Ba         | Sr         | SG         | Yd          | ADM         | VM          | Ash        | FC          | P%           | S%          | FSI        |
|-------------------|---------|-------------|-------------|-------------|-------------|-------------|------------|------------|------------|-------------|-------------|-------------|------------|-------------|--------------|-------------|------------|
| A                 | 9       | 0.32        | 24.6        | 7.8         | 67.4        | 0.04        | 40         | 24         | 1.5        | 92.7        | 1.19        | 26.2        | 4.3        | 68.4        | 0.020        | 0.26        | 8.0        |
| A                 | 201     | 0.51        | 23.4        | 14.2        | 61.9        | 0.03        |            |            | 1.5        | 86.3        | 1.42        | 25.8        | 6.3        | 66.4        | 0.018        |             |            |
| <b>average A</b>  |         | <b>0.42</b> | <b>24.0</b> | <b>11.0</b> | <b>64.6</b> | <b>0.03</b> | <b>40</b>  | <b>24</b>  | <b>1.5</b> | <b>89.5</b> | <b>1.31</b> | <b>26.0</b> | <b>5.3</b> | <b>67.4</b> | <b>0.019</b> | <b>0.26</b> | <b>8.0</b> |
| G                 | 1       | 0.68        | 21.8        | 22.7        | 54.9        | 0.08        | 110        | 138        | 1.5        | 74.7        | 0.36        | 24.8        | 7.8        | 67.0        | 0.100        | 0.38        | 5.0        |
| G                 | 5       | 0.79        | 22.7        | 17.6        | 58.9        | 0.14        | 130        | 64         | 1.5        | 78.0        | 0.93        | 24.3        | 9.0        | 65.7        | 0.118        | 0.41        | 6.0        |
| G                 | 18      | 0.57        | 24.3        | 10.4        | 64.8        | 0.16        |            |            | 1.5        | 88.4        | 0.25        | 24.8        | 8.0        | 67.0        | 0.165        | 0.41        | 6.0        |
| G                 | 202     | 0.58        | 22.6        | 17.7        | 59.2        | 0.19        |            |            | 1.5        | 73.7        | 1.25        | 25.7        | 8.5        | 64.6        | 0.106        |             |            |
| G                 | 203     | 0.53        | 23.3        | 17.0        | 59.2        | 0.12        |            |            | 1.5        | 81.5        | 0.67        | 25.4        | 7.9        | 66.1        | 0.110        |             |            |
| G                 | 205     | 0.00        | 23.3        | 15.9        | 60.7        | 0.19        |            |            | 1.5        | 84.2        | 0.47        | 25.5        | 8.1        | 65.9        | 0.176        |             |            |
| G                 | 101     | 0.34        | 18.3        | 31.8        | 49.5        | 0.12        | 420        | 130        | 1.5        | 50.5        | 0.68        | 21.9        | 8.6        | 68.8        | 0.056        | 0.61        | 5.5        |
| G                 | 102     | 0.35        | 18.0        | 33.0        | 48.7        | 0.15        | 260        | 68         | 1.5        | 50.5        | 1.07        | 21.5        | 11.6       | 65.9        | 0.030        | 0.54        | 7.0        |
| G                 | 103     | 0.37        | 19.4        | 27.2        | 53.0        | 0.10        | 200        | 74         | 1.5        | 64.4        | 1.71        | 22.2        | 7.6        | 68.5        | 0.073        | 0.39        | 4.0        |
| G                 | 113     | 0.33        | 18.4        | 33.0        | 48.2        | 0.12        | 360        | 60         | 1.5        | 52.2        | 1.18        | 21.7        | 9.8        | 67.3        | 0.078        | 0.55        | 7.5        |
| <b>average G</b>  |         | <b>0.45</b> | <b>21.2</b> | <b>22.6</b> | <b>55.7</b> | <b>0.14</b> | <b>247</b> | <b>89</b>  | <b>1.5</b> | <b>69.8</b> | <b>0.86</b> | <b>23.8</b> | <b>8.7</b> | <b>66.7</b> | <b>0.101</b> | <b>0.47</b> | <b>5.9</b> |
| I                 | 105     | 0.60        | 19.9        | 17.8        | 61.7        | 0.06        | 60         | 40         | 1.5        | 79.2        | 0.31        | 24.3        | 6.7        | 68.7        | 0.021        | 0.48        | 3.5        |
| I                 | 204     | 0.00        | 17.0        | 46.9        | 36.1        | 0.08        |            |            | 1.5        | 43.6        | 0.69        | 27.8        | 8.6        | 62.9        | 0.040        |             |            |
| I                 | 206     | 0.00        | 23.5        | 23.2        | 53.4        | 0.03        |            |            | 1.5        | 65.9        | 0.32        | 26.0        | 9.7        | 64.0        | 0.041        |             |            |
| I                 | 209     | 0.00        | 20.9        | 25.1        | 54.0        | 0.04        |            |            | 1.5        | 67.1        | 0.43        | 24.9        | 8.9        | 65.8        | 0.040        |             |            |
| <b>average I</b>  |         | <b>0.15</b> | <b>20.3</b> | <b>28.3</b> | <b>51.3</b> | <b>0.05</b> | <b>60</b>  | <b>40</b>  | <b>1.5</b> | <b>64.0</b> | <b>0.44</b> | <b>25.7</b> | <b>8.5</b> | <b>65.3</b> | <b>0.036</b> | <b>0.48</b> | <b>3.5</b> |
| J                 | 4       | 0.67        | 23.0        | 20.6        | 55.8        | 0.04        | 190        | 130        | 1.5        | 70.5        | 0.51        | 25.8        | 6.7        | 67.0        | 0.101        | 0.42        | 6.5        |
| J                 | 10      | 0.43        | 22.5        | 17.2        | 59.9        | 0.14        |            |            | 1.5        | 75.5        | 0.59        | 23.3        | 7.9        | 68.2        | 0.098        | 0.37        | 7.0        |
| J                 | 11      | 0.55        | 22.2        | 13.3        | 63.9        | 0.18        | 140        | 86         | 1.5        | 83.0        | 0.61        | 25.6        | 5.5        | 68.3        | 0.103        | 0.65        | 4.0        |
| J                 | 12      | 0.55        | 23.2        | 24.8        | 51.5        | 0.11        | 150        | 118        | 1.5        | 63.5        | 0.55        | 28.7        | 5.7        | 65.0        | 0.106        | 0.77        | 5.5        |
| J                 | 13      | 0.63        | 22.7        | 16.4        | 60.3        | 0.07        |            |            | 1.5        | 81.5        | 0.44        | 26.0        | 6.4        | 67.2        | 0.046        | 0.33        | 8.5        |
| J                 | 6       | 0.72        | 22.8        | 18.8        | 57.7        | 0.08        |            |            | 1.5        | 77.4        | 0.52        | 25.3        | 7.3        | 66.9        | 0.046        | 0.37        | 5.0        |
| J                 | 207     | 0.00        | 22.9        | 12.4        | 64.7        | 0.02        |            |            | 1.5        | 87.5        | 0.60        | 24.9        | 6.7        | 67.8        | 0.010        |             |            |
| J                 | 210     | 0.00        | 23.0        | 15.3        | 61.7        | 0.04        |            |            | 1.5        | 83.8        | 0.46        | 25.4        | 7.4        | 66.8        | 0.046        |             |            |
| <b>average J</b>  |         | <b>0.44</b> | <b>22.8</b> | <b>17.4</b> | <b>59.4</b> | <b>0.08</b> | <b>160</b> | <b>111</b> | <b>1.5</b> | <b>77.8</b> | <b>0.54</b> | <b>25.6</b> | <b>6.7</b> | <b>67.1</b> | <b>0.070</b> | <b>0.49</b> | <b>6.1</b> |
| K                 | 2       | 0.85        | 23.8        | 25.5        | 49.9        | 0.06        |            |            | 1.5        | 68.2        | 0.81        | 29.5        | 6.6        | 63.1        | 0.089        | 0.73        | 8.5        |
| K                 | 14      | 0.57        | 25.4        | 14.2        | 59.8        | 0.08        |            |            | 1.5        | 83.4        | 0.33        | 28.2        | 7.2        | 64.2        | 0.078        | 0.78        | 5.0        |
| K                 | 19      | 0.60        | 25.5        | 13.9        | 59.9        | 0.05        | 180        | 78         | 1.5        | 80.9        | 0.52        | 29.0        | 6.3        | 64.2        | 0.046        | 0.70        | 8.0        |
| K                 | 208     | 0.00        | 23.7        | 24.2        | 52.1        | 0.12        |            |            | 1.5        | 73.4        | 0.50        | 28.2        | 6.9        | 64.5        | 0.126        |             |            |
| K                 | 106     | 0.61        | 19.6        | 28.6        | 51.2        | 0.08        |            |            | 1.5        | 63.5        | 0.27        | 26.9        | 7.7        | 65.1        | 0.188        | 0.85        | 8.0        |
| K                 | 107     | 0.55        | 19.3        | 31.1        | 49.1        | 0.11        | 220        | 130        | 1.5        | 65.1        | 0.36        | 26.6        | 7.6        | 65.5        | 0.063        | 0.71        | 8.0        |
| K                 | 108     | 0.64        | 25.8        | 7.9         | 65.6        | 0.11        |            |            | 1.5        | 92.7        | 0.32        | 28.2        | 5.3        | 66.2        | 0.077        | 0.74        | 8.5        |
| K                 | 110     | 0.56        | 22.0        | 24.3        | 53.1        | 0.06        |            |            | 1.5        | 69.2        | 0.37        | 27.5        | 11.3       | 60.8        | 0.037        | 0.68        | 8.0        |
| K                 | 111     | 0.56        | 23.3        | 22.1        | 54.1        | 0.08        |            |            | 1.5        | 75.6        | 0.38        | 28.2        | 9.0        | 62.4        | 0.082        | 0.80        | 7.5        |
| <b>average K</b>  |         | <b>0.55</b> | <b>23.2</b> | <b>21.3</b> | <b>55.0</b> | <b>0.08</b> | <b>200</b> | <b>104</b> | <b>1.5</b> | <b>74.7</b> | <b>0.43</b> | <b>28.0</b> | <b>7.6</b> | <b>64.0</b> | <b>0.087</b> | <b>0.75</b> | <b>7.7</b> |
| L                 | 109     | 0.70        | 24.2        | 18.4        | 56.6        | 0.11        | 170        | 60         | 1.5        | 77.0        | 0.37        | 27.7        | 7.2        | 64.7        | 0.075        | 0.99        | 7.5        |
| L                 | 112     | 0.52        | 18.8        | 27.7        | 53.0        | 0.08        |            |            | 1.5        | 59.4        | 0.39        | 22.7        | 7.5        | 69.4        | 0.044        | 0.38        | 3.5        |
| <b>average L</b>  |         | <b>0.61</b> | <b>21.5</b> | <b>23.1</b> | <b>54.8</b> | <b>0.09</b> | <b>170</b> | <b>60</b>  | <b>1.5</b> | <b>68.2</b> | <b>0.38</b> | <b>25.2</b> | <b>7.4</b> | <b>67.1</b> | <b>0.060</b> | <b>0.69</b> | <b>5.5</b> |
| M                 | 15      | 0.62        | 24.1        | 12.7        | 62.6        | 0.04        | 150        | 42         | 1.5        | 85.6        | 0.29        | 27.7        | 7.8        | 64.3        | 0.046        | 0.64        | 8.0        |
| M                 | 20      | 0.61        | 23.6        | 14.3        | 61.6        | 0.13        |            |            | 1.5        | 82.3        | 0.41        | 27.6        | 7.1        | 64.9        | 0.049        | 0.64        | 7.5        |
| M                 | 24      | 0.68        | 17.7        | 45.6        | 36.0        | 0.14        |            |            | 1.5        | 41.5        | 0.77        | 29.1        | 8.7        | 61.4        | 0.083        | 0.83        | 8.0        |
| <b>average M</b>  |         | <b>0.64</b> | <b>21.8</b> | <b>24.2</b> | <b>53.4</b> | <b>0.10</b> | <b>150</b> | <b>42</b>  | <b>1.5</b> | <b>69.8</b> | <b>0.49</b> | <b>28.1</b> | <b>7.8</b> | <b>63.5</b> | <b>0.059</b> | <b>0.70</b> | <b>7.8</b> |
| N                 | 104     | 0.76        | 27.2        | 15.2        | 56.8        | 0.15        | 260        | 118        | 1.5        | 84.4        | 0.36        | 30.8        | 5.7        | 63.1        | 0.089        | 0.72        | 8.0        |
| P                 | 3       | 0.86        | 28.4        | 10.1        | 60.6        | 0.03        | 140        | 82         | 1.5        | 88.4        | 0.36        | 29.7        | 4.8        | 65.1        | 0.107        | 0.53        | 8.5        |
| P                 | 16      | 0.58        | 26.9        | 8.4         | 64.1        | 0.12        |            |            | 1.5        | 93.9        | 0.40        | 28.0        | 6.8        | 64.9        | 0.098        | 0.74        | 7.0        |
| P                 | 23      | 0.60        | 23.8        | 16.2        | 59.4        | 0.16        | 300        | 350        | 1.5        | 79.1        | 0.39        | 25.1        | 9.1        | 65.5        | 0.157        | 0.70        | 2.5        |
| <b>average P</b>  |         | <b>0.68</b> | <b>26.3</b> | <b>11.6</b> | <b>61.4</b> | <b>0.10</b> | <b>220</b> | <b>216</b> | <b>1.5</b> | <b>87.2</b> | <b>0.38</b> | <b>27.6</b> | <b>6.9</b> | <b>65.2</b> | <b>0.121</b> | <b>0.66</b> | <b>6.0</b> |
| V                 | 21      | 0.76        | 25.4        | 22.8        | 51.0        | 0.07        | 150        | 150        | 1.5        | 65.8        | 0.46        | 32.0        | 8.4        | 59.2        | 0.057        | 0.85        | 7.5        |
| Y                 | 22      | 0.80        | 27.6        | 18.4        | 53.2        | 0.07        | 190        | 146        | 1.5        | 77.9        | 0.70        | 32.7        | 8.0        | 58.5        | 0.045        | 0.83        | 8.0        |
| Y                 | 7       | 0.87        | 27.7        | 22.6        | 48.8        | 0.03        | 110        | 56         | 1.5        | 68.4        | 0.63        | 32.2        | 5.9        | 31.3        | 0.028        | 0.72        | 7.5        |
| <b>average Y</b>  |         | <b>0.84</b> | <b>27.7</b> | <b>20.5</b> | <b>51.0</b> | <b>0.05</b> | <b>150</b> | <b>101</b> | <b>1.5</b> | <b>73.1</b> | <b>0.67</b> | <b>32.5</b> | <b>6.9</b> | <b>44.9</b> | <b>0.037</b> | <b>0.78</b> | <b>7.8</b> |
| AB                | 8       | 0.74        | 27.4        | 26.6        | 45.2        | 0.01        | 280        | 300        | 1.5        | 61.2        | 0.42        | 33.1        | 7.4        | 59.2        | 0.079        | 0.77        | 8.0        |
| AC                | 25      | 0.91        | 31.1        | 8.2         | 59.8        | 0.20        |            |            | 1.5        | 92.6        | 0.55        | 34.2        | 3.7        | 61.6        | 0.109        | 0.56        | 7.0        |
| AE                | 26      | 3.52        | 25.8        | 12.1        | 58.6        | 0.12        | 220        | 150        | 1.5        | 76.3        | 1.05        | 31.8        | 7.1        | 60.1        | 0.062        | 0.64        | 0.5        |
| AE                | 27      | 3.11        | 27.1        | 9.5         | 60.3        | 0.03        |            |            | 1.5        | 85.7        | 0.80        | 33.1        | 5.0        | 61.1        | 0.012        | 0.58        | 1.0        |
| <b>average AE</b> |         | <b>3.32</b> | <b>26.4</b> | <b>10.8</b> | <b>59.4</b> | <b>0.08</b> | <b>220</b> | <b>150</b> | <b>1.5</b> | <b>81.0</b> | <b>0.93</b> | <b>32.4</b> | <b>6.0</b> | <b>60.6</b> | <b>0.037</b> | <b>0.61</b> | <b>0.8</b> |

## SAMPLE COLLECTION AND ANALYSIS

Data for this study were collected from a number of mines to provide a wide distribution of samples from seams so that lateral distribution patterns of phosphorus in a number of seams could be documented. Generally full-seam samples were collected, though for some seams an additional sample representing about 1 metre of hangingwall coal was also collected. Coal samples were analyzed for ash, volatile matter, fixed carbon and phosphorus on a raw basis and washed samples (1.5 specific gravity) were analyzed for sulphur and FSI. Some raw samples were analyzed for barium and strontium. For some seams, 5 centimetres of the hangingwall rock was sampled and analyzed for phosphorus. Analytical data for two mines is reported in Table 1.

Some samples were prepared for petrographic and SEM work. Samples were crushed to pass a 20 mesh screen, mixed 50/50 with a binder and compacted under pressure and a temperature of 140°C. Petrographic analyses involved counting 300 grains using oil immersion. This number is only sufficient to estimate petrographic distributions. Where ever possible geophysical logs were collected for holes close to the sample sites.

## A MODEL FOR PHOSPHORUS MOBILITY IN COAL-FORMING ENVIRONMENTS

Phosphorus may be removed from vegetation during humification as  $H_2PO_4^{-2}$ . If it remains in solution it may leave the peat as the interstitial water is expelled during compaction. If it remains in the peat it may recrystallize as aluminium or iron phosphates in low pH environments or as apatite in moderate pH environments, assuming that the required cations are available. It is possible to match these environments in general terms to those that form different macerals.

In dry environments, that favour the formation of inertinite and destruction of woody tissue, the phosphorus may remain largely insoluble, finely dispersed in inertinite or authogenic mineral matter. Phosphorus has low volatility and remains in coal during carbonization or ashing in an oxidizing environment (Mahony *et al.*, 1981) and consequently it probably also remains in inertinite formed by forest fires. In this case the phosphorus content of inert macerals may approach that of the original vegetation if it is not subsequently leached out. If the vegetation is completely destroyed by fire then the phosphorus will be dispersed as fine particles, that may or may not settle back into the swamp.

In wet acid environments phosphorus will be leached out of the vegetation during humification as  $H_2PO_4^{-}$  and in more strongly acid environments as  $H_2PO_4^{-}$ . At pH values of 4 to 5 crandallite group minerals are stable but apatite is soluble. As phosphorus is leached out of the vegetation it combines with aluminum in part extracted from the vegetation and strontium, barium and calcium, either derived from the vegetation or from the interstitial water. Because of the insolubility of crandallite minerals they will

tend to form close to source. Other minerals that will form using the  $Al^{+3}$ ,  $Fe^{+2}$ ,  $Ca^{+2}$ ,  $Ba^{+2}$  and  $Sr^{+2}$  in solution with the available orthophosphoric acid are waverlite  $Al_3(OH)_3(PO_4)_2 \cdot 5H_2O$  and vivianite  $Fe_3(PO_4)_2 \cdot 8H_2O$ . Vivianite has been reported in recent sediments (Coleman, 1966) in association with pyrite. It has not been identified in British Columbia coals, but is reported in other coals (Mahony *et al.*, 1981). At higher pH values aluminum and iron are not soluble, the solubility of orthophosphoric acid is less, and the phosphorus probably crystallizes as apatite ( $Ca_5(PO_4)_3$ ) using available calcium.

The environment that is ideal for the formation of the maximum amount of vitrinite and minimum amount of inertinite is one of moderate pH and saturation below the water table. Within this environment higher pH values are characterized by high contents of structured vitrinite (tellinite or telocollinite) with finely dispersed phosphorous and low contents of inherent mineral matter and unstructured vitrinite. If the pH is somewhat lower, then unstructured vitrinite (gelovitrinite and detrovitrinite, or vitrinite B) will predominate. The phosphorus will be dissolved from the gellified humic material and either, removed from the peat, or redeposited as apatite in available porosity in semifusinite or fusinite when pH values increase. It is reasonable therefore to expect higher phosphorus concentrations in structured vitrinite than in unstructured vitrinite, which has been completely gellified. Phosphorus contents will be higher in inertinite-rich seams if they contain a high proportion of porous semifusinite and fusinite, which are generally generated by burning or charring woody material.

Environments which are generally wet with moderate pH, but have dry periods when inertinite macerals form, will experience some mobilization of phosphorus. If the inertinite has a high percentage of semifusinite derived from woody plants, then some of the phosphorus may be redeposited as apatite in semifusinite lumen. If at a later time there is introduction of less acid water, then apatite may crystallize on fractures in the coal and the surrounding rocks. If it crystallizes in coal on cleats it will be preferentially concentrated in the structured vitrinite because this maceral usually develops the best micro-cleats.

Liptinite material probably contained high concentrations of phosphorus prior to peatification. Concentrations could be in the percent range, in which case 1% liptinite could account for 0.01% phosphorus in the peat. In medium-volatile coals the liptinite is largely destroyed but variations in phosphorus content related to variations in original liptinite content may remain and produce unpredictable variations in concentration.

Phosphorus is most easily removed from highly acid peat swamps, in which there is not a lot of Ca, Al and Fe available to form insoluble compounds with the orthophosphate. As the interstitial water is removed during compaction the phosphorus is carried into the surrounding rocks. There are a number of studies indicating that hangingwall and footwall rock is sometimes enriched in phosphorus (Dixon *et al.*, 1964).

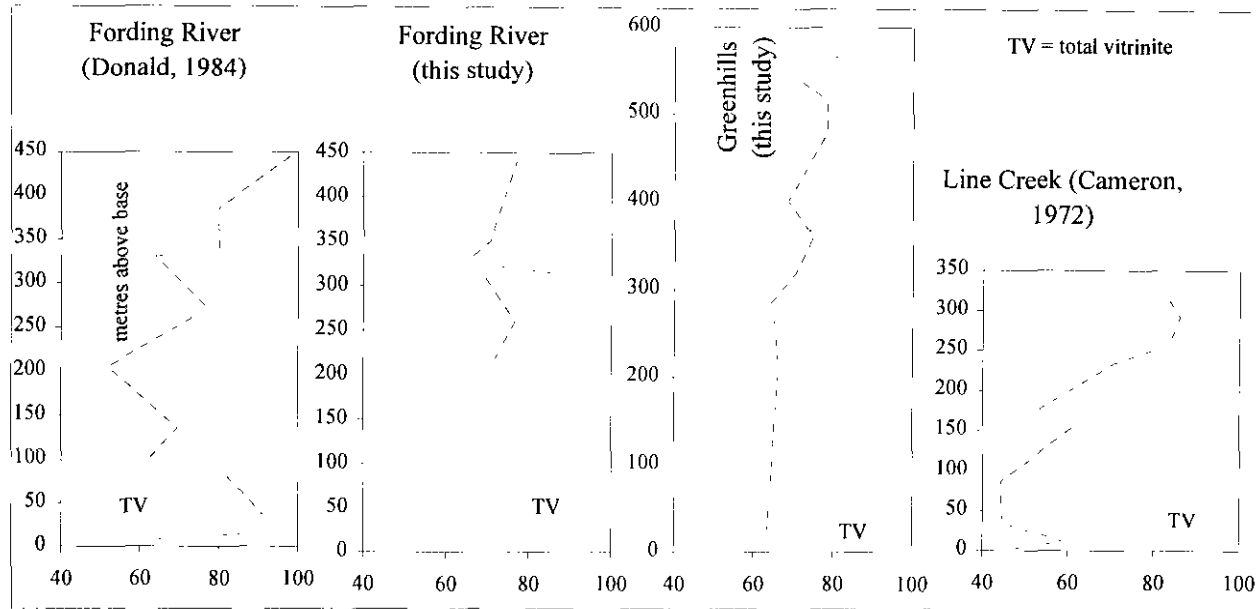


Figure 4: Total vitrinite *versus* distance from base of Mist Mountain Formation for a number of sections in the Elk Valley coalfield. TV = total vitrinite.

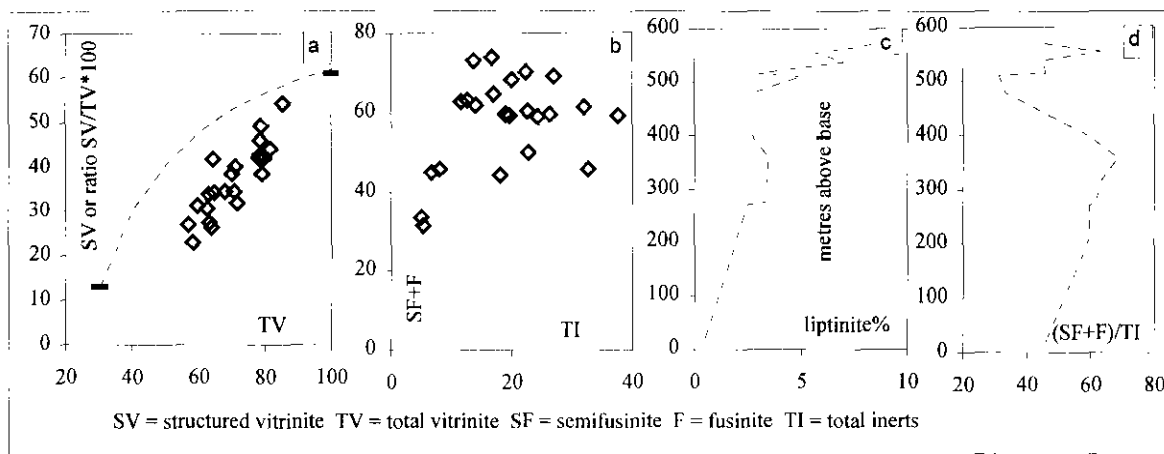


Figure 5: Maceral *versus* maceral and maceral *versus* depth relationships: (a) structured vitrinite *versus* total vitrinite and ratio of structured vitrinite/ total vitrinite *versus* total vitrinite; (b) semifusinite+fusinite *versus* total inerts; (c) structured inertinite (semifusinite+fusinite) *versus* distance from base of Mist Mountain Formation; (d) liptinite *versus* distance from base of Mist Mountain Formation. SF = semifusinite. F = fusinite TV = total vitrinite. SV = structured vitrinite TI = total inerts.

It appears that the phosphorus distribution in coal is probably complex. Phosphorus mobilized out of gellified humic material (unstructured vitrinite) may precipitate as apatite in semifusinite porosity or crystallize as apatite on cleats, which are concentrated in structured vitrinite. Some structured vitrinite and possibly liptinites may retain near original contents of phosphorus. Semifusinite based on its porosity may contain high concentrations of remobilized phosphorus, whereas unstructured vitrinite may be largely flushed of phosphorus. Phosphorus in structured vitrinite and semifusinite will be very difficult to remove, whereas phosphorus on cleats may be more easy to remove.

If the phosphorus is removed from the peat (mainly the gellified humic material), then it may be recycled upwards from the dead vegetation into the overlying growing vegetation and therefore effectively migrate upwards through the swamp. In this case, because a small initial source of phosphorus is constantly reused by new vegetation the total phosphorus content of the seam may be

less than expected, based on the amount of vegetation represented by the seam. In this situation there need be no process of phosphorus removal at work to explain phosphorus contents of coal that are lower than those of vegetation. If the upper part of the seam is rich in semifusinite, then the phosphorus will be trapped in the hangingwall coal, otherwise it may move into the unconsolidated overlying sediments or be redispersed through decomposing vegetation by acid peat waters. In this case it will probably crystallize as crandallite between macerals in the lower pH environments deeper in the peat swamp. The phosphorus content of a seam will be controlled by the initial amount of phosphorus leached from the footwall rocks. There need be no additional source of phosphorus as the peat accumulates as long as the phosphorus is effectively recycled upwards into the growing vegetation. If the process is effective, then there should be an inverse correlation between thickness and phosphorus content of the seam and there should be a

tendency for the phosphorus contents to be higher in hangingwall coal. There is sometimes a weak tendency for higher phosphorus in hangingwall coal as seen in striplog data in Ward *et al.*, (1996), Ryan and Grieve, (1995) and Gluskoter *et al.* (1977). No inverse correlation of phosphorus content and seam thickness has been observed, but variations in rank and petrography may have masked the effect.

## REGIONAL PETROGRAPHY

A total of 38 petrographic analyses were completed on full seam samples (Table 2) from two general areas in the Elk Valley coalfield. There is a general tendency for vitrinite to increase and inertinite to decrease up section (Cameron, 1972); Grieve, 1993; Donald, 1994) and is seen in the present study (Figure 4). Cameron and Donald suggest that this is related to a progressive change in vegetation type from grasses low in the section to trees higher in the section. Grieve suggests that it may be due to higher ground water levels in coal forming environments higher in the section. A swamp dominated by grasses, if burnt over by summer fires, would probably generate a higher proportion of fine inertinite (inertodetrinite) derived from charring and seams low in the section are characterized by high percentages of inertinite and inertodetrinite (Figure 5d).

There are a number of other progressive changes in petrography up section that are important. The proportion of structured vitrinite to total vitrinite increases as the amount of total vitrinite increases (Figure 5a). This is also documented by Diessel (1992, page 99) for Carboniferous and Permian coals. There is an increase in the amount of liptinite up section (Figure 5c), which is largely related to rank. Few papers discuss the relationship between the petrographic composition of a seam and the lithology of the footwall and hangingwall rocks. Cameron (1972) did observe a correlation between the amount of sandstone in the hangingwall and the amount of inertodetrinite in the seam. If there is a relationship between interburden lithology and seam petrography, then this might provide a preliminary way of estimating phosphorus content and other coal-quality parameters that depend on petrography.

## PETROGRAPHY AND PHOSPHORUS DATA

As a start to analyzing the data, raw phosphorus *versus* distance from base of Mist Mountain Formation. profiles are constructed for a number areas (Figure 6). There are general similarities and it appears that there are at least three intervals in the coal section (at about 200, 400 and 550 metres) where the phosphorus tends to be higher.

The model discussed above proposes that there should be a correlation between structured vitrinite plus structured inertinite and P contents. Correlation matrixes for phosphorus and maceral data from this study and that of Ward *et al.* (1996) indicate that for data sets with higher

Table 2  
Preliminary petrography for samples from 2 areas Elk Valley coalfield

| VOLUME PERCENTS |      |           |           |               |                |                |                 |              |          |           |                 |             |                |          |
|-----------------|------|-----------|-----------|---------------|----------------|----------------|-----------------|--------------|----------|-----------|-----------------|-------------|----------------|----------|
| sample          | seam | liptinite | tellinite | telocollinite | desmocollinite | detrovitrinite | total reactives | semifusinite | fusinite | macrinite | inertodetrinite | total inert | mineral matter | ash wt % |
| 9               | A    | 0         | 2         | 25            | 35             | 1              | 63              | 14           | 1        | 7         | 10              | 33          | 4              | 7        |
| 102             | G    | 0         | 3         | 18            | 19             | 5              | 45              | 11           | 0        | 5         | 11              | 27          | 29             | 39       |
| 103             | G    | 0         | 6         | 28            | 26             | 3              | 63              | 7            | 0        | 5         | 5               | 17          | 19             | 28       |
| 112             | G    | 2         | 11        | 25            | 23             | 2              | 63              | 4            | 0        | 3         | 6               | 12          | 25             | 35       |
| 113             | G    | 0         | 6         | 23            | 20             | 6              | 56              | 4            | 1        | 3         | 5               | 12          | 32             | 42       |
| 101             | G1   | 0         | 15        | 27            | 21             | 8              | 71              | 4            | 0        | 2         | 7               | 12          | 17             | 25       |
| 5               | G    | 3         | 8         | 28            | 30             | 1              | 70              | 10           | 1        | 6         | 5               | 23          | 7              | 12       |
| 10              | G    | 3         | 5         | 34            | 21             | 2              | 64              | 17           | 1        | 6         | 2               | 27          | 9              | 14       |
| 18              | G    | 1         | 11        | 29            | 31             | 0              | 71              | 13           | 2        | 4         | 3               | 22          | 7              | 11       |
| 1               | G    | 2         | 10        | 20            | 26             | 2              | 60              | 14           | 1        | 2         | 8               | 24          | 16             | 24       |
| 105             | I    | 1         | 16        | 31            | 29             | 1              | 77              | 7            | 0        | 3         | 6               | 16          | 7              | 11       |
| 4               | J    | 2         | 7         | 25            | 33             | 0              | 68              | 11           | 1        | 3         | 5               | 20          | 12             | 19       |
| 6               | J    | 2         | 6         | 26            | 33             | 2              | 71              | 10           | 1        | 3         | 4               | 19          | 10             | 16       |
| 12              | J    | 2         | 6         | 19            | 25             | 5              | 57              | 14           | 0        | 3         | 6               | 23          | 20             | 29       |
| 13              | J    | 3         | 7         | 24            | 29             | 1              | 65              | 15           | 0        | 4         | 7               | 26          | 9              | 14       |
| 11              | J4   | 3         | 6         | 21            | 31             | 1              | 63              | 19           | 1        | 6         | 6               | 32          | 5              | 9        |
| 19              | K    | 4         | 7         | 31            | 32             | 3              | 78              | 9            | 0        | 3         | 2               | 14          | 8              | 13       |
| 107             | K    | 4         | 8         | 27            | 27             | 4              | 69              | 2            | 0        | 3         | 5               | 11          | 20             | 29       |
| 108             | K    | 2         | 15        | 41            | 33             | 0              | 91              | 3            | 1        | 1         | 2               | 7           | 2              | 4        |
| 110             | K1   | 1         | 8         | 30            | 30             | 10             | 79              | 2            | 0        | 1         | 3               | 6           | 15             | 23       |
| 106             | K2   | 1         | 9         | 27            | 20             | 7              | 65              | 7            | 0        | 2         | 3               | 12          | 23             | 33       |
| 2               | K    | 3         | 5         | 27            | 28             | 1              | 63              | 10           | 1        | 2         | 4               | 17          | 20             | 29       |
| 109             | L    | 1         | 4         | 35            | 27             | 4              | 71              | 2            | 0        | 1         | 5               | 9           | 21             | 30       |
| 15              | M    | 2         | 6         | 19            | 36             | 2              | 64              | 13           | 0        | 2         | 4               | 20          | 16             | 24       |
| 17              | M    | 4         | 6         | 34            | 33             | 4              | 81              | 7            | 1        | 2         | 3               | 13          | 6              | 10       |
| 20              | M    | 5         | 10        | 28            | 37             | 1              | 80              | 11           | 1        | 2         | 2               | 17          | 4              | 6        |
| 104             | N1   | 4         | 9         | 24            | 36             | 4              | 77              | 6            | 1        | 1         | 3               | 11          | 12             | 19       |
| 3               | P    | 3         | 8         | 28            | 39             | 1              | 79              | 9            | 1        | 3         | 1               | 14          | 7              | 12       |
| 16              | P    | 3         | 6         | 14            | 34             | 1              | 58              | 22           | 0        | 7         | 9               | 38          | 4              | 7        |
| 21              | V1   | 3         | 7         | 36            | 28             | 4              | 78              | 2            | 0        | 2         | 2               | 5           | 17             | 25       |
| 7               | Y    | 5         | 16        | 21            | 31             | 6              | 79              | 2            | 0        | 2         | 1               | 5           | 16             | 24       |
| 22              | Y4   | 3         | 8         | 32            | 29             | 6              | 78              | 3            | 0        | 1         | 3               | 8           | 14             | 21       |
| 8               | AB   | 7         | 5         | 20            | 32             | 7              | 72              | 2            | 1        | 2         | 1               | 7           | 22             | 31       |
| 25              | AC   | 6         | 8         | 40            | 30             | 1              | 85              | 7            | 0        | 3         | 2               | 12          | 3              | 5        |
| 27              | AE   | 8         | 8         | 33            | 27             | 2              | 79              | 7            | 1        | 5         | 5               | 18          | 3              | 6        |

minor amounts of gelovitrinite added to detrovitrinite

minor amounts of micrinite added to inertodetrinite

phosphorus contents, phosphorus correlates with structured vitrinite (tellinite or telocollinite) and structured inertinite (semifusinite and fusinite) (Table 3). Phosphorus correlates with mineral matter in one data set (hole 15177), which is characterized by low phosphorus contents. Phosphorus does not correlate with liptinite or micrinite which is probably developed from liptinite. There are therefore two major variables, the amount of structured vitrinite and structured inertinite, that influence the concentration of phosphorus in a coal. A plot of structured vitrinite plus structured inertinite *versus* P% for data set 1 (Table 3) does in fact have a slightly better correlation coefficient (0.38) than values for telocollinite (0.33) or semifusinite (0.31) (Figure 7), though all these coefficients are marginally significant.

The data can also be displayed using triangular plots, in which the three corners of the triangle are inertinite, structured vitrinite and unstructured vitrinite plotted on an

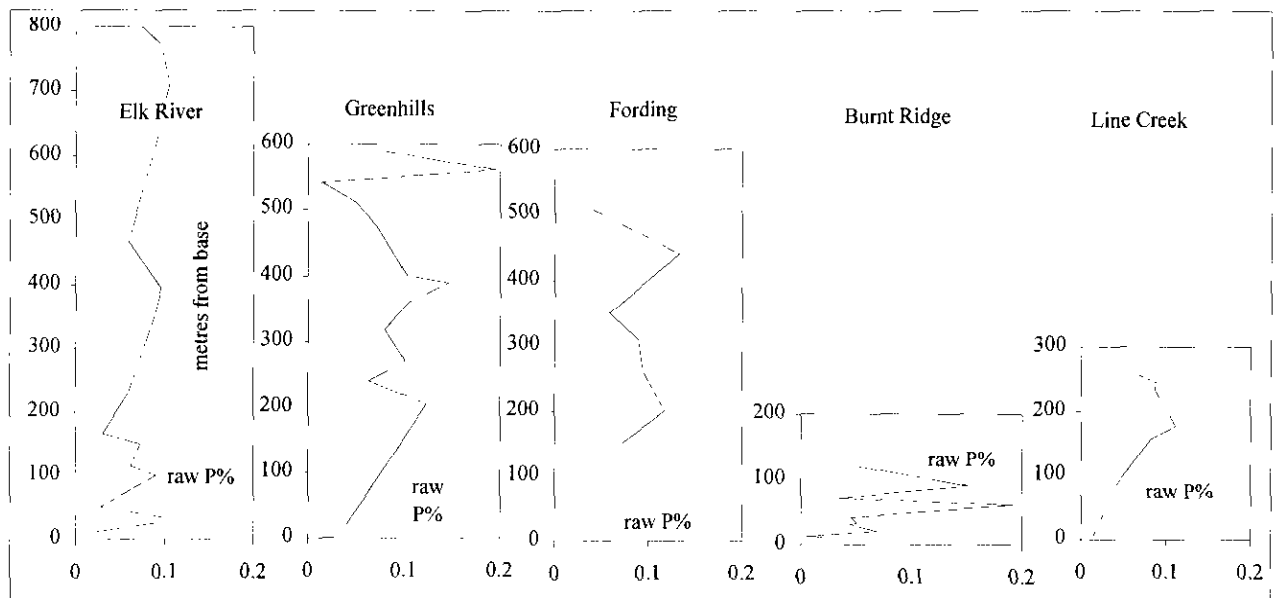


Figure 6: Phosphorus profiles for generalized stratigraphic sections of the Mist Mountain Formation, Elk Valley Coalfield.

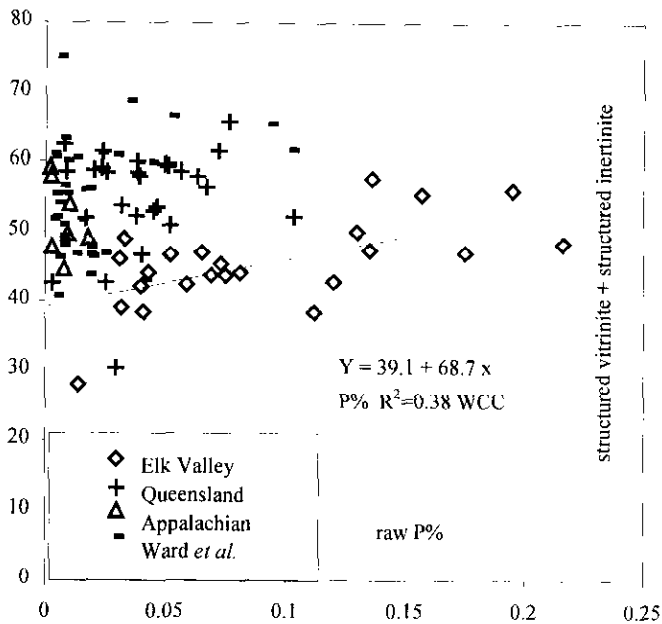


Figure 7: Raw phosphorus versus (structured vitrinite + structured inertinite) plot for coals from Elk Valley coalfield, Australia and eastern USA. Diamonds = Elk Valley data, Cross = Australian data from Ward *et al.* (1996), dash = data from Queensland Coal Board, Triangle = Appalachian data from Price *et al.* (1987).

ash free basis. Phosphorus contents are posted next to the plotted position of the data (Figures 8, 9 and 10). Though there is considerable scatter in the data there is a distinct tendency for phosphorus concentrations to decrease towards the unstructured vitrinite corner. The petrography of the 1.5 specific gravity wash samples is somewhat different from that of the raw petrographic samples, however by posting a phosphorus ease-of-washing number next to the data in a triangular plot it is possible to estimate the ease of extraction of phosphorus from the three maceral groups (Figures 8 and 9). This approach differentiates phosphorus disseminated in structured vitrinite from phosphorus on cleats in vitrinite, because the

later will be easier to wash out. Phosphorus is very difficult to remove from unstructured vitrinite and about equally difficult to remove from inertinite and structured vitrinite.

The petrographic data and phosphorus data add support to the model outlined above and provide an explanation for why, though apatite is present in the porosity in semifusinite and fusinite, the total phosphorus content often correlates with the reactive content of seams. Previously Ryan and Grieve (1995) and Ward *et al.*, (1966) explained this by assuming that inertinite in vitrinite-rich seams contained a higher proportion of phosphorus than inertinite in vitrinite-poor seam. Apatite contains about 17% phosphorus and therefore a semifusinite grain with 10% porosity could have a phosphorus content of 1.7% and if grains of this composition made up 10% of the seam then they would contribute 0.17% phosphorus to the sample. High phosphorus concentrations in vitrinite-rich samples can be explained if the remaining small percentage of inertinite has apatite filled porosities in the range of 5 to 20% and that in inertinite rich, phosphorus poor, samples the apatite-filled porosity is less than 1%. Obviously the explanation is feasible but it is difficult to derive a process that causes inertinite-poor samples to have a higher proportion of semifusinite and fusinite. In fact data from this study indicates either no correlation between structured inertinite and total inertinite or at low inertinite contents the proportion of structured inertinite decreases (Figure 5b). Other authors (Grieve, 1993) have found that the ratio of semifusinite+fusinite to total inertinite is constant for varying concentrations of inertinite.

Some samples were analyzed for barium and strontium concentrations (Table 1). A number of studies indicate that despite reported occurrences of apatite in coal, phosphorus often correlates with strontium (Gluskoter *et al.*, 1977), probably because of the presence of goyazite. Generally phosphorus concentrations in

Table 3  
Correlation matrixes for Elk Valley and Australian data  
from Ward *et al.* (1996). mic=micrinite

|     | P% raw | lipinite                                  | tellinite | telocollinite | desmoV | detroV | semi.fusinite | fusinite | macrinite | inertetrinite | min matter |  |
|-----|--------|-------------------------------------------|-----------|---------------|--------|--------|---------------|----------|-----------|---------------|------------|--|
|     | A      | B                                         | C         | D             | E      | F      | G             | H        | I         | J             | K          |  |
| A   | 1.00   | GREENHILLS                                |           |               |        |        |               |          |           |               |            |  |
| B   | -0.05  | 1.00                                      |           |               |        |        |               |          |           |               |            |  |
| C   | .01    | .25                                       | 1.00      |               |        |        |               |          |           |               |            |  |
| D   | .33    | .29                                       | .00       | 1.00          |        |        |               |          |           |               |            |  |
| E   | -.16   | -.08                                      | .01       | -.20          | 1.00   |        |               |          |           |               |            |  |
| F   | -.19   | .35                                       | .20       | -.10          | -.23   | 1.00   |               |          |           |               |            |  |
| G   | .31    | -.53                                      | -.33      | -.43          | -.07   | -.56   | 1.00          |          |           |               |            |  |
| H   | .15    | -.15                                      | -.03      | .13           | .05    | -.42   | .08           | 1.00     |           |               |            |  |
| I   | .20    | -.22                                      | -.36      | -.10          | -.11   | -.43   | .63           | .15      | 1.00      |               |            |  |
| J   | -.07   | -.39                                      | -.43      | -.57          | -.06   | -.27   | .61           | .01      | .54       | 1.00          |            |  |
| K   | -.45   | -.07                                      | .02       | -.36          | -.29   | .57    | -.34          | -.20     | -.59      | -.09          | 1          |  |
| A   | 1.00   | FORDING                                   |           |               |        |        |               |          |           |               |            |  |
| B   | .13    | 1.00                                      |           |               |        |        |               |          |           |               |            |  |
| C   | -.20   | .15                                       | 1.00      |               |        |        |               |          |           |               |            |  |
| D   | -.13   | .09                                       | .44       | 1.00          |        |        |               |          |           |               |            |  |
| E   | .08    | .64                                       | .30       | .52           | 1.00   |        |               |          |           |               |            |  |
| F   | -.16   | -.30                                      | -.30      | -.36          | -.36   | 1.00   |               |          |           |               |            |  |
| G   | .20    | -.34                                      | -.18      | -.59          | -.34   | -.11   | 1.00          |          |           |               |            |  |
| H   | .58    | .28                                       | .12       | .19           | .41    | -.24   | -.13          | 1.00     |           |               |            |  |
| I   | .03    | -.39                                      | -.33      | -.58          | -.54   | -.17   | .65           | -.35     | 1.00      |               |            |  |
| J   | .22    | -.43                                      | -.27      | -.63          | -.62   | .03    | .57           | -.44     | .70       | 1.00          |            |  |
| K   | .02    | -.35                                      | -.71      | -.69          | -.80   | .40    | .22           | -.22     | .49       | .51           | 1          |  |
| A   | 1.00   | Goonyella lower seam riverside hole 15177 |           |               |        |        |               |          |           |               |            |  |
| B   | -.47   | 1.00                                      |           |               |        |        |               |          |           |               |            |  |
| C   | -.10   | -.04                                      | 1.00      |               |        |        |               |          |           |               |            |  |
| F   | -.57   | .45                                       | .69       | ND            | ND     | 1.00   |               |          |           |               |            |  |
| G   | -.01   | .19                                       | -.81      | ND            | ND     | -.57   | 1.00          |          |           |               |            |  |
| H   | -.40   | .28                                       | .76       | ND            | ND     | .66    | -.51          | 1.00     |           |               |            |  |
| I   | -.21   | .36                                       | -.75      | ND            | ND     | -.29   | .79           | -.52     | 1.00      |               |            |  |
| mic | -.57   | .11                                       | .03       | ND            | ND     | .37    | -.05          | .32      | .04       |               |            |  |
| J   | .15    | -.15                                      | -.81      | ND            | ND     | -.72   | .71           | -.76     | .72       | 1.00          |            |  |
| K   | .53    | -.45                                      | -.50      | ND            | ND     | -.65   | .02           | -.54     | -.08      | .27           | 1          |  |
| A   | 1.00   | Goonyella lower seam riverside hole 15176 |           |               |        |        |               |          |           |               |            |  |
| B   | -.07   | 1.00                                      |           |               |        |        |               |          |           |               |            |  |
| C   | .79    | .14                                       | 1.00      |               |        |        |               |          |           |               |            |  |
| F   | .33    | .32                                       | .62       | ND            | ND     | 1.00   |               |          |           |               |            |  |
| G   | -.80   | -.20                                      | -.93      | ND            | ND     | -.64   | 1.00          |          |           |               |            |  |
| H   | .47    | .13                                       | .58       | ND            | ND     | .25    | -.50          | 1.00     |           |               |            |  |
| I   | -.44   | .24                                       | -.60      | ND            | ND     | -.55   | .65           | -.30     | 1.00      |               |            |  |
| mic | -.26   | .65                                       | .05       | ND            | ND     | .49    | -.20          | .02      | -.02      |               |            |  |
| J   | -.61   | .04                                       | -.80      | ND            | ND     | -.56   | .82           | -.20     | .86       | 1.00          |            |  |
| K   | -.15   | -.36                                      | -.41      | ND            | ND     | -.50   | .20           | -.54     | -.17      | -.11          | 1          |  |

plants are 20 to 40 times higher than concentrations of aluminum, barium and strontium and 10 to 20 times less than that of calcium (Mason, 1966, page 228). The proportions of these elements in Goyazite is Sr/P=1.4, Ba/P=2.2 and Al/P=1.3. Consequently there has to be an external source of barium, strontium and aluminum to crystallize goyazite or gorceixite using phosphorus from the vegetation. Average concentrations of strontium in vegetation and fresh water are <100 ppm and 1 ppm respectively, whereas the average content in samples from

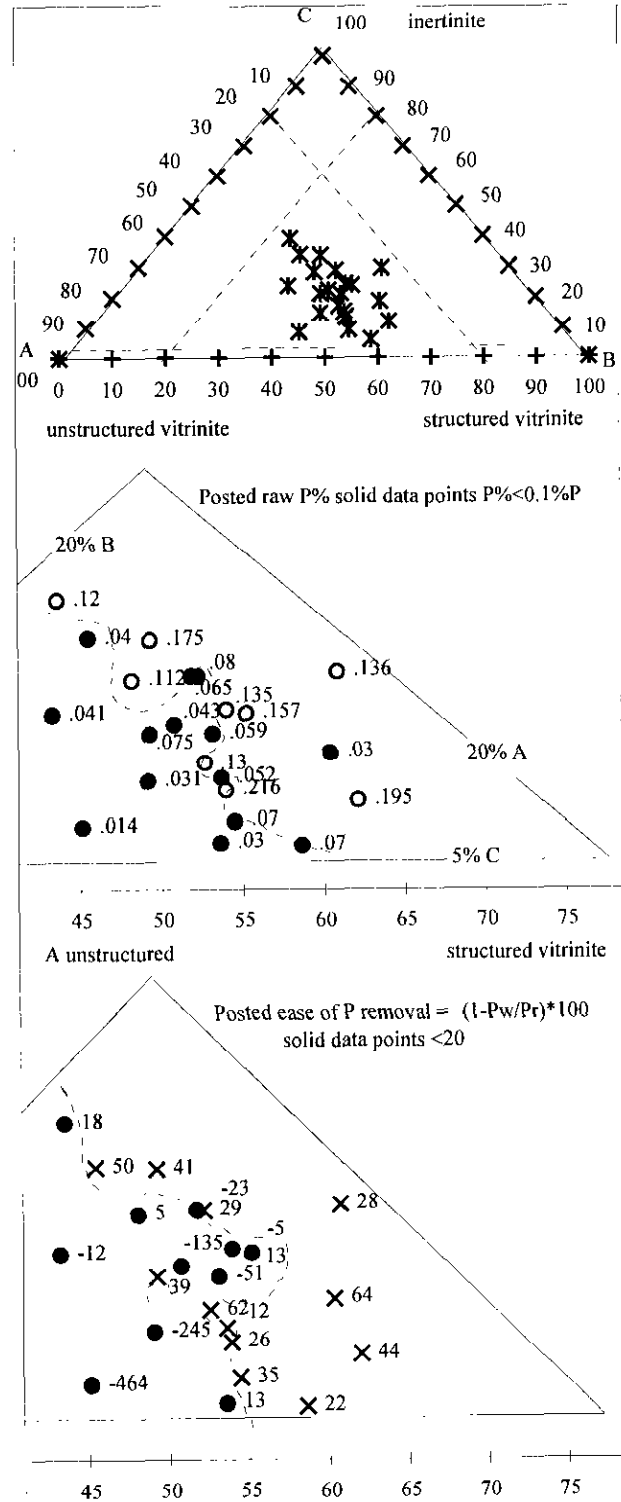


Figure 8: Triangular plots of maceral composition with posted phosphorus contents from Greenhills mine samples. Triangles B and C are the area enclosed by dashed lines in triangle A. Contour lines separate higher P concentrations from lower concentrations (plot B) and difficult to wash samples from easier to wash samples.

this study is 113 ppm. Correlation matrixes indicate that both strontium and barium correlate weakly with structured vitrinite and mineral matter but do not correlate with inertinite or unstructured vitrinite (Table 4). This supports an association of crandallite minerals with

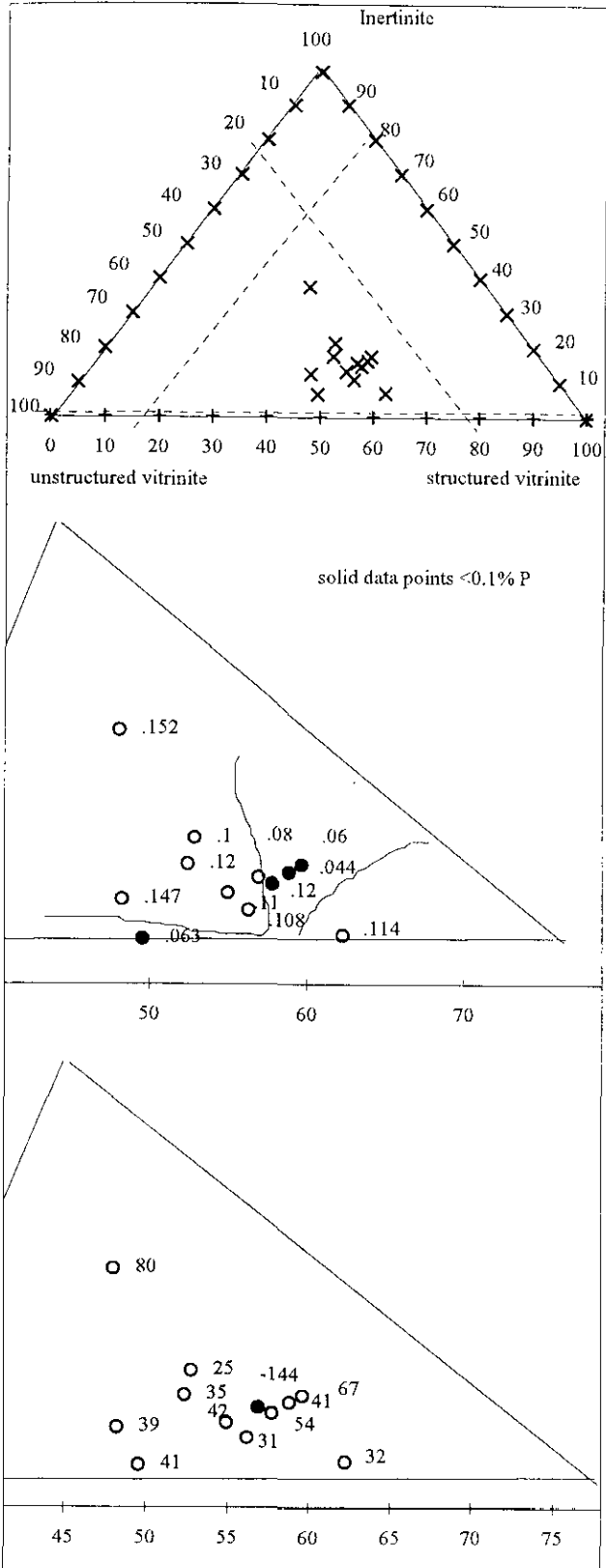


Figure 9: Triangular plots of maceral composition with posted phosphorus contents, Fording mine. Format similar to Figure 8.

Figure 10: On right. Triangular plots of maceral composition with posted phosphorus contents; data from Ward *et al.* (1996). Circle plots =Warkworth, Cross =Tahmoor, Star= Hole 15176, Diamond =hole 15177.

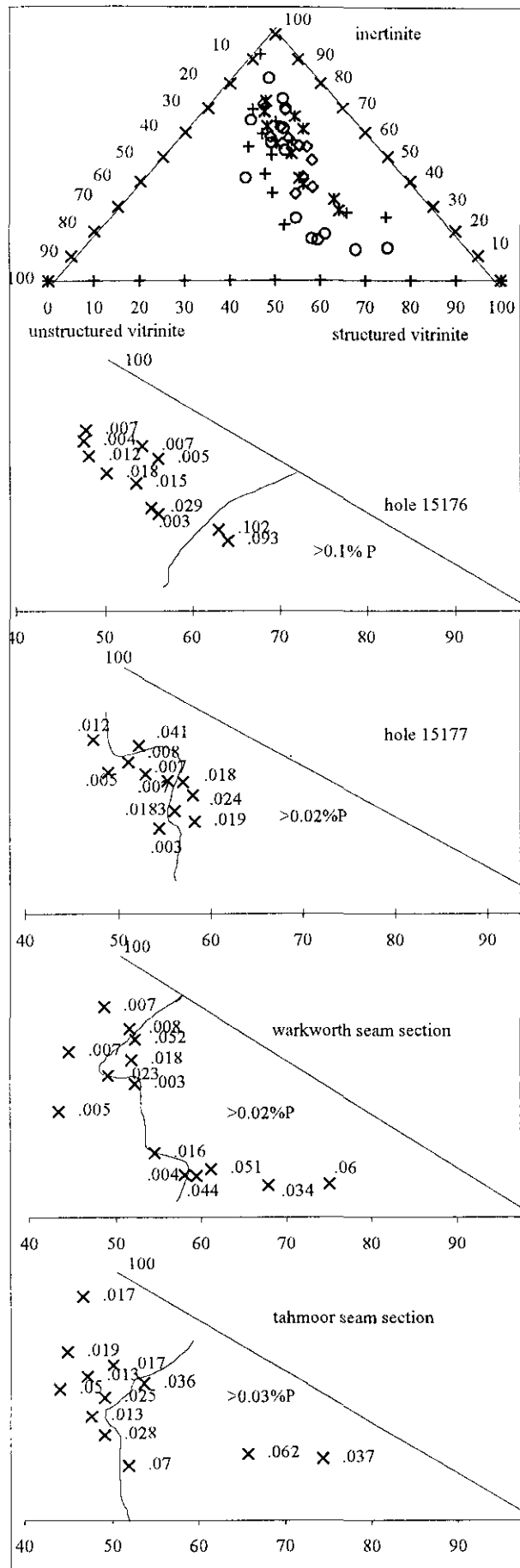


Table 4  
Correlation matrix for Ba and Sr versus all petrography data

|    | Ba   | lipinitite | telinitite | telocollinitite | desmoV | detroV | semi fusinite | fusinite | macramite | inertedetrinite | min matter |
|----|------|------------|------------|-----------------|--------|--------|---------------|----------|-----------|-----------------|------------|
|    | Ba   | A          | B          | C               | D      | E      | F             | G        | H         | I               | J          |
| Ba | 1.00 |            |            |                 |        |        |               |          |           |                 |            |
| A  | .43  | 1.00       |            |                 |        |        |               |          |           |                 |            |
| B  | .10  | .25        | 1.00       |                 |        |        |               |          |           |                 |            |
| C  | .21  | .29        | .00        | 1.00            |        |        |               |          |           |                 |            |
| D  | -.07 | -.08       | .01        | -.20            | 1.00   |        |               |          |           |                 |            |
| E  | .00  | .35        | .20        | -.10            | -.23   | 1.00   |               |          |           |                 |            |
| F  | -.12 | -.53       | -.33       | -.43            | -.07   | -.56   | 1.00          |          |           |                 |            |
| G  | -.30 | -.15       | -.03       | .13             | .05    | -.42   | .08           | 1.00     |           |                 |            |
| H  | -.49 | -.22       | -.36       | -.10            | -.11   | -.43   | .63           | .15      | 1.00      |                 |            |
| I  | -.55 | -.39       | -.43       | -.57            | -.06   | -.27   | .61           | .01      | .54       | 1.00            |            |
| J  | .27  | -.07       | .02        | -.36            | -.29   | .57    | -.34          | -.20     | -.59      | -.09            | 1.00       |
| Sr | 1.00 |            |            |                 |        |        |               |          |           |                 |            |
| A  | .08  | 1.00       |            |                 |        |        |               |          |           |                 |            |
| B  | .12  | .25        | 1.00       |                 |        |        |               |          |           |                 |            |
| C  | .23  | .29        | .00        | 1.00            |        |        |               |          |           |                 |            |
| D  | -.60 | -.08       | .01        | -.20            | 1.00   |        |               |          |           |                 |            |
| E  | .11  | .35        | .20        | -.10            | -.23   | 1.00   |               |          |           |                 |            |
| F  | -.13 | -.53       | -.33       | -.43            | -.07   | -.56   | 1.00          |          |           |                 |            |
| G  | -.02 | -.15       | -.03       | .13             | .05    | -.42   | .08           | 1.00     |           |                 |            |
| H  | -.48 | -.22       | -.36       | -.10            | -.11   | -.43   | .63           | .15      | 1.00      |                 |            |
| I  | -.08 | -.39       | -.43       | -.57            | -.06   | -.27   | .61           | .01      | .54       | 1.00            |            |
| J  | .50  | -.07       | .02        | -.36            | -.29   | .57    | -.34          | -.20     | -.59      | -.09            | 1.00       |

structured vitrinite and also in that phosphorus does not correlate with ash that the source for the barium and strontium is probably the extraneous ash.

The strontium and barium data do not correlate well with raw phosphorus because of the presence of apatite. There is however a better correlation of Sr+Ba with wash phosphorus indicating that some apatite is being removed, but crandallite minerals are remaining. Assuming that all the strontium and barium occurs in crandallite minerals and that the average ratio of Ba+Sr to phosphorus in these minerals is about 2, it is then possible to estimate the total amount of phosphorus present in crandallite minerals rather than apatite. It appears that the crandallite minerals account for up to 0.02% phosphorus and therefore account for less than half the phosphorus present in most samples.

## SCANNING ELECTRON MICROSCOPE WORK

A number of samples were studied using back scattered electron imaging technique on a Philips XL30 scanning electron microscope (SEM). Pellets analyzed by the SEM were made with a binder doped with one part in five of calcium fluoride. This increased the average atomic number of the binder and provided a better back scattered definition of the coal grains. The effect was to outline grains of the transoptic binder and produce a

groundmass mosaic pattern, which made it easier to locate coal fragments. The polished surfaces of pellets were photographed using a close-up lens. The colour print film negatives were then mounted as slides and the negative image enlarged using a projection and colour photocopy

## SCANNING ELECTRON MICROSCOPE WORK

A number of samples were studied using back scattered electron imaging technique on a Philips XL30 scanning electron microscope (SEM). Pellets analyzed by the SEM were made with a binder doped with one part in five of calcium fluoride. This increased the average atomic number of the binder and provided a better back scattered definition of the coal grains. The effect was to outline grains of the transoptic binder and produce a groundmass mosaic pattern, which made it easier to locate coal fragments. The polished surfaces of pellets were photographed using a close-up lens. The colour print film negatives were then mounted as slides and the negative image enlarged using a projection and colour photocopy technique. This provided a cheap enlargement of the mount surface that was used as a map to locate grains under the microscope and in the SEM. Generally it was easier to locate grains in the SEM, which at minimum magnification has a field of view of approximately 3 mm, than under the microscope, which with a 20 power objective has a field of view of 1 mm. Grains were photographed under the microscope and then probed using the SEM after carbon coating. After SEM analysis, by carefully removing the carbon coating it was possible in many cases to reveal the etching caused by the EDS (energy dispersive spectrometer) full frame scan and locate and re-photograph the grains under the optical microscope (Photo 1). It should be noted that the photomicrograph is a mirror image and the SEM videoprint is a true image. This procedure ensured that the petrography of the grain areas probed could be completely described.

Using back scattered electron images, minerals with higher average atomic number appear bright where as the coal fragments remain dark. It is easy to adjust the brightness for the coarser grains to differentiate between quartz, kaolinite, carbonates and phosphorus minerals. The EDS provided X-ray spectra of individual minerals allowing positive identification.

Back scattered electron scans of the mounts identified phosphorus minerals within maceral fragments, often in semifusinite, and occasionally as isolated grains. No phosphorus minerals were observed filling microfractures. The most conspicuous phosphorus mineral identified was apatite (Photo 2), which filled lumen in semifusinite, often in association with kaolinite. Kaolinite is probably the most common cell-filling material, sometimes completely and other times partially filling cells (Photos 3 and 4). Occasionally rounded grains of gorceixite were identified. It was noticeable that whereas the apatite filled cell lumen the gorceixite formed rounded grains and was much rarer and did not obviously fill cells (Photo 2).

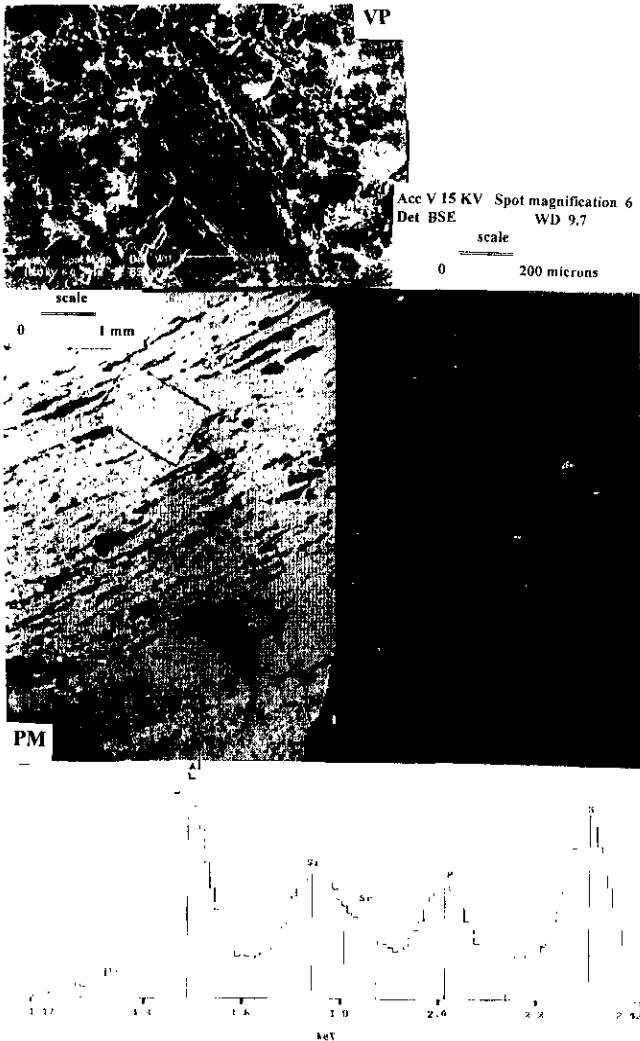


Photo 1: Grain of tellinite filled with liptinite; photomicrographs (PM) of grain before and after SEM EDS analysis showing square burn area on photomicrograph. Also videoprint (VP) of grain in SEM. Frame area analyzed was tellinite with minor liptinite. Scan revealed presence of aluminum, silica, phosphorus and possibly Strontium. The 0.1 millimetre scale bar applies to all photomicrographs and scale bar and operating conditions are also provided for the SEM videoprint.

An EDS X-ray scan in spot mode was used to identify elements in the mineral grains. Phosphorus minerals were differentiated by the relative proportions of calcium, barium, strontium and aluminum accompanying the phosphorus. Detection of calcium and phosphorus and absence of aluminum was assumed to confirm the presence of apatite whereas the presence of phosphorus and aluminum and absence of a large calcium peak was assumed to confirm the presence of the crandallite group minerals (Figure 11). Vivianite,  $(Fe_3(PO_4)_2 \cdot 8H_2O)$  was not identified. In a number of cases it appeared that siderite was associated with crandallite minerals and they might be derived from the alteration of vivianite. It is not always possible to distinguish between gorceixite (barium rich) and goyazite (strontium rich). Generally the crandallite minerals contained both elements and it is difficult to estimate relative proportions of strontium because its peak is masked by the silica peak.

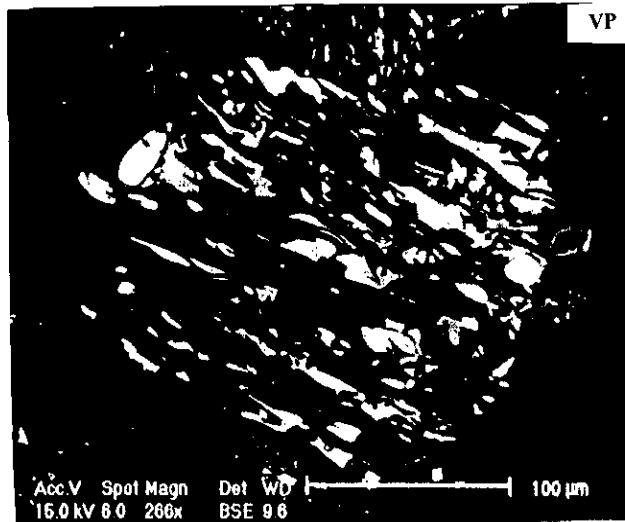


Photo 2: Apatite in phytal porosity in semifusinite. Duller mineral half filling cell in centre is kaolinite and rounded grains on left and right edge of coal fragment are crandallite possibly gorceixite.

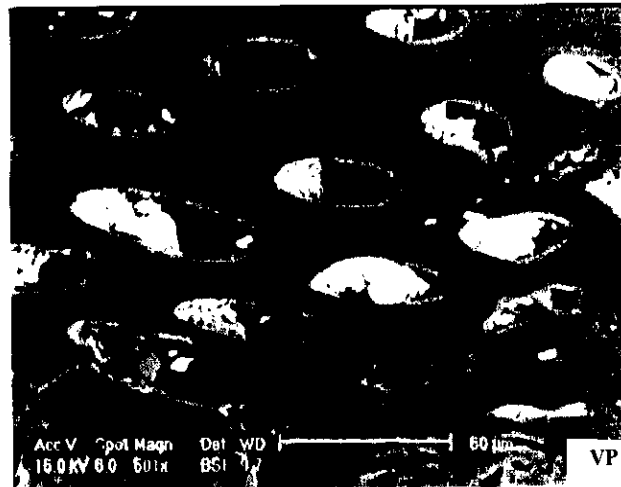


Photo 3 : Kaolinite partially filling cells in semifusinite; note the increase in brightness of cell walls.

Small areas of macerals, free from inclusions, were analyzed in EDS mode using a spot scan, in which an area of less than 5 microns is x-rayed in an attempt to measure dispersed phosphorus levels in different macerals. Spot EDS scans of different macerals failed to detect any phosphorus while at the same time detecting moderate sulphur peaks (Figure 12). The organic sulphur content of these coals averages about 0.6%, and therefore the phosphorus peak should be in the range of 1/50 to 1/10 the size of the sulphur peak based on phosphorus concentrations of 0.012% to 0.06%. Peaks of this size were within detection range based on the size of the sulphur peak. Consequently it appears that phosphorus in all macerals is no longer uniformly distributed and has either been removed, or has concentrated into distinct phosphorus minerals within the macerals.

Some fragments of tellinite and telocollinite contained very small, micron-sized, inclusions of minerals,

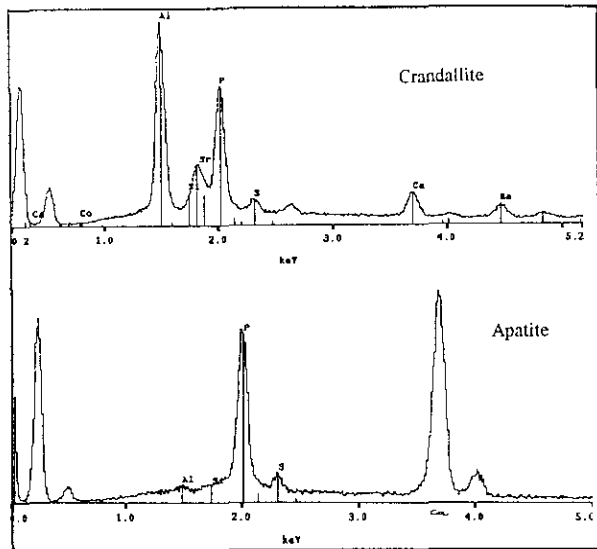


Figure 11: X-ray scans of apatite and crandallite group minerals (goyazite and gorceixite) from samples in this study.

sometimes outlining internal maceral structure. Spot scans of these grains identified them as crandallite minerals, kaolinite or apatite. The grains were so fine that it was easy to miss the fact that they were of varying composition. The occurrence of very small grains of goyazite dispersed in structured vitrinite is important because it explains the correlation of strontium and phosphorus seen in the work of Gluskoter *et al.* (1977) and the correlation of phosphorus with structured vitrinite seen in some of the data in Ward *et al.* (1996) and in this study (Figures 8, 9 and 10). The preferential presence of crandallite group minerals finely dispersed in structured vitrinite also explains why strontium and barium tend to correlate with these macerals (Table 4). The small grains appear to have crystallized out of the enclosing maceral. It is likely that the strontium and aluminum were derived from an external source because the macerals are deficient in these elements compared to phosphorus.

As mentioned, semifusinite contains easily identifiable apatite in cell lumen. Other macerals such as tellinite, telocollinite and desmocollinite contain finely dispersed mineral matter. In an attempt to get integrated phosphorus concentrations of these macerals, EDS scans of 20 x 20 micron frames were made with a count time of 300 seconds real time, which is equivalent to about 200 seconds live time (dead time varied from 30% to 33%). A scan of a mass of liptinite (Photo 5) did not detect phosphorus and apparently this maceral does not contain high levels of dispersed phosphorus. Other macerals do contain measurable amounts of phosphorus within 20 x 20 micron frames that include fine inclusions. The EDS scans on 20 x 20 micron frames indicate that the phosphorus content of structured vitrinite grains (Photo 6a, 6b) is very variable depending on how many dispersed crandallite grains were in the EDS frames. However the average phosphorus counts were about 1/3 that of sulphur counts. The average counts for unstructured vitrinite were about 1/6 that of sulphur. The numerical average wash sulphur

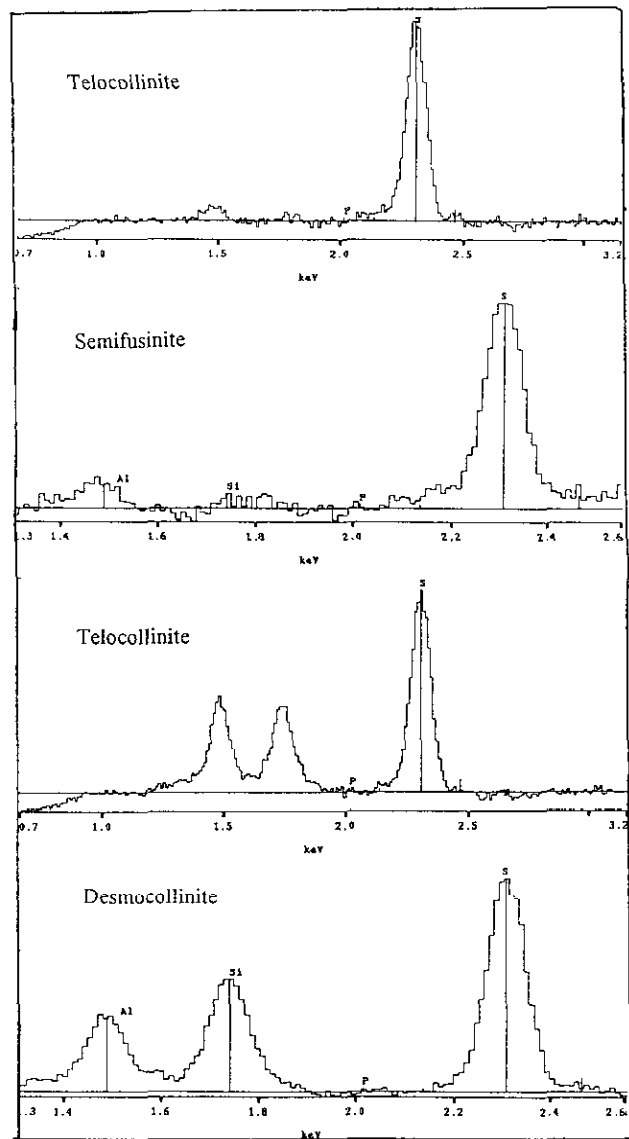


Figure 12: EDS spot scans of inclusion-free areas of macerals.

for the data in Table 1 is 0.62%. If the sulphur and phosphorus K $\alpha$  peaks have roughly the same relationship to concentration, then this implies a background distribution of phosphorus of very roughly of up to 0.3% in tellinite. This agrees with the data in Ward *et al.* (1996), which indicates about 0.25% phosphorus in 100% telovitrinite. This concentration is not excessive in terms of what would be expected in the original vegetation and therefore adds weight to the argument that the phosphorus is in the process of being "sweated out" of the maceral and not being added to it. In unstructured vitrinite the SEM data indicates up to 0.1% phosphorus, which appears to be associated with the finely dispersed mineral matter as indicated by strong aluminum and silica peaks (Photo 7)

It is not possible to quantify the amount of phosphorus occurring in semifusinite and structured vitrinite and compare the total to the phosphorus content of the sample; however the SEM work indicates that much of the phosphorus is as apatite in semifusinite or as crandallite minerals in structured vitrinite. The data indicates that very little phosphorus remains uniformly distributed in the

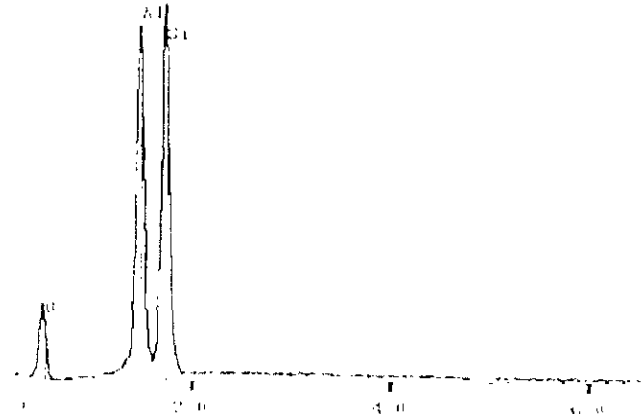


Photo 4: Grain of semifusinite with cells filled with kaolinite, SEM videoprint and spot scan of kaolinite.

macerals or scattered as detrital or cleat filling material. Ward *et al.* (1996) identified some phosphorus minerals occurring in late fractures but this does not appear to be a common occurrence in the Australian coals and has not been observed in this study. The amount of apatite in semifusinite grains varies based on the phytal porosity and on percentage filled by apatite. If semifusinite grain contained 5% apatite filled lumen then the grain as a whole would contain about 0.85% P. Porosities of 5% or higher

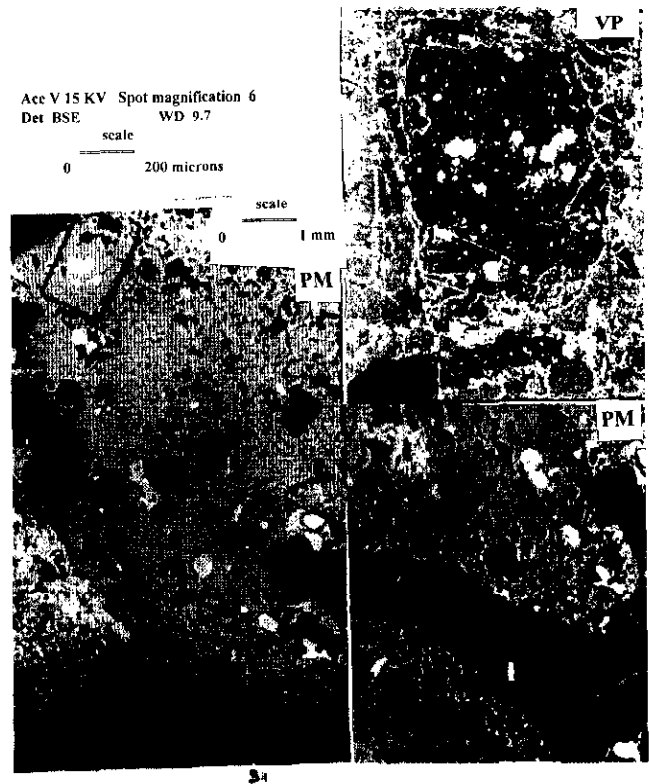


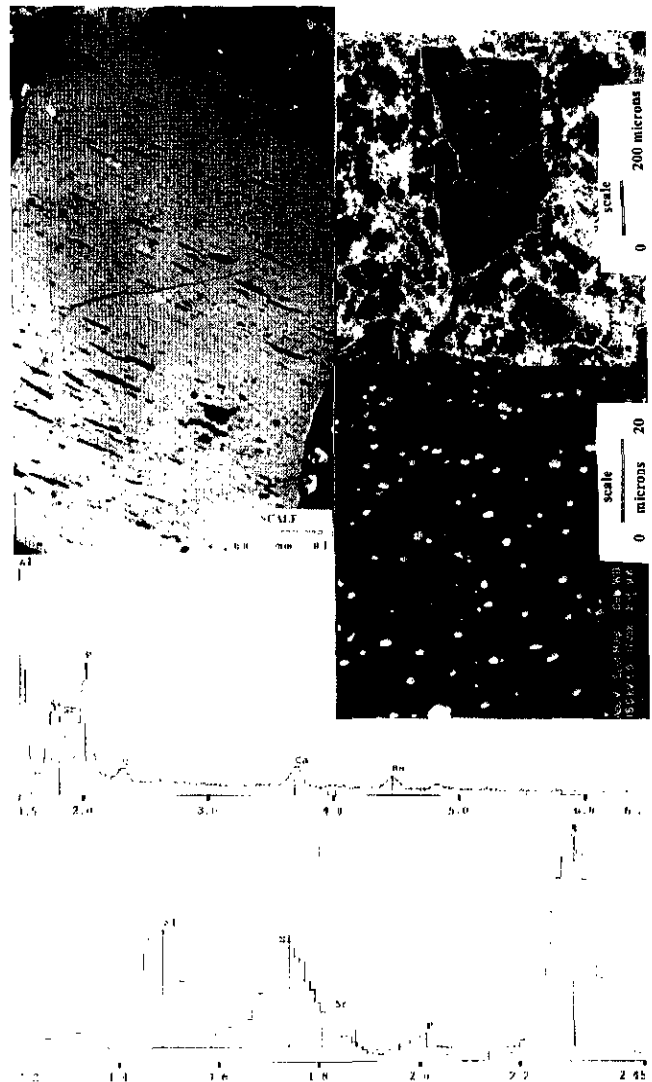
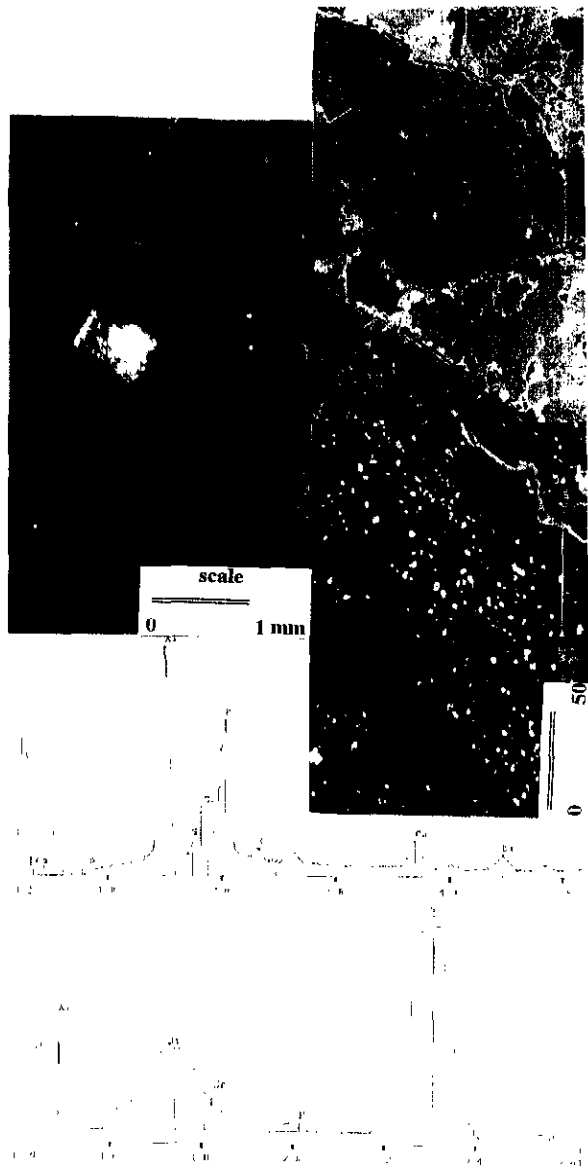
Photo 5: Desmocollinite with large area of lipitine. Photomicrograph, SEM videoprint and x ray spectra of a 20 x 20 micron area of lipitine. Some area of desmocollinite was scanned but no phosphorus was detected.

are not uncommon and consequently these grains contain more phosphorus than the original vegetation and clearly indicate addition of phosphorus to the maceral.

The SEM data confirms the association of phosphorus with structured inertinite and structured vitrinite as seen in Figures 8, 9 and 10 and eliminates the apparent contradiction of phosphorus appearing in semifusinite but the total concentration often correlating with percent reactives as discussed Ryan and Grieve (1995) and Ward *et al.* (1996).

### LATERAL VARIATIONS OF PHOSPHORUS WITHIN SINGLE SEAMS

Data (Figure 6) indicate that certain seams consistently have higher phosphorus concentrations. Based on Figure 7 this is explained by the average petrography in terms of the sum of structured vitrinite plus structured inertinite. However variations within a seam are



Photos 6a and 6b: Photomicrograph, SEM videoprint and x ray spectra of desmocolinite or tellinite grain with dispersed kaolinite and crandallite minerals. Upper x-ray scan is a spot scan and lower scan is a frame scan of the area outlined in the photomicrograph.

not explained by this relationship and appear to be dependent on variations in the smaller component of semifusinite. A small percentage of semifusinite mineralized with apatite has the potential to drastically increase the phosphorus-content of a seam. For example a 1% increase in semifusinite with a 20% apatite filled porosity can increase the phosphorus content of a sample by 0.035%. Much larger changes in the proportion of structured vitrinite would be required to produce the same change in phosphorus concentration.

It is suggested that the regional water table at the time of coal formation controls the general petrography of a seam, which in turn controls the average phosphorus content. Lateral changes in the phosphorus content of a seam are caused by variations in the amount of semifusinite. Variations in the amount of semifusinite are related to the availability of trees and the degree of charring by forest fires. Seams derived predominantly from grasses may have high inertinite contents but low semifusinite and fusinite contents and therefore will have

moderate or low phosphorus contents. For example the base seam in the Mist Mountain section (Ryan and Grieve, 1995), which is characterized by low phosphorus and high inertinite contents is composed predominantly of macrinite and inertodetrinite with low phytal porosity.

There is sufficient data for three seams to produce phosphorus content maps covering an area of approximately 120 square kilometres (Figure 13). There is some uncertainty concerning seam correlation but the data sets do come from seams occupying similar levels in the stratigraphy. For two of the seams the phosphorus contents are quite consistent but the third seam data is more variable.

There is a high phosphorus seam in the lower part of the section in most of the mines in southeast British Columbia that extends north to the Elk River property at the northern end of the Elk Valley coalfield (Grieve, 1992). It is not known if the seams represent the same stratigraphic horizon.

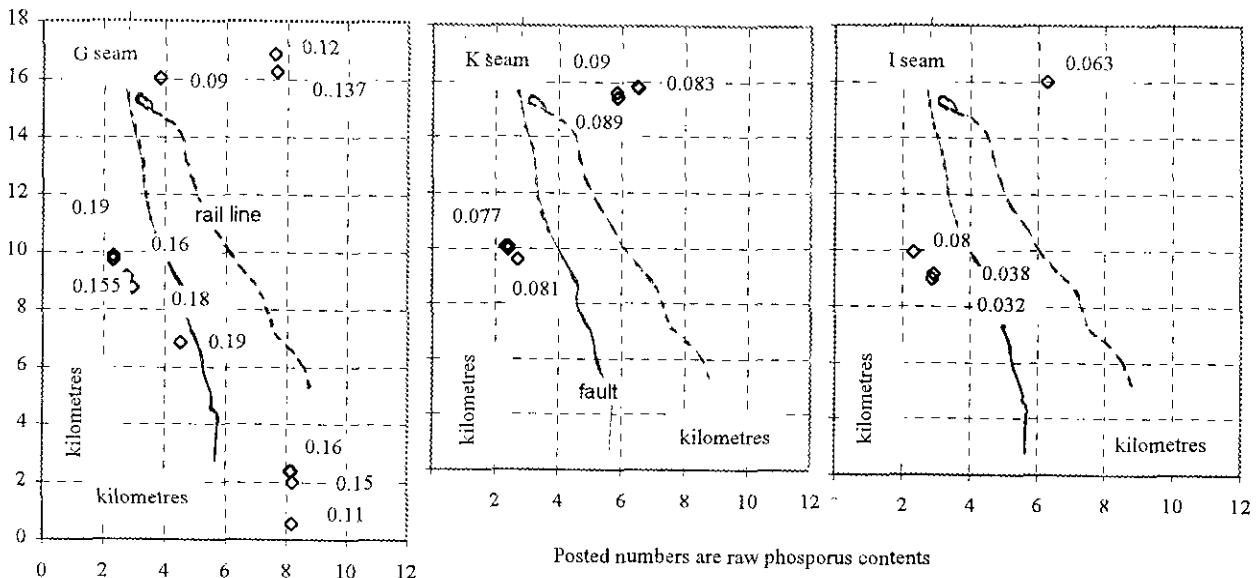


Figure 13: Maps indicating position and concentration of phosphorus in three seams.

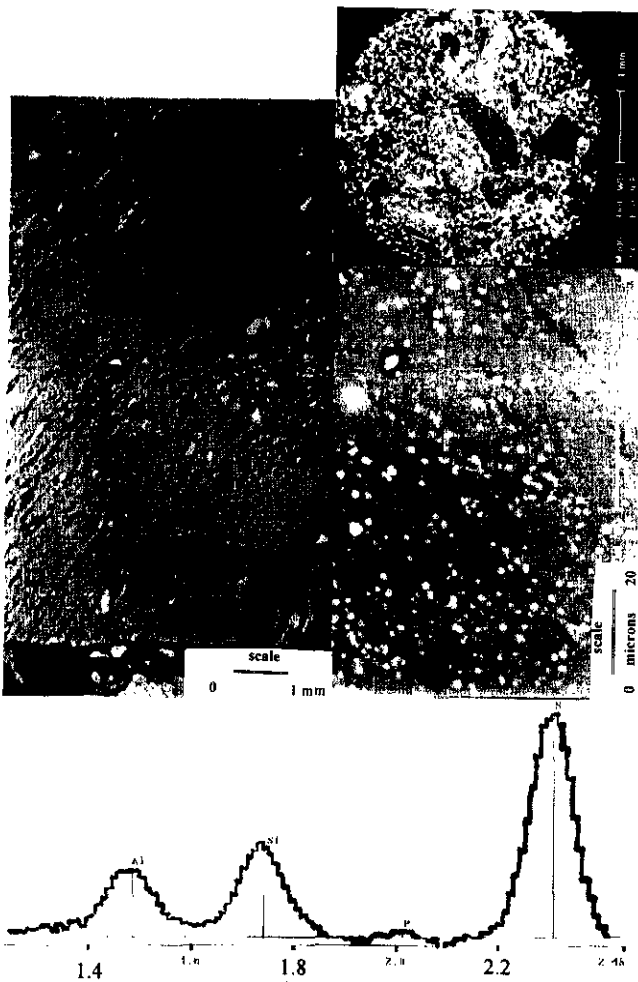


Photo 7: Photomicrograph, SEM videoprint and x ray spectra of desmocollinite with finely dispersed kaolinite and minor phosphorus.

## RELATIONSHIP BETWEEN IN SEAM PHOSPHORUS CONTENT AND HANGINGWALL LITHOLOGY

Lateral variations in phosphorus content of seams are related to petrography. But it is little help in a mining environment to know that a petrographic analysis will provide some indication of changes in phosphorus content. What would be more helpful would be some flag in the regional lithology or structure that signals changes in both petrography and phosphorus content. The observation that the amount of inertodetrinite correlates with the amount of sandstone in the hangingwall (Cameron, 1972) may mean that seams with sandstone hangingwalls have less structured inertinite and therefore less phosphorus.

If there is a relationship between interburden lithology and seam petrography, then this might provide a preliminary way of estimating phosphorus content and other coal-quality parameters that depend on petrography. In an attempt to find useful field criteria for flagging seams with high phosphorus contents, a number of drill holes were examined where a gamma log and phosphorus concentration of the coal were available. Various features such composition, sharpness of hangingwall and footwall and presence of overlying fining or coarsening upwards successions were noted. An unsuccessful attempt was made to correlate these geophysical log features with the phosphorus content of the enclosed seam. If the enclosing rock lithology is correlated with the phosphorus content of the coal seam, then the features defining the correlation appear to be too subtle to be identified on geophysical logs.

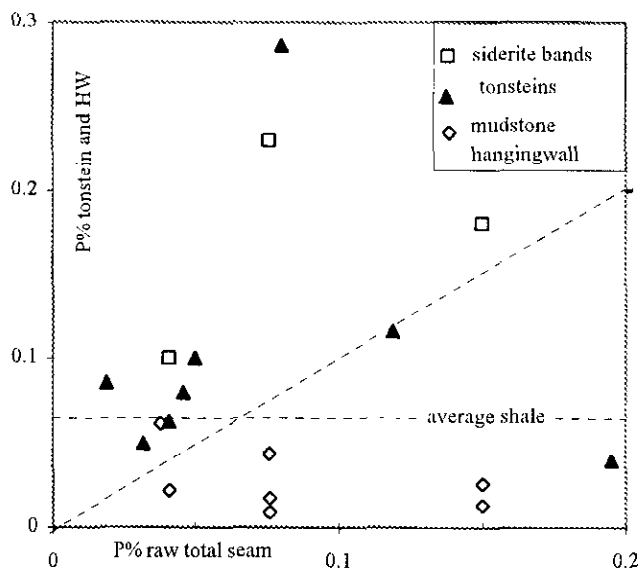


Figure 14: Plot of average seam phosphorus content *versus* hangingwall rock samples and in-seam tonsteins and siderite-rich bands.

A number of in-seam tonstein and siderite-rich bands and hangingwall rock samples were collected. The latter represented about 5 centimetres of contact rock. These samples provide some insight into the movement of phosphorus. In nearly all cases the hangingwall samples contain more phosphorus than the seams as whole (Figure 14) and in that the seam phosphorus content is less than believed to be in the original vegetation, this implies an outward movement of. Most of the hangingwall rock samples have higher phosphorus contents than the average for shale (0.065%). The phosphorus did not originate from, or find a home in, the tonstein bands, which generally have lower phosphorus contents than the seams. There is an association of siderite with phosphorus, which probably relates to temporary low pH environments in the swamp that cause the precipitation of siderite and apatite.

## COMPARISON TO OTHER COALFIELDS

Phosphorus concentrations in coal from the Gates and Gething formations in the Peace River coalfield are generally lower than those in the Elk Valley coalfield (Grieve 1992). In fact there is a consistent decrease in average raw phosphorus content with age of the Jura-Cretaceous coal-bearing formations. The oldest Mist Mountain Formation has an average of 0.076% followed by the younger Gething Formation (0.063%) and the youngest Gates Formation (0.043%). This may correlate with the amount of structured inertinite in coals from the different formations. A preliminary examination of Gething Formation coals indicated that a lot of the inertinite is macrinite (Ryan, 1997). The amount of structured inertinite in a coal is related to the frequency of wildfires (Lamberson and Bustin, 1966) and is therefore related to climate; specifically the amount of precipitation and the oxygen content of the atmosphere, which has varied over geological time.

There is insufficient data to compare phosphorus concentrations in the Elk Valley with those in the Crowsnest coalfield to the south. The lowermost seam in the Crowsnest coalfield has low phosphorus concentrations but data on seams higher in the section is sparse.

Some data has been located for some Australian coals (Ward *et al.*, 1996 and Queensland Coal Board, 1995) and for Appalachian coals (Price and Gransden, 1987). The Elk valley coals are distinguished from the Australian coals by the presence of some high values (Figure 7). Appalachian coals have distinctly lower phosphorus concentrations. There is no obvious petrographic reason for the difference in concentrations; for example the Elk Valley coals do not have more semifusinite than the Australian coals. However there is some uncertainty in the petrographic data because of differences in the way the macerals were described and there is a mixing of raw and wash data. The difference in average phosphorus concentrations may be explained by global climate or vegetation changes over time.

## CONCLUSIONS

It is proposed that much of the phosphorus in coal originates from the parent vegetation, in which there is ample to account for all that is found in coal. In fact vegetation contains on average 10 times as much phosphorus as coal and either phosphorus is lost from vegetation during coalification or growing vegetation scavenges phosphorus from underlying humus. Within the coal, macerals are divided into three groups based on their phosphorus content. The phosphorus content of structured inertinite is variable to high depending on how much apatite is introduced into the phytal porosity. The phosphorus content of structured vitrinite is moderate and probably close to that of the original vegetation. It is partially sweated out of the original vegetation and finely dispersed as crandallite minerals. Phosphorus has been largely removed from unstructured vitrinite and inertinite but some may remain associated with kaolinite.

Petrography and analytical data confirm that, in coal from the Elk Valley coalfield, the structured inertinite and vitrinite phosphorus association. Correlation data indicates that the barium and strontium tend to be associated with the finely dispersed phosphorus in structured vitrinite.

Scanning electron microscope work confirms that much of the visible phosphorus occurs as apatite or occasionally as gorceixite occupying lumen (cells or phytal porosity) in the semifusinite or fusinite. However there are also finely dispersed grains of apatite and goyazite in tellinite and telocollinite. This explains why regional studies reveal a positive correlation between phosphorus and reactive maceral contents of seams.

The phosphorus content of seams in the Elk Valley Mist Mountain Formation is related to the sum of structured vitrinite plus structured inertinite. However variations within a single seam are related to small changes

in the amount of semifusinite, which can have very high concentrations of phosphorus.

Because much of the phosphorus is present as phosphorus minerals enclosed by coal macerals it is difficult to liberate and remove during washing. Inert maceral fragments tend to accumulate in the intermediate size range in crushed coal and in the intermediate specific gravity splits. However it will be difficult for a wash plant to make use of these differentiation's. The best way of reducing the average content of phosphorus in the clean coal is by blending the ROM coal. This will require good advanced knowledge of phosphorus concentrations in the seams so that the information can be built into long range mine plans.

## ACKNOWLEDGMENTS

Sample collection was aided by Martin Zral senior geologist Greenhills coal mine, who was particularly helpful and Ken Komenac senior geologist at the Fording River coal mine. Many of the samples were crushed and split by the author at facilities at the Greenhills mine and thanks are extended to Gail Van Dale and the personnel at the lab for risking my active presence in their world. The SEM work used a machine at the University of British Columbia, Department of geological Sciences and was conducted with considerable help from Mati Raudsepp, Director of Analytical Services. The paper benefited from a detailed editorial review by Dave Lefebure.

## REFERENCES

Bertine, K.K. and Goldberg, E.D. (1971): Fossil Fuel Combustion and the Major Sedimentary Cycle; *Science*, Volume 173, pages 233-235.

Britch, C. (1981): The Greenhills Surface Coal Mining Project; *Canadian Institute of Mining and Metallurgy Bulletin*, Volume 74, pages 155-160.

Burchill, P., Howarth, R.W., Richards, D.G. and Sword, B.J. (1990): Solid-State Nuclear Magnetic Resonance Studies of Phosphorus and Boron in Coals and Combustion Residues; *Fuel*, Volume 69, pages 421-428.

Cameron, A.R. (1972): Petrography of Kootenay Coals in the Upper Elk River and Crowsnest Areas, British Columbia and Alberta; in *Proceedings of the First Geological Conference on Western Canadian Coal*, Mellon, C.B. Kramers, J.W and Seagel, E.J., Editors, *Alberta Research Council*, Information Series, Number 60, pages 31-46.

Coleman, J.M. (1966): Ecological Changes in a Massive Fresh-Water Clay Sequence; *Gulf Coast Association of Geological Societies*, Transactions, Volume 16, pages 159-174.

Cook, A.C. (1962): Fluorapatite Petrifications in a Queensland Coal; *Australian Journal of Science*, Volume 25, page 94.

Diessel, C.F.K. (1992): Coal Bearing Depositional Systems; *Springer-Verlag*, page 26.

Dixon, K., Skipsey, E. and Wats, J.T. (1964): The Distribution and Composition of Inorganic matter in British Coal; part 1- Initial Study of Seams from the East Midlands Division of the National Coal Board; *Journal Inst. Fuel*, Volume 37, pages 485-493.

Donald, R.L. (1984): Sedimentology of the Mist Mountain Formation; University of British Columbia, unpublished M.Sc. Thesis, pages 1-180.

Donald, R.L. and Bustin, R.M. (1987): Depositional Environments of the Coal-Bearing Mist Mountain Formation, Eagle Mountain, Southeast Canadian Rocky Mountains; *Canadian Petroleum Geology, Bulletin*, Volume 35, pages 389-415.

Finkelman, R.B. (1980): Modes of Occurrence of Trace Elements in Coal; unpublished Ph.D. Thesis, *University of Maryland*, 301 pages.

Francis, W. (1961): Coal: Its Formation and Composition; *Edward Arnold*, London, England.

Gluskoter, J.J., Ruch, R.R., Miller, W.G., Cahill, R.A., Dreher, G.B. and Kuhn, J.K. (1977): Trace Elements in Coal: Occurrence and Distribution; *Illinois State Geological Survey*, Circular 499.

Grieve, D.A. and Holuszko, M.E. (1991): Trace Elements, Mineral Matter and Phosphorus in British Columbia Coals; in *Geological Fieldwork 1990*, B.C. Ministry of Energy, Mines and Petroleum Resources, paper 1990-1 pages 361-370.

Grieve D.A. (1992): Phosphorus in British Columbia Coking Coals; *B.C. Ministry of Energy, Mines and Petroleum Resources*, open file 1992-20, pages 1-23.

Grieve, D.A. (1993): Geology and Rank Distribution of the Elk Valley Coalfield Southeastern British Columbia; *B.C. Ministry of Energy, Mines and Petroleum Resources*, Bulletin 82, pages 1-188.

Harris, L.A., Barrett, H.E. and Kopp, O.C. (1981): Element Concentrations and their Distribution in Two Bituminous Coals of Different Paleoenvironments; *International Journal of Coal Geology*, Volume 1, pages 175-193.

Hill, P.A. (1988): Tonsteins of Hat Creek, British Columbia: A Preliminary Study; *International Journal Of Coal Geology*, Volume 10, pages 155-175.

Hill, P.A. (1990): Vertical Distribution of Elements in Deposit No. 1, Hat Creek, British Columbia: A Preliminary Study; *International Journal of Coal Geology*, Volume 15, pages 77-111.

Karner, F.R., Schobert, H.H., Falcone, S.K. and Benson, S.A. (1986): Elemental Distribution and Association with Inorganic and Organic Components in North Dakota Lignites; In, *Mineral Matter and Ash in Coal*, American Chemical Society (ACS) Symposium Series 301, Editor, M. Joan Comstock, pages 70-89.

Kramer, P.J. and Kozlowski, T.T. (1979): Physiology of Woody Plants; Academic Press, *Harcourt Brace Jovanovich, Publishers*, Table 10-2.

Lamberson, M.N. and Bustin, R.M. (1996): The Formation of Inertinite-rich Peats in Mid Cretaceous Gates Formation: Implications for Interpretation of Mid Albian History of Paleowildfire; *Paleogeography*,

- Paleoclimatology, Paleoecology*, Number 120, pages 235-260.
- Ledig and Botkin (1974): *Silvae Genetica*; Volume 23, pages 188-192.
- Mahony, B., Moulson, I. and Wilkinson, H.C. (1981): Study of the Relation Between the Phosphorus Content of Coal and Coke; *Fuel*, Volume 60, pages 355-358.
- Marschner, H. (1986): Mineral Nutrition of Higher Plants; *Academic Press, Harcourt Brace Jovanovich, Publishers*, London, Table 12-4.
- Mason, B. (1966): Principles of Geochemistry; *John Wiley and Sons*, London, page 228.
- Powell, M.A. (1987): The Inorganic Geochemistry of Two Western U.S. Coals: Emery Coal Field, Utah and Powder River Coal Field, Wyoming; unpublished Ph.D Thesis, *University of Western Ontario*, London, Ontario, pages 1-178..
- Price, J.T. and Gransden, J.F. (1987): Metallurgical Coals in Canada: Resources, Research and Utilization; *Energy Mines and Resources Canada*, CANMET report 87-2E, pages 1-71.
- Queensland Coal Board (1995): Queensland Coals, Physical and Chemical Properties, Colliery and Company; Editor, 61 Mary Street, Brisbane, Queensland 4000, Australia, pages 1-121.
- Ryan, B.D. and Grieve, D.A. (1996): Source and Distribution of Phosphorus in British Columbia Coal Seams; in Geological fieldwork 1995, Grant, B. and Newell, J.M., Editors, *B.C. Ministry of Energy, Mines and Petroleum Resources*, paper 1996-1, pages 277-294.
- Ryan, B.D. (1997): Coal Quality Variations in the Gething Formation Northeast British Columbia (93O,J,I); in Geological fieldwork 1996, *B.C. Ministry of Employment and Investment*, paper 1997-1 pages 373-397.
- Salisbury, B.F., and Ross, C. (1969): Plant Physiology; *Wadsworth Publishing Company Inc.*, Belmont, California, Table 10-2.
- Shah, N., Girard, P., Mezerette, C. and Vergnet, A.M. (1992): Wood to Charcoal Conversion in a Partial Combustion Kiln: An Experimental Study to Understand and Upgrade the Process; *Fuel*, Volume 71, pages 105-115.
- Taplin, A.C. (1976): General Geology and Geological Practices at the Fording River Coal; *Canadian Institute of Mining and Metallurgy*, District 6 Meeting Vancouver, British Columbia, October 15 1976, page 13.
- Van Den Busche, B.G. and Grieve, D.A. (1990): Phosphorus in British Columbia Coking Coals, in Geological fieldwork 1989, *B.C. Ministry of Energy, Mines and Petroleum Resources*, Paper 1990-1, pages 427-430.
- Ward, C.R., Corcoran, J.F., Saxby, J.D. and Read H.W. (1996): Occurrence of Phosphorus Minerals in Australian Coal Seams; *International Journal of Coal Geology*, Volume 30, pages 185-210.
- Wedepohl, K.H. (1978): Handbook of Geochemistry, Volume II, part 5, *Springer-Verlag*, Berlin, pages 1-301.





## A REVIEW OF SULPHUR IN COAL: WITH SPECIFIC REFERENCE TO THE TELKWA DEPOSIT, NORTH-WESTERN BRITISH COLUMBIA

By Barry Ryan, B.C. Geological Survey Branch  
and  
Angelo Ledda, Manalta Coal Limited, Calgary

**KEYWORDS:** Telkwa coal, sulphur forms, sulphur origin, petrography.

### INTRODUCTION

The Jura-Cretaceous coal seams of the Currier, Mist Mountain, Gething and Gates formations generally formed in delta or strand plain environments with little marine influence. The sulphur contents of coal from these formations is therefore generally low, nearly always less than 1 % and often less than 0.5 %. Coal-bearing formations of the Cretaceous Nanaimo and Skeena groups were deposited in coastal areas with more marine influence. Consequently sulphur contents are more variable and tend to be higher. It is therefore important to study aspects of sulphur in Cretaceous coal seams such as the seams in the Skeena Group at Telkwa (Figure 1).

This paper studies sulphur in some of the Telkwa coal seams and also provides a short review of some of the voluminous literature on sulphur in coal.

### TYPES, SOURCES AND EVOLUTION OF SULPHUR IN COAL

#### Types of sulphur in coals

Sulphur occurs in coal as sulphides, organic sulphur, elemental sulphur and sulphate. The most important forms are sulphide, mainly as pyrite ( $\text{FeS}_2$ ), and organic sulphur. Sulphate sulphur usually occurs in small amounts, often in sulphate minerals formed during oxidation of coal. Pearson and Kwong (1979) suggest that, in coals with low pyrite concentrations, organic sulphur can oxidize to form gypsum, which can also be introduced by ground-water. Elemental sulphur occurs in trace amounts.

Organic sulphur is bound in a number of forms. Markuszewski *et al.* (1980) classifies organic sulphur into four types.

- Aliphatic or aromatic thiols. Aromaticity refers to the tendency of carbon in coals of higher rank to form hexagonal rings similar to the structure of graphite. Aliphaticity refers to the ability of carbon hydrogen complexes to form chains as in most of the oils. This molecular structure tends to disappear at higher ranks. Thiols are hydrogen sulphur pairs, which in this case are incorporated into the above structures.
- Aliphatic, aromatic or mixed sulphide (thioethers). This is a radical+sulphur+radical bond, in which the ring or chain structures form the radicals.
- Aliphatic aromatic or mixed disulphides. This a radical+sulphur+sulphur+radical molecule;
- Heterocyclic compounds of thiophene type. This is a ring structured molecule containing carbon and a single sulphur atom. The thiophenic group is thermally the most stable and predominates at higher ranks, whereas the thiols are converted or lost. During carbonization much of the thiol-held sulphur is lost. For medium-volatile coals about 30 % of the organic sulphur is lost during carbonization.

Sulphur in sulphides occurs in coal predominantly as pyrite and sometimes marcasite. Many other sulphides can occur, but usually in trace amounts. Often trace metals in coal are associated with the pyrite fraction.

#### Sources of sulphur in coal

Primary sulphur (S) in coal can originate from sea water, fresh water, vegetation and extraneous mineral matter. Secondary sulphur can be introduced during (syngenetic) or after (epigenetic) coal formation by ground water, which is probably remobilizing sulphur that originated in sea water or as loosely held organic sulphur in the vegetation.

Fresh water contains 0 to 10 ppm S and therefore, even if there is prolonged circulation of fresh water through the peat, can not donate much sulphur to the coal.

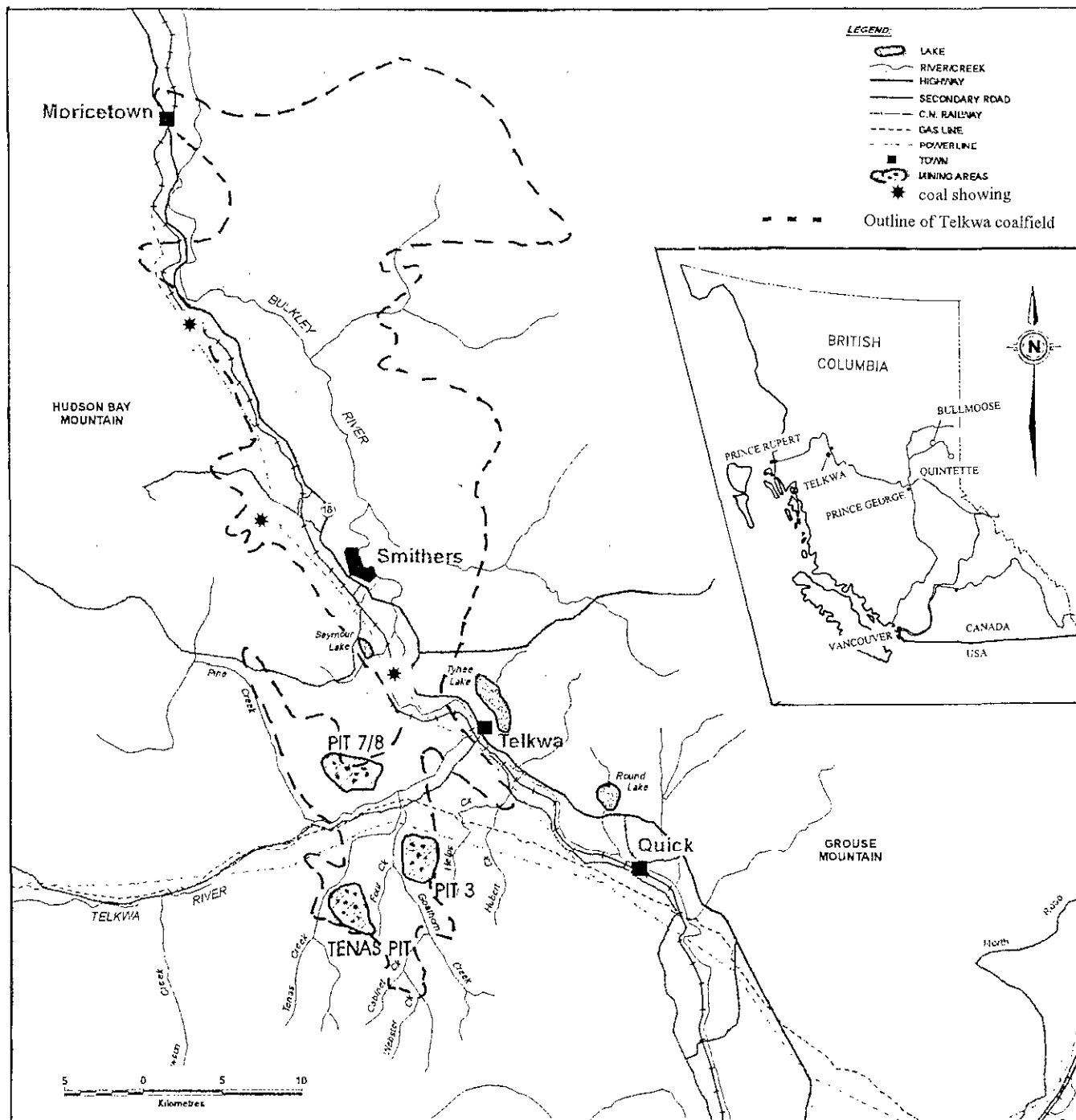


Figure 1: Regional map of the Telkwa coalfield indicating location of the proposed pits.

It is unlikely that much sulphur in coal comes from extraneous mineral matter. If the mineral matter contains sulphides, then they could provide a source of  $SO_4$  and  $H_2S$  to the coal, but amounts would usually be small. Even though pyrite is often found in parting material in coal, the sulphur probably originated in the coal. Partings formed by degradation of biomass may contain high concentrations of sulphur liberated from the biomass. Partings composed of extraneous mineral matter will have variable sulphur contents depending on the degree of marine influence and introduction of sulphur.

Vegetation generally has between 0.01 % and 0.5 % S on a dry basis with marine influenced vegetation having higher concentrations. Plants that grow in brackish water have higher organic sulphur contents than fresh water species, probably because they have adapted to a high sulphur environment. A number of authors quote average concentrations of sulphur in vegetation; Salisbury (1969) considers 0.1 % S to be adequate for higher plants; Altschuler *et al.* (1983) provides sulphur concentrations ranging from 0.01 % to 0.15 % for dry grass with the root material having the highest concentrations; Rankama and Sahama (1950) give an

average of 0.4 % S for angiosperms; Wedepohl (1978) quotes an average for mean concentration plants of 0.5 % S. These concentrations will increase as the vegetation is coalified and volatile matter lost. Even with a 50 % weight loss, which would double these concentrations, there is not enough sulphur in most vegetation to explain sulphur concentrations in coal of over 0.5 %.

If a coal seam contains more than about 0.5 % sulphur, then some of the sulphur was probably derived from sea water, which contains on average 0.265 % SO<sub>4</sub> or 885 ppm S (SO<sub>4</sub> contains 33.4 % S). If a swamp contains 40 % sea water, then this accounts for a total amount of introduced S of:  $0.4 \times 0.265 \times 0.334 =$  about 0.035 % S.

Water-saturated peat can compact by a factor of 5 or more as it is transformed into bituminous coal. If all the sulphur from the water is taken up by the coal, then 0.035 % S in the peat could increase to a concentration of 0.2 % S or more in bituminous coal. This could account for about 0.37 % pyrite if all the S was used to make pyrite. Many coal seams, with sulphur concentrations in excess of 1 % formed over a protracted time, during which sea water was percolating through the peat and continually providing additional SO<sub>4</sub>. Sulphur was extracted from sea water and formed pyrite or increased the organic sulphur content of the coal. This implies repeated influxes of sea water and a hiatus, during which the swamp vegetation did not sink into a hydrological environment isolated from sea water.

Sea water is denser than fresh water and it is interesting to consider various ways that it can be introduced into a paralic environment. One possibility is that occasional high tides cause an influx of sea water over the top of the fresh-water saturated swamp. The sea water sinks and mixes with the underlying fresh water aided by the density difference and various gases, such as methane and carbon dioxide, that are migrating upwards through the swamp. The result is a temporary brackish water environment, that increases the sulphur content of the interstitial water. Over a period of years repeated high tides are able to supply sufficient SO<sub>4</sub> to the swamp to explain sulphur concentrations higher than 1 %. Because the influxes are repeated only once or twice a year they do not inhibit plant growth. Other scenarios exist for the introduction of sea water, such as the percolation of sea water through unconsolidated permeable hangingwall rocks. Models of the hydrology of salt water influxes mixing with fresh water may give some insights as to how sulphur contents vary laterally within seams.

Sea water also introduces large quantities of sodium (10500 ppm), chlorine (1900 ppm), magnesium (1350 ppm) and potassium (380 ppm) along with the 885 ppm sulphur (average concentrations for sea water, Mason, 1966). These extra elements introduced into the swamp generally stay in solution and are eventually dewatered from the peat or expelled as the rank increases. The magnesium, iron and calcium may be trapped in the coal as carbonates, though generally sea

water does not introduce much iron (<1 ppm) or calcium (400 ppm).

Secondary sulphur includes sulphur remobilized during coalification to form syngenetic pyrite, which is often found on cleats. This sulphur may originate from less stable, organic sulphur compounds that break down at low rank or from sulphate rich interstitial water that is squeezed out of the coal as it is compacted and rank increases.

Various studies summarized by Chou (1990) indicate that most of the sulphur in coals with less than 1 % sulphur comes from the original vegetation. For coals with more sulphur, an increasing proportion comes from sea water. Price and Shieh (1979) using sulphur isotope data found that 63 % of the sulphur in high sulphur coals (>0.8 % sulphur) is derived from sea water by sulphate reduction and the rest is derived from the original vegetation. For low sulphur coals the proportion of sulphur derived from sea water decreases to 13 %.

## Origin of pyrite in coal

It is important when visually estimating the amount of pyrite in a seam to understand the relationship to sulphur contents. Pyrite (FeS<sub>2</sub>) has a density of 5.01 g/cc and therefore is about 3.5 times denser than coal. A 1 % visual estimate of the volume of pyrite in a coal seam translates into 3.5 weight % FeS<sub>2</sub>, or about 1.9 weight percent sulphur.

Pyrite in coal typically forms from H<sub>2</sub>S and Fe in solution. The process involves bacterial reduction of SO<sub>4</sub> to H<sub>2</sub>S at pH values of 7 to 4.5 followed by the combining of H<sub>2</sub>S, elemental sulphur and ferrous iron oxide (FeO) to form pyrite and water. This is the only way pyrite can form in peats and low rank coals. Consequently the presence of bacteria and the required pH range are very important controls on pyrite formation in coals. The SO<sub>4</sub> may come from sea water or vegetation, but neither of these sources provide iron, which is usually in plentiful supply and comes from other sources. It is probably derived from the breakdown of clay minerals and is possibly carried in solution as stabilized organic colloids (Price and Shieh, 1979).

The availability of iron influences the amount of pyrite and of secondary organic sulphur formed. Sulphur derived from H<sub>2</sub>S is much more easily converted into pyrite than into organic sulphur. Therefore if an iron source is not available, then some of the H<sub>2</sub>S may stay in solution and escape the swamp. Sources of iron can be limited in a number of ways. The water feeding the swamp may be clean fresh water containing little clay. The water may have a very low pH, which makes it easier for humic acids to flocculate clays before they have a chance to disperse through the swamp. Alternatively the water may be saline and saline water flocculates iron containing colloids (Price and

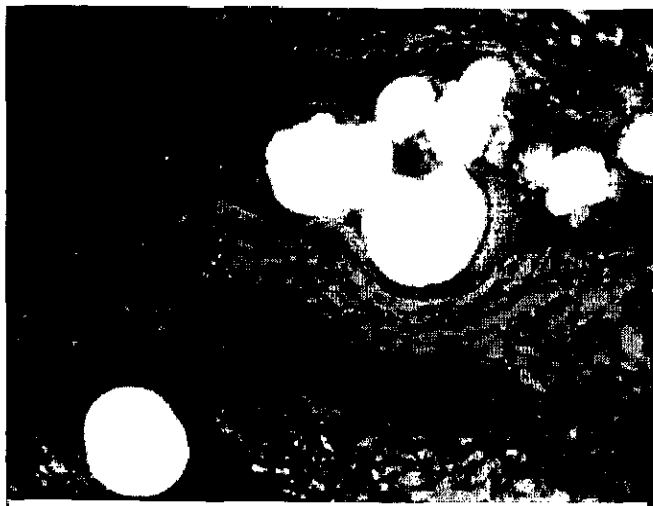


Photo 1: Framboidal pyrite in C seam. All photos taken in oil Immersion 50x10 power with a field of view of about 1.5 millimetres.



Photo 2: Fine euhedral pyrite in 1 seam.

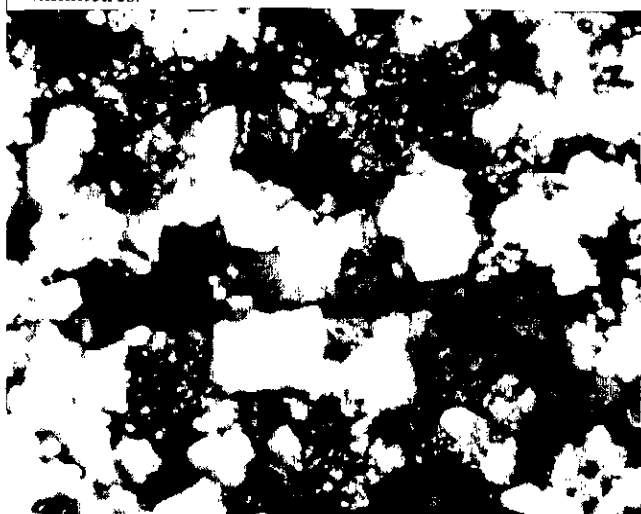


Photo 3: Coarse pyrite in a matrix of detrovitrinite and finely dispersed mineral matter; 1 Upper seam.



Photo 4: Pyrite filling fractured inertinite in 1 seam.

and Shieh, 1979). The last case explains why marine-influenced swamps do not have the highest sulphur contents for coal-forming environments. Despite the availability of a lot of  $H_2S$ , there is not a lot of iron available to make pyrite and though some  $H_2S$  is converted to organic sulphur some escapes from the swamp.

The Eh and pH environments required by the bacteria to generate  $H_2S$  determine the relative amount of pyrite formed in coal. They also influence the preservation of vegetation and the formation of vitrinite and inertinite. At optimum pH conditions (7 to 4.5) bacteria can use  $SO_4$  from sea water or true organic sulphur to generate  $H_2S$ , which is then used to make pyrite. Therefore, the organic sulphur content can decrease in some high sulphur coals because it is used to make pyrite (Diessel,

1992). For Australian Permian coals with total sulphur contents above about 1 per cent, organic sulphur contents decrease and pyrite contents increase markedly. This effect, which has implications for acid rock drainage (ARD) because it increases the ratio of pyrite to total sulphur, is not seen in coals from Telkwa.

Within a maceral the concentration of organic sulphur tends to decrease in proximity to pyrite grains; the extent of the affected area increases as the size of the grain becomes larger. This is interpreted to indicate that  $H_2S$  is more easily combined with Fe to form pyrite than in being adsorbed into the maceral as organic sulphur (Harvey and Demir, 1992). After the coal was heated the sulphur content around pyrite grains increased because sulphur, released as the pyrite oxidized, was infused into the surrounding coal as elemental sulphur.

## Pyrite morphology and genesis

Pyrite can have at least four easily recognized forms as described by Diessel (1992):

- framboidal pyrite composed of fine radiating octahedral crystals, which form spheroids within the macerals;
- euhedral pyrite, which occurs as small (1-10 microns) isolated crystals and cell-filling pyrite within macerals;
- coarse pyrite, which generally surrounds maceral fragments;
- late pyrite in cleats fractures or as nodules.

Other forms include cauliflower pyrite, which appears to develop from framboidal pyrite and dendritic pyrite, which may also be a development from framboidal pyrite. Concretions and cone-in-cone pyrite are late forming and fill cell voids, mainly in semifusinite. The different forms of pyrite crystallize at different times during peat formation and probably under slightly different conditions.

Framboidal pyrite (Photo 1) is composed of spherical clusters of very fine, needle-shaped pyrite crystals ( $<2 \mu\text{m}$ ). The  $\text{H}_2\text{S}$  used to make framboidal pyrite is usually derived from bacterial reduction of sulphur in vegetation and therefore this form of pyrite forms at the beginning of diagenesis of the peat swamp. Its formation probably does not depend on the availability of  $\text{SO}_4$  from sea water. It is usually associated with vitrinite, though its formation predates vitrinite formation as indicated by evidence of compaction and flow of the maceral around the pyrite.

Cohen *et al.*, (1984) suggest a close association of framboid formation and microbial activity. They found that pyrite framboids often formed in rootlet material in mangrove swamps, indicating that the  $\text{H}_2\text{S}$  generating bacteria were part of the root system and were not introduced later during peat accumulation. Love (1957) has noted the common morphology between framboidal pyrite and microbial organisms and it is possible that the pyrite is actually replacing bacterial structures. Caruccio *et al.*, (1977) describe a situation where framboidal pyrite formed in submerged vegetation over a period of 30 years. Obviously, if ideal conditions of low pH, available  $\text{SO}_4$  and available ferrous iron exist, then framboidal pyrite can form rapidly.

Altschuler *et al.* (1983) found that the amount of framboidal pyrite increased downwards through peat at the expense of organic sulphur, indicating that sulphur for making framboidal pyrite was being derived from the vegetation by bacterial activity. This reflects pH conditions, which were more favourable for bacteria deeper in the swamp. They suggested two ways of releasing the sulphur as  $\text{H}_2\text{S}$  from the vegetation: one, indiscriminate release of all organic sulphur in anaerobic conditions followed by reduction of any sulphate

available; or two, degradation of organic sulphur by heterotrophic sulphur reducing bacteria. If the swamp is rapidly submerged the increase of framboidal pyrite with depth at the expense of the organic sulphur will be preserved. If, however, there is a hiatus during which saline water is introduced into the top part of the buried peat, then there will be an increase in total sulphur and pyrite in the top part of the seam.

Fine, euhedral pyrite is often found in what appear to be cavities in desmocollinite (Photo 2) or filling cells in semifusinite, which sometimes also contains amorphous pyrite. Euhedral pyrite can also occur associated with disseminated mineral matter. This form of pyrite therefore must crystallize after formation of semifusinite, which may form by charring or burning vegetation during a period of low water table in the swamp (Lamberson *et al.*, 1996). The peat is then submerged, possibly in brackish water, and pyrite crystallizes in the cell porosity.

Inertinite is enriched in the upper part of many seams and consequently euhedral pyrite may predominate in the upper part of seams. Euhedral pyrite found in vitrinite may have the same origin as framboidal pyrite, but the larger crystals and association with cavities imply existence of a stable, probably aqueous environment and a some what later origin.

Euhedral pyrite may form from the direct precipitation of  $\text{FeS}_2$ , which forms from elemental sulphur and ferrous iron. The elemental sulphur is formed from the oxidation of bacterially-generated  $\text{H}_2\text{S}$  (Altschuler *et al.*, 1983); the ferrous iron is available because higher pH has reduced solubility. These conditions, initially moderate to low pH followed by higher Eh and pH values, are similar to those required for the formation of inertinite and suggest a fluctuating water table.

Coarse pyrite, large clusters of framboids or cauliflower pyrite probably form late in diagenesis when permeable roof rock permits an influx of sulphate-rich sea water. Conditions still permit the bacterial reduction of  $\text{SO}_4$  and the formation of pyrite. The peat has undergone some humification, which makes it more susceptible to addition of organic sulphur. The pyrite forms between maceral grains and there is less evidence of compaction around the pyrite. At Tenas Creek this form of pyrite is associated with detrovitrinite clearly indicating a late emplacement (Photo 3).

Coarse pyrite is nearly always found in the seams adjacent to the roof and less commonly the floor. Its concentration will depend in large part on the lithology of the roof rocks. Rocks that indicate a marine incursion, or are more permeable, may signal increased coarse pyrite in the upper part of the underlying seam. This will not necessarily increase the wash sulphur content of the seam, because coarse pyrite is not intergrown with the macerals and is relatively easy to remove in a wash plant.

Epigenetic pyrite forms along fractures and cleats in the coal. It therefore forms after biogenic coalification when the coal is mature enough to fracture or form



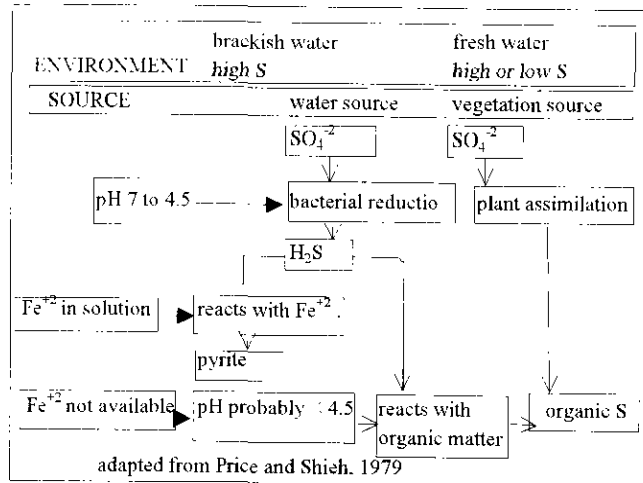
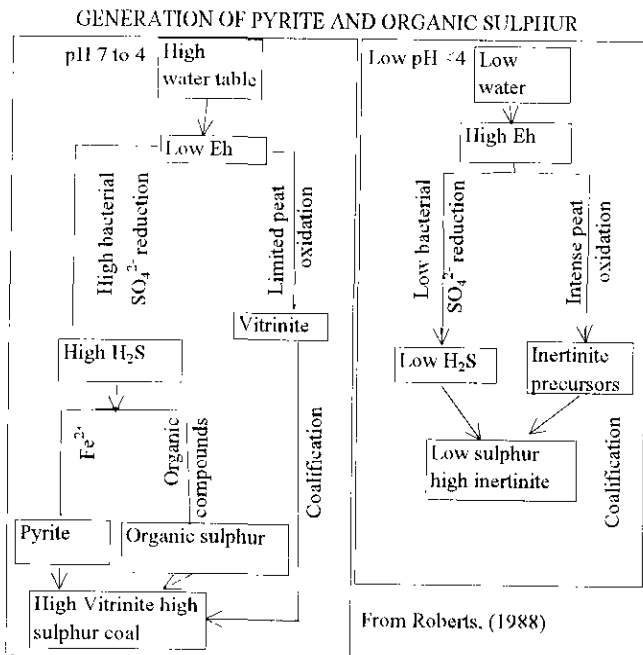


Figure 3: Pyrite formation models suggested by Roberts (1988), and Price and Shieh (1979)

In limnic coals, which do not contain sulphur introduced by sea water, there should be a positive correlation between the contents of reactive macerals and organic sulphur and an inverse relationship between the contents of organic sulphur and fine framboidal pyrite. The total amount of sulphur in the seam should remain fairly constant, decreasing somewhat as the percentage of semifusinite and fusinite increase, because formation of these macerals is probably accompanied by fire and some volatilization of sulphur. The ratio of pyritic sulphur to total sulphur should tend to increase as the percentage of inert macerals increases.

In paralic coals, the organic sulphur content of coal can be increased by the addition of sulphur derived from sea water. If ferrous iron oxide is not readily available, or is highly soluble because of lower pH conditions, then bacterially generated H<sub>2</sub>S can react directly with the vegetation to form organic sulphur compounds (Chou, 1990).

Sulphur is taken up by the pre-liptinite macerals, especially sporinite, which are very efficient at incorporating sulphur. Demir and Harvey (1991) found that the sulphur content in sporinite was higher than in all other macerals and the vegetal precursor. They suggest that macerals rich in hydrogen and aliphatic constituents, which remain fairly stable during the early stages of coalification, are very efficient at taking up any sulphur available as H<sub>2</sub>S. The concentration of sulphur in these macerals can range up to 5% (Demir and Harvey, 1991), but because they make up generally less than 10% of the coal, they do not effect the average organic sulphur concentration of the coal as much as organic sulphur in vitrinite.

The organic sulphur concentration of vitrinite, which usually makes up more than 50% of the coal, varies from about 0.4% to 5%. Consequently variation in vitrinite contents have a significant effect on the total sulphur content of the coal. Sulphur contents of some vitrinites are higher than in the original vegetation, indicating addition of sulphur from sea water sulphate or redistributed of the original organic sulphur.

The inert macerals generally have less organic sulphur than the reactive macerals and contents range from 0.2% to 3.5%. The mean organic sulphur contents decrease in the order semifusinite > fusinite > macrinite (Demir and Harvey, 1991) and are generally less than in the precursor vegetation. Burning of the peat causing sulphur volatilization can explain the low sulphur content in fusinite, but not necessarily in macrinite, from which sulphur may have been removed by bacterial activity prior to charring.

## ASSOCIATION OF MACERALS AND SULPHUR

The previous sections partially discuss the relationships between pyrite and organic sulphur and the different macerals. The general environmental processes that influence these relationships are discussed here. The key word is influence; there may not be strong linkages between maceral composition and the environment in which the original vegetation grew, died and matured into coal. The more important processes considered here are changes in water salinity, effects of fire, oxidation, humification, gellification and putrefaction (Diessel, 1992) and sediment influx. On the more specific and local scale they can, in part, be represented by;

- the presence of SO<sub>4</sub> from sea water;
- changes in the level of the water table level, which influences the risk of fires in the swamp;
- changes in the Eh of the water;
- changes in the pH of the water, which together with Eh influence the processes of humification, gellification and putrefaction;
- the amount of clay available, which provides iron for making pyrite.

These five parameters are used to help demonstrate possible relationships between coal compositions and various environments (Figure 2). Figure 2 combines diagrams proposed for maceral formation by Diessel (1992) and diagrams proposed for pyrite formation by Roberts (1988), Price and Shieh, (1979, Figure 3) and Ryan (1997). The five parameters are organized in a hierarchy such that 28 branch-ends are formed. The end of each branch represents a particular coal type, which is described in terms of the relative contents of sulphur, ash, inertinite, vitrinite and liptinite. Figure 2 provides a rough template for working from environment to coal composition or backwards from composition to a number of possible environments.

The level of the water table is one of the most important factors influencing coal formation. Under conditions of high water table, influxes of sea water may be frequent (paralic environment) increasing total sulphur content. The Eh is generally low and fires are rare decreasing the inertinite content and increasing the preservation of vitrinite. If pH conditions are in the range 4.5 to 7, bacterial activity will reduce available  $\text{SO}_4$  to  $\text{H}_2\text{S}$ . If the  $\text{SO}_4$  originates from sea water, then the coal will have higher sulphur and pyrite concentrations than if the  $\text{SO}_4$  originates from vegetation. If the paralic environment does not have periodic influxes of clays to provide iron to make pyrite, then  $\text{H}_2\text{S}$  will either stay in solution and migrate out of the swamp or remain in the coal as additional organic sulphur.

Low water tables, which are associated with a higher potential for fires and an increased inertinite content, are more likely to be found in limnic environments. There will be less chance for introduction of marine  $\text{SO}_4$  and sulphur and pyrite contents should be low. Fluctuations in the water table level may result in high Eh and variable pH environments, which will effect vitrinite and organic sulphur contents. A low water table may be associated with a lot of bio-degradation, which will increase the inherent ash of the remaining biomass and contents of inertinite and pre-exinite macerals, which are very resistant to decay and enriched in sulphur. Therefore, higher inherent ash contents may accompany higher sulphur and low vitrinite contents.

In water with intermediate pH values preservation of vitrinite, especially structured vitrinite, is favoured. Under higher pH conditions, which do not favour the solubility of  $\text{Fe}^{+2}$ , bacterial or fungal attack of vegetation decreases vitrinite content and pyrite is less likely to form. In this case, if the water table is low or fluctuating, then the  $\text{H}_2\text{S}$  may form a gas and escape. The resulting coal will have low organic and pyritic sulphur concentrations and a high content of inertinite. The  $\text{H}_2\text{S}$  can also move downwards in solution through the peat layers into low pH environments where bacteria are not active and in this case the  $\text{H}_2\text{S}$  may combine with the organic material to form organic sulphur. This environment is one of gellification and preservation of unstructured vitrinite. The resulting coal will have a high content of organic sulphur and vitrinite and low pyrite contents.

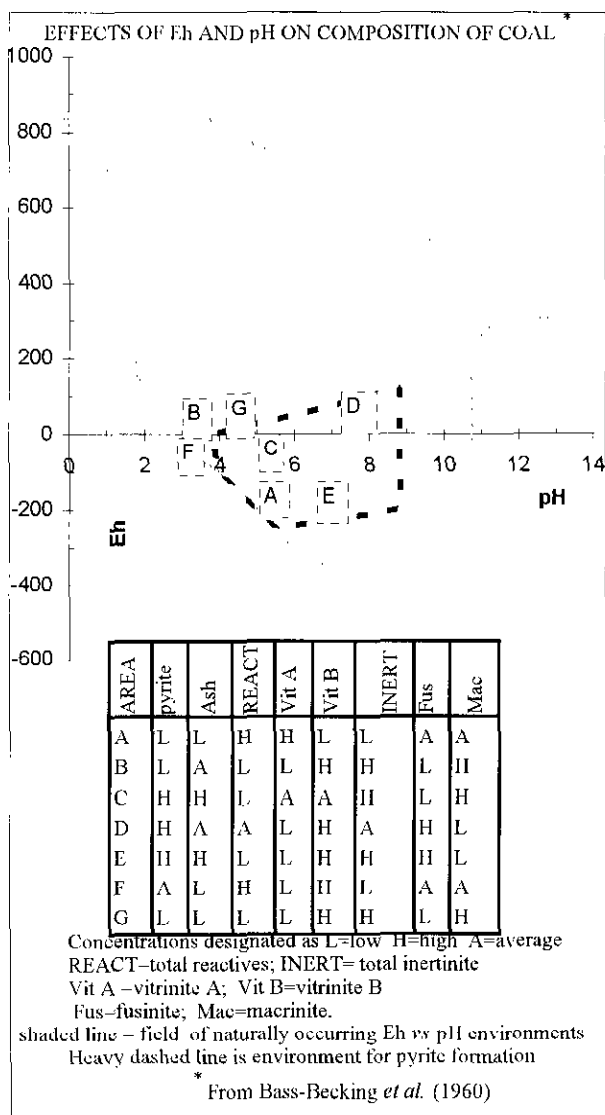


Figure 4: Coal formation model adapted from Bass-Becking *et al.* (1960) adapted to show possible relationships between sulphur and maceral concentrations.

The pH, Eh and water table levels also influence the composition of the ash. Peats deposited in a marine influenced environment often have higher pH values and increased bacterial activity. This results in high concentrations of H, N and S originating from bacterial remains in the coal. Marine influenced coals are also often associated with alkali-rich ashes because clays are less degraded in high pH environments. At low pH values, often associated with limnic environments, montmorillonite is altered to kaolinite, which flocculates at swamp margins and not their interiors.

There is a relationship between the availability of calcium and concentrations of ash and pyrite in seams. The availability of Ca from sea water increases pH values and makes the swamp waters alkaline favouring the activity of bacteria. Pyrite-rich seams are often associated with alkaline floor sediments or penicontemporaneous marls. This may act to balance the ARD potential of high pyrite coals.

Ryan (1996) discussed possible environments for the formation of coals in the Gething Formation from northeast BC, using a pH versus Eh diagram derived from Baas-Becking (1960). Many Gething coal seams have low concentrations of pyrite and ash and moderate to high inertinite contents. The inertinite has a high proportion of macrinite, which has lost its cell structure and probably formed from biomass that had previously experienced some humification. Based on these characteristics Gething coals should plot in area F in Figure 4 and branches 13 to 16 (Figure 2). The low pH values inhibit bacterial activity and the formation of pyrite and flocculate clays at the margin of the peat swamp helping to keep waters in the rest of the swamp clear. They would also alter clay minerals to kaolinite. The end result is that the inherent mineral matter will be kaolinite-rich with low base/acid ratios.

Roberts (1988) studied paralic coals from South Africa, which do not have a strong marine influence. He discussed the effects of high and low water tables on the composition of coal. His models are illustrated by branches 9-12 and 21-24 (Figure 2). He found that total sulphur correlated with vitrinite in coals, which probably formed under high water table conditions and moderate pH conditions. Coals formed under low water table conditions, high Eh and low pH values were characterized by high inertinite and low sulphur contents. Inertinite-rich coals of Australian cratonic basins (Hunt, 1989) are characterized by moderate sulphur contents that also correlate with vitrinite content. They may have formed in environments 21-24, Figure 2.

Based on a study of the Upper Freeport coal seams in Pennsylvania, Cecil *et al.* (1979) proposed three environments. The first, an intermittent aerobic peat environment, is characterized by low pH, high ash, semifusinite and macrinite contents and low sulphur concentrations. The intermittent oxidizing conditions inhibit the formation of H<sub>2</sub>S and therefore pyrite, but increase the amount of inerts and ash in the coal (branches 9, 10, 23, 24 on Figure 2 and area B on Figure 4).

The second is an anaerobic peat environment with pH values >4.5. This environment is characterized by high ash, sulphur, exinite and micrinite contents. The intermittent pH value is ideal for the production of H<sub>2</sub>S and bacterial destruction of vitrinite. Removal of vitrinite increases the percentage of exinite (branches 5 to 8 on Figure 2 and area C on Figure 4).

The third is an anaerobic peat environment with pH values <4.5. The low pH in this environment coupled by the high water table produces a coal with low ash and sulphur contents and high vitrinite contents (branches 9 and 10, Figure 2 and area A, Figure 4).

Renton and Bird (1991) state that the swamp environment plays a large part in defining both the content of pyrite and the maceral composition of the coal. In swamp environments with pHs > 4.5, high ash, pyritic sulphur and exinite concentrations are associated with peat that evolves to coals with low vitrinite contents (branches 5 and 6 in Figure 2 or area D in Figure 4).

The vitrinite will probably be desmocollinite associated with a lot of disseminated mineral matter. Environments where pH is less than <4.5, the resulting coals have low pyrite contents and high contents of bright vitrinite (tellinite and telocollinite) (branches 3 and 4 in Figure 2).

Lamberson *et al.* (1996) suggest that most inertinite is formed by fires, which burn the peat surface when it dries out. Many authors correlate low water tables during peat formation with the increased development of inertinite in coals, but often the exact process responsible for forming the inertinite is not well explained. Lamberson *et al.* point out that it is difficult to find a process other than burning, charring or smoldering that will increase the reflectance of organic material. This method of forming inertinite may make it easier to form inertinite-rich coals that are not associated with a lot of fine mineral matter or sulphur. In this case the inherent mineral matter could be carried away as smoke and the sulphur volatilized as SO<sub>4</sub>. It is harder to understand how burning or smoldering in the dried peat bed can produce coals with large amounts of macrinite, which has lost most of its cell structure.

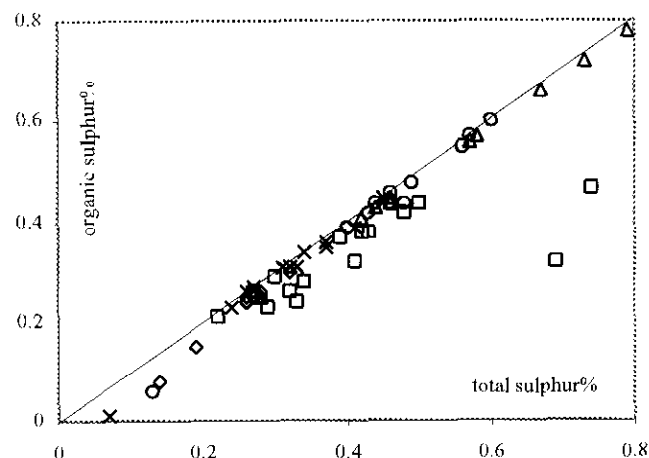


Figure 5: Plot of organic sulphur versus total sulphur for a number of Mist Mountain seams. Diamond, Rmax= 1.38 per cent. Triangle, Rmax= 1.36 per cent. Circle, Rmax=1.35 per cent. Cross, Rmax=1.25 per cent. Square, Rmax=0.9 per cent.

## SULPHUR FORMS IN COALS OF DIFFERENT RANK

The way organic sulphur is held in coal changes as rank increases, but this is not necessarily associated with a release of sulphur. Hydrogen sulphide gas is not generated from coal below temperatures of above 200°C (Hunt, 1979). As rank increases, so does the aromaticity of the coal so that some of the sulphur bound as thiols is restructured into heterocyclic compounds of thiophene type. If the sulphur is lost from coals, then on average the amount of organic sulphur in coal should decrease as the rank increases. Data from a number of seams from the Mist Mountain Formation (Figure 5) do not reveal any change in the relationship between total sulphur and organic sulphur for seams ranging in rank

Table 1  
ANALYTICAL DATA TENAS CREEK AREA

| sample                                      | seam    | from        | to  | ARM  | ADM  | VM              | Ash   | FC                    | TS%  | PS%  | OS%  | 1.6 yld                | ADM  | VM                 | Ash  | FC   | TS%  | PS%  | OS%  |      |
|---------------------------------------------|---------|-------------|-----|------|------|-----------------|-------|-----------------------|------|------|------|------------------------|------|--------------------|------|------|------|------|------|------|
| TK96-10                                     | C       | 0           | 20  | HW   | 4.59 | 0.61            | 23.7  | 13.9                  | 61.8 | 3.13 | 1.4  | 1.62                   | 81.0 | 0.51               | 25   | 9.07 | 65.4 | 1.44 | 0.54 | 0.82 |
| TK96-11                                     | C       | 20          | 40  | COAL | 4.45 | 0.69            | 25    | 21.5                  | 52.8 | 1.06 | 0.3  | 0.72                   | 70.6 | 0.66               | 25.2 | 14.6 | 59.6 | 0.97 | 0.21 | 0.73 |
| TK96-12                                     | C       | 40          | 72  | COAL | 4.56 | 0.61            | 23.7  | 18.2                  | 57.5 | 1.11 |      |                        | 77.5 | 0.71               | 25.4 | 11.9 | 61.9 | 1.11 |      |      |
| TK96-13                                     | C       | 72          | 103 | COAL | 4.24 | 0.7             | 21    | 36.1                  | 42.2 | 6.5  |      |                        | 30.0 | 0.47               | 29   | 7.19 | 63.4 | 1.67 |      |      |
| TK96-14                                     | C       | 103         | 132 | COAL | 7.66 | 0.6             | 28.3  | 6.18                  | 64.9 | 1.57 | 0.54 | 0.98                   | 96.5 | 0.52               | 29.2 | 4.22 | 66   | 1.18 | 0.36 | 0.78 |
| TK96-15                                     | C       | 132         | 160 | COAL | 6.45 | 0.59            | 25.9  | 7.14                  | 66.4 | 1.28 |      |                        | 98.3 | 0.5                | 26.2 | 6.58 | 66.7 | 1.18 |      |      |
| TK96-16                                     | C       | 160         | 170 | FW   | 5.77 | 0.75            | 25    | 18.3                  | 55.9 | 0.91 | 0.16 | 0.71                   | 75.1 | 0.51               | 26.3 | 10.2 | 63   | 0.89 | 0.06 | 0.8  |
| TK96-17                                     | C       | MDSTFW rock |     |      | 3.39 | 0.76            | 16.5  | 69.4                  | 13.3 | 5.1  |      |                        |      |                    |      |      |      |      |      |      |
| mass wt averages                            |         |             |     |      | 0.65 | 23.8            | 21.3  |                       | 3.01 |      |      |                        |      |                    | 9.31 |      | 1.09 |      |      |      |
| Channel                                     | C seam  |             |     |      | 0.7  | 24.5            | 16.6  | 58.2                  | 1.91 |      |      |                        |      |                    |      |      |      |      |      |      |
| TK96-1                                      | 1 U     | 0           | 16  | IHW  | 5.31 | 0.83            | 24.2  | 8.54                  | 66.5 | 1.33 | 0.45 | 0.79                   | 94.1 | 0.64               | 24   | 6.2  | 69.2 | 1.31 | 0.44 | 0.79 |
| TK96-2                                      | 1 U     | 16          | 28  | COAL | 3.04 | 0.68            | 20.9  | 30.9                  | 47.5 | 7.3  | 3.52 | 3.62                   | 46.6 | 0.42               | 22.8 | 13.1 | 63.7 | 1.21 | 0.38 | 0.74 |
| TK96-3                                      | 1 U     | 28          | 33  | MDST | 2.45 | 0.68            | 16.2  | 68                    | 15.2 | 2.49 |      |                        |      |                    | nd   |      | nd   |      |      |      |
| TK96-4                                      | 1 U     | 33          | 58  | COAL | 5.03 | 0.51            | 31.4  | 6.09                  | 62   | 1.96 |      |                        | 95.5 | 0.24               | 31.6 | 4.32 | 63.8 | 1.85 |      |      |
| TK96-5                                      | 1 U     | 58          | 78  | COAL | 8.03 | 0.67            | 26.8  | 7.4                   | 65.1 | 4.43 |      |                        | 91.6 | 0.5                | 28.3 | 2.65 | 68.6 | 1.4  |      |      |
| TK96-6                                      | 1 U     | 78          | 94  | COAL | 6.51 | 0.64            | 28.9  | 4.99                  | 65.5 | 2    | 0.61 | 1.34                   | 96.3 | 0.45               | 30   | 3.77 | 65.8 | 1.64 | 0.42 | 1.17 |
| TK96-7                                      | 1 U     | 94          | 117 | COAL | 6.9  | 0.53            | 28.2  | 3.97                  | 67.3 | 1.82 |      |                        | 96.9 | 0.41               | 28.6 | 3.09 | 67.9 | 1.59 |      |      |
| TK96-8                                      | 1 U     | 117         | 146 | COAL | 7.96 | 0.59            | 24.2  | 7.7                   | 67.6 | 1.42 |      |                        | 95.6 | 0.54               | 24.9 | 6    | 68.5 | 1.3  |      |      |
| TK96-9                                      | 1 U     | 146         | 180 | FW   | 6.45 | 0.5             | 24.4  | 15.5                  | 59.6 | 1.19 | 0.33 | 0.84                   | 76.9 | 0.53               | 25.5 | 8.96 | 65   | 1.11 | 0.23 | 0.86 |
| mass wt averages                            |         |             |     |      | 0.61 | 24.6            | 17.85 |                       | 2.61 |      |      |                        |      |                    |      | 6.41 |      | 1.39 |      |      |
| Channel                                     | 1 Upper |             |     |      | 0.6  | 24.8            | 14.6  | 60                    | 2.72 |      |      |                        |      |                    |      |      |      |      |      |      |
| TRC-05C-15                                  | 1       | 0           | 4   | SLST | 3.52 | 0.86            | 12.5  | 80.6                  | 6.07 | 0.42 |      |                        |      |                    |      |      |      |      |      |      |
| TRC-05C-14                                  | 1       | 4           | 10  | MDST | 5.5  | 0.85            | 11.8  | 72.6                  | 14.9 | 0.51 |      |                        |      |                    |      |      |      |      |      |      |
| TRC-05C-1                                   | 1       | 10          | 35  | COAL | 8.72 | 0.7             | 23.5  | 12.8                  | 63   | 0.71 | 0.09 | 0.61                   | 94.5 | 0.95               | 23.9 | 9.59 | 65.6 | 0.66 | 0.05 | 0.61 |
| TRC-05C-2                                   | 1       | 35          | 64  | COAL | 5.8  | 0.82            |       | 15.8                  |      | 0.57 |      |                        | 87.9 | 0.65               | 23   | 10.7 | 65.8 | 0.59 |      |      |
| TRC-05C-3                                   | 1       | 64          | 94  | COAL | 7.58 | 0.74            |       | 8.17                  |      | 0.69 |      |                        | 95.1 | 0.96               | 25.2 | 5.27 | 68.6 | 0.65 |      |      |
| TRC-05C-4                                   | 1       | 94          | 124 | COAL | 7.42 | 0.67            |       | 12.5                  |      | 0.56 |      |                        | 93.6 | 0.87               | 22.2 | 9.76 | 67.2 | 0.52 |      |      |
| TRC-05C-5                                   | 1       | 124         | 154 | COAL | 9.46 | 0.8             | 25.5  | 6.06                  | 67.7 | 0.76 | 0.13 | 0.54                   | 97.3 | 0.64               | 25.9 | 4.69 | 68.7 | 0.73 | 0.12 | 0.52 |
| TRC-05C-6                                   | 1       | 154         | 184 | COAL | 7.43 | 0.8             |       | 10.3                  |      | 1.05 |      |                        | 92.4 | 0.98               | 24.4 | 7.14 | 67.5 | 0.92 |      |      |
| TRC-05C-7                                   | 1       | 184         | 214 | COAL | 8.15 | 0.75            |       | 16                    |      | 0.64 |      |                        | 86.3 | 0.93               | 24.5 | 9.97 | 64.6 | 0.59 |      |      |
| TRC-05C-8                                   | 1       | 214         | 244 | COAL | 12   | 0.77            |       | 21.3                  |      | 0.63 |      |                        | 70.0 | 1.08               | 26.8 | 6.27 | 65.9 | 0.7  |      |      |
| TRC-05C-9                                   | 1       | 244         | 274 | COAL | 9.45 | 0.78            |       | 22.5                  |      | 0.79 |      |                        | 73.7 | 0.99               | 25.3 | 10.6 | 63.1 | 0.75 |      |      |
| TRC-05C-10                                  | 1       | 274         | 304 | COAL | 7.61 | 0.86            | 20.6  | 29.8                  | 48.7 | 0.6  | 0.18 | 0.4                    | 53.0 | 1.04               | 23.1 | 12.9 | 62.9 | 0.72 | 0.1  | 0.6  |
| TRC-05C-11                                  | 1       | 304         | 334 | COAL | 8.82 | 0.78            |       | 7.82                  |      | 0.77 |      |                        | 94.1 | 1.03               | 24.7 | 5.16 | 69.2 | 0.75 |      |      |
| TRC-05-12                                   | 1       | 334         | 359 | COAL | 7.61 | 0.73            | 22    | 11.6                  | 65.7 | 0.6  | 0.08 | 0.51                   | 91.3 | 1.23               | 22.4 | 7.84 | 68.5 | 0.59 | 0.05 | 0.54 |
| TRC-05-13                                   | 1       | 359         | 369 | COAL | 7.12 | 0.75            | 20.5  | 19.6                  | 59.1 | 0.57 |      |                        |      |                    |      |      |      |      |      |      |
| mass wt averages                            |         |             |     |      | 0.77 | 22.1            | 16.59 |                       | 0.68 |      |      |                        |      |                    | 8.14 |      | 0.67 |      |      |      |
| Channel                                     | 1 Seam  |             |     |      | 0.9  | 24.8            | 14.3  | 60                    | 1.67 |      |      |                        |      |                    |      |      |      |      |      |      |
| ARM as-received moisture                    |         |             |     |      |      | FW foot wall    |       | OS organic sulphur    |      |      |      | TS total sulphur       |      | PS pyritic sulphur |      |      |      |      |      |      |
| 1.6 yld float yield at 1.6 specific gravity |         |             |     |      |      | HW hanging wall |       | AD air-dried moisture |      |      |      | from to in centimetres |      |                    |      |      |      |      |      |      |

from 0.9 % to 1.38 %. It is not clear what happens to the organic sulphur in liptinite when it is progressively destroyed at higher ranks. Any organic sulphur lost during this transformation probably escapes in bitumen that moves out of the coal and leaves behind sulphur-free grains of micrinite.

## THE TELKWA COALFIELD

The Telkwa coalfield is in central British Columbia, centered on the town of Smithers. It extends from north of Smithers to south of Telkwa for about 50 kilometres along the Bulkley River (Figure 1). The coalfield contains a potential coal resource of approximately 850 million tonnes (Ryan and Dawson, 1994). The Telkwa coal property, which occupies less than 10 percent of the whole field, is 15 kilometres south of Smithers and is centered on the confluence of the Telkwa River and Goathorn Creek. Coal on the property is generally high-volatile A bituminous and is considered to be an

excellent thermal coal with some weak coking coal potential. Exploration in the last few years has been successful in finding more reserves in the southwest corner of the license block near Tenas Creek (Figure 1) and about 21 million tonnes of raw, surface mineable coal have been outlined in this area. This increases the raw coal, surface mineable reserve at Telkwa to about 50 million tonnes which makes the property more attractive for development as a thermal coal mine. At present Manalta Coal Limited is proceeding with development plans and has submitted a report to various ministries of the British Columbia Government as part of the environmental impact assessment process.

The geology of the Telkwa Coalfield is discussed in a number of papers (Koo, 1984, Bustin and Palsgrove, 1997) and is shown on regional geology maps of Tipper (1976), MacIntyre *et al.* (1989) and Ryan (1993). Coal-bearing rocks belong to the Skeena Group of Lower Cretaceous age and are assigned to the Red Rose Formation of Albian age and possibly also to the older

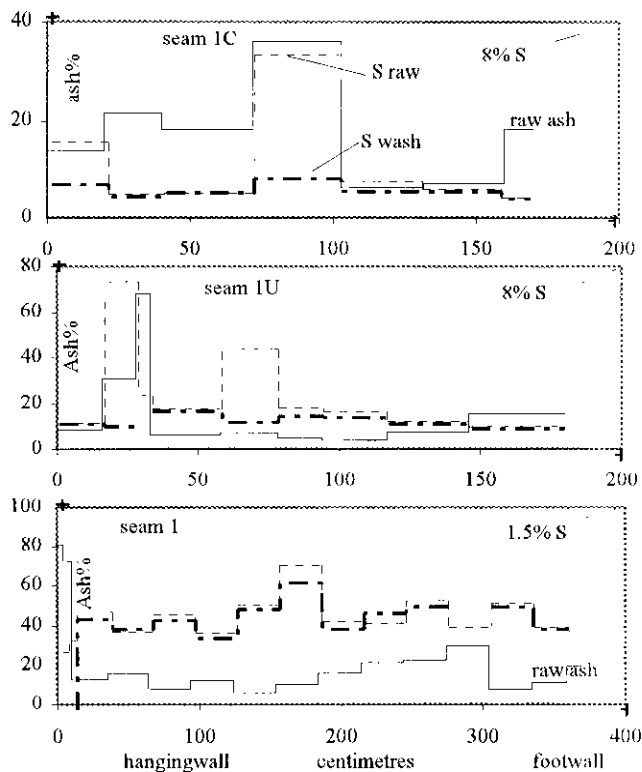


Figure 6: Ash and sulphur striplogs for seams 1, 1U and C. Ash on the left axis and maximum sulphur on the right axis.

Kitsun Creek Formation of Hauterivian age. Coal-bearing rocks outcrop north of Smithers, south of Smithers in the Bulkley River, north of the Telkwa River in the vicinity of Pine Creek, east and west of Goathorn Creek, and at the headwaters of Tenas and Cabinet Creeks (Figure 1). Cretaceous rocks of Hauterivian age outcrop along the northeast edge of the coalfield and contain only traces of coal.

Sulphur in the coal at Telkwa and Quinsam was studied by Holuszko *et al.* (1993). This study continues this investigation at Telkwa, specifically in the Tenas Creek area. In 1996 a test pit was dug in the Tenas Creek area, which is now considered to contain the best mining potential on the property and is expected to be the first area mined. The authors sampled the three mineable seams during the bulk sampling and collected increment and full seam samples. Samples were subjected to a number of analyses, petrographic investigation and scanning electron microscope work.

## EXPLORATION HISTORY

There is a long history of exploration and mining in the southern part of the Telkwa coalfield. In the Telkwa area coal seams were mined in 1903 on Goathorn Creek, previously called Goat Creek (Dowling, 1915). From 1913 to 1915 the Transcontinental Exploration syndicate sank a shaft and constructed 2 tunnels in the Cabinet Creek area (previously Cabin Creek), which intersected

five seams of semi-anthracite (Dowling, 1915). During the period from 1930 to 1970, six small underground mines and one surface mine operated in the Telkwa River-Goathorn Creek area and about 480 000 tonnes of coal were mined. More recently a small tonnage of coal was mined in the Goathorn Creek area by Lloyd Gething during the 1970s and early 1980s.

The recent exploration activity at Telkwa is recorded in a number of geological assessment reports submitted to the B.C. Ministry of Energy, Mines and Petroleum Resources (now part of the Ministry of Employment and Investment) and on file in Victoria (Handy and Cameron, 1982, 1983, 1984; McKinstry, 1990 and Ledda, 1992, 1993, 1994). The property was intensively explored in the period 1978 to 1989 by Crowsnest Resources Limited, when over 350 exploration holes were drilled and a large test pit excavated in the area east of Goathorn Creek. In 1992 Manalta Coal Limited acquired the property. Since then it has carried out a number of major programs, which concentrated on the areas north of the Telkwa River, east of Goathorn Creek and east of Tenas Creek. Mineable coal reserves have now been outlined in all three areas.

## LOCAL STRATIGRAPHY AND STRUCTURE

The stratigraphy of the Cretaceous Skeena Group on the Telkwa Coal property was divided into four units by Bustin and Palsgrove (1997). The lowest unit, which is 20 to 100 metres thick, rests unconformably on a basement of Lower Jurassic volcanic rocks of the Telkwa Formation, Hazelton Group. The unit is non-marine and is distinguished by an abundance of coarse clastics. It contains a single coal zone composed of up to 12 component coal beds, together referred to as Seam 1, which has a cumulative coal thickness ranging up to 12 metres and averaging 7 metres in the Tenas Creek area (Figure 1).

The coal formed in poorly drained areas adjacent to braided rivers. The combination of basement relief and poorly defined drainage patterns accounts for the variable character of Seam 1. There were occasional influxes of sea water, which periodically flooded, part or all, of the coal swamps causing both lateral and stratigraphic increase in sulphur contents of the Seam 1 coal beds.

Unit 2, which does not contain coal, is composed of from 60 to 170 metres of shallow marine mudstones and siltstones.

The major coal-bearing zone, which comprises seams 2 to 10, is within Unit 3, which averages 85 metres in thickness. The unit was deposited in an estuarine mud flat environment that experienced repeated influxes of sea water alternating with regressions and deposition of channel sands. The unit is composed of siltstones, mudstones, sandstones and coal. The seams with higher sulphur contents are generally overlain by

Table 2  
Petrography Tenas Creek Area

| sample          | lipinitite | telinitite | telocollinite | desmocollinite | detrovitrinite | total reactives | semifusinite             | fusinite | macrinite | micrinite | inertodetrinite | total inerts | mineral matter | ash wt % |
|-----------------|------------|------------|---------------|----------------|----------------|-----------------|--------------------------|----------|-----------|-----------|-----------------|--------------|----------------|----------|
| <b>C Seam</b>   |            |            |               |                |                |                 |                          |          |           |           |                 |              |                |          |
| TK96-10         | 3          | 6          | 17            | 25             | 1              | 53              | 13                       | 0        | 16        | 0         | 9               | 38           | 9              | 14       |
| TK96-11         | 1          | 10         | 16            | 20             | 3              | 50              | 17                       | 0        | 10        | 0         | 12              | 39           | 11             | 17       |
| TK96-12         | 1          | 9          | 19            | 19             | 8              | 57              | 12                       | 0        | 10        | 0         | 11              | 33           | 10             | 16       |
| TK96-13         | 1          | 10         | 10            | 24             | 19             | 64              | 3                        | 0        | 2         | 0         | 1               | 6            | 29             | 39       |
| TK96-14         | 2          | 8          | 28            | 29             | 2              | 70              | 17                       | 1        | 3         | 0         | 8               | 30           | 1              | 1        |
| TK-96-15        | 2          | 10         | 28            | 32             | 5              | 77              | 6                        | 0        | 7         | 0         | 8               | 22           | 2              | 3        |
| TK96-16         | 2          | 7          | 32            | 31             | 1              | 73              | 10                       | 1        | 2         | 0         | 4               | 17           | 10             | 16       |
| Av %            | 2          | 9          | 22            | 26             | 6              | 63              | 11                       | 0        | 7         | 0         | 8               | 26           | 10             | 15       |
| Av mmf          | 2          | 10         | 24            | 29             | 6              | 71              | 13                       | 0        | 8         | 0         | 8               | 29           |                |          |
| <b>seam 1 U</b> |            |            |               |                |                |                 |                          |          |           |           |                 |              |                |          |
| TK96-01         | 2          | 7          | 12            | 22             | 4              | 47              | 19                       | 0        | 19        | 1         | 12              | 51           | 2              | 3        |
| TK96-02         | 2          | 6          | 17            | 27             | 4              | 57              | 9                        | 0        | 7         | 0         | 8               | 24           | 18             | 27       |
| TK96-04         | 1          | 4          | 46            | 29             | 2              | 82              | 8                        | 0        | 6         | 0         | 1               | 16           | 2              | 3        |
| TK96-05         | 1          | 3          | 34            | 14             | 6              | 58              | 22                       | 0        | 11        | 0         | 6               | 39           | 3              | 5        |
| TK96-06         | 3          | 2          | 31            | 25             | 4              | 66              | 14                       | 1        | 12        | 0         | 4               | 32           | 2              | 3        |
| TK96-07         | 2          | 4          | 30            | 26             | 2              | 66              | 14                       | 0        | 14        | 0         | 4               | 33           | 1              | 2        |
| TK96-08         | 2          | 5          | 16            | 19             | 5              | 47              | 20                       | 0        | 17        | 2         | 11              | 50           | 3              | 5        |
| TK96-09         | 1          | 2          | 29            | 19             | 5              | 56              | 19                       | 0        | 11        | 1         | 6               | 37           | 8              | 12       |
| Av %            | 2          | 4          | 27            | 23             | 4              | 60              | 16                       | 0        | 12        | 0         | 7               | 35           | 8              | 8        |
| Av mmf          | 2          | 6          | 35            | 30             | 5              | 79              | 21                       | 0        | 16        | 1         | 9               | 46           |                |          |
| <b>seam 1</b>   |            |            |               |                |                |                 |                          |          |           |           |                 |              |                |          |
| TRC-05-02       | 3          | 8          | 22            | 20             | 7              | 60              | 12                       | 0        | 10        | 1         | 11              | 35           | 6              | 9        |
| TRC-05-03       | 1          | 6          | 28            | 25             | 2              | 62              | 14                       | 1        | 13        | 0         | 7               | 35           | 2              | 4        |
| TRC-05-04       | 5          | 5          | 8             | 22             | 2              | 42              | 18                       | 0        | 16        | 1         | 14              | 49           | 8              | 13       |
| TRC-05-06       | 2          | 9          | 19            | 28             | 4              | 62              | 12                       | 0        | 10        | 0         | 8               | 30           | 8              | 12       |
| TRC-05-07       | 2          | 8          | 18            | 31             | 7              | 66              | 13                       | 0        | 6         | 0         | 7               | 26           | 8              | 13       |
| TRC-05-08       | 1          | 3          | 28            | 33             | 1              | 67              | 13                       | 0        | 4         | 0         | 5               | 22           | 11             | 18       |
| TRC-05-10       | 2          | 6          | 21            | 22             | 8              | 59              | 10                       | 0        | 5         | 0         | 6               | 21           | 20             | 29       |
| TRC-05-11       | 2          | 7          | 18            | 31             | 2              | 60              | 18                       | 1        | 15        | 0         | 5               | 39           | 1              | 2        |
| TRC-05-12       | 3          | 11         | 9             | 15             | 5              | 42              | 20                       | 3        | 19        | 0         | 10              | 52           | 6              | 9        |
| TRC-05-5        | 1          | 10         | 20            | 29             | 2              | 62              | 14                       | 1        | 11        | 0         | 9               | 35           | 3              | 5        |
| TRC-05-1        | 2          | 8          | 21            | 24             | 7              | 61              | 11                       | 1        | 8         | 0         | 11              | 30           | 9              | 14       |
| TRC-05-9        | 0          | 6          | 29            | 27             | 3              | 66              | 9                        | 1        | 5         | 0         | 4               | 19           | 16             | 24       |
| Av %            | 2          | 7          | 20            | 25             | 4              | 59              | 13                       | 1        | 10        | 0         | 8               | 33           | 8              | 13       |
| Av mmf          | 3          | 10         | 27            | 34             | 6              | 79              | 18                       | 1        | 14        | 0         | 11              | 44           |                |          |
| SG coal         | 1.3        |            | SG rock       |                | 2.5            |                 | ratio min matter/ash=1.2 |          |           |           |                 |              |                |          |

sandstone. The cumulative coal thickness in unit 3 averages 20.5 metres in areas considered for development.

Unit 3 is overlain by the sandstone-rich unit 4, which is over 100 metres thick, contains no economic coal and represents a major shallow marine transgression.

Outcrop on the Telkwa coal property is sparse and an understanding of the structural geology and seam stratigraphy has evolved as information from drilling and a number of geophysical surveys have become available. Bedding generally dips shallowly southeast or east and is disrupted by at least two generations of faulting. The first generation of faults occurred in the Late Cretaceous and are represented by east-dipping thrusts and reverse faults, that offset the east dip of the sediments east of Goathorn Creek. The younger Tertiary, steep-dipping faults trend northwest or

northeast. Folding in the Late Cretaceous (Evenchick, 1991) has produced open folds that trend northwest with shallow plunges, shallow-dipping west limbs and steeper-dipping east limbs.

The Tenas Creek area, which is underlain by Unit 1, is folded into an open northwest trending syncline. Dips on the west limb range from 9° to 22° and those on the east limb are steepened up to 45°. The resource in the area is contained in Seam 1, which contains a number of coal beds, three of which feature in the mine plans. The lowest bed (1 seam) averages 3.45 metres in thickness and is overlain by a siltstone parting, which attains a maximum thickness of 2.5 metres. 1 Upper seam, which averages 1.9 metres in thickness, overlies the siltstone split. The upper-most C seam averages 1.5 metres and is separated from 1 Upper seam by 13 metres of interbanded sandstone and mudstone. Open pit mineable reserves at Tenas Creek are estimated to be 21 million tonnes based on data from 187 drillholes, which provide a hole spacing of about 150 metres (Manalta Coal Limited, 1997).

The quality of coal from Unit 1 has been studied in the Goathorn Creek- Telkwa River and Pine Creek areas, but not in the Tenas Creek area. In 1989 Matheson (Matheson and Van Den Bussche, 1990) drilled a number of short holes, 6 of which intersected 1 seam near the Telkwa River and Goathorn Creek. In 2 of the holes sulphur contents range from 0.23 to 3.52 and increase towards the hangingwall but for the rest of the seam are less than 0.5 %.

Holuszko *et al.*, (1993) studied 9 samples of coal from Hole GSB89-1 (Matheson and van Den Bussche, 1990) now considered to have penetrated unit 1 coals. The sulphur content averaged 3.53 % and reached 9.7 % in the hangingwall coal. The upper part of the seam was enriched in vitrinite (94.6 %), which was associated with increased amounts of coarse pyrite. The size and amount of pyrite decreased downwards through the seam in conjunction with the vitrinite content, which averages 65 % in the lower parts. More of the data collected as part of the 1989 drill program is described in Matheson *et al.* (1994). Holes GSB89-3 and GSB89-4, which intersected splits of 1 seam, both have low sulphur contents of 0.42 % and total reactives contents of 76 % and 84 %.

## SAMPLING PROGRAM

Samples were collected from the three major seams (C Seam, 1 Upper and 1 Seam) in the Tenas Creek area. Seven samples were collected from C seam, nine from 1 Upper, and fourteen from 1 Seam. Sampling increments averaged about 30 centimetres. In addition full seam channel samples were collected. Raw and samples washed at 1.6 specific gravity were subjected to proximate and sulphur form analyses (Table 1). The petrographic compositions of most of the samples were measured using polished samples and an oil immersion lens. Three hundred grains per sample were identified, which is sufficient to provide an estimate of trends in petrography (Table 2). The major macerals were

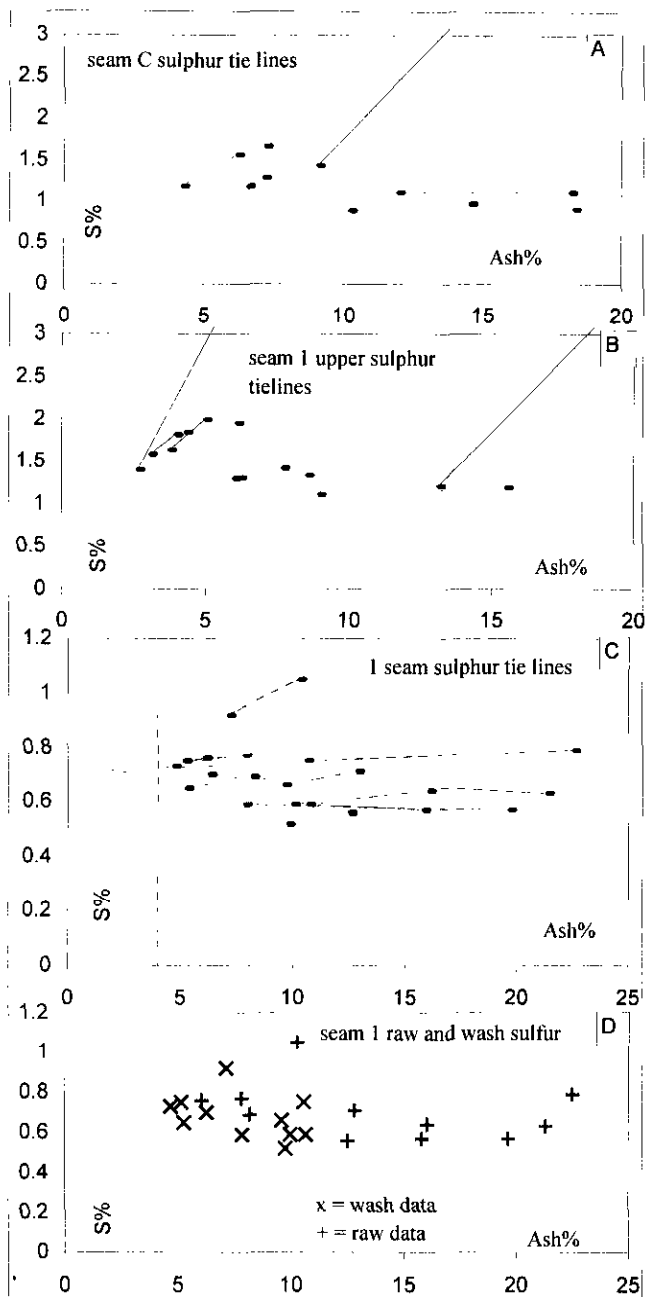


Figure 7: Sulphur versus ash tieline plots for seams 1, 1U and C. Lines join raw and 1.6 specific gravity wash data points.

identified included the vitrinite sub macerals tellinite, telocollinite, detrovitrinite and desmocollinite and the inertinite sub macerals semifusinite, fusinite, inertodetrinite and macrinite. No attempt was made to quantify the small quantities of micrinite and gelovitrinite or to subdivide the liptinites.

## DATA INTERPRETATION

### Coal quality data

The average raw total sulphur contents of the three seams decrease downwards, with C seam being

characterized by high sulphur in the hangingwall coal and a rock split (Figure 6). Sulphur in 1 Upper is concentrated above a rock split and sulphur in 1 seam, which is the thickest seam, correlates with low ash increments. The striplog pattern indicates that the two upper seams each experienced influxes of sulphur from the hangingwall and associated with deposition of a mudstone split.

The weighted average sulphur content of all the C seam samples is 1.91 % compared to a channel sample value of 3.01 %. The difference probably indicates the difficulty of collecting a representative sample of the seam because it contains irregularly distributed concentrations of coarse pyrite. The total sulphur content of C Seam is higher in hangingwall coal, indicating that there was some marine influence. Also the organic sulphur content is higher than in 1 seam (Table 1) indicating some hydrogen sulphide in seams C and 1U was generated in the coal swamp below the mudstone split, but that there was insufficient iron available to combine with all the  $H_2S$  as pyrite. The coarse pyrite in the hangingwall coal and associated with the split is easily removed (Figure 6).

The weight averaged sulphur content of 1 Upper is 2.61 % using the increment samples, which agrees quite well with the single full channel result of 2.71 %. The highest sulphur content (7.3 %) occurs just above a mudstone split. If the 28 centimetres of coal and 5 centimetre mudstone split are removed then the average seam sulphur drops to 1.9 %. The high sulphur above the split indicates that a lot of sulphur has percolated downwards through permeable hangingwall rocks into the upper part of the seam after it was buried. The mudstone split isolated the lower part of the seam from the sulphate-rich waters. The hanging wall portion of the coal could be mined separately, but the high raw sulphur values are deceptive because a lot of it is coarse pyrite that is easily washed out. In fact in this case the float sulphur for the increment samples (heavy dashed lines, Figure 6) above the mudstone are no higher than float sulphur values below the split and separate handling of the upper part of the seam would not effect the clean coal sulphur content.

The channel sample of 1 seam has sulphur content (1.67 %) higher than for the average of the increment samples (0.68 %) suggesting that there is some coarse pyrite in the seam. Sulphur contents are not higher in the hangingwall coal consequently there is no evidence of marine sulphate percolating downwards into the seam. Sulphur contents (Figure 6) are only slightly reduced by washing.

Raw and wash total sulphur data from drill cores is of necessity used to predict the sulphur contents of planned product coal from a wash plant. This introduces the problems of size consist and specific gravity (SG). Drillcore is washed at a top size of about 10 millimetres and experiences better liberation than coal entering a wash plant, which is usually crushed to a size range of 50-0 millimetres. The second problem results from the fact that the core is washed to a fixed SG whereas a plant

operates at variable densities to produce a constant ash concentration. The average wash ash concentration of the drillcore data rarely matches the clean coal ash specifications from a wash plant. The average sulphur concentration of the drillcore data, therefore, must be increased to account for the decrease in wash plant liberation and must be adjusted to reflect SG variations between the wash drillcore ash concentration and clean ash specifications for the plant.

Sulphur *versus* ash tieline plots provide one way of adjusting sulphur contents to different ash concentrations and they also give insights into the form of the sulphur. Tieline plots for the three seams (Figure 7 a, b, c) indicate clearly the different washing tracts for sample with coarse pyrite and those with finely dispersed pyrite or organic sulphur. The former form steep lines with positive slope and the latter flat lines some with negative slope. The background sulphur concentrations in seams C, 1 Upper and 1 are about 1.2 %, 1.2 % and 0.7 %. The tielines for seam 1 are projected to lower ash concentrations with dashed lines. An approximate estimate of sulphur at a lower ash concentration could be derived by averaging the projected sulphur intercepts on a vertical ash line in this case 4 % (chosen for the sake of clarity). In comparison Figure 7d is a plot of all sulphur data *versus* ash and estimating sulphur from this diagram would provide a higher sulphur concentration than the technique above. Neither technique is without faults, but the tieline approach may provide a better estimate.

In general the Texas Creek samples tend to have a lower organic/total sulphur ratio than coals from the Mist Mountain Formation (Figures 5 and 8b). With the exception of two samples with very high organic sulphur contents, there is more organic sulphur in the wash than raw samples (Figure 8a) and organic sulphur contents tend to increase as the ash decreases. The two samples with high organic sulphur are the hangingwall coal from C (1.62 %) and coal above the split in 1U (3.62 %). The organic sulphur contents of both these samples, which also have high pyritic sulphur, are reduced to less than 1 % after washing without extensive loss of coal. This means that some of the coal has very high organic sulphur contents. Removing small quantities of it with the ash does not drastically decrease the yield, but does decrease the total sulphur content of the wash product.

A lot of the coarse pyrite is associated with detrovitrinite and finely disseminated ash (Photo 1). The association of detrovitrinite, fine ash and coarse pyrite could indicate an environment of moderate pH, in which vitrinite formed, followed by generation of H<sub>2</sub>S at a fairly high pH with limited introduction of iron and a moderate amount of disruption and biodegradation of the humus.

The pyritic sulphur concentrations of most of the samples increase as the coal is washed (Figure 8a) because most of the pyrite is finely dispersed in vitrinite and is concentrated as the ash is removed. The sulphur content of the ash is low, probably less than 0.2 % and consequently it would be better to wash the coal to a

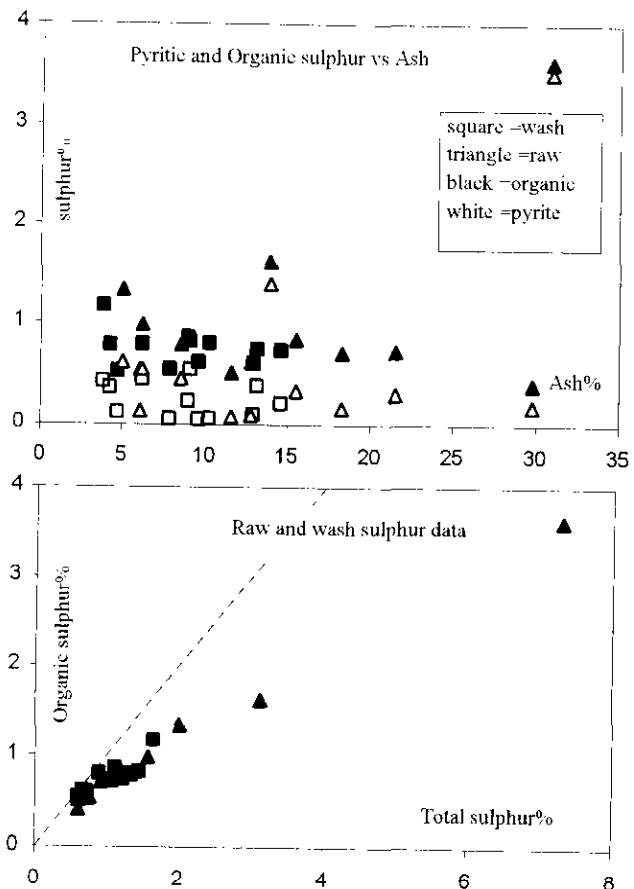


Figure 8: Wash pyrite, raw pyrite and organic sulphur *versus* ash plots for seams 1, 1U and C.

higher ash concentration to maintain clean coal sulphur contents at the 1 % level.

Some useful information about weathering, rank and petrography can be deciphered from inherent or bed moisture content of coal. It is always useful to generate a plot of as-received moisture *versus* ash to see if there are any significant variations in these parameters on a seam by seam basis because this information is always readily available. The predicted as-received moistures at zero percent ash vary from 11 % to 7 % (Figure 9) and decrease to zero at ash values varying from 65 % to 81 %, which is equivalent to about 100 % mineral matter, because of the weight loss that occurs when the mineral matter is ashed. The lower ash at zero moisture for 1 Upper Seam may indicate a more calcareous ash, which often signifies a marine influence and more sulphur, especially pyritic sulphur. The higher moisture in 1 seam at zero ash may indicate that the samples were weathered or that the seam contains a higher proportion of vitrinite. In fact the mineral matter free average total reactivities contents of the seams are 79 % for seams 1 and 1U and 70 % for C. The easiest way of separating the effects of petrography from those of weathering is by using an ash *versus* FSI plot (Ryan, 1996) or by doing oxidation tests (the light transmittance test is the best for high-volatile A through medium-volatile bituminous ranks). Another important aspect of as-received moisture is the fact that it can give an indication of the

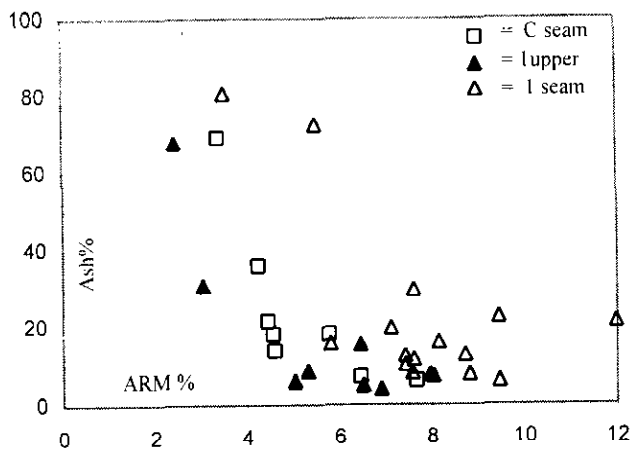


Figure 9: As-received moisture *versus* ash for seams 1, 1U and C.

Run-Of-Mine moisture content of the coal. Based on a 20 % ash and the data in Figure 6, a moisture content averaging about 7 % seems reasonable. This value in conjunction with product moisture specifications should be factored into plant recovery calculations.

### Petrography data and relationship to sulphur distribution

The petrographic composition of 6 samples from C seam, 8 samples of 1 Upper seam and 12 samples of 1 seam were measured (Table 2) and the data presented as striplogs for the three seams (Figure 10). The seams are characterized by total reactivities contents that range from 70 % to 80 % on a mineral-matter-free basis. A lot of the inertinite occurs as macrinite or inertodetrinite and there is not much semifusinite with well preserved cell structure and very little fusinite. Samples contain moderate to low contents of liptinite considering their rank of high-volatile bituminous.

The striplogs indicate that there are no major variations in petrography through the seams. There is a tendency for the upper part of the seams to be vitrinite poor and this correlates with the presence of coarse pyrite which occurs above the splits in C and 1U seams. There are also some correlations in cross plots that provide hints to the controls of maceral formation. There is a good correlation between semifusinite plus fusinite *versus* total inerts (Figure 11e), which is also apparent in data sets for Mist Mountain coals (Cameron, 1972 and Grieve, 1993 ). But the proportion of semifusinite+fusinite is higher in the Elk Valley samples (dashes in Figure 11e). The correlation between semifusinite+fusinite in both areas implies a similar origin, or inter-relationship of origins for the formation of structured inertinite and massive inertinite and consequently both may be related to fire, smoldering or charring. There is a similar relationship between the amount of structured vitrinite *versus* total vitrinite (Figure 11a) and the proportion of structured vitrinite increases as the amount of total vitrinite increases. The formation of desmocollinite and inertovitrinite implies a

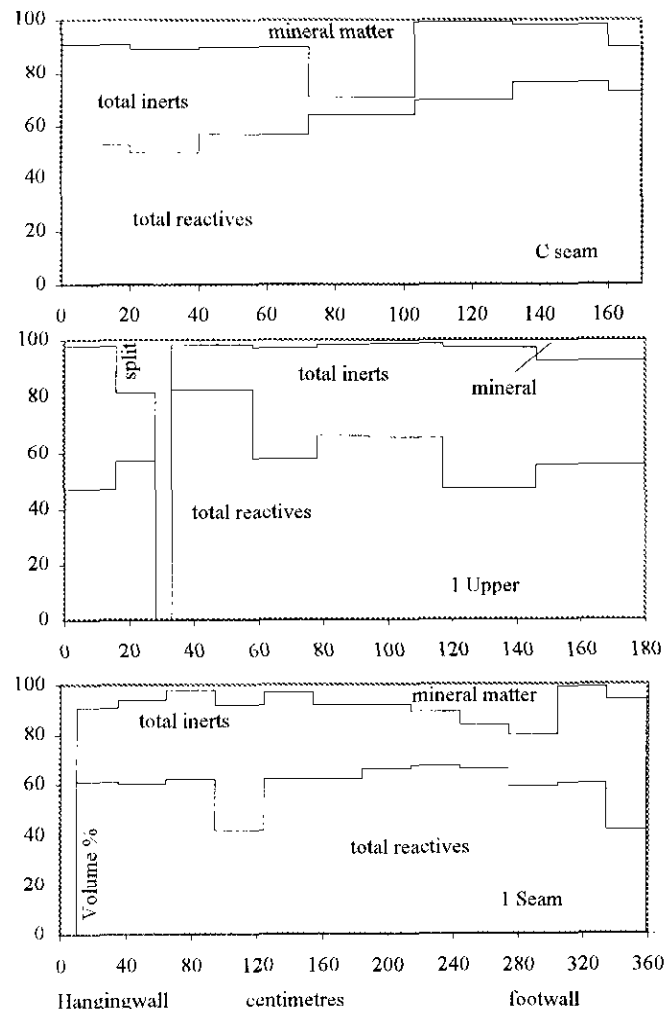


Figure 10: Striplogs of basic petrography for seams 1, 1U and C.

high degree of degradation of humus. There is a weak negative correlation of liptinite with total reactivities (Figure 11b) implying that, as observed by other authors, liptinite is more resistant to biodegradation than previtrinite material.

It is easy to recognize the various forms of pyrite in the three seams. Coarse pyrite is concentrated in the upper part of Seam 1 Upper above the split (Photo 3). Below the split the pyrite occurs as fine framboids or euhedral grains usually scattered in vitrinite (Photo 1, 2). The euhedral pyrite fills cavities in desmocollinite or semifusinite and generally the coal does not appear to have compacted around the grains implying a latter origin than framboidal pyrite around which the coal is compacted. There is very little visible pyrite in 1 Seam, which contains some pyrite filling fractures in inertinite

(Photo 4). This is evenly distributed through the seam and was probably the last morphology of pyrite to be implaced. It is difficult to quantify the various forms of pyrite and compare the amounts to changes in petrographic composition. This can be done in an approximate fashion by generating a correlation matrix between macerals proportions and the sulphur analytical

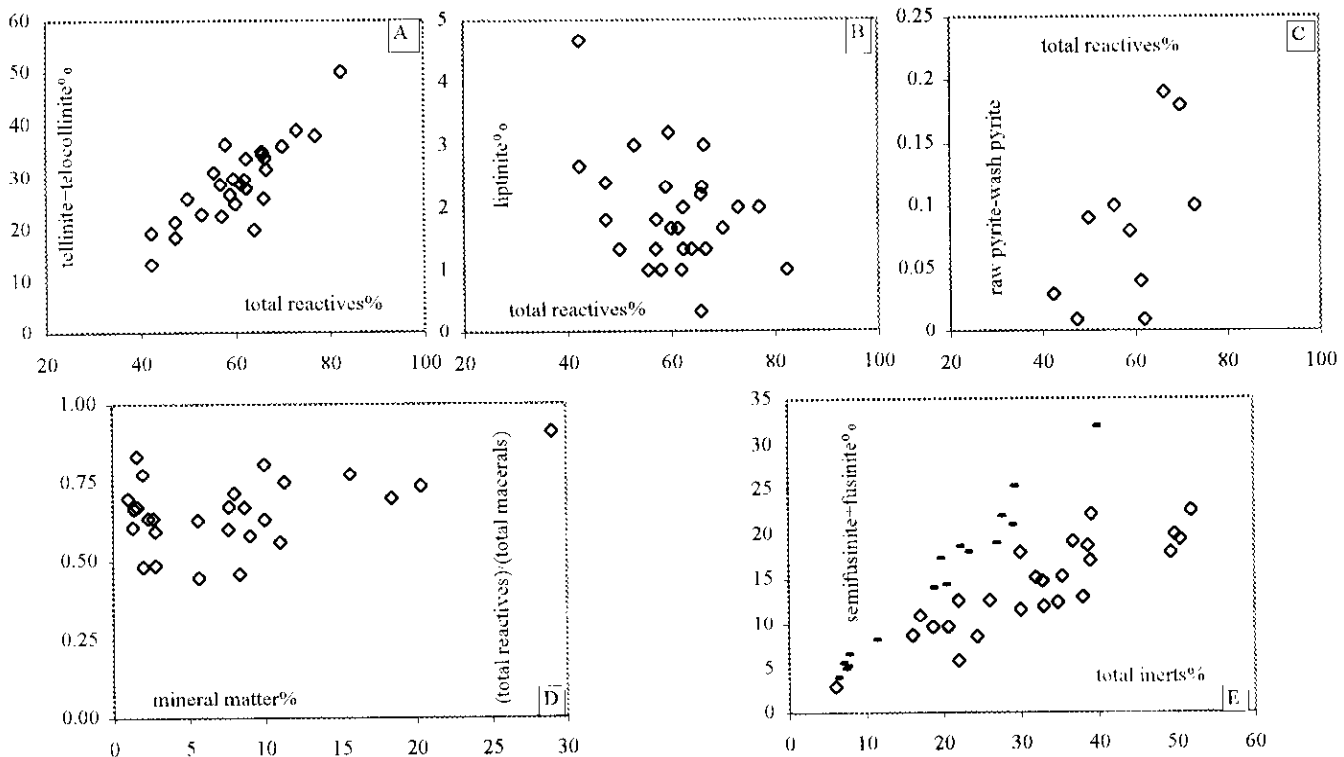


Figure 11: Maceral cross plots for various maceral and sulphur combinations; a/ structured vitrinite *versus* total vitrinite; b/ liptinite *versus* total reactives; c/ easily removed pyrite *versus* total reactives; proportion of total reactives *versus* per cent mineral matter; structured inertinite *versus* total inertinite for Telkwa (diamonds) and Elk Valley coals. Dash data from Grieve, (1993), diamond data from Tenas Creek.

Table 3

Partial correlation matrix for sulphur and petrographic data

|              | liptinite | telinite | telocollinite | desmocollinite | detrovitrinite | total reactives | semifusinite | macrinite | inertodetrinite | total inerts | mineral matter |
|--------------|-----------|----------|---------------|----------------|----------------|-----------------|--------------|-----------|-----------------|--------------|----------------|
| C seam       |           |          |               |                |                |                 |              |           |                 |              |                |
| TS% R        | -0.2      | 0.1      | -0.7          | -0.1           | 0.8            | -0.1            | -0.6         | -0.2      | -0.7            | -0.6         | 0.8            |
| PS% R        | 0.8       | -0.6     | -0.5          | -0.2           | -0.4           | -0.5            | 0.0          | 0.8       | 0.2             | 0.6          | -0.1           |
| OS% R        | 0.9       | -0.7     | -0.4          | -0.1           | -0.5           | -0.4            | -0.1         | 0.7       | 0.2             | 0.5          | -0.1           |
| VM% W        | -0.2      | 0.2      | 0.0           | 0.3            | 0.5            | 0.5             | -0.3         | -0.8      | -0.6            | -0.6         | 0.3            |
| Ash% W       | -0.4      | 0.1      | -0.3          | -0.7           | -0.1           | -0.7            | 0.3          | 0.4       | 0.5             | 0.4          | 0.2            |
| TS% W        | 0.1       | 0.0      | -0.7          | -0.1           | 0.7            | -0.1            | -0.5         | 0.1       | -0.5            | -0.4         | 0.6            |
| PS% W        | 0.7       | -0.4     | -0.5          | -0.2           | -0.2           | -0.5            | 0.3          | 0.7       | 0.4             | 0.7          | -0.3           |
| OS% W        | 1.0       | -1.0     | 0.3           | 0.6            | -1.0           | 0.3             | -0.7         | 0.1       | -0.6            | -0.3         | -0.1           |
| 1 upper seam |           |          |               |                |                |                 |              |           |                 |              |                |
| TS% R        | -0.1      | 0.1      | -0.1          | 0.1            | 0.2            | 0.0             | -0.4         | -0.5      | 0.1             | -0.4         | 0.8            |
| PS% R        | -0.1      | 0.4      | -0.4          | 0.8            | -0.6           | 0.1             | -0.9         | -0.7      | 0.1             | -0.7         | 0.9            |
| OS% R        | -0.1      | 0.3      | -0.3          | 0.8            | -0.5           | 0.2             | -0.9         | -0.7      | 0.0             | -0.8         | 0.9            |
| VM% W        | -0.1      | -0.5     | 0.9           | 0.2            | -0.3           | 0.8             | -0.2         | -0.4      | -0.9            | -0.5         | -0.6           |
| Ash% W       | -0.1      | 0.3      | -0.5          | 0.2            | 0.1            | -0.3            | -0.3         | -0.2      | 0.4             | -0.1         | 0.9            |
| TS% W        | 0.1       | -0.1     | 0.7           | 0.5            | -0.6           | 0.8             | -0.5         | -0.3      | -0.7            | -0.5         | -0.6           |
| PS% W        | 0.9       | 0.6      | -0.5          | 0.6            | -0.7           | 0.0             | -0.3         | 0.5       | 0.4             | 0.2          | -0.3           |
| OS% W        | 0.6       | -0.7     | 0.8           | 0.0            | 0.5            | 0.8             | 0.0          | 0.0       | -0.8            | -0.1         | -0.6           |
| I seam       |           |          |               |                |                |                 |              |           |                 |              |                |
| TS% R        | -0.5      | 0.3      | 0.2           | 0.4            | -0.2           | 0.4             | -0.3         | -0.1      | -0.3            | -0.2         | -0.1           |
| PS% R        | -0.1      | -0.7     | 0.6           | 0.3            | 0.4            | 0.5             | -0.7         | -0.7      | -1.0            | -0.8         | 0.7            |
| OS% R        | -0.5      | 0.5      | 0.0           | 0.3            | -0.4           | 0.2             | 0.2          | 0.2       | 0.9             | 0.3          | -0.7           |
| VM% W        | -0.8      | -0.3     | 0.7           | 0.8            | -0.6           | 0.8             | -0.3         | -0.5      | -0.7            | -0.6         | -0.1           |
| Ash% W       | 0.4       | -0.2     | -0.1          | -0.5           | 0.8            | -0.1            | -0.5         | -0.4      | 0.1             | -0.3         | 0.8            |
| TS% W        | -0.6      | 0.1      | 0.4           | 0.5            | -0.1           | 0.5             | -0.4         | -0.3      | -0.5            | -0.5         | 0.1            |
| PS% W        | -0.5      | -0.2     | 0.5           | 0.7            | -0.3           | 0.6             | -0.4         | -0.4      | -0.6            | -0.5         | 0.1            |
| OS% W        | 0.3       | -0.8     | 0.5           | -0.1           | 0.9            | 0.3             | -0.7         | -0.7      | -0.2            | -0.7         | 0.7            |

data (Table 3). This reveals some weak correlations between pyritic and organic sulphur and the various macerals. This is probably because there is not a lot of sulphur form data and there is not a lot of variation in the maceral data.

Organic sulphur in high sulphur seams C and 1U tends to correlate with liptinite content whereas in the low sulphur 1 seam there are no consistent correlations. Coarse pyrite, which is a large component of the raw pyrite contents in seams C and 1U, does not appear to correlate consistently with any particular maceral. A better measure of coarse pyrite is the difference between wash and raw pyrite and this value does tend to correlate with total reactives (Figure 11c). Fine pyrite, which is probably well represented by the wash pyrite contents in seams C and 1U, correlates with liptinite and other reactive macerals in seam 1U.

### Washability data

The washing characteristics of the three seams at Telkwa are estimated using a plot of wash ash *versus* coal recovery (Figure 12), which gives an indication of the relative ease of washing. Coal recovery is calculated as:

coal recovery =

$$\text{yield} \times (100 - \text{wash ash} \times R) / (100 - \text{raw ash} \times R)$$

where R = wt mineral matter/wt ash.

Data for easy washing seams plots in the top left corner of the diagram and seams that are more difficult to wash plot in the lower right. It is apparent that

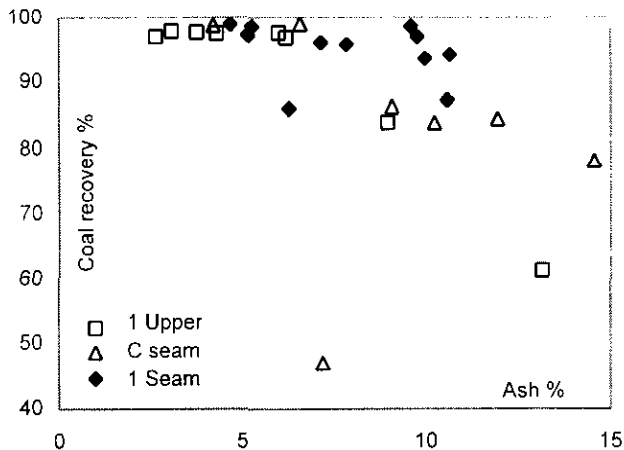


Figure 12: Wash ash *versus* coal recovery data for seams 1, 1U and C.

relative ease of washing of the three seams is 1 Upper > C > 1 Seam. This sequence agrees with the ash *versus* yield plots from full washability data for the seams (Figure 13). Coal recovery correlates positively with the inert macerals and negatively with detrovitrinite probably because of the association of finely disseminated mineral matter with this maceral.

Full seam samples of the three seams were subjected to size analysis and washability incorporating 11 SG fractions. Samples were crushed and screened at top sizes of 9.6, 6.0, 0.6 and 0.15 millimetres. Sulphur data for the three seams indicates that there is some liberation of pyrite into the finer sizes, but only from the 6.0 to 0.15 millimetre size range (Table 4). The 9.6 to 6.0 millimetre size material experienced a net pyrite gain, because there was little liberation of pyrite into finer sizes and some pyrite-free fine coal or ash particles ended up in finer sizes after the crushing and screening process. Pyrite is liberated from the 6.0 to 0.6 millimetre size range and this pyrite is pushed into the 0.15 to 0.0 millimetre size range.

It is possible to estimate the amount of coarse and fine pyrite in the samples using the washability data. For example, the total sulphur of seam 1 for the upper 9.6 to 6.0 millimetre size range is 3.13 % and this is easily reduced to about 1.65 % (Figure 13), probably by the removal of coarse pyrite. The organic sulphur content of this sample is 0.95 % so that 1.65% - 0.95% = 0.7% is an estimate of the amount of fine pyrite in the sample. Table 4 documents the sulphur form and liberation data interpreted from the washability data. The 1 Upper seam contains more coarse than fine pyrite, whereas C seam contains about equal amounts of coarse and fine pyrite. The 1 seam, which contains low concentrations of both coarse and fine pyrite, is the easiest to wash. The coarse pyrite is concentrated in the 9.6 to 6.0 millimetre size fraction of all three seams.

The form, association and size of pyrite grains in the Telkwa seams are all critical to estimating how easy it will be to remove the pyrite and lower the sulphur concentration of the clean coal. It is important to know the sulphur concentration that can be achieved by practical washing methods. It can be uneconomic to

crush coal to a fine size-consist, or to intensely wash it with a low recovery, to obtain a low sulphur product. It might be more practical to remove the sulphur during the end use of the coal, for example by scrubbers in modern coal power plants.

The sulphur is distributed in the coal as organic sulphur, fine pyrite (framboidal or euhedral) and coarse pyrite. The fine pyrite is enclosed by vitrinite and will be difficult to liberate it tends to occur throughout the seam. The coarse pyrite, which is concentrated in the hangingwall coal, appears to be easily liberated and occurs detached grains in the petrographic mounts.

## ACID ROCK DRAINAGE IMPLICATIONS

This paper does not address the issue of acid rock drainage (ARD) at Telkwa. There are a number of consultant reports covering the ARD included in the Telkwa Coal Project Report (Manalta Coal Limited, 1997). However because the title does include the two words sulphur and Telkwa it is appropriate to emphasize some very general points.

Mining disturbs much larger volumes of interburden rock than coal seams. It is therefore important to concentrate acid rock drainage studies more on the interburden rock rather than on the coal. Sulphur in coal occurs in organic and pyritic forms. The organic sulphur does not oxidize and does not take part in acid forming reactions. Pyrite can oxidize to form sulphuric acid and ferrous iron hydroxides. This is the basis of the acid rock drainage problem.

When coal seams are mined, they produce three controlled product streams; the clean coal, which leaves the site; the coarse refuse and the fine tailings material. Only pyrite is that is easily washed out of the coal stays on the mine lease, either in tailing material (fine framboidal or euhedral pyrite) or in the coarse rejects (coarse pyrite).

Different forms of pyrite are more or less susceptible to oxidation under similar conditions. Framboidal pyrite composed of many very small crystals has the highest surface area to volume ratio and therefore can oxidize rapidly. The rapid generation of acid can overwhelm the natural neutralizing capacity of surrounding rock even if on a stoichiometric basis it contains sufficient capacity to do the job. Luckily most of the framboidal pyrite will end up in the tailings and can therefore be placed in a non-oxidizing environment.

Coarse pyrite oxidizes slower than fine pyrite and therefore places less stress on the neutralizing capacity of the surrounding rocks. This type of pyrite is most likely to end up in the coarse rejects. When determining a safe ratio of neutralizing potential to acid generating potential it is important to consider the relative percentages of the various forms of pyrite. This can be estimated for coal, either from core samples, or from bulk samples using sulphur form data and wash sulphur concentrations (Table 4).

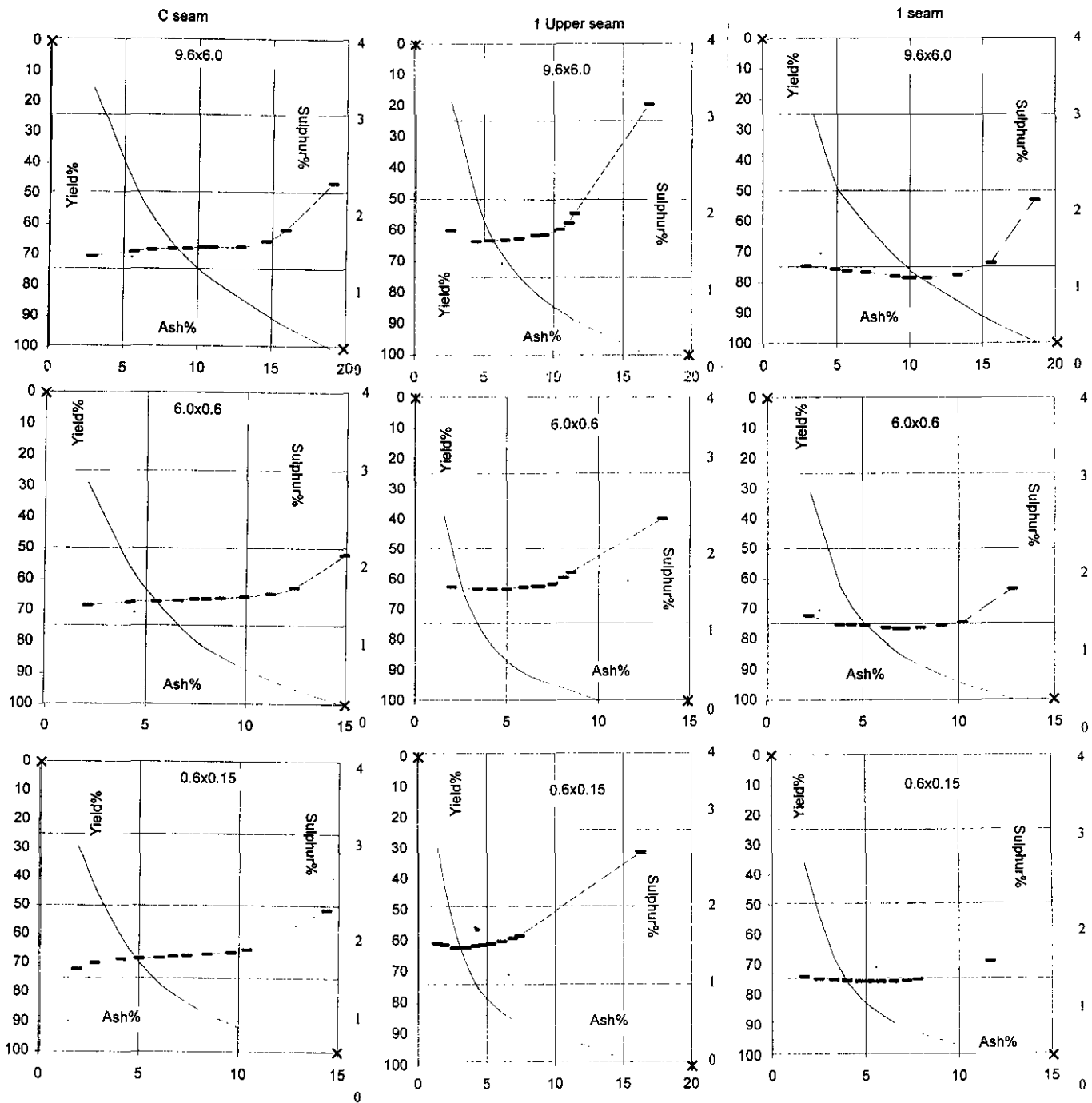


Figure 13: Washability data for seams 1, 1 Upper and C. Sulphur and ash versus yield data is illustrated for three size ranges.

Often it is hangingwall rock material that contains elevated concentrations of pyrite. Some of this material is mined as hangingwall dilution and is trucked with the raw coal to the plant where it will be rejected at the breaker and can then be handled separately from general interburden rock.

## CONCLUSIONS

The average sulphur contents of the three seams sampled at Telkwa vary from 0.7 % to 3 % on a raw basis and 0.6 % to 1.4 % on a 1.6 SG float basis. The C

seam is moderately enriched in marine sulphur, which with available iron has formed framboidal and euhedral pyrite through out the seam. The limited supply of iron has resulted in high concentrations of organic sulphur in hangingwall coal.

The upper part of 1 Upper seam is enriched in marine sulphur and coarse pyrite, indicating an influx of brackish water soon after burial. The formation of the coarse pyrite post dates formation of the framboidal and euhedral pyrite because it is external to the macerals and often associated with detrovitrinite. The organic sulphur content is moderately high through out the seam

indicating a marine influence during accumulation of the vegetation in an environment lacking a ready source of iron but suitable for the generation of H<sub>2</sub>S.

The lowest 1 seam, which is the thickest, has the lowest concentration of sulphur. Pyrite concentrations are low and occur as fracture filling in inertinite, indicating crystallization after some amount of coalification.

The hangingwall rock lithology may well be a good indication of how much coarse pyrite exists in 1 Upper. Unfortunately there may be no field clues as to variations in the organic sulphur content of the seam. Any obvious increase in bright lithotypes in 1 seam will probably correlate with an increase in organic sulphur. In the other seams an increase in bright lithotypes may correlate with an increase in framboidal and euhedral pyrite, both of which are difficult to wash out.

Coarse pyrite is moderately easy to wash out of the coal. Other forms of pyrite are more difficult to wash out because they are associated with the coal. It is better to wash the coal to a higher ash content rather than to force coal into the reject stream in order to achieve minor reductions in sulphur concentrations.

Table 4  
Sulphur liberation and sulphur form data

| 1 Upper Seam |       |      |      |      |      |      |      |
|--------------|-------|------|------|------|------|------|------|
| size mm      | A     | TS   | PS   | OS   | WS   | CP   | FP   |
| 9.5 x 6.0    | 9.1   | 3.13 | 2.14 | 0.95 | 1.65 | 1.48 | 0.7  |
| 6 x 0.6      | -13.2 | 2.41 | 1.57 | 0.82 | 1.6  | 0.81 | 0.78 |
| 0.6 x 0.15   | -0.2  | 2.62 | 1.77 | 0.81 | 1.6  | 1.02 | 0.79 |
| 0.15 x 0     | 4.6   | 3.76 | 2.99 | 0.69 |      |      |      |
| C Seam       |       |      |      |      |      |      |      |
| 9.5 x 6.0    | 3.4   | 2.04 | 1.33 | 0.71 | 1.3  | 0.74 | 0.59 |
| 6 x 0.6      | -2.4  | 1.86 | 1.13 | 0.73 | 1.35 | 0.51 | 0.62 |
| 0.6 x 0.15   | -0.8  | 2.01 | 1.08 | 0.9  | 1.35 | 0.66 | 0.45 |
| 0.15 x 0     | 2.2   | 2.69 | 1.71 | 0.86 |      |      |      |
| 1 Seam       |       |      |      |      |      |      |      |
| 9.5 x 6.0    | 10.6  | 2.18 | 1.44 | 0.72 | 0.9  | 1.28 | 0.18 |
| 6 x 0.6      | -8.1  | 1.51 | 0.84 | 0.66 | 0.95 | 0.56 | 0.29 |
| 0.6 x 0.15   | -4.9  | 1.25 | 0.53 | 0.71 | 0.96 | 0.29 | 0.25 |
| 0.15 x 0     | -0.4  | 1.7  | 0.89 | 0.74 |      |      |      |

A = pyrite liberation from size as % of total pyritic sulphur  
a minus sign indicates pyrite loss  
TS total sulphur PS pyritic sulphur OS organic sulphur  
WS wash sulphur CP coarse pyritic sulphur  
FP fine pyritic sulphur

## ACKNOWLEDGMENTS

The paper benefited from a detailed editorial review by Dave Lefebure.

## REFERENCES

- Altschuler, Z.S., Schnepfe, C.C., Silber, C.C. and Simon F.O. (1983): Sulphur Diagenesis in Everglades Peat and Origin of Pyrite in Coal; *Science*, Volume 221, Number 4607, pages 221-226.
- Bass-Becking, L.G.M., Kaplan, L.R. and Moore, D. (1960): Limits of the Natural Environment in Terms of pH and Oxidation-Reduction Potentials; *Journal of Geology*, Volume 68, pages 243-283.
- Cameron, A.R. (1972): Petrography of Kootenay Coals in the Upper Elk River and Crowsnest Areas, British Columbia and Alberta; in Proceedings of the First Geological Conference on Western Canadian Coal, Mellon, C.B. Kramers, J.W and Seagel, E.J., Editors, *Alberta Research Council*, Information Series No.60, pages 31-46.
- Caruccio, F.T., Ferm, J.C., Horne, J., Geidel, G. and Baganz, B. (1977): Paleoenvironments of Coal and its Relation to Drainage Quality; *U.S. Environmental Protection Agency*, Report No. R-802597-02, by Industrial Environmental Research Laboratory, pages 1-76.
- Cecil, C.B., Stanton, R.W., Dulong, F.T. and Renton, J.J. (1979): Geological Factors that Control Mineral Matter in Coal; *Carboniferous Coal Guidebook*, Department of Geology and Geography, West Virginia University, West Virginia, Bulletin B-37-3, Supplement, pages 43-56.
- Cohen A.D., Spackman, W. and Dolsen, P. (1984): Occurrence and Distribution of Sulphur in Peat-Forming Environments of Southern Florida; *International Journal of Coal Geology*, Volume 4, pages 73-96.
- Chou, C.L. (1990): Geochemistry of Sulphur in Coal; *ACS Symposium Series* Number 429, Geochemistry of Sulphur in Fossil Fuels, pages 30-52.
- Demir, I. and Harvey, R. (1991): Variation of Organic Sulphur in Macerals of Selected Illinois Basin Coals; *Organic Geochemistry*, Pergamon Press, Exiter, England, Volume 16, pages 525-533.
- Diessel, C.F.K. (1992): Coal-Bearing Depositional Systems; *Spring-Verlag*, Berlin, Heidelberg, pages 155-157.
- Dowling, D.B. (1915): Coal Fields of British Columbia; *Geological Survey of Canada*, Memoir 69, pages 189-222. 739.
- Evenchick, C.A. (1991): Geometry, Evolution and Tectonic Framework of the Skeena Fold Belt, North-Central British Columbia; *Tectonics*, Volume 10, No. 3, pages 527-546.

- Grieve, D.A. (1993): Geology and Rank Distribution of the Elk Valley Coalfield, Southeastern British Columbia; B.C. Ministry of Energy, Mines and Petroleum Resources, Bulletin 82, pages 1-188.
- Handy, D. and Cameron, S. (1982):\_ Telkwa Exploration Report; Coal Assessment Number 238, Report on file Ministry of Employment and Investment.
- Handy, D. and Cameron, S. (1983):\_ Telkwa Exploration Report; Coal Assessment Number 239, Report on file Ministry of Employment and Investment.
- Handy, D. and Cameron, S. (1984):\_ Telkwa Exploration Report; Coal Assessment Number 240, Report on file *Ministry of Employment and Investment*.
- Harvey, R.D. and Demir, I (1992): Characterization of Organic Sulphur in Macerals and Chars; *Illinois State Geological Survey, Open File Series, 1992-1*.
- Holuszko, M.E. Matheson, A. and Grieve, D.A. (1993): Pyrite Occurrences in Telkwa and Quinsam Coal Seams; in *Geological Fieldwork 1992, B.C. Ministry of Employment and Investment, Paper 1993*, pages 527-536.
- Hunt, J.W. (1989): Permian Coals of Eastern Australia: A Geological Control of Petrographic Variation; *International Journal of Coal Geology, Volume 12*, pages 589-634.
- Hunt, J.M. (1979): Petroleum Geochemistry and Geology; San Francisco, *W.H. Freeman*, page 617.
- Koo, J. (1983): The Telkwa, Red Rose and Klappan Coal Measures in Northwestern British Columbia; in *Geological Fieldwork 1983, B.C. Ministry of Energy, Mines and Petroleum Resources, Paper 1984-1* pages 81-90.
- Lamberson, M.N., Bustin, R.M., Kalkreuth, W.D. and Pratt, K.C. (1996): The Formation of Inertinite-rich Peats in the Mid Cretaceous Gates Formation: Implications for Interpretation of Mid Albian History of Paleowildfire; *Paleogeography, Paleoclimatology, Paleoecology, Volume 120*, pages 235-260.
- Ledda, A. (1992): Telkwa Exploration Report; Coal Assessment Number 828, Report on file *Ministry of Employment and Investment*.
- Ledda, A. (1994): Telkwa Exploration Report; Coal Assessment Number 844, Report on file *Ministry of Employment and Investment*.
- Love, L.G. (1957): Micro-Organisms and the Presence of Syngenetic Pyrite; *Geological Society London, Quarterly Journal, Volume 113*, pages 97-108.
- MacIntyre, D., Desjardins, P., Tercier, P. and Koo, J. (1989): Geology of the Telkwa River Area NTS 93L/11; *B.C. Ministry of Energy, Mines and Petroleum Resources, Open File 1989-16*.
- McKinstry, B. (1990): Telkwa Exploration Report; Coal Assessment Number 700, Report on file *Ministry of Employment and Investment*.
- Manalta Coal Limited (1997): The Telkwa Coal Project, Application for a Project Approval Certificate; On file at the Ministry of Employment and Investment, Victoria.
- Markuszewski, R., Fan, C.W., Greer, R.T. and Wheelock, T.D. (1980): Evaluation of the Removal of Organic Sulphur from Coal; Symposium on New Approaches in Coal Chemistry, *American Chemical Society, Pittsburgh, PA, November 12-14*, pages 25-37.
- Mason, B. (1966): Principles of Geochemistry; *John Wiley and Sons Inc., New York*, pages 192-207.
- Matheson, A. and Van Den Bussche, B. (1990): Subsurface Coal Sampling Survey, Telkwa Area, Central British Columbia (93L/11); in *Geological Fieldwork 1989, B.C. Ministry of Energy, Mines and Petroleum Resources, Paper 1990-1* pages 445-448.
- Matheson, A., Grieve, D.A., Goodarzi, F. and Holuszko, M.E. (1994): Selected Thermal Coal Basins of British Columbia; *B.C. Ministry of Energy, Mines and Petroleum Resources, Paper 1994-3*, pages 449-454.
- Bustin, R.M. and Palsgrove, R.J (1997): Lithofacies and Depositional Environments of the Telkwa Coal Measures, Central British Columbia, Canada; *International Journal of Coal Geology, Volume 34*, pages 21-52.
- Pearson, D.E., and Kwong, J. (1979): Mineral Matter as a Measure of Oxidation of a Coking Coal; *Fuel, Volume 58*, pages 66-68.
- Price, F.T. and Shieh, Y.T. (1979): The Distribution and Isotopic Composition of Sulphur in Coals from the Illinois Basin; *Economic Geology, Volume 74*, pages 1445-1461.
- Rankama and Sahama (1950): in *Handbook of Geochemistry, Volume II, part 5*, Wedepohl, K.H, Springer-Verlag, Berlin, 1978, page 16L5.
- Renton, J.J and Bird, D.S. (1991): Association of Coal Macerals, Sulphur, Sulphur Species and Iron Disulphide Minerals in three Columns of the Pittsburgh Coal; *International Journal of Coal Geology, Volume 17*, pages 21-50.
- Roberts, D.L. (1988): The Relationship between Macerals and Sulphur Content of some South African Permian Coals; *International Journal of Coal Geology, Volume 10*, pages 399-410.
- Ryan, B.D. (1993): Geology of the Telkwa Coalfield, British Columbia; *B.C. Ministry of Energy, Mines and Petroleum Resources, Open File 1993-21*.
- Ryan, B.D. and Dawson, F.M. (1993): Potential Coal and Coalbed Methane Resource of the Telkwa Coalfield Central British Columbia (93L/11); in *Geological Fieldwork 1993, Grant, B. and Newell, J.M., Editors, B.C. Ministry of Energy, Mines and Petroleum Resources, Paper 1994-1*. pages 225-243.

- Ryan, B.D. (1997): Coal Quality Variations in the Gething Formation Northeast British Columbia (93O,J,I); in *Geological Fieldwork 1996, B.C. Ministry of Employment and Investment*, Paper 1997-1 pages 373-397.
- Salisbury, F.B. and Ross, C. (1969): *Plant Physiology*; Wadsworth Publishing Company, Inc. Belmont, California, page 194.
- Spears, D.A. and Caswell, S.A. (1986): Mineral Matter in Coals: Cleat Minerals and their Origin in some Coals from the English Midlands; *International Journal of Coal Geology*, Volume 6, pages 107-125.
- Tipper, H.W. and Richards, T.A. (1976): Jurassic Stratigraphy and History of North-central British Columbia; *Geological Survey of Canada Memoir* 270, pages 1-73.
- Wedepohl, K.H. (1978): *Handbook of Geochemistry*, Volume II, part 5, *Springer-Verlag*, Berlin, pages 16L1-16L19.





## OKANAGAN AGGREGATE POTENTIAL PROJECT

By Alex Matheson, Roger Paulen, Peter T. Bobrowsky and Nick Massey

**KEYWORDS:** Aggregate potential, Okanagan, sand and gravel, inventory, database.

### INTRODUCTION

The Okanagan Aggregate Potential Project was initiated in 1996 by the Geological Survey Branch of the Ministry of Employment and Investment (Matheson et al, 1996). The aim is to evaluate the aggregate potential of the Okanagan from the United States/Canada border to the Shuswap Lakes. The major parts of sixteen, 1:50,000 map sheets were covered over a five week period, and a total of 267 pits were examined. An additional 41 sites had yet to be evaluated.

Additional funding made available to the Ministry of Employment and Investment by the Ministry of Municipal Affairs and Housing, the Regional District of Central Okanagan, the City of Kelowna and the Ministry of Transport and Highways, enabled the Geological Survey Branch to complete the site examinations of the remaining 41 pits from the previous year, as well as an additional 19 new pits. The 60 pits were examined in the field over a ten day period in August, 1997.

### GEOGRAPHIC LOCATION

The demand for aggregate is greatest near densely populated areas where the need for sand and gravel reflects the active construction industry. Numerous pits in the Shuswap area and near settlements such as Salmon Arm (82 L/11), Vernon (82 L/6), Kelowna (82 E/14), Penticton (82 E/5), and Keremeos (82 E/4) form the majority of active aggregate extraction operations.

The sixteen map sheets covered for this study include 82/ E 3, 4, 5, 6, 11, 12, 13, 14, and 82/L 3, 4, 5, 6, 11, 12, 13, 14, covering a north/south corridor some 80 kilometres wide and 200 kilometres long.

### Field Work

Pits identified in the study area were photographed and documented under the following notations: name of pit, unique identity number and license, licensee or operator and development status. Additional data included measuring pit dimensions and exposed sections that would allow the interpretation of facies, depositional history and quarry type. A hand-held global positioning system unit and the 1:50,000 N.T.S. maps were used to accurately

define the pit location which was then plotted using UTM coordinates on the N.T.S. maps and soil maps for the Okanagan Valley.

### Data Compilation

A database was compiled consisting of the licensing information, field observations, air-photo interpretations, delineation and identification of landforms. The aggregate pits have been digitized as points on the sixteen map sheets. This information will later be combined with water well-logging and previous geotechnical reports to create attributes for each pit for display in ARC-view, and the GIS software used for plotting the data.

### CONCLUSIONS - DISCUSSION

#### Locating Future Deposits

Exploration for future deposits should be in the low-lying areas where glaciofluvial deposits tend to be common. When urban development and expansion have limited the aggregate potential for these areas, smaller but similar deposits located adjacent to the large valleys could be used in the future. Such landforms may be located on the aggregate potential maps, and with ground truthing and more detailed air-photo interpretation, will allow accurate identification of aggregate resources for future use.

#### Value of Aggregate Program

There will always be a demand for aggregate and consequentially it is essential to have a well documented inventory for future use in general development planning for construction, and the resulting infrastructure of transportation networks. Thus, an inventory and evaluation of potential aggregate resources in areas of British Columbia should be completed, so that they may be used in a more effective manner.

### REFERENCES CITED

- Matheson, A., MacDougall, D., Bobrowsky, P.T., Massey, N.W.D. (1996): Okanagan Aggregate Potential Project, in Geological Fieldwork 1996, B.C. Ministry of Employment and Investment, Paper 1997-1, pages 347-352.





British Columbia Geological Survey  
Geological Fieldwork 1997

## Regional Geochemistry Program

# REGIONAL GEOCHEMICAL SURVEY PROGRAM: REVIEW OF 1997 ACTIVITIES

By Wayne Jackaman, Stephen Cook and Ray Lett

**KEYWORDS:** Applied geochemistry, stream sediments, lake sediments, till, mineral exploration, multi-element, reconnaissance-scale, Regional Geochemical Survey.

## INTRODUCTION

British Columbia's Regional Geochemical Survey (RGS) program is a valuable source of high-quality baseline geochemical information. The program supports the exploration and development of B.C.'s mineral resources by providing geochemical results from reconnaissance-scale surveys that are used to map regional geochemical trends, assist mineral potential evaluations and aid regional metallogenic studies and geologic interpretations.

Since 1976, the RGS program has conducted stream sediment and water surveys in over forty 1:250 000 NTS map areas (Figure 30-1). In addition, several lake sediment and water surveys and numerous geochemical research studies have been completed. At present, the RGS database contains analytical determinations, field observations and sample location information for 41 981 stream sediment and water sample sites and 2343 lake sediment and water sample sites. All components of sample collection, preparation and analysis are closely monitored to ensure consistency and conformance to standards set by the National Geochemical Reconnaissance (NGR) Program.

This report provides a summary of 1997 geochemical data releases for British Columbia, and outlines new projects initiated during the 1997 field season. During 1997, new geochemical data was published for stream sediment and water surveys conducted in the McConnell Creek (NTS 94D) and Toodoggone River (NTS 94E) map areas. In addition, lake sediment and water geochemical data was released for surveys completed in the Pinchi Lake area of the Nechako Plateau (parts of NTS 93K) as part of the federal-provincial Nechako NATMAP project, and for the Gataga River area of the northern Kechika Trough (parts of NTS 94M and 104P). Results of a lake sediment and water survey covering the Babine porphyry belt (parts of NTS 93L and 93M) as part of the NATMAP project are scheduled to be released in January 1998. Till geochemical data for two survey areas in the Babine Lake and Adams Plateau area were also released this year.

Project activities during 1997 included a reconnaissance-scale stream sediment and water program in the Mesilinka River (NTS 94C) area of north-central British Columbia, plus regional till surveys and other geochemical studies conducted as part of multi-disciplinary mapping and mineral resource programs in the Nechako-Babine and Eagle Bay regions (Figure 30-1).

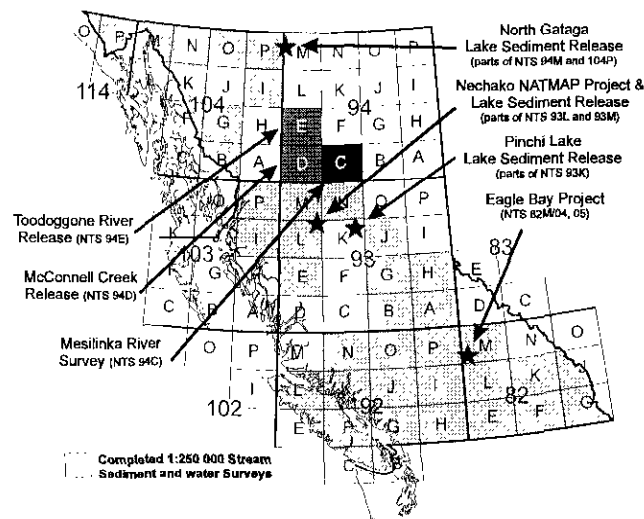


Figure 30-1. Location map of RGS and related projects.

## STREAM SEDIMENT SURVEYS

### McConnell Creek and Toodoggone River RGS Data Releases

Reconnaissance-scale RGS programs were completed in the McConnell Creek (NTS 94D) and Toodoggone River (NTS 94E) 1:250 000 map areas in September, 1996. This region is well known for its geological and metallogenic diversity and is considered to have high potential for additional discoveries of gold-copper porphyry, gold silver epithermal, skarn, vein and basaltic copper deposits.

Stream sediment samples, stream water samples and field observations were systematically collected from 1885 sites over a total area of 18 500 square kilometres. Survey results were released as Open File B.C. RGS 45 and 46 on July 10, 1997. Immediately following the release over 750 claim units were staked by exploration companies and prospectors targeting the numerous base and precious metal anomalies identified in the data packages (Jackaman, 1997a,b).

### 1997 Mesilinka River RGS Program

During July and August, a truck and helicopter supported sample collection program was conducted in the

Mesilinka River (NTS 94C) 1:250 000 map area. Over the 13 500 square kilometre survey area stream sediment, stream water and field observations were collected from 1008 sample sites at an average density of 1 site every 12 square kilometres.

Stream sediment samples will be analyzed for precious and base metals, pathfinder and rare earth elements (Table 30-1). Water samples are being analyzed for pH, fluoride, uranium and sulphate. Survey results are scheduled to be released in July, 1998.

## LAKE SEDIMENT SURVEYS

### Pinchi Lake and North Gataga Data Releases

Geochemical data from two lake sediment surveys in central British Columbia were released in 1997. Results of the Pinchi Lake survey (413 sites; Cook *et al.*, 1997a), in the Fort St. James area of the Nechako Plateau, were released in January, while results of the North Gataga survey (445 sites; Cook *et al.*, 1997b) in the northern Kechika Trough were released in August. The surveys are joint projects of the Geological Survey Branch and the Geological Survey of Canada.

The Pinchi Lake survey area straddles the Pinchi fault zone between the Quesnel and Cache Creek terranes. Geochemical results of this survey, a contribution to the Nechako NATMAP Project, outline prospective new areas for porphyry gold-copper and molybdenum mineralization. Maximum element concentrations of up to 65 ppm molybdenum (median: 4 ppm), 250 ppm copper (median: 50 ppm), 650 ppm nickel (median: 35 ppm), 17 ppb gold (median: 2 ppb), 316 ppm arsenic (median: 5.9 ppm) and 8.4 ppm antimony (median: 0.8 ppm) in lake sediments were recorded. The North Gataga survey covers an area of Devonian-Ordovician siliciclastic and carbonate rocks which are prospective for sedimentary-exhalative (sedex) zinc-lead-barite deposits. This survey, together with a stream sediment geochemical survey (Jackaman *et al.*, 1996) that covered more mountainous terrain to the south, complement recent bedrock mapping in the Kechika Trough by Ferri *et al.* (1997, in press). Maximum concentrations of 6600 ppm zinc (median: 112 ppm), 30 ppm lead (median: 4 ppm), 3100 ppm barium (median: 680 ppm), 100 ppm molybdenum (median: 6 ppm), 500 ppm nickel (median: 16 ppm), 28 ppb gold (median: 1 ppb) and 9 ppm antimony (median: 0.7 ppm) occur in lake sediments of this area.

### New Data Release: Babine Porphyry Belt

Results of a lake sediment geochemical survey of the Babine porphyry belt (Cook *et al.*, 1998) are to be released at the Cordilleran Roundup in January 1998. The Babine survey (332 sites) was conducted in June 1996 in conjunction with bedrock mapping, surficial geology mapping and till geochemistry programs of the Nechako NATMAP Project. The survey area is centred on northern

Table 30-1.

## ROUTINE STREAM SEDIMENT AND WATER ANALYTICAL SUITE

| Element           |      | Analytical Method | Detection Limit | Unit |
|-------------------|------|-------------------|-----------------|------|
| Antimony          | Sb   | AAS-H/INAA        | 0.2/0.1         | ppm  |
| Arsenic           | As   | AAS-H/INAA        | 0.2/0.5         | ppm  |
| Barium            | Ba   | INAA              | 50              | ppm  |
| Bismuth           | Bi   | AAS-H             | 0.2             | ppm  |
| Bromine           | Br   | INAA              | 0.5             | ppm  |
| Cadmium           | Cd   | AAS               | 0.2             | ppm  |
| Cerium            | Ce   | INAA              | 3               | ppm  |
| Cesium            | Cs   | INAA              | 1               | ppm  |
| Chromium          | Cr   | INAA              | 5               | ppm  |
| Cobalt            | Co   | AAS/INAA          | 2/1             | ppm  |
| Copper            | Cu   | AAS               | 2               | ppm  |
| Fluorine          | F    | ION               | 40              | ppm  |
| Gold              | Au   | INAA              | 2               | ppb  |
| Hafnium           | Hf   | INAA              | 1               | ppm  |
| Iron              | Fe   | AAS/INAA          | 0.02/0.01       | %    |
| Lanthanum         | La   | INAA              | 0.5             | ppm  |
| Lead              | Pb   | AAS               | 2               | ppm  |
| Loss on Ignition  | LOI  | GRAV              | 0.1             | %    |
| Lutetium          | Lu   | INAA              | 0.05            | ppm  |
| Manganese         | Mn   | AAS               | 5               | ppm  |
| Mercury           | Hg   | AAS               | 10              | ppb  |
| Molybdenum        | Mo   | AAS/INAA          | 2/1             | ppm  |
| Nickel            | Ni   | AAS/INAA          | 2/20            | ppm  |
| Rubidium          | Rb   | INAA              | 5               | ppm  |
| Samarium          | Sm   | INAA              | 0.1             | ppm  |
| Scandium          | Sc   | INAA              | 0.1             | ppm  |
| Silver            | Ag   | AAS               | 0.2             | ppm  |
| Sodium            | Na   | INAA              | 0.01            | %    |
| Tantalum          | Ta   | INAA              | 0.5             | ppm  |
| Terbium           | Tb   | INAA              | 0.5             | ppm  |
| Thorium           | Th   | INAA              | 0.2             | ppm  |
| Tungsten          | W    | INAA              | 1               | ppm  |
| Uranium           | U    | INAA              | 0.5             | ppm  |
| Vanadium          | V    | AAS               | 5               | ppm  |
| Ytterbium         | Yb   | INAA              | 0.2             | ppm  |
| Zinc              | Zn   | AAS               | 2               | ppm  |
| pH (Waters)       | pH   | GCE               | 0.1             |      |
| Uranium (Waters)  | UW   | LIF               | 0.05            | ppb  |
| Fluoride (Waters) | FW   | ION               | 20              | ppb  |
| Sulphate (Waters) | SO 4 | TURB              | 1               | ppm  |

AAS atomic absorption spectroscopy  
 AAS-H hydride generation AAS  
 AAS-F flameless AAS  
 GCE glass combination electrode  
 LIF laser-induced fluorescence  
 INAA instrumental neutron activation analysis  
 GRAV weight differential  
 ION specific ion electrode  
 TURB turbidimetric

Babine Lake, immediately east of Smithers, and covers all or part of six 1:50,000 scale map areas. This area includes the past-producing Bell and Granisle copper mines as well as exploration prospects such as the Hearne Hill, Nak, Morrison and Lennac Lake porphyry copper deposits.

## TILL SURVEYS

### Eagle Bay and Babine Data Releases

Till geochemical data for two areas in central B.C. were released during 1997. Regional data for a survey of

the Adams Plateau area (Adams Lake Plateau and North Barriere Lake areas; NTS 82M/4, 5) of the Shuswap Highland (Bobrowsky *et al.*, 1997) in southern B.C. was released in April. In addition, regional till geochemical data for a part of the Babine porphyry belt (Old Fort Mountain map area; NTS 93M/1), was released via the internet in May (Levson *et al.*, 1997a).

### **1997 Till Geochemical Surveys**

Till geochemical surveys were conducted in two areas during 1997: the Adams Plateau area (Bobrowsky *et al.*, this volume), and the Ootsa Lake-Nechako River area (Levson *et al.*, this volume). Results of the two surveys will complement previous till geochemical studies just released in the Eagle Bay and Nechako-Babine areas, respectively.

## **OTHER GEOCHEMICAL PROJECTS**

### **Massive Sulphide Geochemical Pathfinders Project**

Geochemical sampling initiated in 1996 (Sibbick *et al.*, 1997) and completed in 1997 (Lett *et al.*, this volume) was designed to study the geochemical expression of typical Kootenay terrane soil, till and vegetation. Soil, till, rock, tree bark and twig samples were obtained for eight target areas in conjunction with regional till geochemical surveys in the Eagle Bay area (NTS 82M/4, 5; 92P/1, 8; Bobrowsky *et al.*, 1997a,b; this volume). The study areas are Birk Creek, Cam Claims, Harper property, Homestake Mine, Samatosum Mine, Spar property and Win Property. Samples were analysed for up to 50 elements by thermal neutron activation, aqua regia digestion-inductively coupled plasma emission spectroscopy and aqua regia digestion-ultrasonic nebulizer inductively coupled plasma emission spectroscopy. A small number of soil and till samples from the Harper and Homestake areas were also analysed for up to 70 elements using enzyme leach-inductively coupled plasma mass spectroscopy. The lower detection limits obtainable with aqua regia digestion-ultrasonic nebulizer inductively coupled plasma emission spectroscopy reveal arsenic, bismuth, silver, selenium and mercury variations that improve the effectiveness of till and soil geochemistry for detecting different types of massive sulphide and gold mineralization.

### **Collection of New Control Reference Standard**

All geochemical samples submitted to contract laboratories for analytical work contain a range of control reference standards to monitor analytical accuracy. Ideally, the standards used in any given survey span a concentration range, from background to anomalous levels, for elements associated with target mineral deposits. In the case of lake sediments, a variety of in-house and certified CANMET control standards are used, but there is

a dearth of gold standards at appropriate concentration levels. Natural gold concentrations in most lakes are very low (generally about 1 ppb), and sediment standards with moderately high gold concentrations in the 10 ppb range are rare. Furthermore, artificially mixed and diluted standards generally yield imprecise and unsatisfactory results. To fulfill this requirement for an appropriate control standard, a bulk lake sediment sample was collected in August 1997 from Clisbako Lake, located approximately 100 kilometres west of Quesnel near Nazko in the Fraser Plateau. This lake is adjacent to the Clisbako epithermal gold prospect. Prior orientation studies here (Cook, 1997) identified elevated concentrations of gold (median: 9 ppb), arsenic (median: 25.5 ppm) and antimony (median: 3.1 ppm) in organic sediments. The standard was collected by repeatedly dropping a Hornbrook sampler from a zodiac anchored at several locations in the western part of the lake, where earlier work had identified particularly homogenous elevated gold concentrations in the 10-12 ppb range. Approximately 125 litres of wet sediment were obtained. When dry, the sediment will be disaggregated in a ceramic ringmill and mixed to create the standard.

### **RGS Interpretive Studies**

Several types of interpretive methods, including element sum ranking, may be used to interpret regional geochemical data. To assess the usefulness of element sum ranking in the search for volcanogenic massive sulphide (VMS) deposits in Carboniferous-Jurassic Cache Creek Group and Upper Triassic Kutcho Formation rocks in the Nechako NATMAP study area, this technique was used to identify RGS stream sediment sites with elevated combined copper-zinc-lead-silver data rankings in the western half of the Manson River (NTS 93N) map area. Sites were ranked, and two watersheds in the Takla Lake area within the top five percentiles of the combined data rankings were selected for follow-up investigations. A variety of geochemical media were sampled in an effort to verify and enhance the anomalies. Stream sediments, moss mats, stream waters and rock samples are presently being analyzed for trace elements by a variety of methods; results will be available in 1998.

### **Till Dispersal Studies**

Till dispersal studies in the vicinity of Babine porphyry belt copper prospects, initiated in 1996 in association with V. Levson (Levson *et al.*, 1997b), continued during 1997 near the Dorothy and Hearne Hill prospects. Till and profile sampling was conducted at these sites, as part of the Nechako NATMAP Project, to document glacial dispersal and investigate copper concentrations in various soil horizons. Studies were also previously conducted near the Nak, Trail Peak and Lennac prospects in the Babine belt. Results will be reported in 1998.

## Lake Sediment Orientation Studies: Hill-Tout Lake

Lake sediment orientation studies previously conducted at Hill-Tout Lake (Cook, 1997), near the Dual porphyry copper prospect south of Houston, identified large variations in sediment metal concentrations between the three distinct sub-basins of the lake. Additional fieldwork was conducted in 1997, as part of the Nechako NATMAP Project, to further investigate the stream sediment and water geochemical inputs to the lake basins. It is expected that this information will help to further refine regional geochemical exploration guidelines for lakes, such as Hill-Tout, which are located in the rugged western margin of the Nechako Plateau. As original water samples collected at the lake were analyzed by ICP-ES methods, additional surface and bottom-water samples were obtained for ICP-MS analysis, which yields superior data for relevant trace elements such as copper. An Open File report documenting sediment and water geochemistry, and implications for regional geochemical exploration, is currently being prepared (Cook and Wyatt, in preparation).

## REFERENCES CITED

- Bobrowsky, P.T., Leboe, E.R., Dixon-Warren, A., Ledwon, A., MacDougall, D. and Sibbick, S.J. (1997): Till Geochemistry of the Adams Lake Plateau-North Barriere Lake Area (82M/4, 5); *B.C. Ministry of Employment and Investment*, Open File 1997-9, 26 pages.
- Paulen, R.C., Bobrowsky, P.T., Little, E.C., Prebble, A.C. and Ledwon, A. (1998): Drift Exploration in the Southern Kootenay Terrane; in *Geological Fieldwork 1997*, *B.C. Ministry of Employment and Investment*, Paper 1998-1, (this volume).
- Cook, S.J. and Wyatt, G.J. (in preparation): Sediment and Water Geochemistry of Hill-Tout Lake, Central British Columbia (93E/14, 15); *B.C. Ministry of Employment and Investment*, Open File.
- Cook, S.J. (1997): Regional and Property-Scale Application of Lake Sediment Geochemistry in the Search for Buried Mineral Deposits in the Southern Nechako Plateau Area, British Columbia (93C, E, F, K, L); in *Interior Plateau Geoscience Project: Summary of Geological, Geochemical and Geophysical Studies*, L.J. Diakow and J.M. Newell, Editors, *B.C. Ministry of Employment and Investment*, Paper 1997-2, pages 175-203.
- Cook, S.J., Jackaman, W., McCurdy, M.W., Day, S.J. and Friske, P.W.B. (1997a): Regional Lake Sediment and Water Geochemistry of part of the Fort Fraser Map Area, British Columbia (93K/9, 10, 15, 16); *B.C. Ministry of Employment and Investment*, Open File 1996-15, 33 pages.
- Cook, S.J., Jackaman, W., Friske, P.W., Day, S.J., Coneys, A.M. and Ferri, F. (1997b): Regional Lake Sediment and Water Geochemistry of the Northern Kechika Trough, British Columbia (94M/2, 3, 4, 5, 6, 12; 104P/8, 9, 10, 15, 16); *B.C. Ministry of Employment and Investment*, Open File 1997-15, 30 pages.
- Cook, S.J., Lett, R.E.W., Levson, V.M., Jackaman, W., Coneys, A.M. and Wyatt, G.J. (1998): Regional Lake Sediment and Water Geochemistry of the Babine Porphyry Belt, Central British Columbia (93L/9, 16; 93M/1, 2, 7, 8); *B.C. Ministry of Employment and Investment*, Open File 1997-17.
- Ferri, F., Rees, C., Nelson, J. and Legun, A. (1997): Geology of the Northern Kechika Trough (94L/14,15; 94M/3,4,5,6,12; 104P/8,9,15,16); *B.C. Ministry of Employment and Investment*, Open File 1997-14.
- Ferri, F., Rees, C., Nelson, J. and Legun, A. (in press): Geology of the Northern Kechika Trough; *B.C. Ministry of Employment and Investment*, Geoscience Map.
- Jackaman, W., Lett, R. and Sibbick, S. (1996): Geochemistry of the Gataga Mountain Area (Parts of 94L/7, 8, 9, 10, 11, 14, 15); *B.C. Ministry of Employment and Investment*, Open File 1996-18.
- Jackaman, W. (1997a): British Columbia Regional Geochemical Survey - McConnell Creek (94D); *B.C. Ministry of Employment and Investment*, BC RGS 45.
- Jackaman, W. (1997b): British Columbia Regional Geochemical Survey - Toodoggone River (94E); *B.C. Ministry of Employment and Investment*, BC RGS 46.
- Lett, R.E., Bobrowsky, P., Hoy, T. and Yeow, A. (1998): South Kootenay project: Geochemical Pathfinders for Massive Sulphide Deposits; in *Geological Fieldwork 1997*, *B.C. Ministry of Employment and Investment*, Paper 1998-1, (this volume).
- Levson, V.M., Cook, S.J., Huntley, D.H., Stumpf, A.J. and Hobday, J. (1997a): Preliminary Till Geochemistry - Old Fort Mountain Area (93M/1); *B.C. Ministry of Employment and Investment*, Open File 1997-18.
- Levson, V.M., Meldrum, D.G., Cook, S.J., Stumpf, A.J., O'Brien, E.K., Churchill, C., Coneys, A.M. and Broster, B.E. (1997b): Till Geochemical Studies in the Babine Porphyry Belt: Regional Surveys and Deposit-Scale Studies (93L/16, 93M/1, 2, 7, 8); in *Geological Fieldwork 1996*, Lefebure, D.V., McMillan, W.J. and McArthur, G., Editors, *B.C. Ministry of Employment and Investment*, Paper 1997-1, pages 457-466.
- Levson, V.M., Stumpf, A. and Stuart, A. (1998): Quaternary Geology Studies in the Smithers and Hazelton Map Areas (93L and M): Implications for Exploration; in *Geological Fieldwork 1997*, *B.C. Ministry of Employment and Investment*, Paper 1998-1, (this volume).
- Sibbick, S.J., Runnels, J.L. and R.E. Lett (1997): Eagle Bay Project Regional Hydrogeochemical survey and geochemical orientation studies in *Geological Fieldwork 1996*, Lefebure, D.V., McMillan, W.J. and McArthur, G., Editors, *B.C. Ministry of Employment and Investment*, Paper 1997-1, pages 423-426.

**Mineral Deposit Research Unit  
The University of British Columbia**

# THE STYLE AND ORIGIN OF ALTERATION ON THE LIMONITE CREEK PROPERTY, CENTRAL BRITISH COLUMBIA (93L/12)

By C.L. Deyell, J.F.H. Thompson, L.A. Groat, J.K. Mortensen, R.M. Friedman,  
Department of Earth and Ocean Sciences, University of British Columbia, and  
W.D. Tompson, Telkwa Gold Corporation.

**KEYWORDS:** High sulphidation system, advanced argillic alteration, porphyry environment, Eocene intrusions, weathering and exotic limonites.

## INTRODUCTION

This report summarizes the nature and mineralogy of alteration zones on the Limonite Creek Property in north central British Columbia. Research to date has included two field seasons involving extensive sampling of drill core, mineralogical classification of alteration, and limited geochemistry. Dating of intrusions that occur in the area of alteration has been initiated and one result is reported herein. Extensive deposits of exotic limonite also occur on and adjacent to the Limonite Creek property. These deposits are assumed to have been derived from the weathering and oxidation of extensive pyrite in the alteration zones. Research is also being directed towards the nature and origin of the limonite, but only a brief summary of these results is included in this paper.

property lies along a mountain ridge at an elevation of 1275 to 1400 metres, approximately one to two kilometres north of Limonite Creek, a tributary of the Zymoetz (Copper) River. Access is by helicopter only, although the Telkwa River logging road runs within seven kilometres south of the prospect.

The Limonite Creek property has been owned and explored by Telkwa Gold Corporation since 1994. Exploration activities have included over 6000 feet of diamond drilling, airborne geophysics, induced polarization and soil geochemical surveys. Previously, Cyprus Canada Inc. conducted geological mapping, rock, water and soil geochemical analyses, a transient electromagnetic (TEM) survey, and diamond drilling in 1992. Noranda Exploration Co. Ltd., Evergreen Explorations, and Pacific Petroleum Ltd. also evaluated the property in the 1960's.

## REGIONAL GEOLOGY

The Limonite Creek property is located within the Stikine terrane (Figure 1) and is underlain by Lower to Middle Jurassic volcanic rocks of the Telkwa Formation. The Telkwa Formation consists of a varied assemblage of marine and non-marine calc-alkaline volcanic rocks, which form the basal part of the Hazelton Group. Five distinctive facies are recognized in the Telkwa Formation (Tipper and Richards, 1976). The Howson Subaerial Facies dominates the Telkwa Pass area, the Howson Range, and most of the Telkwa Range. This facies is described by Tipper and Richards (1976) as an assemblage of bright red, maroon, purple, pink, grey and green, well-bedded, slightly deformed pyroclastic flows and sedimentary rocks, dominantly of andesitic to dacitic composition.

Volcanic rocks of the Telkwa Formation are locally intruded by calc-alkaline stocks and batholiths of Early Jurassic age. These intrusions, termed Topley intrusions (Wordsworth et al., 1993), are thought to be contemporaneous with the Telkwa Formation and have K-Ar ages ranging from 173-205 Ma (Tipper and Richards, 1976). The intrusions form a series of bodies coincident with the Skeena Arch, of which the Howson Batholith is one of the largest. This batholith comprises mainly tonalite and granodiorite and has a K-Ar hornblende age of  $193 \pm 8$  Ma (recalculated from Wanless et al., 1974).

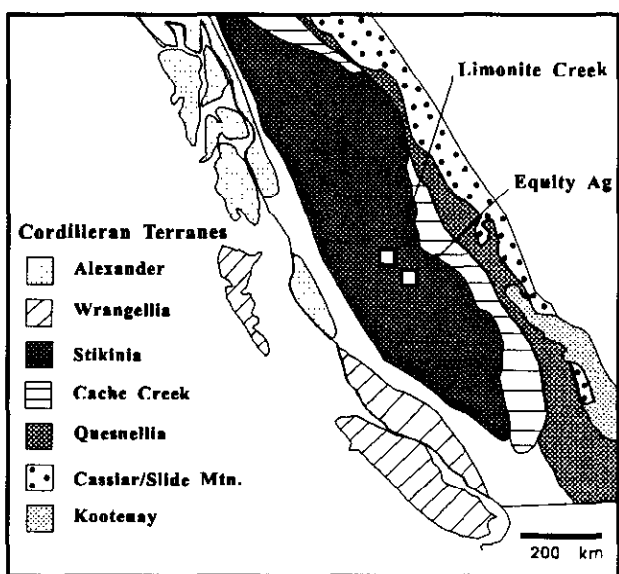


Figure 1. Location of the Limonite Creek property within Stikinia, Central British Columbia.

The Limonite Creek property is located in Telkwa Pass, approximately 50 kilometres southwest of Smithers, in the Omineca Mining District of British Columbia. The

Younger intrusions in this region include the Late Cretaceous Bukley (ca. 70-88 Ma) and Eocene Nanika intrusive suites of the western Skeena Arch, as well as the Eocene Babine Igneous suite in the Babine Lake area to the east. Coeval Upper Cretaceous volcanic rocks of the Brian Boru Formation are locally preserved in the western Skeena Arch and Eocene volcanic rocks of the Ottsa Lake Formation are widespread across the west-central British Columbia region. Both Late Cretaceous and Eocene intrusive suites are associated with mineral deposits in the region. A quartz monzonite associated with the Equity Deposit (Cyr et al., 1984) gave an U-Pb age of  $60.1 \pm 0.2$  Ma, which is likely part of the Nanika intrusive suite. Prior to this study, U-Pb dating of rocks in the Telkwa Pass-Limonite Creek area has not been carried out.

## PROPERTY GEOLOGY

The geology of the Limonite Creek property has been determined from mapping and drill core logging during exploration programs (Tompson (1997); Tompson and Cuttle (1994)) and fieldwork during this study.

The Limonite Creek prospect area is dominated by green and lesser maroon rhyodacitic, dacitic, and andesitic tuffs and flows which are interpreted to belong to the Telkwa Formation. The volcanic rocks are dominated by mafic to intermediate fragmental units with lesser massive and flow-banded units usually of more felsic composition. Bedding is difficult to recognize and most units exhibit a strong foliation trending  $060-090^\circ$ . As shown in Figure 2, these volcanic rocks are intruded by several stocks of dioritic to granodioritic compositions. An irregular body of porphyritic granodiorite occurs in the eastern part of the property, approximately 300 metres south of the camp. The intrusion is weakly altered with biotite partially replaced by chlorite and traces of disseminated pyrite. The intrusion was sampled for U-Pb dating (sample LC-08).

The Limonite Creek prospect is bounded to the east by a coarse to medium grained diorite to granodiorite and to the west by a weakly porphyritic granodiorite. The intrusion to the east shows weak to moderate propylitic alteration and abundant epidote veins close to the contact with the altered volcanic rocks. The majority of

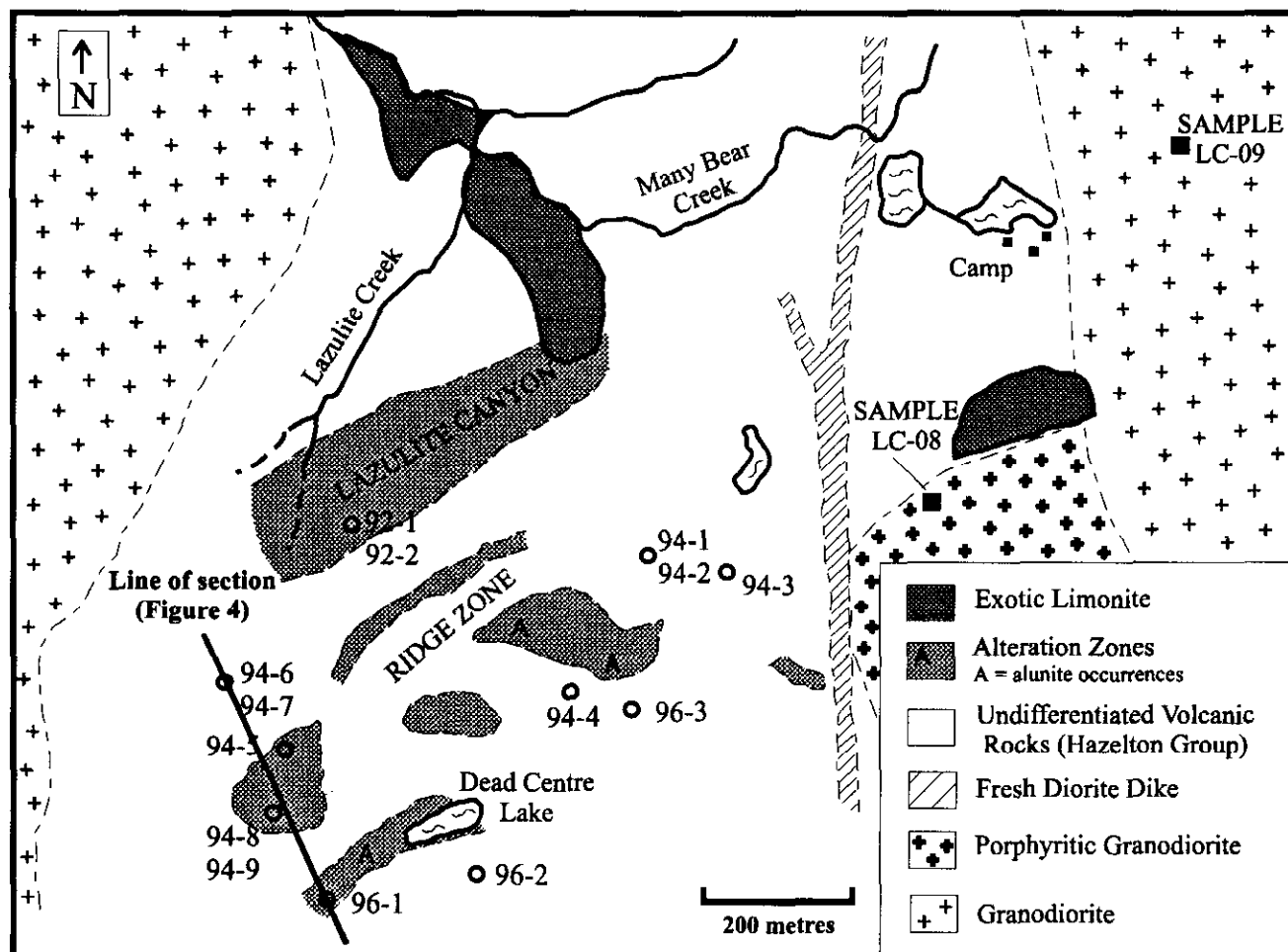


Figure 2: Generalized geological map of the Limonite Creek area showing intense alteration zones, exotic limonite occurrences, drill holes, sample sites for U-Pb dating, and line of section for Figure 4.

this intrusion displays only minor alteration but does contain rare milky white quartz veins with minor chalcopyrite. This intrusion was also sampled for U-Pb dating (sample LC-09), but results are not available at this time.

Both extrusive and intrusive rocks within the Limonite Creek prospect area are cross-cut by numerous late narrow basalt and diorite dike swarms. In the eastern part of the map, a prominent dike with northerly strike cuts across altered and unaltered volcanic rocks and various intrusive units (Figure 2).

## GEOCHRONOLOGY

The sample of porphyritic granodiorite (sample LC-08) was prepared for U-Pb dating using standard mineral separation techniques. The sample yielded abundant, high quality, clear, colourless, stubby prismatic zircon with rounded cross sections and simple terminations. No cores or zoning were observed in these grains. The highest quality and coarsest nonmagnetic grains were selected for analysis and were air abraded to reduce the effects of surface-correlated Pb loss. These grains were split into three fractions which were dissolved, chemically separated and analyzed employing the techniques listed in Mortensen et al. (1995). All work was carried out at the Geochronology Laboratory of the Department of Earth and Ocean Sciences at the University of British Columbia.

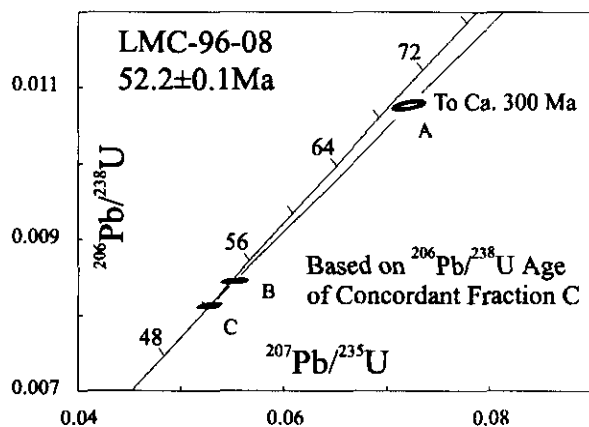


Figure 3: Concordia diagram for sample LC-08. Ellipses are plotted at the  $2\sigma$  level of precision.

Three analyzed zircon fractions for sample LC-08 are plotted on Figure 3 and the U-Pb data are listed in Table 1. The best estimate for the age of the rock,  $52.2 \pm 0.1$  Ma, is based on the  $^{206}\text{Pb}/^{238}\text{U}$  age for concordant fraction C. Fractions A and B give older Pb/U and Pb/Pb ages, which suggests the presence of minor inherited zircon. A regression line through the data give a poorly constrained upper intercept of ca. 300 Ma, which is interpreted as the average age of inherited zircon in fractions A and B.

## ALTERATION

The characterization of alteration assemblages at Limonite Creek is based on drill core logging and petrography, as well as analyses by X-ray Diffraction (XRD), Scanning Electron Microscopy (SEM), and a hand-held infra-red spectrometer (PIMA). Alteration zones identified on the property include intense acid sulphate and advanced argillic zones and widespread sericitic and propylitic assemblages. The mineralogy of each alteration type is given in Table 2.

The location of intense alteration at surface is shown on Figure 2. Relationships among alteration assemblages observed in drill core are complex (Figure 4) although based on the limited data, regions of strong alteration appear to form subvertical zones (the lightly shaded areas in Figure 4). In individual drill holes, intervals of siliceous and acid sulphate alteration are generally bound by advanced argillic alteration. This in turn grades to sericitic and finally propylitic-dominated assemblages. Alteration zones containing anhydrite (and/or gypsum) are generally confined to the periphery of the alteration system and are concentrated at depth.

### Acid Sulphate Alteration (AS)

Acid sulfate alteration is characterized by the presence of alunite in the alteration assemblage. This alteration type is concentrated near the Ridge Zone, on the south side of the Limonite Creek property, and particularly in DH 94-5, 94-8, and 94-9. It also occurs at much greater depth (approximately 200 metres) in DH 96-2 but the relationship between these zones is unclear. AS altered rocks display a variety of textures from massive and sugary to fine-grained and distinctly foliated units. Original rock textures are rarely preserved and alunite crystals are found either in massive alunite-quartz (+/- pyrophyllite) clusters or concentrated in linear zones.

As noted in Table 2, alunite is always associated with quartz, in varying amounts, and very commonly with pyrophyllite. Simple to complex zoning patterns are evident in alunite crystals from both transmitted light petrography as well as detailed SEM examinations. Energy Dispersive Spectrometry (EDS) analyses show alunite compositions always have mixed K and Na contents and commonly may approximate natroalunite compositions. EDS analyses also show complex zoning patterns of Ca and Sr within individual alunite grains.

Accessory minerals associated with the AS assemblage are listed in Table 2. Pyrophyllite contents in AS altered rocks are highly variable, ranging from trace amounts to greater than 30 volume

Table 1: U-Pb Analytical data

| Fraction <sup>1</sup> | Wt    | U <sup>2</sup> | Pb <sup>3</sup> | <sup>206</sup> Pb <sup>4</sup> | Pb <sup>5</sup> | <sup>206</sup> Pb <sup>6</sup> | Isotopic ratios (1σ,%) <sup>7</sup> |                                     |                                      | Apparent ages (2σ, Ma) <sup>7</sup> |                                      |
|-----------------------|-------|----------------|-----------------|--------------------------------|-----------------|--------------------------------|-------------------------------------|-------------------------------------|--------------------------------------|-------------------------------------|--------------------------------------|
|                       | mg    | Ppm            | ppm             | <sup>204</sup> Pb              | Pg              | %                              | <sup>206</sup> Pb/ <sup>238</sup> U | <sup>207</sup> Pb/ <sup>235</sup> U | <sup>207</sup> Pb/ <sup>206</sup> Pb | <sup>206</sup> Pb/ <sup>238</sup> U | <sup>207</sup> Pb/ <sup>206</sup> Pb |
| <b>LMC-96-08</b>      |       |                |                 |                                |                 |                                |                                     |                                     |                                      |                                     |                                      |
| A c,N1,p,s            | 0.117 | 173            | 1.9             | 198                            | 77              | 13.3                           | 0.01076 (0.27)                      | 0.0722 (1.0)                        | 0.04865 (0.88)                       | 69.0 (0.4)                          | 131 (41/42)                          |
| B c,N1,p,s            | 0.130 | 196            | 1.8             | 279                            | 52              | 14.7                           | 0.00845 (0.12)                      | 0.0552 (0.97)                       | 0.04741 (0.90)                       | 54.2 (0.1)                          | 70 (42/43)                           |
| C c,N1,p,s            | 0.128 | 160            | 1.4             | 259                            | 43              | 15.5                           | 0.00813 (0.14)                      | 0.0528 (0.93)                       | 0.04710 (0.84)                       | 52.2 (0.1)                          | 54 (40/41)                           |

Notes: Analytical techniques are listed in Mortensen et al. (1995).

<sup>1</sup> Upper case letter = fraction identifier; All zircon fractions air abraded; Grain size, intermediate dimension: c= <180 μm and >134 μm, m=<134 μm and >104 μm; Magnetic codes: Franz magnetic separator sideslope at which grains are nonmagnetic (N) or Magnetic (M); e.g., N1=nonmagnetic at 1°; Field strength for all fractions =1.8A; Front slope for all fractions=20°; Grain character codes: p=prismatic, s=stubby, t=tabular.

<sup>2</sup> U blank correction of 1pg ± 20%; U fractionation corrections were measured for each run with a double <sup>233</sup>U-<sup>235</sup>U spike (about 0.005/amu).

<sup>3</sup> Radiogenic Pb

<sup>4</sup> Measured ratio corrected for spike and Pb fractionation of 0.0035/amu ± 20% (Daly collector) and 0.0012/amu ± 7% and laboratory blank Pb of 10-45pg ± 20%. Laboratory blank Pb concentrations and isotopic compositions based on total procedural blanks analysed throughout the duration of this study.

<sup>5</sup> Total common Pb in analysis based on blank isotopic composition

<sup>6</sup> Radiogenic Pb

<sup>7</sup> Corrected for blank Pb, U and common Pb. Common Pb corrections based on Stacey Kramers model (Stacey and Kramers, 1975) at the age of the rock or the <sup>207</sup>Pb/<sup>206</sup>Pb age of the fraction.

percent in zones transitional between AS and AA alteration. Minor kaolinite/dickite is locally associated with the AS assemblage. Where it does occur, it tends to form fine-grained aggregates and patches interstitial to the quartz-alunite assemblage. Occurrences of topaz are also noted, particularly in DH 94-8 and DH 94-5. Zoned woodhouseite-svanbergite [CaAl<sub>3</sub>(PO<sub>4</sub>)(SO<sub>4</sub>)(OH)<sub>6</sub> - SrAl<sub>3</sub>(PO<sub>4</sub>)(SO<sub>4</sub>)(OH)<sub>6</sub>] grains occur only in DH 94-4.

Sulphide minerals associated with the AS assemblage include pyrite and locally traces of chalcopyrite, covellite, colusite [Cu<sub>26</sub>V<sub>2</sub>(As, Sn, Sb)<sub>6</sub>S<sub>32</sub>], sphalerite, and enargite. Trace sphalerite and enargite are found at approximately 220 metres depth in DH 96-2 (Tompson, 1997). Colusite is slightly more abundant, but only occurs in this zone.

### Advanced Argillic Alteration (AA)

Advanced argillic alteration is characterized by the presence of quartz and pyrophyllite with other accessory minerals (Table 2). This alteration type is concentrated roughly in the same area as AS alteration, but is also found locally north of the Ridge Zone in DH 94-7 and 94-2. AA zones are also found at greater depth in DH 96-2, as well as in DH 96-1 and 96-3. AA assemblages most commonly occur as massive to highly broken, mottled, pale white to cream-coloured units. Original rock textures are commonly destroyed, but where preserved, pyrophyllite commonly replaces plagioclase

phenocrysts. Pyrophyllite veinlets are also found locally cutting siliceous or AS assemblages.

Minor diaspore has been found in AA altered rocks from localities across the Limonite Creek property. Kaolinite/dickite occurrences are rare, and woodhouseite-svanbergite grains have been recognized only in DH 94-4. Pyrite is the only common sulphide mineral found within this assemblage. Traces of covellite are noted in core from the 1996 drill holes. Hematite occurs locally in significant concentrations, forming a distinct dark grey to black, massive quartz-pyrophyllite-hematite rock.

### Aluminous Alteration (AL)

Aluminous alteration is defined by the presence of aluminous minerals such as andalusite and lazulite. Lazulite is found only rarely in outcrop within Lazulite Canyon as well as locally in DH 94-6. Andalusite is much more common, although its distribution is limited to an area west of the Ridge Zone in DH 94-6 and 94-7. Quartz is always found associated with andalusite in this assemblage, with variable amounts of pyrophyllite and pyrite. Where associated with pyrophyllite, andalusite grains commonly exhibit ragged edges and are surrounded by masses of fine grained pyrophyllite. This may indicate retrograde reactions. Due to the range of accessory minerals associated with this assemblage, AL textures are highly variable.

Table 2 Alteration types and mineral assemblages at Limonite Creek

| Alteration Type        | Major Minerals                   | Associated minerals                                                                                                                                   |
|------------------------|----------------------------------|-------------------------------------------------------------------------------------------------------------------------------------------------------|
| Acid Sulphate (AS)     | alunite-quartz                   | pyrophyllite, muscovite, rutile, pyrite, kaolinite/dickite, +/- topaz, zunyite, woodhouseite-svanbergite, chalcopyrite, colusite, covellite, enargite |
| Advanced Argillic (AA) | pyrophyllite - quartz            | alunite, muscovite, kaolinite/dickite, diaspore, pyrite, rutile, +/- covellite, woodhouseite-svanbergite                                              |
| Aluminous (AL)         | quartz - andalusite +/- lazulite | pyrophyllite, muscovite, pyrite +/- kaolinite/dickite, diaspore, hematite, chalcopyrite, barite                                                       |
| Silicic (SL)           | quartz                           | muscovite, alunite, pyrophyllite, pyrite, rutile +/- barite                                                                                           |
| Sericitic (SR)         | muscovite-quartz                 | pyrite, hematite, anhydrite/gypsum +/- rutile, ilmenite                                                                                               |
| Anhydrite-Quartz (AQ)  | anhydrite (+/- gypsum) - quartz  | muscovite, pyrite, paragonite +/- pyrophyllite, topaz, kaolinite                                                                                      |
| Propylitic (PR)        | chlorite and/or epidote - quartz | muscovite, albite, carbonate, anhydrite, pyrite +/- kaolinite, montmorillonite                                                                        |

Textures may range from massive and clay-rich to strongly foliated, usually soft and sericite-rich, to green, massive, and strongly veined rocks with chlorite-filled amygdules.

### Silicic Alteration (SI)

Silicic alteration (SI) is defined by significant silicification and minor accessory minerals in the alteration assemblage. SI zones are concentrated in DH 94-5 and 94-7, and are also found locally in brecciated zones at surface in the Ridge Zone. Common accessory minerals in this assemblage include muscovite, found either concentrated in veins of goethite (after pyrite) or locally intergrown through the matrix. SI alteration is always partially to strongly oxidized and commonly cross-cut by extensive goethite-filled fractures; only trace amounts of fresh pyrite are preserved within quartz clasts. Locally, quartz breccia zones contain quartz grains and fine-grained clasts set in a goethite matrix.

### Sericitic Alteration (SR)

Sericitic alteration is characterized by a muscovite-quartz assemblage with variable amounts of pyrite, chlorite and locally anhydrite/gypsum, paragonite, hematite, and ilmenite. SR alteration is widely distributed across the Limonite Creek property, commonly occurring in a zone transitional between AS, AA or SI zones and propylitic alteration. Texturally, the SR alteration assemblage is highly variable, ranging from massive muscovite-quartz to chlorite-rich zones with original porphyritic textures preserved. Where SR alteration is transitional to AS or AA alteration, minor amounts of alunite and/or pyrophyllite may occur associated with the muscovite-quartz assemblage. Paragonite, identified by XRD, is found only at depth in DH 96-1 and 96-2. The

presence of illite, as noted in Tompson (1997) and Tompson and Cuttle (1994), has not been confirmed.

### Anhydrite-Quartz Alteration (AQ)

Anhydrite-quartz alteration is found distal to the most intense altered zones. The assemblage is concentrated at depth in DH 96-1 and near surface in the vicinity of DH 92-2 and DH 94-2. Where present, AQ alteration is intermediate between sericitic and propylitic assemblages. Significant amounts of montmorillonite occur in DH 92-2 (with lesser amounts in 94-2), associated with gypsum-muscovite-quartz alteration. At greater depths in DH 96-1, the AQ assemblage is found as massive zones intermixed with lesser SR alteration. Veins of anhydrite-quartz are also commonly found cross-cutting SR and/or PR assemblages in zones located to the east of the Ridge Zone, particularly in DH 92-1, 94-1 and 94-2.

### Propylitic Alteration (PR)

Propylitic alteration assemblages are widely distributed peripheral to zones of more intense alteration and are commonly gradational into SR assemblages. The most common propylitic assemblage consists of chlorite with variable muscovite, quartz, and pyrite. Epidote-, carbonate-, and albite-rich assemblages occur locally. Secondary albite has only been recognized in narrow intervals from DH 94-4 and 94-9 where it is usually associated with abundant hematite. Epidote is a common accessory mineral in chlorite-rich propylitic alteration and locally forms massive zones in DH 92-2 and rarely in DH 94-2. Epidote is also a common constituent of quartz-rich veins which cross-cut propylitic and locally sericite-rich assemblages. Carbonate is present in only a few samples of epidote-bearing alteration from localities to the NE of the Ridge zone in DH 92-2 and DH 94-1.

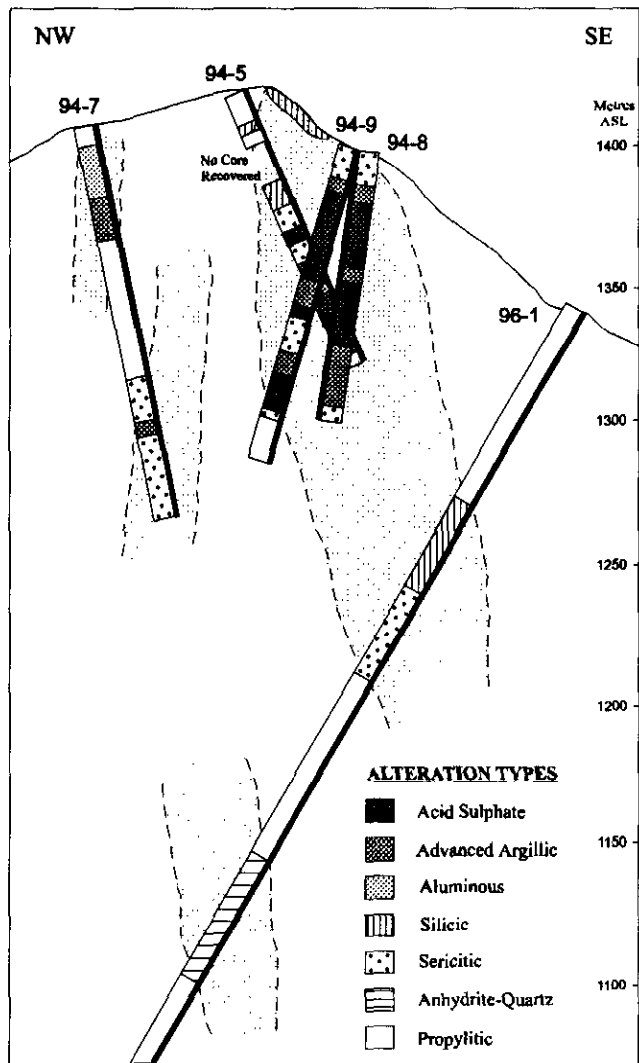


Figure 4: Cross-section through the southwest end of the Ridge zone showing the dominant alteration assemblage in each interval (see Figure 2 for location).

## EXOTIC LIMONITE

Exotic limonites are defined by Blanchard (1968) as those that have "precipitated from iron-bearing solutions which have moved so far from their source that the source can no longer be identified specifically". The term is used at Limonite Creek for three major surface limonite deposits. The largest of these is exposed on the slopes north of Limonite Creek and covers an area of approximately 50 acres. It was reported to be up to 10.5 metres thick (British Columbia Minister of Mines, 1957). Drilling of this limonite zone during 1997 indicated a thickness of at least 7 metres. Two other limonite zones occur on the property to the north and south of the alteration zones (Figure 2). The 'Middle Deposit' is located near the camp and is actively forming from groundwater discharging along its northern edge. Drilling in 1997 determined a minimum thickness of 6 metres. The third deposit is exposed along the southern

banks of Many Bear Creek and appears to be a relatively thin blanket of limonite developed on coarse talus.

In all three of the exotic deposits, limonite is actively forming from acidic, iron-rich solutions as sheets, layers, and terraces parallel to the slope in each area. The measured pH of surface waters associated with the limonites ranges from 3.4 to 6.5. As the limonite precipitates, it commonly incorporates abundant organic matter in the form of pine needles, twigs, and leaves which remain trapped as successive layers accumulate. As a result, the limonite often consists of friable, very porous, light, relatively soft masses with abundant visible organic matter. Locally however, the limonite forms much denser, competent, and compact layers. Along the banks of Many Bear Creek, limonite also locally occurs as a matrix in masses of limonite-cemented pebbles and cobbles.

XRD analyses on selected limonite samples indicate that the exotic deposits are dominated by pure goethite. Sequential extraction techniques using a buffered ammonium oxalate solution (Schwertmann et al., 1982) however demonstrate that the limonite is precipitated from solution at surface initially as ferrihydrite, which over time transforms to crystalline goethite. Trace element analyses of limonite depth profiles have shown that limonites contain trace amounts of Cu, Zn and Mn (maximum of 518, 38 and 90 ppm respectively). Analyses of surface waters actively precipitating the limonitic material are currently in progress.

## DISCUSSION

The alteration at Limonite Creek consists of irregular zones of acid-sulphate, advanced argillic, aluminous and silicic alteration within broader zones of sericitic and widespread propylitic alteration. These alteration mineral assemblages and their distribution are characteristic of high sulphidation systems (e.g., Arribas, 1995). Although significant mineralization has not been found to date on the Limonite Creek property, extensive pyrite and minor amounts of copper-rich sulphides and sulphosalts occur; these minerals are also characteristic of high sulphidation systems.

The presence of andalusite-rich aluminous alteration, and the predominance of pyrophyllite with only minor kaolinite, suggest that most of the alteration formed at temperatures above 250°C (Reyes, 1990; Hemley et al., 1980). This suggests that the alteration formed at greater depths than typical high sulphidation epithermal deposits. Alteration assemblages of these types occur in the upper parts of some porphyry deposits (e.g., El Salvador, Gustafson and Hunt, 1975) and are characteristic of parts of the Equity Silver deposit (Wojdak, 1974), which is located approximately 90 kilometres southeast of Limonite Creek (Figure 1). The presence of locally extensive anhydrite-quartz alteration at Limonite Creek, particularly

at depth in DH 96-1, is also consistent with a porphyry environment.

The U-Pb age for sample for the porphyritic granodiorite (LC-08) of  $52.2 \pm 0.1$  Ma is interpreted to be post-alteration, due to the lack of significant alteration within this intrusion. The age of alteration, therefore, is probably early or pre-early Eocene. The date of the major granodiorite intrusion to the east (sample LC-09), which shows moderate epidote alteration at the contact with the altered volcanic rocks, may constrain the age of the alteration more closely. At the Equity Silver deposit, the Eocene (ca. 50-52 Ma) intrusions are largely post-mineral but the 60 Ma intrusion appears to be related directly to mineralization. The alteration at Limonite Creek may be similar in age to Equity Silver, but a significantly older age cannot be ruled out. Direct dating of alunite is required to determine the actual age of alteration at Limonite Creek.

The alteration zones at Limonite Creek are extensively oxidized at surface with in-situ replacement of pyrite by goethite and local redistribution of goethite. Oxidation persists to at least 135 metres in structures intersected in drill holes. Surface oxidation generated low pH waters that transported dissolved iron to exotic limonites where iron was first precipitated as ferrihydrite subsequently converting to goethite. The extent and thickness of exotic limonites attests to the amount of pyrite in the Limonite Creek alteration zones and the efficiency of transport of iron in low pH waters. Mobilization of iron is a characteristic of the weathering of many high sulphidation alteration systems, which are dominated by pyrite-rich zones with negligible buffering capacity.

## ACKNOWLEDGEMENTS

Telkwa Gold Corporation provided extensive field and financial support that made this project possible. Drilling of the exotic limonites was also aided by W.H. McRae and J.T. Thomas Drilling. Critical reviews by James Lang and Tim Baker greatly improved this paper.

## REFERENCES CITED

- Arribas, A. Jr. (1995): Characteristics of high-sulphidation epithermal deposits, and their relation to magmatic fluid, in *Magmas, Fluids and Ore Deposits*, J.F.H. Thompson, Editor, *Mineralogical Association of Canada*, Short Course Volume 23, pages 419-454.
- Blanchard, R. (1968): Interpretation of Leached Outcrops (Nevada Bureau of Mines Bulletin 66); Nevada Bureau of Mines, Nevada, 196 pages.
- British Columbia Minister of Mines (1957): Annual Report 1957; *Minister of Mines, Province of British Columbia*, page 12.
- Cyr, J.B., Pease, R.B. and Schroeter, T.G. (1984): Geology and Mineralization at Equity Silver Mine; *Canadian Journal of Earth Sciences*, Volume 79, pages 947-968.
- Gustafson, L.B. and Hunt, J.P. (1975): The porphyry copper deposit at El Salvador, Chile; *Economic Geology*, Volume 70, pages 875-912.
- Hemley, J.J., Montoya, J.W., Marinenko, J.W., and Luce, R.W. (1980): Equilibria in the system  $Al_2O_3$ - $SiO_2$ - $H_2O$  and some general implications for alteration/mineralization processes; *Economic Geology*, Volume 75, pages 210-228.
- Mortensen, J. K., Ghosh, D.K. and Ferri, F. (1995): U-Pb Geochronology of Intrusive Rocks Associated with Copper-Gold Porphyry Deposits in the Canadian Cordillera; in, *Porphyry Deposits of the Northwestern Cordillera of North America*, Schroeter, T.G., Editor, *Canadian Institute of Mining, Metallurgy and Petroleum*, Special Volume 46, pages 142-158.
- Reyes, A.G. (1990): Petrology of Philippine geothermal systems and the application of alteration mineralogy to their assessment; *Journal of Volcanology and Geothermal Research*, Volume 43, pages 279-309.
- Schwertmann, U., Schulze, D.G., and Murad, E. (1959): Identification of ferrihydrite in soils by dissolution kinetics, differential X-ray diffraction, and Mossbauer spectroscopy; *Journal of the Soil Science Society of America*, Volume 46, pages 869-875.
- Stacey, J.S. and Kramers, J.D. (1975): Approximation of Terrestrial Lead Isotope Evolution by a Two-Stage Model; *Earth and Planetary Science Letters*, Volume 26, pages 207-221.
- Tipper, H.W. and Richards, T.A. (1976): Jurassic Stratigraphy and History of North-Central British Columbia; *Geological Survey of Canada*, Bulletin 270.
- Tompson, W.D. and Cuttle, J.F. (1994): Exploration of the Acid-Sulfate Epithermal Prospects: Limonite Creek Area; internal report for Limonite Creek Limited Partnership.
- Tompson, W.D. (1997): Exploration of the High Sulphidation Epithermal Prospects - Limonite Creek Area; internal report for Telkwa Gold Corp.
- Wanless, R.K., Stevens, R.D., Lachance, G.R. and Delabio, R.D.N. (1974): Age determinations and Geological Studies: K-Ar Isotopic Ages; *Geological Survey of Canada*, Report 12. Paper 74-2.
- Wojdak, P.J. (1974): Alteration of the Sam Goosly copper-silver-antimony deposit, British Columbia; unpublished M.Sc. thesis, *University of British Columbia*, 116 pages.
- Woodsworth, G.J., Anderson, R.G., and Armstrong, R.L. (1991): Plutonic Regimes; in *Geology of the Cordilleran Orogen in Canada*, H. Gabrielse and C.J. Yorath Editors, *Geological Survey of Canada*, Geology of Canada, No. 4, pages 491-531.



# GEOLOGY AND U-Pb GEOCHRONOLOGY OF INTRUSIVE ROCKS ASSOCIATED WITH MINERALIZATION IN THE NORTHERN TAHTSA LAKE DISTRICT, WEST-CENTRAL BRITISH COLUMBIA

By M.E. Lepitre, Mineral Deposit Research Unit, J.K. Mortensen, R.M. Friedman, Department of Earth and Ocean Sciences, University of British Columbia, and S.J. Jordan, Mineral Deposit Research Unit.

**KEYWORDS:** Bulkley Suite, U-Pb, porphyry deposit, Huckleberry, Whiting Creek, Bergette, Tahtsa Lake District, Cretaceous, Stikine Terrane.

drive road. The Bergette property is located along the access road to the Berg property and is accessible by all terrain vehicle.

## INTRODUCTION

The Bulkley Suite of intrusions are spatially associated with numerous important mineral occurrences in west-central British Columbia. Previous K-Ar dating studies indicated that the Bulkley Suite ranges in age from 70 to 84 Ma (Carter, 1981). The purpose of this study is to better constrain the timing of Bulkley Suite magmatism and associated mineralization in the northern Tahtsa Lake District. The mineral deposits in the study area that are suggested to be related to Bulkley Suite intrusions include Huckleberry, Whiting Creek, Emerald Glacier and Bergette. There are six closely related intrusive phases in the Whiting Creek area, several of which have associated mineralization. In order to resolve the timing of emplacement of the different intrusive phases in the Whiting Creek area, as well as any regional trends in magmatism, precise age constraints are needed. Uranium-lead geochronological studies were undertaken in order to obtain the necessary precision.

## LOCATION AND ACCESS

The northern Tahtsa Lake District is located in west-central British Columbia (Figure 32-1), within the Whitesail Lake map sheet (NTS 93E). The study area is situated near the western margin of the Intermontane morphogeological belt, within the transitional zone between the Coast Plutonic Complex to the west and the Interior Plateau to the east. Access to the area is by means of forestry service roads south of Houston, British Columbia. The forestry service roads are generally in good condition, and are well maintained due to continuing forestry activity and the impending opening of Huckleberry mine. The Whiting Creek property is accessible by four wheel drive vehicle on an exploration road from the main access road. Although there are roads to the north of Whiting Creek, vehicle access is not always possible beyond the creek due to occasional high water levels. Access to the inactive Emerald Glacier mine and areas to the north (the Sibola Stock) are by a steep, four wheel

## REGIONAL GEOLOGY

The project area is located near the western margin of the Intermontane Belt within the Stikine tectonostratigraphic terrane (Figure 32-1). Stikinia is composed of volcanic and sedimentary strata of Lower Devonian to Middle Jurassic age (Monger et al., 1991), and supracrustal sequences of Middle Jurassic to Early Tertiary age, which are intruded by several suites of intrusive rocks. Monger et al. (1991) suggested that all of the components of Stikinia are interrelated components of a complex island arc terrane. Stikinia is in fault contact with the Cache Creek Terrane to the east, whereas the nature of the contact with the terranes to the west has been largely obscured by Cretaceous and Tertiary intrusions. Stikinia is thought to have been accreted to the North American continent by late Middle Jurassic time or possibly earlier (Monger et al., 1991).

Stikinia is comprised of arc assemblages consisting of interbedded volcanic and marine strata. Triassic volcanic assemblages (Takla, Stuhini and Lewes River groups) are unconformably overlain by Lower to Middle Jurassic Hazelton Group volcanic and sedimentary rocks. These rocks, which are dominantly volcanic rocks (pyroclastic) of calc-alkaline composition, were deposited in both marine and non-marine settings.

Overlying the volcanic and marine strata are Middle Jurassic to Early Tertiary supracrustal sequences, which record the effects of the amalgamation and collision of the Stikine terrane (Yorath, 1991). In the study area, the supracrustal sequences are represented by the Ashman Formation of the Bowser Lake Group overlain by the Skeena Group.

Intrusive suites of various ages and compositions were emplaced into the rocks described above. These suites include the Late Triassic Stikine Suite, the Early to Middle Jurassic Topley Suite, the Middle Jurassic Three Sisters Suite, the Late Jurassic to Early Cretaceous Francois Lake Suite, the Late Cretaceous Bulkley Suite, and the Tertiary Nanika, Babine, Quanchus, and Goosly Lake Suites (Woodsworth et al., 1991).

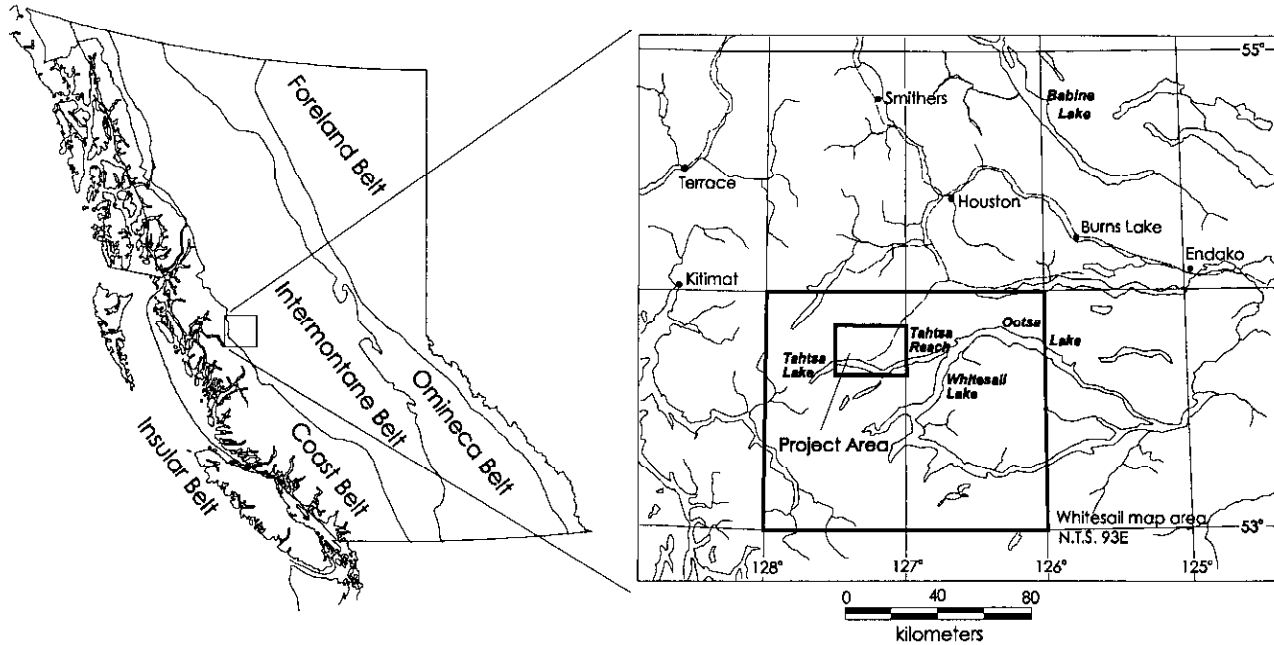


Figure 32-1. Location map for the study area with respect to the main morphogeological belts in the Canadian Cordillera, and showing the main access road.

## LOCAL GEOLOGY

The general geology of the northern Tahtsa Lake District is shown in Figure 32-2. The following geological description is taken mainly from MacIntyre (1985). The most areally extensive unit in this region is the Telkwa Formation of the Lower to Middle Jurassic Hazelton Group. These rocks consist of lapilli tuff, lithic tuff, crystal tuff, tuff breccia and minor amounts of porphyritic augite andesite, dacite, tuffaceous siliceous argillite and pebble conglomerate. The Hazelton Group rocks are overlain by the Middle Jurassic Ashman Formation of the Bowser Lake Group, which are in turn overlain by the Early Cretaceous Skeena Group. The Bowser Lake Group marine sedimentary rocks, which occur in a fault-bounded block just south of the Sibola Stock (Figure 32-2), consist of interbedded pebble conglomerate, sandstone, siltstone, shale, and minor tuff. In the project area the Skeena Group consists of a basal conglomerate unit, an amygdaloidal basalt unit and a marine sedimentary unit. The Skeena Group is unconformably overlain by the Kasalka Group. The Kasalka Group as defined by MacIntyre (1985) comprises both volcanic and comagmatic plutonic rocks.

Several intrusive suites were emplaced into the volcanic and sedimentary strata described above. These include the Bulkley Suite intrusions, the Coast intrusions and the Nanika intrusions (Woodsworth et al. 1991). The known distribution of the Bulkley intrusions defines a vaguely north-south trend. Although the intrusions occupy back arc position with respect to coeval plutonism in the Coast Plutonic Complex, they are calc-alkaline in composition (MacIntyre, 1985), suggesting generation in an arc setting, rather than in a back arc setting.

### Intrusives in the Huckleberry Area

Two small stocks of hornblende-biotite-feldspar porphyry intrude and hornfels Hazelton Group volcanic rocks in the Huckleberry area. Both intrusions have associated Cu +/- Mo mineralization. Post-mineral lamprophyre and microdiorite dykes crosscut both intrusions.

### Intrusives in the Whiting Creek Area

Several intrusions including small stocks and northwest trending dykes that belong to the Bulkley Suite were emplaced into Hazelton Group volcanic rocks in the Whiting Creek area (Figure 32-3). The intrusive phases in the area consist of: quartz porphyry, quartz monzonite porphyry, monzonite porphyry, quartz monzonite of the Whiting Stock, hornblende-biotite-feldspar porphyry dykes, and rhyolite dykes (Cann and Smit, 1995).

### Sibola Stock

The Sibola Stock is a large intrusive body that is compositionally zoned from relatively minor quartz monzodiorite to more typical quartz monzonite. It is similar in both composition and texture to the Whiting Stock. Dykes of several compositions, including biotite-feldspar porphyry and aplite, crosscut the Stock (Figure 32-2).

### Intrusives in the Bergette Area

The Bergette property is located near the northern margin of the Sibola Stock. There are several intrusive

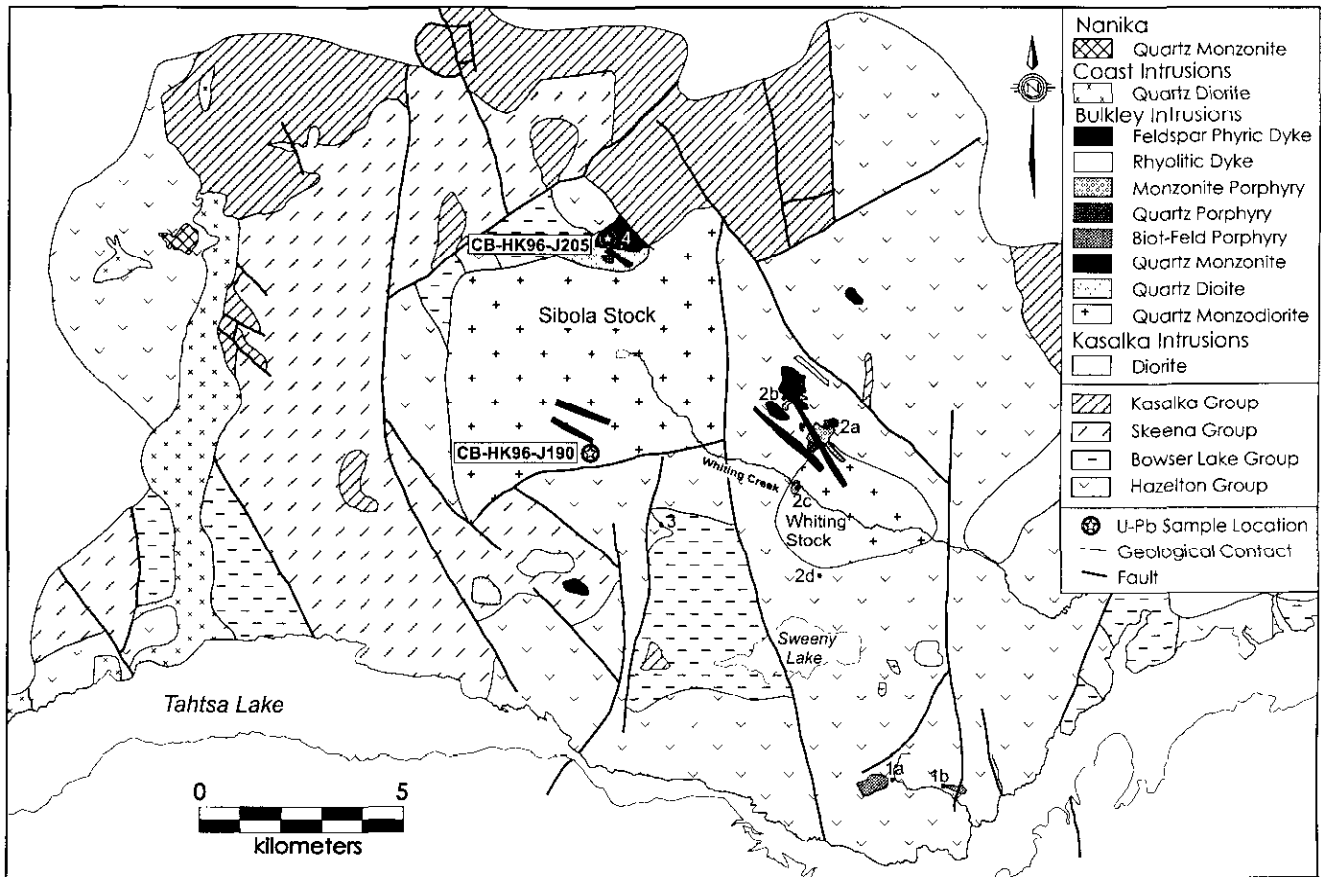


Figure 32-2. Map showing the general geology of the northern Tahtsa Lake District, the locations of the deposits studied, and the locations of U-Pb samples dated in this study. 1. Huckleberry (a) Main Zone (b) East Zone; 2. Whiting Creek (a) Ridge Zone (b) Rusty Zone (c) Creek Zone (d) Sweeny Zone; 3. Emerald Glacier; 4. Bergette.

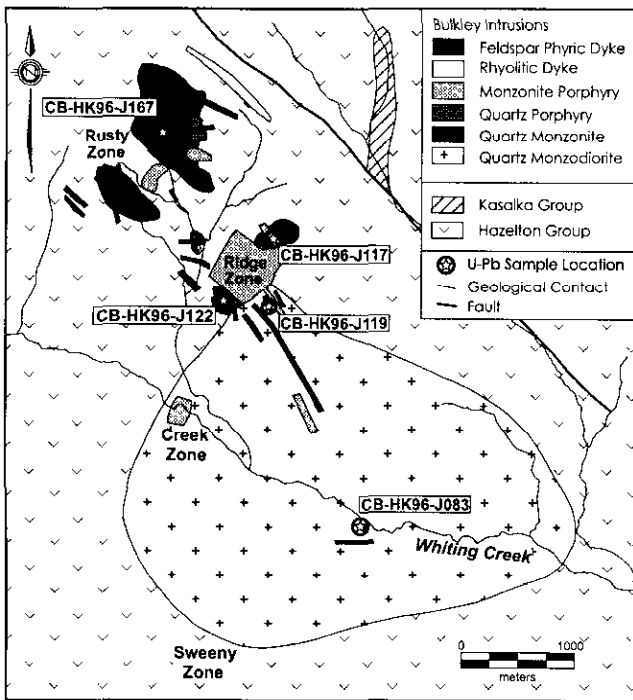


Figure 32-3. Map of the geology of the Whiting Creek area, showing the mineralized zones and the U-Pb sample locations.

phases assigned to the Bulkley Suite in the Bergette area (Figure 32-4). The intrusive phases as described by Church (1971) include a fine grained biotite-hornblende quartz diorite (border phase of Sibola Stock), a porphyritic biotite hornblende quartz monzonite, a quartz porphyry, a breccia body, and northwest-trending feldspar porphyry dykes.

### MINERALIZATION

The Late Cretaceous Bulkley Suite intrusions are associated with numerous mineral occurrences in west-central British Columbia, including copper-molybdenum and molybdenum-tungsten porphyry deposits (McMillan et al., 1995). Several different styles of porphyry-style Cu and/or Mo mineralization are observed in the study area, as well as a quartz-base metal vein deposit.

### Huckleberry

Mineralization occurs in two zones in the Huckleberry area: the Main Zone and the East Zone (Jackson and Illerbrun, 1995). The sulfide mineralization occurs as a system of stockwork fractures and veins hosted both within

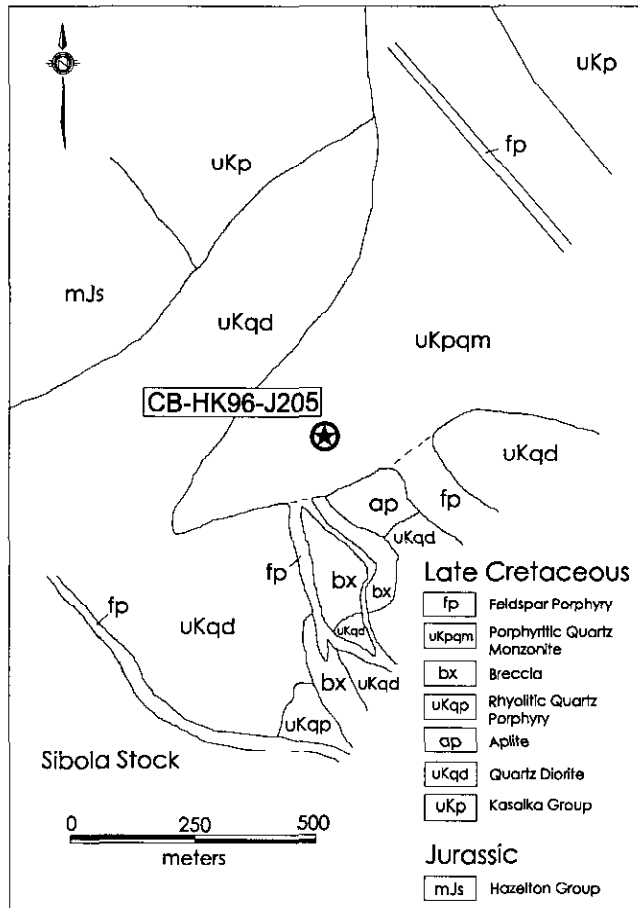


Figure 32-4. Geology of the Bergette area after Church (1971). U-Pb sample location is shown as a circled star.

hornfelsed volcanic rocks and the East Zone Stock. Copper mineralization occurs as chalcopyrite and rare bornite, and minor molybdenum mineralization is present as molybdenite.

### Whiting Creek

In the Whiting Creek area, mineralization is divided into four zones: The Ridge Zone, the Rusty Zone, the Creek Zone, and the Sweeny Zone (Figure 32-3). In the Ridge Zone, mineralization occurs as a quartz-molybdenum stockwork hosted by both the quartz porphyry and the surrounding hornfelsed volcanic rocks. Copper is relatively minor in this zone, except where it is associated with the monzonite porphyry which intrudes the quartz porphyry. The Rusty Zone is a poorly defined zone of Cu-Mo mineralization that appears to be spatially associated with an altered quartz monzonite porphyry stock, which lies immediately to the north of the mineralized zone. Copper grades appear to be somewhat higher here than in the Ridge Zone (Cann and Smit, 1995). Mineralization in the Creek Zone occurs peripheral to a small stock of monzonite porphyry that lies entirely within the Whiting Stock. Sweeny Zone mineralization occurs in hornfelsed volcanic rocks near a small granodiorite intrusion to the

south of the Whiting Stock. The area is covered in overburden and the mineralized zone is very poorly defined. Minor disseminated Cu and Mo mineralization is present and appears to decrease rapidly away from the intrusion.

### Emerald Glacier

The Emerald Glacier deposit is a northwest-trending, sheared quartz vein which cuts the Bowser Lake Group south of the Sibola Stock (Figure 32-2). Sulfides present in the vein include galena, sphalerite, chalcopyrite and pyrite. MacIntyre (1985) suggested that the Emerald Glacier deposit is genetically related to the Sibola Stock based mainly on the close spatial association.

### Bergette

Two styles of mineralization were observed in the Bergette area by Church (1971). These styles were: (1) healed cracks containing gypsum, pyrite, and minor molybdenite with quartz and fluorite hosted in the quartz porphyry; and (2) thin fracture fillings and disseminations of pyrite, chalcopyrite and minor molybdenite with quartz hosted within the west marginal section of Sibola Stock. Although the copper mineralization at the Bergette property appears to be associated with the porphyritic quartz monzonite and the margin of Sibola Stock, formally described mineralized zones have not been assigned (MacIntyre, 1985).

## PREVIOUS GEOCHRONOLOGICAL STUDIES

Several previous geochronological studies have been completed on Bulkley Suite intrusions in the northern Tahtsa Lake District. Results of these studies are summarized in Table 32.1. Carter (1981) obtained a K-Ar biotite age of 82 +/- 6 Ma for the Main Zone Stock at Huckleberry. New U-Pb zircon dates of 83.5 +/- 0.3 Ma for both the Main Zone and the East Zone stocks were reported by Friedman and Jordan (1997). Several intrusive phases at Whiting Creek have been dated by K-Ar methods, including the quartz monzonite (Whiting Stock), the monzonite porphyry, and a biotite-feldspar porphyry dyke. The K-Ar ages obtained for these intrusions are 81.3 +/- 5.4 Ma, 84.1 +/- 5.8 Ma, and 76.0 +/- 4.4 Ma, respectively (MacIntyre, 1985). No isotopic dating studies have previously been undertaken for the Sibola Stock. Church (1971) reported a K-Ar age of 76.7 +/- 5 Ma for the quartz monzonite porphyry at Bergette. Based on this previous work in the study area and other more regional studies (summarized in Christopher and Carter, 1976) the Bulkley Suite is considered to range in age from 70 to 84 Ma (Carter, 1981).

Table 32.1 Summary of previous geochronological studies completed on Bulkley Suite intrusions in the northern Tahtsa Lake District.

| LOCATION             | ROCK TYPE                             | METHOD         | AGE                 | REFERENCE                 |
|----------------------|---------------------------------------|----------------|---------------------|---------------------------|
| <b>HUCKLEBERRY</b>   | Granodiorite Porphyry                 | K-Ar (biotite) | 82 +/-6 Ma          | Carter, 1981              |
|                      | East Zone Stock                       | U-Pb (zircon)  | 83.5 +/-0.3 Ma      | Friedman and Jordan, 1997 |
|                      | Main Zone Stock                       | U-Pb (zircon)  | 83.5 +/-0.3/-0.4 Ma | Friedman and Jordan, 1997 |
| <b>WHITING CREEK</b> | Quartz Monzonite (Whiting Stock)      | K-Ar (biotite) | 81.3 +/-5.4 Ma      | MacIntyre, 1985           |
|                      | Monzonite Porphyry                    | K-Ar (biotite) | 84.1 +/-5.8 Ma      | MacIntyre, 1985           |
|                      | Quartz-biotite-feldspar porphyry Dyke | K-Ar (biotite) | 76.0 +/-4.4 Ma      | MacIntyre, 1985           |
| <b>BERGETTE</b>      | Quartz Monzonite Porphyry             | K-Ar (biotite) | 76.7 +/-5.0 Ma      | Church, 1971              |

## U-Pb GEOCHRONOLOGY

Previous geochronological studies completed in the Northern Tahtsa Lake District have consisted mainly of K-Ar biotite ages (Table 32.1). These analyses are relatively imprecise, and biotite, which has a relatively low closure temperature, is susceptible to resetting during even minor thermal events. With the existing database it was therefore impossible to resolve individual intrusive events in the region. A uranium-lead geochronological study of the various intrusive phases in the project area was undertaken in order to better constrain the timing of magmatism and related mineralization.

### Analytical techniques

Accessory minerals were separated from the samples using conventional crushing, grinding, Wilfley table, heavy liquid, and magnetic separation techniques. All sample preparation and analyses were completed in the Geochronology Laboratory at the University of British Columbia as described by Mortensen et al. (1995).

### Analytical Results

Seven samples were collected for U-Pb dating from the northern Tahtsa Lake District. Five of these samples are representative of the various intrusive phases in the Whiting Creek area. The other two samples are from the Sibola Stock and the quartz monzonite porphyry at Bergette. Sample locations are shown on Figures 32-2, 32-3 and 32-4.

#### *Whiting Stock (CB-HK96-J083)*

Abundant high quality zircon was recovered from a sample of the Whiting Stock. The zircon grains form euhedral stubby to elongate prisms (l:w = 2-3), with rare clear inclusion and no visible zoning or cores. Three fractions were analyzed (fractions A-C, Table 32.2). Two fractions of clear, honey yellow euhedral titanite were

also analyzed (fractions T1-T2, Table 32.2). All fractions of both zircon and titanite gave concordant analyses (Figure 32-5a), although fractions B and T1 appear to have experienced minor Pb loss. A crystallization age of 81.9 +/- 0.5 Ma, based on the total range of  $^{206}\text{Pb}/^{238}\text{U}$  ages for the three oldest concordant fractions that did not suffer Pb loss, is assigned to the rock unit. The titanite age is identical to the zircon age, indicating that the Whiting Stock cooled rapidly through the closure temperature of the U-Pb system in titanite (~600°C; Heaman and Parrish, 1991).

#### *Monzonite Porphyry (CB-HK96-J117)*

Good quality, clear, euhedral zircon in the form of stubby to elongate prisms (l:w = 2-3), was recovered from a sample of the monzonite porphyry. Excess pyrite in the sample was removed prior to hand-picking the zircon fractions for dating by floating it off in dilute nitric acid. Three zircon fractions were analyzed (Table 32.2), all of which yielded overlapping concordant ages (Figure 32-5b). Fraction A gave an imprecise analysis, and the best estimate for the crystallization age of the unit, based on the total range of  $^{206}\text{Pb}/^{238}\text{U}$  ages for the other two fractions, is 80.4 +/- 0.3 Ma.

#### *Biotite Feldspar Porphyry Dyke (CB-HK96-J119)*

Abundant good quality clear, euhedral zircon with few inclusions and no visible zoning or cores was recovered from a sample of the biotite feldspar porphyry dyke. Three zircon morphologies were observed: elongate prisms (l:w = 3), stubby prisms (l:w = 2), and equant grains. One fraction of each morphology was analyzed (Table 32.2). Fraction A and B yielded concordant ages with overlapping error ellipses (Figure 32-5c). Fraction C falls to the right of concordia and gives older Pb/U ages and is interpreted to have contained an inherited zircon component. The crystallization age for this sample, based on the total range of  $^{206}\text{Pb}/^{238}\text{U}$  ages of concordant fractions A and B, is 79.6 +/- 0.5 Ma.

Table 32.2. U-Pb Analytical Data.

| Fraction description <sup>1</sup>                                | Wt (mg) | U <sup>2</sup> (ppm) | Pb* <sup>3</sup> (ppm) | <sup>206</sup> Pb/ <sup>204</sup> Pb <sup>4</sup> | Pb <sup>5</sup> (pg) | <sup>208</sup> Pb <sup>6</sup> (%) | <sup>206</sup> Pb/ <sup>238</sup> U <sup>7</sup> (+/- % 1σ) | <sup>207</sup> Pb/ <sup>235</sup> U <sup>7</sup> (+/- % 1σ) | <sup>207</sup> Pb/ <sup>206</sup> Pb <sup>7</sup> (+/- % 1σ) | <sup>207</sup> Pb/ <sup>206</sup> Pb Age <sup>7</sup> (Ma +/- % 2σ) |
|------------------------------------------------------------------|---------|----------------------|------------------------|---------------------------------------------------|----------------------|------------------------------------|-------------------------------------------------------------|-------------------------------------------------------------|--------------------------------------------------------------|---------------------------------------------------------------------|
| <b>Whiting Stock (sample: CB-HK96-J083)</b>                      |         |                      |                        |                                                   |                      |                                    |                                                             |                                                             |                                                              |                                                                     |
| A: N1,+180,s                                                     | 0.15    | 454                  | 6                      | 3153                                              | 17                   | 8.8                                | 0.01278 (0.16)                                              | 0.0842 (0.23)                                               | 0.04777 (0.16)                                               | 87.9 +7.6/-7.7                                                      |
| B: N1,+180,s                                                     | 0.097   | 469                  | 6                      | 2518                                              | 14                   | 8.6                                | 0.01260 (0.13)                                              | 0.0827 (0.22)                                               | 0.04762 (0.15)                                               | 80.5 +7.2/-7.2                                                      |
| C: N1,+180,e                                                     | 0.069   | 469                  | 6                      | 2174                                              | 12                   | 8.9                                | 0.01274 (0.10)                                              | 0.0838 (0.24)                                               | 0.04768 (0.20)                                               | 83.5 +9.4/-9.5                                                      |
| T1: 0.6-1.8,eq,u                                                 | 0.32    | 353                  | 5                      | 481                                               | 196                  | 16.6                               | 0.01262 (0.14)                                              | 0.0831 (0.51)                                               | 0.04771 (0.42)                                               | 85 +20/-20                                                          |
| T2: 0.6-1.8,eq,u                                                 | 0.54    | 475                  | 7                      | 541                                               | 402                  | 17                                 | 0.01283 (0.19)                                              | 0.0843 (0.45)                                               | 0.04767 (0.33)                                               | 83 +16/-16                                                          |
| <b>Monzonite Porphyry (sample: CB-HK96-J117)</b>                 |         |                      |                        |                                                   |                      |                                    |                                                             |                                                             |                                                              |                                                                     |
| A: N1,+134,e                                                     | 0.094   | 239                  | 3                      | 103                                               | 214                  | 12.5                               | 0.01262 (0.65)                                              | 0.0828 (2.2)                                                | 0.04758 (1.9)                                                | 78 +86/-91                                                          |
| B: N1,+134,s                                                     | 0.105   | 229                  | 3                      | 970                                               | 20                   | 12.1                               | 0.01254 (0.11)                                              | 0.0822 (0.28)                                               | 0.04758 (0.21)                                               | 79 +10/-10                                                          |
| C: N1,+134,s                                                     | 0.118   | 251                  | 3                      | 2784                                              | 8                    | 12.9                               | 0.01257 (0.12)                                              | 0.0827 (0.22)                                               | 0.04772 (0.16)                                               | 85.5 +7.4/-7.4                                                      |
| <b>Biotite Feldspar Porphyry Dyke (sample: CB-HK96-J119)</b>     |         |                      |                        |                                                   |                      |                                    |                                                             |                                                             |                                                              |                                                                     |
| A: N2,+180,e                                                     | 0.48    | 629                  | 8                      | 6631                                              | 35                   | 10                                 | 0.01244 (0.21)                                              | 0.0816 (0.23)                                               | 0.04761 (0.08)                                               | 79.8 +3.8/-3.8                                                      |
| B: N2,134-180,s                                                  | 0.238   | 720                  | 9                      | 4576                                              | 29                   | 9.4                                | 0.01238 (0.13)                                              | 0.0812 (0.22)                                               | 0.04755 (0.14)                                               | 76.7 +6.6/-6.6                                                      |
| C: N2,134-180,eq                                                 | 0.166   | 766                  | 10                     | 7323                                              | 14                   | 10                                 | 0.01260 (0.11)                                              | 0.0831 (0.18)                                               | 0.04781 (0.09)                                               | 89.8 +4.3/-4.3                                                      |
| <b>Quartz Porphyry (sample: CB-HK96-J122)</b>                    |         |                      |                        |                                                   |                      |                                    |                                                             |                                                             |                                                              |                                                                     |
| A: N2,-104,e                                                     | 0.06    | 894                  | 11                     | 3629                                              | 12                   | 8.3                                | 0.01288 (0.09)                                              | 0.0846 (0.19)                                               | 0.04766 (0.13)                                               | 82.4 +6.0/-6.0                                                      |
| B: N2,-104,e                                                     | 0.057   | 851                  | 11                     | 4833                                              | 8                    | 8.2                                | 0.01296 (0.13)                                              | 0.0852 (0.20)                                               | 0.04767 (0.10)                                               | 83.1 +4.9/-4.9                                                      |
| C: N2,-104,e                                                     | 0.048   | 1108                 | 14                     | 2529                                              | 17                   | 7.7                                | 0.01284 (0.09)                                              | 0.0844 (0.21)                                               | 0.04767 (0.15)                                               | 83.0 +7.2/-7.2                                                      |
| <b>Quartz Monzonite Porphyry (sample: CB-HK96-J167)</b>          |         |                      |                        |                                                   |                      |                                    |                                                             |                                                             |                                                              |                                                                     |
| A: N1,+134,e                                                     | 0.108   | 541                  | 7                      | 5541                                              | 9                    | 8.8                                | 0.01320 (0.10)                                              | 0.0873 (0.17)                                               | 0.04796 (0.10)                                               | 97.5 +4.7/-4.8                                                      |
| B: N1,+134,s                                                     | 0.132   | 552                  | 7                      | 5026                                              | 12                   | 8.5                                | 0.01294 (0.08)                                              | 0.0851 (0.17)                                               | 0.04766 (0.11)                                               | 82.4 +5.0/-5.0                                                      |
| C: N1,-134,e                                                     | 0.152   | 550                  | 7                      | 9467                                              | 7                    | 8.8                                | 0.01285 (0.09)                                              | 0.0849 (0.16)                                               | 0.04793 (0.09)                                               | 95.6 +4.1/-4.1                                                      |
| <b>Sibola Stock (sample: CB-HK96-J190)</b>                       |         |                      |                        |                                                   |                      |                                    |                                                             |                                                             |                                                              |                                                                     |
| A: N1,+134,eq                                                    | 0.11    | 165                  | 2                      | 1543                                              | 9                    | 11.6                               | 0.01230 (0.27)                                              | 0.0808 (0.53)                                               | 0.04766 (0.39)                                               | 83 +18/-19                                                          |
| B: N1,+134,s                                                     | 0.17    | 177                  | 2                      | 2121                                              | 11                   | 11.7                               | 0.01233 (0.08)                                              | 0.0809 (0.21)                                               | 0.04759 (0.15)                                               | 79.0 +7.1/-7.1                                                      |
| C: N1,+134,e                                                     | 0.098   | 191                  | 2                      | 1677                                              | 9                    | 13.4                               | 0.01230 (0.09)                                              | 0.0807 (0.23)                                               | 0.04757 (0.17)                                               | 77.8 +8.0/-8.0                                                      |
| D: N1,+134,t,u                                                   | 0.101   | 220                  | 3                      | 1472                                              | 12                   | 12.1                               | 0.01221 (0.09)                                              | 0.0801 (0.24)                                               | 0.04759 (0.18)                                               | 78.8 +8.4/-8.5                                                      |
| <b>Bergette Quartz Monzonite Porphyry (sample: CB-HK96-J205)</b> |         |                      |                        |                                                   |                      |                                    |                                                             |                                                             |                                                              |                                                                     |
| A: N1,+134,e                                                     | 0.2     | 577                  | 7                      | 3159                                              | 28                   | 11.2                               | 0.01212 (0.11)                                              | 0.0796 (0.22)                                               | 0.04765 (0.16)                                               | 82.0 +7.4/-7.4                                                      |
| B: N1,+134,e                                                     | 0.155   | 505                  | 6                      | 4203                                              | 14                   | 11.6                               | 0.01169 (0.25)                                              | 0.0775 (0.29)                                               | 0.04807 (0.16)                                               | 102.6 +7.7/-7.7                                                     |
| C: N1,+134,s                                                     | 0.18    | 509                  | 6                      | 3246                                              | 22                   | 11.1                               | 0.01218 (0.10)                                              | 0.0799 (0.19)                                               | 0.04757 (0.11)                                               | 78.1 +5.4/-5.4                                                      |
| D: N1,-134,e                                                     | 0.127   | 372                  | 5                      | 2202                                              | 16                   | 11.6                               | 0.01209 (0.12)                                              | 0.0793 (0.26)                                               | 0.04759 (0.19)                                               | 78.8 +9.2/-9.2                                                      |

<sup>1</sup>Upper case letter = fraction identifier; All zircons are air abraded, except were indicated (u=unabraded); N1, N2 = non-magnetic at given degrees side slope on the Frantz isodynamic separator; 0.6-1.8 = magnetic at 0.6 amps field strength and non-magnetic at 1.8 amps field strength (20° side slope) on the Frantz; Front slope for all fractions = 20°; Grain size (intermediate dimension) is given in microns; Grain character codes: e=elongate; s=stubby; eq=equant; t=tabular.

<sup>2</sup> U blank correction of 1pg +/- 20%; U fractionation corrections were measured for each run with a double <sup>233</sup>U-<sup>235</sup>U spike (approximately 0.005/amu).

<sup>3</sup> Radiogenic Pb.

<sup>4</sup> Measured ratio corrected for spike, Pb fractionation of 0.0035 to 0.0043/amu +/- 20% (Daly collector; based on repeated analysis of Pb standard NBS 981), and laboratory blank Pb of 10pg +/- 20%. Laboratory blank Pb concentrations and isotopic compositions based on total procedural blanks analyzed throughout the duration of this study.

<sup>5</sup> Total common Pb in analysis based on blank isotopic composition.

<sup>6</sup> Radiogenic Pb.

<sup>7</sup> Corrected for blank Pb, U and common Pb. Common Pb corrections based on Stacey Kramers model (Stacey and Kramers, 1975) at the age of the rock or the <sup>207</sup>Pb/<sup>206</sup>Pb age of the fraction.

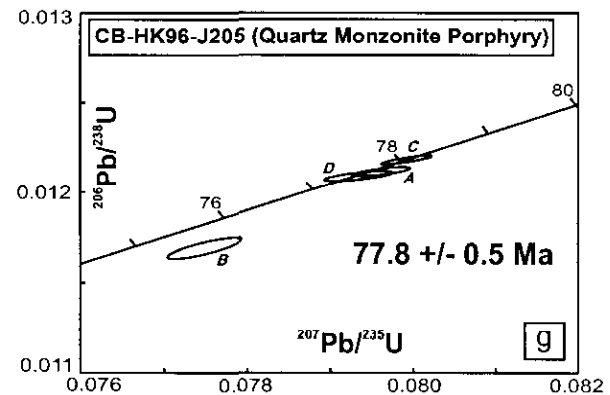
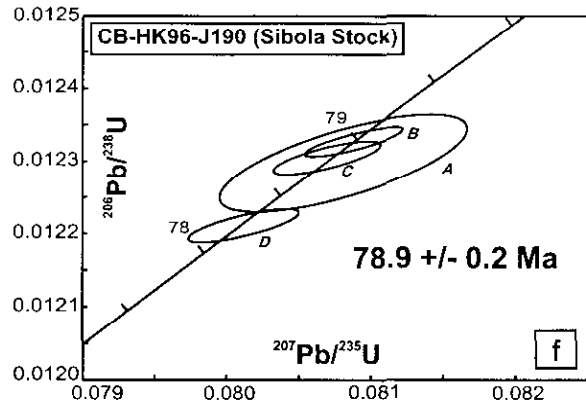
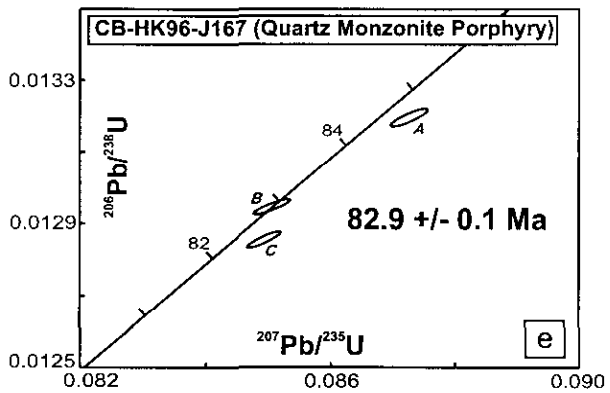
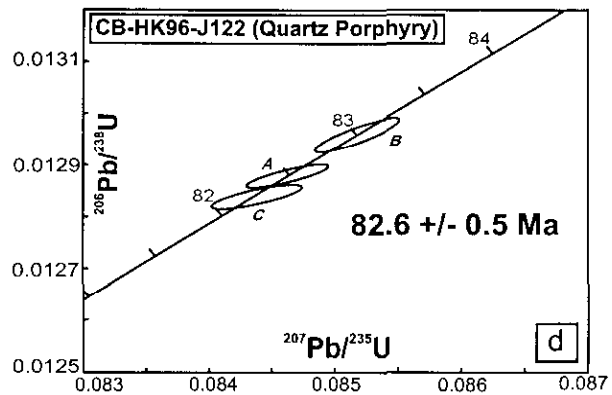
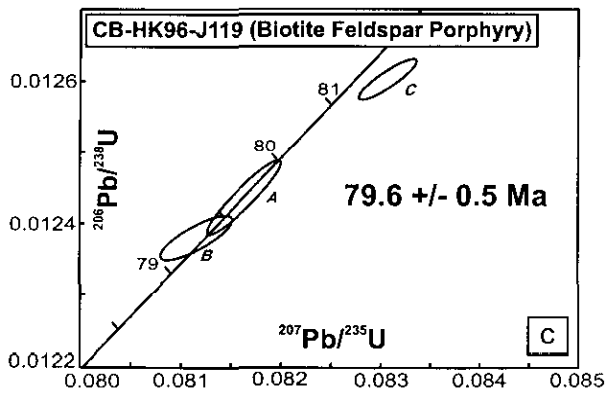
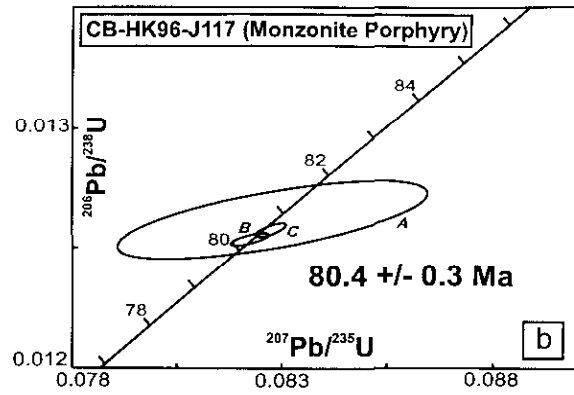
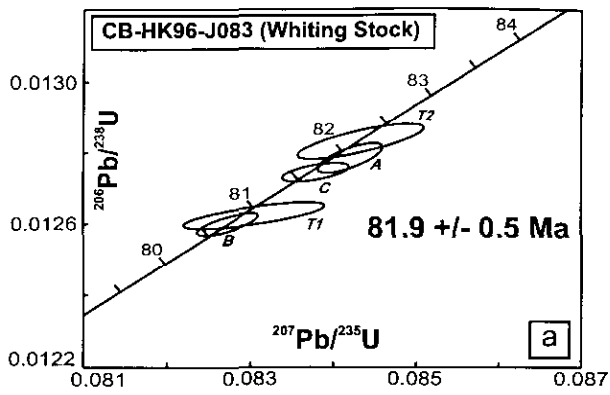


Figure 32-5. U-Pb concordia plots for samples from the Whiting Creek area (Figure 32-5a-e), Sibola Stock (Figure 32-5f) and the Bergette area (Figure 32-5g).

### **Quartz Porphyry (CB-HK96-J122)**

Clear, elongate (l:w = 3-4) euhedral zircon with no visible inclusions, zonation or cores was recovered from a sample of the quartz porphyry. Excess pyrite was removed using dilute nitric acid. Three fractions were analyzed (Table 32.2), all of which gave concordant ages (Figure 32-5d). The age based on the total range of  $^{206}\text{Pb}/^{238}\text{U}$  ages for these three fractions is 82.6 +/- 0.5 Ma.

### **Quartz Monzonite Porphyry (CB-HK96-J167)**

Abundant clear, euhedral zircon was recovered after excess pyrite was removed by nitric acid floatation. Zircon was elongate (l:w = 2-3) with no visible zonation, cores or inclusions. Three fractions were analyzed (Table 32.2). The data shows considerable scatter (Figure 32-5c), and the following interpretation is preliminary. Fraction A is interpreted as having contained an inherited zircon component, whereas fraction C appears to have suffered Pb loss as well as having contained an inherited component. A preliminary age of 82.9 +/- 0.1 Ma is assigned to this unit, based on concordant fraction B.

### **Sibola Stock (CB-HK96-J190)**

Abundant excellent quality, euhedral zircon was recovered from a sample of the Sibola Stock. Four zircon morphologies were observed, including elongate (l:w = 4), stubby (l:w = 2), equant and tabular grains. No zoning, cores or inclusions were visible. One fraction from each morphology was analyzed (Table 32.2). All of the analyses plot on concordia (Figure 32-5f). The analysis for fraction A is relatively imprecise and unabraded fraction D displays minor Pb loss. An age of 78.9 +/- 0.2 Ma, based on the range of  $^{206}\text{Pb}/^{238}\text{U}$  ages for overlapping concordant fractions B and C, is therefore assigned to the unit.

### **Quartz Monzonite Porphyry (CB-HK96-J205)**

Abundant good quality euhedral zircon was recovered from a sample of the quartz monzonite porphyry from Bergette. Zircons were elongate to stubby (l:w = 2-3) and showed no visible zoning, cores or inclusions. Four fractions were analyzed (Table 32.2), three of which yielded overlapping concordant ages (Figure 32-5g). Fraction B is interpreted as having undergone Pb loss. An age of 77.8 +/- 0.5 Ma is assigned to the rock unit, based on the range of  $^{206}\text{Pb}/^{238}\text{U}$  ages for the three concordant fractions.

## **DISCUSSION**

The new high precision data generated in this study, together with the U-Pb data reported by Friedman and Jordan (1997) clearly demonstrates that magmatism in the northern Tahtsa Lake District spanned at least 5 to 7 million years. The data also shows a younging trend in the age of magmatism from south to north within the project area. Porphyry-style mineralization with wide variations in Cu/Mo ratios has been recognized in the area. Friedman

and Jordan (1997) argued that the age of mineralization at Huckleberry is approximated by the age of the associated intrusions (83.5 +/- 0.5 Ma), based on inferred rapid cooling through the biotite closure temperature (Carter, 1981). The mineralization in the Bergette area cannot be older than 77.8 +/- 0.5 Ma, which is the age of the host intrusion. The main phases of mineralization in the Whiting Creek area occurred at 82.6 +/- 0.5 Ma in the Ridge Zone and 82.9 +/- 0.1 Ma in the Rusty Zone, based on the ages of the associated intrusions. Mineralization in the Whiting Creek area is therefore intermediate in age between that at Huckleberry and that at Bergette. Although mineralization at the Ridge and Rusty zones is very similar in age, the two zones have quite different proportions of Cu and Mo, possibly suggesting two separate mineralizing events. The intrusive contact relationship of the Whiting Stock into the quartz porphyry in the Ridge Zone inferred from drill hole data by Cann and Smit (1995) is confirmed by the new age data.

As previously noted, the calc-alkaline nature of the Bulkley Suite in the study area (MacIntyre, 1985) suggests generation in an arc rather than a back arc setting. Broadly coeval magmatism has been documented in the Coast Plutonic Complex up to 100 km to the west of the study area (Woodsworth et al., 1991). However, the isotopic age constraints for the igneous rocks to the west are relatively imprecise, and it is therefore possible that the intrusions in the study area represent a brief eastward excursion of the locus of arc magmatism. It is interesting to note that Engebretson et al. (1985) have postulated an increase in orthogonal relative motion between the subducting oceanic plate to the west (Kula Plate or Farallon Plate) and the North American Plate from 100 to 75 Ma, based on fixed hotspot reference frame studies. This could provide a possible mechanism for the suggested eastward shift of the locus of arc magmatism. Further geochronological and geochemical studies of both the Bulkley Suite intrusions and the Coast Plutonic Complex to the west of the study area are necessary in order to fully evaluate this hypothesis.

## **ACKNOWLEDGEMENTS**

This paper is part of a B.Sc. thesis completed at the UBC Department of Earth and Ocean Sciences by the first author. John Thompson's enthusiasm and broad expertise in Cordilleran mineral deposits was very much appreciated during the field work and during subsequent discussions about the study area. The project was funded by the Mineral Deposit Research Unit as a part of the Magmatic Hydrothermal Project.

## **REFERENCES CITED**

- Cann, R.M., Smit, H., 1995. The Whiting Creek Copper-molybdenum porphyry, west-central British Columbia. *In* *Porphyry Deposits of the North-*

- western Cordillera of North America. *Edited by* T. G. Schroeter. Canadian Institute of Mining, Metallurgy and Petroleum, Special Volume 46, p. 458-466.
- Carter, N.C., 1981. Porphyry Copper and Molybdenum Deposits, west-central British Columbia. British Columbia Ministry of Energy, Mines and Petroleum Resources, Bulletin 64, 150 pages.
- Christopher, P.A., Carter, N.C., 1976. Metallogeny and Metallogenic Epochs for Porphyry Mineral Deposits in the Canadian Cordillera. *In* Porphyry Deposits of the Canadian Cordillera. *Edited by* A. Sutherland Brown. Canadian Institute of Mining and Metallurgy, Special Volume 15, p. 64-71.
- Church, B.N., 1971. Bergette. British Columbia Ministry of Energy, Mines and Petroleum Resources, GEM, p. 147-157.
- Engelbreton, D.C., Cox, A., Gordon, R.G., 1985. Relative Motions Between Oceanic and Continental Plates in the Pacific Basin. Geological Society of America, Special Paper 206, 59 pages.
- Friedman, R.M., Jordan, S., 1997. U-Pb ages for intrusive rocks at the Huckleberry porphyry copper deposit, Tahtsa Lake District, Whitesail Lake Map Area, West-central British Columbia (93E/11). *In* Geological Fieldwork 1996, *Edited by* D.V. Lefevre, W.J. McMillan, J. G. McArthur. British Columbia Ministry of Employment and Investment, Paper 1997-1, p. 219-225.
- Heaman, L., Parrish, R.R., 1991. U-Pb geochronology of accessory minerals. *In* Applications of Radiogenic Isotope Systems to Problems in Geology. *Edited by* L. Heaman and J. N. Ludden. Mineralogical Association of Canada, Short Course Handbook, 19, p. 59-102.
- Jackson, A., Illerbrun, K., 1995. Huckleberry porphyry copper deposit, Tahtsa Lake district, west-central British Columbia. *In* Porphyry Deposits of North-western Cordillera of North America. *Edited by* T.G. Schroeter. Canadian Institute of Mining, Metallurgy and Petroleum, Special Volume 46, p. 313-321.
- MacIntyre, D.G., 1985. Geology and mineral deposits of the Tahtsa Lake District, west-central British Columbia. British Columbia Ministry of Energy, Mines and Petroleum Resources, Bulletin 75, 82 pages.
- McMillan, W.J., Thompson, J.F.H., Hart, C., Johnston, S.T., 1995. Regional geological and tectonic setting of porphyry copper, molybdenum, gold and tungsten deposits in British Columbia and Yukon. *In* Porphyry Deposits of the North-western cordillera of North America. *Edited by* T.G. Schroeter, Canadian Institute of Mining, Metallurgy and Petroleum, Special Volume 46, p. 40-57.
- Monger, J.W.H., Wheeler, J.O., Tipper, H.W., Gabrielse, H., Harms, T., Struik, L.C., Campbell, R.B., Dodds, C.J., Gehrels, G.E., O'Brien, J., 1991. Part B. Cordilleran terranes. *In* Upper Devonian to Middle Jurassic assemblages. *In* Geology of the Cordilleran Orogen in Canada. *Edited by* H. Gabrielse and C.J. Yorath. Geological Survey of Canada, Chapter 8, Geology of Canada, No. 4., p. 281-327.
- Mortensen, J.K., Ghosh, D.K. and Ferri, F., 1995. U-Pb geochronology of intrusive rocks associated with copper-gold porphyry deposits in the Canadian Cordillera. *In* Porphyry Deposits of North-western cordillera of North America. *Edited by* T. G. Schroeter, Canadian Institute of Mining, Metallurgy of Petroleum, Special Volume 46, p. 142-158.
- Stacey, J.S. and Kramer, J.D., 1975. Approximation of Terrestrial Lead Isotope Evolution by a Two-Stage Model. Earth and Planetary Science Letters, 26, p. 207-221.
- Woodsworth, G.J., Anderson, R.G., Armstrong, R.L., 1991. Plutonic regimes. *In* Geology of the Cordilleran Orogen in Canada. *Edited by* H. Gabrielse and C.J. Yorath. Geological Survey of Canada, Chapter 15, Geology of Canada, No. 4, p. 491-531.
- Yorath, C.J., 1991. Upper Jurassic to Paleogene assemblages. *In* Geology of the Cordilleran Orogen in Canada. *Edited by* H. Gabrielse and C.J. Yorath. Geological Survey of Canada, Chapter 9, Geology of Canada, No. 4, p. 329-371.



# U-Pb GEOCHRONOLOGY, Pb ISOTOPIC SIGNATURES AND GEOCHEMISTRY OF AN EARLY JURASSIC ALKALIC PORPHYRY SYSTEM NEAR LAC LA HACHE, B.C.

By Robin J. Whiteaker, Getty Copper Corporation, Vancouver, B.C., J.K. Mortensen and Richard M. Friedman, Department of Earth and Ocean Sciences, University of British Columbia

Keywords: Ann property, Quesnel Terrane, Lac La Hache, alkalic porphyry, U-Pb geochronology, Pb isotopes, geochemistry, Early Jurassic, mineralization, alteration.

## INTRODUCTION

The Ann property is located within the Quesnel Terrane of the Intermontane Belt in south-central British Columbia (Figures 33-1 and 33-2). It is approximately 19 kilometres northeast of Lac La Hache, B.C., near the northwestern edge of map sheet 92P14W (approximate coordinates: latitude 51°58'N, longitude 121°19'W). Topography in the region consists of moderately sloping hills and wide densely forested valleys.

Previous field work has shown that the geology of the Ann property resembles that of other alkaline copper-gold porphyry systems in the Quesnel terrane (most notably Mt. Polley, Copper Mountain and Afton/Ajax).

The focus of this study was to constrain the timing of mineralization, and to place the volcanic and intrusive units in the study area into a regional tectonic framework. New U-Pb dates, trace-Pb isotopic analyses and some whole rock geochemistry are reported for rocks within the Spout/Peach Lake study area (Figure 33-2). It is hoped that possible correlations with other copper-gold porphyry deposits in the southern Canadian Cordillera may be made, ultimately leading to a more focused and improved approach to mineral exploration in this region.

The southern half of the Ann property (Figure 33-3) was chosen for detailed study based primarily on the fact that this includes areas of less subdued relief and reasonably good exposure, and was also the focus of recent trenching and drilling activity. Field samples used for geochronologic, trace-Pb isotopic and geochemical work were collected from the Ann property and other localities within the Spout/Peach Lake study area.

Detailed petrology, structural data, distribution of lithologic units, and the nature of hydrothermal alteration and mineralization for rocks at the Ann property study area are not presented in this paper; for further discussions concerning this research the reader may refer to Whiteaker (1996).

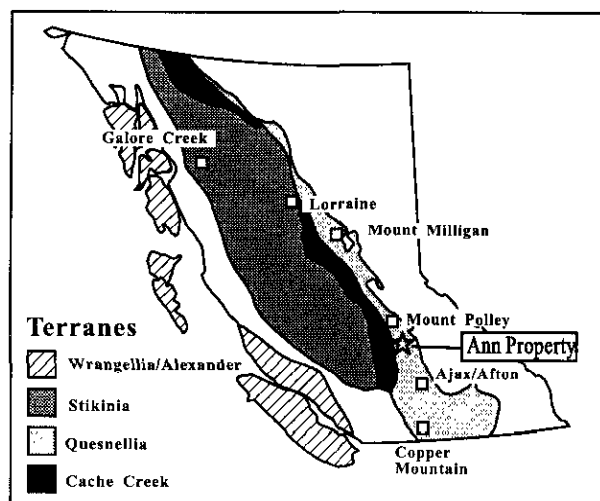


Figure 33-1. Location of the Ann property and the distribution of significant alkalic copper-gold porphyry systems in the Canadian Cordillera.

## PREVIOUS WORK

Previous regional-scale mapping in the study area (Campbell and Tipper, 1971) shows it to be underlain by Early Jurassic alkalic plutons, dykes and small dioritic to syenitic stocks. These rocks intrude broadly coeval volcanic rocks and sediments of the Late Triassic-Early Jurassic Nicola Group, which consist mainly of augite-phyric andesite to basaltic flows, volcanic breccias and tuffs and associated argillite, greywacke, limestone and clastic breccias. Regionally developed plutonic rocks include granodiorite to quartz-monzonite (Takomkane batholith), quartz diorite and syenodiorite. Subsequent detailed mapping and exploration throughout the study area was performed by Asarco Exploration Co. (Gale, 1991) and Regional Resources Ltd./GWR Resources Inc. (von Guttenberg, 1994; Blann, 1995), who recognized similar lithologies.

No previous isotopic ages are available for rocks at the Ann property. Leech et al. (1963) reported a K-Ar biotite date of  $187 \pm 14$  Ma for the Takomkane batholith that lies to the east of the study area. Calderwood et al. (1990) reported a preliminary U-Pb zircon upper intercept age of  $207 \pm 5$  Ma for the same body.

## REGIONAL GEOLOGY

The Nicola Group is an assemblage of submarine and subareal arc volcanic and volcanoclastic rocks and related sediments that is interpreted to have been produced above an east-dipping subduction-accretion zone. This arc apparently developed outboard of ancestral North America during the Late Triassic and was active into Early Jurassic time (Mortimer, 1987). The volcanic rocks were subsequently intruded by broadly coeval intrusions of alkalic to calc-alkalic composition that may in part represent plutonic roots to the arc volcanoes (Preto 1979, Saleken and Simpson, 1984).

The Nicola Group has been divided into four lithologic assemblages (Monger 1989): a western volcanic

belt composed of mafic to felsic, calc-alkalic volcanic and volcanoclastic rocks; a central volcanic belt consisting predominantly of alkalic to calc-alkalic basalt and andesite flows, volcanic breccias and lahars; an eastern volcanic belt composed primarily of alkalic intermediate and mafic flow and fragmental rocks; and an eastern sedimentary assemblage of greywacke, argillite, tuff and limestone, which is overlain by volcanic rocks of the eastern volcanic belt. Lithologies within the Nicola Group across the study area suggest correlation with the central and/or eastern volcanic belt of Monger (1989). Preto (1972) suggests that active faulting during Nicola volcanism may have controlled the emplacement and shape of subsequent intrusive bodies. East-west and northwest trending faults are interpreted to be cut by north trending structures (Preto, 1979).

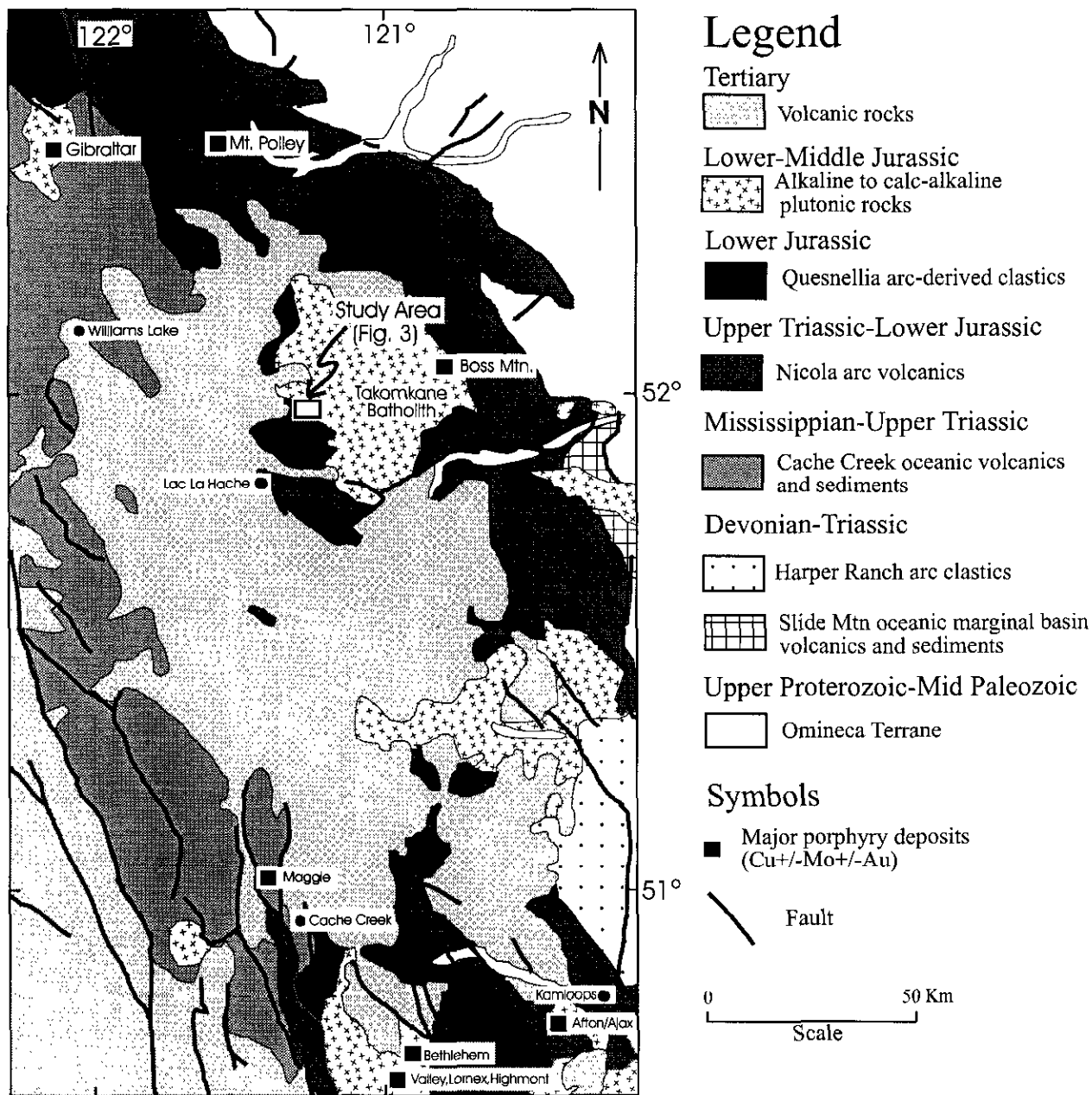


Figure 33-2. Regional geology of the southern Canadian cordillera near the Ann property study area (modified from Wheeler and McFeely, 1991).

## LOCAL GEOLOGY

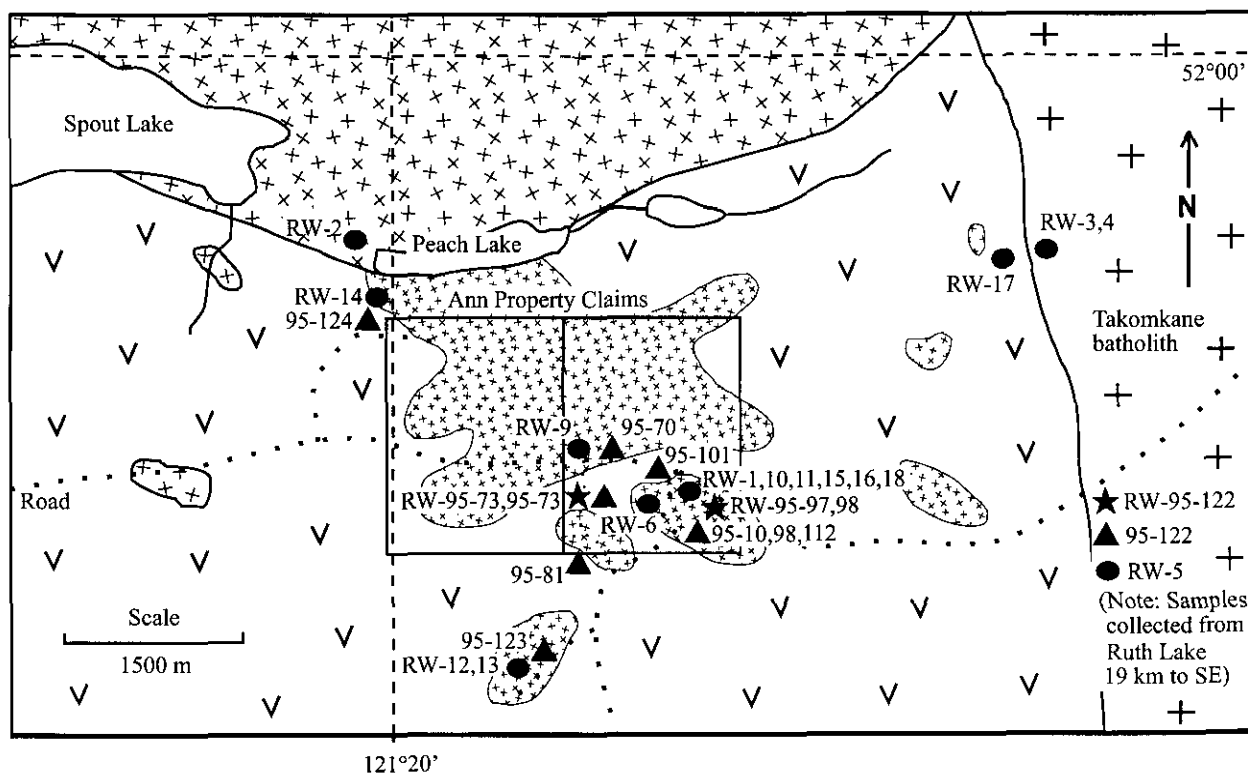
The general scarcity of outcrop and extensive overburden in the study area, coupled with the fact that almost all of the rocks on the property display weak to intense propylitic to potassic alteration, make field identification and correlation of lithologic units difficult. On the basis of detailed surface mapping, drill core logging and petrographic studies several distinct lithologic units, alteration types and styles of mineralization have been defined.

Nicola Group rocks which underlie the study area include massive basalt and basalt-dominated polymictic breccias, and augite- and hornblende-phyric andesite and basalt. These rocks commonly display pervasive propylitic alteration (chlorite-epidote-calcite-sericite), but where directly in contact with intrusive bodies are intensely potassically altered (potassium feldspar ±

biotite ± magnetite), and locally hornfelsed. Very strong propylitic and potassic alteration of Nicola Group volcanic rocks has destroyed much of the primary textures which often makes petrographic distinction between basaltic or andesitic protoliths difficult.

Local outcrops of pyroclastic beds, limestone and minor clastic breccia outside of the Ann property (Figure 33-3) exhibit weak to strong propylitic alteration and/or skarning.

Feldspar-porphyritic andesite (possibly a high-level comagmatic Nicola intrusion) also occurs on the property. This unit is interpreted to be Late Triassic-Early Jurassic in age based on both local stratigraphic sequences and evidence which suggests that propylitic alteration throughout this unit may be related to an adjacent, cross-cutting monzonite intrusion (considered to be Early Jurassic in age; see later discussion).



### Legend

Late Triassic-Early Jurassic

⊕ Takomkane batholith: granodiorite and qtz-monzodiorite

⊕⊕ Spout-Peach Lake Monzonite

\*\*\* Diorite-Monzodiorite-Syenite Intrusive Suite

V Nicola Group volcanic, volcanoclastic and sedimentary rocks

Sample Locations

★ U-Pb Geochronology

● Trace-Pb Isotopes

▲ Whole Rock Geochemistry

Figure 33-3. Simplified geology of the Spout/Peach Lake study area near the Ann property (after Campbell and Tipper, 1971; von Guttenberg, 1994; Blann, 1995; Whiteaker, 1996), showing geochronologic, trace-Pb isotope and geochemical sample sites.

Several intrusive bodies are exposed within the study area and appear to be part of a large polyphase intrusive suite that consists of dominantly fine-medium grained diorite, monzonite and syenite, with minor pyroxenite and gabbro. Locally, this intrusive suite contains abundant, variably resorbed, angular xenoliths of mafic volcanic, gabbroic and granitic composition. On the southeast portion of the Ann property, the intrusive suite is cut by a medium-grained, unmineralized, quartz-hornblende-feldspar porphyry (QHFP) dyke. In addition, numerous 5 to 20 cm wide, hydrothermal breccia bodies cut the diorite-monzodiorite complex. One of these breccia bodies has been intercepted in a recent drillhole adjacent to the QHFP dyke; at this locality the breccia contains fine-coarse grained blebs of pyrite-chalcopyrite-magnetite  $\pm$  bornite (Whiteaker, 1996), as well as elevated gold and silver values (Blann, 1995).

Intrusive rocks throughout the study area display both pervasive and structurally-controlled hydrothermal alteration. Generally the rocks show moderate to intense propylitic (chlorite-epidote-calcite-sericite) to potassic (potassium feldspar-biotite-magnetite  $\pm$  chlorite  $\pm$  epidote  $\pm$  albite) alteration. In places, severe potassic 'flooding' of diorite-monzodiorite has entirely obliterated primary rock textures and mineralogy. In outcrop, these rocks weather a distinctive chalky pinkish-white colour and commonly contain abundant resistant circular green epidote 'patches' and veins enclosed by pink potassium feldspar.

Mineralization in the study area appears to be intimately associated with zones of strong-intense potassic and propylitic alteration. The mineralization occurs primarily within dioritic to monzodioritic intrusive rocks, but is locally common within Nicola volcanic rocks adjacent to these intrusions. Sulphides (pyrite-chalcopyrite  $\pm$  bornite) occur mainly as sparse disseminations and replacements of mafic minerals, but are also prominent within potassium feldspar epidote-chlorite - magnetite  $\pm$  albite veinlets. Some malachite fracture coatings are present across the Ann property where roadcuts have exposed mineralized Nicola volcanic rocks.

Unmineralized, multilithic intrusive breccias (mafic volcanic, diorite and syenite fragments), crop-out locally throughout the southern portion of the Ann property and are exposed for widths of up to 150 m. The relationship between these breccias and the polyphase intrusive suite is not known.

Numerous red-orange to pinkish, narrow (<15cm wide) syenite-monzonite dykes occur across the Ann property and cross-cut both the Early Jurassic intrusions and the Late Triassic volcanic rocks. These dykes may suggest a deep late-stage potassic (syenitic) core to the intrusive complex.

The Takomkane batholith crops on the eastern side of the study area (Figure 33-3). The subsurface lateral extent of this large granodiorite to quartz-monzonite body, with respect to the rocks and stratigraphy at the Ann property, is presently unknown.

Relatively fresh mafic volcanic rocks of presumed Tertiary age unconformably overlie both the Late Triassic Nicola volcanic rocks and the Early Jurassic intrusions on the Ann property. These rocks include dark-grey to black amygdaloidal hornblende porphyritic basalt and feldspar porphyritic basalt. Although these units are regionally widespread, they have been almost entirely removed from the immediate study area by Pleistocene glaciation.

## GEOCHRONOLOGY

No previous isotopic age data exists for any of the intrusive bodies or volcanic rocks on the Ann property. Dating of other alkalic copper-gold porphyry systems within the Quesnel Terrane has produced U-Pb dates that mainly range from 210 to 200 Ma (Early Jurassic; Mortensen et al., 1995). The only exceptions are intrusions in the Mount Milligan area, which have yielded U-Pb zircon ages of  $183 \pm 3$  Ma (Mortensen et al., 1995).

Age control for rocks at the Spout/Peach Lake study area was essential to help determine the relative timing of the emplacement of intrusions into the Late Triassic Nicola Group volcanic rocks and the genesis of mineralization on the property, and to facilitate correlation of associated Cu-Au mineralization on the Ann property with that of other alkalic porphyry systems in the Canadian Cordillera. In addition, the age of the Takomkane batholith, a large calc-alkalic pluton, which lies directly to the east of the Ann property is, at present, poorly constrained. Available dates for the Takomkane batholith are a K-Ar biotite age of  $187 \pm 14$  Ma (Leech et al., 1963) and a U-Pb zircon upper intercept age of  $207 \pm 5$  Ma (Calderwood et al., 1990).

U-Pb zircon and titanite analytical data for a diorite phase of the diorite-monzodiorite intrusive complex, a quartz-hornblende-feldspar porphyry dyke, a porphyritic andesite (possibly a high level, subvolcanic intrusion) and the Takomkane batholith are presented here. Sample localities are shown on Figure 33-3. Mineral separations and isotopic analyses were carried out at the University of British Columbia Geochronology Laboratory, using analytical methodology as described in Mortensen et al. (1995). The analytical data are given in Table 33-1 and plotted on conventional U-Pb concordia diagrams in Figure 33-4 (a), (b), (c) and (d).

### Feldspar-Porphyritic Andesite

A small outcrop of porphyritic andesite occurs on the west side of the study area (sample RW-95-73, Figure 33-3). Contacts with surrounding units are not exposed, and the aphanitic groundmass and moderate alteration masks the exact nature of this unit. It is interpreted to represent a high-level (sub-volcanic) intrusion associated with Nicola Group volcanic rocks. Field relationships suggest that it cross-cuts basalt-dominated polyolithic breccia and has itself been intruded and propylitically altered by an adjacent xenolithic

monzonite stock. A small amount of inclusion-free, pale amber, subhedral to euhedral zircon grains was recovered from the sample. Three fractions form a linear array just below concordia between 200-187 Ma (Figure 33-4a). A weighted average of the  $^{207}\text{Pb}/^{206}\text{Pb}$  ages of the three analyses is  $203.9 \pm 4.2$  Ma, which is interpreted to be the crystallization age of the unit. Two unabraded fractions of titanite were also analyzed (Table 33-1). The analyses are discordant with  $^{206}\text{Pb}/^{238}\text{U}$  ages of 194 Ma and 172 Ma, likely reflecting post-crystallization Pb-loss.

## Diorite

A sample of diorite was collected from an outcrop recently exposed by the construction of a drill-road near

an outcrop of the QHFP dyke (sample RW-95-97, Figure 33-3). Based on core logging, extensive feldspar staining and observed field relationships, this diorite is interpreted to be a phase of the main diorite-monzodiorite intrusion. The sample yielded a small number of tabular to equant, pale yellow zircons as well as clear to amber-yellow, broken, subhedral titanite grains. Two fractions of abraded zircon were analyzed. Both yielded discordant results indicative of the presence of an older inherited zircon component. No meaningful age could be determined from the zircon analyses. Three fractions of unabraded titanite were also analyzed. All three fractions give concordant analyses, with a total range of age of  $^{206}\text{Pb}/^{238}\text{U}$  ages of  $203 \pm 4$  Ma which is interpreted as the age of crystallization for the diorite phase (Figure 33-4b).

Table 33-1. U-Pb analytical data.

| Fraction <sup>1</sup>                                                            | Wt<br>mg | U <sup>2</sup><br>ppm | Pb* <sup>3</sup><br>ppm | $^{206}\text{Pb}^4$<br>ppm | Pb <sup>5</sup><br>pg | $^{208}\text{Pb}$<br>% | Isotopic ratios (1σ,%) <sup>7</sup> |                                  |                                   | Apparent ages (2σ, Ma) <sup>7</sup> |                                   |
|----------------------------------------------------------------------------------|----------|-----------------------|-------------------------|----------------------------|-----------------------|------------------------|-------------------------------------|----------------------------------|-----------------------------------|-------------------------------------|-----------------------------------|
|                                                                                  |          |                       |                         |                            |                       |                        | $^{206}\text{Pb}/^{238}\text{U}$    | $^{207}\text{Pb}/^{235}\text{U}$ | $^{207}\text{Pb}/^{206}\text{Pb}$ | $^{206}\text{Pb}/^{238}\text{U}$    | $^{207}\text{Pb}/^{206}\text{Pb}$ |
| <b>RW-95-73: Porphyritic andesite; UTM 616750E, 5757500N</b>                     |          |                       |                         |                            |                       |                        |                                     |                                  |                                   |                                     |                                   |
| AA: t,200,s                                                                      | 0.135    | 90                    | 4                       | 242                        | 105                   | 35.2                   | 0.03055 (0.24)                      | 0.2094 (0.87)                    | 0.04972 (0.72)                    | 194.0 (0.9)                         | 182 (33)                          |
| BB: t,180,s                                                                      | 0.118    | 388                   | 12                      | 115                        | 814                   | 17.8                   | 0.02705 (0.55)                      | 0.1904 (1.7)                     | 0.05107 (1.4)                     | 172.0 (1.9)                         | 244 (64)                          |
| A: N1,80-100,s,a                                                                 | 0.046    | 592                   | 20                      | 5129                       | 10                    | 15.4                   | 0.03155 (0.10)                      | 0.2183 (0.20)                    | 0.05018 (0.13)                    | 200.3 (0.4)                         | 203.4 (5.9)                       |
| B: N1,80-100,s                                                                   | 0.049    | 668                   | 21                      | 1021                       | 62                    | 14.6                   | 0.02983 (0.10)                      | 0.2065 (0.19)                    | 0.05020 (0.15)                    | 189.5 (0.4)                         | 204.5 (6.9)                       |
| C: N1,80-100,s                                                                   | 0.028    | 736                   | 23                      | 909                        | 43                    | 15.4                   | 0.02950 (0.11)                      | 0.2042 (0.37)                    | 0.05019 (0.30)                    | 187.4 (0.4)                         | 204 (14)                          |
| <b>RW-95-97: Diorite; UTM 617850E, 5757720N</b>                                  |          |                       |                         |                            |                       |                        |                                     |                                  |                                   |                                     |                                   |
| AA: t,90-180,s                                                                   | 0.300    | 105                   | 5                       | 72                         | 1202                  | 40.7                   | 0.03201 (1.0)                       | 0.2129 (3.7)                     | 0.04825 (3.1)                     | 203.1 (4.0)                         | 112 (146)                         |
| BB: t,90-180,s                                                                   | 0.265    | 108                   | 5                       | 106                        | 668                   | 40.3                   | 0.03202 (0.61)                      | 0.2198 (2.2)                     | 0.04978 (1.8)                     | 203.2 (2.5)                         | 185 (86)                          |
| CC: t,90-180,s                                                                   | 0.290    | 117                   | 6                       | 94                         | 918                   | 39.6                   | 0.03231 (0.71)                      | 0.2214 (2.6)                     | 0.04969 (2.1)                     | 205.0 (2.8)                         | 181 (100)                         |
| B: N5,+134,s                                                                     | 0.032    | 570                   | 18                      | 916                        | 39                    | 10.5                   | 0.03051 (0.15)                      | 0.2276 (0.32)                    | 0.05410 (0.22)                    | 193.7 (0.6)                         | 375 (10)                          |
| C: N5,+134,s                                                                     | 0.030    | 484                   | 18                      | 986                        | 34                    | 11.0                   | 0.03626 (0.12)                      | 0.3522 (0.26)                    | 0.07046 (0.18)                    | 229.6 (0.5)                         | 94.7 (7.2)                        |
| <b>RW-95-98: Quartz-hornblende-feldspar porphyry dyke; UTM 617850E, 5757750N</b> |          |                       |                         |                            |                       |                        |                                     |                                  |                                   |                                     |                                   |
| A: N5,90-120,e                                                                   | 0.113    | 990                   | 22                      | 719                        | 236                   | 6.0                    | 0.02327 (0.18)                      | 0.1602 (0.40)                    | 0.04995 (0.28)                    | 148.3 (0.5)                         | 193 (13)                          |
| B: N5,90-120,e                                                                   | 0.166    | 954                   | 26                      | 847                        | 350                   | 5.7                    | 0.02888 (1.0)                       | 0.1992 (1.1)                     | 0.05003 (0.25)                    | 183.5 (3.8)                         | 197 (12)                          |
| C: N5,70-100,s                                                                   | 0.179    | 1236                  | 28                      | 811                        | 413                   | 6.8                    | 0.02328 (0.26)                      | 0.1601 (0.34)                    | 0.04987 (0.17)                    | 148.3 (0.8)                         | 189.1 (8.1)                       |
| A2: N5,70-100,s                                                                  | 0.020    | 1162                  | 27                      | 925                        | 40                    | 6.4                    | 0.02441 (0.10)                      | 0.1683 (0.31)                    | 0.05001 (0.23)                    | 155.5 (0.3)                         | 195 (11)                          |
| B2: N5,70-100,s                                                                  | 0.034    | 1394                  | 32                      | 1000                       | 71                    | 6.9                    | 0.02386 (0.10)                      | 0.1646 (0.40)                    | 0.05002 (0.34)                    | 152.0 (0.3)                         | 196 (16)                          |
| <b>RW-95-122: Takomkane batholith; UTM 635750E, 5743125N</b>                     |          |                       |                         |                            |                       |                        |                                     |                                  |                                   |                                     |                                   |
| AA: t,+149,s                                                                     | 0.940    | 92                    | 4                       | 235                        | 78                    | 37.1                   | 0.03053 (0.27)                      | 0.2119 (0.94)                    | 0.05033 (0.77)                    | 193.9 (1.0)                         | 210 (36)                          |
| BB: t,+149,s                                                                     | 0.810    | 71                    | 3                       | 253                        | 472                   | 36.5                   | 0.03045 (0.25)                      | 0.2111 (0.87)                    | 0.05027 (0.70)                    | 193.4 (0.9)                         | 207 (33)                          |
| A: N1,+149,s,a                                                                   | 0.584    | 278                   | 8                       | 7996                       | 38                    | 8.7                    | 0.03048 (0.14)                      | 0.2097 (0.15)                    | 0.04989 (0.05)                    | 193.6 (0.5)                         | 189.8 (2.1)                       |
| B: N1,+149,s,a                                                                   | 0.525    | 226                   | 7                       | 7187                       | 31                    | 8.4                    | 0.03004 (0.28)                      | 0.2088 (0.31)                    | 0.05041 (0.18)                    | 190.8 (1.1)                         | 214.1 (8.5)                       |
| C: N1,+149,s,a                                                                   | 0.092    | 247                   | 7                       | 3099                       | 14                    | 8.3                    | 0.03045 (0.11)                      | 0.2097 (0.23)                    | 0.04996 (0.15)                    | 193.3 (0.4)                         | 193.3 (6.9)                       |

Notes: Analytical techniques are listed in Mortensen et al. (1995).

<sup>1</sup> Upper case letter(s) = fraction identifier; t=titanite; all others zircon. N1, N5 = nonmagnetic at given degrees side slope on Franz isodynamic magnetic separator. Front slope for all fractions=20°. Grain size given in microns. a = abraded, e=elongate prisms, s=stubby to equant grains.

<sup>2</sup> U blank correction of  $1\text{pg} \pm 20\%$ ; U fractionation corrections were measured for each run with a double  $^{233}\text{U}$ - $^{235}\text{U}$  spike (about 0.005/amu).

<sup>3</sup>Radiogenic Pb.

<sup>4</sup>Measured ratio corrected for spike and Pb fractionation of  $0.0043/\text{amu} \pm 20\%$  (Daly collector) and  $0.0012/\text{amu} \pm 7\%$  (Faraday collector) and laboratory blank Pb of  $10\text{pg} \pm 20\%$ . Laboratory blank Pb concentrations and isotopic compositions based on total procedural blanks analysed throughout the duration of this study.

<sup>5</sup>Total common Pb in analysis based on blank isotopic composition.

<sup>6</sup>Radiogenic Pb.

<sup>7</sup>Corrected for blank Pb, common Pb, and U. Common Pb corrections based on Stacey Kramers model (Stacey and Kramers, 1975) at the age of the rock or the  $^{207}\text{Pb}/^{206}\text{Pb}$  age of the fraction.

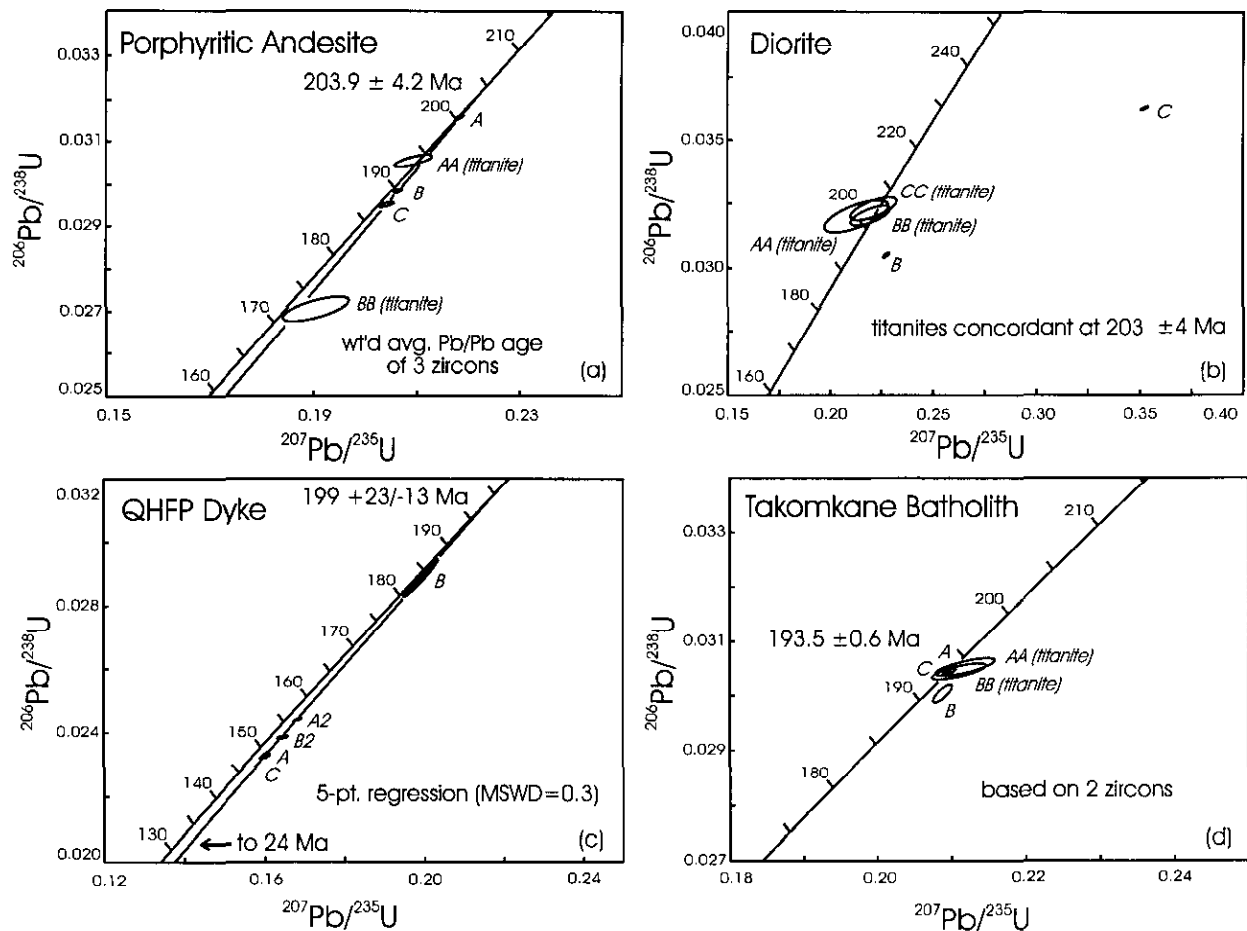


Figure 33-4. U-Pb concordia plots for samples from Ann property study area and the Takomkane batholith. Ellipses are plotted at the  $2\sigma$  level of precision.

### Quartz-Hornblende-Feldspar Porphyry (QHFP) Dyke

A quartz-hornblende-feldspar porphyry dyke (QHFP dyke) was sampled in a freshly uncovered outcrop in a road cut near an area of recent drilling in the diorite unit (sample RW-95-98, Figure 33-3). A relatively fresh sample was collected which provided a small number of small transparent light-yellow to orange-amber euhedral zircons of tabular and prismatic morphology. This unit had previously been inferred to be of Tertiary age. However, five fractions of unabraded zircons define a linear array with upper and lower concordia intercept ages of  $199 \pm 23/-13$  Ma and 24 Ma, respectively (MSWD=0.3) (Figure 33-4c). Because of the fine grain size of the zircons and the small amount recovered, none of the fractions were abraded prior to dissolution. The data array reflects moderate to strong post-crystallization Pb-loss, however there is no indication of any inherited zircon component present. The upper intercept of 199 Ma is therefore interpreted as the best estimate for the crystallization age of the rock.

### Takomkane Batholith

Medium-grained, equigranular, fresh to very weakly altered granodiorite was collected from a steep outcrop at the southern end of Ruth Lake approximately 19 kilometres southeast of the study area (Figure 33-3; approximate coordinates: latitude  $51^{\circ}49'30''$  N, longitude  $121^{\circ}01'30''$  W). The Takomkane batholith is exposed nearer to the Ann property but in heavily forested, low, marshy areas where the granodiorite shows moderate weathering and is therefore unsuited for geochronological study. The granodiorite sample yielded abundant high-quality, coarse, transparent and pale amber, euhedral zircons. Inclusion-free zircons were chosen and divided into three fractions which were strongly abraded. Two of the three zircon fractions were concordant with  $^{206}\text{Pb}/^{238}\text{U}$  ages of  $193.5 \pm 0.6$  Ma (Figure 33-4d), which is interpreted to be the crystallization age of the unit. A third zircon fraction is slightly discordant, reflecting a trace amount of inheritance coupled with minor Pb-loss. Two fractions of euhedral, medium-yellow titanite were also analyzed and yielded concordant analyses with a  $^{206}\text{Pb}/^{238}\text{U}$  age of  $193.7 \pm 1.2$  Ma.

## Geochronology Discussion

New U-Pb ages reported here for rocks on and near the Ann property lead to the following conclusions:

- The presumed Early Jurassic age of diorite on the Ann property has been confirmed at  $203 \pm 4$  Ma.
- An Early Jurassic age of  $203.9 \pm 4.2$  for a feldspar-porphyrific andesite body suggests that intrusive rocks and at least some of the Nicola Group volcanic rocks in the area are coeval.
- Although the new U-Pb age for the QHFP dyke is not tightly constrained, it indicates that the dyke is also an Early Jurassic intrusion and clearly not Tertiary as previously suggested by Blann (1995) and von Guttenberg (1994).
- The tightly constrained U-Pb zircon age of  $193 \pm 0.6$  Ma for the Takomkane batholith supercedes an earlier reported U-Pb age of  $207 \pm 5$  Ma for this body (Calderwood et al., 1990). Both samples were collected from essentially the same outcrop near Ruth Lake, close to the centre of the batholith. Different phases of the Takomkane have been reported (Campbell and Tipper, 1971) and may result in slight variations in cooling histories from the core to the outer edge of the pluton. A K-Ar biotite date of  $187 \pm 14$  Ma for the Takomkane batholith (Leech et al, 1963) was done on a sample collected near the northeast corner of the pluton and probably reflects relatively slow cooling of the batholith through the argon blocking temperature of the biotite. The calc-alkalic Takomkane batholith therefore is clearly younger than the smaller alkalic intrusions on the Ann property.

## TRACE Pb ISOTOPIC ANALYSIS

Trace Pb isotopic compositions were determined for potassium feldspars from intrusive bodies and for sulphide samples collected both regionally and within the study area (Figure 33-3). The purpose of this study was to attempt to relate the different styles of regional and local mineralization and alteration with intrusive suites interpreted to be genetically linked with mineralization. Analytical results are presented in Table 33-2 and plotted on Figure 33-5 (a), (b) and (c). Several conclusions can be drawn from the data set:

Pb isotopic compositions of sulphide samples collected from hydrothermal breccia bodies in the study area, as well as veins hosted within the diorite-monzodiorite intrusive complex (samples 10, 11, 15, 16 and 18), and a mineralized monzodiorite body (samples 12 and 13) to the southwest of the study area are very similar to those from feldspar from both altered diorite in the study area and altered monzonite (sample 2) collected west of Peach Lake. The feldspar Pb compositions are thought to represent primary igneous compositions, whereas the sulphide Pb compositions provide an isotopic 'fingerprint' for the hydrothermal system that produced the mineralization. The data

suggest that the mineralizing fluids were ultimately derived from the dioritic to monzonitic magmas.

Sulphides that occur in fracture-controlled veins (sample 14) within a moderately altered monzonitic intrusive body southwest of Peach Lake (Figure 33-3) give much more radiogenic Pb isotopic compositions than other sulphides and feldspars analyzed from the Ann property. This likely indicates that the Peach Lake occurrence is unrelated to other occurrences in the study area, and may be considerably younger.

Feldspar Pb analyses from unaltered massive granodiorite and from a potassium feldspar-pegmatite phase of the Takomkane batholith (samples 5 and 3, 4 respectively) define a field that is distinct from the other feldspar and sulphide samples analyzed from the study area. These data suggest that the Takomkane batholith was not genetically related to mineralization and alteration in the study area.

A bornite-chalcopyrite skarn (sulphide sample 17) that occurs northeast of the Ann property less than 300 metres from an outcrop of the Takomkane batholith (Figure 33-3) shows a similar trace Pb isotopic signature to those within the study area. This suggests that the skarn-forming event was related to the same magmatic/hydrothermal event that formed other mineral occurrences in the area, rather than to the Takomkane batholith, as had previously been thought.

## WHOLE ROCK GEOCHEMISTRY

Whole rock chemical compositions for a limited suite of intrusive and volcanic rocks on or near the Ann property are given in Table 33-3. Samples comprise Nicola Group basalt, porphyritic andesite, diorite, gabbro, quartz-hornblende-feldspar porphyry (QHFP), monzonite, monzodiorite, Takomkane granodiorite and Tertiary (?) basalt. An attempt was made to select the freshest samples available for each unit of interest.

Nicola Group volcanic rocks and intrusions of the diorite-monzodiorite suite are alkaline to mildly sub-alkaline. However, the QHFP dyke and the Takomkane batholith both lie in the sub-alkaline field of an alkaline affinity diagram (Figure 33-6a).

Widespread metasomatic overprinting and the fine grained nature of Nicola group volcanic rocks mask geochemical differences between andesitic and basaltic protoliths; however whole rock geochemical analysis suggests a basaltic composition (Table 33-3) for at least some of the volcanic rocks.

A plot of  $\text{Na}_2\text{O}$  versus  $\text{K}_2\text{O}$  subdivides intrusive alkaline rocks into high-potassic, potassic and sodic series (Figure 33-6b). All intrusive samples collected at the Ann Property (with the exception of the QHFP dyke) plot in the potassic field. Trace element compositions place all intrusive bodies sampled within the volcanic arc granitoid field on a Rb versus (Y+Nb) discrimination diagram.

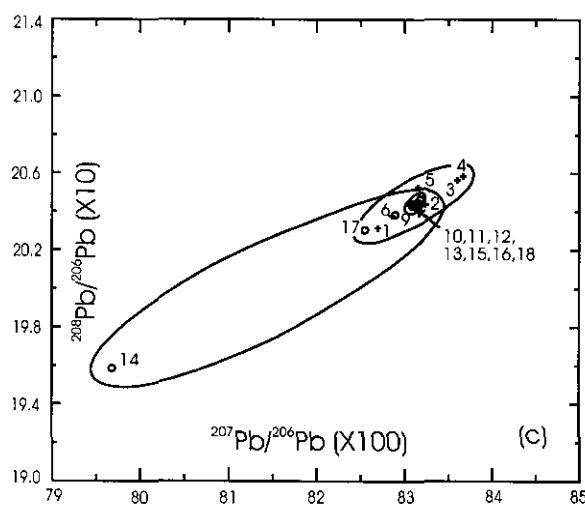
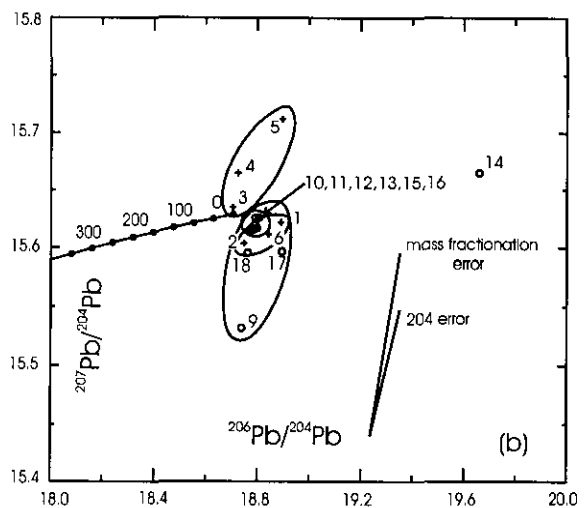
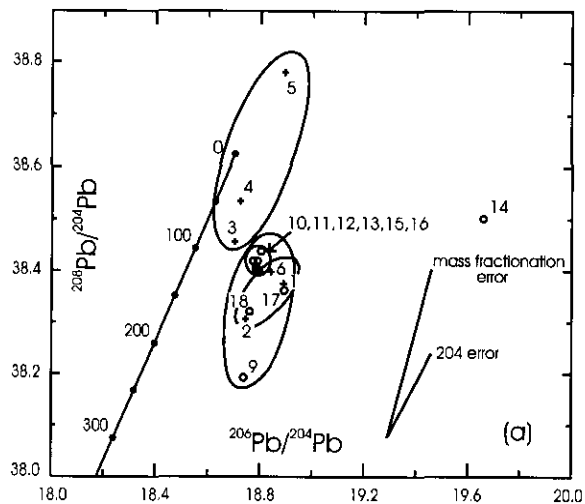


Figure 33-5. Trace-Pb isotope plots of (a)  $^{208}\text{Pb}/^{204}\text{Pb}$  vs.  $^{206}\text{Pb}/^{204}\text{Pb}$ , (b)  $^{207}\text{Pb}/^{204}\text{Pb}$  vs.  $^{206}\text{Pb}/^{204}\text{Pb}$  and (c)  $^{208}\text{Pb}/^{206}\text{Pb}$  versus  $^{207}\text{Pb}/^{206}\text{Pb}$  for sulphide (circles) and feldspar (crosses) samples collected across the Ann Property study area.

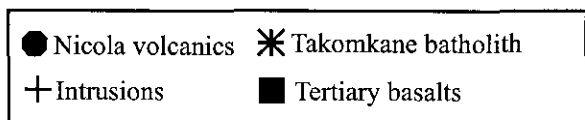
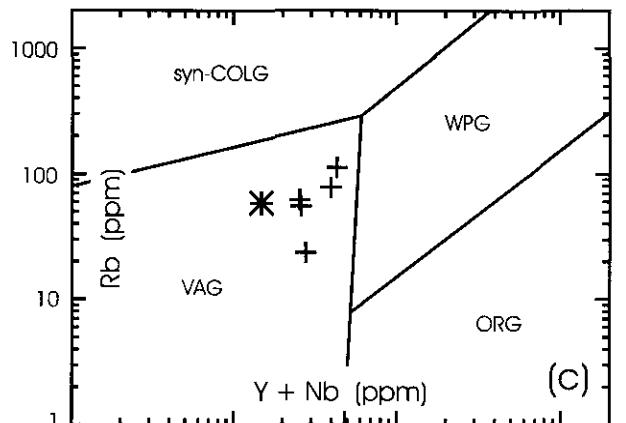
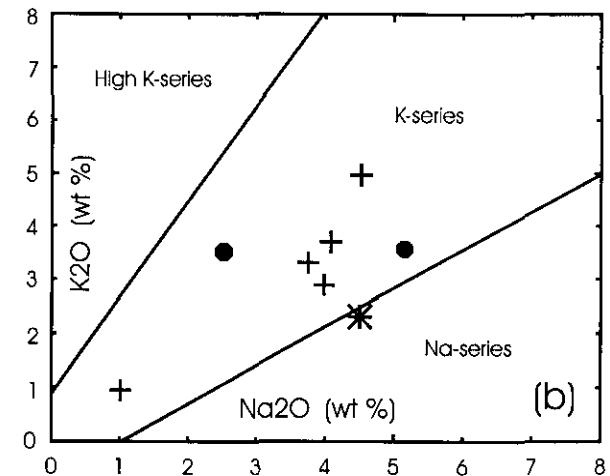
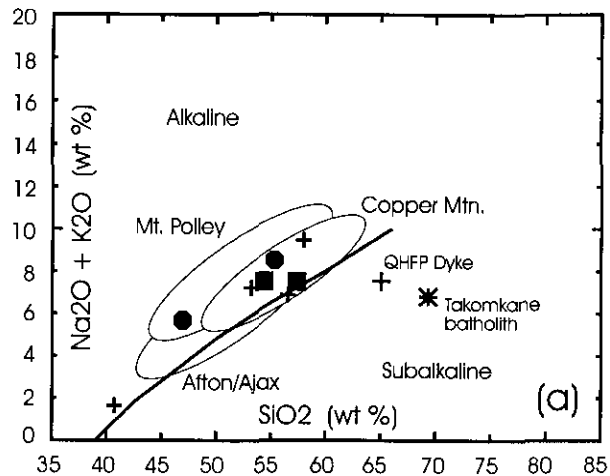


Figure 33-6. Classification of intrusive and volcanic rocks as plotted on (a) alkaline affinity diagram (Irvine and Barager, 1971), (b)  $\text{Na}_2\text{O}$  vs.  $\text{K}_2\text{O}$  (Middlemost, 1975) and (c) on a tectonic affinity diagram which plots Rb vs. Y+Nb (Pearce et al., 1984); abbreviations are volcanic arc granite (VAG), ocean ridge granite (ORG), within plate granite (WPG) and syn-collisional granite (syn-COLG).

Table 33-2. Common-Pb isotopic data.

| Sample Number | Description <sup>1</sup> / Occurrence                                                                   | Location (UTM)      | <sup>208</sup> Pb/ <sup>204</sup> Pb<br>(± 1σ, %) | <sup>207</sup> Pb/ <sup>204</sup> Pb<br>(± 1σ, %) | <sup>206</sup> Pb/ <sup>204</sup> Pb<br>(± 1σ, %) | <sup>208</sup> Pb/ <sup>206</sup> Pb<br>(± 1σ, %) | <sup>207</sup> Pb/ <sup>204</sup> Pb<br>(± 1σ, %) |
|---------------|---------------------------------------------------------------------------------------------------------|---------------------|---------------------------------------------------|---------------------------------------------------|---------------------------------------------------|---------------------------------------------------|---------------------------------------------------|
| RW-1          | o,f,a; diorite phase of intrusive complex at Ann property study area                                    | 617850E<br>5757750N | 38.375 (0.071)                                    | 15.622 (0.067)                                    | 18.89 (0.069)                                     | 20.315 (0.018)                                    | 82.701 (0.017)                                    |
| RW-2          | o,f,a; monzitic intrusion near west end of Peach Lake                                                   | 614240E<br>5760200N | 38.307 (0.004)                                    | 15.604 (0.003)                                    | 18.745 (0.003)                                    | 20.435 (0.002)                                    | 83.242 (0.001)                                    |
| RW-3          | o,f,u; pegmatitic-granodiorite from western edge of Takomkane batholith                                 | 621500E<br>5760400N | 38.456 (0.012)                                    | 15.635 (0.008)                                    | 18.702 (0.011)                                    | 20.563 (0.005)                                    | 83.604 (0.007)                                    |
| RW-4          | o,f,u; pegmatitic granodiorite from western edge of Takomkane batholith                                 | 621500E<br>5760400N | 38.535 (0.005)                                    | 15.665 (0.003)                                    | 18.722 (0.003)                                    | 20.583 (0.004)                                    | 83.674 (0.001)                                    |
| RW-5          | o,f,u; Takomkane grandiorite collected at SE end of Ruth Lake                                           | 635750E<br>5743125N | 38.780 (0.019)                                    | 15.712 (0.016)                                    | 18.894 (0.017)                                    | 20.525 (0.009)                                    | 83.158 (0.006)                                    |
| RW-6          | o,f,a; potassically altered diorite phase of study area intrusive complex                               | 617500E<br>5757500N | 38.398 (0.011)                                    | 15.612 (0.009)                                    | 18.842 (0.01)                                     | 20.379 (0.004)                                    | 82.860 (0.003)                                    |
| RW-9          | o,py-cp,a; potassically altered xenolithic monzonite intrusion                                          | 616750E<br>5757800N | 38.193 (0.065)                                    | 15.532 (0.065)                                    | 18.737 (0.065)                                    | 20.384 (0.007)                                    | 82.897 (0.005)                                    |
| RW-10         | c,py; hydrothermal breccia/vein-fill hosted within diorite-monzodiorite intrusive complex at study area | 617850E<br>5757750N | 38.401 (0.007)                                    | 15.617 (0.003)                                    | 18.796 (0.005)                                    | 20.431 (0.005)                                    | 83.088 (0.003)                                    |
| RW-11         | c,py; hydrothermal breccia/vein-fill hosted within diorite-monzodiorite intrusive complex at study area | 617850E<br>5757750N | 38.438 (0.005)                                    | 15.626 (0.003)                                    | 18.804 (0.004)                                    | 20.441 (0.003)                                    | 83.100 (0.003)                                    |
| RW-12         | c,py; vein-fill within moderately altered monzodiorite intrusion                                        | 617000E<br>5756125N | 38.419 (0.03)                                     | 15.615 (0.03)                                     | 18.772 (0.03)                                     | 20.466 (0.003)                                    | 83.183 (0.003)                                    |
| RW-13         | c,py; vein-fill within moderately altered monzodiorite intrusion                                        | 617000E<br>5756125N | 38.419 (0.005)                                    | 15.626 (0.005)                                    | 18.790 (0.005)                                    | 20.447 (0.001)                                    | 83.164 (0.002)                                    |
| RW-14         | c,py; vein-fill within monzonitic intrusion SW of Peach Lake                                            | 614240E<br>5759700N | 38.502 (0.01)                                     | 15.665 (0.009)                                    | 19.659 (0.01)                                     | 19.585 (0.003)                                    | 79.686 (0.002)                                    |
| RW-15         | c,py; hydrothermal breccia hosted within diorite-monzodiorite intrusive complex at study area           | 617850E<br>5757750N | 38.402 (0.01)                                     | 15.620 (0.005)                                    | 18.789 (0.008)                                    | 20.439 (0.006)                                    | 83.136 (0.006)                                    |
| RW-16         | c,py; hydrothermal breccia hosted within diorite-monzodiorite intrusive complex at study area           | 617850E<br>5757750N | 38.405 (0.005)                                    | 15.616 (0.005)                                    | 18.784 (0.005)                                    | 20.446 (0.001)                                    | 83.139 (0.001)                                    |
| RW-17         | o,bo; skarn near western edge of Takomkane batholith                                                    | 621275E<br>5760300N | 38.362 (0.005)                                    | 15.597 (0.003)                                    | 18.893 (0.004)                                    | 20.305 (0.003)                                    | 82.553 (0.003)                                    |
| RW-18         | c,py; vein-fill associated with hydrothermal breccia hosted within study area intrusive complex         | 617850E<br>5757750N | 38.3219 (0.03)                                    | 15.596 (0.026)                                    | 18.760 (0.03)                                     | 20.427 (0.007)                                    | 83.134 (0.013)                                    |

<sup>1</sup> o=outcrop sample; c=core sample; f=feldspar; py=pyrite; cp=chalcopyrite; bo=bornite; a=altered; u=unaltered

Table 33-3. Whole rock chemical analyses and normative mineralogy for volcanic and intrusive rocks.

| Sample# |      | 95-10 | 95-112 | 95-122 | 95-123  | 95-124 | 95-98 | 95-70  | 95-73  | 95-81  | 95-101 |
|---------|------|-------|--------|--------|---------|--------|-------|--------|--------|--------|--------|
| Rock    |      | Gabb  | Dior   | Grdior | Mnzdior | Mnz    | QHFP  | NiBsIt | NiPrAn | TPBsIt | TABsIt |
| SiO2    | wt % | 40.22 | 52.49  | 68.83  | 57.47   | 55.56  | 61.2  | 46.2   | 54.58  | 52.53  | 54.51  |
| Al2O3   | wt % | 15.43 | 18.52  | 16.12  | 18.15   | 17.82  | 14.27 | 16.04  | 20.12  | 18.45  | 17.04  |
| TiO2    | wt % | 1.15  | 0.61   | 0.23   | 0.66    | 0.54   | 0.38  | 1.07   | 0.44   | 1.21   | 0.71   |
| Fe2O3   | wt % | 16.28 | 7.93   | 2.69   | 6.34    | 7.21   | 3.61  | 13.04  | 7.3    | 7.25   | 6.93   |
| MnO     | wt % | 0.27  | 0.26   | 0.09   | 0.18    | 0.17   | 0.08  | 0.19   | 0.08   | 0.13   | 0.13   |
| MgO     | wt % | 6.91  | 2.99   | 0.94   | 1.81    | 2.47   | 3.88  | 6.15   | 2.21   | 2.47   | 2.13   |
| CaO     | wt % | 16.04 | 8.1    | 3.49   | 4.61    | 7.37   | 3.31  | 9.55   | 5.05   | 6.5    | 5.87   |
| Na2O    | wt % | 0.88  | 3.76   | 4.42   | 4.44    | 3.9    | 3.72  | 2.33   | 5.02   | 3.73   | 3.65   |
| K2O     | wt % | 0.75  | 3.36   | 2.35   | 4.95    | 2.88   | 3.37  | 3.26   | 3.39   | 3.55   | 3.48   |
| P2O5    | wt % | 0.84  | 0.56   | 0.1    | 0.48    | 0.36   | 0.21  | 0.57   | 0.48   | 0.74   | 0.56   |
| Cr2O3   | wt % | 0.01  | 0.01   | 0.01   | 0.01    | 0.01   | 0.02  | 0.01   | 0.01   | 0.01   | 0.01   |
| SUM     | wt % | 98.78 | 98.59  | 99.27  | 99.1    | 98.29  | 94.05 | 98.41  | 98.68  | 96.57  | 95.02  |
| LOI     | wt % | 0.88  | 0.83   | 0.64   | 0.91    | 1.2    | 5.51  | 1.05   | 1.03   | 3.05   | 4.32   |

|    |     |      |      |     |      |     |      |     |      |      |      |
|----|-----|------|------|-----|------|-----|------|-----|------|------|------|
| Ba | ppm | 279  | 989  | 799 | 1247 | 862 | 1235 | 566 | 815  | 1511 | 1572 |
| Rb | ppm | 24   | 61   | 61  | 115  | 56  | 73   | 95  | 56   | 87   | 108  |
| Sr | ppm | 1300 | 1291 | 558 | 739  | 949 | 656  | 827 | 1105 | 1035 | 974  |
| Nb | ppm | <5   | <5   | <5  | 7    | <5  | 12   | <5  | <5   | 11   | <5   |
| Zr | ppm | 88   | 127  | 125 | 185  | 107 | 165  | 102 | 166  | 197  | 193  |
| Y  | ppm | 25   | 25   | 15  | 35   | 25  | 25   | 21  | 23   | 24   | 26   |
| Th | ppm | <5   | <5   | 11  | <5   | <5  | 19   | <5  | <5   | <5   | <5   |
| U  | ppm | <5   | <5   | <5  | <5   | <5  | <5   | <5  | <5   | <5   | <5   |

#### Normative Mineralogy

|      |       |       |       |       |       |       |       |       |       |       |       |
|------|-------|-------|-------|-------|-------|-------|-------|-------|-------|-------|-------|
| Qtz  | mol % | 0     | 0     | 57.8  | 0     | 2.84  | 39.53 | 0     | 0     | 0     | 9.09  |
| Cor  | mol % | 0     | 0     | 0.19  | 0     | 0     | 0     | 0     | 0.07  | 0     | 0     |
| Zir  | mol % | 0.02  | 0.04  | 0.02  | 0.05  | 0.03  | 0.03  | 0.03  | 0.05  | 0.06  | 0.05  |
| Or   | mol % | 0     | 17.99 | 7.38  | 27.6  | 15.99 | 13.72 | 15.95 | 18.32 | 20.1  | 19.13 |
| Alb  | mol % | 0     | 26.61 | 21.07 | 37.57 | 32.87 | 22.96 | 6.17  | 38.02 | 32.05 | 30.43 |
| An   | mol % | 29.13 | 21.49 | 8.94  | 14.1  | 21.23 | 8.44  | 19.57 | 20.35 | 22.12 | 18.41 |
| Lc   | mol % | 3.6   | 0     | 0     | 0     | 0     | 0     | 0     | 0     | 0     | 0     |
| Ne   | mol % | 6.4   | 3.95  | 0     | 0     | 0     | 0     | 11.12 | 3.17  | 0     | 0     |
| Di   | mol % | 22.3  | 11.96 | 0     | 4.72  | 11.18 | 2.05  | 16.74 | 0     | 4.44  | 5.53  |
| Hy   | mol % | 0     | 0     | 4.09  | 4.43  | 13.63 | 12.15 | 0     | 0     | 6.93  | 14.36 |
| Oliv | mol % | 29.94 | 15.36 | 0     | 8.75  | 0     | 0     | 26.7  | 18.03 | 9.32  | 0     |
| Cs   | mol % | 4.47  | 0     | 0     | 0     | 0     | 0     | 0     | 0     | 0     | 0     |
| Cr   | mol % | 0.01  | 0.02  | 0.01  | 0.02  | 0.02  | 0.02  | 0.02  | 0.02  | 0.02  | 0.02  |
| Ap   | mol % | 0.89  | 0.66  | 0.07  | 0.59  | 0.44  | 0.19  | 0.62  | 0.57  | 0.93  | 0.68  |
| Ilm  | mol % | 3.24  | 1.92  | 0.43  | 2.17  | 1.77  | 0.91  | 3.08  | 1.4   | 4.03  | 2.3   |

#### Lithology Abbreviations

|                      |                                          |
|----------------------|------------------------------------------|
| Gabb=Gabbro          | QHFP=Quartz-Hornblende-Feldspar Porphyry |
| Dior=Diorite         | NiBsIt=Nicola Basalt                     |
| Grdior=Granodiorite  | NiPrAn=Nicola Porphyritic Andesite       |
| Mnzdior=Monzodiorite | TPBsIt=Tertiary Porphyritic Basalt       |
| Mnz=Monzonite        | TABsIt=Tertiary Amygdaloidal Basalt      |

#### Normative Mineralogy Abbreviations

|               |                |                 |
|---------------|----------------|-----------------|
| Qtz=quartz    | An=anorthite   | Oliv=olivine    |
| Cor=corundum  | Lc=leucite     | Cs=DiCaSilicate |
| Zir=zircon    | Ne=nepheline   | Cr=chromite     |
| Or=orthoclase | Di=diopside    | Ap=apatite      |
| Alb=albite    | Hy=hypersthene | Ilm=illmenite   |



A plot of Na<sub>2</sub>O versus K<sub>2</sub>O subdivides intrusive alkaline rocks into high-potassic, potassic and sodic series (Figure 33-6b). All intrusive samples collected at the Ann Property (with the exception of the QHFP dyke) plot in the potassic field. Trace element compositions place all intrusive bodies sampled within the volcanic arc granitoid field on a Rb versus (Y+Nb) discrimination diagram (Figure 33-6c).

Alkalic porphyry deposits of the Canadian Cordillera have been divided into silica-saturated and silica-unsaturated categories by Lang et al. (1995). Silica-unsaturated types are associated with alkalic rocks that have leucite and/or nepheline in their modal or normative mineralogy, (e.g., Mount Polley, Galore Creek and Lorraine); whereas silica-saturated systems (e.g., Copper Mountain, Afton-Ajax and Mount Milligan) are associated with alkalic rocks with modal or normative quartz and lacking feldspathoids. No quartz or feldspathoids were observed during petrographic examination of intrusive and volcanic rocks from the study area. Normative mineralogy, however, shows that samples of gabbro and diorite from the Ann property are nepheline-leucite-normative and nepheline-normative respectively (Table 33-3). As well, samples of Nicola

Group basalt and porphyritic andesite are nepheline-normative. Except for a monzodiorite sample collected from an adjacent property none of the rocks on the study area are quartz-normative. Preliminary normative chemical analyses of rocks at and near the Ann property therefore suggest that it should be classified as a silica-undersaturated alkalic porphyry system.

## DISCUSSION AND CONCLUSIONS

Lithological assemblages, and styles of alteration and mineralization throughout the Ann property study area indicate that it is an alkalic Cu-Au porphyry system similar to other alkalic deposits within Quesnellia. The study area is underlain by an Early Jurassic diorite-monzodiorite intrusive suite emplaced into Late Triassic-Early Jurassic Nicola Group volcanic rocks. The latter rocks consist of massive and polymictic mafic volcanic breccia, augite-phyric andesite, feldspar-hornblende-phyric basalt and porphyritic andesite. Collectively these rocks are interpreted to form part of a comagmatic volcanic sequence (Figure 33-7) that is thought to be coeval with the local stocks, sills and dykes.

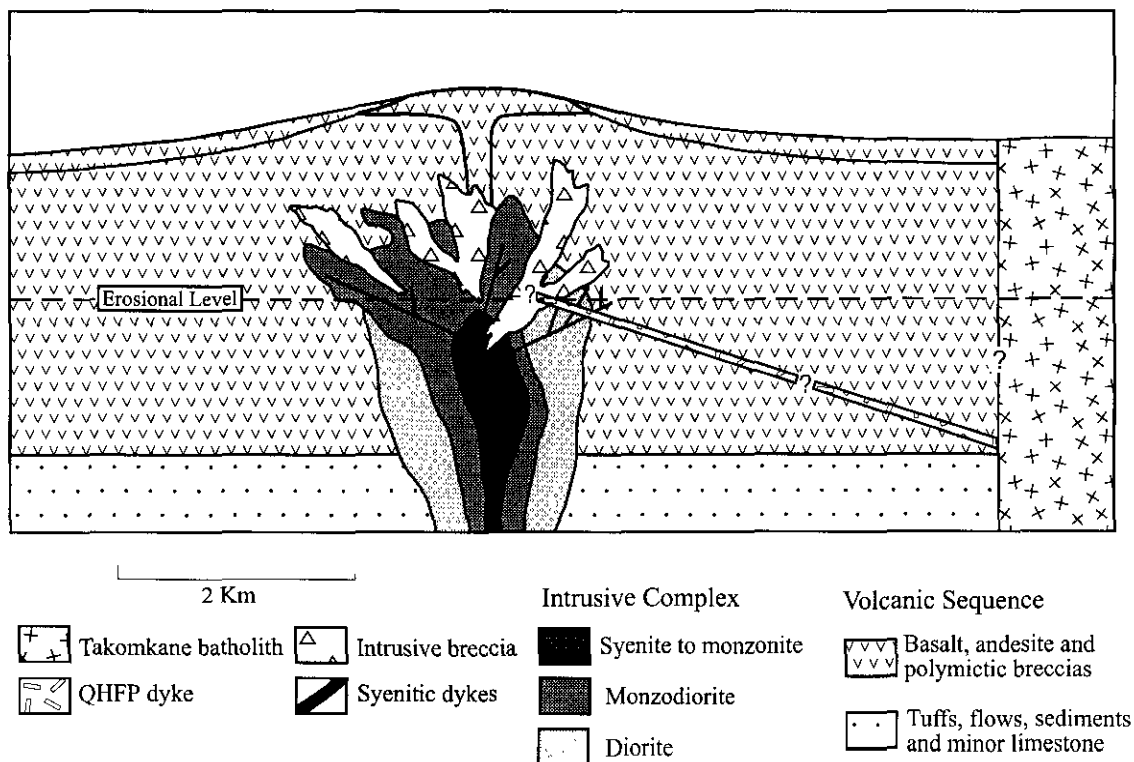


Figure 33-7. Idealized cross-section through the Late Triassic to Middle Jurassic volcanic and intrusive complex at the Ann property study area. Spatial relationships between volcanic and intrusive rocks at the study area, the quartz-hornblende-feldspar porphyry dyke (QHFP), and the Takomkane batholith are speculative.

Geochemically all the intrusive and volcanic rocks at the Ann Property are of alkaline affinity with the exception of the younger Takomkane granodiorite batholith and a quartz-hornblende-feldspar porphyry dyke (QHFP dyke) which are calc-alkaline. On an Rb versus (Y+Nb) diagram all intrusive rocks in the study area, as well as the Takomkane batholith, plot within the island arc granitoid field. The volcanic rocks and the diorite-monzodiorite intrusive suite are cut by a large unmineralized polyolithic intrusive breccia containing angular to subrounded fragments of mafic volcanic and intrusive rocks of dioritic to syenitic composition. An unmineralized calc-alkalic quartz-hornblende-feldspar porphyry dyke (QHFP dyke) cross-cuts the intrusive complex and may be related to regional calc-alkaline magmatic activity.

Hydrothermal alteration throughout the study area is complex and variable. Potassic alteration has affected primarily plutonic rocks and is characterized by potassium feldspar-biotite-magnetite  $\pm$  chlorite  $\pm$  epidote  $\pm$  sulphide  $\pm$  albite assemblage. Within this alteration package are small, generally east-west trending zones of intense potassic feldspar 'flooding' where alteration is characterized by a secondary potassic feldspar-epidote-biotite-magnetite and sparsely disseminated pyrite-chalcopyrite  $\pm$  bornite assemblage. Surrounding the potassic zone are propylitically to potassically altered intrusive phases, Nicola Group volcanic rocks and intrusive breccias. These most commonly contain a secondary mineral assemblage of epidote-magnetite-chlorite-potassium feldspar-calcite-sericite-biotite  $\pm$  albite  $\pm$  pyrite  $\pm$  chalcopyrite  $\pm$  bornite.

Mineralization at the Ann property study area is both fracture-controlled and disseminated. It is most closely associated with zones of moderate to intense potassic-propylitic alteration. Sulphides (pyrite-chalcopyrite  $\pm$  bornite) occur mainly as disseminations and mafic replacement but are locally abundant in veinlets with potassic feldspar-epidote-chlorite  $\pm$  magnetite  $\pm$  albite.

Elevated copper-gold values are known to exist within narrow zones of hydrothermal breccia that cut the diorite-monzodiorite suite at the Ann property adjacent to the QHFP dyke. This type of mineralization (pyrite-chalcopyrite-bornite with gold and abundant magnetite), occurs in veinlets (<1-2 cm), and as disseminated blebs interstitial to brecciated and potassically to albitically altered breccia clasts. The role, if any, of the nearby QHFP dyke in concentrating and remobilizing sulphides and gold associated with hydrothermal brecciation is uncertain.

Trace Pb isotope analyses were performed on feldspars from intrusive bodies and sulphide samples collected both regionally and from the Ann property. The data suggests that the mineralizing fluids that formed the Cu-Au mineralization within the diorite-monzodiorite intrusive complex and regionally were derived from dioritic to monzonitic magmas. Feldspars from the Takomkane batholith have distinctly different isotopic signatures than the other feldspar and sulphide samples analyzed and therefore may be unrelated to mineralization and alteration in the study area.

New U-Pb zircon and titanite ages for rocks at the Ann property and for the Takomkane batholith support previous tectonostratigraphic interpretations that these plutonic bodies represent intrusions emplaced into Quenellia during Middle Jurassic time either during, or just prior to, accretion with cratonic North America. The alkalic diorite-monzodiorite intrusive complex was emplaced during Early Jurassic ( $203 \pm 4$  Ma) time into a Late Triassic-Early Jurassic Nicola Group volcanic sequence. The Early Jurassic age for a porphyritic andesite ( $203.9 \pm 4.2$  Ma) suggests that Nicola Group volcanism continued into Early Jurassic time in the area.

The alkaline intrusive bodies of the Ann Property most closely compare to the mainly Early Jurassic (208-199 Ma) Copper Mountain Suite of plutons, as defined by Woodsworth et al. (1991). This plutonic suite forms a roughly linear, northwest-trending belt of small alkalic intrusions stretching the length of Quesnellia and typically range from diorite to syenite in composition (Lang et al., 1995, and Woodsworth et al., 1991). The Copper Mountain Suite of intrusions hosts several important Cu-Au  $\pm$  Mo porphyry-style deposits, including Mount Polley, Afton-Ajax, Copper Mountain and Galore Creek. The Guichon Plutonic Suite is a mainly latest Triassic to Early Jurassic (210-200 Ma) group of large, primarily calc-alkalic, granodiorite plutons which also scatter along the length of Quesnellia. These intrusions typically have elongate shapes suggesting emplacement may have been controlled by either pre- or synplutonic faults (Gabrielse, 1991). However, the new U-Pb zircon date of  $193 \pm 0.6$  Ma (Early Jurassic) reported here for the calc-alkalic Takomkane batholith indicates a slightly younger age than the rest of the Guichon Plutonic Suite in which it has previously been included. This younger date alone does not preclude the possibility of inclusion within the Guichon Suite but rather may indicate emplacement of this suite over a longer period of time than had previously been thought.

Both the Copper Mountain and Guichon Suites are spatially and temporally related to volcanic rocks of the Nicola Group (Mortimer, 1986). The Guichon Suite has been linked to the calc-alkalic western facies of the Nicola Group island arc assemblage (Monger, 1985), and the smaller, alkalic plutons of the Copper Mountain Suite may be related, as comagmatic equivalents, to the alkaline rocks of the central and eastern Nicola volcanic facies (Barr et al., 1976). Petrographic observations of both volcanic and intrusive rock types coupled with new geochronology for the Ann property alkalic diorite-monzodiorite intrusive complex support the interpretation that the system correlates with the Copper Mountain Suite of intrusions that were emplaced into a central or eastern facies of the Nicola Group. Preto (1979) concluded that these intrusions represent subvolcanic roots of a Late Triassic to Early Jurassic, west-facing island arc.

Despite strong geochemical differences, the alkalic intrusions at the Ann Property and the calc-alkalic Takomkane batholith show a relatively close spatial and temporal relationship. This indicates that both alkaline

and subalkaline magmatism occurred during Early Jurassic time in this area, but does not resolve the question of whether a genetic link exists between these two intrusive suites.

## ACKNOWLEDGEMENTS

This paper forms part of a B.Sc. thesis by the senior author at the Department of Earth and Ocean Sciences, UBC. Financial and technical support were provided by the Ministry of Employment and Investment, Energy and Minerals Division, Mines Branch in Kamloops and by the Mineral Deposits Research Unit (MDRU) at the Department of Earth and Ocean Sciences, UBC. The patient assistance of Fiona Childe was indispensable throughout both U-Pb age-dating and trace-Pb isotope analyses. Critical reviews of the manuscript by Bill McMillan, John Thompson, Jim Lang, Mike Cathro and Vic Preto greatly improved this paper both in content and form.

## REFERENCES

- Barr, D.A., Fox, P.E., Northcote, K.E. and Preto, V.A., (1976): The alkaline suite of porphyry deposits: A summary; Porphyry Deposits of the Canadian Cordillera (A. Sutherland Brown, ed.), *Canadian Institute of Mining and Metallurgy*, Special Volume 15, pages 359-367.
- Blann, D.E., (1995): Ann Property; G.W.R. Resources Inc., Unpublished Report.
- Calderwood, A.R., van der Heyden, P. and Armstrong, R.L., (1990): Geochronometry of the Thuya, Takomkane, Raft and Baldy batholiths, south-central British Columbia; *GAC-MAC*, Program with Abstracts, Volume 15, page A19.
- Campbell, R.B. and Tipper, H.W., (1971): Geology of the Bonaparte Lake Map-Area, British Columbia; *Geological Survey of Canada*, Memoir 363.
- Gabrielse, H. and Yorath, C.J., (1991): Tectonic synthesis, Geology of the Cordilleran Orogen in Canada (H. Gabrielse and C.J. Yorath, eds.); *Geological Survey of Canada*, Geology of Canada, No. 4, DNAG Volume G2, pages 677-705.
- Gale, R.E., (1991): Assessment report on the geology and drilling of the Ann 1 and 2 claims; *Asarco Exploration Company of Canada Ltd.*, Unpublished report.
- Irvine, T.N. and Baragar, W.R.A., (1971): A guide to the chemical classification of the common volcanic rocks; *Canadian Journal of Earth Sciences*, Volume 8, pages 523-548.
- Lang, J.R., Lueck, B., Mortensen, J.K., Russell, J.K., Stanley, C.R. and Thompson, J.F.H., (1995): Triassic-Jurassic silica-undersaturated and silica-saturated alkalic intrusions in the Cordillera of British Columbia: Implications for arc magmatism; *Geology*, Volume 23, pages 451-454.
- Leech, G.B., Lowdon, J.A., Stockwell, C.H., and Wanless, R.K., (1963): Age determinations and geological studies; *Geological Survey of Canada*, Paper 63-17, 140 pages.
- Middlemost, E.A.K., (1975): *Magma and Magmatic Rocks*; Longman Group Limited, Essex.
- Monger, J.W.H., (1989): Geology, Hope Map Sheet, British Columbia; *Geological Survey of Canada*, Map 41-1989, 1:250,000.
- Monger, J.W.H., (1985): Structural evolution of the southwestern Intermontane Belt, Ashcroft and Hope map-areas, British Columbia; Current Research, Part A, *Geological Survey of Canada*, Paper 85-1A, pages 349-358.
- Mortensen, J.K., Ghosh, D.K. and Ferri, F., (1995): U-Pb geochronology of intrusive rocks associated with copper-gold porphyry deposits in the Canadian Cordillera (T.G. Schroeter ed.); *Canadian Institute of Mining, Metallurgy and Petroleum*, Special Volume 46, pages 142-158.
- Mortimer, N., (1987): The Nicola Group: Late Triassic and Early Jurassic subduction-related volcanism in British Columbia; *Canadian Journal of Earth Science*, Volume 24, pages 2521-2536.
- Pearce, J.A., Harris, N.B.W. and Tindle, A.G., (1984): Trace element discrimination diagrams for the tectonic interpretation of granitic rocks; *Journal of Petrology*, Volume 25, pages 956-983.
- Preto, V.A.G., (1972): Geology of Copper Mountain; *British Columbia Ministry of Energy, Mines and Petroleum Resources*, Bulletin 59, 87 pages.
- Preto, V.A.G., (1979): Geology of the Nicola Group between Merritt and Princeton; *British Columbia Ministry of Energy, Mines and Petroleum Resources*, Bulletin 69, 90 pages.
- Saleken, L.W. and Simpson, R.G., (1984): Cariboo-Quesnel gold belt: A geological overview; *Western Miner*, April, pages 15-20.
- Stacey, J.S. and Kramers, J.D. (1975): Approximation of Terrestrial Lead Isotope Evolution by a Two-Stage Model; *Earth and Planetary Science Letters*, Volume 26, pages 207-221.
- von Guttenberg, R., (1994): Ann Property; *Regional Resources Ltd/G.W.R. Resources Inc.*, Unpublished Report.
- Wheeler, J.O. and McFeely, P., (1991): Tectonic assemblage map of the Canadian Cordillera and adjacent parts of the United States of America; *Geological Survey of Canada*, Map 1712A, scale 1:2,000,000.
- Whiteaker, R.J., (1996): The Geology, Geochronology and Mineralization of an Early Jurassic Porphyry System near Lac La Hache, B.C. Unpublished B.Sc. Honours thesis, *University of British Columbia*, Vancouver, B.C.
- Woodsworth G.J., Anderson, R.G., and Armstrong, R.L., (1991): Plutonic regimes, Geology of the Cordilleran Orogen in Canada (H. Gabrielse and C.J. Yorath, eds.); *Geological Survey of Canada*, Geology of Canada, No. 4, DNAG Volume G2, pages 491-531.

